British Journal of Pharmacology (1999) 126, 537–550
http://www.stockton-press.co.uk/bjp

REVIEW ARTICLE

Leukocyte-endothelial cell adhesion: avenues for therapeutic intervention

[1]Julián Panés, [2]Michael Perry & *,[3]D. Neil Granger

[1]Department of Gastroenterology, Institut d'Investigacions Biomèdiques August Pi i Sunyer, Hospital Clínic, Barcelona, Spain; [2]School of Physiology and Pharmacology, University of New South Wales, Sydney, Australia; and [3]Department of Molecular and Cellular Physiology, Louisiana State University Medical Center, Shreveport, Louisiana, U.S.A.

Keywords: Inflammation; leukocyte-endothelial cell adhesion; nuclear factor-kappa B; cytokines; lipid mediators; glucocorticoids; antisense oligonucleotides; selectins; β2-integrins

Abbreviations: AP-1, activation protein-1; CAM, cell adhesion molecule; ESL, E-selectin ligand; ICAM, intercellular adhesion molecule; IL, interleukin; mAb, monoclonal antibody; NF-κB, nuclear factor kappa-B; MAdCAM, mucosal address in cell adhesion molecule; ODN oligodeoxynucleotide; PSGL-1, P-selectin glycoprotein ligand-1; PSL, P-selectin ligand; PECAM, platelet endothelial cell adhesion molecule; TFD, transcription factor decoy; TNF-α, tumour necrosis factor-alpha; VCAM, vascular cell adhesion molecule; VLA, very late antigens

Introduction

Leukocyte-endothelial cell adhesion has been implicated in the pathogenesis of a variety of diseases that affect different organ systems. Examples of such diseases include atherosclerosis, gastric ulcers, haemorrhagic shock, myocardial infarction, stroke, and malaria (Korthuis *et al*., 1994; Panés & Granger, 1998). The recognition that leukocytes must firmly adhere to vascular endothelial cells in order to mediate the organ dysfunction and tissue injury associated with these diseases has resulted in an intensive effort to define the factors that modulate this cell-cell interaction. A major focal point of this effort has been directed towards identifying and characterizing the adhesion glycoproteins that enable leukocytes to bind to vascular endothelial cells. Data derived from both *in vitro* (isolated leukocytes binding to monolayers of cultured endothelial cells) and *in vivo* (intravital microscopic examination of venules) models of leukocyte-endothelial cell adhesion have revealed the relative contributions of different leukocyte and endothelial cell adhesion molecules (CAMs) to the adhesion responses elicited by various inflammatory stimuli. These studies have also led to an appreciation of the potential cellular and molecular loci that can be targeted to interfere with leukocyte-endothelial cell adhesion. As a result, there is a widely held view that several of these loci also represent novel and potentially powerful therapeutic sites for treatment of acute and chronic inflammatory diseases. The major objective of this review is to discuss some of the major potential targets for therapeutic intervention against inflammation that relate to the process of leukocyte-endothelial cell adhesion and more specifically to the regulation of endothelial CAM expression. That discussion is preceded by a brief description of the major CAMs that participate in the recruitment of leukocytes into inflamed tissue and how the expression of these CAMs is coordinated to ensure an orderly sequence of cell-cell interactions.

*Author for correspondence at: Department of Molecular and Cellular Physiology, LSU Medical Center, 1501 Kings Highway, Shreveport, Louisiana 71130-3932, U.S.A.
E-mail: dgrang@lsumc.edu

Adhesion Molecules

Both leukocyte and endothelial CAMs participate in slowing the leukocyte as it exits the capillary and enters the postcapillary venule, which is the major site of leukocyte-endothelial cell adhesion. The initial low affinity interaction between leukocytes and venular endothelium is manifested as a rolling behaviour. Rolling leukocytes can then become firmly adherent (stationary) on the vessel wall, where the process of transendothelial leukocyte migration can occur if a chemotactic signal is generated in the perivascular compartment. Each of the three stages of leukocyte recruitment (Figure 1), i.e., rolling, firm adhesion (adherence) and transendothelial migration, involves the participation of different families of adhesion molecules, including the selectins, β-integrins, and supergene immunoglobulins (Table 1).

Selectins

L-selectin The selectins are a family of lectin-like molecules that mediate leukocyte rolling. L-selectin is normally expressed on most circulating leukocytes while its ligand is only present on activated endothelium. L-selectin is shed from the surface of activated neutrophils, which consequently limits the ability of these cells to roll on endothelial cells (Tedder *et al*., 1995a). Mutant mice that are genetically deficient in L-selectin exhibit an attenuated leukocyte recruitment after an inflammatory stimulus (Tedder *et al*., 1995b). L-selectin binds to a number of different CAMs expressed on the endothelial cell (Table 1) including P-selectin, E-selectin and GlyCAM.

P-selectin This adhesion molecule is expressed on the surface of activated endothelial cells and platelets. It is stored in Weibel-Palade bodies in endothelial cells and in alpha-granules in platelets. When endothelial cells are stimulated (e.g. with thrombin or histamine), P-selectin is mobilized to the surface of activated endothelial cells within minutes, after which it is either recycled back inside the cell membrane or shed into the plasma (Tedder *et al*., 1995a). During inflammation, endothelial P-selectin acts to recruit leukocytes into postcapillary venules, while platelet-associated P-selectin promotes the aggregation of leukocytes with platelets to form thrombi (Kunkel *et al*., 1996). Endothelial cells can also synthesize and

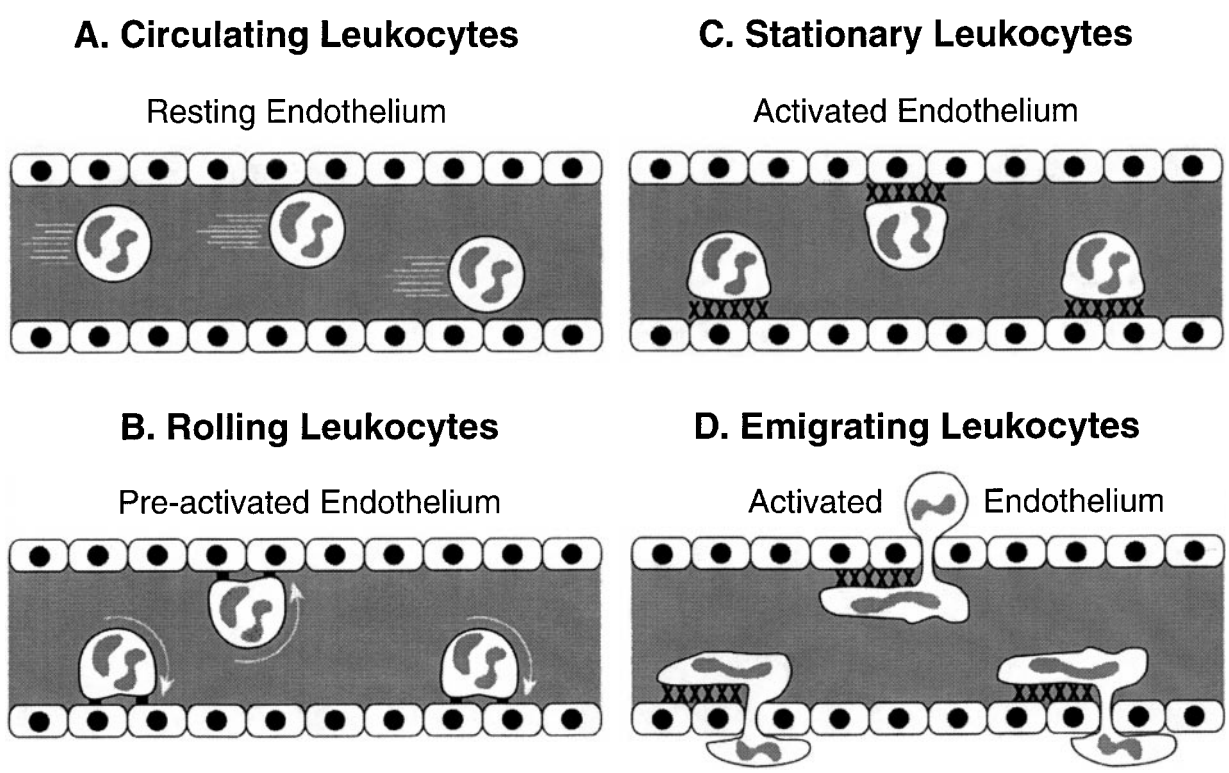

Figure 1 Steps in the recruitment of leukocytes in postcapillary venules. (A) illustrates that in the absence of an inflammatory stimulus, leukocytes are largely flowing in the stream of red cells with no adhesive interactions with venular endothelium. (B) illustrates the low affinity interaction between leukocytes and endothelium that is mediated by selectins and manifested as rolling. (C) illustrates that activation of leukocytes and/or endothelial cells can result in stationary adhesion of leukocytes. (D) illustrates that firmly adherent leukocytes can emigrate from venules into the adjacent interstitial compartment, usually along a chemotactic gradient.

express P-selectin in response to endotoxin or cytokines. However, important species difference have been observed in the response to these stimuli: whereas tumour necrosis factor-alpha (TNF-α) and endotoxin increase expression of P-selectin in murine endothelial cells (Eppihimer *et al*., 1996; Pan *et al*., 1998b), they do not do so in human endothelial cells (Yao *et al*., 1996). This differential response may be related to differences in the P-selectin promoter among species (Pan *et al*., 1998a). Leukocytes normally express several ligands for P-selectin, including L-selectin and P-selectin glycoprotein ligand-1 (PGSL-1) (Panés & Granger, 1998).

E-selectin Unlike P-selectin, the expression of E-selectin on endothelial cells is entirely under transcriptional control. While E-selectin is not constitutively expressed on endothelial cells, its synthesis (and expression) can be induced by cytokines such as interleukin-1 (IL-1) and TNF-α or by endotoxin (Fries *et al*., 1993). E-selectin expression is detected as early as 2 h after endotoxin stimulation and returns to baseline values by 8 h. This contrasts with P-selectin which has an early peak derived from the preformed pool, a further transcription-dependent elevation that peaks at about 5 h, followed by a sustained level of expression beyond 12 h (Eppihimer *et al*., 1996). Ligands on the leukocyte for E-selectin include L-selectin and E-selectin ligand (ESL).

Integrins

Integrins are heterodimeric proteins consisting of alpha and beta subunits. These glycoproteins are expressed on the surface of leukocytes, where they can mediate leukocyte-endothelial cell adhesion within a few minutes after an inflammatory stimulus. The specificity of the various integrins depends on their molecular structure. The integrins associated with leukocyte adhesion belong to the beta-1, beta-2 and beta-7 subfamilies. Members of the beta-2 subfamily contain one of four different alpha chains designated CD11a, CD11b, CD11c, and CD11d that are coupled to a common beta chain, CD18 (see Table 1). The heterodimer CD11a/CD18 is expressed on the surface of most leukocytes and interacts with ICAM-1 and ICAM-2 on endothelial cells to cause firm adhesion (Marlin & Springer, 1987). This integrin is not stored to any appreciable degree within the leukocyte so upregulation most likely results from a conformational change that allows the leukocyte to interact with ICAM-1 (Panés & Granger, 1998).

The heterodimers CD11b/CD18 and CD11c/CD18, expressed by granulocytes and monocytes, are stored in granules and on activation of the leukocyte are rapidly mobilized to the cell surface by fusion with the cell membrane (Panés & Granger, 1998). Activation by inflammatory mediators such as PAF or cytokines such as TNF-α results in a 10–30 fold increase in expression of these integrins on the cell surface. CD11b/CD18 interacts with ICAM-1 on endothelium while the ligand for CD11c/CD18 remains uncertain. The role for the recently described CD11d/CD18 (Shelley *et al*., 1998) in leukocyte recruitment has not been established. Immunoneutralization of these integrins by appropriately directed antibodies will prevent the adhesion of activated leukocytes to activated endothelium. The adhesion of unstimulated leukocytes to endothelial cells is mediated by CD11a/CD18-ICAM-1 interactions while activated leukocytes use both CD11a/CD18 and CD11b/CD18 to bind to ICAM-1 on the endothelium. The biologic importance of the beta-2 integrins was demonstrated

Table 1 Adhesion molecules involved in leukocyte-endothelial cell adhesion

Adhesion Molecule	*Location*	*Expression*		*Ligand*	*Function*
		Constitutive	*Inducible*		
Selectin family					
L-Selectin	All leukocytes	Yes	No (shed on activation)	P-selectin, E-selectin, GlyCAM, CD14, MAdCAM	Rolling
P-Selectin	Endothelial cells, platelets	Yes	Yes	L-selectin, PSGL-1, PSL	Rolling
E-Selectin	Endothelial cells	No	Yes	L-selectin, CLA, SSEA, ESL	Rolling
Integrin family					
CD11a/CD18	All leukocytes	Yes	No	ICAM-1, ICAM-2	Adherence, emigration
CD11b/CD18	Granulocytes, monocytes	Yes	Yes	ICAM-1	Adherence, emigration
CD11c/CD18	Granulocytes, monocytes	Yes	Yes	?	?
$\alpha_4\beta_1$ (VLA)	Lymphocytes, monocytes, eosinophils basophils	Yes	No	VCAM-1, extra-cellular matrix molecules	Adherence
$\alpha_4\beta_7$	Lymphocytes	Yes	No	MAdCAM-1, VCAM-1 fibronectin	Adherence
Immunoglobulin superfamily					
ICAM-1	Endothelium, monocytes	Yes	Yes	CD11a/CD18 CD11b/CD18 CD43	Adherence, emigration
ICAM-2	Endothelium	Yes	No	CD11a/CD18	Adherence, emigration
VCAM-1	Endothelium	No	Yes	$\alpha_4\beta_1$, $\alpha_4\beta_7$	Adherence
PECAM-1	Endothelium, leukocytes, platelets	Yes	No	PECAM-1 (homo-philic)	Adherence, emigration
MAdCAM-1	Endothelium (intestine)	Yes	Yes	L-selectin, $\alpha_4\beta_7$	Adherence, emigration

CLA, cutaneous lymphocyte antigen; ESL, E-selectin ligand; ICAM, intercellular adhesion molecule; MAdCAM, mucosal address in cell adhesion molecule; PECAM, platelet-endothelial cell adhesion molecule; PSGL, P-selectin glycoprotein ligand; PSL, P-selectin ligand; SSEA, sialyl stage-specific embryonic antigen; VCAM, vascular cell adhesion molecule; VLA, very late antigen.

dramatically by the identification of its deficiency in humans. Leukocyte adhesion deficiency is an autosomal recessive trait, characterized by recurrent infections, impaired pus formation and would healing, and abnormalities of many adhesion dependent functions of granulocytes, monocytes and lymphoid cells (Anderson *et al*., 1985). Features of this disorder can be attributed to deficiency of the cell-surface expression of the entire CD11/CD18 complex, which is, in turn, a result of heterogeneous mutations of the CD18 gene (Anderson *et al*., 1985). A major role for the beta-2 integrins in mediating leukocyte-endothelial cell adhesion is also supported by experimental results obtained in mutant mice that are genetically deficient in CD18 (Eppihimer *et al*., 1997; Horie *et al*., 1997a).

Heterodimers of the beta-1 and beta-7 subfamilies also contribute to recruitment of different leukocyte populations. The beta-1 integrin $\alpha4\beta1$ (also designated as very late antigen-4 [VLA-4]) mediates the adhesion of lymphocytes, monocytes, eosinophils and natural killer cells to activated endothelial cells, which express the counter-receptor, vascular cell adhesion molecule-1 (VCAM-1) (Elices *et al*., 1990). The beta-7 integrin $\alpha4\beta7$ is found on lymphocytes that colonize the gut and gut-associated lymphoid tissue. This integrin binds to mucosal address in cell adhesion molecule-1 (MAdCAM-1) on the high endothelial venules of lymphoid tissue and mediates the normal homing of lymphocytes to Peyer's patches (Tsuzuki *et al*., 1996). It also binds to VCAM-1 under conditions of inflammation.

Immunoglobulin superfamily

Five members of the immunoglobulin (Ig) superfamily act as adhesion molecules; ICAM-1, ICAM-2, VCAM-1, platelet endothelial cell adhesion molecule-1 (PECAM-1) and MAdCAM-1. ICAM-1 is normally found on the surface of endothelial cells, but its expression can be significantly increased upon endothelial activation with cytokines or endotoxin. This upregulation varies from one vascular bed to another and, in general, those beds with high constitutive expression like the lung show less upregulation than vascular beds with low constitutive expression (e.g., skeletal muscle or heart). Following endotoxin challenge, peak ICAM-1 expression occurs at around 5 h and remains elevated for 24 h (Panés *et al*., 1995). ICAM-1 binds to CD11a/CD18 and CD11b/CD18 on leukocytes and peak levels of ICAM-1 expression are associated with maximum leukocyte adherence. A soluble isoform of ICAM-1 (sICAM-1), which represents shed fragments of endothelial ICAM-1, can be detected in plasma during inflammation (Komatsu *et al*., 1997). While there is some evidence suggesting that sICAM-1 binds to CD11/CD18 on leukocytes, the functional consequences of this binding remains unclear. However, the importance of ICAM-1 in mediating the recruitment of leukocytes has been demonstrated using both ICAM-1 blocking antibodies and ICAM-1 deficient mice. ICAM-2 is constitutively expressed on endothelial cells and this expression is not influenced by the level of activation of the endothelial cell. ICAM-2 binds to

CD11a/CD18 but with a lower affinity than ICAM-1 (Panés & Granger, 1998).

VCAM-1, which can bind to both $\alpha4\beta1$ and $\alpha4\beta7$ on leukocytes, mediates the trafficking of monocytes and lymphocytes. While the constitutive level of VCAM-1 expression is significantly lower than that of ICAM-1, profound increases in VCAM-1 density on endothelial cells are noted 5–9 h after cytokine stimulation (Henninger *et al*., 1997). PECAM-1, which is constitutively expressed on platelets, leukocytes and endothelial cells, mediates the adhesion of both platelets and leukocytes to endothelial cells (*via* homophilic interactions) and the migration of leukocytes through endothelial cells (Muller *et al*., 1993) as well as migration of these cells through the perivascular basement membrane (Wakelin *et al*., 1996). While cytokine challenge does not result in an increased expression of PECAM-1 on endothelial cells, the adhesion molecule is redistributed to the borders of adjacent endothelial cells where it participates in endothelial cell-cell interactions that affect leukocyte transmigration and microvascular permeability (Romer *et al*., 1995).

MAdCAM-1 is expressed on high endothelial venules. MAdCAM-1 serves as a ligand for L-selectin and $\alpha4\beta7$ integrin and it is involved in lymphocyte homing to Peyer's patches.

Modulation of leukocyte-endothelial cell adhesion

Data derived from both *in vitro* and *in vivo* studies have implicated a number of chemical and physical factors that can influence both the time-course and magnitude of leukocyte-endothelial cell adhesion. The principal physical influence on the adhesion process is shear stress, a force that is generated by the movement of blood in postcapillary venules. Venular wall shear stress determines the level of leukocyte rolling and firm adhesion, and it dictates the contact area between rolling leukocytes and the endothelial cell surface. Reductions in venular blood flow (shear stress) facilitate leukocyte rolling and adhesion, while increases in blood flow tend to oppose leukocyte-endothelial cell adhesion. At low shear rates, the contact time between adhesion molecules on leukocytes and endothelial cells is increased thereby allowing greater opportunity for formation of the strong adhesive bonds that is necessary for a rolling leukocyte to become stationary (Panés & Granger, 1998).

A large number of biological chemicals have been identified that either inhibit or promote leukocyte-endothelial cell adhesion (see Table 2). Most of the chemicals identified as modulators of leukocyte adhesion fall into the category of pro-adhesive agents. Some of these agents, such as histamine, platelet activating factor and IL-8, can rapidly (within 2–3 mins) increase the level of activation and/or expression of adhesion molecules on leukocytes (e.g., CD11b/CD18) and/or endothelial cells (e.g., P-selectin). Other pro-adhesive agents, such as the cytokine TNF-α, act more slowly to promote leukocyte adhesion by enhancing the transcription-dependent expression of endothelial cell adhesion molecules that act to extend and further increase the leukocyte rolling (E-selectin) and adherence/emigration (ICAM-1) responses.

The list of endogenous anti-adhesive chemicals that have been identified to date is relatively small. These agents tend to exert their inhibitory actions on both the leukocyte and endothelial cell, and the underlying mechanisms of action remain poorly understood. Some of the anti-adhesive compounds (nitric oxide, PGI2, and adenosine) are also potent vasodilators, which raises the possibility that their actions *in vivo* can be attributed to increases in venular shear rate. However, there is substantial evidence suggesting that increased shear rates account for only a small component of the inhibitory effect on leukocyte-endothelial cell adhesion. Nitric oxide and glucocorticoids appear to exert at least some of their effects by inhibiting the transcription-dependent expression of endothelial cell adhesion molecules (Panés & Granger, 1998).

Table 2 Modulation of leukocyte-endothelial cell adhesion

	Target	
	Endothelium	*Leukocyte*
Antiadhesive		
Cytokines	IL-4, IL-10, IL-13	IL-4, IL-10, IL-13
Prostaglandins		Prostaglandin I_2
Other	Adenosine	Adenosine
	Nitric oxide	Nitric oxide
	Glucocorticoids	
Proadhesive		
Cytokines	TNFα, TNFγ	TNF-α
	IL-1, IL-4, IFN-γ	IL-1, IL-3, IL-5
Chemokines		IL-8, MCP-1
Lipid mediators	Leukotriene B_4	Leukotriene B_4
	PAF	PAF
	LPS	LPS
		C3b, C5a
Peptides	Histamine	Neuropeptides

The table lists examples and is not intended to be a comprehensive list of all mediators under each category.

Targets for therapeutic intervention

The cellular and molecular basis for the recruitment of leukocytes to sites of inflammation is highly complex and multifactorial, however there is sufficient experimental evidence in the literature to outline the key elements and sequential nature of this process. As illustrated in Figure 2, the inflammatory response involves the participation of multiple cell types, including circulating leukocytes, vascular endothelial cells, and perivascular cells (e.g., mast cells, macrophages), with the latter cells contributing to the initiation and perpetuation of inflammation through the generation of a variety of inflammatory mediators. Following the primary insult (infection, injury, or hypersensitivity reaction), macrophages and mast cells are stimulated (e.g., by activated complement) to release mediators, such as histamine, oxygen radicals, platelet activating factor, leukotrienes, and cytokines. The engagement of histamine, leukotrienes and certain other mediators with their receptors on endothelial cells results in the rapid mobilization of P-selectin from its preformed pool in Weibel-Palade bodies to the cell surface. Hence, within minutes there is an increased recruitment of rolling leukocytes in postcapillary venules that allows for an enhanced exposure of the previously circulating cells to other mediators liberated from the inflamed tissue. The slowly rolling leukocytes are exposed to PAF, leukotrienes, and other mediators that rapidly activate, and then promote the shedding of, L-selectin on leukocytes. As the L-selectin is shed, there is a corresponding increase in the expression and activation of $\beta2$-integrins on leukocytes. The newly expressed and/or activated CD11/CD18 can then bind to its counter-receptor ICAM-1, which is constitutively expressed on endothelial cells. The $\beta2$-integrin/ICAM-1 adhesive interactions enable the inflamed tissue to recruit firmly adherent and emigrating

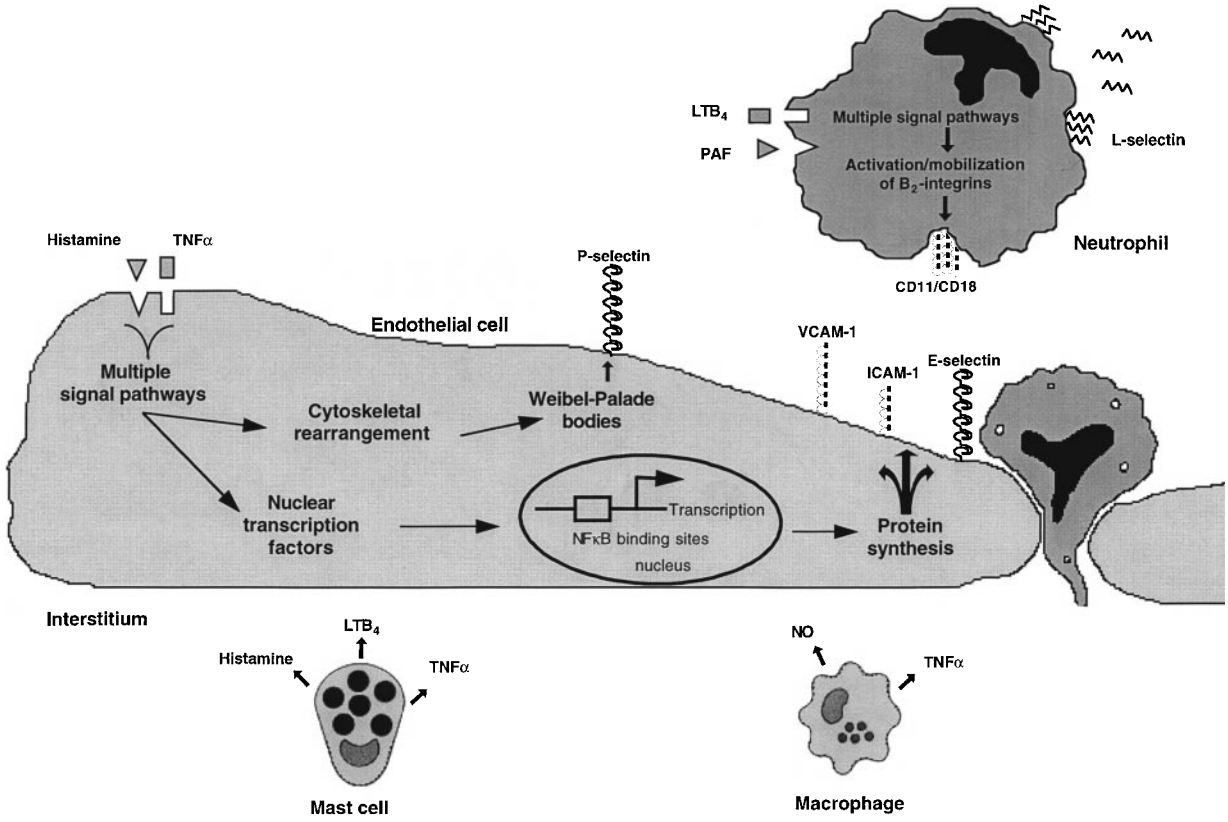

Figure 2 Mechanisms underlying the expression of adhesion molecules on leukocytes and endothelial cells at the onset of inflammation. Perivascular cells such as mast cells and macrophages initiate the response by releasing a variety of inflammatory mediators. Engagement of lipid mediators (LTB_4 and PAF) with receptors on neutrophils results in the activation of β_2-integrins (CD11/CD18). Engagement of histamine with its receptor (H1) on endothelial cells results in the rapid mobilization of preformed P-selectin from its storage site (Weibel-Palade bodies). Engagement of cytokines (e.g., TNFα) to their receptors on endothelial cells lead to the activation of nuclear transcription factors (e.g., NF-κB) that stimulates the synthesis of adhesion glycoproteins, such as VCAM-1, ICAM-1, and E-selectin, which are subsequently expressed on the cell surface.

leukocytes within a few minutes after the initial insult. This intimate interaction also allows PECAM-1, which is constitutively expressed on both endothelial cells and leukocytes, to promote the homophilic adhesion and emigration of leukocytes.

While the rapid inducers of leukocyte rolling, adherence and emigration are eliciting their actions, mast cell- and macrophage-derived cytokines engage with their receptors on endothelial cells. This ultimately (*via* specific signalling pathways) leads to the activation of nuclear transcription factors that modulate the biosynthesis of endothelial cell adhesion molecules that mediate leukocyte rolling (E-selectin) and adherence (ICAM-1, VCAM-1). Consequently, within a few hours (2–4) after the initial inflammatory insult, there is a profound increase in the density of virtually all endothelial cell adhesion molecules that participate in the trafficking of leukocytes during inflammation. As a result of this increased endothelial CAM expression, the recruitment of leukocytes can be sustained at both a higher level and for a longer duration.

The sequence of events described above suggest that there are several potential cellular and molecular loci that can be targeted to interfere with the leukocyte-endothelial cell adhesion associated with inflammation. The following section addresses three potential targets for therapeutic intervention against inflammation that relate to the process of leukocyte-endothelial cell adhesion. These are: (1) inflammatory mediator release and receptor engagement, (2) adhesion molecule synthesis, and (3) adhesion molecule function.

Inflammatory mediators

Experimental findings A large number of mediators have been implicated in the initiation of leukocyte-endothelial cell adhesion during inflammation (Table 2). Several experimental strategies have been employed to assess the contribution of specific mediators to this facet of the inflammatory response. These include: (1) detection of the mediator at sites of inflammation characterized by leukocyte adhesion, (2) demonstration that leukocyte-endothelial cell adhesion can be induced by exposure of non-inflamed venules to an exogenous source of mediator, and (3) inhibition of leukocyte adhesion by agents known to either antagonize or inhibit the production of the mediator. Several inflammatory mediators, including histamine, PAF, LTB4, cytokines, and chemokines have been shown to promote leukocyte rolling, adherence and/or emigration when applied directly to postcapillary venules (Panés & Granger, 1998). A role for specific leukocyte and/or endothelial cell adhesion molecules in mediating these actions has been demonstrated for most of the mediators using either monoclonal antibodies directed against the CAMs (Zimmerman *et al*., 1994a) or mice that are genetically deficient in a specific CAM (Kunkel *et al*., 1996; Xu *et al*., 1994). In some instances (e.g., histamine and cytokines), corroborative *in vivo* evidence of CAM involvement has been obtained from quantitative estimates of endothelial CAM expression in different vascular beds after administration of the inflammatory mediator (Eppihimer *et al*., 1996; Henninger *et al*., 1997).

Antagonists to histamine (Kurose *et al*., 1994c), PAF (Kubes *et al*., 1990b), leukotrienes (Zimmerman *et al*., 1990), IL-8 (Mulligan *et al*., 1993) and TNF-α (Appleyard *et al*., 1996) have been shown to prevent or attenuate the leukocyte-endothelial cell adhesion observed in different models of acute or chronic inflammation. For example, the histamine receptor (H1) antagonist hydroxyzine has been shown to markedly reduce the leukocyte-endothelial cell adhesion and consequent microvascular injury elicited by *Clostridium difficile* toxin A (Kurose *et al*., 1994c). Both PAF- (e.g., WEB 2086) and LTB4-receptor (SC41930) receptor antagonists have proven effective in reducing the leukocyte adhesion observed in tissues exposed to either ischaemia and reperfusion (Kubes *et al*., 1990a; Zimmerman *et al*., 1990) or to inhibition of nitric oxide biosynthesis (Arndt *et al*., 1993). Finally, a role for LTB4 in mediating the leukocyte-endothelial cell adhesion induced by non-steroidal anti-inflammatory drugs, such as aspirin and indomethacin, has been demonstrated using both an LTB4-receptor antagonist (SC41930) and a leukotriene biosynthesis inhibitor (L663,536) (Asako *et al*., 1992).

The involvement of inflammatory mediators in leukocyte-endothelial cell adhesion has also been addressed using agents that are known to stabilize or inhibit the function of perivascular cells that produce and release inflammatory mediators. Mast cell stabilizers have been shown to attenuate the leukocyte-endothelial cell adhesion elicited in postcapillary venules by either ischaemia-reperfusion (Kurose *et al*., 1997), oxidized low density lipoproteins (Liao & Granger, 1996), *Helicobacter pylori* (Kurose *et al*., 1994b), or *Clostridium difficile* toxin A (Kurose *et al*., 1994c). Kupffer cells, the resident macrophages of the liver, have also been implicated in the recruitment of adherent leukocytes. It was shown that treatment with gadolinium chloride, which reduces Kupffer cell function, reduces the recruitment of adherent leukocytes in terminal hepatic venules to the same low level as observed after administration of a TNF-α blocking antibody in a model of ischaemia-reperfusion (Horie *et al*., 1997b).

Therapeutic applications A number of drugs have been developed to antagonize the actions of inflammatory mediators. While many of these drugs, including antihistamines and mast cell stabilizers are widely used in the treatment of inflammation, there is no evidence that directly implicates inhibition of leukocyte-endothelial cell adhesion as a primary mode of action. Nonetheless, data derived from experimental models of inflammation suggest that these agents are likely to interfere with the expression of either leukocyte or endothelial CAM. It also reasonable to assume that the new generation of mediator-directed therapeutic agents such as soluble IL-1 receptor antagonists or TNF-α antibodies, which have proven anti-inflammatory actions in the clinical setting (Fisher *et al*., 1994; Targan *et al*., 1997), exert at least part of their effect through inhibition of endothelial CAM expression.

A major advantage of inflammatory mediator antagonists is their ability to suppress different components of the inflammatory response. For example, PAF and LTB4 antagonists may also act by interfering with the ability of granulocytes to produce oxygen radicals, release proteases, and increase the expression of β2-integrins. Similarly, cytokine-directed inhibitors can blunt the inflammatory responses of macrophages, mast cells, and circulating leukocytes, all of which release mediators that can amplify the expression of endothelial CAMs. However, a major disadvantage of inflammatory mediator-directed therapeutic strategies is their reliance on the assumption that a single mediator can orchestrate all or most of the redundant processes that contribute to leukocyte recruitment. The large number of mediators that can elicit the upregulation of leukocyte rolling receptors alone would argue against the wisdom of this strategy. Nonetheless, it is reasonable to assume that administration of several antagonists should prove more effective in inhibiting the CAM expression associated with inflammation.

Adhesion molecule synthesis

An important target for therapeutic intervention against inflammation that relates to the process of leukocyte-endothelial cell adhesion is endothelial CAM biosynthesis. Targeting this process has the potential to impact the expression of all endothelial CAMs and consequently exert a profound inhibitory effect on leukocyte recruitment. While there are several strategies that can be used to inhibit the biosynthesis of endothelial CAMs, some of these have recently received considerable attention and appear to hold much promise.

Nuclear transcription factors Inducible gene expression is a key regulatory mechanism that requires transcriptional activator proteins whose DNA binding or transcription activity is induced upon exposure of cells to specific stimuli. Of the many transcription factors that have been described, nuclear factor kappa-B (NF-κB) and activation protein-1 (AP-1) appear to be particularly relevant to the regulation of genes involved in the inflammatory cascade. Both factors represent families of polypeptides with related DNA-binding activity but distinct transactivating potential.

NF-κB is an inducible, multisubunit transcription factor of higher eukaryotes. The DNA-binding forms of NF-κB exist as dimeric complexes composed of various combinations of members of the Rel/NF-κB family of polypeptides. NF-κB dimers (e.g., p50/p65) are normally sequestered in the cytosol of unstimulated cells *via* noncovalent interactions with a class of inhibitory proteins called IκBs. These inhibitory proteins prevent nuclear transport and DNA binding of NF-κB/Rel proteins. Signals that induce NF-κB activation cause the dissociation and subsequent degradation of IκB proteins, which allows NF-κB dimers to enter the nucleus and induce gene expression (May & Ghosh, 1988).

NF-κB plays an important role in the expression of a large number of inducible genes, many of which contribute to the cellular responses to stress, injury and inflammation. Consequently, NF-κB can be activated by signals that are associated with such states, including cytokines (such as IL-1 and TNF-α), bacterial endotoxins, and pro-apoptotic and necrotic stimuli such as oxygen free radicals, u.v. light and gamma-irradiation. When cells are exposed to these pathogenic stimuli, a cascade of events leads to the phosphorylation and subsequent degradation of IκB, resulting in NF-κB liberation and its entry into the nucleus, where it activates gene expression (Baeuerle, 1998). NF-κB activation is triggered by the phosphorylation and subsequent conjugation of IκB with ubiquitin, which makes IκB a substrate for degradation by the proteasome proteolytic pathway. Peptide aldehyde inhibitors of the proteasome such as calpain inhibitor 1 and MG-132 (Brown *et al*., 1995) have been shown to block the degradation of IκB and consequent activation of NF-κB that is elicited by TNF-α.

AP-1 is another transcription factor that is composed of homo- and heterodimers of the products of the jun and fos proto-oncogenes. AP-1 subunits include c-jun, jun-B, jun-D, c-Fos, Fos-B, Fra-1 and Fra-2 (Karin & Smeal, 1992). AP-1

activity is induced by many stimuli, including phorbol esters (which activate protein kinase C), polypeptide hormones, cytokines and hydrogen peroxide (Angel & Karin, 1991; Roebuck *et al*., 1995). Several mechanisms account for the regulation of AP-1 activity, including phosphorylation and postranslational modification (Angel & Karin, 1991).

Transcription factors and adhesion molecule expression

Binding sites for NF-κB have been identified in the promoter regions of the genes for E-selectin, VCAM-1 and ICAM-1, while a binding site for AP-1 has been localized on the promoter region of the ICAM-1 gene. Point mutations which decrease NF-κB binding to κB elements result in diminished cytokine-induced E-selectin expression on cultured endothelial cells, suggesting that NF-κB plays an important role in cytokine induction of the E-selectin gene (Essani *et al*., 1996). Two closely spaced functional κB elements have also been identified in the MAdCAM-1 promoter (Takeuchi & Baichwal, 1995). The increased ICAM-1 expression on endothelial cells exposed to hydrogen peroxide (Lo *et al*., 1993) appears to be mediated through AP-1, and independent of κB elements (Roebuck *et al*., 1995). Therefore, hydrogen peroxide and cytokines appear to activate ICAM-1 gene transcription in endothelial cells through distinct cis-regulatory elements within the ICAM-1 promoter.

It was recently demonstrated that inhibitors of the proteasomal degradation pathway for IκB lead to decreased nuclear accumulation of NF-κB and the subsequent abrogation of TNF-α induced cell-surface expression of E-selectin, VCAM-1, and ICAM-1 in endothelial cells (Read *et al*., 1995). This response has important functional consequences because proteasome inhibitors also block both the adherence and emigration of leukocytes in human endothelial cell monolayers.

Therapeutic applications Recent evidence indicates that the transcription factors AP-1 and NF-κB are major targets for some of the commonly used anti-inflammatory drugs including glucocorticoids, aspirin, salicylates, gold salts and D-penicillamine. Glucocorticoids activate the glucocorticoid receptor (GR) in the cytosol, which then form GR-GR homodimers that bind a specific DNA sequence termed the glucocorticoid response element (GRE). Increased transcription of genes bearing a GRE in their promoter region follows. In addition to positive regulation of gene expression, glucocorticoids inhibit the expression of a wide variety of genes involved in the inflammatory process.

An improved understanding of the anti-inflammatory mechanism of glucocorticoids came from the observation that ligand activated GR inhibits AP-1 and NF-κB mediated transcription (reviewed in Cato & Wade, 1996). For example, glucocorticoids inhibit the NF-κB mediated expression of adhesion molecules ICAM-1 (Tailor *et al*., 1997), VCAM-1 (Tessier *et al*., 1996), and E-selectin (Brostjan *et al*., 1997). Glucocorticoids also inhibit the AP-1 expression of collagenases I and IV (Handel, 1997). Several mechanisms for the mutual antagonism between GR and NF-κB, and between GR and AP-1, have been proposed. For example, a direct protein-protein interaction between the GR and NF-κB has been proposed that will prevent the binding of GR and NF-κB to their respective DNA response elements (Ray & Prefontaine, 1994) (Figure 3). Similarly, binding of GR to Jun and Fos has been thought to cause mutual inhibition of GR and AP-1 DNA binding (Sakurai *et al*., 1997). Glucocorticoids also increase transcription of the gene for IκB, thereby increasing the formation of this protein which binds to activated NF-κB in the nucleus. The IκB protein probably induces the dissociation of NF-κB from κB sites on target genes and causes NF-κB to move to the cytoplasm (Scheinman *et al*., 1995).

Recent evidence shows that in human inflammatory bowel disease (Ardite *et al*., 1998) and in asthma (Adcock, 1996), cessation of the inflammatory activity in response to steroid treatment is associated with disappearance of NF-κB from nuclear extracts of intestinal or bronchial mucosa, and that failure to abrogate NF-κB activation results in persistence of the inflammatory process. In patients with steroid-resistant asthma, there appears to be an exaggerated activation of AP-1 that binds to and therefore sequesters activated GR inside the nucleus; this would reduce the availability of GR to inhibit NF-κB, which is normally activated in such patients (Adcock *et al*., 1995).

Gold salts significantly inhibit AP-1 DNA binding in nuclear extracts at concentrations of 5 mM, which is within the range achieved in the serum of rheumatoid arthritis patients under this treatment. Gold salts have also been shown to inhibit IL-1 induced expression of NF-κB and AP-1 dependent transfected reporter genes (Williams *et al*., 1992) and to inhibit DNA binding activity of NF-κB *in vitro* (Yang *et al*., 1995). Consistent with these effects on pro-inflammatory transcription factors is the observation that gold salts inhibit expression of ICAM-1 and VCAM-1 in endothelial cells (Koike *et al*., 1994). D-penicillamine inhibits AP-1 DNA binding in nuclear extracts in the presence of free radicals, presumably by forming disulphide bonds with the cysteine residues in the DNA binding domains of Jun and Fos (Handel *et al*., 1996). Aspirin and sodium salicylate also inhibit activation of NF-κB (Kopp & Ghosh, 1994). It has been shown that salicylate inhibits activation of NF-κB by preventing phosphorylation and subsequent degradation of IκB, and this results in blockade of the TNF-induced increase in mRNA levels of ICAM-1, VCAM-1 and E-selectin, and a dose-dependent inhibition of TNF-induced surface expression of these adhesion molecules (Pierce *et al*., 1996). Indomethacin, a nonsalicylate cyclo-oxygenase inhibitor, has no effect on surface expression of adhesion molecules, suggesting that the effects of salicylate are not due to inhibition of cyclo-oxygenase (Pierce *et al*., 1996).

Proteasome inhibitors have been tested in experimental models of inflammation with promising results. In a rat model of experimental colitis induced by peptidoglycan/polysaccharide, proteasome inhibition using MG-341 significantly suppressed the upregulation of VCAM-1 and iNOS in the colon and this was associated with a reduction of colonic inflammation (Conner *et al*., 1997).

Systemic inhibition of NF-κB activation in humans for prolonged periods carries some risk since there is the potential for severe immunosuppression and enhanced cytokine-induced cytotoxicity (Beg & Baltimore, 1996; Wang *et al*., 1996). Removal of the p65 gene is lethal to the mouse embryo (Beg *et al*., 1995) and p50 knockout mice breed normally but have increased susceptibility to infections (Sha *et al*., 1995). However, because both NF-κB and AP-1 are inducible transcription factors that act in response to environmental stimuli, it may be possible to titrate the dose of an NF-κB directed inhibitor within a dynamic range to achieve a therapeutic, and subtoxic, response.

Antisense oligonucleotides The potential side effects and nonspecific actions of the currently used transcription factor inhibitors have led to a search for drugs that rely on an

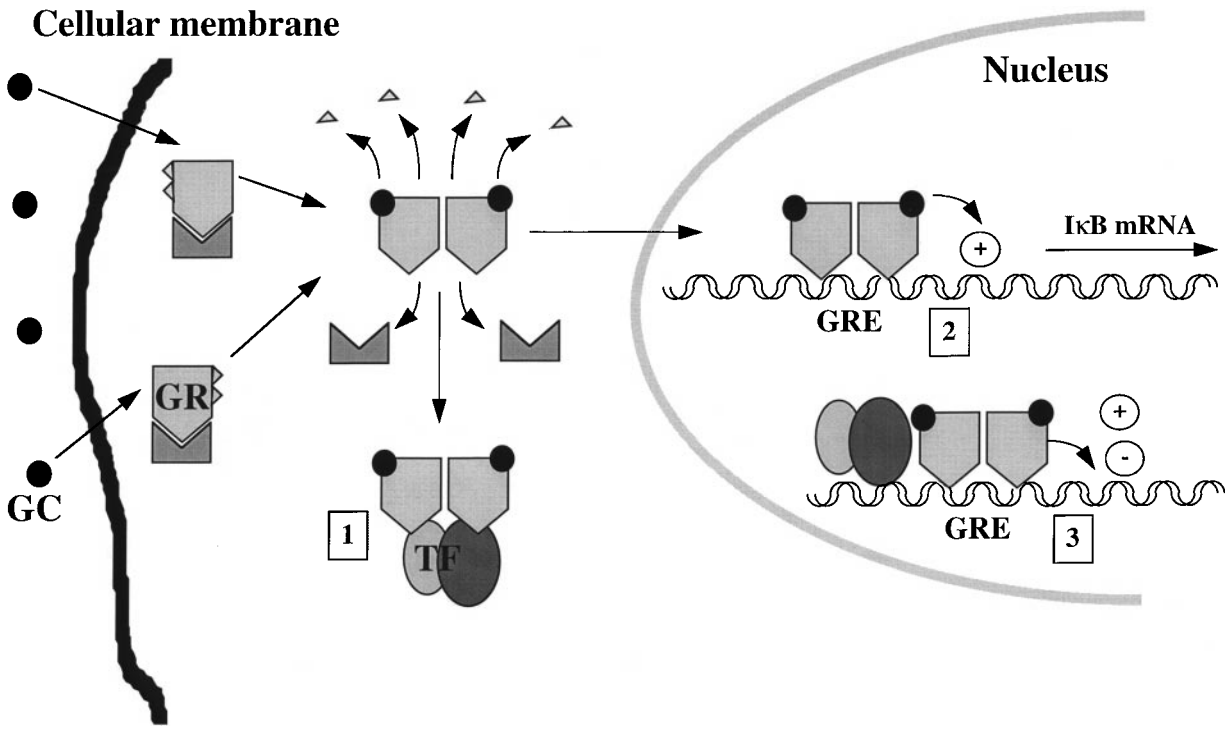

Figure 3 Mechanisms used by the glucocorticoid receptor to inhibit transactivation by transcription factors. (1) After the glucocorticoid (GC) activates its receptor (GR), a direct protein-protein interaction between GR and transcription factors (TF) will prevent the binding of TF to the respective DNA response elements. (2) Binding of GR to the promoter region of the IκB gene results in transactivation; IκB binding NF-κB will prevent binding or displace NF-κB from κB sites. (3) Binding of GR to glucocorticoid responsive elements modulates TF-induced transactivation.

alternative strategy for regulation of protein synthetic pathways that are specifically related to the inflammatory process. One such approach that has already yielded significant results is the use of antisense oligodeoxynucleotides (ODNs) (Agrawal, 1996).

Antisense ODNs are single stranded DNA sequences complimentary to a specific messenger RNA (mRNA). In theory, antisense ODNs, through base pairing of complementary bases, specifically bind to a mRNA thereby blocking the expression of the gene product (Sharma & Narayanan, 1995) (Figure 4). The mechanism of antisense ODN inhibition may involve multiple modalities, including the induction of RNAase H activity through the formation of an DNA:RNA hybrid, steric hindrance that interferes with translation, and inhibition of mRNA processing and transport from the nucleus (Sharma & Narayanan, 1995). Although ODNs can undeniably hit their intended targets, when an antisense molecule elicits a biological response, it can be difficult to determine whether the response was elicited because the reagent interacted specifically with its target RNA, or because some non-antisense reaction – involving other nucleic acids or proteins – took place. In order to distinguish between antisense and non-antisense effects, ODNs with an altered (scrambled) nucleotide sequence of the antisense are employed. The ability of ODNs to act as sequence-specific inhibitors of gene expression depends on their entry into the cytoplasm and/or nucleus. Since ODNs are negatively charged, they cannot passively diffuse through cellular membranes. Instead, they appear to enter cells *via* the processes of adsorptive and fluid-phase endocytosis (Yakubov *et al*., 1989). The identity of cell membrane proteins that bind ODNs is unclear, however a number of heparin binding proteins such as fibroblast growth factors and vascular endothelial growth factors have been implicated in this process (Guvakova *et al*., 1995). Of particular interest is the observation that ODNs may enter cells *via* an interaction with the heparin binding protein CD11b/CD18 (Benimetsaya *et al*., 1997). This suggests that ODNs may be preferentially taken up by activated leukocytes and thereby exert a more profound influence on leukocyte function. Upon entering the cell, in order to be effective, antisense ODNs must be resistant to nucleases, and have sequence-specific effects (Agrawal, 1996). Although questions of ODN specificity remain, there is growing evidence that antisense molecules can be useful pharmacological tools when applied carefully.

Therapeutic applications Antisense molecules have been produced to block the production of specific subunits of NF-κB. In murine embryonic stem cells, antisense ODN raised against p65 elicit a significant reduction in p65 mRNA, and have profound effects on cell adhesion properties (Sokoloski *et al*., 1993). Treatment of neutrophils with antisense phosphorothioate ODN to the p65 subunit of NF-κB results in a reduction in the expression of p65 and effectively abolishes the upregulation of CD11b normally elicited by either formyl-met-leu-phe and tissue plasminogen activator, indicating that antisense oligomers to p65 can interfere with neutrophil adhesion molecules (Narayanan *et al*., 1993). Antisense oligonucleotides to p65/p50 also reduce the expression of CD11b/CD18 on stimulated monocytic HL60 cells (Sokoloski *et al*., 1993), and the expression of E-selectin, ICAM-1, and VCAM-1 on stimulated human umbilical vein endothelial cells (Lee *et al*., 1995). A likely consequence of these actions of p65 ODNs is a profound diminution of the inflammatory response in mice with TNBS-induced colitis, as well as in IL-10 deficient mice with colitis. In both models of colitis, administration of p65 antisense was more effective in treating the inflammatory disease than glucocorticoids (Neurath *et al*., 1996).

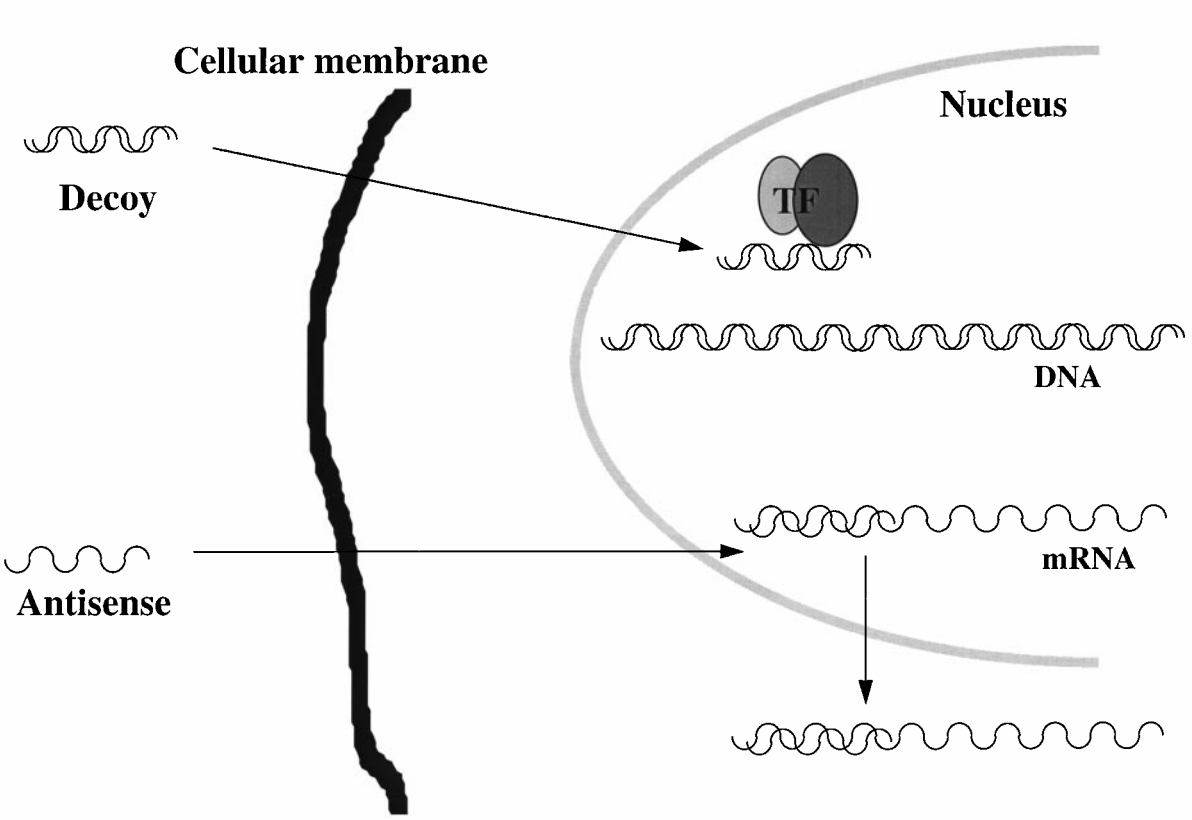

Figure 4 Target sites for decoy and antisense ODNs. Antisense ODNs are single stranded DNA sequences that specifically bind to mRNA, thereby blocking expression of the gene product. Transcription factor (TF) decoys are double stranded ODNs that compete for protein binding with the authentic binding elements, thereby interfering with gene regulation.

ISIS 2302, an antisense phosphorothioate ODN to human ICAM-1, appears to selectively inhibit cytokine-induced ICAM-1 expression in a variety of human cells *in vitro* and *in vivo* (Bennett *et al*., 1994; Yacyshyn *et al*., 1998). Furthermore, a recent pilot study in patients with Crohn's disease showed that administration of this drug reduced ICAM-1 expression in intestinal mucosa and resulted in a significant decrease in corticosteroid usage relative to placebo treated patients (Yacyshyn *et al*., 1998). A murine analogue, ISIS 3082, has been shown to be active in multiple models of inflammation, including dextran-sulphate induced colitis (Bennett *et al*., 1997), allograft rejection (Stepkowski *et al*., 1994), and endotoxin-induced neutrophil recruitment in the lung (Kumasaka *et al*., 1996). Two studies have shown that treatment of stimulated human umbilical vein endothelial cells with antisense ODNs directed against ICAM-1, E-selectin, or VCAM-1 results in selective inhibition of protein expression and a corresponding reduction of monocyte (or HL-60 cell) adhesion to the cultured endothelial cells (Bennett *et al*., 1994; Lee *et al*., 1995).

Decoy oligonucleotides Another strategy used to inhibit components of the inflammatory response is decoy ODNs that specifically interfere with regulatory proteins (Morishita *et al*., 1998). Inhibition of sequence-specific DNA-binding proteins can be achieved with double-stranded ODNs containing the specific binding elements. The transcription factor decoy (TFD) competes for protein binding with the authentic binding elements and consequently interfere with gene regulation (Figure 4). The mechanism of TFD action is distinct from the antisense approach in that the production of the target protein is unaffected and only its capacity to bind to the regulatory DNA element is affected. The TFD strategy is particularly attractive for several reasons: (1) the potential drug targets (transcription factors) are plentiful and readily identifiable, (2) synthesis of the sequence-specific decoy is relatively simple and can be targeted to specific tissues, (3) knowledge of the exact molecular structure of the target transcription factor is unnecessary, and (4) decoy ODNs may be more effective than antisense ODNs in suppressing an inflammatory reaction by virtue of their capacity to inhibit transcription of the multiple genes activated by a given transcription factor. Like antisense ODNs, the same critical parameters for optimal function exist, i.e., TFDs must be nuclease resistant, be taken up by cells, and have sequence-specific effects. A major concern regarding the use of TFDs is nonspecific effects, particularly those of phosphorothioate-substituted ODNs. Non-sequence-specific inhibition may occur from blockade of cell surface receptor activity or interference with other proteins (Gibson, 1996). Furthermore, TFDs containing guanine cytosine dinucleotides may result in immune activation (Khaled *et al*., 1996). To address these concerns, careful controlled experiments must be performed to eliminate the potential nonspecific effects of TFDs-mediated therapy. Furthermore, scrambled ODNs with several mutations in the consensus sequence should be used as controls.

Therapeutic applications Based on evidence showing NF-κB activation and increased adhesion molecule expression in tissues exposed to ischaemia-reperfusion, the value of treatment with decoy ODN against NF-κB has been evaluated in this model of acute inflammation (Morishita *et al*., 1997). In

rats, intracoronary administration of NF-κB decoy ODNs before or after coronary artery occlusion markedly reduces the size of the myocardial infarct measured at 24 h after reperfusion. The selectivity of the NF-κB decoy ODN effect was confirmed by the finding that the reduction in infarct size was not observed in rats treated with antisense ODN directed against the iNOS gene. The specificity of the NF-κB decoy in inhibiting cytokine and adhesion molecule expression was also confirmed by *in vitro* experiments using human and rat coronary artery endothelial cells that were transfected with the NF-κB decoy; the decoy ODN inhibited the expression of ICAM-1, VCAM-1 and E-selectin (Morishita *et al*., 1997). In another study of rats subjected to myocardial ischaemia-reperfusion, the efficacy of a decoy ODN against NF-κB was confirmed by an enhanced recovery of left ventricular function and coronary flow in rats treated with the NF-κB decoy ODN, compared to groups of rats receiving a scrambled decoy or placebo. The protection against ischaemic damage afforded by the NF-κB decoy ODN was associated with less neutrophil adherence to endothelial cells and a lower tissue level of IL-8 (Sawa *et al*., 1997). The findings of these two studies suggest that *in vivo* administration of decoy ODNs against NF-κB may be an effective therapeutic strategy for treatment of myocardial ischaemia.

In a recent study, the two approaches to modulate gene expression were compared, i.e., the ability of an antisense that binds to the mRNA for the ReIA subunit of NF-κB to inhibit cytokine production by TNF-stimulated splenocytes was compared to the responses observed in splenocytes receiving a decoy with double-stranded ODNs that bind the NF-κB protein. TNF-α expression was reduced by both treatments, as were the levels of IL-2. However, the antisense effects did not last beyond 24 h, whereas the decoy ODN was shown to inhibit cytokine production even at 72 h after the initial TNF-stimulation (Khaled *et al*., 1998).

Limitations to the application of decoy or antisense ODN strategies to modulate transcription factor activity are similar to those discussed above in relation to drugs that block NF-κB activation, with potential inhibition of normal physiological responses as the major concern. Therefore, the application of decoy ODN strategies as gene therapy may be limited to the treatment of those acute inflammatory conditions (e.g., ischaemia-reperfusion) in which activation of transcription factors plays a pivotal role.

Adhesion molecule function

The experimental approach for attenuation of leukocyte-endothelial cell adhesion that has received the most attention is inhibition of adhesion molecule function. This strategy has proven to be very effective in limiting both acute and chronic forms of inflammation in animal models and has received limited attention in the clinical setting. In most of these studies, inhibition of adhesion molecule function was achieved through immunoneutralization with monoclonal antibodies that target specific adhesion glycoproteins. Another strategy has involved the administration of soluble isoforms of the adhesion molecules expressed either on leukocytes (e.g., soluble P-selectin glycoprotein ligand-1 [PSGL-1]) or endothelial cells (e.g., sICAM-1).

Monoclonal antibodies (mAbs) have been applied to both *in vitro* and *in vivo* models of inflammation in order to define the specific contribution of leukocyte and endothelial cell adhesion glycoproteins to different steps in the recruitment of leukocytes, i.e., rolling, adherence, and emigration. The same mAbs have also been applied to a variety of animal models of inflammation, including arthritis, malaria, meningitis, acute allograft rejection, haemorrhagic shock, and sepsis (Korthuis *et al*., 1994). In many model systems, the mAbs have been shown to blunt the recruitment of leukocytes and to diminish the tissue injury that usually accompanies the inflammatory response. The magnitude of the inhibitory effect exhibited by the mAb varies with the model studied and the adhesion molecule targeted. Monoclonal antibodies directed against either the common β-subunit of CD11/CD18 or ICAM-1 appear to offer the highest degree of protection in models of ischaemia-reperfusion injury (Kurose *et al*., 1994a). P-selectin-directed mAbs have also shown efficacy in similar models, but part of this protective action has been attributed to an attenuation of leukocyte-platelet aggregation (Kubes *et al*., 1994; Weyrich *et al*., 1993). There are, on the other hand, relatively few reports describing a protective action of E-selectin specific mAbs in experimental models of inflammation. The latter observation may reflect a limited blocking function of the mAbs employed or the absence of a role for E-selectin in these models of inflammation. A limitation in interpreting negative findings with mAbs is the uncertainty regarding whether blocking doses are achieved *in vivo*. Target levels are generally based on the minimum mAb concentration required to achieve maximal inhibition of leukocyte adhesion *in vitro*. Experience gained from open-labelled clinical trials (Kavanaugh *et al*., 1994) indicates that blocking doses are more difficult to achieve *in vivo* than predicted from *in vitro* neutrophil binding assays. Another potential limitation of prolonged mAb usage, at least in chronic models of inflammation, is immunogenicity.

Another approach to blocking adhesion molecule function that is gaining attention in the experimental setting is administration of soluble forms of adhesion receptors, such as ICAM-1, sialyl-Lewis X (SLex), and PSGL-1. It has been shown, for example, that administration of soluble SLex (a fucose-containing carbohydrate ligand to P-selectin found on leukocytes) is as effective as a P-selectin mAb in attenuating leukocyte rolling in inflamed mesenteric venules, while a control, fucose-deficient form of the oligosaccharide was without effect (Zimmerman *et al*., 1994b). Similarly, it has been shown that soluble PGSL-1 administered to rats reduces the renal dysfunction and necrosis normally caused by ischaemia-reperfusion (Takada *et al*., 1997). A soluble human form of PSGL-1 has also been tested in a feline model of myocardial ischaemia-reperfusion injury (Hayward *et al*., 1998). The P-selectin antagonist significantly reduced the reperfusion-induced neutrophil accumulation and myocardial necrosis, and it preserved endothelium-dependent vasorelaxation in reperfused coronary arteries. A recombinant form of soluble murine ICAM-1 was recently shown to be effective in reducing the leukocyte-endothelial cell adhesion elicited in mouse mesenteric venules by ischaemia-reperfusion (Kusterer *et al*., 1998). Hence, the results obtained from all of the experimental studies employing soluble adhesion molecules or their ligands suggest that these agents may be as effective as other anti-adhesion strategies in limiting the accumulation of leukocytes that occurs in ischaemia-reperfusion and other inflammatory conditions.

Therapeutic applications Clinical trials employing mAbs to leukocyte or endothelial cell adhesion molecules have met with varying success. Monoclonal antibodies directed against the β2-integrins have been used in patients receiving bone marrow grafts. In one study, a mAb against CD18 was unable to prevent bone marrow rejection in adult leukaemic recipients

(Baume *et al*., 1989), while in another clinical series, a CD11a-specific mAb prevented failure of bone marrow grafts in HLA-mismatched young recipients (van Dijken *et al*., 1990). The latter mAb (CD11a) was shown to be ineffective in reversing acute rejection in renal transplant recipients (Le Mauff *et al*., 1991).

The outcome of clinical trials employing ICAM-1 specific mAbs appear to be more promising. A phase 1 clinical study using an anti-ICAM-1 mAb as part of the initial immunosuppressive regimen for renal allograft recipients (judged to be at high risk for delayed allograft rejection) demonstrated a lower incidence of both acute graft rejection and delayed graft function (Haug *et al*., 1993). The same ICAM-1 specific mAb has been shown to produce an improved clinical response in an open-label, dose escalating phase I-II study in patients with severe rheumatoid arthritis (Kavanaugh *et al*., 1994). For both indications (kidney transplantation, rheumatoid arthritis), the dosing regimen required to achieve the pharmacokinetic target was much higher than that estimated based on *in vitro* blocking experiments. Furthermore, a high incidence of ICAM-1 mAb anti-idiotype antibodies was found in the kidney transplant patients receiving the murine anti-human ICAM-1 mAb. However, this antigenicity problem should be alleviated with humanized mAbs.

Conclusions

The therapeutic potential of drugs that target leukocyte-endothelial cell adhesion for treatment of acute and chronic inflammatory diseases seems promising. While several key steps in the inflammatory cascade that result in leukocyte recruitment appear amenable to pharmacologic inhibition, the challenges posed by the potential for disruption of alternate physiological processes as well as immune suppression are significant. However, these limitations may be overcome by research that focuses on the identification and characterization of chemical pathways that uniquely serve the process of leukocyte-endothelial cell adhesion, either at the level of receptor activation, adhesion molecule biosynthesis, and/or adhesion molecule function. The development of safe and effective drugs that target these molecular components of the inflammatory response may yield novel, improved therapies for the debilitating disorders associated with inflammation.

DN Granger is supported by grants from the National Institutes of Health (HL26441 and DK43785) and Dr J Panés by grant SAF 97/0040 from Comision Interministerial de Ciencia y Tecnologia.

References

ADCOCK, I.M. (1996). Steroid resistance in asthma. Molecular mechanisms. *Am. J. Respir. Crit. Care Med.,* **154,** S58–S61.

ADCOCK, I.M., LANE, S.J., BROWN, C.R., LEE, T.H. & BARNES, P.J. (1995). Abnormal glucocorticoid receptor-activator protein 1 interaction in steroid-resistant asthma. *J. Exp. Med.,* **182,** 1951–1958.

AGRAWAL, S. (1996). Antisense oligonucleotides: towards clinical trials. *Trends Biotechnol.,* **14,** 376–387.

ANDERSON, D.C., SCHMALSTIEG, F.C., SHEARER, W., BECKER, F.-K., KOHL, S., SMITH, C.W., TOSI, M.F. & SPRINGER, T. (1985). Leukocyte LFA-1, OKM1, p150,95 deficiency syndrome: functional and biosynthetic studies of three kindreds. *Fed Proc.,* **44,** 2671–2677.

ANGEL, P. & KARIN, M. (1991). The role of Jun, Fos and the AP-1 complex in cell-proliferation and transformation. *Biochim. Biophys. Acta.,* **1072,** 129–157.

APPLEYARD, C.B., MCCAFFERTY, D.M., TIGLEY, A.W., SWAIN, M.G. & WALLACE, J.L. (1996). Tumour necrosis factor mediation of NSAID-induced gastric damage: role of leukocyte adherence. *Am. J. Physiol.,* **270,** G42–G48.

ARDITE, E., PANÉS, J., MIRANDA, M., SALAS, A., ELIZALDE, J.I., SANS, M., ARCE, Y., BORDAS, J.M., FERNÁNDEZ-CHECA, J.C. & PIQUÉ, J.M. (1998). Effects of steroid treatment on activation of nuclear factor κB in patients with inflammatory bowel disease. *Br. J. Pharmacol.,* **124,** 431–433.

ARNDT, H., RUSSELL, J.B., KUROSE, I., KUBES, P. & GRANGER, D.N. (1993). Mediators of leukocyte adhesion in rat mesenteric venules elicited by inhibition of nitric oxide synthesis. *Gastroenterology,* **105,** 675–680.

ASAKO, H., KUBES, P., WALLACE, J., GAGINELLA, T., WOLF, R.E. & GRANGER, D.N. (1992). Indomethacin-induced leukocyte adhesion in mesenteric venules: role of lipoxygenase products. *Am. J. Physiol.,* **262,** G903–G908.

BAEUERLE, P.A. (1998). Pro-inflammatory signaling: last pieces in the NF-kappaB puzzle? *Curr. Biol.,* **8,** R19–R22.

BAUME, D., KUENTZ, M., PICO, J.L., BEAUJEAN, F., CORDONNIER, C., VERNANT, J.P., HAYAT, M. & BERNARD, A. (1989). Failure of a CD18/anti-LFA1 monoclonal antibody infusion to prevent graft rejection in leukemic patients receiving T-depleted allogeneic bone marrow transplantation. *Transplantation,* **47,** 472–474.

BEG, A.A. & BALTIMORE, D. (1996). An essential role for NF-κB in preventing TNF-a-induced cell death. *Science,* **274,** 782–784.

BEG, A.A., SHA, W.C., BRONSON, R.T., GHOSH, S. & BALTIMORE, D. (1995). Embryonic lethality and liver degeneration in mice lacking the ReIA component of NF-κB. *Nature,* **376,** 167–170.

BENIMETSKAYA, L., LOIKE, J.D., KHALED, Z., LOIKE, G., SILVERSTEIN, S.C., CAO, L., EL KHOURY, J., CAI, T.Q. & STEIN, C.A. (1997). Mac-1 (CD11b/CD18) is an oligodeoxynucleotide-binding protein [see comments]. *Nat. Med.,* **3,** 414–420.

BENNETT, C.F., CONDON, T.P., GRIMM, S., CHAN, H. & CHIANG, M.Y. (1994). Inhibition of endothelial cell adhesion molecule expression with antisense oligonucleotides. *J. Immunol.,* **152,** 3530–3540.

BENNETT, C.F., KORNBRUST, D., HENRY, S., STECKER, K., HOWARD, R., COOPER, S., DUTSON, S., HALL, W. & JACOBY, H.I. (1997). An ICAM-1 antisense oligonucleotide prevents and reverses dextran sulfate sodium-induced colitis in mice. *J. Pharmacol. Exp. Ther.,* **280,** 988–1000.

BROSTJAN, C., ANRATHER, J., CSIZMADIA, V., NATARAJAN, G. & WINKLER, H. (1997). Glucocorticoids inhibit E-selectin expression by targeting NF-κB and not ATF/c-Jun. *J. Immunol.,* **158,** 3836–3844.

BROWN, K., GERSTBERGER, S., CARLSON, L., FRANZOSO, G. & SIEBENLIST, U. (1995). Control of IκB-a proteolysis by site-specific, signal-induced phosphorylation. *Science,* **267,** 1485–1488.

CATO, A.C. & WADE, E. (1996). Molecular mechanisms of anti-inflammatory action of glucocorticoids. *Bioessays,* **18,** 371–378.

CONNER, E.M., BRAND, S., DAVIS, J.M., LAROUX, F.S., PALOMBELLA, V.J., FUSELER, J.W., KANG, D.Y., WOLF, R.E. & GRISHAM, M.B. (1997). Proteasome inhibition attenuates nitric oxide synthase expression, VCAM-1 transcription and the development of chronic colitis. *J. Pharmacol. Exp. Ther.,* **282,** 1615–1622.

ELICES, M.J., OSBORN, L., TAKADA, Y., CROUSE, C., LUHOWSKYJ, S., HEMLER, M. & LOBB, R.R. (1990). VCAM-1 on activated endothelium interacts with the leukocyte integrin VLA-4 at a site distinct from the VLA-4/fibronectin binding site. *Cell,* **60,** 577–584.

EPPIHIMER, M.J., RUSSELL, J., ANDERSON, D.C., WOLITZKY, B.A. & GRANGER, D.N. (1997). Endothelial cell adhesion molecule expression in gene-targeted mice. *Am. J. Physiol.,* **273,** H1903–H1908.

EPPIHIMER, M.J., WOLITZKY, B., ANDERSON, D.C., LABOW, M.A. & GRANGER, D.N. (1996). Heterogeneity of expression of E- and P-selectins in vivo. *Circ. Res.,* **79,** 560–569.

ESSANI, N.A., MCGUIRE, G.M., MANNING, A.M. & JAESCHKE, H. (1996). Endotoxin-induced activation of the nuclear transcription factor κB and expression of E-selectin messenger RNA in hepatocytes, Kupffer cells, and endothelial cells in vivo. *J. Immunol.,* **156,** 2956–2963.

FISHER, C.J., JR., SLOTMAN, G.J., OPAL, S.M., PRIBBLE, J.P., BONE, R.C., EMMANUEL, G., NG, D., BLOEDOW, D.C. & CATALANO, M.A. (1994). Initial evaluation of human recombinant interleukin-1 receptor antagonist in the treatment of sepsis syndrome: a randomized, open-label, placebo-controlled multicenter trial. The IL-1RA Sepsis Syndrome Study Group. *Crit. Care Med.,* **22,** 12–21.

FRIES, J.W., WILLIAMS, A.J., ATKINS, R.C., NEWMAN, W., LIPSCOMB, M.F. & COLLINS, T. (1993). Expression of VCAM-1 and E-selectin in an in vivo model of endothelial activation. *Am. J. Pathol.,* **143,** 725–737.

GIBSON, I. (1996). Antisense approaches to the gene therapy of cancer. *Cancer Metastasis Rev.,* **15,** 287–299.

GUVAKOVA, M.A., YAKUBOV, L.A., VLODAVSKY, I., TONKINSON, J.L. & STEIN, C.A. (1995). Phosphorothioate oligodeoxynucleotides bind to basic fibroblast growth factor, inhibit its binding to cell surface receptors, and remove it from low affinity binding sites on extracellular matrix. *J. Biol. Chem.,* **270,** 2620–2627.

HANDEL, M.L. (1997). Transcription factors AP-1 and NF-κB: where steroids meet the gold standard of anti-rheumatic drugs. *Inflamm. Res.,* **46,** 282–286.

HANDEL, M.L., WATTS, C.K., SIVERTSEN, S., DAY, R.O. & SUTHERLAND, R.L. (1996). D-penicillamine causes free radical-dependent inactivation of activator protein-1 DNA binding. *Mol. Pharmacol.,* **50,** 501–505.

HAUG, C.E., COLVIN, R.B., DELMONICO, F.L., AUCHINCLOSS, H., JR., TOLKOFF RUBIN, N., PREFFER, F.I., ROTHLEIN, R., NORRIS, S., SCHARSCHMIDT, L. & COSIMI, A.B. (1993). A phase I trial of immunosuppression with anti-ICAM-1 (CD54) mAb in renal allograft recipients. *Transplantation,* **55,** 766–772.

HAYWARD, R., CAMPELL, B., SHIN, Y.K., SCALIA, R. & LEFER, A.M. (1998). Recombinant soluble P-selectin glycoprotein ligand protects against myocardial ischemic reperfusion injury in cats. *Cardiovasc. Res.,* (in press).

HENNINGER, D.D., PANÉS, J., EPPIHIMER, M., RUSSELL, J., GERRITSEN, M., ANDERSON, D.C. & GRANGER, D.N. (1997). Cytokine-induced VCAM-1 and ICAM-1 expression in different organs of the mouse. *J. Immunol.,* **158,** 1825–1832.

HORIE, Y., WOLF, R., ANDERSON, D.C. & GRANGER, D.N. (1997a). Hepatic leukostasis and hypoxic stress in adhesion molecule-deficient mice after gut ischaemia/reperfusion. *J. Clin. Invest.,* **99,** 781–788.

HORIE, Y., WOLF, R., RUSSELL, J., SHANLEY, T.P. & GRANGER, D.N. (1997b). Role of Kupffer cells in gut ischaemia/reperfusion-induced hepatic microvascular dysfunction in mice. *Hepatology,* **26,** 1499–1505.

KARIN, M. & SMEAL, T. (1992). Control of transcription factors by signal transduction pathways: the beginning of the end. *Trends Biochem. Sci.,* **17,** 418–422.

KAVANAUGH, A.F., DAVIS, L.S., NICHOLS, L.A., NORRIS, S.H., ROTHLEIN, R., SCHARSCHMIDT, L.A. & LIPSKY, P.E. (1994). Treatment of refractory rheumatoid arthritis with a monoclonal antibody to intercellular adhesion molecule 1. *Arthritis Rheum.,* **37,** 992–999.

KHALED, A.R., BUTFILOSKI, E.J., SOBEL, E.S. & SCHIFFENBAUER, J. (1998). Use of phosphorothioate-modified oligodeoxynucleotides to inhibit NF-κB expression and lymphocyte function. *Clin. Immunol. Immunopathol.,* **86,** 170–179.

KHALED, Z., BENIMETSKAYA, L., ZELTSER, R., KHAN, T., SHARMA, H.W., NARAYANAN, R. & STEIN, C.A. (1996). Multiple mechanisms may contribute to the cellular anti-adhesive effects of phosphorothioate oligodeoxynucleotides. *Nucleic Acids Res.,* **24,** 737–745.

KOIKE, R., MIKI, I., OTOSHI, M., TOTSUKA, T., INOUE, H., KASE, H., SAITO, I. & MIYASAKA, N. (1994). Gold sodium thiomalate down-regulates intercellular adhesion molecule-1 and vascular cell adhesion molecule-1 expression on vascular endothelial cells. *Mol. Pharmacol.,* **46,** 599–604.

KOMATSU, S., FLORES, S., GERRITSEN, M.E., ANDERSON, D.C. & GRANGER, D.N. (1997). Differential up-regulation of circulating soluble and endothelial cell intercellular adhesion molecule-1 in mice. *Am. J. Pathol.,* **151,** 205–214.

KOPP, E. & GHOSH, S. (1994). Inhibition of NF-κB by sodium salicylate and aspirin. *Science,* **265,** 956–959.

KORTHUIS, R.J., ANDERSON, D.C. & GRANGER, D.N. (1994). Role of neutrophil-endothelial cell adhesion in inflammatory disorders. *J. Crit. Care,* **9,** 47–71.

KUBES, P., IBBOTSON, G., RUSSELL, J., WALLACE, J.L. & GRANGER, D.N. (1990a). Role of platelet-activating factor in ischaemia/reperfusion-induced leukocyte adherence. *Am. J. Physiol.,* **259,** G300–G305.

KUBES, P., KUROSE, I. & GRANGER, D.N. (1994). NO donors prevent integrin-induced leukocyte adhesion but not P-selectin-dependent rolling in postischemic venules. *Am. J. Physiol.,* **267,** H931–H937.

KUBES, P., SUZUKI, M. & GRANGER, D.N. (1990b). Platelet-activating factor-induced microvascular dysfunction: role of adherent leukocytes. *Am. J. Physiol.,* **258,** G158–G163.

KUMASAKA, T., QUINLAN, W.M., DOYLE, N.A., CONDON, T.P., SLIGH, J., TAKEI, F., BEAUDET, A., BENNETT, C.F. & DOERSCHUK, C.M. (1996). Role of the intercellular adhesion molecule-1 (ICAM-1) in endotoxin-induced pneumonia evaluated using ICAM-1 antisense oligonucleotides, anti-ICAM-1 monoclonal antibodies, and ICAM-1 mutant mice. *J. Clin. Invest.,* **97,** 2362–2369.

KUNKEL, E.J., JUNG, U., BULLARD, D.C., NORMAN, K.E., WOLITZKY, B.A., VESTWEBER, D., BEAUDET, A.L. & LEY, K. (1996). Absence of trauma-induced leukocyte rolling in mice deficient in both P-selectin and intercellular adhesion molecule 1. *J. Exp. Med.,* **183,** 57–65.

KUROSE, I., ANDERSON, D.C., MIYASAKA, M., TAMATANI, T., PAULSON, J.C., TODD, R.F., RUSCHE, J.R. & GRANGER, D.N. (1994a). Molecular determinants of reperfusion-induced leukocyte adhesion and vascular protein leakage. *Circ. Res.,* **74,** 336–343.

KUROSE, I., ARGENBRIGHT, L.W., WOLF, R., LIANXI, L. & GRANGER, D.N. (1997). Ischaemia/reperfusion-induced microvascular dysfunction: role of oxidants and lipid mediators. *Am. J. Physiol.,* **272,** H2976–H2982.

KUROSE, I., GRANGER, D.N., EVANS, D.J., JR., EVANS, D.G., GRAHAM, D.Y., MIYASAKA, M., ANDERSON, D.C., WOLF, R.E., CEPINSKAS, G. & KVIETYS, P.R. (1994b). Helicobacter pylori-induced microvascular protein leakage in rats: role of neutrophils, mast cells, and platelets. *Gastroenterology,* **107,** 70–79.

KUROSE, I., POTHOULAKIS, C., LA MONT, J.T., ANDERSON, D.C., PAULSON, J.C., MIYASAKA, M., WOLF, R. & GRANGER, D.N. (1994c). Clostridium difficile toxin A-induced microvascular dysfunction. Role of histamine. *J. Clin. Invest.,* **94,** 1919–1926.

KUSTERER, K., BOJUNGA, J., ENGHOFER, M., HEIDENTHAL, E., USADEL, K.H., KOLB, H. & MARTIN, S. (1998). Soluble ICAM-1 reduces leukocyte adhesion to vascular endothelium in ischaemia-reperfusion injury in mice. *Am. J. Physiol.,* **275,** G377–G380.

LE MAUFF, B., HOURMANT, M., ROUGIER, J.P., HIRN, M., DANTAL, J., BAATARD, R., CANTAROVICH, D., JACQUES, Y. & SOULILLOU, J.P. (1991). Effect of anti-LFA1 (CD11a) monoclonal antibodies in acute rejection in human kidney transplantation. *Transplantation,* **52,** 291–296.

LEE, C.H., CHEN, H.H., HOKE, G., JONG, J.S., WHITE, L. & KANG, Y.H. (1995). Antisense gene suppression against human ICAM-1, ELAM-1, and VCAM-1 in cultured human umbilical vein endothelial cells. *Shock,* **4,** 1–10.

LIAO, L. & GRANGER, D.N. (1996). Role of mast cells in oxidized low-density lipoprotein-induced microvascular dysfunction. *Am. J. Physiol.,* **271,** H1795–H1800.

LO, S.K., JANAKIDEVI, K., LAI, L. & MALIK, A.B. (1993). Hydrogen peroxide-induced increase in endothelial adhesiveness is dependent on ICAM-1 activation. *Am. J. Physiol.,* **264,** L406–L412.

MARLIN, S.D. & SPRINGER, T.A. (1987). Purified intercellular adhesion molecule-1 (ICAM-1) is a ligand for lymphocyte function-associated antigen (LFA-1). *Cell,* **51,** 813–819.

MAY, M.J. & GHOSH, S. (1998). Signal transduction through NF-κB. *Immunol. Today,* **19,** 80–88.

MORISHITA, R., HIGAKI, J., TOMITA, N. & OGIHARA, T. (1998). Application of transcription factor 'decoy' strategy as means of gene therapy and study of gene expression in cardiovascular disease. *Circ. Res.,* **82,** 1023–1028.

MORISHITA, R., SUGIMOTO, T., AOKI, M., KIDA, I., TOMITA, N., MORIGUCHI, A., MAEDA, K., SAWA, Y., KANEDA, Y., HIGAKI, J. & OGIHARA, T. (1997). In vivo transfection of cis element 'decoy' against nuclear factor-kappaB binding site prevents myocardial infarction. *Nat. Med.,* **3,** 894–899.

MULLER, W.A., WEIGL, S.A., DENG, X. & PHILLIPS, D.M. (1993). PECAM-1 is required for transendothelial migration of leukocytes. *J. Exp. Med.,* **178,** 449 – 460.

MULLIGAN, M.S., JONES, M.L., BOLANOWSKI, M.A., BAGANOFF, M.P., DEPPELER, C.L., MEYERS, D.M., RYAN, U.S. & WARD, P.A. (1993). Inhibition of lung inflammatory reactions in rats by an anti-human IL-8 antibody. *J. Immunol.,* **150,** 5585 – 5595.

NARAYANAN, R., HIGGINS, K.A., PEREZ, J.R., COLEMAN, T.A. & ROSEN, C.A. (1993). Evidence for differential functions of the p50 and p65 subunits of NF-kappa B with a cell adhesion model. *Mol. Cell. Biol.,* **13,** 3802 – 3810.

NEURATH, M.F., PETTERSSON, S., MEYER ZUM BÜSCHENFELDE, K.H. & STROBER, W. (1996). Local administration of antisense phosphorothioate oligonucleotides to the p65 subunit NF-κB abrogates established experimental colitis in mice. *Nat. Med.,* **2,** 998 – 1004.

PAN, J., XIA, L. & MCEVER, R.P. (1998a). Comparison of promoters for the murine and human P-selectin genes suggests species-specific and conserved mechanisms for transcriptional regulation in endothelial cells. *J. Biol. Chem,* **273,** 10058 – 10067.

PAN, J., XIA, L., YAO, L. & MCEVER, R.P. (1998b). Tumour necrosis factor-alpha- or lipopolysaccharide-induced expression of the murine P-selectin gene in endothelial cells involves novel kappaB sites and a variant activating transcription factor/cAMP response element. *J. Biol. Chem.,* **273,** 10068 – 10077.

PANÉS, J. & GRANGER, D.N. (1998). Leukocyte-endothelial cell interactions: molecular mechanisms and implications in gastrointestinal disease. *Gastroenterology,* **114,** 1066 – 1090.

PANÉS, J., PERRY, M.A., ANDERSON, D.C., MANNING, A., LEONE, B., CEPINSKAS, G., ROSENBLOOM, C.L., MIYASAKA, M., KVIETYS, P.R. & GRANGER, D.N. (1995). Regional differences in constitutive and induced ICAM-1 expression in vivo. *Am. J. Physiol.,* **269,** H1955 – H1964.

PIERCE, J.W., READ, M.A., DING, H., LUSCINSKAS, F.W. & COLLINS, T. (1996). Salicylates inhibit IκB-a phosphorylation, endothelial-leukocyte adhesion molecule expression, and neutrophil transmigration. *J. Immunol.,* **156,** 3961 – 3969.

RAY, A. & PREFONTAINE, K.E. (1994). Physical association and functional antagonism between the p65 subunit of transcription factor NF-kappa B and the glucocorticoid receptor. *Proc. Natl. Acad. Sci. U.S.A.,* **91,** 752 – 756.

READ, M.A., NEISH, A.S., LUSCINSKAS, F.W., PALOMBELLA, V.J., MANIATIS, T. & COLLINS, T. (1995). The proteasome pathway is required for cytokine-induced endothelial-leukocyte adhesion molecule expression. *Immunity,* **2,** 493 – 506.

ROEBUCK, K.A., RAHMAN, A., LAKSHMINARAYANAN, V., JANAKIDEVI, K. & MALIK, A.B. (1995). H2O2 and tumour necrosis factor-alpha activate intercellular adhesion molecule 1 (ICAM-1) gene transcription through distinct cis-regulatory elements within the ICAM-1 promoter. *J. Biol. Chem.,* **270,** 18966 – 18974.

ROMER, L.H., MCLEAN, N.V., YAN, H.C., DAISE, M., SUN, J. & DE LISSER, H.M. (1995). IFN-g and TNF-a induce redistribution of PECAM-1 (CD31) on human endothelial cells. *J. Immunol.,* **154,** 6582 – 6592.

SAKURAI, H., SHIGEMORI, N., HISADA, Y., ISHIZUKA, T., KAWASHIMA, K. & SUGITA, T. (1997). Suppression of NF-κB and AP-1 activation by glucocorticoids in experimental glomerulonephritis in rats: molecular mechanisms of anti-nephritic action. *Biochim. Biophys. Acta.,* **1362,** 252 – 262.

SAWA, Y., MORISHITA, R., SUZUKI, K., KAGISAKI, K., KANEDA, Y., MAEDA, K., KADOBA, K. & MATSUDA, H. (1997). A novel strategy for myocardial protection using in vivo transfection of cis element 'decoy' against NF-κB binding site: evidence for a role of NF-κB in ischaemia-reperfusion injury. *Circulation,* **96,** II280 – II285.

SCHEINMAN, R.I., GUALBERTO, A., JEWELL, C.M., CIDLOWSKI, J.A. & BALDWIN, A.S., JR. (1995). Characterization of mechanisms involved in transrepression of NF-κB by activated glucocorticoid receptors. *Mol. Cell. Biol.,* **15,** 943 – 953.

SHA, W.C., LIOU, H.C., TUOMANEN, E.I. & BALTIMORE, D. (1995). Targeted disruption of the p50 subunit of NF-kappa B leads to multifocal defects in immune responses. *Cell,* **80,** 321 – 330.

SHARMA, H.W. & NARAYANAN, R. (1995). The therapeutic potential of antisense oligonucleotides. *Bioessays,* **17,** 1055 – 1063.

SHELLEY, C.S., DA SILVA, N., GEORGAKIS, A., CHOMIENNE, C. & ARNAOUT, M.A. (1998). Mapping of the human CD11c (ITGAX) and CD11d (ITGAD) genes demonstrates that they are arranged in tandem separated by no more than 11.5 kb. *Genomics,* **49,** 334 – 336.

SOKOLOSKI, J.A., SARTORELLI, A.C., ROSEN, C.A. & NARAYANAN, R. (1993). Antisense oligonucleotides to the p65 subunit of NF-κB block CD11b expression and alter adhesion properties of differentiated HL-60 granulocytes. *Blood,* **82,** 625 – 632.

STEPKOWSKI, S.M., TU, Y., CONDON, T.P. & BENNETT, C.F. (1994). Blocking of heart allograft rejection by intercellular adhesion molecule-1 antisense oligonucleotides alone or in combination with other immunosuppressive modalities. *J. Immunol.,* **153,** 5336 – 5346.

TAILOR, A., DAS, A.M., GETTING, S.J., FLOWER, R.J. & PERRETTI, M. (1997). Subacute treatment of rats with dexamethasone reduces ICAM-1 levels on circulating monocytes. *Biochem. Biophys. Res. Commun.,* **231,** 675 – 678.

TAKADA, M., NADEAU, K.C., SHAW, G.D. & TILNEY, N.L. (1997). Prevention of late renal changes after initial ischaemia/reperfusion injury by blocking early selectin binding. *Transplantation,* **64,** 1520 – 1525.

TAKEUCHI, M. & BAICHWAL, V.R. (1995). Induction of the gene encoding mucosal vascular address in cell adhesion molecule 1 by tumour necrosis factor alpha is mediated by NF-κB proteins. *Proc. Natl. Acad. Sci. U.S.A.,* **92,** 3561 – 3565.

TARGAN, S.R., HANAUER, S.B., VAN DEVENTER, S.J., MAYER, L., PRESENT, D.H., BRAAKMAN, T., DEWOODY, K.L., SCHAIBLE, T.F. & RUTGEERTS, P.J. (1997). A short-term study of chimeric monoclonal antibody cA2 to tumour necrosis factor alpha for Crohn's disease. Crohn's Disease cA2 Study Group. *N. Engl. J. Med.,* **337,** 1029 – 1035.

TEDDER, T.F., STEEBER, D.A., CHEN, A. & ENGEL, P. (1995a). The selectins: vascular adhesion molecules. *FASEB J.,* **9,** 866 – 873.

TEDDER, T.F., STEEBER, D.A. & PIZCUETA, P. (1995b). L-selectin-deficient mice have impaired leukocyte recruitment into inflammatory sites. *J. Exp. Med.,* **181,** 2259 – 2264.

TESSIER, P.A., CATTARUZZI, P. & MCCOLL, S.R. (1996). Inhibition of lymphocyte adhesion to cytokine-activated synovial fibroblasts by glucocorticoids involves the attenuation of vascular cell adhesion molecule 1 and intercellular adhesion molecule 1 gene expression. *Arthritis Rheum.,* **39,** 226 – 234.

TSUZUKI, Y., MIURA, S., SUEMATSU, M., KUROSE, I., SHIGEMATSU, T., KIMURA, H., HIGUCHI, H., SERIZAWA, H., YAGITA, H., OKUMURA, K. & ISHII, H. (1996). a4 integrin plays a critical role in early stages of T lymphocyte migration in Peyer's patches of rats. *Intl. Immunol.,* **8,** 287 – 295.

VAN DIJKEN, P.J., GHAYUR, T., MAUCH, P., DOWN, J., BURAKOFF, S.J. & FERRARA, J.L. (1990). Evidence that anti-LFA-1 in vivo improves engraftment and survival after allogeneic bone marrow transplantation. *Transplantation,* **49,** 882 – 886.

WAKELIN, M.W., SANZ, M.J., DEWAR, A., ALBELDA, S.M., LARKIN, S.W., BOUGHTON-SMITH, N., WILLIAMS, T.J. & NOURSHARGH, S. (1996). An anti-platelet-endothelial cell adhesion molecule-1 antibody inhibits leukocyte extravasation from mesenteric microvessels in vivo by blocking the passage through the basement membrane. *J. Exp. Med.,* **184,** 229 – 239.

WANG, C.Y., MAYO, M.W. & BALDWIN, A.S., JR. (1996). TNF- and cancer therapy-induced apoptosis: potentiation by inhibition of NF-κB. *Science,* **274,** 784 – 787.

WEYRICH, A.S., MA, X.Y., LEFER, D.J., ALBERTINE, K.H. & LEFER, A.M. (1993). In vivo neutralization of P-selectin protects feline heart and endothelium in myocardial ischaemia and reperfusion injury. *J. Clin. Invest.,* **91,** 2620 – 2629.

WILLIAMS, D.H., JEFFERY, L.J. & MURRAY, E.J. (1992). Aurothioglucose inhibits induced NF-κB and AP-1 activity by acting as an IL-1 functional antagonist. *Biochim. Biophys. Acta.,* **1180,** 9 – 14.

XU, H., GONZALO, J.A., ST-PIERRE, Y., WILLIAMS, I.R., KUPPER, T.S., COTRAN, R.S., SPRINGER, T.A. & GUTIERREZ-RAMOS, J.C. (1994). Leukocytosis and resistance to septic shock in intercellular adhesion molecule 1-deficient mice. *J. Exp. Med.,* **180,** 95 – 109.

YACYSHYN, B.R., BOWEN-YACYSHYN, M.B., JEWELL, L., TAMI, J.A., BENNETT, C.F., KISNER, D.L. & SHANAHAN, W.R. (1998). A placebo-controlled trial of ICAM-1 antisense oligonucleotide in the treatment of Crohn's disease. *Gastroenterology,* **14,** 1133 – 1142.

YAKUBOV, L.A., DEEVA, E.A., ZARYTOVA, V.F., IVANOVA, E.M., RYTE, A.S., YURCHENKO, L.V. & VLASSOV, V.V. (1989). Mechanism of oligonucleotide uptake by cells: involvement of specific receptors? *Proc. Natl. Acad. Sci. U.S.A.,* **86,** 6454 – 6458.

YANG, J.P., MERIN, J.P., NAKANO, T., KATO, T., KITADE, Y. & OKAMOTO, T. (1995). Inhibition of the DNA-binding activity of NF-κB by gold compounds in vitro. *FEBS Lett.,* **361,** 89–96.

YAO, L., PAN, J., SETIADI, H., PATEL, K.D. & MCEVER, R.P. (1996). Interleukin 4 or oncostatin M induces a prolonged increase in P-selectin mRNA and protein in human endothelial cells. *J. Exp. Med.,* **184,** 81–92.

ZIMMERMAN, B.J., GUILLORY, D.J., GRISHAM, M.B., GAGINELLA, T.S. & GRANGER, D.N. (1990). Role of leukotriene B4 in granulocyte infiltration into the postischemic feline intestine. *Gastroenterology,* **99,** 1358–1363.

ZIMMERMAN, B.J., HOLT, J.W., PAULSON, J.C., ANDERSON, D.C., MIYASAKA, M., TAMATANI, T., TODD, R.F.R., RUSCHE, J.R. & GRANGER, D.N. (1994a). Molecular determinants of lipid mediator-induced leukocyte adherence and emigration in rat mesenteric venules. *Am. J. Physiol.,* **266,** H847–H853.

ZIMMERMAN, B.J., PAULSON, J.C., ARRHENIUS, T.S., GAETA, F.C.A. & GRANGER, D.N. (1994b). Thrombin receptor peptide-mediated leukocyte rolling in rat mesenteric venules: role of P-selectin and sialyl Lewis X. *Am. J. Physiol.,* **267,** H1049–H1053.

(Received September 2, 1998
Revised October 27, 1998
Accepted November 3, 1998)

British Journal of Pharmacology (1999) 125, 551–554
http://www.stockton-press.co.uk/bjp

SPECIAL REPORT

Effects of a new C5a receptor antagonist on C5a- and endotoxin-induced neutropenia in the rat

[1]Anna Short, [2]Allan K. Wong, [1]Angela M. Finch, [2]Gerald Haaima, [1]Ian A. Shiels, [2]David P. Fairlie & *,[1]Stephen M. Taylor

[1]Department of Physiology and Pharmacology, University of Queensland, St. Lucia, Queensland 4072, Australia and [2]Centre for Drug Design and Development, University of Queensland, St. Lucia, Queensland 4072, Australia

A new C5a receptor antagonist, the cyclic peptide Phe-[Orn-Pro-D-cyclohexylalanine-Trp-Arg], (F-[OPdChaWR]), was tested for its ability to antagonize the neutropenic effects of both C5a and endotoxin in rats. Human recombinant C5a (2 μg kg^{-1} i.v.) caused rapid neutropenia, characterized by an 83% decrease in circulating polymorphonuclear leukocytes (PMNs) at 5 min. Administration of F-[OPdChaWR] (0.3–3 mg kg^{-1} i.v.), did not affect the levels of circulating PMNs but, when given 10 min prior to C5a, it inhibited the C5a-induced neutropenia by up to 70%. Administration of *E. Coli* lipopolysaccharide (LPS, 1 mg kg^{-1} i.v.) also caused neutropenia with an 88% decrease in circulating PMNs after 30 min. When rats were pretreated with F-[OPdChaWR] (0.3–10 mg kg^{-1} i.v.) 10 min prior to LPS, there was a dose-dependent antagonism of the neutropenia caused by LPS, with up to 69% reversal of neutropenia observed 30 min after LPS administration. These findings suggest that C5a receptor antagonists may have therapeutic potential in the many diseases known to involve either endotoxin or C5a.

Keywords: C5a; C5a antagonist; lipopolysaccharide; endotoxic shock; neutropenia

Abbreviations: ARDS, adult respiratory distress syndrome; Fmoc, fluorenylmethoxycarbonyl; fMLP, formylmethionyl-leucyl-phenylalanine; HPLC, high performance liquid chromatography; LPS, lipopolysaccharide; PAF, platelet activating factor; PMNs, polymorphonuclear leukocytes

Introduction Activation of the complement system has been implicated in a wide range of inflammatory disease states, including septic shock and adult respiratory distress syndrome (ARDS), which can occur as a consequence of bacterial infection (Martin & Silverman, 1992). The 74 amino acid peptide complement factor 5a (C5a) is a potent anaphylatoxin with key roles in the inflammatory and immune response, and is thought to be a major pathogenic factor in sepsis (Stevens *et al*., 1986) and ARDS (Mulligan *et al*., 1996). A drug which blocks the effects of C5a may be a useful therapeutic agent in these and other immunoinflammatory diseases. As yet, there are no C5a receptor antagonists available clinically.

Endotoxic shock is an acute disease state characterized by systemic hypotension (Lundberg *et al*., 1987), pulmonary hypertension (Marceau *et al*., 1987), depletion of circulating leukocytes and platelets, activation of the complement system (Smedegard *et al*., 1989), and can lead to the development of multiple organ failure (Seidenfeld *et al*., 1986). The tissue damage and organ dysfunction is associated with the migration of PMNs from the blood into the interstitium (Ahmed *et al*., 1996). The first stage of this process is adherence of the PMNs to vascular endothelium, and this results in a drop in circulating PMNs, or neutropenia (Smedegard *et al*., 1989). An agent which inhibited this process would have the potential to reduce tissue damage in inflammatory diseases such as sepsis.

Lipopolysaccharide (LPS) is a major component of the cell wall of gram-negative bacteria, and induces rapid endotoxic shock when injected intravenously in the rat (Smith *et al*., 1985). The hypotension caused by intravenous administration of LPS can be blocked by inhibitors of the inducible form of nitric oxide synthase (Szabo *et al*., 1996) as well as by a thromboxane A_2 receptor antagonist (Altavilla *et al*., 1994), while the neutropenia has been reported to be inhibited by a platelet activating factor (PAF) receptor antagonist in the early stages (Coughlan *et al*., 1994) or by lipid A analogues (Soejima *et al*., 1996). The effects of a specific C5a receptor antagonist have not been previously described in this, or any other animal model. In this report we describe the effects of a new C5a antagonist, the cyclic peptide Phe-[Orn-Pro-dCha-Trp-Arg], or F-[OPdChaWR], on C5a- and LPS-induced neutropenia in the rat.

Methods Female Wistar rats (250–350 g) were anaesthetized with i.p. ketamine (80 mg kg^{-1}) and xylazine (12 mg kg^{-1}). A polyethylene catheter was inserted in the femoral vein and rats were infused i.v. over 2 min with 0.2 ml of either F-[OPdChaWR] (0.3–10 mg kg^{-1}) or sterile, pyrogen-free saline for controls. Rats were dosed i.v. 10 min later with 0.2 ml of either C5a (2 μg kg^{-1}) or LPS (1 mg kg^{-1}) or the appropriate vehicle control, each infused over a 1 min period. Blood samples (0.2 ml) were collected periodically over a 150 min period, layered on to an equal volume of Histopaque-Ficoll solution, then centrifuged at 400 × *g* for 30 min at room temperature. The supernatant was discarded, and distilled water was added to the remaining pellet and shaken for 40 s to lyse the red blood cells. Dulbecco's phosphate buffered saline (10 × concentrate) was added to restore isotonicity before being centrifuged at 400 × *g* for 10 min at 4°C. This process lysed the red blood cells leaving a pellet of PMNs, which were washed and resuspended in 0.1 ml saline, and cell number was

* Author for correspondence.

counted on a haemocytometer. Staining of cells with Diff Quik showed purity of PMNs was 95–98% by this method. PMN counts were expressed as a per cent of the blood concentrations obtained immediately prior to C5a or LPS challenge. The apparent binding affinity of F-[OPdChaWR] on isolated rat PMNs was determined using a com-petition binding assay with [^{125}I]-C5a as described previously (Finch et al., 1997).

F-[OPdChaWR] was synthesized as follows. The linear peptide FOPdChaWR was synthesized using butoxycarbonyl (Boc)-Arg(Tosyl)-Pam resin employing *in situ* neutralization protocols for Boc chemistry (Schnolzer *et al.*, 1992). The terminal Phe was introduced as fluorenylmethoxycarbonyl (Fmoc)-Phe to protect the N terminus during cyclisation. The peptide was cleaved and deprotected using 10% 1 : 1 p-cresol-thiocresol in anhydrous HF (0°C, 60 min). Cyclisation was effected using 5 eq benzotriazole1-yl-oxy-tris-(dimethylamino)-phosphoniumhexa-fluorophosphate and 10 eq diisopropylethylamine in dimethyl-formamide (10^{-4} M, 15 h). After cyclisation the Fmoc group was removed (1 : 1 piperidine-DMF, 15 min) and the crude peptide was purified by HPLC. The cyclised product was characterized by electrospray mass spectroscopy ($M+H^+ = 854.5$) giving M_r 853.5 (calculated for $C_{45}H_{65}N_{11}O_6 = 853.5$ monoisotopic). Details of the synthetic methods for other antagonists of C5a receptors have been recently described (Wong *et al.*, 1998).

Human recombinant C5a, lipopolysaccharide (serotype 055 : B5), Histopaque Ficoll (density 1077) solution and phosphate buffered saline were purchased from Sigma (St Louis, MO, U.S.A.). [^{125}I]-C5a was purchased from New England Nuclear (MA, U.S.A.). Dilutions of drugs were made in 0.2 ml sterile pyrogen-free saline on the day of experimentation and brought to 37°C before intravenous infusion.

Statistical significance of results was determined using a non-parametric ANOVA with a Dunn's post-test at all time points. Receptor binding values were expressed as a per cent of the maximal response. Nonlinear regression was performed on these values to calculate the concentration of peptide that caused a 50% inhibition of [^{125}I]-C5a binding (IC_{50}) to isolated rat PMNs. All data are expressed as mean ± s.e. mean.

Results The chemical structure of F-[OPdChaWR] is shown in Figure 1. Cyclisation of the molecule was achieved *via* the sidechain of ornithine and the carboxyterminus of arginine. Human recombinant C5a and F-[OPdChaWR] demonstrated competitive inhibition of [^{125}I]-C5a binding to isolated rat PMNs, with $-\log IC_{50}$ values of 9.78 ± 0.12 and 7.57 ± 0.29 respectively (Figure 2).

The baseline level of circulating PMNs in rats was $2.04 \pm 0.25 \times 10^6$ cells ml^{-1} ($n = 25$). Intravenous injection of 2 μg kg^{-1} C5a caused a rapid, transient neutropenia, which reached a maximum at 5 min, and returned to baseline by 30 min (Figure 3). Intravenous administration of F-[OPdChaWR], 10 min prior to the C5a injection, resulted in dose-dependent reductions in C5a-induced neutropenia over the 30 min observation period. The maximal inhibition (70 ± 8%; $n = 3$) of C5a-induced neutropenia was observed at 5 min with 3 mg kg^{-1} F-[OPdChaWR]. Intravenous administration of F-[OPdChaWR] (0.3–3 mg kg^{-1}) alone had no effect on PMN levels prior to C5a (Figure 3), and a dose of 1 mg kg^{-1} did not affect PMN levels throughout a 150 min time period (data not shown).

Intravenous injection of 1 mg kg^{-1} LPS caused a decrease in blood PMN levels which reached a maximum at 30 min and returned to baseline at 150 min (Figure 3). Intravenous administration of F-[OPdChaWR], (0.3–10 mg kg^{-1}) 10 min prior to LPS, resulted in a dose-dependent inhibition of LPS-induced neutropenia. A dose of 10 mg kg^{-1} F-[OPdChaWR] inhibited LPS-induced neutropenia by 69 ± 4% ($n = 3$) from the maximum value observed at 30 min.

Receptor selectivity of the C5a antagonist was ascertained by examining the activity against the degranulating peptide, formylmethionyl-leucyl-phenylalanine (fMLP) in human PMNs. Concentrations of F-[OPdChaWR] up to 1 mM were ineffective in altering the response of the PMNs to a maximally effective concentration of fMLP (1 μM), while the concentration of F-[OPdChaWR] reducing the secretory reponse to a maximally effective concentration of C5a (100 nM) (Wong *et al.*, 1998) by 50% was 40 nM (Finch & Taylor, unpublished data).

Discussion Acute endotoxaemia is characterized by a number of prominent haemodynamic disturbances, such as hypotension (Lundberg *et al.*, 1987) and neutropenia (Till *et al.*, 1982). Hypotension is mediated by nitric oxide, and inhibitors of the inducible form of nitric oxide synthetase were effective in blocking the decreased blood pressure (Szabo *et al.*, 1996) as was a thromboxane A_2 receptor antagonist (Altavilla *et al.*, 1994). The neutropenia which

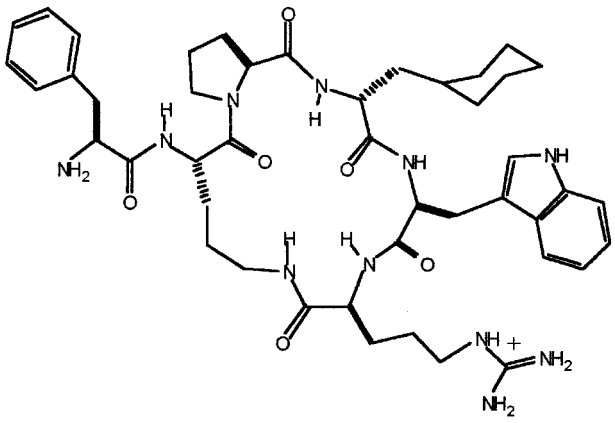

Figure 1 Structure of F-[OPdChaWR].

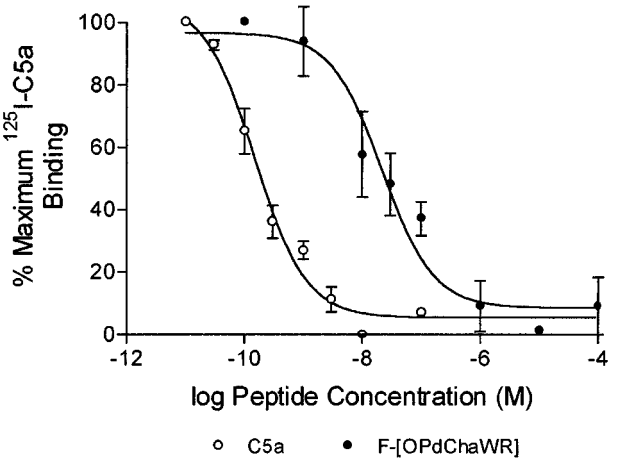

Figure 2 Inhibition of [^{125}I]-C5a binding to rat PMNs by increasing concentrations of human recombinant C5a or F-[OPdChaWR]. Data are expressed as a per cent of maximal binding of [^{125}I]-C5a. Results shown from PMNs from three animals.

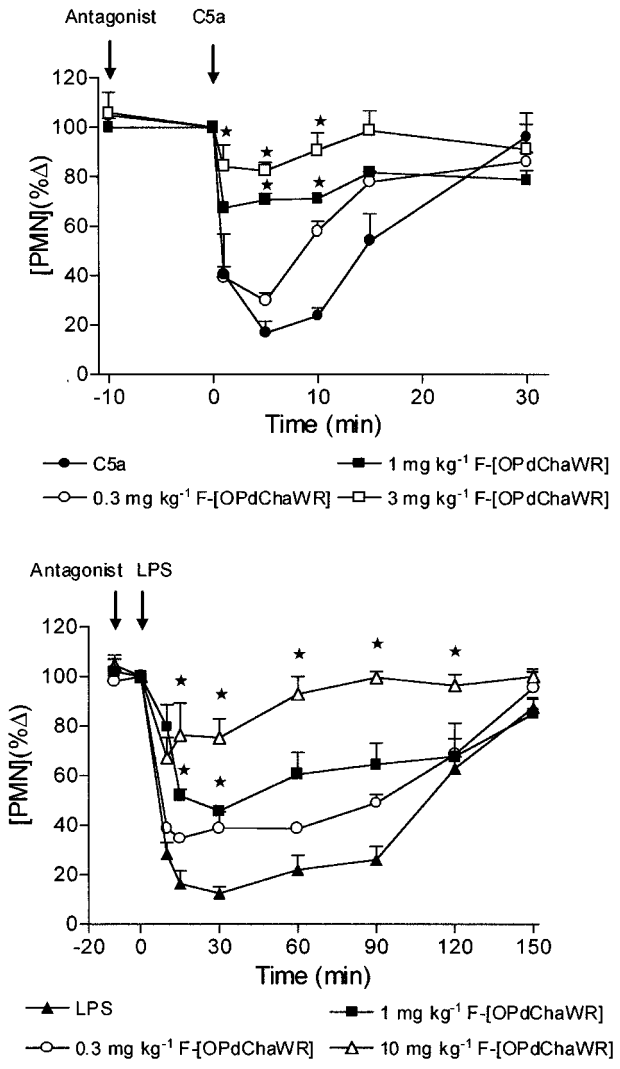

Figure 3 Inhibition of C5a- and LPS-induced neutropenia in the rat by F-[OPdChaWR]. Neutropenia was induced by i.v. 2 μg kg^{-1} C5a or 1 mg kg^{-1} LPS 10 min after i.v. F-[OPdChaWR] (0.3–10 mg kg^{-1}). PMN concentrations are expressed as per cent of the zero time value. *indicates $P<0.05$ compared to C5a- or LPS-control value. ($n=3-4$ rats for each experiment).

occurs represents the first stage of diapedesis, and this extravasation of activated PMNs can lead to organ dysfunction and failure (Seidenfeld *et al.*, 1986). Any agent which could prevent the adherence and subsequent migration of PMNs into the interstitium has therapeutic potential to reduce tissue damage in shock syndromes such as ARDS or endotoxemia. Of the synthetic agents produced to date, only an inhibitor of PAF receptors (Coughlan *et al.*, 1994) and a lipid A analogue (Soejima *et al.*, 1996) have been demonstrated to attenuate neutropenia caused by LPS.

The serum complement system is activated by LPS, and this leads to the generation of the anaphylatoxin C5a (Smedegard *et al.*, 1989). Intravenous administration of C5a in animals results in haemodynamic changes, such as hypotension and neutropenia (Smedegard *et al.*, 1989). The hypotension is blocked by inhibitors of cyclo-oxygenase, suggesting that vasodilator prostanoids mediate the decreased blood pressure, while neutropenia is not affected by these agents (Drapeau *et al.*, 1993). The neutropenic effects of C5a are due to the rapid and transient expression of intracellular adhesion molecules (ICAMs) on neutrophils (Foreman *et al.*, 1996) as well as P-selectin on vascular endothelial cells (Coughlan *et al.*, 1994), resulting in the adherence of PMNs to the endothelium and a subsequent decrease in circulating levels of PMNs. This expression of ICAMs and P-selectin is caused by the activity of C5a on its receptors.

In the rat, administration of a high dose of LPS (50 mg kg^{-1} i.v.) led within 5 min to the generation of high circulating concentrations of C5a (0.6 μg ml^{-1}) which returned to baseline levels within 30 min (Smedegard *et al.*, 1989). The neutropenia caused by C5a was rapid and transient and paralleled the circulating levels of C5a. This report prompted our present study, to determine if the neutropenia to LPS could be inhibited by a C5a receptor antagonist. We used a lower dose of LPS (1 mg kg^{-1}) in the present study to reduce the risk of mortality during the experiment, and our results demonstrate a similar level of neutropenia (*circa* 90%) as for the higher dose of LPS used by the earlier investigators.

In the present experiments, the neutropenia to i.v. C5a was inhibited, in a dose-dependent fashion, by a new C5a receptor antagonist designed and synthesized in our laboratories. When administered prior to LPS, a dose-dependent inhibition of the LPS-induced neutropenia was also seen. The highest dose of F-[OPdChaWR] tested in this study, 10 mg kg^{-1}, did not entirely block the neutropenia to LPS at the early time points, although complete blockade was produced 60 min after LPS administration. Coughlan *et al.* (1994) have reported that a PAF receptor antagonist, CV-3988, inhibited the neutropenia to i.v. LPS in the first 20 min but was ineffective after this time. The incomplete inhibition of neutropenia in the first 15–30 min in the present experiments may reflect a PAF-induced component, and further experiments are necessary to determine if this is the case. The lipid A analogue, B464, has been reported to attenuate the neutropenia to LPS in the guinea-pig and reduce lung injury to LPS (Soejima *et al.*, 1996) but its activity in the rat model has not yet been reported.

The first C5a receptor antagonist developed by modification of the carboxyterminal region of C5a was reported by Konteatis *et al.* (1994). To date, there have been no reports of *in vivo* activity for this, or any other antagonist derived from C5a. We have developed a series of analogues, involving cyclisation and modification of C-terminal analogues of C5a, and some of these have increased binding affinity and antagonist potency (Wong *et al.*, 1998). We used human recombinant C5a in our experiments to determine receptor binding parameters and to cause neutropenia. Human C5a bound effectively to rat PMNs and a dose of 2 μg kg^{-1} caused a similar level of neutropenia as did 12 μg kg^{-1} rat C5a des arg (Smedegard *et al.*, 1989). The new compound tested in the present study, a cyclised peptide, has an apparent binding affinity of 27 nM against [^{125}I]-C5a in intact rat PMNs. Administration of the compound prior to C5a or LPS did not cause neutropenia, indicating that the compound does not activate PMN C5a receptors *in vivo*, and no agonist activities have been discerned for this compound in human foetal artery or human PMNs *in vitro* to date (unpublished data). Drapeau *et al.* (1993) have reported that neutropenia is more sensitive to C5a and C5a agonist peptides than are alterations in blood pressure. The present study did not involve blood pressure measurements, and the effects of new C5a antagonists on this and on other effects of C5a in the rat remain to be determined.

In summary, the present study has demonstrated the *in vivo* effectiveness of a new C5a receptor antagonist which inhibited

the adherence of PMNs to the vascular endothelium induced by either C5a or LPS. Our results also suggest that C5a is a major mediator inducing neutropenia following LPS. Current studies are underway to determine the pharmacological activities of new C5a receptor antagonists in this and other models of immunoinflammatory diseases where C5a is implicated as a major pathogenic factor.

This work was supported by a URG grant from the University of Queensland.

References

AHMED, N., THORLEY, R., XIA, D., SAMOLS, D. & WEBSTER, R.O. (1996). Transgenic mice expressing rabbit C-reactive protein exhibit diminished chemotactic factor-induced alveolitis. *Am. J. Respir. Crit. Care Med.,* **153,** 1141 – 1147.

ALTAVILLA, D., CANALE, P., SQUADRITO, F., SARDELLA, A., AMMENDOLIA, L., URNA, G., IOCULANO, M., SQUADRITO, G. & CAPUTI, A.P. (1994). Protective effects of BAY U 3405, a thromboxane A2 receptor antagonist, in endotoxin shock. *Pharmacol. Res.,* **30,** 137 – 151.

COUGHLAN, A.F., HAU, H., DUNLOP, L.C., BERNDT, M.C. & HANCOCK, W.W. (1994). P-selectin and platelet-activating factor mediate initial endotoxin-induced neutropenia. *J. Exp. Med.,* **179,** 329 – 334 .

DRAPEAU, G., BROCHU, S., GODIN, D., LEVESQUE, L., RIOUX, F. & MARCEAU, F. (1993). Synthetic C5a receptor agonists. Pharmacology, metabolism and in vivo cardiovascular and hematologic effects. *Biochem. Pharmacol.,* **45,** 1289 – 1299.

FINCH, A.M., VOGEN, S.M., SHERMAN, S.A., KIRNARSKY, L., TAYLOR, S.M. & SANDERSON, S.D. (1997). Biologically active conformer of the effector region of human C5a and modulatory effects of N-terminal receptor binding determinants on activity. *J. Med. Chem.,* **40,** 877 – 884.

FOREMAN, K.E., GLOVSKY, M.M., WARNER, R.L., HORVATH, S.J. & WARD, P.A. (1996). Comparative effect of C3a and C5a on adhesion molecule expression on neutrophils and endothelial cells. *Inflammation,* **20,** 1 – 9.

KONTEATIS, Z.D., SICILIANO, S.J., VAN RIPER, G., MOLINEAUX, C.J., PANDYA, S., FISCHER, P., ROSEN, H., MUMFORD, R.A. & SPRINGER, M.S. (1994). Development of C5a receptor antagonists. Differential loss of functional responses. *J. Immunol.,* **153,** 4200 – 4205.

LUNDBERG, C., MARCEAU, F. & HUGLI, T.E. (1987). C5a-induced hemodynamic and hematologic changes in the rabbit. Role of cyclooxygenase products and polymorphonuclear leukocytes. *Am. J. Pathol.,* **128,** 471 – 483.

MARCEAU, F., LUNDBERG, C. & HUGLI, T.E. (1987). Effects of the anaphylatoxins on circulation. *Immunopharmacology,* **14,** 67 – 84.

MARTIN, M.A. & SILVERMAN, H.J. (1992). Gram-negative sepsis and the adult respiratory distress syndrome. *Clin. Infect. Dis.,* **14,** 1213 – 1228.

MULLIGAN, M.S., SCHMID, E., BECK SCHIMMER, B., TILL, G.O., FRIEDL, H.P., BRAUER, R.B., HUGLI, T.E., MIYASAKA, M., WARNER, R.L., JOHNSON, K.J. & WARD, P. A. (1996). Requirement and role of C5a in acute lung inflammatory injury in rats. *J. Clin. Invest.,* **98,** 503 – 512.

SCHNOLZER, M., ALEWOOD, P., JONES, A., ALEWOOD, D. & KENT, S.B. (1992). In situ neutralization in Boc-chemistry solid phase peptide synthesis. Rapid, high yield assembly of difficult sequences. *Int. J. Pept. Protein. Res.,* **40,** 180 – 193.

SEIDENFELD, J.J., POHL, D.F., BELL, R.C., HARRIS, G.D. & JOHANSON JR.,W.G. (1986). Incidence, site, and outcome of infections in patients with the adult respiratory distress syndrome. *Am. Rev. Respir. Dis.,* **134,** 12 – 16.

SMEDEGARD, G., CUI, L.X. & HUGLI, T.E. (1989). Endotoxin-induced shock in the rat. A role for C5a. *Am. J. Pathol.,* **135,** 489 – 497.

SMITH, E.F.D., TEMPEL, G.E., WISE, W.C., HALUSHKA, P.V. & COOK, J.A. (1985). Experimental endotoxemia in the rat: efficacy of prostacyclin or the prostacyclin analog iloprost. *Circ. Shock.,* **16,** 1 – 7.

SOEJIMA, K., ISHIZAKA, A., URANO, T., SAYAMA, K., SAKAMAKI, F., NAKAMURA, H., TERASHIMA, T., WAKI, Y., TASAKA, S., FUJISHIMA, S., KAWATA, T., CHRIST, W.J. & KANAZAWA, M. (1996). Protective effect of B464, a lipid A analog, on endotoxin-induced cellular responses and acute lung injury. *Am. J. Respir. Crit. Care. Med.,* **154,** 900 – 906.

STEVENS, J.H., P, O.H., SHAPIRO, J.M., MIHM, F.G., SATOH, P.S., COLLINS, J.A. & RAFFIN, T.A. (1986). Effects of anti-C5a antibodies on the adult respiratory distress syndrome in septic primates. *J. Clin. Invest.,* **77,** 1812 – 1816.

SZABO, C., BRYK, R., ZINGARELLI, B., SOUTHAN, G.J., GAHMAN, T.C., BHAT, V., SALZMAN, A.L. & WOLFF, D.J. (1996). Pharmacological characterization of guanidinoethyldisulphide (GED), a novel inhibitor of nitric oxide synthase with selectivity towards the inducible isoform. *Br. J. Pharmacol.,* **118,** 1659 – 1668.

TILL, G.O., JOHNSON, K.J., KUNKEL, R. & WARD, P.A. (1982). Intravascular activation of complement and acute lung injury. Dependency on neutrophils and toxic oxygen metabolites. *J. Clin. Invest.,* **6,** 1126 – 1135.

WONG, A.K., FINCH, A.M., PIERENS, G.K., CRAIK, D.J., TAYLOR, S.M. & FAIRLIE, D.P. (1998). Small Molecular probes for G protein-coupled C5a receptors. Conformationally constrained antagonists derived from the C-terminus of the human plasma protein C5a. *J. Med. Chem.,* **41,** 3417 – 3425.

(Received September 9, 1998,
Revised October 26, 1998,
Accepted November 5, 1998)

British Journal of Pharmacology (1999) 126, 555–558
http://www.stockton-press.co.uk/bjp

SPECIAL REPORT

Antagonism by acetyl-RYYRIK-NH_2 of G protein activation in rat brain preparations and of chronotropic effect on rat cardiomyocytes evoked by nociceptin/orphanin FQ

*,[1]H. Berger, [1]E. Albrecht, [2]G. Wallukat & [1]M. Bienert

[1]Forschungsinstitut für Molekulare Pharmakologie, Alfred-Kowalke-Str. 4, D-10315 Berlin, Germany; [2]Max-Delbrück-Centrum für Molekulare Medizin, Robert-Rössle-Straße 10, D-13125 Berlin, Germany

For the further elucidation of the central functions of nociceptin/orphanin FQ (noc/OFQ), the endogenous ligand of the G protein-coupled opioid receptor-like receptor ORL1, centrally acting specific antagonists will be most helpful. In this study it was found that the hexapeptide acetyl-RYYRIK-NH_2 (Ac-RYYRIK-NH_2), described in literature as partial agonist on ORL1 transfected in CHO cells, antagonizes the stimulation of [^{35}S]-GTPγS binding to G proteins by noc/OFQ in membranes and sections of rat brain. The antagonism of the peptide was competitive, of high affinity (Schild constant 6.58 nM), and specific for noc/OFQ in that the stimulation of GTP binding by agonists for the μ-, δ-, and κ-opioid receptor was not inhibited. The hexapeptide also fully inhibited the chronotropic effect of noc/OFQ on neonatal rat cardiomyocytes. It is suggested that Ac-RYYRIK-NH_2 may provide a promising starting point for *in vivo* tests for antagonism of the action of noc/OFQ and for the further development of highly active and specific antagonists.

Keywords: Nociceptin; orphanin FQ; [^{35}S]-GTPγS; rat brain membranes; rat cardiomyocytes; acetyl-RYYRIK-NH_2; antagonism

Abbreviations: Ac-RYYRIK-NH_2, acetyl-RYYRIK-NH_2; DAMGO, [D-Ala^2, N-Me-Phe^4, Gly^5-ol]-enkephalin; DPDPE, [D-Pen^2, D-Pen^5]-enkephalin; GTPγS, guanosine 5′-O-(γ-thio)triphosphate; noc/OFQ, nociceptin/orphanin FQ; ORL1, opioid receptor-like receptor.

Introduction The isolation of the endogenous ligand for the opioid receptor-like receptor ORL1, the heptadecapeptide FGGFTGARKSARKLANQ, named nociceptin (Meunier *et al*., 1995) or orphanin FQ (Reinscheid *et al*., 1995), marked the beginning of a new area in opioid and brain research (Rowe, 1996). Although nociceptin/orphanin FQ (noc/OFQ) shows some structural analogy to opioid peptides, particularly dynorphin A, and acts at the molecular and cellular levels in almost the same way as the classical μ-, δ-, and κ-opioids do, it produces pharmacological effects that oppose, or at least differ from, those of opioids. In the rat, noc/OFQ supraspinally suppresses opioid-mediated analgesia but seems to act spinally as an analgesic. In brain, it suppresses spatial learning, impairs motor performance, influences the release of pituitary hormones, and induces feeding. When administered intravenously, it exhibits smooth muscle relaxant, antinatriuretic and diuretic properties. Furthermore, stimulated immune function appears also to be regulated by noc/OFQ (reviewed by Meunier, 1997; Darland *et al*., 1998; Taylor & Dickenson, 1998). The multiple functions of noc/OFQ, which may be deduced from its pharmacological effects, should provide new insights into brain physiology and may lead to therapeutic applications, e.g., in the management of pain. However, our present knowledge about the pharmacological profile of the peptide is likely to be incomplete and additional functions may be expected.

For the further elucidation of the function of noc/OFQ, specific antagonists will be most helpful. From a combinatorial library of acetylated hexapeptide amides, Dooley *et al*. (1997) identified some hexapeptides that showed partial agonist activity in Chinese hamster ovary (CHO) cells transfected with ORL1 and in the inhibition of electrically induced contractions of mouse *vas deferens*. We thought that such short peptides might provide a promising starting point for the development of specific antagonists of noc/OFQ. Surprisingly, we found in this study that in a native preparation of rat brain membranes one of these peptides identified by Dooley *et al*. (1997), Ac-RYYRIK-NH_2, is a specific antagonist for the activation of G proteins, as measured by stimulation of binding of a GTP analogue, by the activated noc/OFQ receptor. Furthermore, the peptide was also found to antagonize the chronotropic effect of noc/OFQ on spontaneously beating cultured neonatal rat heart cells.

Methods Noc/OFQ and the hexapeptide Ac-RYYRIK-NH_2 were synthesized in our institute. The selective agonists for the μ- and δ-opioid receptor, [D-Ala^2, N-Me-Phe^4, Gly^5-ol]-enkephalin (DAMGO) and [D-Pen^2, D-Pen^5]-enkephalin (DPDPE), respectively, were obtained from Sigma (Deisenhofen, Germany), the κ-opioid receptor agonist U-504,88 was from RBI (Massachusetts, U.S.A.). Guanosine 5′-O-(γ-[^{35}S]-thio)triphosphate ([^{35}S]-GTPγS) was from NEN (Boston, MA, U.S.A.).

Noc/OFQ- and opioid-stimulated [^{35}S]-GTPγS binding to cerebral cortex membranes and coronal brain sections obtained from male Wistar rats was determined as described earlier (Albrecht *et al*., 1998). Briefly, 20 μg of membrane protein was incubated with the compounds in 50 mM Tris (pH 7.4) containing: 100 mM NaCl, 1 mM $MgCl_2$, 0.15 mM bacitracin, 100 μM GDP and 1 mg ml^{-1} BSA and about 70 pM [^{35}S]-GTPγS at 30°C for 120 min with and without the hexapeptide

*Author for correspondence at: Research Institute of Molecular Pharmacology, Alfred-Kowalke-Str. 4, D10315 Berlin, Germany. E-mail: berger@tmp-berlin.de

Ac-RYYRIK-NH_2. The binding of the GTP tracer to the membranes was determined after filtration through Whatman GF/B filters. Slide-mounted sections were incubated in buffer containing 2 mM GDP (Sim *et al.*, 1995) with the compounds and [^{35}S]-GTPγS for 120 min at 25°C. The slides were exposed to UR-imaging plates (FUJI Photo Film Co., Japan) for 16 h, together with ^{14}C-microscales (Amersham) for quantification. The plates were scanned and analysed using the Bio-Imaging Analyzer System BAS-3000 (FUJI) linked to the micro computer imaging device system from Imaging Research Inc. (St. Catherines, Canada). Rat heart cells were obtained from ventricles of 1–2-day-old Wistar rats and cultured as described earlier (Wallukat *et al.*, 1991). The chronotropic response was measured 5 min after the cumulative addition of noc/OFQ with and without Ac-RYYRIK-NH_2.

Data are expressed as means ± s.e.mean. EC_{50} values for the stimulation of [^{35}S]-GTPγS binding by noc/OFQ in absence and presence of different concentrations of Ac-RYYRIK-NH_2 were calculated from the concentration-response curves by nonlinear regression using the program GraphPad Prism 2.01 (GraphPad Software, Inc., San Diego, U.S.A.), and the constant for the inhibition by Ac-RYYRIK-NH_2 was calculated by linear regression of the corresponding Schild plot.

Results The EC_{50} value for the stimulation of binding of [^{35}S]-GTPγS to membranes of rat cortex by noc/OFQ was found to be 11.36 ± 1.83 nM ($n = 5$), which compares well with the EC_{50} of 9.11 nM as found earlier (Albrecht *et al.*, 1998). Increasing concentrations of Ac-RYYRIK-NH_2 shifted the concentration-response curve for noc/OFQ to the right (Figure 1), and from the corresponding Schild plot the inhibition constant K_a of the hexapeptide was calculated to be 6.58 ± 0.69 nM ($n = 5$). The peptide did not antagonize the stimulation of GTPγS binding by agonists of the μ-, δ-, and κ-opioid receptor in membranes of rat cortex (Figure 2) as well as in sections of rat brain at the level of striatum (Figures 3 and 4, data for δ- and κ-agonists not shown). With membranes the high concentration of 10 μM Ac-RYYRIK-NH_2, 1000 fold higher than its inhibitory constant, produced a small effect by its own, which added to the amount of bound [^{35}S]-GTPγS stimulated by the opioid agonists (Figure 2). With much lower potency, as compared to the stimulation of GTP binding in brain membranes, noc/OFQ increased the beating rate of spontaneously beating cardiomyocytes in cultured neonatal rat heart cells, the maximum effect reaching 65% of that of the β-adrenergic agonist isoprenaline. Ac-RYYRIK-NH_2 (1 and 10 μM) did not influence the beating rate but blocked the noc/OFQ-stimulated response (Figure 5).

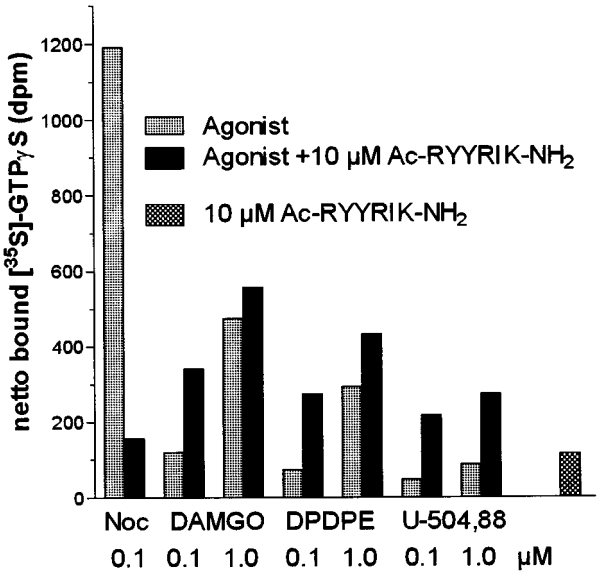

Figure 2 Effect of the hexapeptide Ac-RYYRIK-NH_2 on the stimulation of binding of [^{35}S]-GTPγS to rat cortex membranes by noc/OFQ and agonists for the μ-(DAMGO), δ-(DPDPE), and κ-opioid (U-504,88) receptor. Data are expressed as differences between binding in presence and absence of the compounds tested and are representative of three separate experiments.

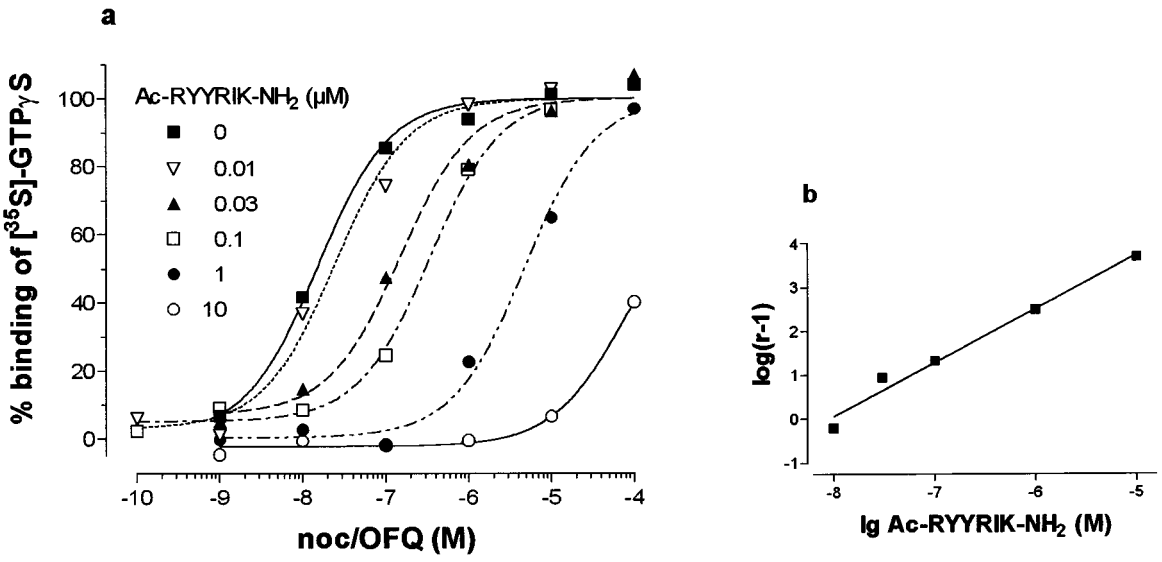

Figure 1 Effect of increasing concentrations of the hexapeptide Ac-RYYRIK-NH_2 on the concentration-response curve for the noc/OFQ-stimulated binding of 70 pM [^{35}S]-GTPγS to rat cortex membranes (a) and the corresponding Schild plot (b). Values in (a) are expressed as binding above basal and are normalized with the saturation value at 10 μM noc/OFQ taken as 100%. The data shown are representative of five separate experiments.

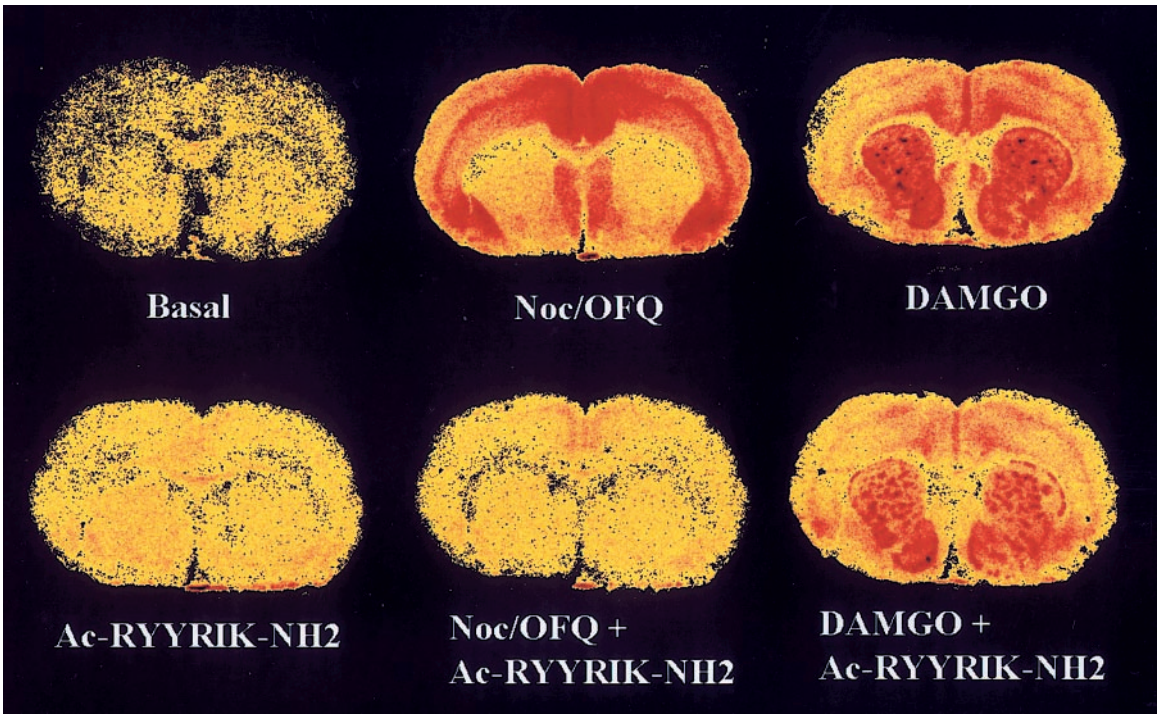

Figure 3 Distributions of basal, 1 μM noc/OFQ- and 5 μM DAMGO-stimulated [^{35}S]-GTPγS binding in absence and presence of 10 μM (noc/OFQ) or 20 μM (DAMGO) hexapeptide Ac-RYYRIK-NH$_2$ in representative sections of rat brain at the level of the caudate putamen. The sections were incubated in Tris buffer/2 mM GDP/100 mM NaCl with 80 pM tracer for 2 h at 25°C.

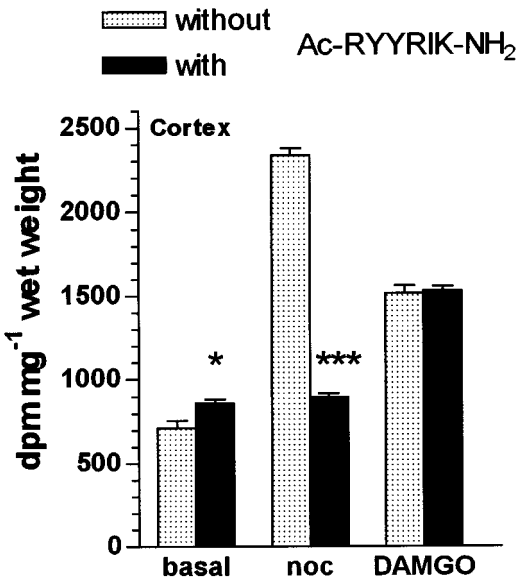

Figure 4 Influence of the hexapeptide Ac-RYYRIK-NH$_2$ on basal, noc/OFQ-, and DAMGO-stimulated [^{35}S]-GTPγS binding to cortex in adjacent coronal sections (six for each sample) obtained from rat brain. Conditions as in Figure 3. *$P<0.05$ and ***$P<0.001$ versus samples without Ac-RYYRIK-NH$_2$.

Discussion For the further elucidation of the function of noc/OFQ, specific antagonists will be most helpful. Presently, no centrally acting specific antagonist is available. A truncated analogue of noc/OFQ, [Phe^1 Ψ(CH$_2$-NH)Gly^2]nociceptin(1-13)-NH$_2$, was found to act as specific competitive antagonist in two peripheral noc/OFQ-sensitive preparations, the electrically stimulated guinea-pig ileum and mouse *vas deferens* (Guerrini *et al*., 1998), but not at central sites where it acted as full agonist (Xu *et al*., 1998). The hexapeptide Ac-RYYRIK-NH$_2$ was earlier identified as partial agonist in the stimulation of GTPγS binding to G proteins by the activated ORL1 receptor when transfected in CHO cells (Dooley *et al*., 1997). In our study the peptide was found to antagonize the stimulation of GTPγS binding by noc/OFQ, but not by agonists of the classical opioid receptors μ, δ, and κ, *in vitro* in rat brain preparations (Figures 1–4) with high affinity, as seen from the low Schild constant of 6.58 nM. Clearly, the hexapeptide is here a competitive receptor antagonist since it did not depress the maximal effect of noc/OFQ (Figure 1). Furthermore, in competition experiments using ^{3}H-Tyr^{14}-noc/OFQ as labelled ligand (Albrecht *et al*., 1998), we found that Ac-RYYRIK-NH$_2$ had an affinity for the noc/OFQ receptor in rat brain membranes which was only 3 fold lower when compared with noc/OFQ (data not shown). However, we found the affinity of Ac-RYYRIK-NH$_2$ to be much higher (K_D 0.3 nM) than reported for mouse ORL1 transfected into CHO cells (K_D 1.5 nM, Dooley *et al*., 1997). As stimulation of GTP binding to G proteins reflects the activation of G proteins by the receptor, and the coupling of receptor and G proteins can influence receptor affinity, it is suggested that the exact mechanism of this coupling differs between native membrane preparations and cells transfected with the receptor. This may lead to the observed differences in the receptor affinities and in the relations of the intrinsic efficacies of noc/OFQ and Ac-RYYRIK-NH$_2$ between the two systems.

Because effects of peripherally administered noc/OFQ on cardiovascular parameters are becoming increasingly recognized (see review by Meunier, 1997), we tested its action on cultured neonatal rat heart cells and found that it dose-dependently evoked a positive chronotropic response by elevating the beating rate of the cardiomyocytes (Figure 5). The exact mechanism and significance of this activity remains

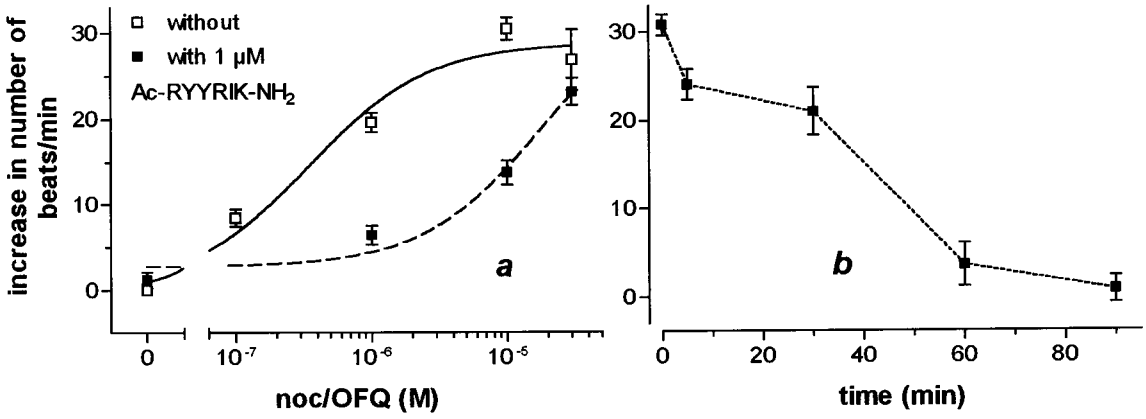

Figure 5 Concentration-response curve for the influence of noc/OFQ on the beating rate of spontaneously beating cardiomyocytes in cultured neonatal rat heart cells in absence and presence of the hexapeptide Ac-RYYRIK-NH_2 (a) and kinetics of the inhibiting effect of 10 μM hexapeptide Ac-RYYRIK-NH_2 on the beating rate induced by 10 μM noc/OFQ before (b). The basal beating rate was 150 ± 4.5 beats min^{-1}; $n = 20-38$.

to be elucidated. It seems, however, to be clear, that the chronotropic response is receptor-mediated, since the receptor antagonist Ac-RYYRIK-NH_2 inhibited the response (Figure 5).

By specifically antagonizing the activation of G proteins by the noc/OFQ receptor in rat brain membranes, the hexapeptide Ac-RYYRIK-NH_2 inhibits the primary events in triggering the biological effects of noc/OFQ. Therefore, this peptide should now provide a starting point for *in vivo* tests for antagonism of the action of noc/OFQ in the CNS and, considering its antagonistic action on cardiomyocytes, also in other tissues. Furthermore, its short sequence and the fact that it does not contain a free N- and C-terminal make it a convenient starting structure for the further development of highly active and specific antagonists.

The authors thank M. Georgi, H. Hans and M. Wegener for technical assistance and Dr M. Beyermann for the synthesis of noc/OFQ.

References

ALBRECHT, E., SAMOVILOVA, N.N., OSWALD, S., BAEGER, I. & BERGER, H. (1998). Nociceptin (orphanin FQ): High-affinity and high-capacity binding site coupled to low-potency stimulation of guanylyl-5′-O-(gamma-thio)-triphosphate binding in rat brain membranes. *J. Pharmacol. Exp. Ther.*, **286,** 896–902.

DARLAND, T., HEINRICHER, M.M. & GRANDY, D.K. (1998). Orphanin FQ/nociceptin: a role in pain and analgesia, but so much more. *Trends Neurosci.*, **21,** 215–221.

DOOLEY, C.T., SPAETH, C.G., BERZETEIGURSKE, I.P., CRAYMER, K., ADAPA, I.D., BRANDT, S.R., HOUGHTEN, R.A. & TOLL, L. (1997). Binding and in vitro activities of peptides with high affinity for the nociceptin/orphanin FQ receptor, ORL1. *J. Pharmacol. Exp. Ther.*, **283,** 735–741.

GUERRINI, R., CALO, G., RIZZI, A., BIGONI, R., BIANCHI, C., SALVADORI, S. & REGOLI, D. (1998). A new selective antagonist of the nociceptin receptor. *Br. J. Pharmacol.*, **123,** 163–165.

MEUNIER, J.C. (1997). Nociceptin/orphanin FQ and the opioid receptor-like ORL1 receptor. *Eur. J. Pharmacol.*, **340,** 1–15.

MEUNIER, J.C., MOLLEREAU, C., TOLL, L., SUAUDEAU, C., MOISAND, C., ALVINERIE, P., BUTOUR, J.L., GUILLEMOT, J.C., FERRARA, P., MONSARRAT, B., MAZARGUIL, H., VASSART, G., PARMENTIER, M. & COSTENTIN, J. (1995). Isolation and structure of the endogenous agonist of opioid receptor-like ORL(1) receptor. *Nature,* **377,** 532–535.

REINSCHEID, R.K., NOTHACKER, H.P., BOURSON, A., ARDATI, A., HENNINGSEN, R.A., BUNZOW, J.R., GRANDY, D.K., LANGEN, H., MONSMA, F.J. & CIVELLI, O. (1995). Orphanin FQ: A neuropeptide that activates an opioidlike G protein-coupled receptor. *Science,* **270,** 792–794.

ROWE, P.M. (1996). Excitement over orphanin FQ/nociceptin. *Lancet,* **347,** 606.

SIM, L.J., SELLEY, D.E. & CHILDERS, S.R. (1995). In vitro autoradiography of receptor-activated G proteins in rat brain by agonist-stimulated guanylyl 5′-[gamma-[S-35]thio]triphosphate binding. *Proc. Natl. Acad. Sci. U.S.A.,* **92,** 7242–7246.

TAYLOR, F. & DICKENSON, A. (1998). Nociceptin/orphanin FQ. A new opioid, a new analgesic? *Neuroreport,* **9,** R65–R70.

WALLUKAT, G., NEMECZ, G., FARKAS, T., KUEHN, H. & WOLLENBERGER, A. (1991). Modulation of the beta-adrenergic response in cultured rat heart cells. I. Beta-adrenergic supersensitivity is induced by lactate via a phospholipase A2 and 15-lipoxygenase involving pathway. *Mol. Cell. Biochem.,* **102,** 35–47.

XU, I.S., WIESENFELDHALLIN, Z. & XU, X.J. (1998). [Phe1 Psi(CH_2-NH)Gly(2)]-nociceptin-(1-13)NH_2, a proposed antagonist of the nociceptin receptor, is a potent and stable agonist in the rat spinal cord. *Neurosci. Lett.,* **249,** 127–130.

(Received October 1, 1998
Revised November 6, 1998
Accepted November 13, 1998)

British Journal of Pharmacology (1999) 126, 559–562
http://www.stockton-press.co.uk/bjp

SPECIAL REPORT

Deficiency of nitric oxide in polycation-induced airway hyperreactivity

*,[1]Herman Meurs, [1]Fineke E. Schuurman, [1]Michiel Duyvendak & [1]Johan Zaagsma

[1]Department of Molecular Pharmacology, University Centre for Pharmacy, A. Deusinglaan 1, 9713 AV Groningen, The Netherlands

Using a perfused guinea-pig tracheal tube preparation, we investigated the role of endogenous nitric oxide (NO) in polycation-induced airway hyperreactivity (AHR) to methacholine. Intraluminal (IL) administration of the NO synthase inhibitor N^{ω}-nitro-L-arginine methyl ester (L-NAME; 100 μM) caused a 1.8 fold increase in the maximal contractile response (E_{max}) to IL methacholine compared to control, without an effect on the pEC_{50} ($-\log_{10}$ EC_{50}). The polycation poly-L-arginine (100 μg ml^{-1}, IL) similarly enhanced the E_{max} for methacholine; however, the pEC_{50} value was also increased, by one $\log_{10}$ unit. L-NAME had no effect on the enhanced methacholine response of poly-L-arginine-treated airways, while the enhanced agonist response was completely normalized by the polyanion heparin (25 u ml^{-1}, IL). In addition, the effect of L-NAME was fully restored in the poly-L-arginine plus heparin treated airways. The results indicate that, in addition to enhanced epithelial permeability, a deficiency of endogenous NO contributes to polycation-induced AHR. The latter finding may represent a novel mechanism of AHR induced by eosinophil-derived cationic proteins in allergic asthma.

Keywords: Nitric oxide; N^{ω}-nitro-L-arginine methyl ester; poly-L-arginine; heparin; methacholine; airway hyperreactivity; tracheal perfusion; guinea-pig

Abbreviations: AHR, airway hyperreactivity; cNOS, constitutive nitric oxide synthase; EL, extraluminal; E_{max}, maximal effect; IL, intraluminal; KH, Krebs-Henseleit; L-NAME, N^{ω}-nitro-L-arginine methyl ester; MBP, major basic protein; NO, nitric oxide; ΔP, differential (hydrostatic) pressure; P_{inlet}, (hydrostatic) pressure at the inlet; P_{outlet}, (hydrostatic) pressure at the outlet; pEC_{50}, $-\log_{10}$ of the concentration causing 50% of effect

Introduction Eosinophil-derived cationic polypeptides, particularly major basic protein (MBP), a highly charged protein rich in arginine and lysine residues, have been implicated in the development of airway hyperreactivity (AHR) in allergic asthma (Gleich *et al*., 1993).

Among the possible mechanisms involved, polycation-induced dysfunction of the airway epithelium appears to play a prominent role. Thus, MBP is highly cytotoxic to airway epithelial cells and induces pathological alterations similar to those found in the airways of asthmatic patients (Motojima *et al*., 1989). Furthermore, enhanced levels of MBP have been reported in the bronchoalveolar lavage fluid of asthmatic patients, which were correlated with both the degree of epithelial denudation and the severity of AHR (Wardlaw *et al*., 1988).

MBP has been demonstrated to induce AHR *in vivo*, an effect that could be closely mimicked by synthetic cationic polypeptides such as poly-L-arginine and poly-L-lysine (Uchida *et al*., 1993) and inhibited by polyanions such as heparin (Coyle *et al*., 1993a), indicating the involvement of cationic charge. In an intact guinea-pig tracheal tube preparation *in vitro*, perfusion of the luminal surface with polycations increased the responsiveness to intraluminally, but not to extraluminally, applied methacholine, directly demonstrating that cationic peptides may indeed induce AHR by alterations of the epithelial layer (Coyle *et al*., 1993b).

Although overt epithelial damage appeared not to be required for cationic protein-induced AHR (Uchida *et al*., 1993; Coyle *et al*., 1993b), a reduced barrier function causing increased airway permeability may be involved (Omari *et al*., 1993; Hulsmann *et al*., 1996). In addition, it has been proposed that polycations like MBP may inhibit the agonist-induced release of an epithelium-derived relaxing factor (Flavahan *et al*., 1988).

One of the epithelium-derived relaxing factors appears to be nitric oxide (NO), which may be generated from agonist-induced activation of constitutive NO synthase (cNOS) isozymes present in the epithelium (Nijkamp *et al*., 1993; Kobzik *et al*., 1993). Recently, we have demonstrated that a deficiency of endogenous cNOS-derived NO is involved in allergen-induced AHR after the early asthmatic reaction (De Boer *et al*., 1996; Schuiling *et al*., 1998), which may be due to a reduced availability of the substrate L-arginine (Meurs *et al*., 1998). Since it has been recently reported that polycations, including MBP and poly-L-arginine, may reduce cellular uptake of L-arginine (Hirschmann *et al*., 1998), we hypothesized that limitation of substrate for cNOS activity induced by eosinophil-derived or synthetic polycationic peptides may cause a reduced contractile agonist-induced NO production and subsequent AHR to these agonists. Using a perfused guinea-pig tracheal tube preparation, this hypothesis was tested by assessing the effects of the nonselective NOS inhibitor N^{ω}-nitro-L-arginine methyl ester (L-NAME) on the airway constriction induced by intraluminal (IL) application of methacholine in untreated and poly-L-arginine-treated airways.

Methods *Tracheal perfusion* Specified pathogen-free Dunkin Hartley guinea-pigs (Harlan, Heathfield, U.K.), weighing 600–800 g, were used in this study. The animals were killed by

*Author for correspondence.

a sharp blow on the head and exsanguinated. The tracheas were rapidly removed and placed in Krebs-Henseleit (KH) solution (37°C) of the following composition (mM): NaCl 117.50, KCl 5.60, $MgSO_4$ 1.18, $CaCl_2$, 2.50, NaH_2PO_4 1.28, $NaHCO_3$ 25.00, D-glucose 5.50; gassed with 5% CO_2 and 95% O_2; pH 7.4.

The tracheas were prepared free of serosal connective tissue and cut into two halves of approximately 17 mm before mounting in a perfusion setup, as described previously (De Boer *et al*., 1996). To this aim, the tracheal preparations were attached at each side to stainless steel perfusion tubes fixed in a Delrin perfusion holder. The holder with the trachea was then placed in a water-jacketed organ bath (37°C) containing 20 ml of gassed KH (the serosal or extraluminal (EL) compartment). The lumen was perfused with recirculating KH from a separate 20 ml bath (mucosal or IL compartment) at a constant flow rate of 18 ml min^{-1}. Two axially centred side-hole catheters connected with pressure transducers (TC-XX, Viggo-Spectramed B.V., Bilthoven, The Netherlands) were situated at the distal and proximal ends of the trachealis to measure hydrostatic pressures (P_{outlet} and P_{inlet}, respectively). The signals were fed into a differential amplifier to obtain the difference between the two pressures ($\Delta P = P_{inlet} - P_{outlet}$), which was plotted on a flatbed chart recorder. ΔP reflects the resistance of the tracheal segment to perfusion and is a function of the mean diameter of the trachea between the pressure taps (Munakata *et al*., 1989). The transmural pressure in the trachea was set at 0 cm H_2O. At the perfusion flow rate used, a baseline ΔP of 0.1–1.0 cm H_2O was measured, depending on the diameter of the preparation.

After a 45 min equilibration period with three washes with fresh KH (both IL and EL), 1 μM isoprenaline was added to the EL compartment for maximal smooth muscle relaxation to assess basal tone. After three washes during at least 30 min, the trachea was exposed to EL 40 mM KCl in KH to obtain a receptor-independent reference response. Subsequently, the preparation was washed four times with KH during 45 min until basal tone was reached and a cumulative concentration response curve was made with IL methacholine. When used, L-NAME (100 μM), poly-L-arginine (100 μg ml^{-1}) and heparin (25 u ml^{-1}) were applied to the IL reservoir, 40 min prior to agonist-addition.

Data analysis To compensate for differences in ΔP due to variation in resting internal diameter of the preparations used, IL responses of the tracheal tube preparations to methacholine were expressed as a percentage of the response induced by EL administration of 40 mM KCl. The contractile effect of 10 mM methacholine (highest concentration) was defined as E_{max} (De Boer *et al*., 1996). Using this E_{max}, the sensitivity to methacholine was evaluated as pEC_{50} ($-\log_{10}$ EC_{50}) value. Data are expressed as means ± s.e.mean. Statistical analysis was performed using the Student's *t*-test for unpaired observations. A P value <0.05 was considered statistically significant.

Chemicals Methacholine chloride, poly-L-arginine hydrochloride (mol wt 5000–15000), heparin sodium and L-N^{ω}-nitro arginine methyl ester were obtained from Sigma Chemical Co. (St. Louis, MO, U.S.A.).

Results IL perfusion of the airways with the NOS inhibitor L-NAME (100 μM) caused a significant 1.8 fold increase in the E_{max} of IL methacholine compared to control ($P<0.001$), without a significant effect on the pEC_{50} of the agonist (Figure 1, Table 1). A comparable 1.6 fold ($P<0.001$) increase in methacholine E_{max} was caused by the synthetic polycation poly-L-arginine (100 μg ml^{-1}, IL), while the pEC_{50} was significantly enhanced from 2.86 ± 0.12 to 3.90 ± 0.17 ($P<0.001$). Very remarkably, L-NAME had no additional effect on the methacholine responsiveness of the poly-L-arginine-treated airways (Figure 1, Table 1).

The enhanced responsiveness to methacholine in the presence of poly-L-arginine was completely reversed by coperfusion with the polyanion heparin (25 u ml^{-1}), while heparin by itself had no effect on the methacholine response of untreated airways (Figure 1, Table 1). In addition, the effect of L-NAME was fully restored in the airways treated with poly-L-arginine plus heparin (Figure 1, Table 1).

L-NAME, poly-L-arginine, as well as heparin had no effect on basal airway tone (not shown).

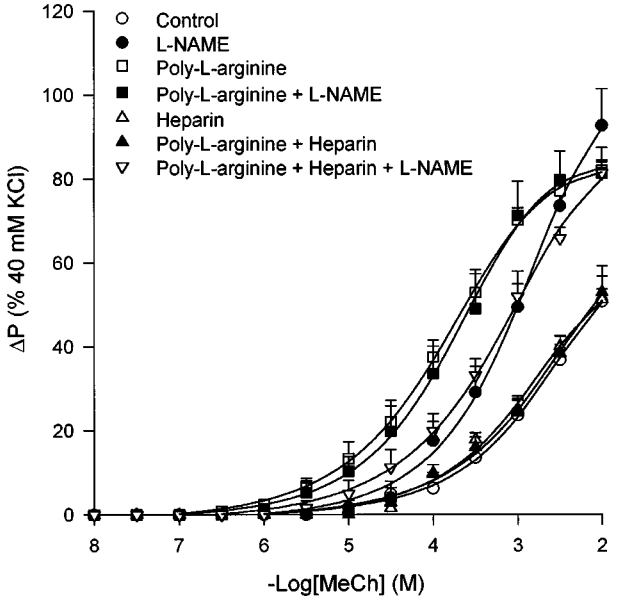

Figure 1 Effect of 100 μM L-NAME, 100 μg ml^{-1} poly-L-arginine, 100 μg ml^{-1} poly-L-arginine + 100 μM L-NAME, 25 u ml^{-1} heparin, 100 μg ml^{-1} poly-L-arginine + 25 u ml^{-1} heparin, and 100 μg ml^{-1} poly-L-arginine + 25 u ml^{-1} heparin + 100 μM L-NAME on methacholine-induced constriction of intact perfused guinea-pig tracheae. Methacholine-induced constriction of the perfused airway preparations was measured as an increase in differential pressure (ΔP) at constant flow and normalized to the response of 40 mM KCl (EL). Results are means ± s.e.mean of 3–8 experiments.

Table 1 Effects of (combinations of) L-NAME (100 μM), poly-L-arginine (100 μg ml^{-1}) and heparin (25 u ml^{-1}) on the responsiveness to methacholine of intact perfused guinea-pig tracheae

	E_{max} (% KCl)	pEC_{50} (−log M)	n
Control	50.7 ± 2.9	2.86 ± 0.12	8
L-NAME	92.7 ± 8.7***	3.14 ± 0.18	4
Heparin	51.2 ± 5.5	3.02 ± 0.12	3
Poly-L-arginine	81.9 ± 2.0***	3.90 ± 0.17***	6
+ L-NAME	81.2 ± 6.1***	3.78 ± 0.14***	5
+ Heparin	52.9 ± 6.4†††	2.92 ± 0.10††	3
+ Heparin + L-NAME	81.3 ± 3.1***	3.27 ± 0.14†	4

Results are means ± s.e.mean of *n* experiments. Statistical analysis: ***$P<0.001$ compared to Control; †$P<0.05$, ††$P<0.01$ and †††$P<0.001$ compared to poly-L-arginine.

Discussion This *in vitro* study demonstrates for the first time that a deficiency of cNOS-derived NO is involved in polycation-induced enhanced airway responsiveness. Thus, using the NOS inhibitor L-NAME, we confirmed the previous finding that methacholine-induced constriction of guinea-pig tracheal tube preparations is functionally antagonized by agonist-induced cNOS-derived NO (Nijkamp *et al*., 1993; De Boer *et al*., 1996), while the enhanced airway responsiveness to methacholine in poly-L-arginine perfused airways, which was also noted by others (Coyle *et al*., 1993b), was insensitive to the NOS inhibitor. The deficiency of NO supports the previous hypothesis of Flavahan *et al*. (1988) that loss of an epithelium derived relaxing factor may contribute to polycation-induced enhanced contractility. This hypothesis was based on the observation that MBP caused an increase in airway smooth muscle responsiveness in guinea-pig tracheal ring preparations that was dependent on the presence of intact epithelium (Flavahan *et al*., 1988).

In accordance with previous studies (Coyle *et al*., 1993b; Omari *et al*., 1993), we found that both the maximal response and the sensitivity to the contractile agonist were enhanced in the presence of poly-L-arginine. Since inhibition of cNOS by L-NAME in the control airways increased the E_{max}, but not the sensitivity (pEC_{50}) to methacholine, deficient NOS activity in the poly-L-arginine-treated airways may have contributed to the increased E_{max} in these airways. The enhanced sensitivity to IL methacholine in the poly-L-arginine-treated airways may reflect an enhanced epithelial permeability for the agonist due to disruption of the diffusion barrier, since this effect can be mimicked by both mechanical (Munakata *et al*., 1989) and chemical (Coyle *et al*., 1993b) denudation of the airway epithelium. It should, however, be noted that the increase in pEC_{50} for methacholine by one $\log_{10}$ unit is approximately one order of magnitude smaller than that observed after denudation (Munakata *et al*., 1989; Coyle *et al*., 1993b) and than the difference in pEC_{50} values of EL and IL applied methacholine (ΔpEC_{50} (EL-IL)) previously noted in our own study (De Boer *et al*., 1996), indicating that the epithelial barrier function is only partially lost.

In line with previous observations by Coyle *et al*. (1993b), the poly-L-arginine-induced AHR to methacholine was effectively blocked by the polyanion heparin, indicating that cationic charge interactions may underly the development of the enhanced agonist responsiveness. This is also true for the reduced NOS activity by the polycation, since the effect to L-NAME was fully restored by coperfusion of poly-L-arginine with heparin.

The present findings are obviously of interest with respect to the mechanism of allergen-induced AHR *in vivo*. Thus, using a guinea-pig model of allergic asthma, characterized by allergen-induced early and late allergic reactions, airway eosinophilia and AHR after both reactions (Santing *et al*., 1994), we have recently established that a deficiency of cNOS-derived NO contributes to the increased *ex vivo* responsiveness of isolated perfused tracheae to methacholine and histamine after the early allergic reaction, at 6 h after inhalational challenge of the animals with ovalbumin aerosol (De Boer *et al*., 1996). Using the same animal model, a reduced production or effectiveness of endogenous NO was similarly found to contribute to the AHR to histamine *in vivo* after the early allergic reaction (Schuiling *et al*., 1998), while evidence for a deficiency of cNOS-derived NO modulating airway reactivity was recently also found in patients with severe asthma (Ricciardolo *et al*., 1997). Therefore, it can be proposed that polycationic peptides released by activated eosinophils in the inflamed airways may contribute to the deficiency of bronchodilating cNOS-derived NO and subsequent AHR in allergic asthma.

The mechanism of polycation-induced NO deficiency remains to be established. However, one possible mechanism could be polycation-induced inhibition of the cellular uptake of L-arginine by cationic aminoacid transporters, as indicated very recently in rat and guinea-pig alveolar macrophages (Hirschmann *et al*., 1998).

In conclusion, the present data demonstrate that a deficiency of NO is involved in polycation-induced AHR, which could represent a novel mechanism of AHR induced by eosinophil-derived cationic polypeptides in allergic asthma.

References

COYLE, A.J., ACKERMAN, S.J. & IRVIN, C.G. (1993a). Cationic proteins induce airway hyperresponsiveness dependent on charge interactions. *Am. Rev. Respir. Dis.,* **147,** 896–900.

COYLE, A.J., MITZNER, W. & IRVIN, C.G. (1993b). Cationic proteins alter smooth muscle function by an epithelium-dependent mechanism. *J. Appl. Physiol.,* **74,** 1761–1768.

DE BOER, J., MEURS, H., COERS, W., KOOPAL, M., BOTTONE, A.E., VISSER, A.C., TIMENS, W. & ZAAGSMA, J. (1996). Deficiency of nitric oxide in allergen-induced airway hyperreactivity to contractile agonists after the early asthmatic reaction. An *ex vivo* study. *Br. J. Pharmacol.,* **116,** 1109–1116.

FLAVAHAN, N.A., SLIFMAN, N.R., GLEICH, G.J. & VANHOUTTE, P.M. (1988). Human eosinophil major basic protein causes hyperreactivity of respiratory smooth muscle. *Am. Rev. Respir. Dis.,* **138,** 685–688.

GLEICH, G.J., ADOLPHSON, C.R. & LEIFERMAN, K.M. (1993). The biology of the eosinophilic leukocyte. *Annu. Rev. Med.,* **44,** 85–101.

HIRSCHMANN, J., HEY, C., HAMMERMANN, J.G., FOLKERTS, J.G., NIJKAMP, F.P., GLEICH, G.J., WESSLER, I. & RACKÉ, K. (1998). Inhibition of L-arginine transport in rat and guinea pig alveolar macrophages (AMϕ) by poly-cationic peptides. *Br. J. Pharmacol.,* **123,** 177P.

HULSMANN, A.R., RAATGREEP, H.R., DEN HOLLANDER, J.C., BAKKER, W.H., SAXENA, P.R. & DE JONGSTE, J.C. (1996). Permeability of human isolated airways increases after hydrogen peroxide and poly-L-arginine. *Am. J. Respir. Crit. Care Med.,* **153,** 841–846.

KOBZIK, L., BREDT, D.S., LOWENSTEIN, C.J., DRAZEN, J., GASTON, B., SUGARBAKER, D. & STAMLER, J.S. (1993). Nitric oxide synthase in human and rat lung: immunocytochemical and histochemical localization. *Am. J. Respir. Cell. Mol. Biol.,* **9,** 371–377.

MEURS, H., DE BOER, J., DUYVENDAK, M., SCHUURMAN, F.E. & ZAAGSMA, J. (1999). Role for L-arginine, but not for superoxide anions, in the deficiency of nitric oxide after the allergen-induced early asthmatic reaction in guinea pigs (abstract). *Clin. Exp. Allerg,* (in press).

MOTOJIMA, S., FRIGAS, E., LOWGERING, D.A. & GLEICH, G.J. (1989). Toxicity of eosinophil cationic proteins for guinea pig tracheal epithelium *in vitro*. *Am. Rev. Respir. Dis.,* **139,** 801–805.

MUNAKATA, M., HUANG, I., MITZNER, W. & MENKES, H. (1989). Protective role of epithelium in the guinea pig airway. *J. Appl. Physiol.,* **66,** 1547–1552.

NIJKAMP, F.P., VAN DER LINDE, H.J. & FOLKERTS, G. (1993). Nitric oxide synthesis inhibitors induce airway hyperresponsiveness in the guinea pig *in vivo* and *in vitro*. *Am. Rev. Respir. Dis.,* **148,** 727–734.

OMARI, T., SPARROW, M.P., CHURCH, M.K., HOLGATE, S.T. & ROBINSON, C. (1993). A comparison of the effects of polyarginine and stimulated eosinophils on the responsiveness of the bovine isovolumic bronchial segment preparation. *Br. J. Pharmacol.,* **109,** 553–561.

RICCIARDOLO, F.L.M., DI MARIA, G.U., MISTRETTA, A., SAPIENZA, M.A. & GEPETTI, P. (1997). Impairment of bronchoprotection by nitric oxide in severe asthma. *Lancet,* **350,** 1297–1298.

SANTING, R.E., OLYMULDER, C.G., ZAAGSMA, J. & MEURS, H. (1994). Relationships among allergen-induced early and late phase airway obstructions, bronchial hyperreactivity, and inflammation in conscious, unrestrained guinea pigs. *J. Allergy Clin. Immunol.,* **93,** 1021 – 1030.

SCHUILING, M., ZUIDHOF, A.B., BONOUVRIE, A.A., VENEMA, N., ZAAGSMA, J. & MEURS, H. (1998). Role of nitric oxide in the development and partial reversal of allergen-induced airway hyperreactivity in conscious, unrestrained guinea-pigs. *Br. J. Pharmacol.,* **123,** 1450 – 1456.

UCHIDA, D.A., ACKERMAN, S.J., COYLE, A.J., LARSEN, G.L., WELLER, P.F., FREED, J. & IRVIN, C.G. (1993). The effect of human eosinophil granule major basic protein on airway responsiveness in the rat *in vivo*. A comparison with polycations. *Am. Rev. Respir. Dis.,* **147,** 982 – 988.

WARDLAW, A.J., DUNNETTE, S., GLEICH, G.J., COLLINS, J.V. & KAY, A.B. (1988). Eosinophils and mast cells in bronchoalveolar lavage in subjects with mild asthma. *Am. Rev. Respir. Dis.,* **137,** 62 – 69.

(Received September 19, 1998
Revised November 12, 1998
Accepted November 19, 1998)

British Journal of Pharmacology (1999) 126, 563–567
http://www.stockton-press.co.uk/bjp

SPECIAL REPORT

Cyclo-oxygenase-2 mediates P2Y receptor-induced reactive astrogliosis

[1]Roberta Brambilla, *,[2]Geoffrey Burnstock, [1]Albino Bonazzi, [1]Stefania Ceruti, [1]Flaminio Cattabeni & [1]Maria P. Abbracchio

[1]Institute of Pharmacological Sciences, University of Milan, Via Balzaretti 9, 20133 Milan, Italy and [2]Autonomic Neuroscience Institute, Royal Free Hospital School of Medicine, Rowland Hill Street, London NW3 2PF, England, U.K.

Excessive cyclo-oxygenase-2 (COX-2) induction may play a role in chronic neurological diseases characterized by inflammation and astrogliosis. We have previously identified an astroglial receptor for extracellular nucleotides, a P2Y receptor, whose stimulation leads to arachidonic acid (AA) release, followed, 3 days later, by morphological changes resembling reactive astrogliosis. Since COX-2 may be upregulated by AA metabolites, we assessed a possible role for COX-2 in P2Y receptor-mediated astrogliosis. A brief challenge of rat astrocytes with the ATP analogue α,β-methylene ATP (α,βmeATP) resulted, 24 h later, in significantly increased COX-2 expression. The selective COX-2 inhibitor NS-398 completely abolished α,βmeATP-induced astrocytic activation. Constitutive astroglial COX-1 or COX-2 did not play any role in purine-induced reactive astrogliosis. PGE_2, a main metabolite of COX-2, also induced astrocytic activation. These data suggest that a P2Y receptor mediates reactive astrogliosis *via* induction of COX-2. Antagonists selective for this receptor may counteract excessive COX-2 activation in both acute and chronic neurological diseases.

Keywords: ATP; cyclo-oxygenase-2; inflammation; astrogliosis; P2Y receptors

Abbreviations: AA, arachidonic acid; AP-1, activator protein-1; ASA, acetylsalicylic acid; COX, cyclo-oxygenase; GFAP, glial fibrillary acidic protein; α,βmeATP, α,β-methylene ATP; β,γmeATP, β,γ-methylene ATP; PGD_2, prostaglandin D_2; PGE_2, prostaglandin E_2

Introduction Recent reports have implicated cyclo-oxygenase-2 (COX-2) in a variety of neurological disorders, including chronic pain and inflammation (Dolan *et al*., 1998), acute (e.g., ischaemia; Ohtsuki *et al*., 1996) as well as chronic (e.g., Alzheimer's disease; Tocco *et al*., 1997) neurodegenerative diseases characterized by a marked inflammatory component and activation of astroglial cells (Ohtsuki *et al*., 1996; Blom *et al*., 1997; Tocco *et al*., 1997). A key role for the inducible enzyme in the pathogenesis of these disorders is also supported by the results of epidemiological studies showing that steroidal as well as non-steroidal anti-inflammatory drugs lower the risk of developing Alzheimer's disease (Breitner *et al*., 1994).

Extracellular ATP exerts its effects through P2 receptors: these are ligand-gated ion channels (P2X receptors) or G-protein-coupled receptors (P2Y receptors) (Abbracchio & Burnstock, 1994). In brain, ATP has been implicated both in fast neuro-neuronal communication *via* P2X receptors, and in regulation of several properties of astrocytes *via* P2Y receptors, some of which may be involved in mechanisms of neural injury following massive ATP release during trauma and ischaemia (Neary *et al*., 1996). We have previously shown that a brief (2 h) challenge of rat brain astrocytes with the relatively hydrolysis-resistant ATP analogues α,β-methylene ATP (α,βmeATP) and β,γ-methylene ATP (β,γmeATP) results, 3 days later, in marked concentration-dependent elongation of astrocytic processes which intensively stain for the astroglial marker GFAP (glial fibrillary acidic protein) (Bolego *et al*., 1997). This effect, which reproduces *in vitro* the astrocytic hypertrophy known to occur in *in vivo* reactive astrogliosis (Ridet *et al*., 1997) was abolished by pertussis toxin, suggesting the involvement of a P2Y receptor. Astrocytic activation by ATP analogues was not due to modulation of either phospholipase C or adenylyl-cyclase activity (Bolego *et al*., 1997), nor to changes of the intracellular Ca^{2+} concentrations (Centemeri *et al*., 1997), but to a rapid activation of phospholipase A_2 and arachidonic acid (AA) release (Bolego *et al*., 1997). Arachidonic acid is a substrate for both constitutive COX-1 and mitogen-activated COX-2 (Wu, 1996). The involvement of COX-2-mediated production of proinflammatory cytokines and PGE_2 by astrocytes in neurodegeneration has been suggested (Blom *et al*., 1997). A specific aim of the present study was therefore to evaluate a role for the inducible enzyme in P2Y receptor-mediated reactive astrogliosis.

Methods *Rat astrocytic cultures* Primary astrocytic cultures were established from rat corpus striatum of 7-day-old pups as previously described (Bolego *et al*., 1997). Cells were initially plated in serum-supplemented medium and after 24 h placed in chemically defined serum-free medium.

Treatment of cultures Challenge with the various agents and treatment with inhibitors are summarized in Figure 1. Briefly, at day 2 of culture, cells were challenged for 2 h with various agents (either α,βmeATP, AA, PGE_2 or PGD_2), washed and placed in drug-free medium until the end of the experiment (day 5 of culture). In selected experiments where effects of inhibitors were examined, either acetylsalicylic acid (ASA) or NS-398 were added to cultures 30 min before α,βmeATP and maintained in the medium throughout the challenge with the purine analogue (short protocol). To assess the role of inducible COX-2 in purine-induced reactive astrogliosis, cells

* Author for correspondence; E-mail: g.burnstock@ucl.ac.uk

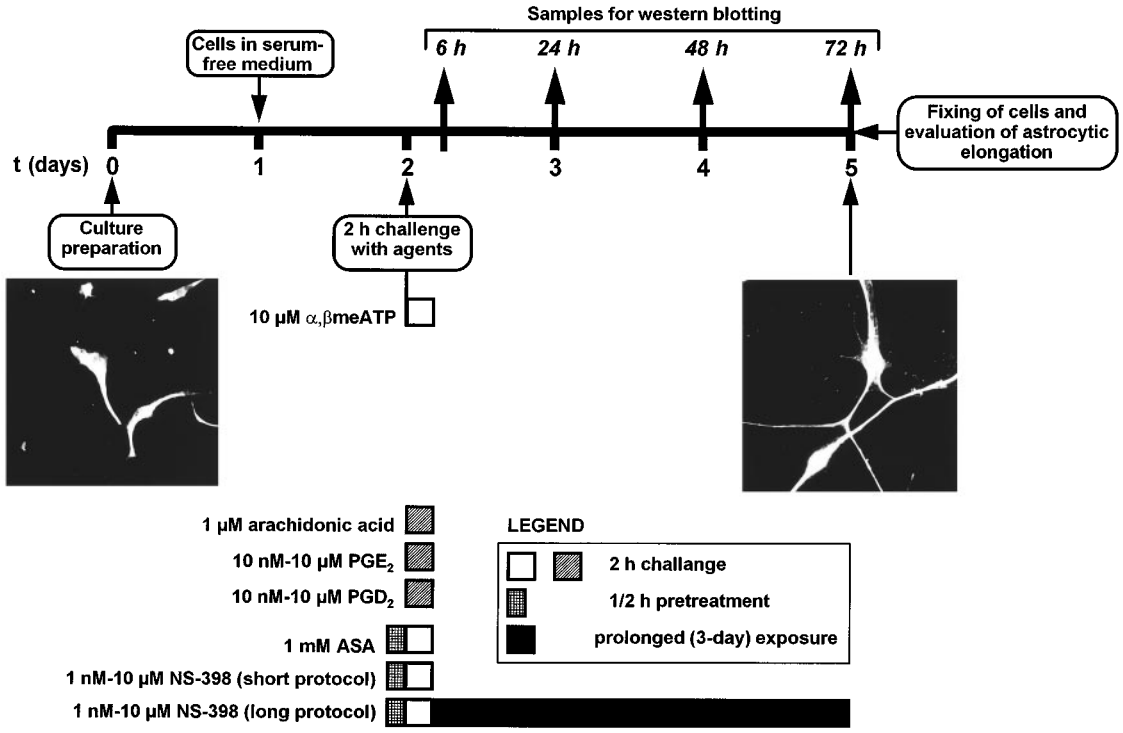

Figure 1 The experimental protocol used to assess a role for COXs in purine-mediated reactive astrogliosis. Rat striatal astrocytic cells were initially established in complete medium, placed in serum-free medium at day 1 to favour morphological differentiation resembling reactive astrogliosis, and challenged at day 2 with either purine analogues (e.g. α,βmeATP) or other agents (see text). After challenge, cells were grown for a further 3 days in drug-free medium, fixed, stained with an anti-GFAP antibody for determination of the elongation of astrocytic processes. Left panel: micrograph depicting control astrocytes with typical bipolar shape. Right panel: activated astrocytes showing increased length of astrocytic processes. In selected experiments, samples for evaluation of COX-2 by Western blot were taken at various periods after challenge with α,βmeATP, as indicated. To evaluate a role of constitutive COXs, ASA and NS-398 were added to the cultures 30 min before challenge with the purine analogue and maintained for the 2 h challenge period (short protocol). To evaluate the role of inducible COX-2, NS-398 was also maintained in the culture medium for the entire duration of the experiment (long protocol).

challenged with α,βmeATP in the presence of NS-398 were washed and maintained in medium containing NS-398 at the same concentration up to cell fixing (long protocol). Neither NS-398 nor ASA had any effect on process length when tested alone.

Immunofluorescence staining and analysis of GFAP-positive astrocytic processes Astrocytes were identified by indirect immunofluorescence staining using rabbit anti-GFAP immunoglobulins (1 : 500, DAKO) followed by biotinylated donkey anti-rabbit secondary antibody and streptavidin-fluorescein (Bolego *et al*., 1997). The length of GFAP-positive astrocytic processes (mean μm cell$^{-1}\pm$s.e.mean) was measured using a Zeiss fluorescence microscope equipped with a fluorescein filter and connected to an image video system (video camera, NIH Image 1.47 software on a Macintosh computer). The cellular processes of at least 75 cells sample^{-1} were analysed under blind conditions. Cells were chosen at random. The absolute control value was 141 ± 5.6 μm cell^{-1} (mean$\pm$s.e.mean of 24 independent experiments). To enable a more immediate evaluation, data were expressed as per cent of a corresponding control set.

Western blot analysis This was performed as previously described (Abbracchio *et al*., 1997). Briefly, 20 mg of total protein from each sample (see Figure 1) was loaded on 11% sodium-dodecylsulphate polyacrylamide gels and blotted onto nitrocellulose filters. Filters were incubated with goat polyclonal anti-rat anti-COX-2 antibody (1 : 3,000, Santa Cruz Biotechnology) followed by a secondary anti-goat antibody (conjugated to horseradish peroxidase, 1 : 4000) and visualized with ECL Western blotting kit (Amersham U.K.). Semiquantitative evaluation of autoradiograms was performed by densitometric analysis on a computerized image analyser (see above).

Results The experimental protocol utilized in the present study is shown in Figure 1. Exposure of cultures to α,βmeATP under conditions that elicited the formation of reactive astrocytes (Figure 1) resulted, 24 h after agonist challenge, in increased expression of COX-2, as evaluated by Western blot analysis (Figure 2a). The amount of enzyme was still increased with respect to control cultures 48 h after challenge and returned to basal levels 72 h after challenge with the purine analogue. Under these experimental conditions a marked elongation of GFAP-positive astrocytic processes was detected (see Figure 1 and solid column in Figure 2b). Maintenance of cells in the continuous presence of the selective COX-2 inhibitor NS-398 (Futaki *et al*., 1994) after challenge with the purine analogue (see 'long protocol' in Figure 1) resulted in a concentration-dependent attenuation of astrocytic elongation (Figure 2b). A trend to decreased reactive astrogliosis was already observed in the presence of NS-398 (0.001 μM); inhibition was statistically significant at 0.01 μM; complete abolition of α,βmeATP-induced reactive astrogliosis was observed at all other concentrations of inhibitor tested (Figure 2b), suggesting a specific role for the inducible enzyme in the

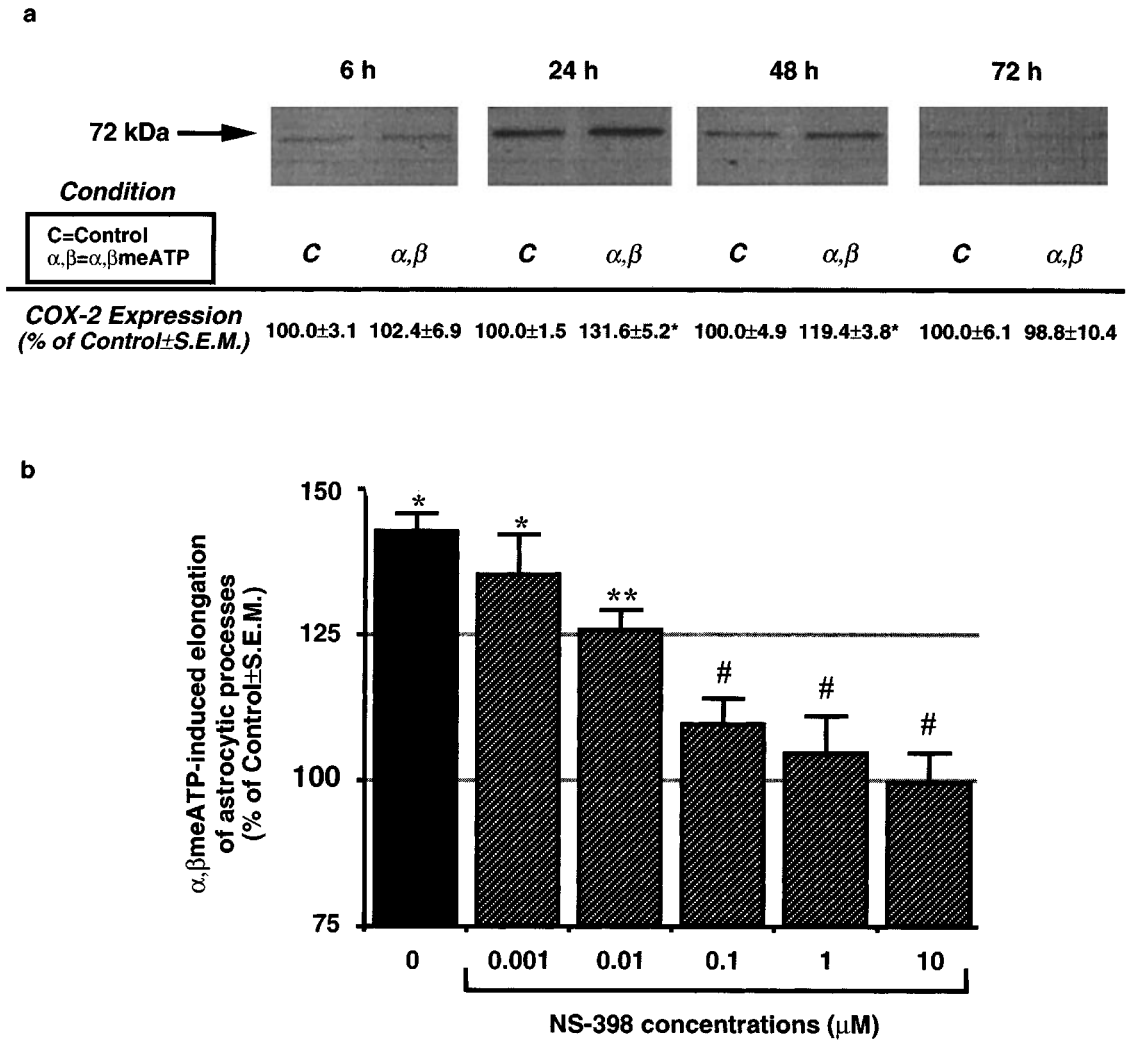

Figure 2 Involvement of inducible COX-2 in P2Y receptor-mediated reactive astrogliosis. (a) Cells were challenged with α,βmeATP (10 μM) for 2 h, placed in agonist-free medium, and the presence of COX-2 assessed at 6, 24, 48 and 72 h by immunoblot analysis with a specific ant-COX-2 antibody. Results (area × optical density of the 72 kDa MW COX-2 band) are expressed as mean per cent ± s.e.mean of the corresponding control value from four independent experiments run in triplicate. COX-2 was significantly increased at 24 and 48 h (*$P<0.05$, 1-way ANOVA, Scheffé's F-test). (b) Under the experimental conditions, a marked astrocytic activation was found, as demonstrated by increased elongation of GFAP-positive astrocytic processes (expressed as percentage of control mean μm cell^{-1} ± s.e.mean; see solid column; *$P<0.05$, 1-way ANOVA, F-test). If, after challenge with the purine analogue, cells were maintained in the presence of NS-398 to selectively inhibit the inducible enzyme (long protocol, Figure 1), a concentration-dependent inhibition of α,βmeATP-induced astrocytic elongation was found (hatched columns; **$P<0.05$ vs both control and α,βmeATP alone, $^{\#}P<0.05$ vs α,βmeATP alone and not statistically different from control, 1-way ANOVA, F-test).

formation of reactive astrocytes. Other non-selective inhibitors of COX-2 (e.g., dexamethasone, which also blocks phospholipase A_2) also abolished purine-induced reactive astrogliosis (data not shown).

Western blot experiments revealed a low, but significant, amount of COX-2 also in control unstimulated astrocytes (Figure 2a), suggesting that COX-2 may be constitutively expressed in these cells. Therefore, we designed specific experiments aimed at testing a possible role for constitutive COXs in purine-induced astrogliosis. Cultures were exposed to NS-398 (0.001 – 10 μM) to selectively block constitutive COX-2, or to ASA (1 mM) (which irreversibly inhibits both COX-1 and COX-2; Kalgutkar *et al*., 1998) immediately before and throughout challenge with α,βmeATP (short protocol). ASA was used at a concentration high enough to irreversibly inactivate all the COXs enzymes present during challenge with the purine analogue, i.e., to ensure abolition of the contribution made by the constitutively expressed enzymes. After challenge, cells were washed, placed in drug-free medium, and grown for a further 3 days before morphological analysis. Under these conditions, no inhibition of purine-induced astrocytic elongation was detected (Table 1), hence ruling out a role for constitutive COXs and suggesting that any effect seen after treatment with the purine analogue must result from cloning of new enzyme. Data with NS-398 (Figure 2b) suggest that this is indeed COX-2.

We have previously shown that, in a similar way to ATP analogues, exposure of cultures to AA elicits the formation of reactive astrocytes (Bolego *et al*., 1997). Since PGE_2 and PGD_2 have been implicated as functionally important COX products in brain (Blom *et al*., 1997; Minghetti *et al*., 1997), in the present study we have also examined these prostaglandins for their ability to trigger reactive astrogliosis. The exogenous addition of the inflammatory PGE_2 (but not PGD_2) mimicked the effects evoked by P2Y receptor activation, resulting in statistically significant and concentration-dependent elonga-

Table 1 Effect of NS-398 and acetylsalicylic acid (ASA) inhibition of COX-2 on elongation of astrocytic processes

Inhibitor	*Conditions*	*Length of process* (% of Control ± s.e.mean)
NS-398	α,βmeATP	137.0 ± 5.0*
	α,βmeATP + 0.1 μM NS-398	130.9 ± 6.4**
	α,βmeATP + 1 μM NS-398	136.3 ± 8.2**
	α,βmeATP + 10 μM NS-398	126.4 ± 4.4**
ASA	α,βmeATP	140.5 ± 4.2*
	α,βmeATP + 1 mM ASA	167.7 ± 6.7**

Constitutive COXs were inhibited by the presence of NS-398 or ASA before and throughout challenge with α,βmeATP (short protocol, Figure 1). Neither NS-398 nor ASA significantly inhibited the astrocytic elongation induced by α,βmeATP (*$P<0.05$ vs control, **$P<0.05$ vs control and not statistically different from α,βmeATP alone, 1-way ANOVA, F-test).

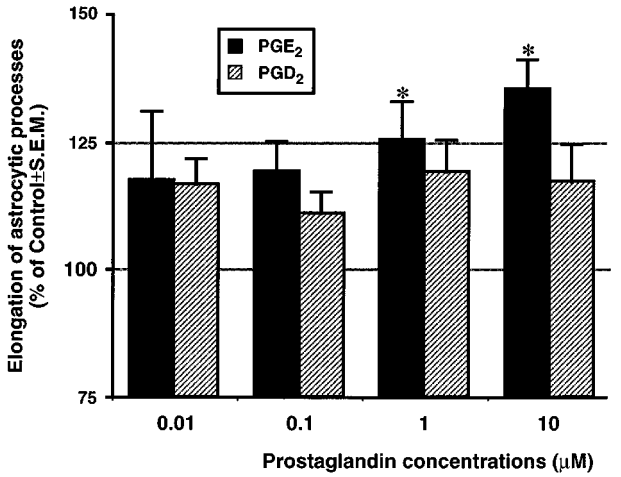

Figure 3 Exogenously applied PGE_2, but not PGD_2, can mimic P2Y receptor-mediated reactive astrogliosis. Cultures were challenged for 2 h with the concentrations of prostaglandins indicated, washed, grown for a further 3 days in drug-free medium, fixed, stained and assessed for elongation of the astrocytic processes. Results are the mean ± s.e.mean of three independent experiments run in quadruplicate. *$P<0.05$, 1-way ANOVA, F-test.

tion of astrocytic processes (Figure 3). This suggests that PGE_2 is likely to represent the main AA metabolite involved in purine-induced reactive astrogliosis.

Discussion Our results show that ATP may trigger reactive astrogliosis *via* activation of a P2Y receptor linked to induction of COX-2. Transductional signalling to COX-2 induction involves an early activation of phospholipase A_2 and AA release; this may hence act as an inducer of the COX-2 gene *via* the protein kinase-C/mitogen-activated kinase pathway (Neary *et al*., 1996). Regulation of COX-2 transcription by activator protein-1 (AP-1) has been reported (Wu, 1996); interestingly we and others have previously shown that exposure of astrocytes to ATP results in induction of the *Jun* and *Fos* transcriptional factors (Neary *et al*., 1996; Bolego *et al*., 1997) and formation of AP-1 complexes (Neary *et al*., 1996). Data also point to PGE_2 as a main COX-2 metabolite in P2Y receptor-mediated reactive astrogliosis; this is consistent with previous results demonstrating increases of this inflammatory mediator in a human post-mortem astrocytic culture (Blom *et al*., 1997).

A relationship between extracellular P2 receptors and prostanoid production was proposed back in the 1970s (Burnstock *et al*., 1975). The ability of astroglial cells to release prostanoids upon activation of P2 receptors was demonstrated in the late 1980s (Pearce *et al*., 1989). Our results establish for the first time a specific correlation between activation of G protein-coupled P2Y receptors on astrocytes and induction of COX-2. Enhanced COX-2 activity in neurological diseases may contribute to neuronal damage *via* production of free radicals during AA conversion (Katsuki & Okuda, 1995). In addition, COX-2 products may potentiate brain damage by increasing oedema and by delivery of proinflammatory cells into the brain. Moreover, whereas neuron-derived prostanoids seem to be more involved in functions related to synaptic transmission and neural plasticity, reactive astrocytes and microglial cells are likely to be the major sources of prostaglandins in pathological conditions (Minghetti *et al*., 1997). A specific pathogenic role for astroglial COX-2 is also suggested by the demonstration that PGE_2 largely potentiated release of pro-inflammatory cytokine interleukin-6 from both astroglioma cell lines and post-mortem human astrocytes (Blom *et al*., 1997). PGE_2 has been also recently associated with release of reactive oxygen and other radicals in neurotoxicity induced by the prion protein (Brown *et al*., 1996). On this basis, selective inhibitors of COX-2 have been suggested to be beneficial for the therapy of central nervous system diseases characterized by neurodegenerative events (Ohtsuki *et al*., 1996; Blom *et al*., 1997), chronic inflammation and pain (Dolan, *et al*., 1998), while avoiding the gastrointestinal, renal and haematopoietic adverse effects typical of mixed COX-1/COX-2 inhibitors (Flower, 1996). Our results suggest that such a goal may be achieved by selectively blocking astroglial P2Y receptors mediating reactive astrogliosis. In previous work, we have shown that the non-selective P2 receptor antagonist suramin can concentration-dependently block the formation of reactive astrocytes by ATP analogues (Bolego *et al*., 1997). However, suramin also has a variety of additional activities on membrane channels, G proteins and enzymes. Selective antagonists of the astroglial P2Y receptor devoid of effects on other biological targets are hence highly desirable: these may represent a novel class of anti-inflammatory agents.

This work was partially supported by the European Union BIOMED2 Programme BMH4 CT96-0676. The authors are grateful to Professor G.C. Folco, Institute of Pharmacological Sciences, Milan, Italy, for invaluable suggestions on the experimental protocol, to Dr Alicia Hernandez (ibidem) for useful discussion, and to Roy Jordan for editorial assistance.

References

ABBRACCHIO, M.P. & BURNSTOCK, G. (1994). Purinoceptors: are there families of P2X and P2Y purinoceptors? *Pharmacol. Ther.,* **64,** 445–475.

ABBRACCHIO, M.P., RAINALDI, G., GIAMMARIOLI, A.M., CERUTI, S., BRAMBILLA, R., CATTABENI, F., BARBIERI, D., FRANCESCHI, C., JACOBSON, K.A. & MALORNI, W. (1997). The A_3 adenosine receptor mediates cell spreading, reorganization of actin cytoskeleton, and distribution of Bcl-XL: studies in human astroglioma cells. *Biochem. Biophys. Res. Commun.,* **241,** 297–304.

BLOM, M.A.A., VAN TWILLERT, M.G., DE VRIES, S.C., ENGEL, S.F., FINCH, C.E., VEERHUIS, R. & EIKELENBOOM, P. (1997). NSAIDS inhibit the IL-1β-induced IL-6 release from human post-mortem astrocytes: the involvement of prostaglandin E_2. *Brain Res.,* **777,** 210–218.

BOLEGO, C., CERUTI, S., BRAMBILLA, R., PUGLISI, L., CATTABENI, F., BURNSTOCK, G. & ABBRACCHIO, M.P. (1997). Characterization of the signalling pathways involved in ATP and basic fibroblast growth factor-induced astrogliosis. *Br. J. Pharmacol.,* **121,** 1692–1699.

BREITNER, J.C.S., GAU, B.A., WELSH, K.A., PLASSMAN, B.L., MCDONALD, W.M., HELMS, M.J. & ANTHONY, J.C. (1994). Inverse association of anti-inflammatory treatments and Alzheimer's disease: initial results of a control co-twin study. *Neurology,* **44,** 227–232.

BROWN, D.R., SCHMIDT, B. & KRETZSCHMAR, H.A. (1996). Role of microglia and host prion protein in neurotoxicity of a prion protein fragment. *Nature,* **380,** 345–347.

BURNSTOCK, G., COCKS, T., PADDLE, B. & STASZEWSKA-BARCZAK, J. (1975). Evidence that prostaglandin is responsible for the 'rebound contraction' following stimulation of non-adrenergic, non-cholinergic ('purinergic') inhibitory nerves. *Eur. J. Pharmacol.,* **31,** 360–362.

CENTEMERI, C., BOLEGO, C., ABBRACCHIO, M.P., CATTABENI, F., PUGLISI, L., BURNSTOCK, G. & NICOSIA, S. (1997). Characterization of the Ca^{2+} responses evoked by ATP and other nucleotides in mammalian brain astrocytes. *Br. J. Pharmacol.,* **121,** 1700–1706.

DOLAN, S., O'SHAUGHNESSY, P.J. & NOLAN, A.M. (1998). Up-regulation of COX-2 and prostaglandin EP3 receptor mRNA expression in spinal cord in a clinical model of chronic inflammation. *Eur. J. Neurosci.,* **10,** 77.

FLOWER, R.J. (1996). New directions in cyclooxygenase research and their implications for NSAID-gastropathy. *Ital. J. Gastroenterol.,* **28,** 23027.

FUTAKI, N., TAKAHASHI, S., YOKOYAMA, M., ARAI, I., HIGUCHI, S. & OTOMO, S. (1994). NS-398, a new anti-inflammatory agent selectively inhibits prostaglandin G/H synthase/cyclooxygenase (COX-2) activity in vitro. *Prostaglandins,* **47,** 55–59.

KALGUTKAR, A.S., CREWS, B.C., ROWLINSON, S.W., GARNER, C., SEIBERT, K. & MARNETT, L.J. (1998). Aspirin-like molecules that covalently inactivate cyclooxygenase-2. *Science,* **280,** 1268–1270.

KATSUKI, H. & OKUDA, S. (1995). Arachidonic acid as a neurotoxic and neurotrophic substance. *Prog. Neurobiol.,* **46,** 607–636.

MINGHETTI, L., POLAZZI, E., NICOLINI, A., CREMINON, C. & LEVI, G. (1997). Up-regulation of cyclooxygenase-2 expression in cultured microglia by prostaglandin E_2, cyclic AMP and non-steroidal anti-inflammatory drugs. *Eur. J. Neurosci.,* **9,** 934–940.

NEARY, J.T., RATHBONE, M.P., CATTABENI, F., ABBRACCHIO, M.P. & BURNSTOCK, G. (1996). Trophic actions of extracellular nucleotides and nucleosides on glial and neuronal cells. *Trends Neurosci.,* **19,** 13–18.

OHTSUKI, T., KITAGAWA, K., YAMAGATA, K., MANDAI, K., MABUCHI, T., MATSUSHITA, K., YANAGIHARA, T. & MATSUMOTO, M. (1996). Induction of cyclooxygenase-2 mRNA in gerbil hippocampal neurons after transient forebrain ischaemia. *Brain Res.,* **736,** 353–356.

PEARCE, B., MURPHY, S., JEREMY, J., MORROW, C. & DANDONA, P. (1989). ATP-evoked Ca^{2+} mobilization and prostanoid release from astrocytes: P2-purinergic receptors linked to phosphoinositide hydrolysis. *J. Neurochem.,* **52,** 971–977.

RIDET, J.L., MALHOTRA, S.K., PRIVAT, A. & GAGE, F.H. (1997). Reactive astrocytes: cellular and molecular cues to biological function. *Trends Neurosci.,* **20,** 570–577.

TOCCO, G., FREIRE-MOAR, J., SCHREIBER, S.S., SAKHI, S.H., AISEN, P.S. & PASINETTI, G.M. (1997). Maturational regulation and regional induction of cyclooxygenase-2 in rat brain: implications for Alzheimer's disease. *Exp. Neurol.,* **144,** 339–349.

WU, K.H. (1996). Cyclooxygenase 2 induction: molecular mechanisms and pathophysiological roles. *J. Lab. Clin. Med.,* **128,** 242–245.

(Received September 21, 1998
Revised October 26, 1998
Accepted November 4, 1998)

British Journal of Pharmacology (1999) 126, 568–571
http://www.stockton-press.co.uk/bjp

SPECIAL REPORT

Modulation of noradrenergic neuronal firing by selective serotonin reuptake blockers

*,[1]Steven T. Szabo, [1]Claude de Montigny & [1]Pierre Blier

Neurobiological Psychiatry Unit, McGill University, Montreal, Canada, H3A 1A1

Using *in vivo* extracellular unitary recording, the effect of short term (2-day) and long-term (21-day) administration of the selective 5-HT reuptake inhibitor (SSRI) paroxetine (10 mg kg^{-1} day^{-1}, s.c. using osmotic minipumps) was examined on the spontaneous firing activity of locus coeruleus noradrenergic neurons. Long-term but not short-term treatment significantly decreased firing activity. Thus, it appears that enhancing 5-HT neurotransmission by sustained SSRI administration leads to a reduction of the firing rate of noradrenergic neurons. The SSRI paroxetine therefore alters the activity of noradrenergic neurons with a delay that is consistent with its therapeutic action in depression and panic disorder.

Keywords: Antidepressant; noradrenaline; major depression; panic disorder; serotonin (5-HT); selective serotonin reuptake inhibitor (SSRI)

Abbreviations: SSRI, selective serotonin reuptake inhibitor

Introduction The pathophysiology underlying major depression and panic disorder is poorly understood, however, more is known about the mechanisms of action of the antidepressant drugs used to treat these disorders (reviewed by Blier & de Montigny, 1997). For instance, selective 5-HT reuptake inhibitors (SSRIs) have been shown to enhance 5-HT neurotransmission in projecting brain areas by increasing 5-HT release as a result of a progressive desensitization of somatodendritic and terminal 5-HT autoreceptors which normally exert a negative feedback influence on the function of 5-HT neurons. Since SSRIs and other antidepressant drugs require an administration of about 2 weeks before exerting a detectable therapeutic effect, the blockade of 5-HT uptake *per se* cannot account for their therapeutic efficacy in major depression and panic disorder. In the treatment of panic disorder, when a SSRI is administered at a starting dose equivalent to that utilized in the treatment of major depression, an exacerbation of the symptoms often occurs (van Vilet *et al*., 1996). Consequently, the starting dose is routinely decreased by at least half to avoid this deterioration and then it is progressively titrated to the upper range of the therapeutic window. These clinical observations suggest that panic disorder patients, contrary to depressed patients, might have an increased hypersensitivity of certain 5-HT receptor subtypes. The beneficial effects of the drugs in panic disorder occur gradually at about the same rate as for the treatment of major depression.

It is well established that noradrenergic neurons modulate the 5-HT system. Dorsal raphe 5-HT neurons receive noradrenergic projections from the locus coeruleus (Baraban & Aghajanian, 1980; Anderson *et al*., 1977; Loizou, 1969), a nucleus which gives rise to more than 90% of noradrenergic innervation of the brain. The noradrenergic neurons located in the locus coeruleus modulate the activity of 5-HT neurons in the dorsal raphe nucleus *via* excitatory α_1-adrenoceptors (Baraban & Aghajanian, 1980). In turn, noradrenergic neurons of the locus coeruleus receive dense 5-HT projections which have revealed an inhibitory role of 5-HT using different experimental approaches (Vertes & Kocsis, 1994; Léger & Descarries, 1978; Cedarbaum & Aghajanian, 1978). This modulation is indicated by several lines of evidence. For instance, lesioning of 5-HT neurons with a selective 5-HT neurotoxin produces an elevation of firing rate of noradrenergic neurons (Haddjeri *et al*., 1997). The noradrenergic system is in itself a neuronal system which has been implicated in the antidepressant response. Consequently, the therapeutic effect of drugs selective for the 5-HT system, like SSRIs, could in fact be mediated in part by a modification of the efficacy of 5-HT transmission in the locus coeruleus. Changes in noradrenergic function in various brain areas by antidepressant drugs may play a crucial role in controlling 5-HT output, and noradrenergic/5-HT interactions may ultimately be relevant to onset antidepressant efficacy and/or to their side effects. In the present study, electrophysiological experiments were performed in male rats undergoing short-term (2-day) and long-term (21-day) treatment with the SSRI paroxetine where the spontaneous neuronal firing rate of locus coeruleus noradrenergic neurons was determined since this parameter controls in large part the release of noradrenaline in the brain.

Methods The experiments were carried out in male Sprague Dawley rats (Charles River, St. Constant, Québec, Canada) weighing between 300–325 g, kept under standard laboratory conditions (12:12 light-dark cycle with access to food and water *ad libitum*). Two groups of rats were treated with paroxetine (10 mg kg^{-1} day^{-1}) for either 3 weeks or 2 days and one group of rats was treated with citalopram (20 mg kg^{-1} day^{-1}) for 3 weeks delivered by osmotic minipumps (ALZA, Palo Alto, CA, U.S.A.) inserted subcutaneously. Two groups of rats were treated with a vehicle (a 50% v/v ethanol/water solution) for 3 weeks or 2 days *via* osmotic minipumps implanted subcutaneously to act as respective controls for the treated groups. The rats were tested with the minipumps in place. Electrophysiological experiments were performed on rats anaesthetized with chloral hydrate (400 mg kg^{-1}, i.p.) and mounted in a stereotaxic apparatus (David Kopf Instruments). Supplemental doses (100 mg kg^{-1}, i.p.) were given to prevent any nociceptive reaction to pinching of the hind paw. Body temperature was maintained at 37°C

*Author for correspondence.

throughout the experiment utilizing a thermistor-controlled heating pad (Seabrook Medical Instruments, Inc.). Extracellular unitary recording of noradrenergic neurons of the locus coeruleus were conducted with single-barrelled glass micropipettes pre-loaded with fibreglass filaments (to facilitate filling) being pulled in a conventional manner, with the tips broken back to 1–3 μm and filled with a 2 M NaCl solution. Their impedance range was between 2 and 4 MΩ. A burr hole was drilled 1 mm posterior to lambda and 1 mm lateral to midline for locus coeruleus neurons recordings. Locus coeruleus noradrenergic neurons were recorded with micropipettes lowered at −0.7 mm interaural and 1.1–1.4 mm lateral. Spontaneously active noradrenergic neurons of the locus coeruleus were identified using the following criteria: regular firing rate (1–5 Hz) and positive action potential of long duration (0.8–1.2 ms) exhibiting a characteristic burst discharge in response to nociceptive pinch of the contralateral hind paw. Noradrenergic neurons were recorded for at least 1 min to establish basal firing rate. In order to determine possible changes of spontaneous firing activity of noradrenergic neurons, four to five electrode descents were carried out through this nucleus in control and treated rats.

All results were expressed as mean ± s.e.mean. Of single neuron values. Statistical comparisons of values obtained in control and paroxetine treated rats were carried out using one-way analysis of variance followed by *post hoc* Tukey Test.

Results Systematic electrode descents into the locus coeruleus were carried out in rats treated with paroxetine for 2 and 21 days as well as with their respective controls. The spontaneous firing activity of locus coeruleus noradrenergic neurons in treatment and control groups were recorded (Figure 1). The 2-day paroxetine treated rats ($n=5$) did not significantly differ in spontaneous firing rate activity when compared to control rats ($n=7$). However, the 21-day paroxetine treated rats ($n=8$) resulted in a significant 52% decrease in the mean spontaneous firing rate when compared to that of the control rats (Figure 2). Similar results were obtained with the other SSRI citalopram after a 21-day treatment ($n=5$ rats; 1.69 ± 0.08 Hz, $n=54$ neurons) resulting in a 36% significant decrease when compared to that of control rats. However, this attenuation of firing activity was significantly different from that obtained in the paroxetine group.

Discussion Previous results from our laboratory have demonstrated that acute injection of SSRIs like paroxetine has no effect on the spontaneous firing activity of locus coeruleus noradrenergic neurons (Béïque *et al*., 1998). The results of the present study indicate that the long-term 21-day treatment but not the short-term 2-day paroxetine treatment greatly reduced the spontaneous firing rate of the locus coeruleus noradrenergic neurons. In contrast, the acute and short-term administration of a SSRI reduces the firing rate of 5-HT neurons of the dorsal raphe nucleus in the rodent brain (de Montigny *et al*., 1981; Quinaux *et al*., 1982). However, these neurons regain their normal firing rate after long-term treatment (Blier & de Montigny, 1983). This has been shown to be due to desensitization of the somatodendritic 5-HT_{1A} autoreceptor which controls their firing activity (Blier & Montigny, 1983). The terminal 5-HT autoreceptor controlling 5-HT release also desensitizes following long-term SSRI administration (Blier *et al*., 1988). These two modifications, in the presence of sustained 5-HT reuptake blockade, result in an increased amount of 5-HT release per action potential in the forebrain.

The difference observed between the paroxetine and citalopram groups after 21 days of treatment cannot be attributed to different degrees of 5-HT reuptake blockade as these regimens were shown to produce a similar effect on the 5-HT reuptake process (Piñeyro *et al*., 1994; Mongeau *et al*., 1998). The difference may rather stem from the weak but significant anti-cholinergic potency of paroxetine. Indeed, since acetylcholine exerts an excitatory effect on noradrenergic neurons firing (Guyenet *et al*., 1977), then the antagonism of an endogenous acetylcholine activation by paroxetine, but not citalopram, might have lead to the greater decrease of noradrenergic firing by the former drug.

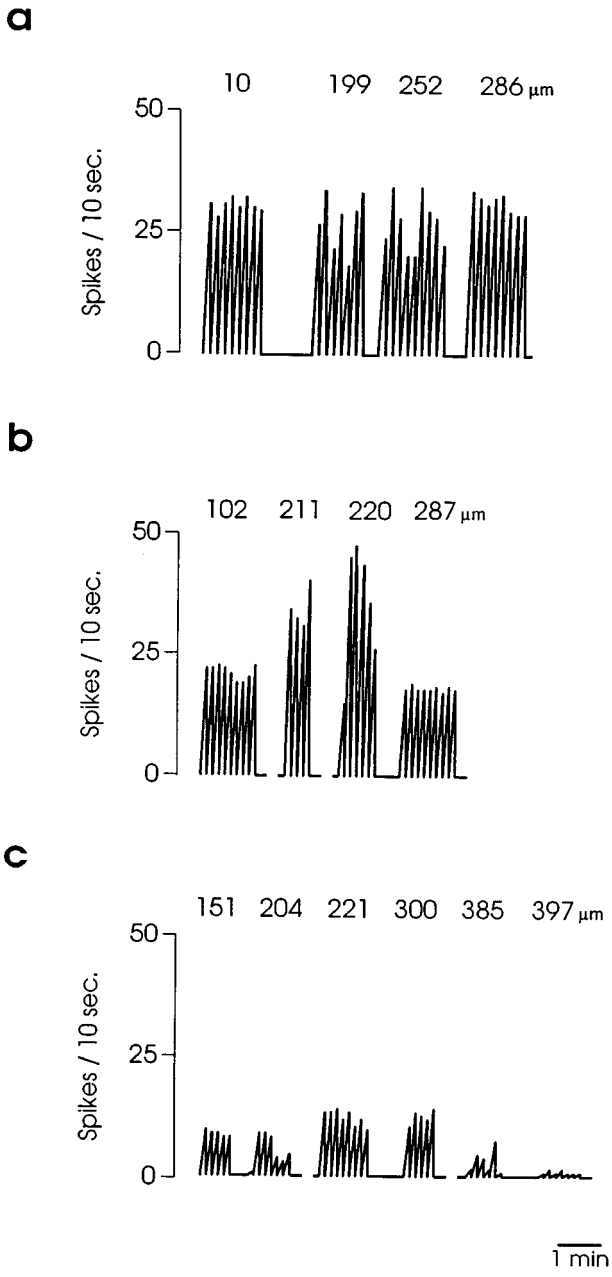

Figure 1 Integrated firing rate histograms of locus coeruleus noradrenergic neurons, recorded in one electrode descent in the locus coeruleus showing their spontaneous firing activity in control (A), 2-day paroxetine treatment (10 mg kg^{-1} day^{-1}) (B), and 21-day paroxetine treatment (10 mg kg^{-1} day^{-1}) (C). The breaks in the lines in between neurons indicate approximately 5-min time laps. The number above each neuron indicates the depth from the floor of the fourth ventricle at which it was recorded.

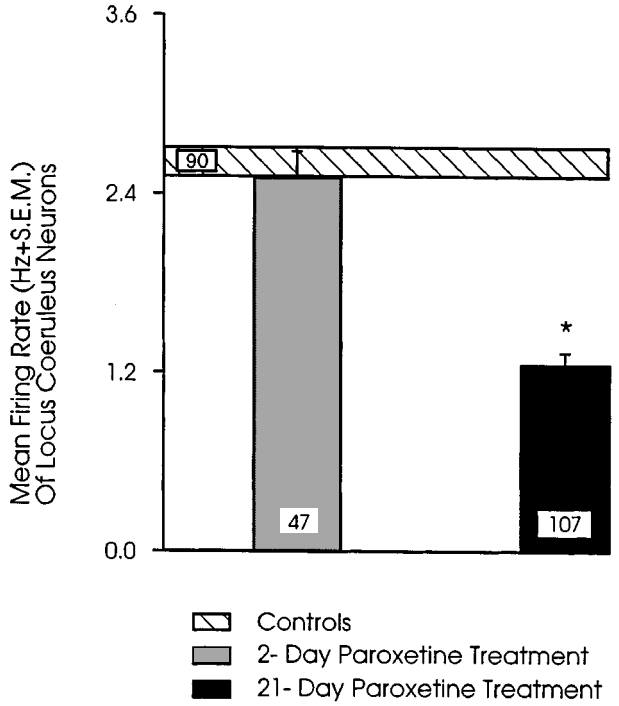

Figure 2 Effects of 2- and 21-day paroxetine treatments (10 mg kg^{-1} day^{-1}) on the firing activity of locus coeruleus neurons. The shaded area represents the range (s.e.mean $\times 2$) of the mean firing activity of neurons recorded in control rats. $^*P<0.05$ (Tukey Test) when compared to the control value. The number of neurons recorded is displayed in each box.

The present findings are interesting when taken into the context of the time course needed for SSRIs to exert their therapeutic efficacy of major depression and panic disorder. The increase in 5-HT release resulting from long-term SSRI treatment would theoretically lead to an increased activation of 5-HT_{2A} receptors on noradrenergic locus coeruleus neurons (Haddjeri *et al*., 1997). This would yield an increased inhibitory response and ultimately a decrease in firing activity of locus coeruleus noradrenergic neurons which is what we have observed. SSRIs thus decrease the locus coeruleus firing rate and may ultimately also attenuate noradrenaline release in projection areas. This in turn may have a profound impact on the α_2-adrenergic heteroreceptors on the 5-HT terminals, thus diminishing the inhibitory influence on these noradrenergic receptors and contributing to the increase of 5-HT neurotransmission by the SSRI.

The present findings might also be related to the initial exacerbation of panic disorder generally observed with usual starting doses of SSRI for major depression. The acute and short-term administration of SSRIs produces in general a small increase in extracellular 5-HT concentration in several postsynaptic structures (Romero *et al*., 1996), but has no effect on noradrenergic neuronal firing rate (Béïque *et al*., 1998). It is thus possible that increased symptoms upon SSRI treatment initiation symptoms may in fact be attributable to an increase in 5-HT synaptic availability not counteracted by an attenuation of noradrenergic firing activity. However, as the treatment is prolonged, 5-HT neurotransmission is further increased but noradrenergic neurotransmission is attenuated. The latter effect may contribute to the anxiolytic and anti-panic effect of SSRI since an enhancement of noradrenergic firing and release achieved with the α_2-adrenoceptor antagonist yohimbine can produce anxiety in healthy volunteers and trigger panic attacks in patients with panic disorder (Charney *et al*., 1984). The decrease in firing activity of locus coeruleus noradrenergic neurons combined with the increase in 5-HT neurotransmission may thus be the adaptive mechanisms whereby SSRIs eventually exert their therapeutic effect in some anxiety disorders. In contrast, this attenuated noradrenergic tone could explain in part the fatigue and asthenia sometimes reported following long-term SSRI treatment in major depression. Indeed, these symptoms occasionally remain in the presence of markedly improved mood (Feighner *et al*., 1991).

This work was supported by the Medical Research Council of Canada (MRC; grants MA 6444 and MT 11014). S.T.S. is in receipt of a Max Stern Fellowship Award and P.B. of a MRC Scientist award.

References

ANDERSON, C., PASQUIER, D.A., FORBES, W.B. & MORGANE, P.J. (1977). Locus coeruleus-to-dorsal raphe imput examined by electrophysiological and morphological methods. *Brain Res. Bull.,* **2,** 209–221.

BARABAN, J.M. & AGHAJANIAN, G.K. (1980). Suppression of serotonergic neuronal firing by alpha-adrenoceptor antagonists: evidence against GABA mediation. *Eur. J. Pharmacol.,* **66,** 287–294.

BÉÏQUE, J.C., DE MONTIGNY, C., BLIER, P. & DEBONNEL, G. (1998). Venlafaxine: Discrepancy between *in vivo* 5-HT and NE reuptake blockade and affinity for reuptake sites. *Synapse,* (in press).

BLIER, P., CHAPUT, Y. & DE MONTIGNY, C. (1988). Long-term 5-HT reuptake blockade, but not monoamine oxidase inhibition, decreases the function of terminal 5-HT autoreceptors: An electrophysiological study in the rat brain. *Naunyn-Scmiedeberg's Arch. Pharmacol.,* **337,** 246–254.

BLIER, P. & DE MONTIGNY, C. (1983). Electrophysiological investigations on the effect of repeated zimelidine administration on serotonergic neurotransmission in the rat. *J. Neurosci.,* **3,** 1270–1278.

BLIER, P. & DE MONTIGNY, C. (1997). Serotonergic neurons and 5-HT receptors in the CNS. *Handbook of Experimental Pharmacology,* **129,** 727–750.

CEDARBAUM, J.M. & AGHAJANIAN, G.K. (1978). Afferent projections to the rat locus coeruleus as determined by a retrograde tracing technique. *J. Comp. Neurol.,* **178,** 1–16.

CHARNEY, D.S., HENINGER, G.R. & BREIER, A. (1984). Noradrenergic function in panic anxiety: effects of yohimbine in healthy subjects and patients with agoraphobia and panic disorder. *Arch. Gen. Psychiatry.,* **43,** 1155–1161.

DE MONTIGNY, C., BLIER, P., CAILLÉ, G. & KOUASSI, E. (1981). Pre- and postsynaptic effect of zimelidine and norzimelidine on the serotonergic system: single cell studies in the rat. *Acta Psychiat. Scand.,* **63,** S79–S80.

FEIGHNER, J.P. & BOYER, W.F. (1991). Selective Re-uptake Inhibitors: The Clinical Use of Citalopram, Fluoxetine, Fluvoxamine, Paroxetine, and Sertraline. *Persp. Psychiat.,* **1,** 133–139.

GUYENET, P.G. & AGHAJANIAN, G.K. (1977). Excitation of neurons in the nucleus locus coeruleus by substance P and related peptides. *Brain Res.,* **136,** 178–184.

HADDJERI, N., DE MONTIGNY, C. & BLIER, P. (1997). Modulation of the firing activity of noradrenergic neurones in the rat locus coeruleus by the 5-hydroxytryptamine system. *Br. J. Pharmacol.,* **120,** 865–875.

LÉGER, L. & DESCARRIES, L. (1978). Serotonin nerve terminals in the locus coeruleus of the adult rat: An autoradiographic study. *Brain Res.,* **145,** 1 – 13.

LOIZOU, L.A. (1969). Projections of the nucleus locus coeruleus in the albino rat. *Brain Res.,* **15,** 563 – 569.

MONGEAU, R., WEISS, M., DE MONTIGNY, C. & BLIER, P. (1998). Milnacipran. Effect of acute, short-term and long-term administration on rat locus coeruleus noradrenergic and dorsal raphe serotonergic neurons. *Neuropharmacology,* **37,** 905 – 918.

PIÑEYRO, G., BLIER, P., DENNIS, T. & DE MONTIGNY, C. (1994). Desensitization of the neuronal 5-HT carrier following its long-term blockade. *J. Neurosci.,* **14,** 3036 – 3047.

QUINAUX, N., SCUVÉE-MOREAU, J. & DRESSE, A. (1982). Inhibition of in vitro and ex vivo uptake of noradrenaline and 5-hydroxytryptamine by five antidepressants; correlation with reduction of spontaneous firing rate of central monoaminergic neurones. *Naunyn-Schmiedeberg's Arch. Pharmacol.,* **319,** 66 – 70.

ROMERO, L., BEL, N., ARTIGAS, F., DE MONTIGNY, C. & BLIER, P. (1996). Effect of pindolol on the function of pre- and postsynaptic 5-HT_{1A} receptors: In vivo microdialysis and electrophysiological studies in the rat brain. *Neuropsychopharmacology,* **15,** 349 – 360.

VAN VILET I.M., DEN BOER, J.A., WESTENBERG, H.G. & SLAAP, B.R. (1996). A double-blind comparative study of brofaromine and fluvoxamine in outpatients with panic disorder. *J. Clin. Psychopharmacol.,* **16,** 299 – 306.

VERTES, R.P. & KOCSIS, B. (1994). Projections of the dorsal raphe nucleus to brainstem: PHA-L analysis in the rat. *J. Comp. Neurol.,* **340,** 11 – 26.

(Received August 10, 1998
Revised October 12, 1998
Accepted November 6, 1998)

British Journal of Pharmacology (1999) 126, 572–574
http://www.stockton-press.co.uk/bjp

SPECIAL REPORT

Attenuation of haloperidol-induced catalepsy by a 5-HT_{2C} receptor antagonist

*,[1]C. Reavill, [1]A. Kettle, [1]V. Holland, [1]G. Riley & [1]T. P. Blackburn

[1]Department of Neuroscience Research, SmithKline Beecham Pharmaceuticals, New Frontiers Science Park, Third Avenue, Harlow, Essex CM19 5AW, England

Atypical neuroleptics produce fewer extrapyramidal side-effects (EPS) than typical neuroleptics. The pharmacological profile of atypical neuroleptics is that they have equivalent or higher antagonist affinity for 5-HT_2 than for dopamine D_2 receptors. Our aim was to identify which 5-HT_2 receptor contributed to the atypical profile. Catalepsy was defined as rats remaining immobile over a horizontal metal bar for at least 30 s, 90 min after dosing. Radioligand binding assays were carried out with homogenates of human recombinant 5-HT_{2A}, 5-HT_{2B} and 5-HT_{2C} receptors expressed in Human Embryo Kidney (HEK293) cells. Haloperidol (1.13 mg kg^{-1} i.p.) induced catalepsy in all experiments. The selective 5-$HT_{2C/2B}$ receptor antagonist, SB-228357 (0.32–10 mg kg^{-1} p.o.) significantly reversed haloperidol-induced catalepsy whereas the 5-HT_{2A} and 5-HT_{2B} receptor antagonists, MDL-100907 (0.003–0.1 mg kg^{-1} p.o.) and SB-215505 (0.1–3.2 mg kg^{-1} p.o.) respectively did not reverse haloperidol-induced catalepsy. The data suggest a role for 5-HT_{2C} receptors in the anticataleptic action of SB-228357.

Keywords: $5HT_{2C}$ and Dopamine D_2 receptor antagonists; catalepsy

Abbreviations: D_2, dopamine 2; 5-HT_2, serotonin 2; EPS, extrapyramidal side-effects; HEK, human embryo kidney; IC_{50} inhibitor constant; K_D, dissociation equilibrium constant; K_i, inhibitor constant; pK_i, negative logarithm of inhibitor constant

Introduction Clozapine and the new generation of 'atypical' neuroleptics such as olanzapine are less liable than typical neuroleptics to cause extrapyramidal side-effects (EPS) when used to treat schizophrenia (Meltzer, 1996). As well as being dopamine D_2 receptor antagonists, the atypical neuroleptics are high affinity antagonists at $5HT_2$ receptors. This property may be responsible for their atypical profile (Meltzer *et al.*, 1989). Therefore, we have investigated whether 5-$HT_{2A/2B/2C}$ receptor subtypes modulate haloperidol-induced catalepsy.

Methods Male Sprague Dawley rats (200–250 g; Charles River) were housed in groups of six under a 12 h light dark cycle (lights on 0700 h) with free access to food and water. To test for catalepsy, rats were positioned so that their hindquarters were on the bench and their forelimbs rested on a 1 cm diameter horizontal bar, 10 cm above the bench. The length of time the rats maintained this position was recorded by stopwatch to a maximum of 120 s. This procedure occurred 30, 60 and 90 min after drug administration. Rats were judged to be cataleptic, and assigned a score of '1' if they maintained this position for 30 s or more; otherwise, they were assigned a score of '0'. As the raw data were derived from a non-linear quantal scoring scheme, a logistic regression analysis in SAS-RA© (SAS Institute Inc.) was used to analyse the data at the 90 min time point. MDL-100907 (R-(+)-α-(2,3-dimethoxyphenyl)-1-[2-(4-fluorophenyl) ethyl]-4-piperidinemethanol) (0.003–0.1 mg kg^{-1}), SB-215505 (6-chloro-5-methyl-1-(5-quinolylcarbamoyl) indoline) (0.1–3.2 mg kg^{-1}) and SB-228357 (1-5[-fluoro-3-(3-pyridyl)phenyl-carbamoyl]-5-methoxy-6-trifluoromethylindoline) (0.32–10 mg kg^{-1}) were ground in one drop of BRIJ-35 and diluted in 1% methylcellulose and administered at 2 ml kg^{-1} p.o.. Haloperidol was dissolved with an equal weight of tartaric acid and injected at 1 ml kg^{-1} i.p. immediately after the $5HT_2$ receptor antagonists. In all experiments, each treatment group consisted of six rats and the assessor was blind to the treatments.

Radioligand binding assays were carried out with homogenates of human recombinant 5-HT_{2A}, 5-HT_{2B} and 5-HT_{2C} receptors expressed in Human Embryo Kidney (HEK293) cells (Kennett *et al.*, 1997). Washed membranes were incubated with ten concentrations (1×10^{-11} M – 1×10^{-5} M) of test compounds and 0.5 nM [^{3}H]-ketanserin (5-HT_{2A}), 8 nM [^{3}H]-5-HT (5-HT_{2B}) or 0.6 nM [^{3}H]-mesulergine (5-HT_{2C}) for 30–45 min at 37°C in a pH 7.4 50 mM tris buffer. K_i (dissociation equilibrium constant, mol l^{-1} of the drug) values were calculated from the IC_{50} (Cheng & Prusoff, 1973) using the K_D: 5-HT_{2A} 0.7 nM, 5-HT_{2B} 11.0 nM and 5-HT_{2C} 0.58 nM. pK_i values were calculated as the negative logarithm of the molar K_i.

Results Haloperidol produced a significant cataleptic response in the range 0.38–3.76 mg kg^{-1} (Figure 1, top panel). Maximal effect (6/6 cataleptic rats) occurred at a dose of 1.13 mg kg^{-1} ($P<0.01$) and this dose was used in subsequent experiments for challenge with the 5-HT_2 receptor antagonists. SB-228357 significantly attenuated haloperidol-induced catalepsy at 0.32–10 mg kg^{-1}. At 10 mg kg^{-1} catalepsy was only seen in one of the six rats ($P<0.01$; Figure 1 bottom panel). Neither MDL-100907 nor SB-215505 reduced haloperidol-induced catalepsy ($P>0.05$ in each case; Figure 2).

In the radioligand binding studies (Table 1), SB-228357 had a high affinity for the 5-HT_{2C} receptor with 100 and 10 fold selectivity over the 5-HT_{2A} and 5-HT_{2B} receptors respectively. MDL-100907 was at least 700 and 16 fold selective for the 5-HT_{2A} receptor over the 5-HT_{2B} and 5-HT_{2C} receptor respectively. SB-215505 was 30 fold selective for the 5-HT_{2B}

*Author for correspondence.

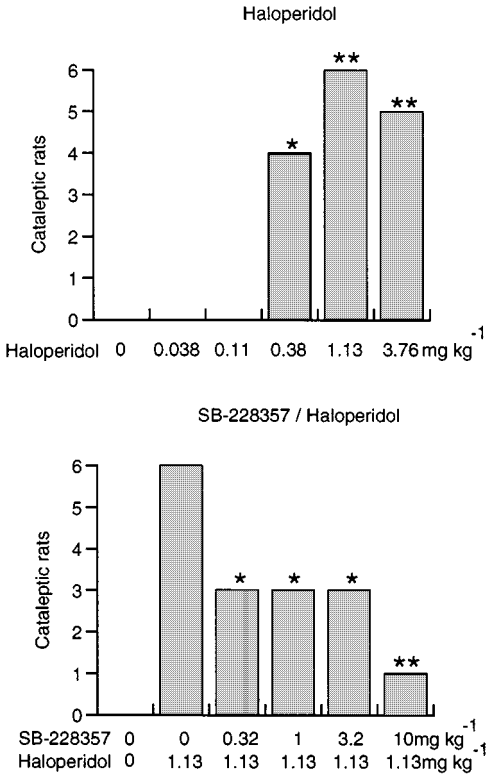

Figure 1 Each bar shows the number of cataleptic rats, 90 min after administration of haloperidol (top) and after pretreatment with SB-228357 (bottom). Significant haloperidol-induced catalepsy (top), or significant antagonism of the haloperidol effect (bottom) denoted by * = $P<0.05$; ** = $P<0.01$.

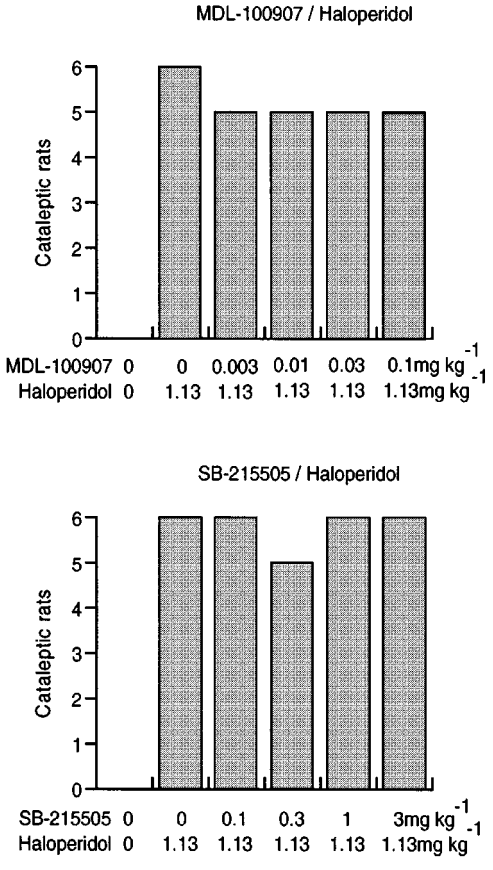

Figure 2 Each bar shows the number of cataleptic rats 90 min after administration of haloperidol and pretreatment with MDL-100907 and SB-215505.

over the 5-HT_{2A} receptor, and only marginally selective over the 5-HT_{2C} receptor. Ritanserin had a high affinity for all three receptors (Table 1).

Discussion Serotoninergic mechanisms are known to influence neuroleptic-induced catalepsy (Balsara *et al*., 1979), and 5-HT_2 receptor antagonism has been suggested to confer a favourable side-effect profile to neuroleptics (Meltzer *et al*., 1989). There is clinical evidence to support this as the mixed 5-$HT_{2A/2C}$ receptor antagonist, mianserin has been shown to reduce neuroleptic-induced akathisia (Poyurovsky & Weizman, 1997).

Other workers have attempted to discover if 5-HT_2 receptor antagonists modulate catalepsy. Kalkman *et al*. (1998) used SB-200646 and failed to show attenuation of loxepine-induced catalepsy. However, SB-200646 has only moderate affinity ($pK_i = 6.9$) and selectivity for the 5-HT_{2C} receptor (Kennett *et al*., 1994). Bligh-Glover *et al*. (1995) showed that ritanserin attenuated the catalepsy induced by low doses (0.25–0.375 mg kg^{-1}) of haloperidol but not high doses (0.75 mg kg^{-1}). However while ritanserin had a high affinity for 5-HT_2 receptors (Table 1) it is a non-selective compound. The recent discovery of high affinity and more selective 5-HT_2 receptor antagonists has enabled further investigation of the role of these receptors in catalepsy.

Further evidence has recently been provided that 5-HT_{2C} receptor antagonism may produce a favourable outcome in states of motor disturbance. Thus, oro-facial dyskinesias elicited by stimulation of subthalamic 5-HT_{2C} receptors are blocked by the 5-HT_{2C} receptor antagonist, SDZ SER 082 (Eberle-Wang *et al*., 1996), and injection of the 5-HT_{2C} receptor antagonist, SB-206553 (5-methyl-1-(3-pyridylcarbamoyl)-2,3-dihydropyrrolo[2,3-f]indole), into the substantia nigra zona reticulata produces an antiparkinsonian effect in the rat (Fox *et al*., 1998). Furthermore, 60% of striatal 5-HT-mediated phosphoinositide hydrolysis is accounted for by 5-HT_{2C} receptors despite there being 3 fold fewer striatal 5-HT_{2C} than 5-HT_{2A} receptors (Wolf & Schutz, 1997).

MDL-100907, has been reported to have 100 fold selectivity for the 5HT_{2A} over the 5-HT_{2C} receptor (5-HT_{2A} $K_i = 0.85$ nM; 5-HT_{2C} $K_i = 87$ nM, Kehne *et al*., 1996), although our data (Table 1) show this compound to have less than 100 fold selectivity. MDL-100907 is in clinical development for schizophrenia, following an 'atypical' profile in preclinical tests (Kehne *et al*., 1996). In these experiments, antagonism of apomorphine-induced stereotypy was used as a method of predicting EPS liability. In our study, MDL-100907 failed to attenuate haloperidol-induced catalepsy at doses that were active in the rat 5-HTP head twitch model (Kehne *et al*., 1996). Kalkman *et al*. (1998) have shown that MDL-100151 (R-(±)-α-(2,3- dimethoxyphenyl)-1- [2 -(4-fluorophenyl)ethyl]-4-piperi-

Table 1 Receptor radioligand binding profile of 5-HT_2 receptor antagonists [$pK_i \pm$s.e.mean (n)]

	pK_i *5-HT_{2A}*	pK_i *5-HT_{2B}*	pK_i *5-HT_{2C}*
MDL-100907	8.86±0.08 (4)	6.02±0.03 (4)	7.66±0.09 (3)
Ritanserin	9.42±0.05 (5)	9.25±0.06 (3)	9.65±0.07 (5)
SB-215505	6.77±0.23 (3)	8.3±0.05 (6)	7.66±0.09 (4)
SB-228357	6.97±0.06 (16)	8.14±0.08 (14)	9.14±0.07 (16)

dinemethanol), the racemate of MDL-100907, is cataleptogenic at a dose of 0.3 mg kg^{-1}. This could explain why MDL-100907 failed to attenuate catalepsy. In contrast, SB-228357 had a pronounced anticataleptic profile. This compound had a high affinity for the 5-HT_{2C} receptor and is 100 and 10 fold selective over the 5-HT_{2A} and 5-HT_{2B} receptor respectively (Table 1). This suggests that 5-HT_{2C} receptor antagonism, or possibly mixed 5-$HT_{2C/2B}$ receptor antagonism is the optimum profile for antagonising haloperidol-induced catalepsy. However, there was no evidence that SB-215505 blocked the cataleptic response. This compound has a high affinity for the 5-HT_{2B} receptor and is moderately selective over both 5-HT_{2A} and 5-HT_{2C} receptors (Table 1).

By deduction, our data suggest that 5-HT_{2C} receptor antagonism, and not 5-HT_{2A} or 5-HT_{2B} receptor antagonism, is likely to be the mechanism by which 'atypical' antipsychotic drugs lack EPS.

References

BALSARA, J.J., JADHAV, J.H. & CHANDOKAR, A.G. (1979). Effect of drugs influencing central serotonergic mechanisms on haloperidol-induced catalepsy. *Psychopharmacol.,* **62,** 67 – 69.

BLIGH-GLOVER, W., JASKIW, G.E., VRTUNSKI, B., UBOGY, D. & MELTZER, H.Y. (1995). 5-HT2 receptor antagonists can attenuate submaximal haloperidol-induced catalepsy in rats. *Schiz. Res.,* **15,** 153 – 154.

CHENG, Y.C. & PRUSSOF, W.H. (1973). Relationship between inhibition constant (K_i) and the concentration of inhibitor which causes 50% inhibition (IC_{50}) of an enzymatic reaction. *Biochem. Pharmacol.,* **92,** 881 – 894.

EBERLE-WANG, K., LUCKI, I. & CHESSELET, M.-F. (1996). A role for the subthalamic nucleus in 5-HT_{2C}-induced oral dyskinesia. *Neuroscience,* **72,** 117 – 128.

FOX, S.H., MOSER, B. & BROTCHIE, J.M. (1998). Behavioural effects of 5-HT2C receptor antagonism in the substantia nigra zona reticulata of the 6-hydroxydopamine-lesioned rat model of Parkinson's Disease. *Exp. Neurol.,* **151,** 35 – 49.

KALKMAN, H.O., NEUMANN, V., NOZULAK, J. & TRICKLEBANK, M.D. (1998). Cataleptogenic effect of subtype selective 5-HT receptor antagonists in the rat. *Eur. J. Pharmacol.,* **343,** 201 – 207.

KEHNE, J.H., BARON, B.M., CARR, A.A., CHANEY, S.F., ELANDS, J., FELDMAN, D.J., FRANK, R.A., VAN GIERSBERGEN, P.L.M., MCCLOSKEY, T.C., JOHNSON, M.P., MCCARTY, D.R., POIROT, M., SENYAH, Y., SIEGEL, B.W. & WIDMAIER, C. (1996). Preclinical characterization of the potential of the putative atypical antipsychotic MDL 100,907 as a potent 5-HT_{2A} antagonist with a favorable CNS safety profile. *J. Pharmacol. Exp. Ther.,* **277,** 968 – 981.

KENNETT, G.A., WOOD, M.D., BRIGHT, F., TRAIL, B., RILEY, G., HOLLAND, V., AVENELL, K.Y., STEAN, T., UPTON, N., BROMIDGE, S., FORBES, I.T., BROWN, A.M., MIDDLEMISS, D.N. & BLACKBURN, T.P. (1997). SB 242084, a selective and brain penetrant 5-HT_{2C} receptor antagonist. *Neuropharmacology,* **36,** 609 – 620.

KENNETT, G.A., WOOD, M.D., GLEN, A., GREWAL, S., FORBES, I., GADRE, A. & BLACKBURN, T.P. (1994). *In vivo* properties of SB 200646A, a 5-$HT_{2C/2B}$ receptor antagonist. *Br. J. Pharmacol.,* **111,** 797 – 802.

MELTZER, H.Y. (1996). Pre-clinical pharmacology of atypical antipsychotic drugs: a selective review. *Br. J. Psychiat.,* **168,** (Suppl. 29), 23 – 31.

MELTZER, H.Y., MATSUBARA, S. & LEE, M.A. (1989). Classification of typical and atypical antipsychotic drugs on the basis of dopamine D-1, D-2 and serotonin$_2$ pKi values. *J. Pharmacol. Exp. Ther.,* **251,** 238 – 246.

POYUROVSKY, M. & WEIZMAN, A. (1997). Serotonergic agents in the treatment of acute neuroleptic-induced akathisia: open-label study of buspirone and mianserin. *Int. Clin. Psychopharmacol.,* **12,** 263 – 268.

WOLF, W.A. & SCHUTZ, L.J. (1997). The serotonin 5-HT_{2C} receptor is a prominent serotonin receptor in basal ganglia: evidence from functional studies on serotonin-mediated phosphinositide hydrolysis. *J. Neurochem.,* **69,** 1449 – 1458.

(Received August 14, 1998
Revised November 3, 1998
Accepted November 9, 1998)

British Journal of Pharmacology (1999) 126, 575–580
http://www.stockton-press.co.uk/bjp

Rate-dependent blockade of a potassium current in human atrium by the antihistamine loratadine

*,[1]William J. Crumb Jr.

[1]Department of Pediatrics, Division of Cardiology, Tulane University School of Medicine,1430 Tulane Avenue, New Orleans, Louisiana 70112-2699, U.S.A.

1 The antihistamine loratadine is widely prescribed for the treatment of symptoms associated with allergies. Although generally believed to be free of adverse cardiac effects, there are a number of recent reports suggesting that loratadine use may be associated with arrhythmias, in particular atrial arrhythmias.

2 Nothing is known regarding the potassium channel blocking properties of loratadine in human cardiac cells. Using the whole-cell patch clamp technique, the effects of loratadine on the transient outward K current (I_{to}), sustained current (I_{sus}), and current measured at -100 mV (I_{K1} and I_{ns}), the major inward and outward potassium currents present in human atrial myocytes, were examined in order to provide a possible molecular mechanism for the observed atrial arrhythmias reported with loratadine use.

3 Loratadine rate-dependently inhibited I_{to} at therapeutic concentrations with 10 nM loratadine reducing I_{to} amplitude at a pacing rate of 2 Hz by $34.9 \pm 6.0\%$. In contrast, loratadine had no effect on either I_{sus} or current measured at -100 mV.

4 These results may provide a possible mechanism for the incidences of supraventricular arrhythmias reported with the use of loratadine.

Keywords: Antihistamine loratadine; human; potassium current; transient outward current; atria

Abbreviations: I_{K1}, inwardly rectifying potassium current; I_{ns}, non-selective cation current; I_{sus}, sustained current; I_{to}, transient outward potassium current

Introduction

Antagonists to H_1-histamine receptors are commonly prescribed for the treatment of allergies, urticarial diseases, and symptomatic relief of upper respiratory infections. Recently, members of this family of compounds such as terfenadine and astemizole have been associated with rare but potentially life-threatening adverse cardiac events (Craft, 1985; Davies *et al*., 1989; Bishop & Gaudry, 1989; Monahan *et al*., 1990; Lindquist & Edwards, 1997). For instance, terfenadine use has been associated with serious ventricular arrhythmias such as torsade de pointe and sudden death (Davies *et al*., 1989; Monahan *et al*., 1990). Terfenadine and astemizole have subsequently been shown to block one or more cardiac potassium channels and it is believed this action may underlie the observed arrhythmias (Woosley *et al*., 1993; Salata *et al*., 1995; Rampe *et al*., 1993; Crumb *et al*., 1995c).

In contrast to terfenadine and astemizole, the antihistamine loratadine is generally believed to be free of adverse cardiac effects. However, there are a number of recent reports suggesting that loratadine use may be associatd with arrhythmias, in particular atrial arrhythmias (Lindquist & Edwards, 1997; Aust Adv Drug React Bull, 1996 ; Haria *et al*., 1994). In human atrium, the transient outward K current (I_{to}), sustained current (I_{sus}), and current measured at -100 mV (which consists of the inwardly rectifying K current, I_{K1}, and the non-selective cation current, I_{ns}), represent the major inward and outward K currents and thus play an important role in the resting potential, shape and duration of the human atrial action potential. Blockade of any of these potassium currents may be potentially arrhythmogenic. To date, nothing is known regarding the potassium channel blocking properties of loratadine in human cardiac cells. Therefore, the present study was undertaken to characterize the effects of loratadine on I_{to}, I_{sus}, and current measured at -100 mV in isolated human atrial myocytes in order to provide a possible molecular mechanism for the observed arrhythmias reported with loratadine use.

Methods

Human tissue was obtained, in accordance with Tulane University School of Medicine Institutional guidelines. Myocytes were isolated from specimens of human right atrial appendage obtained during surgery from hearts of five patients (ages 40–67 years) undergoing cardiopulmonary bypass. All atrial specimens were described as grossly normal at the time of excision and all patients had normal P waves on electrocardiography. Some patients had received cardioactive drugs including calcium channel blockers and digitalis. The cell isolation procedure has been described in detail in Crumb *et al*. (1995a).

Isolated human atrial myocytes were superfused with an 'external' solution that consisted of (in mmol l^{-1}): 137 NaCl, 4 KCl, 1 $MgCl_2$, 1.8 $CaCl_2$, 11 Glucose, 10 HEPES; adjusted to a pH of 7.4 with NaOH. Glass pipettes were filled with an 'internal' solution that consisted of (in mmol l^{-1}): 120 K-aspartate, 20 KCl, 4 Na-ATP, 5 EGTA, 5 HEPES; adjusted to a pH of 7.2 with KOH. Loratadine was kindly provided by Almirall Prodesfarma (Barcelona, Spain) and dissolved in 100% DMSO to make concentrated stock solutions (1 mM).

*Author for correspondence.
E-mail: wcrumb@tmcpop.tmc. tulane.edu

Loratadine was added to the bath solution from this concentrated stock (final DMSO concentration less than 0.01%) or from another more diluted stock solution (100 μM) made in distilled, deionized water.

Experiments were performed in the presence of 200 μM Cd^{2+} to block the L-type Ca current and at a holding potential of -60 mV to inactivate the sodium current. All experiments were performed at room temperature (22–23°C) so that peak I_{to} could be accurately distinguished from the capacitive current. The transient outward current was measured by subtracting the amplitude of the current measured at the end of the depolarizing voltage pulse (sustained current) from peak current amplitude. The sustained current was measured at the end of a depolarizing pulse to $+60$ mV.

Acceptable atrial myocytes were rod-shaped and lacked any visible blebs on the surface. Currents were measured using the whole-cell variant of the patch clamp method (Hamill *et al.*, 1981). Currents were digitized at 3–5 kHz and filtered at 1 kHz. Pipette tip resistance were approximately 1.0–2.0 MΩ when the pipettes were filled with the internal solution. Analogue capacity compensation and 40–60% series resistance (R_s) compensation was used in all experiments to yield voltage drops across uncompensated R_s of less than 3 mV. Paired and unpaired Student's *t*-test was used for statistical analysis. Data are presented as mean ± s.e.mean.

For exponential fits of data (e.g., fits of time course of current decay and I_{to} recovery), a single exponential fit was accepted as the fit of choice whenever the following criteria were met: (a) the amplitude parameters obtained from the least squares fit were all of the same sign and (b) when a negative value for the AIC (asymptotic information criteria) statistic was obtained when comparing a one versus a two exponential fit (Akaike, 1974; Horn, 1987).

Results

Figure 1 shows the effects of loratadine on K^+ currents recorded from an isolated human atrial myocyte. In the absence of drug, application of voltage pulses from -100 mV to $+60$ mV elicited a family of currents characteristic of human atrial myocytes. At potentials negative to -70 mV, an inward current, which reflects the combination of the inwardly rectifying potassium current (I_{K1}) and the inward component of a non-selective cation current (Crumb *et al.*, 1995b), was elicited. At more depolarized potentials, a current was elicited which decays rapidly to a steady-state (see Figure 1, control). The decaying current represents the transient outward potassium current (I_{to}) while the current remaining after the decay of I_{to}, commonly referred to as the sustained current (I_{sus}) is distinct and consists of two currents, a potassium current designed Kv 1.5 (Wang *et al.*, 1993) and the non-selective cation current (Crumb *et al.*, 1995b). A reduction in the amplitude of any of these currents can alter the shape and duration of the cardiac action potential and thus may be potentially arrhythmogenic.

While pacing slowly (0.1 Hz), addition of 100 nM loratadine to the solution bathing the cell, a concentration associated with arrhythmias in humans (Hilbert *et al.*, 1987), produced no noticeable change in the amplitude of either inward or outward currents. This is clearly illustrated by the lack of a definable loratadine-sensitive current (Figure 1). Similar results were observed in four additional cells.

Since I_{to} is sensitive to pacing rate and the actions of many ion channel blocking drugs are rate-dependent, it is possible that the effects of loratadine on I_{to} may be frequency-dependent. To test this hypothesis, the effects of loratadine on the timecourse of recovery of I_{to} were examined using a 2-pulse protocol consisting of a 500 ms conditioning pulse to $+60$ mV followed by a test pulse to $+60$ mV after a variable recovery period at the holding potential (-60 mV) (Figure 2). As illustrated in Figure 2, the timecourse of I_{to} recovery was significantly slower in the presence of loratadine (100 nM) compared with control and was best fit with a single exponential relationship. The time constant of recovery (τ) obtained in the presence of drug was 107.7 ± 9.3 ms, significantly slower than in the absence of drug (63.5 ± 5.0 ms) ($n = 6$, $P < 0.05$). These results

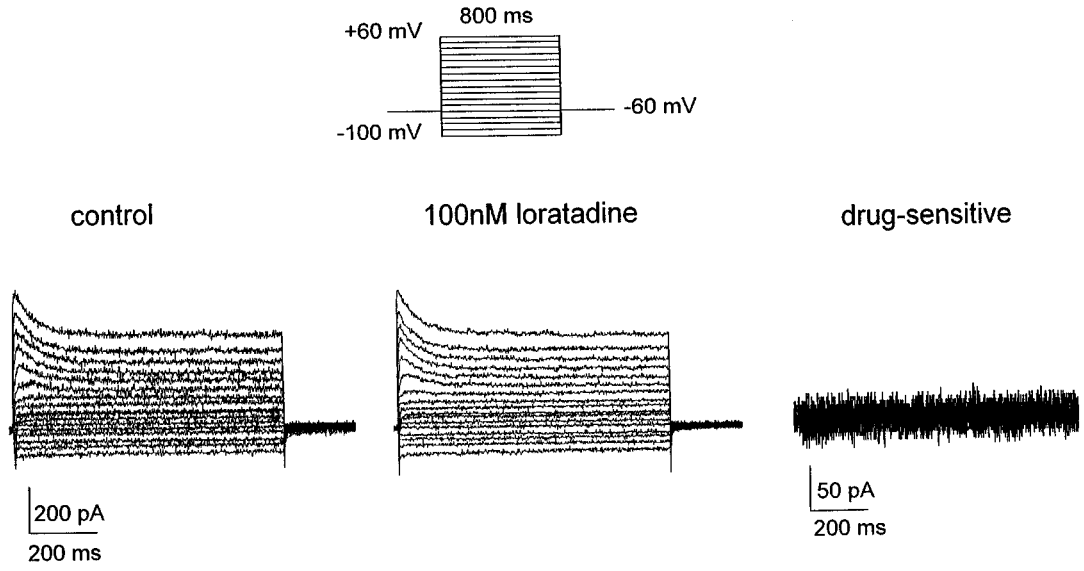

Figure 1 Effects of 100 nM loratadine on potassium currents recorded from an isolated human atrial myocyte. A family of currents were elicited by the protocol shown before and after addition of 100 nM loratadine to the bath solution. Currents were elicited at a pacing rate of 0.1 Hz. The drug-sensitive currents represent control-loratadine currents. Note the lack of effect on current amplitude.

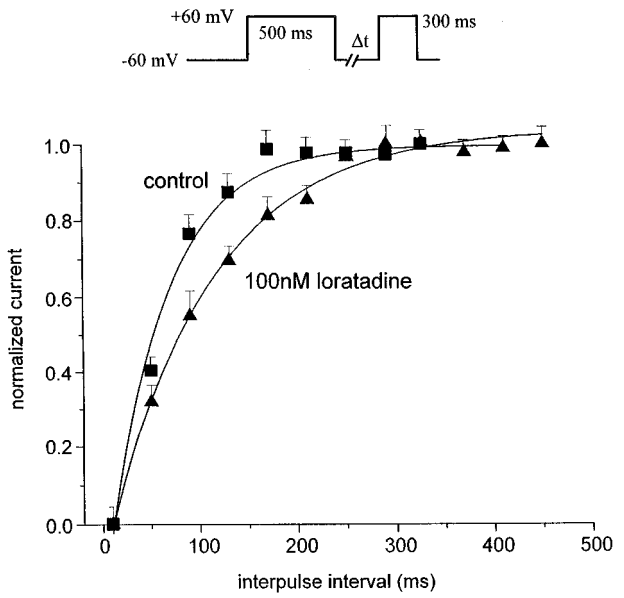

Figure 2 Recovery kinetics of I_{to} before and after 100 nM loratadine. A plot of the I_{to} recovery kinetics obtained from a human atrial myocyte before and after exposure to 100 nM loratadine. Currents were elicited by the indicated protocol. Data points were fit with a single exponential function of the form -0.85 exp $(-\times/104.1$ ms$)+0.998$ after loratadine and -0.92 exp $(-\times/59.0$ ms$)+1.00$ before loratadine.

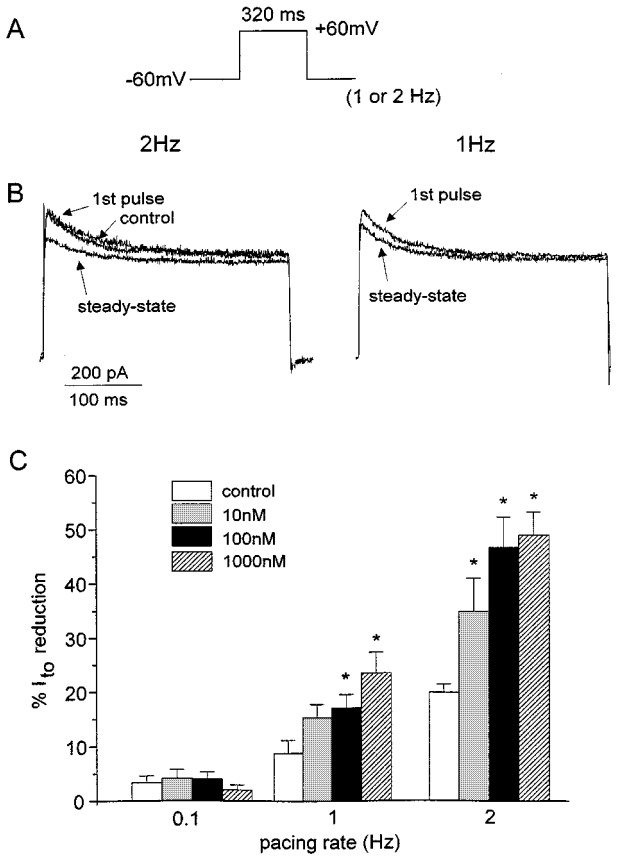

Figure 3 Effects of pacing rate in the presence of 100 nM loratadine on I_{to} recorded from an isolated human atrial myocyte. (A) Pulse protocol. (B) Reduction in amplitude of I_{to} in a cell paced at 1 and 2 Hz. Illustrated are the first and steady-state currents of a 30 pulse rate train. Currents were elicited by the pulse protocol in panel A. (C) Rate- and concentration-dependent reduction of I_{to} by loratadine. % reduction of I_{to} at a given pacing rate was calculated as the reduction in current amplitude of the last pulse in the rate train (30 pulses) relative to the first pulse in the rate train. Symbols are mean$\pm$s.e. ($n=5-16$). Asterisks indicate value is significantly different from control.

suggest that at higher pacing rates a reduction in I_{to} amplitude might be observed in the presence of loratadine.

Figure 3 illustrates the effects of pacing rate on loratadine inhibition of I_{to}. To more accurately characterize the effects of loratadine on I_{to}, the current measured at the end of the voltage pulse was subtracted from the peak current (Crumb *et al.*, 1995b). After a 20 s interval at the holding potential in the presence of 100 nM loratadine, application of a depolarizing voltage pulse elicited a current which was virtually identical in amplitude to that observed in the absence of drug indicating a lack of tonic block (Figure 3B). In 100 nM loratadine, tonic reduction of I_{to} was $4.1\pm1.3\%$, I_{sus} was 6.6 ± 2.1, and the current measured at -100 mV was $6.6\pm4.2\%$ ($n=5$). At pacing rates which simulate either a resting heart rate (1 Hz) or a heart rate achieved during moderate exercise (2 Hz), 100 nM loratadine caused a pronounced reduction in the amplitude of I_{to} (Figure 3B and C). Interestingly, the rate-dependent effects of loratadine were also observed at therapeutic concentrations (i.e. 10 nM) (Figure 3C). For instance, at a frequency of 1 Hz, 10 nM loratadine produced a $15.3\pm2.4\%$ ($n=5$) reduction in I_{to} amplitude, not significantly different from control ($8.8\pm2.3\%$, $n=16$) (Figure 3C). At higher pacing rates, (2 Hz), 10 nM loratadine markedly reduced I_{to} amplitude by $34.9\pm6.0\%$ ($n=5$), significantly greater than that observed in the absence of loratadine ($19.9\pm1.5\%$, $n=16$) ($P<0.05$) (Figure 3C). In contrast, loratadine produced only a negligibly greater blockade of I_{sus} when compared to control even at the highest pacing rate tested (2 Hz) ($1.1\pm0.7\%$ greater than control with 10 nM, $3.6\pm2.6\%$ with 100 nM, $6.9\pm2.9\%$ with 1 μM, $n=5-6$). Even at a concentration of 10 μM, loratadine produced only a small reduction in the amplitude of the current measured at -100 mV when paced at 2 Hz ($8.3\pm3.7\%$, $n=5$).

As suggested in Figure 3, the kinetics of I_{to} decay appeared to be faster in the presence of loratadine than in its absence. The kinetics of I_{to} decay were measured once a steady-state level of current reduction was achieved at either 1 or 2 Hz in the presence of loratadine and compared to that measured in the absence of loratadine (control) at the same pacing rate. The decay of I_{to} could be well fit with a single exponential function with values ranging between 50 and 80 ms in the absence of drug. Fits obtained from cells before and after exposure to loratadine are shown in Figure 4. As indicated, in the presence of loratadine I_{to} current decay tended to be faster, although this tendency did not reach significance at any concentration or pacing rate ($P=0.06$).

The combination of a reduction in I_{to} amplitude and a tendency to 'speed-up' I_{to} decay kinetics suggests that in the presence of loratadine the amount of current exiting the cell through transient outward channels during depolarizations at pacing rates of 1 Hz or greater will be reduced. This hypothesis was tested by calculating the I_{to} current integral in the presence and absence of loratadine at pacing rates of 1 and 2 Hz. As illustrated in Figure 5, in the presence of 100 nM loratadine the total amount of current leaving the cell during a depolarizing pulse was dramatically and significantly reduced when compard to control (Figures 5A and B) ($P<0.05$). Interestingly, the ability of 10 nM loratadine to reduce total current exiting the cell was not significantly different from that observed for 100 nM (Figure 5D).

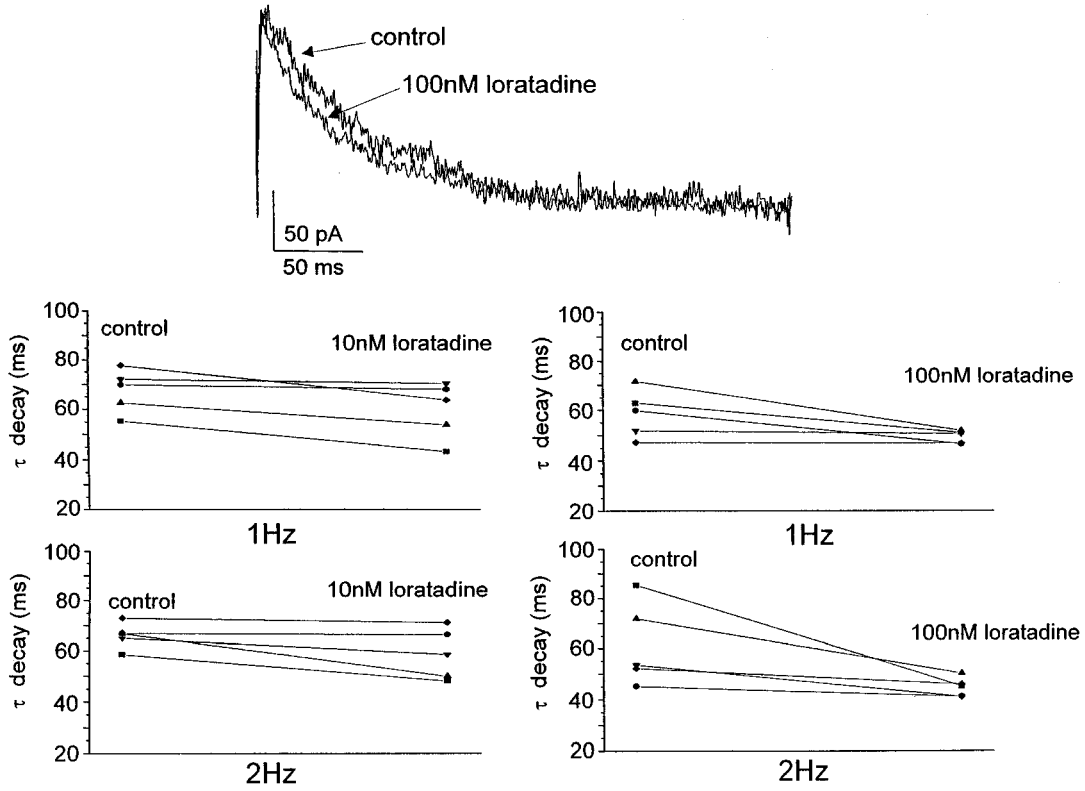

Figure 4 Effect of loratadine on I_{to} decay kinetics. Examples of current traces recorded in the absence and presence of 100 nM loratadine are shown at top of figure. Currents illustrated were recorded after current amplitude had reached a steady-state and were elicited by a series of 30 pulses (320 ms) to +60 mV from a holding potential of −60 mV (pacing rate = 2 Hz). For clarity, end of pulse current has been subtracted from peak current and currents have been superimposed. Plots of decay time constants measured from cells before and after exposure to either 10 or 100 nM loratadine are also shown. Currents were fit with a single exponential function.

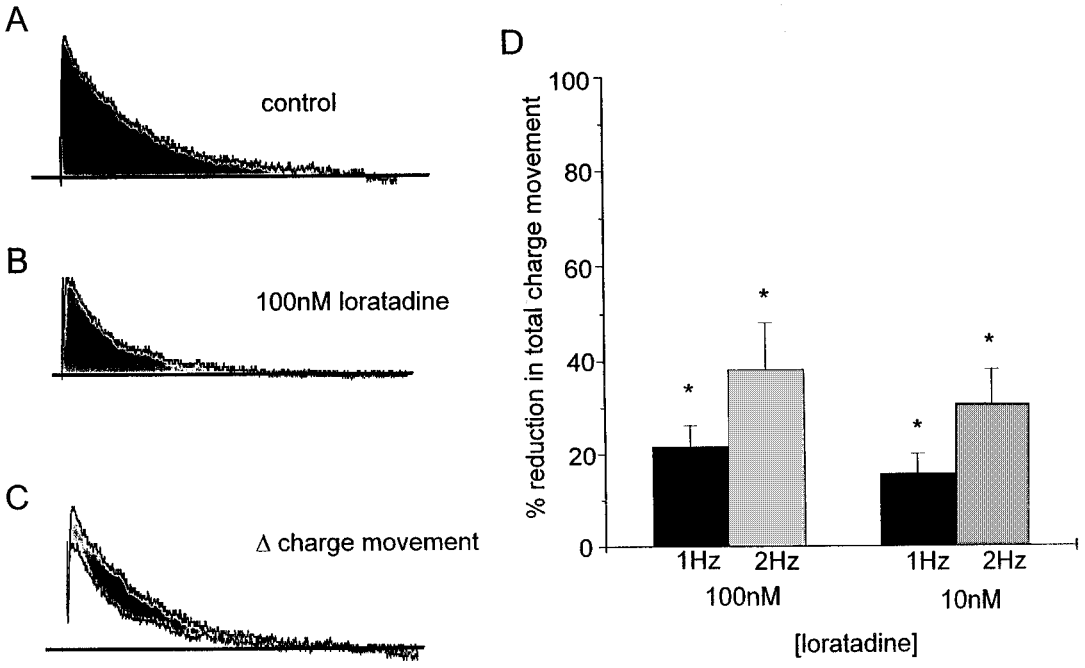

Figure 5 Effect of loratadine on I_{to} total charge movement in human atrial myocytes. (A) Example of the integrated current in the absence of drug (26 pA ms^{-1}). Steady-state current has been subtracted from peak current. Line indicates zero current. Currents illustrated were recorded after current amplitude had reached a steady-state and were elicited by a series of 30 pulses (320 ms) to +60 mV from a holding potential of −60 mV (pacing rate = 2 Hz). (B) Current recorded from same cell after addition of 100 nM loratadine (15.5 pA ms^{-1}). (C) Change in total charge exiting through I_{to} channels induced by 100 nM loratadine. Shaded area indicates the loratadine-sensitive integrated current. (D) Plot of the % reduction in total charge movement measured in cells before and after exposure to loratadine at the indicated pacing rates. All values were significantly different from control, indicated by asterisks. Data are mean ± s.e.mean ($n = 5$).

Discussion

The major finding of this study is that loratadine blocks I_{to} recorded from human atrial myocytes and significantly reduces the amount of I_{to} current exiting the myocyte in a rate-dependent manner at concentrations achieved therapeutically and during an overdose (Hilbert *et al*., 1978). At therapeutic concentrations (10 nM), loratadine significantly blocked I_{to} at pacing rates which mimic elevated heart rates (2 Hz) while at concentrations which may be achieved during an overdose (100 nM) (Hilbert *et al*., 1987), I_{to} was blocked at pacing rates which simulate both normal (1 Hz) and elevated heart rates (Figure 3). These results provide a possible molecular mechanism for the reported supraventricular arrhythmias associated with the use of loratadine. The reduction caused by loratadine in the total amount of I_{to} current exiting the myocyte (Figure 5) may be arrhythmogenic since I_{to} is an important repolarizing current in human atrium and has been shown to modulate atrial action potential shape and duration (Shibata *et al*., 1989).

The block of I_{to} by loratadine (10–100 nM) described in the present study is in marked contrast to a previous report in which loratadine at concentrations up to 1 μM exhibited no blocking actions on I_{to} recorded from rat ventricle (Ducic *et al*., 1997). These differences may reflect species differences in the molecular nature of I_{to} or in the fact that the previous report did not examine the effects of rate on the blocking action of loratadine. In fact, in the present study when cells were paced slowly (0.1 Hz), loratadine even at concentrations up to 1 μM produced only a very modest reduction in the amplitude of I_{to} similar to previous reports (Figure 3).

Use of non-sedating antihistamines has been associated with cardiac arrhythmias (Craft, 1985; Davies *et al*., 1989; Bishop & Gaudry, 1989; Monahan *et al*., 1990; Lindquist & Edwards, 1997). Although the occurrence of such cardiotoxic side effects is rare, it is nonetheless important to recognize since these arrhythmias can be life threatening. The adverse cardiac effects associated with antihistamines are typified by terfenadine which has been associated with prolongation of the QT interval and torsade de pointes (Davies *et al*., 1989; Monahan *et al*., 1990; Lindquist & Edwards, 1997). Providing a possible mechanism for these arrhythmias, terfenadine has been shown to block several cardiac potassium channels including I_{to}, I_{sus} and the delayed rectifier (I_{Kr}) in human heart as well as in other species and expression systems (Woosley *et al*., 1993; Salata *et al*., 1995; Rampe *et al*., 1993; Crumb *et al*., 1995c). Block of I_{Kr} and/or I_{sus} by terfenadine is believed to be in part responsible for the reported incidences of QT prolongation and torsade de pointes.

There are several reports of loratadine associated adverse cardiac events in patients in particular atrial arrhythmias. Reports of palpitations and arrhythmias have been reported to the Australian ADR Advisory Committee (1996) and a number of reports of supraventricular arrhythmias have been reported to the United States Food and Drug Administration (Haria *et al*., 1994). Recently, an examination of adverse drug reaction (ADR) reports obtained from the World Health Organization ADR database indicates several hundred incidences of loratadine associated 'rate and rhythm disorders' and more than a dozen incidences of sudden cardiac death (Lindquist & Edwards, 1997). In addition to atrial arrhythmias, loratadine use has also been associated with ventricular arrhythmias. One case report associates loratadine use with QT prolongation and ventricular arrhythmias in a patient with a history of both atrial and ventricular arrhythmias (Good *et al*., 1994).

In summary, the present study describes the block of the potassium current I_{to} in human atrial myocytes by loratadine. This potassium channel blockade may provide a mechanism for the rare incidences of supraventricular arrhythmias reported with the use of this antihistamine. Although untested, it is intriguing to speculate that block of I_{to} in human ventricle may be similarly arrhythmogenic. The observation that a marked reduction in repolarizing current is observed with therapeutic concentrations of loratadine at rates mimicking elevated heart rates suggests that care should be taken in administering this antihistamine in patients with an existing tachyarrhythmia or under conditions where heart rate may be elevated (i.e. exercise or stress).

The author would like to thank Drs Nabil Munfakh, Herman A. Heck and Lynn H. Harrison Jr. of Louisiana State University Hospital for kindly providing atrial specimens.

References

AKAIKE, H. (1974). A new look at the statistical model identification. *IEEE Trans Automatic Control. AC.,* **19,** 716–723.

BISHOP, R.O. & GAUDRY, P.L. (1989). Prolonged Q-T interval following astemizole overdose. *Arch. Emerg. Med.,* **6,** 63–65.

CRAFT, T.M. (1985). Torsade de pointes after astemizole overdose. *Br. Med. J.,* **292,** 660.

CRUMB, W.J., PIGOTT, J.D. & CLARKSON, C.W. (1995a). Comparison of the transient outward current in young and adult human atrial myocytes. Evidence for developmental changes. *Am. J. Physiol.,* **268,** H1335–H1342.

CRUMB, W.J., PIGOTT, J.D. & CLARKSON, C.W. (1995b). Description of a nonselective cation current in human atrium. *Circ. Res.,* **77,** 950–956.

CRUMB, W.J., WIBLE, B., ARNOLD, D.J., PAYNE, J.P. & BROWN, A.M. (1995c). Blockade of multiple human cardiac potassium currents by the antihistamine terfenadine: Possible mechanism for terfenadine-associated cardiotoxicity. *Mol. Pharmacol.,* **47,** 181–190.

DAVIES, A.J., HARINDRA, V., MCEWAN, A. & GHOSE, R.R. (1989). Cardiotoxic effect with convulsions in terfenadine overdose. *Br. Med. J.,* **298,** 325.

DUCIC, I., KO, C.M., SHUBA, Y. & MORAD, M. (1997). Comparative effects of loratadine and terfenadine on cardiac K channels. *J. Cardiovasc. Pharmacol.,* **30,** 42–54.

GOOD, A.P., ROCKWOOD, R. & SCHAD, P. (1994). Loratadine and ventricular tachycardia. *Am. J. Cardiol.,* **74,** 207.

HAMILL, O.P., MARTY, A., NEHER, E., SAKMANN, B. & SIGWORTH, F.J. (1981). Improved patch-clamp techniques for high-resolution current recording from cells and cell-free membrane patches. *Pflugers Arch.,* **391,** 85–100.

HARIA, M., FITTON, A. & PETERS, D.H. (1994). Loratadine: a reappraisal of its pharmacological properties and therapeutic use in allergic disorders. *Drugs,* **48,** 617–637.

HILBERT, J., RADWANSKIE, E., WEGLEIN, R., LUC, V., PERENTESIS, G., SYMCHOWICZ, S. & ZAMOAGLIONE, N. (1987). Pharmacokinetics and dose proportionality of loratadine. *J. Clin. Pharmacol.,* **27,** 694–698.

HORN, R. (1987). Statistical methods for model discrimination. *Biophys. J.,* **51,** 255–263.

LINDQUIST, M. & EDWARDS, I.R. (1997). Risk of non-sedating antihistamines. *Lancet,* **349,** 1322.

MONAHAN, B.P., FERGUSON, C.L., KILLEAVY, E.S., LLOYD, B.K., TROY, J. & CANTILENA, L.R. (1990). Torsade de pointes occurring in association with terfenadine use. *JAMA,* **264,** 2788–2790.

POSSIBLE ARRHYTHMIAS DUE TO LORATADINE? More help please. (1996). *Aust. Adv. Drug React. Bull.,* **15,** 3.

RAMPE, D., WIBLE, B., BROWN, A.M. & DAGE, R.C. (1993). Effects of terfenadine and its metabolites on a delayed rectifier K channel cloned from human heart. *Mol. Pharmacol.,* **44,** 1240–1246.

SALATA, J.J., JURKIEWICZ, N.K., WALLACE, A.A., STUPIENSKI, R.F., GUINOSSO, P.J. & LYNCH, J.J. (1995). Cardiac electrophysiological actions of the histamine H1-antagonists astemizole and terfenadine compared with chlorpheniramine and pyrilamine. *Circ. Res.,* **76,** 110–119.

SHIBATA, E.F., DRURY, T., REFSUM, H., ALDRETE, V. & GILES, W. (1989). Contributions of a transient outward current to repolarization in human atrium. *Am. J. Physiol.,* **257,** H1773–H1781.

WANG, Z., FERMINI, B. & NATTEL, S. (1993). Sustained depolarization-induced outward current in human atrial myocytes: evidence for a novel delayed rectifier potassium current similar to Kv 1.5 cloned channel currents. *Circ. Res.,* **73,** 1061–1076.

WOOSLEY, R.L., CHEN, Y., FRIEMAN, J.P. & GILLIS, R.A. (1993). Mechanism of the cardiotoxic actions of terfenadine. *JAMA,* **268,** 1532–1536.

(Received August 4, 1998
Accepted October 6, 1998)

British Journal of Pharmacology (1999) 126, 581–584
http://www.stockton-press.co.uk/bjp

The effects of specific antibody fragments on the 'irreversible' neurotoxicity induced by Brown snake (*Pseudonaja*) venom

*,[1]R.G.A. Jones, [2]L. Lee & [1]J. Landon

[1]Department of Chemical Pathology, The Medical College of St. Bartholomew's Hospital, Charterhouse Square, London EC1M 6BQ and [2]Therapeutic Antibodies U.K. Ltd, The Medical College of St. Bartholomew's Hospital, Charterhouse Square, London EC1M 6BQ

1 Brown snake (*Pseudonaja*) venom has been reported to produce 'irreversible' post synaptic neurotoxicity (Harris & Maltin, 1981; Barnett *et al*., 1980).

2 A murine phrenic nerve/diaphragm preparation was used to study the neurotoxic effects of this venom and pre- and post-synaptic components were distinguished by varying the temperature and frequency of nerve stimulation. There were no myotoxic effects and the neurotoxicity proved irreversible by washing alone.

3 The effects of a new Fab based ovine antivenom have been investigated and proved able to produce a complete, rapid (<1 h) reversal of the neurotoxicity induced by Brown snake venom. A reversal was also possible when the antivenom addition was delayed for a further 60 min.

4 We believe that this is the first time such a reversal has been shown.

Keywords: Neurotoxicity; reversal; Brown snake *Pseudonaja*; antivenom; Fab; ovine; antibodies

Abbreviations: CSL $F(ab')_2$, CSL Brown Snake Antivenom

Introduction

Australia is home to some of the most poisonous snakes in the world (White & Pounder, 1984). Brown snakes (*Pseudonaja sp*.) account for most bites and fatalities (Sutherland, 1992; Jelinek & Breheny, 1990) and the clinical features of such envenoming include disseminated intravascular coagulation and, on occasion, generalized neurotoxicity (Judd & White, 1994). The venom contains both pre- and post-synaptic neurotoxins (Barnett *et al*., 1979) and the pre-synaptic component, textilotoxin, is the most potent and complex toxin ever isolated from a snake venom.. This phospholipase A_2 neurotoxin has a molecular weight of approximately 72 kD and comprises five non-covalently linked subunits (Tyler *et al*., 1987a; Su *et al*., 1983; Simpson *et al*., 1993). Its exact mechanism of action remains unknown, but is dependant on both temperature and the frequency of nerve stimulation. In addition, textilotoxin is said to be unaffected by antitoxin treatment once the initial binding phase is completed (Lloyd *et al*., 1991; Simpson *et al*., 1993; Hamilton *et al*., 1980; Cull-Candy *et al*., 1976).

Two post-synaptic based neurotoxins have also been isolated. One (pseudonajatoxin-a) is reported to bind 'irreversibly' to nicotinic acetylcholine receptors (Barnett *et al*., 1980) and is unusually large with 117 amino acid residues, seven disulphide bonds and a molecular weight of 12 kD (Barnett *et al*., 1979; 1980). The second (pseudonajatoxin-b) blocks acetylcholine receptors on mammalian skeletal muscle only weakly and reversibly (Tyler *et al*., 1987b).

It is not known which of the three neurotoxins are clinically important, but Harris & Maltin (1981) reported that the neurotoxic effects of whole venom are of a predominantly post-synaptic type lasting, *in vivo*, for 2–3 days. They also reported that the effects of the venom could not be reversed *in vitro*, by a conventional antivenom. This has important implications for the treatment of Brown snake envenomation and, therefore, experiments were performed to determine if a new ovine Fab based antivenom could reverse its neurotoxic effects.

*Author for correspondence at: Department of Reproductive Physiology, St Bartholomews' Hospital, 48–53 Bartholomew Close, London EC1A 7BE.

Methods

Antivenom

The antivenom was prepared by immunizing sheep with a maximum of 1 mg/28 days of equal amounts of venom from four *Pseudonaja* species; *P. textilis*, *P. nuchalis*, *P. affinis* and *P. inframacula*, in order to maximize the cross reactivity of the final product (Venom Supplies Limited, P.O. Box 547, Tanuda 5352, South Australia). Ten ml of blood kg^{-1} body weight was collected from each sheep 2 weeks after each immunization, once adequate antibody titres had been achieved (30 weeks post primary immunization), and the serum was separated and its IgG fraction partially purified by precipitation with sodium sulphate (final concentration 18%) at 25°C for 15 min with mixing. The precipitate, after pelleting by centrifugation, was washed twice with 18% sodium sulphate, reconstituted in saline (0.9% sodium chloride) and the IgG partially digested with papain to yield Fab fragments (Rawat *et al*., 1994). Commercially available CSL Brown Snake Antivenom (CSL $F(ab')_2$) was purchased from CSL Ltd., Melbourne, Australia, and dialyzed against saline to remove the cresol preservative.

In vitro *neurotoxicity*

Left phrenic nerve-hemidiaphragm preparations were isolated from 20–35 g male, out-bred white mice (Kitchen, 1984; Bulbring, 1946). Each preparation was bathed in 60 ml Krebs buffer (mM 118 NaCl; 25 $NaHCO_3$; 1.0 $NaH_2PO_4.H_2O$; 4.8 KCl; 1.9 $CaCl_2.2H_2O$; 1.2 $MgSO_4.7H_2O$; 11.1 D glucose) maintained at 32°C, and supplied with 95% O_2 + 5% CO_2. A

silicone anti-foaming agent (Sigma) diluted 1 in 60,000 was added to prevent excess foaming in the tissue bath. Indirect stimulation (*via* the nerve) was supplied using a supramaximal voltage (~3 V, 0.2 Hz, 0.2 ms) and muscle contractions were recorded using an isometric transducer linked to a Lectromed Ltd amplifier (HF cut 150 Hz) and chart recorder (MX216–100), with tissue holder-electrodes from Harvard Apparatus Ltd. This was continued for at least 30 min until a consistent response was produced after which venom was added (t_0), and washed out after 30 min (t_{30}) and again after a further 30 min (t_{60}). The decrease in contractions was calculated as a percentage based on the extent of the contractions just before venom addition. The myotoxic effects of the venom were assessed by applying a short burst of direct (muscle) stimulation (0.2 Hz, 1 ms, ~50 V) before venom addition and at 30 min intervals thereafter.

The ability of the antivenom to neutralize the neurotoxic effects of the venom was assessed by mixing a fixed venom concentration (5 mg l^{-1}) with antivenom and incubating at 37°C for 30 min before addition to the hemidiaphragm preparation (t_0). An identical dose cycle was used to that shown above. The ability of the antivenom to reverse neurotoxicity was assessed by exposing the preparation to venom (5 mg l^{-1}) for 30 min before washing and then replacing the bathing solution with Krebs buffer containing antivenom for the remainder of the experiment. Late reversal of neurotoxicity was assessed by exposing the preparation to venom as above, washing after 30 min (t_{30}) and stimulating for a further 60 min before replacing the bathing solution with Krebs buffer containing antivenom (t_{90}) for the remainder of the experiment. Finally reversal of neurotoxicity by antivenom was assessed under more favourable conditions for pre-synaptic (textilotoxin) neurotoxicity, namely by stimulation at a higher temperature (37°C) and frequency (1.0 Hz).

Control responses under identical conditions but without venom or antivenom were also performed.

In vivo *toxicity*

In vivo toxicity and neutralization was determined by intravenous LD_{50} and ED_{50} assays (Theakston & Reid, 1983; Laing *et al*., 1992) using 18–20 g male mice.

Results

Venom effects on the phrenic nerve/diaphragm

A dose of 5 mg l^{-1} venom produced a rapid neurotoxic effect (Figure 1) with 95% blockade of the contractions within 30 min which was unaffected by two washes with Krebs buffer. No direct (myotoxic) action was found at this, or higher venom concentrations (25 mg l^{-1}, data not shown).

Neutralization of neurotoxicity by premixing venom and antivenom

Antivenom at a concentration of 200 mg l^{-1} Fab produced complete neutralization of the venom (5 mg l^{-1}) neurotoxicity (Figure 2). Halving the antivenom concentration to 100 mg l^{-1} Fab resulted in only a 40–60% blockade of the response which was reversed by washing. Complete neutralization using 200 mg l^{-1} Fab antivenom was also possible at a higher temperature and frequency (37°C 1.0 Hz^{-1}; data not shown). A concentration of 400 mg l^{-1} of CSL $F(ab')_2$ antivenom resulted in a 40–50% blockade of the response which was reversed by washing.

Reversal of neurotoxicity

Antivenom, at a concentration of 200 mg l^{-1} of Fab, produced complete reversal of neurotoxicity within 50 min of its addition (Figure 3) and an equimolar concentration of specific IgG (600 mg l^{-1}) produced a similar effect (data not shown). A concentration of 400 mg $l^{-1}$of CSL $F(ab')_2$

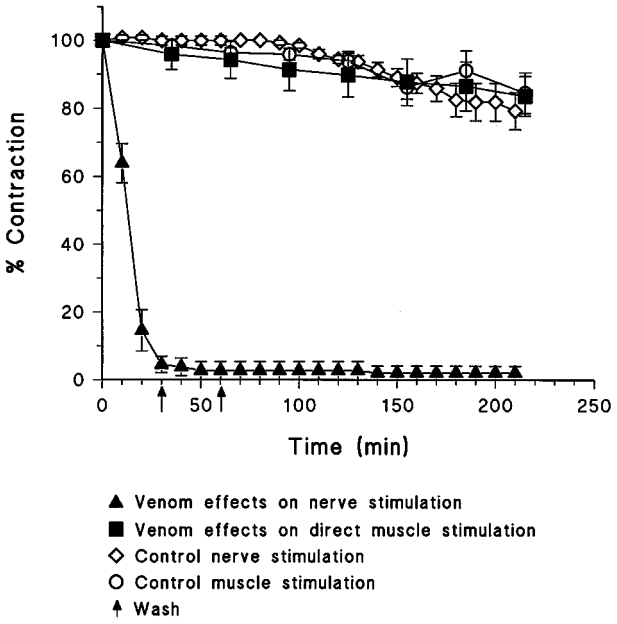

Figure 1 Effects of *Pseudonaja* venom (5 mg l^{-1}) on the mouse phrenic nerve/diaphragm at 32°C, with a stimulation frequency of 0.2 Hz (±s.e.mean, $n=5$), with controls ($n=4$).

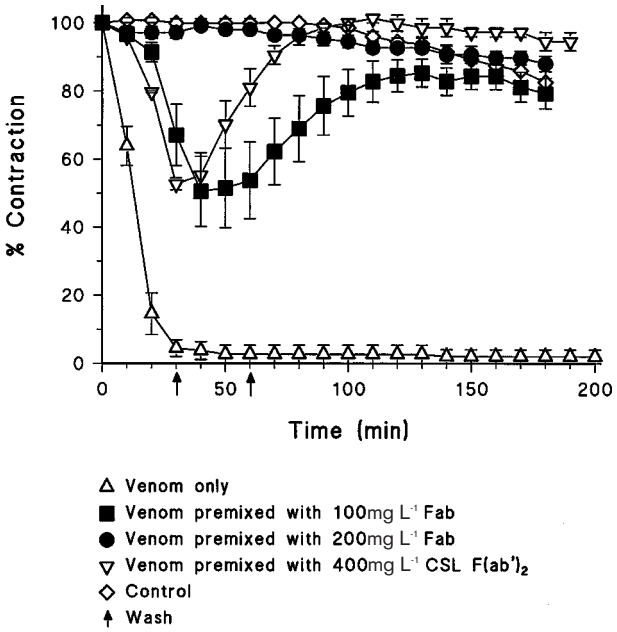

Figure 2 Neutralization of the neurotoxicity of *Pseudonaja* venom at 32°C with a stimulating frequency of 0.2 Hz *via* the nerve (±s.e.mean). Five mg l^{-1} venom alone ($n=5$) and premixed with Fab antivenom ($n=4$) or CSL $F(ab')_2$ ($n=3$). Control without venom or antivenom ($n=4$).

antivenom produced a significantly slower reversal. The effect of the Fab antivenom was slightly slower and less marked (94% control) at 37°C and, when combined with a high stimulating frequency (1.0 Hz, 37°C), only reversed 44% of the blockade (Figure 4).

Late reversal of neurotoxicity

Addition of antivenom (200 mg l^{-1} Fab) under the standard conditions (0.2 Hz, 32°C) 90 min after venom again produced complete reversal of neurotoxicity (Figure 3), while an 81% reversal was achieved when the temperature was raised to 37°C (Figure 4). When the higher temperature is combined with stimulation at 1.0 Hz only a 29% reversal could be attained (Figure 4).

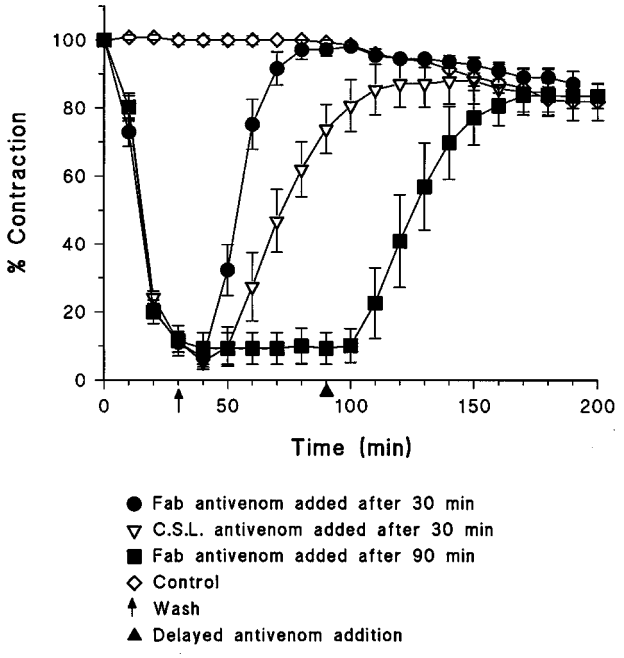

Figure 3 Antivenom reversal of *Pseudonaja* venom neurotoxicity at 32°C with a stimulating frequency of 0.2 Hz *via* the nerve (±s.e.mean). Venom (5 mg l^{-1}) induced neurotoxicity with antivenom added after 30 min, 200 mg l^{-1} Fab ($n=4$) or 400 mg l^{-1} CSL F(ab′)$_2$ ($n=4$) and the delayed addition of 200 mg l^{-1} Fab after 90 min ($n=4$). Control without venom or antivenom ($n=4$).

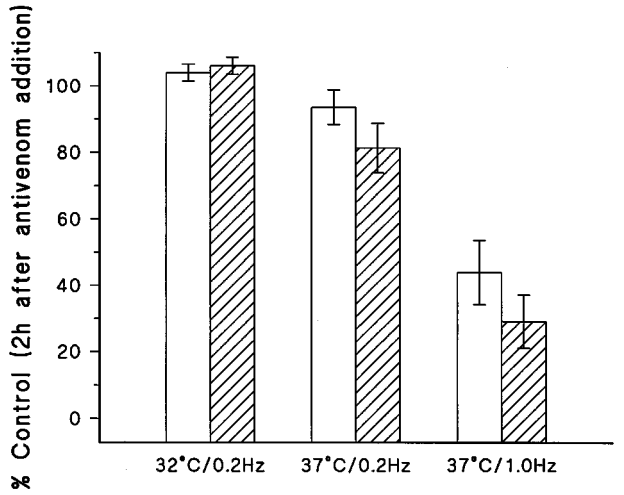

Figure 4 Effects of temperature and stimulation frequency on the reversal of neurotoxicity. Antivenom addition 30 min (open bars) and 90 min after venom (hatched bars), ±s.e.mean ($n=4$).

In vivo *toxicity*

In vivo the venom had an $LD_{50}=47$ μg kg^{-1} (95% confidence limits from probit analysis = 26–79). The ovine Fab based antivenom had an ED_{50} value of 74 mg kg^{-1} against $2\times LD_{50}$ (95% confidence limits = 47–100). Commercially available equine CSL F(ab′)$_2$ based antivenom had an ED_{50} value of 626 mg kg^{-1} against $2\times LD_{50}$ (95% confidence limits = 463–789).

Discussion

In this study Brown snake venom, in agreement with previous reports, caused no myotoxicity but effectively complete neurotoxicity that could not be reversed by washing (Sutherland *et al*., 1981; Harris & Maltin, 1981; Su *et al*., 1983).

After pre-mixing, 200 mg l^{-1} of the ovine Fab antivenom appeared to neutralize completely all the toxic components of the venom both *in vitro* and *in vivo*. Reducing the concentration *in vitro* to 100 mg l^{-1} resulted in a transitory and partial reduction of the twitch response which could be reversed to control levels by washing. A higher concentration (400 mg l^{-1}) of CSL F(ab′)$_2$ antivenom produced similar findings.

Harris & Maltin (1981) demonstrated, by measuring endplate potentials, that Brown snake venom neurotoxicity was predominantly of a post synaptic type and, in contrast to the present studies, could not be reversed by the delayed addition of antivenom despite preventing the development of neurotoxicity when added 10 min before the venom. No apparent explanation can be found for this difference, however, antivenom which still contained the preservative cresol was used by Harris & Maltin.

We have shown for the first time that sufficient amounts of an antivenom can rapidly (<1 h) and totally reverse the neurotoxicity produced by this venom. This reversal could also be demonstrated following the late addition of antivenom, an important factor in effective snake bite therapy. A slower reversal could also be produced by the CSL F(ab′)$_2$ antivenom using a higher concentration (400 mg l^{-1}).

A fast antibody induced reversal of neurotoxicity has previously been described for a post synaptic neurotoxin (toxin α) purified from spitting cobra (*Naja nigricollis*) venom, and is unique to antibodies raised to part of the toxin which is distinct from the toxic site (Boulain & Menz 1982; Boulain *et al*., 1982; 1985; Gatineau *et al*., 1988; Guenneugues *et al*., 1997; Menez *et al*., 1982; 1984). Due to the rapid rate of reversal of Brown snake venom neurotoxicity and the polyclonal nature of the antivenoms, a similar mechanism of reversal is suggested, with a subset of antibody clones specific for an epitope on the toxin(s) which is distinct from the toxic site, resulting in a modification of a flexible region and destablizing the toxin receptor complex (Boulain & Menz 1982; Boulain *et al*., 1982; 1985; Gatineau *et al*., 1988; Guenneugues *et al*., 1997; Menez *et al*., 1982; 1984; Zinn-Justin *et al*., 1993). This is despite the unusual structure and large size (12 kD) of pseudonajatoxin-a, the venom's predominant post-synaptic toxin (Barnett *et al*., 1979; 1980; Tyler *et al*., 1987b).

Our findings indicate that although the antivenom could produce complete reversal of neurotoxicity normally (0.2 Hz, 32°C), it was possible to reveal the presence of an irreversible neurotoxic component at an increased temperature (37°C) and

with high frequency nerve stimulation (1.0 Hz). Presumably this must represent only a minor venom constituent. Pre mixing experiments under these conditions showed that sufficient antibody was present to fully neutralize this component. These irreversible features are highly indicative of the pre-synaptic phospholipase neurotoxin, textilotoxin (Simpson *et al*., 1993; Lloyd *et al*., 1991; Su *et al*., 1983).

The new Fab based antivenom was found to be 8.5 times more effective *in vivo* and more than twice as effective *in vitro* compared to the current clinical treatment (CSL $F(ab')_2$).

The *in vitro* neurotoxic effects of this venom could also be reversed by the specific IgG. However, *in vivo* due to their small size, Fab fragments have a different pharmacokinetic profile and are able to quickly penetrate the interstitial space resulting in a greater volume of distribution than intact IgG (Smith *et al*., 1979). This, it is hoped, will allow a more rapid transfer to Fab antibody into the synapse than can be achieved with conventional IgG or $F(ab')_2$ based antivenoms, and would be more likely to result in a quick reversal of neurotoxicity.

In conclusion, the venom is devoid of myotoxic effects, and the ability of an antivenom to produce a full and rapid (<1 h) reversal of Brown snake venom induced neurotoxicity, is shown here for the first time.

We would like to thank Dr David Smith for critically reviewing the manuscript.

References

BARNETT, D., HOWDEN, M.E.H. & SPENCE, I. (1979). Pre- and post synaptic neurotoxins in the venom of the common brown snake (*Pseudonaja t.textilis*). *Proc. Aust. Physiol. Pharmacol. Soc.,* **10,** 240.

BARNETT, D., HOWDEN, M.E.H. & SPENCE, I. (1980). A neurotoxin of novel structural type from the venom of the Australian common brown snake. *Naturwissenschaften,* **67,** 405–406.

BOULAIN, J.C., FROMAGEOT, P. & MENEZ, A. (1985). Further evidence showing that neurotoxin-acetylcholine receptor dissociation is accelerated by monoclonal neurotoxin-specific immunoglobulin. *Mol. Immunol.,* **22,** 553–556.

BOULAIN, J.C. & MENEZ, A. (1982). Neurotoxin-specific immunoglobulins accelerate dissociation of the neurotoxin-acetylcholine receptor complex. *Science,* **217,** 732–733.

BOULAIN, J.C., MENEZ, A., COUDERC, J., FAURE, G., LIACOPOULOS, P. & FROMAGEOT, F. (1982). Neutralizing monoclonal antibody specific for *Naja nigricollis* toxin α: Preparation, characterization, and localization of the antigenic binding site. *Biochemistry,* **21,** 2910–2915.

BULBRING, E. (1946). Observations on the isolated phrenic nerve diaphragm preparation of the rat. *Br. J. Pharmacol.,* **1,** 38–61.

CULL-CANDY, S.G., FOHLMAN, J., GUSTAVSSON, D., LULLMAN-RAUCH, R. & THESLEFF, S. (1976). The effects of taipoxin and notexin on the function and fine structure of the murine neuromuscular junction. *Neuroscience,* **1,** 175–180.

GATINEAU, E., LEE, C.Y., FROMAGEOT, P. & MENEZ, A. (1988). Reversal of snake neurotoxin binding to mammalian acetylcholine receptor by specific antiserum. *Eur. J. Biochem.,* **171,** 535–539.

GUENNEUGUES, M., DREVET, P., PINKASFELD, S., GILQUIN, B., MENEZ, A. & ZINN-JUSTIN, S. (1997). Picosecond to hour time scale dyanmics of a 'three finger' toxin: Correlation with its toxic and antigenic properties. *Biochemistry,* **36,** 16097–16108.

HAMILTON, R.C., BROAD, A.J. & SUTHERLAND, S.K. (1980). Effects of Australian eastern brown snake (*Pseudonaja textilis*) venom on the ultrastructure of nerve terminals on the rat diaphragm. *Neurosci. Lett.,* **19,** 45–50.

HARRIS, J.B. & MALTIN, C.A. (1981). The effects of the subcutaneous injection of the crude venom of the Australian Common Brown snake, *Pseudonaja textilis* on the skeletal neuromuscular system. *Br. J. Pharmacol.,* **73,** 157–163.

JELINEK, G.A. & BREHENY, F.X. (1990). Ten years of snake bites at Fremantle hospital. *Med. J. Aust.,* **153,** 658–661.

JUDD, M. & WHITE, J. (1994). In: *A south Australian handbook on bites and stings*. pp. 9–10. South Australian Museum and Women's and Children's Hospital: Adelaide.

KITCHEN, I. (1984). Neuromuscular blocking drugs and the rat phrenic nerve hemidiaphragm preparation. In: *Textbook of In Vitro Practical Pharmacology*. pp. 79–83. Oxford: Blackwell Scientific Publications.

LAING, G.D., THEAKSTON, R.D., LEITE, R.P., DA SILVA, W.D. & WARRELL, D.A. (1992). Comparison of the potency of three Brazilian *Bothrops* antivenoms using *in vivo* rodent and *in vitro* assays. *Toxicon,* **30,** 1219–1225.

LLOYD, D.R., NICHOLSON, G.M., SPENCE, I., CONNOR, M., TYLER, M.I. & HOWDEN, M.E.H. (1991). Frequency-dependent neuromuscular blockade by textilotoxin *in vivo*. *Toxicon,* **29,** 1266–1269.

MENEZ, A., BOULAIN, J.C., BOUET, F., COUDERC, J., FAURE, G., ROUSSELET, A., TREMEAU, O., GATINEAU, E. & FROMAGEOT, P. (1984). On the molecular mechansisms of neutralisation of a cobra neurotoxin by specific antibodies. *J. Physiol. Paris,* **79,** 196–206.

MENEZ, A., BOULAIN, J.C., FAURE, G., COUDERC, J., LIACOPOULOS, P., TAMIYA, N. & FROMAGEOT, P. (1982). Comparison of the toxic and antigenic regions in toxin α isolated from *Naja nigricollis* venom. *Toxicon,* **20,** 95–103.

RAWAT, S., LAING, G., SMITH, D.C., THEAKSTON, D. & LANDON, J. (1994). A new antivenom to treat eastern coral snake (*Micrurus fulvius fulvius*) envenoming. *Toxicon,* **32,** 185–190.

SIMPSON, L.L., LAUTENSLAGER, G.T., KAISER, I.I. & MIDDLEBROOK, J.L. (1993). Identification of the site at which phospholipase A2 neurotoxins localise to produce their neuromuscular blocking effects. *Toxicon,* **31,** 13–26.

SMITH, T.W., LLOYD, B.L., SPICER, N. & HABER, E. (1979). Immunogenicity and kinetics of distribution and elimination of sheep digoxin-specific IgG and Fab fragments in the rabbit and baboon. *Clin. Exp. Immunol.,* **36,** 384–396.

SU, M.J., COULTER, A.R., SUTHERLAND, S.K. & CHANG, C.C. (1983). The presynaptic neuromuscular blocking effect and phosphlipase A_2 activity of textilotixin, a potent toxin isolated from the venom of the Australian brown snake, *Pseudonaja textilis*. *Toxicon,* **21,** 143–151.

SUTHERLAND, S.K. (1992). Deaths from snake bite in Australia, 1981–1991. *Med. J. Aust.,* **157,** 740–746.

SUTHERLAND, S.K., CAMPBELL, D.G. & STUBBS, A.E. (1981). A study of the major Australian snake venoms in the monkey (*Macaca fascicularis*). II. Myolytic and haematological effects of venoms. *Pathology,* **13,** 705–715.

THEAKSTON, R.D. & REID, H.A. (1983). Development of simple standard assay procedures for the characterization of snake venom. *Bull. World Health Organ.,* **61,** 949–956.

TYLER, M.I., BARNETT, D., NICHOLSON, P., SPENCE, I. & HOWDEN, M.E.H. (1987a). Studies on the subunit structure of textilotoxin, a potent neurotoxin from the venom of the Australian common brown snake (*Pseudonaja textilis*). *Biochim. Biophys. Acta,* **915,** 210–216.

TYLER, M.I., SPENCE, I., BARNETT, D. & HOWDEN, M.E.H. (1987b). Pseudonajatoxin b: Unusual amino acid sequence of a lethal neurotoxin from the venom of the Australian common brown snake, *Pseudonaja textilis*. *Eur. J. Biochem.,* **166,** 139–143.

WHITE, J. & POUNDER, D.J. (1984). Fatal snakebite in Australia. *Am. J. Forensic Med. Pathol.,* **5,** 137–143.

ZINN-JUSTIN, S., ROUMESTAND, C., DREVET, P., MENEZ, A. & TOMA, F. (1993). Mapping of new 'neutralising' epitopes of a snake curaremimetic toxin by proton nuclear magnetic resonance spectroscopy. *Biochemistry,* **32,** 6884–6891.

(Received July 3, 1998
Revised September 28, 1998
Accepted October 9, 1998)

British Journal of Pharmacology (1999) 126, 585–594
http://www.stockton-press.co.uk/bjp

Canine external carotid vasoconstriction to methysergide, ergotamine and dihydroergotamine: role of 5-$HT_{1B/1D}$ receptors and α_2-adrenoceptors

*,[1,2]Carlos M. Villalón, [2]Peter De Vries, [1]Gonzalo Rabelo, [1]David Centurión, [1]Araceli Sánchez-López & [2]Pramod Saxena

[1]Sección de Terapéutica Experimental, Departamento de Farmacología y Toxicología, CINVESTAV, I.P.N., Apdo. Postal 22026, 14000 México D.F., México; and [2]Department of Pharmacology, Faculty of Medicine and Health Sciences, Erasmus University Rotterdam, P.O. Box 1738, 3000 DR Rotterdam, The Netherlands

1 The antimigraine drugs methysergide, ergotamine and dihydroergotamine (DHE) produce selective vasoconstriction in the external carotid bed of vagosympathectomized dogs anaesthetized with pentobarbital and artificially respired, but the receptors involved have not yet been completely characterized. Since the above drugs display affinity for several binding sites, including α-adrenoceptors and several 5-HT_1 and 5-HT_2 receptor subtypes, this study has analysed the mechanisms involved in the above responses.

2 Intracarotid (i.c.) infusions during 1 min of methysergide (31–310 μg min^{-1}), ergotamine (0.56–5.6 μg min^{-1}) or DHE (5.6–31 μg min^{-1}) dose-dependently reduced external carotid blood flow (ECBF) by up to 46 ± 4, 37 ± 4 and 49 ± 5%, respectively. Blood pressure and heart rate remained unchanged.

3 The reductions in ECBF by methysergide were abolished and even reversed to increases in animals pre-treated with GR127935 (10 μg kg^{-1}, i.v.).

4 The reductions in ECBF by ergotamine and DHE remained unchanged in animals pre-treated (i.v.) with prazosin (300 μg kg^{-1}), but were partly antagonized in animals pre-treated with either GR127935 (10 or 30 μg kg^{-1}) or yohimbine (1000 μg kg^{-1}). Pre-treatment with a combination of GR127935 (30 μg kg^{-1}) and yohimbine (1000 μg kg^{-1}) abolished the responses to both ergotamine and DHE. The above doses of antagonists were shown to produce selective antagonism at their respective receptors.

5 These results suggest that the external carotid vasoconstrictor responses to methysergide primarily involve 5-$HT_{1B/1D}$ receptors, whereas those to ergotamine and DHE are mediated by 5-$HT_{1B/1D}$ receptors as well as α_2-adrenoceptors.

Keywords: Carotid artery; dihydroergotamine; dog; ergotamine; GR127935; 5-hydroxytryptamine (5-HT); 5-$HT_{1B/1D}$ receptors; methysergide; prazosin; yohimbine

Abbreviations: DHE, dihydroergotamine; ECBF, external carotid blood flow; HR, heart rate; 5-HT, 5-hydroxytryptamine; i.c., intracarotid; L-NAME, L-N^G-nitroarginine methyl ester; MAP, mean arterial blood pressure

Introduction

Several lines of pharmacological evidence show that serotonin (5-hydroxytryptamine; 5-HT) and the antimigraine drug sumatriptan constrict the carotid vascular bed in vagosympathectomized animals *via* 5-HT_1-like receptors (Den Boer *et al*., 1991b; Villalón *et al*., 1995). Using the potent and selective 5-$HT_{1B/1D}$ receptor antagonist, GR127935 (N-[4-Methoxy-3-(4-methyl-1-piperazinyl)phenyl]-2′-methyl-4′ (5-methyl-1, 2,4-oxadiazol-3-yl) [1,1,-biphenyl]-4-carboxamide hydrochloride monohydrate) (see Pauwels, 1996; Skingle *et al*., 1996), it was subsequently demonstrated that these vasoconstrictor 5-HT_1-like receptors correspond to 5-$HT_{1B/1D}$ subtypes (De Vries *et al*., 1996; Villalón *et al*., 1996). Additionally, it has been previously demonstrated that the classical antimigraine agents methysergide, ergotamine and dihydroergotamine (DHE) exert a selective vasoconstrictor action in the carotid vascular bed of several species, including dogs (Saxena, 1974b; Saxena *et al*., 1983), pigs (Saxena & Verdouw, 1984; Den Boer *et al*., 1991a), cats (Spierings & Saxena, 1980) and monkeys (Mylecharane *et al*., 1978).

Surprisingly, very little is known about the receptor mechanisms involved in the external carotid vasoconstriction induced by methysergide, ergotamine and DHE in the dog. In this respect, we have shown that vasoconstriction in the canine external carotid bed may be mediated by activation of 5-$HT_{1B/1D}$ receptors (Villalón *et al*., 1996), α_1- and α_2-adrenoceptors (Villalón & Terrón, 1994; Terrón *et al*., 1996), but not by 5-HT_2 (Villalón *et al*., 1995) or D_2 receptors (Villalón & Terrón, 1994). Indeed, as shown in Table 1, ergotamine and DHE are able to interact with a wide variety of receptors mediating vasoconstriction, including 5-$HT_{1/2}$ receptors and $\alpha_{1/2}$-adrenoceptors, whereas methysergide seems to interact mainly with 5-$HT_{1/2}$ receptors. In the light of these findings, the present study set out to characterize the pharmacological profile of the receptors involved in the vasoconstriction of the canine external carotid vascular bed in response to methysergide, ergotamine and DHE, with particular emphasis on verifying the possible involvement of the 5-$HT_{1B/1D}$ receptor subtypes and α_1- and α_2-adrenoceptors. For this purpose, we made use of antagonists at 5-$HT_{1B/1D}$ receptor subtypes (GR127935;

*Author for correspondence; E-mail: carlos_villalon@infosel.net.mx

Skingle *et al*., 1996), α_1- (prazosin) and α_2- (yohimbine) adrenoceptors (Hoffman & Lefkowitz, 1996), after determining the doses of these antagonists that produce selective blockade at their respective receptors. Preliminary results of this investigation have been communicated to the XIIIth International Congress of Pharmacology (Villalón *et al*., 1998).

Methods

General

Experiments were carried out in a total of 72 dogs (15–31 kg) not selected for breed or sex. The animals were anaesthetized with an intravenous (i.v.) bolus injection of sodium pentobarbitone (30 mg kg^{-1}) and additional amounts (1 mg kg^{-1}, i.v.) were provided when required. All dogs were intubated with an endotracheal tube and artificially respired with room air; for this purpose, a Palmer ventilation pump was used at a rate of 20 strokes min^{-1} and a stroke volume of 13–16 ml kg^{-1}, as previously established by Kleinman & Radford (1964). Catheters were placed in the inferior vena cava *via* a femoral vein for the administration of antagonist drugs and in the aortic arch *via* a femoral artery, connected to a Statham pressure transducer (P23 ID), for the measurement of blood pressure. After drug administration, the venous catheter was flushed with 3 ml of saline. Mean blood pressure (MAP) was calculated from the systolic (SAP) and diastolic (DAP) arterial pressures: MAP = DAP + (SAP-DAP)/3. Heart rate was measured with a tachograph (7P4F, Grass Instrument Co., Quincy, MA, U.S.A.) triggered from the blood pressure signal. The right common carotid artery was dissected free and the corresponding internal carotid and occipital arteries were ligated. Thereafter, an ultrasonic flow probe (4 mm R-Series) connected to an ultrasonic T201D flowmeter (Transonic Systems Inc., Ithaca, N.Y., U.S.A.) was placed around the right common carotid artery, and the flow through this artery was considered as the external carotid blood flow (for further details, see Villalón *et al*., 1993). Bilateral cervical vagosympathectomy was systematically performed in order to produce one of the main features of migraine, i.e. external carotid vasodilatation (Saxena & De Vlaam-Schluter, 1974). The agonists were administered into the carotid artery by a Harvard model 901 pump (Harvard Apparatus Co. Inc., Millis, MA, U.S.A.) with a catheter inserted into the right cranial thyroid artery. Blood pressure, heart rate and external carotid blood flow were recorded simultaneously by a model 7D polygraph (Grass Instrument Co., Quincy, MA, U.S.A.). The body temperature of the animals was maintained between 37–38°C.

Experimental protocol

After a stable haemodynamic condition for at least 30 min, baseline values of blood pressure, heart rate and external carotid blood flow were determined. At this point, the dogs were divided into two groups ($n = 56$ and 16, respectively). The first group ($n = 56$) was subdivided into three subgroups. In the first subgroup ($n = 8$), the effects of sequential 1 min intracarotid (i.c.) infusions of methysergide (31, 100 and 310 μg min^{-1}) were analysed in animals pre-treated i.v. with either saline (0.1 ml kg^{-1}, $n = 4$) or GR127935 (10 μg kg^{-1}; $n = 4$). In the second and third subgroups ($n = 24$ each), the effects of cumulative 1 min i.c. infusions of ergotamine (0.56, 1, 1.8, 3.1 and 5.6 μg min^{-1}) or DHE (5.6, 10, 18 and 31 μg min^{-1}), respectively, were analysed in animals pre-treated with i.v. infusions of either ($n = 4$ each) saline (0.1 ml kg^{-1}), GR127935 (10 μg kg^{-1}), GR127935 (30 μg kg^{-1}), prazosin (300 μg kg^{-1}), yohimbine (1000 μg kg^{-1}) or the combination of GR127935 (30 μg kg^{-1}) and yohimbine (1000 μg kg^{-1}). In the second group ($n = 16$), all animals received subsequent 1 min i.c. infusions of clonidine (1 μg min^{-1}), phenylephrine (10 μg min^{-1}) and sumatriptan (30 μg min^{-1}). Then, this group of animals was subdivided into four subgroups ($n = 4$ each). In these subgroups, the responses to clonidine, phenylephrine and sumatriptan were reanalysed after i.v. administration of either prazosin (300 μg kg^{-1}), yohimbine (1000 μg kg^{-1}), GR127935 (30 μg kg^{-1}) or the combination of GR127935 (30 μg kg^{-1}) and yohimbine (1000 μg kg^{-1}).

The dose-intervals between the different doses of methysergide ranged between 5 and 10 min, as in each case we waited

Table 1 Pharmacological profile of several agonists and antagonists used in the present study

Receptor	*Methysergide*	*Ergotamine*	*DHE*	*GR127935*	*Prazosin*	*Yohimbine*
5-HT_{1A}	7.63[a,*]	8.37[a,*]	9.30[b]	7.20[e]	5.00[a,*]	6.86[a,*]
r5-HT_{1B}	5.82[a,*]	8.69[a,*]	7.85[b]	8.50[d]	5.10[a,*]	5.46[a,*]
h5-HT_{1B}	n.d.	n.d.	9.22[b]	9.90[c]/9.00[d]	n.d.	n.d.
h5-HT_{1D}	n.d.	n.d.	8.60[b]	8.90[c]/8.60[d]	n.d.	n.d.
5-$HT_{1B/1D}$	8.42[a,*]	7.60[a,*]	7.65[b]	n.d.	7.12[a,*]	7.12[a,*]
5-ht_{1E}	6.64[e]	6.22[e]	6.22[b]	6.20[c]/5.40[d]	n.d.	5.90[e]
5-ht_{1F}	7.47[e]	6.77[e]	6.96[b]	7.30[c]/6.40[d]	n.d.	7.04[e]
5-HT_{2A}	8.57[a,*]	7.69[a,*]	8.54[b]	7.20[c]/7.80[d]	4.95[a,*]	5.95[a,*]
5-HT_{2B}	u.a.[f]	8.17[g,†]	7.70[g,†]	6.20[d]	n.d.	7.90[f,$]
5-HT_{2C}	8.90[h,*]	7.25[a,*]	7.48[a,*]/7.43[b]	6.20[c]/7.00[d]	4.70[a,*]	4.37[a,*]
5-ht_{5A}	7.20[h,*]	8.40[h,*]	n.d.	5.20[e]	n.d.	6.00[h,*]
5-HT_{5B}	6.90[h,*]	8.50[h,*]	n.d.	n.d.	n.d.	6.00[h,*]
5-ht_{6}	6.43[h,*]	n.d.	7.88[h,*]/8.00[b]	5.80[d]	n.d.	n.d.
5-HT_{7}	7.90[h,*]	7.49[h,*]	6.82[h,*]/7.82[b]	5.50[c]/6.20[d]	n.d.	5.55[i]
α_1	5.64[j]	8.00[k]	8.00[b]	<6.00[c]	9.24[j]	6.39[j]
α_2	5.59[j]	8.20[k]	8.00[b]	<6.00[c]	5.33[j]	6.82[j]
D_2	6.70[j]	8.50[k]	7.00[k]	<5.00[c]	<6.00[j]	6.22[j]

[a]Hoyer (1988); [b]Leysen *et al*., (1996); [c]Pauwels (1996); [d]Price *et al*. (1997); [e]Adham *et al*., (1993); [f]Baxter *et al*. (1994); [g]Glusa & Roos (1996); [h]Hoyer *et al*. (1994); [i]Bard *et al*. (1993); [j]Leysen (1985); [k]Leysen & Gommeren (1984). All values have been presented as pK_iexcept for: $, pA_2; †, pEC_{50}; *, pK_D. Abbreviations: u.a., unsurmountable antagonist; n.d., not determined. r5-HT_{1B} refer to the rodent 5-HT_{1B} and receptor; h5-HT_{1B} and h5-HT_{1D} refer to the previously called 5-$HT_{1D\beta}$ and 5-$HT_{1D\alpha}$ human receptor binding sites, respectively (Hartig *et al*. (1996); 5-$HT_{1B/1D}$ refers to the, then called, 5-HT_{1D} receptor binding site in calf caudate membrane, at which time the experimental conditions allowed the inclusion of the 5-HT_{1B} (5-$HT_{1D\beta}$) and 5-HT_{1D} (5-$HT_{1D\alpha}$) receptor sites.

until the blood flow had returned completely to baseline values. Moreover, after the administration of an antagonist or saline a period of about 10 min was allowed to elapse before the responses to the respective agonists were elicited.

Data presentation and statistical analysis

All data have been expressed as the means ± s.e.mean. The peak changes in external carotid blood flow (calculated as percent change from baseline) by methysergide, ergotamine and DHE after pre-treatment with a dose of a particular antagonist were compared to the respective responses by these agonists in saline-pre-treated animals by Student's unpaired *t*-test. Furthermore, the peak percent changes in external carotid blood flow by clonidine, phenylephrine and sumatriptan before and after antagonist treatment were compared by using Student-Newman-Keuls test, once an analysis of variance (randomized block design) had revealed that the samples represented different populations (Steel & Torrie, 1980). Statistical significance was accepted at $P<0.05$ (two-tailed).

Drugs

Apart from the anaesthetic (sodium pentobarbitone), the drugs used in the present study (obtained from the sources indicated) were the following: phenylephrine hydrochloride, clonidine hydrochloride and prazosin hydrochloride (Sigma Chemical Company, St. Louis, MO, U.S.A.); GR127935 and sumatriptan succinate (gifts from Dr M. Skingle, Glaxo Group Research, Ware, Herts, U.K. and Dr H.E. Connor, Glaxo Group Research, Stevenage, Hertfordshire, U.K. respectively); methysergide maleate, DHE mesylate and ergotamine tartrate (gift: Sandoz A.G., Basel, Switzerland). All compounds were dissolved in physiological saline. When needed, 5% (vv^{-1}) propylene glycol (prazosin) was added; this vehicle had no effect on the haemodynamic variables. GR127935 was solubilized according to the instructions of the supplier by heating the dispersion in bidistilled water to about 70°C for 10 s and then allowing to cool down to room temperature. All doses of antagonists refer to the respective salts, whereas those of the agonists refer to the free base.

Results

Systemic haemodynamic variables

Baseline values of mean arterial blood pressure, heart rate and external carotid blood flow in the 72 vagosympathectomized dogs were, respectively, 142 ± 5 mmHg, 178 ± 8 beats min^{-1} and 163 ± 21 ml min^{-1}. No significant differences were observed in the initial values between the 18 subgroups. As depicted in Table 2, these haemodynamic variables remained essentially unchanged after i.v. administrations of saline, GR127935, yohimbine, or the combination of GR127935 and yohimbine, at all doses tested. Only prazosin produced a significant decrease in both mean blood pressure and external carotid blood flow by 29 ± 15 and 29 ± 16%, respectively, without affecting the corresponding carotid vascular conductance (not shown). This prazosin-induced hypotension and the resulting decrease in external carotid blood flow has previously been reported to be attributable to its α_1-adrenoceptor blocking properties (Terrón *et al*, 1996). In any case, these effects were not accompanied by changes in heart rate (Table 2), as previously shown by Massingham & Hayden (1975).

Initial effects of methysergide, ergotamine and DHE on external carotid blood flow

As shown in Figure 1, i.c. infusions (during 1 min) of methysergide (31, 100 and 310 $\mu g\ min^{-1}$), ergotamine (0.56, 1, 1.8, 3.1 and 5.6 $\mu g\ min^{-1}$) and DHE (5.6, 10, 18 and 31 $\mu g\ min^{-1}$) produced dose-dependent decreases in external carotid blood flow, without changes in mean blood pressure or heart rate (not shown). The above responses, which were immediate in onset, are drug-induced as 1 min i.c. infusions of the corresponding volumes of saline did not affect any haemodynamic parameter for the duration of the experiments (data not shown). The duration of action of ergotamine and DHE could not be established, as external carotid blood flow did not return to baseline values, as previously reported (Saxena, 1974a; Villalón *et al*., 1992). In contrast, the duration of action of methysergide was 2.0 ± 0.7, 7.0 ± 1.2 and 9.0 ± 1.9 min after 31, 100 and 310 $\mu g\ min^{-1}$, respectively. The apparent rank order of potency obtained in the present experiments was ergotamine > DHE > methysergide (Figure 1).

Effects of GR127935 on the methysergide-induced external carotid vasoconstriction

As depicted in Figure 2, in animals pre-treated with 10 $\mu g\ kg^{-1}$ of GR127935, the decreases in external carotid blood flow by methysergide were abolished and even reversed to an external carotid vasodilatation.

Effects of GR127935, prazosin, yohimbine or the combination of GR127935 and yohimbine on the ergotamine- and DHE-induced external carotid vasoconstriction

As shown in Figures 3 (ergotamine) and 4 (DHE), 10 $\mu g\ kg^{-1}$ of GR127935 only partly blocked the external carotid vasoconstrictor responses to ergotamine and DHE. Interest-

Table 2 Mean arterial blood pressure (MAP), heart rate (HR) and external carotid blood flow (ECBF) values before and after different i.v. treatments

Treatment	*Dose* ($\mu g\ kg^{-1}$)	n	*MAP* (mmHg) *Before*	*MAP* (mmHg) *After*	*HR* (beats min^{-1}) *Before*	*HR* (beats min^{-1}) *After*	*ECBF* (ml min^{-1}) *Before*	*ECBF* (ml min^{-1}) *After*
Saline	0.1†	12	152 ± 11	152 ± 12	176 ± 12	173 ± 11	151 ± 8	153 ± 6
GR127935	10	12	141 ± 6	148 ± 5	183 ± 7	182 ± 8	163 ± 13	155 ± 13
GR127935	30	8	137 ± 5	145 ± 6	181 ± 5	181 ± 7	134 ± 12	127 ± 9
Prazosin	300	8	143 ± 8	101 ± 14*	184 ± 8	188 ± 10	171 ± 21	122 ± 15*
Yohimbine	1000	8	143 ± 6	138 ± 10	171 ± 8	186 ± 14	177 ± 32	139 ± 22
GR127935 + Yohimbine	30 + 1000	8	138 ± 5	128 ± 7	176 ± 9	199 ± 18	170 ± 19	143 ± 18

All values have been presented as means ± s.e.mean. †, ml kg^{-1}; *$P<0.05$ vs before values.

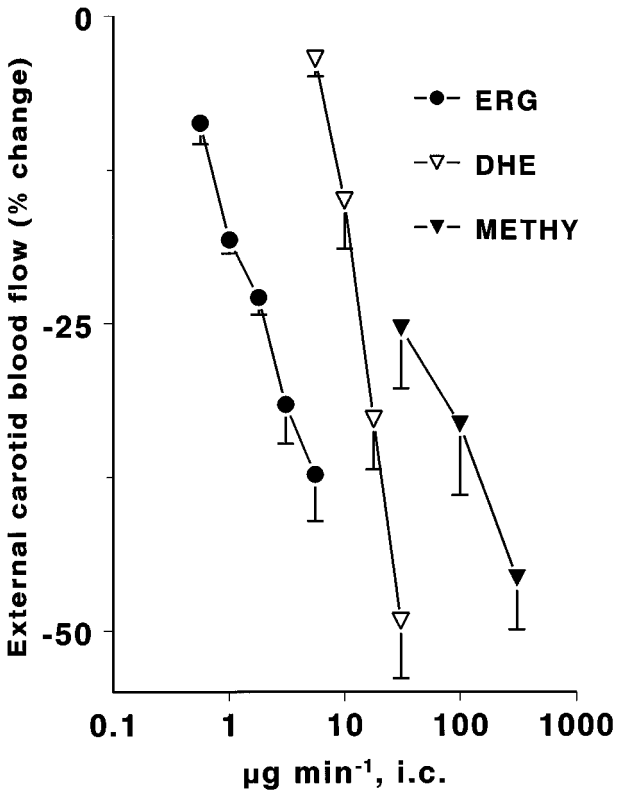

Figure 1 Comparative effects (expressed as per cent change from baseline values) of 1 min i.c. infusions ($n=4$ each) of ergotamine (ERG), dihydroergotamine (DHE) and methysergide (METHY) on external carotid blood flow in vagosympathectomized dogs. All values have been presented as means ± s.e.mean.

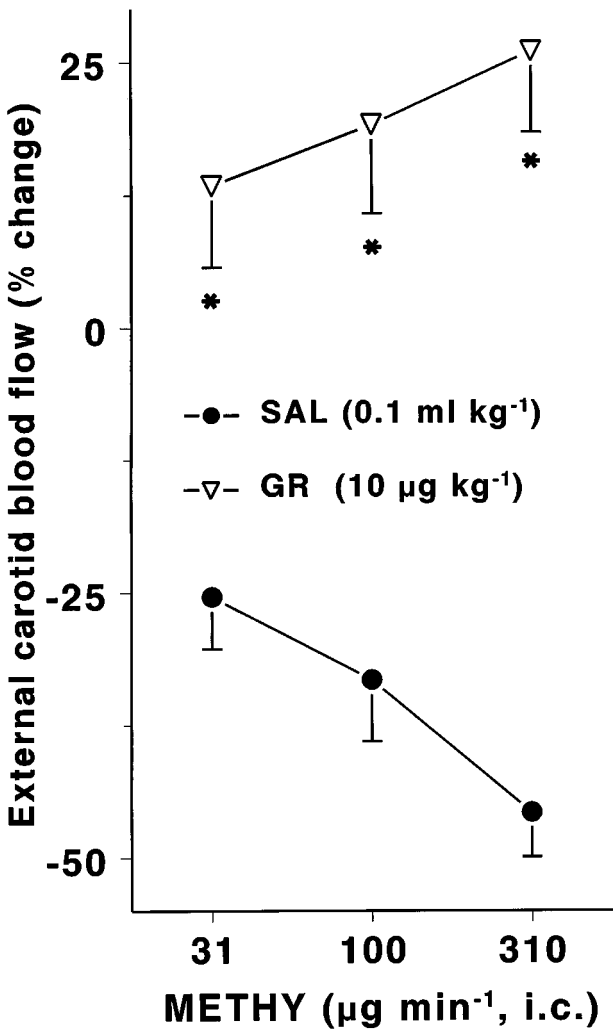

Figure 2 Percentage changes from baseline values by 1 min i.c. infusions of methysergide (METHY; 31–310 μg min^{-1}) in external carotid blood flow in animals pre-treated (i.v.; $n=4$ each) with either saline (SAL; 0.1 ml kg^{-1}) or GR127935 (GR; 10 μg kg^{-1}). All values have been presented as means ± s.e.mean. $^*P<0.05$ vs response in saline-pre-treated animals.

ingly, a higher dose of GR127935 (30 μg kg^{-1}) did not produce a further blockade. Moreover, whereas prazosin (300 μg kg^{-1}) did not affect the ergotamine- and DHE-induced decreases in external carotid blood flow, yohimbine (1000 μg kg^{-1}) brought about a partial blockade. Significantly, the combination of GR127935 (30 μg kg^{-1}) and yohimbine (1000 μg kg^{-1}) completely blocked the external carotid vasoconstriction induced by ergotamine (Figure 3) and DHE (Figure 4). The above doses of antagonists, as explained below, were shown to produce selective antagonism at their respective receptors.

Effects of GR127935, prazosin, yohimbine and the combination of GR127935 and yohimbine on the external carotid vasoconstriction produced by clonidine, phenylephrine and sumatriptan

As depicted in Figure 5, GR127935 (30 μg kg^{-1}) selectively antagonized the external carotid vasoconstriction to sumatriptan, as the responses to clonidine and phenylephrine remained unaffected. Similarly, prazosin (300 μg kg^{-1}) exclusively abolished the phenylephrine-induced decreases in external carotid blood flow, leaving the clonidine- and sumatriptan-induced changes intact. Lastly, while yohimbine (1000 μg kg^{-1}) abolished only the clonidine-induced carotid vascular effects, the combination of GR127935 (30 μg kg^{-1}) and yohimbine (1000 μg kg^{-1}) completely blocked the clonidine-, as well as the sumatriptan-induced constriction of the canine carotid vascular bed. It should be pointed out that the external carotid vasoconstrictor responses to phenylephrine, clonidine and sumatriptan are highly reproducible, as they remained essentially unchanged in control animals receiving two subsequent bolus injections of physiological saline (Villalón & Terrón, 1994; Villalón *et al*, 1996).

Discussion

General

The major findings of the present study in vagosympathectomized dogs were that: (i) the methysergide-induced external carotid vasoconstriction was abolished, and even reversed to carotid vasodilatation, by the selective 5-HT$_{1B/1D}$ receptor antagonist, GR127935 and (ii) the external carotid vasoconstrictor responses by ergotamine and DHE were only partly antagonized by GR127935 or yohimbine, but were completely blocked by the combination of GR127935 and yohimbine. Apart from the implications discussed below, these data indicate that the vasoconstrictor responses to ergotamine and DHE in the external carotid vascular bed involve both 5-HT$_{1B/1D}$ receptors and α_2-adrenoceptors, whereas methysergide seems to exert external carotid vasoconstriction primarily *via* 5-HT$_{1B/1D}$ receptors.

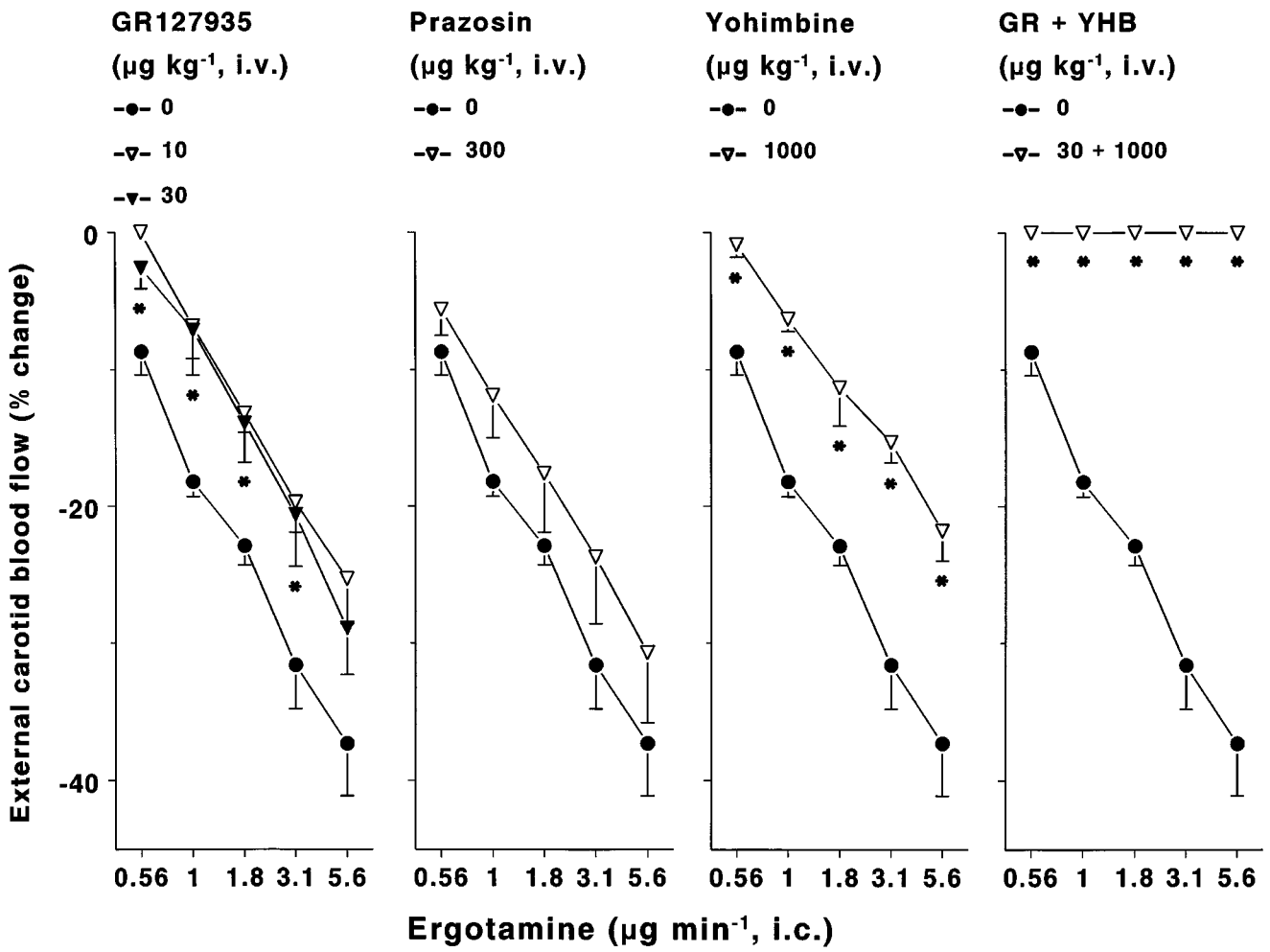

Figure 3 Percentage changes from baseline values of external carotid blood flow by 1 min i.c. infusions of ergotamine (0.56–5.6 μg min^{-1}) in animals pre-treated (i.v.; $n=4$ each) with either saline (0.1 ml kg^{-1}), GR127935 (10 or 30 μg kg^{-1}), prazosin (300 μg kg^{-1}), yohimbine (1000 μg kg^{-1}) or the combination of GR127935 (GR; 30 μg kg^{-1}) and yohimbine (YHB; 1000 μg kg^{-1}). All values have been presented as means$\pm$s.e.mean. For the sake of clarity, the responses to ergotamine in saline-pre-treated animals are shown in all panels. *$P<0.05$ vs response in saline-pre-treated animals.

Receptors involved in the methysergide-induced carotid vasoconstrictor responses

As previously observed using i.v. administrations (Villalón *et al*., 1996), 1 min i.c. infusions of methysergide dose-dependently decreased external carotid blood flow, an effect which has been suggested to be due to an agonist action of the ergot derivative at smooth muscle 5-HT$_1$-like receptors (Saxena & Verdouw, 1984; Martin, 1994). As methysergide did not affect heart rate or blood pressure, these data suggest that under our experimental conditions methysergide induced a selective vasoconstriction in the external carotid circulation. A complete blockade of the methysergide-induced carotid vasoconstriction was observed after treatment with 10 μg kg^{-1} of GR127935; this dose of GR127935 has previously been shown to abolish sumatriptan-induced external carotid vasoconstriction without affecting that to noradrenaline or oxymetazoline (Villalón *et al*., 1996). In the present study, our results further demonstrate that doses of GR127935 up to 30 μg kg^{-1} selectively abolish sumatriptan-induced canine external carotid vasoconstriction, since the corresponding responses to phenylephrine and clonidine remained unaltered (Figure 5), as expected from its binding profile (see Table 1). Thus, these data show that methysergide constricts the external carotid vasculature predominantly *via* the 5-HT$_{1B/1D}$ receptor subtypes, at which methysergide displays high affinities (see Table 1). In view of the complete blockade by GR127935, as well as the low affinities exhibited by methysergide at α_1- and α_2-adrenoceptors (see Table 1), we decided not to further analyse the effects of prozosin or yohimbine on the methysergide-induced external carotid vasoconstriction.

Contribution of 5-HT$_{1B/1D}$ receptors in the carotid vasoconstrictor responses to ergotamine and DHE

One minute i.c. infusions of ergotamine and DHE induced dose-dependent decreases in the external carotid blood flow, without affecting heart rate or mean arterial blood pressure. Thus, these findings suggest that such responses were caused by a selective constriction in the external carotid vascular bed. Notwithstanding, unlike methysergide, the responses to ergotamine and DHE were of long duration, as previously observed *in vivo* (Saxena, 1974a; Den Boer *et al*., 1991a; Villalón *et al*., 1992; De Vries *et al*., 1998b) and *in vitro* (Müller-Schweinitzer & Weidmann, 1978; MaassenVanDen-Brink *et al*., 1998). Although there is no clear-cut explanation for this difference, it has been suggested, albeit not categorically proven, that it may be due to a slow dissociation

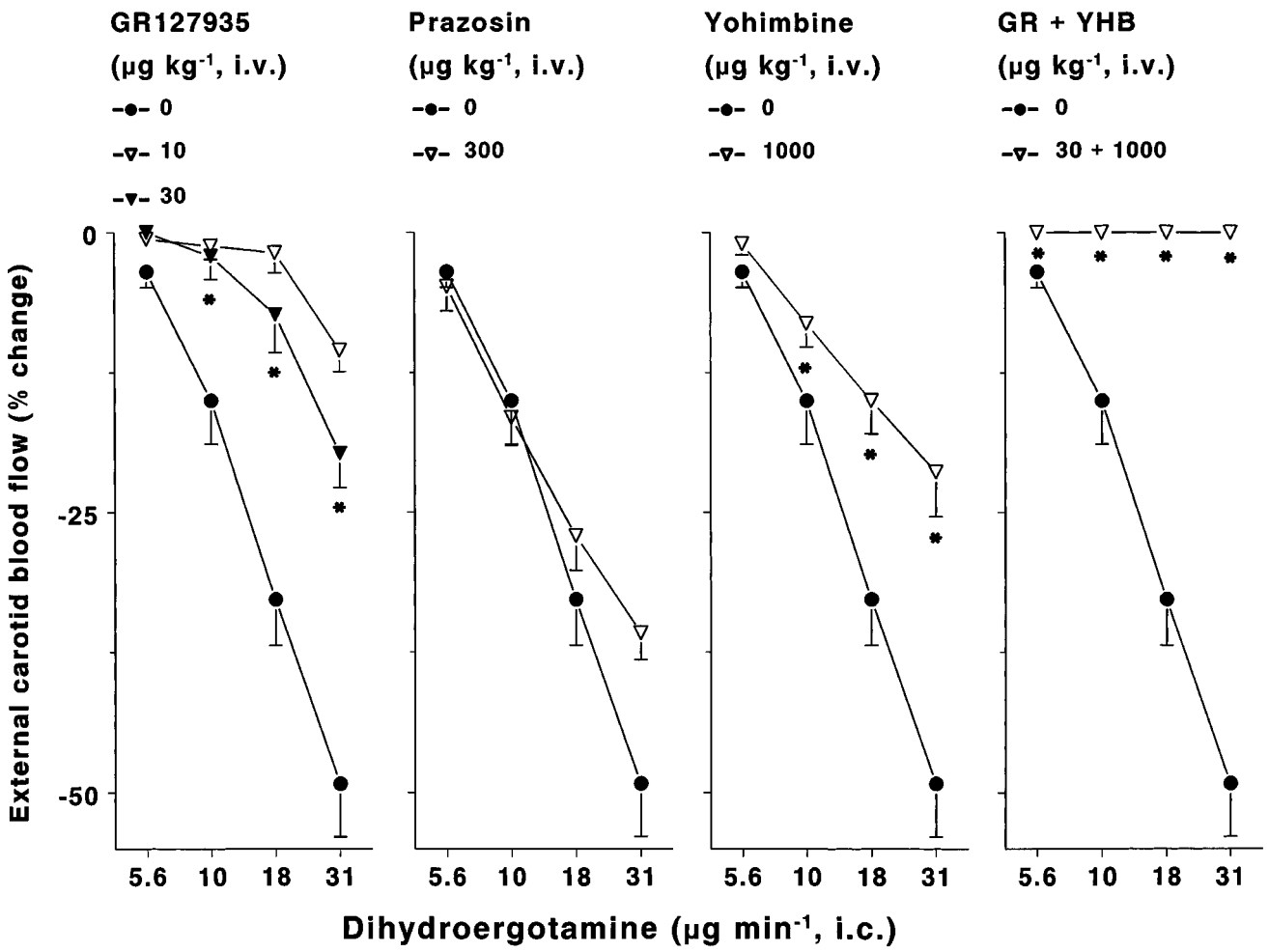

Figure 4 Percentage changes from baseline values of external carotid blood flow by 1 min i.c. infusions of dihydroergotamine (5.6–31 μg min^{-1}) in animals pre-treated (i.v.; $n=4$ each) with either saline (0.1 ml kg^{-1}), GR127935 (10 or 30 μg kg^{-1}), prazosin (300 μg kg^{-1}), yohimbine (1000 μg kg^{-1}) or the combination of GR127935 (GR; 30 μg kg^{-1}) and yohimbine (YHB; 1000 μg kg^{-1}). All values have been presented as means ± s.e.mean. For the sake of clarity, the responses to dihydroergotamine in saline-pre-treated animals are shown in all panels. *$P<0.05$ vs response in saline-pre-treated animals.

from its receptors or a sequestration and subsequent diffusion out of a local nonsaturable compartment (Müller-Schweinitzer & Weidmann, 1978; Martin *et al*., 1995).

Regarding the possible receptor mechanisms involved in the vasoconstrictor responses to ergotamine and DHE, previous results in anaesthetized dogs have shown that the external carotid vasoconstrictor responses to ergotamine and DHE are not mediated by 5-HT$_2$ receptors, whereas only part of the effects seem to be mediated by phentolamine-sensitive α-adrenoceptors (Saxena *et al*., 1983). Moreover, 5-HT$_1$-like receptors are only partly involved in the ergotamine- and DHE-induced constriction of the carotid vasculature in pigs (Den Boer *et al*., 1991a). Since 5-HT$_1$-like receptors mediating porcine as well as canine carotid vasoconstriction are similar to the 5-HT$_{1B/1D}$ receptor subtypes (De Vries *et al*., 1996; Villalón *et al*., 1996; Saxena *et al*., 1998), we decided to explore the possible involvement of 5-HT$_{1B/1D}$ receptors in the present study. Indeed, the responses to ergotamine and DHE in dogs were, in contrast to the methysergide- and sumatriptan-induced effects, only partly antagonized by 10 μg kg^{-1} of GR127935; the fact that pre-treatment with a higher dose of GR127935 did not produce any further blockade, implies that the ergotamine- and DHE-induced external carotid vasoconstriction involves a mixed population of receptors. Thus, we suggest that the responses to ergotamine and DHE are partly mediated *via* 5-HT$_{1B/1D}$ receptors, but a considerable part is mediated *via* GR127935-resistant receptors. Consistent with these findings, we have recently shown that ergotamine and DHE act, at least partly, *via* GR127935-sensitive 5-HT$_{1B/1D}$ receptors in the porcine carotid vascular bed, but additional receptors/mechanisms seem to be involved (De Vries *et al*., 1998b).

Contribution of α_1- and/or α_2-adrenoceptors in the carotid vasoconstrictor responses to ergotamine and DHE

As discussed above, a considerable part of the external carotid vasoconstriction by both ergotamine and DHE is mediated by non-5-HT$_{1B/1D}$ receptors. These GR127935-resistant receptors may be of the α-adrenoceptor class, as (i) agonists at α_1- and α_2-adrenoceptors can produce potent vasoconstrictor responses in the carotid circulation of dogs (Villalón & Terrón, 1994; Terrón *et al*., 1996) and pigs (Willems, E.W., personal communication); and (ii) ergotamine and DHE display high affinities at α_1- and α_2-adrenoceptors (Table 1).

Nevertheless, 300 μg kg^{-1} of prazosin, a dose which is 3 fold higher than that required to abolish methoxamine-

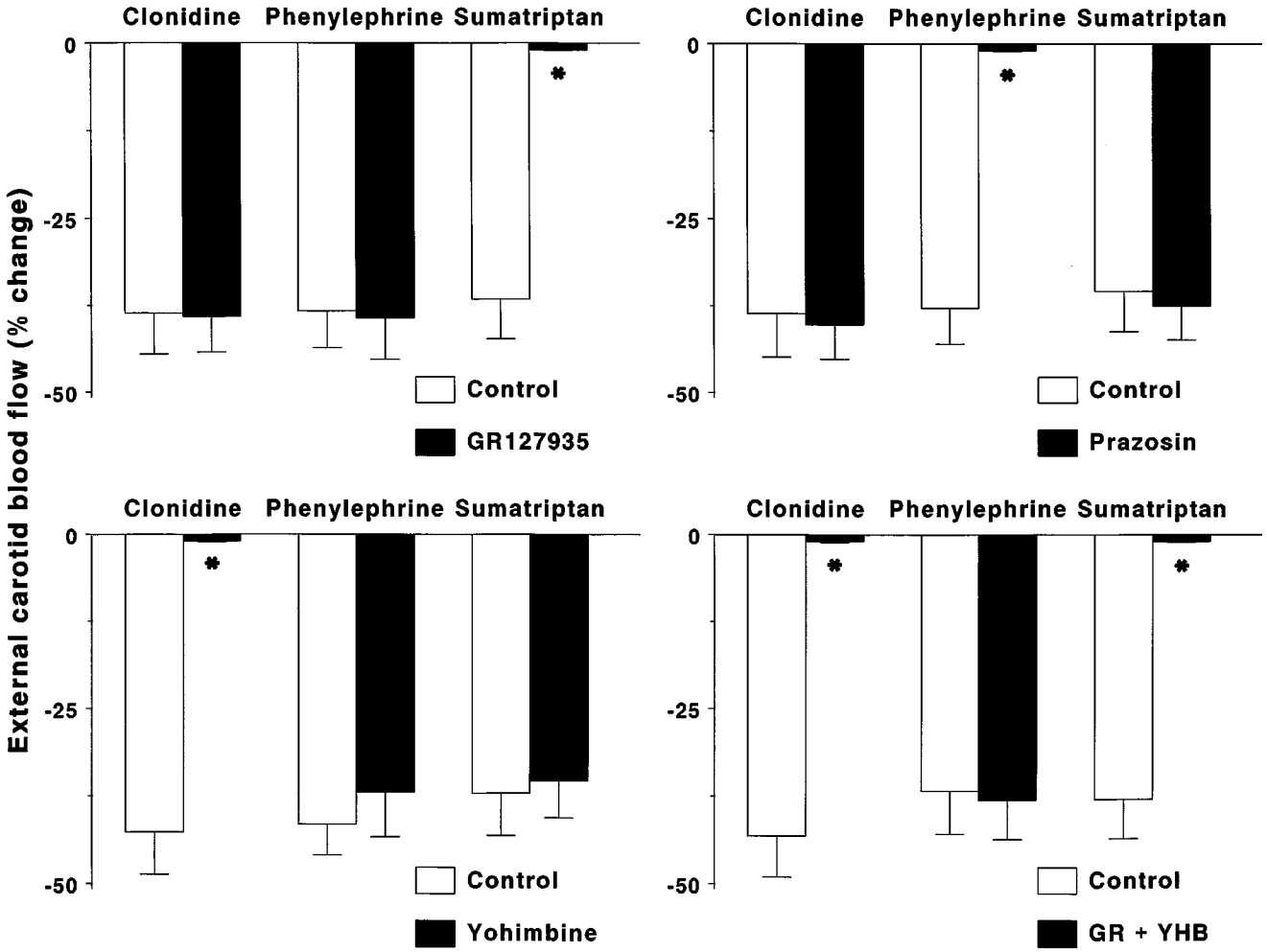

Figure 5 Percentage changes from baseline values of external carotid blood flow by 1 min i.c. infusions of clonidine (1 μg min^{-1}), phenylephrine (10 μg min^{-1}) or sumatriptan (30 μg min^{-1}) before and after i.v. administration ($n=4$ each) of either GR127935 (30 μg kg^{-1}), prazosin (300 μg kg^{-1}), yohimbine (1000 μg kg^{-1}) or the combination of GR127935 (GR; 30 μg kg^{-1}) and yohimbine (YHB; 1000 μg kg^{-1}) in vagosympathectomised dogs. All values have been presented as means$\pm$s.e.mean. *$P<0.05$ after vs before.

induced canine external carotid vasoconstriction (Terrón *et al*., 1996), did not affect the vasoconstrictor responses to either ergotamine (Figure 3) or DHE (Figure 4). These results suggest that ergotamine and DHE do not display α_1-adrenoceptor agonist properties under our experimental conditions. Indeed, this suggestion is strengthened by our results showing that the above dose of prazosin produced a selective and complete blockade of the α_1-adrenoceptor-mediated external carotid vasoconstriction induced by phenylephrine (Figure 5). It might still be argued that ergotamine and DHE could have behaved as α-adrenoceptor antagonists. Nonetheless, at such low total doses (5.6 and 31 μg for ergotamine and DHE, respectively) these ergot derivatives did not modify the external carotid vasoconstrictor responses to phenylephrine and clonidine (data not shown).

Contrasting with prazosin, yohimbine was capable of producing a partial blockade of the vasoconstrictor responses to ergotamine and DHE (see Figures 3 and 4) at a dose (1000 μg kg^{-1}) that selectively abolished clonidine-induced canine external carotid vasoconstriction (Figure 5). Taken together, the above results imply that α_2-, but not α_1-adrenoceptors, are involved, as previously suggested by other studies (Müller-Schweinitzer & Weidmann, 1978; Kalkman, 1983; Müller-Schweinitzer, 1984).

Nevertheless, it must be recognized that yohimbine also displays moderate affinity for other receptors, including α_1-adrenoceptors and 5-HT$_{1B/1D}$ receptors (see Table 1); thus, it is reasonable to assume that the above dose of the drug could have been high enough to block these, and other, receptors. Yet, lower doses of yohimbine (100 and 300 μg kg^{-1}, i.v.) did not completely block clonidine-induced external carotid vasoconstriction and higher doses (3000 μg kg^{-1}, i.v.) were not selective in our model as they also blocked phenylephrine-induced external carotid vasoconstriction (data not shown). Indeed, other *in vivo* studies have shown that yohimbine displays moderate selectivity for α_2- over the α_1-adrenoceptor in anaesthetized cats (Ramage & Tomlinson, 1985) and dogs (Shepperson *et al*., 1981).

However, as shown in Figure 5, the antagonism produced by 1000 μg kg^{-1} of yohimbine at external carotid α_2-receptors was selective, since this dose completely blocked the clonidine-induced carotid vascular effects without affecting those to sumatriptan (mediated by 5-HT$_{1B/1D}$ receptors; Villalón *et al*., 1996) and phenylephrine (mediated by α_1-adrenoceptors; Villalón & Terrón, 1994). In any case, the latter suggestion is validated by the fact that prazosin, at doses producing selective α_1-adrenoceptor antagonism did not affect the responses to ergotamine and DHE. Although beyond the scope of the

present investigation, further studies using highly selective agonists and antagonists will be required to ascertain which specific subtype(s) of the α_2-adrenoceptor is (are) producing vasoconstriction.

Possible involvement of other receptors in the carotid vasoconstrictor responses to ergotamine and DHE

As discussed above, the constriction of the canine carotid vascular bed by ergotamine and DHE is likely to be mediated by 5-$HT_{1B/1D}$ receptors, as well as α_2-adrenoceptors. The question remains open, however, whether additional receptors and/or mechanisms play a role in their effects. For this reason we studied the effects of a combination of GR127935 and yohimbine on the carotid vascular responses by the ergot alkaloids. Indeed, after simultaneous, selective blockade of both 5-$HT_{1B/1D}$ receptors and α_2-adrenoceptors, the carotid vascular effects of ergotamine and DHE are abolished. Therefore, the above results, taken collectively, suggest that the vasoconstriction of the carotid vascular bed induced by ergotamine and DHE in vagosympathectomized dogs is primarily mediated by both 5-$HT_{1B/1D}$ receptors and α_2-adrenoceptors.

On the other hand, since methysergide, ergotamine and DHE (as well as GR127935 and yohimbine) display also moderate affinity for 5-HT_{1F} receptors (see Table 1), its potential role cannot be categorically excluded in the present study, particularly when considering that mRNA for 5-ht_{1F} receptors has been shown in cranial blood vessels (Bouchelet *et al*., 1996). Indeed, sumatriptan, which displays reasonable affinity (pK_i: 7.64) for the recombinant 5-ht_{1F} receptor (Adham *et al*., 1993), also produced a GR127935-sensitive vasoconstriction in the canine external carotid bed (Villalón *et al*., 1996). Notwithstanding, two recent findings from our laboratory apparently argue against the role of 5-HT_{1F} receptors (and simultaneously reinforce the role of 5-HT_{1B} receptors): (i) 1 min i.c. infusions of LY344864 ($1-3100\ \mu g\ min^{-1}$), a selective 5-HT_{1F} receptor agonist (Phebus *et al*., 1997), did not produce canine external carotid vasoconstriction (unpublished); and (ii) SB224289 ($300\ \mu g\ kg^{-1}$), a selective 5-HT_{1B} ligand with very low affinity (pK_i: <5.0) for 5-HT_{1F} receptors (Hagan *et al*., 1997), completely blocked 5-HT- as well as sumatriptan-induced canine external carotid vasoconstriction (De Vries *et al*., 1998a).

Possible involvement of external carotid vasodilator mechanisms by ergot derivatives

Interestingly, after treatment with GR127935, not only was the methysergide-induced carotid constriction abolished, but a clear vasodilator response was unmasked. We have previously demonstrated that the 5-HT-induced external carotid vasodilatation in GR127935-pretreated vagosympathectomized dogs is mediated *via* 5-HT_7 receptors (Villalón *et al*., 1997a), as shown in other vascular preparations (Saxena *et al*., 1998). Therefore, it is tempting to suggest that methysergide could have acted *via* smooth muscle relaxant 5-HT_7 receptors, for which the compound displays high affinity (see Table 1). Nevertheless, this seems less likely, as methysergide behaves as a silent antagonist at other cardiovascular 5-HT_7 receptors, including those mediating feline tachycardia (Villalón *et al*., 1997b) and rat hypotension (Saxena & Lawang, 1985). Alternatively, methysergide may have stimulated an endothelial receptor resulting in the release of nitric oxide, possibly of the 5-HT_{2B} receptor subtype, as shown previously for other ergot derivatives in the porcine pulmonary circulation (Glusa & Roos, 1996). In support of this contention, the methysergide-induced carotid dilatory response was inhibited in animals treated with the nitric oxide synthetase inhibitor L-N^G-nitroarginine methyl ester (L-NAME; unpublished observations).

As opposed to methysergide, ergotamine and DHE did not induce any vasodilator effects in the external carotid circulation, even after complete blockade of the vasoconstrictor effects by GR127935 and yohimbine. This seems to argue the possible involvement of endothelial dilatory (5-HT) receptors, as these ergot derivatives have been shown to be potent agonists at the (5-HT_{2B}) receptors mediating endothelium-dependent vasorelaxation of porcine isolated pulmonary arteries (Glusa & Roos, 1996). It should be noted, however, that yohimbine has been shown to possess high antagonist affinity at 5-HT_{2B} receptors (Table 1) and, therefore, may have inhibited the potential ergot-induced vasorelaxant effects at these receptors. In this context, in view of the low affinity displayed by yohimbine at 5-HT_7 receptors (Table 1), it is highly unlikely that 5-HT_7 receptors mediate the potential ergotamine- and DHE-induced external carotid vasodilatation.

In conclusion, our results show that in vagosympathectomized, anaesthetized dogs, methysergide constricts the external carotid vascular bed predominantly *via* GR127935-sensitive 5-$HT_{1B/1D}$ receptors. After administration of GR127935, an external carotid vasodilator (possibly endothelial) component was unmasked. Additionally, the present results show the predominant involvement of both 5-$HT_{1B/1D}$ receptors and α_2-adrenoceptors, but not α_1-adrenoceptors, in the external carotid constriction by ergotamine and DHE. The therapeutic efficacy of these classical antimigraine drugs is likely to be mediated by these receptors, as constriction of the carotid vascular bed is highly predictive of antimigraine potential (Saxena *et al*., 1997). In this context, we have clearly demonstrated that the decrease in carotid blood flow by antimigraine agents is exclusively due to vasoconstriction of carotid arteriovenous anastomoses (for references see Saxena, 1995; Saxena *et al*., 1997), which have been suggested to be in a dilated state during migraine headaches (e.g. Heyck, 1969; Saxena, 1995). Lastly, although we cannot categorically exclude other, possibly novel receptors/mechanisms, as shown recently in the porcine carotid vasculature (De Vries *et al*., 1998b), it seems that, if present at all, these are of minor importance in the dog external carotid vascular bed.

The technical assistance of Mr Arturo Contreras is gratefully acknowledged. The authors also thank CONACyT (Mexico City, Mexico) and the pharmaceutical companies (see Drugs Section) for their support.

References

ADHAM, N., KAO, H.T., SCHECHTER, L.E., BARD, J., OLSEN, M., URQUHART, D., DURKIN, M., HARTIG, P.R., WEINSHANK, R.L. & BRANCHEK, T.A. (1993). Cloning of another human serotonin receptor (5-HT_{1F}): a fifth 5-HT_1 receptor subtype coupled to the inhibition of adenylate cyclase. *Proc. Natl. Acad. Sci. U.S.A.,* **90,** 408–412.

BARD, J.A., ZGOMBICK, J., ADHAM, N., VAYSSE, P., BRANCHEK, T.A. & WEINSHANK, R.L. (1993). Cloning of a novel human serotonin receptor (5-HT_7) positively linked to adenylate cyclase. *J. Biol. Chem.,* **268,** 23422–23426.

BAXTER, G.S., MURPHY, O.E. & BLACKBURN, T.P. (1994). Further characterization of 5-hydroxytryptamine receptors (putative 5-HT_{2B}) in rat stomach fundus longitudinal muscle. *Br. J. Pharmacol.,* **112,** 323–331.

BOUCHELET, I., COHEN, Z., CASE, B., SEGUELA, P. & HAMEL, E. (1996). Differential expression of sumatriptan-sensitive 5-hydroxytryptamine receptors in human trigeminal ganglia and cerebral blood vessels. *Mol. Pharmacol.,* **50,** 219–223.

DEN BOER, M.O., HEILIGERS, J.P.C. & SAXENA, P.R. (1991a). Carotid vascular effects of ergotamine and dihydroergotamine in the pig: no exclusive mediation via 5-HT_1-like receptors. *Br. J. Pharmacol.,* **104,** 183–189.

DEN BOER, M.O., VILLALÓN, C.M., HEILIGERS, J.P.C., HUMPHREY, P.P.A. & SAXENA, P.R. (1991b). Role of 5-HT_1-like receptors in the reduction of porcine cranial arteriovenous anastomotic shunting by sumatriptan. *Br. J. Pharmacol.,* **102,** 323–330.

DE VRIES, P., HEILIGERS, J.P.C., VILLALÓN, C.M. & SAXENA, P.R. (1996). Blockade of porcine carotid vascular response to sumatriptan by GR127935, a selective 5-HT_{1D} receptor antagonist. *Br. J. Pharmacol.,* **118,** 85–92.

DE VRIES, P., SÁNCHEZ-LÓPEZ, A., CENTURIÓN, D., HEILIGERS, J.P.C., SAXENA, P.R. & VILLALÓN, C.M. (1998a). The canine external carotid vasoconstrictor 5-HT_1 receptor: blockade by 5-HT_{1B} (SB224289), but not by 5-HT_{1D} (BRL15572) receptor antagonists. *Eur. J. Pharmacol.,* **362,** 69–72.

DE VRIES, P., VILLALÓN, C.M., HEILIGERS, J.P.C. & SAXENA, P.R. (1998b). Characterisation of 5-HT receptors mediating constriction of porcine carotid arteriovenous anastomoses; involvement of 5-$HT_{1B/1D}$ and novel receptors. *Br. J. Pharmacol.,* **123,** 1561–1570.

GLUSA, E. & ROOS, A. (1996). Endothelial 5-HT receptors mediate relaxation of porcine pulmonary arteries in response to ergotamine and dihydroergotamine. *Br. J. Pharmacol.,* **119,** 330–334.

HAGAN, J.J., SLADE, P.D., GASTER, L., JEFFREY, P., HATCHER, J.P. & MIDDLEMISS, D.N. (1997). Stimulation of 5-HT_{1B} receptors causes hypothermia in the guinea pig. *Eur. J. Pharmacol.,* **331,** 169–174.

HARTIG, P.R., HOYER, D., HUMPHREY, P.P.A. & MARTIN, G.R. (1996). Alignment of receptor nomenclature with the human genome: classification of 5-HT_{1B} and 5-HT_{1D} receptor subtypes. *Trends Pharmacol. Sci.,* **17,** 103–105.

HEYCK, H. (1969). Pathogenesis of migraine. *Res. Clin. Stud. Headache,* **2,** 1–28.

HOFFMAN, B.B. & LEFKOWITZ, R.J. (1996). Catecholamines, sympathomimetic drugs and adrenergic receptor antagonists. In *Goodman & Gilman's The Pharmacological Basis of Therapeutics*. eds. Hardman, J.G., Limbird, L.E., Molinoff, P.B., Ruddon, R.W. & Goodman Gilman, A., pp. 199–248: McGraw-Hill Book Co.

HOYER, D. (1988). Functional correlates of serotonin 5-HT_1 recognition sites. *J. Rec. Res.,* **8,** 59–81.

HOYER, D., CLARKE, D.E., FOZARD, J.R., HARTIG, P.R., MARTIN, G.R., MYLECHARANE, E.J., SAXENA, P.R. & HUMPHREY, P.P. (1994). International Union of Pharmacology classification of receptors for 5-hydroxytryptamine (Serotonin). *Pharmacol. Rev.,* **46,** 157–203.

KALKMAN, H.O. (1983). The cardiovascular profile of ergotamine in pithed rats; evidence for α_2-mimetic activity in arteries and veins. In *Vascular serotonin receptors (Ph.D. Thesis, University of Amsterdam)*, 83–94. Amsterdam: Rodopi.

KLEINMAN, L.I. & RADFORD, E.P. (1964). Ventilation standards for small mammals. *J. Appl. Physiol.,* **19,** 360–362.

LEYSEN, J.E. (1985). Serotonergic binding sites. In *Serotonin and the cardiovascular system*. eds. Vanhoutte, P.M., 43–62. New York: Raven Press.

LEYSEN, J.E. & GOMMEREN, W. (1984). In vitro binding profile of drugs used in migraine. In *The pharmacological basis of migraine therapy*. eds. Amery, W.K., Van Neuten, J.M. & Wauquier, A., 255–266. London: Pitman Publishing Ltd.

LEYSEN, J.E., GOMMEREN, W., HEYLEN, L., LUYTEN, W.H., VAN DE WEYER, I., VANHOENACKER, P., HAEGEMAN, G., SCHOTTE, A., VAN GOMPEL, P., WOUTERS, R. & LESAGE, A.S. (1996). Alniditan, a new 5-hydroxytryptamine$_{1D}$ agonist and migraine-abortive agent: ligand-binding properties of human 5-hydroxytryptamine$_{1D\alpha}$, human 5-hydroxytryptamine$_{1D\beta}$, and calf5-hydroxytryptamine$_{1D}$ receptors investigated with [^{3}H]5-hydroxytryptamine and [^{3}H]alniditan. *Mol. Pharmacol.,* **50,** 1567–1580.

MAASSENVANDENBRINK, A., REEKERS, M., BAX, W.A., BERRARI, M.D. & SAXENA, P.R. (1998). Coronary side-effect potential of current and prospective antimigraine drugs. *Circulation,* **98,** 25–30.

MARTIN, G.R. (1994). Vascular receptors for 5-hydroxytryptamine: distribution, function and classification. *Pharmacol. Ther.,* **62,** 283–324.

MARTIN, G.R., MARTIN, R.S. & WOOD, J. (1995). Long-acting 5-HT_{1D} receptor agonist effects of dihydroergotamine. Studies using a model to differentiate slow drug-receptor dissociation from diffusion. In *Experimental headache models*. eds. Olesen, J. & Moskowitz, M.A., 163–167. Philadelphia: Lippincott-Raven Publishers.

MASSINGHAM, R. & HAYDEN, M.L. (1975). A comparison of the effects of prazosin and hydrallazine on blood pressure, heart rate and plasma renin activity in conscious renal hypertensive dogs. *Eur. J. Pharmacol.,* **30,** 121–124.

MÜLLER-SCHWEINITZER, E. (1984). Alpha-adrenoceptors, 5-hydroxytryptamine receptors and the action of dihydroergotamine in human venous preparations obtained during saphenectomy procedures for varicose veins. *Naunyn-Schmiedeberg's Arch. Pharmacol.,* **327,** 299–303.

MÜLLER-SCHWEINITZER, E. & WEIDMANN, H. (1978). Basic pharmacological properties. In *Ergot alkaloids and related compounds*. eds. Berde, B. & Schild, H.O., pp. 87–232. Berlin, Heidelberg, New York: Springer Verlag.

MYLECHARANE, E.J., SPIRA, P.J., MISBACH, J., DUCKWORTH, J.W. & LANCE, J.W. (1978). Effects of methysergide, pizotifen and ergotamine in the monkey cranial circulation. *Eur. J. Pharmacol.,* **48,** 1–9.

PAUWELS, P.J. (1996). Pharmacological properties of a putative 5-$HT_{1B/D}$ receptor antagonist GR127935. *CNS Drug Rev.,* **2,** 415–428.

PHEBUS, L.A., JOHNSON, K.W., ZGOMBICK, J.M., GILBERT, P.J., VAN BELLE, K., MANCUSO, V., NELSON, D.L., CALLIGARO, D.O., KIEFER, JR, A.D., BRANCHEK, T.A. & FLAUGH, M.E. (1997). Characterization of LY344864 as a pharmacological tool to study 5-HT_{1F} receptors: binding affinities, brain penetration and activity in the neurogenic dural inflammation model of migraine. *Life Sci.,* **61,** 2117–2126.

PRICE, G.W., BURTON, M.J., COLLIN, L.J., DUCKWORTH, M., GASTER, L., GÖTHERT, M., JONES, B.J., ROBERTS, C., WATSON, J.M. & MIDDLEMISS, D.N. (1997). SB-216641 and BRL-15572-compounds to pharmacologically discriminate h5-HT_{1B} and h5-HT_{1D} receptors. *Naunyn-Schmiedeberg's Arch. Pharmacol.,* **356,** 312–320.

RAMAGE, A.G. & TOMLINSON, A. (1985). The effect of yohimbine, WY 26392 and idazoxan on sympathetic nerve activity. *Eur. J. Pharmacol.,* **109,** 153–160.

SAXENA, P.R. (1974a). Selective carotid vasoconstriction by ergotamine as a relevant mechanism in its antimigraine action. *Arch. Neurobiol.,* **37,** S301–S315.

SAXENA, P.R. (1974b). Selective vasoconstriction in carotid vascular bed by methysergide: possible relevance to its antimigraine effect. *Eur. J. Pharmacol.,* **27,** 99–105.

SAXENA, P.R. (1995). Cranial arteriovenous shunting, an *in vivo* animal model for migraine. In *Experimental headache models*. eds. Olesen, J. & Moskowitz, M.A., pp. 189–198. Philadelphia: Lippincott-Raven Publishers.

SAXENA, P.R. & DE VLAAM-SCHLUTER, G.M. (1974). Role of some biogenic substances in migraine and relevant mechanism in antimigraine action of ergotamine-studies in an experimental model for migraine. *Headache,* **13,** 142–163.

SAXENA, P.R., DE VRIES, P. & VILLALÓN, C.M. (1998). 5-HT_1-like receptors: a time to bid good-bye. *Trends Pharmacol. Sci.,* **19,** 311–316.

SAXENA, P.R., FERRARI, M.D., DE VRIES, P. & VILLALÓN, C.M. (1997). Pharmacological overview of new 5-HT_{1D} receptor agonists in development for the acute treatment of migraine. In *Headache treatment: trial methodology and new drugs*. eds. Olesen, J. & Tfelt-Hansen, P., pp. 229–241. New York: Lippincott-Raven publishers.

SAXENA, P.R., KOEDAM, N.A., HEILIGERS, J. & HOF, R.P. (1983). Ergotamine-induced constriction of cranial arteriovenous anastomoses in dogs pretreated with phentolamine and pizotifen. *Cephalalgia,* **3,** 71–81.

SAXENA, P.R. & LAWANG, A. (1985). A comparison of cardiovascular and smooth muscle effects of 5-hydroxytryptamine and 5-carboxamidotryptamine, a selective agonist of 5-HT_1 receptors. *Arch. Int. Pharmacodyn. Ther.,* **277,** 235–252.

SAXENA, P.R. & VERDOUW, P.D. (1984). Effects of methysergide and 5-hydroxytryptamine on carotid blood flow distribution in pigs: further evidence for the presence of atypical 5-HT receptors. *Br. J. Pharmacol.,* **82,** 817–826.

SHEPPERSON, N.B., DUVAL, N., MASSINGHAM, R. & LANGER, S.Z. (1981). Pre- and postsynaptic alpha adrenoceptor selectivity studies with yohimbine and its two diastereoisomers rauwolscine and corynanthine in the anesthetized dog. *J. Pharmacol. Exp. Ther.,* **219,** 540–546.

SKINGLE, M., BEATTIE, D.T., SCOPES, D.I.T., STARKEY, S.J., CONNOR, H.E., FENIUK, W. & TYERS, M.B. (1996). GR127935: a potent and selective 5-HT_{1D} receptor antagonist. *Behav. Brain Res.,* **73,** 157–161.

SPIERINGS, E.L. & SAXENA, P.R. (1980). Antimigraine drugs and cranial arteriovenous shunting in the cat. *Neurology,* **30,** 696–701.

STEEL, R.G.D. & TORRIE, J.H. (1980). *Principles and procedures of statistics. A biomedical approach* (2nd edition), Tokyo: McGraw-Hill Kogakusha Ltd.

TERRÓN, J.A., RAMIREZ-SAN JUAN, E., HONG, E. & VILLALÓN, C.M. (1996). Role of $alpha_1$-adrenoceptors in the reduction of external carotid blood flow induced by buspirone and ipsapirone in the dog. *Life Sci.,* **58,** 63–73.

VILLALÓN, C.M., BOM, A.H., DEN BOER, M.O., HEILIGERS, J.P. & SAXENA, P.R. (1992). Effects of S9977 and dihydroergotamine in an animal experimental model for migraine. *Pharmacol. Res.,* **25,** 125–137.

VILLALÓN, C.M., CENTURIÓN, D., LUJÁN-ESTRADA, M., TERRÓN, J.A. & SÁNCHEZ-LÓPEZ, A. (1997a). Mediation of 5-HT-induced external carotid vasodilatation in GR127935-pretreated vagosympathectomized dogs by the putative 5-HT_7 receptor. *Br. J. Pharmacol.,* **120,** 1319–1327.

VILLALÓN, C.M., HEILIGERS, J.P.C., CENTURIÓN, D., DE VRIES, P. & SAXENA, P.R. (1997b). Characterization of putative 5-HT_7 receptors mediating tachycardia in the cat. *Br. J. Pharmacol.,* **121,** 1187–1195.

VILLALÓN, C.M., RABELO, G., SÁNCHEZ, A., CENTURIÓN, D., DE VRIES, P. & SAXENA, P.R. (1998). Pharmacological profile of the receptors involved in the external carotid vasoconstrictor response to ergotamine, dihydroergotamine and methysergide in the dog. *Naunyn-Schmiedeberg's Arch. Pharmacol.,* **358,** R229.

VILLALÓN, C.M., RAMIREZ-SAN, JUAN, E., CASTILLO, C., CASTILLO, E., LOPEZ-MUNOZ, F.J. & TERRÓN, J.A. (1995). Pharmacological profile of the receptors that mediate external carotid vasoconstriction by 5-HT in vagosympathectomized dogs. *Br. J. Pharmacol.,* **116,** 2778–2784.

VILLALÓN, C.M., SÁNCHEZ-LÓPEZ, A. & CENTURIÓN, D. (1996). Operational characteristics of the 5-HT_1-like receptors mediating external carotid vasoconstriction in vagosympathectomized dogs; close resemblance to the 5-HT_{1D} receptor subtype. *Naunyn-Schmiedeberg's Arch. Pharmacol.,* **354,** 550–556.

VILLALÓN, C.M. & TERRÓN, J.A. (1994). Characterization of the mechanisms involved in the effects of catecholamines on the canine external carotid blood flow. *Can. J. Physiol. Pharmacol.,* **72,** 165.

VILLALÓN, C.M., TERRÓN, J.A. & HONG, E. (1993). Role of 5-HT_1-like receptors in the increase in external carotid blood flow induced by 5-hydroxytryptamine in the dog. *Eur. J. Pharmacol.,* **240,** 9–20.

(Received August 17, 1998
Revised September 28, 1998
Accepted October 28, 1998)

British Journal of Pharmacology (1999) 126, 595–606
http://www.stockton-press.co.uk/bjp

Non-specific action of methoxamine on I_{to}, and the cloned channels hKv 1.5 and Kv 4.2

[1]Chris Parker, [1]Qi Li & *,[1]David Fedida

[1]Department of Physiology, Queen's University Kingston, Kingston, Ontario, K7L 3N6, Canada

1 The α_1-adrenoceptor agonist methoxamine acted independently of receptor activation to reduce I_{to} and the sustained outward current in rat ventricular myocytes, and hKv 1.5 and Kv 4.2 cloned K^+ channel currents. Two hundred μM methoxamine reduced I_{to} by 36% in the presence of 2 μM prazosin, and by 37 and 38% after preincubation of myocytes with either N-ethylmaleimide or phenoxybenzamine ($n=6$). The EC_{50} values at +60 mV for direct reduction of I_{to}, hKv 1.5, and Kv 4.2 by methoxamine were 239, 276, and 363 μM, respectively, with Hill coefficients of 0.87–1.5.

2 Methoxamine accelerated I_{to} and Kv 4.2 current inactivation in a concentration- and voltage-dependent manner. Apparent rate constants for methoxamine binding and unbinding gave K_d values in agreement with EC_{50} values measured from dose-response relations. The voltage-dependence of block supported charged methoxamine binding to a putative intracellular site that sensed ~20% of the transmembrane electrical field.

3 In the presence of methoxamine, deactivating Kv 4.2 tail currents displayed a distinct rising phase, and were slowed relative to control, such that tail current crossover was observed. These observations support a dominant mechanism of open channel block, although closed channel block could not be ruled out.

4 Single-channel data from hKv 1.5 patches revealed increased closed times with blank sweeps and decreased burst duration in the presence of drug, and a reduction of mean channel open time from 1.8 ms in control to 0.4 ms in 500 μM methoxamine. For this channel, therefore, both open and closed channel block appeared to be important mechanisms for the action of methoxamine.

Keywords: Methoxamine; transient outward current; hKv 1.5; Kv 4.2; channel block

Abbreviations: CTL, control; δ, fraction of transmembrane electric field sensed by a singly-charged drug molecule at its receptor site; Mox, methoxamine; NEM, N-ethylmaleimide; PE, phenylephrine; PhBz, phenoxybenzamine; Pz, prazosin; τ_{block}, time constant of block of current by drug; $\tau_{deactivation}$, time constant of deactivation of tail currents; τ_{decay}; time constant of current decay in the presence of drug; τ_{inact}; time constant of control current inactivation

Introduction

Inhibition of repolarizing K^+ currents in cardiac muscle in response to α-adrenoceptor stimulation by hormones, neurotransmitters, and drugs is one mechanism of positive inotropy in the heart, which becomes increasingly important pathophysiologically when α_1-adrenoceptors are increased in proportion to other adrenoceptor subtypes, such as during heart failure (Hwang *et al*., 1996). Many previous studies of α_1-adrenoceptor-mediated responses in cardiac tissues have used the α-adrenoceptor-specific agonist methoxamine (Fedida *et al*., 1990), since methoxamine lacks activity at β-adrenoceptors. Structurally, methoxamine is related to phenylephrine, but has greater specificity for the α_1-adrenoceptor subtypes. Several studies, however, have demonstrated that methoxamine, especially at high concentrations, can produce pharmacological responses that differ from those observed in response to phenylephrine. In sinoatrial nodal cells, for example, methoxamine reduced the slow inward (I_{si}) and the hyperpolarization-activated (I_h) currents, whereas phenylephrine, in the presence of pindolol, increased both of these currents (Satoh & Hashimoto, 1988). The authors speculated that methoxamine may have had non-specific actions in addition to its activity at α_1-adrenoceptors. Here we have investigated prazosin-insensitive actions of methoxamine on I_{to} in isolated rat ventricular cardiac myocytes, and in further experiments we have studied methoxamine block of current carried by two cloned potassium channels, hKv 1.5 and Kv 4.2. The results suggest that methoxamine can inhibit voltage-gated K^+ currents independently of α_1-adrenoceptor activation.

*Author for correspondence at: Department of Physiology, University of British Columbia, 2146 Health Sciences Mall, Vancouver, British Columbia V6T 1Z3, Canada.

Methods

Myocyte isolation and cell culture

Hearts were rapidly removed from male rats weighing between 150 and 250 g previously anaesthetized with sodium pentobarbitone (80 mg kg^{-1}, i.p.), and ventricular cells were isolated as previously described for rabbit myocytes (Braun *et al*., 1990). hKv 1.5 or Kv 4.2 were stably or transiently transfected into human embryonic kidney 293 (HEK) cells using the vector pCDNA3 (Invitrogen, San Diego, CA, U.S.A.). Transfected cells were plated on glass coverslips in 25 mm Petri dishes, and maintained in Modified Eagle's Medium (MEM) at 37°C in an air/5% CO_2 incubator until use. Cells transiently expressing hKv 1.5 or Kv 4.2 were detected by co-transfection with pHook-1 (Invitrogen), as previously described (Zhang *et al*., 1997).

Electrophysiological solutions

For whole-cell recording from myocytes, the pipette filling solution contained (in mM): KCl, 20; K-aspartate, 120; EGTA, 1; $MgCl_2$, 1; HEPES, 5; Na_2ATP, 4; GTP, 0.1; pH 7.2 with KOH. For HEK cells, K-aspartate was substituted by KCl. The bath solution for both cell types contained (in mM): NaCl, 135; KCl, 5; sodium acetate, 2.8; $MgCl_1$, 1; HEPES, 10; $CaCl_2$, 1; pH 7.4 with NaOH. For cell-attached recordings, the pipette was filled with this bath solution and the membrane potential was zeroed with a solution that contained (in mM): KCl, 135; $MgCl_2$, 1; HEPES, 10; $CaCl_2$, 1; dextrose, 10; pH 7.4 with KOH. For myocyte experiments, bath solutions were continuously bubbled with 100% O_2, and contained 5 μM propranolol to block β-adrenergic stimulation, and 300 μM $CdCl_2$ to block calcium and calcium-activated currents. Methoxamine (Mox), phenylephrine (PE), phenoxybenzamine (PhBz), and N-ethylmaleimide (NEM) were prepared in water just prior to use, at appropriate stock concentrations. Prazosin (Pz) was dissolved in ethanol at 2 mM, and protected from light. The concentration of ethanol in the bath solution never exceeded 0.1%. When cells were exposed to methoxamine, effects on membrane currents usually reached a steady-state within 1–2 min so that drug exposure times rarely exceeded 5 min. All chemicals were from Sigma Chemical Co. (St. Louis, MO, U.S.A.).

Electrophysiological procedures and analysis

All experiments were carried out at 22–23°C. Whole-cell recordings were made using an Axopatch 200A amplifier (Axon Instruments, Foster City, CA, U.S.A.). Patch electrodes were pulled from thin-walled borosilicate glass (TW150, World Precision Instruments, FL, U.S.A.) and had resistances of 1.5–3.0 MΩ. Capacity compensation and 75–85% series resistance compensation were used in all measurements. In some experiments involving HEK cells, leak subtraction was applied to data. Data were filtered at 5–10 kHz before digitization and stored on a microcomputer for later analysis using pClamp6 software (Axon Instruments). The transient outward current (I_{to}) amplitude from rat ventricular myocytes was taken to represent the peak outward current measured during depolarizing voltage steps, as described previously (Apkon & Nerbonne, 1988). The dose-response curves (Figures 2B, 4D, and 5B) for current inhibition produced by methoxamine were computer-fitted to a Hill equation:

$$f = \max/[1 + (EC_{50}/[D]^{n_H})] \quad (1)$$

where f is the percentage current block ($f = [1 - I_{drug}/I_{control}] \times 100\%$) at drug concentration [D], max is the maximum fitted level of block, EC_{50} is the concentration producing half-maximal inhibition, and n_H is the Hill coefficient.

In rat ventricular myocytes, outward currents evoked upon depolarization contain at least two kinetic components, the first of which activates and inactivates rapidly (I_{to}), while the kinetics of the second are at least 10 fold slower, as previously described (Apkon & Nerbonne, 1991). Thus, peak outward current was taken to represent predominantly I_{to}, with only a negligible contribution from the second, slowly-activating sustained component of the outward current. I_{to} and the sustained current component also differ in their voltage-dependence of steady-state inactivation, and this can be used to separate them (Apkon & Nerbonne, 1991). After a 1 s conditioning step to −100 mV, outward currents evoked at a test potential of +60 mV exhibited both transient and sustained components (Figure 3A). After a conditioning step to −60 mV the sustained current was preferentially inactivated with only minimal effects on the peak outward current, whereas a prepulse to 0 mV inactivated both currents, and left only a small residual current representing leak and other non-inactivating currents. I_{to} was isolated by subtracting current traces recorded using a conditioning potential of 0 mV from those recorded using a conditioning potential of −60 mV. Single-exponential fits to this difference current, measured under control conditions, were taken to represent the time constant of inactivation (τ_{inact}) of I_{to}. For Kv 4.2, control current traces were better fit to a second order exponential function, and the fast inactivation time constant in control was denoted τ_{inact}. In the presence of drug, I_{to} and Kv 4.2 currents were fit to second-order exponentials, and the fast time constants of current decay in the presence of each concentration of drug were denoted τ_{decay}, since they represented both inactivation and block of current by drug. We extracted time constants of methoxamine block (τ_{block}) as an approximation of the drug-channel interaction kinetics as previously described (Slawsky & Castle, 1994; Snyders & Yeola, 1995), using:

$$1/\tau_{decay} = 1/\tau_{block} + 1/\tau_{inact} \quad (2)$$

and values of τ_{inact} measured as indicated above. In addition we calculated first order rate constants for block, using:

$$1/\tau_{block} = k_{+1}\,[D] + k_{-1} \quad (3a)$$

and

$$K_d = k_{-1}/k_{+1} \quad (3b)$$

in which k_{+1} and k_{-1} are the apparent rate constants of binding and unbinding for the drug, respectively, and K_d is the equilibrium dissociation constant. For single channel analysis, blank sweeps were averaged and subtracted from all current traces to compensate for leak and capacity currents. Data were filtered at 1 kHz for presentation and analysis. Experimental values are given as means ± s.e.mean. For the data in Figures 1E, 4C and 5C, repeated measures ANOVA was used to determine significance. In all other cases, paired or unpaired *t*-tests were used, as appropriate. A value of $P < 0.05$ was considered statistically significant.

Results

Methoxamine can reduce outward currents independently of α_1-adrenoceptor activation

In isolated rat ventricular myocytes, methoxamine reduced the amplitude of the outward currents, and this effect had both prazosin-sensitive and prazosin-insensitive components, as illustrated by the data in Figure 1A–D. Addition of 200 μM methoxamine (B) reduced the amplitude of transient and sustained outward currents compared with control (A) across the entire potential range where currents could be measured. After wash, 2 μM prazosin was added to the bath solution (C), which has been shown to inhibit α-adrenergic responses in isolated cardiac myocytes (Fedida *et al*., 1991; Li *et al*., 1996). Even in the presence of prazosin, however, 200 μM methoxamine was still able to reduce current amplitude (D), although this effect was not as great as that observed with methoxamine alone. Specifically, at +60 mV, 200 μM methoxamine in the presence of prazosin was able to reduce peak outward current (I_{to}, see Methods) to 69.5 ± 0.4% ($n = 6$) of control. After washout, some cells were exposed for a second time to the same concentration of methoxamine and prazosin, which resulted in a reduction of I_{to} to 69.2 ± 0.7% of control ($n = 5$),

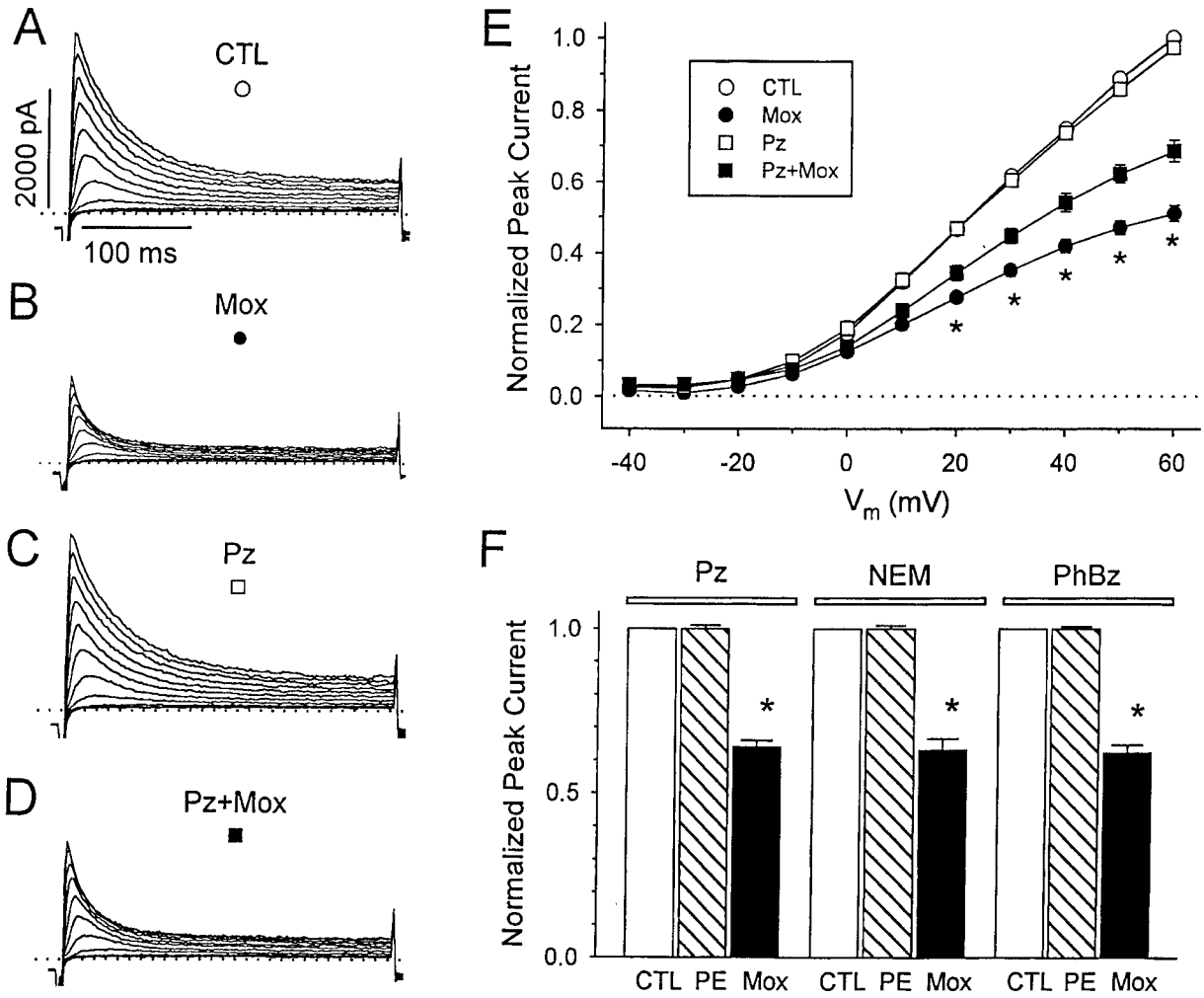

Figure 1 Methoxamine directly blocks outward currents in rat ventricular myocytes. A–D, currents from a representative myocyte during depolarizations from −80 mV to between −20 and +60 mV, in 10 mVsteps at a pulse frequency of 0.2 Hz. Dotted lines denote zero current level. Control (CTL, A) and with 200 μM methoxamine (Mox, B) after 5 min exposure. After 15 min of wash in control solution the cell was exposed to 2 μM prazosin (Pz, C) and then 200 μM methoxamine plus 2 μM prazosin (Pz+Mox, D). (E) mean peak I_{to} current-voltage relations in control and during exposure to prazosin or methoxamine, or both ($n=6$). For each cell, I_{to} was normalized to peak current in control solution measured at +60 mV. Symbols are as marked in panels A–D. * Indicates significant differences between current amplitudes in methoxamine alone compared with both methoxamine and prazosin, $P<0.05$. (F) block of signal transduction does not prevent the action of methoxamine. Effects of 100 μM phenylephrine (PE) and 200 μM methoxamine (Mox) on I_{to} amplitude in the presence of 2 μM prazosin (Pz), or after 30 min pretreatment with 50 μM N-ethylmaleimide (NEM) or 1 μM phenoxybenzamine (PhBz), as indicated. Currents were measured at +60 mV, and were normalized to I_{to} amplitude in the absence of α-agonist, but in the presence of Pz, NEM, or PhBz. Data are means±s.e.mean ($n=6$). * indicates a significant difference from control, $P<0.05$.

which was not significantly different from that produced by the first exposure. Phenylephrine is approximately ten times more potent than methoxamine in stimulating α_1-adrenoceptors (Yang & Endoh, 1994), and addition of 100 μM phenylephrine resulted in a significant decrease in I_{to} amplitude that was completely blocked by 2 μM prazosin ($n=5$).

Mean current-voltage relations for peak current reduction in response to methoxamine are shown in Figure 1E. Both the prazosin-sensitive and -insensitive actions of methoxamine affected current at all positive potentials. However, while the prazosin-sensitive action of methoxamine was relatively potential-independent, the prazosin-insensitive inhibition of I_{to} increased at the more positive potentials studied, greater than +20 mV. These data suggest that methoxamine reduced I_{to} in a manner that was both dependent upon, and independent of α-adrenoceptor activation. The increasing block of I_{to} at more positive potentials caused by methoxamine in the presence of prazosin was fitted with a Woodhull equation (Woodhull, 1973) which allowed calculation of the fraction of the electric field (δ) sensed by a singly charged drug molecule at its receptor site. From data in Figure 1E, a value of $\delta=0.18$ was obtained.

Prazosin is a competitive antagonist of α-adrenoceptors. To explore the possibility that methoxamine was merely overcoming prazosin block, cells were exposed to the alkylating agents NEM or PhBz (Figure 1F). NEM, which alkylates sulphhydryl groups, has been shown to inhibit GTP-binding proteins, including G-proteins (Ueda *et al.*, 1990). There is substantial molecular homogeneity between cardiac α_1-adrenoceptors and the primary sequences of other members of the G-protein-binding superfamily (Harrison *et al.*, 1991), and it appears that in mammalian cardiac cells, the effects of α_1-adrenoceptor stimulation are primarily transduced *via* G-proteins (Im & Graham, 1990; Wu *et al.*, 1992; Nakaoka *et al.*, 1994), and it has been demonstrated that NEM can inhibit α_1-adrenoceptor-mediated responses (Liebau *et al.*, 1989). PhBz

irreversibly alkylates α-adrenoceptors, with relative specificity for the α_1 subtypes, and its use as an α-adrenoceptor antagonist has been well described (Minneman *et al*., 1994).

Preincubation of isolated cardiac myocytes for 30 min with either 50 μM NEM or 1 μM PhBz failed to prevent the reduction of peak outward current observed in response to methoxamine (Figure 1F). The mean reduction of I_{to} in response to 200 μM methoxamine in NEM- or PhBz-pretreated cells was 37.0±3.5% ($n=6$, mean±s.e.mean), and 37.8±2.4% ($n=6$) respectively, as shown by the solid bars in Figure 1F. These results are comparable with, and not significantly different from, the mean reduction observed in response to methoxamine in the presence of prazosin, which was 36.0±1.9% ($n=6$). In contrast to methoxamine, all three agents antagonized the action of 100 μM phenylephrine. These data also suggest that methoxamine resulted in an inhibition of I_{to} that was not mediated through α_1-adrenergic receptor pathways.

Inhibition of I_{to} by methoxamine is concentration dependent

The non-specific action of methoxamine was concentration-dependent, as illustrated in Figure 2. Increasing concentrations of methoxamine, in the presence of 2 μM prazosin, decreased both the peak and steady-state levels of the outward currents recorded on depolarization (Figure 2A). As described previously for adult rat ventricular myocytes, depolarization-activated outward currents are composed of at least two kinetically distinct components: one that activates and inactivates rapidly (I_{to}), and one that activates and inactivates slowly (Apkon & Nerbonne, 1991). Since the more rapid of these components activates approximately 10 fold faster and inactivates approximately 30 fold faster than the slowly-activating component, the peak outward current predominantly reflects I_{to}, whereas the plateau current remaining after 100 ms should largely reflect the contribution of the second slower component. For purposes of analysis, therefore, we have considered only the effects of methoxamine on the peak transient current as a reflection of drug effects on I_{to}. In the dose-response relation in Figure 2B, data points correspond to percentage current block by methoxamine of the peak current in response to a depolarizing voltage step to +60 mV from a holding potential of −80 mV. The solid line was fitted to the data using equation [1]. The EC_{50} at +60 mV was 239 μM, and n_H was 1.5. The threshold for non-specific inhibition of I_{to} by methoxamine was between 10 and 50 μM, and the peak amplitude of I_{to} was then decreased by methoxamine in a concentration-dependent manner. The concentration of methoxamine that resulted in a maximum reduction of I_{to} was difficult to determine, as concentrations greater than 1 mM were often toxic to the myocytes. Based on the results of the fit to the Hill equation, it is likely that a maximum reduction of I_{to} of about 75% could be achieved at concentrations of methoxamine greater than 2–5 mM.

Methoxamine accelerates I_{to} inactivation in a concentration and voltage-dependent manner

In addition to decreasing I_{to} amplitude, increasing concentrations of methoxamine also apparently accelerated the rate of I_{to} decay. However, methoxamine reduced not only I_{to}, but also the sustained outward current component as well. Therefore, in order to measure the rate of I_{to} decay alone, we separated these two current components using a voltage protocol based on the differences in voltage-dependence of

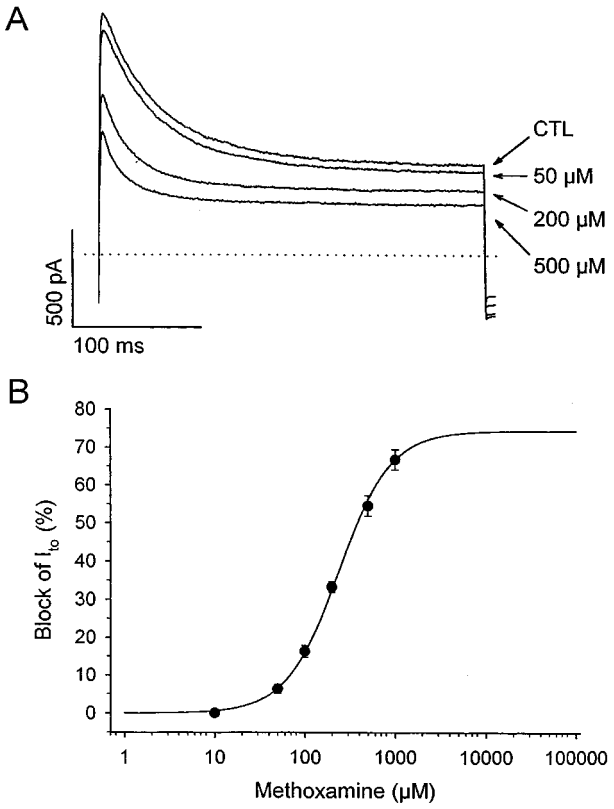

Figure 2 Concentration-dependence of non-specific action of methoxamine on I_{to} in rat ventricular myocytes. (A) currents recorded during steps to +60 mV from −80 mV in the presence of 2 μM prazosin (CTL), and in response to 50, 200, and 500 μM methoxamine in the presence of prazosin, as indicated. (B) dose-response curve for the non-specific action of methoxamine. Data are means±s.e.mean from 6–14 cells at each concentration. Solid line was fit to data using equation [1]. The EC_{50} value was 239 μM and the Hill coefficient, n_H, was 1.5, with a maximum expected block of 75%.

steady-state inactivation of I_{to} and the sustained current component. Outward currents were measured at +60 mV after 1 s conditioning pulses to −100, −60, or 0 mV, as shown in Figure 3A. After a −100 mV prepulse, outward current comprised both transient and sustained components, but after a conditioning prepulse to −60 mV, the sustained component was largely inactivated with little effect on peak current. Both components were inactivated by a 0 mV prepulse. I_{to} and the sustained current component were isolated by subtraction as described in the Methods, and are illustrated in the lower panel of Figure 3A. The current traces in the inset to Figure 3B show I_{to} under control conditions and in the presence of 200 and 500 μM methoxamine, as indicated. Control currents were fitted with a single exponential function, whereas in the presence of drug, currents have been fitted to a double exponential decay (solid lines). There is a clear concentration-dependent acceleration of current decay in the presence of the drug. In controls, during 250 ms depolarizations, I_{to} inactivation at +60 mV had a time constant, τ_{inact} of 34.6±1.2 ms ($n=9$). In the presence of methoxamine and prazosin the rapid time constant of current decay, τ_{decay}, accelerated with increasing concentrations of methoxamine. From these data we extracted the concentration-dependence of $(1/\tau_{block})$ as described in the Methods and shown in Figure 3B. $1/\tau_{block}$ increased linearly over a wide range of drug concentrations, and τ_{block} was taken as an approximation of the time course of drug-channel interaction (Slawsky & Castle, 1994). From

equation [3a] the best least-squares fit to $1/\tau_{block}$, as indicated by the solid line in Figure 3B, resulted in an apparent association rate constant, k_{+1}, of 8.9×10^4 M^{-1} s^{-1}, and an apparent dissociation rate constant, k_{-1}, of 32.9 s^{-1}. Using equation [3b], the calculated K_d was 307 μM, which is in agreement with the EC_{50} value of 239 μM obtained from the dose-response curve (Figure 2B).

τ_{block} also decreased in a voltage-dependent manner, while time constants obtained from monoexponential fits to control current inactivation (τ_{inact}) showed little voltage-dependence over the same potential range (Figure 3C, □). On the other hand, τ_{decay}, measured in the presence of 200 μM methoxamine, decreased from a value of 28.8 ± 1.9 ms at +10 mV to a value of 11.6 ± 1.0 ms at +60 mV. From these measurements we extracted values for τ_{block} (Figure 3C, ●), which decreased from 103 ± 13.9 ms at +10 mV to 15.9 ± 1.9 ms at +60 mV. The values indicate that an increase in the electrical gradient accelerated block, which supports the idea that τ_{block} reflects the time course of channel block by a positively charged form of methoxamine. In addition, the data support the observations described in Figure 1, where the degree of block increased at the more positive potentials studied.

Methoxamine inhibits hKv 1.5 and Kv 4.2 currents

Data presented in Figure 1 suggested that methoxamine reduced both peak (I_{to}) and sustained outward currents recorded from myocytes, and it was therefore of interest to examine individual cloned channel currents to find out which, if any, were preferentially blocked by the non-specific action of methoxamine. Both Kv 4.2 and hKv 1.5 are thought to be important components of outward current in cardiac tissue. Kv 4.2 and Kv 4.3 are thought to underlie I_{to} in rat and human ventricular myocytes (Barry *et al*., 1995;

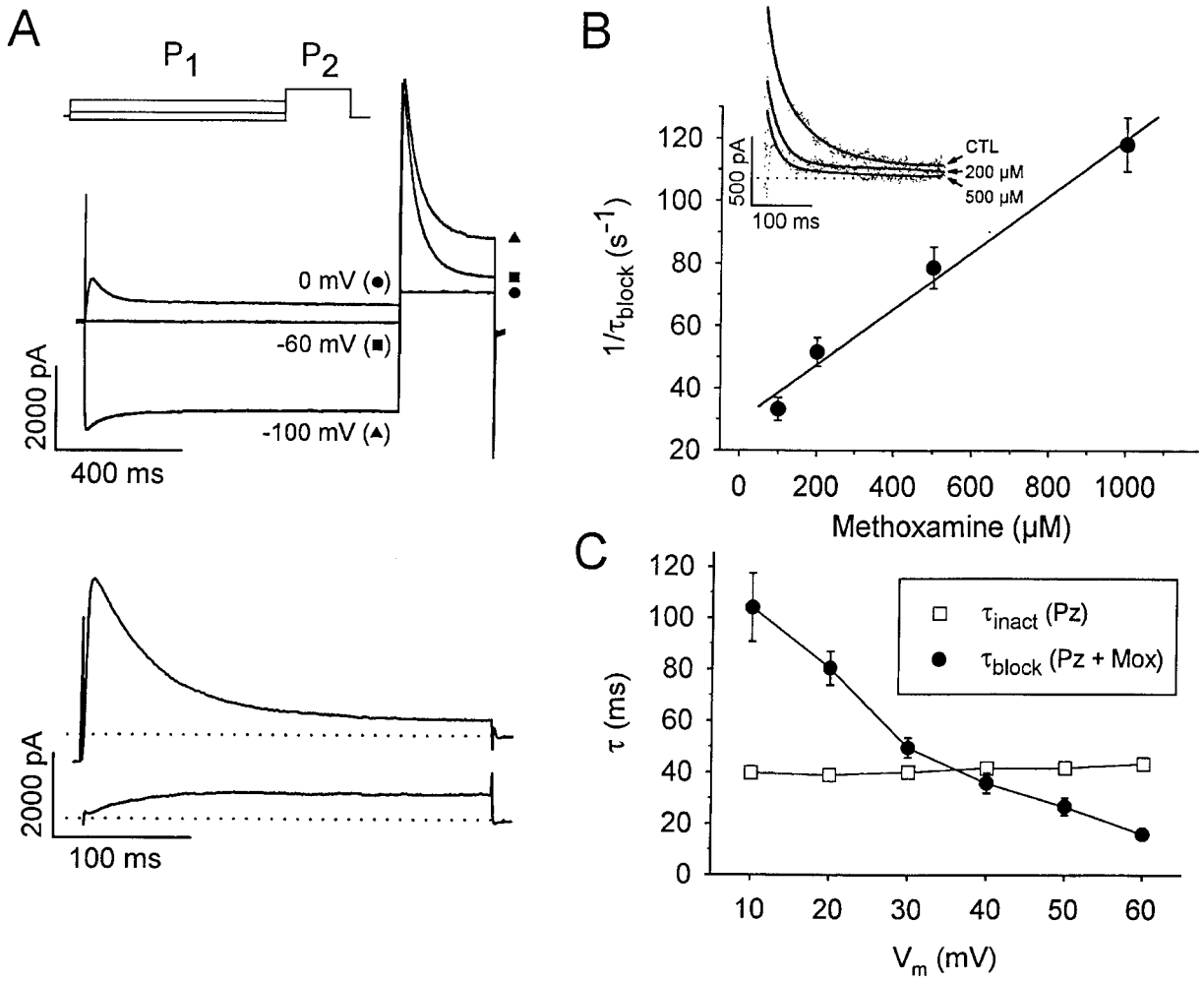

Figure 3 Concentration- and voltage-dependent kinetics of I_{to} block due to the non-specific action of methoxamine. (A) outward currents evoked from rat ventricular myocytes during a step to +60 mV (P_2), preceded by a 1 s conditioning prepulse (P_1) to −100 mV, −60 mV, or 0 mV, as indicated in the top panel. The lower panel shows difference currents isolating I_{to} (above) and the sustained outward current (below), derived as described in the Methods. Dotted lines indicate zero current level. (B) inset shows isolated I_{to} currents at +60 mV in control (CTL), and in the presence of 200 and 500 μM methoxamine, as indicated. Control currents were fit to a single exponential function, and currents in the presence of drug were fit to a double exponential (solid lines). The time constant for drug-channel interaction (τ_{block}) was extracted as described in the Methods. In the main panel, $1/\tau_{block}$ values have been plotted vs methoxamine concentration. The solid lines fit to data using equation [3a] gave apparent association (k_{+1}) and dissociation (k_{-1}) rate constants of 8.9×10^4 M^{-1} s^{-1} and 32.9 s^{-1} respectively. The K_d value from equation [3b] was 307 μM. Data are means ± s.e.mean from 5–10 cells at each concentration of methoxamine, and 2 μM prazosin was continuously present. (C) voltage-dependent acceleration of I_{to} inactivation by methoxamine in rat ventricular myocytes. Inactivation time constants were obtained from fits to the relaxation phase of I_{to} (see Methods) during 300 ms voltage steps from −80 mV. Control current inactivation was fit to a single exponential function, yielding τ_{inact}. In 2 μM prazosin and 200 μM methoxamine, the current decay was accelerated and τ_{block} was extracted as described in the Methods. τ_{block} values between +10 to +60 mV were accelerated, but τ_{inact} were not voltage dependent. Data are means ± s.e.mean ($n = 5–10$ at each voltage).

Dixon *et al*., 1996). hKv 1.5, cloned from human heart (Tamkun *et al*., 1991; Fedida *et al*., 1993) is thought to be a component of sustained current (Fedida *et al*., 1993; Wang *et al*., 1993), perhaps I_{Kur} in human myocytes (Feng *et al*., 1997). hKv 1.5 and Kv 4.2 were heterologously expressed in HEK cells, which lack α_1-adrenoceptors (Theroux *et al*., 1996), and currents expressed in these cells failed to show any response to phenylephrine ($n=6$). Figure 4A illustrates current traces obtained from an HEK cell transfected with hKv 1.5, in response to depolarizing voltage steps to +60 mV, during exposure to a range of methoxamine concentrations. hKv 1.5 currents are relatively slowly inactivating and the effect of methoxamine was to reduce both peak and sustained hKv 1.5 current amplitude with less of an acceleration of the rate of current decay than seen for I_{to} in myocytes. Current traces obtained in the presence of methoxamine activated initially as in control (see Figure 4A), but reached a lower peak and subsequently decayed more quickly. Untransfected HEK cells are known to contain a small endogenous voltage-activated delayed rectifier current. The average magnitude of this endogenous current, measured in untransfected HEK cells at +60 mV and at 300 ms, was 274±32 pA ($n=10$), and current tracings from a typical cell, obtained in response to a series of depolarizations over the range of −80 to +80 mV, are shown in the top panel of Figure 4B. The lower panel of Figure 4B illustrates typical drug-sensitive endogenous currents, in the presence of 200 μM and 1 mM methoxamine. This endogenous current was insensitive to concentrations of methoxamine <200 μM ($n=6$), and partial inhibition was noted at concentrations >500 μM. This suggests that the reduction of sustained currents observed in hKv 1.5-transfected cells with <500 μM methoxamine must represent solely block of hKv 1.5 current. Even with 1 mM methoxamine, the average magnitude of the methoxamine-sensitive current, measured at +80 mV, was 89 pA. Nonetheless, to minimize the contributions of this endogenous current, our analyses of expressed hKv 1.5 cloned channel currents included only those cells that contained relatively large currents, such that the methoxamine-sensitive endogenous

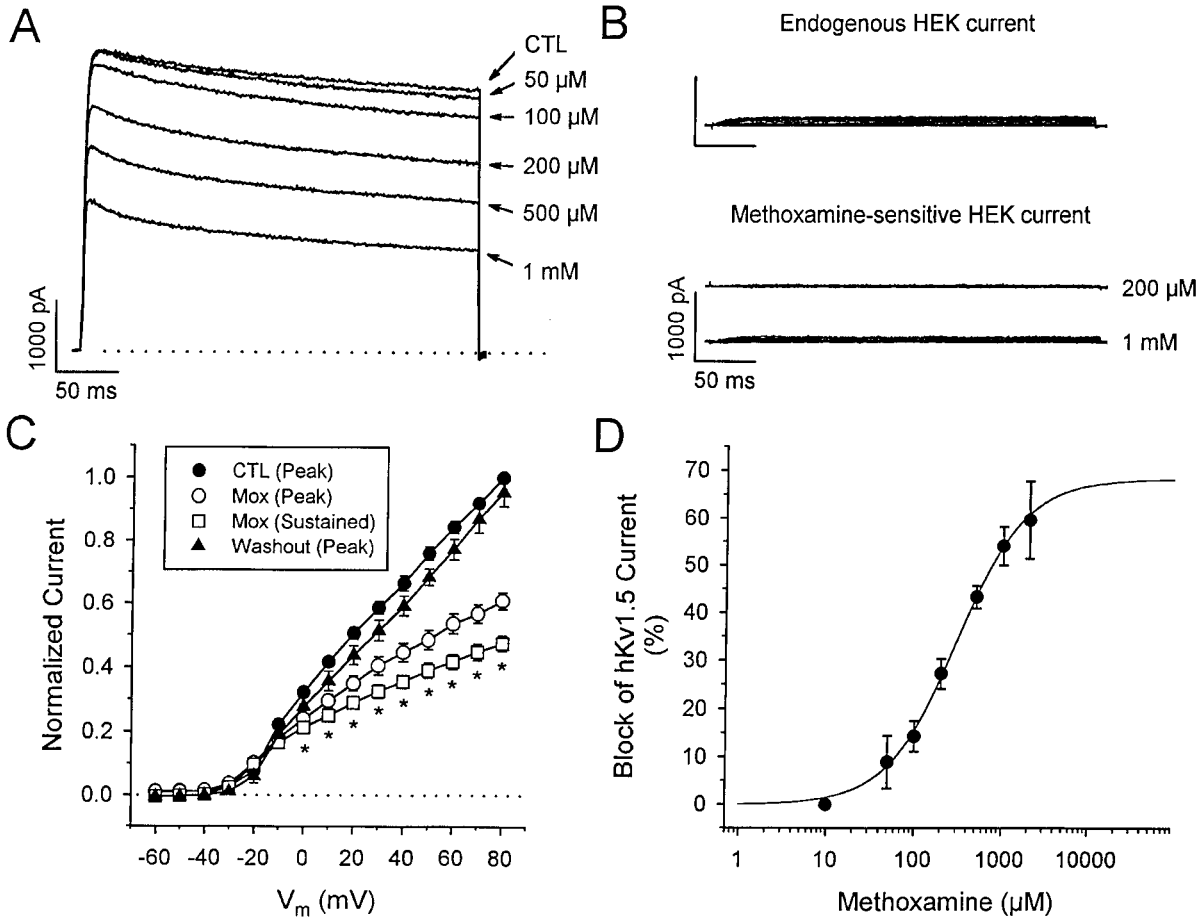

Figure 4 Reduction of hKv 1.5 current by methoxamine. (A) transfected HEK cell hKv 1.5 currents at +60 mV in control (CTL) and during exposure to a range of methoxamine concentrations as indicated. 2 μM prazosin was present in the bath at all times. The dotted line indicates zero current level. (B) endogenous HEK current in untransfected cells. The top panel shows typical endogenous currents in response to depolarizations over the range of −80 to +80 mV, from a holding potential of −80 mV. The lower panel illustrates the small methoxamine-sensitive endogenous currents obtained by subtracting currents in the presence of the indicated concentration of methoxamine from the corresponding currents in the absence of drug. The voltage-step protocol is the same as that described above. (C) normalized I-V relationships for peak control ($n=5$), peak ($n=5$) and sustained ($n=5$) hKv 1.5 currents in the presence of 500 μM methoxamine and peak current after washout ($n=4$), as indicated. Peak and sustained (at 300 ms) hKv 1.5 currents were individually normalized to peak and sustained current, respectively, measured at +80 mV under control conditions. *denotes statistically significant difference of both peak and sustained current amplitudes from control, $P<0.05$. (D) dose-response for the block of sustained hKv 1.5 current at +60 mV by methoxamine. The data are means±s.e.mean ($n=5$). The solid line represents a fit of the data to equation [1]. At +60 mV, the EC_{50} was 276 μM with $n_H=1.2$, and a maximum expected block of 65.5%.

current would be expected to contribute less than 3% of the total measured methoxamine-sensitive hKv 1.5 current. Mean peak (○) and sustained (□) current-voltage relations for cells exposed to 500 μM methoxamine are shown in Figure 4C, and illustrate the large effects of methoxamine on peak hKv 1.5 current, as well as reversibility of the drug action on washout (▲). Block of hKv 1.5 current by methoxamine was voltage- (Figure 4C) and concentration-dependent (Figure 4D). Fit to current-voltage data positive to +20 mV gave a value for $\delta = 0.18$, similar to that determined for I_{to} with methoxamine and prazosin (see text to Figure 1). Data points in Figure 4D were well fit by equation [1], which yielded an EC_{50} value, at +60 mV, of 276 μM, and $n_H = 1.2$, with a maximum level of block of 65.5% predicted from the fit.

The response of Kv 4.2 channel currents to methoxamine was similar to that observed for I_{to}. Threshold drug actions were observed at 50 μM and consisted predominantly of an acceleration of the rate of current decay. Higher concentrations of methoxamine not only accelerated the rate of Kv 4.2 current decay, but also reduced peak current, with little effect of methoxamine on the initial activation of the currents relative to control (Figure 5A). As for hKv 1.5 data, at drug concentrations greater than 500 μM, the methoxamine-sensitive endogenous current was small, and would be expected to compose less than 5% of the total methoxamine-sensitive current in all Kv 4.2-transfected cells included in analyses. The EC_{50} for steady-state Kv 4.2 current reduction was 363 μM, with $n_H = 0.87$, with a maximum expected block of 95% predicted from the fit of the data in Figure 5B. I-V relationships for cells in control solution (Figure 5C, ●, $n = 10$) and in the presence of 100 μM (□, $n = 6$) and 500 μM (○, $n = 7$) methoxamine again illustrate a voltage-dependence of block, and a fit of the current-voltage data positive to +20 mV in the presence of 500 μM methoxamine yielded a value of $\delta = 0.21$. For Kv 4.2 the control current inactivation was bi-exponential with fast time constants that were relatively voltage-independent in control (data not shown). The time constant for drug-channel interaction (Figure 5D; $1/\tau_{block}$, ●) was again concentration-dependent as for I_{to}. From equation [3a] the best least-squares fit to these data, as indicated by the solid line in Figure 5D, gave an apparent k_{+1} of 3.2×10^4 M^{-1}s^{-1}, and $k_{-1} = 8.3$ s^{-1}. From equation [3b], the calculated K_d was 388 μM, which is in close agreement with the EC_{50} value of 363 μM obtained from the dose-response curve (Figure 5B).

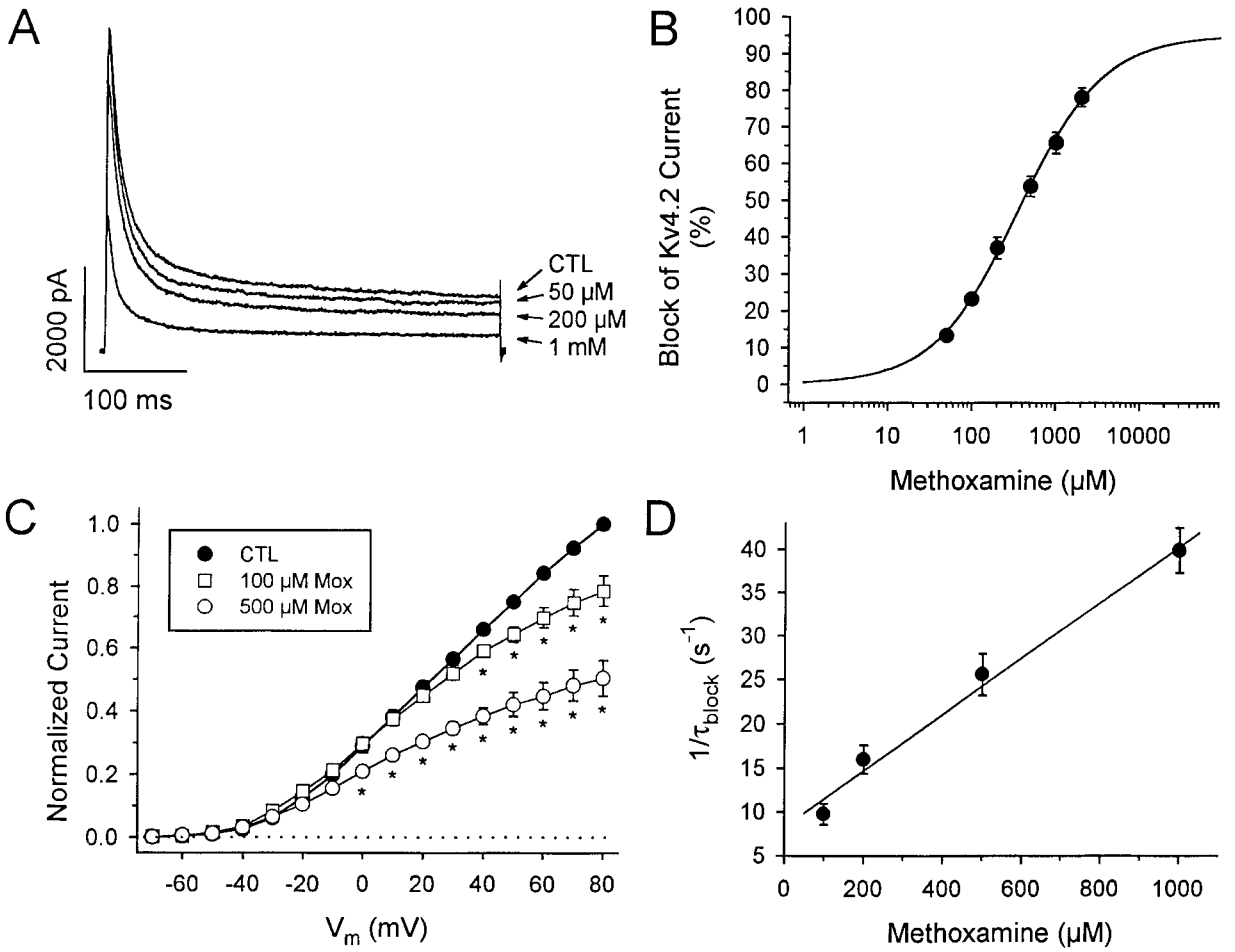

Figure 5 Reduction of Kv 4.2 current by methoxamine. (A) Kv 4.2 transfected HEK cell currents at +60 mV in control (CTL), and in the presence of 50, 200 μM, and 1 mM methoxamine, as indicated. (B) dose-response relation for Kv 4.2 current block by methoxamine. Current was measured at 300 ms and data points are means±s.e.mean ($n = 6$ at each concentration). The solid line was fit to data using equation [1]. The EC_{50} was 363 μM with $n_H = 0.87$, and a maximum expected block of 95%. (C) normalized mean I-V relations for Kv 4.2 current in control ($n = 6$), 100 μM ($n = 5$), and 500 μM ($n = 6$) methoxamine, as indicated. Currents were normalized to control currents at +80 mV, measured at 300 ms. *denotes statistically significant difference from control current amplitude, $P < 0.05$. (D) $1/\tau_{block}$ values plotted vs methoxamine concentration. τ_{block} values were extracted as described in the Methods from fits to the rapid phase of Kv 4.2 decay in the presence of methoxamine. From equation [3a] the best least-squares fit to these data, as indicated by the solid line in Figure 7D, gave an apparent k_{+1} of 3.2×10^4 M^{-1} s^{-1}, and $k_{-1} = 8.3$ s^{-1}. From equation [3b], the calculated K_d was 388 μM. Data are means±s.e.mean ($n = 5-9$ at each concentration).

Methoxamine modifies Kv 4.2 tail currents

Under control conditions, at −40 mV, Kv 4.2 current deactivated with a time constant ($\tau_{deactivation}$) of 24.4±1.6 ms ($n=6$), which represents the closing of channels from the open state. In the presence of methoxamine, the peak tail current amplitude was reduced relative to control, but also displayed an initial rising phase that was not observed in the absence of drug ($n=8$). This rising phase was more pronounced with higher doses of methoxamine, and represents unblock of open channels previously inhibited by methoxamine. Figure 6A shows representative tail currents obtained at −40 mV, after 100 ms depolarizations in control conditions, and in the presence of 100, 500 μM or 1 mM methoxamine. Not only was the peak more reduced and the rising phase more pronounced at higher methoxamine concentrations, but subsequent decay of the tail currents was significantly slowed in the presence of methoxamine, and this effect was dose-dependent (Figure 6B). This had the result that tail currents recorded at the higher concentrations of methoxamine crossed over the control tail current (Figure 6A, inset). These data indicate that upon repolarization, methoxamine dissociated from blocked channels, allowing these channels to become conducting and resulting in the rising phase of tail current. Subsequently, a dynamic equilibrium was reached, wherein a fraction of these open, unblocked channels became blocked again, delaying the irreversible closing of these channels and resulting in the slowed rate of tail current decay relative to control.

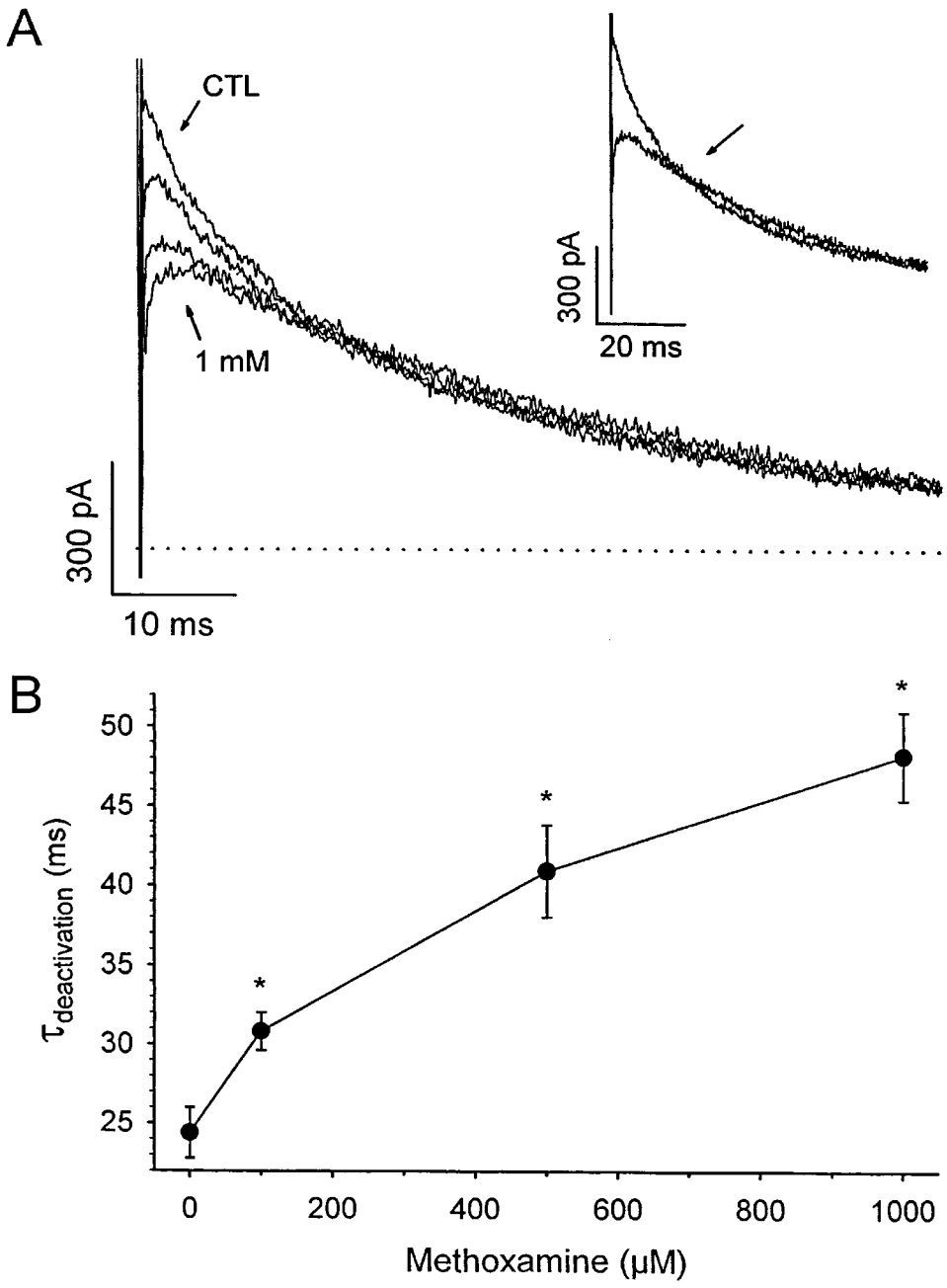

Figure 6 Methoxamine modifies Kv 4.2 deactivating tail currents. (A) typical deactivating tail currents in control (CTL), 100 μM, 500 μM, and 1 mM methoxamine. Peak tail current amplitudes decreased with increasing dose. The cell was held at −80 mV, and tails were recorded at −40 mV after a 100 ms depolarization to +50 mV. Dotted line indicates zero current level. Inset panel shows crossover of tail in control and 1 mM methoxamine and crossover point is arrowed. (B) slowing of rate of decay of tail currents with increasing doses of methoxamine. Tail currents in control and in the presence of drug were obtained as in (A) and were computer-fitted to a single exponential function to obtain the deactivation time constant, $\tau_{deactivation}$, at each concentration of drug. Data are means±s.e.mean ($n=6$). *denotes significant difference from control (i.e. 0 μM methoxamine), $P<0.05$.

Methoxamine block of single Kv channels

For single-channel recording, HEK cells were depolarized in high K^+ solution containing 2 μM prazosin. Pipettes contained 5 mM K^+ solution and patches containing one or a few hKv 1.5 channels were held at a transmembrane potential of -80 mV and depolarized to $+60$ mV, at 0.5 Hz. Representative control sweeps are presented in Figure 7A, and tracings recorded with 500 μM methoxamine in the bath solution are illustrated in Figure 7B. Under control conditions, hKv 1.5 channels opened in multiple bursts that were characterized by frequent brief closings. These kinetics for hKv 1.5 have been reported

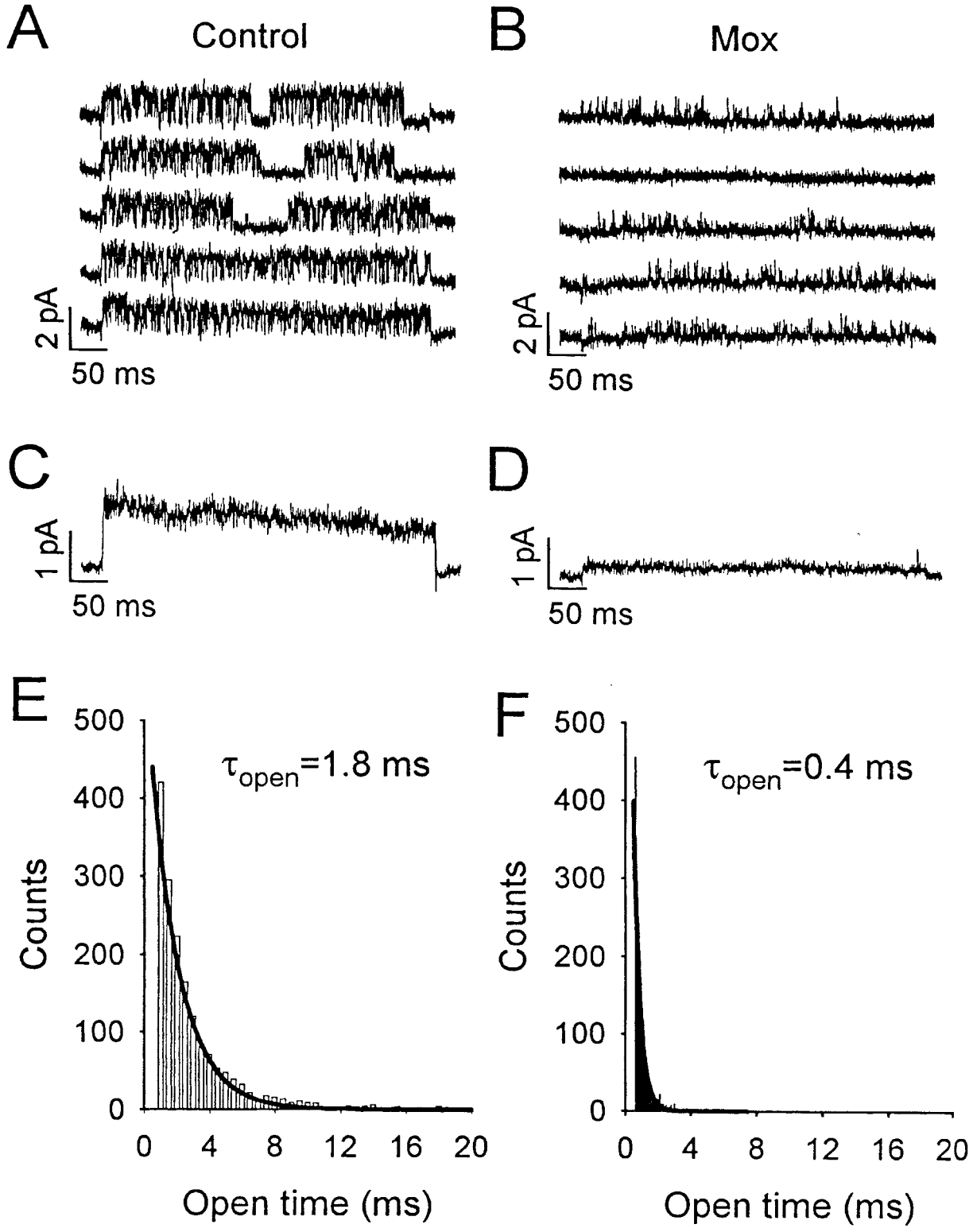

Figure 7 Effects of methoxamine on hKv 1.5 single channels in cell-attached patches with 140 mM K^+ in the bath (see Methods). (A and B) cells were held at -80 mV and single-channel currents obtained at $+60$ mV, in control and in 500 μM methoxamine. Each sweep was recorded during 500 ms depolarizations. (C and D) ensemble averages ($n=20$) in control and in 500 μM methoxamine. (E and F) open-channel dwell time distributions in control and 500 μM methoxamine. Bin widths were 0.5 ms in E and 0.1 ms in F. Solid lines are single-exponential fits to data, with $\tau_{open} = 1.8 \pm 0.01$ ms in control, and 0.4 ± 0.06 ms in methoxamine.

previously from our laboratory (Chen & Fedida, 1998) and are quite different from the maintained openings with few closings that characterize the endogenous current in HEK cells (data not shown). In the presence of methoxamine, burst duration was greatly reduced, rapid closings within bursts became even more frequent, and the channel rarely opened to its full amplitude. The mean single channel current in control solution, as determined by a Gaussian fit to an all-points amplitude histogram (data not shown) was 1.1 ± 0.01 pA, which corresponds to a single channel conductance of 9 pS, consistent with that reported previously for hKv 1.5 (Grissmer *et al*., 1994). In the presence of methoxamine, however, the mean single channel current amplitude was significantly reduced to 0.3 ± 0.01 pA. These two actions of 500 μM methoxamine had the effect of reducing the ensemble-average current by 73% (Figure 7D) relative to control (Figure 7C). This may be compared with the 43% reduction of hKv 1.5 current observed in the whole cell configuration (Figure 4C). In addition, methoxamine significantly decreased the mean channel open time of hKv 1.5. Fits to open channel dwell time distributions for a cell in control solution (Figure 7E) and following addition of methoxamine (Figure 7F) yielded time constants (τ_{open}), corresponding to mean channel open times, of 1.8 ± 0.01 ms and 0.4 ± 0.06 ms, respectively. Similar results were seen in four other cells.

Discussion

Methoxamine has both α_1-adrenoceptor-dependent and α_1-adrenoceptor-independent actions

Methoxamine and phenylephrine have both been widely used in studies of α-adrenergic effects on cardiac ionic currents. In our studies, both phenylephrine and methoxamine reduced peak I_{to} amplitude in rat ventricular myocytes, but the response to phenylephrine was prevented by prazosin, whereas prazosin could reduce, but not abolish, the response to methoxamine (Figure 1). Similarly, preincubation of ventricular cells with prazosin, NEM, or PhBz prevented the action of phenylephrine, but failed to prevent the reduction in I_{to} observed during exposure to 200 μM methoxamine (see Figure 1F). This suggests that although prazosin, NEM, and PhBz act to disrupt different stages of the α-adrenergic signal transduction pathway, the non-specific action of methoxamine was not dependent on receptor activation, or on signal transduction by heterotrimeric G-proteins.

Methoxamine reduced both peak (I_{to}) and sustained outward currents in rat ventricular myocytes, independently of α_1-adrenoceptor stimulation, so we examined the action of methoxamine on two classes of Kv channels. These were Kv 4.2, a rapidly inactivating channel thought to underlie I_{to} (Barry *et al*., 1995; Dixon *et al*., 1996) and hKv 1.5, a slowly-inactivating delayed rectifier-type of channel thought to contribute to sustained outward current (Van Wagoner *et al*., 1996; Feng *et al*., 1997). Our data demonstrated that methoxamine could reduce the whole-cell currents recorded from hKv 1.5 and Kv 4.2 in HEK cells (Figures 4 and 5) which express no detectable endogenous α_1-adrenoceptors (Theroux *et al*., 1996).

Concentration- and voltage-dependence of receptor-independent action of methoxamine

In the presence of prazosin, methoxamine decreased the amplitudes of I_{to}, hKv 1.5, and Kv 4.2 in a concentration- and voltage-dependent manner. The EC_{50}s for observed fractional block were similar for all three currents, and Hill coefficients were also similar, suggesting a single binding site model in each case. In myocytes, methoxamine characteristically increased the rate of decay of I_{to} (Figure 3). This was similar to data obtained for Kv 4.2 (Figure 5), but appeared to be much less important an effect for hKv 1.5 (Figure 4). We extracted a methoxamine-dependent time constant for block, τ_{block} (Figures 3 and 5), which decreased with increasing drug concentrations. The calculated K_d values, at +60 mV, were in good agreement with EC_{50} values obtained from dose-response relations (Figures 2B and 5B).

The observed voltage-dependence of I_{to} (Figure 1E), hKv 1.5 (Figure 4C) and Kv 4.2 (Figure 5C) inhibition, increasing with potential, is expected if the positively charged form of methoxamine (at pH 7.4, with $pK_a = 9.2$) blocks the channel and therefore responds to changes in membrane potential. Uncharged methoxamine could cross the plasma membrane and become protonated and charged within the cell, and then reach a putative intracellular binding site. This is supported by single channel data in Figure 7 where methoxamine was added to the bath solution and the external face of the membrane at the recording site was shielded by the pipette. The fraction of the membrane electrical field (δ) sensed by the drug at its receptor site was determined to be 0.18 for I_{to} and for hKv 1.5, and 0.21 for Kv 4.2. These values are similar to those for quinidine (Fedida, 1997) and quaternary ammonium compounds (Choi *et al*., 1993), and suggests that positively charged agents may bind to a common intracellularly-accessible site (Snyders & Yeola, 1995).

Non-specific action of methoxamine is consistent with both open- and closed-channel block

Methoxamine accelerated the rate of decay of I_{to} and Kv 4.2 without markedly affecting the initial time course of activation (Figures 2A and 5A), which is generally suggestive of a mechanism of open-channel block (Slawsky & Castle, 1994). In the presence of higher concentrations of methoxamine, the reduction in peak I_{to}, hKv 1.5 and Kv 4.2 currents can be explained by rapid drug-channel interaction according to the first-order rate constant given by $k_{+1}[D]$. In the presence of methoxamine, deactivating Kv 4.2 tail currents showed a distinct rising phase that was not observed under control conditions, and decay of the current tails was significantly slowed in the presence of drug (Figure 6). These observations are consistent with a simple open channel block scheme for methoxamine and Kv 4.2:

$$\mathrm{C} \underset{4\beta}{\overset{\alpha}{\rightleftharpoons}} \mathrm{O} \underset{k_{-1}}{\overset{k_{+1}[D]}{\rightleftharpoons}} \mathrm{OB} \downarrow \mathrm{I}$$

In this model, α and 4β refer to standard opening and closing rate constants, respectively, between the last closed (C) and open (O) states in a Hodgkin-Huxley four-subunit model, (I) is the inactivated state, and k_{+1} and k_{-1} are the apparent binding and unbinding rates for methoxamine and Kv 4.2, which were calculated to be 3.2×10^4 M^{-1} s^{-1} and 8.3 s^{-1}, respectively (Figure 5D). Since the unbinding rate is relatively fast, upon repolarization tail currents in the presence of drug should exhibit a rising phase indicative of the OB→O transition. Subsequently, these unblocked open channels can reblock, which slows tail current decay according to the relative values of 4β and $k_{+1}[D]$. If drug binding is sufficiently rapid relative

to channel closing, a 'crossover' of tail currents can be observed, as is the case for quinidine (Snyders *et al*., 1992; Fedida, 1997), and was demonstrated by data in Figure 6.

In addition to accelerating the rate of decay of whole cell current, methoxamine decreased the mean hKv 1.5 single channel open time, consistent with rapid association and dissociation of the drug and the channel, and supportive of open-channel block. However, mean single channel current was also reduced, which may reflect brief openings not visualized at our bandwidth (1 kHz), or alternatively, alteration of the channel conductance by methoxamine. The number of blank sweeps also increased during methoxamine, and this increase in channel closed times strongly suggests an additional interaction with resting or closed states of hKv 1.5.

Implications for previous studies

Methoxamine has been a widely-used agonist to study the role of α_1-adrenergic modulation of cardiac function, and the concentrations of drug used in these studies vary widely over the range of 10^{-6}–10^{-2} M. In rat ventricular myocytes a 25–50% reduction in the magnitude of the outward K^+ currents was observed in response to 20 μM methoxamine (Apkon & Nerbonne, 1988). At this concentration of methoxamine, the non-specific component of I_{to} inhibition is negligible (Figure 2B) compared to the α_1-adrenoceptor-mediated response. Many studies, however, have used higher concentrations (e.g. >100 μM methoxamine), at which there is likely to be a significant non-specific component to the observed action that cannot be overlooked. In the absence of prazosin, 100 μM methoxamine resulted in $\sim$35% reduction of I_{to} in rat ventricular cells (Fedida & Bouchard, 1992), at which concentration our results indicate that I_{to} would be reduced by $\sim$15% due to a non-specific action alone. Yang *et al*. (1996) routinely used 100 μM methoxamine to examine positive inotropy in isolated rabbit myocardium, and methoxamine concentrations up to 1 mM have been used to demonstrate modulation of I_{to} in hyperthyroid rabbit myocytes (Shimoni & Banno, 1993). Interestingly, in rabbit atrium, 200 μM methoxamine has also been shown to decrease the I_{to} mean single channel open time (Braun *et al*., 1990). This result is similar to our α-adrenoceptor-independent action on single hKv 1.5 channels, although we noted additional closed channel effects (Figure 7). All these results suggest that great caution must be exercised in the use of methoxamine as an α-agonist in systems which possess significant numbers of voltage-gated K^+ channels or where ion channel modulation itself is being directly studied.

Interestingly, other compounds that interact with adrenoceptors have also been shown to have channel-blocking properties. The α-antagonist phentolamine can block ATP-sensitive K^+ (K_{ATP}) channels in rabbit ventricle (Wilde *et al*., 1994) and pancreatic β-cells (Plant & Henquin, 1990), as can the specific α_2-antagonist yohimbine. Dicentrene, an alkaloid α-antagonist, inhibits I_{to}, I_K, and the sodium current (I_{Na}) in guinea-pig ventricular cells independently of adrenoceptor binding (Su *et al*., 1994). To our knowledge, however, this is the first report of an α-adrenoceptor agonist with K^+ channel-blocking properties.

Supported by grants from the Heart and Stroke Foundation of Ontario and the Medical Research Council of Canada to David Fedida. The authors would like to thank Shunping Lin for valuable assistance in data collection.

References

APKON, M. & NERBONNE, J.M. (1988). α_1-adrenergic agonists selectively suppress voltage-dependent K^+ currents in rat ventricular myocytes. *Proc. Natl. Acad. Sci. U.S.A.,* **85,** 8756–8760.

APKON, M. & NERBONNE, J.M. (1991). Characterization of two distinct depolarization-activated K^+ currents in isolated adult rat ventricular myocytes. *J. Gen. Physiol.,* **97,** 973–1011.

BARRY, D.M., TRIMMER, J.S., MERLIE, J.P. & NERBONNE, J.M. (1995). Differential expression of voltage-gated K^+ channel subunits in adult rat heart: Relation to functional K^+ channels. *Circ. Res.,* **77,** 361–369.

BRAUN, A.P., FEDIDA, D., CLARK, R.B. & GILES, W.R. (1990). Intracellular mechanisms for α_1-adrenergic regulation of the transient outward current in rabbit atrial myocytes. *J. Physiol. (Lond.),* **431,** 689–712.

CHEN, F.S.P. & FEDIDA, D. (1998). On the mechanism by which 4-aminopyridine occludes quinidine block of the cardiac K^+ channel, hKv 1.5. *J. Gen. Physiol.,* **111,** 539–554.

CHOI, K.L., MOSSMAN, C., AUBÉ, J. & YELLEN, G. (1993). The internal quaternary ammonium receptor site of *Shaker* potassium channels. *Neuron,* **10,** 533–541.

DIXON, J.E., SHI, W.M., WANG, H.S., MCDONALD, C., YU, H., WYMORE, R.S., COHEN, I.S. & MCKINNON, D. (1996). Role of the Kv 4.3 K^+ channel in ventricular muscle-A molecular correlate for the transient outward current. *Circ. Res.,* **79,** 659–668.

FEDIDA, D., SHIMONI, Y. & GILES, W.R. (1990). α-Adrenergic modulation of the transient outward current in rabbit atrial myocytes. *J. Physiol. (Lond.),* **423,** 257–277.

FEDIDA, D., BRAUN, A.P. & GILES, W.R. (1991). α_1-Adrenoceptors reduce background K^+ current in rabbit ventricular myocytes. *J. Physiol. (Lond.),* **441,** 673–684.

FEDIDA, D., WIBLE, B., WANG, Z., FERMINI, B., FAUST, F., NATTEL, S. & BROWN, A.M. (1993). Identity of a novel delayed rectifier current from human heart with a cloned K^+ channel current. *Circ. Res.,* **73,** 210–216.

FEDIDA, D. (1997). Gating charge and ionic currents associated with quinidine block of human Kv 1.5 delayed rectifier K^+ channels. *J. Physiol. (Lond.),* **499,** 661–675.

FEDIDA, D. & BOUCHARD, R.A. (1992). Mechanisms for the positive inotropic effect of α_1-adrenoceptor stimulation in rat cardiac myocytes. *Circ. Res.,* **71,** 673–688.

FENG, J.L., WIBLE, B., LI, G.R., WANG, Z.G. & NATTEL, S. (1997). Antisense oligodeoxynucleotides directed against Kv 1.5 mRNA specifically inhibit ultrarapid delayed rectifier K^+ current in cultured adult human atrial myocytes. *Circ. Res.,* **80,** 572–579.

GRISSMER, S., NGUYEN, A.N., AIYAR, J., HANSON, D.C., MATHER, R.J., GUTMAN, G.A., KARMILOWICZ, M.J., AUPERIN, D.D. & CHANDY, K.G. (1994). Pharmacological characterization of five cloned voltage-gated K^+ channels, types Kv 1.1, 1.2, 1.3, 1.5, and 3.1, stably expressed in mammalian cell lines. *Mol. Pharmacol.,* **45,** 1227–1234.

HARRISON, J.K., PEARSON, W.R. & LYNCH, K.R. (1991). Molecular characterization of α_1- and α_2-adrenoceptors. *TIPS,* **12,** 62–67.

HWANG, K.C., GRAY, C.D., SWEET, W.E., MORRAVEC, C.S. & IM, M.-J. (1996). α_1-adrenergic receptor coupling with G_h in the failing human heart. *Circulation,* **94,** 718–726.

IM, M.-J. & GRAHAM, R.M. (1990). A novel guanine nucleotide-binding protein coupled to the α_1-adrenergic receptor. I. Identification by photolabeling of membrane and ternary complex preparations. *J. Biol. Chem.,* **265,** 18944–18951.

LI, G.R., FENG, J.L., WANG, Z.G., FERMINI, B. & NATTEL, S. (1996). Adrenergic modulation of ultrarapid delayed rectifier K^+ current in human atrial myocytes. *Circ. Res.,* **78,** 903–915.

LIEBAU, S., HOHLFELD, J. & FORSTERMANN, U. (1989). The inhibition of α_1-adrenoceptor-mediated contraction of rabbit pulmonary artery by Ca^{2+}-withdrawal, pertussis toxin, and N-ethylmaleimide. *Naun. Schmied. Arch. Pharmacol.,* **339,** 496–502.

MINNEMAN, K.P., THEROUX, T.L., HOLLINGER, S., HAN, C. & ESBENSHADE, T.A. (1994). Selectivity of agonists for cloned α_1-adrenergic receptor subtypes. *Mol. Pharmacol.,* **46,** 929–936.

NAKAOKA, H., PEREZ, D.M., BAEK, K.J., DAS, T., HUSAIN, A., MISONO, K., IM, M.-J. & GRAHAM, R.M. (1994). G_h: a GTP-binding protein with transglutaminase activity and receptor signalling function. *Science,* **264,** 1593–1595.

PLANT, T.D. & HENQUIN, J.C. (1990). Phentolamine and yohimbine inhibit ATP-sensitive K^+ channels in mouse pancreatic β-cells. *Br. J. Pharm.,* **101,** 115–120.

SATOH, H. & HASHIMOTO, K. (1988). Effect of α_1-adrenoceptor stimulation with methoxamine and phenylephrine on spontaneously beating rabbit sino-atrial node cells. *Naun. Schmied. Arch. Pharmacol.,* **337,** 415–422.

SHIMONI, Y. & BANNO, H. (1993). α-Adrenergic modulation of transient outward current in hyperthyroid rabbit myocytes. *Am. J. Physiol. Heart Circ. Physiol.,* **264,** H74–H77.

SLAWSKY, M.T. & CASTLE, N.A. (1994). K^+ channel blocking actions of flecainide compared with those of propafenone and quinidine in adult rat ventricular myocytes. *J. Pharmacol. Exp. Ther.,* **269,** 66–74.

SNYDERS, D.J., KNOTH, K.M., ROBERDS, S.L. & TAMKUN, M.M. (1992). Time-, voltage-, and state-dependent block by quinidine of a cloned human cardiac potassium channel. *Mol. Pharmacol.,* **41,** 322–330.

SNYDERS, D.J. & YEOLA, S.W. (1995). Determinants of antiarrhythmic drug action - Electrostatic and hydrophobic components of block of the human cardiac hKv 1.5 channel. *Circ. Res.,* **77,** 575–583.

SU, M.J., NIEH, Y.C., HUANG, H.W. & CHEN, C.C. (1994). Dicentrine, an α-adrenoceptor antagonist with sodium and potassium channel blocking activities. *Naunyn-Schmiedebergs Arch. Pharm.,* **349,** 42–49.

TAMKUN, M.M., KNOTH, K.M., WALBRIDGE, J.A., KROEMER, H., RODEN, D.M. & GLOVER, D.H. (1991). Molecular cloning and characterization of two voltage-gated K^+ channel cDNAs from human ventricle. *FASEB J.,* **5,** 331–337.

THEROUX, T.L., ESBENSHADE, T.A., PEAVY, R.D. & MINNEMAN, K.P. (1996). Coupling efficiencies of human α_1-adrenergic receptor subtypes: Titration of receptor density and responsiveness with inducible and repressible expression vectors. *Mol. Pharmacol.,* **50,** 1376–1387.

UEDA, H., MISAWA, H., KATADA, T., UI, M., TAKAGI, H. & SATOH, M. (1990). Functional reconstitution of purified G_i and G_o with μ-opioid receptors in guinea-pig striatal membranes pretreated with micromolar concentrations of N-ethylmaleimide. *J. Neurochem.,* **54,** 841–848.

VAN WAGONER, D.R., KIRIAN, M. & LAMORGESE, M. (1996). Phenylephrine suppresses outward K^+ currents in rat atrial myocytes. *Am. J. Physiol. Heart Circ. Physiol.,* **271,** H937–H946.

WANG, Z., FERMINI, B. & NATTEL, S. (1993). Sustained depolarization-induced outward current in human atrial myocytes: Evidence for a novel delayed rectifer K^+ current similar to Kv 1.5 cloned channel currents. *Circ. Res.,* **73,** 1061–1076.

WILDE, A.A., VELDKAMP, M.W., VAN GINNEKEN, A.C. & OPTHOF, T. (1994). Phentolamine blocks ATP sensitive potassium channels in cardiac ventricular cells. *Cardiovasc. Res.,* **28,** 847–850.

WOODHULL, A.M. (1973). Ionic blockage of sodium channels in nerve. *J. Gen. Physiol.,* **61,** 687–708.

WU, D., KATZ, A., LEE, C.-H. & SIMON, M.I. (1992). Activation of phospholipase C by α_1-adrenergic receptors is mediated by the α subunits of G_q family. *J. Biol. Chem.,* **267,** 25798–25802.

YANG, H. & ENDOH, M. (1994). Dissociation of the positive inotropic effect of methoxamine from the hydrolysis of phosphoinositide in rabbit ventricular myocardium: a comparison with the effects of phenylephrine and the subtype of the α_1 adrenoceptor involved. *J. Pharm. Exp. Ther.,* **269,** 732–742.

YANG, H.T., NOROTA, I., ZHU, Y. & ENDOH, M. (1996). Methoxamine-induced inhibition of the positive inotropic effect of endothelin via α_1-adrenoceptors in the rabbit heart. *Eur. J. Pharmacol.,* **296,** 47–54.

ZHANG, X., ANDERSON, J.W. & FEDIDA, D. (1997). Characterization of nifedipine block of the human heart delayed rectifier, hKv 1.5. *J. Pharmacol. Exp. Ther.,* **281,** 1247–1256.

(Received June 23, 1998
Revised September 30, 1998
Accepted November 4, 1998)

British Journal of Pharmacology (1999) 126, 607–612
http://www.stockton-press.co.uk/bjp

Pharmacological diversity between native human 5-HT_{1B} and 5-HT_{1D} receptors sited on different neurons and involved in different functions

[1]Manuela Marcoli, [1]Guido Maura, [2]Claudio Munari, [3]Antonio Ruelle & *,[1]Maurizio Raiteri

[1]Dipartimento di Medicina Sperimentale, Sezione di Farmacologia e Tossicologia, Università di Genova, Viale Cembrano 4, 16148 Genova, Italy; [2]Clinica Neurochirurgica, Università di Genova, Ospedale S. Martino, Largo Rosanna Benzi 10, 16132 Genova, Italy; and [3]Divisione di Neurochirurgia, Ospedali Galliera, Via A. Volta 8, 16128 Genova, Italy

1 The releases of [^{3}H]5-hydroxytryptamine ([^{3}H]5-HT) and of endogenous glutamic acid and their modulation through presynaptic h5-HT_{1B} autoreceptors and h5-HT_{1D} heteroreceptors have been investigated in synaptosomal preparations from fresh neocortical samples obtained from patients undergoing neurosurgery.

2 The inhibition by 5-HT of the K^+ (15 mM)-evoked overflow of [^{3}H]5-HT was antagonized by the 5-HT_{1B}/5-HT_{1D} receptor ligand GR 127935, which was ineffective on its own; this drug was previously found to behave as a full agonist at the h5-HT_{1D} heteroreceptor regulating glutamate release.

3 The recently proposed selective h5-HT_{1B} receptor ligand SB-224289 also prevented the effect of 5-HT at the autoreceptor, being inactive on its own; in contrast, SB-224289, at 1 μM, was unable to interact with the h5-HT_{1D} heteroreceptor.

4 The inhibitory effect of 5-HT on the K^+-evoked overflow of glutamate was antagonized by the h5-HT_{1D} receptor ligand BRL-15572; added in the absence of 5-HT the compound was without effect. BRL-15572 (1 μM) was unable to modify the effect of 5-HT at the autoreceptor regulating [^{3}H]5-HT release.

5 The selective 5-HT_{1A} receptor antagonist (+)-WAY 100135, previously found to be an agonist at the h5-HT_{1D} heteroreceptor regulating glutamate release, could not interact with the h5-HT_{1B} autoreceptor when added at 1 μM.

6 It is concluded that native h5-HT_{1B} and h5-HT_{1D} receptors exhibit a hitherto unexpected pharmacological diversity.

Keywords: Human cerebral cortex; 5-hydroxytryptamine release; glutamate release; 5-hydroxytryptamine-glutamate interaction; human native 5-hydroxytryptamine receptors; h5-HT_{1B} receptor; h5-HT_{1D} receptor

Abbreviations: BRL-15572, 1-phenyl-3-[4-(3-chlorophenyl)piperazin-1-yl] phenylpropan-2-ol dihydrochloride; GR 127935, N-[4-methoxy-3-(4-methyl-1-piperazinyl)phenyl]-2′-methyl-4′-(5-methyl-1,2,4-oxa-diazol-3-yl)[1,1,-biphenyl]-4-carboxamide; SB-224289, 2,3,6,7-tetrahydro-1′-methyl-5-[2′-methyl-4′-(5-methyl-1,2,4-oxadiazol-3-yl)biphenyl-4-carbonyl]furo[2,3-f]indole-3-spiro-4′-piperidine hydrochloride salt; (+)-WAY 100135, (S)-(+)N-tert-butyl-3-[4-(2-methoxyphenyl) piperazin-1-yl]-2-phenylpropionamide dihydrochloride

Introduction

At least five 5-HT_1 receptor subtypes have been recognized, 5-HT_{1A}, 5-HT_{1B} (former nomenclature: 5-$HT_{1D\beta}$), 5-HT_{1D} (formerly termed 5-$HT_{1D\alpha}$), 5-HT_{1E} and 5-HT_{1F}. All subtypes are seven transmembrane, G-protein coupled receptors and all are thought to be negatively linked to adenylyl cyclase (Hoyer *et al*., 1994; Martin & Humphrey, 1994).

Human 5-HT_{1B} (h5-HT_{1B}) and 5-HT_{1D} (h5-HT_{1D}) receptors have been reported to have relatively low (63%) overall amino acid homology; in apparent contrast, for a series of 19 structurally diverse compounds, the two cloned human receptors were found to be nearly indistinguishable in their binding affinities (Hartig *et al*., 1992; Weinshank *et al*., 1992).

Subsequently, however, the classical 5-HT_2 receptor antagonist ketanserin was proposed to permit discrimination between h5-HT_{1B} and h5-HT_{1D} receptors (Kaumann *et al*., 1994; Pauwels & Colpaert, 1995; Zgombick *et al*., 1995). More recently, using recombinant h5-HT_{1B} and h5-HT_{1D} receptors, the novel compounds SB-216641, SB-224289 and BRL-15572 have been found to discriminate the two subtypes. In binding studies on receptors expressed in CHO cells SB-216641 and SB-224289 had, respectively, 25 and 80 fold higher affinity for h5-HT_{1B} than h5-HT_{1D} receptors; conversely, BRL-15572 had 60 fold higher affinity for h5-HT_{1D} than h5-HT_{1B} receptors. In functional assays ([^{35}S]-GTPγS binding and cyclic AMP accumulation) with the above cloned receptor expression system, SB-216641 and BRL-15572 displayed agonist intrinsic activity at both h5-HT_{1B} and h5-HT_{1D} receptors (Price *et al*., 1997), whereas SB-224289 behaved as an inverse agonist (Gaster *et al*., 1998).

Functional studies with native human brain 5-HT receptors are relatively rare and have been almost exclusively focused on autoreceptors mediating feedback inhibition of 5-HT release (Schlicker *et al*., 1985; 1997; Galzin *et al*., 1992; Maura *et al*., 1993; Raiteri, 1994; Fink *et al*., 1995). These autoreceptors were initially classified as h5-HT_{1B} based exclusively on their insensitivity to ketanserin (Maura *et al*., 1993; Fink *et al*., 1995). More recently, Schlicker *et al*. (1997) found that SB-216641 is a preferential ligand at native h5-HT_{1B} receptors in human neocortex, in agreement with the above results with

* Author for correspondence.

cloned receptors, although the compound was an antagonist at the autoreceptors devoid of any intrinsic activity.

A functional model of native brain h5-HT$_{1D}$ receptor has recently been proposed: neocortical glutamatergic neurons in human cerebrocortex possess release-inhibiting heteroreceptors that, based on their sensitivity to sumatriptan and to ketanserin, were proposed to belong to the h5-HT$_{1D}$ subtype (Maura *et al*., 1998). Interestingly, GR 127935, a compound described as a potent and selective 5-HT$_{1B}$/5-HT$_{1D}$ receptor antagonist (Skingle *et al*., 1993; 1996), inhibited glutamate release similarly to sumatriptan, thus behaving as a full agonist at native h5-HT$_{1D}$ receptors (Maura *et al*., 1998). Recently the h5-HT$_{1D}$ ligand BRL-15572 has been reported to behave as a potent antagonist at native h5-HT$_{1D}$ heteroreceptors in human atrial appendages (Schlicker *et al*., 1997).

To establish that native h5-HT$_{1B}$ and h5-HT$_{1D}$ receptors have distinct (and possibly opposing) function in the human brain and can be differentially acted upon by drugs is of great importance. Release-regulating 5-HT autoreceptors and 5-HT heteroreceptors regulating glutamate release have therefore been compared using various selective 5-HT receptor ligands and monitoring [^{3}H]-5-hydroxytryptamine ([^{3}H]-5-HT) and endogenous glutamate release from human neocortical synaptosomes. Based on the data obtained, at least six compounds appear to permit a clear-cut pharmacological discrimination between h5-HT$_{1B}$ and h5-HT$_{1D}$ native receptors.

Methods

Characteristics of human specimens

Samples of human cerebral cortex were obtained from 11 female and seven male patients (aged 19–70 years). The tissues had to be removed from patients undergoing neurosurgery either to remove deeply located tumours or to treat epilepsy resistant to antiepileptic drugs. Samples of frontal (6), temporal (9) and parietal (3) lobes were used. Since no significant differences between results obtained from the two groups of patients were observed, data have been pooled. Immediately after removal, the tissue was placed in a physiological salt solution kept at 2–4°C.

Release experiments

Crude synaptosomes were prepared within 2 h, at 2–4°C. The tissue was homogenized in 40 vol of 0.32 M sucrose, buffered at pH 7.4 with phosphate. The homogenate was centrifuged (5 min at $1000 \times g$), to remove nuclei and debris, and synaptosomes were isolated from the supernatant by centrifugation at $12{,}000 \times g$ for 20 min. The synaptosomal pellet was then resuspended in a physiological medium having the following composition (mM): NaCl 125, KCl 3, $MgSO_4$ 1.2, $CaCl_2$ 1.2, NaH_2PO_4 1, $NaHCO_3$ 22 and glucose 11 (aerated with 95% O_2 and 5% CO_2); pH 7.2–7.4. Protein was determined according to Bradford (1976).

Synaptosomes were incubated 15 min at 37°C in 95% O_2 and 5% CO_2, either with [^{3}H]-5-HT (final concentration 0.08 μM) or without radioactive label (experiments of glutamate release). Experiments of both [^{3}H]-5-HT and endogenous glutamate release were performed with the same tissue sample when a sufficient amount of tissue was available (six out of 18 patients). Identical aliquots of the synaptosomal suspension (0.6–1 mg of protein) were distributed in a set of parallel superfusion chambers maintained at 37°C (Raiteri *et al*., 1974). Superfusion was then started with standard medium aerated with 95% O_2 and 5% CO_2, at a rate of 0.6 ml min^{-1}, and continued for 48 min. At min 39 synaptosomes were depolarized by a 90-s pulse of KCl (15 mM) replacing an equimolar concentration of NaCl. Fraction collection began at min 36, according to the following scheme: two 3-min samples (basal release) before and after one 6-min sample (basal release plus release evoked by high-K^+). When 5-HT was used as an agonist in experiments of [^{3}H]-5-HT release, citalopram (1 μM) (a 5-HT uptake inhibitor) was present from the beginning of superfusion. Agonists were added concomitantly with high K^+, antagonists were present from 8 min before depolarization.

Amino acid determination

The amount of endogenous glutamate released or remaining in the synaptosomes after superfusion was measured by h.p.l.c. The glutamate content of synaptosomes was measured in the supernatant obtained after homogenization (Ultra Turrax, max speed, 20 s) in ice-cold distilled water and centrifugation at $20{,}000 \times g$ for 10 min. The analytical method (Tonnaer *et al*., 1983) involved precolumn derivatization with *o*-phthalaldehyde followed by separation on C_{18} reverse phase chromatography column (Chrompack. 10 cm × 4.6 mm, 3 μm) and three solvent discontinuous gradient, from 23% methanol in acetate buffer 0.1 M pH 6 to 46% methanol in acetate buffer 0.1 M pH 5.8, in 22 min, at a rate of 0.9 ml min^{-1}.

Calculation

The amount of endogenous glutamate released in each fraction collected was expressed as pmol mg^{-1} synaptosomal protein. The radioactivity released in each fraction was calculated as a percentage of the synaptosomal tritium at the onset of the respective collection period. The depolarization-evoked release (overflow) was estimated by subtracting basal release from total release. Depolarization-evoked overflow in the presence of drugs was calculated as percentage variation with respect to the control. Means ± s.e.mean of the given numbers of experiments are presented throughout. The data presented in the Figures were compared by two-tailed Student's *t*-test.

Materials

5-Hydroxytryptamine (5-HT) creatinine sulphate was purchased from Calbiochem. Los Angeles, CA, U.S.A. The following drugs were gifts: N-[4-methoxy-3-(4-methyl- 1-piperazinyl)phenyl]-2′-methyl-4′-(5-methyl-I,2,4-oxa-diazol-3-yl)[1,1,-biphenyl]-4-carboxamide (GR 127935; Glaxo Group Research, Greenford, U.K.); (S)-(+)N-tert-butyl-3-[4-(2-methoxyphenyl)piperazin-1-yl]-2-phenylpropionamide dihydrochloride ((+)-WAY 100135; Wyeth Research, Berkshire, U.K.); 2,3,6,7-tetrahydro-1′-methyl-5-[2′-methyl-4′-(5-methyl-1,2,4- oxadiazol-3-yl) biphenyl-4-carbonyl] furo[2,3-f] indole- 3-spiro-4′-piperidine hydrochloride salt (SB-224289) and 1-phenyl-3-[4-(3-chlorophenyl)piperazin-1-yl]phenylpropan-2-ol dihydrochloride (BRL-15572) (SmithKline Beecham Pharmaceuticals, Harlow, Essex, U.K)

Results

Human cerebral cortex synaptosomes were labelled with [^{3}H]-5-HT and depolarized in superfusion with KCl (15 mM). Basal tritium release was 1.10 ± 0.09% min^{-1} and K^+-evoked

overflow amounted to 3.50±0.15% ($n=6$). The overflow of tritium elicited by K^+ depolarization was inhibited by 40% when 5-HT (0.1 μM) was added to the superfusion medium, in keeping with previously reported results (Maura *et al*., 1993).

The inhibitory effect of 5-HT was totally prevented by GR 127935 (1 μM) (Figure 1), a drug classified as a selective mixed 5-HT$_{1B}$/5-HT$_{1D}$ receptor antagonist (Skingle *et al*., 1993; 1996). GR 127935 (1 μM), added on its own, had no effect on the basal (not shown) or the K^+-evoked tritium release from synaptosomes prelabelled with [^{3}H]-5-HT (Figure 1).

SB-224289, a recently proposed selective h5-HT$_{1B}$ receptor ligand (Roberts *et al*., 1997; Gaster *et al*., 1998), abolished the effect of 5-HT when present in the superfusion medium at 1 μM. At this concentration, SB-224289 did not modify, on its own, the basal (not shown) or the K^+-evoked release of tritium (Figure 1).

The inhibition by 5-HT of the K^+-evoked tritium overflow remained unchanged when BRL-15572 (1 μM), a recently proposed selective h5-HT$_{1D}$ receptor ligand (Price *et al*., 1997; Schlicker *et al*., 1997), was added to the superfusion medium at 1 μM (Figure 1). At this concentration, the compound had little effect on its own.

The selective 5-HT$_{1A}$ receptor antagonist (+)-WAY 100135 (1 μM; Fletcher *et al*., 1993) was also unable to prevent the inhibitory effect of 5-HT and, added alone at 1 μM, did not affect the basal release (not shown) or the K^+-evoked overflow of tritium (Figure 1).

Figure 2 illustrates the results obtained in experiments in which human cerebral cortex synaptosomes were depolarized with KCl (15 mM) and the release of endogenous glutamate was monitored. Basal glutamate release before the onset of the K^+ stimulation amounted to 290±38 pmol mg^{-1} protein ($n=6$); the K^+-evoked glutamate overflow was 505±43 pmol mg^{-1} protein ($n=6$). The overflow of glutamate provoked by high-K^+ had previously been found to be strongly dependent on the presence of Ca^{2+} ions in the superfusion medium (Maura *et al*., 1998).

When 5-HT (0.1 μM) was added concomitantly with the depolarizing stimulus, the glutamate overflow elicited by K^+ (15 mM) was inhibited by 40% (Figure 2), which is in keeping with the concentration-response curve of 5-HT obtained previously, under identical experimental conditions (Maura *et al*., 1998).

The inhibitory effect of 5-HT (0.1 μM) on the K^+-evoked glutamate overflow from human neocortical synaptosomes

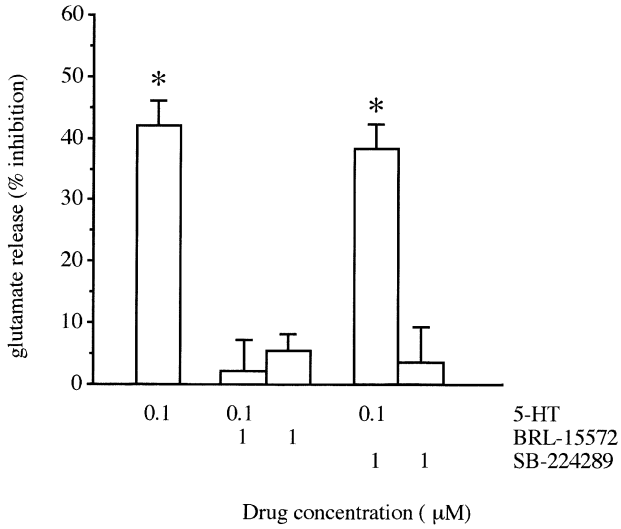

Figure 2 Antagonism by BRL-15572 or SB-224289 of the inhibition by 5-HT of the K^+-evoked glutamate overflow from human cerebrocortical synaptosomes. Data are expressed as per cent inhibition of the K^+-evoked overflow of glutamate. The agonist was added concomitantly with high-K^+; the antagonists 8 min before. For more technical details see Methods. Data are means ±s.e.mean of 3–4 independent experiments, each consisting of three replicate chambers for each condition. *$P<0.005$ when compared to control K^+-evoked overflow.

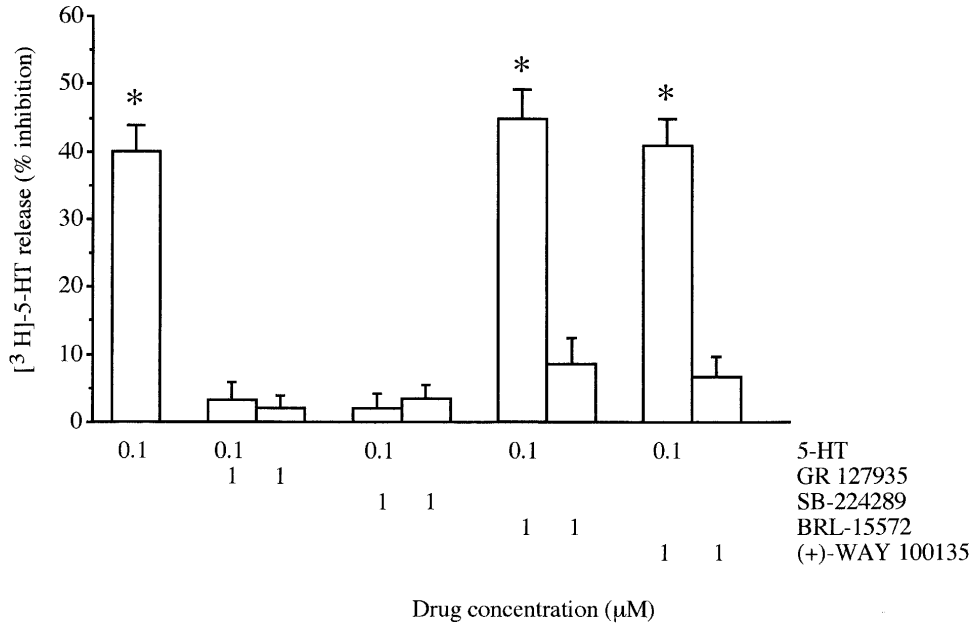

Figure 1 Antagonism by GR 127935, SB-224289, BRL-15572 or (+)-WAY 100135 of the inhibition by 5-HT of the K^+-evoked [^{3}H]-overflow from human cerebrocortical synaptosomes prelabelled with [^{3}H]-5-HT. Data are expressed as per cent inhibition of the K^+-evoked overflow of tritium. The agonist was added concomitantly with high-K^+; the antagonists 8 min before. For more technical details see Methods. Data are means±s.e.mean of 3–6 independent experiments, each consisting of three replicate chambers for each condition. *$P<0.005$ when compared to control K^+-evoked overflow.

was completely prevented by BRL-15572 (1 μM). At this concentration, the compound alone had no effect on the basal release (not shown) or the K^+-evoked overflow of glutamate (Figure 2). In contrast SB-224289 (1 μM) had no significant effect alone or on the 5-HT inhibition of glutamate overflow elicited by depolarization (Figure 2).

To facilitate comparison between the pharmacology of native h5-HT$_{1B}$ auto- and h5-HT$_{1D}$ heteroreceptors, the present data and the results previously obtained with human cerebral cortex have been summarized in Table 1.

Discussion

In the human cerebral cortex, the 5-HT autoreceptor located on serotonergic terminals and which mediates inhibition of 5-HT release probably represents the most important function of the h5-HT$_{1B}$ receptor subtype (Fink *et al*., 1995). Recently, a sumatriptan- and ketanserin-sensitive 5-HT heteroreceptor mediating inhibition of glutamate release was found to exist on glutamatergic nerve terminals of human brain cortex and proposed to represent a functional model for the h5-HT$_{1D}$ subtype (Maura *et al*., 1998). The compounds listed in Table 1 are ligands at h5-HT$_{1B}$/h5-HT$_{1D}$ receptors, based largely on studies with recombinant receptors and, more rarely, with native human CNS receptors. The analysis of these compounds in release experiments with superfused human neocortex synaptosomes has now been completed and the Table summarizes their classification as agonists or antagonists (or inactive molecules) at the native h5-HT$_{1B}$ and h5-HT$_{1D}$ receptors considered.

Sumatriptan, a h5-HT$_{1B}$/h5-HT$_{1D}$ ligand, is an agonist at both auto- and heteroreceptors (Maura *et al*., 1993; 1998). The drug also behaved as a h5-HT$_{1B}$/h5-HT$_{1D}$ receptor agonist in experiments with slices of human cerebral cortex, where it was found to inhibit [^{3}H]-GABA release (Feuerstein *et al*., 1996).

Methiothepin has often been shown to be an antagonist at native human brain 5-HT$_{1B}$/5-HT$_{1D}$ receptors. It blocked h5-HT$_{1B}$ terminal autoreceptors both in slices (Schlicker *et al*., 1985; Galzin *et al*., 1992) and in synaptosomes (Maura *et al*., 1993; Fink *et al*., 1995). Methiothepin also antagonized 5-HT and sumatriptan at the h5-HT$_{1D}$ heteroreceptors regulating glutamate release (Maura *et al*., 1998).

Ketanserin was the first compound proposed to permit discrimination between h5-HT$_{1B}$ and h5-HT$_{1D}$ (Kaumann *et al*., 1994; Pauwels & Colpaert, 1995). Ketanserin exhibited marked selectivity ($\sim$ 70 fold) for the recombinant h5-HT$_{1D}$ relative to the h5-HT$_{1B}$ receptor (Zgombick *et al*., 1995). Accordingly, we recently found that ketanserin antagonized the sumatriptan-induced inhibition of glutamate release, whereas the sumatriptan-sensitive human neocortex autoreceptor was ketanserin-insensitive (Maura *et al*., 1993; Fink *et al*., 1995). It has to be noted that the affinity and resulting selectivity of ketanserin for the 5-HT$_{1D}$ receptor is species dependent: the drug is only 5 fold selective for the guinea-pig 5-HT$_{1D}$ receptor relative to the guinea-pig 5-HT$_{1B}$ subtype (Zgombick *et al*., 1997).

We find here that GR 127935 is a terminal autoreceptor h5-HT$_{1B}$ antagonist, devoid of intrinsic activity (Figure 1), whereas at the h5-HT$_{1D}$ heteroreceptor regulating glutamate release, GR 127935 was recently reported to behave as a full agonist (Maura *et al*., 1998). The compound is usually classified as a 'mixed 5-HT$_{1B}$/5-HT$_{1D}$ receptor antagonist', based on functional data from experimental animals (Skingle *et al*., 1993; 1996). However, GR 127935 has been tested in several works carried out with recombinant h5-HT$_{1B}$ and h5-HT$_{1D}$ receptors and the data obtained, although in part controversial, possibly due to the different properties of the transfection hosts and differences in receptor expression levels, show that GR 127935 can display intrinsic activity. GR 127935 was a full agonist in HeLa cells expressing h5-HT$_{1D}$ and h5-HT$_{1B}$ receptors (Walsh *et al*., 1995), and NIH-3T3 fibroblast expressing h5-HT$_{1D}$ receptors. It was a partial agonist in Y-1 adrenocortical cells expressing h5-HT$_{1B}$ receptors (Zgombick *et al*., 1996); whereas, similarly to what observed in our present work, GR 127935 was an antagonist at cloned h5-HT$_{1B}$ receptors, in transfected CHO cells, while showing intrinsic agonist activity at the h5-HT$_{1D}$ subtype (Pauwels & Colpaert, 1995; Pauwels *et al*., 1997). Interestingly, GR-127935 showed partial agonist activity at recombinant h5-HT$_{1D}$ receptors in a cell line where no receptor reserve existed (Watson *et al*., 1996).

Metergoline is known as a high affinity ligand at 5-HT$_{1B}$/5-HT$_{1D}$ receptors (Hamblin & Metcalf, 1991; Bruinvels *et al*., 1992). Strong intrinsic activity was observed with the drug at cloned h5-HT$_{1D}$ receptors, but not at the h5-HT$_{1B}$ subtype (Pauwels *et al*., 1996). In keeping with these results, we found metergoline unable to antagonize 5-HT at the h5-HT$_{1D}$ heteroreceptor regulating glutamate release; instead, metergoline inhibited the K^+-evoked overflow of glutamate (Maura *et al*., 1998), thus behaving as a h5-HT$_{1D}$ receptor agonist (Table 1). Conversely, at the concentration displaying maximal agonist activity at the h5-HT$_{1D}$ heteroreceptor, metergoline blocked 5-HT at the autoreceptors regulating 5-HT release in the human neocortex (Galzin *et al*., 1992; Maura *et al*., 1993) and it should therefore be considered as a potent antagonist at the native h5-HT$_{1B}$ subtype.

SB-224289 has been classified as a selective 5-HT$_{1B}$ receptor antagonist (Roberts *et al*., 1997; 1998; Gaster *et al*., 1998). Accordingly, the compound blocked the effect of 5-HT on the terminal autoreceptor in human neocortex synaptosomes. Added to the superfusion medium in absence of exogenous 5-HT, SB-224289 had no effect on the K^+-evoked overflow of [^{3}H]-5-HT. In contrast, at the heteroreceptors regulating glutamate release SB-224289 was unable to prevent the action of 5-HT; moreover, in the absence of 5-HT, it did not inhibit the K^+-evoked overflow of glutamate. Thus SB-224289 is a pure antagonist at the h5-HT$_{1B}$ autoreceptor at concentrations which have no effect on the h5-HT$_{1D}$ heteroreceptor.

BRL-15572 behaved as a pure antagonist at the h5-HT$_{1D}$ heteroreceptor regulating glutamate release in human cere-

Table 1 Pharmacological profiles of the h5-HT$_{1B}$ autoreceptor and of the h5-HT$_{1D}$ heteroreceptor regulating glutamate release in human cerebral cortex

Drugs	*h5-HT$_{1B}$ autoreceptor*	*h5-HT$_{1D}$ heteroreceptor*
Sumatriptan	Agonist[a]	Agonist[b]
Methiothepin	Antagonist[a,c]	Antagonist[b]
Ketanserin	Inactive[a,c]	Antagonist[b]
GR 127935	Antagonist	Agonist[b]*
Metergoline	Antagonist[a,d]	Agonist[b]*
SB-224289	Antagonist	Inactive
BRL-15572	Inactive	Antagonist
(+)-WAY 100135	Inactive	Agonist[b]*

[a]Data from Maura *et al*. (1993); [b]Maura *et al*. (1998); [c]Fink *et al*. (1995); [d]Galzin *et al*. (1992). *Full agonist; maximal effect at 1 μM, as with 5-HT or sumatriptan (Maura *et al*., 1998).

brocortex, while exhibiting little or no affinity for the h5-HT$_{1B}$ autoreceptor. In a recent paper (Schlicker *et al*., 1997), BRL-15572 was reported to block the effect of 5-HT on the electrically-evoked release of [^{3}H]-noradrenaline from human atrial appendages, an effect mediated by presynaptic h5-HT$_{1D}$ heteroreceptors on noradrenergic terminals (Molderings *et al*., 1996).

The 5-HT$_{1A}$ receptor antagonist (+)-WAY 100135 had previously been found to inhibit the K^+-evoked overflow of glutamate from human neocortex synaptosomes. Actually, in experiments run in parallel with sumatriptan, the inhibition caused by (+)-WAY 100135 (1 μM) did not differ significantly from that caused by sumatriptan (1 μM), the maximally effective concentration of this drug (Maura *et al*., 1998). Thus (+)-WAY 100135, similarly to GR 127935, metergoline and spiperone (Maura *et al*., 1998), appears to be a full agonist at h5-HT$_{1D}$ heteroreceptors regulating glutamate release. On the other hand, (+)-WAY 100135 (1 μM) was unable to reduce the action of 5-HT on the autoreceptor; moreover, the compound had no effect on [^{3}H]-5-HT release, in the absence of 5-HT, indicating poor, if any, affinity for the h5-HT$_{1B}$ autoreceptor (Table 1). Our data are in good agreement with those recently reported by Davidson *et al*. (1997) showing that (+)-WAY 100135 had much higher affinity for recombinant h5-HT$_{1D}$ than h5-HT$_{1B}$ receptors and behaved as a partial agonist in [^{35}S]-GTPγS binding.

To conclude, our functional studies of native h5-HT$_{1B}$ and h5-HT$_{1D}$ receptors in the cerebral cortex clearly show that the two receptors, originally reported to be pharmacologically indistinguishable (Weinshank *et al*., 1992), exhibit in fact a strikingly different pharmacology. Oddly enough, the diversity between these two receptor subtypes, as it emerges from the data summarized in Table 1, appears much more convincing than for other receptor systems, for instance the muscarinic receptors, where subtypes have often been proposed on the basis of relatively modest quantitative differences between antagonist affinities.

The finding that compounds which, based on experiments with laboratory animals, are known as pure receptor antagonists (GR 127935, metergoline, (+)-WAY 100135), exhibit high intrinsic activity at native h5-HT$_{1D}$ heteroreceptors, whereas none of the antagonists tested show intrinsic activity at h5-HT$_{1B}$ autoreceptors, deserves some comments. As previously mentioned, intrinsic agonist activity is sometimes displayed in recombinant systems by otherwise pure receptor antagonists due to excessive receptor expression and consequent receptor reserve (Hoyer & Boddeke, 1993). It is usually thought that these drugs would be silent antagonists in native tissues, unless a large receptor reserve exists. If this is true, our data might reflect the existence of a high reserve of h5-HT$_{1D}$ heteroreceptors, but not of h5-HT$_{1B}$ autoreceptors, in the human cerebral cortex. In any case, considering the variability of the results obtained with cell systems expressing recombinant receptors, but also the species variations in ligand affinities previously observed (see Zgombick *et al*., 1997), it is evident that functional studies with native human receptors remain of unique importance.

The pharmacological diversity of human 5-HT$_{1B}$ and 5-HT$_{1D}$ receptors augurs well for the potential development of receptor-selective drugs. In particular, the clear differences existing between release-regulating h5-HT$_{1B}$ terminal autoreceptors and h5-HT$_{1D}$ glutamate terminal heteroreceptors in human brain opens the possibility to develop drugs that are selective autoreceptor antagonists or heteroreceptor agonists, or both, and which may represent novel therapeutic agents potentially useful in conditions characterized by defective serotonergic transmission or/and excessive glutamatergic transmission, including depression, epilepsy and neurodegenerative diseases.

Supported by grants from Telethon – Italy (Grant no. 869) and from the Italian M.U.R.S.T. The authors wish to thank Mrs Maura Agate for her help in preparing the manuscript.

References

BRADFORD, M.M. (1976). A rapid and sensitive method for the quantification of microgram quantities of protein utilizing the principle of protein-dye binding. *Anal. Biochem.,* **72,** 248 – 254.

BRUINVELS, A.T., LERY, H., NOZULAK, J., PALACIOS, J.M. & HOYER, D. (1992). 5-HT$_{1D}$ binding sites in various species: similar pharmacological profile in dog, monkey, calf, guinea-pig and human brain membranes. *Naunyn-Schmiedeberg's Arch. Pharmacol.,* **346,** 243 – 248.

DAVIDSON, C., HO, M., PRICE, G.W., JONES, B.J. & STAMFORD, J.A. (1997). (+)-WAY 100135, a partial agonist, at native and recombinant 5-HT$_{1B/1D}$ receptors. *Br. J. Pharmacol.,* **121,** 737 – 742.

FEUERSTEIN, T.J., HÜRING, H., VAN VELTHOVEN, V., LÜCKING, C.H. & LANWEHRMEYER, G.B. (1996). 5-HT$_{1D}$-like receptors inhibit the release of endogenously formed [^{3}H]GABA in human, but not in rabbit, neocortex. *Neurosci. Lett.,* **209,** 210 – 214.

FINK, K., ZENTNER, J. & GÖTHERT, M. (1995). Subclassification of presynaptic 5-HT autoreceptors in the human cerebral cortex as 5-HT$_{1D\beta}$ receptors. *Naunyn-Schmiedeberg's Arch. Pharmacol.,* **352,** 451 – 454.

FLETCHER, A., BILL, D.J., BILL, S.J., CLIFFE, I.A., DOVER, G.M., FORSTER, E.A., HASKINS, J.T., JONES, D., MANSELL, H.L. & REILLY, Y. (1993). WAY 100135: a novel, selective antagonist at presynaptic and postsynaptic 5-HT$_{1A}$ receptors. *Eur. J. Pharmacol.,* **237,** 283 – 291.

GALZIN, A.M., POIRIER, M.F., LISTA, A., CHODKIEWICZ, J.P., BLIER, P., RAMDINE, R., LOÔ, H., ROUX, F.X., REDONDO, A. & LANGER, S.Z. (1992). Characterization of the 5-hydroxytryptamine receptor modulating the release of 5-[^{3}H]hydroxytryptamine in slices of the human neocortex. *J. Neurochem.,* **59,** 1293 – 1301.

GASTER, L.M., BLANEY, F.E., DAVIES, S., DUCKWORTH, D.M., HAM, P., JENKINS, S., JENNINGS, A.J., JOINER, G.F., KING, F.D., MULHOLLAND, K.R., WYMAN, P.A., HAGAN, J.J., HATCHER, J., JONES, B.J., MIDDLEMISS, D.N., PRICE, G.W., RILEY, G., ROBERTS, C., ROUTLEDGE, C., SELKIRK, J. & SLADE, P.D. (1998). The selective 5-HT$_{1B}$ receptor inverse agonist 1′-methyl-5-[[2′-methyl-4′-(5-methyl-1,2,4-oxadiazol-3-yl)biphenyl-4-yl]carbonyl]-2,3,6,7-tetrahydrospiro[furo[2,3-*f*]indole-3,4′-piperidine] (SB-224289) potently blocks terminal 5-HT autoreceptor function both *in vitro* and *in vivo*. *J. Med. Chem.,* **41,** 1218 – 1235.

HAMBLIN, M.W. & METCALF, M.A. (1991). Primary structure and functional characterization of a human 5-HT$_{1D}$-type serotonin receptor. *Mol. Pharmacol.,* **40,** 143 – 148.

HARTIG, P.R., BRANCHEK, T.A. & WEINSHANK, R.L. (1992). A subfamily of 5-HT$_{1D}$ receptor genes. *Trends Pharmacol. Sci.,* **13,** 152 – 159.

HOYER, D. & BODDEKE, H.W.G.M. (1993). Partial agonists, full agonists, antagonists: dilemmas of definition. *Trends Pharmacol. Sci.,* **14,** 270 – 275.

HOYER, D., CLARKE, D.E., FOZARD, J.R., HARTIG, P.R., MARTIN, G.R., MYLECHARANE, E.J., SAXENA, P.R. & HUMPHREY, P.A. (1994). International Union of Pharmacology classification of receptors for 5-hydroxytryptamine (serotonin). *Pharmacol. Rev.,* **2,** 157 – 203.

KAUMANN, A.J., FRENKEN, M., POSIVAL, H. & BROWN, A.M. (1994). Variable participation of 5-HT$_1$-like receptors and 5-HT$_2$ receptors in serotonin-induced contraction of human isolated coronary arteries. *Circulation,* **90,** 1141 – 1153.

MARTIN, G.R. & HUMPHREY, P.P.A. (1994). Classification Review. Receptors for 5-hydroxytryptamine: current perspectives on classification and nomenclature. *Neuropharmacology,* **33,** 261 – 273.

MAURA, G., MARCOLI, M., TORTAROLO, M., ANDRIOLI, G.C. & RAITERI, M. (1998). Glutamate release in human cerebral cortex and its modulation by 5-hydroxytryptamine acting at h5-HT$_{1D}$ receptors. *Br. J. Pharmacol.,* **123,** 45 – 50.

MAURA, G., THELLUNG, S., ANDRIOLI, G.C., RUELLE, A. & RAITERI, M. (1993). Release-regulating serotonin 5-HT$_{1D}$ autoreceptors in human cerebral cortex. *J. Neurochem.,* **60,** 1179 – 1182.

MOLDERINGS, G.J., FRÖLICH, D., LIKUNGU, J. & GÖTHERT, M. (1996). Inhibition of noradrenaline release via presynaptic 5-HT$_{1D\alpha}$ receptors in human atrium. *Naunyn-Schmiedeberg's Arch. Pharmacol.,* **353,** 272 – 280.

PAUWELS, P.J. & COLPAERT, F.C. (1995). The 5-HT$_{1D}$ receptor antagonist GR 127,935 is an agonist at cloned human 5-HT$_{1D\alpha}$ receptor sites. *Neuropharmacology,* **34,** 235 – 237.

PAUWELS, P.J., PALMIER, C., WURCH, T. & COLPAERT, F.C. (1996). Pharmacology of cloned human 5-HT$_{1D}$ receptor-mediated functional responses in stably transfected rat C6-glial cell lines: further evidence differentiating human 5-HT$_{1D}$ and 5-HT$_{1B}$ receptors. *Naunyn-Schmiedeberg's Arch. Pharmacol.,* **353,** 144 – 156.

PAUWELS, P.J., TARDIF, S., PALMIER, C., WURCH, T. & COLPAERT, F.C. (1997). How efficacious are 5-HT$_{1B/D}$ receptor ligands: an answer from GTPγS binding studies with stably transfected C6-glial cell lines. *Neuropharmacology,* **36,** 499 – 512.

PRICE, G.W., BURTON, M.J., COLLIN, L.J., DUCKWORTH, M., GASTER, L., GÖTHERT, M., JONES, B.J., ROBERTS, C., WATSON, J.M. & MIDDLEMISS, D.N. (1997). SB-216641 and BRL-15572-compounds to pharmacologically discriminate h5-HT$_{1B}$ and h5-HT$_{1D}$ receptors. *Naunyn-Schmiedeberg's Arch. Pharmacol.,* **356,** 312 – 320.

RAITERI, M. (1994). Functional studies of neurotransmitter receptors in human brain. *Life Sci.,* **54,** 1635 – 1647.

RAITERI, M., ANGELINI, F. & LEVI, G. (1974). A simple apparatus for studying the release of neurotransmitters from synaptosomes. *Eur. J. Pharmacol.,* **25,** 411 – 414.

ROBERTS, C., BELENGUER, A., MIDDLEMISS, D.N. & ROUTLEDGE, C. (1998). Differential effects of 5-HT$_{1B/1D}$ receptor antagonists in dorsal and median raphe innervated brain regions. *Eur. J. Pharmacol.,* **346,** 175 – 180.

ROBERTS, C., PRICE, G.W., GASTER, L., JONES, B.J., MIDDLEMISS, D.N. & ROUTLEDGE, C. (1997). Importance of 5-HT$_{1B}$ receptor selectivity for 5-HT terminal autoreceptor activity: an *in vivo* microdialysis study in the freely-moving guinea-pig. *Neuropharmacology,* **36,** 549 – 557.

SCHLICKER, E., BRANDT, F., CLASSEN, K. & GÖTHERT, M. (1985). Serotonin release in human cerebral cortex and its modulation via serotonin receptors. *Brain Res.,* **331,** 337 – 341.

SCHLICKER, E., FINK, K., MOLDERINGS, G.J., PRICE, G.W., DUCKWORTH, M., GASTER, L., MIDDLEMISS, D.N., ZENTNER, J., LIKUNGU, J. & GÖTHERT, M. (1997). Effects of selective h5-HT$_{1B}$ (SB-216641) and h5-HT$_{1D}$ (BRL-15572) receptor ligands on guinea-pig and human 5-HT auto- and heteroreceptors. *Naunyn-Schmiedeberg's Arch. Pharmacol.,* **356,** 321 – 327.

SKINGLE, M., BEATTIE, D.T., SCOPES, D.I.C., STARKEY, S.J., CONNOR, H.E., FENIUK, W. & TYERS, M.B. (1996). GR127935: a potent and selective 5-HT$_{1D}$ receptor antagonist. *Behav. Brain Res.,* **73,** 157 – 161.

SKINGLE, M., SCOPES, D.I.C., FENIUK, W., CONNOR, H.E., CARTER, M.C., CLITHEROW, J.W. & TYERS, M.B. (1993). GR 127935: a potent orally active 5-HT$_{1D}$ receptor antagonist. *Br. J. Pharmacol.,* **110,** 9P.

TONNAER, J.A.D.M., ENGELS, G.M.H., WIEGANT, V.M., BURBACH, J.P.H., DE JONG, W. & DE WIED, D. (1983). Proteolytic conversion of angiotensins in rat brain tissue. *Eur. J. Biochem.,* **131,** 415 – 421.

WALSH, D.M., BEATTIE, D.T. & CONNOR, H.E. (1995). The activity of 5-HT$_{1D}$ receptor ligands at cloned human 5-HT$_{1D\alpha}$ and 5-HT$_{1D\beta}$ receptors. *Eur. J. Pharmacol.,* **287,** 79 – 84.

WATSON, J.M., BURTON, M.J., PRICE, G.W., JONES, B.J. & MIDDLEMISS, D.N. (1996). GR127935 acts as a partial agonist at recombinant human 5-HT$_{1D\alpha}$ and 5-HT$_{1D\beta}$ receptors. *Eur. J. Pharmacol.,* **314,** 365 – 372.

WEINSHANK, R.L., ZGOMBICK, J.M., MACCHI, M.J., BRANCHEK, T.A. & HARTIG, P.R. (1992). Human serotonin 1D receptor is encoded by a subfamily of two distinct genes: 5-HT$_{1D\alpha}$ and 5-HT$_{1D\beta}$ *Proc. Natl. Acad. Sci. U.S.A.,* **89,** 3630 – 3634.

ZGOMBICK, J.M., BARD, J.A., KUCHAREWICZ, S.A., URQUHART, D.A., WEINSHANK, R.L. & BRANCHEK, T.A. (1997). Molecular cloning and pharmacological characterization of guinea pig 5-HT$_{1B}$ and 5-HT$_{1D}$ receptors. *Neuropharmacology,* **36,** 513 – 524.

ZGOMBICK, J.M., SCHECHTER, L.E., ADHAM, N., KUCHAREWICZ, S.A., WEINSHANK, R.L. & BRANCHEK, T.A. (1996). Pharmacological characterizations of recombinant human 5-HT$_{1D\alpha}$ and 5-HT$_{1D\beta}$ receptor subtypes coupled to adenylate cyclase inhibition in clonal cell lines: apparent differences in drug intrinsic efficacies between human 5-HT$_{1D}$ subtypes. *Naunyn-Schmiedeberg's Arch. Pharmacol.,* **354,** 226 – 236.

ZGOMBICK, J.M., SCHECHTER, L.E., KUCHAREWICZ, S.A., WEINSHANK, R.L. & BRANCHEK, T.A. (1995). Ketanserin and ritanserin discriminate between recombinant human 5-HT$_{1D\alpha}$ and 5-HT$_{1D\beta}$ receptor subtypes. *Eur. J. Pharmacol. Mol. Pharmacol. Section,* **291,** 9 – 15.

(Received July 16, 1998
Revised October 29, 1998
Accepted November 4, 1998)

British Journal of Pharmacology (1999) 126, 613–620
http://www.stockton-press.co.uk/bjp

Effect of prolonged administration of a urinary kininase inhibitor, ebelactone B on the development of deoxycorticosterone acetate-salt hypertension in rats

*,[1]Hiroshi Ito, [1]Masataka Majima, [1]Shin-ichi Nakajima, [1]Izumi Hayashi, [1]Makoto Katori & [2]Tohru Izumi

[1]Department of Pharmacology, Kitasato University School of Medicine, Kitasato 1-15-1, Sagamihara, Kanagawa 228, Japan and [2]Internal Medicine, Kitasato University School of Medicine, Kitasato 1-15-1, Sagamihara, Kanagawa 228, Japan

1 The effect of prolonged administration of a carboxypeptidase Y-like kininase inhibitor, ebelactone B (EB) (2-ethyl-3, 11-dihydroxy-4, 6, 8, 10, 12-pentamethyl-9-oxo-6-tetradecenoic 1, 3-lactone), on the development of deoxycorticosterone acetate (DOCA)-salt hypertension was tested.

2 The systolic blood pressure (SBP) of non-treated 6-week-old Sprague-Dawley strain rats was gradually increased by DOCA-salt treatment from 137 ± 2 mmHg ($n = 11$) to 195 ± 7 mmHg at 10 weeks of age.

3 With daily oral administration of lisinopril (5 mg kg^{-1}, twice a day), which is an inhibitor of angiotensin converting enzyme, a major kininase in plasma, the development of hypertension was not suppressed.

4 By contrast, administration of EB (5 mg kg^{-1}, twice a day), completely inhibited the development of hypertension (SBP: 146 ± 1 mmHg, $n = 5$, 10 weeks old). The reduced SBP at 10 weeks of age was equal to the SBP before any treatment (142 ± 1 mmHg, $n = 5$).

5 Direct determination of mean blood pressure (MBP) in conscious, unrestrained rats confirmed that MBP elevation was completely inhibited by EB.

6 Continuous subcutaneous infusion (5 mg kg^{-1} day^{-1}) of HOE140, a bradykinin B_2 receptor antagonist, restored the elevation of SBP, which was suppressed by EB.

7 The weights of left ventricle of DOCA-salt treated rats 10-weeks-old (0.36 ± 0.02 g 100 g body $weight^{-1}$, $n = 11$) was significantly reduced by EB (0.27 ± 0.01, $n = 5$), as were the sodium levels in serum, cerebrospinal fluid and erythrocyte.

8 These findings suggested that EB is effective in preventing salt-related hypertension presumably by eliminating sodium retention.

Keywords: Ebelactone B; deoxycorticosterone acetate-salt hypertension; bradykinin; kininase

Abbreviations: ACE, angiotensin converting enzyme; CPY, carboxypeptidase Y; DOCA, deoxycorticosterone acetate; EB, ebelactone B; MBP, mean blood pressure; NEP, neutral endopeptidase; SBP, systolic blood pressure; SD, Sprague-Dawley

Introduction

A wide variety of antihypertensive agents can reduce established genetic or secondary hypertension, and several antihypertensive agents capable of improving the patient's quality of life are now available. However, fewer drugs have been developed for the prevention of hypertension. Some researchers have tried to predict high blood pressure in childhood so that action can be taken to prevent hypertension in the adults (Zinner *et al*., 1971; Klein *et al*., 1977; Holland & Beresford, 1977; Higgins *et al*., 1980; Levine *et al*., 1980; Lauer *et al*., 1991). Even in a genetically hypertensive model, namely, the spontaneously hypertensive rats, it was suggested that the initial phase is critical in the development of hypertension (Unger & Rettig, 1990). In the present experiment, we administered a urinary kininase inhibitor with the aim of preventing the development of hypertension in models in which short-duration administration was effective in reducing high blood pressure (Majima *et al*., 1995).

We previously reported that the renal kallikrein kinin system showed an antihypertensive action, suppressing the development of hypertension when sodium retention in the body was induced (Majima & Katori, 1994). This was due to kinin generated through the action of kallikrein secreted from the connecting tubules of the kidney (Scicli & Carretero, 1986), and may be potentiated when kinin degradation in the kidney is inhibited. In rat urine, we found a novel urinary kininase, a carboxypeptidase Y (CPY)-kininase, some of whose characteristics resembled those of a carboxypeptidase from yeast (Kuribayashi *et al*., 1993). This serine protease was a major kininase in rat urine in terms of kinin-degrading activity (Kuribayashi *et al*., 1993), and is also secreted in human urine (Saito *et al*., 1995). In addition, a microbial product, ebelactone B (EB), was found. It was isolated from Actinomycetes, and is a potent inhibitor of carboxypeptidase Y-like kininase (Majima *et al*., 1994a). EB showed kinin-dependent diuretic and natriuretic actions in anaesthetized rats (Majima *et al*., 1994a), and transiently but significantly reduced the high blood pressure in a deoxycorticosterone acetate (DOCA)-salt model on short-term administration (Majima *et al*., 1995).

In the present experiment, we tested the preventive effect on the development of hypertension by a prolonged administration of EB from the first day of DOCA-salt treatment.

* Author for correspondence.

Methods

Animals

Male Sprague-Dawley strain (SD) rats (specific pathogen-free, 6-weeks-old, SLC, Hamamatsu, Japan) were used. All animals were housed at a constant humidity ($60 \pm 5\%$) and temperature ($25 \pm 1°C$), and kept on a 12-h light/12-h dark cycle throughout the experiments. All rats were given normal rat chow containing 0.3% sodium, NMF (Oriental Yeast Corp., Tokyo, Japan). The number of animals (n) used for each experiment is stated in the corresponding section. This study was performed in accordance with the guidelines for animal experiments of Kitasato University School of Medicine.

Induction of hypertension and administration of kininase inhibitors

At 6 weeks of age, the drinking water was replaced with 1% NaCl solution after resection of the left kidney, and weekly subcutaneous administration of deoxycorticosterone acetate solution (5 mg kg^{-1} $week^{-1}$, 5 mg ml^{-1} in physiological saline containing 50 mg ml^{-1} of gum arabic) was started for 4 weeks as reported previously (Majima *et al*., 1991).

One day after the start of DOCA-salt treatment, EB (5 mg kg^{-1}, suspended in 1% CMC at a concentration of 15 mg ml^{-1}; a gift from the Institute of Microbial Chemistry, Tokyo, Japan), lisinopril (5 mg kg^{-1}, suspended in 1% CMC at a concentration of 15 mg ml^{-1}; a gift from Shionogi Pharmaceutical Corp., Osaka, Japan) or BP102 (sinorphan, 30 mg kg^{-1}, dissolved in 1% CMC at a concentration of 90 mg/ml, a gift from Shionogi Pharmaceutical Corp., Osaka, Japan) was administered twice a day for 4 weeks by oral administration. BP102 was developed as a prodrug of the neutral endopeptidase (NEP) inhibitor thiorphan, which was the first synthetic inhibitor of NEP (Roques *et al*., 1980). Control animals received only vehicle solution, and two further control groups were prepared. One group is unilateral nephrectomised rats without 1% NaCl solution and subcutaneous injection of DOCA. Another group is unilateral nephrectomised rats with DOCA-treatment without giving 1% NaCl solution.

Doses used in the present experiment were selected as follows. The previous report (Majima *et al*., 1995), we administered EB at doses of 5 and 15 mg kg^{-1} (twice a day). The hypotensive effects were not increased with higher doses. Thus, we selected the dose of 5 mg kg^{-1}. In case of BP102, diuretic effects were not different between the doses of 30 and 100 mg kg^{-1} (twice a day), suggesting that 30 mg kg^{-1} was a maximal dose. In the preliminary experiments, lisinopril (5 mg kg^{-1}, twice a day) completely blocked the development of hypertension in young spontaneously hypertensive rats. Thus, this dose was selected in these experiments.

Measurement of blood pressure

The systolic blood pressure (SBP) of unanaesthetized rats was determined twice a week with a tail-cuff plethysmograph (Ueda model UR1000, Ueda Seisakusho, Tokyo Japan) as reported previously (Majima *et al*., 1991; 1993a; 1994b) twice a week for 4 weeks from the start of experiment. Mean arterial blood pressure (MBP) was determined for 1 h in conscious and unrestrained rats, as reported previously (Majima *et al*., 1993a; 1994b) 1 day after determination of the SBP. The rats were anaesthetized with light ether anaesthesia soon after the SBP determination by tail-cuff method, and a polyethylene cannula (PE-10, Clay Adams, Parsippany, NJ, U.S.A.) was inserted into the abdominal aorta through the femoral artery under light ether anaesthesia and the cannula was connected to a PE-50 cannula (Clay Adams, Parsippany, NJ, U.S.A.) and exteriorized in the interscapular region.

On the next day, a blood pressure transducer (TP-200T, Nihon Kohden, Tokyo, Japan) was attached to the other end of the intra-arterial cannula, and the mean arterial blood pressure was monitored on a polygraph (WS-641-G, Nihon Kohden, Tokyo, Japan) (Majima *et al*., 1995). Starting 30 min after the connection of the transducer, recordings were made for over 1 h in the rats, which were kept in separate cages.

Weights of left ventricle of heart and of kidney

Immediately after blood collection, rats were exsanguinated and the hearts and kidneys were excised under ether anaesthesia, and were fixed with a 10% formaldehyde solution. After removal of the atrium and right ventricle from the fixed hearts, the left ventricles were weighed (Majima *et al*., 1993a). The hearts (non-treated) from rats without nephrectomy, which received no salt water were also weighed. The kidneys were also weighed after removal of the *capsula fibrosa*.

Blood collection

One hour after MBP determination, a half ml of blood was collected from the carotid artery at 10 weeks of age through a cannula into glass tubes without anticoagulant under light ether anaesthesia. Collected blood was left at room temperature for 2 h, and then centrifuged at $1500 \times g$ for 15 min at 25°C in order to obtain serum. Blood (1 ml) was also collected directly into tubes containing ice-chilled iso-osmotic lithium chloride solution, for determination of the sodium concentration of the erythrocytes. During the blood collection, there was no volume replacement.

Collection of urine and measurement of urinary levels of sodium

Twenty-four hour urine samples from individual rats were collected using metabolic cages 24 h after determination of SBP at 7 and 9 weeks of age. The volume of urine and drinking water were recorded at the end of the 24 h period. Urinary sodium levels were determined electrometrically using electrodes selective for sodium ions, respectively (Majima *et al*., 1993a). Sodium balance was approximately calculated as the amounts of sodium excreted in urine over 24 h subtracted from the sodium intake.

Collection of urine and measurement of urinary active kallikrein

Twenty-four hour urine samples from individual rats were collected using metabolic cages after determination of SBP at 7 and 9 weeks of age. The volume of urine and drinking water were recorded at the end of the 24 h period.

The active kallikrein in the 24 h urine was measured using a peptidyl fluorogenic substrate selective for glandular kallikrein, Pro-Phe-Arg-methyl-coumarinylamide (Peptide Institute, Minoh, Osaka, Japan), as reported previously (Majima *et al*., 1993a). One arbitrary unit was defined as the amount of urinary kallikrein that released 1×10^{-10} mol 7-amino-4-methylcoumarin from 1 μl of urine in 10 min at 37°C.

Measurement of urinary kinin secretion

Free kinin was measured in the urine collected *via* catheters (PE-10, Clay Adams, Parsippany, NJ, U.S.A.) inserted into ureters of rats under sodium pentobarbitone anaesthesia (60 mg kg^{-1}, s.c.). During urine collection, physiological saline was infused (6 ml kg^{-1} h^{-1}) to the femoral vein. The kinin levels were determined with a bradykinin enzyme immunoassay kit (Markit-M, Dainippon Pharmaceutical Corp., Osaka, Japan) after extraction with ethanol (Majima *et al*., 1991; 1993a; 1994b). Extracted kinin fraction was purified with a Sep-Pak C_{18} column (Waters Associates, Milford, MA, U.S.A.) (Kauker *et al*., 1984). Kinin was separated by high-performance liquid chromatography by the method reported previously (Shima *et al*., 1992; Majima *et al*., 1993a). Four weeks after the start of DOCA-salt treatment (10-weeks-old), EB (5 mg kg^{-1}, suspended in 1% CMC at a concentration of 15 mg ml^{-1}) was orally administered. Urinary kinin excretion during the first 30 min was determined. The excretion of urinary kinin in control rats which did not receive EB, was also measured.

Measurement of sodium levels in serum and in erythrocytes

The levels of sodium in the sera were determined by ion-selective electrodes, as reported previously (Majima *et al*., 1991). The sodium concentration in the erythrocytes (RBC[Na]i), which was a marker for sodium retention, was determined using atomic absorption spectrophotometry (McCormic *et al*., 1989), as reported previously (Majima *et al*., 1993a; 1994b; 1995). The sodium concentrations in the erythrocytes were expressed as mmol l^{-1} RBC.

Measurement of sodium levels in cerebrospinal fluid

Immediately before the blood collection, cerebrospinal fluid from rats (Waynfortii, 1988), was obtained by aspiration from the cisterna magna with a 26-gauge needle under light ether anaesthesia. All rats were kept on the sloped stand which was prepared to aspirate the cerebrospinal fluid easily (Waynfortii, 1988). The levels of sodium in the cerebrospinal fluid were determined with an atomic absorption spectrophotometer, as a marker for the sodium retention (Majima *et al*., 1994b).

Continuous administration of a bradykinin antagonist

A bradykinin antagonist, HOE140 (5 mg kg^{-1} day^{-1}, dissolved in physiological saline, infusion rate; 12 μl day^{-1}, Peptide Institute) was administered from the first day of DOCA-salt treatment by continuous subcutaneous infusion using a micro-osmotic pump (Alzet model 2002, Alza Corp, Palo Alto, CA, U.S.A.) implanted under the skin of back. Control animals received physiological saline (12 μl day^{-1}) using the same type pump. From the first day of DOCA-salt treatment, EB (5 mg kg^{-1}, twice a day, suspended in 1% CMC at a concentration of 15 mg ml^{-1}) was administered twice a day for 2 weeks by oral administration. SBP was determined by tail cuff method and urinary sodium levels were determined using the method described above (Majima *et al*., 1993a).

Statistical analysis

Values were expressed as means $\pm$ s.e.mean. Factorial ANOVA and repeated measures ANOVA with the *post-hoc* test were used to evaluate the significance of differences. For comparison between two groups, Student's *t*-test was used. A P value less than 0.05 was considered to be significant.

Results

Effects of kininase inhibitors on systemic blood pressure of DOCA-salt treated rats

The SBP of non-treated SD strain rats (6-weeks-old) was 137 ± 2 mmHg, and DOCA-salt treatment gradually increased the SBP to 155 ± 3 and 195 ± 7 mmHg, at 8 and 10 weeks of age, respectively (Figure 1). The daily oral administration of the angiotensin converting enzyme (ACE) inhibitor lisinopril from the first day of DOCA-salt treatment did not suppress the development of hypertension (156 ± 5 and 210 ± 10 mmHg, at 8 and 10 weeks of age, respectively). The SBP of rats treated with BP102 (30 mg kg^{-1}, p.o.), which is an inhibitor of neutral endopeptidase, remained at low levels (146 ± 1 and 160 ± 4 mmHg, at 8 and 10 weeks of age, respectively). At 10 weeks of age, SBP of BP102-treated rats was slightly increased, and the difference of SBP between at 6 weeks of age and at 10 weeks of age was statistically significant (ANOVA was used to evaluate the significance of differences). By contrast, administration of EB (5 mg kg^{-1}, p.o.), an inhibitor for rat urinary kininase, completely inhibited the development of hypertension (SBP: 138 ± 1 and 146 ± 1 mmHg, at 8 and 10 weeks of age, respectively).

The results from the direct determination of blood pressure in conscious, unrestrained rats 10-weeks-old (Table 1) were confirmed by those from the tail cuff determination. MBP was reduced by EB (112 ± 1 mmHg) to that in the non-treated rats (110 ± 2 mmHg). There was no significant difference between the control groups (non-treated rats, uninephrectomized rats, and uninephrectomized rats with DOCA treatment) and EB-treated rats.

Effects of kininase inhibitors on weights of left ventricles of heart and kidneys

The left ventricle weight of the vehicle-treated rats (0.36 ± 0.02 g 100 g body $weight^{-1}$), 4 weeks after the start of DOCA-salt treatment (10-weeks-old) was significantly higher than the left ventricle weight of the EB-treated rats (0.27 ± 0.01 g 100 g body $weight^{-1}$). The left ventricle weight of the EB-treated rats was the same as the left ventricle weight of non-treated rats (0.28 ± 0.01 g 100 g body $weight^{-1}$) (Table 1). The left kidney weight of vehicle-treated rats (0.76 ± 0.01 g 100 g body $weight^{-1}$) (10-weeks-old) was significantly higher than the left kidney weight of the EB-treated rats (0.55 ± 0.01 g 100 g body $weight^{-1}$).

Effects of kininase inhibitors on water intake, urine volume, and balance of water and sodium

The urine volume at both 7 and 9 weeks of age were not changed significantly with these kininase inhibitors (Table 2). The same was true in water intake in these animals (Table 2). The tentatively calculated values of sodium balance are shown in Table 2. The amounts of sodium excreted in urine over 24 h were subtracted from the sodium intake, which were derived from the drinking water and food in each rat. As shown in Table 2, sodium retention seen in vehicle- and lisinopril-treated rats was significantly suppressed by BP102 and EB at both 7 and 9 weeks of age.

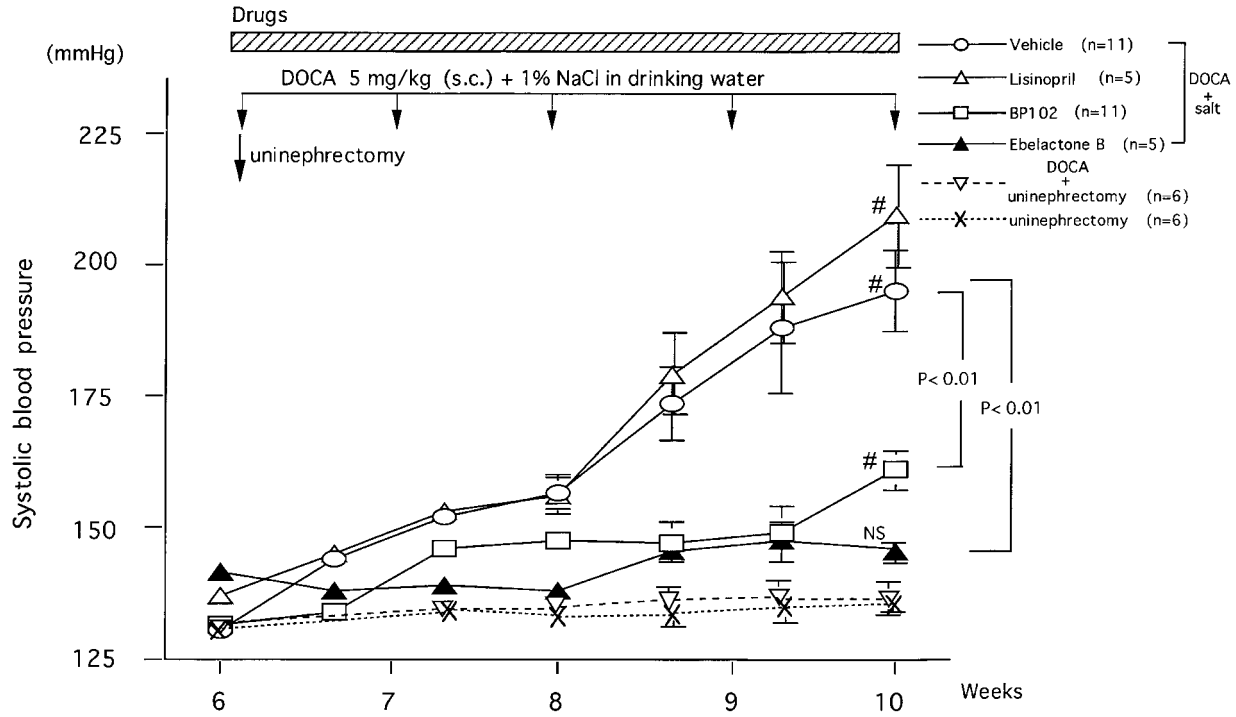

Figure 1 Effects of ebelactone B, BP102 and lisinopril on the development of deoxycorticosterone acetate-salt hypertension. Values are means ± s.e.mean. After unilateral nephrectomy at 6 weeks of age, deoxycorticosterone acetate (5 mg kg^{-1}, s.c.) was administered once a week, and ebelactone B (5 mg kg^{-1}), BP102 (30 mg kg^{-1}), or lisinopril (5 mg kg^{-1}) was administered orally twice a day from immediately after the surgery for 4 weeks. Values in rats receiving these three compounds are shown in comparison with those in rats receiving vehicle. The results of unilateral nephrectomized group with DOCA and unilateral nephrectomized group without DOCA-salt also showed. # comparison of values at 6 and 10 weeks of age. ANOVA was used to evaluate the significance of differences.

Table 1 Effects of ebelactone B, BP102 and lisinopril on the mean blood pressure, weights of left ventricle and right kidney, and body weight in deoxycorticosterone acetate-salt treated rats

				DOCA-salt + uninephrectomy			
(10 weeks)	*Uninephrectomy* (n = 6)	*DOCA + uninephrectomy* (n = 6)	*Vehicle* (n = 11)	*Lisinopril* (n = 5)	*BP102* (n = 11)	*Ebelactone B* (n = 5)	*Non treated* (n = 5)
Mean blood pressure (mmHg)	103 ± 3	105 ± 2	162 ± 9	173 ± 5	120 ± 2*	112 ± 1*	110 ± 2
Left ventricle weight (g 100 g BW^{-1})	0.26 ± 0.01	0.27 ± 0.01	0.36 ± 0.02	0.40 ± 0.01	0.29 ± 0.01**	0.27 ± 0.01**	0.28 ± 0.01
Kidney weight (g 100 g BW^{-1})	0.51 ± 0.03	0.50 ± 0.03	0.76 ± 0.01	0.86 ± 0.05	0.60 ± 0.02***	0.55 ± 0.02***	0.33 ± 0.03
Body weight (g)	330 ± 6.42	328 ± 6.25	296 ± 6.24	291 ± 9.85	315 ± 5.69	311 ± 5.87	337 ± 6.12

Values are means ± s.e.mean. Non-treated: results from rats that underwent neither uninephrectomy nor deoxycorticosterone acetate-salt treatment. ANOVA was used to evaluate the significance of differences. *, **, *** $P<0.05$.

Effects of kininase inhibitors on urinary kallikrein excretions

Urinary active kallikrein secretions in BP102-treated rats were 174 and 226% of those in vehicle rats at 7 and 9 weeks of age, respectively, and in EB-treated rats, were 168 and 236% of those in vehicle rats at 7 and 9 weeks of age, respectively. By contrast, lisinopril (89 and 55% of vehicle rats at 7 and 9 weeks of age, respectively) did not increase the excretion of urinary active kallikrein at either age (Table 2).

Effects of a urinary kininase inhibitor, EB on urinary kinin excretion

The amounts of urinary kinin in DOCA-salt treated rats (10-weeks-old) without EB were 113 ± 29 pg 30 min^{-1} ($n=4$). With EB (5 mg kg^{-1}, p.o.), urinary kinin excretion was increased to 477 ± 154 pg 30 min^{-1} during the first 30 min.

Effects of kininase inhibitors on sodium concentration in serum, cerebrospinal fluid and erythrocytes

The serum sodium levels in rats treated with EB (138 ± 1 mmol l^{-1}) and BP102 (136 ± 1 mmol l^{-1}) were significantly reduced, compared with the levels of vehicle-treated rat (142 ± 1 mmol l^{-1}); whereas lisinopril treatment (144 ± 1 mmol l^{-1}) had no effect on the serum sodium levels (Table 3).

The sodium levels in cerebrospinal fluid in rats treated with EB (127 ± 3 mmol l^{-1}) and BP102 (126 ± 2 mmol l^{-1}) were also less than those in vehicle-treated rats (144 ± 2 mmol l^{-1}). Lisinopril (141 ± 2 mmol l^{-1}) did not reduce the levels (Table 3).

The sodium levels in the erythrocytes of rats treated with EB (5.2 ± 0.3 mmol l^{-1}) and BP102 (5.3 ± 0.3 mmol l^{-1}) were also reduced, compared with vehicle-treated rats (6.3 ± 0.5 mmol l^{-1}). However, lisinopril (5.9 ± 0.3 mmol l^{-1}) showed no significant effect (Table 3).

Effects of HOE140 on systemic blood pressure in EB-treated rats

Continuous subcutaneous infusion of HOE140 to DOCA-salt treated rats, which received oral administration of EB, caused more rapid increase in SBP (167 ± 3 mmHg, $n = 5$, at 8 weeks of age), in comparison with SBP in vehicle-treated rats (145 ± 3 mmHg, $n = 5$, at 8 weeks of age) (Figure 2).

Discussion

We previously reported that Brown Norway Katholiek (BN-Ka) rats, which secrete no kinin in the urine because of a deficiency of kininogens, developed DOCA-salt hypertension more rapidly than in normal rats of the same strain (Brown Norway Kitasato rats, BN-Ki rats) (Majima *et al*., 1991). We found that a major kininase in urine was CPY-like exopeptidase, and was inhibited by a microbial product, ebelactone B, isolated from Actinomycetes (Majima *et al*., 1994a). EB did not inhibit kininases in plasma. The short-term administration of EB (4–7 days) to DOCA-salt treated rats resulted in transient but significant reductions in SBP and MBP during the developmental stages of DOCA-salt hypertension in normal BN-Ki and SD strain rats, which can generate kinin in the urine, however, kininogen-deficient BN-Ka rats showed no reduction in blood pressure (Majima *et al*., 1995). These results suggested that EB reduced blood pressure through an action on the kallikrein-kinin system. EB abolished the retention of sodium in the body, with concomitant increases in urinary sodium excretion even in short-term experiments (Majima *et al*., 1995).

In the present experiment, to test the effects of prolonged administration of EB on the initiation of hypertension in a DOCA-salt hypertensive model, we administered EB from the first day of DOCA-salt treatment throughout the 4-week experimental period (Figure 1). EB completely inhibited the development of hypertension throughout the experimental period and increased urinary kinin excretions. The preventive effect on hypertension development was kinin-dependent, judging from the effect of continuous and simultaneous infusion of HOE140 (Figure 2). By contrast, the ACE inhibitor lisinopril did not reduce the blood pressure. These effects of kininase inhibitors were confirmed from the mean

Table 2 Effects of ebelactone B, BP102 and lisinopril on excretion of urinary active kallikrein, intake of 1% NaCl solution, urine volume, and the balance of water and sodium

				DOCA-salt + uninephrectomy		
	Uninephrectomy (n = 6)	*DOCA + uninephrectomy* (n = 6)	*Vehicle* (n = 11)	*Lisinopril* (n = 5)	*BP102* (n = 11)	*Ebelactone B* (n = 5)
Urinary kallikrein activity (AU day^{-1})						
7 weeks	67 ± 24.8	82 ± 15.3	69 ± 8.9	61 ± 30.5	120 ± 27.3*	116 ± 3.6*
9 weeks	83 ± 32.7	95 ± 23.1	79 ± 18.1	44 ± 8.3	180 ± 55.1**	187 ± 35.1**
24 h intake volume (ml 24 h^{-1} rat^{-1})						
7 weeks	30 ± 4.2	28 ± 3.0	59 ± 7.6	76 ± 14.7	37 ± 2.8	40 ± 3.6
9 weeks	31 ± 4.1	32 ± 3.5	66 ± 4.6	90 ± 10.7	53 ± 4.1	49 ± 3.5
24 h urine volume (ml 24 h^{-1} rat^{-1})						
7 weeks	22 ± 2.0	18 ± 4.3	48 ± 9.4	70 ± 14.1	28 ± 3.2	27 ± 3.5
9 weeks	24 ± 3.1	21 ± 4.4	57 ± 4.1	84 ± 12.0	36 ± 2.8	32 ± 2.3
intake volume – urine volume (ml 24 h^{-1} rat^{-1})						
7 weeks	8 ± 3.3	10 ± 3.2	11 ± 4.1	6 ± 3.4	9 ± 3.1	13 ± 2.3
9 weeks	7 ± 3.6	11 ± 3.9	9 ± 3.8	6 ± 3.3	17 ± 3.3	17 ± 3.1
Sodium intake – urinary sodium (mg 24 h^{-1} rat^{-1})						
7 weeks	1.7 ± 0.9	9.6 ± 2.1	115 ± 10.1	129 ± 12.3	68 ± 7.2*	57 ± 7.1*
9 weeks	0.8 ± 1.2	10.3 ± 2.5	378 ± 25.8	465 ± 27.6	294 ± 18.7**	267 ± 19.5**

Urine was collected for 24 h, and active kallikrein excretion over 24 h was measured using a peptidyl fluorogenic substrate selective for glandular kallikrein as described in Methods. Values are means ± s.e.mean. ANOVA was used to evalue the significance of differences. *, ** $P < 0.05$.

Table 3 Effects of ebelactone B, BP102 and lisinopril on the sodium levels in the serum, cerebrospinal fluid and erythrocytes

				DOCA-salt + uninephrectomy		
(10 weeks)	*Uninephrectomy* (n = 6)	*DOCA + uninephrectomy* (n = 6)	*Vehicle* (n = 11)	*Lisinopril* (n = 5)	*BP102* (n = 11)	*Ebelactone B* (n = 5)
Serum sodium levels (mmol l^{-1})	138 ± 1	137 ± 1	142 ± 1	144 ± 1	136 ± 1*	138 ± 1*
Sodium levels in CSF (mmol l^{-1})	130 ± 3	132 ± 3	144 ± 2	141 ± 2	126 ± 2**	127 ± 3**
RBC [Na]i (mmol l^{-1})	5.1 ± 0.2	5.0 ± 0.3	6.3 ± 0.5	5.9 ± 0.3	5.3 ± 0.3***	5.2 ± 0.3***

Each sample was collected at 10 weeks of age as described in Methods. RBC[Na]i; sodium concentration in erythrocytes. Values are means ± s.e.mean. Values in rats receiving ebelactone B, BP102 or lisinopril were compared with those in rats of the same age receiving vehicle, and ANOVA was used to evaluate the significance of differences. *, **, *** $P < 0.05$.

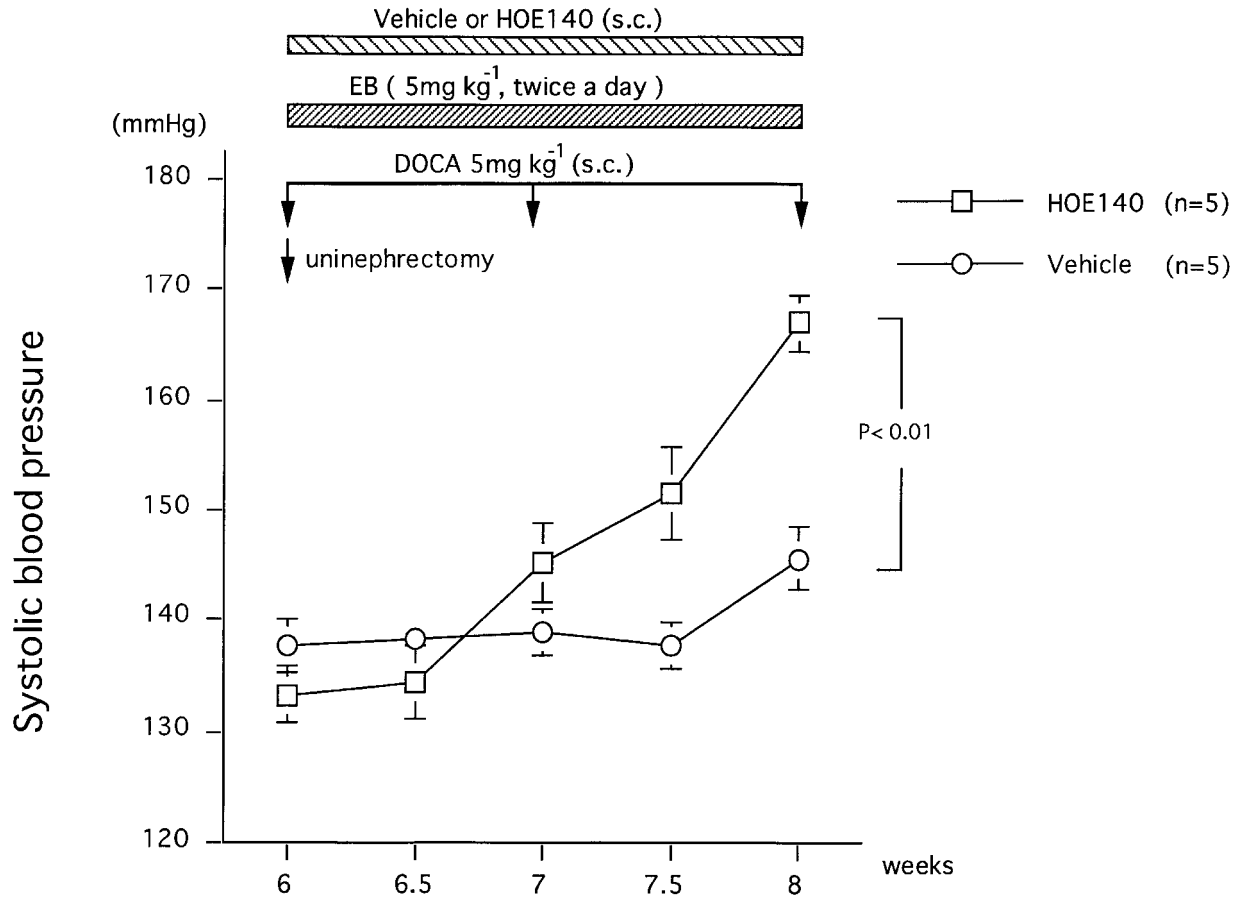

Figure 2 Effects of HOE140 on the development of deoxycorticosterone acetate-salt hypertension in rats under ebelactone B treatment. Values are means ± s.e.mean obtained. After uninephrectomy at 6 weeks of age, deoxycorticosterone acetate (5 mg kg^{-1}, s.c.) was administered once a week. Ebelactone B (5 mg kg^{-1}) was administered orally twice a day from the first day of deoxycorticosterone acetate-salt treatment. HOE140 was continuously infused subcutaneously using a micro-osmotic pump (5 mg kg^{-1} day^{-1}, dissolved in physiological saline). ANOVA was used to evaluate the significance of differences.

blood pressure determined through the indwelling cannula (Table 1). Furthermore, the weights of left ventricle treated with EB were the same as those of rats without DOCA-salt treatment, although significant increases in the weights of left ventricle were observed in DOCA-salt treated rats receiving only vehicle solutions (Table 1). The increase in left ventricular weight may be a consequence of the increased after-load caused by the elevated arterial blood pressure. The kidney weight in vehicle and lisinopril-treated rats were larger than those in EB- and BP102-treated rats. This may be due to the dilatation of renal tubules which was usually observed in the kidney of DOCA-salt treated rats, which secreted a greater volume of urine.

The lack of any antihypertensive effect of ACE inhibitors in DOCA-salt hypertension in rats, which had been reported already by others (Pham *et al.*, 1993), was also confirmed in the present experiment, even though the administration was started at the pre-hypertensive stage (Figure 1). Although ACE (kininase II) is a predominant kininase in rat plasma (Majima *et al.*, 1993b), and though administration of the ACE inhibitor, captopril causes a significant increase in blood kinin levels (Majima *et al.*, 1994a; Nakagawa & Nasjletti, 1988), lisinopril induced no hypotensive response, suggesting that the increased blood kinin levels were not related to the hypotensive response. Plasma renin activity was suppressed markedly in this DOCA-salt model (Majima *et al.*, 1991). These may be reasons for the lack of the antihypertensive effect of ACE inhibitors in DOCA-salt hypertension.

EB decreased the sodium levels in serum together with those in the cerebrospinal fluids and erythrocytes (Table 3), suggesting that EB prevented sodium retention in the body. The increase in sodium concentration of erythrocyte was reported to be a good marker of sodium retention (McCormic *et al.*, 1989), and the increase in sodium levels in cerebrospinal fluid after intracisternal infusion of high sodium solution caused a continuous increase in systemic blood pressure with the concomitant increase in the sympathetic nerve discharge. The 24 h urine volume in rats receiving vehicle solutions or lisinopril tended to be larger than that in rats treated with EB, possibly because of pressure diuresis, or the increased intake of sodium from drinking water (Table 2). The sodium levels in the cerebrospinal fluid and the erythrocytes may be reduced as a result of the lack of sodium retention. In another hypertensive model, spontaneously hypertensive rats, we preliminary tested the effect of EB. Two weeks administration of EB (15 mg kg^{-1} day^{-1}) to spontaneously hypertensive rats (4-weeks-old) reduced SBP from 165 ± 3 (vehicle) to 146 ± 3 mmHg (EB) ($n=5$, $P<0.05$). These suggested that EB may be effective in a model other than DOCA-salt hypertension.

NEP has been reported to be another major kininase in rat urine (Kuribayashi *et al.*, 1993). BP102, a prodrug of the NEP inhibitor thiorphan, significantly inhibited the development of hypertension (Figure 1). However, its potency was weaker than that of the CPY-like kininase inhibitor EB in spite of using the maximal dosage of BP102 and EB. Since the optimal pH of NEP was around 8, and that of CPY-like kininase around 6,

the pH of the urine of rats fed normal chow (around 6) was more suitable for CPY-like kininase to show high protease activity. The actual contribution of CPY-like kininase to the degradation of endogenous kinin may be greater than that of NEP. Thus, EB may exert more complete suppression of the development of DOCA-salt hypertension than BP102. Although the difference of kinetic parameters such as bioavailability was not tested in the present study, the diuretic action of EB was also greater than that of BP102 (Majima *et al*., 1994a; Nakajima *et al*., 1998).

We have previously reported that renal kallikrein secretion from DOCA-salt treated rats was increased compared with that from rats receiving no DOCA-salt treatment, and that the kallikrein secretion from DOCA-salt treated animals peaked 3 weeks after the start of DOCA-salt treatment and thereafter declined (Katori *et al*., 1992). It was reported that DOCA-salt treatment caused renal injury in parallel with the development of hypertension (Dworkin *et al*., 1984; Raij *et al*., 1989). The reduction in kallikrein secretion in the late phase of this hypertensive model may be a reflection of the damage to the renal tubules from which the kallikrein was secreted. In the present experiments, there was no significant reduction in the secretion of urinary kallikrein during ACE inhibitor treatments, although some researchers have reported the reduction in the urinary kallikrein secretion after ACE inhibitors (Zacharieva *et al*., 1996). The reduction in high blood pressure by EB and BP102 may prevent renal injury, because as shown in the present study, urinary secretion of renal kallikrein remained at a higher level in rats receiving these kininase inhibitors (Table 2).

In conclusion, the present results indicated that EB, a urinary CPY-like kininase inhibitor, is a promising agent in terms of the novel concept of preventing the development of hypertension by abolishing sodium retention through the inhibition of kinin degradation.

References

DWORKIN, L.D., HOSTETTER, T.H., RENNKE, H.G. & BRENNER, B.M. (1984). Hemodynamic basis for glomerular injury in rats with deoxycorticosterone-salt hypertension. *J. Clin. Pharmacol.,* **73,** 1448–1461.

HIGGINS, M.W., KELLER, J.B., METZNER, H.L., MOORE, F.E. & OSTRANDER, L.D. (1980). Studies of blood pressure in Tecumseh, Michigan. II. Antecedents in childhood of high blood pressure in young adults. *Hypertension,* **2** (suppl I): I-117–I-123.

HOLLAND, W.W. & BERESFORD, S.A.A. (1977). Factors influencing blood pressure in children. In *Epidemiology and Control of Hypertension*. ed. Paul O. pp. 375–386. New York: Grune & Stratton, Inc.

KATORI, M., MAJIMA, M., MOHSIN, SSJ., HANAZUKA, M., MIZOGAMI, S. & OH-ISHI, S. (1992). Essential role of kallikrein-kinin system in suppression of blood pressure rise during the developmental stage of hypertension induced by deoxycorticosterone acetate-salt in rats. *Agent Action,* **38** (suppl III): 235–242.

KAUKER, M.L., CROFTON, J.T., SHARE, L. & NASJLETTI, A. (1984). Role of vasopressin in regulation of renal kinin excretion in Long- Evans and diabetes insipidus rats. *J Clin. Invest.,* **73,** 824–831.

KLEIN, B.E., HENNEKENS, C.H., JESSE, M.J., GOURLEY, J.E. & BLUMENTHAL, S. (1977). Longitudinal studies of blood pressure in offspring of hypertensive mothers. In *Epidemiology and Control of Hypertension*. Paul O. (ed). pp. 387–395. New York, Grune & Stratton, Inc.

KURIBAYASHI, Y., MAJIMA, M., KATORI, M. & KATO, H. (1993). Major kininases in rat urine are neutral endopeptidase and carboxypeptidase Y-like exopeptidase. *Biomed Res.,* **14,** 191–201.

LAUER, R.M., BURNS, T.L., CLARKE, W.R. & MAHONEY, L.T. (1991). Childhood predictors of future blood pressure. *Hypertension,* **18**, 3(suppl I): I-74–I-81.

LEVINE, R.S., HENNEKENS, C.H., DUNCAN, R.C., ROBERTSON, E.G., GOURLEY, J.E., CASSADY, J.C. & GELBAND, H. (1980). Blood pressure in infant twins: Birth to 6 months of age. *Hypertension,* **2** (suppl): 29–33.

MAJIMA, M., IKEDA, Y., KURIBAYASHI, Y., MIZOGAMI, S., KATORI, M. & AOYAGI, T. (1995). Ebelactone B, an inhibitor of urinary carboxypeptidase Y-like kininase, prevents the development of deoxycorticosterone acetate-salt hypertension in rats. *Eur. J. Pharmacol.,* **284,** 1–11.

MAJIMA, M. & KATORI, M. (1994). Sodium accumulation induces hypertension in kininogen-deficient Brown Norway Katholiek rats. *Jpn. Heart J.,* **35,** 494–495.

MAJIMA, M., KATORI, M., HANAZUKA, M., MIZOGAMI, S., NAKANO, T., NAKAO, Y., MIKAMI, R., URYU, H., OKAMURA, R., MOHSIN, SSJ. & OHISHI, S. (1991). Suppression of rat deoxycorticosterone-salt hypertension by the kallikrein-kinin system. *Hypertension,* **17,** 806–813.

MAJIMA, M., KURIBAYASHI, Y., IKEDA, K., ADACHI, H., KATO, M., KATORI, M. & AOYAGI, T. (1994a). Diuretic and natriuretic effect of ebelactone B in anesthetized rats by inhibition of a urinary carboxypeptidase Y-like kininase. *Jap. J. Pharmacol.,* **65,** 79–82.

MAJIMA, M., MIZOGAMI, S., KURIBAYASHI, Y., KATORI, M. & OH-ISHI, S. (1994b). Hypertension induced by a nonpressor dose of angiotensin II in kininogen-deficient rats. *Hypertension,* **24,** 111–120.

MAJIMA, M., SHIMA, C., SAITO, M., KURIBAYASHI, Y., KATORI, M. & AOYAGI, T. (1993b). Poststatin, a novel inhibitor of bradykinin-degrading enzymes in rat urine. *Eur. J. Pharmacol.,* **232,** 181–190.

MAJIMA, M., YOSHIDA, O., MIHARA, H., MUTO, T., MIZOGAMI, S., KURIBAYASHI, Y., KATORI, M. & OH-ISHI, S. (1993a). High sensitivity to salt in kininogen-deficient Brown Norway Katholiek rats. *Hypertension,* **22,** 705–714.

MCCORMIC, C.P., HENNESSY, J.F., RAUCH, A.L. & BUCKALEW, V.M. (1989). Erythrocyte sodium concentration and Rb uptake in weaning Dahl rats. *Am. J. Hypertens.,* **2,** 604–609.

NAKAGAWA, M. & NASJLETTI, A. (1988). Plasma kinin concentration in deoxycorticosterone-salt hypertension. *Hypertension,* **11,** 411–415.

NAKAJIMA, S., MAJIMA, M., ITO, H., HAYASHI, I., YAJIMA, Y. & KATORI, M. (1998). Effects of a neutral endopeptidase inhibitor, BP102, on the development of deoxycorticosterone acetate-salt hypertension in kininogen-deficient Brown Norway Katholiek rats. *Int. J. Tiss. Reac.,* **XX,** 45–56.

PHAM, I., GOZALEZ, W., AMRANI, A., OURNIE-ZALUSKI, M., PHILIPPE, M., LABOULANDINE, I., ROQUES, B. & MICHEL, J. (1993). Effects of converting enzyme inhibitor and neutral endopeptidase inhibitor on blood pressure and renal function in experimental hypertension. *J. Pharmacol. Exp. Ther.,* **265,** 1339.

RAIJ, L., DALMASSO, A.P., STANLEY, N.A. & FISH, A.J. (1989). Renal injury in DOCA-salt hypertensive C5-sufficient and C5-deficient mice. *Kidney Int.,* **36,** 582–592.

ROQUES, B.P., FOURNIE-ZALUSKI, M.C., SOROCA, E., LECOMTE, J.M., MALFROY, B., LLORENS, C. & SCHWARTZ, J.C. (1980). The enkephalinase inhibitor thiorphan shows antinociceptive activity in mice. *Nature,* **288,** 286.

SAITO, M., MAJIMA, M., KATORI, M., SANJOU, Y., SUYAMA, I., SHIOKAWA, H., KOSHIBA, K. & AOYAGI, T. (1995). Degradation of bradykinin in human urine byarboxypeptidase Y-like exopeptidase and neutral endopeptidase and their inhibition by ebelactone B and phosphoramidon. *Int. J. Tiss. Reac.,* **XVII,** 181–190.

SCICLI, A.G. & CARRETERO, O.A. (1986). Renal kallikrein-kinin system. *Kidney Int.,* **29,** 120–130.

SHIMA, C., MAJIMA, M. & KATORI, M. (1992). A stable metabolite, Arg-Pro-Pro-Gly-Phe, of bradykinin in the degradation pathway in human plasma. *Jpn. J. Pharmacol.,* **60,** 111–119.

UNGER, T. & RETTIG, R. (1990). Development of genetic hypertension: Is there a critical phase? *Hypertension,* **16,** 615–616.

WAYNFORTII, H.B. (1988). *Experimental and Surgical Technique in the Rat*. London, UK, Academic Press, 59–61.

ZACHARIEVA, S., TORBOVA, S., ORBETZOVA, M., BORISSOVA, A.M., ANDONOVA, K. & SHEITANOVA, S. (1996). Effects of perindopril treatment on plasma and urine of kallikrein activity and the stable metabolite of prostaglandin E2 in patients with essential hypertension. *Meth. Findings Exper. Clin. Pharm.,* **18,** 205–209.

ZINNER, S.H., LEVEY, P.S. & KASS, E.H. (1971). Familial aggregation of blood pressure in childhood. *N. Engl. J. Med.,* **284,** 401–404.

(Received October 12, 1998
Revised November 2, 1998
Accepted November 6, 1998)

British Journal of Pharmacology (1999) 126, 621–626
http://www.stockton-press.co.uk/bjp

Assessment of the effects of endothelin-1 and magnesium sulphate on regional blood flows in conscious rats, by the coloured microsphere reference technique

[1]P.A. Kemp, *,[1]S.M. Gardiner, [1]J.E. March, [2]P.C. Rubin & [1]T. Bennett

[1]School of Biomedical Sciences, University of Nottingham Medical School, Queens Medical Centre, Nottingham NG7 2UH, England; and [2]School of Medical and Surgical Sciences, University of Nottingham Medical School, Queens Medical Centre, Nottingham NG7 2UH, England

1 There is evidence to suggest that magnesium (Mg^{2+}) is beneficial in the treatment of a number of conditions, including pre-eclampsia and acute myocardial infarction. The mode of action of Mg^{2+} in these conditions is not clear, although the vasodilator properties of Mg^{2+} are well documented both *in vitro* and *in vivo*.

2 Previously, we demonstrated that i.v. infusion of magnesium sulphate ($MgSO_4$) alone, or in the presence of vasoconstrictors, caused increases in flow and conductance in the common carotid, internal carotid and hindquarters vascular beds, in conscious rats. Therefore, the objective of the present study was to investigate the regional and subregional changes in haemodynamics in response to the vasoconstrictor peptide endothelin-1 (ET-1) and $MgSO_4$ in more detail, using the coloured microsphere reference technique.

3 Infusion of ET-1 and $MgSO_4$ had similar effects on heart rate and mean arterial pressure as in our previous study. Infusion of ET-1 caused a rise in mean arterial pressure and a fall in heart rate, and infusion of $MgSO_4$ returned mean arterial pressure to control levels with no effect on heart rate.

4 The responses to $MgSO_4$ in the presence of ET-1 showed considerable regional heterogeneity with blood flow increasing (e.g. skeletal muscle), decreasing (e.g. stomach) or not changing (e.g. kidney). Of particular interest was the finding that $MgSO_4$ caused increases in flow in the cerebral and coronary vascular beds.

5 This, and our previous studies, have shown that $MgSO_4$ can reverse vasoconstriction in a number of vascular beds, and indicate that this compound may have therapeutic benefit in conditions associated with vasospasm.

Keywords: Endothelin-1; magnesium sulphate; blood flow; coloured microspheres

Abbreviations: $MgSO_4$, magnesium sulphate; Mg^{2+}, magnesium; ET-1, endothelin-1

Introduction

There is evidence to suggest that magnesium (Mg^{2+}) is beneficial in the treatment of a number of conditions, including pre-eclampsia (Lucas *et al*., 1995; Eclampsia Trial Collaborative Group, 1995) and acute myocardial infarction (Woods *et al*., 1992). The mode of action of Mg^{2+} in these conditions is not clear, although vasodilator properties of Mg^{2+} are well documented both *in vitro* (Altura & Altura, 1980, 1982; Altura & Turlapaty, 1981; Kimura *et al*., 1989; Skajaa *et al*., 1990; Szabo *et al*., 1991, 1992; Noguera & D'Ocon, 1993), and *in vivo* (Seelig *et al*., 1983; Dipette *et al*., 1987; Nishio *et al*., 1989; Chi *et al*., 1990; Ram *et al*., 1991; Sipes *et al*., 1991; Perales *et al*., 1991; Kemp *et al*., 1993, 1994).

Woods (1991) suggested that Mg^{2+} is a coronary vasodilator, and that some of the beneficial effect of Mg^{2+} in the treatment of acute myocardial infarction may be due to the prevention and relief of coronary vasospasm associated with the condition. Also, infusion of Mg^{2+} has been shown to be useful in coronary artery bypass surgery (Marichal *et al*., 1992), and to suppress exercise-induced angina in patients with variant angina (Kugiyama *et al*., 1988). The ability of Mg^{2+} to prevent seizures in pre-eclampsia could also be due to its vasodilator action (Perales *et al*., 1991; Belfort & Moise, 1992; Kemp *et al*., 1993). It is believed that the seizures may be caused by cerebral ischaemia, brought about by cerebral vasospasm, and that Mg^{2+} is effective in preventing or relieving the vasospasm and, therefore, the cerebral ischaemia (Perales *et al*., 1991; Belfort & Moise, 1992; Kemp *et al*., 1993).

Previously, we investigated the effect of intravenous infusion of magnesium sulphate ($MgSO_4$) alone, or in the presence of vasoconstrictors, on regional haemodynamics in conscious rats, using chronically implanted pulsed Doppler flow probes. The effects of $MgSO_4$ were studied in the common and internal carotid vascular beds (Kemp *et al*., 1993), and in the renal, mesenteric and hindquarters vascular beds (Kemp *et al*., 1994) in separate experiments. $MgSO_4$ alone, or in the presence of vasoconstrictor peptides, caused increases in flow and conductance in the common carotid, internal carotid and hindquarters vascular beds; the vasodilator effects of $MgSO_4$ were particularly marked in the hindquarters vascular bed in the presence of endothelin (Kemp *et al*., 1994). However, in those studies, we were unable to measure coronary flow. Furthermore, although internal carotid flow and conductance increased during infusion of $MgSO_4$, we could not be certain that the changes we measured were a reflection of changes only in the cerebral vascular bed. In addition, any change in brain blood flow due to variation in vertebral arterial haemodynamics would not have been detected, although Wellers *et al*. (1976) demonstrated that, in anaesthetized rats, blood flow

* Author for correspondence.

through the right vertebral artery was mainly distributed extracranially. For these various reasons we were interested in investigating the subregional changes in haemodynamics in response to $MgSO_4$ in more detail. Therefore, in the present study we used the coloured microsphere technique (Kowallik *et al*., 1991; Hakkinen *et al*., 1995) to determine, in conscious rats, the influence of $MgSO_4$ on regional and subregional blood flows in the presence of exogenous endothelin-1 (ET-1).

Methods

Left atrial catheter implantation

Male, Long Evans rats ($n=16$ in total) had left atrial catheters implanted for injection of microspheres. The method used for left atrial catheter implantation was a modified version of that described by Wicker & Tarazi (1982).

Rats were anaesthetized (sodium methohexitone, 60 mg kg^{-1}, i.p., supplemented as required), intubated, and put on to a ventilator. A thoracotomy was performed through the fourth left intercostal space, the pericardium was opened, and a tie was placed around the tip of the left atrium. The base of the atrium was clamped between a pair of forceps to prevent bleeding, and then a small cut was made in the wall of the atrial appendage. A saline-filled (heparinized saline, 15 u ml^{-1}) catheter (Portex polythene tubing, I.D. 0.28 mm), with a flared end, was inserted into the atrium and tied in place. The forceps holding the base of the atrium were then released and blood was drawn back into the catheter to check that it was positioned correctly. The catheter was flushed, and the chest wall was closed around the catheter. A drain was inserted through the chest wall and negative pressure was applied to reinflate the lungs. The drain was removed, the hole closed, and the rat was removed from the ventilator. The catheter was tunnelled under the skin to exit at the back of the neck, protruding 1–2 cm, and the end was heat sealed. The animals were allowed to recover from the anaesthetic and left for 3–4 days, before arterial and venous catheters were inserted.

Arterial and venous catheterization

Under anaesthesia (as above) an arterial catheter was inserted into the distal abdominal aorta (*via* the ventral caudal artery) and two venous catheters were inserted into the jugular vein for the infusion of drugs. All catheters were tunnelled under the skin to exit at the same site as the atrial catheter.

At this stage, an extension was attached to the atrial catheter and all the catheters were fed through a flexible spring, which was attached to a harness worn by the rat. The animals were allowed to recover for 24 h before experiments began. The arterial catheter was connected, overnight, to an infusion pump (heparinized saline 7.5 u ml^{-1}, 0.4 ml h^{-1}), *via* a fluid-filled swivel (Brown *et al*., 1976). When experiments began, the catheters were connected to pumps for drug infusion, reference sample withdrawal, and microsphere injection. The arterial catheter was connected to a pressure transducer and arterial pressure was measured, when it was not required for reference sample withdrawal.

Coloured microsphere technique

Yellow, red and blue Dye-Trak polystyrene microspheres (Triton Technology Inc., San Diego, U.S.A.), 15 μm in diameter, were used. The microspheres were sonicated and vortexed immediately prior to injection. Approximately 100,000 yellow, 100,000 red, and 200,000 blue spheres, in 0.2 ml of 0.02% Tween in saline, were injected (0.8 ml min^{-1}, Sage pump, model 351) into the left atrium, followed by 0.3 ml of saline. Starting 10 s before, and continuing for 55 s following injection of the spheres, a reference sample was withdrawn (Sage pump, model 351) from the distal abdominal aorta at a rate of 0.85 ml min^{-1}. At the end of the experiment the animals were killed (Euthatal, sodium pentobarbitone solution, 200 mg ml^{-1}, 0.3–0.5 ml) and the tissues of interest removed and weighed (see below). The coloured microspheres were extracted from the tissue and blood by overnight digestion with 4 M potassium hydroxide, followed by vacuum filtration through 10 μm pore filters (Triton Technology Inc.). The filters were carefully folded, to prevent sphere loss, and placed in a 1-ml Eppendorf tube. Dyes were recovered in 200 μl of dimethylformamide. The tubes were vortexed and centrifuged, and 50 μl of the supernatant was taken for spectrophotometry. The dye mixtures were scanned, between 340 and 800 nm, in a Beckman DU 650 spectrophotometer, and the scans saved to disk. On computer, the scans were copied to the Dye-Trak matrix inversion program (Triton Technology Inc.), which corrects for overlap of the absorption spectra of the colours; sample weights were added, and blood flows calculated (Kowallik *et al*., 1991).

One group of animals ($n=8$) was given an i.v. infusion of $MgSO_4$ (220 μmol min^{-1} at 0.15 ml min^{-1}) (Kemp *et al*., 1993) for 7 min, beginning 20 min after the onset of ET-1 infusion (12.5 pmol min^{-1} at 0.3 ml h^{-1}) (Kemp *et al*., 1993), and the other group ($n=8$) was infused with isotonic saline in place of ET-1 and $MgSO_4$. In both groups of animals, three measurements of flow were made in the way described above. Yellow spheres were injected immediately before onset of saline (control group) or ET-1 (experimental group). Red spheres were injected 20 min after onset of saline (control group) or ET-1 (experimental group), and blue spheres were injected during the last min of saline (control group) or $MgSO_4$ (experimental group) infusion. Blood pressure and heart rate were monitored throughout the experiment, except for during the three flow measurement periods when the arterial catheter was required for reference sample withdrawal. Measurements of mean arterial pressure and heart rate were made just before and immediately after each flow measurement.

At the end of the experiment animals were killed, and the kidneys, adrenal glands, spleen, stomach, testicles, heart (ventricles only), tongue, eyes, and brain were removed whole. Samples of small intestine, hindquarters and head skin, and hindquarters muscle were taken. The tissues were then weighed, and tissue and reference samples were processed, as described above, for removal of spheres from the tissues, and for estimation of amount of dye of each colour present in the samples. Calculations of blood flow, corrected for weight, were made as described above.

For reasons unknown, some samples of skin and hinquarters muscle could not be filtered and it was not possible, therefore, to estimate flow in those samples. Therefore, the numbers of measurements made for those tissues were: Head skin: Control group ($n=7$), Experimental group ($n=6$); Hindquarters skin: Control group ($n=4$), Experimental group ($n=4$); Hindquarters muscle: Control group ($n=8$), Experimental group ($n=7$). For all other tissues $n=8$ in both groups.

Data analysis

All data are given as means ± s.e.mean. Flow data were compared by analysis of variance followed by *post hoc*

Bonferroni/Dunn test. Heart rate and pressure changes relative to baseline, changes relative to pre-saline or $MgSO_4$ and changes relative to pre-measurement values, were analysed by Friedman's test (Theodorsson-Norheim, 1987). A P value <0.05 was taken as significant.

Drugs

$MgSO_4$ was dissolved in distilled water. ET-1 (Peptide Institute, Osaka, Japan) was dissolved in isotonic saline containing 1% bovine serum albumin (Sigma).

Results

Heart rate and mean arterial pressure

There were no significant changes in heart rate in the control group during the experiment. However, mean arterial pressure showed a small, but significant, increase after the first measurement (Table 1). In the experimental group, the changes seen in heart rate and mean arterial pressure were similar to those seen in the previous studies during infusion of ET-1 and $MgSO_4$ (Kemp *et al*., 1994). Infusion of ET-1 caused a significant rise in mean arterial pressure and a reduction in heart rate. Subsequent co-infusion with $MgSO_4$ caused mean arterial pressure to return to baseline levels, with no significant effect on heart rate (Table 1).

Effects of ET-1 and $MgSO_4$ on regional and subregional blood flows

Effects on cranial flow (brain, eye, tongue, cranial skin) There were no significant differences in baseline flows between groups, for any of the tissues measured, except the head skin in which the baseline flow was slightly, but significantly, higher in the experimental group compared to the control group. During infusion of saline (control group) there were no significant changes in tissue blood flows (Table 2). In the experimental group infusion of ET-1 had no effect on brain or eye blood flow, but reduced flow through the cranial skin. $MgSO_4$ had no effect on blood flow through the eyes or cranial skin, but increased brain and tongue blood flows to above baseline levels (Table 2).

Effects on coronary flow Baseline values for flow through the heart were not significantly different between the two groups. In the control group there was a significant increase in flow to the heart after the first measurement of flow, which was still apparent in the second measurement (Table 2). Infusion of ET-1 had no significant effect on blood flow to the heart, but $MgSO_4$ caused a large increase in flow to above the baseline value (Table 2).

Effects on flow in the kidneys, adrenal glands, spleen, stomach and small intestine Baseline flows for all tissues, except the stomach, were not significantly different between groups (Table 2). Resting flow through the stomach was significantly higher in the control group than in the experimental group (Table 2). In all tissues measured, except for the adrenal glands, there were no significant changes in flow during infusion of saline. The adrenal glands were combined for flow measurement because of their small size, and, like the heart, showed a significant increase in flow in the control group after the first flow measurement, with no further change after that (Table 2). Infusion of ET-1 caused significant reductions in flow through the kidneys and adrenal glands, and infusion of $MgSO_4$ had no significant effect on these reductions in flow. In the spleen, infusion of ET-1 and $MgSO_4$ had no significant effects. Infusion of ET-1 caused a significant rise in blood flow to the stomach, which returned towards baseline levels during infusion of $MgSO_4$ (Table 2).

Effects on flow in the hindquarters region (testicles, hindlimb skin, hindlimb muscle) In all tissues measured, baseline flows were not different between groups (Table 2) and flow was unaffected by infusion of saline. Infusion of ET-1 caused a significant reduction in flow to the testicles, with no significant change in flow taking place during infusion of $MgSO_4$. In the hindquarters skin, infusion of ET-1 and $MgSO_4$ caused little change in blood flow. In hindquarters muscle, infusion of ET-1 did not cause a significant reduction in blood flow; however, infusion of $MgSO_4$ caused a significant increase in flow (Table 2).

Discussion

The results from this study, using the coloured microsphere technique to measure flow, produced values for resting flows in all tissues that compared well to measurements made by other workers using either radio-labelled, or coloured, microspheres to measure flow in rats (Malik *et al*., 1976; Ishise *et al*., 1980; Wicker & Tarazi, 1982; Hakkinen *et al*., 1995). Our observations substantiate the finding of Hakkinen *et al*. (1995) that coloured microspheres are a suitable alternative to radio-labelled spheres for measuring blood flow in rats.

In our previous study (Kemp *et al*., 1993) we found that ET-1 caused a fall in common and internal carotid blood flow,

Table 1 Heart rate and mean arterial pressure measured just before, and immediately after, each determination of flow

	Control group			*Experimental group*		
Heart rate	*Control* (beats min^{-1})	*Saline* (beats min^{-1})	*Saline* (beats min^{-1})	*Control* (beats min^{-1})	*ET-1* (beats min^{-1})	*ET-1* + Mg^{2+} (beats min^{-1})
Before	385±8	403±14	398±10	368±10	298±25†	260±12†
After	389±9	396±7	373±14	365±14	264±18*	265±12
Mean arterial pressure	*Control* (mmHg)	*Saline* (mmHg)	*Saline* (mmHg)	*Control* (mmHg)	*ET-1* (mmHg)	*ET-1* + Mg^{2+} (mmHg)
Before	106±3	111±3†	114±3†	108±4	146±4†	111±3‡
After	110±3	114±2	116±2	112±4	140±4	111±3

Values are means±s.e.mean; *denotes a significant change in the post-measurement value compared to the pre-measurement value; †denotes significantly different from the first measurement (control); ‡denotes significantly different from the second measurement (ET-1).

Table 2 Subregional blood flows (ml min^{-1} 100 g^{-1}) in conscious Long Evans rats in control ($n=8$) and experimental groups ($n=8$); Values are means ± s.e.mean

	Control group			*Experimental group*		
	Control (ml min^{-1} 100 g^{-1})	*Saline* (ml min^{-1} 100 g^{-1})	*Saline* (ml min^{-1} 100 g^{-1})	*Control* (ml min^{-1} 100 g^{-1})	*ET-1* (ml min^{-1} 100 g^{-1})	*ET-1* + Mg^{2+} (ml min^{-1} 100 g^{-1})
Head skin	21±3	20±2	15±2	27±5*	12±2†	11±2†
Tongue	95±25	79±16	85±14	60±8	40±7	116±22†‡
Eyes	165±20	169±14	172±22	170±14	140±10	178±6
Brain	125±10	139±10	132±16	123±9	124±9	170±13†‡
Heart	403±24	523±31†	581±26†	393±24	265±17	614±57†‡
Left kidney	505±37	575±70	503±57	464±44	186±11†	178±22†
Right kidney	389±79	470±81	370±86	431±44	145±23†	204±14†
Adrenal glands	565±46	837±87†	848±72†	583±46	244±24†	388±26†
Spleen	241±16	338±60	371±107	355±27	256±23	287±45
Stomach intestine	269±22	285±19	261±17	217±30	162±25	166±24
Stomach	233±14	193±15	194±17	108±13*	212±13†	129±15‡
Testicles	41±3	47±4	51±3	40±3	29±2†	25±2†
Hindquarters skin	19±3	21±6	19±4	18±4	7±1	5±1†
Hindquarters muscle	14±2	16±2	14±2	12±2	8±1	17±4†‡

The first flow measurement was made immediately before infusion of saline (control) or ET-1 (experimental). The second flow measurement was made 20 min after onset of saline or ET-1 infusion, and immediately before onset of $MgSO_4$ infusion. The third flow measurement was made in the last minute of a 7 min infusion of $MgSO_4$. Values are means ± s.e.mean; *denotes a significant difference between the control values for the two groups; †denotes significantly different from the first flow measurement (control); ‡denotes significantly different from the second flow measurement (ET-1).

and infusion of $MgSO_4$ caused flow to increase in both vessels, in the presence of ET-1. Torregrosa *et al*., (1994) showed that ET-1 caused a reduction in cerebral blood flow in the conscious goat, but found that $MgSO_4$ caused an increase in flow, in the presence of ET-1, only when given directly into the cerebroarterial supply, and not when given as an intravenous infusion. In the present study, ET-1 and $MgSO_4$ had heterogeneous effects on blood flow through the cranial tissues supplied by the internal carotid artery. Infusion of ET-1 reduced flow only in the skin, and $MgSO_4$ caused increases in flow only in the tongue and brain. Although ET-1 did not cause a reduction in flow to the brain, infusion of $MgSO_4$ markedly increased cerebral blood flow, in the presence ET-1. This shows that $MgSO_4$ is able to increase cerebral blood flow, and provides further evidence that $MgSO_4$ may have the ability to relieve cerebral vasospasm (Perales *et al*., 1991; Belfort & Moise, 1992; Kemp *et al*., 1993). Heterogeneous haemodynamic effects of ET-1 and $MgSO_4$ were not confined to the cranial tissues and possible explanations are considered below.

At first sight our findings of a lack of effect of ET-1 on cerebral blood flow appears at odds with the report from Macrae *et al*. (1993) showing severe reductions in cerebral blood flow in response to ET-1. However, those workers applied ET-1 directly to the adventitial surface of the exposed middle cerebral artery, rather than giving the peptide intravenously. Using the latter route of administration, Takahashi *et al*. (1992) found, as we did, that ET-1 did not affect cerebral blood flow. Since ET-1 caused a significant increase in systemic arterial blood pressure with no change in cerebral blood flow, there would have been a decrease in calculated cerebral vascular conductance. Under these circumstances this cerebral vasoconstriction is likely to have been an autoregulatory response.

In the heart, there was a significant increase in flow after the first injection of microspheres in the control group. In contrast, there was a fall in flow during infusion of ET-1 in the experimental group, although this was not significant. However, infusion of $MgSO_4$, in the presence of ET-1, caused a large increase in flow to levels significantly higher than the baseline value. These findings demonstrate that $MgSO_4$ is capable of increasing flow to the heart in rats, and supports the view that $MgSO_4$ may be beneficial in the treatment of acute myocardial infarction because of its ability to improve coronary flow (Woods, 1991).

In our previous study, using Doppler flow probes (Kemp *et al*., 1994), renal and mesenteric flows were significantly reduced by ET-1. Renal flow was not affected significantly by infusion of $MgSO_4$, but the reduction in flow in the mesenteric vascular bed was attenuated by a small, but significant, amount by $MgSO_4$. In the present study, the kidneys showed the same pattern of changes as in the previous study. Interestingly, flow through the stomach rose significantly during infusion of ET-1 and returned to control level in the presence of $MgSO_4$. Flow in the spleen was unaffected by ET-1 and $MgSO_4$. Thus, it appears there might be substantial variation in the changes in inter-organ flow, not apparent from monitoring with Doppler probes. A vasodilator effect of ET-1 in the stomach has also been reported by Allcock *et al*., (1995) in the anaesthetized, ganglion-blocked rat. In that study the vasodilator effect of ET-1 was shown to be converted to a vasoconstriction in the presence ET_A-, and/or ET_B-receptor antagonists. Allcock *et al*. (1995) suggested these observations were consistent with the ability of ET-1 to stimulate local prostanoid production. If this was the case, our finding that $MgSO_4$ suppressed the ET-1 induced gastric hyperaemia may indicate an inhibitory influence of $MgSO_4$ on prostanoid synthesis, although this is not consisitent with the ability of $MgSO_4$ to stimulate prostacyclin production (Laurant *et al*., 1992).

In our earlier study (Kemp *et al*., 1994), flow to the hindquarters region was unaffected by infusion of ET-1. However, $MgSO_4$ alone, and in the presence of ET-1, caused a marked increase in hindquarters flow. In the present study, the testicles showed a significant reduction in blood flow during infusion of ET-1, which was unaffected by $MgSO_4$. Although hindquarters muscle blood flow was not altered by infusion of ET-1, infusion of $MgSO_4$ caused an increase in flow which was significantly different to basal flow and flow in the presence of ET-1 alone. The increase in flow caused by $MgSO_4$ (42%) was comparable to that seen in the hindquarters region, in the previous study, in the presence of ET-1 (46%).

The striking heterogeneity in the regional and subregional haemodynamic effects of ET-1 and $MgSO_4$ is likely to be due to the wide range of interacting factors which influence microvascular behaviour. In addition to those considered above, we (Kemp *et al*., 1994) have suggested there might be contributions from baroreflex-mediated sympathoadrenal and neurohumoral activation. As pointed out by Malmström *et al.* (1997) a further factor to be considered is the variation in endothelial permeability between different vascular beds, since this will influence tissue access of exogenous substances administered intravenously.

In conclusion this, and our previous studies, have shown that $MgSO_4$ can reverse vasoconstriction in a number of vascular beds, and indicate that this compound may have therapeutic benefit in conditions associated with vasospasm.

This work was supported by a grant (BHF 91/10) from the British Heart foundation.

References

ALLCOCK, G.H., WARNER, T.D. & VANE, J.R. (1995). Roles of endothelin receptors in the regional and systemic vascular responses to ET-1 in the anaesthetized ganglion-blocked rat: use of selective antagonists. *Br. J. Pharmacol.,* **116,** 2482 – 2486.

ALTURA, B.M. & ALTURA, B.T. (1981). Magnesium ions and contraction of vascular smooth muscle. *Fed. Proc.,* **40,** 2672 – 2679.

ALTURA, B.M. & TURLAPATY, P.D.M.V. (1982). Withdrawal of magnesium enhances coronary arterial spasms produced by vasoactive agents. *Br. J. Pharmacol.,* **77,** 649 – 659.

ALTURA, B.T. & ALTURA, B.M. (1980). Withdrawal of magnesium causes vasospasm while elevated magnesium produces relaxation of tone in cerebral arteries. *Neurosci. Lett.,* **20,** 323 – 327.

BELFORT, M.A. & MOISE JR K.J. (1992). Effect of magnesium sulphate on maternal brain blood flow in preeclampsia: A randomized, placebo-controlled study. *Am. J. Obstet. Gynecol.,* **167,** 661 – 666.

BROWN, Z.W., AMIT, Z. & WEEKS, J.R. (1976). Simple flow-thru swivel for infusions into unrestrained animals. *Pharmacol. Biochem. Behav.,* **5,** 363 – 365.

CHI, O.Z., POLLACK, P. & WEISS, H.R. (1990). Effects of magnesium sulphate and nifedipine on regional cerebral blood flow during middle cerebral artery ligation in the rat. *Arch. Int. Pharmacodyn. Ther.,* **304,** 196 – 205.

DIPETTE, D.J., SIMPSON, K. & GUNTUPALLI, J. (1987). Systemic and regional hemodynamic effect of acute magnesium administration in the normotensive and hypertensive state. *Magnesium,* **6,** 136 – 149.

ECLAMPSIA TRIAL COLLABORATIVE GROUP. (1995). Which anticonvulsant for women with eclampsia? Evidence from the collaborative eclampsia trial. *Lancet,* **345,** 1455 – 1463.

HAKKINEN, J.P., MILLER, M.W., SMITH, A.H. & KNIGHT, D. (1995). Measurement of organ blood flow with coloured microspheres in the rat. *Cardiovasc. Res.,* **29,** 74 – 79.

ISHISHE, S., PEGRAM, B.L., YAMAMOTO, J., KITAMURA, Y. & FROHLICH, E.D. (1980). Reference sample microsphere method: cardiac output and blood flows in conscious rat. *Am. J. Physiol.,* **233,** H443 – H449.

KEMP, P.A., GARDINER, S.M., BENNETT, T. & RUBIN, P.C. (1993). Magnesium sulphate reverses carotid vasoconstriction caused by endothelin-1, angiotensin II and neuropeptide-Y, but not that caused by N^G-nitro-L-arginine methyl ester, in conscious rats. *Clin. Sci.,* **85,** 175 – 181.

KEMP, P.A., GARDINER, S.M., MARCH, J.E., BENNETT, T. & RUBIN, P.C. (1994). Effects of N^G-nitro-L-arginine methyl ester on regional haemodynamic responses to $MgSO_4$ in conscious rats. *Br. J. Pharmacol.,* **111,** 325 – 331.

KIMURA, T., YASUE, H., SAKAINO, N., ROKUTANDA, M., JOUGASAKI, M. & ARAKI, H. (1989). Effects of magnesium on the tone of isolated human coronary arteries. *Circulation,* **79,** 1118 – 1124.

KOWALLIK, P., SCHULZ, R., GUTH, B.D. & SCHADE, A. (1991). Measurement of regional myocardial blood flow with coloured microspheres. *Circulation,* **83,** 974 – 982.

KUGIYAMA, K., YASUE, H., OKUMURA, K., GOTO, K., MINODA, K., MIYAGI, H., MATSUYAMA, K., KOJIMA, A., KOGA, Y. & TAKAHASHI, M. (1988). Suppression of exercise-induced angina by magnesium sulphate in patients with variant angina. *J. Am. Coll. Cardiol.,* **12,** 1177 – 1183.

LAURANT, P., MOUSSARD, C., ALBER, D., HENRY, J.C. & BERTHELOT, A. (1992). *In vivo* and *in vitro* magnesium effects on aortic prostacyclin generation in DOCA-salt hypertensive rats. *Prostaglandins Leukot. Essent. Fatty Acids,* **47,** 183 – 186.

LUCAS, M.J., LEVENO, K.J. & CUNNINGHAM, F.G. (1995). A comparison of magnesium sulphate with phenytoin for the prevention of eclampsia. *New Engl. J. Med.,* **333,** 201 – 205.

MACRAE, I.M., ROBINSON, M.J., GRAHAM, D.I., REID, J.L. & McCULLOCH, J. (1993). Endothelin-1-induced reductions in cerebral blood flow: Dose dependency, time course, and neuropathological consequences. *J. Cereb. Blood Flow Metab.,* **13,** 276 – 284.

MALIK, A.B., KAPLAN, J.E. & SABA, T.M. (1976). Reference sample method for cardiac output and regional blood flow determination in the rat. *J. Appl. Physiol.,* **40,** 472 – 475.

MALMSTRÖM, R.E., BALMER, K.C. & LUNDBERG, J.M. (1997). The neuropeptide Y (NPY) Y_1 receptor antagonist BIBP 3226: equal effects on vascular responses to exogenous and endogenous NPY in the pig *in vivo*. *Br. J. Pharmacol.,* **121,** 595 – 603.

MARICHAL, A., HESS, W. & SCHIEBER, G. (1992). Haemodynamics in patients undergoing coronary artery bypass grafting after magnesium aspartate infusion. *Anaesthetist,* **41,** 752 – 759.

NISHIO, A., GREBREWOLD, A., ALTURA, B.T. & ALTURA, B.M. (1989). Comparative vasodilator effects of magnesium salts on rat mesenteric arterioles and venules. *Arch. Int. Pharmacodyn. Ther.,* **298,** 139 – 163.

NOGUERA, M.A. & D'OCON, M.P. (1993). Modulatory role of magnesium on the contractile response of rat aorta to several agonists in normal and calcium-free medium. *J. Pharm. Pharmacol.,* **45,** 697 – 700.

PERALES, A.J., TORREGROSA, G., SALOM, J.B., MIRANDA, F.J., ALABADI, J.A., MONLEON, J. & ALBORCH, E. (1991). In vivo and in vitro effects of magnesium sulphate in the cerebrovascular bed of the goat. *Am. J. Obstet. Gynecol.,* **165,** 1534 – 1538.

RAM, Z., SADEH, M., SHACKED, I., SAHAR, A. & HADANI, M. (1991). Magnesium sulphate reverses experimental delayed cerebral vasospasm after subarachnoid hemorrhage in rats. *Stroke,* **22,** 922 – 927.

SEELIG, J.M., WEI, E.P., KONTOS, H.A., CHOI, S.C. & BECKER, D.P. (1983). Effect of changes in magnesium ion concentration on cat cerebral arterioles. *Am. J. Physiol.,* **245,** H22 – H26.

SIPES, S.L., CHESTNUT, D.H., VINCENT JR R.D., WEINER, C.P., THOMPSON, C.S. & CHATTERJEE, M.S. (1991). Does magnesium sulphate alter the cardiovascular response to vasopressor agents in gravid ewes? *Anesthesiology,* **75,** 1010 – 1018.

SKAJAA, K., FORMAN, A. & ANDERSSON, K.-E. (1990). Effects of magnesium on isolated human foetal and maternal uteroplacental vessels. *Acta Physiol. Scand.,* **139,** 551 – 559.

SZABO, C., FARAGO, M., DORA, E., HORVATH, I. & KOVACH, A.G.B. (1991). Endothelium-dependent influence of small changes in extracellular magnesium concentration on tone of feline middle cerebral arteries. *Stroke,* **22,** 785 – 789.

SZABO, C., HARDEBO, J. & SALFORD, L.G. (1992). Role of endothelium in the responses of human intracranial arteries to a slight reduction of extracellular magnesium. *Exp. Physiol.,* **77,** 209 – 211.

TAKAHASHI, H., NAKANISHI, T., NISHIMURA, M., TANAKA, H. & YOSHIMURA, M. (1992). Effects of endothelin-1 and inhibition of nitric oxide production with N^G-monomethyl-L-arginine on arterial pressure and regional blood flow in anaesthetized rats. *J. Cardiovasc. Pharmacol.,* **20,** S176 – S178.

THEODORSSON-NORHEIM, E. (1987). Friedman and Quade tests: BASIC computer program to perform non-parametric two-way analysis of variance and multiple comparisons on ranks of several related samples. *Comput. Biol. Med.,* **17,** 85 – 99.

TORREGROSA, G., PERALES, A.J., SALOM, J.B., MIRANDA, F.J., BARBERA, M.D. & ALBORCH, E. (1994). Different effects of Mg^{2+} on endothelin-1 and 5-hydroxytryptamine-elicited responses in goat cerebrovascular bed. *J. Cardiovasc. Pharmacol.,* **23,** 1004 – 1010.

WELLERS, D., WOUTERS, L., NIJKAMP, F.P. & WYBREN DE JONG. (1976). Distribution of blood flow supplied by the vertebral artery in rats: Anatomical, functional and pharmacological aspects. *Experientia,* **32,** 85 – 87.

WICKER, P. & TARAZI, R.C. (1982). Coronary blood flow measurements with left atrial injection of microspheres in conscious rats. *Cardiovasc. Res.,* **16,** 580 – 586.

WOODS, K.L. (1991). Possible pharmacological actions of magnesium in acute myocardial infarction. *Br. J. Clin. Pharmacol.,* **32,** 3 – 10.

WOODS, K.L., FLETCHER, F., ROFFE, C. & HAIDER, Y. (1992). Intravenous magnesium sulphate in suspected acute myocardial infarction: results of the second Leicester intravenous magnesium intervention trial (LIMIT-2). *Lancet,* **339,** 1553 – 1558.

(Received July 29, 1998
Revised October 21, 1998
Accepted November 6, 1998)

British Journal of Pharmacology (1999) 126, 627–638
http://www.stockton-press.co.uk/bjp

Electrophysiological examination of the effects of sustained flibanserin administration on serotonin receptors in rat brain

[1]Lynne E. Rueter & *,[1]Pierre Blier

[1]Neurobiological Psychiatry Unit, McGill University, 1033 Pine Avenue, W. Montréal, Canada H3A 1A1

1 5-HT_{1A} receptor agonists have proven to be effective antidepressant medications, however they suffer from a significant therapeutic lag before depressive symptoms abate. Flibanserin is a 5-HT_{1A} receptor agonist and 5-HT_{2A} receptor antagonist developed to possibly induce a more rapid onset of antidepressant action through its preferential postsynaptic 5-HT_{1A} receptor agonism.

2 Flibanserin antagonized the effect of microiontophoretically-applied DOI in the medial prefrontal cortex (mPFC) following 2 days of administration, indicating antagonism of postsynaptic 5-HT_{2A} receptors. This reduction in the effect of locally-applied DOI was no longer present following 7-day flibanserin administration.

3 Two-day flibanserin administration only marginally reduced the firing activity of dorsal raphe (DRN) 5-HT neurons. Following 7 days of administration, 5-HT neuronal firing activity had returned to normal and the somatodendritic 5-HT_{1A} autoreceptors were desensitized.

4 The responsiveness of postsynaptic 5-HT_{1A} receptors located on CA_3 hippocampus pyramidal neurons and mPFC neurons, examined using microiontophoretically-applied 5-HT and gepirone, was unchanged following a 7-day flibanserin treatment.

5 As demonstrated by the ability of the 5-HT_{1A} receptor antagonist WAY 100635 to selectively increase the firing of hippocampal neurons in 2- and 7-day treated rats, flibanserin enhanced the tonic activation of postsynaptic 5-HT_{1A} receptors in this brain region.

6 The results suggest that flibanserin could be a therapeutically useful compound putatively endowed with a more rapid onset of antidepressant action.

Keywords: Flibanserin; 5-HT_{1A} receptors; 5-HT_{2A} receptors; BMY 7378; WAY 100635; LSD; dorsal raphe nucleus; medial prefrontal cortex; hippocampus; electrophysiology

Abbreviations: DOI, (±)-2,5-dimethoxy-4-iodoamphetamine hydrochloride; DRN, dorsal raphe nucleus; LSD, lysergic acid diethylamide; mPFC, medial prefrontal cortex; SSRI, selective serotonin reuptake inhibitors; 5-HT, serotonin

Introduction

Serotonin (5-HT)$_{1A}$ receptor agonists have been shown to be effective antidepressant drugs despite some difficulty of titrating the dose to obtain this therapeutic action without inducing cumbersome side effects (see Robinson *et al*., 1990; Wilcox *et al*., 1996; Stahl *et al*., 1998). Nevertheless, these compounds suffer from the same therapeutic lag as other antidepressant medications used to date, i.e. 2–3 weeks of administration are required before antidepressant action is observed. It has been hypothesized that this delay in the therapeutic response results from the initial action of 5-HT_{1A} agonists at the somatodendritic 5-HT_{1A} autoreceptors located on the serotonergic neurons (Blier & de Montigny, 1987). Following their acute or short-term administration, 5-HT neuronal firing is diminished, thereby resulting in a decrease in endogenous 5-HT release in projection areas (Fornal *et al*., 1994; Blier & de Montigny, 1987; Dong *et al*., 1997; Bosker *et al*., 1996; Kreiss & Lucki, 1997). However, following long-term administration, the somatodendritic 5-HT_{1A} autoreceptors are desensitized, thereby allowing normal firing activity and subsequent release of 5-HT despite the ongoing presence of 5-HT_{1A} agonists (Blier & de Montigny, 1987; Dong *et al*., 1997; Kreiss & Lucki, 1997). Normalized levels of synaptic 5-HT plus the presence of 5-HT_{1A} receptor agonists then leads to an enhanced activation of the postsynaptic 5-HT_{1A} receptors located in limbic structures (Haddjeri *et al*., 1998). It has been hypothesized that this enhanced tonic activation underlies the antidepressant response in multiple classes of antidepressant treatments (Blier & de Montigny, 1994).

Recent advances in drug development have concentrated on shortening the therapeutic lag. Two major approaches have been delineated. First, attempts have been made to block, using the preferential presynaptic 5-HT_{1A} receptor antagonist pindolol (Romero *et al*., 1996), the initial inhibition of 5-HT neuronal firing due to the activation of the somatodendritic 5-HT_{1A} autoreceptors. In five of six double blind studies, conjunctive therapy of selective 5-HT reuptake inhibitors (SSRI) and pindolol has been shown to have a more rapid onset of antidepressant action (Pérez *et al*., 1997; Tome *et al*., 1997; Berman *et al*., 1997; Thomas *et al*., 1997; Zanardi *et al*., 1997; 1998). In addition, an open label study has found a similar reduction in the therapeutic lag of the 5-HT_{1A} agonist buspirone by the concurrent administration of pindolol (Blier *et al*., 1997). The latter observation, if confirmed in a double-blind study, would indicate that an enhanced tonic activation of postsynaptic 5-HT_{1A} receptors is truly a main determinant of the antidepressant response.

The second approach in drug development has been to bypass autoreceptor activation altogether by developing compounds with preferential activity at the postsynaptic 5-HT_{1A} receptors (de Montigny & Blier, 1991). Flibanserin (BIMT 17) has been described as a 5-HT_{1A} agonist with selective activity at postsynaptic 5-HT_{1A} receptors as well as a

* Author for correspondence.

5-HT_{2A} receptor antagonist (K_i of 7.3 and 6.9, respectively) but with no significant affinity for other receptors (Borsini *et al*., 1995a; b). This combination of properties could lead to a rapid increase in 5-HT_{1A} receptor-mediated inhibition as well as a decrease in 5-HT_2 receptor-mediated excitation of postsynaptic neurons. Studies demonstrating an enhanced inhibition of the postsynaptic membrane with the coadministration of a 5-HT_{1A} agonist and a 5-HT_2 antagonist support this contention (Ashby *et al*., 1994). Acute experiments with flibanserin have been somewhat conflicting regarding the preferential activity of flibanserin at the postsynaptic membrane. Borsini *et al*. (1995a) demonstrated that 8-OH-DPAT increased the firing of cortical neurons at low doses and decreased the firing at high doses, a biphasic effect suggestive of pre- and postsynaptic components to the action of this compound, whereas flibanserin dose-dependently only inhibited cortical firing. The results of this indirect evaluation were interpreted as a preferential activity of flibanserin in some postsynaptic areas. However, this study was possibly complicated by the affinity of the comparison drug, 8-OH-DPAT, for the 5-HT_7 receptor. In contrast, we found that, given intravenously, flibanserin was most potent on 5-HT neurons (Rueter *et al*., 1998b). In this same study, however, flibanserin was more potent at postsynaptic 5-HT_{1A} receptors when applied locally and it acted as a partial agonist in the hippocampus but as a full agonist in the cortex. The present study was designed to further delineate the properties of flibanserin. In order to better mimic the conditions under which human patients would receive the compound, flibanserin was given systemically in a sustained fashion. The effects of 2- and 7-day treatments of flibanserin on 5-HT_{1A} and/or 5-HT_{2A} receptors in the dorsal raphe nucleus (DRN), medial prefrontal cortex (mPFC), and CA_3 region of the hippocampus of the rat were investigated using *in vivo* single unit recording and microiontophoresis. In some experiments, the 5-HT_{1A} receptor agonist gepirone was used as an active reference drug.

Methods

Animal preparation and drug administration

Under halothane anaesthesia, pairs of male Sprague-Dawley rats were implanted with osmotic minipumps (Alza, Palo Alto, CA, U.S.A) that delivered either flibanserin, gepirone or their vehicle. This mode of administration more closely approaches the blood levels of psychotropic drugs achieved in patients given the much faster metabolism of such agents in rodents that in humans. Flibanserin was dissolved in deionized water with several drops of acetic acid and gepirone in water only. The concentrations of flibanserin (2.5, 5, or 10 mg kg^{-1} day^{-1}) and gepirone (15 mg kg^{-1} day^{-1}) were determined based on the mean body weight of the animals during the 2- or 7-day treatment. All experiments were performed with the minipumps in place. After implantation, rats were housed in standard conditions with free access to food and water. Principles established by the Canadian Committee on Animal Care were followed at all times.

For electrophysiological experiments, rats were anaesthetized with chloral hydrate (400 mg kg^{-1}, i.v.) and placed in a stereotaxic frame with the nose bar set 3 mm below the ear bars. In order to maintain a full anaesthetic state in which there was no reaction to a tail or paw pinch, chloral hydrate supplements of 100 mg kg^{-1} were given as needed. Burr holes were drilled over the DRN (anterior 0.9, lateral 0, in reference to interaural 0), the mPFC (anterior 3.0, lateral 0.8, in reference to bregma) or the hippocampus (anterior 4.0, lateral 4.0, in reference to lambda), and electrodes were lowered to the target areas (DRN DV: 5.0–6.5; mPFC DV: 1.0–3.5; hippocampus CA_3 region DV: 3.5–4.2, in reference to dura; Paxions & Watson, 1982). In order to limit the number of animals used, more than one site was examined in each rat.

For extracellular recordings in the DRN, single barrel glass electrodes were pulled in the conventional manner in order to achieve a tip with a 2–7 MΩ impedance and were filled with 2 M NaCl solution. DRN 5-HT neurons were identified based on their established characteristics (Aghajanian, 1978). For sampling the mean firing rate, neurons were recorded during five successive penetrations, 100–200 μm apart, formed in a star pattern.

Extracellular recordings in the mPFC and hippocampus were performed with five-barrel glass electrodes pulled to a tip with an impedance of 0.8–1.2 MΩ. The central barrel was filled with a 2 M NaCl solution and served as the recording barrel. Depending upon the experiment, two of the side barrels were filled with the following solutions: 5-HT creatinine sulphate (5 mM in 200 mM NaCl, pH 3.5–4.0), (±)-2,5-dimethoxy-4-iodoamphetamine hydrochloride (DOI; 50 mM in 200 mM NaCl, pH 4.0), BMY 7378 (50 mM in 200 mM NaCl, pH 3.0; RBI), or gepirone (25 mM in 200 mM NaCl, pH 5.0). The final two side barrels were filled with 2 M NaCl to serve as an automatic current balance and quisqualic acid (1.5 mM in 400 mM NaCl, pH 8.0) to activate or maintain the neuronal firing.

For all multibarrel electrodes, currents of −10 nA were used to retain the microiontophoretic solutions between experimental ejections. Medial PFC and hippocampus CA_3 pyramidal neurons were identified based on their respective characteristics (Ashby *et al*., 1990; Kandel & Spencer, 1961). Because hippocampus CA_3 pyramidal neurons and the majority of mPFC neurons do not discharge spontaneously in the anaesthetized rat, a leak or small to moderate ejection current of quisqualate (0 to −50 nA in the mPFC; +1 to −4 nA in the hippocampus) was used to activate the neurons within their physiological range without affecting their responsiveness to 5-HT and 5-HT receptor agonists (Ranck, 1975; Ashby *et al*., 1990). Microiontophoretic ejections were made for 50 s periods, with the exception of 5-HT during its concurrent application with BMY 7378. The antagonism of the effect of DOI applied by iontophoresis in the mPFC was carried out after the 2-day treatment period, presumably before adaptative changes would occur with more prolonged administration, to ensure that flibanserin was present in sufficient concentrations in the brain.

Intravenous drug administrations were made through a catheter inserted into a lateral tail vein. For consecutive injections, a minimum of 2 min elapsed before the subsequent injection. Lysergic acid diethylamide (LSD), dissolved in 0.9% saline, was used to assess the functioning of the presynaptic 5-HT_{1A} autoreceptors because this intravenous probe has always provided results consistent with alterations of 5-HT_{1A} receptor responsiveness, unlike the more selective 5-$HT_{1A/7}$ agonist 8-OH-DPAT (Blier *et al*., 1987; Blier & de Montigny, 1987; Shen *et al*., 1993). The tonic inhibition of the postsynaptic hippocampal neurons was assessed using two methods. First, the ability of the microiontophoretic application of the 5-HT_{1A} receptor antagonist, BMY 7378, (Chaput & de Montigny, 1988) to disinhibit hippocampal neurons was investigated in 2-day treated rats. Second, the 5-HT_{1A} receptor antagonists BMY 7378 and WAY 100635 (Fletcher *et al*., 1996) were

dissolved in 0.9% saline and used to assess the degree of 5-HT_{1A} receptor-mediated inhibition of the postsynaptic neurons induced by the sustained administration of flibanserin for 2 and 7 days. The degree to which the antagonists could disinhibit the firing of hippocampal neurons has been determined to be a measure of the tonic activation of postsynaptic 5-HT_{1A} receptors (Haddjeri *et al*., 1998). Two minutes prior to the intravenous administration of WAY 100635 or BMY 7378, the firing activity of the quisqualate-activated CA_3 pyramidal neurons was decreased to about 5 Hz in order to more readily allow the detection of enhancements in firing following administration of the antagonists in control and treated rats.

The degree of tonic activation of postsynaptic 5-HT_{1A} receptors in the mPFC was not determined in a manner analogous to that used in the hippocampus for the following reasons. First, both of the selective 5-HT_{1A} antagonists available, BMY 7378 and WAY 100635, have been shown to inhibit mPFC neuronal firing when given alone (Rueter *et al*., 1998b). Second, the aim of the present study was to compare the effects of sustained flibanserin administration with other antidepressant drugs, and, to date, the tonic activation of postsynaptic receptors has only been assessed in the hippocampus.

Drugs

Flibanserin (BIMT 17; 1-[2-[4-(3-trifluoromethyl phenyl) piperazin-1-yl] ethyl] benzimidazol-[1H]-2-one; Boehringer Ingelheim, Ontario, Canada), chloral hydrate, gepirone (Bristol Myers Squibb, Wallingford, CT, U.S.A), LSD (lysergic acid diethylamide), 5-HT creatinine sulphate (Sigma, Mississauga, ON, Canada), DOI ((±)-2,5-dimethoxy-4-iodoamphetamine hydrochloride; Research Biochemical International (RBI), Natick, MA, U.S.A), quisqualic acid, WAY 100635 (N-{2-[4(2-methoxyphenyl)-1-piperazinyl]ethyl}-n-(2-pyridinyl) cyclohexanecarboxamide trimydroxychloride; Wyeth Ayerst, Princeton, NJ, U.S.A), BMY 7378 (8-[2-[4-(2-methoxyphenyl)-1-piperazinyl]ethyl]-8-azaspirol [4,5]-decane-7,9-dione dihydrochloride Bristol-Myers Squibb, Wallingford, CT, U.S.A).

Data analysis

For 2-day administration of flibanserin, the means ± s.e.mean of DRN 5-HT neuronal firing rates were determined for each dose of flibanserin and their paired controls and were analysed with a one-way analysis of variance (ANOVA) with *post hoc* Newman-Keuls. The firing rates following 7-day administration were analysed with a Student's *t*-test. The effect of LSD on DRN 5-HT neuronal firing activity was assessed, converted to percentage of baseline, and analysed with a Student's *t*-test. For the inhibition of the recorded neuron by microiontophoretic application of 5-HT, DOI and gepirone, the resultant inhibition was analysed online by computer. The effects of different ejection values upon the number of spikes suppressed in treated and control rats were analysed with two-way repeated measures ANOVA with *post hoc* Newman-Keuls. The degree of disinhibition of the recorded cell by the i.v. administration of BMY 7378 or WAY 100635 was measured and converted into percentage of baseline in order to allow comparison between cells and analysed using two-way repeated measures ANOVAs with *post hoc* Newman Keuls (2-day administration experiments) or a Student's *t*-test (7-day administration experiments).

Table 1 Mean firing rates of DRN 5-HT neurons following 2-day systemic administration of flibanserin and control vehicle

	Number of neurons	*Firing rate* (Hz; mean ± s.e.mean)
Control	58	1.16 ± 0.09
Flibanserin		
(2.5 mg kg^{-1} × 2 days)	46	0.93 ± 0.07*
(5 mg kg^{-1} × 2 days)	41	0.87 ± 0.10*
(10 mg kg^{-1} × 2 days)	45	0.84 ± 0.08*

*$P < 0.05$ when compared to the control group.

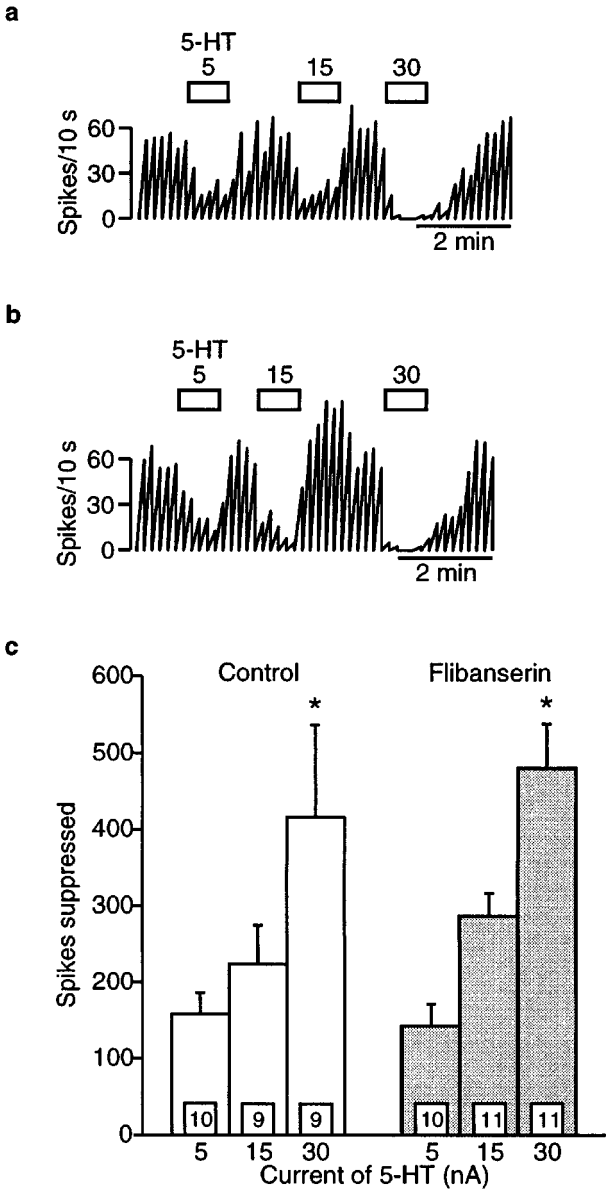

Figure 1 Effects of microiontophoretically-applied 5-HT on mPFC neurons in rats treated for 2 days with (b) 5 mg kg^{-1} day^{-1} flibanserin or (a) vehicle (delivered using an osmotic minipump implanted subcutaneously) as depicted in integrated firing rate histograms. The rectangles above the traces indicate the time of microiontophoretic ejections with the ejection values in nA denoted above the rectangles. Quisqualate was used to activate the neurons. (c) Mean ± s.e.mean of the number of spikes suppressed by microiontophoretically-applied 5-HT. Five to six rats were used in each treatment group. The number of neurons recorded is indicated in the boxes at the bottom of each column. *$P < 0.05$ when compared to respective 5 and 15 nA ejection values.

Results

Effect of 2-day flibanserin treatment on DRN 5-HT neuronal firing activity

A 2-day administration of flibanserin (2.5, 5 and 10 mg kg^{-1} day^{-1}) significantly decreased the firing rate of DRN 5-HT neurons by 20–27% ($F_{3,186}=3.1$, $P=0.03$). There was no significant difference in the mean firing rate of 5-HT neurons between any of the doses of flibanserin (Table 1). Since the inhibitory effect of flibanserin appeared to be already maximal at 5 mg kg^{-1} day^{-1}, this dose was chosen for further experiments after 2 and 7 days of administration.

Effects of microiontophoretically-applied 5-HT and DOI on mPFC neurons in 2-day flibanserin-treated and control rats

The microiontophoretic application of 5-HT current-dependently inhibited the firing of mPFC neurons in both flibanserin-treated (5 mg kg^{-1} day^{-1}) and control rats ($F_{2,35}=24.9$, $P<0.0001$). There was, however, no difference in the number of spikes suppressed by 5-HT between flibanserin-treated rats and their paired controls ($F_{1,19}=0.1$, $P=0.8$; Figure 1).

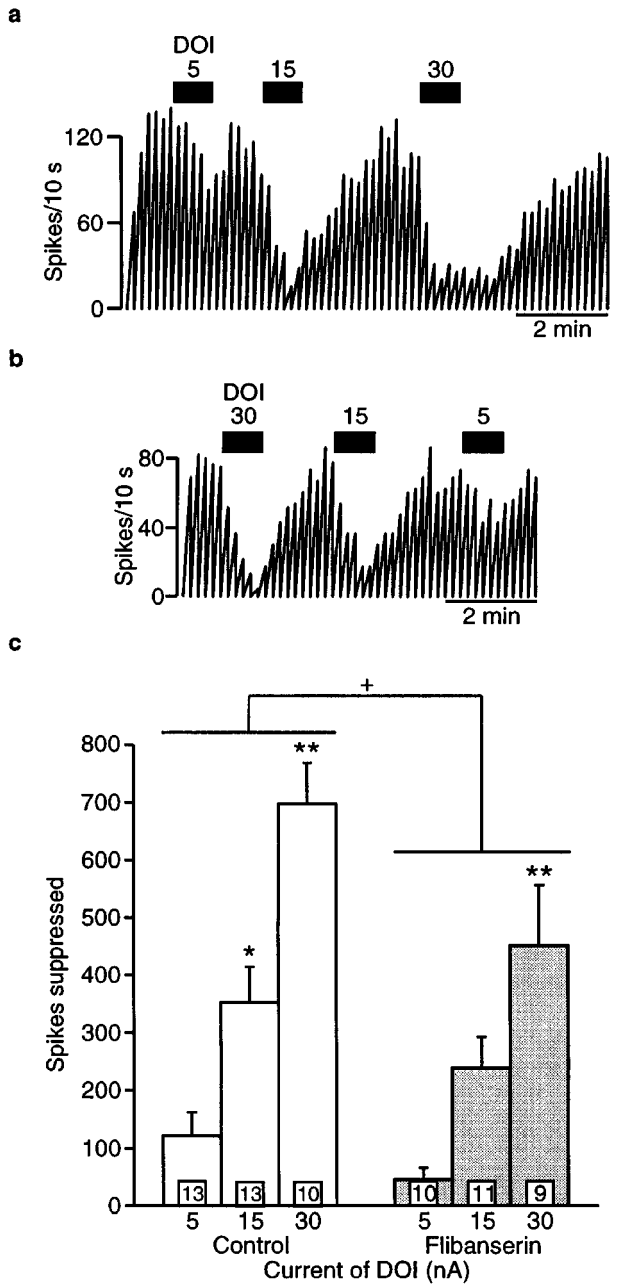

Figure 2 Effects of microiontophoretically-applied DOI on mPFC neurons in rats treated for 2 days with (b) 5 mg kg^{-1} day^{-1} flibanserin or (a) vehicle (delivered using an osmotic minipump implanted subcutaneously) as depicted in integrated firing rate histograms. The rectangles above the traces indicate the time of microiontophoretic ejections with the ejection values in nA denoted above the rectangles. Quisqualate was used to activate the neurons. (c) Mean ± s.e.mean of the number of spikes suppressed by microiontophoretically-applied DOI. Five to six rats were used in each treatment group. The number of neurons recorded is indicated in the boxes at the bottom of each column. *$P<0.05$ when compared to respective 5 nA ejection value. **$P<0.05$ when compared to respective smaller ejection values. +$P<0.05$ for overall effect of treatment.

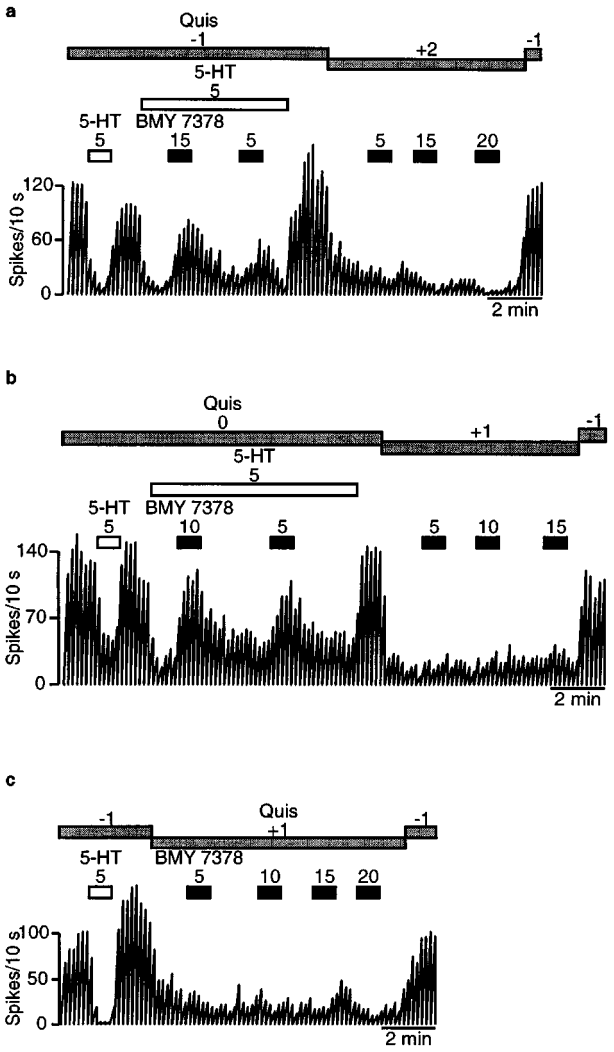

Figure 3 Examples of integrated firing rate histograms of hippocampus CA_3 pyramidal neurons in rats treated for 2 days with (a) vehicle control, (b) 5 mg kg^{-1} day^{-1} flibanserin, and (c) 15 mg kg^{-1} day^{-1} gepirone (delivered using an osmotic minipump implanted subcutaneously) during the microiontophoretic application of the 5-HT_{1A} receptor antagonist BMY 7378. The experiments were carried out three times. The rectangles above the traces indicate the time of microiontophoretic ejections with the ejection values in nA denoted above the rectangles. Note that BMY 7378 antagonizes the effects of locally-applied 5-HT (a and b) but not that of systemically-administered flibanserin or gepirone (b and c).

The microiontophoretic application of DOI current-dependently inhibited the firing of mPFC neurons in both treated and control rats ($F_{2,35}=44.6$, $P<0.0001$). The ability of DOI to inhibit mPFC neurons was significantly decreased in 2-day flibanserin treated rats ($F_{1,25}=5.4$, $P=0.03$; Figure 2). These results support the notion that 5-HT exerts its inhibitory effect on neuronal firing rate in the mPFC *via* more than the 5-HT_{2A} receptor subtype.

Effect of microiontophoretically-applied BMY7378 on hippocampus CA_3 pyramidal neurons in rats treated for 2 days with flibanserin or gepirone

In a first series of experiments, the ability of the local application of the 5-HT_{1A} receptor antagonist BMY 7378 to antagonize the actions of compounds at the postsynaptic 5-HT_{1A} receptors in the hippocampus, the effect of microiontophoretically-applied BMY 7378 was determined during concurrent local application of 5-HT. The inhibition of hippocampal neurons induced by 5-HT (Figure 3a,b), an effect previously demonstrated to be entirely attributable to 5-HT_{1A} receptor activation in this paradigm (Chaput & de Montigny, 1988; Blier *et al*., 1993a,b), was reversed by BMY 7378. In contrast, local application of BMY 7378 was not able to disinhibit neuronal firing when serotonergic compounds were given systemically in a sustained fashion (flibanserin: 2.5,5, and 10 mg kg^{-1} day^{-1}; gepirone: 15 mg kg^{-1} day^{-1}, Figure 3).

Effect of intravenous injection of WAY 100635 and BMY 7378 on the firing activity of hippocampus CA_3 pyramidal neurons following 2 days of flibanserin or gepirone administration

In order to determine the extent to which the systemic 2-day administration of flibanserin (5 mg kg^{-1} day^{-1}), and gepirone (15 mg kg^{-1} day^{-1}) was enhancing the tonic activation of postsynaptic 5-HT_{1A} receptors in the hippocampus, the ability of BMY 7378 to disinhibit the firing of these neurons was tested. Briefly, if the presence of the 5-HT_{1A} receptor agonists is tonically inhibiting the hippocampal neurons, the administration of a 5-HT_{1A} receptor antagonist should displace the agonists from the postsynaptic receptors thereby removing the inhibition. With the inhibition removed, the firing rate of the hippocampal neuron should increase (Haddjeri *et al*., 1998). For these experiments, BMY 7378 was initially chosen based on its consistent ability to antagonize the inhibitory effect of flibanserin on postsynaptic neuronal firing (Rueter *et al*., 1998). BMY 7378, in cumulative doses, inhibited the firing rate

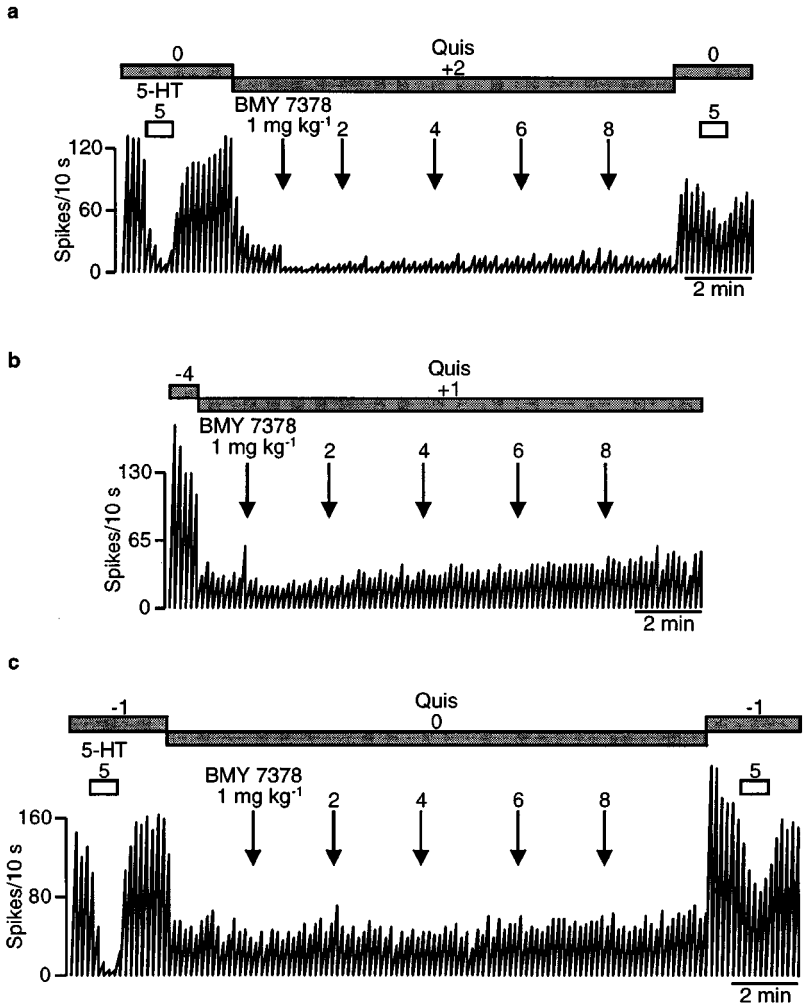

Figure 4 Examples of integrated firing rate histograms of hippocampus CA_3 pyramidal neurons in rats treated for 2 days with (a) vehicle control, (b) 5 mg kg^{-1} day^{-1} flibanserin, (c) 15 mg kg^{-1} day^{-1} gepirone (delivered using an osmotic minipump implanted subcutaneously) during the i.v. administration of cumulative doses of BMY 7378. The rectangles above the traces indicate the time of microiontophoretic ejections with the ejection values in nA denoted above the rectangles. Arrows indicate the time of i.v. injections with the cumulative doses of BMY 7378 denoted above the arrow. Note the presence of BMY 7378 significantly antagonizes the effect of microiontophoretically-applied 5-HT.

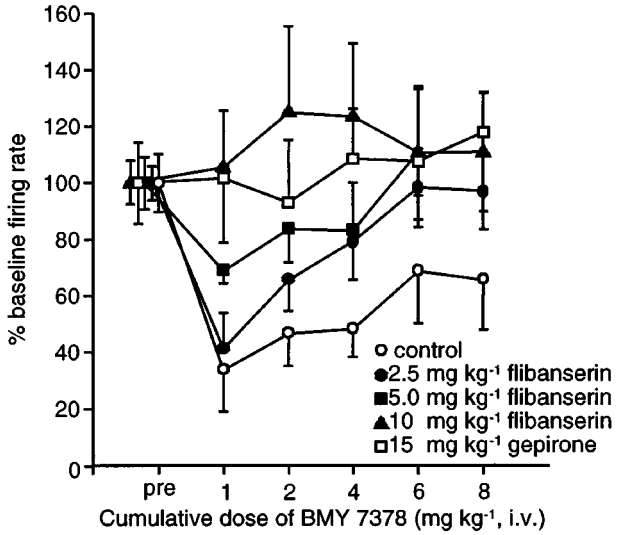

Figure 5 Effects of the cumulative i.v. administration of BMY 7378 on the percentage of baseline firing rate of hippocampus CA_3 pyramidal neurons following 2-day administration of flibanserin, gepirone, and vehicle (delivered using an osmotic minipump implanted subcutaneously; mean ± s.e.mean). Four to five rats were used in each treatment group. Due to the complexity of the figure, indicators of significant differences between the doses of BMY 7378 and between the treatments are not included here.

of hippocampal neurons in the control rats, indicative of it being a partial agonist in the hippocampus (Figures 4 and 5). Following the 2-day administration of flibanserin (2.5,5, and 10 mg kg^{-1} day^{-1}) and gepirone (15 mg kg^{-1} day^{-1}), BMY 7378 induced either a smaller inhibition, no change, or an increase in hippocampal firing rate. The relative increases in firing activity were dependent upon the increasing doses of the agonists ($F_{4,17}=4.0$, $P=0.02$; Figures 4 and 5).

Due to the inhibition of hippocampal neurons caused by the partial agonistic properties of BMY 7378, further experiments were conducted in control and 2-day flibanserin treated rats (5 mg kg^{-1} day^{-1}), utilizing a WAY 100635 pretreatment intended to minimize the inhibition induced by BMY 7378. However, it was found that WAY 100635 itself significantly increased the firing rate of hippocampal neurons in flibanserin-treated but not control rats ($F_{\text{dose of 5-HT1A antagonist, }6,40}=4.3$, $P=0.002$; $F_{\text{treatment }1,7}=6.7$, $P=0.04$; Figure 6). The subsequent administration of cumulative doses of BMY 7378 did not further increase the firing activity.

Effects of 7-day flibanserin treatment on DRN 5-HT neuronal firing activity and the functioning of the somatodendritic 5-HT_{1A} autoreceptor

There was no difference in the firing rates of DRN 5-HT neurons between rats treated for 7 days with 5 mg kg^{-1} day^{-1} flibanserin or vehicle controls (0.97 ± 0.07 versus 1.01 ± 0.07 Hz, respectively; $t_{103}=0.4$, $P=0.7$).

The ability of the 5-HT agonist LSD to inhibit the firing activity of DRN 5-HT neurons was significantly reduced in rats treated for seven days with flibanserin ($t_6=4.9$, $P=0.003$; Figure 7). Whereas 10 μg kg^{-1} of LSD was sufficient to completely suppress the firing of 5-HT neurons in most control rats, at least 20 μg kg^{-1} was required to achieve the same effect in flibanserin-treated rats (% inhibition of neuronal firing activity induced by 10 μg kg^{-1} LSD: control 96 ± 2%, $n=4$, flibanserin-treated 31 ± 13%, $n=4$; $t_6=4.9$, $P=0.003$).

Effect of microiontophoretically-applied gepirone and DOI on mPFC neurons in 7-day flibanserin-treated and control rats

Microiontophoretically-applied gepirone current dependently inhibited the firing rate of mPFC neurons, measured as spikes suppressed, in both control and flibanserin treated rats (5 mg kg^{-1} day^{-1}, $F_{2,34}=50.5$, $P<0.0001$; Figure 8a, b and c). There was no difference in the ability of gepirone to inhibit firing between control and 7-day treated rats ($F_{1,20}=0.6$, $P=0.4$; Figure 8c).

Similarly, microiontophoretically-applied DOI current dependently inhibited the firing rate of mPFC neurons in both control and flibanserin treated rats (spikes suppressed; $F_{2,33}=72.8$, $P<0.0001$: Figure 8a, b and d). However, unlike the results seen following 2-day flibanserin administration, there was no difference between control and treated animals ($F_{1,18}=1.0$, $P=0.3$; Figure 8d).

Effect of microiontophoretically-applied 5-HT and gepirone on hippocampus CA_3 pyramidal neurons in 7-day flibanserin-treated and control rats

Microiontophoretically-applied 5-HT current-dependently inhibited the firing activity of hippocampal neurons in both control and flibanserin-treated rats (5 mg kg^{-1} day^{-1}, spikes suppressed; $F_{2,40}=32.4$, $P<0.0001$; Figure 9a, b and c). There was no difference in the ability of 5-HT to suppress neuronal firing between the control and treated rats ($F_{1,21}=0.4$, $P=0.5$: Figure 9c). In addition, microiontophoretically-applied gepirone current-dependently inhibited the firing rate of hippocampal neurons (spikes suppressed; $F_{2,36}=27.6$, $P<0.0001$; Figure 9a, b and d), with there being no difference between the control and treated rats ($F_{1,20}=1.2$, $P=0.3$; Figure 9d).

Effect of the intravenous injection of WAY 100635 on the firing activity of hippocampus CA_3 pyramidal neurons following 7 days of flibanserin administration

WAY 100635 (250 μg kg^{-1}, i.v.) significantly antagonized the inhibition induced by the microiontophoretic application of 5-HT ($F_{1,6}=81.1$, $P<0.001$), and there was no difference in the antagonism induced by WAY 100635 between the flibanserin-treated (5 mg kg^{-1} day^{-1}) animals and the controls ($F_{1,6}=1.0$, $P=0.4$; Figure 10c). Furthermore, WAY 100635 did not alter the firing rate of hippocampal neurons in control rats (Figure 10a and d). In contrast, there was a significant increase of 34% in the firing rate of hippocampal neurons in the 7-day flibanserin-treated rats following the i.v. administration of WAY 100635 ($t_8=3.1$, $P=0.02$: Figure 10b and d).

Discussion

Sustained administration of the 5-HT_{1A} receptor agonist/5-HT_{2A} receptor antagonist flibanserin induced several changes in the 5-HT system of the rat. First, DRN 5-HT neuronal firing activity was reduced by only 25% following 2-day administration of flibanserin, and this inhibition of firing activity was not dose-dependent. Following 7 days of sustained flibanserin administration, 5-HT neuronal firing had recovered to normal levels probably due to the desensitization of the somatodendritic 5-HT_{1A} autoreceptors. Second, as expected, a 2-day flibanserin treatment significantly attenuated the effect of microiontophoretically-applied DOI in the mPFC. However, this ability of flibanserin to antagonize DOI was no

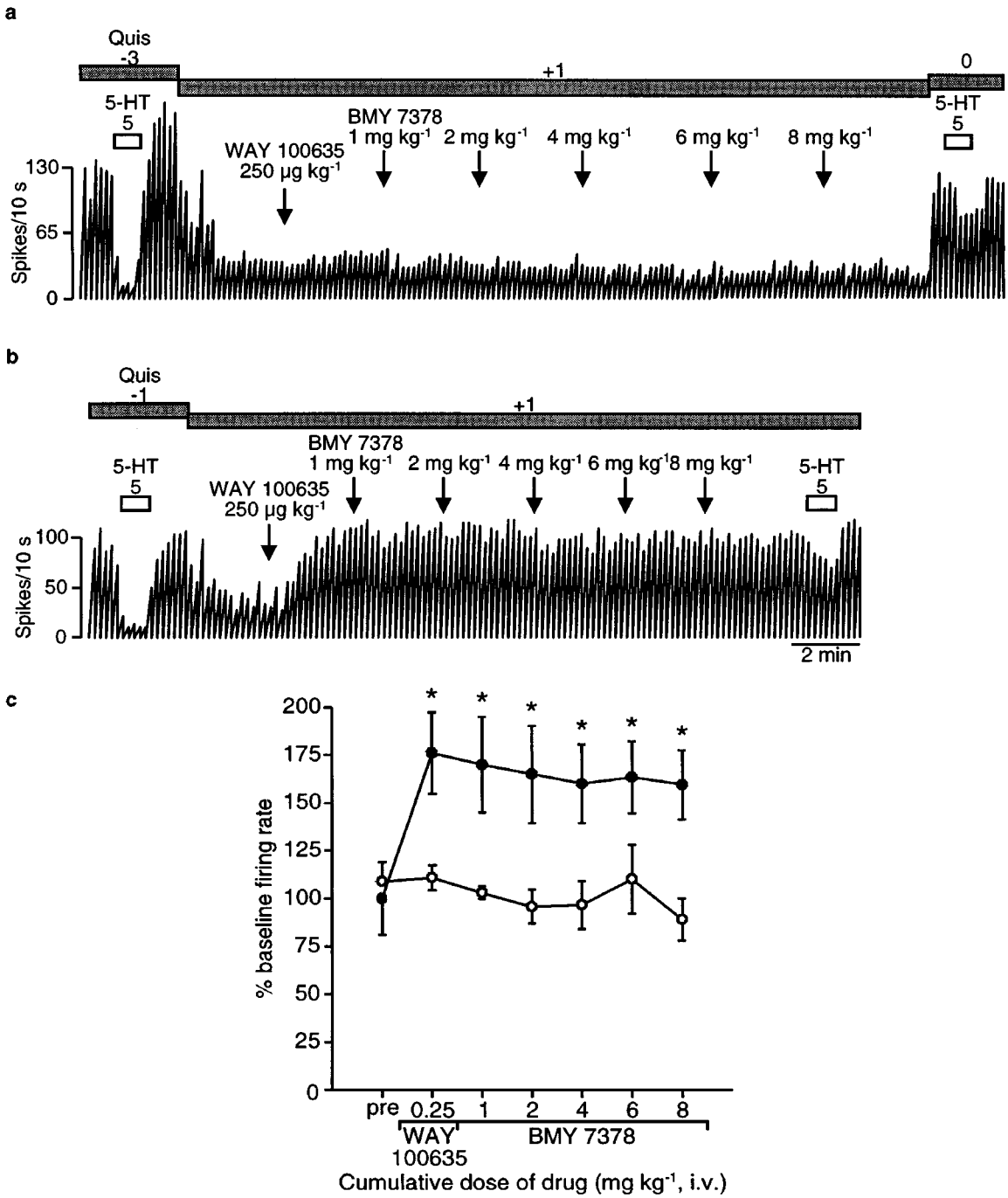

Figure 6 Effects of the i.v. administration of the 5-HT_{1A} receptor antagonist WAY 100635 and cumulative doses of BMY 7378 on the basal firing rate of hippocampus CA_3 pyramidal neurons in rats treated for 2 days with (b) 5 mg kg^{-1} day^{-1} flibanserin or (a) vehicle (delivered using an osmotic minipump implanted subcutaneously) as depicted in integrated firing rate histograms. The rectangles above the traces indicate the time of microiontophoretic ejections with the ejection values in nA denoted above the rectangles. Arrows indicate the time of i.v. injections with the dose of WAY 100635 and the cumulative doses of BMY 7378 denoted above the arrow. (c) Mean $\pm$ s.e.mean values for the percentage of baseline firing rate of hippocampal neurons in response to the i.v. administration of WAY 100635 and subsequent cumulative doses of BMY 7378. The open circles depict the results obtained in control rats and the filled circles those observed in flibanserin-treated rats. Five rats were used in each treatment group. $^*P<0.05$ when compared to the preinjection value and to control values.

longer present following 7-day flibanserin administration indicating a fairly rapid change in the functioning of the postsynaptic 5-HT_{2A} receptors in the mPFC. In contrast, there was no effect of flibanserin on the ability of microiontophoretically-applied 5-HT or the 5-HT_{1A} receptor agonist gepirone to inhibit either mPFC or hippocampus CA_3 pyramidal neurons after 2 or 7 days of flibanserin administration. Finally, sustained flibanserin administration, for either 2 or 7 days, significantly enhanced the tonic activation of the postsynaptic 5-HT_{1A} receptors in the hippocampus.

The decrease in DRN 5-HT neuronal firing activity seen following 2 days of flibanserin administration and the recovery to normal following a longer period of treatment with the desensitization of the somatodendritic 5-HT_{1A} autoreceptors was a finding similar to those reported for other 5-HT_{1A} receptor agonists (Blier & de Montigny, 1987; Dong *et al.*, 1997; Godbout *et al.*, 1991). However, there were notable differences between flibanserin and these other 5-HT_{1A} receptor agonists. First, the degree of inhibition of 5-HT neuronal firing activity seen following two days of adminis-

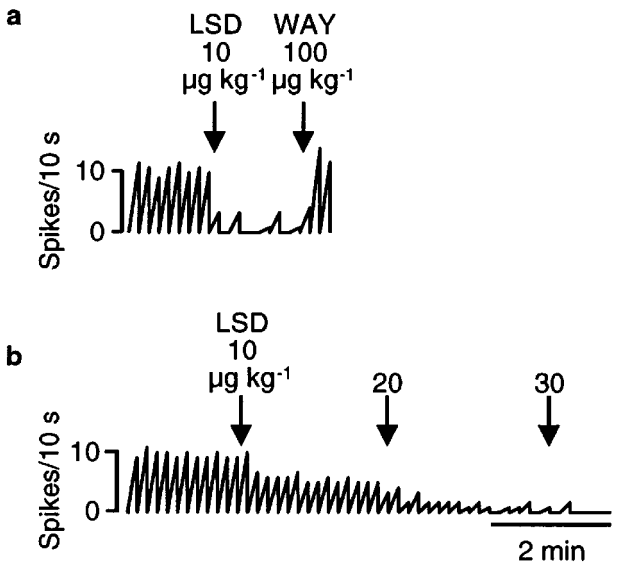

Figure 7 Effects of the i.v. administration of LSD on the firing rates of DRN 5-HT neurons in control (a) and 7 day flibanserin-treated rats (5 mg kg^{-1} day^{-1}; b) (delivered using an osmotic minipump implanted subcutaneously) as depicted in integrated firing rate histograms. Arrows indicate the time of injection with the cumulative dose of LSD ($\mu g\ kg^{-1}$) denoted above the arrows. Note the inhibitory effect of LSD was reversed by the i.v. administration of the selective 5-HT_{1A} receptor antagonist WAY 100635.

tration of flibanserin (about 25%; 2.5–10 mg kg^{-1} day^{-1}) was markedly smaller than that seen with either 15 mg kg^{-1} day^{-1} of gepirone (80%; Blier & de Montigny, 1987) and ipsapirone (75%; Dong *et al.*, 1997), or 10 mg kg^{-1} day^{-1} of tandospirone (70%: Godbout *et al.*, 1991). Second, the ability of flibanserin to inhibit DRN 5-HT neuronal firing activity was not dose-dependent, i.e. increasing the dose of flibanserin 2–4 fold did not significantly alter the degree of inhibition (Table 1), unlike the other 5-HT_{1A} agonists mentioned above and BAY X 3702 (6%, 42%, 77% with 0.5, 1.0 and 1.25 mg kg^{-1} day^{-1} for 2 days; Dong *et al.*, 1998). Finally, unlike a 7-day sustained administration with gepirone and ipsapirone, the firing rate of 5-HT neurons had recovered fully following 7 days of flibanserin administration. Nevertheless, the desensitization of the somatodendritic 5-HT_{1A} autoreceptors seen with sustained flibanserin administration did develop as with other 5-HT_{1A} agonists (Figure 7; Blier & de Montigny, 1987; Dong *et al.*, 1997; Godbout *et al.*, 1991). Recent studies investigating the time course of changes in the 5-HT_{1A} autoreceptors in the DRN following sustained administration of the SSRI fluoxetine and paroxetine suggest that there is a gradual desensitization of the autoreceptors during periods of enhanced stimulation of 5-HT_{1A} receptors (Le Poul *et al.*, 1995; 1997). It is thus possible to hypothesize that the full recovery of 5-HT neuronal firing activity following 7 days of flibanserin administration was due to the fact that there was a limited

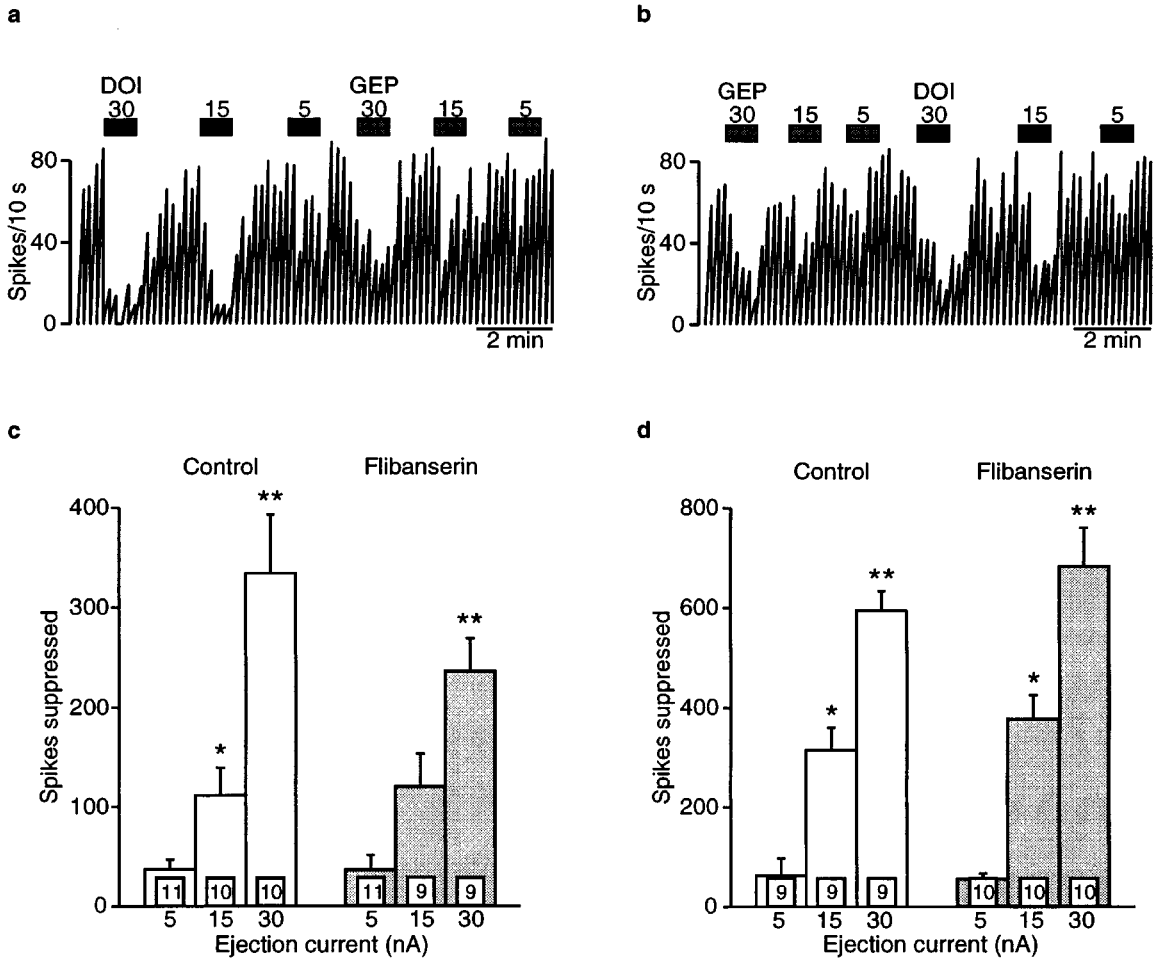

Figure 8 Effects of microiontophoretically-applied gepirone and DOI on mPFC neurons in rats treated for 7 days with (b) 5 mg kg^{-1} day^{-1} flibanserin or (a) vehicle (delivered using an osmotic minipump implanted subcutaneously) as depicted in integrated firing rate histograms. The rectangles above the traces indicate the time of microiontophoretic ejections with the ejection values in nA denoted above the rectangles. Quisqualate was used to activate the neurons. (c) Mean ± s.e.mean of the number of spikes suppressed by microiontophoretically-applied gepirone. (d) Mean ± s.e.mean of the number of spikes suppressed by microiontophoretically-applied DOI. Four to five rats were used for each treatment group. The number of neurons recorded is indicated in the boxes at the bottom of each column. $*P<0.05$ when compared to respective 5 nA ejection value. $**P<0.05$ when compared to respective smaller ejection values.

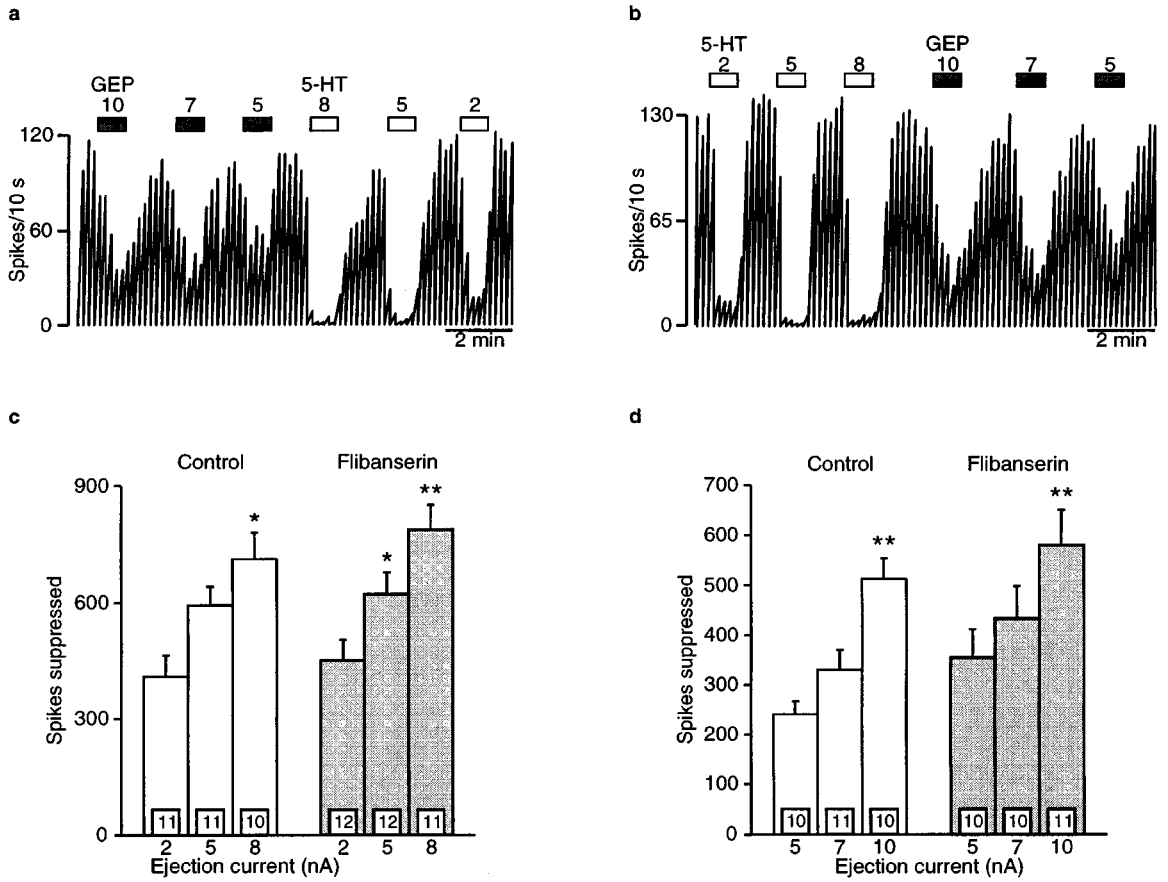

Figure 9 Effects of microiontophoretically-applied 5-HT and gepirone on hippocampus CA_3 pyramidal neurons in rats treated for 7 days with (b) 5 mg kg^{-1} day^{-1} flibanserin or (a) vehicle (delivered using an osmotic minipump implanted subcutaneously) as depicted in integrated firing rate histograms. The rectangles above the traces indicate the time of microiontophoretic ejections with the ejection values in nA denoted above the rectangles. Quisqualate was used to activate the neurons. (c) Mean $\pm$ s.e.mean of the number of spikes suppressed by microiontophoretically-applied 5-HT. (d) Mean $\pm$ s.e.mean of the number of spikes suppressed by microiontophoretically-applied gepirone. Six to seven rats were used for each treatment group. The number of neurons recorded is indicated in the boxes at the bottom of each column. $^{*}P<0.05$ when compared to respective 5 nA ejection value. $^{**}P<0.05$ when compared to respective smaller ejection values.

degree of firing inhibition and, therefore, a desensitization of the somatodendritic 5-HT_{1A} autoreceptors was sufficient to readily reverse the inhibitory effects of the compound.

Flibanserin significantly antagonized the inhibitory effect of DOI at the 5-HT_{2A} receptors in the mPFC following 2 days of administration (Figure 2). This finding is consistent with the 5-HT_{2A} receptor antagonistic properties of flibanserin. Since flibanserin has a greater affinity for 5-HT_{1A} receptors than for 5-HT_{2A} receptors, this result indicates that the dose of 5 mg kg^{-1} day^{-1} was most likely sufficient to act on both of these receptors (Figure 2; Borsini *et al.*, 1995b). It is interesting to note that, while 5-HT_{2A} receptors in the cortex have generally been described as excitatory, the microiontophoretic application of the 5-HT_2 receptor agonist DOI inhibits the firing of mPFC neurons (Ashby *et al.*, 1990; unpublished results from our laboratory). The ability of a 5-HT_{2A} receptor antagonist to block this inhibition further suggests that at least a subgroup of 5-HT_{2A} receptors in the mPFC may be inhibitory. The antagonism of cortical 5-HT_{2A} receptors was not present following 7-day flibanserin administration (Figure 8). This suggests an increase in the sensitivity of the 5-HT_{2A} receptors in cortex. Previous studies investigating the chronic administration of 5-HT_2 receptor antagonists have consistently reported a decrease in the density of 5-HT_{2A} receptors, but the findings regarding the sensitivity of these receptors following long-term treatment have been contradictory (Blackshear & Sanders-Bush, 1982; Akiyoshi *et al.*, 1994; Stoltz *et al.*, 1983; Darmani *et al.*, 1992). Some studies have found a desensitization of the 5-HT_{2A} receptors while others have shown a supersensitivity of behaviours mediated by these receptors during the withdrawal period. Indeed, it has been suggested that receptor responsiveness is a more accurate picture of the functioning of these receptors than receptor binding parameters (Smith *et al.*, 1990). While none of these previous studies have reported an increased functioning of these receptors during the treatment with a 5-HT_2 receptor antagonist, the present study suggests that a supersensitivity of 5-HT_{2A} receptors may occur during 5-HT_{2A} receptor antagonist administration. In contrast, it may be that the purported increased sensitivity of the 5-HT_{2A} cortical receptors following the 7-day administration with flibanserin may not have been due to the 5-HT_{2A} receptor antagonistic properties of flibanserin but rather to its 5-HT_{1A} receptor agonistic properties. A 7-day administration with gepirone has indeed been shown to increase 5-HT_2 receptor-mediated behaviours despite a decreased number of cortical 5-HT_2 binding sites (Yocca *et al.*, 1991).

There is one further intriguing aspect to the changes in cortical 5-HT_2 receptors following long-term administration of 5-HT_2 receptor antagonists. Kidd *et al.* (1990) have shown that chronic administration of the 5-HT_2 receptor antagonist ritanserin, a treatment regimen that decreases the number of

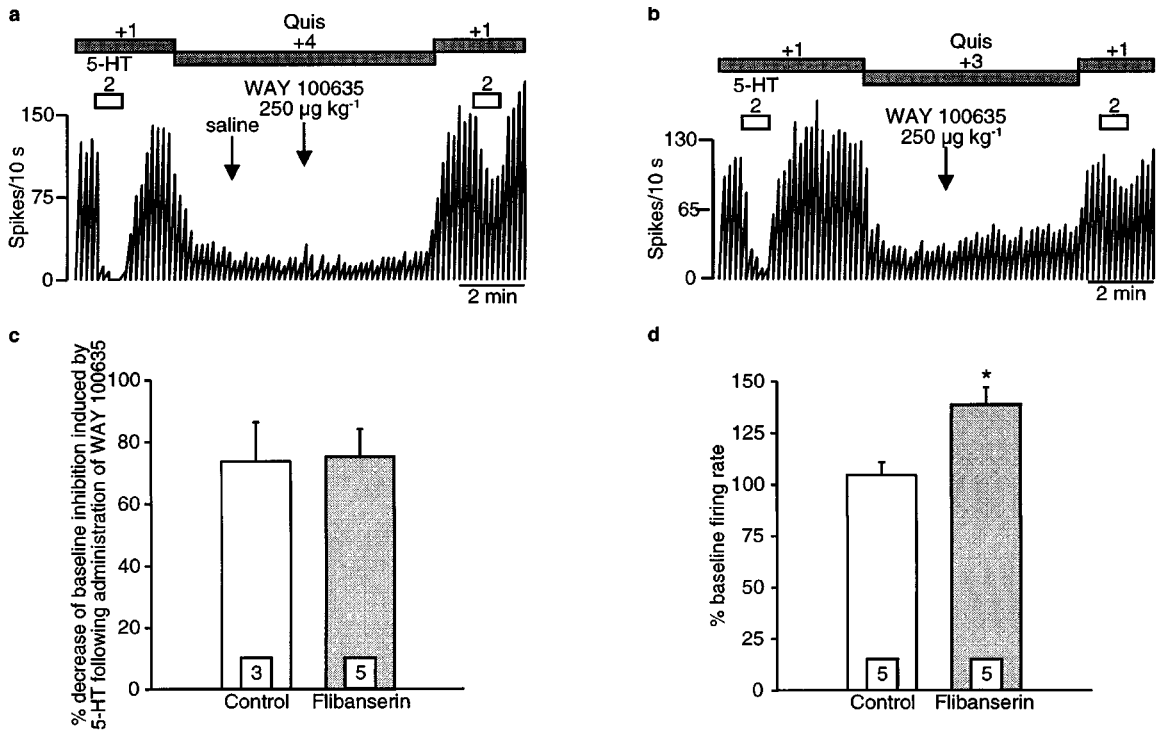

Figure 10 Effects of the i.v. administration of the selective 5-HT_{1A} receptor antagonist WAY 100635 on the basal firing rate of hippocampus CA_3 pyramidal neurons in rats treated for 7 days with (b) 5 mg kg^{-1} day^{-1} flibanserin or (a) vehicle (delivered using an osmotic minipump implanted subcutaneously) as depicted in integrated firing rate histograms. The rectangles above the traces indicate the time of microiontophoretic ejections with the ejection values in nA denoted above the rectangles. Arrows indicate the time of i.v. injections with the dose of WAY 100635 denoted above the arrow. (c) Mean ± s.e.mean values for the percentage decrease in the ability of microiontophoretically-applied 5-HT to inhibit the firing of hippocampal neurons after the administration of WAY 100635 (250 μg kg^{-1}, i.v.). (d) Mean ± s.e.mean values for the percentage of baseline firing rate of hippocampal neurons following the i.v. administration of 250 μg kg^{-1} WAY 100635. The number of neurons recorded is indicated in the boxes at the bottom of each column. $^*P<0.05$.

5-HT_2 receptor binding sites in cortex, decreased the inhibitory effect of the 5-HT_{1A} agonist receptor 8-OH-DPAT on 5-HT release. Moreover, repeated administration of the 5-HT_2 receptor agonist, DOI, which also downregulates 5-HT_2 receptors in the cortex, attenuated the 5-HT_{1A} receptor-mediated inhibitory action of 8-OH-DPAT on DRN 5-HT neuronal firing (Kidd *et al*., 1991). 8-OH-DPAT is known to inhibit 5-HT neuronal firing *via* a feedback loop, most likely extending from the cortex (Blier & de Montigny, 1987; Ceci *et al*., 1994). Thus, the sustained interaction of flibanserin on cortical 5-HT_{2A} receptors may be contributing to the lack of a dose-dependent effect of flibanserin on the firing activity of DRN 5-HT neurons following 2-day administration and/or the normalization of DRN 5-HT neuronal firing activity seen following 7 days of flibanserin administration.

Several experiments in the present study were designed to examine the degree of tonic inhibition of hippocampus CA_3 pyramidal neurons following 2-day flibanserin administration. BMY 7378 was chosen because, in acute administration studies, it was found to more consistently antagonize flibanserin than did the more selective 5-HT_{1A} receptor antagonist WAY 100635 (Rueter *et al*., 1998). First, the ability of the local application of the 5-HT_{1A} receptor antagonist BMY 7378 to reverse the ongoing inhibition of hippocampal neurons induced by flibanserin was investigated. While the local application of BMY 7378 could reverse the inhibition caused by the local application of 5-HT, it could not reverse the inhibition caused by the systemically-administered flibanserin (Figure 3). Given that systemically-administered flibanserin could be acting on 5-HT_{1A} receptors on the hippocampal neuron located outside the small region affected by the microiontophoretic ejection of BMY 7378 (i.e. on the dendrites of pyramidal neurons, Blier *et al*., 1993a,b), this result was not necessarily surprising. The second set of experiments were designed to reverse the inhibition induced by systemically-administered flibanserin using the systemic injection of BMY 7378. However, results indicated that BMY 7378 significantly inhibited neuronal firing in controls. In the presence of flibanserin, the inhibitory effect of BMY 7378 was attenuated in a dose-dependent fashion. At the highest dose of flibanserin used, BMY 7378 actually increased hippocampus neuronal firing above baseline levels (Figures 4 and 5). Thus, these experiments demonstrated a tonic inhibition of CA_3 pyramidal neurons by flibanserin mediated by the postsynaptic 5-HT_{1A} receptors. Nevertheless, the inhibition of firing activity induced by the apparent partial agonistic properties of BMY 7378 was troubling. Therefore, a third set of experiments was performed, utilizing a pretreatment of WAY 100635 intended to block this putative agonistic action of BMY 7378, thereby leaving only the disinhibition of the hippocampal neuron. As expected, in control rats, pretreatment with WAY 100635 prevented the inhibitory action of BMY 7378. However, WAY 100635, by itself, significantly disinhibited the firing activity of the hippocampal neurons, further supporting an enhanced tonic activation of the postsynaptic 5-HT_{1A} receptors following a 2-day flibanserin administration (Figure 6). An enhancement of the tonic activation of the postsynaptic 5-HT_{1A} receptors has been demonstrated following long-term treatment with several types of antidepressant treatments (Haddjeri *et al*., 1998). Such an increased tonic activation after 2 days of treatment, as was the case with flibanserin, so far has been reported with the dual 5-HT/norepinephrine reuptake blockade, as well as with a monoamine oxidase inhibitor and pindolol, two strategies putatively endowed with a more rapid

onset of action and/or a greater efficacy (Rueter *et al*., 1998a; Haddjeri *et al*., 1998).

Similar to the 2-day treatment, the disinhibition of hippocampus neuronal firing induced by the i.v. administration of WAY 100635 indicated that the 7-day flibanserin treatment increased the tonic activation of the postsynaptic 5-HT_{1A} receptors in the CA_3 region of the hippocampus (Figure 10). There was, however, no difference in the ability of WAY 100635 to block the effects of locally-applied 5-HT between flibanserin-treated and control animals (Figure 10c), suggesting the selective disinhibition of postsynaptic neurons was a reflection of the systemic levels of flibanserin combined with the presumably normal extracellular levels of 5-HT. It may be considered somewhat surprising that the disinhibition induced by the i.v. administration of WAY 100635 was not significantly larger following 7-day flibanserin administration when compared to the effects seen at 2 days of administration given that the DRN 5-HT neuronal firing had returned to normal levels. However, it is yet unclear whether there is a linear relationship between the degree of disinhibition and the clinical efficacy of an antidepressant treatment (Haddjeri *et al*., 1998).

In summary, flibanserin induced a desensitization of the somatodendritic 5-HT_{1A} autoreceptors which allowed a recovery of normal 5-HT neuronal firing activity in a shorter time period than other 5-HT_{1A} agonists. In addition, there was an enhanced tonic activation of the postsynaptic 5-HT_{1A} receptors in the hippocampus at both 2 and 7 days of flibanserin administration, an effect obtained in a significantly shorter period of drug administration than that seen with other antidepressant compounds. However, one has to consider that the degree of activation of multiple subtypes of postsynaptic 5-HT receptors other than the 5-HT_{1A} subtype by endogenous 5-HT was still dependent on the recovery of the firing rate of 5-HT neurons during sustained flibanserin administration. Nevertheless, these results suggest that flibanserin could be an effective antidepressant drug that may have a more rapid onset of action than classical antidepressant drugs.

This work was supported in part by the Medical Research Council of Canada (grant MT-11014), the Fonds de la Recherche en Santé de Québec and Boehringer Ingelheim. L.R. is the recipient of a Fellowship from the Royal Victoria Hospital (Montréal, Canada). P.B. is the recipient of a Medical Research Council of Canada Scientist Award.

References

AGHAJANIAN, G.K. (1978). Feedback regulation of central monoaminergic neurons: Evidence from single-cell recording studies. In *Essays in Neurochemistry and Neuropharmacology*. ed. Youdim, M.B.H., Lovenberg, W., Sharman, D.F., & Lagnando, J.R. pp. 1–32. New York: Wiley.

AKIYOSHI, J., TSUCHIYAMA, K., MIZOBE, Y., NAKAMURA, M., KURANAGA, H. & NAGAYAMA, H. (1994). Effects of chronic mianserin administration on serotonin metabolism and receptors in the 5-hydroxytryptophan depression model. *Prog. Neuro-Psychopharmacol. Biol. Psychiat.,* **18,** 165–179.

ASHBY, JR C.R., EDWARDS, E. & WANG, R.Y. (1994). Electrophysiological evidence for a functional interaction between 5-HT_{1A} and 5-HT_{2A} receptors in the rat medial prefrontal cortex: an iontophoretic study. *Synapse,* **17,** 173–181.

ASHBY, JR C.R., JIANG, L.H., KASSER, R.J. & WANG, R.Y. (1990). Electrophysiological characterization of 5-hydroxytryptamine$_2$ receptors in the rat medial prefrontal cortex. *J. Pharmacol. Exp. Ther.,* **252,** 171–178.

BERMAN, R.M., DARNELL, A.M., MILLER, H.L., ANAND, A. & CHARNEY, D.S. (1997). Effect of pindolol in hastening response to fluoxetine in the treatment of major depression: a double-blind, placebo-controlled trial. *Am. J. Psychiat.,* **154,** 37–43.

BLACKSHEAR, M.A. & SANDERS-BUSH, E. (1982). Serotonin receptor sensitivity after acute and chronic treatment with mianserin. *J. Pharmacol. Exp. Ther.,* **221,** 303–308.

BLIER, P., BERGERON, R. & DE MONTIGNY, C. (1997). Selective activation of postsynaptic 5-HT_{1A} receptors induces rapid antidepressant response. *Neuropsychopharmacology,* **16,** 333–338.

BLIER, P. & DE MONTIGNY, C. (1987). Modification of 5-HT neuron properties by sustained administration of the 5-HT_{1A} agonist gepirone: Electrophysiological studies in the rat brain. *Synapse,* **1,** 470–480.

BLIER, P. & DE MONTIGNY, C. (1994). Current advances and trends in the treatment of depression. *Trends Pharmacol. Sci.,* **15,** 220–226.

BLIER, P., DE MONTIGNY, C. & TARDIF, D. (1987). Short-term lithium treatment enhances responsiveness of postsynaptic 5-HT_{1A} receptors without altering 5-HT autoreceptor sensitivity: An electrophysiological study in the rat brain. *Synapse,* **1,** 225–232.

BLIER, P., LISTA, A. & DE MONTIGNY, C. (1993a). Differential properties of pre- and postsynaptic 5-hydroxytryptamine$_{1A}$ receptors in the dorsal raphe and hippocampus: I - Effect of spiperone. *J. Pharmacol. Exp. Ther.,* **265,** 7–15.

BLIER, P., LISTA, A. & DE MONTIGNY, C. (1993b). Differential properties of pre- and postsynaptic 5-hydroxytryptamine$_{1A}$ receptors in the dorsal raphe and hippocampus: II - Effect of pertussis and cholera toxins. *J. Pharmacol. Exp. Ther.,* **265,** 16–23.

BORDET, R., THOMAS, P. & DUPUIS, B. (1998). Effect of pindolol on onset of action of Paroxetine in the treatment of major depression: intermediate analysis of a double-blind, placebo-controlled trial. *Am. J. Psychiat.,* **155,** 1346–1351.

BORSINI, F., CECI, A., BIETTI, G. & DONETTI, A. (1995a). BIMT 17, a 5-HT_{1A} receptor agonist/5-HT_{2A} receptor antagonist, directly activates postsynaptic 5-HT inhibitory responses in the rat cerebral cortex. *Naunyn-Schmiedeberg's Arch. Pharmacol.,* **352,** 283–290.

BORSINI, F., GIRALDO, E., MONFERINI, E., ANTONINI, G., PARENTI, M., BIETTI, G. & DONETTI, A. (1995b). BIMT 17, a 5-HT_{2A} receptor antagonist and 5-HT_{1A} receptor full agonist in rat cerebral cortex. *Naunyn-Schmiedeberg's Arch. Pharmacol.,* **352,** 276–282.

BOSKER, F.J., DE WINTER, T.Y.C.E., KLOMPMAKERS, A.A. & WESTENBERG, H.G.M. (1996). Flesinoxan dose-dependently reduces extracellular 5-hydroxytryptamine (5-HT) in rat median raphe and dorsal hippocampus through activation of 5-HT_{1A} receptors. *J. Neurochem.,* **66,** 2546–2555.

CECI, A., BASCHIROTTO, A. & BORSINI, F. (1994). The inhibitory effect of 8-OH-DPAT on the firing activity of dorsal raphe serotoninergic neurons in rats is attenuated by lesion of the frontal cortex. *Neuropharmacology,* **33,** 709–713.

CHAPUT, Y. & DE MONTIGNY, C. (1988). Effects of the 5-hydroxytryptamine$_1$ receptor antagonist BMY 7378, on 5-hydroxytryptamine neurotransmission: Electrophysiological studies in the rat central nervous system. *J. Pharmacol. Exp. Ther.,* **246,** 359–370.

DARMANI, N.A., MARTIN, B.R. & GLENNON, R.A. (1992). Behavioural evidence for differential adaptation of the serotonergic system after acute and chronic treatment with (±)-1-(2,5-dimethoxy-4-iodophenyl)-2-aminopropane (DOI) or ketanserin. *J. Pharmacol. Exp. Ther.,* **262,** 692–698.

DE MONTIGNY, C. & BLIER, P. (1991). Development of selective agonists of postsynaptic 5-HT_{1A} receptors: a future direction in the pharmacotherapy of affective disorders? In *Current Practices and Future Developments in the Pharmacotherapy of Mental Disorders*. ed. Meltzer, H.Y, & Nerozzi, D. pp. 99–103. New York: Elsevier Science Publishers.

DONG, J., DE MONTIGNY, C. & BLIER, P. (1997). Effect of acute and repeated versus sustained administration of the 5-HT_{1A} agonist ipsapirone: electrophysiological studies in the rat hippocampus and dorsal raphe. *Naunyn-Schmiedeberg's Arch. Pharmacol.,* **356,** 303–311.

DONG, J., DE MONTIGNY, C. & BLIER, P. (1998). Full agonistic properties of Bay X 3702 on presynaptic and postsynaptic 5-HT_{1A} receptors electrophysiological studies in the rat hippocampus and dorsal raphe. *J. Pharmacol. Exp. Ther.,* (in press).

FLETCHER, A., FORSTER, E.A., BILL, D.J., BROWN, G., CLIFFE, I.A., HARTLEY, J.E., JONES, D.E., MCLENACHAN, A., STANHOPE, K.J., CRITCHLEY, D.J.P., CHILDS, K.J., MIDDEFELL, V.C., LANFUMEY, L., CORRADETTI, R., LAPORTE, A.-M., GOZLAN, H., HAMON, M. & DOURISH, C.T. (1996). Electrophysiological, biochemical, neurohormonal, and behavioural studies with WAY-100635, a potent, selective and silent 5-HT_{1A} receptor antagonist. *Behav. Brain Res.,* **73,** 337–353.

FORNAL, C.A., LITTO, W.J., METZLER, C.W., MARROSU, F., TADA, K. & JACOBS, B.L. (1994). Single-unit responses of serotonergic dorsal raphe neurons to 5-HT_{1A} agonist and antagonist drug administration in behaving cats. *J. Pharmacol. Exp. Ther.,* **270,** 1345–1358.

GODBOUT, R., CHAPUT, Y., BLIER, P. & DE MONTIGNY, C. (1991). Tandospirone and its metabolite, 1-(2-pyrimidinyl)-piperazine- I. Effects of acute and long-term administration of tandospirone on serotonin neurotransmission. *Neuropharmacology,* **30,** 679–690.

HADDJERI, N., BLIER, P. & DE MONTIGNY, C. (1998). Long-term antidepressant treatments result in a tonic activation of forebrain 5-HT_{1A} receptors. *J. Neurosci.,* **18,** 10150–10156.

KANDEL, E.R. & SPENCER, W.A. (1961). Electrophysiology of hippocampal neurons. II. Afterpotentials and repetitive firing. *J. Neurophysiol.,* **24,** 243–259.

KIDD, E.J., GARRATT, J.C. & MARSDEN, C.A. (1991). Effects of repeated treatment with 1-(2,5-dimethoxy-4-iodophenyl)-2-aminopropane (DOI) on the autoregulatory control of dorsal raphe 5-HT neuronal firing and cortical 5-HT release. *Eur. J. Pharmacol.,* **200,** 131–139.

KIDD, E.J., LEYSEN, J.E. & MARSDEN, C.A. (1990). Chronic 5-HT_2 receptor antagonist treatment alters 5-HT_{1A} autoregulatory control of 5-HT release in rat brain in vivo. *J. Neurosci. Meth.,* **34,** 91–98.

KREISS, D.S. & LUCKI, I. (1997). Chronic administration of the 5-HT_{1A} receptor agonist 8-OH-DPAT differentially desensitizes 5-HT_{1A} autoreceptors of the dorsal and median raphe nuclei. *Synapse,* **25,** 107–116.

LE POUL, E., LAARIS, N., DOUCET, E., LAPORTE, A.M., HAMON, M. & LANFUMEY, L. (1995). Early desensitization of somatodendritic 5-HT_{1A} autoreceptors in rats treated with fluoxetine or paroxetine. *Naunyn-Schmeideberg's Arch. Pharmacol.,* **352,** 141–148.

LE POUL, E., LAARIS, N., HAMON, M. & LANFUMEY, L. (1997). Fluoxetine-induced desensitization of somatodendritic 5-HT_{1A} autoreceptors in independent of gluococorticoid(s). *Synapse,* **27,** 303–312.

PAXINOS, G. & WATSON, C. (1982). In *The Rat Brain in Stereotaxic Coordinates*. New York: Academic Press.

PÉREZ, V., GILABERTE, I., FARIES, D., ALVAREZ, E. & ARTIGAS, F. (1997). Randomised, double-blind, placebo-controlled trial of pindolol in combination with fluoxetine antidepressant treatment. *Lancet,* **349,** 1594–1597.

RANCK, J.B. (1975). Behavioural correlates and firing repertories of neurons in the dorsal hippocampal formation of unrestrained rats. In *The Hippocampus*. ed. Isaacson, I. & Robert, L. pp. 207–244. New York: Plenum.

ROBINSON, D.S., RICKELS, K., FEIGHNER, J., FABRE, JR L.F., GAMMANS, R.E., SHROTRIYA, R.C., ALMS, D.R., ANDARY, J.J. & MESSINA, M.E. (1990). Clinical effects of the 5-HT_{1A} partial agonists in depression: A composite analysis of buspirone in the treatment of depression. *J. Clin. Psychopharmacol.,* **10,** 67S–76S.

ROMERO, L., BEL, N., ARTIGAS, F., DE MONTIGNY, C. & BLIER, P. (1996). Effect of pindolol at pre- and postsynaptic 5-HT_{1A} receptors: in vivo microdialysis and electrophysiological studies in the rat brain. *Neuropsychopharmacology,* **15,** 349–360.

RUETER, L.E., DE MONTIGNY, C. & BLIER, P. (1998a). Electrophysiological characterization of the effect of long-term duloxetine administration on the rat serotonergic and noradrenergic systems. *J. Pharmacol. Exp. Ther.,* **285,** 404–412.

RUETER, L.E., DE MONTIGNY, C. & BLIER, P. (1998b). In vivo electrophysiological assessment of the agonistic properties of flibanserin at pre- and postsynaptic 5-HT_{1A} receptors in the rat brain. *Synapse,* **29,** 392–405.

SHEN, Y., MONSMA, F.J., METCALF, M.A., JOSE, P.A., HAMBLIN, M.W. & SIBLEY, D.W. (1993). Molecular cloning and expression of a 5-hydroxytryramine 7 serotonin receptor subtype. *J. Biol. Chem.,* **268,** 18200–18204.

SMITH, R.L., BARRETT, R.J. & SANDERS-BUSH, E. (1990). Adaptation of brain 5-HT_2 receptors after mianserin treatment: receptor sensitivity, not receptor binding, more accurately correlates with behaviour. *J. Pharmacol. Exp. Ther.,* **254,** 484–488.

STAHL, S.M., KAISER, L., ROESCHEN, J., KEPPEL HESSELINK, J.M. & ORAZEM, J. (1998). Effectiveness of ipsapirone, a 5-HT-1A partial agonist, in major depressive disorder: support for the role of 5-HT-1A receptors in the mechanism of action of serotonergic antidepressants. *Int. J. Neurpsychopharmacol,* **1,** 11–18.

STOLTZ, J.F., MARSDEN, C.A. & MIDDLEMISS, D.N. (1983). Effect of chronic antidepressant treatment and subsequent withdrawal on [^{3}H]-5-hydroxytryptamine and [^{3}H]-spiperone binding in rat frontal cortex and serotonin receptor mediated behaviour. *Psychopharmacology,* **80,** 150–155.

TOME, M.B., ISAAC, M.T., HARTE, R. & HOLLAND, C. (1997). Paroxetine and pindolol: a randomized trial of serotonergic autoreceptor blockade in the reduction of antidepressant latency. *Int. Clin. Psychopharmacol.,* **12,** 81–89.

WILCOX, C.S., FERGUSON, J.M., DALE, J.L. & HEISER, J.F. (1996). A double-blind trial of low- and high-dose ranges of gepirone-ER compared with placebo in the treatment of depressed outpatients. *Psychopharmacol. Bull.,* **32,** 335–342.

YOCCA, F.D., EISON, A.S., HYSLOP, D.K., RYAN, E., TAYLOR, D.P. & GIANUTSOS, G. (1991). Unique modulation of central 5-HT_2 receptor binding sites and 5-HT_2 receptor-mediated behaviour by continuous gepirone treatment. *Life Sci.,* **49,** 1777–1785.

ZANARDI, R., FRANCINI, L., GASPERINI, M., PEREZ, J. & SMERALDI, E., (1998). Selective serotonin reuptake inhibitors alone and in association with pindolol in the treatment of delusional depression. *Eur. Neuropsycholpharmacol.,* **8,** (Suppl. 2), S98.

ZANARDI, R., ARTIGAS, F., FRANCHINI, L., SFORZINI, L., GASPERINI, M., SMERALDI, E. & PEREZ, J. (1997). How long pindolol should be associated to paroxetine to improve the antidepressant response? *J. Clin. Psychopharmacol.,* **17,** 446–450.

(Received May 6, 1998
Revised October 1, 1998
Accepted November 6, 1998)

British Journal of Pharmacology (1999) 126, 639–648
http://www.stockton-press.co.uk/bjp

N-substituted analogues of S-nitroso-*N*-acetyl-D,L-penicillamine: chemical stability and prolonged nitric oxide mediated vasodilatation in isolated rat femoral arteries

*,[1]I.L. Megson, [1]S. Morton, [2]I.R. Greig, [2]F.A. Mazzei, [2]R.A. Field, [2]A.R. Butler, [3]G. Caron, [3]A. Gasco, [3]R. Fruttero & [1]D.J. Webb

[1]Clinical Pharmacology Unit, University of Edinburgh, Western General Hospital, Edinburgh EH4 2XU; [2]School of Chemistry, University of St. Andrews, St. Andrews, Fife KY16 9ST; [3]Dipartimento di Scienza e Tecnologia del Farmaco, Universita degli Studi di Torino, Torino, Italy

1 Previous studies show that linking acetylated glucosamine to S-nitroso-*N*-acetyl-D,L-penicillamine (SNAP) stabilizes the molecule and causes it to elicit unusually prolonged vasodilator effects in endothelium-denuded, isolated rat femoral arteries. Here we studied the propanoyl (SNPP; 3 carbon side-chain), valeryl (SNVP; 5C) and heptanoyl (SNHP; 7C) N-substituted analogues of SNAP (2C), to further investigate other molecular characteristics that might influence chemical stability and duration of vascular action of S-nitrosothiols.

2 Spectrophotometric analysis revealed that SNVP was the most stable analogue in solution. Decomposition of all four compounds was accelerated by Cu(II) and cysteine, and neocuproine, a specific Cu(I) chelator, slowed decomposition of SNHP. Generation of NO from the compounds was confirmed by electrochemical detection at 37°C.

3 Bolus injections of SNAP (10 μl; 10^{-8}–10^{-3} M) into the perfusate of precontracted, isolated rat femoral arteries taken from adult male Wistar rats (400–500 g), caused concentration-dependent, transient vasodilatations irrespective of endothelial integrity. Equivalent vasodilatations induced by SNVP and SNHP were transient in endothelium-intact vessels but failed to recover to pre-injection pressures at moderate and high concentrations (10^{-6}–10^{-3} M) in those denuded of endothelium. This sustained effect (>1 h) was most prevalent with SNHP and was largely reversed by the NO scavenger, haemoglobin.

4 We suggest that increased lipophilicity of SNAP analogues with longer sidechains facilitates their retention by endothelium-denuded vessels; subsequent slow decomposition within the tissue generates sufficient NO to cause prolonged vasodilatation. This is a potentially useful characteristic for targeting NO delivery to areas of endothelial damage.

Keywords: Nitric oxide; S-nitrosothiols; vasodilatation; SNAP analogues

Abbreviations: ACh, acetylcholine; ANOVA, analysis of variance; Cys, cysteine; EDHF, endothelium-derived hyperpolarizing factor; Hb, ferrohaemoglobin; GTN, glyceryl trinitrate; T½, half-life; NCu, neocuproine; NO, nitric oxide; SNP, sodium nitroprusside; SNAP, S-nitroso-*N*-acetyl-D,L-penicillamine; SNHP, S-nitroso-*N*-heptanoyl-D,L-penicillamine; SNPP, S-nitroso-*N*-propanoyl-D,L-penicillamine; SNVP, S-nitroso-*N*-valeryl-D,L-penicillamine; P, partition coefficient; PTCA, percutaneous transluminal coronary angioplasty; PE, phenylephrine

Introduction

Nitric oxide (NO) synthesized in the endothelium of blood vessels (Palmer *et al*., 1987; 1988; Palmer & Moncada, 1989) is recognized to be an important factor in control of local blood flow and of blood pressure in animals (Aisaka *et al*., 1989; Rees *et al*., 1989; Gardiner *et al*., 1990; Chu *et al*., 1991) and man (Vallance *et al*., 1989; Haynes *et al*., 1993). In addition, NO is known to inhibit platelet adhesion and aggregation (Radomski *et al*., 1987a,b; 1990), smooth muscle mitogenesis (Garg & Hassid, 1989) and monocyte adhesion (Lefer, 1997). Endothelial dysfunction resulting in reduced NO synthesis is thought to play an important role in atherogenesis (Chappell *et al*., 1987; Harrison *et al*., 1987; Forstermann *et al*., 1988; Guerra *et al*., 1989), and physical damage to the endothelium during percutaneous transluminal coronary angioplasty (PTCA) is a major contributory factor in the high incidence of thrombus formation and restenosis following this procedure (Langford *et al*., 1994). Current NO donor drugs, including the organic nitrates (such as glyceryl trinitrate; GTN) and sodium nitroprusside (SNP) do not improve outcome in patients with unstable angina or myocardial infarction or following PTCA.

S-Nitrosothiols (general formula R-S-N=O) undergo thermal decomposition in solution to disulphides, generating NO in the process (Williams, 1985). They present a potential alternative to existing NO donors, particularly as they do not appear to engender vascular tolerance (Harowitz *et al*., 1983; Bauer & Fung, 1991), an undesirable feature of prolonged administration of organic nitrates. Other potential advantages over current NO donors are their relative platelet (De Belder *et al*., 1994) and arterial selectivity (MacAllister *et al*., 1995) which might make them particularly attractive in the treatment of thrombotic and arterial disease. However, the therapeutic potential of the investigated S-nitrosothiols, such as S-nitroso-*N*-acetyl-D,L-penicillamine (SNAP; Figure 1a) and S-nitrosoglutathione (GSNO), is limited by the unpredictable nature of their decomposition, due in part to the catalytic effect of trace Cu(I) ions (Dicks *et al*., 1996; Gordge *et al*., 1996; Al-Sa'doni

* Author for correspondence; E-mail: ian.megson@ed.ac.uk

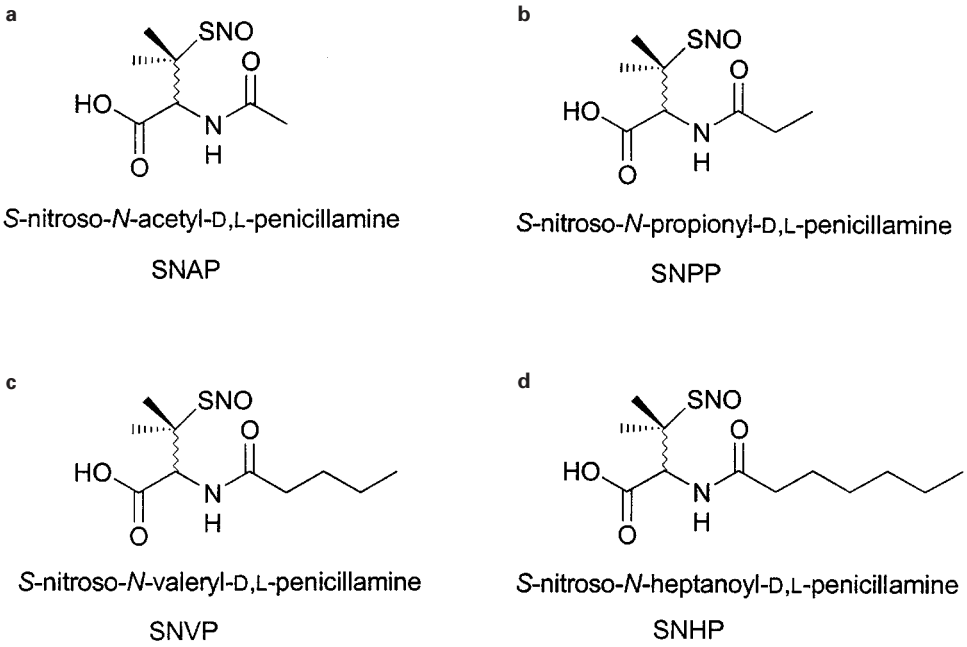

Figure 1 Structural formulae and full generic names for (a) SNAP, (b) SNPP, (c) SNVP and (d) SNHP.

et al., 1997). Accelerated decomposition in the presence of Cu(II) (De Man *et al*., 1996) is now thought to be mediated by prior reduction to Cu(I) by thiols and might contribute to copper-mediated inhibition of atherogenesis (Ferns *et al*., 1997). *In vivo*, decomposition may also be accelerated by direct transfer of NO^+ to reduced tissue thiols (transnitrosation; Askew *et al*., 1995) and by enzyme-dependent mechanisms (Askew *et al*., 1995; Gordge *et al*., 1996). Therapeutic effects of existing S-nitrosothiols might be improved by increasing their stability *in vitro* and by introducing a means of targeting delivery to damaged vessels deprived of endogenous NO.

Recently, we reported that a novel S-nitrosated glyco-amino acid, consisting of SNAP coupled to acetylated glucosamine (RIG200), was substantially more stable than the parent compound *in vitro*. Furthermore, we showed that it caused prolonged (>4 h), NO-mediated vasodilatation in endothelium-denuded rat isolated femoral arteries, whilst responses to SNAP itself were transient (Megson *et al*., 1997). Both RIG200 and SNAP caused transient vasodilatation in endothelium-intact vessels. We speculated that removal of the endothelium facilitates retention of RIG200 and suggested that lipophilicity of the compound by the acetylated glucosamine might be responsible for the effect. Here, we further test our hypothesis using novel N-substituted analogues of SNAP synthesized with different carbon side-chain lengths (C3–7; Figure 1b,c and d). We envisaged that increasing alkyl side-chain length would increase lipophilicity and *in vitro* stability. We also anticipated that SNAP analogues with longer side-chains would be more likely to cause sustained vasodilatation in endothelium-denuded vessels, similar to RIG200. Selectivity for endothelium-denuded vessels could lead to targeting of NO donors to vessels with endothelial injury caused by atherosclerosis or surgical procedures such as PTCA.

Methods

Decomposition of SNAP analogues in vitro

2.5 mM solutions of SNAP and RIG200 in oxygenated (95% O_2, 5% CO_2) Krebs buffer (composition in mM): NaCl 118, KCl 4.7, $CaCl_2$ 2.5, $MgSO_4$ 1.2, KH_2PO_4 1.2, $NaHCO_3$ 25 and glucose 5.5, were incubated in the dark at 24°C. Care was taken to use the same Krebs solution to dilute SNAP and its analogues in order to ensure identical copper ion content. The decrease in absorbance at a wavelength (λ) of 341 nm was measured using a Phillips PU 8720 ultraviolet/visible scanning spectrophotometer (path length = 1 cm).

Experiments at 24°C were repeated in the presence of either an intermediate concentration of $CuSO_4$ (1 μM; Askew *et al*., 1995), or the specific Cu(I) chelator, neocuproine (NCu; 1 μM; (Dicks *et al*., 1996; Al Sa'doni *et al*., 1997) in order to establish the effect of Cu(I) on the decomposition rate. Decomposition was also compared in the presence of the reduced thiol, cysteine (Cys; 1 mM). Rate constants were derived according to the following equation:

$$k = \frac{Ln2}{T\frac{1}{2}}$$

where T ½ = the observed half-life of S-nitrosothiols in solution.

NO release from S-nitrosothiols (10^{-5} M) in Krebs buffer solution at 37°C was confirmed using an isolated NO electrode (World Precision Instruments, Aston, Hertfordshire, U.K.). The electrode was calibrated with NO generated *in situ* from $NaNO_2$ (10^{-7}–10^{-6} M) acidified in ascorbic acid (1 mM). The role of Cu(I) and reduced thiols in decomposition was assessed using $CuSO_4$ (1 μM), NCu (10 μM) and Cys (10 μM).

Ionization constants and lipophilicity parameters in n-octanol/water of N-substituted analogues of SNAP

The pH-metric method (Avdeef, 1993) was used to measure the ionization constant (pK_a) and the logarithm of the partition coefficient in *n*-octanol/water of the neutral form of SNAP and SNVP ($\log P^N$). The method is based on the principle that there is a shift in the aqueous acid-base titration curve of a protogenic substance when a second phase (namely *n*-octanol) is added (Figure 2). The technique requires two successive titrations; first, the solute in water is titrated against standard acid or base to deduce the ionization constant (pK_a). The titration is then repeated in the presence of *n*-octanol and a new ionization constant p_0K_a is determined. The shift in the

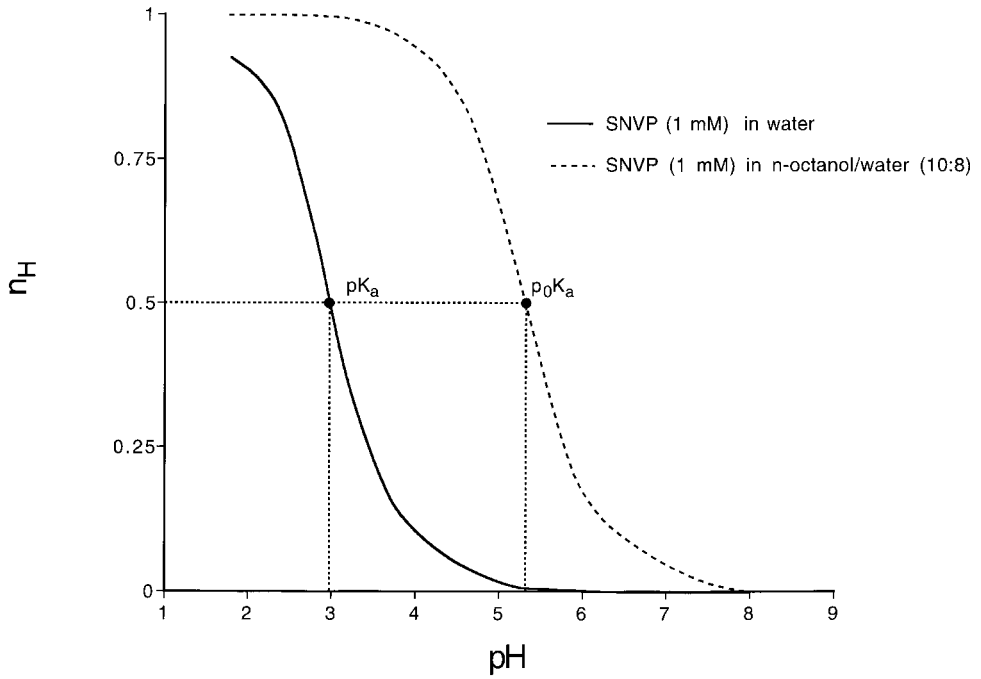

Figure 2 Difference (Bjerrum) plots for SNVP (1 mM) in water and in *n*-octanol/water (10 : 8; both $n=4$) where n_H is the proportion of SNVP that is not ionised. These pK_a values were used to derive the partition coefficient (log P^N) for SNVP. Similar experiments were carried out for SNAP and results are presented in Table 2.

ionization constant is in response to the partitioning of some of the substance into the organic phase. This shift in pK_a for a generic acid (HA) is used in the calculation of P^N as shown in the following equation:

$$P^N_{HA} = \frac{(10^{(p_0K_a - pK_a)} - 1)}{r}$$

where r is the ratio of *n*-octanol to water.

All potentiometric titrations were performed using GLpKa apparatus (Sirius Analytical Instruments Ltd, Forrest Row, East Sussex, U.K.).

For the determination of the pK_a of SNAP and SNVP, 15 ml aqueous solutions ($n=4$) were initially acidified to pH 1.8 with HCl. The solutions were then titrated under nitrogen at $25.0 \pm 0.1^\circ$C with standardized KOH to pH 8. pK_a values were obtained by difference (Bjerrum) plots (Figure 2) and the values obtained were refined by a weighted nonlinear least-squares procedure.

For the experimental determination of log P^N, titrations of SNAP and SNVP (1 mM), containing volumes of *n*-octanol (1 ml organic solvent/15 ml water to 10 ml organic solvent/8 ml water) were performed in the pH range 1.8–8.0 ($n=4$). The same conditions and calculation procedures used for the determination of pK_a values were adopted. The pH-metric approach does not permit measurement of log P lower than -0.5, thus the log P of the anionic species (log P^A) could not be experimentally determined.

The experimental log P^N value for SNAP (0.96) was used to calculate the corresponding values for the other SNAP analogues by a Rekker type approach (Avdeef, 1993; Mannhold *et al*., 1995; Caron *et al*., 1997).

Biological activity

Preparation Experiments were performed on isolated segments of femoral artery from adult male Wistar rats (400–500 g; $n=36$) using the perfusion technique described previously (Flitney *et al*., 1992; Megson *et al*., 1997). Briefly, animals were sacrificed by cervical dislocation and both femoral arteries were cannulated immediately distal to the epigastric arterial branch. Arterial segments (7–8 mm long) were dissected free and transferred to perspex organ bath chambers (1 ml volume) at 37°C where they were perfused (0.6 ml min^{-1}; Gilson minipuls 3, Anachem, Luton, U.K.) and superfused (1 ml min^{-1}; Watson Marlow 302S; Watson Marlow, Falmouth, U.K.) with fresh oxygenated Krebs buffer solution. Twin vessels were precontracted with phenylephrine (PE) and perfusion pressure was monitored by a differential pressure transducer (T; Sensym SCX 15ANC, Farnell Electronic Components, Leeds, U.K.) located upstream.

The apparatus permits exclusive drug delivery to the luminal surface of the vessel by bolus injection (10 μl) through a resealable rubber septum into the perfusate immediately upstream of the vessel (transit time to artery $\sim$3 s, through lumen $\sim$300 ms). Injections of vehicle (Krebs buffer) had no effect on perfusion pressure. Vasodilator responses in control vessels could be compared to those perfused with supramaximal concentrations of the recognized NO scavenger, ferrohaemoglobin (Martin *et al*., 1985). Where possible, two vessels from each animal were used in parallel; one being denuded of endothelium, the other with endothelium intact.

Experimental protocols

All experiments were carried out in a darkened laboratory in order to protect photolabile drugs and to prevent photorelaxation of vessels (Megson *et al*., 1995). Drugs were dissolved and diluted in PE-containing Krebs solution and kept on ice prior to use.

Endothelial function of precontracted arteries was assessed using ferrohaemoglobin (Hb; 10 μM); Hb scavenges endogenous NO and the resultant vasoconstriction is a measure of basal NO activity. This technique was preferred to cholinergic, endothelium-dependent relaxation because, in this perfusion system, the endothelium is already highly stimulated to produce NO by flow, and responses to cholinergic stimuli are,

as a result, typically small (Flitney *et al*., 1992; Megson *et al*., 1997). In addition, a significant proportion of ACh-induced vasodilatation is believed to be due to release of endothelium-derived hyperpolarizing factor (EDHF; Cohen & Vanhoutte, 1995). In experiments where the endothelium was removed, air was passed through the lumen until such time as the vessel was unresponsive to Hb (5–10 min). Denudation invariably caused an increase in pressure due to loss of endothelium-derived NO. Pressure was restored to its original level by appropriate reduction in PE concentration ($\sim 0.5 \times$ original concentration). Selected vessels were taken for immunohistochemical staining to confirm endothelial denudation (5 μm paraffin sections, fixed in formalin (10%; 24 h), treated with biotinylated constitutive NO synthase antibodies coupled to avidin (avidin-biotin complex) and visualized ($n=8$ endothelium-denuded; $n=8$ endothelium-intact).

Vasodilator responses to bolus injections of SNAP and its analogues

Bolus injections of increasing concentrations of SNAP, SNPP, SNVP or SNHP (10 μl; 10^{-8}–10^{-3} M) were made sequentially into the perfusate of precontracted, endothelium-intact or -denuded vessels. Responses were deemed to have recovered once pressure was maintained for more than 5 min. Time intervals between injections of S-nitrosothiol were matched between intact and denuded vessels for each individual experiment. Responses to 10^{-3} M concentrations were allowed to recover for a period of 1 h, after which vessels were perfused with Hb (10 μM). In order to assess the role of extracellular NO in vasodilatation induced by SNAP and its N-substituted analogues in endothelium-denuded vessels, sequential bolus injections of S-nitrosothiols were also made into perfusate containing Hb (10 μM).

Drugs and reagents

All chemicals except the S-nitrosothiols were obtained from Sigma Ltd. (Poole, Dorset, U.K.). Met-Hb was reduced to the ferro-form using sodium dithionite as described previously (Martin *et al*., 1985).

SNAP was prepared using an established method (Field *et al*., 1978). Ultraviolet/visible spectral analysis confirmed an absorption peak at $\lambda = 341$ nm, characteristic for S-nitrosothiols. The extinction coefficient (ε) at this wavelength was 1168 $M^{-1}\,cm^{-1}$. SNAP is soluble in Krebs buffer at concentrations up to 10 mM. The N-substituted analogues of SNAP were synthesized by the acylation of D,L-penicillamine followed by S-nitrosation (details will be published elsewhere). All were soluble to concentrations up to 2.5 mM after ultrasonication.

Analysis of results

Signals from the pressure transducers were processed by a MacLab/4e analogue-digital converter and displayed through 'Chart' software (AD Instruments, Sussex, U.K.) on a Macintosh Performa 630 microcomputer. Vasodilator response amplitude was expressed as a percentage of PE-induced pressure existing prior to the first in a series of drug application (percentage pressure change; negative values represent relaxation, positive represent constriction). Data are given for percentage pressure change both at the peak of responses and following response recovery as defined earlier. Mean values are given $\pm$ s.e.mean.

P values stated in the text were obtained using two-factor, repeated dose ANOVAs except where otherwise specified. $P<0.05$ was accepted as statistically significant.

Results

Decomposition of SNAP analogues in vitro

Rate constants derived from spectrophotometric studies of decomposition indicated that SNAP was the most stable of the analogues in Krebs buffer alone at 24°C (Table 1). The rate of SNAP and SNPP decomposition was noticeably more variable than SNVP and SNHP. SNVP proved the most stable in Krebs buffer; decomposition was <1% in 1 h, preventing calculation of a rate constant.

Decomposition of all four analogues was accelerated by Cu^{2+} (1 μM; Table 1). SNAP decomposition in the presence of Cu^{2+} was significantly faster than that of the other S-nitrosothiols ($P<0.05$; unpaired student's *t*-test). Interestingly, SNVP decomposition under these conditions stopped after $\sim$30 min, when the concentration reached 78.01 $\pm$ 4.78 of its initial value, preventing determination of a meaningful rate constant. Only the rate of decomposition of SNHP was significantly inhibited by NCu (10 μM; Table 1; $P<0.05$), although the variabilty seen with SNAP and SNPP in Krebs alone was not evident in the presence of NCu.

Cys (1 mM) accelerated decomposition of all four analogues and the rate of decomposition in the presence of Cys was not significantly different between the analogues (Table 1).

Generation of NO from the decomposition of SNAP and its analogues (10 μM) was confirmed at 37°C using an isolated

Table 1 Rate constants for N-substituted analogues of SNAP in Krebs buffer alone (control) and in the presence of NCu (10 μM), $CuSO_4$ (1 μM) and Cys (1 mM)

	Rate Constant			
	Control ($\times 10^{-3}$ min^{-1})	*+NCu* ($\times 10^{-3}$ min^{-1})	*+$CuSO_4$* ($\times 10^{-3}$ min^{-1})	*+Cys* ($\times 10^{-3}$ min^{-1})
SNAP	14.7 $\pm$ 2.7	12.7 $\pm$ 0.6	81.1 $\pm$ 17.2	13.9 $\pm$ 3.8
SNPP	12.2 $\pm$ 6.6	9.3 $\pm$ 0.7	31.7 $\pm$ 7.3**	12.9 $\pm$ 5.6
SNVP	–[a]	–[a]	–[b]	18.7 $\pm$ 2.9
SNHP	4.9 $\pm$ 1.0***	2.4 $\pm$ 0.5*	27.6 $\pm$ 5.2**	19.3 $\pm$ 4.4

Results are expressed as means $\pm$ s.e.mean ($n=5$) in 2.5 mM solutions of S-nitrosothiols at 24°C. [a]Insufficient decomposition of SNVP in Krebs alone and Krebs + NCu occurred within 1 h (<1%) to derive rate constants. [b]Decomposition of SNVP in Krebs + $CuSO_4$ was accelerated initially but stopped after $\sim$30 min when the concentration had fallen to 78.01 $\pm$ 4.78%, preventing calculation of a meaningful rate constant. *$P<0.05$; **$P<0.01$ for N-substituted analogues compared to SNAP values recorded under equivalent conditions (unpaired Student's *t*-test).

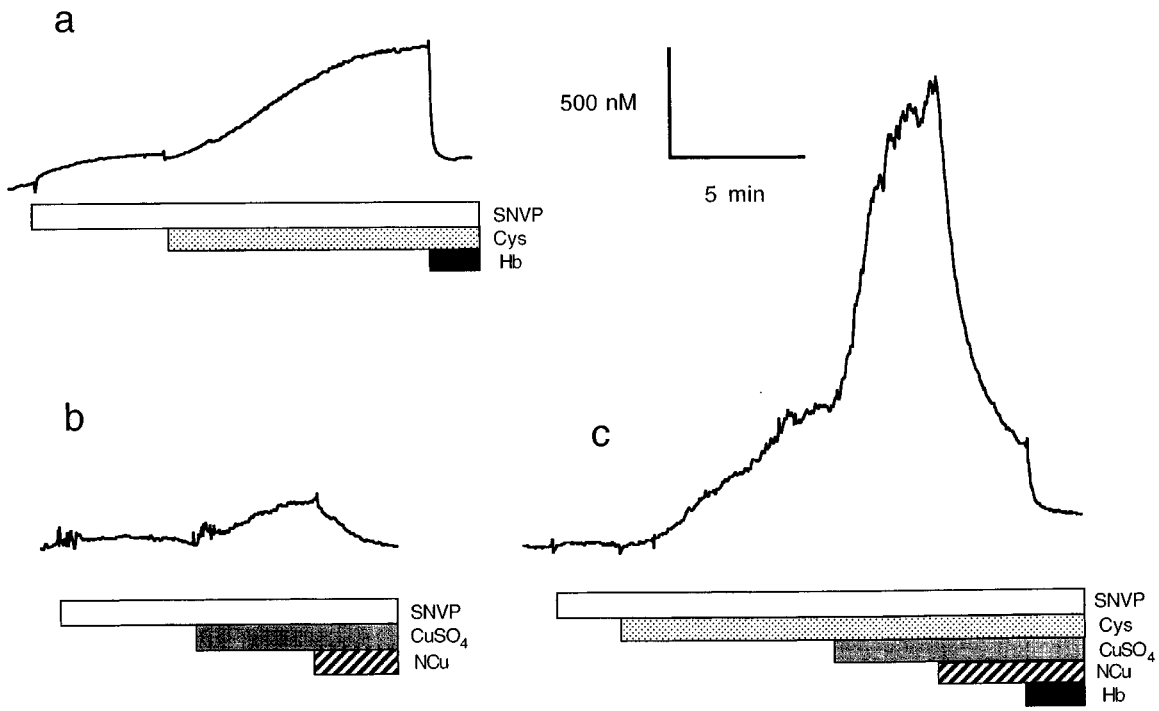

Figure 3 Representative trace for NO concentration detected in solutions of SNVP (10 μM) in saline at 37°C, using an isolated NO electrode. Cys (10 μM; a, c), $CuSO_4$ (1 μM; b, c), NCu (10 μM; b, c) and Hb (10 μM; a, c) were added to the solution as indicated by the horizontal bars.

Table 2 Effect of $CuSO_4$ (1 μM), Cys (10 μM) or both $CuSO_4$ and Cys on maximum NO concentrations measured in 10 μM solutions of SNAP analogues in Krebs buffer

	NO Concentrations			
Compound	*In Krebs buffer* (nM)	*In Krebs + $CuSO_4$* (nM)	*In Krebs + Cys* (nM)	*In Krebs + $CuSO_4$ and Cys* (nM)
SNAP	343.3 ± 171.6	867.7 ± 485.7	1287.9 ± 264.9	1870.9 ± 417.6
SNPP	58.0 ± 13.9*	144.5 ± 88.5*	842.3 ± 328.2	2097.1 ± 914.2
SNVP	30.0 ± 18.9**	389.1 ± 168.4*	682.6 ± 158.1	1780.2 ± 302.1
SNHP	248.9 ± 92.4	623.0 ± 121.0	1029.7 ± 345.8	1749.5 ± 463.0

Results are expressed as means ± s.e.mean ($n = 5$ for each). *$P < 0.05$; **$P < 0.01$ for N-substituted analogues compared to SNAP values recorded under equivalent conditions (unpaired Student's t-test).

NO electrode. The results largely support the spectrophotometric data in that SNAP generates NO significantly more rapidly than the other analogues and that NO generation is accelerated by addition of Cu^{2+} or Cys (results for SNVP are illustrated in Figure 3; similar experiments with other analogues are summarized in Table 2). Addition of Cu^{2+} and Cys together greatly accelerated decomposition; NO generation reached a peak value of $\sim 1.5-2.5$ μM after 2 min (Figure 3c). Addition of an excess of NCu (10 μM) in experiments involving Cu^{2+} reversed the Cu-mediated accelerated NO release (Figure 3b) but did not affect NO generated spontaneously or in the presence of Cys. Addition of Hb (10 μM) at any point during experiments caused a rapid (< 1 min) fall in NO concentration to levels at or near zero (Figure 3a and c).

Biological activity

Vessel parameters Vessels were pre-contracted to pressures of 101.2 ± 3.7 mmHg with PE (7.89 ± 0.52 μM; $n = 68$). Pressure in endothelium intact vessels increased by 78.1 ± 9.0% ($n = 32$; $P < 0.001$; unpaired student's t-test) on perfusion with Hb (10 μM). Pressure in denuded vessels failed to increase significantly above pre-contraction levels on perfusion with Hb (+1.2 ± 3.8%; $n = 36$).

Vasodilator responses in endothelium-intact vessels Bolus microinjections of all four S-nitrosothiols caused dose-dependent vasodilatation in endothelium-intact arteries (Figures 4 and 5a). PD_2 values were calculated as 5.83 ± 0.17 (SNAP; $n = 8$), 5.74 ± 0.39 (SNPP; $n = 8$), 5.09 ± 0.31 (SNVP; $n = 8$) and 5.66 ± 0.23 (SNHP; $n = 8$). There was no significant difference between responses ($P > 0.05$, ANOVA) or PD_2 values ($P > 0.05$, Student's t-test) for these compounds. Vasodilator responses to S-nitrosothiols recovered to or above pre-injection pressures at all but the highest injected concentration (Figures 4a and 6a). Responses to 10^{-3} M bolus injections of SNPP and SNHP failed to recover fully after washout. Perfusion with Hb 1 h after washout of 10^{-3} M bolus injections of SNAP analogues caused perfusion pressure to rise significantly above pre-injection pressure (Figure 4a; +71.7 ± 14.5% after SNAP, $n = 8$; +57.3 ± 7.1% for SNPP, $n = 8$; +51.9 ± 7.5% for SNVP, $n = 8$ and +49.0 ± 16.9% for SNHP; $n = 8$).

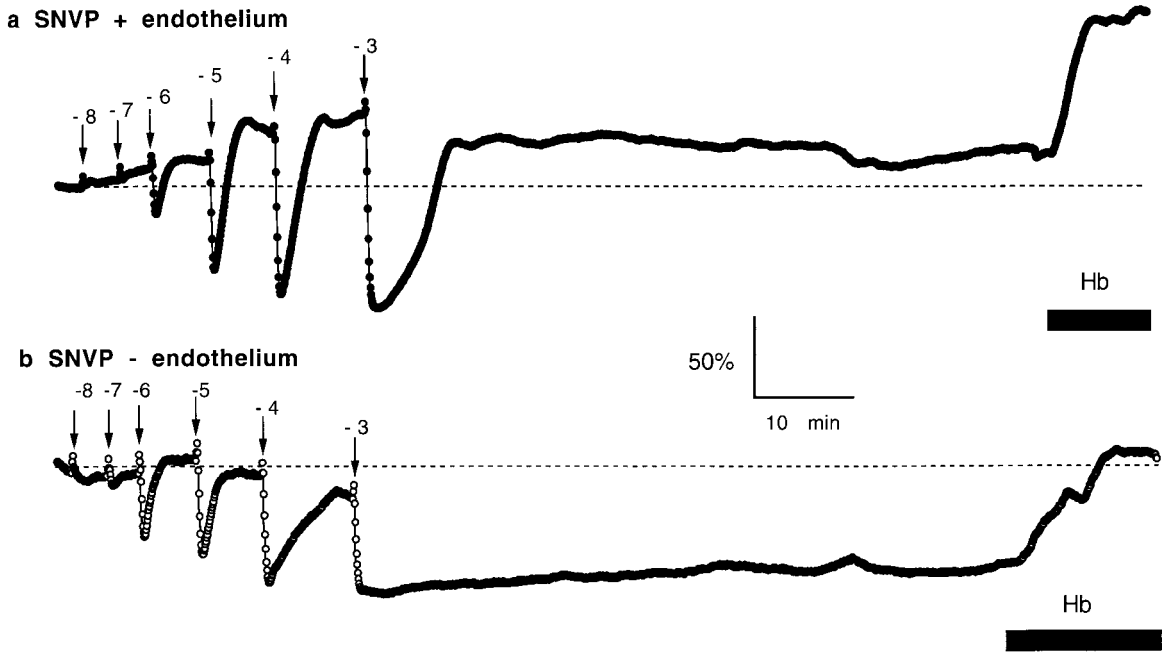

Figure 4 Representative pressure recordings of vasodilatations elicited by sequential bolus injections (10 μl) of SNVP (log M concentrations as indicated) in (a) endothelium-intact and (b) endothelium-denuded rat femoral arteries. Perfusion with 10 μM Hb is indicated by the horizontal bar.

Vasodilator responses in endothelium-denuded vessels Peak amplitude of responses to SNVP and SNHP compounds was significantly enhanced in endothelium-denuded vessels compared to intact vessels ($P<0.01$ and $P<0.05$ respectively, $n=8$ for both compounds) but not for SNAP and SNPP ($P>0.05$). The extent to which SNAP and SNPP responses recovered following bolus injections was not different in endothelium denuded vessels compared with intact vessels (Figure 6b; $P>0.05$ for both compounds). However, in denuded vessels, responses to SNVP and SNHP were sustained at concentrations $>10^{-6}$ M (Figure 6b; $P<0.01$ for both compounds). Sustained vasodilatation was clearly related to the length of the N-substituted side-chain, and was most pronounced with SNHP. Sustained responses were largely reversed by Hb to $99.0\pm7.1\%$ of pre-injection pressure following SNAP; $82.6\pm7.2\%$ following SNPP; $94.2\pm7.9\%$ following SNVP and $81.6\pm7.0\%$ following SNHP ($n=8$ for all four compounds).

Inhibition of responses in endothelium-denuded vessels by Hb Vasodilator responses in endothelium-denuded vessels during perfusion with Hb (10 μM) were significantly attenuated (Figure 5c; $P<0.05$, $n=7$ for all four compounds) and recovered to, or above, pre-injection levels (Figure 6c) with all four analogues; sustained vasodilatation was not evident in Hb-perfused vessels.

Lipophilicity and sustained vasodilatation

Excellent agreement was achieved between experimental and calculated values for SNVP (2.53 and 2.47 ± 0.022 respectively), confirming the validity of the Rekker-type approach for determining partition coefficients and demonstrates the lack of intramolecular effects in this series of S-nitrosothiols. Ionization constants do not vary significantly from shorter to longer molecules, thus all the derivatives have the same degree of ionization and are 99.9% ionized at physiological pH. The log P of the anionic species (log P^A) is generally assumed to be three orders of magnitude lower than log P^N (Avdeef, 1996). In addition, according to their chemical structures, it is reasonable to assume that the anionic forms are not affected by any intramolecular effects, thus their logarithm of partion coefficient (log P^A) are linearly correlated with log P^N (Fruttero *et al*., 1998) which can be used as the general lipophilicity descriptors for SNAP and its derivatives.

A logarithmic plot of calculated values for P^N against response recovery following a bolus injection (10^{-3} M) for each of the S-nitrosothiols (Figure 7), shows a linear correlation ($r^2=0.998$), suggesting that lipophilicity (Testa *et al*., 1996) might be an important factor in determining the degree of sustained vasodilatation exhibited by this group of compounds.

Discussion

Our results show that the N-substituted chain length of SNAP analogues is an important determinant of the rate of decomposition of the compounds in solution, their lipophilicity, and their ability to cause sustained vasodilatation in endothelium-denuded isolated rat femoral arteries.

Increasing the length of the alkyl sidechain of SNAP clearly affected *in vitro* stability (Table 1), with SNVP proving the least prone to decomposition. The stability of S-nitrosothiols is affected by steric factors as it involves the dimerization of two thiyl radicals ($RS^{\bullet}$, Bainbrigge *et al*., 1997) and it is apparent that this process is most effectively retarded by a 5C side chain. Decomposition of SNAP, SNPP, and SNHP were greatly accelerated in the presence of Cu^{2+}, as would be predicted from previous observations (De Man *et al*., 1996; Dicks *et al*., 1996; Gordge *et al*., 1996; Al-Sa'doni *et al*., 1997). However, SNVP decomposition, though accelerated initially, stopped when the concentration reached $\sim80\%$ of its original value. The reason for this apparent resistance of SNVP to Cu-mediated decomposition is unknown but it may involve chelation of Cu ions by the resulting disulphide, in a process

similar to that reported previously for GSNO (Swift, 1989). NCu significantly inhibited decomposition of SNHP and greatly reduced the variability in decompostion seen with SNAP and SNPP in Krebs buffer alone (Table 1). This result suggests that sufficient trace Cu(I) in Krebs buffer exists to accelerate SNHP decomposition, and that changing Cu(I) levels from day-to-day are responsible for inconsistencies in SNAP and SNPP decomposition. Interestingly, the exquisite sensitivity of SNAP to trace Cu(I) is not apparently shared by SNVP, again implying that the valeryl sidechain imparts resistance to Cu(I) catalysis.

The rate of decomposition of SNAP analogues was accelerated by Cys and, interestingly, decomposition of all four compounds in the presence of Cys occurred at similar rates (Table 1). This observation might help to explain why S-nitrosothiols with widely varying thermal stabilities *in vitro* have similar biological properties, and suggests that transnitrosation to Cys might be a key mechanism for decomposition *in vivo*.

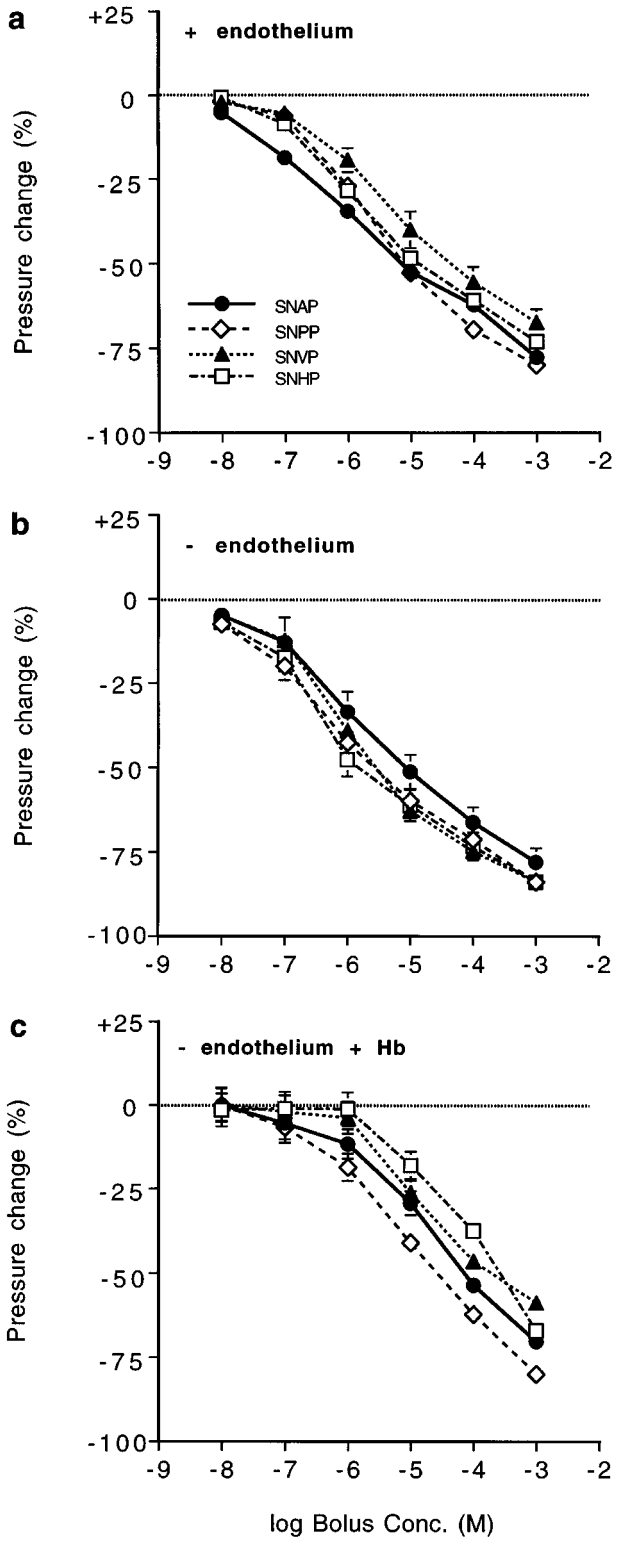

Figure 5 Concentration-response curves for peak amplitude of responses to bolus injections (10 μl) of N-substituted S-nitrosothiols into the perfusate of (a) endothelium-intact vessels, (b) endothelium-denuded vessels and (c) endothelium-denuded vessels perfused with 10 μM Hb ($n=8$ for all compounds under each condition). There was no statistical significant difference between responses to any of the SNAP analogues in either (a) or (b) ($P>0.05$; repeated dose, 2 factor ANOVAs). Responses to SNVP and SNHP, but not the other analogues, were significantly enhanced in (b) compared to (a) and responses to all four analogues were significantly inhibited by Hb (c; $P<0.05$).

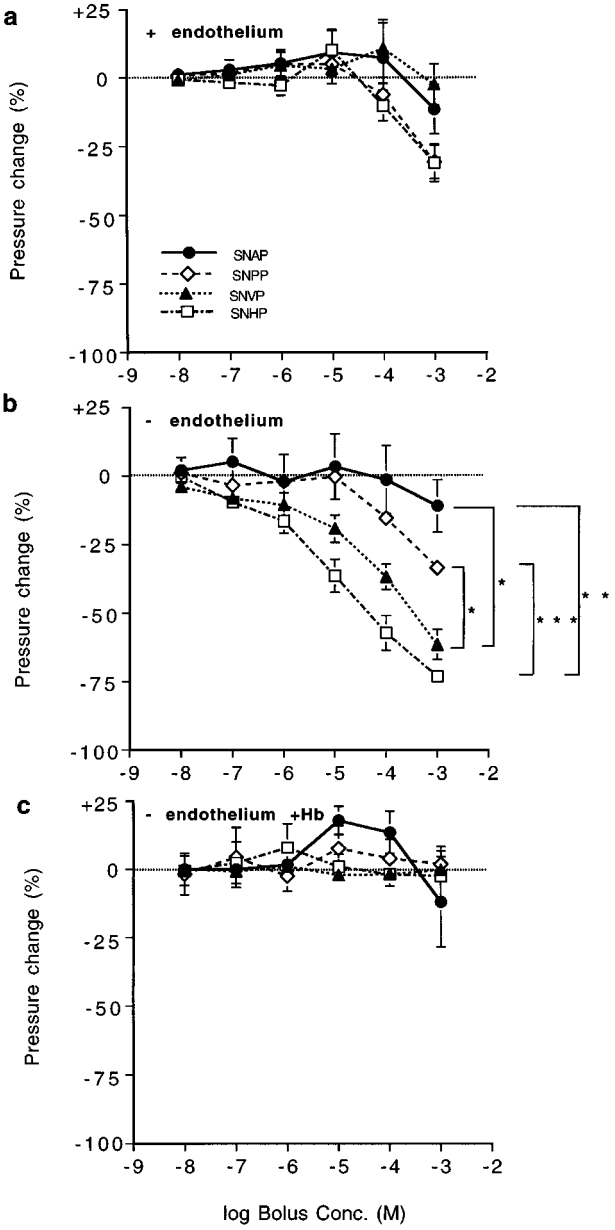

Figure 6 Concentration-recovery curves (means$\pm$s.e.mean) for bolus injections (10 μl) of N-substituted S-nitrosothiols into the perfusate of (a) endothelium-intact vessels, (b) endothelium denuded vessels and (c) endothelium-denuded vessels perfused with 10 μM Hb ($n=8$ for all compounds under each condition). Significant differences in (b) are as shown (*$P<0.05$, **$P<0.01$, ***$P<0.001$). Responses to the four analogues were not significantly different from each other in (a) and (c; $P>0.05$; repeated dose, 2 factor ANOVAs).

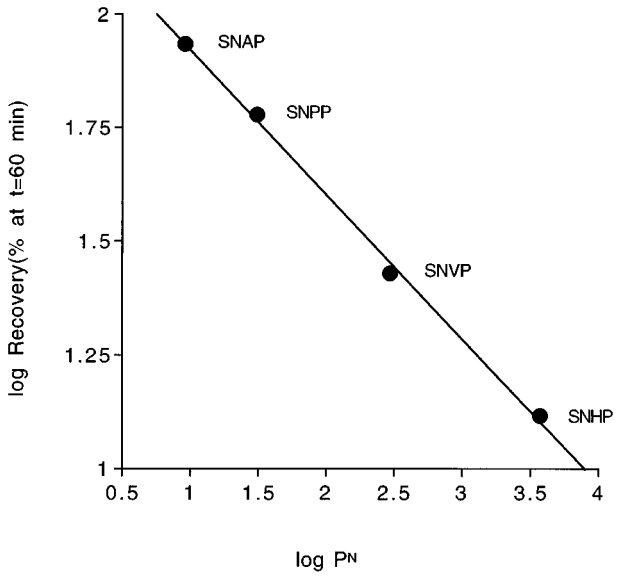

Figure 7 Logarithmic plot of partition coefficient (P^N) of N-substituted analogues of SNAP against response recovery to bolus injections of compounds (10 μl; 10^{-3} M). Recovery is expressed as the pressure attained at $t=60$ min after bolus washout as a percentage of pre-injection pressure ($n=8$). The relationship is linear, with a correlation coefficient (r^2) of 0.998.

SNVP, of all the compounds, generated NO most slowly in Krebs buffer alone (Table 2), as predicted by spectrophotometric studies. Accelerated NO generation in the presence of either Cu^{2+} or Cys (Figure 3a and b) reflected Cu^{+}-mediated catalysis and transnitrosation respectively. We propose that the markedly accelerated NO generation seen in the presence of both Cys and Cu^{2+} (Figure 3 and Table 2) is due to Cys-mediated reduction of Cu^{2+} to Cu^{+}, facilitating Cu^{+}-mediated catalysis of S-nitrosothiol decomposition. This, added to transnitrosation from SNAP analogues to Cys, forming unstable S-nitrosocysteine, would explain the rapid release of NO under these conditions. The results indicate that in the presence of Cys, different SNAP analogues generate similar amounts of NO, perhaps explaining comparable biological effects.

Vasodilator responses to bolus injections of SNAP analogues The lack of discrimination of arteries to bolus injections of SNAP and its analogues (Figure 5a), despite large variations in thermal stability (Table 1), lends weight to the argument that S-nitrosothiol decomposition in vascular tissue is accelerated by a process common to all of these compounds. In general, responses to all four compounds were transient in intact vessels (Figures 4 and 6), with only responses to the highest dose on occasion failing to recover fully to pre-injection pressure (Figure 6a). The rebound contraction sometimes seen in endothelium intact vessels following bolus injections (Figure 4a) were similar to those seen with RIG200 (Megson *et al*., 1997); an effect that might be due to desensitization of vessels to endothelium-derived NO following delivery of exogenous NO. Hb-mediated vasoconstriction at the end of experiments reflected scavenging of endothelium-derived NO and confirmed the endothelial integrity of the vessels (Figure 4a).

Peak amplitudes of vasodilator responses to SNVP and SNHP were significantly increased in endothelium-denuded vessels (Figure 5b), perhaps reflecting hypersensitivity of vessels to exogenous NO once deprived of endothelium-derived NO (Moncada *et al*., 1991). However, these two analogues were also the ones that caused sustained vasodilatation in endothelium-denuded vessels (Figure 6b), suggesting that the apparent increase in peak amplitude of responses might be due to the falling perfusion pressure caused by the sustained effects of preceding injections, rather than to hypersensitivity (Figures 4b and 6b). The prolonged responses to moderate and high concentrations ($10^{-6}-10^{-3}$ M) of SNVP and SNHP (Figure 6b), which lasted for >1 h after washout, were largely reversed by Hb and were therefore predominently NO-mediated (Figure 4b). Some vessels ($n=5/16$) still had reduced tone ($<17\%$) even during Hb perfusion, perhaps suggesting an alternative mechanism for sustained vasodilatation, involving either NO from a source inaccessible to Hb, or an NO-independent mechanism. However, this possibility is not supported by evidence from our other experiments in which vasodilatations in response to S-nitrosothiols in endothelium-denuded vessels during Hb perfusion, invariably recovered to pre-injection pressure (Figure 6c). The peak amplitude of responses in endothelium-denuded vessels to all four compounds was significantly inhibited by perfused Hb (Figure 5c), implying that the transient element of responses is, at least in part, due to NO released at a site accessible to intraluminal Hb.

The precise mechanism by which some S-nitrosothiols cause sustained vasodilatation clearly requires further investigation but our studies suggest that the effect is correlated to lipid solubility (Figure 7). We hypothesize that sustained vasodilatation is due to retention of lipophilic S-nitrosothiols in lipid-rich compartments of sub-endothelial layers of denuded arteries. Retained compounds decompose slowly to release NO which causes dilatation of vessels for >1 h after bolus washout. Penetration of compounds is sufficiently shallow to facilitate scavenging of NO by intraluminal Hb, which does not penetrate the basement membrane of arteries (Hongo *et al*., 1988).

These properties require confirmation in human vessels and ultimately *in vivo*, but S-nitrosothiols that cause prolonged vasodilatation specifically in vessels with endothelial injury could be beneficial following PTCA, particularly if they prove to have anti-mitogenic properties and inhibitory effects on platelet aggregation. S-nitrosothiols could also be useful in the treatment of atherosclerosis where compounds might not only be selectively retained in areas of endothelial damage but, in light of their lipophilicity, also in regions of lipid deposition.

We acknowledge support from the BHF (Junior Research Fellowship to ILM; FS/95061), from the Rollo Trust (St Andrews) and from MURST (Torino). Professor D.J. Webb is supported by a Research Leave Fellowship from the Wellcome Trust (WT0526330).

References

AISAKA, K., GROSS, S.S., GRIFFITH, O.W. & LEVI, R. (1989). N^G-Methyl arginine, an inhibitor of endothelium-derived nitric oxide synthesis, is a potent pressor agent in the guinea pig: does nitric oxide regulate blood pressure in vivo? *Biochem. Biophys. Res. Commun.*, **160,** 881–886.

AL-SA'DONI, H.H., MEGSON, I.L., BISLAND, S.K., BUTLER, A.R. & FLITNEY, F.W. (1997). Neocuproine, a selective Cu(I) chelator, and the relaxation of rat vascular smooth muscle by S-nitrosothiols. *Br. J. Pharmacol.*, **121,** 1047–1050.

ASKEW, S.C., BUTLER, A.R., FLITNEY, F.W., KEMP, G.D. & MEGSON, I.L. (1995). Chemical mechanism underlying the vasodilator and platelet anti-aggregating properties of S-nitroso-N-acetyl-D,L-penicillamine and S-nitrosoglutathione. *Bioorg. Med. Chem.,* **3,** 1–9.

AVDEEF, A. (1996). Assessment of distribution-pH profiles. In *Lipohilicity in Drug Action and Toxicology*. ed. Pliska, V., Testa, B. & van de Waterbeemd, H: Weinheim, VCH Publishers.

AVDEEF, A. (1993). pH-metric Log P: refinement of partition coefficients and ionization constants of multiprotic substances. *J. Pharm. Sci.,* **82,** 183–190.

BAINBRIGGE, N., BUTLER, A.R. & GORBITZ, C.H. (1997). The thermal stability of S-nitrosothiols: experimental studies and ab initio calculations on model compounds. *J. Chem. Soc. Perkin Trans., 2,* 351–353.

BAUER, J.A. & FUNG, H.L. (1991). Differential hemodynamic effects and tolerance properties of nitroglycerin and an S-nitrosothiol in experimental heart failure. *J. Pharmacol. Exp. Ther.,* **256,** 249–254.

CARON, G., GAILLARD, P., CARRUPT, P.A. & TESTA, B. (1997). Lipophilicity behaviour of model and medicinal compounds containing a sulfide, sulfoxide or sulfone moiety. *Helvetica. Chimica. Acta.,* **80,** 449–462.

CHAPPELL, S.P., LEWIS, M.J. & HENDERSON, A.H. (1987). Effect of lipid feeding on endothelium-dependent relaxation in rabbit aorta preparations. *Cardiovasc. Res.,* **21,** 34–38.

CHU, A., CHAMBERS, D.E., LIN, C.-C., KEUHL, W.D., PALMER, R.M.J., MONCADA, S. & COBB, F. (1991). Effects of inhibition of nitric oxide formation on basal vasomotion and endothelium-dependent responses of the coronary arteries in awake dogs. *J. Clin. Invest.,* **87,** 1964–1968.

COHEN, R.A. & VANHOUTTE, P.M. (1995). Endothelium-dependent hyperpolarisation: beyond nitric oxide and cyclic GMP. *Circulation,* **92,** 3337–3349.

DE BELDER, A.J., MACALLISTER, R., RADOMSKI, M.W. & MONCADA, S. (1994). Effects of S-nitroso-glutathione in the human forearm circulation: evidence for selective inhibition of platelet activation. *Cardiovasc. Res.,* **28,** 691–694.

DE MAN, G., DE WINTER, B.Y., BOECKXSTAENS, G.E., HERMAN, A.G. & PELCKMANS, P.A. (1996). Effect of Cu^{2+} on relaxations to the nitrergic neurotransmitter, NO and S-nitrosothiols in the rat fundus. *Br. J. Pharmacol.,* **119,** 990–996.

DICKS, A.P., SWIFT, H.R., WILLIAMS, D.L.H., BUTLER, A.R., AL-SA'DONI, H.H. & COX, B.G. (1996). Identification of Cu^{+} as the effective reagent in nitric oxide formation from S-nitrosothiols (RSNO). *J. Chem. Soc. Perkin. Trans., 2,* 481–487.

FERNS, G.A.A., LAMB, D.J. & TAYLOR, A. (1997). The possible role of copper ions in atherogenesis: the Blue Janus. *Atherosclerosis,* **133,** 139–252.

FIELD, L., DILTS, R.V., RAVICHANCHRAN, R., LENHERT, P.G. & CARNAHAN, G.E. (1978). An unusually stable thionitrite from N-acetyl-D,L-penicillamine: X-ray structure and molecular structure of 2-(acetylamino)-2-carboxy-1, 1-dimethylethylthionitrite. *J. Chem. Soc. Chem. Commun.,* 249–250.

FLITNEY, F.W., MEGSON, I.L., FLITNEY, D.E. & BUTLER, A.R. (1992). Iron-sulphur cluster nitrosyls, a novel class of nitric oxide generator: mechanism of vasodilator action on rat isolated tail artery. *Br. J. Pharmacol.,* **107,** 842–848.

FORSTERMANN, U., MUGGE, A., ALHEID, U., HAVERICH, A. & FROLICH, J.C. (1988). Selective attenuation of endothelium-mediated vasodilation in atherosclerotic human coronary arteries. *Circ. Res.,* **62,** 185–190.

FRUTTERO, R., CARON, G., FORNATTO, E., BOSCHI, D., ERMONDI, G., GASCO, A., CARRUPT, P.A. & TESTA, B. (1998). Mechanisms of liposomes/water partitioning of (p-methylbenzyl)alkylamines. *Pharm. Res.,* **15,** 1407–1413.

GARDINER, S.M., COMPTON, A.M., KEMP, P.A. & BENNETT, T. (1990). Regional and cardiac haemodynamic effects of N^{G}-nitro-L-arginine methyl ester in conscious, Long Evans rats. *Br. J. Pharmacol.,* **101,** 625–631.

GARG, U.C. & HASSID, A. (1989). Nitric oxide-generating vasodilators and 8-bromo-cyclic guanosine monophosphate inhibit mitogenesis and proliferation of cultured rat vascular smooth muscle cells. *J. Clin. Invest.,* **83,** 1774–1777.

GORDGE, M.P., MEYER, D.J., HOTHERSHALL, J., NEILD, G.H., PAYNE, N.N. & NORONHA-DUTRA, A. (1996). Role of a copper (I)-dependent enzyme in the anti-platelet action of S-nitrosoglutathione. *Br. J. Pharmacol.,* **114,** 1083–1089.

GUERRA, R.J., BROTHERTON, A.F.A., GOODWIN, P.J., CLARK, C.R., ARMSTRONG, M.L. & HARRISON, D.G. (1989). Mechanism of abnormal endothelium-dependent relaxation in atherosclerosis: implications for altered autocrine and paracrine functions of EDRF. *Blood Vessels,* **26,** 300–314.

HAROWITZ, J.D., ANTMAN, E.M., LORELL, B.H., BARRY, W.H. & SMITH, T.W. (1983). Potentiation of the cardiovascular effects of nitroglycerin by N-acetylcysteine. *Circulation,* **68,** 1247–1253.

HARRISON, D.G., ARMSTRONG, M.L., FRIEMAN, P.C. & HEISTAD, D.D. (1987). Restoration of endothelium-dependent relaxation by dietary treatment in atherosclerosis. *J. Clin. Invest.,* **80,** 1808–1811.

HAYNES, W.G., NOON, J.P., WALKER, B.R. & WEBB, D.J. (1993). L-NMMA increases blood pressure in man. *Lancet,* **342,** 931–932.

HONGO, K., OGAWA, H., KASSELL, N., NAKAGOMI, T., SASAKI, T., TSUKAHARA, T. & LEHMAN, M. (1988). Comparison of intraluminal and extraluminal inhibitory effects of haemoglobin on endothelium-dependent relaxation of rabbit basilar artery. *Stroke,* **19,** 1550–1555.

LANGFORD, E.J., BROWN, A.S., WAINWRIGHT, R.J., DE BELDER, A.J., THOMAS, M.R., SMITH, R.E.A., RADOMSKI, M.W., MARTIN, J.F. & MONCADA, S. (1994). Inhibition of platelet activity by S-nitrosoglutathione during coronary angioplasty. *Lancet,* **344,** 1458–1460.

LEFER, A.M. (1997). Nitric oxide: nature's naturally occurring leukocyte inhibitor. *Circulation,* **95,** 553–554.

MACALLISTER, R.J., CALVER, A.L., RIEZEBOS, J., COLLIER, J. & VALLANCE, P. (1995). Relative potency of nitrovasodilators on human blood vessels: an insight into the targetting of nitric oxide delivery. *J. Pharmacol. Exp. Ther.,* **273,** 1529–1537.

MANNHOLD, R., REKKER, R.F., SONNTAG, C., TERLAAK, A.M. & DROSS, K. (1995). Comparative evaluation of the predictive power of calculation procedures for molecular lipophilicity. *J. of Pharm. Sci.,* **84,** 1410–1419.

MARTIN, W., VILLANI, G.M., JOTHIANANDAN, D. & FURCHGOTT, R.F. (1985). Selective blockade of endothelium-dependent and glyceryl trinitrate-induced relaxation by hemoglobin, and by methylene blue in the rabbit aorta. *J. Pharmacol. Exp. Ther.,* **232,** 708–716.

MEGSON, I.L., FLITNEY, F.W., BATES, J. & WEBSTER, R.N. (1995). "Repriming" of vascular smooth muscle photorelaxation is dependent on endothelium-derived nitric oxide. *Endothelium,* **3,** 39–46.

MEGSON, I.L., GREIG, I.R., GRAY, G.A., WEBB, D.J. & BUTLER, A.R. (1997). Prolonged effect of a novel S-nitrosated glyco-amino acid in endothelium-denuded rat femoral arteries: potential as a slow release nitric oxide donor drug. *Br. J. Pharmacol.,* **122,** 1617–1624.

MONCADA, S., REES, D.D., SCHULZ, R. & PALMER, R.M.J. (1991). Development and mechanism of a specific supersensitivity to nitrovasodilators following inhibition of nitric oxide synthase in vivo. *Proc. Natl. Acad. Sci. U.S.A.,* **88,** 2166–2170.

PALMER, R.M.J., ASHTON, D. & MONCADA, S. (1988). Vascular endothelial cells synthesise nitric oxide from L-arginine. *Nature,* **333,** 664–666.

PALMER, R.M.J., FERRIGE, A.G. & MONCADA, S. (1987). Nitric oxide release accounts for the biological activity of EDRF. *Nature,* **327,** 524–526.

PALMER, R.M.J. & MONCADA, S. (1989). A novel citrulline-forming enzyme implicated in the formation of nitric oxide by vascular endothelial cells. *Biochem. Biophys. Res. Commun.,* **158,** 348–352.

RADOMSKI, M.W., PALMER, R.M.J. & MONCADA, S. (1987a). Endogenous nitric oxide inhibits human platelet adhesion to vascular endothelium. *Lancet,* **2,** 1057–1058.

RADOMSKI, M.W., PALMER, R.M.J. & MONCADA, S. (1987b). The role of nitric oxide and cGMP in platelet adhesion to vascular endothelium. *Biochem. Biophys. Res. Commun.,* **148,** 1482–1489.

RADOMSKI, M.W., PALMER, R.M.J. & MONCADA, S. (1990). An L-arginine: nitric oxide pathway present in human platelets regulates aggregation. *Proc. Natl. Acad. Sci. U.S.A.,* **87,** 5193–5197.

REES, D.D., PALMER, R.M.J. & MONCADA, S. (1989). Role of endothelium-derived nitric oxide in the regulation of blood pressure. *Proc. Natl. Acad. Sci. U.S.A.,* **86,** 3375–3378.

SWIFT, H. (1989). PhD Thesis. Department of Chemistry, University of Durham, Durham, U.K.

TESTA, B., CARRUPT, P.A., GAILLARD, P. & TSAI, R.S. (1996). Intramolecular interactions encoded in lipophilicity: their nature and significance. In *Lipophilicity in Drug Action and Toxicology*. ed. Pliska, V., Testa, B. & van de Waterbeemd, H. pp. 49–71. Weinheim: VCH Publishers.

VALLANCE, P., COLLIER, J. & MONCADA, S. (1989). Effects of endothelium-derived nitric oxide on peripheral arterial tone in man. *Lancet,* **334,** 997–1000.

WILLIAMS, D.L.H. (1985). S-nitrosation and the reactions of S-nitroso compounds. *Chem. Soc. Rev.,* **14,** 171–196.

(Received August 3, 1998
Revised November 2, 1998
Accepted November 9, 1998)

British Journal of Pharmacology (1999) 126, 649–656
http://www.stockton-press.co.uk/bjp

Bradykinin B_1 and B_2 receptors, tumour necrosis factor α and inflammatory hyperalgesia

*,[1,3]S. Poole, [2]B.B. Lorenzetti, [2]J.M. Cunha, [1]F.Q. Cunha & [1]S.H. Ferreira

[1]Department of Pharmacology, Faculty of Medicine of Ribeirão Preto, University of São Paulo, Avenida Bandeirantes, 3900, 14049-900- Ribeirão Preto, São Paulo, Brazil; and [2]Department of Pharmacology, University Federal Paraná, Curitiba, Paraná, Brazil

1 The effects of BK agonists and antagonists, and other hyperalgesic/antihyperalgesic drugs were measured (3 h after injection of hyperalgesic drugs) in a model of mechanical hyperalgesia (the end-point of which was indicated by a brief apnoea, the retraction of the head and forepaws, and muscular tremor).

2 DALBK inhibited responses to carrageenin, bradykinin, DABK, and kallidin.

3 Responses to kallidin and DABK were inhibited by indomethacin or atenolol and abolished by the combination of indomethacin + atenolol.

4 DALBK or HOE 140, given 30 min before, but not 2 h after, carrageenin, BK, DABK and kallidin reduced hyperalgesic responses to these agents.

5 A small dose of DABK + a small dose of BK evoked a response similar to the response to a much larger dose of DABK or BK, given alone.

6 Responses to BK were antagonized by HOE 140 whereas DALBK antagonized only responses to larger doses of BK. The combination of a small dose of DALBK with a small dose of HOE 140 abolished the response to BK.

7 The hyperalgesic response to LPS (1 μg) was inhibited by DALBK or HOE 140 and abolished by DALBK + HOE 140. The hyperalgesic response to LPS (5 μg) was not antagonized by DALBK + HOE 140.

8 These data suggest: (a) a predominant role for B_2 receptors in mediating hyperalgesic responses to BK and to drugs that stimulate BK release, and (b) activation of the hyperalgesic cytokine cascade independently of both B_1 and B_2 receptors if the hyperalgesic stimulus is of sufficient magnitude.

Keywords: Inflammatory hyperalgesia; bradykinin; [des-Arg^9]BK; [des-Arg^9, Leu^8]BK; tumour necrosis factor alpha; interleukin-8; prostaglandin E_2

Abbreviations: ATEN, Atenolol; BK, bradykinin; DABK, [des-Arg^9]BK; DALBK, [des-Arg^9, Leu^8]BK; Cg, carrageenin; D-Arg^0-Hyp^3-Thi^5-Dtic^7-Oic^8-BK, HOE 140; INDO, indomethacin; IL, interleukin; IU, international unit; i.pl., intraplantar; LPS, lipopolysaccharide; PGE_2, prostaglandin E_2; TNFα, tumour necrosis factor α

Introduction

Bradykinin (BK) is an important inflammatory mediator involved in oedema formation and serves as a trigger for inflammatory pain (Steranka *et al*., 1988; Dray & Perkins, 1993; Hall, 1997). BK activates and sensitizes pain receptors (nociceptors). Activation of nociceptors causes immediate overt pain (Armstrong *et al*., 1957; Sicuteri *et al*., 1965; Ferreira, 1972; Whalley *et al*., 1987), whereas sensitization of nociceptors is responsible for the development of inflammatory hyperalgesia (Ferreira, 1972; Ferreira *et al*., 1978a). BK exerts its biological activities by stimulating two receptor subtypes, B_1 and B_2 (see Hall, 1997, for a review). B_2 receptors have been localized to sensory neurones (Steranka *et al*., 1988; Nagy *et al*., 1993). B_1 receptors have been reported to be present on sensory neurones or ganglia, especially after induction, in some models (Segond-von Banchet *et al*., 1996; Seabrook *et al*., 1997) but not in a model of persistent inflammatory hyperalgesia (Davis *et al*., 1996).

BK has been shown to be hyperalgesic in models of inflammation, in both behavioural and electrophysiological studies (Dray *et al*., 1988; Lang *et al*., 1990; Handwerker & Reeh, 1991). Until a few years ago it was believed that the acute inflammatory events, such as oedema and inflammatory pain, were mediated solely by B_2 receptors, since HOE 140, a B_2 receptor antagonist, inhibited the hyperalgesic effect of BK and was anti-hyperalgesic in experimental models of inflammatory pain, including carrageenin-evoked hyperalgesia (Beresford & Birch, 1992; Heapy *et al*., 1991; Ferreira *et al*., 1993). More recently, it was shown that both B_1 and B_2 receptors play an important role in mechanical and thermal hyperalgesia, notably when the hyperalgesia is persistent and subsequent to an earlier inflammatory insult, suggesting the induction of B_1 receptors at the site of injury by inflammatory mediators, such as cytokines (Perkins *et al*., 1993; Perkins & Kelly, 1993). Consistent with this notion, in models of mechanical and thermal hyperalgesia, hyperalgesic responses to IL-1β were inhibited by the BK B_1 receptor antagonist DALBK (Davis & Perkins, 1994; Perkins & Kelly, 1994; Perkins *et al*., 1995)

In a model of inflammatory (mechanical) hyperalgesia, responses to carrageenin and bacterial endotoxin (lipopolysaccharide, LPS) were initiated by BK, acting on BK_2

*Author for correspondence.
[3]Current address: Division of Endocrinology, National Institute for Biological Standards and Control, Blanche Lane, South Mimms, Potters Bar, Herts EN6 3QG, England, U.K.

receptors, which stimulated the release of tumour necrosis factor α (TNFα). The TNFα induced the production of IL-1β and IL-6, which stimulated the production of cyclo-oxygenase products, and IL-8, which stimulated production of sympathomimetic amines (Cunha *et al*., 1992; Ferreira *et al*., 1993). These data are consistent with data obtained in another model of inflammatory hyperalgesia: inflammatory hyperalgesia caused by Freund's complete adjuvant, to which TNFα and IL-1β contributed (Garabedian *et al*., 1995; Woolf *et al*., 1996, 1997; Banner *et al*., 1998) and with a report that BK evoked the release of TNFα from macrophage monolayers (Tiffany & Burch, 1989).

The aim of the present study was to investigate further, in a model of inflammatory (mechanical) hyperalgesia, the BK-initiated, TNFα-driven, cytokine cascade and to investigate the relative contributions of the two BK receptor subtypes, B_1 and B_2 to this stimulation.

Methods

Animals

Male Wistar rats, weighing 130–180 g, were housed in temperature controlled rooms (22–25°C) with water and food *ad libitum* until use.

Nociceptive test

A constant pressure of 20 mmHg (measured using a sphygmomanometer), was applied (*via* a syringe piston moved by compressed air) to an area of 15 mm^2 of the dorsal surface of the hind paws of rats, and discontinued when they presented a typical 'freezing reaction'. The freezing reaction was signalled by a brief apnoea, concomitant with the retraction of the head and forepaws and a reduction in the escape movements which animals frequently made to escape from the position imposed by the experimental situation. Usually, the apnoea was associated with successive waves of muscular tremor. For each animal, the latency to the onset of the freezing reaction (from the time of first application of the pressure) was measured before administration (zero time) and again, 3 h after administration of a hyperalgesic agent. The intensity of hyperalgesia was quantified as the reduction in reaction time, calculated by subtracting the value of the second measurement from that of the first (Ferreira *et al*., 1978b, 1988, Cunha *et al*., 1998). Reaction times were typically 32–34 s (with s.e.means of 0.5–1.0 s) before injection and 2–4 s after stimulation with hyperalgesic agents. Multiple paw treatments did not alter basal reaction times. Different individuals prepared the solutions to be injected, made the injections, and measured the reaction times.

Experimental protocol

Hyperalgesia was measured 3 h after injection of hyperalgesic agents (agonists), each injected in 100 μl, into the hind paws (intraplantar, i.p.l.) of rats. Anti-hyperalgesic agents (antagonists and antibodies) were injected i.pl. (50 or 100 μl, into the paw to be injected with a hyperalgesic agent) except for HOE

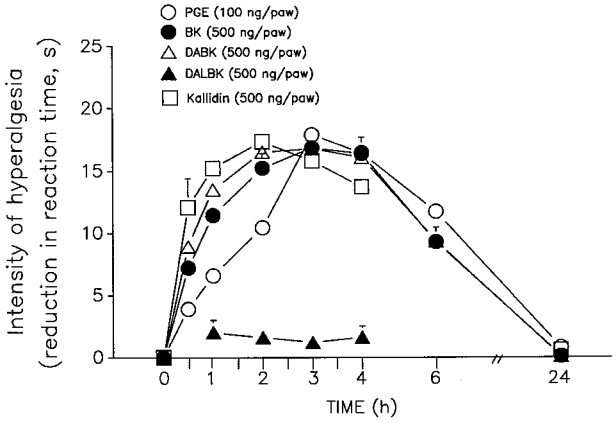

Figure 2 Time course of the development of responses to hyperalgesic agents. The intensity of hyperalgesia was measured in injected paws 0.5–24 h after injection of PGE_2 (PGE, 100 ng paw^{-1}, open circles), BK (500 ng paw^{-1}, filled circles), DABK (500 ng paw^{-1}, open triangles), DALBK (500 ng paw^{-1}, filled triangles), kallidin (500 ng paw^{-1}, open squares). All substances were injected i.pl. in a volume of 100 μl. Vertical bars are s.e.means in groups of five animals.

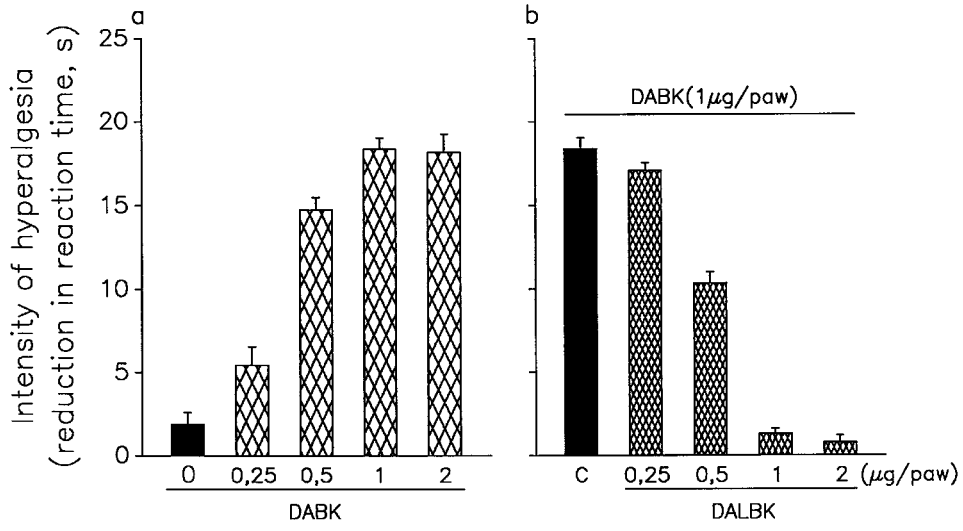

Figure 1 Dose-dependence of hyperalgesia evoked by DABK and its inhibition by DALBK. (a) The intensity of hyperalgesia in injected paws after injection of DABK (0.25–2.0 μg paw^{-1}). (b) The inhibitory effect of DALBK (0.25–2.0 μg paw^{-1}) on the hyperalgesic response to DABK (1 μg,), injected into the same paws, 30 min later. Hyperalgesia was measured 3 h after injection of DABK. Vertical bars are s.e.means in groups of five animals.

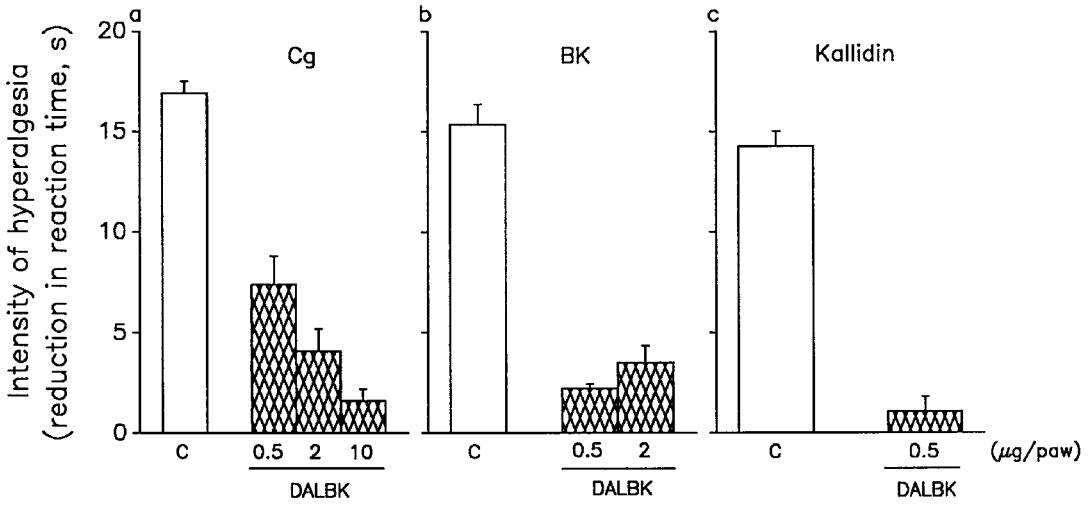

Figure 3 The inhibitory effect of DALBK (0.5–10.0 μg paw^{-1}) on the hyperalgesic responses to (a) carrageenin (100 μg), (b) BK (500 ng) and (c) kallidin (500 ng). DALBK was injected into paws to be injected with one of the three hyperalgesic agents, 30 min before the hyperalgesic agent. Hyperalgesia was measured 3 h after injection of hyperalgesic agents. Vertical bars are s.e.means in groups of five animals.

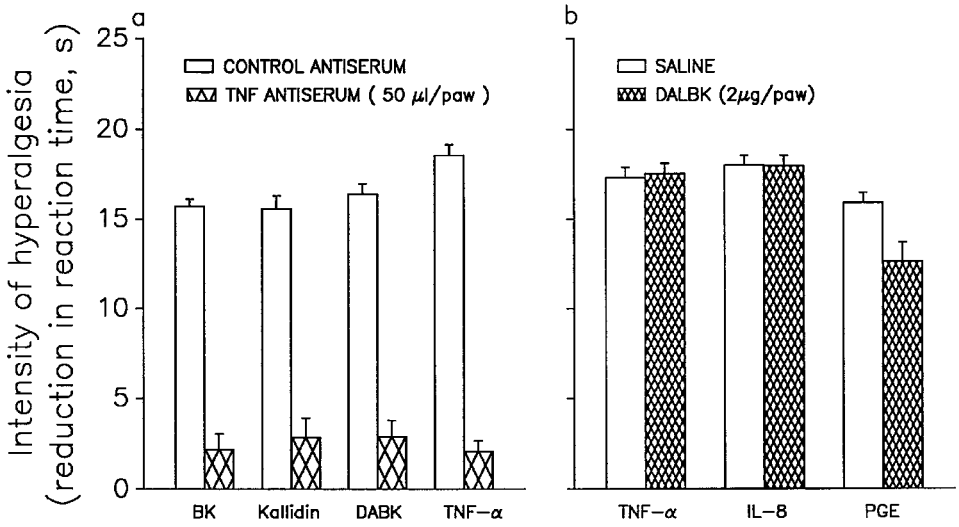

Figure 4 (a) Inhibition by a sheep anti-murine TNFα serum (50 μl paw^{-1}) of the hyperalgesic effects of BK (500 ng), kallidin (500 ng), DABK (500 ng) and murine TNFα (2.5 pg). Anti-murine TNFα serum (hatched columns) or pre-immune control serum (open columns) was injected into paws to be injected with one of the four hyperalgesic agents, 30 min before the hyperalgesic agent. (b) Effect of DALBK (2.0 μg paw^{-1}) on the hyperalgesic responses to TNFα (2.5 pg), IL-8 (0.1 ng) and PGE_2 (100 ng). DALBK (2 μg paw^{-1}) was injected into paws to be injected with one of the three hyperalgesic agents, 30 min before the hyperalgesic agent. Hyperalgesia was measured 3 h after injection of hyperalgesic agents. Vertical bars are s.e.means in groups of five animals.

140, which was injected subcutaneously (s.c., 200 μl), 30 min before or 2 h after hyperalgesic agents. Results are presented as means $\pm$ s.e.means of groups of five animals.

Drugs

The following drugs were obtained from the sources indicated. Recombinant murine TNFα (NIBSC preparation coded 88/532, 200,000 Units 1 μg ampoule^{-1}), human recombinant interleukin-8 (72 amino acids, NIBSC preparation coded 89/520, 1000 International Units 1 μg ampoule^{-1}), atenolol, BK, [des-Arg^9]BK (DABK), [des-Arg^9, Leu^8]BK (DALBK), kallidin, prostaglandin E_2, PGE_2, (Sigma Chemical Co., St. Louis, MO, U.S.A.), HOE 140 (D-Arg^0-Hyp^3-Thi^5-DTic^7-Oic^8-BK, Hoechst AG, Frankfurt, Germany), sheep anti-murine recombinant TNFα antiserum and pre-immune serum (Dr T. Meager, Division of Immunobiology, NIBSC, Mahadevan *et al.*, 1990), indomethacin (Merck, Sharpe & Dohme Ltd, Hoddesdon, Herts, U.K.), carrageenin (FMC Corporation, Philadelphia, U.S.A.).

Results

Inhibition by DALBK of hyperalgesia evoked by DABK

DABK (0.25–2.0 μg) injected into one hind paw of rats evoked dose-dependent hyperalgesia in injected paws with a dose of DABK (1 μg) evoking the maximum hyperalgesic response to this drug (Figure 1). DALBK (0.25–2.0 μg)

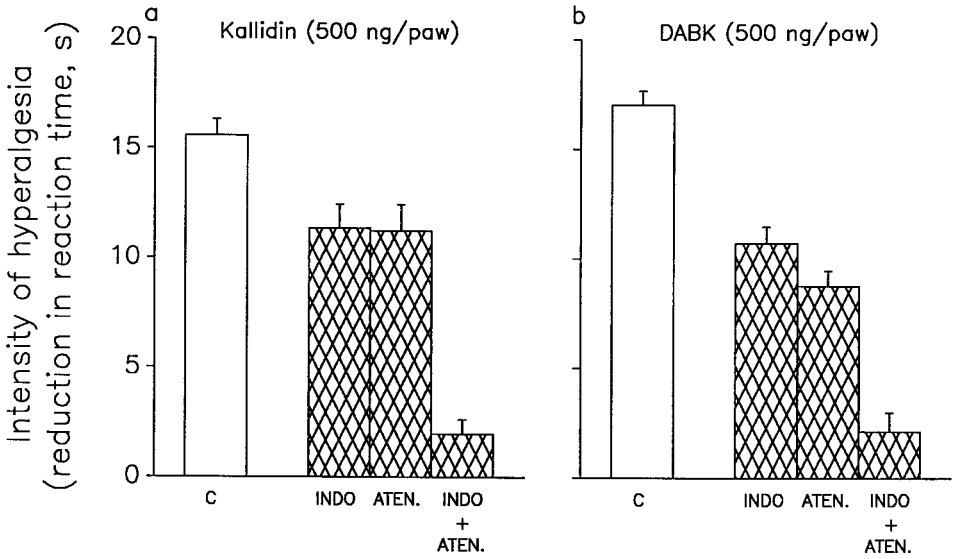

Figure 5 Inhibition by indomethacin (INDO, 100 μg), atenolol (25 μg) and indomethacin + atenolol (INDO, 100 μg + ATEN, 25 μg) of hyperalgesic responses to (a) Kallidin (500 ng) and (b) DABK (500 ng). Indomethacin or atenolol or both were injected into paws to be injected with Kallidin or DABK, 30 min before the hyperalgesic agents. Hyperalgesia was measured 3 h after injection of hyperalgesic agents. Vertical bars are s.e.means in groups of five animals.

injected into hind paws to be injected, 30 min later, with DABK inhibited, in a dose-dependent manner, responses to DABK (1.0 μg) with a dose of DALBK (1.0 μg) abolishing the hyperalgesic response to DABK (1 μg, Figure 1).

Time course of hyperalgesic responses

Injection of the hyperalgesic agents PGE_2 (100 ng), BK (500 ng), DABK (500 ng), and kallidin (500 ng), into one hind paw of rats evoked time-dependent hyperalgesia in injected paws, which began within 30 min of injection, reached a plateau within 2 h (3 h for PGE_2) and was maximum at 3 h after injection (Figure 2). Responses had begun to decline at 6 h (3 h for kallidin) and had returned to pre-injection values within 24 h. The B_1 receptor antagonist DALBK (500 ng, i.pl.) was without effect.

Inhibition by DALBK of responses to carrageenin, BK and kallidin

Carrageenin (100 μg), BK (500 ng) and kallidin (500 ng) evoked hyperalgesic responses, measured 3 h after their injection (i.pl., Figure 3). DALBK, injected into paws to be injected 30 min later with one of the hyperalgesic agents, antagonized the hyperalgesic responses: DALBK (0.5 μg) abolished responses to BK and kallidin whereas DALBK (10.0 μg) was required to abolish the response to carrageenin (Figure 3).

Inhibition by sheep anti-murine TNFα of responses to BK, kallidin, DABK and murine TNFα

BK (500 ng), kallidin (500 ng), DABK (500 ng) and murine TNFα (2.5 pg) evoked hyperalgesic responses, measured 3 h after their injection (i.pl., Figure 4a). The responses were abolished by injection of a sheep anti-murine TNFα serum (50 μl), injected into paws to be injected with one of the four hyperalgesic agents, 30 min before the hyperalgesic agent.

Effect of DALBK on responses to murine TNFα, IL-8 and PGE_2

TNFα (2.5 pg), IL-8 (0.1 ng) and PGE_2 (100 ng) evoked hyperalgesic responses, measured 3 h after their injection (Figure 4b). The responses to TNFα, IL-8 and PGE_2 were little affected by DALBK (2.0 μg, injected into paws to be injected with one of the hyperalgesic agents, 30 min before the hyperalgesic agent).

Inhibition by indomethacin and atenolol of responses to kallidin and DABK

Hyperalgesic responses to kallidin (500 ng, Figure 5a) and DABK (500 ng, Figure 5b) were inhibited by 27 and 37%, respectively by indomethacin (100 μg) and by 27 and 48%, respectively by atenolol (25 μg, each injected into paws to be injected with either kallidin or DABK, 30 min before the hyperalgesic agent). The responses to kallidin and DABK were abolished (-88%) by the combination of indomethacin + atenolol (100 + 25 μg, respectively, Figure 5).

Effects of B_1 and B_2 receptor antagonists on hyperalgesic responses to B_1 and B_2 receptor agonists

DALBK (2 μg, i.pl.), given 30 min before, but not 2 h after, injections (i.pl.) of carrageenin (100 μg), BK (500 ng), DABK (500 ng) and kallidin (500 ng) reduced (by -66 to -92%) the hyperalgesic responses to these agents (Figure 6). Similarly, HOE 140 (1 mg kg^{-1}, s.c.) given 30 min before, but not 2 h after, injections (i.pl.) of carrageenin (100 μg), BK (500 ng), and kallidin (500 ng) reduced (by -72 to -88%) the hyperalgesic responses to carrageenin, BK and kallidin; responses to DABK (500 ng) were not antagonized by HOE 140 (1 mg kg^{-1}, s.c.), given either 30 min before or 2 h after the DABK (Figure 6).

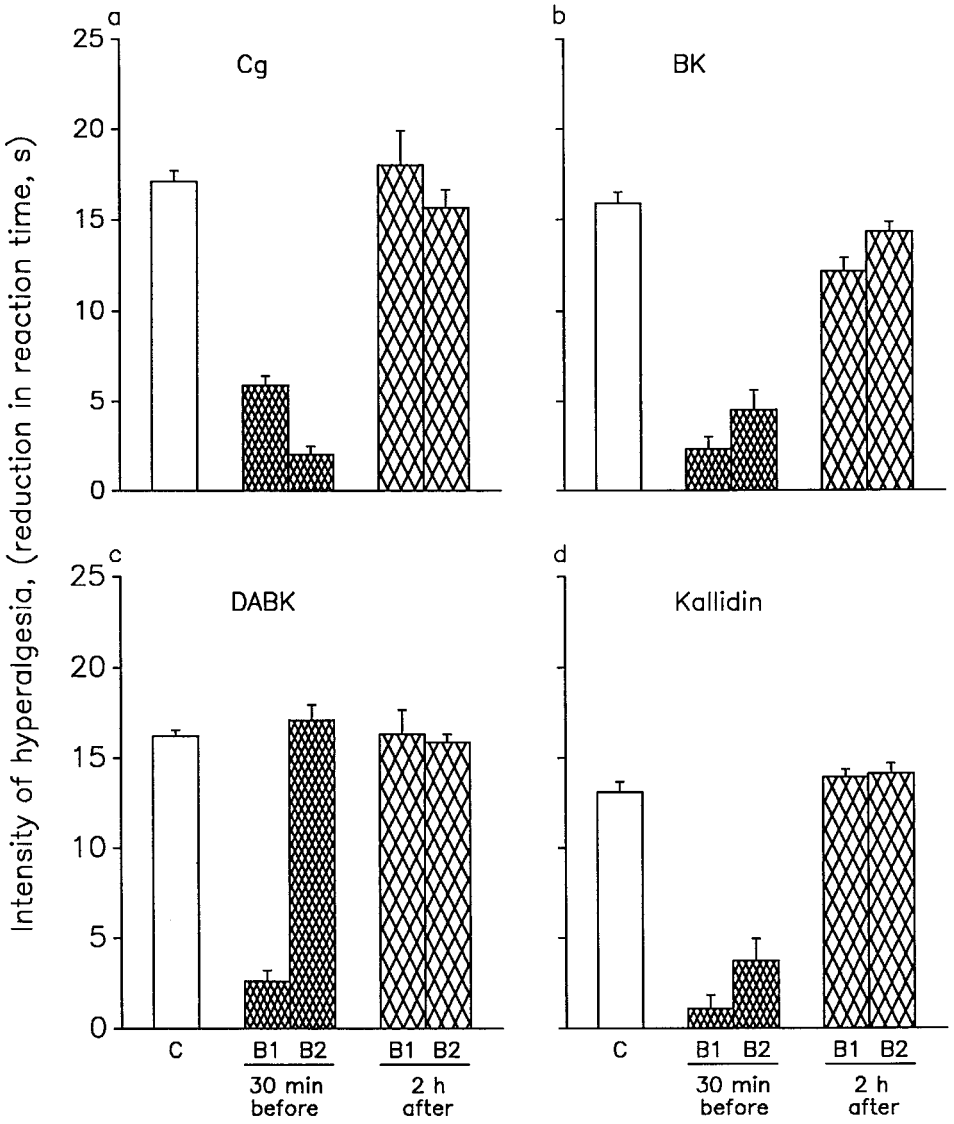

Figure 6 Effects of B_1 and B_2 receptor antagonists on hyperalgesic responses to carrageenin and B_1 and B_2 receptor agonists. DALBK (B_1 antagonist, 2 μg, i.pl.) or HOE 140 (B_2 antagonist, 1 mg kg^{-1}, s.c.) was given either 30 min before or 2 h after injections (i.pl.) of (a) carrageenin (Cg, 100 μg), (b) BK (500 ng), (c) (500 ng) and (d) kallidin (500 ng). Hyperalgesia was measured 3 h after injection of hyperalgesic agents, vertical bars are s.e.means in groups of five animals.

Synergy between the B_1 agonist DABK and BK

The combination of a small dose of the B_1 agonist DABK (100 ng, i.pl.) and BK (25 ng, i.pl.) evoked a hyperalgesic response of 17.9$\pm$0.6 s, compared with responses to DABK (100 ng, i.pl.) and BK (25 ng, i.pl.), each given alone, of 4.1$\pm$0.6 and 5.0$\pm$0.3 s, respectively (Figure 7a). The response to this combination of the two drugs (17.9$\pm$0.6 s) exceeded by 97% the addition of the two individual responses (4.1+5.0=9.1 s) and was similar to the responses to a much larger dose (500 ng) of either DABK or BK, given alone: 16.1$\pm$0.7 and 18.0$\pm$0.6 s, respectively (Figure 7a).

Inhibition of responses to BK by HOE 140 and DALBK

Hyperalgesic responses to BK (25–500 ng, i.pl.) were antagonized by HOE 140 (1 mg kg^{-1}, s.c.), with responses to the smaller doses of BK (25 and 50 ng, i.pl.) abolished and responses to larger doses of BK (100 and 500 ng, i.pl.) reduced by 88 and 67%, respectively (Figure 7b). In contrast, hyperalgesic responses to small doses of BK (25 and 50 ng, i.pl.) were not antagonized by DALBK (500 ng, injected into paws to be injected with BK, 30 min before the BK) whereas hyperalgesic responses to larger doses of BK (100 and 500 ng, i.pl.) were reduced by 27 and 53%, respectively following DALBK (500 ng, Figure 7b). DALBK, even at a small dose (200 ng, i.pl.), was a much more effective antagonist of BK (500 ng) when combined with a small dose of HOE 140 (0.1 mg kg^{-1}, s.c., Figure 7c). When given alone, each antagonist had a marginal effect (−15 and −17%, respectively) upon the response to BK whereas the combination of the two antagonists abolished the response to BK (Figure 7c).

Effects of B_1 and B_2 receptor antagonists on hyperalgesic responses to LPS

Hyperalgesic responses to LPS (1 μg) were inhibited by DALBK (500 ng, i.pl.) and HOE 140 (0.1 mg kg^{-1}, s.c.) by −34 and −76%, respectively. When these doses of the two antagonists were combined, the response to BK was reduced by 88%. In contrast, hyperalgesic responses to LPS (5 μg) were little affected by DALBK (500 ng, i.pl., +13%), HOE 140

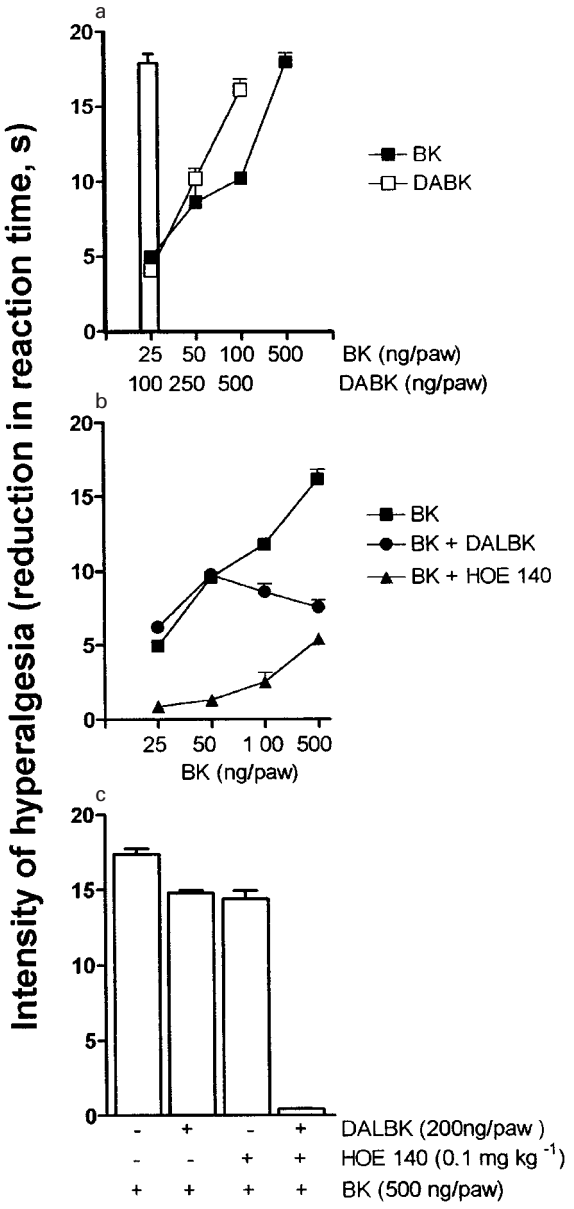

Figure 7 (a) Hyperalgesic responses to injections of BK (25–500 ng, i.pl., filled squares) and DABK (100–500 ng, open squares), each given alone or together (BK, 25 ng + DABK, 100 ng, open column). (b) Inhibition of hyperalgesic responses to BK (25–500 ng, i.pl., filled squares) by DALBK (500 ng, injected into the paws to be injected with BK, filled circles) or HOE 140 (1 mg kg^{-1}, s.c., filled triangles), each given 30 min before the BK. (c) Inhibition of the hyperalgesic response to BK (500 ng, i.pl.) by DALBK (200 ng, injected into the paws to be injected with BK) and HOE 140 (0.1 mg kg^{-1}, s.c.), each given alone (+ −, − +) or together (+ +). Hyperalgesia was measured 3 h after injection of hyperalgesic agents. Vertical bars are s.e.means in groups of five animals.

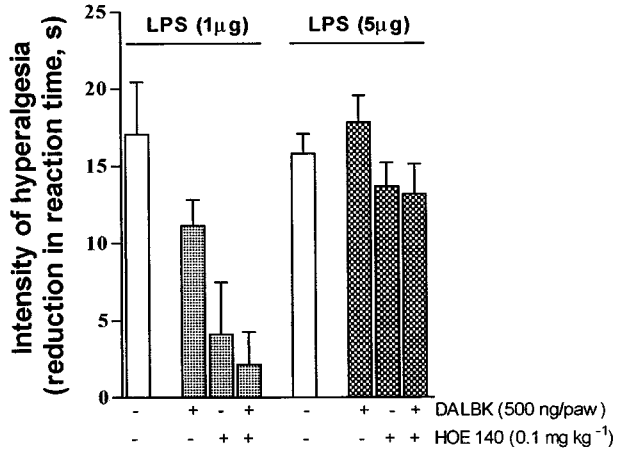

Figure 8 Effects of B_1 and B_2 receptor antagonists on hyperalgesic responses to LPS. DALBK (500 ng, i.pl.) or HOE 140 (0.1 mg kg^{-1}, s.c.), or both were given 30 min before injection (i.pl.) of LPS (1 μg or 5 μg). Hyperalgesia was measured 3 h after injection of LPS. Vertical bars are s.e.means in groups of five animals.

(0.1 mg kg^{-1}, s.c., −13%) or by the combination of these doses of the two antagonists (−17%).

Discussion

In the model of mechanical hyperalgesia utilized in the present study, the inflammatory agent carrageenin induced production of TNFα, which initiated a cascade of cytokine release (Cunha *et al*., 1992). IL-1β and IL-6, induced by TNFα, stimulated the release of hyperalgesic cyclo-oxygenase products (inflammatory hyperalgesia), whereas IL-8, induced by TNFα, stimulated the release of hyperalgesic sympathomimetics (sympathetic hyperalgesia). An early and crucial role for TNFα was proposed because a single injection of this cytokine mimicked the response to carrageenin by inducing production of IL-1β, IL-6 and IL-8, and a single injection of antiserum neutralizing endogenous TNFα abolished the response to carrageenin (Cunha *et al*., 1992). Subsequently, BK, acting upon BK_2 receptors, was identified as a trigger for the induction of TNFα (Ferreira *et al*., 1993): the BK B_2 receptor antagonist HOE 140 (1 mg kg^{-1}) inhibited hyperalgesic responses to BK, carrageenin and smaller doses of LPS (0.5–2 μg). However, the failure of even a large dose of HOE 140 (10 mg kg^{-1}) to inhibit hyperalgesic responses to a larger dose of LPS (5 μg) revealed that the (hyperalgesic) cytokine cascade could be activated independently of BK_2 receptors if the hyperalgesic stimulus were of sufficient magnitude (Ferreira *et al*., 1993). The possible involvement of BK B_1 receptors in the induction of the cytokine cascade was not addressed in the study.

The results of a series of experiments, utilizing a variety of models of hyperalgesia, including mechanical hyperalgesia, indicate a role for BK B_1 receptors in mediating hyperalgesic responses, notably persistent responses to inflammatory stimuli (Perkins & Kelly, 1993, 1994; Davis & Perkins, 1994; Perkins *et al*., 1993, 1995). The present study was undertaken to gain more information about the characteristics of the BK-initiated, TNFα-driven cytokine cascade delineated previously (Cunha *et al*., 1992; Ferreira *et al*., 1993) and to investigate the relative contributions of the two BK receptor subtypes, B_1 and B_2, in this model of mechanical hyperalgesia. The B_1 agonist DABK is here shown to evoke hyperalgesic responses of similar magnitude and duration to responses to BK and kallidin. Also, the B_1 antagonist DALBK antagonized not only hyperalgesic responses to the B_1 agonist DABK, but responses to BK, kallidin and carrageenin. The effect of BK on B_1 receptors is likely to have been due to endogenous conversion of BK to DABK. Consistent with previous results (Dray & Perkins, 1993), these data suggest a role for both B_1 and B_2 receptors in mediating responses to BK, kallidin and carrageenin.

Evidence that the B_1-mediated hyperalgesic effects of DABK, BK, kallidin and carrageenin resulted from the triggering of the same TNFα-driven cascade of cytokines and other mediators shown previously to be induced subsequent to activation of B_2 receptors (Ferreira *et al*., 1993) came from three different experiments. Firstly, an antiserum neutralizing rat TNFα abolished hyperalgesic responses to BK, kallidin and DABK, and the B_1 antagonist DALBK failed to inhibit responses to TNFα, IL-8 and PGE_2. Secondly, indomethacin and atenolol inhibited hyperalgesic responses to kallidin and DABK, and indomethacin + atenolol (given together) abolished responses to kallidin and DABK. Thirdly, the B_1 antagonist DALBK, in common with the B_2 antagonist HOE 140, was effective against BK, kallidin, and carrageenin only when given (30 min) before but not (2 h) after these hyperalgesic agents. Thus, B_1 receptors can have a role both in initiating the (TNFα-driven) cascade of hyperalgesic cytokines (and other mediators) and in mediating responses to one of those cytokines, namely IL-1β (Davis & Perkins, 1994, Perkins & Kelly, 1994; Perkins *et al*., 1995).

The capacity of both the B_1 agonist DABK and BK to evoke maximum hyperalgesic responses suggests a role for both B_1 and B_2 receptors in initiating BK-dependent hyperalgesic responses. This notion is supported by the synergy between the B_1 agonist DABK and BK, with a small dose of each combining to give a response equivalent to that of a $\geqslant 5$ fold larger dose of either drug given alone. The property of the B_2 antagonist HOE 140 to antagonize responses to both small and large doses of BK, in contrast to the B_1 antagonist DALBK, which antagonized only responses to larger doses of BK, suggests that, in the above model, responses to small doses of BK were mediated predominantly *via* B_2 receptors, whereas responses to larger doses of BK activated B_1 receptors in addition to B_2 receptors. Further evidence for a role for B_1 receptors in mediating hyperalgesic responses to larger doses of BK came from the finding that the combination of ineffectual doses (when given alone) of the B_1 antagonist DALBK and the B_2 antagonist HOE 140 abolished the response to a large dose of BK. However, the predominant role of the B_2 receptor in mediating hyperalgesic responses to larger doses of BK (Ferreira *et al*., 1993) was confirmed in that a large dose of the B_2 antagonist HOE 140 was itself sufficient to abolish the hyperalgesic response to a large dose of BK.

The earlier finding (Ferreira *et al*., 1993) that the B_2 antagonist HOE 140 inhibited the hyperalgesic response to a small dose of LPS (1 μg) but not that to a larger dose (5 μg) was confirmed in the present study. Similarly, the B_1 antagonist DALBK has now been shown to also inhibit the hyperalgesic response to a small dose of LPS (1 μg) but not that to a larger dose (5 μg). Indeed, the hyperalgesic response to the larger dose of LPS (5 μg) was not inhibited even by the combination of the B_1 and B_2 antagonists. These data reveal that the (hyperalgesic) cytokine cascade can be activated independently of both B_1 and B_2 receptors if the hyperalgesic stimulus is of sufficient magnitude. Nevertheless, the demonstration of a powerful synergy between (small doses of) B_1 and B_2 receptor antagonists in antagonizing hyperalgesic responses to BK suggests that the combination of B_1 and B_2 receptor antagonists merits further evaluation. This is particularly so in circumstances in which a BK agonist is believed to play a role but in which a B_1 or a B_2 antagonist, administered alone, fails to inhibit the response.

The authors thank Ms I.R. Santos for technical assistance. This work was supported by grants from FAPESP and CNPq (Brazil).

References

ARMSTRONG, D., JEPSON, J.B., KEELE, C.A. & STEWART, J.M. (1957). Pain producing substance in human inflammatory exudates and plasma. *J. Physiol.,* **135,** 350 – 370.

BANNER, L.R., PATTERSON, P., ALLCHORNE, A., POOLE, S. & WOOLF, C.J. (1998). Leukaemia inhibitory factor is an anti-inflammatory and analgesic cytokine. *J. Neurosci.,* **18,** 5456 – 5462.

BERESFORD, I.J.M. & BIRCH, P.J. (1992). Antinociceptive activity of the bradykinin antagonist HOE 140 in rat and mouse. *Br. J. Pharmacol.,* **105,** 1P – 314P.

CUNHA, F.Q., POOLE, S., LORENZETTI, B.B. & FERREIRA, S.H. (1992). The pivotal role of tumour necrosis factor alpha in the development of inflammatory hyperalgesia. *Br. J. Pharmacol.,* **107,** 660 – 664.

CUNHA, F.Q., POOLE, S., LORENZETTI, B.B., VEIGA, F.H. & FERREIRA, S.H. (1998). Cytokine-mediated inflammatory hyperalgesia limited by interleukin-4. *Br. J. Pharmacol.,* In press.

DAVIS, A.J. & PERKINS, M.N. (1994). The involvement of bradykinin B1 and B2 receptor mechanisms in cytokine-induced mechanical hyperalgesia in the rat. *Br. J. Pharmacol.,* **113,** 63 – 68.

DAVIS, C.L., NAEEM, S., PHAGOO, S.B., CAMPBELL, E.A., URBAN, L. & BURGESS, G.M. (1996). B1 bradykinin receptors and sensory neurones. *Br. J. Pharmacol.,* **118,** 1469 – 1476.

DRAY, A., BETTANEY, J., FORSTER, P. & PERKINS, M.N. (1998). Activation of a bradykinin receptor in peripheral nerve and spinal cord in the neonatal rat in vitro. *Br. J. Pharmacol.,* **95,** 1008 – 1010.

DRAY, A. & PERKINS, M. (1993). Bradykinin and inflammatory pain. *Trends Neurosci.,* **16,** 99 – 104.

FERREIRA, S.H. (1972). Prostaglandins, aspirin-like drugs and analgesia. *Nature New Biol.,* **240,** 200 – 203.

FERREIRA, S.H., LORENZETTI, B.B., BRISTOW, A.F. & POOLE, S. (1988). Interleukin-1β as a potent hyperalgesic agent antagonized by a tripeptide analogue. *Nature,* **334,** 698 – 699.

FERREIRA, S.H., LORENZETTI, B.B. & CORREA, F.M.A. (1978b). Central and peripheral antialgesic action of aspirin-like drugs. *Eur. J. Pharmacol.,* **53,** 39 – 48.

FERREIRA, S.H., LORENZETTI, B.B. & POOLE, S. (1993). Bradykinin initiates cytokine mediated inflammatory hyperalgesia. *Br. J. Pharmacol.,* **110,** 1227 – 1231.

FERREIRA, S.H., NAKAMURA, M. & CASTRO, M.S.A. (1978a). The hyperalgesic effects of prostacyclin and prostaglandin E2. *Prostaglandins,* **16,** 31 – 37.

GARABEDIAN, B., POOLE, S., ALLCHORNE, A., WINTER, J. & WOOLF, C.J. (1995). Interleukin-1 beta contributes to the inflammation-induced increase in nerve-growth factor levels and inflammatory hyperalgesia. *Br. J. Pharmacol.,* **115,** 1265 – 1275.

HALL, J.M. (1997). Bradykinin Receptors. *Gen. Pharmac.,* **28,** 1 – 6.

HANDWERKER, H.O. & REEH, P.W. (1991). Pain and Inflammation. In: *Proceedings of the VIth World Congress on Pain*, eds. Bond, M.R., Charlton, J.E. & Woolf, C.J. pp. 59 – 70, Amsterdam: Elsevier Science Publishers BV.

HEAPY, C.G., FARMER, S.C. & SHAW, J.S. (1991). The inhibitory effect of HOE 140 in mouse abdominal constriction assays. *Br. J. Pharmacol.,* **104,** 455P.

LANG, E., NOVAK, A., REEH, P.W. & HANDWERKER, H.O. (1990). Chemosensitivity of fine afferents from rat skin in vitro. *J. Neurophysiol.,* **63,** 887 – 901.

MAHADEVAN, V., MALIK, S.T., MEAGER, A., FIERS, W., LEWIS, G.P. & HART, I.R. (1990). Role of tumor necrosis factor in flavone acetic acid-induced tumor vasculature shutdown. *Cancer Res.,* **50,** 5537 – 5542.

NAGY, I., PABLA, R., MATESZ, C., DRAY, A., WOOLF, C.J. & URBAN, L. (1993). Cobalt uptake enables identification of capsaicin- and bradykinin-sensitive subpopulations of rat dorsal root ganglion cells in vitro. *Neurosci.,* **56,** 241 – 246.

PERKINS, M.N., CAMPBELL, E. & DRAY, A. (1993). Antinociceptive activity of the bradykinin B1 and B2 receptor antagonists, des-Arg9, [Leu8]-BK and HOE 140, in two models of persistent hyperalgesia in the rat. *Pain,* **53,** 191–197.

PERKINS, M.N. & KELLY, D. (1993). Induction of bradykinin B1 receptors in vivo in a model of ultra-violet irradiation-induced thermal hyperalgesia in the rat. *Br. J. Pharmacol.,* **110,** 1441–1444.

PERKINS, M.N. & KELLY, D. (1994). Interleukin-1 beta induced-desArg9bradykinin-mediated thermal hyperalgesia in the rat. *Neuropharmacol.,* **33,** 657–660.

PERKINS, M.N., KELLY, D. & DAVIS, A.J. (1995). Bradykinin B1 and B2 receptor mechanisms and cytokine-induced hyperalgesia in the rat. *Can. J. Physiol. Pharmacol.,* **73,** 832–836.

SEABROOK, G.R., BOWERY, B.J., HEAVENS, R., BROWN, N., FORD, H., SIRINATHSINGHI, D.J., BORKOWSKI, J.A., HESS, J.F., STRADER, C.D. & HILL, R.G. (1997). Expression of B1 and B2 bradykinin receptor mRNA and their functional roles in sympathetic ganglia and sensory dorsal root ganglia neurones from wild-type and B2 receptor knockout mice. *Neuropharmacol.,* **36,** 1009–1017.

SEGOND-VON-BANCHET, G., PETERSEN, M. & HEPPELMANN, B. (1996). Bradykinin receptors in cultured rat dorsal root ganglion cells: influence of length of time in culture. *Neurosci.,* **75,** 1211–1218.

SICUTERI, F., FRANCIULLACCI, F.M., FRANCHI, G. & DEL BIANCO, P.L. (1965). Serotonin-bradykinin potentiation of the pain receptors in man. *Life Sci.,* **4,** 309–316.

STERANKA, L.R., MANNING, D.C. & DEHASS, C.J. (1988). Bradykinin as pain mediator: receptors are localized to sensory neurones and antagonists have analgesic actions. *Proc. Natl. Acad. Sci. U.S.A.,* **85,** 3245–3249.

TIFFANY, C.W. & BURCH, R.M. (1989). Bradykinin stimulates tumour necrosis factor and interleukin-1 release from macrophages. *FEBS Lett.,* **247,** 189–192.

WHALLEY, E.T., CLEGG, S., STEWART, J.M. & VAVREK, R.J. (1987). The effect of kinin agonists and antagonists on the pain response of the human blister base. *Naunyn-Schmiedeberg's Archives of Pharmacology,* **336,** 652–655.

WOOLF, C.J., ALLCHORNE, A., GARABEDIAN, B.S. & POOLE, S. (1997). Cytokines, nerve growth factor and inflammatory hyperalgesia: the contribution of tumour necrosis factor alpha. *Br. J. Pharmacol.,* **121,** 417–424.

WOOLF, C.J., MA, Q.-P., ALLCHORNE, A. & POOLE, S. (1996). Peripheral cell types contributing to the hyperalgesic action of nerve growth factor in inflammation. *J. Neurosci.,* **16,** 2716–2723.

(Received July 28, 1998
Revised November 1, 1998
Accepted November 9, 1998)

British Journal of Pharmacology (1999) 126, 657–664
http://www.stockton-press.co.uk/bjp

$GABA_B$ receptor-mediated stimulation of adenylyl cyclase activity in membranes of rat olfactory bulb

[1]Maria C. Olianas & *,[1]Pierluigi Onali

[1]Section on Biochemical Pharmacology, Department of Neurosciences, University of Cagliari, via Porcell 4, 09124 Cagliari, Italy

1 Previous studies have shown that $GABA_B$ receptors facilitate cyclic AMP formation in brain slices likely through an indirect mechanism involving intracellular second messengers. In the present study, we have investigated whether a positive coupling of $GABA_B$ receptors to adenylyl cyclase could be detected in a cell-free preparation of rat olfactory bulb, a brain region where other G_i/G_o-coupled neurotransmitter receptors have been found to stimulate the cyclase activity.

2 The $GABA_B$ receptor agonist (−)-baclofen significantly increased basal adenylyl cyclase activity in membranes of the granule cell and external plexiform layers, but not in the olfactory nerve-glomerular layer. The adenylyl cyclase stimulation was therefore examined in granule cell layer membranes.

3 The (−)-baclofen stimulation ($pD_2 = 4.53$) was mimicked by 3-aminopropylphosphinic acid ($pD_2 = 4.60$) and GABA ($pD_2 = 3.56$), but not by (+)-baclofen, 3-aminopropylphosphonic acid, muscimol and isoguvacine. The stimulatory effect was counteracted by the $GABA_B$ receptor antagonists CGP 35348 ($pA_2 = 4.31$), CGP 55845 A ($pA_2 = 7.0$) and 2-hydroxysaclofen ($pK_i = 4.22$). Phaclofen (1 mM) was inactive.

4 The (−)-baclofen stimulation was not affected by quinacrine, indomethacin, nordihydroguaiaretic acid and staurosporine, but was completely prevented by pertussis toxin and significantly reduced by the α subunit of transducin, a $\beta\gamma$ scavenger. The $\beta\gamma$ subunits of transducin stimulated the cyclase activity and this effect was not additive with that produced by (−)-baclofen.

5 In the external plexiform and granule cell layers, but not in the olfactory nerve-glomerular layer, (−)-baclofen enhanced the adenylyl cyclase stimulation elicited by the neuropeptide pituitary adenylate cyclase activating polypeptide (PACAP) 38.

6 Conversely, the adenylyl cyclase activity stimulated by either forskolin or Ca^{2+}/calmodulin-(Ca^{2+}/CaM) was inhibited by (−)-baclofen in all the olfactory bulb layers examined.

7 These data demonstrate that in specific layers of rat olfactory bulb activation of $GABA_B$ receptors enhances basal and neurotransmitter-stimulated adenylyl cyclase activities by a mechanism involving $\beta\gamma$ subunits of G_i/G_o. This positive coupling is associated with a widespread inhibitory effect on forskolin- and Ca^{2+}/CaM-stimulated cyclic AMP formation.

Keywords: $GABA_B$ receptors; adenylyl cyclase; G protein $\beta\gamma$ subunits; rat olfactory bulb

Abbreviations: 3-APA, 3-aminopropylphosphinic acid; 3-APPA, 3-aminopropylphosphonic acid; α_{tGDP}, the α subunit of transducin in the GDP-bound form; $\beta\gamma_t$, the $\beta\gamma$ subunits of transducin; BSA, bovine serum albumin; CaM, calmodulin; DTT, dithiothreitol; PACAP, pituitary adenylate cyclase activating polypeptide; PMA, phorbol 12-myristate, 13-acetate

Introduction

The metabotropic $GABA_B$ receptors constitute a distinct subclass of receptors for the inhibitory amino acid GABA (Bowery, 1993). These receptors are widely distributed in the central nervous system, where they are located at both pre- and post-synaptic sites. Drugs acting on $GABA_B$ receptors have been found to be useful in the treatment of spasticity and may have other potential clinical applications, such as absence epilepsy, cognitive impairment and depression (Malcangio & Bowery, 1995; Wojcik & Holopainen, 1992). Recently, the $GABA_B$ receptor has been cloned from rat brain and found to show sequence similarity to the metabotropic receptors for the excitatory neurotransmitter glutamate (Kaupmann *et al*., 1997). These studies have also led to the identification of two molecular forms of the $GABA_B$ receptor which display a different N-terminal sequence but similar pharmacological properties (Kaupmann *et al*., 1997). $GABA_B$ receptors have been shown to interact with pertussis toxin-sensitive G proteins of the G_i/G_o family (Morishita *et al*., 1990) and to activate different signalling mechanisms, including stimulation of K^+ conductance, inhibition of Ca^{2+} channel activities and modulation of cyclic AMP formation (Bowery, 1993; Wojcik & Holopainen, 1992). With regard to the latter mechanism, both inhibitory and stimulatory effects have been reported. Thus, $GABA_B$ receptors have been found to inhibit adenylyl cyclase activity in homogenates of different brain areas (Wojcik & Neff, 1984) and this effect has been shown to be prevented by pertussis toxin, indicating the involvement of G_i/G_o (Xu & Wojcik, 1986). A negative coupling to adenylyl cyclase has also been observed for the cloned receptor expressed in host cells (Kaupmann *et al*., 1997). On the other hand, in brain slice preparations the $GABA_B$ receptor agonist baclofen, besides inhibiting forskolin-stimulated cyclic AMP accumulation, has been found to potentiate the adenylyl cyclase stimulation elicited by different neurotransmitters, such as noradrenaline, vasoactive intestinal peptide, adenosine and prostaglandins (Enna & Karbon, 1984; Hill & Dolphin, 1984; Karbon & Enna, 1985; Watling & Bristow, 1986; Schaad *et al*., 1989). Evidence has been provided that the facilitation of cyclic AMP formation

*Author for correspondence.

occurs indirectly as a consequence of phospholipase A_2 stimulation by $GABA_B$ receptors (Duman *et al*., 1986; Enna & Karbon, 1987). Moreover, baclofen has been found to enhance agonist binding to β-adrenergic receptors, thus suggesting that the $GABA_B$ receptor potentiation of isoproterenol-stimulated cyclic AMP formation may be partially due to an enhanced coupling of β-adrenergic receptor to the adenylyl cyclase stimulatory G protein G_S (Scherer *et al*., 1989).

The recent identification of adenylyl cyclases II and IV, two enzyme isoforms which can be stimulated by G protein $\beta\gamma$ subunits synergistically with activated G_s (Tang & Gilman, 1992), has raised the possibility of a novel mechanism by which $GABA_B$ receptors may directly couple to cyclic AMP stimulation. In fact, by interacting with G_i/G_o, $GABA_B$ receptors may promote the release of a sufficiently high amount of $\beta\gamma$ subunits to stimulate type II/IV adenylyl cyclase activities (Tang & Gilman, 1992). We have recently shown that in rat olfactory bulb, a brain area expressing a high level of type II adenylyl cyclase (Feinstein *et al*., 1991), other G_i/G_o-coupled receptors, such as the acetylcholine muscarinic and opioid receptors, stimulate basal adenylyl cyclase activity and potentiate the responses of G_s-linked neurotransmitter receptors (Olianas & Onali, 1993). In the present study, we report that activation of $GABA_B$ receptors stimulates adenylyl cyclase activity in discrete layers of the rat main olfactory bulb and provide evidence that this positive coupling involves the action of $\beta\gamma$ subunits of G_i/G_o. Part of this work has previously been presented in an abstract form (Olianas & Onali, 1996a).

Methods

Microdissection of olfactory bulb and membrane preparation

Male Sprague-Dawley rats (200–350 g) were killed by decapitation and the olfactory bulbs were rapidly removed and kept on an ice-cold phosphate buffered saline containing 2.5 mM $CaCl_2$. With the use of a tissue slicer, the bulbs were cut into 300 μm thick coronal sections, which were kept in the same saline solution. With the aid of a stereoscopic microscope equipped with a diascopic illuminator base, each slice was free-hand dissected into three portions of the main olfactory bulb: (1) the olfactory nerve-glomerular layer; (2) the external plexiform layer; (3) the granule cell layer plus the white matter. The tissue layers from individual slices were pooled and homogenized in an ice-cold buffer containing (mM): HEPES-NaOH 10, EGTA 1, dithiothreitol (DTT) 1 and $MgCl_2$ 1 (pH 7.4) using a teflon-glass tissue grinder. The homogenate was centrifuged at $27{,}000 \times g$ for 20 min. The pellet was resuspended in the same buffer at a protein concentration of 0.7–1.0 mg ml^{-1} and used immediately for the adenylyl cyclase assay.

Adenylyl cyclase assay

The enzyme activity was assayed by monitoring the conversion of [α-^{32}P]-ATP into [^{32}P]-cyclic AMP. Unless otherwise indicated, the reaction mixture (final volume = 100 μl) contained (mM): HEPES-NaOH buffer (pH 7.4) 50, $MgCl_2$ 2.3, [α-^{32}P]-ATP (70–90 c.p.m. $pmol^{-1}$) 0.2, [^{3}H]-cyclic AMP (80 c.p.m. $nmol^{-1}$) 0.5, GTP 0.1, EGTA 0.3, DTT 1.3, 3-isobutyl-1-methylxanthine 1, phosphocreatine 5, 50 u ml^{-1} of creatine kinase, 50 μg of bovine serum albumin (BSA), 10 μg of bacitracin and 10 kallikrein inhibitor units of aprotinin. The incubation was started by adding the tissue preparation (50–60 μg of protein) and carried out at 30°C for 10 min. [^{32}P]-cyclic AMP was isolated according to Salomon *et al*. (1974). When the effects of the transducin subunits were examined, 10 μl of the membrane preparation (20–25 μg of protein) were preincubated with an equal volume of a solution containing either the $\beta\gamma$ subunits, the α subunit or the appropriate vehicle for 60–90 min at ice-bath temperature. Thereafter (−)-baclofen was added (10 μl) immediately followed by the addition of the reaction mixture (20 μl). The concentration of transducin subunits reported in the figures refer to the final concentrations in the adenylyl cyclase assay. Assays were performed in duplicate.

Intracerebral injection of pertussis toxin

Pertussis toxin was dissolved in a solution containing 50 mM sodium phosphate buffer and 250 mM NaCl (pH 7.4) and injected into the olfactory bulbs (3.0 μg for each bulb) as previously described (Olianas & Onali, 1993). Control animals received an equal volume of vehicle containing 3.0 μg of BSA. At 72 h after the injections, the animals were killed and the membranes were prepared from vehicle- and toxin-treated bulbs. Three tissue preparations were tested.

Protein content was determined by the method of Bradford (1976) using BSA as a standard.

Statistical analysis

Results are given as mean ± s.e.mean. Concentration-response curves were analysed by a least squares curve-fitting computer program (Graph Pad Prism, San Diego, CA, U.S.A.). Agonist concentrations producing half maximal effects (EC_{50} values) were converted to the negative logarithmic form (pD_2), as these values are log-normally distributed. Antagonist pA_2 values were calculated from Arunlakshana-Schild regressions (Arunlakshana & Schild, 1959) in which the log of dose ratios (DR)-1 is plotted as a function of the antagonist concentration. The pA_2 values were calculated by using the PHARM/PCS programme of Tallarida & Murray (1987). In experiments examining the effects of a single concentration of antagonist, the inhibition constant (K_i) was calculated according to the equation:

$$EC_{50}b = EC_{50}a(1 + I/K_i)$$

where $EC_{50}a$ and $EC_{50}b$ are the concentrations of the agonist producing half maximal effect in the absence and in the presence of the antagonist, respectively, and I is the concentration of the antagonist. For comparison with pA_2 values, K_i values were converted to the negative logarithmic form (pK_i). Statistically significant differences between concentration-response curves were determined by two-way analysis of variance. Statistical significance of the difference between means was determined by Student's *t*-test.

Materials

[α-^{32}P]-ATP (30–40 Ci $mmol^{-1}$), [2,8-^{3}H]-cyclic AMP (25 Ci $mmol^{-1}$) were obtained from New England Nuclear-Du Pont (Bad Homburg, Germany). (−)-Baclofen, (+)-baclofen, CGP 55845 A (3-N[1-(S)-(3,4-dichlorophenyl)ethyl] amino-2-(S)-hydroxy-propyl-P-benzyl-phosphinic acid) and CGP 35348 (3-aminopropyl)(diethoxymethyl) phosphinic acid) were obtained from Ciba-Geigy, Basel, Switzerland. Phaclofen, 2-hydroxysaclofen, 3-aminopropylphosphinic acid and 3-aminopropylphosphonic acid were purchased from Tocris Cookson Ltd (Langford, Bristol, U.K.). Muscimol, isoguvacine, GABA, nordihydroguaiaretic acid, indomethacin, phorbol 12-myristate, 13-acetate (PMA), quinacrine and

calmodulin (bovine brain) were from Sigma Chemical Co. (St. Louis, MO, U.S.A.). Pituitary adenylate cyclase-activating polypeptide (PACAP) 38 was from Peninsula Laboratories Inc. (Merseyside, U.K.). Forskolin and pertussis toxin were from Calbiochem (La Jolla, CA, U.S.A.) and Research Biochemical Inc. (Natick, MA, U.S.A.), respectively. Staurosporine was from Kyowa Hakko Kogyo Co (Tokyo, Japan). Transducin $\beta\gamma$ subunits ($\beta\gamma_t$) and α subunit in the GDP-bound form (α_{tGDP}), each purified from bovine retina, were kindly provided by Dr Heidi E. Hamm, Northwestern University, Chicago, IL, U.S.A.. Stock solutions of $\beta\gamma_t$ and α_{tGDP} were made in a storing buffer containing 50% glycerol, 75 mM Tris-HCl, 3.75 mM DTT, 75 μM phenylmethanesulfonyl fluoride (pH 7.3). Dilutions were made in 10 fold diluted storing buffer containing 0.1% BSA immediately before the experiments.

Results

Effects of (−)-baclofen on adenylyl cyclase activity of different layers of main olfactory bulb

As shown in Table 1, the addition of 1 mM (−)-baclofen failed to affect adenylyl cyclase activity of olfactory nerve-glomerular layer. Conversely, in the external plexiform layer and in the granule cell layer, (−)-baclofen stimulated basal adenylyl cyclase activity by 27.7 and 42.6%, respectively. As the stimulatory effect was higher in the granule cell layer, the characterization of the stimulatory effect was performed in tissue samples microdissected from this layer.

Effects of GABA receptor agonists on basal adenylyl cyclase activity

As illustrated in Figure 1A, the stimulatory effect of (−)-baclofen was saturable and concentration-dependent with a pD_2 value of 4.53 ± 0.03. The $GABA_B$ receptor agonist 3-aminopropylphosphinic acid (3-APA) (Hills *et al*., 1989) mimicked the stimulatory effect of (−)-baclofen with a pD_2 of 4.60 ± 0.10. Its maximal stimulation corresponded to approximately 80% of that of (−)-baclofen. Conversely, the less active enantiomer (+)-baclofen (Bowery, 1993) and 3-aminopropylphosphonic acid (3-APPA) were without effects at concentrations up to 1 mM. The stimulation of adenylyl cyclase activity was also observed with GABA ($pD_2 = 3.56 \pm 0.08$), but not with the selective $GABA_A$ receptor agonists muscimol and isoguvacine (Figure 1B).

Effects of $GABA_B$ receptor antagonists

As shown in Figure 2, the adenylyl cyclase stimulation elicited by (−)-baclofen was progressively shifted to the right by increasing concentrations of the $GABA_B$ receptor antagonists CGP 35348 and CGP 55845 A (Bittiger *et al*., 1993). Schild plot analysis of the antagonism yielded a pA_2 value of 4.31 ± 0.06 and a slope of 0.96 ± 0.03 for CGP 35348 and a pA_2 of 7.0 ± 0.2 and a slope of 0.92 ± 0.4 for CGP 55845 A. 2-Hydroxysaclofen, tested at the concentration of 300 μM, counteracted the (−)-baclofen stimulation with a pK_i of 4.22 ± 0.10, whereas phaclofen was inactive at the concentration of 1 mM (results not shown). *Per se*, none of the antagonists tested had effects on basal adenylyl cyclase activity.

Effects of agents affecting phospholipid metabolism

Neither quinacrine (200 μM), a non selective inhibitor of phospholipase A_2, nor indomethacin (10 μM) and nordihy-

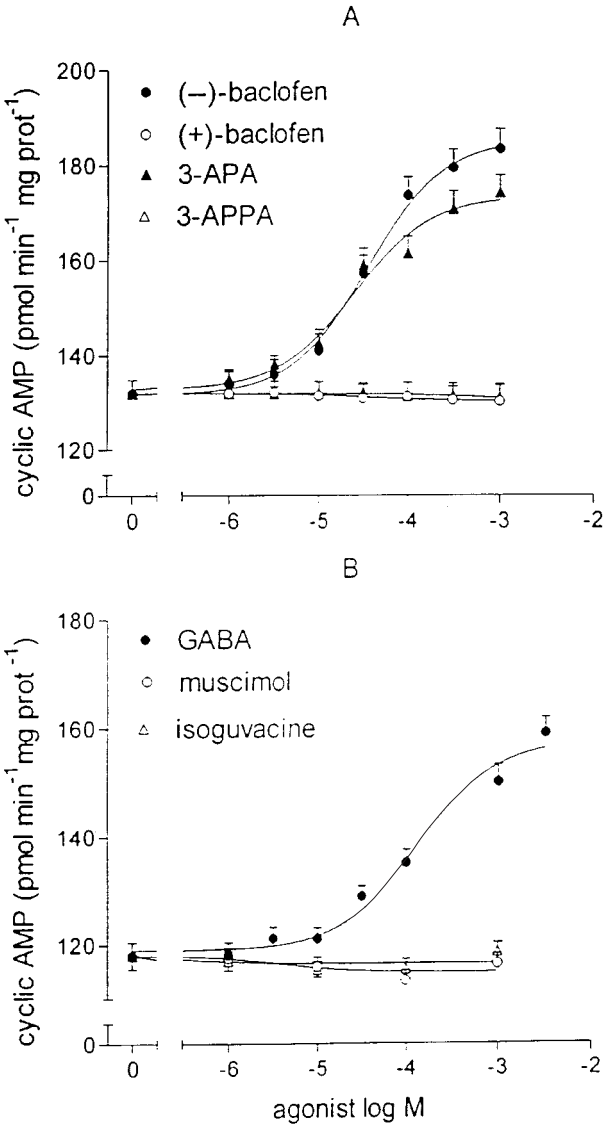

Figure 1 Effects of GABA receptor agonists on adenylyl cyclase activity in membranes of rat olfactory bulb granule cell layer. Data are the mean, and vertical lines show s.e.mean, of 3–5 experiments. 3-APA, 3-aminopropylphosphinic acid; 3-APPA, 3-aminopropylphosphonic acid.

Table 1 Effects of (−)-baclofen on adenylyl cyclase activity of different layers of rat olfactory bulb

Membrane source	n	*Adenylyl cyclase* (pmol min^{-1} mg $protein^{-1}$) *Control*	*(−)-baclofen* (1 mM)
Olfactory nerve-glomerular layer	3	50.1 ± 1.8	51.0 ± 1.5
External plexiform layer	5	82.5 ± 2.3	105.4 ± 2.9*
Granule cell layer	5	120.5 ± 3.8	171.9 ± 4.1*

N = number of determinations. Each experiment was performed on a separate tissue preparation. *$P < 0.001$.

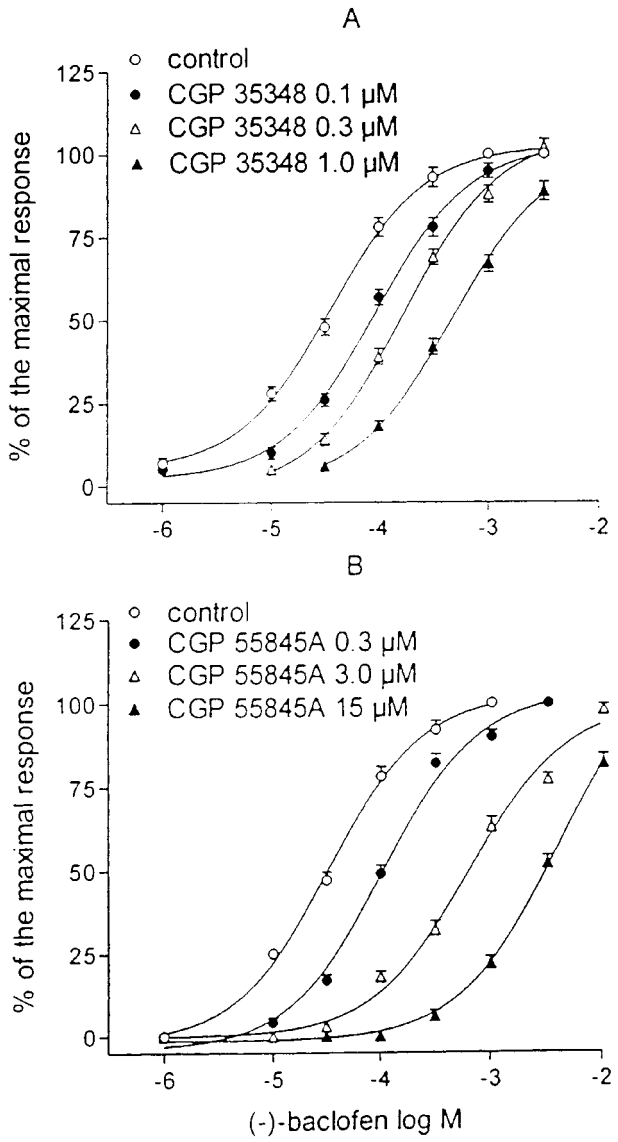

Figure 2 Antagonism of (−)-baclofen-induced stimulation of adenylyl cyclase by CGP 35348 and CGP 55845 A. The enzyme activity stimulated by (−)-baclofen was assayed in the presence of either vehicle (control) or antagonist at the indicated concentrations. Data are the mean, and vertical lines show s.e.mean, of three experiments for each antagonist.

droguaiaretic acid (10 μM), two inhibitors of arachidonic acid metabolism *via* cyclooxygenase and lipoxygenase pathways, respectively, affected the (−)-baclofen stimulation of adenylyl cyclase activity (results not shown). Incubation of membranes with the phorbol ester PMA (1 μM) increased basal adenylyl cyclase activity by 55.5±3.5% and this effect was completely prevented by the coaddition of the protein kinase inhibitor staurosporine (0.5 μM). However, at the same concentration staurosporine did not affect the stimulatory effect of 1 mM (−)-baclofen (results not shown).

Effects of the intracerebral injection of pertussis toxin

As shown in Figure 3, the intrabulbar injection of pertussis toxin completely prevented the adenylyl cyclase stimulation elicited by 1 mM (−)-baclofen. The toxin treatment, however, failed to affect the enzyme stimulation elicited by the β-adrenergic agonist isoproterenol (10 μM).

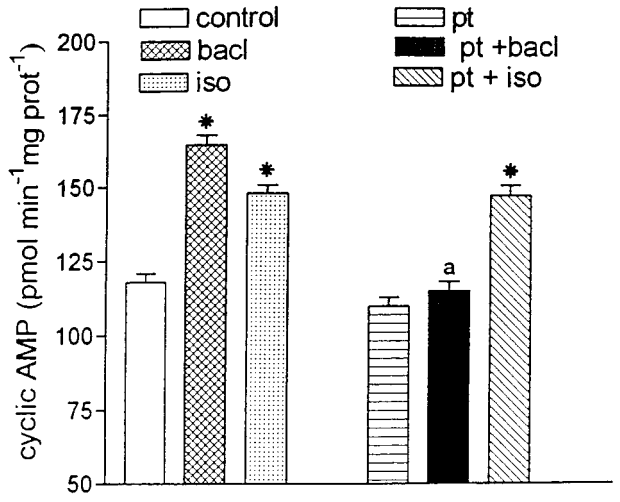

Figure 3 Effects of treatment of rat olfactory bulb with pertussis toxin (pt) on the stimulation of adenylyl cyclase activity by either 1 mM (−)-baclofen (bacl) or 10 μM isoproterenol (iso). Data are the mean, and vertical lines show s.e.mean, of three experiments performed on three separate tissue preparations. $*P<0.001$ vs basal activity; a not significantly different from basal.

Effects of α_{tGDP} and $\beta\gamma_t$

Preincubation of tissue membranes with increasing concentrations of α_{tGDP}, a scavenger of G protein $\beta\gamma$ subunits (Federman *et al.*, 1992), resulted in a progressive reduction of the adenylyl cyclase stimulation by 1 mM (−)-baclofen (Figure 4) At the concentration of 1.5 μM, α_{tGDP} reduced the enzyme stimulation by 75.4±5.0%. Basal adenylyl cyclase activity was slightly reduced by the exposure to α_{tGDP} (~15% reduction at 1.5 μM). On the other hand, incubation of tissue membranes with $\beta\gamma_t$ (0.4 μM) caused a 2 fold stimulation of adenylyl cyclase activity (Figure 5). In membranes pretreated with $\beta\gamma_t$ the addition of 1 mM (−)-baclofen failed to produce a further increase in adenylyl cyclase activity.

Effects of (−)-baclofen on PACAP stimulation of adenylyl cyclase activity

The neuropeptide PACAP 38 (10 nM) increased the adenylyl cyclase activity of olfactory nerve-glomerular layer, external plexiform layer and granule cell layer by 220±7, 150±5 and 80±3%, respectively ($n=3$). The addition of (−)-baclofen (1 mM) failed to affect the PACAP-stimulated enzyme activity in the olfactory nerve-glomerular layer, but potentiated it by 22.5±2.0 and 26.0±3.0% ($P<0.01$, $n=3$) in the external plexiform and granule cell layers, respectively. As shown in Figure 6A, in membranes of granule cell layer (−)-baclofen enhanced the maximal stimulation of the enzyme activity by PACAP 38 without significantly changing the potency of the neuropeptide (pD_2 values were: control 9.74±0.09, (−)-baclofen 9.79±0.10). Moreover, the concurrent stimulation of adenylyl cyclase by PACAP 38 (0.1 nM) resulted in a marked amplification of the stimulatory effect elicited by (−)-baclofen (Figure 6B).

Effects of (−)-baclofen on forskolin- and Ca^{2+}/CaM-stimulated adenylyl cyclase activities

The diterpene forskolin (10 μM) stimulated adenylyl cyclase activity of olfactory nerve-glomerular layer, external plexiform layer and granule cell layer by 17, 7.5 and 3.3 fold, respectively.

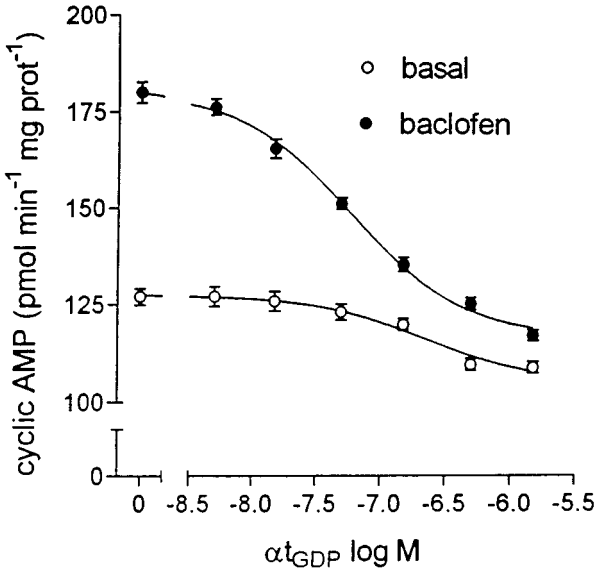

Figure 4 Effect of α_{tGDP} on (−)-baclofen stimulation of adenylyl cyclase activity in membranes of rat olfactory bulb. Tissue membranes were preincubated with the indicated final concentrations of α_{tGDP} for 60 min at ice-bath temperature. Thereafter, adenylyl cyclase activity was assayed in the absence and in the presence of 1 mM (−)-baclofen. Data are the mean, and vertical lines show s.e.mean, of three experiments.

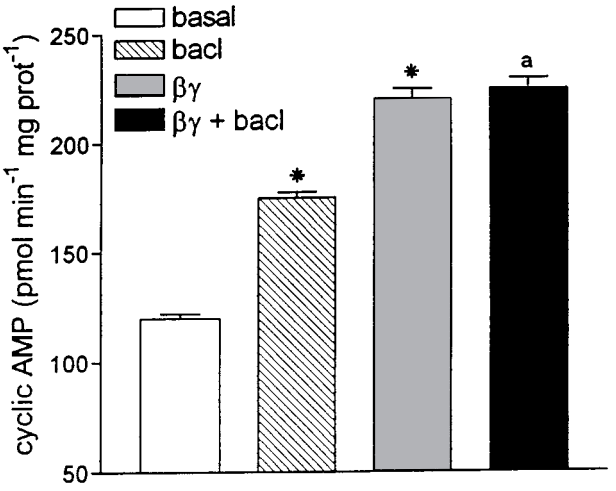

Figure 5 Lack of additivity of the stimulatory effects of $\beta\gamma_t$ and (−)-baclofen on adenylyl cyclase activity of olfactory bulb membranes. Tissue membranes were preincubated for 60 min at ice-bath temperature with either vehicle or $\beta\gamma_t$ at the final concentration of 0.4 μM. Thereafter, adenylyl cyclase activity was assayed in the absence and in the presence of 1 mM (−)-baclofen. Data are the mean, and vertical lines show the s.e.mean, of three experiments. *$P<0.001$ vs basal; [a]not significantly different from $\beta\gamma_t$ alone.

(−)-Baclofen (1 mM) inhibited the forskolin-stimulated enzyme activity by $18\pm2\%$ ($P<0.01$), $10.5\pm1.2\%$ ($P<0.05$) and $16.5\pm1.5\%$ ($P<0.01$) in olfactory nerve-glomerular layer, external plexiform layer and granule cell layer, respectively. The addition of Ca^{2+}/CaM (2 μM free Ca^{2+} and 2.5 μM CaM) enhanced the adenylyl cyclase activity by 290, 250 and 90% in olfactory nerve-glomerular layer, external plexiform layer and granule cell layer, respectively. (−)-Baclofen (1 mM) inhibited the Ca^{2+}/CaM-stimulated enzyme activity by $45\pm5\%$ in the granule cell layer and by $30\pm4\%$ in the other layers ($P<0.001$). As shown in Figure 7, the (−)-baclofen inhibition of Ca^{2+}/CaM-stimulated enzyme activity of the granule cell layer was concentration dependent with a pD_2 of 4.3 ± 0.1. (+)-Baclofen was completely inactive.

Discussion

The present study shows that baclofen causes stimulation of adenylyl cyclase activity in membranes of specific layers of the main olfactory bulb. The pharmacological profile of this response is consistent with the involvement of $GABA_B$ receptors. Thus, the enzyme stimulation displays a marked stereoselectivity to baclofen, with the (−)-enantiomer being the active and the (+)-enantiomer the inactive form (Bowery, 1993). The $GABA_A$ receptor agonists isoguvacine and muscimol fail to stimulate the enzyme activity, further demonstrating the specificity of the (−)-baclofen effect. Analysis of various functional responses has led to the identification of $GABA_B$ receptors with high- and low-affinity for baclofen (Wojcik & Holopainen, 1992). The potency of (−)-baclofen in stimulating adenylyl cyclase activity is in the micromolar range, suggesting the involvement of low-affinity $GABA_B$ receptors. The different pharmacological activity of two GABA analogues 3-aminopropylphosphinic acid and 3-aminopropylphosphonic acid, the first one stimulating adenylyl cyclase with an efficiency slightly lower than that of (−)-baclofen and the second one being completely inactive, agrees with that observed at $GABA_B$ receptors potentiating the β-adrenoceptors-induced stimulation of cyclic AMP accumulation in rat cortical slices (Scherer *et al*., 1988; Pratt *et al*., 1989).

The (−)-baclofen stimulation of adenylyl cyclase activity is antagonized in a concentration-dependent and surmountable manner by the selective $GABA_B$ receptor antagonists CGP 35348 and CGP 55485 A. Both compounds yield Schild plots with slope factors close to unity, indicating a competitive type of inhibition. In terms of absolute values, the antagonist potencies are close to those previously reported to block $GABA_B$ receptors coupled to cyclic AMP regulation in the brain (Knight & Bowery, 1996; Cunningham & Enna, 1996). Also the potency of 2-hydroxysaclofen in antagonizing the (−)-baclofen stimulatory effect ($pK_i=4.2$) agrees with the reported affinity for $GABA_B$ receptors (Bowery, 1993). The lack of blockade by a high concentration of phaclofen (1 mM) indicates that the receptors are insensitive to this drug. Phaclophen-insensitive $GABA_B$ receptors coupled to cyclic AMP have previously been described in rat cortical slices (Scherer *et al*., 1988; Robinson *et al*., 1989).

The (−)-baclofen stimulation of adenylyl cyclase is not affected by quinacrine, indomethacin and nordihydroguaiaretic acid, indicating that in membranes this effect occurs independently of phospholipase A_2 activation and arachidonic acid metabolism. The protein kinase C stimulator PMA causes a significant stimulation of adenylyl cyclase activity and this effect is completely blocked by the protein kinase inhibitor staurosporine, indicating that a protein kinase C-catalyzed phosphorylation can affect cyclic AMP formation. However, staurosporine has no effect on the (−)-baclofen stimulatory effect, ruling out the involvement of protein kinase C.

In vivo treatment with pertussis toxin completely prevents the (−)-baclofen stimulation of adenylyl cyclase activity. This finding correlates with the previous observation that pertussis toxin prevents not only the inhibitory (Xu & Wojcik, 1986) but also the facilitatory effects of $GABA_B$ receptors on cyclic AMP formation (Wojcik *et al*., 1989). The pertussis toxin sensitivity of the $GABA_B$ receptor-mediated stimulation suggests the

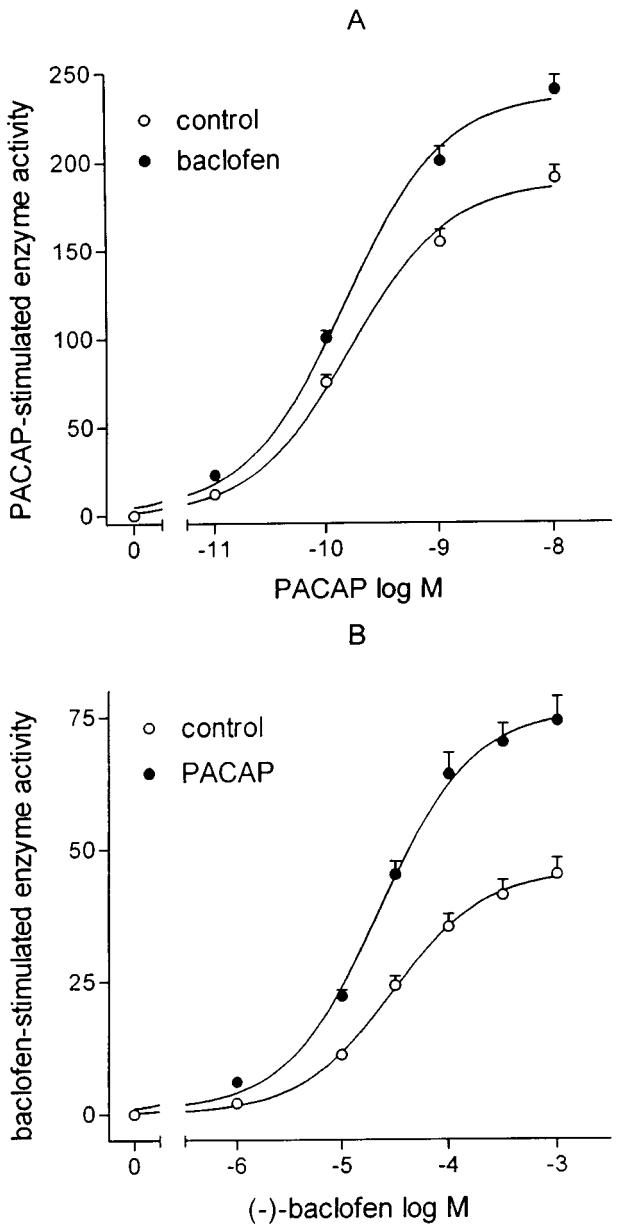

Figure 6 (A) Concentration-dependent stimulation of adenylyl cyclase activity of granule cell layer by PACAP 38 in the absence (control) and in the presence of 1 mM (−)-baclofen. Data are the mean, and vertical lines show the s.e.mean, of three experiments and represent the net stimulation of enzyme activity (reported as pmol cyclic AMP min^{-1} mg^{-1} protein) elicited by PACAP above control values. Control values were: basal 115±3, (−)-baclofen (1 mM) 160±4 pmol cyclic AMP min^{-1} mg^{-1} protein. $P<0.01$ for the difference between the curves by analysis of variance (B): Concentration-dependent stimulation of adenylyl cyclase activity by (−)-baclofen in the absence (control) and in the presence of 0.1 nM PACAP. Data are the mean, and vertical lines show the s.e.mean, of three experiments and represent the net stimulation of enzyme activity (reported as pmol cyclic AMP min^{-1} mg^{-1} protein) elicited by (−)-baclofen above control values. Control values were: basal 112±2, 0.1 nM PACAP 175±4 pmol cyclic AMP min^{-1} mg^{-1} protein. $P<0.01$ for the difference between the curves by analysis of variance.

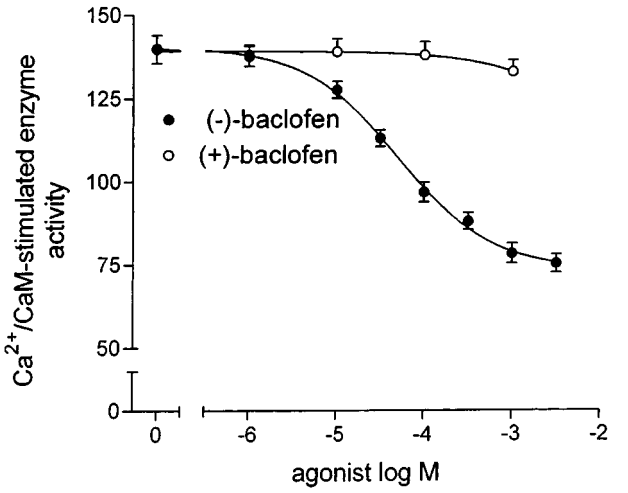

Figure 7 Concentration-dependent inhibition of Ca^{2+} CaM-stimulated adenylyl cyclase activity of granule cell layer by (−)-baclofen and lack of effect by (+)-baclofen. Data are the mean, and vertical lines show the s.e.mean, of three experiments and represent the net stimulation of enzyme activity (reported as pmol cyclic AMP min^{-1} mg^{-1} protein) elicited by the addition of 2.0 μM free Ca^{2+} and 2.5 μM CaM. The concentration of free Ca^{2+} was obtained with an EGTA/Ca^{2+} buffer and was calculated with a computer program (EQCAL, Biosoft, U.K.).

possibility that this response occurs through the release of $\beta\gamma$ subunits from G_i/G_o and the activation of type II/IV adenylyl cyclase isoforms (Tang & Gilman, 1992). We found that the (−)-baclofen stimulation of adenylyl cyclase is markedly reduced by the addition of α_{tGDP}, a $\beta\gamma$ scavenger (Federman *et al.*, 1992). Moreover, exogenously added $\beta\gamma$ subunits of transducin increase the enzyme activity and this effect is not additive with that produced by (−)-baclofen. Because the $\beta\gamma$-induced stimulation of type II/IV adenylyl cyclases is amplified when the enzymes are concomitantly activated by G_s (Tang & Gilman, 1992), we investigated whether $GABA_B$ receptors could enhance the cyclic AMP formation elicited by G_s-coupled neurotransmitter receptors. We found that (−)-baclofen significantly potentiates the stimulation of adenylyl cyclase elicited by PACAP 38, a neurotransmitter that acts through G_s-linked receptors (Olianas & Onali, 1996b). The concurrent activation of PACAP receptors also results in a marked amplification of the (−)-baclofen stimulatory effect, as expected in the case of a synergistic interaction between $\beta\gamma$ subunits and G_s. Taken together, these observations indicate that the positive coupling of $GABA_B$ receptors to cyclic AMP is mediated through $\beta\gamma$ subunits which then activate type II/IV adenylyl cyclases, two enzyme isoforms expressed in the olfactory bulb (Feinstein *et al.*, 1991; Olianas *et al.*, 1998).

As $GABA_B$ receptors have been found to inhibit forskolin-stimulated cyclic AMP formation in the brain (Hill & Dolphin, 1984; Karbon & Enna, 1985), it was important to see whether (−)-baclofen could elicit the same response in the olfactory bulb. It was found that (−)-baclofen inhibits the forskolin-stimulated adenylyl cyclase activity in each layer examined. However, the extent of the maximal inhibition is modest (10–18%), possibly because forskolin stimulates all isoforms of adenylyl cyclase (Tang & Gilman, 1992), including types II and IV which may be stimulated by (−)-baclofen. We therefore examined the effect of (−)-baclofen on the enzyme activity stimulated by Ca^{2+}/CaM, which activates cyclase isoforms I, III and VIII but is inactive on types II and IV (Sunahara *et al.*, 1996). Previous studies have shown that types I and III are expressed in rat olfactory bulb (Xia *et al.*, 1991; Glatt & Snyder, 1993). The Ca^{2+}/CaM-stimulated enzyme activity is inhibited by (−)-baclofen to a greater extent than the forskolin-stimulated activity in each microdissected tissue layer examined. The inhibition occurs at the same agonist

concentrations required to cause the stimulatory effect and is stereospecific. Thus, as previously observed in brain slices (Hill & Dolphin, 1984; Karbon & Enna, 1985), $GABA_B$ receptors can either stimulate or inhibit adenylyl cyclase. This dual control may provide a mechanism by which $GABA_B$ receptors can enhance the signalling of G_s-linked neurotransmitter receptors regulating Ca^{2+}-insensitive adenylyl cyclases and inhibit the Ca^{2+}/CaM-dependent cyclic AMP formation induced by Ca^{2+}-mobilizing neurotransmitters. Interestingly, whereas the inhibitory effect displays a wide distribution in the olfactory bulb, the enhancement of basal and G_s-stimulated adenylyl cyclase activities is only observed in the external plexiform and granule cell layers. Previous studies have demonstrated that in rat olfactory bulb $GABA_B$ receptors are more concentrated in the glomerular layer than in external plexiform and granule cell layers (Bowery *et al*., 1987; Chu *et al*., 1990). Thus, the distribution of the positive coupling to cyclase is not a function of the receptor density but likely depends on the colocalization at specific synaptic sites of $GABA_B$ receptors, G_i/G_o, G_s-linked receptors and type II/IV adenylyl cyclases. While this study was in progress, Uezono *et al*. (1997) reported that in Xenopus oocytes expressing rat brain cortex poly (A)+ RNA and cRNA for type II adenylyl cyclase baclofen induced a $\beta\gamma$-mediated stimulation of cyclic AMP production. To our knowledge, the present study provides the first evidence that in brain membranes, where receptors, G proteins and effector molecules are expressed in native conditions, activation of $GABA_B$ receptors stimulate adenylyl cyclase activity through $\beta\gamma$ subunits.

We are grateful to Dr H.E. Hamm, Northwestern University, Chicago, U.S.A. for the gift of transducin subunits and to Dr W. Froestl, CIBA-GEIGY, Basel, Switzerland, for providing us with CGP 35348 and CGP 55845 A.

References

ARUNLAKSHANA, O. & SCHILD, H.O. (1959). Some quantitative uses of drug antagonists. *Br. J. Pharmacol. Chemother.,* **14,** 48–57.

BITTIGER, H., FROESTL, W., MICKEL, S.J. & OLPE, H.-R. (1993). $GABA_B$ receptor antagonists: from synthesis to therapeutic application. *Trends Pharmacol. Sci.,* **14,** 391–393.

BOWERY, N.G. (1993). $GABA_B$ receptor pharmacology. *Annu. Rev. Pharmacol. Toxicol.,* **33,** 109–147.

BOWERY, N.G., HUDSON, A.L. & PRICE, G.W. (1987). $GABA_A$ and $GABA_B$ receptor site distribution in the rat central nervous system. *Neuroscience,* **20,** 365–383.

BRADFORD, M.M. (1976). A rapid and sensitive method for the quantitation of microgram quantities of protein utilizing the principle of protein-dye binding. *Anal. Biochem.,* **72,** 248–254.

CHU, D.C.M., ALBIN, R.L., YOUNG, A.B. & PENNEY, J.B. (1990). Distribution and kinetics of $GABA_B$ binding sites in rat central nervous system: a quantitative autoradiographic study. *Neuroscience,* **34,** 341–357.

CUNNINGHAM, M.D. & ENNA, S.J. (1996). Evidence for pharmacologically distinct $GABA_B$ receptors associated with cAMP production in rat brain. *Brain Res.,* **720,** 220–224.

DUMAN, R.S., KARBON, E.W., HARRINGTON, C. & ENNA, S.J. (1986). An examination of the involvement of phospholipases A_2 and C in the α-adrenergic and γ-aminobutyric acid receptor modulation of cyclic AMP accumulation in rat brain slices. *J. Neurochem.,* **47,** 800–810.

ENNA, S.J. & KARBON, E.W. (1984). $GABA_B$ receptors and transmitter-stimulated cAMP accumulation in rat brain. *Neuropharmacology,* **23,** 821–822.

ENNA, S.J. & KARBON, E.W. (1987). Receptor regulation: evidence for a relationship between phospholipid metabolism and neurotransmitter receptor-mediated cAMP formation in brain. *Trends Pharmacol. Sci.,* **8,** 21–24.

FEDERMAN, A.D., CONKLIN, B.R., SCHRADER, K.A., RANDALL, R.R. & BOURNE, H.R. (1992). Hormonal stimulation of adenylyl cyclase through G_i protein $\beta\gamma$ subunits. *Nature,* **356,** 159–161.

FEINSTEIN, P.G., SCHRADER, K.A., BAKALAYAR, H.A., TANG, W.-J., KRUPINSKI, J., GILMAN, A.G. & REED, R.R. (1991). Molecular cloning and characterization of a Ca^{2+}/calmodulin-insensitive adenylyl cyclase from rat brain. *Proc. Natl. Acad. Sci. USA,* **88,** 10173–10177.

GLATT, C.E. & SNYDER, S.H. (1993). Cloning and expression of an adenylyl cyclase localized to the corpus striatum. *Nature,* **361,** 536–538.

HILL, D.R. & DOLPHIN, A.C. (1984). Modulation of adenylate cyclase activity by $GABA_B$ receptors. *Neuropharmacology,* **23,** 829–830.

HILLS, J.M., DINGSDALE, R.A., PARSONS, M.E., DOLLE, R.E. & HOWSON, W. (1989). 3-Aminopropylphosphinic acid–a potent, selective $GABA_B$ receptor agonist in the guinea-pig ileum and rat anococcygeus muscle. *Br. J. Pharmacol.,* **97,** 1292–1296.

KARBON, E.W. & ENNA, S.J. (1985). Characterization of the relationship between γ-aminobutyric acid B agonists and transmitter-coupled cyclic nucleotide-generating systems in rat brain. *Mol. Pharmacol.,* **27,** 53–59.

KAUPMANN, K., HUGGEL, K., HEID, J., FLOR, P.J., BISCHOFF, S., MICKEL, S.J., MCMASTER, G., ANGST, C., BITTIGER, H., FROESTL, W. & BETTLER, B. (1997). Expression cloning of $GABA_B$ receptors uncovers similarity to metabotropic glutamate receptors. *Nature,* **386,** 239–246.

KNIGHT, A.R. & BOWERY, N.G. (1996). The pharmacology of adenylyl cyclase modulation by $GABA_B$ receptors in rat brain slices. *Neuropharmacology,* **35,** 703–712.

MALCANGIO, M. & BOWERY, N.G. (1995). Possible therapeutic application of $GABA_B$ receptor agonists and antagonists. *Clin. Neuropharm.,* **18,** 285–305.

MORISHITA, R., KATO, K. & ASANO, T. (1990). $GABA_B$ receptors couple to G proteins G_0, G_0* and G_{11} but not to G_{12}. *FEBS Lett.,* **271,** 231–235.

OLIANAS, M.C. & ONALI, P. (1993). Synergistic interaction of muscarinic and opioid receptors with G_s-linked neurotransmitter receptors to stimulate adenylyl cyclase activity of rat olfactory bulb. *J. Neurochem.,* **61,** 2183–2190.

OLIANAS, M.C. & ONALI, P. (1996a). Positive coupling of $GABA_B$ receptors to adenylyl cyclase in rat olfactory bulb. *Proc. Soc. Neurosci.,* **22,** 1293.

OLIANAS, M.C. & ONALI, P. (1996b). Characterization of the G protein involved in the muscarinic stimulation of adenylyl cyclase of rat olfactory bulb. *Mol. Pharmacol.,* **49,** 22–29.

OLIANAS, M.C., INGIANNI, A. & ONALI, P. (1998). Role of G protein $\beta\gamma$ subunits in muscarinic receptor-induced stimulation and inhibition of adenylyl cyclase activity in rat olfactory bulb. *J. Neurochem.,* **70,** 2620–2627.

PRATT, G.D., KNOTT, C., DAVEY, R. & BOWERY, N.G. (1989). Characterization of 3-aminopropyl phosphinic acid (3-APPA) as a $GABA_B$ agonist in rat brain tissue. *Br. J. Pharmacol.,* **96,** 141P.

ROBINSON, T.N., CROSS, A.J., GREEN, A.R., TOCZEK, J.M. & BOAR, B.R. (1989). Effects of the putative antagonists phaclofen and δ-aminovaleric acid on $GABA_B$ receptor biochemistry. *Br. J. Pharmacol.,* **98,** 833–840.

SALOMON, Y., LONDOS, C. & RODBELL, M. (1974). A highly sensitive adenylate cyclase assay. *Anal. Biochem.,* **58,** 541–548.

SCHAAD, N.C., SCHORDERET, M. & MAGISTRETTI, P.J. (1989). Accumulation of cyclic AMP elicited by vasoactive intestinal peptide is potentiated by noradrenaline, histamine, adenosine, baclofen, phorbol esters, and ouabain in mouse cerebral cortical slices: studies on the role of arachidonic acid metabolites and protein kinase C. *J. Neurochem.,* **53,** 1941–1951.

SCHERER, R.W., FERKANY, J.W. & ENNA, S.J. (1988). Evidence for pharmacologically distinct subsets of $GABA_B$ receptors. *Brain Res. Bull.,* **21,** 439–443.

SCHERER, R.W., FERKANY, J.W., KARBON, E.W. & ENNA, S.J. (1989). γ-Aminobutyric $acid_B$ receptor activation modifies agonist binding to β-adrenergic receptors in rat brain cerebral cortex. *J. Neurochem.,* **53,** 989–991.

SUNAHARA, R.K., DESSAUER, C.W. & GILMAN, A.G. (1996). Complexity and diversity of mammalian adenylyl cyclases. *Annu. Rev. Pharmacol. Toxicol.,* **36,** 461–480.

TALLARIDA, R.J. & MURRAY, R.B. (1987). Manual of Pharmacologic Calculations with Computer Programs. Springer-Verlag, New York.

TANG, W.-J. & GILMAN, A.G. (1992). Adenylyl Cyclases. *Cell,* **70,** 869–872.

UEZONO, Y., UEDA, Y., UENO, S., SHIBUYA, I., YANAGIHARA, N., TOYOHIRA, Y., YAMASHITA, H. & IZUMI, F. (1997). Enhancement by baclofen of the G_s-coupled receptor-mediated cAMP production in Xenopus oocytes expressing rat brain cortex poly(A)+ RNA: a role of G-protein $\beta\gamma$ subunits. *Biochem. Biophys. Res. Comm.,* **241,** 476–480.

WATLING, K.J. & BRISTOW, D.R. (1986). $GABA_B$ receptor-mediated enhancement of vasoactive intestinal peptide-stimulated cyclic AMP production in slices of rat cerebral cortex. *J. Neurochem.,* **46,** 1756–1762.

WOJCIK, W.J. & HOLOPAINEN, I. (1992). Role of central $GABA_B$ receptors in physiology and pathology. *Neuropsychopharmacology,* **6,** 201–214.

WOJCIK, W.J. & NEFF, N.H. (1984). γ-Aminobutyric acid B receptors are negatively coupled to adenylate cyclase in brain, and in the cerebellum these receptors may be associated with granule cells. *Mol. Pharmacol.,* **25,** 24–28.

WOJCIK, W.J., ULIVI, M., PAEZ, X. & COSTA, E. (1989). Islet-activating protein inhibits the β-adrenergic receptor facilitation elicited by γ-aminobutyric $acid_B$ receptors. *J. Neurochem.,* **53,** 753–758.

XIA, Z., REFSDAL, C.D., MERCHANT, K.M., DORSA, D.M. & STORM, D.R. (1991). Distribution of mRNA for the calmodulin-sensitive adenylyl cyclase in rat brain: expression in areas associated with learning and memory. *Neuron,* **6,** 431–443.

XU, J. & WOJCIK, W.J. (1986). γ-Aminobutyric $acid_B$ receptor-mediated inhibition of adenylate cyclase in cultured cerebellar granule cells: blockade by islet activating protein. *J. Pharmacol. Exp. Ther.,* **239,** 568–573.

(Received June 22, 1998
Revised October 30, 1998
Accepted November 9, 1998)

British Journal of Pharmacology (1999) 126, 665–672
http://www.stockton-press.co.uk/bjp

Agonist-inverse agonist characterization at CB_1 and CB_2 cannabinoid receptors of L759633, L759656 and AM630

[1]Ruth A. Ross, [1]Heather C. Brockie, [1]Lesley A. Stevenson, [1]Vicki L. Murphy, [1]Fiona Templeton, [2,3]Alexandros Makriyannis and *,[1]Roger G. Pertwee

[1]Department of Biomedical Sciences, Institute of Medical Sciences, University of Aberdeen, Foresterhill, Aberdeen AB25 2ZD, Scotland; [2]Department of Pharmaceutical Sciences, University of Connecticut, Storrs, Connecticut 06268, U.S.A.; [3]Department of Molecular & Cell Biology, University of Connecticut, Storrs, Connecticut 06268, U.S.A.

1 We have tested our prediction that AM630 is a CB_2 cannabinoid receptor ligand and also investigated whether L759633 and L759656, are CB_2 receptor agonists.

2 Binding assays with membranes from CHO cells stably transfected with human CB_1 or CB_2 receptors using [^{3}H]-CP55940, confirmed the CB_2-selectivity of L759633 and L759656 (CB_2/CB_1 affinity ratios = 163 and 414 respectively) and showed AM630 to have a K_i at CB_2 receptors of 31.2 nM and a CB_2/CB_1 affinity ratio of 165.

3 In CB_2-transfected cells, L759633 and L759656 were potent inhibitors of forskolin-stimulated cyclic AMP production, with EC_{50} values of 8.1 and 3.1 nM respectively and CB_1/CB_2 EC_{50} ratios of >1000 and >3000 respectively.

4 AM630 inhibited [^{35}S]-GTPγS binding to CB_2 receptor membranes ($EC_{50} = 76.6$ nM), enhanced forskolin-stimulated cyclic AMP production in CB_2-transfected cells (5.2 fold by 1 μM), and antagonized the inhibition of forskolin-stimulated cyclic AMP production in this cell line induced by CP55940.

5 In CB_1-transfected cells, forskolin-stimulated cyclic AMP production was significantly inhibited by AM630 (22.6% at 1 μM and 45.9% at 10 μM) and by L759633 at 10 μM (48%) but not 1 μM. L759656 (10 μM) was not inhibitory. AM630 also produced a slight decrease in the mean inhibitory effect of CP55940 on cyclic AMP production which was not statistically significant.

6 We conclude that AM630 is a CB_2-selective ligand that behaves as an inverse agonist at CB_2 receptors and as a weak partial agonist at CB_1 receptors. L759633 and L759656 are both potent CB_2-selective agonists.

Keywords: Cannabinoid CB_1 and CB_2 receptors; AM630; L759633; L759656; CB_2-selective ligands; CB_2-selective agonist; CB_2-selective inverse agonist; [^{35}S]-GTPγS; cyclic AMP

Abbreviations: AM630, 6-iodopravadoline; BSA, bovine serum albumin; CHO, Chinese hamster ovary; CP55940, (−)-3-[2-hydroxy-4-(1,1-dimethylheptyl)phenyl]-4-(3-hydroxypropyl)cyclohexan-1-ol; IBMX, 3-isobutyl-1-methylxanthine; L759633, (6aR,10aR)-3-(1,1-dimethyl-heptyl)-1-methoxy-6,6,9-trimethyl-6a,7,10,10a-tetrahydro-6H-benzo[c]chromene; L759656, (6aR,10aR)-3-(1,1-dimethyl-heptyl)-1-methoxy-6,6-dimethyl-9-methylene-6a,7,8,9,10,10a-hexahydro-6H-benzo[c]chromene; SR141716A, N-(piperidin-1-yl)-5-(4-chlorophenyl)-1-(2,4-dichlorophenyl)-4-methyl-1H-pyrazole-3-carboxamide hydrochloride; SR144528, N-[(1S)-endo-1,3,3-trimethyl bicyclo [2.2.1] heptan-2-yl]-5-(4-chloro-3-methylphenyl)-1-(4-methylbenzyl)-pyrazole-3-carboxamide; WIN55212-2, (*R*)-(+)-[2,3-dihydro-5-methyl-3-[(4-morpholino)methyl]pyrrolo-[1,2,3-de]-1,4-benzoxazin-6-yl](1-naphthyl)methanone

Introduction

Many cannabinoid effects are now known to be mediated by CB_1 receptors that are present in the central nervous system as well as in certain neuronal and nonneuronal peripheral tissues or by CB_2 receptors that are found mainly in cells of the immune system (Pertwee, 1997). Both receptor types are coupled to their effector systems through $G_{i/o}$ proteins (Pertwee, 1997). These discoveries have led to the development of selective ligands for CB_1 and CB_2 receptors. Particularly important have been SR141716A, which behaves as a selective CB_1 receptor inverse agonist (Bouaboula *et al*., 1997; MacLennan *et al*., 1998) and SR144528, which behaves as a selective CB_2 receptor inverse agonist (Rinaldi-Carmona *et al*., 1998).

A less well characterized cannabinoid receptor ligand is 6-iodopravadoline (AM630) (Figure 1). This has been shown to be a selective, competitive antagonist of certain cannabinoid receptor agonists in the mouse isolated *vas deferens* (Pertwee *et al*., 1995) but to possess the properties of a weak cannabinoid CB_1 receptor agonist in the myenteric plexus-longitudinal muscle preparation of guinea-pig small intestine (Pertwee *et al*., 1996). There are also reports that AM630 attenuates cannabinoid-induced stimulation of [^{35}S]-GTPγS binding to mouse and guinea-pig brain membrane preparations (Hosohata *et al*., 1997a,b) and that it behaves as an inverse agonist in Chinese hamster ovary (CHO) cells stably transfected with CB_1 receptors (Landsman *et al*., 1998).

Although there is now good evidence that AM630 is a CB_1 receptor ligand, the question remains as to whether it also interacts with CB_2 receptor, and if so whether it is a CB_2 receptor agonist, antagonist or inverse agonist. Our prediction was that AM630 would be a CB_2 receptor ligand as it is a structural analogue of WIN55212-2, a cannabinoid receptor agonist that is already known to have some degree of selectivity for the CB_2 receptor (Felder *et al*., 1995; Showalter *et al*., 1996). In this investigation we first compared the ability of AM630 to bind to CB_1 and CB_2 receptors and then

* Author for correspondence; E-mail: rgp@aberdeen.ac.uk

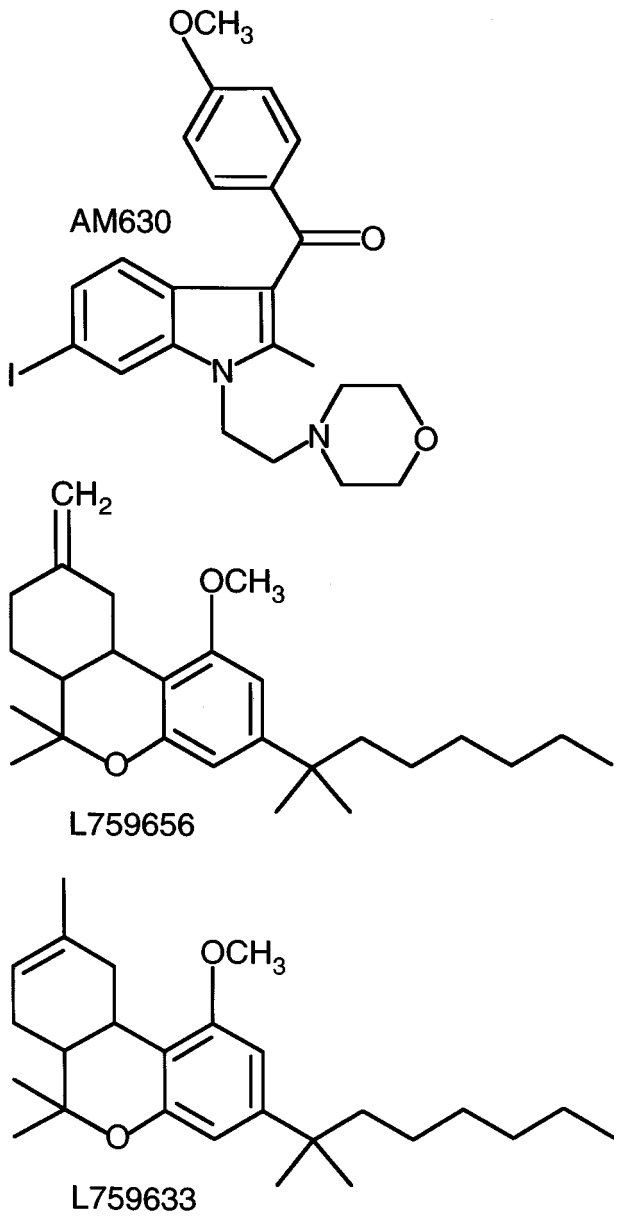

Figure 1 Structures of AM630, L759656 and L759633.

attempted to establish whether it shows agonist, antagonist or inverse agonist activity at each of these receptor types. The pharmacological properties of two other putative cannabinoid receptor ligands were also investigated in the present study. These are L759633 and L759656 (Figure 1), both of which have been reported to have a markedly higher affinity for human CB_2 than human CB_1 receptors (Gareau *et al*., 1996). However, no other information about these compounds has yet been published. Since there is a need for CB_2-selective agonists for use as pharmacological tools, we carried out experiments to establish whether either of these compounds show significant efficacy at CB_1 and/or CB_2 receptors.

Binding assays were performed with membrane preparations of CB_1- or CB_2-transfected CHO cells. The radioactive probe used in most of our binding experiments was [^{3}H]-CP55940, which binds equally well to CB_1 and CB_2 receptors (Showalter *et al*., 1996). The functional assays used exploited the well-established ability of cannabinoid receptor agonists to inhibit forskolin-stimulated cyclic AMP production and of cannabinoid receptor agonists and inverse agonists to modulate [^{35}S]-GTPγS binding (Pertwee, 1997; MacLennan *et al*., 1998). These assays were carried out with CHO cells stably transfected with CB_1 or CB_2 receptors.

Methods

CHO cells

These were stably transfected with cDNA encoding human CB_1 or CB_2 receptors. The CB_1-transfected cells used in binding assays with [^{3}H]-CP55940 or [^{3}H]-WIN55212-2 were supplied by Euroscreen, Brussels ($B_{max} = 23.8$ pmol mg^{-1} protein) and were a gift from Organon. The CB_2-transfected cells used in binding assays with [^{3}H]-CP55940, [^{3}H]-WIN55212-2 or [^{35}S]-GTPγS ($B_{max} = 72.5$ pmol mg^{-1} protein) and the CB_1- and CB_2-transfected cells used in cyclic AMP assays ($B_{max} = 3.5$ pmol mg^{-1} protein and 50.7 pmol mg^{-1} protein respectively) were provided by Drs G. Disney and A. Green, GlaxoWellcome R&D, Medicines Research Centre, Stevenage. Untransfected CHO cells were a gift from Dr Min Zhao, University of Aberdeen. The clones used in cyclic AMP assays were the same as those used in the sPAP reporter assay described by Green *et al*. (1998). Cells were maintained at 37°C and 5% CO_2 in DMEM (f-12 HAM) with 2 mM Glutamine, Geneticin (600 μg ml^{-1}) and Hygromycin (300 μg ml^{-1}). Because receptor overexpression may lead to the activation of effector mechanisms to which receptors in natural membranes are not normally coupled (see Kenakin, 1995), the cyclic AMP assays were performed with cells expressing fewer CB_1 or CB_2 receptors than the cells used in the binding assays.

Membrane preparation

CHO cells were suspended in 50 mM Tris buffer (pH 7.4) and 0.32 M sucrose and homogenized with an Ultra-Turrex homogenizer. The homogenate was diluted with 50 mM Tris buffer (pH 7.4) and centrifuged at 50,000 × *g* for 1 h to isolate the membranes.

Binding experiments

A filtration procedure was used to measure [^{3}H]-CP55940 and [^{3}H]-WIN55212-2 binding. This is a modification of the method described by Compton *et al*. (1993). Binding assays were performed with [^{3}H]-CP55940 or [^{3}H]-WIN55212-2, 1 mM $MgCl_2$, 1 mM EDTA, 2 mg ml^{-1} bovine serum albumin (BSA) and 50 mM Tris buffer, total assay volume 500 μl. Binding was initiated by the addition of cell membranes (20–30 μg protein). Assays were carried out at 30°C for 90 min before termination by addition of ice-cold wash buffer (50 mM Tris buffer, 1 mg ml^{-1} BSA) and vacuum filtration using a 12-well sampling manifold (Brandel Cell Harvester) and Whatman GF/B glass-fibre filters that had been soaked in wash buffer at 4°C for 24 h. Each reaction tube was washed three times with a 4 ml aliquot of buffer. The filters were oven-dried for 60 min and then placed in 5 ml of scintillation fluid (Ultima Gold XR, Packard). Radioactivity was quantified by liquid scintillation spectrometry. Specific binding was defined as the difference between the binding that occurred in the presence and absence of 1 μM unlabelled cannabinoid. Protein assays were performed using a Bio-Rad Dc kit. Unlabelled and radiolabelled cannabinoids were each added in a volume of 50 μl following dilution in assay buffer (50 mM Tris buffer containing 10 mg ml^{-1} BSA). The concentration of [^{3}H]-CP55940 or [^{3}H]-WIN55212-2 used in displacement assays was 0.5 nM. The concentrations of cannabinoids that produced

a 50% displacement of radioligand from specific binding sites (IC_{50} values) were calculated using GraphPad Prism (GraphPad Software, San Diego, U.S.A.). Competitive binding curves were fitted with minimum values for displacement of radioligand from specific binding sites constrained to zero. Dissociation constant (K_i values) were calculated using the equation of Cheng & Prusoff (1973) and dissociation constant values of [^{3}H]-CP55940 and [^{3}H]-WIN55212-2 shown in the footnote to Table 1.

Cyclic AMP assay

Cells (2×10^6 cells ml^{-1}) were preincubated for 30 min at 37°C with cannabinoid and 3-isobutyl-1-methylxanthine (IBMX; 50 μM) in phosphate buffered saline containing 1 mg ml^{-1} BSA (assay buffer) followed by a further 30 min incubation with 2 μM forskolin in a total volume of 500 μl. The reaction was terminated by addition 0.1 M HCl and centrifuged to remove cell debris. The pH was brought to 8–9 using 1 M NaOH and cyclic AMP content was then measured using a radioimmunoassay kit (Biotrak, Amersham). Forskolin and IBMX were dissolved in DMSO.

[^{35}S]-GTPγS assay

CB_2 transfected cells were removed from flasks by scraping, resuspended in homogenization buffer (0.32 M sucrose and 50 mM Tris), and homogenized using an ultra-Turrex homogenizer. The homogenate was diluted with Tris buffer (50 mM, pH 7.4) and centrifuged at 50,000 $\times g$ for 45 min. Cell membranes (20 μg) were incubated in assay buffer containing 2 mg ml^{-1} fatty acid free BSA, 20 μM GDP and 0.1 nM [^{35}S]-GTPγS. The assay buffer contained 50 mM Tris, 10 mM $MgCl_2$, 100 mM NaCl and 0.2 mM EDTA at pH 7.4. Incubations were carried out at 30°C for 90 min in a total volume of 500 μl. The reaction was terminated by the addition of 4 ml of ice-cold wash buffer (50 mM Tris and 1 mg ml^{-1} BSA, pH 7.4) followed by rapid filtration under vacuum through Whatman GF/B glass-fibre filters (pre-soaked in wash buffer) using a 12-tube Brandel cell harvester. The tubes were washed three times with 4 ml of wash buffer. Filters were oven dried, placed in 5 ml of scintillation fluid and bound radioactivity was determined by liquid scintillation counting. Basal binding of [^{35}S]-GTPγS was determined in the presence of 20 μM GDP and absence of cannabinoid. Non-specific binding was determined in the presence of 10 μM GTPγS.

Analysis of data

Values have been expressed as means and variability as s.e.mean or as 95% confidence limits. Mean values have been compared using the Kruskall-Wallis test followed by Dunn's multiple comparison test. A P value <0.05 was considered to be significant. Effects of test compounds on forskolin-stimulated cyclic AMP production have been expressed in percentage terms. This was calculated from the equation $[100 \times (f' - b)]/(f - b)$ where f′, f and b are values of cyclic AMP production (pmol ml^{-1}), f′ in the presence of forskolin and the test compound, f in the presence of forskolin only and b in the absence of both forskolin and the test compound. Drug-induced inhibition of specific [^{35}S]-GTPγS binding was expressed as the percentage decrease below the basal level of [^{35}S]-GTPγS binding using the equation $[100 \times (d' - d)]/d$ where d′ and d are d.p.m. in the presence and absence of the drug respectively. Values for EC_{50}, IC_{50} and maximal effects (E_{max}) and the 95% confidence limits of these values have been calculated by non-linear regression analysis using GraphPad Prism (GraphPad Software, San Diego, U.S.A.).

The ability of AM630 to antagonize CP55940-induced inhibition of forskolin-stimulated cyclic AMP production in CB_2 transfected cells is expressed in terms of the concentration ratio. This has been defined as the concentration of CP55940 that produces a particular degree of inhibition in the presence of AM630 at a concentration, B, divided by the concentration of CP55940 that produces an identical degree of inhibition in the absence of AM630. Since AM630 behaved as an inverse agonist at CB_2 receptors (see Results), it was considered inappropriate to insert concentration ratio values into the Schild equation in order to obtain a K_B value of AM630 at these receptors. Concentration ratio values and their 95% confidence limits have been determined by symmetrical (2 + 2) dose parallel line assays (Colquhoun, 1971), using responses to pairs of agonist concentrations located on the steepest part of each log concentration-response curve. This method was also used to establish whether log concentration-response curves of CP55940 constructed in the presence and absence of AM630 deviated significantly from parallelism.

Drugs

CP55940 {(−)-3-[2-hydroxy-4-(1,1-dimethylheptyl)phenyl]-4-(3-hydroxypropyl)cyclohexan-1-ol} was supplied by Pfizer, WIN55212-2 {(R)-(+)-[2,3-dihydro-5-methyl-3-[(4-morpholino)methyl]pyrrolo-[1,2,3-de]-1,4-benzoxazin-6-yl](1-naphthyl)-methanone} by Research Biochemicals International, SR141716A [N-(piperidin-1-yl)-5-(4-chlorophenyl)-1-(2,4-dichlorophenyl)-4-methyl-1H-pyrazole-3-carboxamide hydrochloride] and SR144528 {N-[(1S)-endo-1,3,3-trimethyl bicyclo [2.2.1] heptan-2-yl]-5-(4-chloro-3-methylphenyl)-1-(4-methylbenzyl)-pyrazole-3-carboxamide} by Sanofi Recherche and L759633 [(6aR,10aR)-3-(1,1-dimethyl-heptyl)-1-methoxy-6,6,9-trimethyl-6a,7,10,10a -tetrahydro -6H-benzo[c]chromene] and L759656 [(6aR,10aR)-3-(1,1-dimethyl-heptyl)-1-methoxy-6,6-dimethyl-9-methylene - 6a,7,8,9,10,10a-hexahydro-6H-benzo[c]chromene] by Merck Frosst. AM630 (6-iodopravadoline) was synthesized in the laboratory of Dr A. Makriyannis. [^{3}H]-CP55940 (126 Ci mmol^{-1}) and [^{3}H]-WIN55212-2 (45 Ci mmol^{-1}) were supplied by NEN Life Science Products. Cannabinoids were stored as 1 mg ml^{-1} stock solutions in ethanol and diluted in assay buffer. At the highest concentrations used, ethanol by itself had no detectable effect on specific binding of [^{3}H]-CP55940, [^{3}H]-WIN55212-2 or [^{35}S]-GTPγS or on forskolin-stimulated cyclic AMP production (data not shown).

Results

Cannabinoid binding experiments

The radioligand binding data shown in Table 1 confirm that CP55940 is a high-affinity non-selective ligand for cannabinoid receptors. The data also confirm L759656 and L759633 to be markedly CB_2-selective, with much lower K_i values in CB_2 transfected cell membranes than in membranes of CB_1 transfected cells. AM630 is also CB_2-selective with a CB_1/CB_2 K_i ratio of 165 in transfected CHO cell membranes. Further experiments showed AM630 to be no less effective in displacing [^{3}H]-CP55940 than [^{3}H]-WIN55212-2 from CB_2 receptors on CHO cell membranes (Table 1). SR144528 was also equally effective in displacing [^{3}H]-CP55940 and [^{3}H]-WIN55212-2 from CB_2 receptors (Table 1).

Table 1 K_i values of CP55940, WIN55212-2, L759656, L759633 and AM630 for displacement of [^{3}H]-CP55940 from CB_1 or CB_2 receptors on CHO cell membranes

Labelled cannabinoid	*Unlabelled cannabinoid*	*CB_1 K_i (nM)*	*CB_2 K_i (nM)*
[^{3}H]-CP55940	CP55940	5.0±0.8	1.8±0.2
	L759633	1043±296	6.4±2.2
	L759656	4888±950	11.8±2.5
	AM630	5152±567	31.2±12.4
	SR144528	>10 μM	5.6±1.1
[^{3}H]-WIN55212-2	AM630	–	37.5±15.4
	SR144528	–	4.1±1.3

K_i values were calculated by the Cheng & Prusoff equation ($n=3$ or 4) using K_D values of 1.2 and 0.8 nM for [^{3}H]-CP55940 in membranes of CB_1 and CB_2 cells respectively and a K_D value of 2.1 nM for [^{3}H]-WIN55212-2 in membranes of CB_2 cells (Ross & Pertwee, unpublished).

Table 2 EC_{50} values for inhibition of forskolin-stimulated cyclic AMP production in CHO cells stably transfected with CB_1 or CB_2 receptors

Cannabinoid	*CB_1 EC_{50} (nM)*	*CB_2 EC_{50} (nM)*	*CB_1 EC_{50}/ CB_2 EC_{50}*
CP55940	2.6±1.0 (7)	2.9±1.4 (9)	0.9
L759633	ca 10 μM (6)	8.1±4.5 (3)	>1000
L759656	>10 μM (6)	3.1±0.6 (4)	>3000
AM630	>10 μM (4)	IA (4)	–
SR144528	>10 μM (3)	IA (4)	–

Forskolin-stimulated cyclic AMP production was normalized to 100% in the absence of cannabinoids. In CB_1-transfected cells, it fell to 52.0±10.0% in the presence of 10 μM L759633, a value significantly less than 100% ($P<0.01$; one-sample t-test) and to 85.7±11.7% in the presence of 10 μM L759656, a value not significantly less than 100% ($P>0.05$; one-sample t-test). Forskolin-stimulated cyclic AMP production in CB_1-transfected cells was not decreased significantly by L759633 or L759656 at concentrations of 100 nM or 1 μM (one-sample t-test). IA indicates that AM630 and SR144528 behaved as inverse agonists in CB_2-transfected cells.

Effects of CP55940, L759656, L759633 and AM630 on cyclic AMP production

Cyclic AMP concentrations in the absence and presence of 2 μM forskolin were 5.1±1.8 and 46.3±13.1 pmol ml^{-1} respectively in CB_1-transfected cells ($n=6$) and 5.6±2.6 and 52.8±11.7 pmol ml^{-1} respectively in CB_2-transfected cells ($n=6$). CP55940 was highly potent in inhibiting forskolin-stimulated cyclic AMP production in both CB_1- and CB_2-transfected cells (Table 2 and Figure 2). The CB_1/CB_2 EC_{50} ratio of 0.9 reflects the non-selective nature of this agonist. In contrast, L759633 and L759656 showed greater potency against forskolin-stimulated cyclic AMP production in CB_2-transfected cells than in CB_1-transfected cells (Table 2 and Figure 2). Indeed, forskolin-stimulated cyclic AMP production in CB_1-transfected cells was not significantly inhibited by L759656 and was only inhibited by L759633 at the highest concentration used (10 μM) (Table 2). The maximal inhibitory effects of CP55940, L759633 and L759656 on forskolin-stimulated cyclic AMP production in CB_2-transfected cells were not significantly different (Figure 2).

AM630 produced a significant inhibitory effect on cyclic AMP production in CB_1-transfected cells, albeit only at concentrations in the micromolar range (Figure 3). More specifically, AM630 concentrations of 1 and 10 μM caused forskolin-stimulated cyclic AMP production in this cell line to fall to 77.5±4.2% ($n=4$) and 54.1±12.4% ($n=8$) of the control value respectively (one-sample t-test). In CB_2-transfected cells, AM630 enhanced the ability of forskolin to stimulate cyclic AMP production at 0.1, 1 and 10 μM, the highest of these concentrations provoking an increase in cyclic AMP production of 5.5 fold (Figure 3). In the absence of forskolin, AM630 had no effect on cyclic AMP production by CB_1- or CB_2-transfected cells ($n=3$; data not shown). Forskolin-stimulated cyclic AMP production in untransfected CHO cells was affected neither by AM630 nor by L759633 or L759656 (data not shown).

Effect of AM630 on GTPγS binding and on CP55940-induced inhibition of cyclic AMP production

In CB_2-transfected cells, the ability of CP55940 to inhibit cyclic AMP production at concentrations of 1 μM or less was abolished by 1 μM AM630 which produced a non-parallel upward shift in the log concentration-response curve of the agonist (Figure 4). At the lower concentration of 100 nM, AM630 produced a significant dextral shift in the log concentration-response curve of CP55940 for inhibition of cyclic AMP production by CB_2-transfected cells that did not deviate significantly from parallelism (Figure 5). The mean value of this shift, with its 95% confidence limits shown in brackets, was 21.3 (3.5 and 649.4). Also shown in Figure 5 is the ability of the established CB_2 receptor antagonist, SR144528, to oppose CP55940-induced inhibition of cyclic AMP production by the same cell line. AM630 also shared the ability of SR144528 to produce a concentration-related inhibition of GTPγS binding to membranes from CB_2-transfected cells (Figure 6). It was 7.4 times less potent than SR144528. However, the maximum degree of inhibition produced by the two compounds was essentially the same.

A further set of experiments with CB_2-transfected cells (Figure 7), showed that inhibition of forskolin-stimulated cyclic AMP production by 10 nM CP55940 (85.5±3.4%; $n=5$) was concentration-dependently reversed by AM630. A 50% reversal was achieved by AM630 at a concentration (EC_{50}) of 128.6±40.6 nM ($n=5$). This is the mean concentration of AM630 that increased forskolin-stimulated cyclic AMP production by CB_2-transfected cells to a level midway between that observed in the presence of 10 nM CP55940 and that observed in the absence of this agonist. A similar method has been used by Rinaldi-Carmona *et al*. (1998) to calculate the concentration of SR144528 that produces a 50% reversal of CP55940-induced inhibition of forskolin-stimulated cyclic AMP production by CB_2-transfected cells.

In CB_1-transfected cells, 1 μM AM630 appeared to produce a 3 fold decrease in the potency of CP55940 for inhibition of forskolin-stimulated cyclic AMP production (Figure 4). However, this effect of AM630 was not statistically significant. Similarly, the inhibitory effect of 10 nM CP55940 on forskolin-stimulated cyclic AMP production by this cell line (89.4±5.6%; $n=4$) appeared to be slightly reversed by 1 μM AM630 although not by higher or lower concentrations of this compound (Figure 7). Again, this effect was not statistically significant. In contrast, it was possible to detect reversal of this inhibitory effect in CB_1-transfected cells by SR141716A. This compound produced a 50% reversal of the inhibitory effect of 10 nM CP55940 on forskolin-stimulated cyclic AMP production at 11.2±3.1 nM ($n=5$).

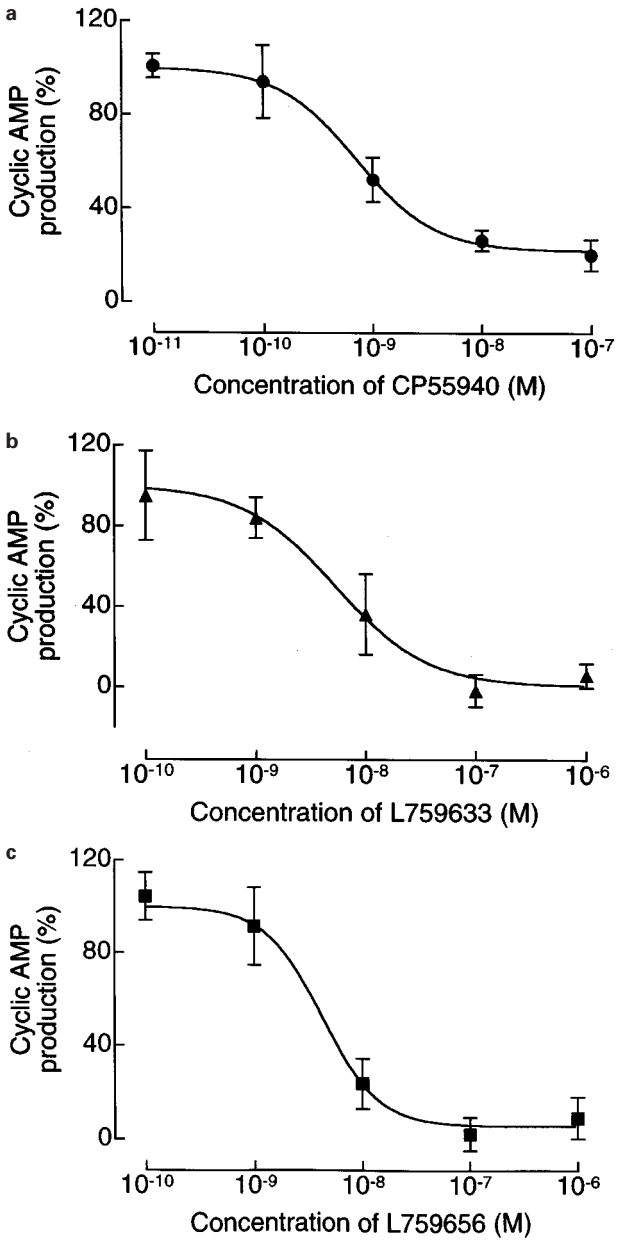

Figure 2 Inhibition by (a) CP55940 ($n=9$), (b) L759633 ($n=3$) and (c) L759656 ($n=4$) of forskolin-stimulated cyclic AMP production in CB_2-transfected CHO cells. Each symbol represents mean percentage change in forskolin-stimulated cyclic AMP production ± s.e.mean. Forskolin-stimulated cyclic AMP production in the absence of any cannabinoid has been normalized to 100%. Mean E_{max} values for CP55940, L759633 and L759656, with 95% confidence limits shown in brackets, were 21.9% (5.1 to 38.7), 0.5% (−25.3 to 26.3%) and 5.9% (−10.6 to 22.4%) respectively (GraphPad Prism).

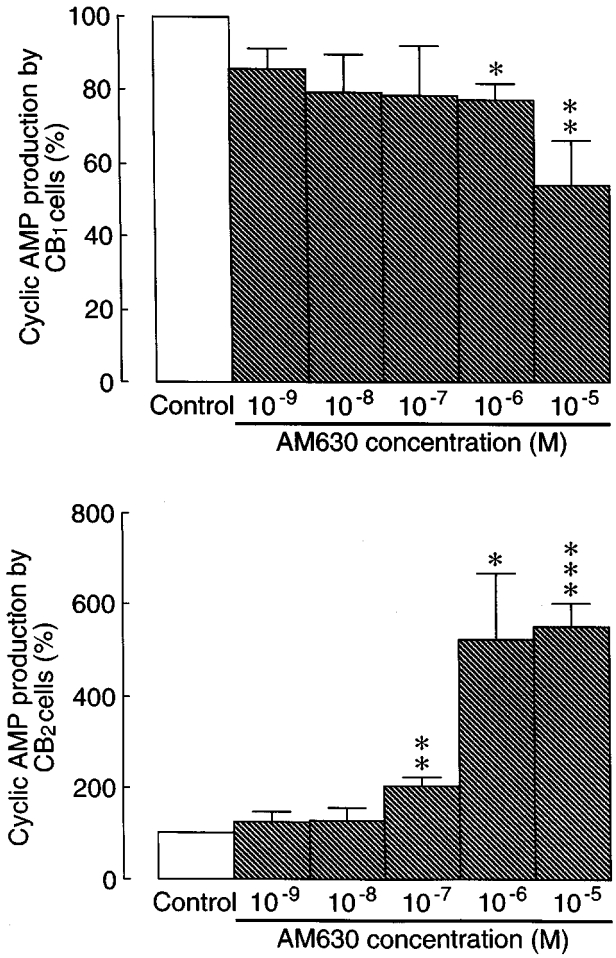

Figure 3 The effect of AM630 on forskolin-stimulated cyclic AMP production in CB_1 and CB_2-transfected CHO cells (± s.e.mean; $n=3$ to 8). Each column represents mean percentage change in forskolin-stimulated cyclic AMP production ± s.e.mean. Forskolin-stimulated cyclic AMP production in the absence of AM630 has been normalized to 100%. Asterisks indicate values significantly less than 100% ($^*P<0.05$; $^{**}P<0.01$; $^{***}P<0.001$; one-sample t-test). The mean EC_{50} value of AM630 for enhancement of forskolin-stimulated cyclic AMP production in the CB_2-transfected cells with its 95% confidence limits shown in brackets is 230.4 nM (48.4 and 1096 nM) (GraphPad Prism).

Discussion

The results obtained showed that L759633 and L759656 bind with higher affinity to CB_2 than CB_1 receptors. Although this confirms previously reported binding data for these compounds (Gareau *et al.*, 1996), the CB_2/CB_1 affinity ratios of L759633 and L759656 were both higher in the previous investigation (793 and >1000 respectively) than reported here (163 and 414 respectively). Consistent with their binding properties, both L759633 and L759656 were markedly more potent as inhibitors of forskolin-stimulated cyclic AMP production in CB_2- than CB_1-transfected cells. Indeed, the CB_1/CB_2 EC_{50} ratios of both compounds in this functional bioassay (>1000 and >3000 respectively) were somewhat greater than their CB_2/CB_1 affinity ratios. Our results also confirm previous reports that CP55940 is a cannabinoid receptor agonist that acts with more or less equal potency at CB_1 and CB_2 receptors (Felder *et al.*, 1995). The ability of L759633 and L759656 to behave as CB_2-receptor agonists has not been reported previously. Clearly, both compounds will be useful pharmacological tools for the study of cannabinoid receptor pharmacology.

AM630 bound to both CB_1 and CB_2 receptors with a CB_2/CB_1 affinity ratio of 165, indicating it to have a similar selectivity for CB_2 binding sites as L759656. Its affinity for CB_2 receptors was 2.6 times less than that of L759656. The K_i value obtained for AM630 in these experiments with CB_2-transfected cell membranes (31.2 nM) is similar to a previously reported K_i value of AM630 (11.2 nM) for displacement of [^{3}H]-CP55940 from a membrane preparation of mouse spleen (Pertwee, 1998), a tissue known to express CB_2 receptors (Munro *et al.*, 1993). Both these K_i values are similar to K_B values of AM630 reported by Pertwee *et al.* (1995) for antagonism of the inhibitory effects of CP55940 (17.3 nM) and WIN55212-2 (36.5 nM) on electrically-evoked contractions of the mouse

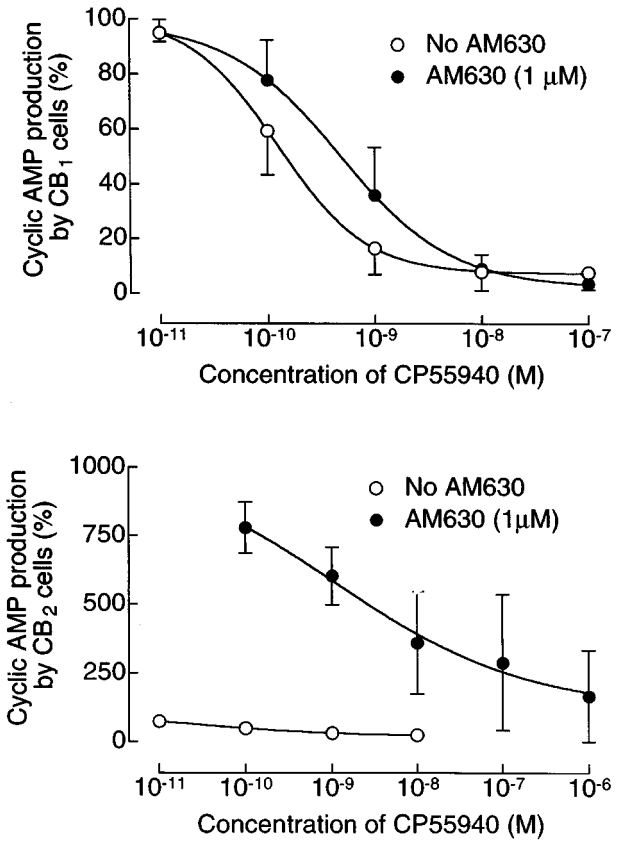

Figure 4 The effect of 1 μM AM630 on CP55940-induced inhibition of forskolin-stimulated cyclic AMP production in CB_1 and CB_2-transfected CHO cells. Each symbol represents mean percentage change in forskolin-stimulated cyclic AMP production $\pm$ s.e.mean ($n=3$). Forskolin-stimulated cyclic AMP production in the absence of AM630 and CP55940 has been normalized to 100%. Mean EC_{50} values of CP55940 in the CB_1-transfected cells with their 95% confidence limits shown in brackets are 0.5 nM (0.2 and 1.2 nM) in the presence of AM630 and 0.2 nM (0.1 and 0.4 nM) in its absence (GraphPad Prism).

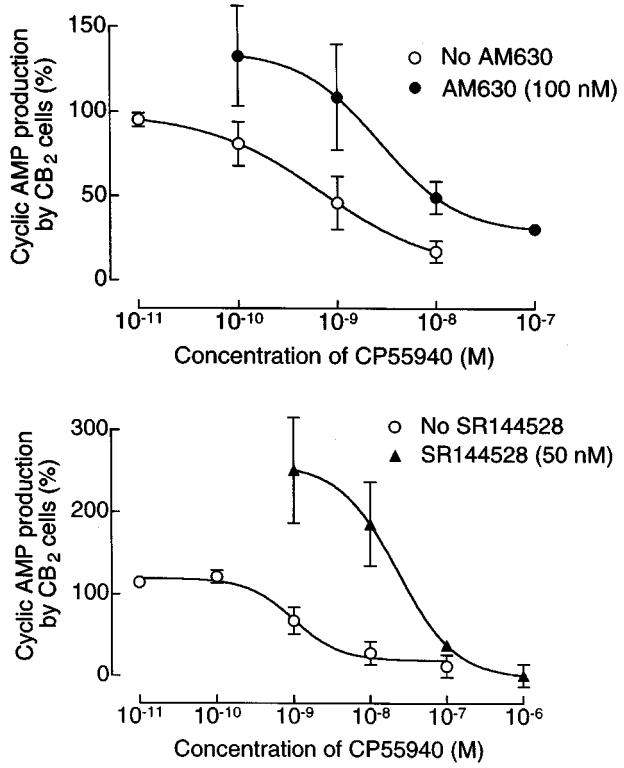

Figure 5 The effect of 100 nM AM630 or 50 nM SR144528 on CP55940-induced inhibition of forskolin-stimulated cyclic AMP production in CB_2-transfected CHO cells. Each symbol represents mean percentage change in forskolin-stimulated cyclic AMP production $\pm$ s.e.mean ($n=3$ or 4). Forskolin-stimulated cyclic AMP production in the absence of AM630, SR144528 and CP55940 has been normalized to 100%. The mean dextral shift in the log concentration-response curve of CP55940 produced by AM630 is 21.3 and its 95% confidence limits are 3.0 and 649.4 (symmetrical (2+2) dose parallel line assay). It did not deviate significantly from parallelism.

isolated *vas deferens*, possibly reflecting the presence in this tissue of CB_2-like cannabinoid receptors that can mediate twitch inhibition (Griffin *et al.*, 1997).

Unlike L759633 and L759656, AM630 did not inhibit forskolin-stimulated cyclic AMP production by CB_2-transfected cells. Instead, it readily reversed the ability of CP55940 to produce this inhibitory effect with an EC_{50} (128.6 nM) approximately one order of magnitude higher than the corresponding EC_{50} value (10 nM) of the established CB_2-selective antagonist, SR144528 (Rinaldi-Carmona *et al.*, 1998). In addition, AM630 alone produced a concentration-dependent enhancement of forskolin-stimulated cyclic AMP production by CB_2-transfected cells. Possibly, AM630 is antagonizing a CB_2 receptor agonist that is being spontaneously released by this cell line. Another possibility is that the CB_2-transfected cells contain constitutively active CB_2 receptors in equilibrium with inactive CB_2 receptors and that AM630 is an inverse agonist that binds preferentially to the receptors in the inactive state thereby decreasing the proportion of constitutively active receptors. A similar mechanism has been proposed to explain the ability of the CB_2 receptor antagonist, SR144528, to enhance forskolin-stimulated cyclic AMP production by CB_2-transfected cells (Rinaldi-Carmona *et al.*, 1998). In line with both suggested mechanisms is our finding that AM630 shares the ability of SR144528 to inhibit GTPγS binding to CB_2 receptors. Thus

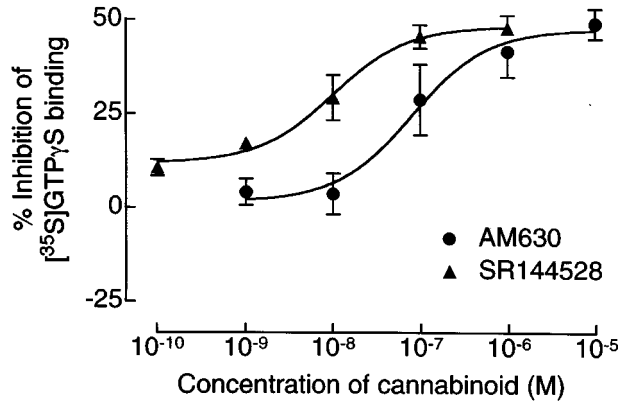

Figure 6 Effects of AM630 and SR144528 on specific binding of [^{35}S]-GTPγS to CB_2-transfected CHO cell membranes. Each symbol represents mean percentage decrease in binding $\pm$ s.e.mean ($n=3$ to 5). The mean EC_{50} values of AM630 and SR144528 for inhibition of [^{35}S]-GTPγS binding with their 95% confidence limits shown in brackets are 76.6 nM (16.5 and 356.2 nM) and 10.4 nM (3.6 and 29.7 nM) respectively. Corresponding values for the maximum degree of inhibition produced are 47.2 $\pm$ 5.8% and 48.5 $\pm$ 2.9% respectively (mean E_{max} values $\pm$ s.e.mean; non-linear regression analysis; GraphPad Prism).

CB_2 receptors are G protein coupled (Pertwee, 1997) and it is to be expected that the binding of GTPγS to G proteins will be stimulated by agonists for G protein-coupled receptors and

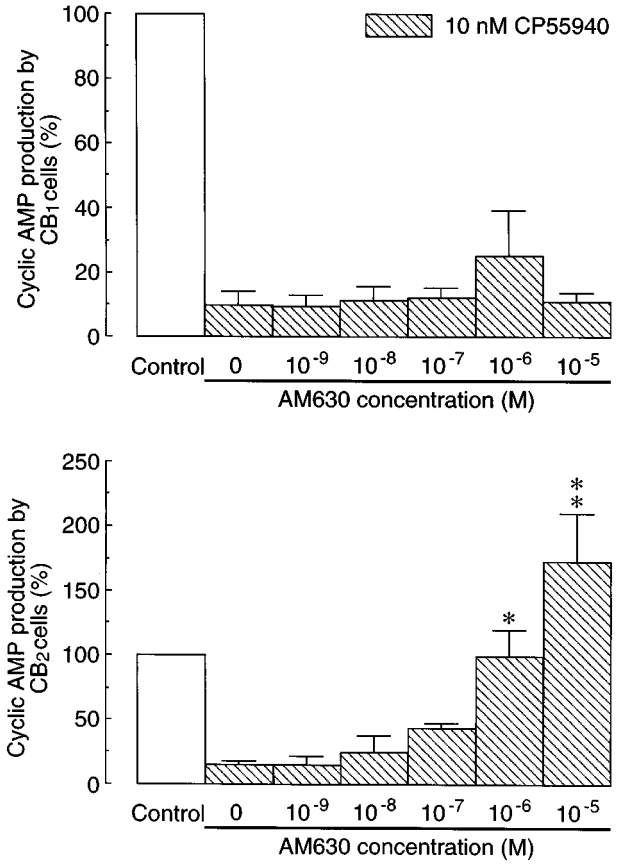

Figure 7 Effects of AM630 on inhibition of forskolin-stimulated cyclic AMP production by 10 nM CP55940 in CB_1- and CB_2-transfected CHO cells (±s.e.mean; $n=4$ to 6). Each column represents mean percentage change in forskolin-stimulated cyclic AMP production. Forskolin-stimulated cyclic AMP production in the absence of AM630 and CP55940 has been normalized to 100%. Asterisks indicate significant differences from forskolin-stimulated cyclic AMP production in the presence of CP55940 and absence of AM630 ($*P<0.05$; $**P<0.01$; Kruskall-Wallis test followed by Dunn's multiple comparison test).

inhibited by inverse agonists for such receptors (Bouaboula *et al*., 1997; Breivogel *et al*., 1997; MacLennan *et al*., 1998). A third possibility is that AM630-induced enhancement of cyclic AMP production in CB_2-transfected cells is mediated by G_s proteins. However, AM630 had no effect on cyclic AMP production by CB_2-transfected cells in the absence of forskolin. Moreover, although there is evidence that, under certain conditions, CB_1 receptors may be coupled to adenylate cyclase through G_s proteins, there is also evidence that CB_2 receptors are not (Glass & Felder, 1997).

Although AM630 antagonizes CP55940 in CB_2-transfected cells, it shares the ability of CP55940 to inhibit forskolin-stimulated cyclic AMP production by CB_1-transfected cells, albeit with an EC_{50} above 1 μM. This finding is consistent with a previous observation that AM630 behaves as a CB_1 receptor agonist in the myenteric plexus-longitudinal muscle preparation of guinea-pig small intestine with an EC_{50} value of 1.9 μM (Pertwee *et al*., 1996), a potency value that is reasonably close to the K_i of AM630 for displacement of [^{3}H]-CP55940 from CB_1-transfected cell membranes (Table 1). AM630 does not seem to behave as a CB_1 receptor agonist in all CB_1 receptor-containing preparations. Landsman *et al*. (1998) have reported that AM630 inhibits [^{35}S]-GTPγS binding to CB_1-transfected cell membranes with an EC_{50} of 0.9 μM. This effect is opposite in direction to that of CB_1 receptor agonists which stimulate [^{35}S]-GTPγS binding (Breivogel *et al*., 1997; MacLennan *et al*., 1998). Hosohata *et al*. (1997a,b) have found AM630 to antagonize cannabinoid-induced stimulation of [^{35}S]-GTPγS binding to mouse and guinea-pig brain membrane preparations with K_B values of 3.1 and 9.3 μM respectively. Thus it would seem that, depending on the CB_1 receptor-containing preparation used, AM630 can behave as a CB_1 receptor agonist, antagonist or inverse agonist. Further experiments are required to establish why this should be. It is noteworthy, however, that in the present investigation, a concentration of AM630 that inhibited forskolin-stimulated cyclic AMP production by CB_1-transfected cells when administered alone (1 μM), appeared to produce a dextral shift in the log concentration-response curve of CP55940 for inhibition of forskolin-stimulated cyclic AMP production by CB_1-transfected cells. This dextral shift was not statistically significant. However, this observation does raise the possibility that high concentrations of AM630 may produce a significant degree of antagonism in this cell line in which case AM630 would possess the mixed agonist-antagonist properties of a CB_1 partial agonist.

In conclusion, our results confirm L759633 and L759656 to have significantly higher affinity for CB_2 than CB_1 receptors (see Introduction). In addition, they show that both these compounds are potent, high-efficacy CB_2 receptor agonists, that L759656 lacks significant activity as a CB_1 receptor agonist and that although L759633 can activate CB_1 receptors, it does so only at micromolar concentrations that are above those at which it is capable of interacting with CB_2 receptors. The pharmacological properties of AM630 are more complex. Thus, we found AM630 to behave as an inverse agonist at CB_2 receptors but as a partial agonist at CB_1 receptors. Further experiments are required to establish the structural features of AM630 responsible for each of these actions.

This work was supported by grants 039538 and 047980 from the Wellcome Trust (to R.G.P. and R.A.R.) and by grants DA3801 (to A.M.) and DA9158 (to A.M. and R.G.P.) from the National Institute on Drug Abuse. We thank Organon for CB_1-transfected cells, GlaxoWellcome for CB_1- and CB_2-transfected cells, Merck Frosst for L759633 and L759656, Pfizer for CP55940 and Sanofi Recherche for SR141716A and SR144158.

References

BOUABOULA, M., PERRACHON, S., MILLIGAN, L., CANAT, X., RINALDI-CARMONA, M., PORTIER, M., BARTH, F., CALANDRA, B., PECCEU, F., LUPKER, J., MAFFRAND, J.-P., LE FUR, G. & CASSELLAS, P. (1997). A selective inverse agonist for central cannabinoid receptor inhibits mitogen-activated protein kinase activation stimulated by insulin or insulin-like growth factor 1. Evidence for a new model of receptor/ligand interactions. *J. Biol. Chem.*, **272,** 22330–22339.

BREIVOGEL, C.S., SIM, L.J. & CHILDERS, S.R. (1997). Regional differences in cannabinoid receptor G-protein coupling in rat brain. *J. Pharmacol. Exp. Ther.*, **282,** 1632–1642.

CHENG, Y.-C. & PRUSOFF, W.H. (1973). Relationship between the inhibition constant (K_I) and the concentration of inhibitor which causes 50 per cent inhibition (IC_{50}) of an enzymatic reaction. *Biochem. Pharmacol.*, **22,** 3099–3108.

COLQUHOUN, D. (1971). *Lectures on Biostatistics*. Oxford University Press., Oxford.

COMPTON, D.R., RICE, K.C., DE COSTA, B.R., RAZDAN, R.K., MELVIN, L.S., JOHNSON, M.R. & MARTIN, B.R. (1993). Cannabinoid structure-activity relationships: correlation of receptor binding and *in vivo* activities. *J. Pharmacol. Exp. Ther.,* **265,** 218 – 226.

FELDER, C.C., JOYCE, K.E., BRILEY, E.M., MANSOURI, J., MACKIE, K., BLOND, O., LAI, Y., MA, A.L. & MITCHELL, R.L. (1995). Comparison of the pharmacology and signal transduction of the human cannabinoid CB_1 and CB_2 receptors. *Mol. Pharmacol.,* **48,** 443 – 450.

GAREAU, Y., DUFRESNE, C., GALLANT, M., ROCHETTE, C., SAWYER, N., SLIPETZ, D.M., TREMBLAY, N., WEECH, P.K., METTERS, K.M. & LABELLE, M. (1996). Structure activity relationships of tetrahydrocannabinol analogues on human cannabinoid receptors. *Bioorg. Med. Chem. Letts.,* **6,** 189 – 194.

GLASS, M. & FELDER, C.C. (1997). Concurrent stimulation of cannabinoid CB1 and dopamine D2 receptors augments cAMP accumulation in striatal neurons: evidence for a G_s linkage to the CB1 receptor. *J. Neuroscience,* **17,** 5327 – 5333.

GREEN, A., O'SHAUGHNESSY, C., DISNEY, G., WHITTINGTON, A., REES, S., LEE, M. & MARSHALL, F. (1998). *Reporter assays for human cannabinoid CB_1 and CB_2 receptors for the identification of novel agonists*. Symposium on the Cannabinoids, Burlington, Vermont, International Cannabinoid Research Society, 102.

GRIFFIN, G., FERNANDO, S.R., ROSS, R.A., MCKAY, N.G., ASHFORD, M.L.J., SHIRE, D., HUFFMAN, J.W., YU, S., LAINTON, J.A.H. & PERTWEE, R.G. (1997). Evidence for the presence of CB_2-like cannabinoid receptors on peripheral nerve terminals. *Eur. J. Pharmacol.,* **339,** 53 – 61.

HOSOHATA, K., QUOCK, R.M., HOSOHATA, Y., BURKEY, T.H., MAKRIYANNIS, A., CONSROE, P., ROESKE, W.R. & YAMAMURA, H.I. (1997a). AM630 is a competitive cannabinoid receptor antagonist in the guinea pig brain. *Life Sci.,* **61,** PL115 – 118.

HOSOHATA, Y., QUOCK, R.M., HOSOHATA, K., MAKRIYANNIS, A., CONSROE, P., ROESKE, W.R. & YAMAMURA, H.I. (1997b). AM630 antagonism of cannabinoid-stimulated [^{35}S]GTPγS binding in the mouse brain. *Eur. J. Pharmacol.,* **321,** R1 – R3.

KENAKIN, T. (1995). Agonist-receptor efficacy I: mechanisms of efficacy and receptor promiscuity. *Trends Pharmacol. Sci.,* **16,** 188 – 192.

LANDSMAN, R.S., MAKRIYANNIS, A., DENG, H., CONSROE, P., ROESKE, W.R. & YAMAMURA, H.I. (1998). AM630 is an inverse agonist at the human cannabinoid CB1 receptor. *Life Sci.,* **62,** PL109 – PL113.

MACLENNAN, S.J., REYNEN, P.H., KWAN, J. & BONHAUS, D.W. (1998). Evidence for inverse agonism of SR141716A at human recombinant cannabinoid CB_1 and CB_2 receptors. *Br. J. Pharmacol.,* **124,** 619 – 622.

MUNRO, S., THOMAS, K.L. & ABU-SHAAR, M. (1993). Molecular characterization of a peripheral receptor for cannabinoids. *Nature,* **365,** 61 – 65.

PERTWEE, R.G. (1997). Pharmacology of cannabinoid CB_1 and CB_2 receptors. *Pharmacol. Ther.,* **74,** 129 – 180.

PERTWEE, R.G. (1998). Cannabinoid receptors and their ligands in brain and other tissues. In *Marihuana and Medicine*. ed. Nahas, G.G., Sutin, K.M. & Agurell, S., Totowa: Humana Press. (in press).

PERTWEE, R.G., FERNANDO, S.R., NASH, J.E. & COUTTS, A.A. (1996). Further evidence for the presence of cannabinoid CB_1 receptors in guinea-pig small intestine. *Br. J. Pharmacol.,* **118,** 2199 – 2205.

PERTWEE, R., GRIFFIN, G., FERNANDO, S., LI, X., HILL, A. & MAKRIYANNIS, A. (1995). AM630, a competitive cannabinoid receptor antagonist. *Life Sci.,* **56,** 1949 – 1955.

RINALDI-CARMONA, M., BARTH, F., MILLAN, J., DEROCQ, J.-M., CASSELLAS, P., CONGY, C., OUSTRIC, D., SARRAN, M., BOUABOULA, M., CALANDRA, B., PORTIER, M., SHIRE, D., BRELIERE, J.-C. & LE FUR, G. (1998). SR 144528, the first potent and selective antagonist of the CB2 cannabinoid receptor. *J. Pharmacol. Exp. Ther.,* **284,** 644 – 650.

SHOWALTER, V.M., COMPTON, D.R., MARTIN, B.R. & ABOOD, M.E. (1996). Evaluation of binding in a transfected cell line expressing a peripheral cannabinoid receptor (CB2): identification of cannabinoid receptor subtype selective ligands. *J. Pharmacol. Exp. Ther.,* **278,** 989 – 999.

(Received July 29, 1998
Revised November 9, 1998
Accepted November 10, 1998)

British Journal of Pharmacology (1999) 126, 673–680
http://www.stockton-press.co.uk/bjp

Suppression of nitric oxide synthase and the down-regulation of the activation of NFκB in macrophages by resveratrol

[1]Shu-Huei Tsai, [2]Shoei-Yn Lin-Shiau & *,[1]Jen-Kun Lin

[1]Institute of Biochemistry, College of Medicine, National Taiwan University, Taipei, Taiwan, R.O.C.; [2]Institute of Toxicology, College of Medicine, National Taiwan University, Taipei, Taiwan, R.O.C.

1 Resveratrol, naringenin and naringin are naturally occurring flavonoids in grapes and grapefruits. The anti-inflammatory effects of these flavonoids have been well documented, but the mechanism is poorly characterized. High concentration of NO are produced by inducible NO synthase (iNOS) in inflammation, and the prevention of the expression of iNOS may be an important anti-inflammatory mechanism. In this study, the effects of these flavonoids on the induction of NO synthase (NOS) in RAW 264.7 cells activated with bacterial lipopolysaccharide (LPS, 50 ng ml^{-1}) were investigated.

2 Resveratrol was found strongly to inhibit NO generation in activated macrophages, as measured by the amount of nitrite released into the culture medium, and resveratrol strongly reduced the amount of cytosolic iNOS protein and steady state mRNA levels. However, the inhibitory abilities of naringenin were lower, and the inhibitory abilities of naringin were almost negligible.

3 In electrophoretic mobility shift assays, the activation of NFκB induced by LPS for 1 h was inhibited by resveratrol (30 μM). Furthermore, in immunoblotting analysis, cells treated with LPS plus resveratrol showed an inhibition of phosphorylation as well as degradation of IκBα, and a reduced nuclear content of NFκB subunits.

4 The flavonoids may be of value for inhibiting the enhanced expression of iNOS in inflammation through down-regulation of NFκB binding activity.

Keywords: Resveratrol; flavonoids; inducible NO synthase; NFκB; RAW 264.7 monocyte/macrophages

Abbreviations: GAPDH, glyceraldehyde-3-phosphate dehydrogenase; IκB, inhibitor κB; iNOS, inducible nitric oxide synthase; LPS, lipopolysaccharide; NFκB, nuclear factor-κB; NO, nitric oxide; PCR, polymerase chain reaction; ROI, reactive oxygen intermediate; RT, reverse transcription

Introduction

Nitric oxide (NO) has a role in mediating macrophage cytotoxicity, regulating blood pressure, and in neurotransmission. NO is synthesized *in vivo* from L-arginine by nitric oxide synthase (NOS) with NADPH and oxygen as substrates. Molecular cloning and sequencing analysis has revealed that there are at least three main types of NOS isoforms. Two Ca^{2+}/calmodulin-dependent isoforms are constitutively expressed in the endothelium of blood vessel and the neuron of the brain. These isoforms synthesize small amounts of NO in response to various agonists that increase intracellular Ca^{2+}. The high output isoform, inducible-NOS (iNOS), is expressed in various cell types following its transcriptional induction (Nathan & Xie, 1994). Among the most important stimuli for induction of iNOS is bacterial endotoxic lipopolysaccharide (LPS) (Stuehr & Marletta, 1985; Ding *et al*., 1988). Low concentrations of NO produced by iNOS are likely to contribute much of the antimicrobial activity of macrophages against certain bacterial pathogens. However, high concentrations of NO and its derivatives, such as peroxynitrite and nitrogen dioxide, are found to play important roles in inflammation and in the multistage processes of carcinogenesis (Ohshima & Bartsch, 1994; Halliwell, 1994).

The promoter region of the mouse gene for iNOS has been characterized (Weisz *et al*., 1994). Several binding sites for transcription factors have been identified in the promoter region of the iNOS gene including NFκB, ISRE, IRF-1 and Oct (Lowenstein *et al*., 1993; Xie *et al*., 1993; Kamijo *et al*., 1994; Martin *et al*., 1994; Goldring *et al*., 1996). Of these transcription factors, only the activation of NFκB has been shown to mediate the enhanced expression of the iNOS gene in macrophages exposed to LPS (Xie *et al*., 1994). The NFκB is an inducible transcription factor originally identified as a hetrodimeric complex consisting of a 50 kDa subunit (p50) and a 65 kDa subunit (p65). A common feature of the regulation of transcription factors belonging to the Rel family is their sequestration in the cytoplasm as inactive complexes with a class of inhibitory molecules known as IκB (Baeuerle & Baltimore, 1996).

Resveratrol is a phytoalexin found in grapes and other plants. The flavonoid naringin is the abundant natural product from grapefruits and related citrus species. The aglycone, naringenin is readily formed from naringin after dietary intake in humans. It is conceivable that resveratrol possesses many biological activities that favour protection against atherosclerosis, including antioxidant activity, modulation of hepatic apolipoprotein and lipid synthesis, inhibition of platelet aggregation as well as the production of anti-atherogenic eicosanoids by human platelet and neutrophils (Soleas *et al*., 1997). In addition, a cancer chemotherapeutic activity of resveratrol has also been described (Jang *et al*., 1997). Naringenin is present in grapefruits mainly as its glycosylated form, naringin. Many biological functions of naringenin and naringin have been studied, including anti-inflammatory, antioxidative (Limasset *et al*., 1993), antimutagenic (Calomme *et al*., 1996) and anticarcinogenic effects (So *et al*., 1996). The

* Author for correspondence at: Institute of Biochemistry, College of Medicine, National Taiwan University, No. 1, Section 1, Jen-ai Road, Taipei, Taiwan, R.O.C.

anti-inflammatory and cancer-preventing characteristics of these flavonoids have been well documented. Nevertheless, how these effects are produced by these flavonoids is not well characterized.

In this study, we have examined the effects of these flavonoids on NO generation, cytosolic iNOS protein, steady state mRNA levels, and gene promoter activity through the translocation of transcription factor NFκB to nucleus. Taken together, these findings indicated that resveratrol could protect against endotoxin-induced inflammation by preventing the activation of NFκB.

Methods

Reagents

LPS (*Escherichia coli* 0127: E8), naringin, naringenin and resveratrol were purchased from Sigma Chemical (St Louis, MO, U.S.A.). Isotopes were obtained from Amersham (Arlington Heights, IL, U.S.A.). Polynucleotide kinase and oligo (dT)18 were obtained from Pharmacia (Piscataway, NJ, U.S.A.).

Cell culture

RAW 264.7 cells were cultured in RPMI-1640 (without phenol red) supplement with 10% endotoxin-free, heat-inactivated, foetal calf serum (GIBCO, Grand Island, NY, U.S.A.), supplemented with 100 units ml^{-1} penicillin, and 100 $\mu g\ ml^{-1}$ streptomycin. When the cells reached a density of $2-3\times10^6$ cells ml^{-1}, they were activated by incubation in medium containing *E. coli* LPS (50 ng ml^{-1}). Various concentrations of test compounds dissolved in DMSO were added together with LPS.

Nitrite assay

The nitrite concentration in the culture medium was measured as an indicator of NO production using the Griess reaction (Kim *et al*., 1995). One hundred microliters of each supernatant was mixed with the same volume of Griess reagent (1% sulphanilamide in 5% phosphoric acid and 0.1% naphthylethylenediamine dihydrochloride in water) and the absorbance of the mixture, at 550 nm, was determined with an enzyme-linked immunosorbent assay plate reader (Dynatech MR-7000; Dynatech Labs, Chantilly, VA, U.S.A.).

Western blots

Total cellular extract was prepared using radio-immunoprecipitation assay buffer (in mM): Tris-HCl (pH 7.4) 50, NaCl 150, 1% Triton X-100, 1% deoxycholate, 0.1% sodium dodecyl sulphate, 1% aprotinin). Total protein (for iNOS and α-tubulin), cytosolic fractions (for Sp1, IκBα, c-Re1, p65 and p50) or nuclear fractions (for Sp1,c-Rel, p65 and p50) containing $30-50$ μg of protein were separated on sodium dodecyl sulphate-polyacrylamide minigels (8% for iNOS, Sp1 and 10% for IκBα, c-Rel, p65 and p50) and transferred to Immobilon polyvinylidene difluoride membranes (Millipore, Bedford, MA, U.S.A.). The membranes were incubated overnight at 37°C with 10% bovine serum albumin in phosphate-buffered saline to block nonspecific immunoglobulins and then incubated with macNOS monoclonal antibody (Transduction Laboratories, Lexington, KY, U.S.A.), anti-IκBα, -c-Rel, -p65, -p50 or -Sp1 polyclonal antibodies (Santa Cruz Biochemicals, Santa Cruz, CA, U.S.A.), anti-phospho (Ser32)-specific IκBα (New England Biolabs, Bevery, MA, U.S.A.), or anti-α-tubulin monoclonal antibody (Oncogene Science, Cambridge, U.K.). iNOS, IκBα, p65, p50, c-Rel, Sp1 and α-tubulin protein were detected by chemiluminescence (ECL, Amersham), or by incubation with the coloregenic substrates: nitro blue tetrazolium (NBT) and 5-bromo-4-chloro-3-indolyl-phosphate (BCIP) as suggested by the manufacture (Sigma Chemical Co.).

RT–PCR and Northern blot

Following stimulation with LPS for 5 h, cells were washed in ice-cold PBS and total RNA was isolated by acid guanidinium thiocyanate-phenol-chloroform extraction (Chomczynski & Sacchi, 1987). Total RNA (5 μg) was converted to cDNA with 1 μM oligo(dT)18, 0.5 mM concentration of each dNTP, Tris-HCl (pH 8.3) (50 mM), KCl (75 mM), $MgCl_2$, (3 mM), 1 unit μl^{-1} RNase inhibitor, and 10 units μl^{-1} Moloney murine leukaemia virus reverse transcriptase at 42°C for 1.5 h. PCR of the cDNA was performed in a final volume of 25 μl containing all four dNTPs (each at 200 μM), KCl (500 mM), $MgCl_2$ (15 mM), 0.1% gelatin, 50 units ml^{-1} Super *Taq* DNA polymerase, and each primer at 0.4 μM. The amplification cycles were 95°C for 30 s, 65°C for 45 s, and 72°C for 2 min. The PCR products were separated by electrophoresis on a 1.8% agarose gel after 35 cycles (497-bp iNOS fragment; 983-bp G3PDH fragment) and visualized by ethidiume bromide staining. Amplification of G3PDH served as a control for sample loading and integrity. PCR was performed on the cDNA using the following sense and antisense primers, respectively; iNOS: CCCTTCCGAAGTTTCTGGCAG-CAGC and GGCTGTCAGAGAGCCTCGTGGCTTTGG; G3PDH: TGAAGGTCGGTGTGAACGGATTTGGC and CATGTAGGCCATGAGGTCCACCAC. Total RNA (25 μg) was denatured with formaldehyde/formamide and incubated at 65°C for 15 min, size-fractioned on 1.2% formaldehyde-containing agarose, and transferred onto Hybond-N nylon membrane (Amershan Corp., Arlington Heights, IL, U.S.A.) in $20\times$ standard saline citrate (3 M sodium chloride and 0.3 M sodium citrate pH 7.0). The blotted membrane was hybridized with iNOS fragment, which was labelled with ^{32}P by using a Random Primer Labelling kit (Amersham). After hybridization, the membrane was washed, dried and autoradiographed with Kodak X-ray film (Rochester, NY, U.S.A.). After hybridization with iNOS-specific probe, the blot was stripped and reprobed with a probe for GAPDH cDNA as a control (Lin & Lin, 1997).

Preparation of extracts and electrophoretic mobility shift assay

Nuclear and cytoplasmic extracts were prepared according to a modified method of Chen *et al*., 1995. At the end of the culture, the cells were suspended in hypotonic buffer A (in mM): HEPES (pH 7.6) 10, KCl 10, EDTA 0.1, DTT 1, phenylmethylsulphonyl fluoride 0.5 for 10 min on ice and vortexed for 10 s. Nuclei were pelleted by centrifugation at $12{,}000\times g$ for 20 s. The supernatants containing cytosolic proteins were collected. A pellet containing nuclei was suspended in buffer C (in mM): HEPES (pH 7.6) 20, EDTA 1, DTT 1, phenylmethylsulphonyl fluoride 0.5, 25% glycerol, 0.4 M NaCl, for 30 min on ice. The supernatants containing nuclear proteins were collected by centrifugation at $12{,}000\times g$ for 20 min and stored at −70°C. For the electrophoretic mobility shift assay, 5 μg of each nuclear extract was mixed with the labelled double-

stranded NFκB oligonucleotide, 5′-AGTTGAGGG-GACTTTCCCAGGC-3′, and incubated at room temperature for 20 min. The incubation mixture included 1 μg of poly (dI-dC) in a binding buffer (in mM) HEPES (pH 7.9) 25, EDTA 0.5, DTT 0.5 NaCl 50, 1% Nonidet P-40, 5% glycerol. The DNA/protein complex was electrophoresed on 4.5% non-denaturing polyacrylamide gels in 0.5 × Tris/borate/EDTA buffer (Tris 0.0445 M, borate 0.0445 M, EDTA 0.001 M). The specificity of binding was also examined by competition with the unlabelled oligonucleotide. Radioactive bands were detected by autoradiography and the bands were cut, solubilized and counted in a beta scintillation counter (Packard Co.).

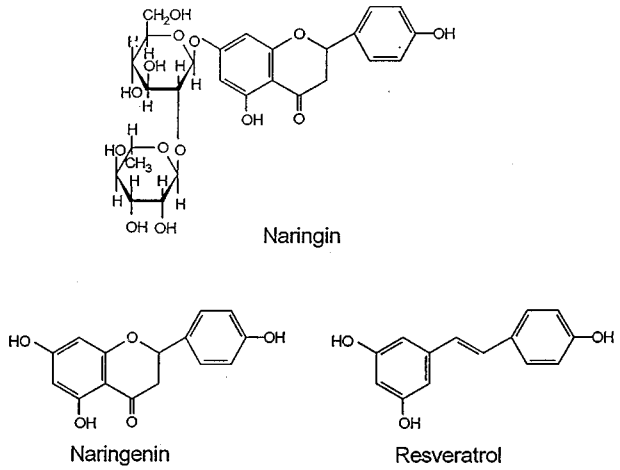

Figure 1 Structures of resveratrol, naringin and naringenin.

Results

Inhibition of NO generation by flavonoids

To investigate the anti-inflammatory effects of the three flavonoids shown in Figure 1, they were tested for their ability to inhibit NO generation in LPS-activated macrophages. The concentration-response curves (Figure 2) were determined 18 h after the flavonoids and LPS had been added to the medium. Resveratrol was found significantly to reduce NO generation, whereas naringenin showed less inhibitory effect over the same concentration range, and the inhibitory ability of naringin was almost negligible. The flavonoids did not interfere the Griess reaction.

Inhibition of iNOS protein

Resveratrol, naringin and naringenin were studied for their effect on iNOS protein in macrophages activated with LPS. Inhibition of iNOS protein by these compounds was detected in concentration-dependent manner (Figure 3). The inhibitory

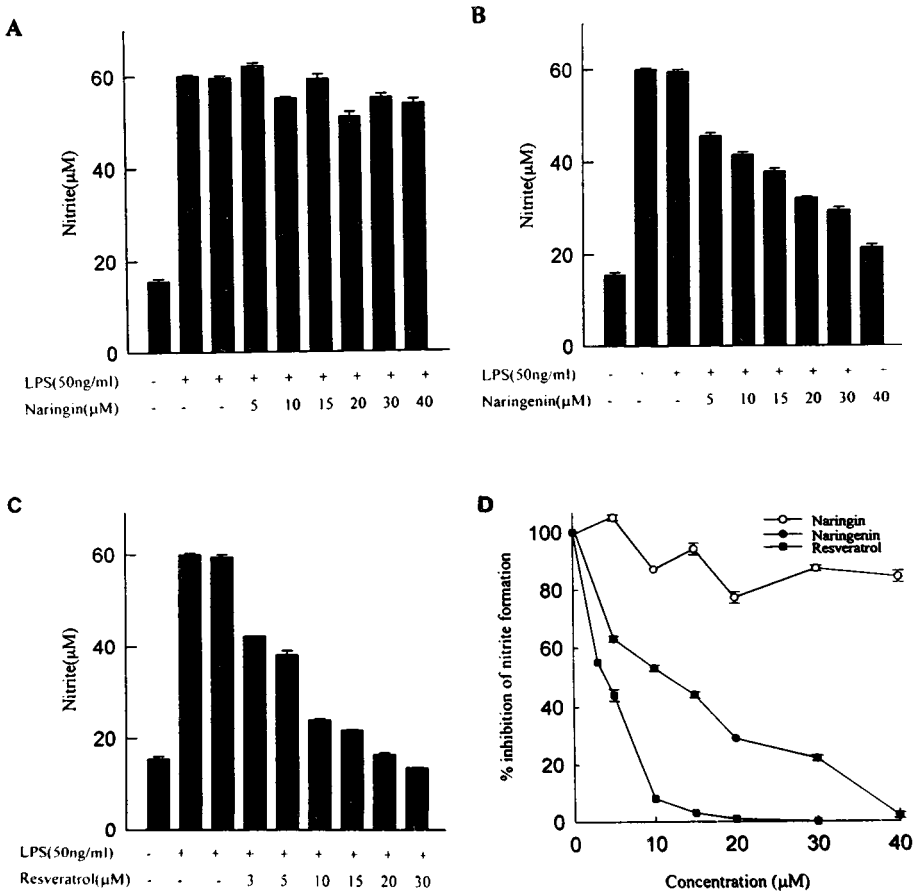

Figure 2 Effects of various concentrations of resveratrol, naringin and naringenin on nitrite release into the culture medium of activated macrophages. RAW 264.7 cells were treated with or without LPS (50 ng ml^{-1}) and various flavonoids or DMSO (0.03%) solvent ((A) naringin; (B) naringenin; (C) resveratrol) for 18 h. At the end of the incubation time, the culture medium was collected for nitrite assay. Each data point is mean ± s.e.mean for three determinations. (D) Rates of nitrite release were measured in activated macrophages in the presence of the indicated concentrations of various flavonoids, and the data was normalized (LPS = 100%).

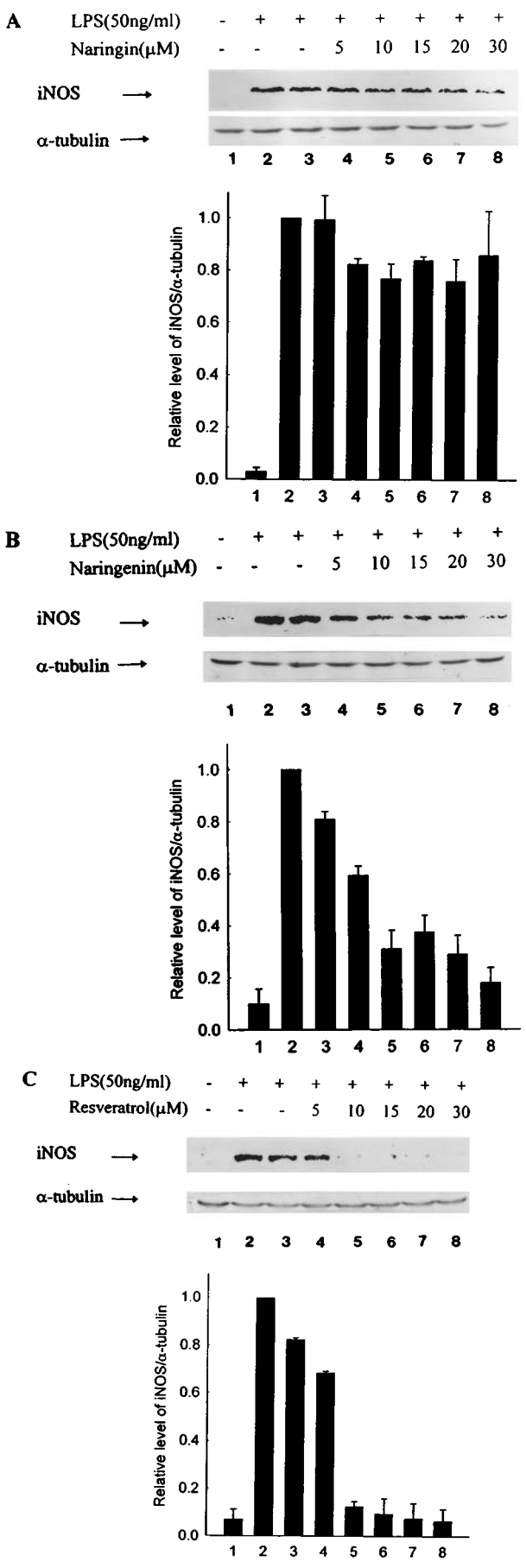

Figure 3 Immuno-blotting analysis of inducible NO systhase in activated macrophages with various flavonoids or solvent only at 18 h ((A) naringin; (B) naringenin; (C) resveratrol). At the end of the incubation time, the total protein was extracted for iNOS protein and α-tubulin analysis by using iNOS and α-tubulin-specific antibodies as described in Methods. Quantification of the iNOS protein expression was performed by densitometric analysis (IS-1000 Digital System) of the immunoblot. Data are expressed as the means ± s.e.mean of the ratio of maximal protein expression observed with LPS as determined by three independent experiments. The ratio of iNOS to α-tubulin protein expression observed with LPS alone is set at 1. The relative level was calculated as the ratio of iNOS to α-tubulin protein expression, which was performed by densitometric analysis of the immunoblot.

activity of naringenin and naringin was less than that of resveratrol. The flavonoid concentrations inhibiting iNOS protein was similar to those for reduction of nitrite formation.

Effects of flavonoids on iNOS gene expression

In order to investigate whether the suppression of iNOS activity by flavonoids was due to reduced iNOS mRNA, a RT–PCR analysis for total mRNA samples extracted from RAW 264.7 cells was carried out. The amplification of cDNA with primers specific for mouse iNOS and GAPDH (as control gene) is shown in Figure 4A. The results indicate that significantly lower levels of iNOS mRNA is expressed in macrophages activated by LPS in the presence of flavonoids than in their absence. Similar levels were obtained from Northern blot analysis of specific iNOS mRNA in cell extracts (Figure 4C). Coincubation of macrophages with LPS plus resveratrol caused almost complete suppression of iNOS mRNA after 5 h induction, and weaker suppression was found in the presence of LPS plus naringenin. Naringin had no effect on LPS-induced iNOS mRNA expression.

Inhibition of flavonoids on LPS-induced nuclear protein with NFκB binding activity

Deletion and mutational analyses have demonstrated that the transcription factor NFκB is involved in the activation of iNOS by LPS. To investigate if the flavonoids selectively inhibited activation of NFκB, analysis of NFκB binding activity by gel mobility shift assay was performed. As shown in Figure 5A, the induction of specific NFκB binding activity by LPS was significantly inhibited by resveratrol (30 μM). On the other hand, inhibition by naringenin was lower, and naringin was almost inactive. The addition of excess unlabelled consensus oligonucleotide completely prevented the band shifts, demonstrating the specificity of the protein/DNA interaction (Figure 5B).

Effect of flavonoids on the phosphorylation and degradation of IκBα

To determine whether the inhibitory action of these flavonoids was due to their effect on the phosphorylation and degradation of IκBα, the phosphorylated and cytoplasmic levels of IκBα protein were examined by immunoblot analysis. After 30 min activation of macrophages by LPS, the serine-phosphorylated IκBα protein was detected by Ser32-phospho-specific IκBα antibody. The results are illustrated in Figure 6A. Resveratrol had a strong ability to inhibit LPS-induced IκBα phosphorylation. In order to confirm the involvement of flavonoids in the prevention of the degradation of IκBα protein, immunoblot analysis of IκBα protein was performed. Figure 6B shows that the cytosolic IκBα protein was detected after 1 h activation, and the inhibitory pattern for resveratrol was similar to the

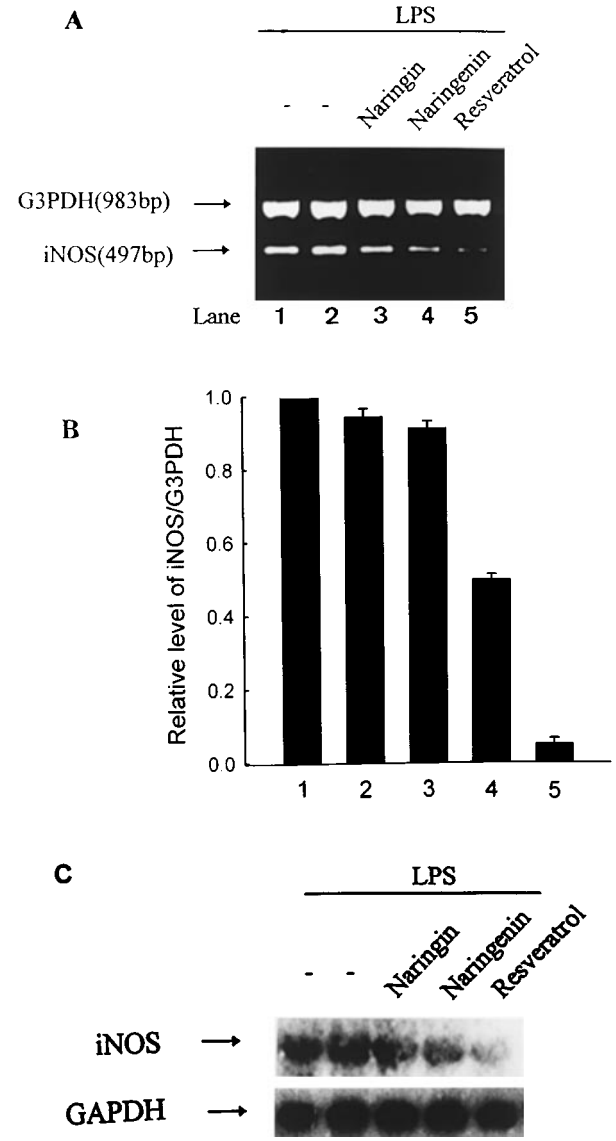

Figure 4 RT–PCR analysis of the expression of iNOS mRNA. (A) RAW 264.7 cells were treated with no flavonoid (lane 1), DMSO (0.03%, lane 2), naringin (30 μM, lane 3), naringenin (30 μM, lane 4), or resveratrol (30 μM, lane 5) before stimulation with LPS (50 ng ml^{-1}) for 5 h. Total RNA was extracted from treated cells and the iNOS mRNA expression was determinated as described in Methods. *G3PDH*, glyceraldehyde-3-phosphate dehydrogenase. (B) Quantification of the iNOS RNA expression was performed by densitometric analysis (IS-1000 Digital System) of the RT–PCR analysis. Data are expressed as the means$\pm$s.e.mean of the ratio of maximal RNA expression observed with LPS in three independent experiments. The ratio of iNOS to G3PDH RNA expression observed with LPS alone is set at 1. The relative level was calculated as the ratio of iNOS to G3PDH RNA expression. (C) Total RNA was extracted from treated cells and assayed for iNOS mRNA expression by Northern blot analysis. Blots were hybridized to ^{32}P-labelled iNOS probe as described in Methods. Signals for GAPDH mRNA for each lane are shown as controls.

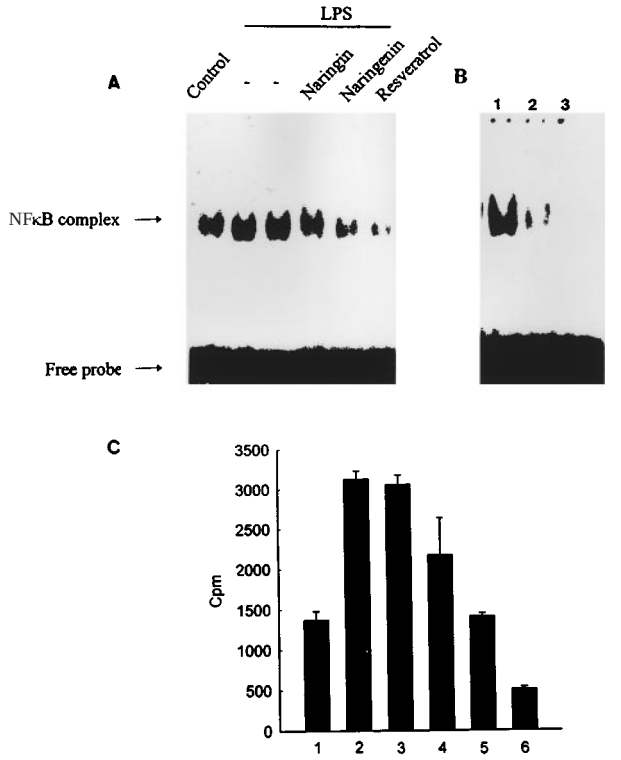

Figure 5 Electrophoretic mobility shift assay using a 5′-end-labelled consensus oligonucleotide for NFκB binding and nuclear extracts from RAW 264.7 cells. (A) RAW 264.7 cells were treated with LPS (50 ng ml^{-1}) without or with different flavonoids (30 μM) or DMSO (0.03%) solvent and then incubated for 1 h. (B) shows competition assay for the identification of NFκB-binding specificity. Lane 1: NFκB complex in LPS-treated RAW 264.7 cells; lane 2: addition of a 25 fold molar excess of the nonradioactive NFκB before adding the [^{32}P]-NFκB element; lane 3: addition of a 50 fold molar excess of the nonradioactive NFκB before adding the [^{32}P]-NFκB element. (C) the actual radioactivity (c.p.m) present in respective bands. Data are expressed as the means$\pm$s.e.mean of the radioactivity (c.p.m.) in three independent experiments.

pattern of inhibition of IκBα phosphorylation. The inhibitory effect of naringenin was lower, and the inhibitory effect of naringin was negligible.

Reduction of nuclear NFκB level by various flavonoids

The above results suggested that flavonoids could reduce iNOS expression by blocking iNOS promoter activation. Since activation of transcription factor NFκB is necessary for iNOS induction, we tested if flavonoids perturbed the distribution of NFκB subunits (c-Rel, p65 and p50) as assessed by nuclear accumulation. As shown in Figure 7, coincubation with LPS plus resveratrol decreased the NFκB proteins in nucleus. Sp1, a nuclear protein was used as control to confirm that there was no contamination with nuclear proteins during extraction of the cytosolic fraction. These results suggest that inhibition of NO production by flavonoids occurs *via* blocking the phosphorylation as well as degradation of IκB protein; thus preventing the translocation of NFκB protein, and finally suppressing NFκB activation in the nucleus.

Discussion

Flavonoids occur ubiquitously in the plant kingdom and are common components of the human diet. The flavonoids exhibit a wide structural diversity; more than 4000 different flavonoids have been identified from various plants. Flavonoids have been shown to have structually-dependent, highly specific effects on a variety of enzymes and are able to interfere with numerous cellular processes, including growth and differentiation (Brandi, 1992). Resveratrol (3,5,4′-trihydroxystilbene) is one of the stilbene family. Naringin (naringenin 7-hesperidoside) is the glycosylated form of naringenin. Here we demonstrated that resveratrol strongly inhibited the induction

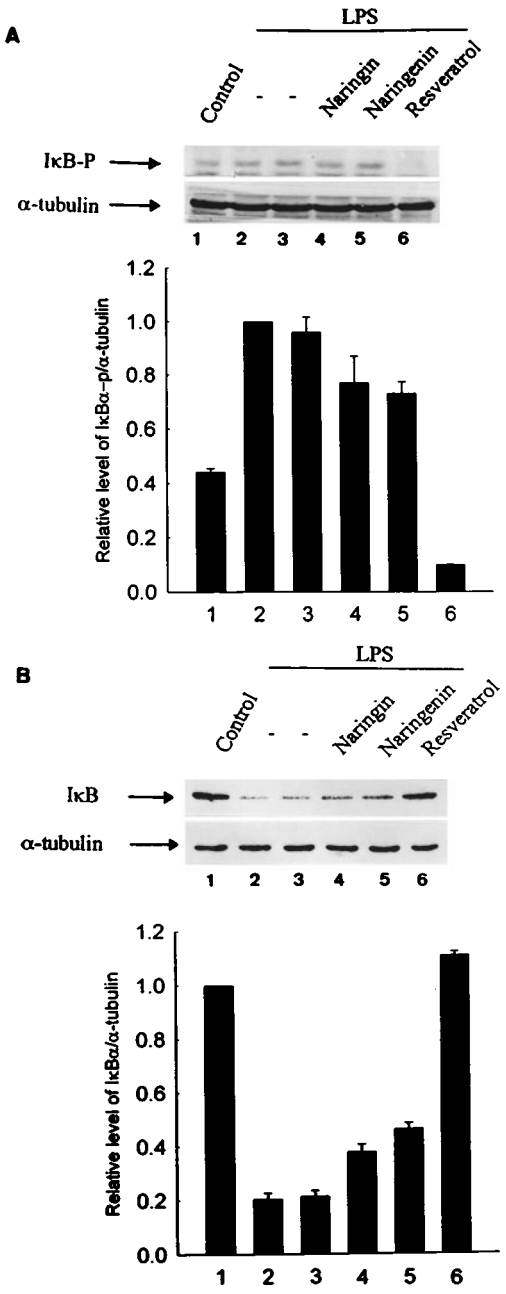

Figure 6 The inhibition by flavonoids of LPS-mediated IκBα phosphorylation and degradation. RAW 264.7 cells were treated with LPS (50 ng ml^{-1}) without or with different flavonoids (30 μM) or DMSO (0.03%) solvent and then incubated for 30 min or 1 h. Cytosolic fractions were prepared and analysed for the content of IκBα protein by Western blot. (A) After 30 min activation, the phosphorylated IκBα was detected by Ser32-phospho-specific antibody. Quantification of the phosphorylated IκBα protein expression was performed by densitometric analysis (IS-1000 Digital System) of the Western blot. Data are expressed as the means ± s.e.mean of the ratio of maximal phosphorylated IκBα observed with LPS in three independent experiments. The ratio of phosphorylated IκBα to α-tubulin protein expression observed with LPS alone is set at 1. The relative level was calculated as the ratio of phosphorylated IκBα to α-tubulin protein expression. (B) The content of IκBα protein was detected after 1 h activation. Quantification of the IκBα protein expression was performed by densitometric analysis (IS-1000 Digital System) of the Western blot. Data are expressed as the means ± s.e.mean of the ratio of maximal IκBα protein expression in three independent experiments. The ratio of IκBα to α-tubulin protein expression observed with control is set at 1. The relative level was calculated as the ratio of IκBα to α-tubulin protein expression.

of iNOS in RAW 264.7 cells activated with LPS with an IC_{50} of 5 μM. Naringenin had less inhibitory activity, and naringin was almost devoid of an inhibitory effect. It is difficult to deduce a structure-activity relationship from these compounds, but it may be noted that naringin is the only compound with a rhamnglucoside group at the 7 position. In addition, our laboratory has observed that tea polyphenols (10 μM) significantly reduce iNOS protein (Lin & Lin, 1997). The tea polyphenols also have an hydroxyl group at the 5 and 7 positions. This suggests that the hydroxy groups of resveratrol and naringenin may be important for the inhibitory activity on iNOS induction. Based on these findings, it seems that those compounds with neighbouring hydroxyl moieties had the most potent anti-inflammatory property, and glycosylation of OH groups reduced this activity.

Mammals are in permanent contact with Gram-negative bacteria and LPS (Schletter *et al.*, 1995). Low doses of LPS are considered beneficial for the host. On the other hand, the presence of a large amount of LPS leads to dramatic pathophysiological reactions such as fever, leukopenia, hypotension and multi-organ failure. LPS stimulates host cells (mainly monocytes/macrophages but also endothelial cells, smooth muscle cells and neutrophils) to produce and release NO by induction of iNOS protein. The iNOS isoform can

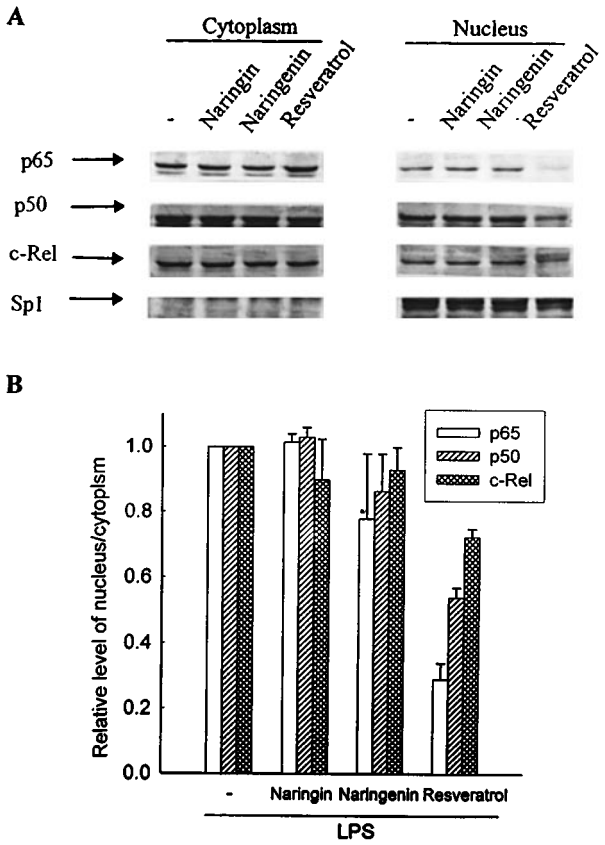

Figure 7 Flavonoids reduced nuclear NFκB levels. RAW 264.7 cells were treated with LPS (50 ng ml^{-1}) without or with different flavonoids (30 μM) and then incubated for 1 h. (A) Cytosolic and nuclear fractions were prepared and analysed for the content of c-Rel, p65, p50 and Sp1 proteins. (B) Quantification of the NFκB (c-Rel, p65 and p50) protein expression was performed by densitometric analysis (IS-1000 Digital System) of the Western blot. Data are expressed as the means ± s.e.mean of the ratio of maximal NFκB nuclear translocation observed with LPS in three independent experiments. The ratio of NFκB nuclear translocation observed with LPS is set at 1. The relative level was calculated as the ratio of nuclear to cytoplasmic NFκB.

produce high, persistent concentrations of NO on induction with endotoxin alone or in combination with cytokines in many cell types. It is expressed in the resting state in other cells, potentially resulting in cytotoxicity, tissue damage, or DNA damage. Here we showed that resveratrol inhibits the expression of iNOS. Thus, resveratrol may act as protectant against the effects of agents which stimulate iNOS induction.

Activation of NFκB is necessary for LPS induction of the iNOS promoter (Xie *et al*., 1994). NFκB is composed mainly of two proteins: p50 and p65. In its unstimulated form, NFκB is present in the cytosol bound to the inhibitory protein, IκB. After stimulation of cells by a variety of agents, IκB becomes phosphorylated and this triggers a proteolytic degradation of IκB. Serine phosphorylation of IκB is sufficient for efficient degradation. On the other hand, stoichiometric phosphorylation of IκB on tyrosine 42 dose not cause a subsequent proteolytic degradation of the IκB but, apparently, is sufficient to release IκB from NFκB and hence activate NFκB (Imbert *et al*., 1996). Our results showed that resveratrol reduces iNOS expression by blocking transcription of its gene, a conclusion supported by the observation that it reduced steady state iNOS mRNA levels, promoter activity (as assessed by gel mobility assay), and nuclear accumulation of NFκB subunits. The mechanisms by which resveratrol can interfere with the activation of NFκB are not clear. One possibility is that resveratrol could interact with ankyrin domains present in IκB, because the phosphorylation of IκB was inhibited by resveratrol. Such an interaction could conceivably hinder IκB phosphorylation and subsequent dissociation of NFκB.

However, whether resveratrol physically interacts with IκB remains to be determined. Cells treated with LPS could generate ROIs by inducing NADPH oxidase activity (Bastian & Hibbs, 1994). We also found that hydroxy radicals can activate protein tyrosine kinase (Lee *et al*., 1996). Furthermore, resveratrol has been found to possess potent protein kinase inhibitory activity and antioxidant activity (Miller & Rice-Evans, 1995; Chen *et al*., 1990; Jayatilake *et al*., 1993). A role for protein tyrosine kinase and ROIs has been implicated in NFκB activation (Bastian & Hibbs, 1994; Baldwin, 1996). Therefore, we postulate that resveratrol might inhibit the activation of NFκB through inhibiting the LPS-induced phosphorylation and degradation of IκBα. It is possible that the anti-inflammatory and anti-cancer properties of the flavonoids may be mediated, at least in part, by inhibition of iNOS expression through down-regulation of NFκB binding activity.

We would like to thank Dr K. F. Fork for the gift of resveratrol. This study was supported by grants from the National Science Council [NSC 87-2316-B-002-011] and the National Health Research Institute [DOH87-HR-403].

References

BAEUERLE, P.A. & BALTIMORE, D. (1996). NFκB: ten years after. *Cell,* **87,** 13–20.

BALDWIN JR, A.S. (1996). The NFκB and IκB proteins: new discoveries and insights. *Annu. Rev. Immunol.,* **14,** 649–681.

BASTIAN, N.R. & HIBBS JR, J.B. (1994). Assembly and regulation of NADPH oxidase and nitric oxide synthase. *Curr. Opin. Immunol.,* **6,** 131–139.

BRANDI, M.I. (1992). Flavonoids: biochemical effects and therapeutic applications. *Bone Miner.,* **19,** S3–S14.

CALOMME, M., PIETERS, L., VLIETINCK, A. & BERGHE, D.M. (1996). Inhibition of bacterial mutagenesis by citrus flavonoids. *Planta Medica,* **62,** 222–226.

CHEN, F., KUHN, D.C., SUN, S.C., GAYDOS, L.J. & DEMERS, L.M. (1995). Dependence and reversal of nitric oxide production on NF-κB in silica and lipopolysaccharide-induced macrophages. *Biochem. Biophys. Res. Commun.,* **214,** 839–846.

CHEN, Y.T., ZHANG, R.L., JIA, Z.J. & JU, Y. (1990). Flavonoids as superoxide scavenger and antioxidants. *Free Rad. Biol. Med.,* **9,** 19–21.

CHOMCZYNSKI & SACCHI, N. (1987). Single-step method of RNA isolation by acid guanidinium thiocyanate-phenol-chloroform extraction. *Anal. Biochem.,* **162,** 156–159.

DING, A.H., NATHAN, C.F. & STUEHR, D.J. (1988). Release of reactive nitrogen intermediates and reactive oxygen intermediates from mouse peritoneal macrophages. *J. Immunol.,* **141,** 2407–2412.

GOLDRING, C.E.P., REVENEAU, S., ALGARTE, M. & JEANNIN, J.-F. (1996). In vivo footprinting of the mouse inducible nitric oxide synthase gene: inducible protein occupation of numerous sites including Oct and NF-IL6. *Nucleic Acid Res.,* **24,** 1682–1687.

HALLIWELL, B. (1994). Free radicals, antioxidants, and human disease: curiosity, cause, or consequence? *Lancet,* **344,** 721–725.

IMBERT, V., RUPEC, R.A., LIVOLSI, A., PAHL, H.L., TRAENCKNER, B.M., MUELLER-DIECKMANN, C., FARAHIFAR, D., ROSSI, B., AUBERGER, P., BAEUERLE, P.A. & PEYRON, J. (1996). Tyrosine phosphorylation of IκB-α activates NF-κB without proteolytic degradation of IκB-α. *Cell,* **86,** 787–798.

JANG, M., CAI, L., UDEANI, G.O., SLOWING, K.V., THOMAS, C.F., BEECHER, W.W., FONG H.H.S., FARNSWORTH, N.R., KINGHORN, A.D., MEHTA, R.G., MOON, R.C., PEZZUTO, J.M. (1997). Cancer chemopreventive activity of resveratrol, a natural product derived from grapes. *Science,* **75,** 218–220.

JAYATILAKE, G.S., JAYASURIYA, H., LEE, E.S., KOONCHANOK, N.M., GEAHLEN, R.L., ASHENDEL, C.L., McLAUGHLIN, J.L. & CHANG, C.J. (1993). Kinase inhibitors from polygonum cuspidatum. *J. Nat. Prod.,* **56,** 1805–1810.

KAMIJO, R., HARADA, H., MATSUYAMA, T., BOSLAND, M., GERECITANO, J., SHAPIRO, D., LE, J., KOH, S.I., KIMURA, T., GREEN, S.J., MAK, T.W., TANIGUCHI, T. & VILCEK, J. (1994). Requirement for transcription factor IRF-1 in NO synthase induction in macrophages. *Science,* **263,** 1613–1615.

KIM, H., LEE, H.S., CHANG, K.T., KO, T.H., BAEK, K.J. & KWON, N.S. (1995). Chloromethyl ketones block induction of nitric oxide synthase in murine macrophages by preventing activation of nuclear factor-κB. *J. Immunol.,* **154,** 4741–4748.

LEE, S.F., HUANG, Y.T., WU, W.S. & LIN, J.K. (1996). Induction of c-Jun protooncogene expression by hydrogen peroxide through hydroxyl radical generation and p60Src tyrosine kinase activation. *Free Rad. Biol. Med.,* **21,** 437–448.

LIMASSET, B., DOUCEN, C.L., DORE, J.C., OJASOO, T., DAMON, M. & PAULET, A.C. (1993). Effects of flavonoids on the release of reactive oxygen species by stimulated human neutrophils. *Biochem. Pharmacol.,* **46,** 1257–1271.

LIN, Y.L. & LIN, J.K. (1997). (−)-Epigallocatechin-3-gallate blocks the induction of nitric oxide synthase by down-regulating lipopolysaccharide-induced activity of transcription factor nuclear factor-κB. *Mol. Pharmacol.,* **52,** 465–472.

LOWENSTEIN, C.J., ALLEY, E.W., RAVAL, P., SNOWMAN, A.M., SNYDER, S.H., RUSSELL, S.W. & MURPHY, A.W. (1993). Macrophage nitric oxide synthase gene: two upstream regions mediate induction by interferon γ and lipopolysccharide. *Proc. Natl. Acad. Sci. U.S.A.,* **90,** 9730–9734.

MARTIN, E., NATHAN, C. & XIE, Q.-W. (1994). Role of interferon regulatory factor 1 in iduction of nitric oxide synthase. *J. Exp. Med.,* **180,** 977–984.

MILLER, N.J. & RICE-EVANS, C.A. (1995). Antioxidant activity of resveratrol in red wine. *Clin. Chem.,* **41,** 1789.

NATHAN, C. & XIE, Q.-W. (1994). Regulation of biosynthesis of nitric oxide. *J. Biol. Chem.,* **269,** 13725–13728.

OHSHIMA, H. & BARTSCH, H. (1994). Chronic infections and inflammatory processes as cancer risk factors: possible role of nitric oxide in carcinogenesis. *Mutat. Res.,* **305,** 253–264.

SCHLETTER, J., HEINE, H., ULMER, A.J. & RIETSCHEL, E.T. (1995). Molecular mechanisms of endotoxin activity. *Ach. Microbiol.,* **164,** 383–389.

SO, F.V., GUTHRIE, N., CHAMBERS, A.F., MOUSSA, M. & CARROLL, K.K. (1996). Inhibition of human breast cancer cell proliferation and delay of mammary tumorigenesis by flavonoids and citrus juices. *Nutr. Cancer,* **26,** 167–181.

SOLEAS, G.J., DIAMANDIS, E.P. & GOLDBERG, D.M. (1997). Resveratrol: a molecule whose time has come? And gone? *Clin. Biochem.,* **30,** 91–113.

STUEHR, D.J. & MARLETTA, M.A. (1985). Mammalian nitrate biosynthesis: mouse macrophages produce nitrite and nitrate in response to *Escherichia coli* lipopolysaccharide. *Proc. Natl. Acad. Sci. U.S.A.,* **82,** 7738–7742.

WEISZ, A., OGUCHI, S., CICATIELLO, L. & ESUMI, H. (1994). Dual mechanism for the control of inducible-type NO synthase gene expression in macrophages during activation by interferon-γ and bacterial lipopolysaccharide. *J. Biol. Chem.,* **269,** 8324–8333.

XIE, Q.-W., KASHIWABARA, Y. & NATHAN, C. (1994). Role of transcription factor NFκB/Rel in induction of nitric oxide synthase. *J. Biol. Chem.,* **269,** 4705–4708.

XIE, Q.-W., WHISNANT, R. & NATHAN, C. (1993). Promoter of the mouse gene encoding calcium-independent nitric oxide synthase confers inducibility by interferon γ and bacterial lipopolysaccharide. *J. Exp. Med.,* **177,** 1779–1784.

(Received June 15, 1998
Revised November 9, 1998
Accepted November 11, 1998)

British Journal of Pharmacology (1999) 126, 681–688
http://www.stockton-press.co.uk/bjp

ATP- and glutathione-dependent transport of chemotherapeutic drugs by the multidrug resistance protein MRP1

*,[1]Johan Renes, [2]Elisabeth G.E. de Vries, [2]Edith F. Nienhuis, [1]Peter L.M. Jansen & [1]Michael Müller

[1]Groningen Institute for Drug Studies, Division of Gastroenterology and Hepatology, University Hospital Groningen, 9700 RB Groningen, The Netherlands and [2]Division of Medical Oncology, University Hospital Groningen, 9700 RB Groningen, The Netherlands

1 The present study was performed to investigate the ability of the multidrug resistance protein (MRP1) to transport different cationic substrates in comparison with *MDR1*-P-glycoprotein (MDR1). Transport studies were performed with isolated membrane vesicles from *in vitro* selected multidrug resistant cell lines overexpressing MDR1 (A2780AD) or MRP1 (GLC_4/Adr) and a *MRP1*-transfected cell line (S1(MRP)).

2 As substrates we used ^{3}H-labelled derivatives of the hydrophilic monoquaternary cation *N*-(4′,4′-azo-*n*-pentyl)-21-deoxy-ajmalinium (APDA), the basic drug vincristine and the more hydrophobic basic drug daunorubicin. All three are known MDR1-substrates.

3 MRP1 did not mediate transport of these substrates *per se*. In the presence of reduced glutathione (GSH), there was an ATP-dependent uptake of vincristine and daunorubicin, but not of APDA, into GLC_4/Adr and S1(MRP) membrane vesicles which could be inhibited by the MRP1-inhibitor MK571.

4 ATP- and GSH-dependent transport of daunorubicin and vincristine into GLC_4/Adr membrane vesicles was inhibited by the MRP1-specific monoclonal antibody QCRL-3.

5 MRP1-mediated daunorubicin transport rates were dependent on the concentration of GSH and were maximal at concentrations $\geqslant$10 mM. The apparent K_M value for GSH was 2.7 mM. Transport of daunorubicin in the presence of 10 mM GSH was inhibited by MK571 with an IC_{50} of 0.4 μM.

6 In conclusion, these results demonstrate that MRP1 transports vincristine and daunorubicin in an ATP- and GSH-dependent manner. APDA is not a substrate for MRP1.

Keywords: Drug resistance; ABC transporter; MDR1; MRP1; ATP-dependent drug transport; GSH; daunorubicin; vincristine; APDA

Abbreviations: ABC transporter, ATP binding cassette transporter; AMP-PCP, β,γ-methyleneadenosine 5′-triphosphate; [^{3}H]-APDA, *N*-(4′,4′-azo-*n*-pentyl)-21-deoxy-[21-^{3}H]ajmalinium; Baf, bafilomycin A_1; FCS, foetal calf serum; GSH, reduced glutathione; GSSG, oxidized glutathione; GS *S*-conjugates, glutathione *S*-conjugates; LTC_4, leukotriene C_4; MDR1, *MDR1*-P-glycoprotein; MRP, multidrug resistance protein; PBS, phosphate-buffered saline; TS, tris/sucrose; V-type ATPase, vacuolar H^+-ATPase

Introduction

Human multidrug resistance is frequently associated with the overexpression of the *MDR1*-P-glycoprotein (MDR1) (Juliano & Ling, 1976) and/or the multidrug resistance protein (MRP1) (Cole *et al*., 1992), two members of the ATP binding cassette (ABC) transporter superfamily (Higgins, 1992). Although they share only 15% amino acid sequence homology, both proteins confer resistance to a broad range of natural product drugs in drug selected cell lines as well as in transfected cells (Loe *et al*., 1996c; Broxterman *et al*., 1995; Gottesman & Pastan, 1993). Currently, it is generally accepted that MDR1 functions as an ATP-dependent transport protein capable of reducing intracellular levels of various natural product drugs (Borst & Schinkel, 1997; Germann, 1996; Ruetz & Gros, 1994a). Most of these drugs, e.g. vinca alkaloids, anthracyclines, epipodophillotoxins, actinomycin D and paclitaxel, have unrelated chemical structures but share the property of being hydrophobic compounds.

*Author for correspondence at: Division of Gastroenterology and Hepatology, University Hospital Groningen, P.O. Box 30.001, Hanzeplein 1, 9700 RB Groningen, The Netherlands.
E-mail: j.w.renes@med.rug.nl

MRP1 was first identified in tumour cells with a multidrug resistant phenotype without overexpression of MDR1 (Cole *et al*., 1992). Although MRP1 is able to confer resistance to drugs which are MDR1 substrates, the substrate specificity of MRP1 seems different from that of MDR1. Transport studies with membrane vesicles isolated from MRP1 overexpressing cells, either *in vitro* selected or transfected, revealed that MRP1 is a transporter of multivalent organic anions, preferentially glutathione *S*-conjugates (GS *S*-conjugates), (Barnouin *et al*., 1998; Loe *et al*., 1996b; 1997; Jedlitschky *et al*., 1996; Müller *et al*., 1994b), but also of sulphate conjugates (Jedlitschky *et al*., 1996) and glucuronides (Jedlitschky *et al*., 1996; Loe *et al*., 1996a). Also oxidized glutathione (GSSG), complexes of reduced glutathione (GSH) with arsenite (Zaman *et al*., 1995) and unmodified compounds in the presence of GSH (Loe *et al*., 1996b; 1997) are MRP1 substrates. In view of its substrate specificity and the ubiquitous expression of *MRP1* in human tissues (Zaman *et al*., 1993) and blood cells (Burger *et al*., 1994), the putative physiological role of MRP1 seems to be cellular extrusion of metabolites of GSH-dependent detoxification reactions (Müller *et al*., 1996).

The molecular basis of the drug specificity of MRP1 is not fully understood. Two models currently exist describing the drug transport mechanism of MRP1. First, MRP1 may be a

transporter of drug conjugates (e.g. GS *S*-conjugates and glucuronide conjugates) (Priebe *et al*., 1998; Jedlitschky *et al*., 1996; Ishikawa *et al*., 1995), however, stable GS *S*-conjugates of vincristine and daunorubicin could not be detected in HPLC-analysed media from *MRP1* transfected cells (Zaman *et al*., 1995). Moreover, there is no evidence that the chemotherapeutic agents to which MRP1 confers resistance, are substrates for GSH- or glucuronic acid conjugation (for review see O'Brien & Tew, 1996; Tew, 1994). Secondly, MRP1 may transport unmodified natural product drugs in the presence of GSH. For example, it has been demonstrated that unmodified vincristine is transported by MRP1 but only in the presence of physiological concentrations of GSH (Loe *et al*., 1996b). Furthermore, resistance to vinca alkaloids and anthracyclines is reversed by GSH depletion in MRP1-overexpressing cells, but not in cells overexpressing MDR1 (Zaman *et al*., 1995; Versantvoort *et al*., 1995). Therefore, GSH appears to play an important role in MRP1-mediated drug resistance. In this study we compared MDR1 and MRP1 with respect to their ability to transport different classes of cationic drugs and investigated the role of GSH in MRP1-mediated transport. We hypothesized that the hydrophobic basic drug daunorubicin has not necessarily to be conjugated with GSH to be a MRP1 substrate (Priebe *et al*., 1998; Ishikawa *et al*., 1995), but is transported by MRP1 in the presence of GSH. We used vincristine as a previously demonstrated MRP1 substrate (Loe *et al*., 1996b) to characterize our experimental system. Furthermore, experiments were performed with the permanently positively charged monoquaternary cationic derivate of the anti-arrhythmic drug ajmaline (*N*-(4′, 4′-azo-*n*-pentyl)-21-deoxy-ajmalinium, APDA) to study the ability of MRP1 to mediate the transport of more hydrophilic cations which are excellent MDR1 substrates *in vitro*.

Methods

Chemicals

N-(4′,4′-azo-*n*-pentyl)-21-deoxy-[21-^{3}H]-ajmalinium [^{3}H]-(APDA) (46 GBq mmol^{-1}) (Müller *et al*., 1994a), was kindly provided by Dr G. Kurz (University of Freiburg, Germany), [G-^{3}H]-vincristine (226 GBq mmol^{-1}) was obtained from Amersham (Little Chalfont, U.K.) and [14,15,19,20-^{3}H(N)]-leukotriene C_4 ([^{3}H]-LTC_4) (4884 GBq mmol^{-1}) and [G-^{3}H]-daunorubicin (46.62 GBq mmol^{-1}) were from NEN (Boston, MA, U.S.A.). Benzonase, grade I protease free, was from Merck (Darmstadt, Germany). ATP, creatine phosphate and creatine kinase were purchased from Boehringer (Mannheim, Germany). The MRP1 inhibitor MK571 was kindly provided by Dr A.W. Ford-Hutchinson (Merck-Frosst, Pointe Claire-Dorval, Quebec, Canada) and the MDR1 inhibitor PSC833 was a kind gift of Novartis (Basel, Switzerland). The monoclonal antibody (mAb) QCRL-3, directed against MRP1, was obtained from Signet Laboratories (Dedham, MA, U.S.A.). β,γ-Methyleneadenosine 5′-triphosphate (AMP-PCP), GSH, the vacuolar H^+-ATPase (V-type ATPase) inhibitor bafilomycin A_1 (Baf) and all other chemicals were from Sigma (St. Louis, MO, U.S.A.).

Cell culture

Culture procedures for the human GLC_4 small cell lung cancer line and its doxorubicin selected multidrug resistant counterpart GLC_4/Adr have been described previously (Zijlstra *et al*., 1987). Culture of the non-small cell lung cancer cell line SW1573/S1, further designated as S1, and of its *MRP1* transfected subline S1(MRP) was performed as reported (Zaman *et al*., 1994) only with stepwise increase of the Geneticin concentration to 0.4 mg ml^{-1} (Gibco, Paisley, U.K.). The human ovarian tumour cell line A2780 was cultured in RPMI1640 medium, supplemented with 10% foetal calf serum (FCS), (Gibco). The multidrug resistant A2780AD line was isolated from the A2780 line by a multistep selection with doxorubicin and maintained in RPMI1640 medium supplemented with 10% FCS as described (Rogan *et al*., 1984).

Preparation of membrane vesicles

Membrane vesicles were prepared as described previously (Müller *et al*., 1994b) with minor modifications. Briefly, cells were harvested, washed with phosphate-buffered saline (PBS, mM: NaCl 137, KCl 2.7, Na_2HPO_4 10.1, KH_2PO_4 1.8, pH 7.4) and centrifuged at $180 \times g$, for 10 min at 4°C. The resulting pellet was diluted 40 fold in hypotonic buffer (1 mM $NaHCO_3$, pH 7.4) and stirred gently in the presence of 100 U Benzonase for 1 h. The cell lysate was centrifuged at $100{,}000 \times g$ for 30 min at 4°C and the remaining pellet was resuspended in 5 ml isotonic TS buffer (10 mM Tris/250 mM sucrose, pH 7.4) and homogenized with a Dounce B homogenizer in the presence of 100 U Benzonase. The crude membrane fraction was layered on top of a 38% (w/v) sucrose solution in 10 mM Tris (pH 7.4) and centrifuged at $280{,}000 \times g$ for 1 h at 4°C in a swing out rotor. The interface layer was collected, diluted to 25 ml in TS buffer and centrifuged at $100{,}000 \times g$ for 30 min at 4°C. The resulting pellet was resuspended in 300–500 μl isotonic buffer. Vesicles were formed by passing the suspension 20 times through a 25 gauge needle. The membrane vesicles were snap frozen in liquid nitrogen and stored at −80°C. Protein content was measured by a Bradford-based Biorad protein assay (Biorad laboratories, Hercules, CA, U.S.A.).

Immunodetection of MRP1 and MDR1

Ten μg protein of each membrane preparation was separated on a SDS/7.5% polyacrylamide gel and transferred to nitrocellulose (Amersham) by electroblotting. MRP1 was detected by the rat monoclonal MRPr1 (1 : 500), kindly provided by Dr R. Scheper, (Free University, Amsterdam, the Netherlands). MDR1 was detected by the monoclonal antibody C219 (1 : 500), (Centocor, Malvern, MA, U.S.A.). MRP2 protein levels were analysed with the monoclonal antibody M_2 III-5, a kind gift of Dr R. Oude Elferink (Academic Medical Centre, Amsterdam, the Netherlands). Primary antibodies were visualized by enhanced chemiluminescence (ECL), (Pierce, Rockford, IL, U.S.A.).

Transport studies

Uptake of [^{3}H]-APDA (300 nM), [^{3}H]-vincristine (300 nM) and [^{3}H]-daunorubicin (600 nM) into membrane vesicles was measured by a rapid filtration technique. Membrane vesicles (50 μg protein) were rapidly thawed and added to the buffer system containing 4 mM ATP or AMP-PCP, 10 mM $MgCl_2$, 10 mM creatine phosphate, 100 μg ml^{-1} creatine kinase, 10 mM Tris pH 7.4 and 250 mM sucrose. After 1 min prewarming at 37°C, the substrate was added (110 μl final volume). At indicated time points, samples (25 μl) were taken and diluted in 1 ml ice cold stopsolution (PBS). These solutions were subsequently filtered through OE66 cellulose

acetate filters, pore size 0.2 μm (Schleicher & Schuell, Dassel, Germany), presoaked in PBS. Filters were rinsed with 5 ml PBS/0.05% Tween 20 followed by 5 ml PBS. After rinsing, the filters were air dried and radioactivity was counted with a liquid scintillation counter. Experiments with [^{3}H]-daunorubicin were performed similarly, except that the PBS stopsolution contained 1 mM ethidium bromide, the filters were presoaked in PBS/1 mM ethidium bromide and the filters were first washed by 5 ml PBS/1 mM ethidium bromide, followed by PBS/0.05% Tween 20 and 5 ml PBS. This method reduced the background binding of [^{3}H]-daunorubicin with 70–80% and resulted in a signal to noise ratio of 10 : 2–3. Experiments with [^{3}H]-LTC_4 (1.5 nM) were performed with 10 μg protein, NC45 nitrocellulose filters, pore size 0.45 μm (Schleicher & Schuell), and 10 mM Tris/250 mM sucrose buffer (pH 7.4) instead of PBS. If required, PSC833, MK571, GSH and/or Baf were added together with the membrane vesicles to the buffer system.

Time course experiments of [^{3}H]-daunorubicin (600 nM) uptake were carried out with membrane vesicles from GLC_4/Adr cells (100 μg protein in 220 μl reaction volume) in the presence of 1 μM Baf and in the presence or the absence of 5 mM GSH. At indicated time points, samples of 25 μl were taken and treated as described above. Aspecific binding of [^{3}H]-daunorubicin was measured at 4°C in the presence of 4 mM ATP and 5 mM GSH and subtracted from all values obtained at 37°C.

Uptake experiments in the presence of the MRP1-specific monoclonal antibody (mAb) QCRL-3 or the control mAb directed against the T-cell marker CD3 (a kind gift of Dr B.J. Kroesen, University Hospital Groningen) were performed for 1 min as described above. The mAbs were added together with the membrane vesicles to the buffer system.

All transport data are presented as the difference of the values measured in the presence of ATP and in the presence of AMP-PCP. The non-hydrolyzable ATP analogue AMP-PCP did not support uptake, demonstrating that ATP hydrolysis was required.

Results

Immunoblot analysis of MRP1 and MDR1

The levels of MRP1 and MDR1 in membrane subfractions were analysed by immunoblotting. Increased levels of the 190 kDa MRP1 (Müller *et al*., 1994b; Roelofsen *et al*., 1997) were detected in membranes from GLC_4/Adr and *MRP1*-transfected S1(MRP) cells, while membranes isolated from A2780, A2780AD, GLC_4 and S1 cells exhibited lower levels (Figure 1). MDR1 was found to be overexpressed in membranes isolated from A2780AD cells. No expression of MDR1 was found in membrane preparations from the other cell lines. MRP2 was not detected in membranes from any of these cell lines (data not shown).

ATP-dependent uptake of cationic drugs in membrane vesicles from MDR1- and MRP1-overexpressing cells

Transport properties of MDR1 and MRP1 were compared with two hydrophobic basic drugs ([^{3}H]-vincristine and [^{3}H]-daunorubicin) and the more hydrophilic cation ([^{3}H]-APDA). Figure 2a shows ATP-dependent uptake of [^{3}H]-APDA, [^{3}H]-vincristine and [^{3}H]-daunorubicin into membrane vesicles from A2780 and A2780AD cells. ATP-dependent uptake of all three substrates into A2780AD membrane vesicles was increased

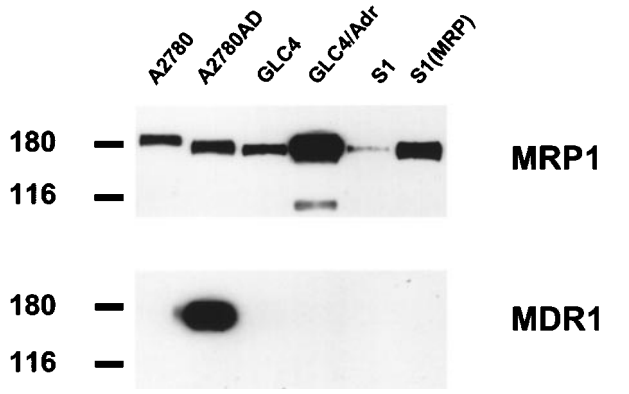

Figure 1 Immunoblot analysis of isolated membrane subfractions. Membrane proteins (10 μg) were resolved on 7.5% SDS–PAGE and transferred to nitrocellulose by electroblotting. Protein levels were analysed with monoclonal antibodies raised against MRP1 (MRPr1) and MDR1 (C219). Primary antibodies were visualized by enhanced chemiluminescence. Sizes of molecular weight markers are indicated in kDa.

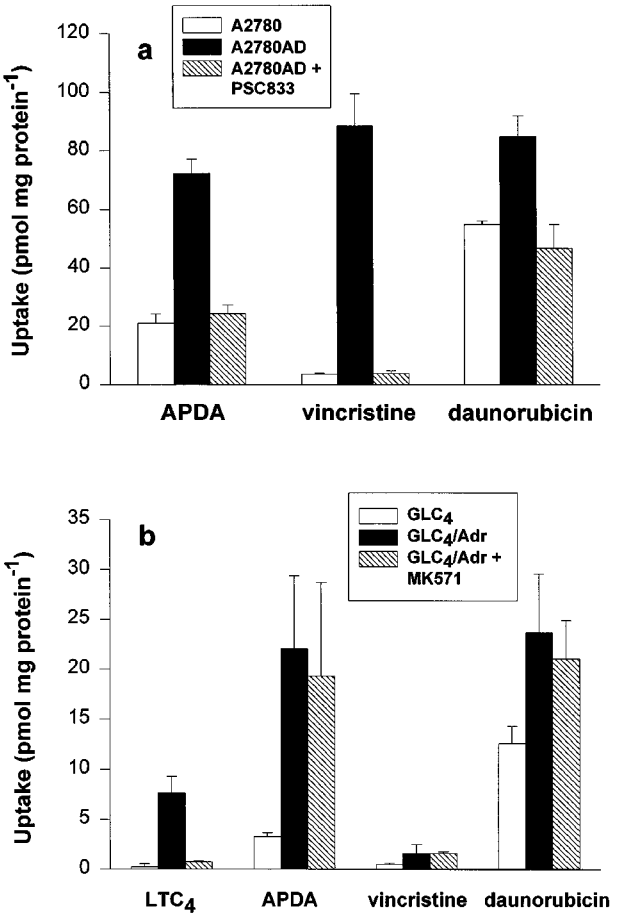

Figure 2 ATP-dependent uptake of cationic drugs into membrane vesicles from MDR1- and MRP1-overexpressing cells. Uptake of [^{3}H]-APDA (300 nM), [^{3}H]-vincristine (300 nM) and [^{3}H]-daunorubicin (300 nM) into membrane vesicles (50 μg) from A2780 and A2780AD cells was measured during 5 min as described under 'experimental procedures'. Uptake into A2780AD membrane vesicles was also measured in the presence of 1 μM of the MDR1 inhibitor PSC833 (a). Similar experiments were performed with membrane vesicles from GLC_4 and from GLC_4/Adr cells either in the absence or the presence of 5 μM of the MRP1 inhibitor MK571 (b). [^{3}H]-LTC_4 was used as control substrate for MRP1-mediated transport. Data shown are means $\pm$s.d. from at least three experiments with at least triplicate determinations.

compared to A2780 membrane vesicles. This uptake was inhibited by the MDR1 inhibitor PSC833. These results indicate that the ATP-dependent transport of [^{3}H]-APDA, [^{3}H]-vincristine and [^{3}H]-daunorubicin into membrane vesicles from A2780AD is mediated by MDR1.

Under the same conditions, transport studies were performed with membrane vesicles from GLC_4 cells and the MRP1-overexpressing GLC_4/Adr cell line (Figure 2b). The cysteinyl-leukotriene LTC_4 was used as a control substrate for MRP1-mediated transport. ATP-dependent transport of [^{3}H]-LTC_4 into membrane vesicles from GLC_4/Adr cells was 16 fold higher than the uptake into GLC_4 membrane vesicles. This was inhibited by the MRP1 inhibitor MK571. In the presence of ATP, uptake of [^{3}H]-APDA and [^{3}H]-daunorubicin into GLC_4/Adr membrane vesicles was significantly higher than into GLC_4 membrane vesicles. [^{3}H]-vincristine uptake was only modestly higher. In contrast to [^{3}H]-LTC_4, uptake of these three cationic compounds into GLC_4/Adr membrane vesicles was not inhibited by MK571. The uptake of [^{3}H]-APDA, [^{3}H]-vincristine and [^{3}H]-daunorubicin into membrane vesicles from S1(MRP) and S1 cells was similar. Furthermore, uptake of all three substrates into S1(MRP) membrane vesicles was not inhibited by MK571 (data not shown). These results indicate that the uptake of [^{3}H]-APDA, [^{3}H]-vincristine and [^{3}H]-daunorubicin *per se* into membrane vesicles from MRP1-overexpressing cells, although ATP-dependent, is not mediated by MRP1.

MRP1-mediated transport of [^{3}H]-vincristine and [^{3}H]-daunorubicin but not of [^{3}H]-APDA in the presence of GSH

Next, we investigated the GSH-dependency of MRP1-mediated transport. The above described non-MRP1-mediated uptake of the monoquaternary cation [^{3}H]-APDA and the weak base [^{3}H]-daunorubicin into GLC_4/Adr membrane vesicles (Figure 2b) might be driven by a proton gradient. To eliminate this uptake we used the vacuolar H^+-ATPase (V-type ATPase) inhibitor bafilomycin A_1 (Baf) to block the potential involvement of proton gradient generating V-type ATPases. Uptake of [^{3}H]-APDA and [^{3}H]-daunorubicin into GLC_4/Adr membrane vesicles in the presence of 1 μM Baf was reduced to 5 and 35% of the control values, respectively, while [^{3}H]-vincristine uptake was only slightly inhibited. In addition, Baf did not alter [^{3}H]-LTC_4 uptake (Table 1). These results indicate that Baf reduces non-MRP1-mediated uptake of cationic compounds into GLC_4/Adr membrane vesicles without affecting the transport activity of MRP1. Therefore, all experiments to investigate the role of GSH in MRP1-mediated cation transport were performed in the presence of 1 μM Baf.

GSH (5 mM) did not affect the uptake [^{3}H]-APDA into GLC_4/Adr membrane vesicles (Figure 3a). However, the uptake of [^{3}H]-vincristine and [^{3}H]-daunorubicin, in the presence of ATP, was stimulated by GSH. This stimulated uptake was inhibited by MK571. With membrane vesicles from S1(MRP) cells, similar results were obtained (Figure 3b). The levels of GSH-mediated uptake of [^{3}H]-vincristine and [^{3}H]-daunorubicin into GLC_4/Adr and into S1(MRP) membrane vesicles correlated with levels of MRP1 protein expression (Figure 1). These data show that MRP1-mediated ATP-dependent transport of daunorubicin appears to be GSH-dependent. To gain more insight into the initial uptake phase, a 2 min time course of [^{3}H]-daunorubicin uptake was measured (Figure 4). Because of a relatively low overexpression of MRP1 in S1(MRP) membrane vesicles, GLC_4/Adr membrane vesicles were used for these experiments. In the presence of 5 mM GSH, the uptake of [^{3}H]-daunorubicin was linear up to 1 min. After 3 min, a steady state uptake of about 30 pmol mg protein^{-1} was reached which did not significantly

Table 1 Uptake of [^{3}H]-LTC_4 and cationic drugs into membrane vesicles from GLC_4/Adr cells in the absence and the presence of Baf

Substrate	*Uptake* (pmol mg protein^{-1}) *Control*	*1 μM Baf*	
[^{3}H]-LTC_4 (1.5 nM)	7.7±1.64	7.8±2.0	ns
[^{3}H]-APDA (300 nM)	22.1±7.34	1.2±1.34	$P<0.001$
[^{3}H]-vincristine (300 nM)	1.6±0.9	0.4±0.02	ns
[^{3}H]-daunorubicin (300 nM)	23.7±5.9	8.4±5.7	$P<0.006$

Uptake of indicated substrates into membrane vesicles from GLC_4/Adr cells (50 μg) were measured for 5 min in the absence or the presence of 1 μM Baf. Data represent mean±s.d. of three independent experiments with quadruplicate determinations. Data were compared by an unpaired two-tailed Student's *t*-test, differences were considered to be significant when $P<0.05$; ns, not significant.

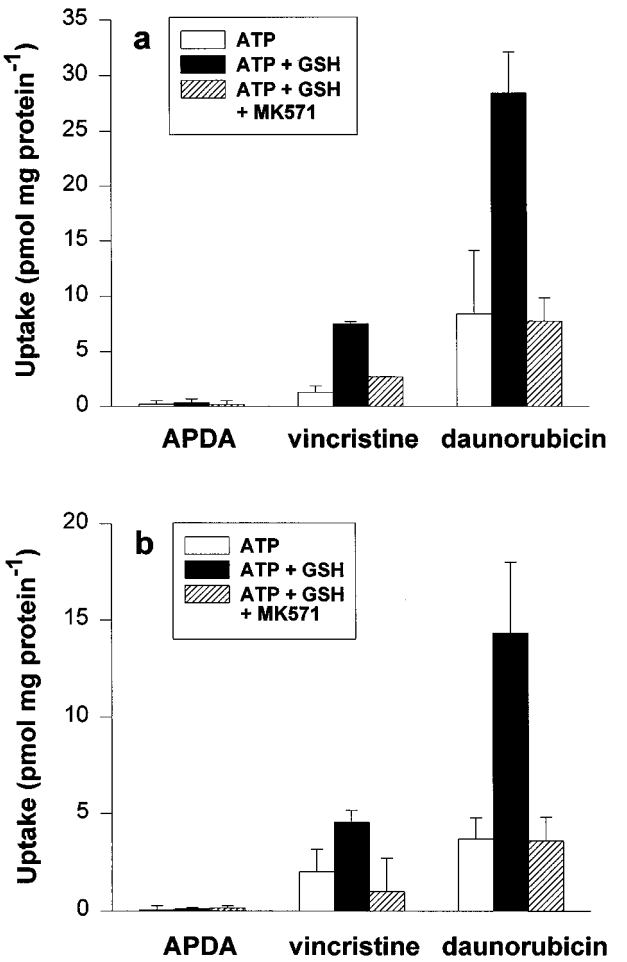

Figure 3 ATP-dependent uptake of cationic drugs in the presence of GSH. (a) represents uptake during 5 min of [^{3}H]-APDA (300 nM), [^{3}H]-vincristine (300 nM) and [^{3}H]-daunorubicin (600 nM) into membrane vesicles prepared from GLC_4/Adr cells in the absence and the presence of 5 mM GSH. Uptake was also measured in the presence of 5 μM MK571. (b) represents the same experiments with *MRP1*-transfected S1 (MRP) cells. All experiments were performed in the presence of 1 μM Baf. Data represent mean±s.d. from at least two experiments with quadruplicate determinations.

change during the next 7 min (data not shown). The non-hydrolyzable ATP analogue AMP-PCP did not stimulate uptake, indicating that GSH-dependent uptake of [^{3}H]-daunorubicin requires ATP hydrolysis. MK571 (2 μM) completely inhibited the GSH-dependent [^{3}H]-daunorubicin uptake.

Inhibition of [^{3}H]-vincristine, [^{3}H]-daunorubicin and [^{3}H]-LTC$_4$ transport with the monoclonal antibody (mAb) QCRL-3

To demonstrate that transport of [^{3}H]-daunorubicin and [^{3}H]-vincristine is specifically mediated by MRP1, uptake of both cations into GLC$_4$/Adr membrane vesicles was measured in the presence of the mAb QCRL-3 which recognizes a conformation dependent MRP1-epitope (Hipfner *et al.*, 1994). [^{3}H]-LTC$_4$ was used as positive control for QCRL-3 inhibition. Results are presented in Figure 5. Transport of all three substrates was inhibited by QCRL-3 with IC$_{50}$'s of 2, 20 and 12 μg ml^{-1} (0.23, 2.3 and 1.4 μg mAb per 50 μg protein) respectively for [^{3}H]-daunorubicin, [^{3}H]-vincristine and [^{3}H]-LTC$_4$. A control mAb directed against the T-cell marker CD3 with an identical isotype as QCRL-3 did not affect [^{3}H]-LTC$_4$ transport and only slightly inhibited transport of [^{3}H]-daunorubicin and [^{3}H]-vincristine (less than 15% at the highest QCRL-3 concentration, data not shown).

Dependency of MRP1-mediated daunorubicin transport on GSH concentration

The effect of different GSH concentrations on MRP1-mediated daunorubicin transport was investigated with GLC$_4$/Adr membrane vesicles. Figure 6 shows that [^{3}H]-daunorubicin transport was stimulated by increased concentrations of GSH with a maximum of 10 mM after which a steady state level was reached. The K_M value was determined to be 2.7 mM.

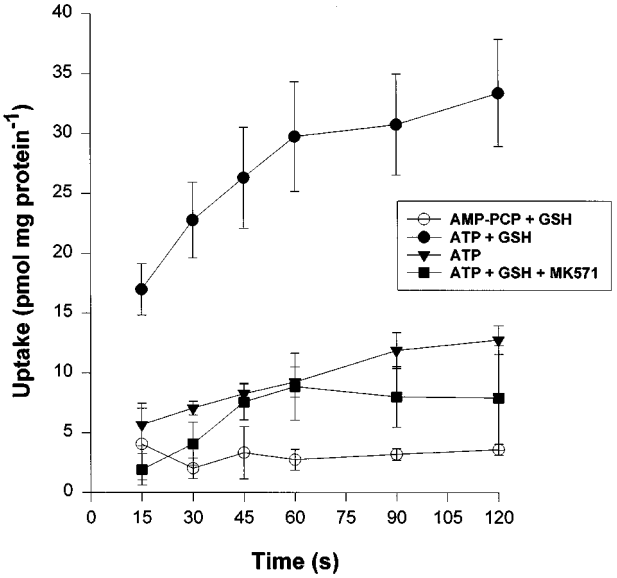

Figure 4 Time course of MRP1-mediated daunorubicin transport. Initial uptake of [^{3}H]-daunorubicin (600 nM) into GLC$_4$/Adr membrane vesicles (100 μg protein, 220 μl final volume) was followed during 2 min with different conditions. All experiments were performed in the presence of 1 μM Baf. GSH and MK571 were added to a final concentration of 5 mM and 2 μM, respectively. Data points are means$\pm$s.d. from at least four independent experiments with quadruplicate measurements. Experiments were performed with two different batches of membrane vesicles.

Determination of IC$_{50}$ value of MK571 for MRP1-mediated daunorubicin transport

The inhibitory effect of MK571 on MRP1-mediated daunorubicin transport was measured in the presence of 10 mM GSH. MK571 effectively inhibited GSH-stimulated [^{3}H]-daunorubicin transport in a dose-dependent manner with an IC$_{50}$ of 0.4 μM (Figure 7).

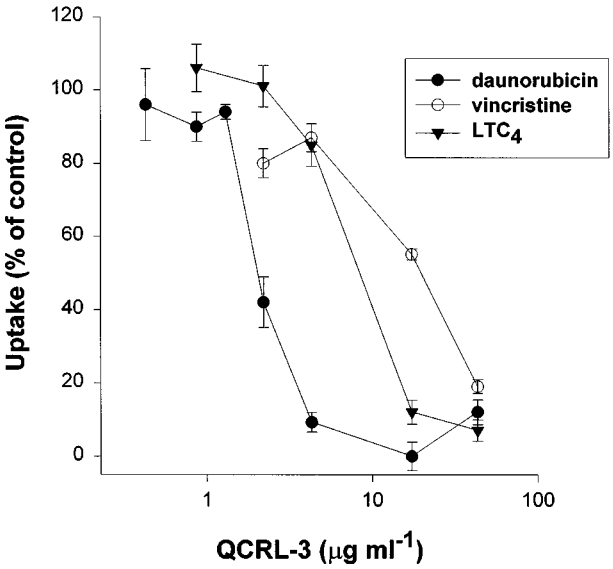

Figure 5 Inhibition of MRP1-mediated transport by the mAb QCRL-3. Uptake of [^{3}H]-daunorubicin (600 nM), [^{3}H]-vincristine (300 nM) into GLC$_4$/Adr membrane vesicles (50 μg) was measured for 1 min in the presence of 1 μM Baf, 5 mM GSH and increasing concentrations of the MRP1 specific mAb QCRL-3. [^{3}H]-LTC$_4$ (1.5 nM) was used as control for MRP1 inhibition by QCRL-3. Data are plotted as percentages of control. Uptake rates of control experiments were 19, 4.3 and 3.9 pmol mg protein^{-1} min^{-1}, respectively, for [^{3}H]-daunorubicin, [^{3}H]-vincristine and [^{3}H]-LTC$_4$. Data points represent means$\pm$s.e.mean of triplicate measurements in a single experiment.

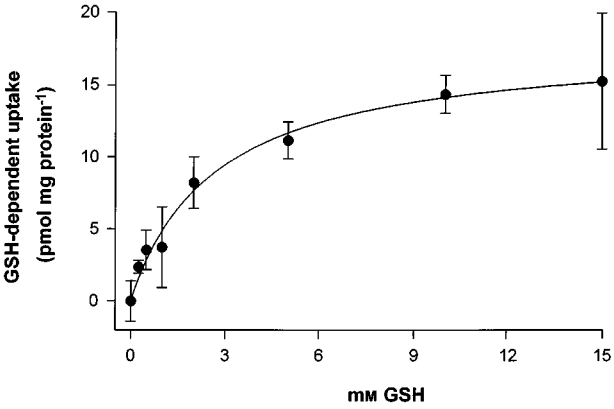

Figure 6 Dependency of MRP1-mediated daunorubicin transport on the GSH concentration. Uptake of [^{3}H]-daunorubicin into GLC$_4$/Adr membrane vesicles was measured for 1 min as described at Figure 5 in the presence of different GSH concentrations. Data points represent the difference between ATP-dependent uptake and ATP-dependent uptake in the presence of GSH. Data points are means$\pm$s.e.mean of at least triplicate measurements in a single experiment. Two additional experiments showed the same results. Curve fitting and calculation of the K_M value was performed with the Graphpad Prism^{TM} program. The initial ATP-dependent uptake of daunorubicin in the absence of GSH was 9.8$\pm$1.4 pmol mg protein^{-1}.

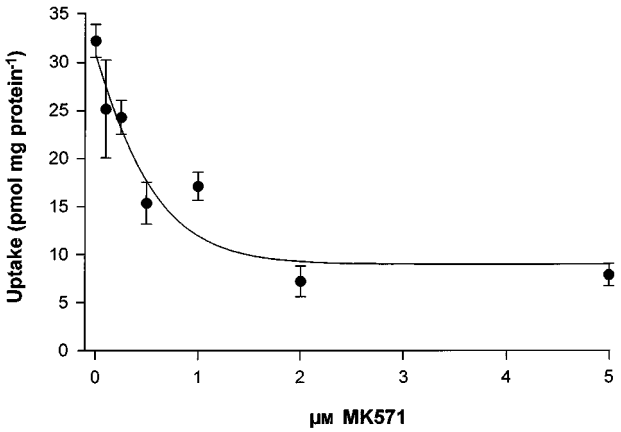

Figure 7 Determination of IC_{50} for MK571 of GSH-dependent daunorubicin transport by MRPI. Uptake of [^{3}H]-daunorubicin into GLC_4/Adr membrane vesicles was measured in the presence of 10 mM GSH with different concentrations of MK571 as described at Figure 5. Data points represent means$\pm$s.e.mean of triplicate measurements in a single experiment. The experiment was performed twice with similar results. Curve fitting and calculation of the IC_{50} value was performed with the Graphpad Prism^{TM} program.

Discussion

MDR1 and MRP1, two distantly related members of the large superfamily of ABC-transporter proteins, are both able to confer resistance of cells against a broad spectrum of natural product drugs (Loe *et al*., 1996c; Broxterman *et al*., 1995; Gottesman & Pastan, 1993). MDR1-related multidrug resistance is most likely due to the ATP-dependent extrusion of unmodified drugs from the cells mediated by the MDR1 protein (Dong *et al*., 1996; Urbatsch *et al*., 1995; Sharom *et al*., 1995; Shapiro & Ling, 1994; Ruetz & Gros, 1994b; Horio *et al*., 1988). Also MRP1-mediated multidrug resistance depends on the transport capacity of MRP1, but the mechanism by which this protein mediates drug transport appears to differ from MDR1. Most MRP1 substrates are organic compounds that need to be conjugated with e.g. GSH before being transported. Also some organic cationic drugs appear to be MRP1 substrates. Although these substrates are not known to form GS *S*-conjugates, it has been shown that the presence of GSH is required for MRP1-associated resistance against the cytotoxicity of these drugs (Versantvoort *et al*., 1995; Zaman *et al*., 1995). This suggests that for MRP1-mediated extrusion of these cations, GSH is required without a need for conjugation. This prompted us to investigate the role of GSH in MRP1-mediated organic cation transport.

We have used three cationic substrates: two more hydrophobic basic drugs [^{3}H]-vincristine and [^{3}H]-daunorubicin and the permanently positively charged organic cation [^{3}H]-APDA. These drugs are substrates for MDR1 as demonstrated by us in this study and by others previously (Müller *et al*., 1994a; Tamai & Safa, 1990; Kamimoto *et al*., 1989). To test the ability of MRP1 to transport these substrates *in vitro* we have used membrane vesicles prepared from the GLC_4/Adr cell line. This cell line was used for two reasons. First, GLC_4/Adr exhibits a very high overexpression of MRP1. This high level could not be found in *MRP1*-transfected cell lines such as S1(MRP) or even not in *Spodoptera frugiperda* or *Trichoplusia ni* (High Five^{TM}) insect cells, overexpressing MRP1 by using the baculovirus expression system (Renes *et al*., unpublished data). Furthermore, it has been demonstrated recently that GLC_4/Adr cells exclusively overexpress *MRP1* but not the isoforms *MRP2*, *MRP3*, *MRP4* and *MRP5* (Kool *et al*., 1997).

We showed that [^{3}H]-APDA and [^{3}H]-daunorubicin, and to a much lower extent [^{3}H]-vincristine, were taken up in membrane vesicles from GLC_4/Adr cells in the presence of ATP but not in the presence of AMP-PCP. However, this uptake was not inhibited by the leukotriene D_4 receptor antagonist and MRP1-inhibitor MK571 (Gekeler *et al*., 1995; Jones *et al*., 1989). This is a clear indication that MRP1, in contrast to MDR1, is not directly involved in ATP-dependent transport of these cationic substrates. We have recently demonstrated that GLC_4/Adr cells have a more pronounced Golgi apparatus and contain more intracellular vesicular structures than GLC_4 cells (van Luyn *et al*., 1998). We therefore speculated that addition of ATP might activate V-type ATPases that are present in membranes of certain intracellular organelles. These V-type ATPases generate a proton-gradient by hydrolyzing ATP and are involved in acidification of intracellular compartments of the endocytotic and exocytotic pathway (for review see Gluck *et al*., 1996; Mellman *et al*., 1986). The crude membrane preparations we used contain plasma membranes as well as intracellular organelles, including acidic vesicular structures which could be responsible for the MRP1-independent uptake of cations. The macrolide antibiotic bafilomycin A_1 (Baf) is known to function as a specific inhibitor for V-type ATPases (Bowman *et al*., 1988). Addition of Baf blocked ATP-stimulated uptake of the cations into GLC_4/Adr membrane vesicles but it did not influence MRP1-mediated transport of [^{3}H]-LTC_4. Therefore, Baf was used in all further experiments.

Several reports have suggested an important role of GSH in MRP1-mediated drug efflux from cells with a multidrug resistant phenotype (O'Brien & Tew, 1996 and references therein). Experiments with MRP1-transfected cells showed that depletion of GSH results in a complete reversal of resistance to vinca alkaloids and anthracyclines (Zaman *et al*., 1995). Furthermore, MRP1 mediates vincristine transport only in the presence of GSH (Loe *et al*., 1996b, this study). Reducing agents such as 2-mercaptoethanol, dithiothreitol and L-cysteine, have been tested but none of these could increase uptake of [^{3}H]-vincristine in membrane vesicles from MRP1 transfected cells (Loe *et al*., 1996b) indicating that it is not the reducing capacity of GSH that is responsible for this effect. GSH itself seems to play an essential role in MRP1-mediated transport of hydrophobic drugs and our findings support this. In this study we show that in the presence of physiological concentrations of GSH, the hydrophobic basic drug daunorubicin is transported by MRP1 in an ATP-dependent manner. The rate of MRP1-mediated daunorubicin transport is dependent on the concentration of GSH. This implies that changes in the intracellular GSH concentration will have a marked effect on the MRP1-mediated daunorubicin transport from drug resistant cells.

The specificity of MRP1-mediated cation transport, in particular of daunorubicin, was demonstrated by the MRP1-specific mAb QCRL-3 (Loe *et al*., 1996b; 1997) and by MK571 inhibition. QCRL-3 inhibited MRP1-mediated transport of daunorubicin in the presence of GSH better than LTC_4 transport. One explanation for this effect may be a difference in binding sites for hydrophobic cations and for anions at MRP1. The competitive inhibitor MK571 inhibited MRP1-mediated GSH-dependent daunorubicin transport in a dose-dependent manner with an IC_{50} value of 0.4 μM. This is similar to what has been reported for LTC_4-inhibition (Leier *et al*., 1994). The difference between MRP1 inhibition by QCRL-3

and by MK571 can be explained by the difference in binding of each of these compounds to MRP1.

The mechanism by which GSH facilitates MRP1-mediated transport of hydrophobic cationic drugs has not yet been fully elucidated. There is no evidence for conjugation of GSH to drugs to which MRP1 confers resistance (O'Brien & Tew, 1996; Zaman *et al*., 1995). There are indications that MRP1 mediates GSH-transport (Rappa *et al*., 1997; Zaman *et al*., 1995), and may function as a co-transporter for GSH and the drug. Thus GSH may be a low affinity substrate for MRP1. From experiments using the vanadate-trapping technique it has been suggested that GSH as well as anticancer drugs directly interact with MRP1 (Taguchi *et al*., 1997). Transport of anionic MRP1-substrates such as GSH- and glucuronide-conjugates are inhibited by hydrophobic (cationic) vinca alkaloids (Loe *et al*., 1996b; Müller *et al*., 1994b) and anthracyclines (Loe *et al*., 1996b). One hypothesis explaining these results is that MRP1 may contain two binding sites: one for hydrophobic compounds and one for hydrophilic compounds. This would allow a similar binding of GSH and the hydrophobic drug as well as binding of hydrophobic compounds conjugated to GSH, glucuronate or sulphate. Further studies are needed to address this important issue.

In conclusion, we showed that in addition to vincristine MRP1-mediated transport of the unmodified anticancer drug daunorubicin is dependent on GSH. APDA is not a substrate for MRP1.

This study is supported by grant RUG 95-1007 from the Dutch Cancer Society. Hans Koning (University Hospital Groningen) is acknowledged for technical assistance. We thank Dr A.W. Ford-Hutchinson for providing MK571 and Dr G. Kurz for the gift of [^{3}H]-APDA. In addition we thank Drs R. Scheper, R. Oude Elferink and B.J. Kroesen for providing monoclonal antibodies and Dr H.W. van Veen (Dept. Microbiology, University of Groningen) for critical comments on the manuscript.

References

BARNOUIN, K., LEIER, I., JEDLITSCHKY, G., POURTIER-MANZANEDO, A., KÖNIG, J., LEHMAN, W-D. & KEPPLER, D. (1998). Multidrug resistance protein-mediated transport of chlorambucil and melphalan conjugated to glutathione. *Br. J. Cancer,* **77,** 201 – 209.

BORST, P. & SCHINKEL, A.H. (1997). Genetic dissection of the function of mammalian P-glycoproteins. *Trends Genet.,* **13,** 217 – 221.

BOWMAN, E.J., SIEBERS, A. & ALTENDORF, K. (1988). Bafilomycins: a class of inhibitors of membrane ATPases from microorganisms, animal cells, and plant cells. *Proc. Natl. Acad. Sci. U.S.A.,* **85,** 7972 – 7976.

BROXTERMAN, H.J., GIACCONE, G. & LANKELMA, J. (1995). MRP and other drug transport-related resistance to natural product agents. *Curr. Opin. Oncol.,* **7,** 532 – 540.

BURGER, H., NOOTER, K., ZAMAN, G.J.R., SONNEVELD, P., VAN WINGERDEN, K.E., OOSTRUM, R.G. & STOTER, G. (1994). Expression of the multidrug resistance-associated protein (MRP) in acute and chronic leukemias. *Leukemia,* **8,** 990 – 997.

COLE, S.P.C., BHARDWAJ, G., GERLACH, J.H., MACKIE, J.E., GRANT, C.E., ALMQUIST, K.C., STEWART, A.J., KURZ, E.U., DUNCAN, A.M. & DEELEY, R.G. (1992). Overexpression of a transporter gene in a multidrug-resistant human lung cancer cell line. *Science,* **258,** 1650 – 1654.

DONG, M., PENIN, F. & BAGGETTO, L.G. (1996). Efficient purification and reconstitution of P-glycoprotein for functional and structural studies. *J. Biol. Chem.,* **271,** 28875 – 28883.

GEKELER, V., ISE, W., SANDERS, H.K., ULRICH, W. & BECK, J. (1995). The leukotriene LTD_4 receptor antagonist MK571 specifically modulates MRP associated multidrug resistance. *Biochem. Biophys. Res. Commun.,* **208,** 345 – 352.

GERMANN, U.A. (1996). P-glycoprotein – A mediator of multidrug resistance in tumour cells. *Eur. J. Cancer,* **32A,** 927 – 944.

GLUCK, S.L., UNDERHILL, D.M., IYORI, M., HOLLIDAY, L.S., KOSTROMINOVA, T.Y. & LEE, B.S. (1996). Physiology and biochemistry of the kidney vacuolar H^+-ATPase. *Annu. Rev. Physiol.,* **58,** 427 – 445.

GOTTESMAN, M.M. & PASTAN, I. (1993). Biochemistry of multidrug resistance mediated by the multidrug transporter. *Annu. Rev. Biochem.,* **62,** 385 – 427.

HIGGINS, C.F. (1992). ABC transporters: from microorganism to man. *Annu. Rev. Cell Biol.,* **67,** 113.

HIPFNER, D.R., GAULDIE, S.D., DEELEY, R.G. & COLE, S.P.C. (1994). Detection of the M_r 190,000 multidrug resistance protein, MRP, with monoclonal antibodies. *Cancer Res.,* **54,** 5788 – 5792.

HORIO, M., GOTTESMAN, M.M. & PASTAN, I. (1988). ATP-dependent transport of vinblastine in vesicles from human multidrug-resistant cells. *Proc. Natl. Acad. Sci. U.S.A.,* **85,** 3580 – 3584.

ISHIKAWA, T., AKIMARU, K., KUO, M.T., PRIEBE, W. & SUZUKI, M. (1995). How does the MRP/GS-X pump export doxorubicin? *J. Natl. Cancer Inst.,* **87,** 1639 – 1640.

JEDLITSCHKY, G., LEIER, I., BUCHHOLZ, U., BARNOUIN, K., KURZ, G. & KEPPLER, D. (1996). Transport of glutathione, glucuronate and sulphate conjugates by the *MRP* gene-encoded conjugate export pump. *Cancer Res.,* **56,** 988 – 994.

JONES, T.R., ZAMBONI, R., BELLEY, M., CHAMPION, E., CHARETTE, L., FORD-HUTCHINSON, A.W., FRENETTE, R., GAUTHIER, J., LEGER, S., MASSON, P., MCFARLENE, C.S., PIECHUTA, H., ROKAH, J., WILLIAMS, H., YOUNG, R.N., DEHAVEN, R.N. & PONG, S.S. (1989). Pharmacology of L-660,711 (MK-571): a novel potent and selective leukotriene D_4 receptor antagonist. *Can. J. Physiol. Pharmacol.,* **67,** 17 – 28.

JULIANO, R.L. & LING, V. (1976). A surface glycoprotein modulating drug permeability in chinese hamster ovary cell mutants. *Biochim. Biophys. Acta.,* **455,** 152 – 162.

KAMIMOTO, Y., GATMAITAN, Z., HSU, J. & ARIAS, I.M. (1989). The function of Gp170, the multidrug resistance gene product in rat liver canalicular membrane vesicles. *J. Biol. Chem.,* **264,** 11693 – 11698.

KOOL, M., DE HAAS, M., SCHEFFER, G.L., SCHEPER, R.J., VAN EIJK, M.J.T., JUIJN, J.A., BAAS, F. & BORST, P. (1997). Analysis of expression of *cMOAT* (*MRP2*), *MRP3*, *MRP4*, and *MRP5*, homologues of the multidrug resistance-associated protein gene (*MRP1*), in human cancer cell lines. *Cancer Res.,* **57,** 3537 – 3547.

LEIER, I., JEDLITSCHKY, G., BUCHHOLZ, U., COLE, S.P.C., DEELEY, R.G. & KEPPLER, D. (1994). The *MRP* gene encodes an ATP-dependent export pump for leukotriene C_4 and structurally related conjugates. *J. Biol. Chem.,* **269,** 27807 – 27810.

LOE, D.W., ALMQUIST, K.C., COLE, S.P.C. & DEELEY, R.G. (1996a). ATP-dependent 17β-estradiol 17-(β-D-glucuronide) transport by multidrug resistance protein (MRP). *J. Biol. Chem.,* **271,** 9683 – 9689.

LOE, D.W., ALMQUIST, K.C., DEELEY, R.G. & COLE, S.P.C. (1996b). Multidrug resistance protein (MRP)-mediated transport of leukotriene C_4 and chemotherapeutic agents in membrane vesicles. *J. Biol. Chem.,* **271,** 9675 – 9682.

LOE, D.W., DEELEY, R.G. & COLE, S.P.C. (1996c). Biology of the multidrug resistance-associated protein, MRP. *Eur. J. Cancer,* **32A,** 945 – 957.

LOE, D.W., STEWART, R.K., MASSEY, T.E., DEELEY, R.G. & COLE, S.P.C. (1997). ATP-dependent transport of Aflatoxin B_1 and its glutathione conjugates by the product of the multidrug resistance protein (*MRP*) gene. *Mol. Pharmacol.,* **51,** 1034 – 1041.

MELLMAN, I., FUCHS, R. & HELENIUS, A. (1986). Acidification of the endocytic and exocytic pathways. *Annu. Rev. Biochem.,* **55,** 663 – 700.

MÜLLER, M., MAYER, R., HERO, U. & KEPPLER, D. (1994a). ATP-dependent transport of amphiphilic cations across the hepatocyte canalicular membrane mediated by mdr1 P-glycoprotein. *FEBS. Lett.,* **343,** 168 – 172.

MÜLLER, M., MEIJER, C., ZAMAN, G.J.R., BORST, P., SCHEPER, R.J., MULDER, N.H., DE VRIES, E.G.E. & JANSEN, P.L.M. (1994b). Overexpression of the gene encoding the multidrug resistance-associated protein results in increased ATP-dependent glutathione *S*-conjugate transport. *Proc. Natl. Acad. Sci. U.S.A.,* **91,** 13033 – 13037.

MÜLLER, M., ROELOFSEN, H. & JANSEN, P.L.M. (1996). Secretion of organic anions by hepatocytes: involvement of homologues of the multidrug resistance protein. *Semin. Liver Dis.,* **16,** 211 – 220.

O'BRIEN, M.L. & TEW, K.D. (1996). Glutathione and related enzymes in multidrug resistance. *Eur. J. Cancer,* **32A,** 967 – 978.

PRIEBE, W., KRAWCZYK, M., KUO, M.T., YAMANE, Y., SAVARAJ, N. & ISHIKAWA, T. (1998). Doxorubicin- and daunorubicin-glutathione conjugates, but not unconjugated drugs, competitively inhibit leukotriene C_4 transport mediated by MRP/GS-X pump. *Biochem. Biophys. Res. Commun.,* **247,** 859 – 863.

RAPPA, G., LORICO, A., FLAVELL, R.A. & SARTORELLI, A.C. (1997). Evidence that the multidrug resistance protein (MRP) functions as a co-transporter for glutathione and natural product drugs. *Cancer Res.,* **57,** 5232 – 5237.

ROELOFSEN, H., VOS, T.A., SCHIPPERS, I.J., KUIPERS, F., KONING, H., MOSHAGE, H., JANSEN, P.L.M. & MÜLLER, M. (1997). Increased levels of the multidrug resistance protein in lateral membranes of proliferating hepatocyte-derived cells. *Gastroenterology,* **112,** 511 – 521.

ROGAN, A.M., HAMILTON, T.C., YOUNG, R.C., KLECKER, R.W. & OZOLS, R.F. (1984). Reversal of adriamycin resistance by verapamil in human ovarium cancer. *Science,* **224,** 994 – 996.

RUETZ, S. & GROS, P. (1994a). A mechanism for P-glycoprotein action in multidrug resistance: are we there yet? *Trends Pharmacol. Sci.,* **15,** 260 – 263.

RUETZ, S. & GROS, P. (1994b). Functional expression of P-glycoproteins in secretory vesicles. *J. Biol. Chem.,* **269,** 12277 – 12284.

SHAPIRO, A.B. & LING, V. (1994). ATPase activity of purified and reconstituted P-glycoprotein from chinese hamster ovary cells. *J. Biol. Chem.,* **269,** 3745 – 3754.

SHAROM, F.J., YU, X., CHU, J.W.K. & DOIGE, C.A. (1995). Characterization of the ATPase activity of P-glycoprotein from multidrug resistant chinese hamster ovary cells. *Biochem. J.,* **308,** 381 – 390.

TAGUCHI, Y., YOSHIDA, A., TAKADA, Y., KOMANO, T. & UEDA, K. (1997). Anti-cancer drugs and glutathione stimulate vanadate-induced trapping of nucleotide on multidrug resistance-associated protein (MRP). *FEBS Lett.,* **401,** 11 – 14.

TAMAI, I. & SAFA, A.R. (1990). Competitive interaction of cyclosporins with the *vinca* alkaloid-binding site of P-glycoprotein in multidrug-resistant cells. *J. Biol. Chem.,* **265,** 16509 – 16513.

TEW, K.D. (1994). Glutathione associated enzymes in anticancer drug resistance. *Cancer Res.,* **54,** 4313 – 4320.

URBATSCH, I.L., SANKARAN, B., WEBER, J. & SENIOR, A.E. (1995). P-glycoprotein is stably inhibited by vanadate-induced trapping of nucleotide at a single catalytic site. *J. Biol. Chem.,* **270,** 19383 – 19390.

VAN LUYN, M.J.A., MÜLLER, M., RENES, J., MEIJER, C., SCHEPER, R.J., NIENHUIS, E.F., MULDER, N.H., JANSEN, P.L.M. & DE VRIES, E.G.E. (1998). Transport of glutathione conjugates into secretory vesicles is mediated by the multidrug-resistance protein 1. *Int. J. Cancer,* **76,** 55 – 62.

VERSANTVOORT, C.H.M., BROXTERMAN, H.J., BAGRIJ, T., SCHEPER, R.J. & TWENTYMAN, P.R. (1995). Regulation by glutathione of drug transport in multidrug-resistant human lung tumour cell lines overexpressing multidrug resistance-associated protein. *Br. J. Cancer,* **72,** 82 – 89.

ZAMAN, G.J.R., FLENS, M.J., VAN LEUSDEN, M.R., DE HAAS, M., MULDER, H.S., LANKELMA, J., PINEDO, H.M., SCHEPER, R.J., BAAS, F., BROXTERMAN, H.J. & BORST, P. (1994). The human multidrug resistance-associated protein MRP is a plasma membrane drug-efflux pump. *Proc. Natl. Acad. Sci. U.S.A.,* **91,** 8822 – 8826.

ZAMAN, G.J.R., LANKELMA, J., VAN TELLINGEN, O., BEIJNEN, J., DEKKER, H., PAULUSMA, C., OUDE ELFERINK, R.P.J., BAAS, F. & BORST, P. (1995). Role of glutathione in the export of compounds from cells by the multidrug-associated protein. *Proc. Natl. Acad. Sci. U.S.A.,* **92,** 7690 – 7694.

ZAMAN, G.J.R., VERSANTVOORT, C.H., SMIT, J.J., EIJDEMS, E.W., DE HAAS, M., SMITH, A.J., BROXTERMAN, H.J., MULDER, N.H., DE VRIES, E.G.E., BAAS, F. & BORST, P. (1993). Analysis of the expression of MRP, the gene for a new putative transmembrane drug transporter, in human multidrug resistant lung cancer cell lines. *Cancer Res.,* **53,** 1747 – 1750.

ZIJLSTRA, J.G., DE VRIES, E.G.E. & MULDER, N.H. (1987). Multifactorial drug resistance in an adriamycin resistant human small cell lung carcinoma cell line. *Cancer Res.,* **47,** 1780 – 1784.

(Received August 10, 1998
Revised November 11, 1998
Accepted November 13, 1998)

British Journal of Pharmacology (1999) 126, 689–696
http://www.stockton-press.co.uk/bjp

An *in vitro* electrophysiological study on the effects of phenytoin, lamotrigine and gabapentin on striatal neurons

*,[1]P. Calabresi, [1]D. Centonze, [1]G. A. Marfia, [1]A. Pisani & [1,2]G. Bernardi

[1]Clinica Neurologica, Dip. Sanità, Università di Roma "Tor Vergata", via O Raimondo 8, 00173, Rome, Italy; [2]IRCCS Ospedale S. Lucia, Rome, Italy

1 We performed intracellular recordings from a rat corticostriatal slice preparation in order to compare the electrophysiological effects of the classical antiepileptic drug (AED) phenytoin (PHT) and the new AEDs lamotrigine (LTG) and gabapentin (GBP) on striatal neurons.

2 PHT, LTG and GBP affected neither the resting membrane potential nor the input resistance/membrane conductance of the recorded cells. In contrast, these agents depressed in a dose-dependent and reversible manner the current-evoked repetitive firing discharge.

3 These AEDs also reduced the amplitude of glutamatergic excitatory postsynaptic potentials (EPSPs) evoked by cortical stimulation. However, substantial pharmacological differences between these drugs were found. PHT was the most effective and potent agent in reducing sustained repetitive firing of action potentials, whereas LTG and GBP preferentially inhibited corticostriatal excitatory transmission. Concentrations of LTG and GBP effective in reducing EPSPs, in fact, produced only a slight inhibition of the firing activity of these cells.

4 LTG, but not PHT and GBP, depressed cortically-evoked EPSPs increasing paired-pulse facilitation (PPF) of synaptic transmission, suggesting that a presynaptic site of action was implicated in the effect of this drug. Accordingly, PHT and GBP, but not LTG reduced the membrane depolarizations induced by exogenously-applied glutamate, suggesting that these drugs preferentially reduce postsynaptic sensitivity to glutamate released from corticostriatal terminals.

5 These data indicate that in the striatum PHT, LTG and GBP decrease neuronal excitability by modulating multiple sites of action. The preferential modulation of excitatory synaptic transmission may represent the cellular substrate for the therapeutic effects of new AEDs whose use may be potentially extended to the therapy of neurodegenerative diseases involving the basal ganglia.

Keywords: Antiepileptic drugs; epilepsy; excitatory amino acids; intracellular recordings; striatum; synaptic transmission

Abbreviations: AED, antiepileptic drug; EPSP, excitatory postsynaptic potentials; GBP, gabapentin; LTG, lamotrigine; PHT, phenytoin; PPF, paired pulse facilitation; RMP, resting membrane potential; TTX, tetrodotoxin

Introduction

Despite substantial progress in the treatment of epileptic seizures made in the past two decades, epilepsy still remains a significant therapeutic challenge. Advances in the understanding of the pathogenesis of this disease have allowed the development of new pharmacological compounds with different mechanisms of action. These new antiepileptic drugs (AEDs), used in monotherapy or in association with traditional drugs, offer hope for patients with uncontrolled epilepsy. Different mechanisms of action have been proposed to explain the clinical effects of old and new AEDs: modulation of voltage-dependent sodium channels, modulation of voltage-dependent calcium channels, enhancement of GABA-mediated neuronal inhibition, reduction of glutamate-mediated excitatory transmission (Harden, 1994; Upton, 1994; Walker & Sander, 1994; Macdonald & Kelly, 1994; Calabresi *et al*., 1996b; Macdonald, 1996). The latter mechanism seems to be particularly important for the therapeutic effects of some new AEDs such as lamotrigine (LTG) and gabapentin (GBP). It has been shown, in fact, that LTG potently inhibited the release of excitatory amino acids evoked by the sodium channel activator veratridine while it was much less effective in inhibiting the release of acetylcholine or GABA (Leach *et al*., 1986). GBP prolonged the onset latency of epileptic seizures following intraperitoneal injection of the glutamate receptor agonist NMDA (Bartoszyk, 1982). Accordingly, the efficacy of GBP against tonic seizure in mice was antagonized by the administration of serine, an agonist at the glycine receptor on the NMDA receptor channel complex (Oles *et al*., 1990).

AEDs may attenuate or prevent seizures through effects on pathologically altered neurons of seizure foci or, alternatively, by reducing the spread of excitation from seizure foci to additional brain regions. It has been suggested that the basal ganglia play an important role in the initiation and propagation of seizure activity (Faeth *et al*., 1954; Engel *et al*., 1978; Amato *et al*., 1982; Gale, 1992). The main excitatory projection to the basal ganglia is represented by the corticostriatal glutamatergic pathway and activity of striatal neurons affects the excitability of the cortex by modulating the thalamocortical glutamatergic pathway (Divac *et al*., 1977; Calabresi *et al*., 1996a). An increased activity of GABAergic striatal neurons may result in an excessive inhibition of the substantia nigra pars reticulata and of the internal segment of the globus pallidus which exert an inhibitory action on the thalamus. This effect may finally result in an increased excitation of the cortex by the thalamus.

In the present study we have evaluated the electrophysiological actions of PHT, a classical AED, and of the new compounds LTG and GBP on striatal projecting spiny cells intracellularly recorded in a corticostriatal slice preparation in order to compare their effects on the intrinsic neuronal activity to those exerted on the excitatory corticostriatal synaptic

* Author for correspondence; E-mail: calabre@uniroma2.it

transmission. An abnormal activity of the corticostriatal glutamatergic pathway has also been postulated to play a pathogenetic role in neurodegenerative diseases involving the basal ganglia such as Parkinson's disease and Huntington's disease (Calabresi *et al*., 1996a). Thus, the characterization of the electrophysiological effects produced by AEDs on the corticostriatal glutamatergic transmission might also provide possible insights for the treatment of these neurodegenerative disorders.

Methods

Preparation and maintenance of the slices

Adult male Wistar rats (150–250 g) were used for all the experiments. The preparation and maintenance of coronal slices have been described previously (Calabresi *et al*., 1990a, 1995a, 1997b, 1998). Briefly, corticostriatal coronal slices (200–300 μm) were prepared from tissue blocks of the brain with the use of a vibratome. A single slice was transferred to a recording chamber and submerged in a continuously flowing Krebs solution (35°C, 2–3 ml min^{-1}) gassed with 95% O_2-5% CO_2. The composition of the control solution was (in mM): NaCl, 126 KCl, 2.5 $MgCl_2$, 1.2 NaH_2PO_4, 1.2 $CaCl_2$, 2.4 Glucose, 11 $NaHCO_3$ 25.

Recording technique

In all the experiments the intracellular recording electrodes were filled with 2 M KCl (30–60 MΩ). An Axoclamp 2A amplifier was used for recordings either in current-clamp or in voltage-clamp mode. In single-electrode voltage-clamp mode the switching frequency was 3 kHz. The headstage signal was continuously monitored on a separate oscilloscope. Traces were displayed on an oscilloscope and stored in a digital system. For synaptic stimulation, bipolar electrodes were used. These stimulating electrodes were located either in the cortical areas close to the recording electrode or in the white matter between the cortex and the striatum in order to activate corticostriatal fibres.

Morphological identification of the recorded cells

In some experiments biocytin (Sigma) was used in the intracellular electrode in order to stain the neurons. In these cases, biocytin at concentration of 2–4% was added to a 0.5 M KCl pipette solution. Slices containing neurons stained with biocytin were fixed in paraformaldehyde (in 0.1 M phosphate buffer at pH 7.4) overnight and processed according to published protocols (Horikawa & Armstrong, 1988). In several cases, sections were further processed to make permanent staining of biocytin loaded cells.

Data analysis and drug applications

Values given in the text and in the figures are mean ± s.e.mean of changes in the respective cell populations. Student's *t*-test (for paired and unpaired observations) was used to compare the means. Drugs were applied by dissolving them to the desired final concentration in the saline and by switching the perfusion from control saline to drug-containing saline. Drug solutions entered the recording chamber within 40 s after a three ways tap had been turned on. Biocytin, tetrodotoxin (TTX), glutamate and phenytoin (PHT) were from Sigma; gabapentin (GBP) and lamotrigine (LTG) were respectively from Parke-Davis and Glaxo-Wellcome. GBP was solved in water while PHT and LTG were solved in DMSO. The maximal final concentration of the solvent was 1 : 300. This concentration of DMSO did not produce *per se* detectable electrophysiological changes.

Results

Properties of the recorded neurons

Conventional sharp-microelectrode intracellular recordings were obtained from 82 electrophysiologically identified 'principal' spiny cells. The main characteristics of these cells have been described in detail previously both *in vivo* (Wilson & Groves, 1980; Calabresi *et al*., 1990b) and *in vitro* (Kita *et al*., 1984; Calabresi *et al*., 1990a, 1998; Jiang & North, 1991; Cepeda *et al*., 1994). These cells had high resting membrane potential (−84 ± 5 mV), relatively low apparent input resistance (38 ± 8 MΩ) when measured at the resting potentials from the amplitude of small (<10 mV) hyperpolarizing electrotonic potentials, action potentials of short duration (1.1 ± 0.3 ms) and high amplitude (102 ± 4 mV). They were silent at rest and showed membrane rectification and tonic firing activity during depolarizing current pulses. In 12 of the 82 recorded spiny neurons, the electrophysiological identification was confirmed by a morphological analysis obtained by using biocytin staining (data not shown).

Effects of PHT, LTG and GBP on intrinsic membrane properties of striatal spiny neurons

Bath application of PHT, LTG and GBP (5–10 min), at the concentrations employed in this study (10–300, 3–300, 10–1000 μM respectively), did not alter intrinsic membrane properties of the recorded cells such as resting membrane potential and current-voltage relationship measured in the subthreshold range. The current-voltage relationship was measured in voltage-clamp recordings before and during the application of the drugs and obtained by measuring the steady-state current during the application of voltage steps (1–3 s duration) both in positive and negative directions from the holding potential ($n = 12$; data not shown).

Effects of PHT, LTG and GBP on the firing activity induced by depolarizing current steps

Striatal spiny neurons responded to a 700 ms depolarizing pulse with a sustained repetitive firing of action potentials which was blocked by the sodium channel blocker TTX (1 μM) (data not shown). In order to compare the effects of different doses of PHT, LTG and GBP we assumed as control value a number of 20–25 action potentials; this frequency of discharge was obtained by injecting 0.6–1 nA of current intensity through the intracellular recording electrode. Bath application (5–10 min) of PHT (10–300 μM), LTG (10–300 μM) and GBP (100–1000 μM), produced a dose-dependent decrease of the number of sodium-dependent action potentials elicited by the current step. This effect was reversible after 25–30 min wash out of the drugs. The minimal effect was obtained with 30 μM PHT, 30 μM LTG and 300 μM GBP, whilst maximal responses were achieved with 300 μM PHT, 300 μM LTG and 1 mM GBP respectively (Figure 1). The potency of these AEDs was expressed as the extrapolated EC_{50} value which was 42.8 μM for PHT, 48.9 μM for LTG, 320.4 μM for GBP (Table 1). It should be noted, however, that PHT and GBP were more

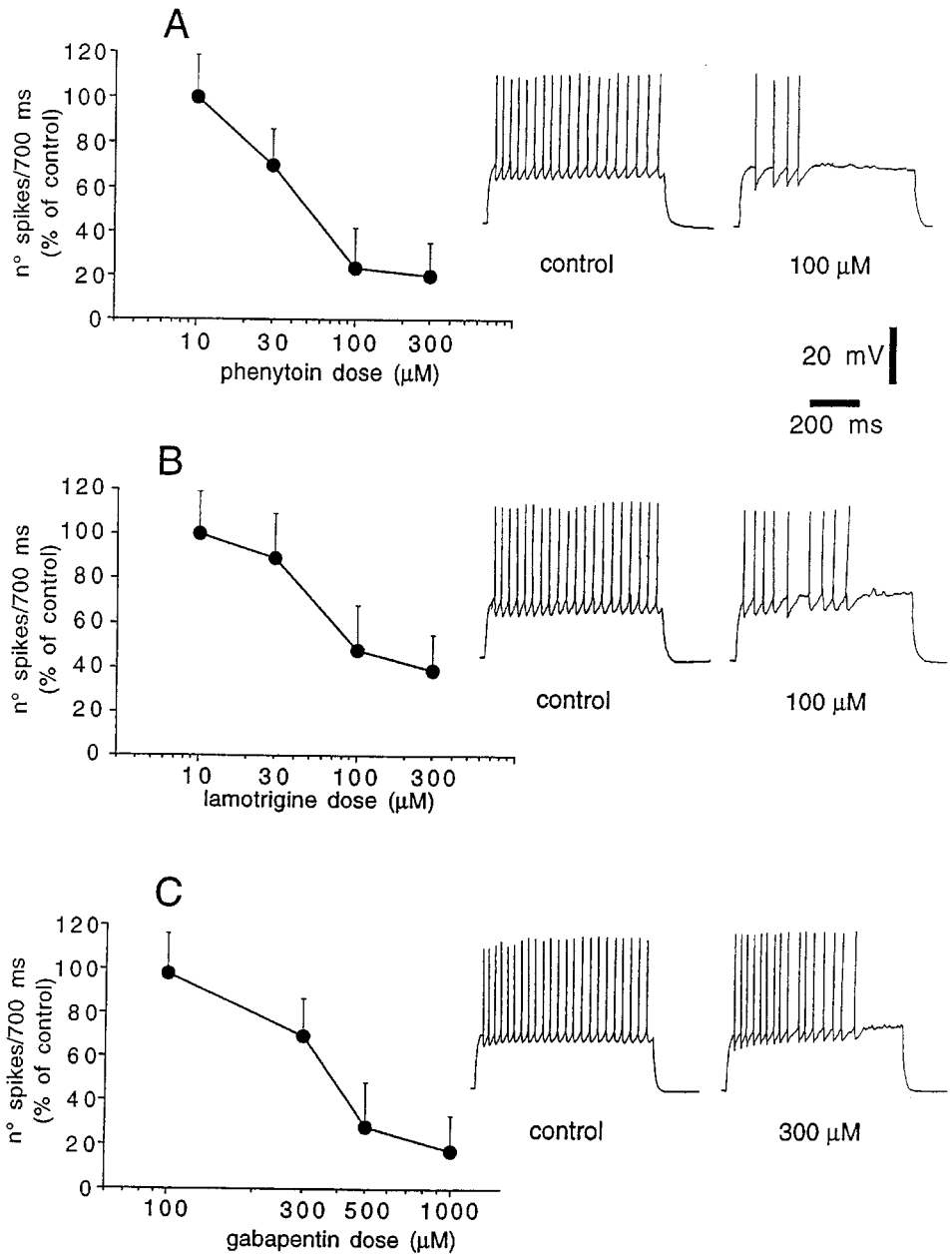

Figure 1 PHT, LTG and GBP inhibit current-evoked firing discharge of striatal spiny neurons. (A) The graph shows the dose-response curve obtained at various concentrations of PHT on the firing activity evoked by pulses of positive current (0.6–1 nA intensity, 700 ms duration). Each data point was obtained from at least four single experiments. The right part of the figure shows single voltage responses to a depolarizing pulse (0.8 nA) recorded from a striatal spiny neuron under control condition and during the application of 100 μM PHT. The resting membrane potential (RMP) of the cell was −87 mV and was constant throughout the experiment. (B) The graph shows the dose-response curve obtained at various concentrations of LTG on the firing activity evoked by pulses of positive current (0.6–1 nA intensity, 700 ms duration). Each data point was obtained from at least four single experiments. The right part of the figure shows single voltage responses to a depolarizing pulse (0.7 nA) recorded from a striatal spiny neuron under control condition and during the application of 100 μM LTG. The RMP of the cell was −90 mV and was constant throughout the experiment. (C) The graph shows the dose-response curve obtained at various concentrations of GBP on the firing activity evoked by pulses of positive current (0.6–1 nA intensity, 700 ms duration). Each data point was obtained from at least four single experiments. The right part of the figure shows single voltage responses to a depolarizing pulse (0.9 nA) recorded from a striatal spiny neuron under control condition and during the application of 300 μM GBP. The RMP of the cell was −85 mV and was constant throughout the experiment.

Table 1

AEDS	*Potency* (EC_{50}, μM): *firing inhibition*	*Potency* (EC_{50}, μM): *EPSP inhibition*	*Relative efficacy: firing inhibition*	*Relative efficacy: EPSP inhibition*
PHT	42.8	33.5	+ + +	+
LTG	48.9	26.7	+	+ + +
GBP	320.4	96.8	+ +	+ +

effective than LTG in reducing action potential discharge. In fact, saturating doses of PHT (300 μM) and of GBP (1 mM) reduced the firing frequency to 20% of the control values. Conversely, saturating doses of LTG (300 μM) reduced the firing discharge to about 40% of the control. Even higher doses of LTG (1 mM, $n=3$) did not cause further reduction of this parameter (data not shown). Interestingly, all these three AEDs were more effective in suppressing the action potentials triggered during the last part of the depolarizing pulse suggesting that a certain activation of the voltage dependent sodium channels was required for the action of these compounds.

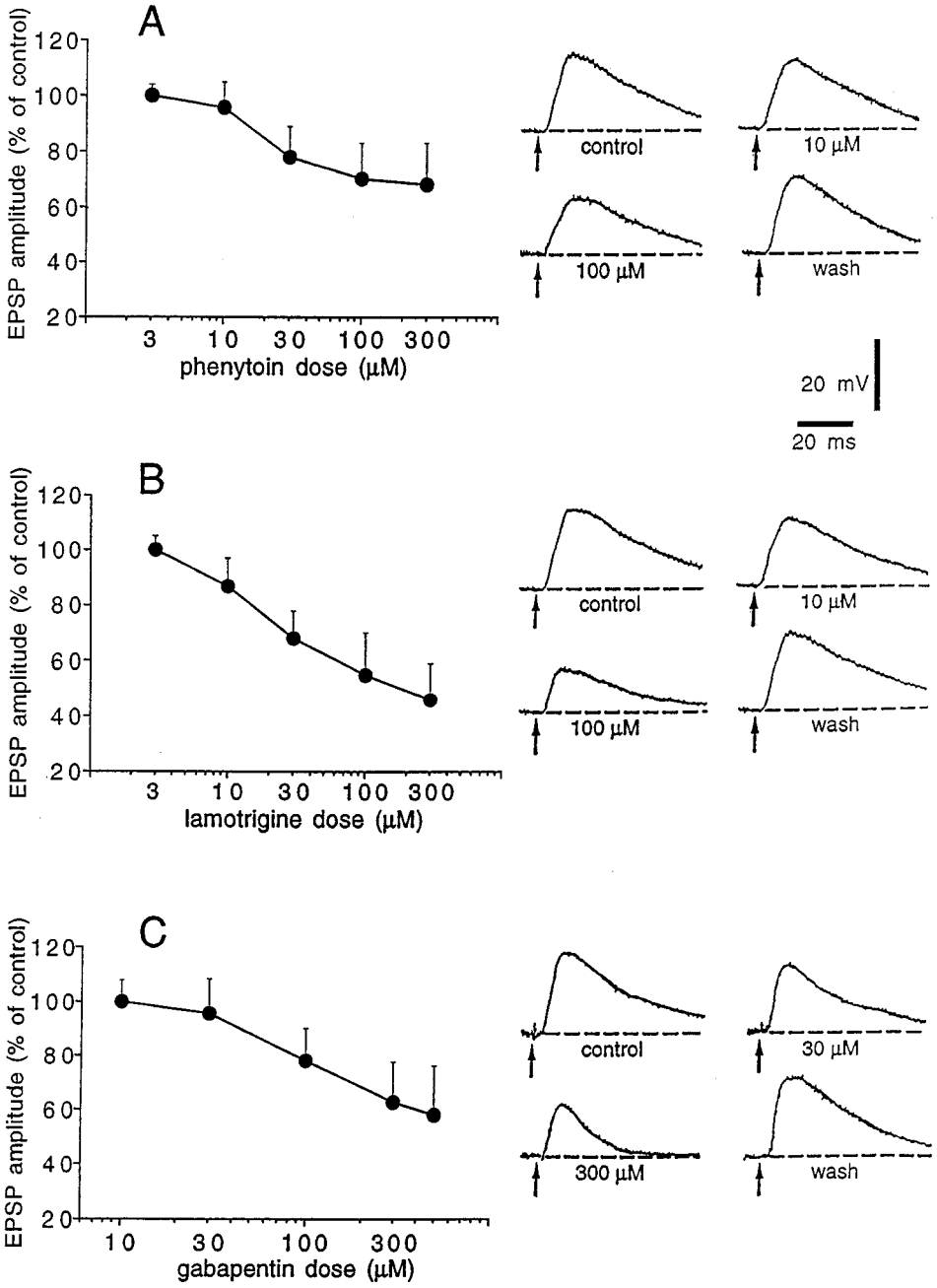

Figure 2 PHT, LTG and GBP inhibit excitatory postsynaptic potentials (EPSPs) evoked by cortical stimulation in striatal spiny neurons. (A) The graph shows the dose-response curve obtained at various concentrations of PHT on the amplitude of corticostriatal EPSPs. Each data point was obtained from at least four single experiments. The right part of the figure shows averages (four single sweeps) of EPSPs recorded from a striatal spiny neuron under control condition, during the application of two different concentrations of PHT and after 30 min of wash out. Each concentration was applied for 10 min. The RMP of the neuron was −89 mV and was constant throughout the experiment. (B) The graph shows the dose-response curve obtained at various concentrations of LTG on the amplitude of corticostriatal EPSPs. Each data point was obtained from at least four single experiments. The right part of the figure shows averages (four single sweeps) of EPSPs recorded from a striatal spiny neuron under control condition, during the application of two different concentrations of LTG and after 30 min of wash out. Each concentration was applied for 10 min. The RMP of the neuron was −89 mV and was constant throughout the experiment. (C) The graph shows the dose-response curve obtained at various concentrations of GBP on the amplitude of corticostriatal EPSPs. Each data point was obtained from at least four single experiments. The right part of the figure shows averages (four single sweeps) of EPSPs recorded from a striatal spiny neuron under control condition, during the application of two different concentrations of GBP and after 30 min of wash out. Each concentration was applied for 10 min. The RMP of the neuron was −88 mV and was constant throughout the experiment.

Effects of PHT, LTG and GBP on corticostriatal glutamatergic EPSPs

Spiny neurons respond to a single cortical stimulation by producing excitatory postsynaptic potentials (EPSPs) whose physiological and pharmacological characteristics have been previously described (Calabresi *et al*., 1990a, 1992a,b; Jiang & North, 1991). We studied the pharmacological action of these three AEDs on corticostriatal glutamatergic EPSPs. Bath application of PHT (3–300 μM), LTG (3–300 μM) and GBP (10–500 μM) significantly reduced the EPSP amplitude in a dose-dependent and reversible manner. The minimal effective concentration of PHT, LTG and GBP was 10, 10 and 100 μM respectively, while maximal inhibitory effects were obtained with 300 μM PHT, 300 μM LTG and 500 μM GBP (Figure 2). The EC_{50} value for this action was 33.5 μM for PHT, 26.7 μM for LTG, 96.8 μM for GBP (Table 1). It has to be stressed that LTG was also more effective than PHT and GBP in reducing the EPSP amplitude. In fact, saturating doses of PHT (300 μM) and GBP (500 μM) decreased the EPSP amplitude respectively to 70 and 55% of the control values. Conversely, saturating doses of LTG (300 μM) reduced the EPSP amplitude to about 45% of the control value.

Effects of PHT, LTG and GBP on paired-pulse facilitation

In order to study whether the depression of corticostriatal synaptic transmission by these compounds was dependent on pre- or postsynaptic sites of action, we measured synaptic responses to a pair of stimuli before, during and after the application of two different concentrations of PHT, LTG and GBP (30 and 100 μM, 30 and 100 μM, 100 and 500 μM respectively). In these experiments interstimulus interval was of 60 ms. Paired-pulse modification of neurotransmission has been studied extensively and is attributed to a presynaptic change in release probability (Manabe *et al*., 1993; Schulz *et al*., 1994). An increase in the ratio of the second pulse response to the first pulse response (EPSP2/EPSP1) indicates a decrease in the release probability. The decrease in transmitter release probability is consistent with the observations that manipulations depressing transmitter release usually increase the magnitude of this ratio also at corticostriatal synapses (Calabresi *et al*., 1997a). PHT and GBP depressed corticostriatal EPSPs without significantly affecting paired-pulse facilitation (PPF). This finding suggests that the inhibitory effect of these AEDs did not exclusively involve a presynaptic site of action. Conversely, the depression of the EPSP by 30 μM LTG, which was similar to those caused by 100 μM PHT and 500 μM GBP, was coupled to a clear increase of PPF as expected by a prevalent presynaptic site of action. Interestingly, at higher concentrations (100 μM), LTG reduced corticostriatal synaptic transmission without changing EPSP2/EPSP1 ratio. The latter observation indicates that, at this higher dose, LTG also affects a postsynaptic site of action (Figure 3).

Effects of PHT, LTG and GBP on membrane depolarizations induced by exogenous glutamate

The experiments dealing with the paired-pulse facilitation raised the possibility that the depression of the EPSP amplitude induced by PHT, GBP but not by low doses of LTG could be caused by a reduction of the sensitivity of the postsynaptic cell to glutamate. In order to explore this possibility, we have measured the amplitude of the membrane depolarizations induced by brief bath application of exogenous glutamate (0.3–1 mM for 10–20 s) before, during and after the administration of these three compounds. As shown in

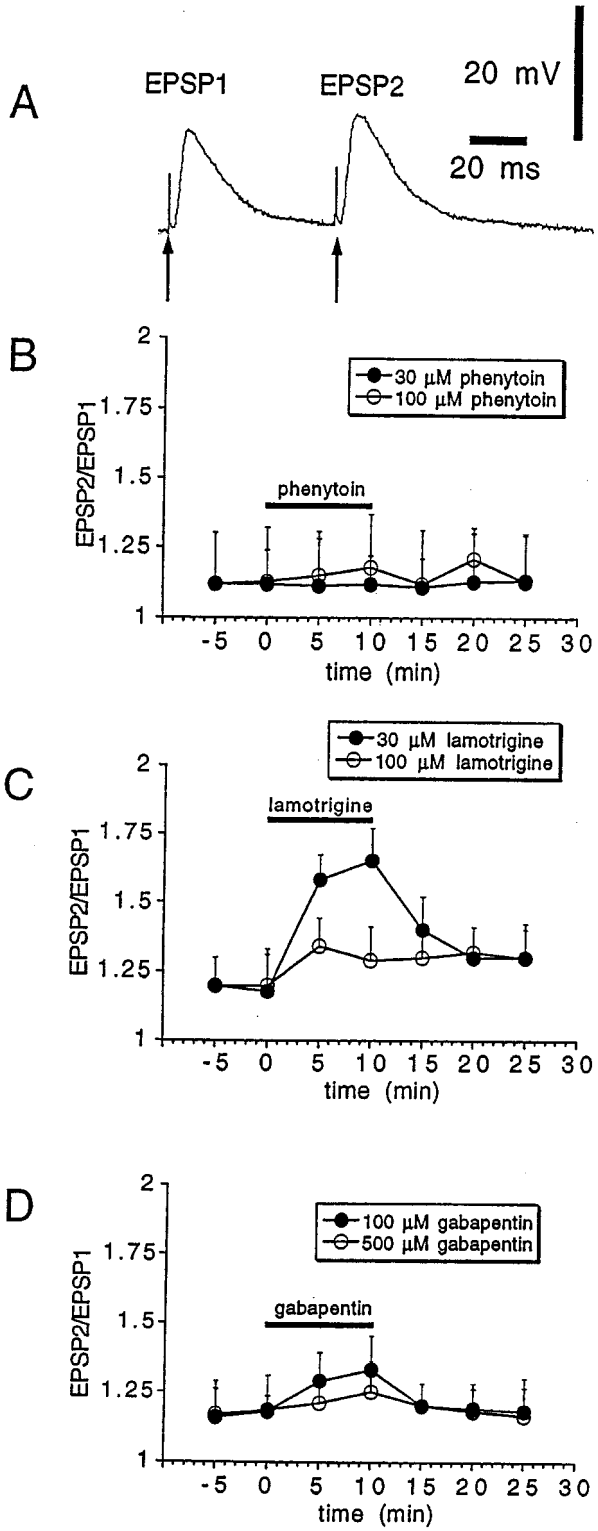

Figure 3 LTG but not PHT and GBP increases paired-pulse facilitation. (A) The trace shows synaptic responses to a pair of stimuli recorded with interstimulus interval of 60 ms under control condition. (B) The graph shows the ratio of the second pulse response to the first pulse response (EPSP2/EPSP1) before, during, and after the application of two different concentrations of PHT (black bar). (C) The graph shows the ratio of EPSP2/EPSP1 before, during, and after the application of two different concentrations of LTG (black bar). (D) The graph shows the ratio of EPSP2/EPSP1 before, during, and after the application of two different concentrations of GBP (black bar).

Figure 4, two different doses of both PTH and GBP, which caused *per se* a depression of cortically-evoked EPSPs uncoupled to change in PPF (30–100 μM and 100–300 μM respectively), decreased in a dose-dependent manner the glutamate-induced membrane depolarizations. We also tested the postsynaptic sensitivity to glutamate before and during the application of lamotrigine. Neither 30 μM nor 100 μM LTG significantly affected the postsynaptic sensitivity to glutamate ($P>0.05$).

Discussion

The main finding of the present study is that PHT, LTG and GBP decrease the excitability of striatal spiny neurons by modulating multiple electrophysiological properties of these cells. Although previous data concerning the mechanisms of action of these AEDs have been obtained by using different experimental preparations (McLean & Macdonald, 1983; Leach *et al*., 1986; Yaari *et al*., 1986; Cheung *et al*., 1992; Rock *et al*., 1993; Kuo & Bean, 1994; Taylor, 1994; Calabresi *et al*., 1996b; Stefani *et al*., 1997), our study represents the first analysis in which multiple electrophysiological effects have been investigated in the same preparation in order to determine the sensitivity of each electrophysiological parameter to these compounds.

Intrinsic resting properties of striatal spiny neurons such as membrane potential, input resistance and membrane conductance were not significantly modified even by high concentrations of PHT, LTG and GBP. In contrast, we found that all these three AEDs depressed both the current-evoked repetitive firing discharge and the amplitude of EPSPs evoked by cortical stimulation. However, substantial pharmacological differences in the potency (EC_{50}) and in the efficacy of these three agents were observed (Table 1). The EC_{50} measured for the inhibitory action on firing activity and synaptic transmission were close for PHT while these values were significantly different for LTG and GBP. Moreover, both LTG and GBP were more effective in reducing corticostriatal EPSPs than the current-evoked firing discharge. These data may suggest that, although these two new AEDs reduce the neuronal excitability by targeting multiple sites of action, they preferentially decrease excitatory synaptic transmission in the striatum. Moreover, PHT was the most potent and effective agent in reducing sustained repetitive firing, whereas LTG showed the major potency and efficacy in reducing corticostriatal EPSPs. GBP was more potent in reducing EPSP amplitude than in decreasing firing frequency, although high concentrations of this drug were also very effective in reducing the latter parameter.

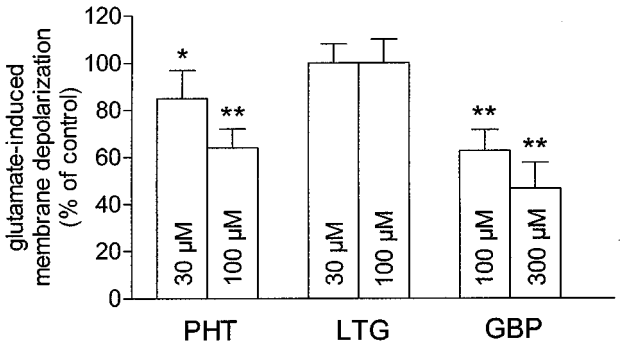

Figure 4 PHT and GBP but not LTG decrease postsynaptic sensitivity to exogenous glutamate. The graph shows that PHT and GBP exert a dose-dependent inhibition of membrane depolarizations induced by brief (10–20 s) applications of exogenous glutamate (0.3–1 mM) while LTG fails to affect these responses. Each data point was obtained from at least four single experiments (* = $P<0.05$; ** = $P>0.01$). These experiments were performed in the presence of 1 μM TTX in order to avoid possible contaminations of the postsynaptic responses by a TTX-sensitive release of excitatory transmitter.

The suppression of voltage-dependent sodium currents, detected as an inhibition of the firing activity, is a common action of many neuroprotective and anticonvulsivant drugs. The interaction with sodium channels has been demonstrated for phenytoin (Yaari *et al*., 1986), carbamazepine (McLean & Macdonald, 1986), oxcarbazepine (Calabresi *et al*., 1995b), gabapentin (Wamil & McLean, 1994), lamotrigine (Cheung *et al*., 1992), felbamate (Pisani *et al*., 1995), riluzole (Benoit & Escande, 1991; Siniscalchi *et al*., 1997). In the present study we have shown that PHT, LTG and GBP interfere with TTX-sensitive action potentials also in striatal neurons. All these three drugs reduced repetitive firing activity in a use-dependent manner as indicated by the evidence that the action potentials occurring in the late phase of the current-induced depolarization were preferentially inhibited. These data may indicate that in the striatum, such as in other brain regions, a sustained activation of the voltage-dependent sodium channels is required for the action of these AEDs presumably by stabilizing sodium channels in the inactivated state.

Synaptic excitatory transmission is emerging as a promising site of intervention for new AEDs and a reduction of glutamatergic transmission has been claimed as part of the mechanism of action of some new anticonvulsants (Walker & Sander, 1994; Macdonald & Kelly, 1994; Calabresi *et al*., 1995b, 1996b; Pisani *et al*., 1995). PHT, LTG and GBP reduced cortically-evoked EPSPs with apparently different relative order of potency and efficacy (Table 1). These differential pharmacological profiles, probably, originate from different mechanisms of action. The experiments dealing with the paired-pulse facilitation, in fact, suggest that LTG affects corticostriatal glutamatergic transmission with a prominent presynaptic site of action whereas PHT and GBP preferentially reduce postsynaptic sensitivity to glutamate. Changes in paired-pulse facilitation of synaptic transmission are commonly considered a good index of a presynaptic mechanism of action (Manabe *et al*., 1993; Schulz *et al*., 1994; Calabresi *et al*., 1997a). Accordingly, LTG reduced corticostriatal EPSPs with a clear increase in PPF and, even at saturating doses, failed to affect the membrane depolarizations induced by exogenous glutamate. Conversely, PHT and GBP decreased corticostriatal EPSPs without affecting the PPF; these AEDs also reduced the membrane depolarizations induced by exogenously-applied glutamate, suggesting a postsynaptic site of action. Interestingly, the doses required to achieve this latter effect were similar to those required to reduce corticostriatal synaptic transmission, indicating that a reduction of postsynaptic sensitivity to glutamate may play a major role in the inhibitory action exerted by PHT and GBP on glutamatergic transmission.

Therapeutic plasma levels of PHT and LTG are usually reported to be around 10–20 μM. The concentration of PHT in the cerebrospinal fluid is equal to the unbound fraction in the plasma (McNamara, 1996). The therapeutic GBP plasma levels are generally in the range of 10–50 μM. Limited data indicate that concentrations of GBP in cerebrospinal fluid are approximately 5–35% of those in plasma while concentrations in brain tissue are approximately 80% of those in plasma (McLean, 1994).

It is interesting to note that the resting membrane potential of striatal spiny neurons recorded *in vitro* is rather negative (around −85 mV in the presence of 2.5 external potassium concentration). If one assumes that the AEDs are exerting at least part of their effects *via* an interaction with the inactivated state of the Na^+ channel population, this could explain why relatively high concentrations of AEDs are required to exert their effects. Nevertheless, it should be considered that striatal spiny neurons intracellularly recorded *in vivo* show a characteristic pattern of spontaneous activity consisting of long periods of silence ('down' state) separated by brief episodes that cause firing discharge ('up' state). These depolarizing episodes were attributed to maintained, coordinated synaptic excitation from cerebral cortex, whereas the 'down' state was attributable to the activation of a strong inwardly rectifying potassium conductance (Calabresi *et al*., 1990b; Wilson & Kawaguchi, 1996). Thus, it is likely that *in vivo* the concentrations of AEDs required to achieve firing and synaptic inhibition during the 'up' state are lower than those necessary to inhibit striatal spiny neurons *in vitro*.

It has recently been proposed the use of old and new AEDs as possible neuroprotective agents in the therapy of acute (ischaemia) and neurodegenerative (Parkinson's disease and Huntington's disease) disorders involving the basal ganglia (Zipp *et al*., 1993; Meldrum, 1994; Lynch *et al*., 1995; Koroshetz & Moskowitz, 1996; Olson *et al*., 1997; Shinotoh *et al*., 1997; Starr *et al*., 1997). Thus, the differential pharmacological profiles reported for PHT, LTG and GBP might help not only in understanding the antiepileptic mechanisms of action of old and new AEDs, but also in the design of new clinical protocols for the treatment of acute and chronic diseases involving the striatum.

We wish to thank M. Tolu for the technical assistance. This study was supported by BIOMED Project to P.C. (No. BMH4-97-2215) and by HURST-CNR Biotechnology Program L-95/95 to G.B.

References

AMATO, G., CRESCIMANNO, G., SORBERA, F. & LA GRUTTA, V. (1982). Relationship between the striatal system and amygdaloid paroxysmal activity. *Exp. Neurol.,* **77,** 492 – 504.

BARTOSZYK, G.D. (1982). Gabapentin and convulsions provoked by excitatory amino acids. *Naunyn Schmiedebergs Arch. Pharmacol.,* **324,** R24.

BENOIT, E. & ESCANDE, D. (1991). Riluzole specifically blocks inactivated Na channels in myelinated nerve fibre. *Pflügers Arch.,* **419,** 603 – 609.

CALABRESI, P., CENTONZE, D., PISANI, A. & BERNARDI, G. (1997a). Endogenous adenosine mediates the presynaptic inhibition induced by aglycemia at corticostriatal synapses. *J. Neurosci.,* **17,** 4509 – 4516.

CALABRESI, P., CENTONZE, D., PISANI, A., SANCESARIO, G., GUBELLINI, P., MARFIA, G.A. & BERNARDI, G. (1998). Striatal spiny neurons and cholinergic interneurons express differential ionotropic glutamatergic responses and vulnerability: implications for ischemia and Huntington's disease. *Ann. Neurol.,* **43,** 586 – 597.

CALABRESI, P., DE MURTAS, M., PISANI, A., STEFANI, A., SANCESARIO, G., MERCURI, N.B. & BERNARDI, G. (1995a). Vulnerability of medium spiny striatal neurons to glutamate: role of Na^+/K^+ ATPase. *Eur. J. Neurosci.,* **7,** 1674 – 1683.

CALABRESI, P., DE MURTAS, M., STEFANI, A., PISANI, A., SANCESARIO, G., MERCURI, N.B. & BERNARDI, G. (1995b). Action of GP47779, the active metabolite of oxcarbazepine, on corticostriatal system. I. Modulation of corticostriatal synaptic transmission. *Epilepsia,* **36,** 990 – 996.

CALABRESI, P., MAGARINOS ASCONE, C., CENTONZE, D., PISANI, A., SANCESARIO, G., D'ANGELO, V. & BERNARDI, G. (1997b). Opposite membrane potential changes induced by glucose deprivation in striatal spiny neurons and in large aspiny interneurons. *J. Neurosci.,* **17,** 1940 – 1949.

CALABRESI, P., MAJ, R., PISANI, A., MERCURI, N.B. & BERNARDI, G. (1992a). Long-term synaptic depression in the striatum: physiological and pharmacological characterization. *J. Neurosci.,* **12,** 4224 – 4233.

CALABRESI, P., MERCURI, N.B. & BERNARDI, G. (1990a). Synaptic and intrinsic control of membrane excitability of neostriatal neurons. II. An in vitro analysis. *J. Neurophysiol.,* **63,** 663 – 675.

CALABRESI, P., MERCURI, N.B. & BERNARDI, G. (1990b). Synaptic and intrinsic control of membrane excitability of neostriatal neurons. I. An in vivo analysis. *J. Neurophysiol.,* **63,** 651 – 662.

CALABRESI, P., PISANI, A., MERCURI, N.B. & BERNARDI, G. (1992b). Long-term potentiation in the striatum is unmasked by removing the voltage-dependent blockade of NMDA receptor channel. *Eur. J. Neurosci.,* **4,** 929 – 935.

CALABRESI, P., PISANI, A., MERCURI, N.B. & BERNARDI, G. (1996a). The corticostriatal projection: from synaptic plasticity to dysfunctions of the basal ganglia. *Trends Neurosci.,* **19,** 19 – 24.

CALABRESI, P., SINISCALCHI, A., PISANI, A., STEFANI, A., MERCURI, N.B. & BERNARDI, G. (1996b). A field potential analysis on the effects of lamotrigine, GP 47779, and felbamate in neocortical slices. *Neurology,* **47,** 557 – 562.

CEPEDA, C., WALSH, J.P., PEACOCK, W., BUCKWALD, N.A. & LEVINE, M.S. (1994). Neurophysiological, pharmacological and morphological properties of human caudate neurons recorded in vitro. *Neuroscience,* **59,** 89 – 103.

CHEUNG, H., KAMP, D. & HARRIS, E. (1992). An in vitro investigation of the action of lamotrigine on neuronal-activated sodium channels. *Epilepsy Res.,* **13,** 107 – 112.

DIVAC, I., FONNUM, F. & STORM-MATHISON, J. (1977). High affinity uptake of glutamate in terminals of corticostriatal axons. *Nature,* **266,** 377 – 378.

ENGEL, J., WOLFSON, L. & BROWN, L. (1978). Anatomical correlates of electrical and behavioral events related to amygdala kindling. *Ann. Neurol.,* **3,** 538 – 544.

FAETH, W.H., WALKER, A.E. & ANDY, O.J. (1954). The propagation of cortical and sub-cortical epileptic discharge. *Epilepsia,* **3,** 37 – 48.

GALE, K. (1992). Subcortical structures and pathways involved in convulsive seizure generation. *J. Clin. Neurophysiol.,* **9,** 264 – 277.

HARDEN, C.L. (1994). New antiepileptic drugs. *Neurology,* **44,** 787 – 795.

HORIKAWA, H. & ARMSTRONG, W.E. (1988). A versatile means of intracellular labelling: injection of biocytin and its detection with avidin conjugates. *J. Neurosci. Methods,* **25,** 1 – 11.

JIANG, Z.-C. & NORTH, R.A. (1991). Membrane properties and synaptic responses of rat striatal neurones in vitro. *J. Physiol.,* **443,** 533 – 553.

KITA, T., KITA, H. & KITAI, S.T. (1984). Passive electrical membrane properties of rat neostriatal neurons in an in vitro slice preparation. *Brain Res.,* **300,** 129 – 139.

KOROSHETZ, W.J. & MOSKOWITZ, M.A. (1996). Emerging treatments for stroke in humans. *Trends Pharmacol. Sci.,* **17,** 227 – 233.

KUO, C.-C. & BEAN, B.P. (1994). Na^+ channels must deactivate to recover from inactivation. *Neuron,* **12,** 819 – 829.

LEACH, M.J., MARDEN, C.M. & MILLER, A.A. (1986). Pharmacological studies on lamotrigine, a novel potential antiepileptic drug: II Neurochemical studies on the mechanism of action. *Epilepsia,* **27,** 490 – 497.

LYNCH III, J.J., YU, S.P., CANZONIERO, L.M.T., SENSI, S.L. & CHOI, D.W. (1995). Sodium channel blockers reduce oxygen-glucose deprivation-induced cortical neuronal injury when combined with glutamate receptor antagonists. *J. Pharmacol. Exp. Ther.,* **273,** 554 – 560.

MACDONALD, R.L. & KELLY, K. (1994). New antiepileptic drug mechanisms of action. In *An appraisal of some new anticonvulsivants - a clinical perspective*. ed. Trimble, M. pp. 35–50. New York: Wiley.

MACDONALD, R.L. (1996). Cellular effects of antiepileptic drugs. In *Epilepsy: a comprehensive textbook*. eds. Engel, J., & Pedley, T.A. pp. 1383–1391. Philadelphia: Lippincott-Raven Publishers.

MCNAMARA, J.O. (1996). Drugs effective in the therapy of the epilepsies. In *Goodman & Gilman's; The pharmacological basis of therapeutics*. eds. Hardman, J.G. & Limbird, L.E. pp. 461–486. New York: McGraw-Hill.

MANABE, T., WYLLIE, D.J.I. & NICOLL, R.A. (1993). Modulation of synaptic transmission and long-term potentiation: effects on paired pulse facilitation and EPSC variance in the CA1 region of the hippocampus. *J. Neurophysiol.,* **70,** 1451–1459.

MCLEAN, M.J. (1994). Clinical pharmacokinetics of gabapentin. *Neurology,* **44** (suppl 5): S17–S22.

MCLEAN, M.J. & MACDONALD, R.L. (1986). Carbamazepine and 10,11-epoxycarbamazepine produce use- and voltage-dependent limitation of rapidly firing action potentials of mouse central neurons in cell culture. *J. Pharmacol. Exp. Ther.,* **238,** 727–737.

MCLEAN, M.J. & MACDONALD, R.L. (1983). Multiple actions of phenytoin on mouse spinal cord neurons in cell culture. *J. Pharmacol. Exp. Ther.,* **227,** 779–789.

MELDRUM, B.S. (1994). The role of glutamate in epilepsy and other CNS disorders. *Neurology,* **44** (suppl 8): S14–S23.

OLES, R.J., SINGH, L., HUGHES, J. & WOODRUFF, G.N. (1990). The anticonvulsant action of gabapentin involves the glycine/NMDA receptor. *Soc. Neurosci.,* **16,** 783.

OLSON, W.L., GRUENTHAL, M., MUELLER, M.E. & OLSON, W.H. (1997). Gabapentin for parkinsonism: a double-blind, placebo-controlled, crossover trial. *Am. J. Med.,* **102,** 60–66.

PISANI, A., STEFANI, A., SINISCALCHI, A., MERCURI, N.B., BERNARDI, G. & CALABRESI, P. (1995). Electrophysiological actions of felbamate on rat striatal neurones. *Br. J. Pharmacol.,* **116,** 2053–2061.

ROCK, D.M., KELLY, K.M. & MACDONALD, R.L. (1993). Gabapentin actions on ligand- and voltage-gated responses in cultured rodent neurons. *Epilepsy Res.,* **16,** 89–98.

SCHULZ, P.E., COOK, E.P. & JOHNSTON, D. (1994). Changes in paired-pulse facilitation suggest presynaptic involvement in long-term potentiation. *J. Neurosci.,* **14,** 5325–5337.

SHINOTOH, H., VINGERHOETS, F.J., LEE, C.S., UITTI, R.J., SCHULZER, M., CALNE, D.B. & TSU, J. (1997). Lamotrigine trial in idiopathic parkinsonism: a double-blind, placebo-controlled, crossover study. *Neurology,* **48,** 1282–1285.

SINISCALCHI, A., BONCI, A., MERCURI, N.B. & BERNARDI, G. (1997). Effects of riluzole on rat cortical neurones: an in vitro electrophysiological study. *Br. J. Pharmacol.,* **120,** 225–230.

STARR, M.S., STARR, B.J. & KAUR, J. (1997). Stimulation of basal and L-DOPA-induced motor activity by glutamate antagonists in animal models of Parkinson's disease. *Neurosci. Biobehav. Rev.,* **21,** 437–446.

STEFANI, A., SPADONI, F. & BERNARDI, G. (1997). Differential inhibition by riluzole, lamotrigine and phenytoin of sodium and calcium currents in cortical neurons: implication for neuroprotective strategies. *Exp. Neurol.,* **147,** 115–122.

TAYLOR, C.P. (1994). Emerging perspective on the mechanism of action of gabapentin. *Neurology,* **44** (suppl 5): S10–S16.

UPTON, N. (1994). Mechanisms of action of new antiepileptic drugs: rational design and serendipitous finding. *Trends Pharmacol. Sci.,* **15,** 456–463.

WALKER, M.C. & SANDER, J.W. (1994). Developments in antiepileptic drug therapy. *Curr. Opin. Neurol.,* **7,** 131–139.

WAMIL, A.W. & MCLEAN, M.J. (1994). Limitation by gabapentin of high-frequency action potential firing by mouse central neurons in cell culture. *Epilepsy Res.,* **17,** 1–11.

WILSON, C.J. & GROVES, P.M. (1980). Fine structure and synaptic connections of the common spiny neuron of the rat neostriatum: a study employing intracellular inject of horse-radish peroxidase. *J. Comp. Neurol.,* **194,** 599–615.

WILSON, C.J. & KAWAGUCHI, Y. (1996). The origins of two-state spontaneous membrane potential fluctuations of neostriatal spiny neurons. *J. Neurosci.,* **16,** 2651–2661.

YAARI, Y., SELTZER, M. & PINCUS, J. (1986). Phenytoin: mechanism of its anticonvulsivant action. *Ann. Neurol.,* **20,** 171–184.

ZIPP, F., BAAS, H. & FISHER, P.A. (1993). Lamotrigine-antiparkinsonian activity by blockade of glutamate release? *J. Neural Transm. Park. Dis. Dement Sect.,* **5,** 67–75.

(Received August 26, 1998
Accepted November 13, 1998)

British Journal of Pharmacology (1999) 126, 697–700
http://www.stockton-press.co.uk/bjp

Effects of angiotensin II receptor blockade on proximal fluid uptake in the rat kidney

*,[1]M.L. Smart, [2]S. Hiranyachattada & [1]P.J. Harris

[1]Department of Physiology, The University of Melbourne, Parkville 3052, Victoria, Australia; [2]Department of Physiology, Faculty of Science, Prince of Songkla University, Hatyai, Songla 90112, Thailand

1 Angiotensin II has a well described dose-dependent biphasic action on proximal tubule fluid uptake, although the concentration and effect of endogenous luminal angiotensin II remain controversial.

2 Shrinking split-droplet micropuncture was used to examine the fluid uptake in response to the luminal application of three AT_1 antagonists (losartan, EXP3174, candesartan).

3 Addition of losartan at 10^{-8} M decreased fluid uptake rate (Jv_a) by $17.5 \pm 2.2\%$ ($P<0.05$). Luminal addition of EXP3174 at concentrations between $10^{-9}-10^{-5}$ M caused a dose-dependent decrease in fluid uptake, with a maximum decrease of $41.0 \pm 9.5\%$ ($P<0.01$) at 10^{-6} M. Candesartan also decreased fluid uptake, by $21.9 \pm 4.9\%$ ($P<0.05$) at 10^{-8} M and $23.6 \pm 5.5\%$ ($P<0.05$) at 10^{-5} M.

4 All three antagonists at a low concentration (10^{-8} M) decreased fluid uptake. EXP3174 and candesartan at a higher concentration (10^{-5} M) also decreased fluid uptake in contrast to the previously reported effect of losartan.

5 We conclude that the endogenous concentration of antiotensin II in the proximal luminal fluid is low and exerts a stimulatory effect on fluid absorption. Losartan at concentrations greater than 10^{-6} M may have a non-selective action on fluid uptake.

Keywords: Angiotensin II; losartan; EXP3174; candesartan; fluid uptake; proximal tubule; kidney

Introduction

The addition of angiotensin II to either the peritubular capillary or the proximal lumen reveals a dose-dependent biphasic effect on fluid absorption. Angiotensin II at low concentrations ($10^{-12}-10^{-10}$ M) stimulates fluid uptake, while high concentrations ($10^{-7}-10^{-5}$ M) inhibit fluid uptake (Harris & Young, 1977; Schuster *et al*., 1984; Wang & Chan, 1990; Li *et al*., 1994). This biphasic response to angiotensin II indicates that sodium and water uptake will either be enhanced or suppressed depending upon the peritubular capillary and luminal concentrations of angiotensin II in the capillary and tubule lumen.

The endogenous concentration of intrarenal angiotensin II and its consequent action on fluid uptake in the proximal tubule lumen is uncertain. Samples of luminal fluid obtained by micropuncture from superficial proximal tubules have been shown to contain a nanomolar concentration of angiotensin II (Seikaly *et al*., 1990; Braam *et al*., 1993; Mitchell *et al*., 1997). Previous studies in our laboratory (Hiranyachattada & Harris, 1996) and by Leyssac *et al*. (1997) concluded that addition of a high concentration of the AT_1 antagonist losartan (10^{-5} M) to the proximal tubule lumen enhanced fluid uptake. Taken together these observations support the existence of high endogenous concentrations of angiotensin II within the luminal fluid, and suggest that, at least in the anaesthetized rat, fluid uptake is suppressed by the endogenous concentration of angiotensin II in the lumen.

The presence of a high luminal AII concentration remains controversial because of a number of contradictory observations. Luminal additions of angiotensin II have been shown to have marked stimulatory effect on fluid uptake (Wang & Chan, 1990; Li *et al*., 1994) that would not be expected if the endogenous angiotensin II concentration was already high. Quan & Baum (1996), who measured proximal tubule fluid uptake following luminal addition of a lower dose of losartan (10^{-8} M), observed a 35% decrease in uptake, adding further to the evidence favouring a low endogenous luminal angiotensin II concentration.

The primary purpose of the present study was to assess the influence of the endogenous concentration of angiotensin II by measuring the effects of angiotensin II receptor blockade on fluid absorption in proximal tubules. We used the AT_1 receptor antagonists, losartan, EXP3174 (a potent active metabolite of losartan) and candesartan, as the predominant angiotensin receptor in the proximal tubule has been reported to be the AT_1 subtype (Sechi *et al*., 1992). A previous study from this laboratory supports this conclusion since AT_2 receptor blockade with PD-123319 did not affect fluid uptake (Hiranyachattada & Harris, 1996).

In addition, the proposal that losartan has a biphasic dose-dependent effect on fluid uptake was examined, since such a response pattern would be a key factor in interpreting the effects of pharmacological blockade of angiotensin II in the lumen.

Methods

Male Sprague-Dawley rats (300 ± 50 g; $n=68$) were anaesthetized with Inactin (100 mg kg^{-1} i.p.) and infused intravenously with 0.9% NaCl at 1.6 ml h^{-1} 100 g bodyweight wt^{-1}. A carotid cannula was inserted to measure the blood pressure, which was continuously recorded on a chart recorder (Rikadenki, Model R-02). The left kidney was prepared for

* Author for correspondence.

micropuncture as previously reported (Harris *et al.*, 1987). After a 1 h equilibration period, shrinking split-drop micropuncture was performed in midproximal convoluted tubule segments visible on the kidney surface. From a double-barreled micropipette Sudan black-stained castor oil was infused into the proximal tubule. Artificial tubular fluid (ATF) (in mM) NaCl 145, $NaHCO_3$ 5, KCl 5 and $CaCl_2$ 1.5, pH 7.4 was then injected from the other barrel of the pipette to split the oil column. Proximal fluid absorption was determined by the rate of change of volume of the shrinking drop and expressed per unit surface area of epithelium (Jv_a). The volume of the shrinking drop was measured using digital analysis of oil-water menisci in successive video frames taken at 1 s intervals. The experiment was terminated if the mean arterial blood pressure of the rat did not remain above 100 mmHg during the measurement period. Fluid uptake rate was determined in 3–5 tubules receiving a vehicle solution (ATF) and then in another 3–5 tubules following introduction of an AT_1 antagonist {losartan, (2-n-butyl-4-chloro-5-hydroxymethyl-1-[(2′-1H-tetrazol-5-yl)biphenyl-4-yl)methyl]imidazole; EXP3174, (2-n-butyl-4-chloro-1-[(2′-1H-tetrazol-5-yl)biphenyl-4-yl)methyl]imidazole-5-carboxylic acid); candesartan, (2ethoxy-1-[[2′-(1H-tetrazol-5-yl)biphenyl-yl]methyl]-1H-benzimidazole-7-(carboxylic acid) in ATF}. Each tubule receiving the antagonist solution was exposed to only one concentration.

Statistics

In each experiment a mean value for Jv_a was determined from both control and treatment measurements. A paired *t*-test was performed for each group (different concentration of AT_1 antagonists) and compared with the corresponding controls. Values are expressed as means ± s.e.mean (n = number of rats).

Results

The first series of experiments were designed to determine the effects of losartan on fluid uptake. Losartan (10^{-8} M) when added to the intratubular solution decreased mean proximal fluid uptake by 17.5% (control 2.24 ± 0.06, treatment $1.87 \pm 0.16 \times 10^{-4}$ mm^3 mm^{-2} s^{-1}; $n=8$, $P<0.05$). However, no effect of losartan on fluid uptake was apparent when applied at 10^{-7} M (control 2.54 ± 0.46, treatment $2.38 \pm 0.17 \times 10^{-4}$ mm^3 mm^{-2} s^{-1}; $n=7$).

When EXP3174 (10^{-5}–10^{-9} M) was added to the intratubular fluid a dose-dependent decrease in fluid absorption was observed. EXP3174 decreased fluid absorption by 38.3% at 10^{-5} M (all values in $\times 10^{-4}$ mm^3 mm^{-2} s^{-1}: control 2.30 ± 0.05, treatment 1.42 ± 0.14; $n=6$, $P<0.05$), 41.0% at 10^{-6} M (control 2.31 ± 0.12, treatment 1.36 ± 0.24; $n=7$, $P<0.01$), 32.4% at 10^{-7} M (control 2.48 ± 0.11, treatment 1.68 ± 0.10; $n=6$, $P<0.01$), 23.5% at 10^{-8} M (control 2.15 ± 0.13, treatment 1.64 ± 0.18; $n=8$, $P<0.05$) and 17.8% at 10^{-9} M (control 2.19 ± 0.08, treatment 1.8 ± 0.11; $n=6$, $P<0.05$). EXP3174 at 10^{-10} M had no significant effect on fluid absorption (control 2.08 ± 0.11, treatment 1.96 ± 0.29; $n=8$).

Addition of candesartan at 10^{-5} M to the intratubular fluid caused a decrease in fluid uptake by 23.6% (control 2.53 ± 0.15, treatment $1.93 \pm 0.14 \times 10^{-4}$ mm^3 mm^{-2} s^{-1}; $n=6$, $P<0.05$). A similar decrease in absorption was also evident at 10^{-8} M, (control 2.47 ± 0.04, treatment $1.93 \pm 0.12 \times 10^{-4}$ mm^3 mm^{-2} s^{-1}; $n=6$, $P<0.01$).

There was no significant difference between the levels of inhibition of fluid absorption with the highest concentration (10^{-5} M) of candesartan and EXP3174.

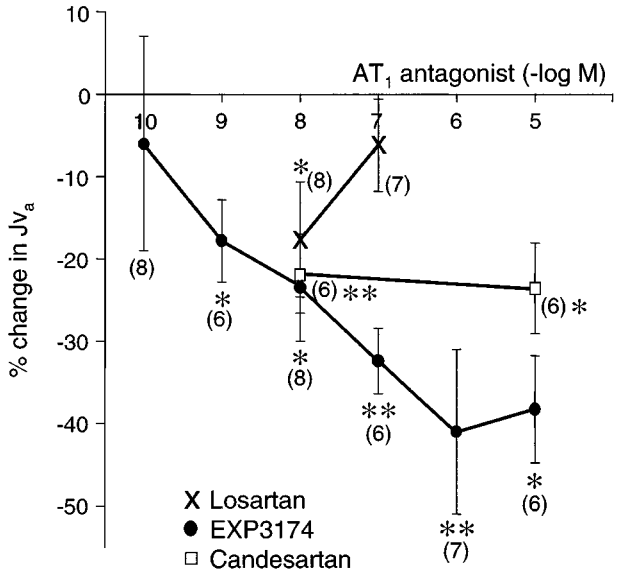

Figure 1 The effect of intratubular AT_1 antagonists on proximal tubular fluid absorption. Data are shown as means ± s.e.mean and presented as percentage changes in fluid absorption compared with control. Figures in parentheses indicate numbers of animals. $^*P<0.05$, $^{**}P<0.01$ (paired *t*-test).

Discussion

The use of several AT_1 receptor antagonists in this study clearly indicates that endogenous luminal angiotensin II acts on apical AT_1 receptors to increase fluid uptake. The addition of an AT_1 antagonist to the tubule lumen would be expected to result in an increase in fluid absorption if a high (inhibitory) endogenous concentration of angiotensin II was present, but a decrease in fluid absorption if a low (stimulatory) endogenous concentration of angiotensin II existed. The results of the present study, where the luminal addition of losartan (10^{-8} M), EXP3174 (10^{-9}–10^{-5} M) and candesartan (10^{-8} and 10^{-5} M) all decreased fluid absorption, support the latter contention. This strongly suggests that, at least in the Inactin anaesthetized rat, the endogenous concentration of angiotensin II in the lumen is within the range associated with stimulation of sodium transport and most likely to be between 10^{-12}–10^{-10} M.

Losartan at 10^{-8} M decreased fluid absorption by 17.5%, supporting the previous finding by Quan & Baum (1996) who perfused rat proximal tubules with losartan (10^{-8} M) and observed a 35% decrease in fluid uptake. Interestingly, this group also observed a 40% decrease in fluid uptake during luminal infusion of enalaprilat (10^{-4} M). The known effects of intravenous losartan on renal function in anaesthetized rats also support the observed decrease in fluid absorption with luminal addition of losartan at 10^{-8} M. Xie *et al.* (1990) observed that intravenous losartan had a powerful inhibitory effect on bicarbonate and fluid absorption, and Zhuo *et al.* (1992) reported that it caused a 9% decrease in fractional proximal fluid absorption. Studies performed in the rabbit aorta, revealed that losartan binds competitively to the AT_1 receptor, and importantly, exhibits no partial agonist effect (Chiu *et al.*, 1990).

This present study is the first to establish a dose response relation between the luminal concentration of EXP3174 and fluid absorption in the presence of endogenous luminal angiotensin II. The dose-dependent decrease in absorption induced by EXP3174 showed a maximum effect of 41% at

10^{-6} M. This inhibition of proximal fluid absorption is in accord with observations made in anaesthetized dogs following intravenous infusion of EXP3174 (0.5 μg kg^{-1} min^{-1}) (Tamaki *et al*., 1993). Fractional excretion of sodium and fractional proximal excretion of sodium were increased, indicating a decrease in sodium absorption in the proximal tubule. The pattern of response also concurs with observations from *in vitro* preparations of rabbit aorta where EXP3174 inhibited angiotensin II-stimulated contractile responses in a dose-dependent manner (Wong *et al*., 1990).

Candesartan applied to the lumen at either a high (10^{-5} M) or low (10^{-8} M) concentration decreased fluid uptake to a similar extent. The lack of dose-dependence may represent saturation of the inhibitory action at a concentration of 10^{-8} M or greater. Candesartan is reported to be an insurmountable antagonist that may interact with the same or a similar site on the AT_1-receptor as losartan (Ojima *et al*., 1997).

All three antagonists, losartan, EXP3174 and candesartan at 10^{-8} M decreased fluid absorption by approximately 20%. At a higher concentration (10^{-5} M), both EXP3174 and candesartan decreased fluid absorption, in contrast with previous observations that losartan at this dose increases transepithelial sodium transport (Hiranyachattada & Harris, 1996; Leyssac *et al*., 1997). The dose-dependent, biphasic effect of losartan is not consistent with selective blockade of luminal AT_1 receptors, and suggests that losartan at high concentrations ($>10^{-6}$ M) has a nonselective effect on sodium absorption. It is not possible to determine the site of this non-selective effect of losartan at concentrations greater than 10^{-6} M from the results of this present study.

Losartan is known to have different pharmacological properties than EXP3174 and candesartan. Firstly, it is a surmountable antagonist as opposed to both EXP3174 and candesartan displaying insurmountable antagonism (Wong *et al*., 1990; Ojima *et al*., 1997). In humans losartan increases uric acid secretion (Burnier *et al*., 1996) although in rats both losartan and EXP3174 both inhibit urate uptake (Edwards *et al*., 1996).

While the evidence presented here points to a low endogenous concentration of luminal angiotensin II, the data from measurements of angiotensin II in fluid samples obtained directly from the proximal tubule lumen (Seikaly *et al*., 1990; Braam *et al*., 1993) cannot be easily dismissed. Measurements obtained from free-flow collection samples revealed nanomolar concentrations of angiotensin II, and may differ from the endogenous level in split-droplets because of angiotensin II filtered at the glomerulus. Although, inspection of the dose-response relations produced by luminal application of exogenous angiotensin II (Wang & Chan 1990; Li *et al*., 1994), suggest that no significant effect of endogenous angiotensin II on fluid absorption would be observed if the concentration was around 10^{-9} M.

It is concluded from the pharmacological studies using AT_1 receptor antagonists that angiotensin II is present in the lumen at a concentration that stimulates sodium reabsorption (around 10^{-12}–10^{-10} M). The use of appropriate concentrations of pharmacological antagonists indicated that losartan has a nonselective action on fluid absorption at concentrations greater than 10^{-6} M. Losartan at a low concentration (10^{-8} M) has a quantitatively similar action on fluid uptake compared with EXP3174 and candesartan at the same dose.

This work was supported by the NH & MRC of Australia. M. Smart received an Australian Postgraduate Award and S. Hiranyachattada received a postgraduate scholarship from the International Development Program. Losartan, EXP3174 and candesartan were a generous gift from Merck and Astra Hassle respectively.

References

BRAAM, B., MITCHELL, K.D., FOX, J. & NAVAR, L.G. (1993). Proximal tubular secretion of angiotensin II in rats. *Am. J. Physiol.,* **264,** F891–F898.

BURNIER, M., ROCH-RAMAL, F. & BRUNNER, H.R. (1996). Renal effects of angiotensin II receptor blockade in normotensive subjects. *Kidney Int.,* **49,** 1787–1790.

CHIU, A.T., MCCALL, D.E., PRICE, W.A., WONG, P.C., CARINI, D.J., DUNCIA, J.V., WEXLER, R.R., YOO, S.E., JOHNSON, A.L. & TIMMERMANS, P.B.M.W.M. (1990). Nonpeptide angiotensin II receptor antagonists. VII. Cellular and biochemical pharmacology of DUP 753, an orally active antihypertensive agent. *J. Pharmacol. Exp. Ther.,* **252,** 711–717.

EDWARDS, R.M., TRIZNA, W., STACK, E.J. & WEINSTOCK, J. (1996). Interaction of nonpeptide angiotensin II receptor antagonists with the urate transporter in rat renal brush-border membranes. *J. Pharmacol. Exp. Ther.,* **276,** 125–129.

HARRIS, P.J., CULLINAN, M., THOMAS, D. & MORGAN, T.O. (1987). Digital image capture and analysis for split-droplet micropuncture. *Pflügers Arch.,* **408,** 615–618.

HARRIS, P.J. & YOUNG, J.A. (1977). Dose-dependent stimulation and inhibition of proximal tubular sodium reabsorption by angiotensin II in the rat kidney. *Pflügers Arch.,* **367,** 295–297.

HIRANYACHATTADA, S. & HARRIS, P.J. (1996). Modulation by locally produced luminal angiotensin II of proximal tubular sodium reabsorption via an AT_1 receptor. *Br. J. Pharmacol.,* **119,** 617–618.

LEYSSAC, P.P., KARLSEN, F.M. & HOLSTEIN-RATHLOU, N.H. (1997). Effect of angiotensin II receptor blockade on proximal tubular fluid reabsorption. *Am. J. Physiol.,* **273,** R510–R517.

LI, L., WANG, Y., CAPPARELLI, A., JO, O.D. & YANAGAWA, N. (1994). Effect of luminal angiotensin II on proximal tubule fluid transport: role of apical phospholipase A_2. *Am. J. Physiol.,* **266,** F202–F209.

MITCHELL, K.D., JACINTO, S.M. & MULLINS, J.J. (1997). Proximal tubular fluid, kidney, and plasma levels of angiotensin II in hypertensive ren-2 transgenic rats. *Am. J. Physiol.,* **273,** F246–F253.

OJIMA, M., INADA, Y., SHIBOUTA, Y., WADA, T., SANADA, T., KUBO, K. & NISHIKAWA K. (1997). Candesartan (CV-11974) dissociates slowly from the angiotensin AT_1 receptor. *Eur. J. Pharmacol.,* **319,** 137–146.

QUAN, A. & BAUM, M. (1996). Endogenous production of angiotensin II modulates rat proximal tubule transport. *J. Clin. Invest.,* **97,** 2878–2882.

SCHUSTER, V.L., KOKKO, J.P. & JACOBSON, H.R. (1984). Angiotensin II directly stimulates sodium transport in rabbit proximal convoluted tubules. *J. Clin. Invest.,* **73,** 507–515.

SECHI, L.A., GRADY, E.F., GRIFFIN, C.A., KALINYAK, J.E. & SCHAMBELAN, M. (1992). Distribution of angiotensin II receptor subtypes in rat and human kidney. *Am. J. Physiol.,* **262,** F236–F240.

SEIKALY, M.G., ARANT, B.S. & SENEY, F.D. (1990). Endogenous angiotensin concentrations in specific intrarenal fluid compartments of the rats. *J. Clin. Invest.,* **86,** 1352–1357.

TAMAKI, T., NISHIYAMA, A., YOSHIDA, H., HE, H., FUKUI, T., YAMAMOTO, A., AKI, Y., KIMURA, S., IWAO, H., MIYATAKE, A. & ABE, Y. (1993). Effects of EXP3174, a non peptide angiotensin II receptor antagonist, on renal hemodynamics and renal function in dogs. *Eur. J. Pharmacol.,* **236,** 15–21.

WANG, T. & CHAN, Y.L. (1990). Mechanism of angiotensin II action on proximal tubular transport. *J. Pharmacol. Exp. Ther.,* **252,** 689–695.

WONG, P.C., PRICE, W.A., CHIU, A.T., DUNCIA, J.V., CARINI, D.J., WEXLER, R.R., JOHNSON, A.L. & TIMMERMANS, P.B.M.W.M. (1990). Nonpeptide angiotensin II receptor antagonist XI. Pharmacology of EXP3174: An active metabolite of DuP753, an orally active antihypertensive agent. *J. Pharmacol. Exp. Ther.,* **255,** 211 – 217.

XIE, M.H., LIU, F.Y., WONG, P.C., TIMMERMANS, P.B.M.W.M. & COGAN, M.G. (1990). Proximal nephron and renal affects of DuP753, a nonpeptide angiotensin II receptor antagonist. *Kidney Int.,* **38,** 473 – 479.

ZHUO, J., THOMAS, D., HARRIS, P.J. & SKINNER, S.L. (1992). The role of endogenous angiotensin II in the regulation of renal haemodynamics and proximal fluid reabsorption in the rat. *J. Physiol.,* **453,** 1 – 13.

(Received May 11, 1998
Revised November 13, 1998
Accepted November 17, 1998)

British Journal of Pharmacology (1999) 126, 701–708
http://www.stockton-press.co.uk/bjp

Pharmacological evidence that inducible nitric oxide synthase is a mediator of delayed preconditioning

[1]J. Imagawa, *,[1]D.M. Yellon & [1]G.F. Baxter

[1]The Hatter Institute for Cardiovascular Studies, University College London Hospital and Medical School, Grafton Way, London, WC1E 6DB, U.K.

1 Brief periods of myocardial ischaemia preceding a subsequent more prolonged ischaemic period 24–72 h later confer protection against myocardial infarction ('delayed preconditioning' or the 'second window' of preconditioning). In the present study, we examined the effects of pharmacological modifiers of inducible nitric oxide synthase (iNOS) induction and activity on delayed protection conferred by ischaemic preconditioning 48 h later in an anaesthetized rabbit model of myocardial infarction.

2 Rabbits underwent a myocardial preconditioning protocol (four 5 min coronary artery occlusions) or were sham-operated. Forty-eight hours later they were subjected to a sustained 30 min coronary occlusion and 120 min reperfusion. Infarct size was determined with triphenyltetrazolium staining. In rabbits receiving no pharmacological intervention, the percentage of myocardium infarcted within the risk zone was $43.9 \pm 5.0\%$ in sham-operated animals and this was significantly reduced 48 h after ischaemic preconditioning with four 5 min coronary occlusions to $18.5 \pm 5.6\%$ ($P < 0.01$).

3 Administration of the iNOS expression inhibitor dexamethasone (4 mg kg^{-1} i.v) 60 min before ischaemic preconditioning completely blocked the infarct-limiting effect of ischaemic preconditioning (infarct size $48.6 \pm 6.1\%$). Furthermore, administration of aminoguanidine (300 mg kg^{-1}, s.c.), a relatively selective inhibitor of iNOS activity, 60 min before sustained ischaemia also abolished the delayed protection afforded by ischaemic preconditioning (infarct size $40.0 \pm 6.0\%$).

4 Neither aminoguanidine nor dexamethasone *per se* had significant effect on myocardial infarct size. Myocardial risk zone volume during coronary ligation, a primary determinant of infarct size in this non-collateralized species, was not significantly different between intervention groups. There were no differences in systolic blood pressure, heart rate, arterial blood pH or rectal temperature between groups throughout the experimental period.

5 These data provide pharmacological evidence that the induction of iNOS, following brief periods of coronary occlusion, is associated with increased myocardial tolerance to infarction 48 h later.

Keywords: Ischaemic preconditioning; second window of protection; nitric oxide synthase; aminoguanidine; dexamethasone; myocardial infarction, rabbit

Abbreviations: AG, aminoguanidine; DX, dexamethasone; hsp72, 72 kDa heat shock protein; cNOS, constitutive nitric oxide synthase; iNOS, inducible nitric oxide synthase; K_{ATP}, ATP-sensitive potassium channel; NF-κB, nuclear factor kappa B; NO, nitric oxide; NOS, nitric oxide synthase; PC, preconditioning; SWOP, second window of preconditioning

Introduction

Preconditioning myocardium with brief periods of ischaemia confers biphasic protection against later sustained ischaemia-reperfusion insult (Yellon *et al*., 1998). An early preconditioning effect appears rapidly after transient ischaemic stimuli and lasts approximately 1 h, while a delayed or 'second window' of preconditioning ('SWOP') develops many hours later and lasts for a few days. The delayed infarct-limiting effect of prior brief ischaemia has been confirmed in dog (Kuzuya *et al*., 1993), rabbit (Marber *et al*., 1993), rat (Yamashita *et al*., 1998) and pig myocardium (Muller *et al*., 1998).

Previously we have demonstrated that delayed preconditioning in rabbit myocardium was dependent on adenosine receptor activation (Baxter *et al*., 1994), protein kinase C activation (Baxter *et al*., 1995) and protein tyrosine kinase activity (Imagawa *et al*., 1997). However, the fact that delayed preconditioning requires many hours to be established suggests that the phenomenon is related to *de novo* synthesis of proteins which mediate or directly induce cardioprotection (Yellon & Baxter, 1995). In line with this inducible cytoprotective protein hypothesis, it has been demonstrated that the 72 kDa heat shock protein (hsp72) is upregulated 24 h after ischaemic preconditioning in rabbit myocardium (Marber *et al*., 1993), and in canine myocardium upregulation of manganese superoxide dismutase 24 h after preconditioning is temporally associated with cardioprotection (Hoshida *et al*., 1993; Kuzuya *et al*., 1993). However, so far evidence that these proteins are directly responsible for the protection observed in delayed preconditioning is elusive. Moreover, myocardial ischaemic stress is a complex stimulus and is known to involve the upregulation of many other proteins which could potentially be involved in the mediation of delayed cardioprotection.

Nitric oxide (NO), generated from various isoforms of nitric oxide synthase (NOS) has the potential to exhibit several beneficial effects in ischaemic tissue. These actions might be direct effects of NO on metabolism, such as reduction in oxygen utilization, or they might be exerted through cyclic GMP signalling. Several pieces of experimental evidence suggest that the inducible form of nitric oxide synthase (iNOS) might be involved in some forms of delayed adaptive

* Author for correspondence; E-mail: s.bush-cavell@ucl.ac.uk

cytoprotection: (i) Dexamethasone was shown to prevent the development of a delayed anti-arrhythmic protection 20 h after pacing-induced preconditioning in the dog (Vegh *et al*., 1994). This finding is compatible with the induction of iNOS since dexamethasone is known to inhibit the expression of iNOS (Radomski *et al*., 1990; Rees *et al*., 1990); (ii) Endotoxin-induced cardioprotection is abolished by treatment with dexamethasone in rats (Wu *et al*., 1996); (iii) We have shown a delayed myocardial protection 24 h after treatment with monophosphoryl lipid A, an endotoxin derivative, in the rabbit (Baxter *et al*., 1996), which could also be related to induction of iNOS; (iv) Aminoguanidine, a relatively selective inhibitor of iNOS activity (Griffiths *et al*., 1993; Misko *et al*., 1993) has been shown to block the delayed pharmacological preconditioning by monophosphoryl lipid A in a rabbit infarct model (Zhao *et al*., 1997) and (v) In a conscious rabbit model of myocardial stunning, Bolli *et al*. (1997) demonstrated that treatment with a non-selective NOS inhibitor, N^{ω}-nitro-L-arginine, and the selective iNOS inhibitors aminoguanidine and S-methylisothiourea blocked the delayed anti-stunning effect of delayed preconditioning. This body of evidence suggests that iNOS may be induced by a variety of stimuli that evoke delayed myocardial protection.

In view of the preceding evidence, we hypothesized that transient ischaemia-reperfusion stress (ischaemic preconditioning), initiates the induction of iNOS and that this enzyme is a mediator of delayed cytoprotection during subsequent prolonged ischaemia through the enhanced generation of NO. We examined if the delayed infarct-limiting effect of ischaemic preconditioning was modified either by inhibition of iNOS induction with dexamethasone given during preconditioning ischaemia, or by inhibition of iNOS activity with aminoguanidine given before prolonged coronary artery occlusion. A preliminary account of these findings was presented to the British Cardiac Society at its annual meeting in May 1998 (Imagawa *et al*., 1998a).

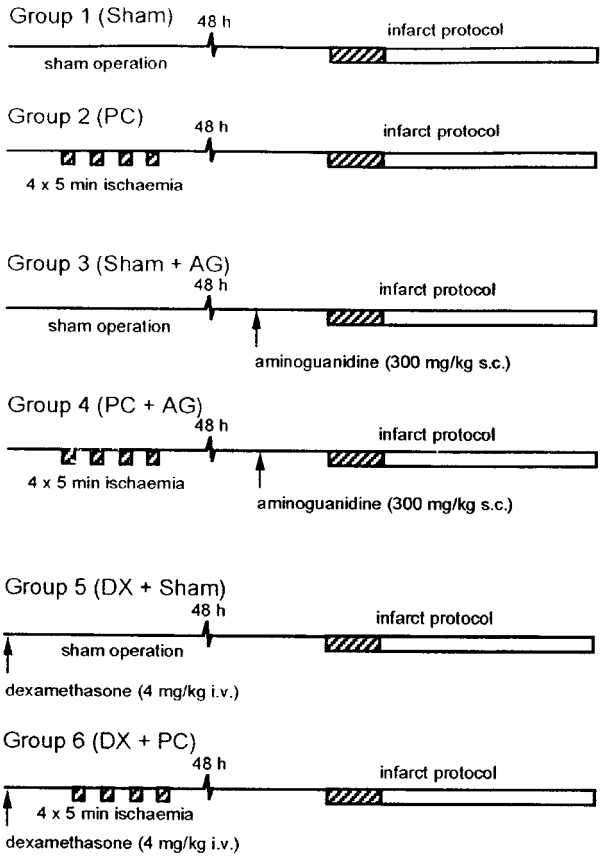

Figure 1 Experimental groups and treatment protocols. Hatched areas indicate periods of myocardial ischaemia induced by coronary artery occlusion. Sham operation consisted of the positioning of a coronary ligature without occlusion. Preconditioning was performed by occlusion of a coronary artery for four 5 min periods each seperated by 10 min reperfusion. All animals were left for 48 h before the infarct protocol was peformed. This consited of 30 min coronary occlusion followed by 120 min reperfusion. Aminoguanidine was given 60 min before the infarct coronary occlusion. Dexamethasone was given 60 min before positioning of the coronary ligature in the sham operation or preconditioning groups.

Methods

Male New Zealand White rabbits (2.1–2.9 kg) were used throughout. Animals were allowed to acclimatize in the institutional animal house for around 1 week after delivery. They were allowed free access to a pelleted diet, water, and fresh hay. The care and use of animals in this work were in accordance with U.K. Home Office guidelines of the Animals (Scientific Procedures) Act 1986. These experiments were divided into two parts as previously described (Marber *et al*., 1993; Baxter *et al*., 1994; 1997; Imagawa *et al*., 1997). Part 1 involved preparation of the animals in which ischaemic preconditioning was performed on day 1. Forty eight hours later, Part 2 of the procedure (myocardial infarction) was performed on day 3.

The experimental protocols are summarized in Figure 1. Animals were randomly assigned into six groups. Group 1 were sham-operated control animals without drug treatment (Sham). Group 2 were preconditioned without drug treatment (PC). Group 3 were sham-operated on day 1 and received aminoguanidine prior to infarction on day 3 (Sham + AG). Group 4 were preconditioned on day 1 and received aminoguanidine prior to infarction on day 3 (PC + AG). Group 5 were sham-operated on day 1 with dexamethasone treatment (DX + Sham). Group 6 were preconditioned on day 1 with dexamethasone treatment (DX + PC).

During preparative surgery all groups received sterile normal saline (0.9% NaCl) infusion (approximately 3 ml kg^{-1}). 60 min before coronary occlusion in the infarct procedure, animals received either saline 1 ml kg^{-1} s.c. (Groups 1, 2, 5 and 6) or aminoguanidine 300 mg kg^{-1} (Groups 3 and 4). Aminoguanidine was dissolved in saline at a concentration of 300 mg ml^{-1}. The dexamethasone-treated groups received dexamethasone 4 mg kg^{-1} i.v. (20 mg ml^{-1} in ampoule) 60 min prior to the first preconditioning coronary occlusion.

Part 1: Ischaemic preconditioning or sham-operation

Animals were anaesthetized with a combination of 2 mg kg^{-1} i.v. diazepam and 0.3 ml kg^{-1} i.m. fentanyl citrate and fluanisone mixture (Hypnorm®). They were intubated with an orotracheal tube using a paediatric laryngoscope and ventilated with room air supplemented with O_2 at a tidal volume of 5 ml kg^{-1} and a rate of approximately 1 Hz (small animal ventilator, Harvard Apparatus, Kent, U.K.). Electrodes were attached to shaved areas on each limb for recording of the surface ECG. The amplified ECG signals were recorded with an ECG amplifier and recorder (RS3400, Gould Instruments, Ilford, U.K.). A marginal ear vein was cannulated to administer drugs. Under antibiotic cover (5 mg kg^{-1} enrofloxacin, s.c.) and with aseptic technique, a median sternotomy and pericar-

diotomy were performed. An anterolateral branch of the circumflex coronary artery was identified, and a 3-0 silk suture (Mersilk type 546, Ethicon, Edinburgh, U.K.) was passed underneath the vessel at a point approximately halfway between the left atrioventricular groove and the apex. The ends of the suture were threaded through a 1.5 cm polypropylene tube to form a snare. The artery was occluded by pulling the ends of the suture taut and clamping the snare onto the epicardial surface. Snaring of the artery caused epicardial cyanosis and regional hypokinesis within 20–30 s and was usually accompanied by ST-segment elevation in the ECG within 1 min. After 5 min of ischaemia, reperfusion was instituted by releasing the snare. Successful reperfusion was confirmed by conspicuous blushing of the previous ischaemic myocardium and gradual resolution of the ECG changes. The preconditioning protocol consisted of four 5 min occlusions, each separated by 10 min reperfusion. After preconditioning, the loose suture was left *in situ*, the thorax was evacuated, and the sternotomy closed. Animals were extubated and allowed to recover from anaesthesia with postoperative analgesia (30 μg kg^{-1} buprenorphine HCl, i.m. and 1 mg kg^{-1} flunixin meglumine, s.c.). Sham-operated animals underwent the same surgical procedure, including pericardiotomy and positioning the coronary artery suture, without coronary occlusion. Approximately 24 h after surgical preparation, an antibiotic and an analgesic (5 mg kg^{-1} enrofloxacin, s.c. and 1 mg kg^{-1} flunixin meglumine, s.c.) were given to all animals.

Part 2: Infarction procedure

On day 3, approximately 48 h after operation on day 1, rabbits were reanaesthetized with a combination of 30 mg kg^{-1} pentobarbitone sodium (i.v.) and 0.15 ml kg^{-1} Hypnorm® (i.m.). Electrodes were attached to the shaved area on each limb for recording of the surface ECG. After the trachea was cannulated *via* a mid-line cervical incision under local anaesthetic (2% lignocaine HCl), animals were ventilated with room air supplemented with O_2 and tidal volume was adjusted as necessary throughout the procedure to maintain arterial pH between 7.3 and 7.5 and pCO_2 at <5.0 kPa. The rate of the ventilation was approximately 1 Hz. The right common carotid artery was cannulated with a short rigid polyethylene cannula attached to a pressure transducer (P23XL, Gould) for continuous recording of arterial blood pressure and intermittent arterial blood gas measurements (AVL993, AVL Medical Instruments U.K. Ltd, Stone, Staffs, U.K.). Rectal temperature was monitored periodically and maintained at 38.5 ± 0.5°C with a heating pad. The thorax was reopened, and the *in situ* coronary ligature was used again for coronary occlusion. The artery was occluded for 30 min, followed by 120 min reperfusion by manipulating the ligature and snare as described above.

At the end of 120 min reperfusion, 1000 i.u. heparin sodium was administered before the heart was excised and Langendorff-perfused with saline solution to remove blood. The ligature was tightened again, and zinc-cadmium sulphide 1–10 μm microspheres were infused through the aorta to delineate the myocardium at risk under ultraviolet light. After freezing, the heart was sliced transversely from apex to base in 2 mm sections. The slices were defrosted, blotted and incubated at 37°C with 1% w/v triphenyltetrazolium chloride in phosphate buffer (pH 7.4) for 10–20 min and fixed in 4% v/v formaldehyde solution for 2–7 days to clearly distinguish between stained viable tissue and unstained necrotic tissue. The volumes of the infarcted tissue and the tissue at risk were determined by a computerized planimetric technique (Summa Sketch II, Summa Graphics, Seymour, CT, U.S.A.).

Materials

We obtained aminoguanidine hemisulphate and triphenyltetrazolium chloride from Sigma Chemical (Poole, U.K.), dexamethasone sodium phosphate from Merck Sharp & Dohme (Hoddesden, U.K.), Hypnorm® from Janssen (Wantage, U.K.), diazepam from CP Pharmaceutical (Clwyd, U.K.), sodium pentobarbitone (Sagatal®) from Rhone Merieux (Dublin, Ireland), lignocaine HCl from Antigen Pharmaceuticals (Roscrea, Ireland), zinc-cadmium sulphide fluorescent microspheres (1–10 μm) from Duke Scientific (Palo Alto, CA, U.S.A.), enrofloxacin (Baytril®) from Bayer (Suffolk, U.K.), flunixin meglumine (Finadyne®) from Schering-Plough (Suffolk, U.K.) and buprenorphine HCl (Vetergesic®) from Reckitt & Colman Products Ltd (Hull, U.K.). All other chemicals were of analytical reagent quality.

Statistical analysis

The data are presented throughout as means $\pm$ s.e.mean. The significance of differences in mean values was evaluated by a one-way ANOVA. When treatment constituted a significant source of variance, Fisher's least significant difference test was used *post hoc* for predetermined individual group comparisons. The null hypothesis was rejected when $P<0.05$.

Results

Mortality and exclusions

A total of 46 rabbits were used for this study. Forty-five animals survived the preparation protocols. During Part 2, six animals were lost due to sustained ventricular fibrillation and/or systemic circulatory failure during the infarct protocol (two in Sham, three in DX + PC and one in DX + Sham) and two hearts (one in PC and one in PC + AG) were excluded due to an ischaemic myocardial risk volume less than 0.4 cm^3 which was a prospectively determined exclusion criterion. One experiment was also excluded due to failure to determine clearly the risk zone in Sham group. The final numbers of animals were 36 (six in each group). Some of these animals had transient ventricular fibrillation during sustained ischaemia which reverted to sinus rhythm either spontaneously or with gentle tapping of the cardiac apex. However, there were no significant differences in the incidence of ventricular fibrillation between groups.

Myocardial infarct size

Ischaemic risk volumes during coronary occlusion were not significantly different between intervention groups at around 1.0 cm^3 (Figure 2a). Percentage of infarction within the risk area was reduced from 43.9 ± 5.0% in Sham group to 18.5 ± 5.6% in PC group ($P<0.01$, Figure 2b). These infarct size values are consistent with our previous observation of infarct limitation associated with delayed preconditioning at 48 h (Baxter *et al*., 1997; Imagawa *et al*., 1997).

The inhibition of iNOS activity by aminoguanidine 60 min prior to sustained ischaemia, had virtually no effect on infarct size in sham-operated animals (39.4 ± 6.0% in Sham + AG group vs 43.9 ± 5.0% in Sham group, $P>0.05$, Figure 2b).

However, this inhibitor completely abolished the delayed protection afforded by ischaemic preconditioning (40.0±6.0% in PC+AG group vs 18.5±5.6% in PC group, $P<0.05$, Figure 2b).

Dexamethasone given prior to the sham-operation had no significant effect on infarct size produced by sustained coronary occlusion 48 h later (46.7±6.7% in DX+Sham group vs 43.9±5.0% in Sham group, $P>0.05$, Figure 2b). However, dexamethasone given before ischaemic preconditioning abolished the delayed infarct-limiting effect of ischaemic preconditioning (48.6±6.1% in DX+PC group vs 18.5±5.6% in PC group, $P<0.01$, Figure 2b). Figure 3 shows the relation between risk region and infarct size for each animal. In all groups, there was a positive correlation between these two variables. These plots indicate that infarct size is dependent on the risk zone size and that distribution of the plots is clearly different between the PC group and the other five groups, indicating that the reduction in infarct size in PC group was independent of risk volume.

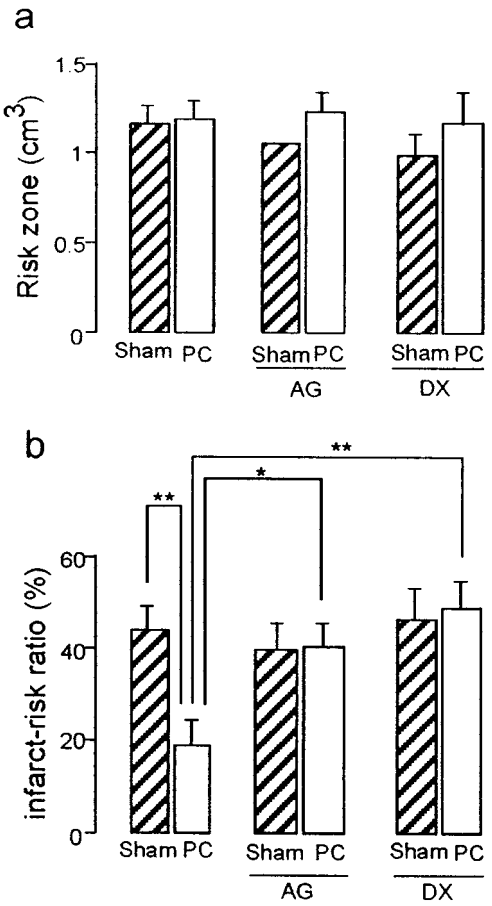

Figure 2 Effects of aminoguanidine (AG) and dexamethasone (DX) on myocardial infarct size assessed after 30 min coronary occlusion followed by 120 min reperfusion in sham-operated (Sham) or ischaemically preconditioned (PC) rabbit hearts. (a) Myocardial risk zone volume. (b) Infarct size as a percentage of risk volume. Vertical bars depict mean with s.e.mean ($n=6$). *$P<0.05$, **$P<0.01$ (1-way ANOVA).

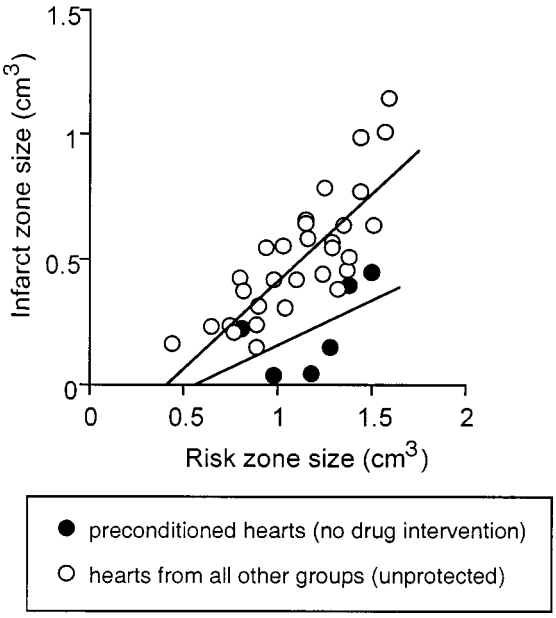

Figure 3 Relation between absolute infarct and risk zone volumes for individual hearts. Closed circles indicate values from preconditioned hearts without any pharmacological inhibitors (protected hearts) ($y=0.36\times-0.20$; $r=0.53$). Open circles indicate values from the remaining five groups of hearts (non-protected hearts) ($y=0.71\times-0.28$; $r=0.81$). The regression line for preconditioned hearts is significantly different from the regression line for all other groups ($P<0.05$, analysis of covariance).

Table 1 Changes in heart rate and systolic blood pressure before and during 30 min ischaemia and 120 min reperfusion

	Baseline	*Ischaemia 5 min*	*Ischaemia 29 min*	*Rep 60 min*	*Rep 120 min*
Heart rate (beats/min)					
Sham	253±14	238±10	235±13	247±17	247±14
PC	218±8	228±8	238±12	229±13	226±13
Sham+AG	251±17	254±16	253±15	252±15	245±15
PC+AG	246±13	248±9	232±10	233±5	227±7
DX+Sham	231±10	247±8	238±6	215±10	213±10
DX+PC	221±17	234±15	228±7	208±12	201±11
Systolic blood pressure (mmHg)					
Sham	79.0±3.0	69.3±4.3	70.7±4.5	69.8±5.0	70.0±5.3
PC	75.7±3.1	67.5±2.7	73.7±5.1	70.8±4.3	73.0±3.9
Sham+AG	85.0±5.8	78.2±4.5	78.7±4.2	75.2±6.6	69.7±4.1
PC+AG	86.7±3.6	78.3±4.9	78.0±5.7	73.7±3.2	69.8±2.6
DX+Sham	82.2±1.9	80.7±1.5	78.8±2.2	77.8±2.7	78.7±3.2
DX+PC	78.5±1.9	74.0±3.8	73.8±1.4	72.7±2.4	74.8±1.8

Data are mean±s.e.mean ($n=6$). Rep, reperfusion; Sham, sham-operated; PC, preconditioned; AG, aminoguanidine; DX, dexamethasone.

Haemodynamic responses and differences in arterial blood gases

Table 1 describes the changes in systolic blood pressure and heart rate during sustained (30 min) coronary occlusion and subsequent 120 min reperfusion. There were no statistically significant differences in these haemodynamic parameters between groups throughout the experimental period. Although baseline blood pressure in PC group was somewhat lower than that in other groups, this was not statistically significant. Of particular note, aminoguanidine prior to coronary occlusion produced no significant effects on blood pressure or heart rate. Since temperature is a mjor determinant of the rate of infarction in ischaemic tissue, rectal temperature was strictly maintained at around 38.5°C (Table 2). Arterial blood pH tended to fall at 29 min after ischaemia and recovered after reperfusion in all groups. However, there were no statistically significant differences in blood pH between groups at any time points (Table 2).

Discussion

The pertinent findings of the present study can be summarized as follows. Four 5 min coronary artery occlusions induced an adaptive response in myocardium (delayed preconditioning) which was associated with reduced myocardial infarct size following sustained coronary artery occlusion 48 h later. This result is consistent with previous reports of delayed preconditioning against infarction (e.g. Marber *et al*., 1993; Baxter *et al*., 1997; Imagawa *et al*., 1997; Qiu *et al*., 1997). A selective inhibitor of iNOS activity, aminoguanidine (Griffiths *et al*., 1993; Misko *et al*., 1993), when given before sustained ischaemia abolished the protection implying that iNOS activity is necessary during sustained ischaemia for the demonstration of delayed preconditioning. Dexamethasone, an inhibitor of iNOS expression (Radomski *et al*., 1990; Rees *et al*., 1990), completely abolished the delayed myocardial protection conferred by ischaemic preconditioning. The major conclusion of the present studies is that the induction and subsequent activation of iNOS appears to be necessary for development of delayed preconditioning in this experimental model. Our findings concur with work by Vegh's group in the canine model that dexamethasone prevents the development of delayed preconditioning against arrhythmias (Vegh *et al*., 1994). While this manuscript was in preparation, a report by Takano *et al*., (1998) was published which supports our data with respect to a role for nitric oxide synthase in delayed preconditioning against infarction in rabbit myocardium.

Effects of aminoguanidine and dexamethasone

Aminoguanidine is a selective inhibitor of iNOS (Griffiths *et al*., 1993; Misko *et al*., 1993). Under some experimental conditions the selectivity of this agent may be limited (Laszlo *et al*., 1995) and therefore we can not rule out the possibility that the constitutive form of NOS (cNOS) was also inhibited by aminoguanidine. However, the data tend to argue against any significant inhibition of cNOS by aminoguanidine in our experiments for the following reasons. First, we showed that aminoguanidine had no effect on infarct size *per se* whereas the inhibition of cNOS by non-selective NOS inhibitors significantly affects myocardial infarct size in this rabbit model of ischaemia-reperfusion (Patel *et al*., 1993; Williams *et al*., 1995). Secondly, the blood pressure in aminoguanidine-treated animals was not significantly higher than that in control animals before and during ischaemia and reperfusion periods in contrast to previous data showing marked hypertensive effects of non-selective NOS inhibitors in rabbits (Patel *et al*., 1993; Williams *et al*., 1995). These results would suggest the selectivity of aminoguanidine for iNOS over cNOS at the dose we used (300 mg kg^{-1}, s.c.).

It has been reported that aminoguanidine has some effects other than NOS inhibition. Among them, an inhibitory effect on the antioxidant enzyme catalase (Ou & Wolff, 1993) might be involved in abrogation of delayed preconditioning by aminoguanidine since upregulation of endogenous antioxidant enzymes has been postulated as a mechanism of delayed preconditioning. However, the IC_{50} for aminoguanidine on catalase activity is reported to be 15 mM (Ou & Wolff, 1993), a value far in excess of the plasma concentration of aminoguanidine estimated from the dose we used. Therefore, we believe it unlikely that aminoguanidine significantly affects catalase activity in our experimental condition.

Dexamethasone has been reported to suppress the expression of iNOS in endothelial cells stimulated with interferon-γ and lipopolysaccharide (Radomski *et al*., 1990). The suppression would be mediated through inhibitory effect of the glucocorticoid on the transcription factor nuclear factor kappa B (NF-κB) (Auphan *et al*., 1995) and concomitant inhibition

Table 2 Changes in rectal temperature and arterial blood pH before and during 30 min ischaemia and 120 min reperfusion

	Baseline	*Ischaemia 5 min*	*Ischaemia 29 min*	*Rep 60 min*	*Rep 120 min*
Rectal temperature (°C)					
Sham	38.4±0.1	38.5±0.1	38.3±0.1	38.5±0.1	38.5±0.1
PC	38.4±0.1	38.4±0.1	38.2±0.2	38.3±0.1	38.4±0.1
Sham+AG	38.5±0.1	38.4±0.1	38.2±0.1	38.5±0.1	38.4±0.1
PC+AG	38.3±0.1	38.3±0.1	38.3±0.1	38.5±0.1	38.5±0.1
DX+Sham	38.6±0.1	38.5±0.1	38.3±0.1	38.4±0.1	38.6±0.1
DX+PC	38.6±0.1	38.5±0.1	38.4±0.0	38.6±0.1	38.5±0.1
Arterial pH					
Sham	7.45±0.01	7.44±0.01	7.40±0.02	7.41±0.01	7.43±0.01
PC	7.45±0.01	7.46±0.02	7.40±0.01	7.46±0.01	7.45±0.01
Sham+AG	7.46±0.02	7.46±0.02	7.43±0.01	7.44±0.01	7.43±0.01
PC+AG	7.46±0.01	7.46±0.01	7.43±0.02	7.45±0.01	7.45±0.01
DX+Sham	7.45±0.01	7.45±0.01	7.42±0.01	7.43±0.02	7.43±0.01
DX+PC	7.41±0.02	7.41±0.02	7.38±0.03	7.41±0.01	7.41±0.02

Data are mean±s.e.mean ($n=6$). Rep, reperfusion; Sham, sham-operated; PC, preconditioned; AG, aminoguanidine; DX, dexamethasone.

of cytokine production (Evans & Zuckerman, 1991). Because NF-κB activates many immunoregulatory genes in response to pro-inflammatory stimuli, the inhibition of its activity by dexamethasone would affect many kinds of biological activities including inducible cyclo-oxygenase (Masferrer *et al*., 1992). Thus dexamethasone is not a specific inhibitor of iNOS expression. At present, we can not exclude the possible involvement of cyclo-oxygenase products, such as prostacyclin, in delayed preconditioning against infarction since these mediators have not been systematically investigated in the phenomenon. However, the complete abrogation of delayed preconditioning by aminoguanidine, which is not a cyclo-oxygenase inhibitor, would suggest that the inhibitory effect of dexamethasone on delayed preconditioning is likely to be due to inhibition of iNOS expression, rather than inhibition of cyclo-oxygenase induction.

Possible mechanisms of iNOS induction

This evidence tends to support the hypothesis that NO may be an important mediator of delayed preconditioning proposed initially by Vegh *et al*. (1994) with respect to antiarrhythmic effects and subsequently by Bolli *et al*., (1997) with respect to anti-stunning effects. The present findings that NO may be a mediator of the infarct-limiting effects of delayed preconditioning are supported by the work of Takano *et al*. (1998) which was published while this manuscript was in preparation. This group reported that aminoguanidine treatment resulted in abolition of delayed preconditioning in rabbits when administered immediately prior to infarction.

Although the results of the present study suggest the involvement of iNOS in delayed cardioprotection conferred by ischaemic preconditioning, the mechanisms responsible for induction of iNOS by brief ischaemia have not been clarified. Our earlier work has clearly established that adenosine receptor activation during preconditioning is necessary for the triggering the development of delayed preconditioning against infarction. However, in other experimental models, it has been shown that a burst of oxygen free radicals is generated during the initial periods of brief, repetitive anoxia, and the radicals, including superoxide anion, are essential for triggering delayed cytoprotection 24 h later in isolated rat myocyte preparations (Zhou *et al*., 1996). Superoxide anion is converted to hydrogen peroxide, a well known activator of nuclear factor kappa B (NF-κB) (Satriano & Achlondorff, 1994). NF-κB is essential for the induction of iNOS by lipopolysaccharide in murine macrophages (Xie *et al*., 1994). Activated NF-κB would mediate the induction of some cytokines, such as tumour necrosis factor α and interleukin-1β, which have been shown to be potent inducers of iNOS in a variety of cells including macrophages, smooth muscle cells and endothelial cells (Moncada & Higgs, 1993). In addition, it has been reported that tyrosine kinase inhibitors abolish both NF-κB activation (Lee *et al*., 1997) and iNOS induction (Kleinert *et al*., 1996; LaPointe & Sitkins, 1996) conferred by stimulation with cytokines in many tissues including cardial myocytes. Therefore, ischaemic preconditioning might induce iNOS through a pathway involving free radicals, cytokines, tyrosine phosphorylation and NF-κB. Our previous data (Imagawa *et al*., 1997) showing inhibitory effects of a tyrosine kinase inhibitor on delayed preconditioning is consistent with this hypothesis.

The time course of iNOS induction after ischaemic preconditioning was not investigated in this study. However, it has been reported that the generation of NO by iNOS is maintained at least 48 h after stimulation with cytokines such as interferon γ and/or lipopolysaccharide in vascular endothelial cells (Radomski *et al*., 1990), colonic epithelial cell line (Kolios *et al*., 1995) and cardiac myocytes (Luss *et al*., 1995). In addition, a brief myocardial ischaemia enhanced production of NO metabolite 24–48 h later (Kim *et al*., 1997). From these results it might be possible that iNOS was activated 48 h after ischaemic preconditioning at which time point we observed delayed cardioprotection although the time course of iNOS induction might vary with experimental conditions.

Cardioprotection by NO

There is good evidence for a cardioprotective effect of NO under conditions of ischaemia and reperfusion. The mechanisms might include the reduction of myocardial oxygen demand concomitant with vasodilatory and negative inotropic effects of NO. However, in the present study the haemodynamic status was not different between any groups. Therefore it is unlikely that delayed protection is mediated by NO-induced decrease in myocardial oxygen demand. It has been reported that NO would protect myocardium from reperfusion injury *via* suppression of the activity of neutrophils (Lefer & Lefer, 1996). A recent report shows that peroxynitrite anion, which is formed by the interaction of superoxide and NO, is also cardioprotective through the inhibition of leukocyte-endothelial cell interactions in rats (Lefer *et al*., 1997). However, in the rabbit model (Birnbaum *et al*., 1997), in contrast to the dog (Chatelain *et al*., 1987) and rat (Hale & Kloner, 1991) models, only a small number of neutrophils infiltrated the myocardial area at risk following 30 min of ischaemia and 4 h reperfusion. Therefore it is unlikely that neutrophils play a major role in formation of myocardial infarction in our experimental model. Alternatively, recent experimental evidence has shown that NO enhances ATP-sensitive K channel (K_{ATP}) activity in rabbit cardiomyocytes (Cameron *et al*., 1996) and vascular smooth muscle cells from rabbit mesenteric arteries (Murphy & Brayden, 1995). We recently showed that a K_{ATP} channel opener, nicorandil, conferred cardioprotection in a rabbit myocardial infarct model (Imagawa *et al*., 1998b). Thus NO might protect ischaemic myocardium through activation of K_{ATP} channels in the rabbit heart. The involvement of K_{ATP} channels has been already reported in hyperthermia-induced (Pell *et al*., 1997), monophosphoryl lipid A-induced (Elliott *et al*., 1996) and adenosine A_1 agonist-induced (Baxter & Yellon, 1998) delayed cardioprotection in a rabbit infarct model. It remains to be determined how opening of K_{ATP} channels protects myocardium from infarction and which channel is relevant to protection, i.e. the mitochondrial or the plasmalemmal K_{ATP} channel. At the present time, we hypothesize that NO is not the sole mediator or final effector molecule of delayed myocardial protection but it may modulate the activity of a distal effector, possibly the K_{ATP} channel.

Conclusion

Our results demonstrate that delayed protection against myocardial infarction conferred by ischaemic preconditioning can be abolished by an iNOS expression inhibitor, dexamethasone, administered prior to preconditioning. Furthermore, in agreement with the recent work of Bolli's group, we observed that aminoguanidine, an inhibitor of iNOS activity, given prior to infarction also blocked the delayed protective effects of ischaemic preconditioning in our rabbit infarct model. Thus, it is likely that the induction and activation of iNOS are

important steps in the development of delayed preconditioning in the rabbit and that NO might be a possible mediator of delayed cardioprotection.

Dr Baxter is supported by a British Heart Foundation personal fellowship (FS 97001). We thank the Hatter Foundation for continued support.

References

AUPHAN, N., DIDONATO, J.A., ROSETTE, C., HELMBERG, A. & KARIN, M. (1995). Immunosuppression by glucocorticoids: inhibition of NFκB activity through induction of IκB synthesis. *Science,* **270,** 286 – 290.

BAXTER, G.F., GOMA, F.M. & YELLON, D.M. (1995). Involvement of protein kinase C in the delayed cytoprotection following sublethal ischemia in rabbit myocardium. *Br. J. Pharmacol.,* **115,** 222 – 224.

BAXTER, G.F., GOMA, F.M. & YELLON, D.M. (1997). Characterisation of the infarct-limiting effect of delayed preconditioning: timecourse and dose-dependency studies in rabbit myocardium. *Basic Res. Cardiol.,* **92,** 159 – 167.

BAXTER, G.F., GOODWIN, R.W., WRIGHT, M.J., KERAC, M., HEADS, R.J. & YELLON, D.M. (1996). Myocardial protection after monophosphoryl lipid A: studies of delayed anti-ischaemic properties in rabbit heart. *Br. J. Pharmacol.,* **117,** 1685 – 1692.

BAXTER, G.F., MARBER, M.S., PATEL, V.C. & YELLON, D.M. (1994). Adenosine receptor involvement in a delayed phase of myocardial protection 24 hours after ischemic preconditioning. *Circulation,* **90,** 2993 – 3000.

BAXTER, G.F. & YELLON, D.M. (1998). Increased myocardial tolerance to ischaermia 24 h after adenosine A1 receptor stimulation: evidence for a role of the ATP-sensitive K+ channel. *Br. J. Pharmacol.,* **123** (proc suppl), 94P (abstract).

BIRNBAUM, Y., PATTERSON, M. & KLONER, R.A. (1997). The effect of CY1503, a sialyl Lewis^x analog blocker of the selectin adhesion molecules, on infarct size and "no-reflow" in the rabbit model of acute myocardial infarction/reperfusion. *J. Mol. Cell. Cardiol.,* **29,** 2013 – 2025.

BOLLI, R., BHATTI, Z.A., TANG, X.-L., QIU, Y., ZHANG, Q., GUO, Y. & JADOON, A.K. (1997). Evidence that late preconditioning against myocardial stunning in conscious rabbits is triggered by the generation of nitric oxide. *Circ. Res.,* **81,** 42 – 52.

CAMERON, J.S., KIBLER, K.K.A., BERRY, H., BARRON, D.N. & SODDER, V.H. (1996). Nitric oxide activates ATP-sensitive potassium channels in hypertrophied ventricular myocytes. *FASEB J.,* **10,** A65.

CHATELAIN, P., LATOUR, J.G., TRAN, D., LORGERIL, M.D., DUPRAS, G. & BOURASSA, M. (1987). Neutrophil accumulation in experimental myocardial infarcts: relation with extent of injury and effect of reperfusion. *Circulation,* **75,** 1083 – 1090.

ELLIOTT, G.T., COMERFORD, M.L., SMITH, M.L. & ZHAO, L. (1996). Myocardial ischemia/reperfusion protection using monophosphoryl lipid A is abrogated by the ATP-sensitive potassium channel blocker, glibenclamide. *Cardiovasc. Res.,* **32,** 1071 – 1080.

EVANS, G.F. & ZUCKERMAN, S.H. (1991). Glucocorticoid-dependent and - independent mechanisms involved in lipopolysaccharide tolerance. *Eur. J. Immunol.,* **21,** 1973 – 1979.

GRIFFITHS, M.J.D., MESSENT, M., MACALLISTER, R.J. & EVANS, T.W. (1993). Aminoguanidine selectively inhibits inducible nitric oxide synthase. *Br. J. Pharmacol.,* **110,** 963 – 968.

HALE, S.L. & KLONER, R.A. (1991). Time course of infiltration and distribution of neutrophils following coronary artery reperfusion in the rat. *Cor. Art. Dis.,* **2,** 373 – 378.

HOSHIDA, S., KUZUYA, T., FUJI, H., YAMASHITA, N., OE, H., HORI, M., SUZUKI, K., TANIGUCHI, N. & TADA, M. (1993). Sublethal ischemia alters myocardial antioxidant activity in canine heart. *Am. J. Physiol.,* **264,** H33 – H39.

IMAGAWA, J., BAXTER, G.F. & YELLON, D.M. (1997). Genistein, a tyrosine kinase inhibitor, blocks the "second window of protection" 48 h after ischemic preconditioning in the rabbit. *J. Mol. Cell. Cardiol.,* **29,** 1885 – 1893.

IMAGAWA, J., BAXTER, G.F. & YELLON, D.M. (1998a). Delayed preconditioning against infarction may involve inducible nitric oxide synthase. *Heart,* **79** (suppl 1), P10.

IMAGAWA, J., BAXTER, G.F. & YELLON, D.M. (1998b). Myocardial protection afforded by nicorandil and ischaemic preconditioning in a rabbit infarct model in vivo. *J. Cardiovasc. Pharmacol.,* **31,** 74 – 79.

KIM, S.-J., GHALEH, B., KUDEJ, R.K., HUANG, C.-H., HINTZE, T.H. & VANTER, S.F. (1997). Delayed enhanced nitric oxide-mediated coronary vasodilation following brief ischemia and prolonged reperfusion in conscious dogs. *Circ. Res.,* **81,** 53 – 59.

KLEINERT, H., EUCHENHOFER, C., IHRIG-BIEDERT, I. & FORSTERMANN, U. (1996). In murine 3T3 fibroblasts, different second messenger pathways resulting in the induction of NO synthase II (iNOS) converge in the activation of transcription factor NFκB. *J. Biol. Chem.,* **271,** 6039 – 6044.

KOLIOS, G., BROWN, Z., ROBSON, R.L., ROBERTSON, D.A. & WESTWICK, J. (1995). Inducible nitric oxide synthase activity and expression in a human colonic epithelial cell line, HT-29. *Br. J. Pharmacol.,* **116,** 2866 – 2872.

KUZUYA, T., HOSHIDA, S., YAMASHITA, N., FUJI, H., OE, H., HORI, M., KAMADA, T. & TADA, M. (1993). Delayed effects of sublethal ischemia on the acquisition of tolerance to ischemia. *Circ. Res.,* **72,** 1293 – 1299.

LAPOINTE, M.C. & SITKINS, J.R. (1996). Mechanisms of interleukin-1β regulation of nitric oxide synthase in cardiac myocytes. *Hypertension,* **27,** 709 – 714.

LASZLO, F., EVANS, S.M. & WHITTLE, B.J.R. (1995). Aminoguanidine inhibits both constitutive and inducible nitric oxide synthase isoforms in rat intestinal microvasculature in vivo. *Eur. J. Pharmacol.,* **272,** 169 – 175.

LEE, B.S., KANG, H.S., PYUN, K.H. & CHOI, I. (1997). Roles of tyrosine kinases in the regulation of nitric oxide synthesis in murine liver cells: modulation of NFκB activity by tyrosine kinases. *Hepatol.,* **25,** 913 – 919.

LEFER, A.M. & LEFER, D.J. (1996). The role of nitric oxide and cell adhesion molecules on the microcirculation in ischemia-reperfusion. *Cardiovasc. Res.,* **32,** 743 – 751.

LEFER, D.J., SCALIA, R., CAMPBELL, B., NOSSULI, T., HAYWARD, R., SALAMON, M., GRAYSON, J. & LEFER, A.M. (1997). Peroxynitrite inhibits leukocyte-endothelial cell interactions and protects against ischemia-reperfusion injury in rats. *J. Clin. Invest.,* **99,** 684 – 691.

LUSS, H., WATKINS, S.C., FREESWICK, P.D., IMRO, A.K., NUSSLER, A.K., BILLAR, T.R., SIMMONS, R.L., DEL-NIDO, P.J. & MCGOWAN, JR, F.X. (1995). Characterization of inducible nitric oxide synthase expression in endotoxemic rat cardiac myocytes in vivo and following cytokine exposure in vitro. *J. Mol. Cell. Cardiol.,* **27,** 2015 – 2029.

MARBER, M.S., LATCHMAN, D.S., WALKER, J.M. & YELLON, D.M. (1993). Cardiac stress protein elevation 24 hours after brief ischemia or heat stress is associated with resistance to myocardial infarction. *Circulation,* **88,** 1264 – 1272.

MASFERRER, J.L., SEIBERT, K., ZWEIFEL, L. & NEEDLEMAN, P. (1992). Endogenous glucocorticoids regulate an inducible cyclooxygenase enzyme. *Proc. Natl. Acad. Sci. U.S.A.,* **89,** 3917 – 3921.

MISKO, T.P., MOORE, W.M., KASTEN, T.P., NOCKOLS, G.A., CORBETT, J.A., TILTON, R.G., MCDANIEL, M.L., WILLIAMSON, J.R. & CURRIE, M.G. (1993). Selective inhibition of the inducible nitric oxide synthase by aminoguanidine. *Eur. J. Pharmacol.,* **223,** 119 – 125.

MONCADA, S. & HIGGS, A. (1993). The L-arginine-nitric oxide pathway. *New Engl. J. Med.,* **329,** 2002 – 2012.

MULLER, C.A., BAXTER, G.F., LATOUF, S.E., MCCARTHY, J., OPIE, L.H. & YELLON, D.M. (1998). Delayed preconditioning against infarction in pig heart after PTCA balloon inflations. *J. Mol. Cell. Cardiol.,* **30,** A (abstract).

MURPHY, M.E. & BRAYDEN, J.E. (1995). Nitric oxide hyperpolarizes rabbit mesenteric arteries via ATP-sensitive potassium channels. *J. Physiol.,* **486,** 47 – 58.

OU, P. & WOLFF, S.P. (1993). Aminoguanidine: A drug proposed for prophylaxis in diabetes inhibits catalase and generates hydrogen peroxide in vitro. *Biochem. Pharmacol.,* **46,** 1139 – 1144.

PATEL, V.C., YELLON, D.M., SINGH, K.J., NEILD, G.H. & WOOLFSON, R.G. (1993). Inhibition of nitric oxide limits infarct size in the in situ rabbit heart. *Biochem. Biophys. Res. Comm.,* **194,** 234–238.

PELL, T.J., YELLON, D.M., GOODWIN, R.W. & BAXTER, G.F. (1997). Myocardial ischaemic tolerance following heat stress is abolished by ATP-sensitive potassium channel blockade. *Cardiovasc. Drugs Ther.,* **11,** 679–686.

QIU, Y., RIZVI, A., TANG, X.L., MANCHIKALAPUDI, S., TAKANO, H., JADOON, A.K., WU, W.-J. & BOLLI, R. (1997). Nitric oxide triggers late preconditioning against myocardial infarction in conscious rabbits. *Am. J. Physiol.,* **273,** H2931–H2936.

RADOMSKI, M.W., PALMER, R.M.J. & MONCADA, S. (1990). Glucocorticoids inhibit the expression of an inducible, but not constitutive nitric oxide synthase in vascular endothelial cells. *Proc. Natl. Acad. Sci. U.S.A.,* **87,** 10043–10047.

REES, D.D., CELLEK, S., PALMER, R.M.J. & MONCADA, S. (1990). Dexamethasone prevents the induction by endotoxin of a nitric oxide synthase and the associated effects of vascular tone: an insight into endotoxin shock. *Biochem. Biophys. Res. Comm.,* **173,** 541–547.

SATRIANO, J. & ACHLONDORFF, D. (1994). Activation and attenuation of transcription factor NFκB in mouse glomerular mesangial cells in response to tumour necrosis factor-α, immunogloblin G, and adenosine 3′:5′-cyclic monophosphate. Evidence for involvement of reactive oxygen species. *J. Clin. Invest.,* **94,** 1629–1636.

TAKANO, H., MANCHIKALAPUDI, S., TANG, X.-L., QIU, Y., RIZVI, A., JADOON, A.K., ZHANG, Q. & BOLLI, R. (1998). Nitric oxide synthase is the mediator of late preconditioning against myocardial infarction in conscious rabbits. *Circulation,* **98,** 441–449.

VEGH, A., PAPP, J.G. & PARRATT, J.R. (1994). Prevention by dexamethasone of the marked antiarrhythmic effects of preconditioning induced 20 h after rapid cardiac pacing. *Br. J. Pharmacol.,* **113,** 1081–1082.

WILLIAMS, M.W., TAFT, C.S., RAMNAUTH, S., ZHAO, Z.-Q. & VINTEN-JOHANSEN, J. (1995). Endogenous nitric oxide (NO) protects against ischaemia-reperfusion injury in the rabbit. *Cardiovasc. Res.,* **30,** 79–86.

WU, S., FURMAN, B.L. & PARRATT, J.R. (1996). Delayed protection against ischaemia-induced ventricular arrhythmias and infarct size limitation by the prior administration of *Escherichia Coli* endotoxin. *Br. J. Pharmacol.,* **118,** 2157–2163.

XIE, Q.W., KASHIWABARA, Y. & NATHAN, C. (1994). Role of transcription factor NFκB/Rel in induction of nitric oxide synthase. *J. Biol. Chem.,* **269,** 4705–4708.

YAMASHITA, N., NOSHIDA, S., TANIGUCHI, N., KUZUYA, T. & HORI, M. (1998). A 'second window of protection' occurs 24 hours after ischemic preconditioning in rat heart. *J. Mol. Cell. Cardiol.,* **30,** 1181–1189.

YAMASHITA, N., NISHIDA, S., HOSHIDA, S., KUZUYA, T., HORI, M., TANIGUCHI, N., KAMADA, T. & TADA, M. (1994). Induction of manganese superoxide dismutase in rat cardiac myocytes increases tolerance to hypoxia 24 hours after preconditioning. *J. Clin. Invest.,* **94,** 2193–2199.

YELLON, D.M. & BAXTER, G.F. (1995). A ''second window of protection'' or delayed preconditioning phenomenon: future horizons for myocardial protection? *J. Mol. Cell. Cardiol.,* **27,** 1023–1034.

YELLON, D.M., BAXTER, G.F., GARCIA-DORADO, D., HEUSCH, G. & SUMERAY, M.S. (1998). Ischaemic preconditioning: present position and future directions. *Cardiovasc. Res.,* **37,** 21–33.

ZHAO, L., WEBER, P.A., SMITH, J.R., COMERFORD, M.L. & ELLIOTT, G.T. (1997). Role of inducible nitric oxide synthase in pharmacological ''preconditioning'' with monophosphoryl lipid A. *J. Mol. Cell. Cardiol.,* **29,** 1567–1576.

ZHOU, X., ZHAI, X. & ASHRAF, M. (1996). Direct evidence that initial oxidative stress triggered by preconditioning contributes to second window of protection by endogenous antioxidant enzyme in myocytes. *Circulation,* **93,** 1177–1184.

(Received September 28, 1998
Revised November 3, 1998
Accepted November 17, 1998)

British Journal of Pharmacology (1999) 126, 709–716
http://www.stockton-press.co.uk/bjp

Endothelium-derived relaxing, contracting and hyperpolarizing factors of mesenteric arteries of hypertensive and normotensive rats

*,[1]S. Sunano, [1]H. Watanabe, [1]S. Tanaka, [1]F. Sekiguchi, & [2]K. Shimamura

[1]Faculty of Pharmaceutical Sciences, Kinki University, 3-4-1 Kowakae, Higashi-osaka, 577 Osaka Japan; [2]Research Institute of Hypertension, Kinki University, 377-2 Ohno-higashi, Osaka-Sayama, 589 Osaka, Japan

1 Differences in the acetylcholine (ACh)-induced endothelium-dependent relaxation and hyperpolarization of the mesenteric arteries of Wistar Kyoto rats (WKY) and stroke-prone spontaneously hypertensive rats (SHRSP) were studied.

2 Relaxation was impaired in preparations from SHRSP and tendency to reverse the relaxation was observed at high concentrations of ACh in these preparations.

3 Relaxation was partly blocked by N^G-nitro-L-arginine (L-NOARG, 100 μM) and, in the presence of L-NOARG, tendency to reverse the relaxation was observed in response to higher concentrations of ACh, even in preparations from WKY. The relaxation remaining in the presence of L-NOARG was also smaller in preparations from SHRSP.

4 The tendency to reverse the relaxation observed at higher concentrations of ACh in preparations from SHRSP or WKY in the presence of L-NOARG were abolished by indomethacin (10 μM).

5 Elevating the K^+ concentration of the incubation medium decreased relaxation in the presence of both indomethacin and L-NOARG.

6 Relaxation in the presence of L-NOARG and indomethacin was reduced by the application of both apamin (5 μM) and charybdotoxin (0.1 μM). This suggests that the relaxation induced by ACh is brought about by both endothelium-derived relaxing factor (EDRF, nitric oxide (NO)) and hyperpolarizing factor (EDHF), which activates Ca^{2+}-sensitive K^+ channels.

7 Electrophysiological measurement revealed that ACh induced endothelium-dependent hyperpolarization of the smooth muscle of both preparations in the presence of L-NOARG and indomethacin; the hyperpolarization being smaller in the preparation from SHRSP than that from WKY.

8 These results suggest that the release of both NO and EDHF is reduced in preparations from SHRSP. In addition, indomethacin-sensitive endothelium-derived contracting factor (EDCF) is released from both preparations; the release being increased in preparations from SHRSP.

Keywords: Mesenteric artery; stroke-prone spontaneously hypertensive rats; nitric oxide; contracting factor; hyperpolarizing factor

Introduction

Vascular contraction is controlled by endothelium-derived factors such as relaxing (EDRF), contracting (EDCF), and hyperpolarizing factors (EDHF) (Pearson & Vanhoutte, 1993). Changes in these factors can be causes of changes in blood pressure. For example, it has been reported that endothelium-dependent relaxation is impaired in the blood vessels of hypertensive rats (Winquist, 1988; Lüscher & Vanhoutte, 1986). Reduced amounts of EDRF, EDHF, or increased amounts of EDCF can impair the relaxation.

In the mesenteric artery, which is thought to be a resistance artery, impaired relaxation has also been observed in the preparation from hypertensive rats (Watt & Thurston, 1989; Jameson *et al*., 1993; Li & Bukoski, 1993; Li *et al*., 1994; Takase *et al*., 1994; Diedrich *et al*., 1990). This is thought to be brought about by the increased release of EDCF, which is a product of arachidonic acid cascade synthesized *via* the cyclo-oxygenase pathway, since relaxation can be restored by agents such as indomethacin (Watt & Thurston, 1989; Jameson *et al*., 1993; Li & Bukoski, 1993; Li *et al*., 1994) or meclofenamate (Takase *et al*., 1994; Diedrich *et al*., 1990), which are known to block that pathway (Mizuno *et al*., 1982).

*Author for correspondence;
E-mail; sunano@phar.kindai.ac.jp

Decreased release of EDRF can also be a cause of impaired relaxation as described above, and as suggested in the aorta of stroke-prone spontaneously hypertensive rats (SHRSP) (Sunano *et al*., 1992). The EDRF in the aorta is known to be nitric oxide (NO), and synthesis of NO can be blocked by agents such as N^G-nitro-L-arginine (L-NOARG) (Moore *et al*., 1990) and N^G-methyl-L-arginine (L-NMMA) (Palmer *et al*., 1988). In the mesenteric artery, however, acetylcholine can still induce relaxation in the presence of these agents, indicating the involvement of a factor(s) other than NO. One of the factors that can induce the relaxation of the mesenteric artery is EDHF (Nagao *et al*., 1992; Parsons *et al*., 1994; Hwa *et al*., 1994; Waldron & Garland, 1994).

In the present experiments, differences in the effects of L-NOARG and indomethacin on endothelium-dependent relaxation between mesenteric arteries from Wistar Kyoto rats (WKY) and SHRSP were studied. In addition, the involvement of EDHF in relaxation and its changes in the preparation from SHRSP were also studied. SHRSP were used, as endothelium-dependent relaxation is more prominently impaired than in conventional spontaneously hypertensive rats (SHR) (Sunano *et al*., 1989), and WKY were used as the control normotensive rats, since SHRSP were originally established from WKY (Okamoto *et al*., 1974).

Methods

Sixteen-week-old SHRSP and age matched WKY were used in these experiments. They were obtained from Dr Okamoto (Okamoto *et al*., 1974) and bred successively in our animal facility. They were fed a normal chow (Funabashi SP) and tap water was given freely. Room temperature was kept at 22°C, with 60% humidity, and a 12 h light-and-dark cycle.

The blood pressure of the rats was measured by means of the tail cuff method. Prior to measurement, the rats were warmed in a cage kept at 40°C for 10 min. This procedure was required to obtain constant and stable blood pressure values.

The rats were killed by bleeding from vena cava after anaesthetizing with CO_2. The mesenterium including the superior mesenteric artery and its branches were excised and immediately immersed in a modified Tyrode's solution. The composition of the modified Tyrode's solution was as follows (mM): NaCl, 137; KCl, 5.4; $CaCl_2$, 2.0; $MgCl_2$, 1.0; $NaHCO_3$, 11.9; NaH_2PO_4, 0.4; glucose, 5.6; which was equilibrated with a gas mixture of 95% O_2 and 5% CO_2 at 37°C. The pH of the solution under these conditions was 7.3. K^+-Tyrode's solution was made by replacing all NaCl in the modified Tyrode's solution with KCl, and the high-K^+ Tyrode's solution containing the desired concentration of K^+ was made by mixing the Tyrode's and K^+-Tyrode's solutions.

Ring preparations of 1.5 mm in width were made from the second branches of the superior mesenteric artery, and they were kept in the modified Tyrode's solution. In six preparations respectively from WKY and SHRSP, the endothelium was damaged by perfusing the vessels with the modified Tyrode's solution containing 0.3% 3-[(3-Cholamidopropyl) dimethylammonio]-1-propane-sulphonate (CHAPS) for 2.5 min. The rings were mounted in an organ bath (MOB-1, Technical Supply, Osaka) under a stretch tension of 1 mN, and tension changes were measured isometrically with a force-displacement transducer (Shinkoh, Nagano, Japan). The temperature of the apparatus was kept at 37°C by circulating water of the same temperature.

The preparations were equilibrated in the modified Tyrode's solution for at least 60 min, and then they were subjected twice to high K^+-induced contractions by changing the solution from the modified to the high-K^+ solution containing 80 mM K^+ for 5 min with an interval of 15 min in between. Endothelium-dependent relaxation was induced by applying acetylcholine (ACh) cumulatively to preparations pre-contracted with 5 μM noradrenaline (NA). We ascertained that this concentration of NA induced submaximal contraction of the preparations and that maximum contraction was achieved at a concentration of 10 μM. Synthesis of NO and the products of the cyclo-oxygenase pathway of the arachidonic acid cascade were blocked with L-NOARG (100 μM) and indomethacin (10 μM), respectively. The involvement of EDHF in relaxation was investigated by increasing the K^+ concentration in the modified Tyrode's solution or by applying tetraethylammonium (TEA), glibenclamide, apamin or charybdotoxin. At the end of the experiments, the preparations were completely relaxed by applying verapamil (10 μM) and papaverine (100 μM), and all tensions were measured in respect to this relaxed level.

Changes in membrane potential were measured by means of microelectrode technique. In this method, glass microelectrodes which had tip resistance of 40–80 MΩ when filled with 3 M KCl were used. Mesenteric artery was mounted on organ bath of 1 ml volume with insect pins. The preparation was continuously superfused with Tyrode's solution at flow rate of 4 ml min^{-1}. Microelectrode was inserted into smooth muscle from outer surface of the preparation.

The drugs used in this experiment were: 3-[(3-Cholamidopropyl) dimethylammonio]-1-propane-sulphate (CHAPS, Sigma, St Louis, MO, U.S.A.), noradrenaline bitartrate (NA, Sigma, St Louis, MO, U.S.A.), sodium nitroprusside (SNP, Sigma, St Louis, MO, U.S.A.), acetylcholine hydrochloride (ACh, Wako, Osaka, Japan), N^G-nitro-L-arginine (Sigma, St Louis MO, U.S.A.), indomethacin (Sigma, St Louis MO, U.S.A.), SQ 29,548 (Cayman Chemical, MI, U.S.A.), tetraethylammonium (TEA, Wako, Osaka, Japan), glibenclamide (Sigma, St Louis, MO, U.S.A.), apamin (Sigma, St Louis, MO, U.S.A.), charybdotoxin (Peptid Inst., Osaka, Japan), verapamil (Wako, Osaka, Japan) and papaverine (Wako, Osaka, Japan).

The values obtained were expressed as the means ± s.e.mean. These values were analysed by the Student's *t*-test and Newman-Keul's multiple comparison test, where *P* values of less than 0.05 were considered to be significant.

Results

Body weight and systolic blood pressure of the rats

Body weights of SHRSP and WKY at 16 weeks of age were 309 ± 4.9 g ($n = 30$) and 395 ± 4.6 g ($n = 30$), respectively, the former being significantly smaller ($P < 0.01$). The systolic blood pressures of SHRSP and WKY were 245 ± 3.5 mmHg ($n = 30$) and 135 ± 1.1 mmHg ($n = 30$), respectively. The systolic blood pressure of the former was significantly higher than those of the latter ($P < 0.01$).

Relaxation of mesenteric arteries induced by sodium nitroprussid (SNP)

SNP induced relaxation of NA (5 μM)-precontracted endothelium-removed preparations both from WKY and SHRSP. The concentration-response curve for the relaxation was almost identical in both preparations; the maximal relaxation observed at 1 mM SNP was 97 ± 1.5 and 98 ± 1.2% of precontraction in preparations from WKY and SHRSP, respectively (data was not shown).

Relaxation induced by ACh

The amplitudes of the precontraction induced by 5 μM NA in the preparations from WKY and SHRSP were 87.2 ± 6.6% ($n = 10$) and 90.6 ± 4.8% ($n = 10$) of 80 mM K^+-induced contraction, respectively; the difference between these values were not significant. The application of ACh to preparations precontracted with 5 μM NA, caused a concentration-dependent relaxing response (Figure 1). In preparations from WKY, the concentration-dependent relaxing response was observed in response to ACh concentrations of up to 1 mM. The maximal relaxation (91.8 ± 1.0% of the pre-contracted value ($n = 12$)) was observed at a concentration of 0.1 μM, and then gradually increased up to 98.3 ± 0.6% ($n = 12$) at 1 mM. In preparations from SHRSP, only low to moderate concentrations of ACh induced relaxation, and tendency to reverse the relaxation appeared as the concentrations of the drug were increased further. Thus, maximal relaxation (65.8 ± 7.7% of the pre-contracted value ($n = 8$)) was observed at an ACh concentration of 0.1 μM. The relaxation by ACh of concentrations higher than 3 nM were significantly smaller in the preparation from SHRSP than that from WKY ($P < 0.05$).

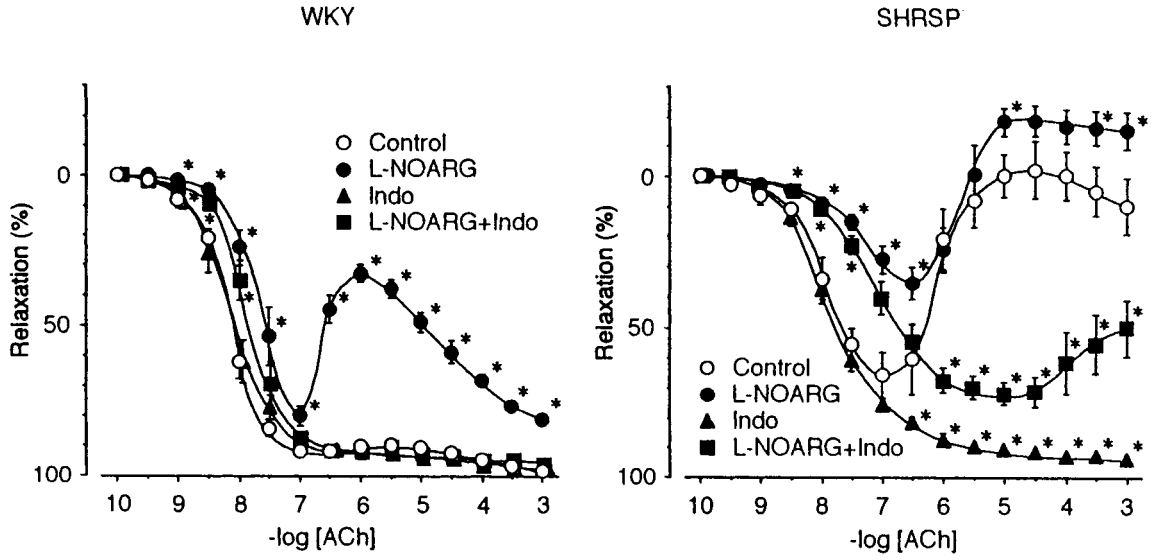

Figure 1 The concentration-response curves for acetylcholine (ACh)-induced relaxation and effects of L-NOARG and indomethacin in mesenteric arteries from WKY and SHRSP. WKY and SHRSP indicate the preparations from WKY and SHRSP, respectively. The preparations were pre-contracted in the presence of 5 μM of noradrenaline (NA), and then ACh was added cumulatively. The relaxation induced by ACh was expressed as a percentage of the NA-induced pre-contraction. Data are means$\pm$s.e.mean from 8–12 preparations. Control, L-NOARG, Indo and L-NOARG+Indo indicate the ACh concentration-response curves in the absence of, in the presence of L-NOARG (100 μM), indomethacin (10 μM) and both, respectively. Asterisks indicate significant differences from respective Control values ($*P<0.05$).

In CHAPS-treated preparations from both WKY and SHRSP, relaxation induced by ACh was markedly reduced, and only 20.2$\pm$5.4% ($n=6$) relaxation was observed even in preparations from WKY.

Effects of L-NOARG and methylene blue on the action of ACh

L-NOARG (100 μM) showed prominent effect on the relaxation of preparations from WKY, especially by ACh at concentrations higher than 0.1 μM (Figure 1, WKY). Relaxation was attenuated, and the preparations tended to contract at higher concentrations of ACh, similarly to that observed in preparations from SHRSP in the absence of L-NOARG. Relaxation at lower concentrations of ACh remained, although its amplitude was reduced. In preparations from SHRSP, L-NOARG attenuated ACh-induced relaxation and the tendency to contract in response to higher concentrations of ACh was augmented (Figure 1, SHRSP). However, the relaxation induced by lower concentrations of ACh still remained, although its magnitude was reduced.

Methylene blue (10 μM) had similar effects to L-NOARG in preparations from both WKY and SHRSP (data was not shown).

Effects of indomethacin and SQ 29,548 on the action of ACh

The ACh-induced relaxation of mesenteric arteries was augmented by indomethacin at a concentration of 10 μM. Augmentation was prominent in preparations from SHRSP, and the tendency to reverse the relaxation at higher concentrations of ACh disappeared (Figure 1, SHRSP). Augmentation of the relaxation induced by indomethacin was not observed in preparations from WKY (Figure 1, WKY). Thus, differences in the responses of preparations from WKY and SHRSP were minimized in the presence of indomethacin.

The effects of indomethacin on preparations from SHRSP were similar to the effects of the drug on preparations from WKY in the presence of L-NOARG (Figure 1). Reduced relaxation of the preparation from WKY in the presence of L-NOARG was recovered, and the tendency to reverse the relaxation observed at higher concentrations of ACh was abolished by the addition of indomethacin (10 μM). In preparations from SHRSP, reduced relaxation in the presence of L-NOARG was also restored, and the tendency to contract was abolished by the addition of indomethacin (Figure 1, SHRSP). Thus, only the relaxation was observed in response to ACh in the presence of both L-NOARG and indomethacin. When the relaxation induced by ACh 1 mM in the presence of L-NOARG and indomethacin were compared between preparations from WKY and SHRSP, they were significantly smaller in preparations from the latter (96.2$\pm$1.1% ($n=12$) vs 50.0$\pm$9.3% ($n=12$), $P<0.01$).

Similarly, SQ 29,548 (100 μM) augmented the relaxation induced by ACh and minimized the tendency to reverse the relaxation in preparations from SHRSP, and attenuated them in both preparations in the presence of L-NOARG, although the effect was less prominent than that of indomethacin (Figure 2).

Influence of increasing K^+ concentration and TEA

This experiment was performed in the presence of L-NOARG and indomethacin. As shown in Figure 3, relaxation induced by ACh was attenuated by increasing K^+ concentration in the incubation medium in both preparations. Similar but weaker effects were observed with 10 mM TEA. In preparations from SHRSP, the effect of this concentration of TEA was similar to that of increasing K^+ concentration to 10 mM. In the preparation from WKY, the amplitude of the maximum relaxation was not altered, although the concentration of ACh required for relaxation increased (data was not shown). Experiments with higher concentrations of TEA could not be performed because of the contractile effects of the drug.

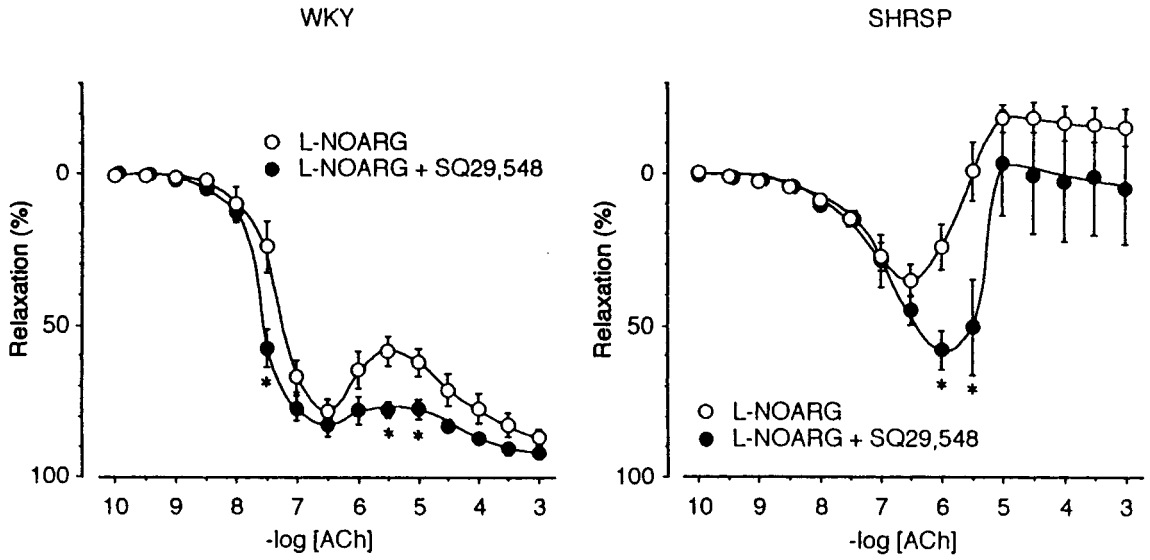

Figure 2 Effect of SQ 29,548 on the relaxation induced by acetylcholine (ACh) in the presence of L-NOARG. ACh was applied in the presence of 100 μM L-NOARG (○) or 100 μM L-NOARG and 100 μM SQ 29,548 (●). Data are means$\pm$s.e.mean from 12 preparations. The others are the same as those in Figure 1. Note that SQ 29,548 augmented the relaxation and minimized the tendency to reverse the relaxation observed at high concentrations of ACh.

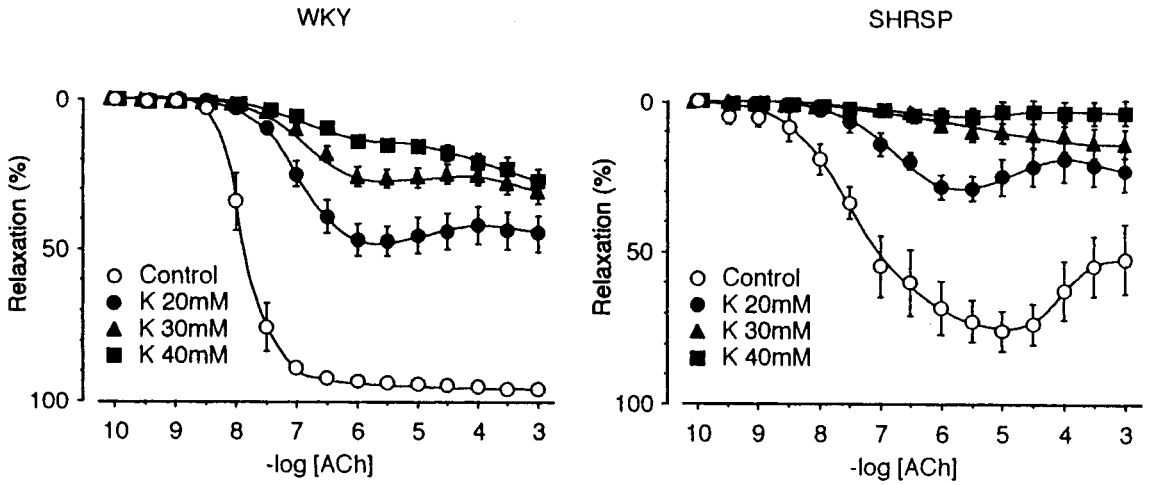

Figure 3 The effect of increasing the K^+ concentration on the response to acetylcholine (ACh). These experiments were performed in the presence of 100 μM L-NOARG and 10 μM indomethacin so that the involvement of nitric oxide and the cyclo-oxygenase pathway of the arachidonic acid cascade could be excluded. The K^+ concentration in the modified Tyrode's solution was increased to 20 mM (●), 30 mM (▲) and to 40 mM (■). The noradrenaline concentration was 5 μM in the control, 3 μM in the K^+ 20 mM, 2 μM in the K^+ 30 mM, and 1 μM in the K^+ 40 mM Tyrode's solution was used to adjust the contraction amplitude. Data are means$\pm$s.e.mean from 12 preparations. Relaxations of ACh of the concentrations higher than 10 nM were significantly smaller in the presence of elevated K^+ than control (5.4 mM K^+). The others are the same as those in Figure 1.

Effects of glibenclamide, apamin and charybdotoxin

Glibenclamide (10 μM) did not significantly affect relaxation induced by ACh in the presence of L-NOARG and indomethacin (data was not shown).

Apamin, up to 5 μM, had no effect on ACh-induced relaxation in the presence of L-NOARG and indomethacin in preparations from WKY (Figure 4, WKY), while it attenuated relaxation and enhanced the tendency to reverse the relaxation at high concentrations of ACh in preparations from SHRSP (Figure 4, SHRSP). Charybdotoxin (ChTX 0.1 μM) shifted ACh concentration-response curve in the presence of L-NOARG and indomethacin to the right but did not alter the maximum relaxation in the preparation from WKY (Figure 4, WKY). The effect of ChTX on the preparation from SHRSP was basically similar to that of apamin and it was stronger than that of apamin (Figure 4, SHRSP). The simultaneous application of apamin and ChTX at the concentrations described above, however, attenuated relaxation markedly in preparations from WKY, and almost blocked relaxation in preparations from SHRSP (Figure 4).

ACh-induced hyperpolarization of smooth muscle

The resting membrane potentials of the smooth muscle of the mesenteric arteries of WKY and SHRSP were -63 ± 1.3 mV ($n=72$) and -59 ± 0.8 mV ($n=84$), respectively. The membrane potential of the latter was significantly smaller

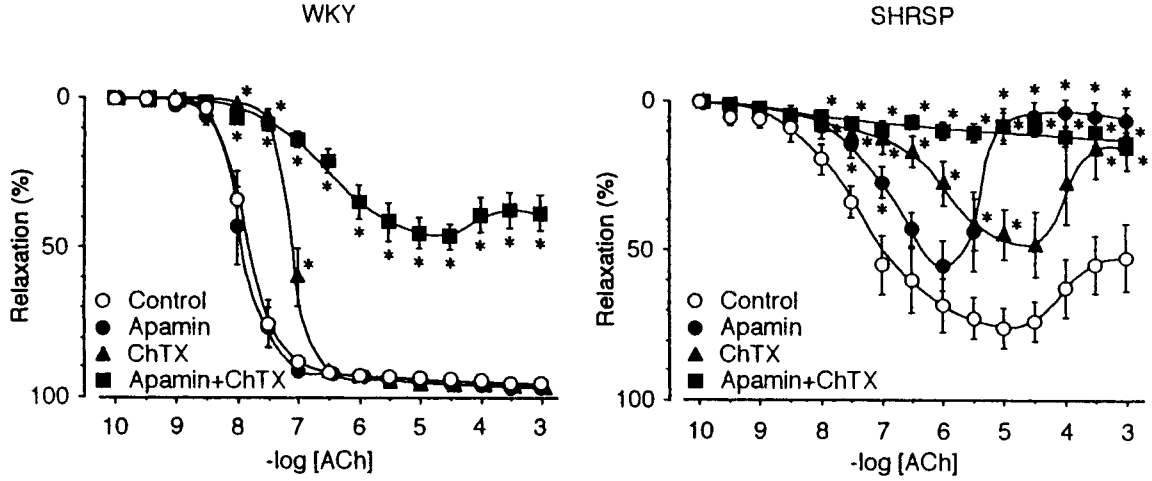

Figure 4 Concentration-response curves for acetylcholine (ACh) in the presence of L-NOARG and indomethacin, and the effects of apamin and charybdotoxin. Control indicates the relaxation curve in the presence of L-NOARG (100 μM) and indomethacin (10 μM). Apamin, ChTX and Apamin + ChTX indicate curves in the presence of apamin (5 μM), charybdotoxin (0.1 μM) and both, respectively in addition to L-NOARG and indomethacin. Data are means $\pm$ s.e.mean of 12 preparations. Asterisks indicate significant difference between control value and values in the presence of respective drug or drugs ($*P<0.05$). The others are the same as in Figure 1.

($P<0.01$). ACh 1 μM hyperpolarized the membrane by 13.9 ± 1.5 mV ($n=11$) and 8.0 ± 1.1 mV ($n=9$) in the arteries of WKY and SHRSP, respectively. The amplitude of hyperpolarization was smaller in preparations from SHRSP ($P<0.01$).

Changes of membrane potential were observed also in the presence of NA (5 μM), L-NOARG (100 μM) and indomethacin (10 μM); the condition was the same that the relaxation by hyperpolarization was studied. Under this condition, the membrane potential was -61 ± 1.0 mV ($n=23$) and -42 ± 0.6 mV ($n=43$), respectively in preparations from WKY and SHRSP. The difference in the membrane potential was also significant ($P<0.01$). Application of 1 μM ACh under the same condition caused hyperpolarization of the smooth muscle membrane in both preparations (Figure 5). The hyperpolarization induced by the application of ACh (1 μM) to preparations from WKY and SHRSP was 18 ± 2.1 mV ($n=6$) and 12 ± 1.3 mV ($n=11$), respectively; the difference between these values being significant ($P<0.01$). It has been ascertained in concentration-response experiment that ACh of 1 μM induced maximal hyperpolarization in smooth muscle of the mesenteric artery both from WKY and SHRSP.

Discussion

In the mesenteric arteries of SHR, ACh-induced relaxation is known to be impaired (Watt & Thurston, 1989; Jameson *et al*., 1993; Li & Bukoski, 1993; Takase *et al*., 1994; Fujii *et al*., 1992) as in other blood vessels (see Lüscher & Vanhoutte, 1986; Winquist, 1988). A similar result has been reported in the mesenteric artery of SHRSP (Diedrich *et al*., 1990), as we confirmed in this study. The impaired relaxation is associated with a contractile response, especially at high concentrations of ACh (Diedrich *et al*., 1990). It has been shown that impaired relaxation of mesenteric artery of SHR and SHRSP is improved by treatment with indomethacin or meclofenamate, which are known to block the cyclo-oxygenase pathway of the arachidonic acid cascade (Watt & Thurston, 1989; Jameson *et al*., 1993; Li & Bukoski, 1993; Takase *et al*., 1994; Diedrich *et al*., 1990; Fujii *et al*., 1992). We confirmed this in this study. Thus, impaired endothelium-dependent relaxation in the mesenteric artery can be explained by the co-release of EDCF which is thought to be a product of the arachidonic acid cascade *via* the cyclo-oxygenase pathway (Mizuno *et al*., 1982). This EDCF would be thromboxane A_2 and/or prostaglandin H_2 as in other blood vessels of SHRSP (Auch-Schwelk *et al*., 1990; Ito *et al*., 1991; Mayhan, 1992), since SQ29,548, a blocker of thromboxane A_2 and prostaglandin H_2 receptors, augmented the maximal relaxation.

However, reduced NO production has also been reported in cultured aortic endothelial cells of SHRSP (Malinski *et al*., 1993; Grunfeld *et al*., 1995). Grunfeld *et al*. (1995) explained that the reduction is brought about by scavenging NO by excessively produced superoxide anion. In the present experiment with mesenteric artery, it was indicated that the release of NO was also reduced in the preparation from SHRSP, since the effect of L-NOARG was smaller in this preparation when compared with that in the preparation from WKY. The inhibition of endothelium-dependent relaxation *via* the inhibition of NO synthesis agrees with result from previous reports (Li *et al*., 1994; Fujii *et al*., 1992), but differs from the findings of Li & Bukoski (1993) who showed that L-NOARG had no effect on the endothelium-dependent relaxation induced by ACh in the mesenteric artery of WKY, although they observed also that ACh-induced relaxation was attenuated in the mesenteric artery of SHR. The cause of this discrepancy is uncertain, but our results indicate that a reduction in NO synthesis, even in preparations from WKY, impairs of endothelium-dependent relaxation in a fashion similar to that in preparations from SHRSP. The tendency to reverse the relaxation appeared in the preparation from WKY in the presence of L-NOARG, may indicate some interaction between NO and EDCF as has been suggested by Auch-Schwelk *et al*. (1992). The effect of methylene blue, which showed a similar effect as L-NOARG on the ACh-induced relaxation, may be explained mainly by the inhibition of cyclic GMP production in the smooth muscle, although inhibition of NO synthesis (Mayer *et al*., 1993) or production of oxygen-derived free radicals which inactivates NO (Wolin *et al*., 1990) may also be involved.

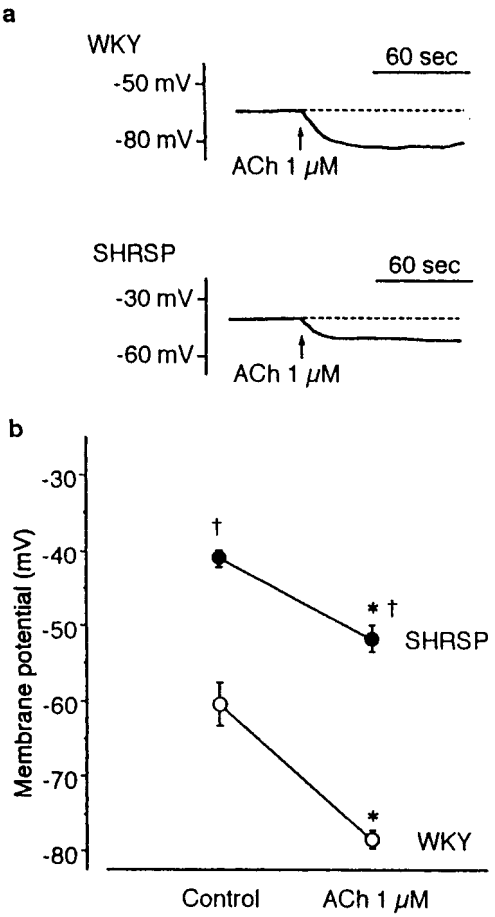

Figure 5 Effect of acetylcholine (ACh) on the membrane potential of the smooth muscle of the rat mesenteric artery. Changes in the membrane potential were measured in the presence of noradrenaline (5 μM), L-NOARG (100 μM) and indomethacin (10 μM). (a) A typical membrane potential recording induced by 1 μM ACh in preparations from WKY and SHRSP. (b) The mean membrane potentials in the preparations from WKY and SHRSP in the absence and presence of ACh. The number of preparations was 23 and 43, respectively for WKY and SHRSP in the absence of ACh (Control), and 6 and 11, respectively for WKY and SHRSP in the presence of ACh (ACh 1 μM). Asterisks indicate significant difference from respective control value ($P<0.01$) and daggers indicate significant difference from the value of WKY ($P<0.01$). Note the smaller hyperpolarization induced by ACh in the preparations from SHRSP.

We also showed that the relaxation induced by ACh was inhibited only partially by L-NOARG. The inability of L-NOARG to block the endothelium-dependent relaxation induced by ACh has also been reported in the mesenteric artery of the rat (Nagao *et al*., 1992; Parsons *et al*., 1994). This indicates that a factor other than NO is also involved in the relaxation (Li *et al*., 1994). One factor which may be involved in the relaxation, especially in the presence of L-NOARG, is EDHF (Fujii *et al*., 1992; McPherson & Angus, 1991; Chen & Suzuki, 1989; Chen *et al*., 1988; Garland & McPherson, 1992; Fujii *et al*., 1993; Waldron & Garland, 1994). We showed in the present experiment that ACh induced hyperpolarization of the smooth muscle membranes of the mesenteric arteries of both WKY and SHRSP in the presence of noradrenaline, L-NOARG and indomethacin. It has been known that NO does not cause hyperpolarization of the membranes of the mesenteric artery in the presence of noradrenaline (Garland & McPherson, 1992). Moreover, the hyperpolarization induced by ACh has been reported not to be blocked by methylene blue or L-NOARG (Fujii *et al*., 1992; Garland & McPherson, 1992), indicating the involvement of an EDHF other than NO in ACh-induced hyperpolarization. Thus, we concluded that an EDHF other than NO is involved in the ACh-induced relaxation of the mesenteric arteries of WKY and SHRSP.

In our experiments, the relaxation induced by ACh in the presence of L-NOARG and indomethacin was markedly attenuated by TEA or by increasing the K^+ concentration in the incubation medium. These results are similar to those from preparations from SHR (Li *et al*., 1994; Fujii *et al*., 1993), and suggest that the relaxation remaining in the presence of L-NOARG is caused by hyperpolarization of the smooth muscle membrane due to an increased K^+ conductance. However, the possible blockage of EDHF release caused by inhibiting the hyperpolarization of the endothelial cell membrane can not be ruled out (Demirel *et al*., 1994).

Li *et al*., (1994) reported that EDHF is involved in the ACh-induced relaxation of the resistance arteries of WKY but not SHR. A similar conclusion was made by Adeagbo & Triggle (1993) in the perfused mesenteric artery. In this study we showed that relaxation induced by K^+ channel activation due to the release of EDHF is impaired in the mesenteric artery of SHRSP. Similar results have recently been reported in endothelium-dependent relaxation in SHR (Kahonen *et al*., 1995). This may be caused by the impaired release of EDHF, as has been proposed in the mesenteric artery of SHR (Fujii *et al*., 1992). Mechanism of the marked difference in membrane potential in mesenteric artery of SHRSP in the presence of NA under condition treated with L-NOARG and indomethacin would be explained by the smaller resting membrane potential (Fujii *et al*., 1992) and higher sensitivity to NA (Kuriyama & Suzuki, 1978). The hyperpolarization by ACh was much still smaller in preparations from SHRSP than in those from WKY, regardless the membrane potential much far from K^+ equivalent potential. In addition, it has been reported that the hyperpolarization by K^+ channel opener was not different in the mesenteric arteries from WKY and SHR (Fujii *et al*., 1992), indicating that K^+ channel itself was not different between these preparations. Thus, the reduction of the release of EDHF in the mesenteric artery of SHRSP was also supported by membrane potential recording.

The hyperpolarization of smooth muscle membranes that causes relaxation may be brought about by activating both ATP-activated (K^+_{ATP}) and/or Ca-activated K^+ channels (K^+_{Ca}). Hyperpolarization due to the former has been shown in a number of blood vessels (Standen *et al*., 1989). In contrast, it was shown in the present experiment with rat mesenteric arteries that relaxation was blocked in the presence of apamin and ChTX, both of which are known to block K^+_{Ca}, but not by glibenclamide, which blocks K^+_{ATP}. It has recently been shown that ACh-induced hyperpolarization of small arterial smooth muscle results from activation of both ChTX-sensitive and apamin-sensitive K^+ channels (Hashitani & Suzuki, 1997). Thus, it can be concluded that the relaxation in the presence of both L-NOARG and indomethacin in WKY and SHRSP mesenteric arteries is brought about by hyperpolarization due to activation of both the small and intermediate K^+_{Ca} conductance in these preparations, although possibility of the involvement of voltage-dependent K^+ channel (Zygmunt *et al*., 1997) remained to be investigated. The proportion of the involvement of these channels may differ between smooth muscles from WKY and SHRSP, since the effect of apamin and ChTX affected the relaxation differently.

In conclusion, endothelium-dependent relaxation in the mesenteric artery of SHRSP was impaired when compared with that of WKY. All of decreased release of NO and EDHF,

and the increased release of indomethacin-sensitive EDCF are involved in impairing relaxation. Present data suggests that the reduced release of NO can potentiate the release or the actions of EDCF, which impairs relaxation. It was also suggested that EDHF exerts is action through the activation of Ca^{2+}-sensitive K^+ channel.

References

ADEAGBO, A.S.O. & TRIGGLE, C.R. (1993). Varying extracellular [K^+]: A functional approach to separating EDHF and EDNO-related mechanisms in perfused rat mesenteric arterial bed. *J. Cardiovasc. Pharmacol.,* **21,** 423–429.

AUCH-SCHWELK, W., KATUSIC, Z.S. & VANHOUTTE, P.M. (1990). Thromboxane A_2 receptor antagonists inhibit endothelium-dependent contraction. *Hypertension,* **15,** 699–703.

AUCH-SCHWELK, W., KATUSIC, Z.S. & VANHOUTTE, P.M. (1992). Nitric oxide inactivates endothelium derived contracting factor in the rat aorta. *Hypertension,* **19,** 442–445.

CHEN, G. & SUZUKI, H. (1989). Some electrical properties of the endothelium-dependent hyperpolarization recorded from rat arterial smooth muscle. *J. Physiol.,* **410,** 91–106.

CHEN, G., SUZUKI, H. & WESTON, A.H. (1988). Acetylcholine releases endothelium-derived hyperpolarizing factor and EDRF from rat blood vessels. *Br. J. Pharmacol.,* **95,** 1165–1174.

DEMIREL, E., RUSKO, J., LASKEY, R.E., ADAMS, D.J. & VAN BREEMEN, C. (1994). TEA inhibits ACh-induced EDRF release: Endothelial Ca^{2+}-dependent K^+ channels contribute to vascular tone. *Am. J. Physiol.,* **267,** H1135–H1141.

DIEDRICH, D., YANG, Z., BUHLER, F.R. & LUSCHER, T.F. (1990). Impaired endothelium-dependent relaxations in hypertensive resistance arteries involve cyclooxygenase pathway. *Am. J. Physiol.,* **258,** H445–H451.

FUJII, K., OHMORI, S., TOMINAGA, M., ABE, I., TAKATA, Y., OHYA, Y., KOBAYASHI, K. & FUJISHIMA, M. (1993). Age-related changes in endothelium-dependent hyperpolarization in the rat mesenteric artery. *Am. J. Physiol.,* **265,** H509–H516.

FUJII, K., TOMINAGA, M., OHMORI, S., KOBAYASHI, K., KOGA, T., TAKATA, Y. & FUJISHIMA, M. (1992). Decreased endothelium-dependent hyperpolarization to acetylcholine in smooth muscle of the mesenteric artery of spontaneously hypertensive rats. *Circulation Res.,* **70,** 660–669.

GARLAND, C.J. & McPHERSON, G.A. (1992). Evidence that nitric oxide does not mediate the hyperpolarization and relaxation to acetylcholine in the rat mesenteric artery. *Br. J. Pharmacol.,* **105,** 429–435.

GRUNFELD, S., HAMILTON, C.A., MESAROS, S., McCLAIN, S.W., DOMINICZAK, A.F., BOHR, D.F. & MALINSKI, T. (1995). Role of superoxide in the depressed nitric oxide production by the endothelium of genetically hypertensive rats. *Hypertension,* **26,** 854–857.

HASHITANI, H. & SUZUKI, H. (1997). K^+ channels which contribute to the acetylcholine-induced hyperpolarization in smooth muscle of the guinea-pig submucosal arteriole. *J. Physiol.,* **501,** 319–329.

HWA, J., GHIBAUDI, L., WILLIAMS, P. & CHATTERJEE, M. (1994). Comparison of acetylcholine-dependent relaxation in large and small arteries of rat mesenteric vascular bed. *Am. J. Physiol.,* **266,** H952–H958.

ITO, T., KATO, T., IWAMA, Y., MURAMATSU, M., SHIMIZU, K., ASANO, H., OKUMURA, K., HASHIMOTO, H. & SATAKE, T. (1991). Prostaglandin H_2 as an endothelium-derived contracting factor and its interaction with endothelium-derived nitric oxide. *J. Hypertension,* **9,** 729–736.

JAMESON, M., DAI, F.-U., LUSCHER, T., SKOPEC, J., DIEDRICH, A. & DIEDRICH, D. (1993). Endothelium-derived contracting factors in resistance arteries of young spontaneously hypertensive rats before development of overt hypertension. *Hypertension,* **21,** 280–288.

KAHONEN, M., MAKYNEN, H., WU, X., ARVOLA, P. & PORSTI, I. (1995). Endothelial function in spontaneously hypertensive rats: influence of quinapril treatment. *Br. J. Pharmacol.,* **115,** 859–867.

KURIYAMA, H. & SUZUKI, H. (1978). Electrical property and chemical sensitivity of vascular smooth muscles in normatensive and spontaneously hypertensive rats. *J. Physiol.,* **285,** 409–424.

LI, J., BIAN, K. & BUKOSKI, R.D. (1994). A non-cyclo-oxygenase, non-nitric oxide relaxing factor is present in resistance arteries of normotensive but not spontaneously hypertensive rats. *Am. J. Med. Sci.,* **307,** 7–14.

LI, J. & BUKOSKI, R.D. (1993). Endothelium-dependent relaxation of hypertensive resistance arteries is not impaired under all conditions. *Circulation Res.,* **72,** 290–296.

LÜSCHER, T.F. & VANHOUTTE, P.M. (1986). Endothelium-dependent contractions to acetylcholine in the aorta of the spontaneously hypertensive rats. *Hypertension,* **8,** 344–348.

MALINSKI, T., KAPTURCZAK, M., DAYHARSH, J. & BOHR, D. (1993). Nitric oxide synthase activity in genetic hypertension. *Biochem. Biophys. Res. Commun.,* **194,** 654–658.

MAYER, B., BRUNNER, F. & SCHMIDT, K. (1993). Inhibition of nitric oxide synthesis by methylene blue. *Biochem. Pharmacol.,* **45,** 367–374.

MAYHAN, W.G. (1992). Role of prostaglandin H_2-thromboxane A_2 in response of arterioles during chronic hypertension. *Am. J. Physiol.,* **262,** H539–H543.

McPHERSON, G.A. & ANGUS, J.A. (1991). Evidence that acetylcholine-mediated hyper-polarization of the rat mesenteric artery does not involve the K^+ channel opened by cromakalim. *Br. J. Pharmacol.,* **103,** 1184–1190.

MIZUNO, K., YAMAMOTO, S. & LANDS, W.E.M. (1982). Effects of non-steroidal anti-inflammatory drugs on fatty acid cyclooxygenase and prostaglandin hydroperoxidase activities. *Prostaglandins,* **23,** 743–757.

MOORE, P.K., AL-SWAYEH, O.A., CHONG, N.W.S., EVANS, R.A. & GIBSON, A. (1990). L-N^G-nitro arginine (L-NOARG), a novel, L-arginine-reversible inhibitor of endothelium-dependent vasodilatation in vitro. *Br. J. Pharmacol.,* **99,** 408–412.

NAGAO, T., ILLIANO, S. & VANHOUTTE, P.M. (1992). Heterogeneous distribution of endothelium-dependent relaxations resistant to N^G-nitro-L-arginine in rats. *Am. J. Physiol.,* **263,** H1090–H1094.

OKAMOTO, K., YAMORI, Y. & NAGAOKA, A. (1974). Establishment of the stroke-prone spontaneously hypertensive rat (SHR). *Circulation Res.,* **34–35** (Suppl), 143–153.

PALMER, R.M.J., REES, D.D., ASHTON, D.S. & MOMCADA, S. (1988). L-arginine is the physiological precursor for the formation of nitric oxide in endothelium-dependent relaxation. *Biochem. Biophys. Res. Commun.,* **153,** 1251–1256.

PARSONS, S.J.W., HILL, A., WALDRON, G.J., PLANE, F. & GARLAND, C.J. (1994). The relative importance of nitric oxide and nitric oxide-independent mechanisms in acetylcholine-evoked dilatation of the rat mesenteric bed. *Br. J. Physiol.,* **113,** 1275–1280.

PEARSON, P. & VANHOUTTE, P.M. (1993). Vasodilator and vasoconstrictor substances produced by the endothelium. *Rev. Physiol. Biochem. Pharmacol.,* **122,** 1–67.

STANDEN, N.B., QUAYLE, J.M., DAVIS, N.W., BRAYDEN, J.E., HUANG, Y. & NELSON, T.M. (1989). Hyperpolarizing vasodilators activate ATP-sensitive K^+ channels in arterial smooth muscle. *Science,* **245,** 177–180.

SUNANO, S., OSUGI, S., KANEKO, K., YAMAMOTO, K. & SHIMAMURA, K. (1992). Effects of chronic treatment with SQ 29852 on spontaneous smooth muscle tone and endothelium-dependent relaxation in aorta of stroke- prone spontaneously hypertensive rats. *J. Cardiovasc. Pharmacol.,* **19,** 602–609.

SUNANO, S., OSUGI, S. & SHIMAMURA, K. (1989). Blood pressure and impairment of endothelium-dependent relaxation in spontaneously hypertensive rats. *Experientia,* **45,** 705–708.

TAKASE, H., DOHI, Y., KOJIMA, M. & SATO, K. (1994). Changes in the endothelial cyclooxygenase pathway in resistance arteries of spontaneously hypertensive rats. *J. Cardiovasc. Pharmacol.,* **23,** 329–330.

WALDRON, G.J. & GARLAND, C.J. (1994). Contribution of both nitric oxide and change in membrane potential to acetylcholine-induced relaxation in the rat small mesenteric artery. *Br. J. Pharmacol.,* **112,** 831–836.

WATT, P.A.C. & THURSTON, H. (1989). Endothelium-dependent relaxation in resistance vessels from the spontaneously hypertensive rats. *J. Hypertension,* **7,** 661–666.

WINQUIST, R.J. (1988). Endothelium-dependent relaxations in hypertensive blood vessels. In: *Relaxing and contracting factors*. ed. Vanhoutte, P.M. pp. 473–494. Clifton, NJ: Humana Press.

WOLIN, M.S., CHERRY, P.D., RODENBURG, J.M., MESSINA, E.J. & KALEY, G. (1990). Methylene blue inhibits vasodilation of skeletal muscle arterioles to acetylcholine and nitric oxide via the extracellular generation of superoxide anion. *J. Pharmacol. Exp. Ther.*, **254,** 872–876.

ZYGMUNT, P.M., EDWARDS, G., WESTON, A.H., LARSSON, B. & HOGESTATT, E.D. (1997). Involvement of voltage-dependent potassium channels in the EDHF-mediated relaxation of rat hepatic artery. *Br. J. Pharmacol.*, **121,** 141–149.

(Received December 4, 1997
Revised November 6, 1998
Accepted November 11, 1998)

British Journal of Pharmacology (1999) 126, 717–729
http://www.stockton-press.co.uk/bjp

Vasorelaxation and inhibition of the voltage-operated Ca^{2+} channels by FK506 in the porcine coronary artery

[1]Toru Yasutsune, [3]Nozomi Kawakami, [1]Katsuya Hirano, [1]Junji Nishimura, [2]Hisataka Yasui, [3]Kenji Kitamura & *,[1]Hideo Kanaide

[1]Division of Molecular Cardiology, Research Institute of Angiocardiology, Faculty of Medicine, Kyushu University, 3-1-1 Maidashi, Higashi-ku, Fukuoka 812-8582, Japan; [2]Cardiovascular Surgery, Research Institute of Angiocardiology, Faculty of Medicine, Kyushu University, 3-1-1 Maidashi, Higashi-ku, Fukuoka 812-8582, Japan; [3]Department of Pharmacology, Fukuoka Dental College, Fukuoka, Japan

1 Using fura-2 fluorometry, the effects of FK506, an immunosuppressant, on changes in cytosolic Ca^{2+} concentrations ($[Ca^{2+}]_i$) and tension were investigated in porcine coronary arterial strips. The effects of FK506 on the activity of voltage-operated Ca^{2+} channels were examined by applying a whole cell patch clamp to the isolated smooth muscle cells of porcine coronary artery.

2 FK506 inhibited the sustained increases in both $[Ca^{2+}]_i$ and tension induced by 118 mM K^+ depolarization and 100 nM U46619 in a concentration-dependent manner (1–30 μM). The extent of inhibition of the K^+-induced contraction was greater than that of the U46619-induced contraction. The increases in $[Ca^{2+}]_i$ and tension induced by histamine and endothelin-1 in the presence of extracellular Ca^{2+} were also inhibited by 10 μM FK506.

3 FK506 (10 μM) had no effect on Ca^{2+} release induced by caffeine or by histamine in the Ca^{2+}-free solution.

4 FK506 (10 μM) had no effect on the $[Ca^{2+}]_i$-tension relationships of the contractions induced by cumulative increases of extracellular Ca^{2+} during K^+ depolarization or stimulation with U46619.

5 In the patch clamp experiments, FK506 (30 μM) partially inhibited the inward current induced by depolarization pulse from −80 mV to 0 mV.

6 In conclusion, FK506 induces arterial relaxation by decreasing $[Ca^{2+}]_i$ mainly due to the inhibition of the L-type Ca^{2+} channels, with no effect on the Ca^{2+} sensitivity of the contractile apparatus.

Keywords: FK506; porcine coronary artery; vasorelaxation; cytosolic Ca^{2+} concentration; voltage-operated Ca^{2+} channel

Abbreviations: $[Ca^{2+}]_i$, cytosolic Ca^{2+} concentration; EGTA, ethyleneglycol-bis(β-aminoethylether)-N,N,N′,N′-tetraacetic acid FKBP, FK506 binding protein; fura-2/AM, fura-2 acetoxymethyl ester; HEPES, N-[2-hydroxyethyl]piperazine-N′-[2-ethanesulphonic acid]; IP_3, inositol 1,4,5-trisphosphate; IP_3R, IP_3 receptor; PSS, physiological salt solution; RyR, ryanodine receptor; VOC, voltage-operated L-type Ca^{2+} channel

Introduction

FK506 (tacrolimus, (−)-(1R, 9S, 12S, 13R, 14S, 17R, 18E, 21S, 23S, 24R, 25S, 27R)-17-allyl-1, 14-dihydroxy-12-[(E)-2-[(1R,3R,4R)- 4-hydroxy-3-methoxycyclohexyl]-1-methylvinyl]-23 , 25- dimethoxy- 13, 19, 21, 27 - tetramethyl - 11, 28 - dioxa - 4-azatricyclo [22.3.1.04.9] octacos-18-ene-2, 3, 10, 16-tetrone hydrate, $C_{44}H_{69}NO_{12}\cdot H_2O$, M.W.: 822.05) is an immunosuppressant widely used in organ transplantations (Starzl *et al*., 1989). FK506 binds to its cytosolic receptor, FK506 binding protein (FKBP), and the resulting complex inhibits the type 2B Ca^{2+}-calmodulin-dependent protein phosphatase, calcineurin, which is essential in T cell activation (Clipstone & Crabtree, 1992; Liu *et al*., 1991; 1992; O'Keefe *et al*., 1992). It is also suggested that calcineurin is involved in other signal transduction pathways regulated by Ca^{2+} (Guerini, 1997). For example, the Ca^{2+}-dependent inactivation of L-type Ca^{2+} channels was partially inhibited by cyclosporin A, another widely used immunosuppressant (Schuhmann *et al*., 1997). Alteration of the Ca^{2+} sensitivity of the contractile apparatus as well as cytosolic Ca^{2+} concentration ($[Ca^{2+}]_i$) has recently been suggested as one of the regulatory mechanisms of smooth muscle contraction (Somlyo & Somlyo, 1994). It is suggested that protein phosphatases, especially type 1 phosphatase, play an important role in regulation of the Ca^{2+} sensitivity of the contractile apparatus of smooth muscle (Somlyo & Somlyo, 1994). However the role of type 2B phosphatase in the regulation of smooth muscle contraction remains to be elucidated.

Recently, it has been proposed that FKBPs form functional complexes with Ca^{2+} release channels and modulate their activity (Marks, 1997). These channels play crucial roles in many cellular functions including smooth muscle contraction, excitation-contraction coupling in striated muscle, T cell activation and fertilization (Himpens *et al*., 1995; Marks, 1992; 1997). FKBPs have been shown to be associated with ryanodine receptors (RyR) and to modulate channel activity, possibly by enhancing cooperation between its four subunits. Interaction with FKBPs stabilized the channel activity of RyR, namely it decreased open probability and increased mean open time of the channel after caffeine activation, and also increased the full conductance level (Brillantes *et al*., 1994; Jayaraman *et al*., 1992; Kaftan *et al*., 1996; Timerman *et al*., 1993). FK506 as well as the related compound, rapamycin, reversed the stabilizing effect of FKBPs, enhanced the caffeine-induced Ca^{2+} release and, in the case of skeletal muscle, enhanced

*Author for correspondence.
E-mail; kanaide@molcar.med.kyushu-u.ac.jp

contractility (Brillantes *et al*., 1994; Kaftan *et al*., 1996). Recently, it was also shown that FKBP12 was associated with IP_3R and stabilized its activity in rat cerebellum (Cameron *et al*., 1995).

Hypertension is one of the common side effects of FK506, indicating that FK506 may directly modulate vascular smooth muscle contractility (Alessiani *et al*., 1993; Armitage *et al*., 1991; Fung *et al*., 1991). However, the effect of FK506 on the tension development of vascular smooth muscle has never been studied.

In the present study, in order to investigate the effect of FK506 on arterial contraction and to elucidate the role of the type 2B phosphatases in the regulation of smooth muscle contraction, we simultaneously measured $[Ca^{2+}]_i$ and tension in porcine coronary arterial strips using the fura-2 front surface fluorometry method. Unexpectedly, FK506 was found to induce arterial relaxation by decreasing $[Ca^{2+}]_i$ level mainly due to inhibition of Ca^{2+} influx in the porcine coronary artery. Therefore, we further evaluated the effects of FK506 on the Ca^{2+} channel activity with a patch clamp technique.

Methods

Preparation of medial strips of porcine coronary artery and fura-2 loading

Fresh pig hearts were obtained from a local slaughterhouse. The left circumflex branches of coronary arteries were immediately isolated and transported to the laboratory in ice cold physiological salt solution (PSS). The composition of normal PSS (mM) was; NaCl 123, KCl 4.7, $NaHCO_3$ 15.5, KH_2PO_4 1.2, $MgCl_2$ 1.2, $CaCl_2$ 1.25, and D-glucose 11.5. A segment of the coronary artery 2–3 cm from the origin were excised. After removing the adventitia, the segment was opened longitudinally, and the endothelium was removed by gently rubbing the internal surface with a cotton swab. The medial preparation was cut into 1 mm width × 5 mm long strips under a binocularscope. The lack of functional endothelium was confirmed by the observation that the addition of 1 μM bradykinin during contraction induced by 118 mM K^+ depolarization did not induce relaxation.

Vascular strips without endothelium were loaded with the Ca^{2+} indicator dye, fura-2, by incubation in oxygenated Dulbecco's modified Eagle medium containing 25 μM fura-2 acetoxymethyl ester (fura-2/AM) and 5% w/v foetal bovine serum for 3–4 h at 37°C. The strips were then washed in normal PSS for more than 1 h to remove the dye remaining in the extracellular space and to equilibrate the strips before starting the specific measurements.

Simultaneous measurement of $[Ca^{2+}]_i$ and tension of the porcine coronary arterial strips

The changes in $[Ca^{2+}]_i$ and tension of the fura-2 loaded vascular strips were simultaneously measured at 37°C as previously described (Hirano *et al*., 1990). The fura-2 loaded strips were mounted vertically to a strain gauge connected at one end of the strip (model TB-612T, Nihon Koden, Tokyo, Japan) whilst the other end was connected to a clamp in a quartz organ bath. Changes in the fluorescence intensity of the fura-2-Ca^{2+} complex were monitored with a front surface fura-2 fluorometer equipped with optic fibres (model CAM-OF-2, Japan Spectroscopic, Tokyo, Japan). The quartz optic fibres were used to transmit alternating (400 Hz) 340 nm and 380 nm excitation light from a xenon lamp to the strips. The surface fluorescence of the strips was collected with glass optic fibres and passed through a 500 nm band-pass filter into a photomultiplier. The quartz and glass optic fibres were arranged in a concentric inner circle (3 mm diameter) and an outer circle (7 mm diameter) at one end of the optic fibres facing the strip. The fluorescence intensities (500 nm emission) at 340 nm and 380 nm excitation were monitored and their ratio (F340/F380) was recorded as an indicator of $[Ca^{2+}]_i$. During a fura-2 equilibration period, the strips were stimulated with 118 mM K^+ deplolarization at 15 min intervals and the resting tension was increased in a stepwise manner. The resting tension was finally adjusted to approximately 300 mg (=2.97 mN) in normal PSS. This was the minimal resting tension yielding maximum tension development in response to depolarization with 118 mM K^+.

Before each experimental protocol, the response to 118 mM K^+ depolarization was recorded as control. Both changes in fluorescence ratio and tension were expressed as a percentage, assigning values in normal PSS (5.9 mM K^+) and at 10 min after the stimulation with 118 mM K^+ depolarization to be 0 and 100%, respectively.

Electrophysiological recordings

Small segments of coronary artery similar to those used for the tension study were incubated in Ca^{2+}-free solution containing 0.05% w/v collagenase P and 0.15% w/v bovine serum albumin (fraction V, essentially fatty acid free) in a shaking water bath at 37°C for 35 min. Thereafter, the tissue was gently agitated with a blunt-tipped pipette to disperse the smooth muscle cells. The debris was filtered and the cells collected by centrifugation at 1000 r.p.m. for 2 min and suspended in fresh Ca^{2+}-free solution containing 0.2% w/v bovine serum albumin and 0.1% w/v trypsin inhibitor (type IIs). The cell suspension was stored at 10°C and experiments were performed at room temperature (25–28°C) within 5 h after harvest. The composition of the Ca^{2+}-free solution (in mM) was NaCl 140, KCl 5.4, $MgCl_2$ 1.2, glucose 12, N-[-2-hydroxyethyl]piperazine-N′-[2-ethanesulphonic acid] (HEPES) 10 (pH = 7.3–7.4).

Patch electrode was manipulated using a three dimensional micromanipulator (Manipulater E; Leitz, Wetzler, Germany). For recording the Ca^{2+} channel currents, high Ba^{2+} solution was superfused in the bath and the pipette was filled with high Cs^+ solution with the following compositions (in mM), respectively; Ba^{2+} solution, $BaCl_2$ 90 and HEPES 5; Cs^+ solution, CsCl 135, $MgCl_2$ 5, EGTA 5, Na_2ATP 5, glucose 12 and HEPES 10; (pH 7.3–7.4). For recording the K^+ channel currents, Ca^{2+}-free solution (described above) was superfused in the bath and the pipette was filled with high K^+ solution with the following ionic composition (in mM); high K^+ solution, KCl 120, glucose 20, $MgCl_2$ 5, EGTA 5, HEPES 10; (pH = 7.3–7.4). The membrane currents were recorded by a whole cell voltage clamp configuration (Hamill *et al*., 1981) through an amplifier (Axopatch 200, Axon Instruments, Burlingame, CA, U.S.A.). Patch electrodes (3–5 MΩ) were prepared with an electrode puller (P-97, Sutter Instrument Co., Novato, CA, U.S.A.), and heat polisher (MF-83, Narishige Scientific Instrument Laboratory, Tokyo, Japan). Data acquisition was compiled using pCLAMP software (Axon Instruments). In the present experiments, the membrane potential was kept at −80 mV and depolarizing pulse to 0 mV was repetitively applied to the cell (300 ms duration, 15 s interval). In preliminary experiments, we confirmed that ethanol (less than 0.1% v/v) did not affect Ca^{2+} channel currents.

Solutions and chemicals

The Ca^{2+}-free PSS used in the fluorometry experiments contained 2 mM ethyleneglycol-bis(β-aminoethylether)-N,N,N′,N′-tetraacetic acid (EGTA) instead of 1.25 mM $CaCl_2$. High (118 mM) K^+ PSS was prepared by replacing an equimolar substitution of KCl for NaCl. The solutions were gassed with a mixture of 5% CO_2 and 95% O_2 and the resulting pH was 7.4.

FK506 was kindly donated by Fujisawa Pharmaceutical Co., Ltd (Osaka, Japan). FK506 was dissolved in ethanol as a stock solution of 10 or 100 mM. The final concentration of ethanol was less than 0.1% v/v. This final concentration of ethanol, *per se*, had no effects on the $[Ca^{2+}]_i$ and tension of the porcine coronary medial strips as previously described (Kuroiwa *et al*., 1993). Fura-2/AM was purchased from Dojindo Laboratories (Kumamoto, Japan). Bovine serum albumin, endothelin-1, nicardipine and trypsin inhibitor were purchased from Sigma (St. Louis, MO, U.S.A.). Bradykinin was purchased from the Peptide Institute, Inc. (Osaka, Japan). U46619 (9,11-dideoxy-9α,11α-methanoepoxy-prostaglandin $F_{2\alpha}$, C_{21}, $H_{34}O_4$, M.W.: 350.5) was purchased from Funakoshi (Tokyo, Japan). Collagenase P was purchased from Boehringer-Manheim (Germany). All other chemicals were of the highest grade commercially available.

Data analysis

All data from the simultaneous measurements of $[Ca^{2+}]_i$ and tension were collected by a computerized data acquisition system (MacLab; Analog Digital instruments, Castle Hill, Australia: Macintosh, Apple Computer, Cupertino, CA, U.S.A.). The data for the representative traces shown in the figures were printed directly from the computer using a laser printer (Laser-Writer II NTX-J, Apple Computer). The data are expressed as the means ± s.e.means of the indicated numbers of experiments. One strip obtained from one animal was used for each experiment, therefore the number of experiments (n value) indicates the number of animals. Statistical analysis was performed using unpaired Student's t-tests and P values of less than 0.05 were considered to be significant.

Results

The effect of FK506 on the increases in $[Ca^{2+}]_i$ and tension induced by high K^+ depolarization

Figure 1 shows the effect of 10 μM FK506 on the increases in $[Ca^{2+}]_i$ and tension induced by 118 mM K^+ depolarization in porcine coronary arterial medial strips. As shown in Figure 1a, when the bathing solution was changed from normal (5.9 mM K^+) PSS to 118 mM K^+ PSS, $[Ca^{2+}]_i$ rapidly increased to produce a sharp peak and then declined slightly to the plateau phase within 10 min. Tension also developed rapidly to the plateau phase. The levels of $[Ca^{2+}]_i$ and tension at the plateau phase were both assigned as 100%. The bathing solution was then changed to normal PSS. At 30 min incubation in normal PSS, subsequent stimulation with 118 mM K^+ depolarization in the absence of FK506 yielded responses of $[Ca^{2+}]_i$ (96.4 ± 2.3%, $n=10$) and tension (103.6 ± 1.5%, $n=10$) similar to those obtained for the first response to 118 mM K^+ depolarization (Figure 1a).

The application of 10 μM FK506 had no effect on $[Ca^{2+}]_i$ or tension at the resting state (Figure 1b). The subsequent stimulation with 118 mM K^+ depolarization at 30 min after application of FK506 caused increases in $[Ca^{2+}]_i$ and tension, which were smaller than those observed in the absence of FK506. The levels of $[Ca^{2+}]_i$ and tension at the plateau phase of contraction in the presence of 10 μM FK506 were 68.6 ± 3.7% and 61.4 ± 2.4% ($n=7$), respectively. Despite the removal of FK506 from the bathing solution, the inhibitory effect on the contraction remained for about 1 h and was thereafter completely reversed (data not shown). There was no difference in the inhibitory effect on high K^+-depolarization-induced contraction between 60 min and 30 min pretreatment with FK506, while there was only an apparently smaller inhibition in the case of 15 min pretreatment (data not shown). Therefore, the effect of FK506 was evaluated using a 30 min pretreatment with FK506.

Figure 1c summarizes the concentration-dependent effect of FK506 on the increases in both $[Ca^{2+}]_i$ and tension induced by 118 mM K^+ depolarization. A significant inhibition of both $[Ca^{2+}]_i$ and tension were observed at 1 μM and higher concentrations. The maximum inhibition was not observed at 30 μM FK506, which was the highest concentration available in less than 0.1% v/v ethanol vehicle. The profile of the concentration-dependent inhibition $[Ca^{2+}]_i$ appeared to be similar to that observed on the tension response. Thus, the decreases in tension were well correlated with the decrease in $[Ca^{2+}]_i$ in the FK506-induced relaxation.

The effects of FK506 on $[Ca^{2+}]_i$ elevation and tension development induced by U46619

In order to compare the effect of FK506 on the voltage-operated Ca^{2+} channels with that on other Ca^{2+}-influx pathways, U46619, a thromboxane A_2 mimetic, was used to induce contraction in porcine coronary artery. Thromboxane A_2 is a platelet-derived potent vasoconstrictor and could play an important role in cardiac allograft rejection (Khirabadi *et al*., 1985), in which blood coagulation and platelet aggregation are occasionally seen. In the porcine coronary artery, the application of 100 nM U46619 induced considerable rapid increases in both $[Ca^{2+}]_i$ and tension, which reached the steady state level within 10–15 min. The steady state level was maintained for more than 1 h (Figure 2a). At 70 min of application, the level of tension (95.4 ± 1.8%, $n=5$) induced by 100 nM U46619 was similar, while the level of $[Ca^{2+}]_i$ (57.7 ± 6.8%, $n=5$) was significantly lower than those obtained with 118 mM K^+ depolarization. FK506 (30 μM) was applied at 10 min and during the steady state of U46619-induced contraction, inducing gradual decreases in $[Ca^{2+}]_i$ and tension (Figure 2b). At 60 min, the inhibitory effect on $[Ca^{2+}]_i$ and tension reached a maximal and steady level. The effect of FK506 was thus evaluated at 60 min after the application. Figure 2c summarizes the concentration-dependent inhibitory effects of FK506 on the contraction induced by U46619. FK506 (1 μM) had no effect on the increase in $[Ca^{2+}]_i$ and tension induced by 100 nM U46619. At 10 μM, FK506 inhibited the tension developed from 95.4 ± 1.8% ($n=5$) to 78.9 ± 2.8% ($n=7$). FK506 thus inhibited the contraction induced by 118 mM K^+ depolarization more potently than that induced by 100 nM U46619.

The effects of FK506 on $[Ca^{2+}]_i$ and tension development induced by endothelin-1 or histamine in normal PSS

The effects of FK506 on contractions induced by endothelin-1 or histamine were examined (Figure 3). FK506 was applied

30 min prior to and during the agonist-induced contractions. Stimulation of strips with 10 nM endothelin-1 in the absence of FK506 induced rapid increases in $[Ca^{2+}]_i$ and tension followed by a slight decline (Figure 3a). The maximum levels of $[Ca^{2+}]_i$ increase and tension development induced by 10 nM endothelin-1 were $91.8 \pm 3.9\%$ and $136.9 \pm 6.0\%$ ($n=7$), respectively. At 60 min of application, the levels of $[Ca^{2+}]_i$ and tension were $71.9 \pm 3.7\%$ and $108.0 \pm 7.0\%$ ($n=7$), respectively. In the presence of 10 μM FK506, although the initial increase in $[Ca^{2+}]_i$ and tension was similar, $[Ca^{2+}]_i$ and tension during the steady state were significantly smaller than those obtained in the absence of FK506. The levels of $[Ca^{2+}]_i$ and tension at the

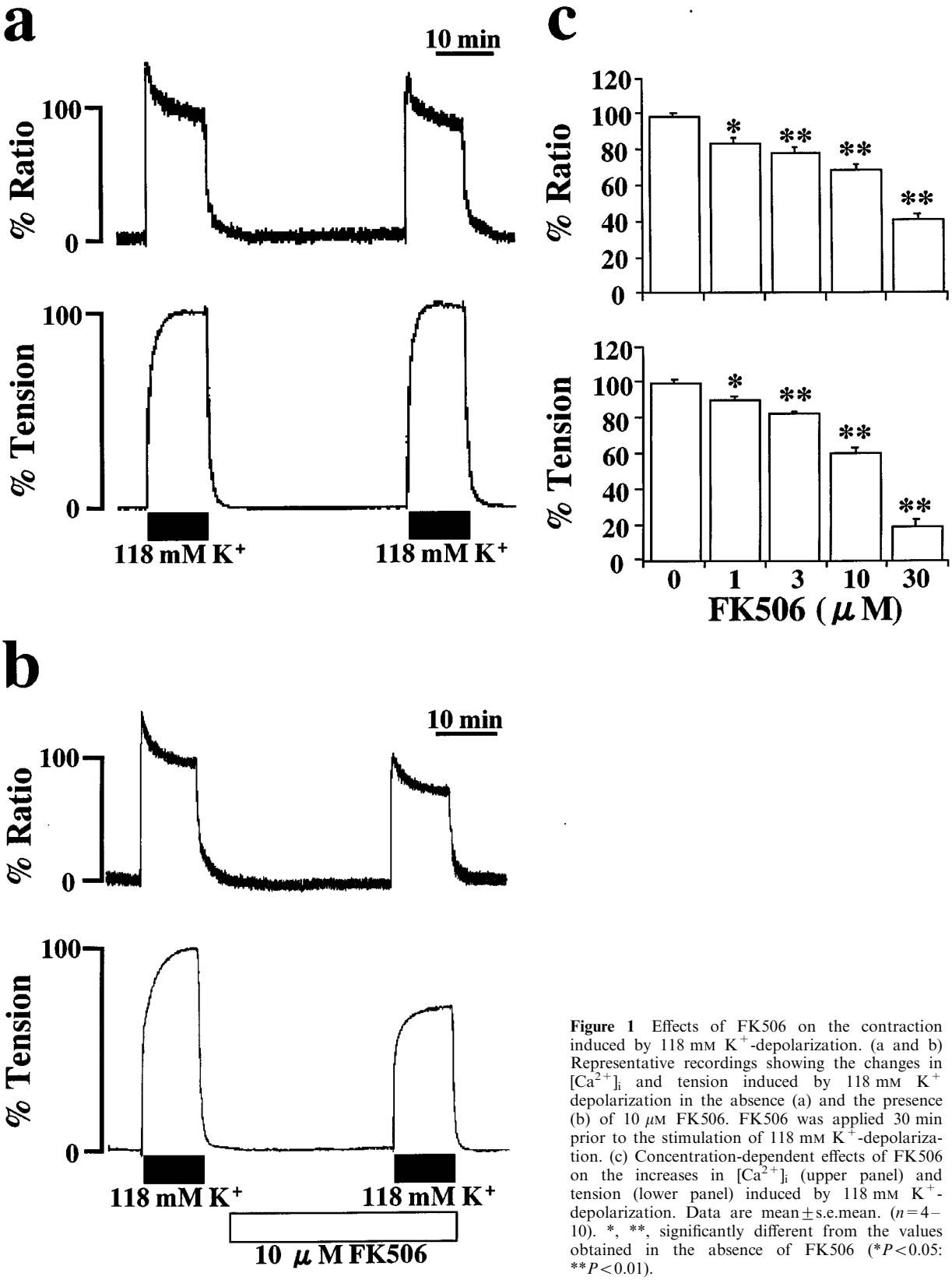

Figure 1 Effects of FK506 on the contraction induced by 118 mM K^+-depolarization. (a and b) Representative recordings showing the changes in $[Ca^{2+}]_i$ and tension induced by 118 mM K^+ depolarization in the absence (a) and the presence (b) of 10 μM FK506. FK506 was applied 30 min prior to the stimulation of 118 mM K^+-depolarization. (c) Concentration-dependent effects of FK506 on the increases in $[Ca^{2+}]_i$ (upper panel) and tension (lower panel) induced by 118 mM K^+-depolarization. Data are mean $\pm$ s.e.mean. ($n=4$–10). *, **, significantly different from the values obtained in the absence of FK506 (*$P<0.05$: **$P<0.01$).

peak were 88.3±12.1% and 122.7±3.8% ($n=9$), respectively. The levels of $[Ca^{2+}]_i$ and tension at 60 min were 45.4±4.1% and 69.0±8.6% ($n=9$), respectively. On the other hand, 10 μM histamine induced rapid increases in both $[Ca^{2+}]_i$ and tension followed by a gradual decline (Figure 3b). In the absence of FK506, the maximum levels of $[Ca^{2+}]_i$ increase and tension development induced by 10 μM histamine were 103.4±5.7% and 122.2±6.8% ($n=7$), respectively. The levels of $[Ca^{2+}]_i$ and tension at 60 min were 33.9±7.7% and 32.3±6.9% ($n=7$), respectively. Treatment with 10 μM FK506 significantly inhibited both the initial contraction (80.7±4.0% for $[Ca^{2+}]_i$; 110.0±5.4% for tension, $n=11$) and the following sustained contraction (25.0±5.8% for $[Ca^{2+}]_i$; 18.6±5.1% for tension at 60 min, $n=11$).

The effects of FK506 on the Ca^{2+} release induced by caffeine and histamine in the Ca^{2+}-free solution

The effect of FK506 on Ca^{2+} release from intracellular stores was examined by using caffeine and histamine as stimuli to

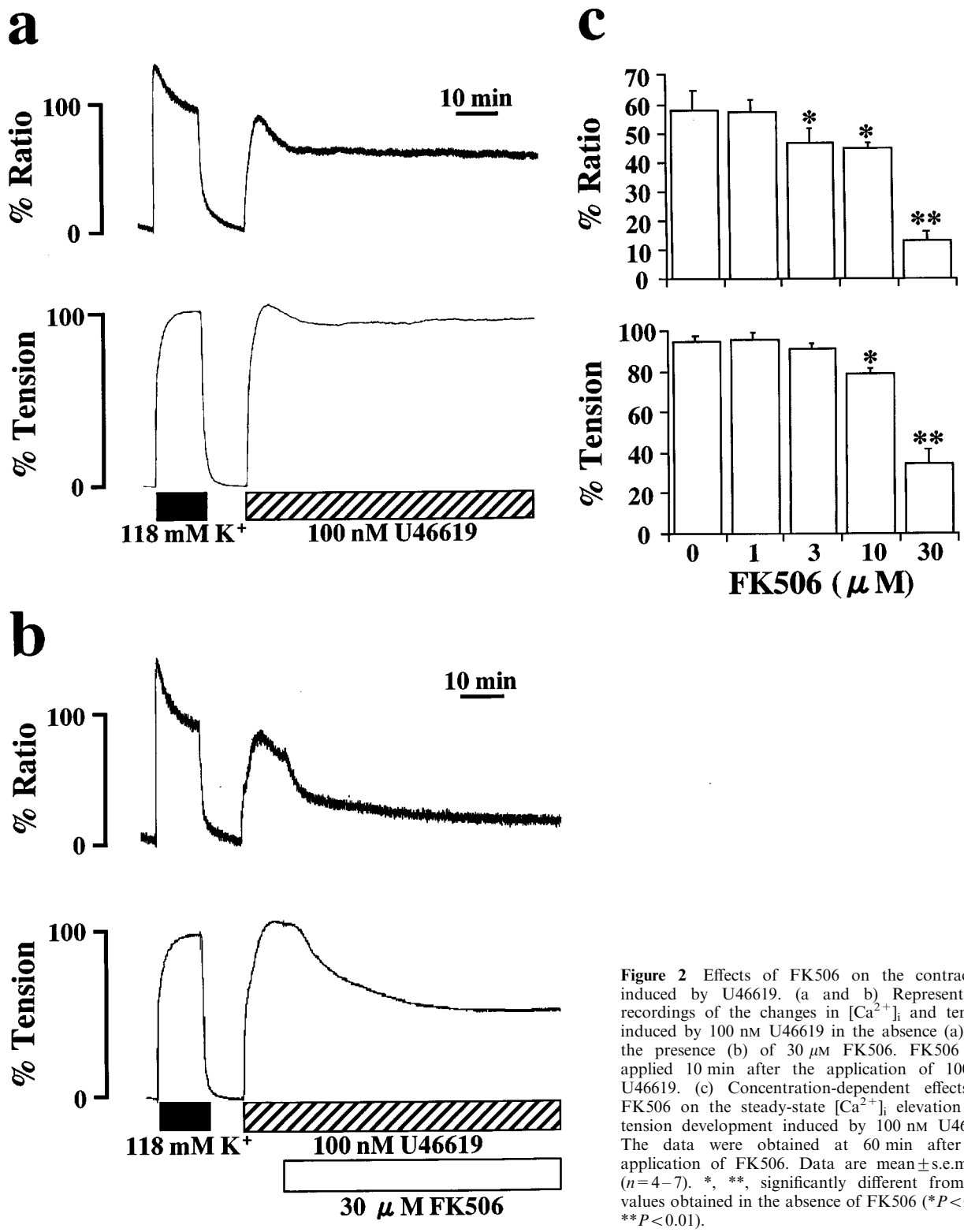

Figure 2 Effects of FK506 on the contraction induced by U46619. (a and b) Representative recordings of the changes in $[Ca^{2+}]_i$ and tension induced by 100 nM U46619 in the absence (a) and the presence (b) of 30 μM FK506. FK506 was applied 10 min after the application of 100 nM U46619. (c) Concentration-dependent effects of FK506 on the steady-state $[Ca^{2+}]_i$ elevation and tension development induced by 100 nM U46619. The data were obtained at 60 min after the application of FK506. Data are mean±s.e.mean. ($n=4-7$). *, **, significantly different from the values obtained in the absence of FK506 (*$P<0.05$; **$P<0.01$).

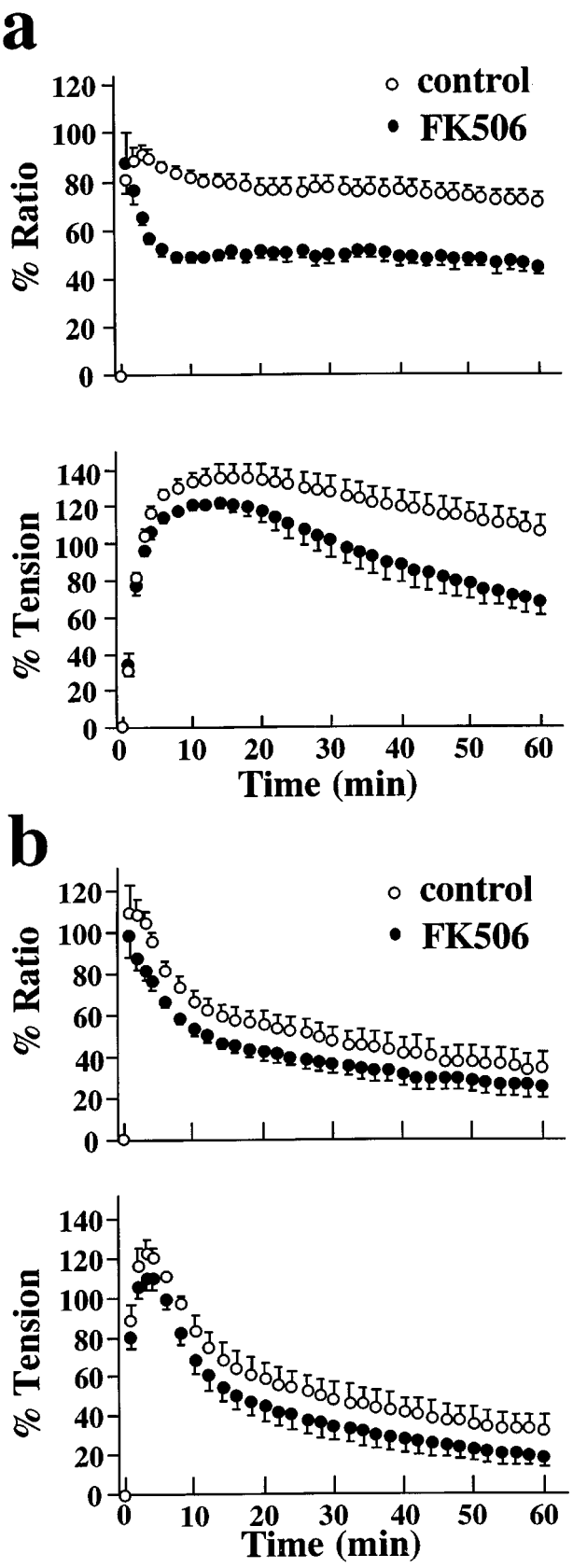

Figure 3 Effects of 10 μM FK506 on the increases in $[Ca^{2+}]_i$ and tension induced by 10 nM endothelin-1 (a) and 10 μM histamine (b) in normal PSS. Time courses of changes in $[Ca^{2+}]_i$ and tension in the presence and absence of FK506 were summarized. FK506 was applied 30 min prior to the applications of endothelin-1 or histamine. Data are mean $\pm$ s.e.mean. ($n=5-9$).

induce two different mechanisms of Ca^{2+} release. Figure 4a shows representative recordings showing the effect of 20 mM caffeine on $[Ca^{2+}]_i$ and tension of the porcine coronary arterial strips in the Ca^{2+}-free PSS. Changing the bathing solution (normal PSS) to the Ca^{2+}-free PSS containing 2 mM EGTA decreased basal $[Ca^{2+}]_i$ level to $-24.8\pm1.2\%$ ($n=5$) in 10 min, whereas the resting tension was unchanged. The following stimulation with 20 mM caffeine induced transient increases in $[Ca^{2+}]_i$ and tension (Figure 4a). The peak levels of $[Ca^{2+}]_i$ and tension were $8.5\pm2.4\%$ and $5.6\pm0.8\%$ ($n=5$), respectively (Figure 4c). FK506 (10 μM) was applied 30 min before the application of caffeine (Figure 4b). The basal $[Ca^{2+}]_i$ level decreased to $-22.3\pm1.7\%$ ($n=6$) in Ca^{2+}-free PSS containing 10 μM FK506. The peak levels of $[Ca^{2+}]_i$ and tension induced by 20 mM caffeine in the presence of 10 μM FK506 were $7.1\pm2.6\%$ and $3.6\pm0.8\%$ ($n=6$), respectively (Figure 4c). These values did not significantly differ from those obtained in the absence of FK506. The caffeine induced increases in $[Ca^{2+}]_i$ and tension were concentration-dependent with the minimum concentration required to induce a maximum response being 20 mM (data not shown). The effects of FK506 on caffeine-induced contractions were also examined at the submaximal concentration, i.e., 10 mM caffeine. The peak levels of $[Ca^{2+}]_i$ elevation and tension induced by 10 mM caffeine were $-4.2\pm0.7\%$ and $1.8\pm0.8\%$ ($n=4$), respectively (Figure 4d). Treatment with 10 μM FK506 had no significant effects on these levels ($-5.1\pm3.9\%$ for $[Ca^{2+}]_i$; $1.7\pm0.5\%$ for tension, $n=5$).

The effects of FK506 on the Ca^{2+} release induced by 10 μM histamine were examined similarly (Figure 5). Stimulation with 10 μM histamine in the Ca^{2+}-free PSS containing 2 mM EGTA induced transient increases in $[Ca^{2+}]_i$ and tension, with the peak levels being $8.9\pm5.5\%$ and $49.8\pm4.5\%$ ($n=9$), respectively (Figure 5a and c). In the presence of 10 μM FK506, histamine-induced increases in $[Ca^{2+}]_i$($-1.3\pm5.1\%$, $n=11$) appeared smaller than that observed in the absence of FK506 but there was no significant difference between them. Tension development seen in the presence of FK506 ($34.5\pm2.7\%$, $n=11$) was significantly smaller than that seen in the absence of FK506 (Figure 5b and c).

The effects of FK506 on the $[Ca^{2+}]_i$-tension relationships during the contraction induced by high K^+ depolarization and U46619

To clarify the effect of FK506 on the Ca^{2+} sensitivity of the contractile apparatus of the coronary arterial smooth muscle, we examined the $[Ca^{2+}]_i$-tension relationship of the contractions induced by the cumulative applications of extracellular Ca^{2+} during stimulation with 118 mM K^+ depolarization and 100 nM U46619. Figure 6 shows representative recordings of the changes in $[Ca^{2+}]_i$ and tension observed in the absence of FK506. The strips were first exposed to Ca^{2+}-free PSS containing 2 mM EGTA for 10 min and then to Ca^{2+}-free PSS without EGTA for 5 min before stimulation with 118 mM K^+ (Figure 5a) and U46619 (Figure 5b). When extracellular Ca^{2+} was applied cumulatively from 0–2.5 mM, graded elevations of $[Ca^{2+}]_i$ and tension were observed. During exposure to 118 mM K^+ depolarization, $[Ca^{2+}]_i$ and tension increased to $110.3\pm6.9\%$ and $111.9\pm3.3\%$ ($n=10$), respectively at an extracellular Ca^{2+} concentration of 2.5 mM. During stimulation with 100 nM U46619, the levels of $[Ca^{2+}]_i$ and tension reached $68.2\pm5.2\%$ and $91.8\pm7.3\%$ ($n=6$), respectively at 2.5 mM extracellular Ca^{2+}. When the effects of FK506 on these contractions were examined, 10 μM FK506 was applied 30 min prior to the cumulative application of

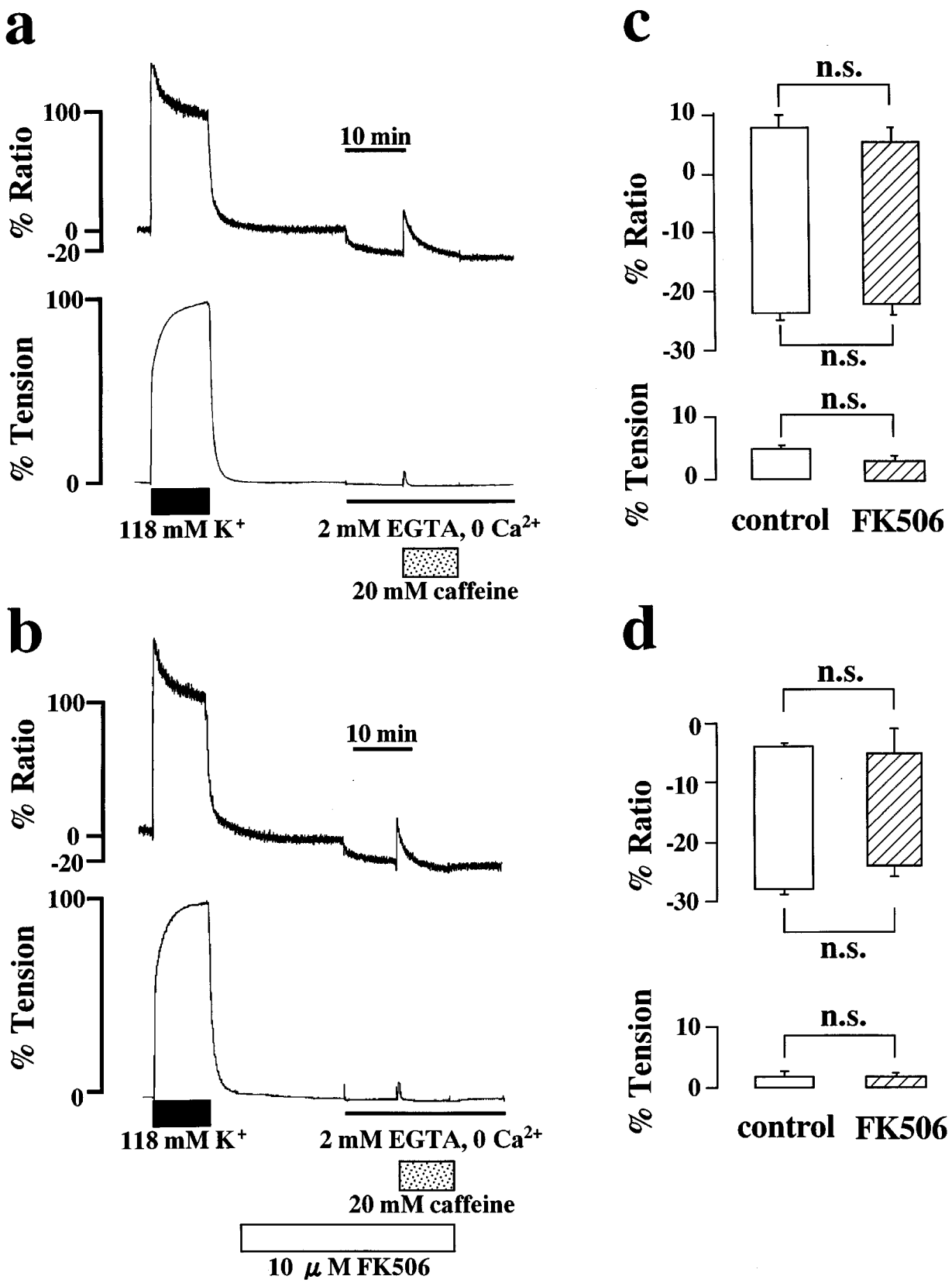

Figure 4 Effects of FK506 on the Ca^{2+} release induced by caffeine. (a and b) Representative recordings showing the elevation of $[Ca^{2+}]_i$ and tension induced by 20 mM caffeine in Ca^{2+}-free PSS containing 2 mM EGTA, in the absence (a) and presence (b) of 10 μM FK506. FK506 was applied 30 min prior to the application of caffeine. (c and d) Summary of the transient elevations in $[Ca^{2+}]_i$ and tension induced by 20 mM (c) and 10 mM (d) caffeine in Ca^{2+}-free PSS containing 2 mM EGTA in the absence and presence of 10 μM FK506. Bottom of the column indicates the level of $[Ca^{2+}]_i$ and tension just before the application of caffeine. Top of the column indicates the peak level of $[Ca^{2+}]_i$ and tension induced by caffeine. Data are mean$\pm$s.e.mean. ($n=6$). n.s., not significant difference.

extracellular Ca^{2+}. Treatment with 10 μM FK506 inhibited the increases in $[Ca^{2+}]_i$ and tension following exposure to both 118 mM K^+ depolarization and 100 nM U46619. $[Ca^{2+}]_i$ and tension increased to 69.3±5.4% and 67.9±4.2% ($n=8$) at 2.5 mM extracellular Ca^{2+} during 118 mM K^+ depolarization in the presence of FK506, respectively. During the stimulation with U46619 in the presence of FK506, $[Ca^{2+}]_i$ and tension increased 52.1±4.6% and 78.1±10.1% ($n=6$) at 2.5 mM extracellular Ca^{2+}, respectively.

The effect of FK506 on the Ca^{2+} sensitivity was evaluated by examining the $[Ca^{2+}]_i$-tension relationships of these contractions (Figure 6c). In the absence of FK506, the

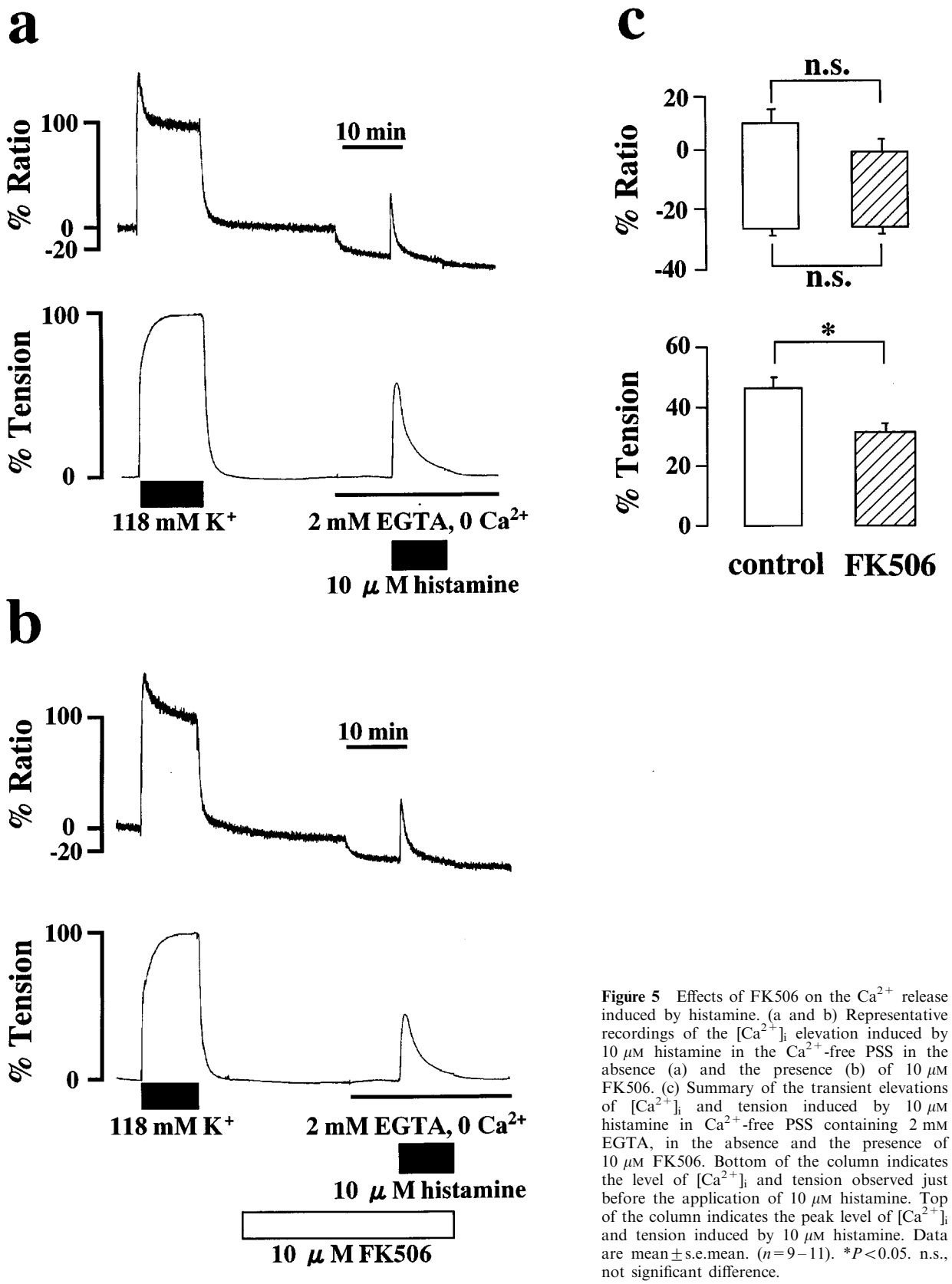

Figure 5 Effects of FK506 on the Ca^{2+} release induced by histamine. (a and b) Representative recordings of the $[Ca^{2+}]_i$ elevation induced by 10 μM histamine in the Ca^{2+}-free PSS in the absence (a) and the presence (b) of 10 μM FK506. (c) Summary of the transient elevations of $[Ca^{2+}]_i$ and tension induced by 10 μM histamine in Ca^{2+}-free PSS containing 2 mM EGTA, in the absence and the presence of 10 μM FK506. Bottom of the column indicates the level of $[Ca^{2+}]_i$ and tension observed just before the application of 10 μM histamine. Top of the column indicates the peak level of $[Ca^{2+}]_i$ and tension induced by 10 μM histamine. Data are mean±s.e.mean. ($n=9-11$). *$P<0.05$. n.s., not significant difference.

$[Ca^{2+}]_i$-tension relation curve of contraction obtained during stimulation with U46619 was to the left of that obtained with 118 mM K^+ depolarization. In both cases, the $[Ca^{2+}]_i$-tension relation curves obtained in the presence of 10 μM FK506 overlapped with those obtained in the absence of FK506. Thus, FK506 did not shift these $[Ca^{2+}]_i$-tension relation curves (Figure 6c).

The effect of FK506 on the Ca^{2+} channel current in the porcine coronary arterial smooth muscle cells

To investigate the mechanism of FK506-induced inhibition of $[Ca^{2+}]_i$ elevation, we performed whole cell voltage clamp experiments of the dispersed porcine coronary arterial smooth muscle cells. When 90 mM Ba^{2+} solution was superfused in the bath and the pipette was filled with 135 mM Cs^+solution, a depolarizing pulse to 0 mV from the holding potential of -80 mV evoked an inward current. The mean amplitude of the inward current was 236 ± 79 pA ($n=6$). Nicardipine (1 μM) completely inhibited this inward current, indicating the involvement of a Ca^{2+} channel current (data not shown). Figure 7a shows the effects of FK506 on the inward current of the porcine coronary artery. Application of 30 μM FK506 immediately inhibited the peak amplitude of the inward current (Figure 7a inset) and the maximum inhibition of the current was obtained 5–10 min after application of FK506 (Figure 7b). Current recovery was not observed within 10 min following removal of FK506. The mean amplitude in the

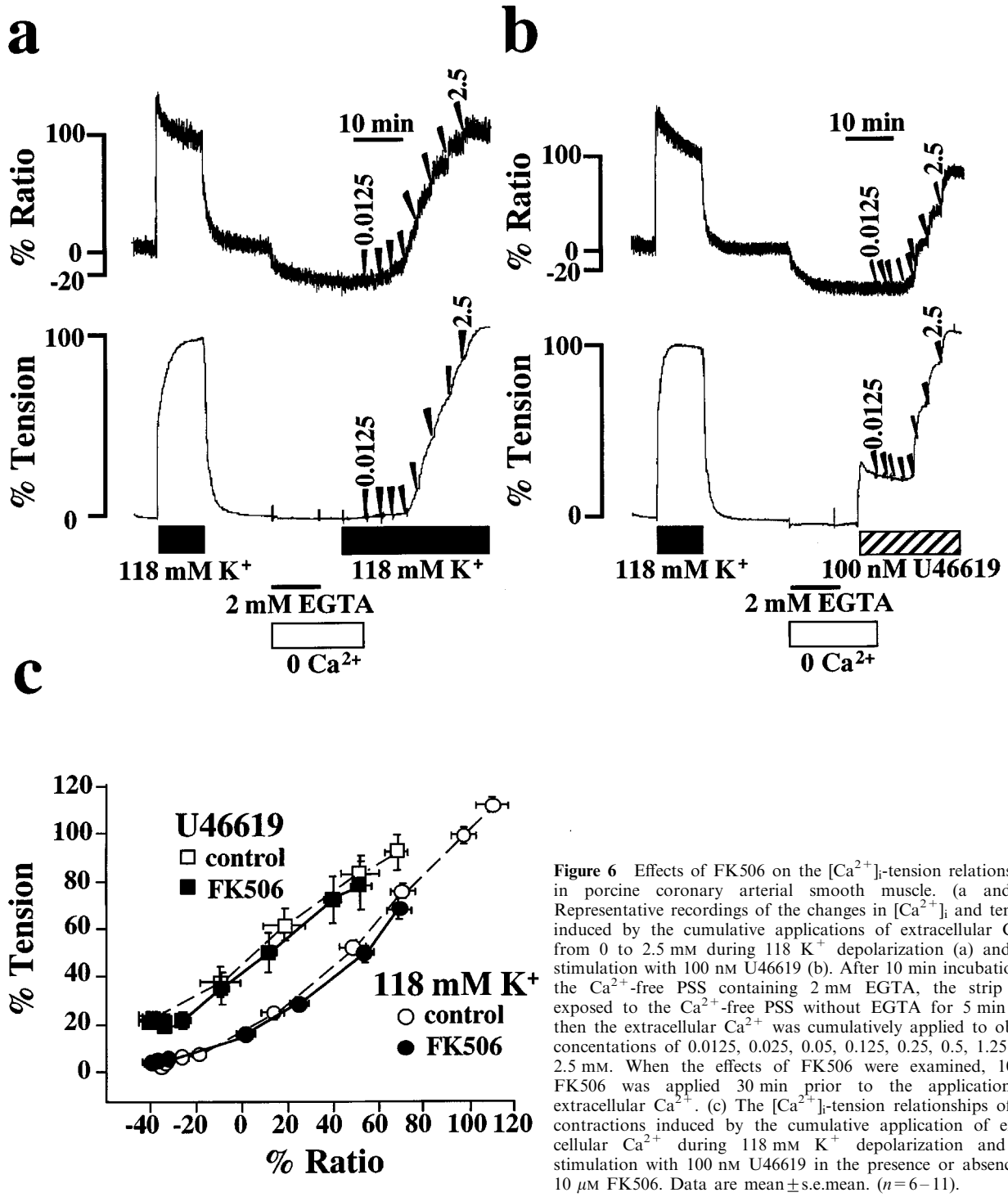

Figure 6 Effects of FK506 on the $[Ca^{2+}]_i$-tension relationships in porcine coronary arterial smooth muscle. (a and b) Representative recordings of the changes in $[Ca^{2+}]_i$ and tension induced by the cumulative applications of extracellular Ca^{2+} from 0 to 2.5 mM during 118 K^+ depolarization (a) and the stimulation with 100 nM U46619 (b). After 10 min incubation in the Ca^{2+}-free PSS containing 2 mM EGTA, the strip was exposed to the Ca^{2+}-free PSS without EGTA for 5 min and then the extracellular Ca^{2+} was cumulatively applied to obtain concentations of 0.0125, 0.025, 0.05, 0.125, 0.25, 0.5, 1.25 and 2.5 mM. When the effects of FK506 were examined, 10 μM FK506 was applied 30 min prior to the application of extracellular Ca^{2+}. (c) The $[Ca^{2+}]_i$-tension relationships of the contractions induced by the cumulative application of extracellular Ca^{2+} during 118 mM K^+ depolarization and the stimulation with 100 nM U46619 in the presence or absence of 10 μM FK506. Data are mean$\pm$s.e.mean. ($n=6-11$).

presence of 30 μM FK506 was 78.6±8.5% of the control ($n=6$; peak height). A lower concentration of FK506 (10 μM) did not show any significant inhibition (105.1±12.5% of the control, $n=3$) (Figure 7c). We also examined the effect of FK506 on the K^+ channel current. An outward K^+ current was evoked by a depolarizing pulse to 0 mV, and FK506 (30 μM) inhibited this current (Figure 7b inset). The outward K^+ current was restored by removal of FK506 (Figure 7b). The mean amplitude in the presence of 30 μM FK506 was 59.7±6.1% of the control ($n=6$; peak height), and of 10 μM FK506 was 81.3±6.3% of the control ($n=3$; peak height) (Figure 7c).

Discussion

In the present study, we found that FK506, an immunosuppressant widely used in organ transplantation, relaxed porcine coronary artery. The relaxing effect of FK506 observed in this study is consistent with previous observations on the canine basilar artery (Nishizawa *et al*., 1993). In the present study, by using the front surface fluorometry of fura-2 and electrophysiological measurement, we found that; (1) FK506 decreased $[Ca^{2+}]_i$ and caused relaxation during the contractions induced not only by high K^+ depolarization but also by agonists such as U46619, histamine and endothelin-1. FK506 decreased $[Ca^{2+}]_i$ during the sustained phase of contractions which are dependent on extracellular Ca^{2+}, suggesting that the decrease in $[Ca^{2+}]_i$ was due to inhibition of Ca^{2+} influx. (2) There were no effects on the relationship between $[Ca^{2+}]_i$ and tension, indicating that the reduction of $[Ca^{2+}]_i$ is the major mechanism of FK506-induced relaxation. Ca^{2+} sensitivity of the contractile apparatus was not affected. (3) The Ca^{2+} release induced by caffeine was not altered by FK506. (4) FK506 inhibited inward current induced by depolarizing pulse in the whole cell voltage clamp experiments, indicating that FK506 inhibits a voltage-operated L-type Ca^{2+} channel (VOC). It is thus suggested that the mechanism of relaxation induced by FK506 is analogous to that of Ca^{2+} channel blockers such as diltiazem and verapamil (Hirano *et al*., 1990).

High external K^+ solution depolarizes membrane potential, activates VOC and induces sustained increases in $[Ca^{2+}]_i$ and tension in vascular smooth muscle (Hirano *et al*., 1990). In the present study, FK506 inhibited the sustained phase of $[Ca^{2+}]_i$ elevation induced by high K^+ depolarization, indicating the inhibition of VOC by FK506. In the case of agonist-induced contractions, at least four different mechanisms should be considered for Ca^{2+} influx pathways. The first and second mechanisms are activation of VOC directly by agonist-induced membrane depolarization, and indirectly by agonist-activated intracellular second messengers or trimeric G proteins (Casteels & Suzuki, 1980; Miyoshi & Nakaya, 1991; Pacaud *et al*., 1991; Scornik & Toro, 1992). U46619 was shown to depolarize membrane potential of porcine coronary artery (Scornik & Toro, 1992). The third mechanism involves so-called receptor-operated Ca^{2+}channels (Bolton, 1979) and the fourth mechanism involves the capacitative Ca^{2+} influx pathway (Parekh & Penner, 1997; Putney, 1990). FK506 had no significant effects on the activity of the capactitative Ca^{2+} influx induced by thapsigargin (data not shown). Since FK506 inhibited K^+ depolarization-induced contractions more potently than U46619-induced contractions, FK506 was suggested to inhibit mainly VOC following contraction induced by depolarization and by agonists. The inhibitory effects of FK506 on VOC was clarified in the electrophysiological experiments. FK506 also inhibited K^+ channel current (Figure 7b and c). Thus, the effects of FK506 on ion channels were not selective to VOC. However, we consider the inhibition of Ca^{2+} channel to be essential for the relaxation of porcine coronary arterial smooth muscle cells because inhibition of K^+ channel current in the depolarized state is regarded to have no effect on the activity of VOC or on the membrane potential. On the other hand, inhibition of Ca^{2+} channels, which is a direct cause of decrease in $[Ca^{2+}]_i$ induces relaxation of smooth muscle in the present study. However, the precise mechanism of inhibition of Ca^{2+} influx by FK506 remains to be elucidated. There is no similarity in chemical structure between FK506 and known Ca^{2+} channel blockers. The type 2B protein phosphatase was shown to be involved in the Ca^{2+}-dependent inactivation of L-type Ca^{2+} channels in smooth muscle (Schuhmann *et al*., 1997). Since the concentration of FK506 required to inhibit VOC was much higher than that required to inhibit the phosphatase, it is possible that the FK506-induced inhibition of the Ca^{2+} influx is not mediated by inhibition of the phosphatase.

It has been recently shown that FKBP12 and FKBP12.6 are associated with the RyR and stabilized the activity of Ca^{2+} release channels in skeletal and cardiac muscle, respectively (Brillantes *et al*., 1994; Kaftan *et al*., 1996). In skeletal muscle, FK506 dissociated FKBP from RyR, enhanced Ca^{2+}release and increased contractility (Brillantes *et al*., 1994). However, in the present study, FK506 had no effect on the caffeine-induced Ca^{2+} release. This finding suggests that, in smooth muscle cells, FKBP may play only a minor role, if any, in the regulation of the channel activity of RyR. It was reported that smooth muscle cells express RyR3, which is different from skeletal (RyR1) or cardiac (RyR2) isoforms (McPherson & Campbell, 1993). This difference in RyR isoform may be linked to the difference in sensitivity to inhibition by FK506. On the contrary, FK506 significantly inhibited the tension development induced by histamine in the Ca^{2+}-free PSS, while the inhibition of $[Ca^{2+}]_i$ elevation was not statistically significant. In the presence of extracellular Ca^{2+}, the initial increases in $[Ca^{2+}]_i$ and tension induced by histamine were inhibited by FK506. It has been shown that FKBP12 formed a functional complex with IP_3R isolated from rat cerebellum and that FK506 dissociated this complex and increased Ca^{2+} flux through IP_3R (Cameron *et al*., 1995). Therefore, it is possible that the inhibition of histamine-induced Ca^{2+} release is not due to the dissociation of an FKBP-IP_3R complex. There is a possibility that FK506 inhibits either histamine binding to the receptor, receptor-G protein interaction or phospholipase C. These possibilities remain to be elucidated. However, since the transient contraction induced by endothelin-1 was not inhibited by FK506, it is unlikely that FK506 worked as a non-selective antagonist. Regarding the observation that the endothelin-induced Ca^{2+} release, as well as the caffeine-induced Ca^{2+} release is resistant to FK506, it is noteworthy that endothelin-1 induced Ca^{2+} release from the caffeine-sensitive store site in the cultured rat aortic smooth muscle cells (Kai *et al*., 1989).

Alteration of the Ca^{2+} sensitivity of the contractile apparatus is now considered to be one of the important regulatory mechanisms of smooth muscle contraction (Somlyo & Somlyo, 1994). However, the regulatory mechanisms of Ca^{2+} sensitivity remain to be elucidated. Protein phosphatases were shown to play an important role in regulation of Ca^{2+} sensitivity. Inhibitors of type 1 and type 2A protein phosphatases such as okadaic acid and calyculin-A have been shown to alter Ca^{2+} sensitivity of the contractile apparatus (Hirano *et al*., 1989). Myosin phosphatases were isolated from smooth muscle and categorized as type 1 phosphatase

(Shimizu *et al*., 1994; Somlyo & Somlyo, 1994). Thus, type 1 phosphatase is considered to be the major phosphatase involved in regulation of the Ca^{2+} sensitivity. In the present study, FK506, an inhibitor of type 2B phosphatase, had no effect on the $[Ca^{2+}]_i$-tension relationship. This argues against a major contribution of type 2B phosphatase to the regulation of Ca^{2+} sensitivity of the contractile apparatus of smooth muscle.

There was an apparent discrepancy in potency of FK506 between the tension study and patch clamp experiment. In the patch clamp experiment, gradual and progressive decline of

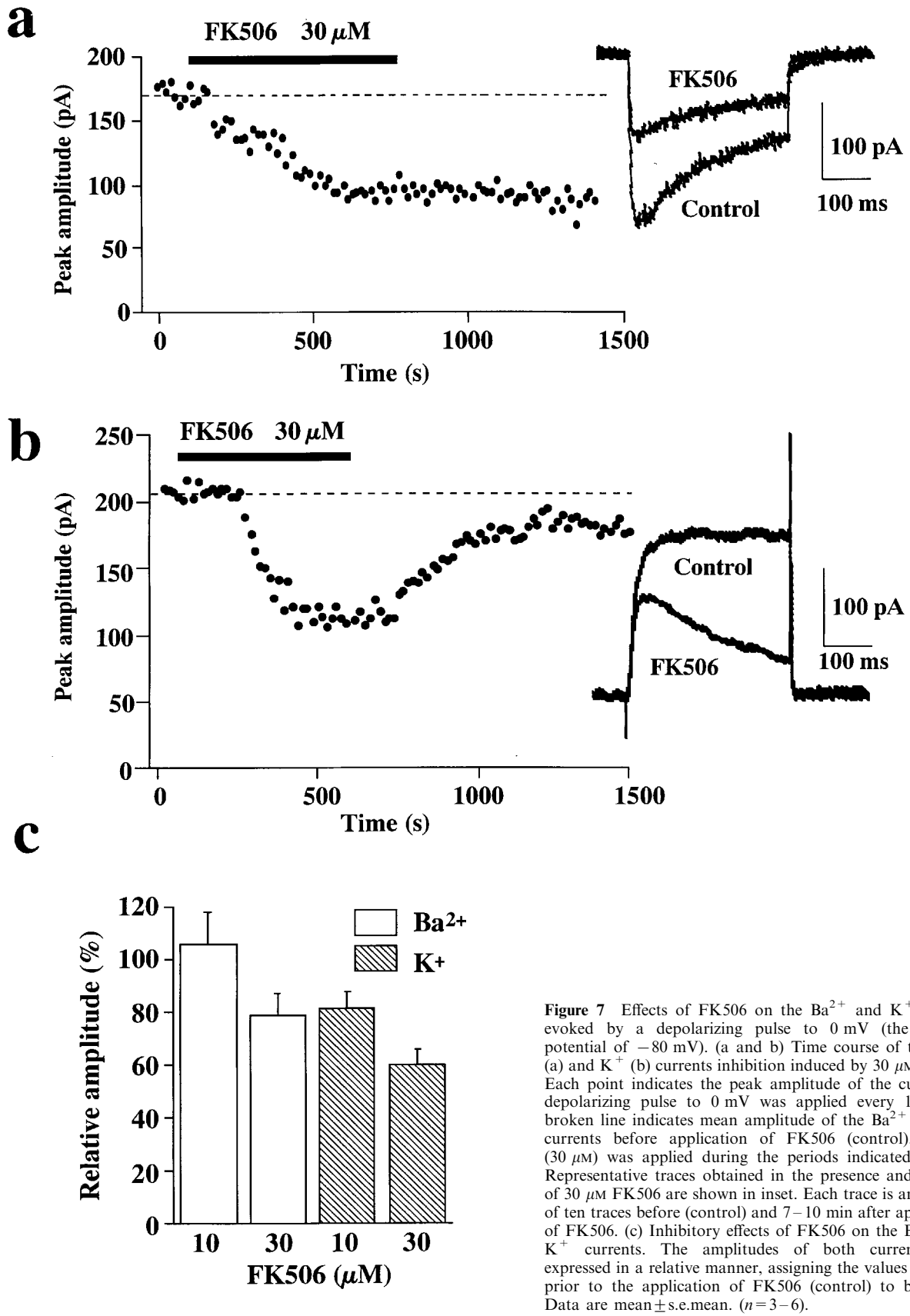

Figure 7 Effects of FK506 on the Ba^{2+} and K^+ current evoked by a depolarizing pulse to 0 mV (the holding potential of −80 mV). (a and b) Time course of the Ba^{2+} (a) and K^+ (b) currents inhibition induced by 30 μM FK506. Each point indicates the peak amplitude of the current. A depolarizing pulse to 0 mV was applied every 15 s. The broken line indicates mean amplitude of the Ba^{2+} and K^+ currents before application of FK506 (control). FK506 (30 μM) was applied during the periods indicated by bar. Representative traces obtained in the presence and absence of 30 μM FK506 are shown in inset. Each trace is an average of ten traces before (control) and 7–10 min after application of FK506. (c) Inhibitory effects of FK506 on the Ba^{2+} and K^+ currents. The amplitudes of both currents were expressed in a relative manner, assigning the values recorded prior to the application of FK506 (control) to be 100%. Data are mean ± s.e.mean. (n = 3–6).

Ca^{2+} channel activity (run down) made it difficult to examine the effects of FK506 after treatment for more than 30 min. In the tension study, however, the vasorelaxing effects of FK506 required at least 30 min treatment to reach steady state. Therefore, it was necessary to use a higher concentration of FK506 to observe the inhibition of Ca^{2+} channel activity with shorter treatment in the patch clamp experiment. The differences in temperature (37°C in the tension study *vs* room temperature in the patch clamp experiment) may have contributed to the difference in potency of FK506 because it has been reported that the binding properties of ligands to Ca^{2+} channel are affected by temperature (Maan & Hosey, 1987). Moreover, in addition to the inhibition of VOC which was confirmed in the patch clamp experiment, other mechanisms such as inhibition of agonist-induced Ca^{2+} influx or Ca^{2+} release could have contributed to decrease in $[Ca^{2+}]_i$ and force in the tension study. These additional effects of FK506 might have caused apparent higher potency in the vasorelaxation than in the inhibition of channel activity.

The plasma concentrations of FK506 in organ recipients are in the range 0.6–25 nM (Alessiani *et al*., 1993; Japanese FK506 study group, 1991). These values are consistent with the K_i value for inhibition of type 2B phosphatase activity (Liu *et al*., 1992). Thus, the concentration shown to induce smooth muscle relaxation was much higher than these values but are similar to those required to dissociate FKBP from RyR and to enhance Ca^{2+} release in cardiac muscle (Kaftan *et al*., 1996). However, the high lipophilicity of FK506 and its repetitive usage in patients might cause its accumulation in cells. It is noteworthy that the intracytoplasmic concentrations of FK506 in mouse splenic T cells and Jurkat cells were 10–900 times higher than extracellularly added concentrations (Dumont *et al*., 1994).

In conclusion, FK506 has been shown to cause relaxation of smooth muscle by decreasing $[Ca^{2+}]_i$ mainly *via* inhibition of Ca^{2+} influx through VOC. FK506 had no effect on the Ca^{2+} sensitivity of contractile apparatus and the extent of relaxation was to be expected from the observed reduction in $[Ca^{2+}]_i$. Thus, the mechanism of relaxation induced by FK506 is analogous to that induced by Ca^{2+} channel blockers. It is unlikely that type 2B protein phosphatase mediates the inhibition of Ca^{2+} influx by FK506 nor that type 2B protein phosphatase plays an important role in the regulation of the Ca^{2+} sensitivity of contractile apparatus in smooth muscle.

We thank Dr Timothy D. Keeley for reading the manuscript. This study was supported in part by Grant-in-aid for Scientific Research (A) (07407022) and (B) (10557072), for Scientific Research on Priority Areas (A) (10177222; 10177228), for Encouragement of Young Scientists (A) (10770308), and for Creative Basic Research Studies of Intracellular Signaling Network from the Ministry of Education, Science, Sports and Culture, Japan, and by The Vehicle Racing Commemorative Foundation, Kimura Memorial Heart Foundation Research Grant, Kaibara Morikazu Medical Science Promotion Foundation, Kanae Foundation for Life & Socio-Medical Science, and Japan Heart Foundation Research Grant.

References

ALESSIANI, M., CILLO, U., FUNG, J.J., IRISH, W., ABU-ELMAGD, K., JAIN, A., TAKAYA, S., VAN THIEL, D. & STARZL, T.E. (1993). Adverse effects of FK 506 overdosage after liver transplantation. *Transplant. Proc.,* **25,** 628–634.

ARMITAGE, J.M., KORMOS, R.L., FUNG, J. & STARZL, T.E. (1991). The clinical trial of FK 506 as primary and rescue immunosuppression in adult cardiac transplantation. *Transplant. Proc.,* **23,** 3054–3057.

BOLTON, T.B. (1979). Mechanisms of action of transmitters and other substances on smooth muscle. *Physiol. Rev.,* **59,** 606–718.

BRILLANTES, A.-M..B., ONDRIAS, K., SCOTT, A., KOBLINSKY, E., ONDRIASOVA, E., MOSCHELLA, M.C., JAYARAMAN, T., LANDERS, M., EHRLICH, B.E. & MARKS, A.R. (1994). Stabilization of calcium release channel (ryanodine receptor) function by FK506-binding protein. *Cell,* **77,** 513–523.

CAMERON, A.M., STEINER, J.P., SABATINI, D.M., KAPLIN, A.I., WALENSKY, L.D. & SNYDER, S.H. (1995). Immunophilin FK506 binding protein associated with inositol 1,4,5-trisphosphate receptor modulates calcium flux. *Proc. Natl. Acad. Sci. U.S.A.,* **92,** 1784–1788.

CASTEELS, R. & SUZUKI, H. (1980). The effect of histamine on the smooth muscle cells of the ear artery of the rabbit. *Pflügers Arch.,* **387,** 17–25.

CLIPSTONE, N.A. & CRABTREE, G.R. (1992). Identification of calcineurin as a key signalling enzyme in T-lymphocyte activation. *Nature,* **357,** 695–697.

DUMONT, F.J., KASTNER, C., IACOVONE, JR F. & FISCHER, P.A. (1994). Quantitative and temporal analysis of the cellular interaction of FK-506 and rapamycin in T-lymphocytes. *J. Pharmacol. Exp. Ther.,* **268,** 32–41.

FUNG, J., ABU-ELMAGD, K., JAIN, A., GORDON, R., TZAKIS, A., TODO, S., TAKAYA, S., ALESSIANI, M., DEMETRIS, A., BRONSTER, O., MARTIN, M., MIELES, L., SELBY, R., REYES, J., DOYLE, H., STIEBER, A., CASAVILLA, A. & STARZL, T. (1991). A randomized trial of primary liver transplantation under immunosuppression with FK 506 vs cyclosporine. *Transplant. Proc.,* **23,** 2977–2983.

GUERINI, D. (1997). Calcineurin: not just a simple protein phosphatase. *Biochem. Biophys. Res. Commun.,* **235,** 271–275.

HAMILL, O.P., MARTY, A., NEHER, E., SAKMANN, B. & SIGWORTH, F.J. (1981). Improved patch-clamp techniques for high-resolution current recording from cells and cell-free membrane patches. *Pflügers Archiv.,* **391,** 85–100.

HIMPENS, B., MISSIAEN, L. & CASTEELS, R. (1995). Ca^{2+} homeostasis in vascular smooth muscle. *J. Vasc. Res.,* **32,** 207–219.

HIRANO, K., KANAIDE, H., ABE, S. & NAKAMURA, M. (1990). Effects of diltiazem on calcium concentrations in the cytosol and on force of contractions in porcine coronary arterial strips. *Br. J. Pharmacol.,* **101,** 273–280.

HIRANO, K., KANAIDE, H. & NAKAMURA, M. (1989). Effects of okadaic acid on cytosolic calcium concentrations and on contractions of the porcine coronary artery. *Br. J. Pharmacol.,* **98,** 1261–1266.

JAPANESE FK 506 STUDY GROUP. (1991). Japanese study of FK 506 on kidney transplantation: results of an early phase II study. *Transplant. Proc.,* **23,** 3071–3074.

JAYARAMAN, T., BRILLANTES, A.-M., TIMERMAN, A.P., FLEISCHER, S., ERDJUMENT-BROMAGE, H., TEMPST, P. & MARKS, A.R. (1992). FK506 binding protein associated with the calcium release channel (ryanodine receptor). *J. Biol. Chem.,* **267,** 9474–9477.

KAFTAN, E., MARKS, A.R. & EHRLICH, B.E. (1996). Effects of rapamycin on ryandodine receptor/Ca^{2+}-release channels from cardiac muscle. *Circ. Res.,* **78,** 990–997.

KAI, H., KANAIDE, H. & NAKAMURA, M. (1989). Endothelin-sensitive intracellular Ca^{2+} store overlaps with caffeine-sensitive one in rat aortic smooth muscle cells in primary culture. *Biochem. Biophys. Res. Commun.,* **158,** 235–243.

KHIRABADI, B.S., FOEGH, M.L. & RAMWELL, P.W. (1985). Urine immunoreactive thromboxane B_2 in rat cardiac allograft rejection. *Transplantation,* **39,** 6–8.

KUROIWA, M., AOKI, H., KOBAYASHI, S., NISHIMURA, J. & KANAIDE, H. (1993). Role of GTP-protein and endothelium in contraction induced by ethanol in pig coronary artery. *J. Physiol.,* **470,** 521–537.

LIU, J., ALBERS, M.W., WANDLESS, T.J., LUAN, S., ALBERG, D.G., BELSHAW, P.J., COHEN, P., MACKINTOSH, C., KLEE, C.B. & SCHREIBER, S.L. (1992). Inhibition of T cell signaling by immunophilin-ligand complexes correlates with loss of calcineurin phosphatase activity. *Biochemistry,* **31,** 3896 – 3901.

LIU, J., FARMER JR, J.D., LANE, W.S., FRIEDMAN, J., WEISSMAN, I. & SCHREIBER, S.L. (1991). Calcineurin is a common target of cyclophilin-cyclosporin A and FKBP-FK506 complexes. *Cell,* **66,** 807 – 815.

MAAN, A.C. & HOSEY, M.M. (1987). Analysis of the properties of binding of calcium-channel activators and inhibitors to dihydropyridine receptors in chick heart membranes. *Circ. Res.,* **61,** 379 – 388.

MARKS, A.R. (1992). Calcium channels expressed in vascular smooth muscle. *Circulation,* **86** (suppl III): III-61 – III-67.

MARKS, A.R. (1997). Intracellular calcium-release channels: regulators of cell life and death. *Am. J. Physiol.,* **272,** (Heart Circ. Physiol., 41), H597 – H605.

MCPHERSON, P.S. & CAMPBELL, K.P. (1993). The ryanodine receptor/Ca^{2+} release channel. *J. Biol. Chem.,* **268,** 13765 – 13768.

MIYOSHI, Y. & NAKAYA, Y. (1991). Angiotensin II blocks ATP-sensitive K^+ channels in porcine coronary artery smooth muscle cells. *Biochem. Biophys. Res. Commun.,* **181,** 700 – 706.

NISHIZAWA, S., PETERSON, J.W., SHIMOYAMA, I., IWASAKI, K. & UEMURA, K. (1993). Therapeutic effect of a new immunosuppressant, FK-506, on vasospasm after subarachnoid hemorrhage. *Neurosurgery,* **32,** 986 – 992.

O'KEEFE, S.J., TAMURA, J., KINCAID, R.L., TOCCI, M.J. & O'NEILL, E.A. (1992). FK-506 and CsA-sensitive activtion of the interleukin-2 promoter by calcineurin. *Nature,* **357,** 692 – 694.

PACAUD, P., LOIRAND, G., BARON, A., MIRONNEAU, C. & MIRONNEAU, J. (1991). Ca^{2+} channel activation and membrane depolarization mediated by Cl^- channels in response to noradrenaline in vascular myocytes. *Br. J. Pharmacol.,* **104,** 1000 – 1006.

PAREKH, A.B. & PENNER, R. (1997). Store depletion and calcium influx. *Physiol. Rev.,* **77,** 901 – 930.

PUTNEY, J.J. & BIRD, G.S. (1993).The signal for capactitative calcium entry. *Cell,* **75,** 199 – 201.

PUTNEY, JR J.W. (1990). Capacitative calcium entry revisited. *Cell Calcium,* **11,** 611 – 624.

SCHUHMANN, K., ROMANIN, C., BAUMGARTNER, W. & GROSCHNER, K. (1997). Intracellular Ca^{2+} inhibits smooth muscle L-type Ca^{2+} channels by activation of protein phosphatase type 2B and by direct interaction with the channel. *J. Gen. Physiol.,* **110,** 503 – 513.

SCORNIK, F.S. & TORO, L. (1992). U46619, a thromboxane A2 agonist, inhibits K_{Ca} channel activity from pig coronary artery. *Am. J. Physiol.,* **262,** C708 – C713.

SHIMIZU, H., ITO, M., MIYAHARA, M., ICHIKAWA, K., OKUBO, S., KONISHI, T., NAKA, M., TANAKA, T., HIRANO, K., HARTSHORNE, D.J. & NAKANO, T. (1994). Characterization of the myosin-binding subunit of smooth muscle myosin phosphatase. *J. Biol. Chem.,* **269,** 30407 – 30411.

SOMLYO, A.P. & SOMLYO, A.V. (1994). Signal transduction and regulation in smooth muscle. *Nature,* **372,** 231 – 236.

STARZL, T.E., TODO, S., FUNG, J., DEMETRIS, A.J., VENKATARAMMAN, R. & JAIN, A. (1989). FK 506 for liver, kidney, and pancreas transplantation. *Lancet,* **2,** 1000 – 1004.

TIMERMAN, A.P., OGUNBUMNI, E., FREUND, E., WIEDERRECHT, G., MARKS, A.R. & FLEISCHER, S. (1993). The calcium release channel of sarcoplasmic reticulum is modulated by FK-506-binding protein. *J. Biol. Chem.,* **268,** 22992 – 22999.

(Received May 29, 1998
Revised November 2, 1998
Accepted November 6, 1998)

British Journal of Pharmacology (1999) 126, 730–734
http://www.stockton-press.co.uk/bjp

Effects of vitamin C and of a cell permeable superoxide dismutase mimetic on acute lipoprotein induced endothelial dysfunction in rabbit aortic rings

[1]L. Fontana, [1]K.L. McNeill, [1]J.M. Ritter & *,[1]P.J. Chowienczyk

[1]Department of Clinical Pharmacology, Guy's, King's and St Thomas' School of Biomedical Sciences, St Thomas' Hospital, Lambeth Palace Road, London SE1 7EH, England

1 Low density lipoprotein (LDL) inhibits endothelium-dependent relaxation. The mechanism is uncertain, but increased production of superoxide anion O_2^- with inactivation of endothelium-derived NO and formation of toxic free radical species have been implicated. We investigated effects of the cell permeable superoxide dismutase mimetic manganese (III) tetrakis (1-methyl-4-pyridyl) porphyrin (MnTMPyP), the free radical scavenger vitamin C and arginine (which may reduce O_2^- formation) on acute LDL-induced endothelial dysfunction in rabbit aortic rings, using LDL prepared by ultracentrifugation of plasma from healthy men and aortic rings from New Zealand white rabbits.

2 LDL (150 μg protein ml^{-1} for 20 min) markedly inhibited relaxation of aortic rings (in Krebs' solution at 37°C and pre-constricted to 80% maximum tension with noradrenaline) to acetylcholine $82 \pm 10\%$ (mean percentage difference between sum of relaxations after each concentration of acetylcholine in the presence and absence of LDL, $\pm$s.e.mean, $n=26$, $P<0.001$) but not to the endothelium-independent agonist nitroprusside.

3 MnTMPyP (10 μM) reduced inhibitory effects of LDL from 124 ± 27 to $56 \pm 17\%$ ($n=6$, $P<0.05$).

4 Vitamin C (1 mM) reduced inhibitory effects of LDL from 59 ± 8 to $22 \pm 5\%$ ($n=6$, $P<0.05$).

5 Inhibitory effects of LDL were similar in the absence or presence of arginine (84 ± 12 *vs* $79 \pm 16\%$, $n=14$, $P=0.55$). Effects of L-arginine (10 mM) did not differ significantly from those of D-arginine (10 mM).

6 Acute (20 min) exposure of aortic rings to LDL impairs endothelium-dependent relaxation which can be partially restored by MnTMPyP and vitamin C. This is consistent with LDL causing increased O_2^- generation.

Keywords: Antioxidants; arginine; endothelium; low density lipoprotein; nitric oxide; oxidative stress; superoxide anion; superoxide dismutase; vitamin C

Abbreviations: cNOS, constitutive NO synthase; LDL, low density lipoprotein; MnTMPyP, manganese (III) tetrakis (1-methyl-4-pyridyl) porphyrin; NO, nitric oxide; O_2^-, superoxide anion; SOD, superoxide dismutase; TBARS, thiobarbituric acid reactive substances

Introduction

Low-density lipoprotein (LDL) acutely inhibits endothelium-dependent relaxation in rabbit aortic rings (Jacobs *et al*., 1990) and, in men with increased serum concentrations of LDL-cholesterol, impaired endothelium-dependent relaxation occurs before development of structurally apparent atherosclerotic lesions (Chowienczyk *et al*., 1992; Zeiher *et al*., 1991). Since endothelium-derived relaxing factors, nitric oxide (NO) in particular, have antiatherogenic actions (Cooke & Tsao, 1994), LDL induced endothelial dysfunction may play a causal role in atherogenesis. The mechanism whereby LDL inhibits endothelium-dependent relaxation remains uncertain, but may involve increased formation of superoxide anion (O_2^-) (Ohara *et al*., 1993) with consequent inactivation of NO (Gryglewski *et al*., 1986). However Cu-Zn superoxide dismutase (SOD) does not restore endothelial function either *in vitro* following acute exposure to LDL (Plane *et al*., 1993) or *in vivo* (García *et al*., 1995). This may be because Cu-Zn SOD does not gain access to intracellular O_2^-. To elucidate the role of O_2^- in lipoprotein induced endothelial dysfunction we examined effects of the cell permeable superoxide dismutase (SOD) mimetic manganese (III) tetrakis (1-methyl-4-pyridyl) porphyrin (MnTMPyP) on the inhibitory effects of LDL on endothelium-dependent relaxation in an isolated rabbit aortic ring preparation. We also examined effects of vitamin C which may be effective in scavenging intra- and extra-cellular O_2^- (Som *et al*., 1983; Halliwell & Gutteridge, 1989). Acute administration of L-arginine restores endothelium-dependent relaxation in both hypercholesterolaemic animals (Cooke *et al*., 1991) and humans (Drexler *et al*., 1991), possibly as a result of decreasing O_2^- production by constitutive NO synthase (cNOS) (Pritchard *et al*., 1995) or by an antioxidant effect (Nagasee *et al*., 1997). An antioxidant effect has been seen with both L- and D-arginine (Nagasee *et al*., 1997) whereas the effect on cNOS is assumed to be specific to L-arginine. We, therefore, examined the ability of L- and D-arginine to prevent inhibitory effects of LDL on endothelium-dependent relaxation in this preparation.

Methods

Preparation of lipoproteins

Native LDL was isolated from healthy men (aged 24–55 years). Venous blood was collected into vacutainers containing

* Author for correspondence; E-mail: p.chowienczyk@umds.ac.uk

EDTA. Plasma was separated by low-speed centrifugation at 4°C and LDL (density, 1.019–1.063 g ml^{-1}) then isolated from the plasma by discontinuous density gradient ultracentrifugation (Chung *et al.*, 1980). Isolated LDL was then dialysed with continuous stirring at 4°C for 24 h against two changes of 10 mM phosphate buffer solution (pH 7.4). The protein concentration was measured (Lowry *et al.*, 1951) and the final concentration of LDL expressed as μg protein ml^{-1}. Oxidative modification of LDL was prevented by the inclusion of EDTA (0.3 mM) in all buffers (Jacobs *et al.*, 1990). Oxidation of LDL was sought by measurement of thiobarbituric acid reactive substances (TBARS) (Yagi, 1976). TBARS were below the limit of detection being less than 1% of values obtained when samples were oxidized by exposure to Cu^{2+} ($CuSO_4$, 1.7 μM) for 3 h.

Experimental protocols

New Zealand white male rabbits (2–2.5 Kg) were sacrificed to obtain the descending thoracic aorta, which were trimmed of adhering tissue and fat. Transverse 2-mm-wide rings were cut and mounted in 3-ml organ baths containing oxygenated Krebs' solution (+EDTA, 0.3 mM), at 37°C. Tissues were placed under 2 g resting tension for 60 min and tension adjusted to 2 g for a further 30 min. Isometric measurements were recorded *via* force transducers (Grass FT03, Austria). Tissues were contracted with increasing doses of noradrenaline (0.06–0.12 μM) to determine a concentration which gave 80% maximum contraction. Repeated (2–4) exposures to this concentration were performed to establish that reproducible contractions were obtained. Relaxation dose-response curves to acetylcholine (10^{-8}–10^{-5} M) were then obtained. Following washout, preconstriction with noradrenaline and relaxation to acetylcholine were repeated during incubation with MnTMPyP (10 μM) alone, LDL (150 μg protein ml^{-1}) alone and LDL with MnTMPyP. After a final washout preconstriction and relaxation to acetylcholine was repeated to ensure that baseline responses were maintained over the time course of the experiment. Similar experiments were performed using vitamin C (1 mM), L-arginine (10 mM) and D-arginine (10 mM). A similar protocol was also used to examine effects of LDL on relaxation to nitroprusside as a non endothelium-dependent control. Doses of MnTMPyP and vitamin C were chosen as the maximum dose which, in pilot studies, had no inhibitory effects on relaxation to acetylcholine. Effects of Cu-Zn SOD (20 units ml^{-1}) were examined in these pilot studies; it was found to have no effect on relaxation to acetylcholine in the presence or absence of LDL.

Data analysis and statistical methods

Results are expressed as means±s.e.mean. The following summary measures were used to express inhibitory effects of drugs (D) alone, LDL (L) alone and LDL in the presence of drugs on percentage relaxation to acetylcholine (R_{ACh}):

$$\%\text{inhibition by drug alone} = [(\Sigma R_{ACh} - \Sigma R_{ACh+D})/\Sigma R_{ACh}] \times 100\%$$

$$\%\text{inhibition by LDL alone} = [(\Sigma R_{ACh} - \Sigma R_{ACh+L})/\Sigma R_{ACh}] \times 100\%$$

$$\%\text{inhibition by LDL in presence of drug} = [(\Sigma R_{ACh+D} - \Sigma R_{ACh+D+L})/\Sigma R_{ACh+D}] \times 100\%$$

where ΣR_{ACh} is the sum of relaxations to each dose of acetylcholine. In addition we calculated values of EC_{50} and E_{max} for the acetylcholine relaxation curves. Differences in these summary statistics between the different drugs were sought using one way analysis of variance (ANOVA). Repeated measures ANOVA was used to assess whether inhibitory properties of LDL differed in the presence or absence of drugs and whether this effect differed between the different drugs. A non-parametric test (paired sign) was also used to test whether inhibitory effects of LDL differed in the presence and absence of each of the drugs. Differences were considered significant if $P<0.05$.

Results

In all experiments incubation with LDL markedly inhibited relaxation to acetylcholine (Figures 1–4). The mean inhibition for all experiments was 82±9.8% ($n=26$, $P<0.001$) and did not differ significantly between experiments in which different drugs (MnTMPyP, vitamin C, arginine) were used. Incubation with LDL did not significantly inhibit relaxation to nitroprusside (per cent inhibition 14±6%, $n=6$, Figure 5). Relaxation to acetylcholine was significantly reduced after incubation with drugs (MnTMPyP, vitamin C, arginine) alone (mean inhibition for all drugs: 18±2%, $n=26$, $P<0.001$). However, the magnitude of the effect was small in comparison with the inhibition produced by LDL (82 *vs* 18%, $P<0.001$) and did

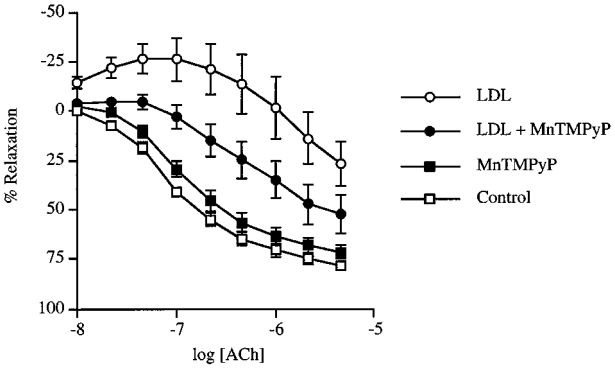

Figure 1 Relaxation of pre-contracted rabbit aortic rings ($n=6$) to acetylcholine at baseline and after 20 min incubation with the cell permeable SOD mimetic manganese (III) tetrakis (1-methyl-4-pyridyl) porphyrin (MnTMPyP) alone (10 μM), LDL alone (150 μg protein ml^{-1}) and LDL plus MnTMPyP.

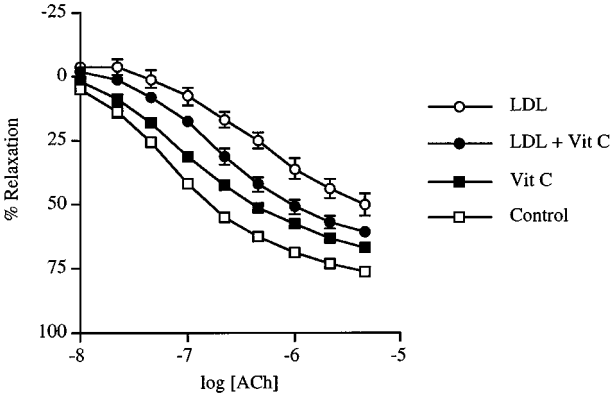

Figure 2 Relaxation of pre-contracted rabbit aortic rings ($n=6$) to acetylcholine at baseline and after 20 min incubation with vitamin C alone (1 mM), LDL alone (150 μg protein ml^{-1}) and LDL plus vitamin C.

not differ significantly for different drugs. Inhibitory effects of LDL were, overall, less marked in the presence of the drugs (MnTMPyP, vitamin C, arginine: $P<0.001$, for all drugs). There was a significant difference between drugs in their effects on preventing inhibition by LDL ($P<0.01$). MnTMPyP produced the most marked effects reducing inhibitory effects of LDL from 124 ± 27 to $56\pm17\%$ ($n=6$, $P<0.05$, Figure 1). Vitamin C also reduced inhibitory effects of LDL from 59 ± 8 to $22\pm5\%$ ($n=6$, $P<0.05$, Figure 2). Inhibitory effects of LDL were similar in the absence or presence of L-arginine (78 ± 12 *vs* $77\pm22\%$, $n=8$, Figure 3) and in the absence or presence of D-arginine (92 ± 24 *vs* $80\pm26\%$, $n=6$, Figure 4). MnTMPyP reduced the change in EC_{50} following incubation with LDL (3.4 ± 0.76 μM in the absence and 0.67 ± 0.24 μM in the presence of MnTMPyP, $n=6$, $P<0.01$) and the change in E_{max} ($51.3\pm10.9\%$ in the absence and $19.9\pm8.2\%$ in the presence of MnTMPyP, $n=6$, $P<0.05$). Vitamin C also reduced the change in EC_{50} following incubation with LDL (0.54 ± 0.17 μM in the absence and 0.14 ± 0.03 μM in the presence of vitamin C, $n=6$, $P<0.05$) and the change in E_{max} ($26.2\pm5.8\%$ in the absence and $6.1\pm2.2\%$ in the presence of vitamin C, $n=6$, $P<0.01$). L- and D-arginine had no significant effect on the change in EC_{50} or E_{max} induced by LDL. Non-parametric testing confirmed significant effects of MnTMPyP and vitamin C but not L- or D-arginine on each measure of LDL induced inhibition of relaxation. Following the final washout and pre-contraction with noradrenaline, relaxation responses to each dose of acetylcholine were not significantly different from those obtained at baseline.

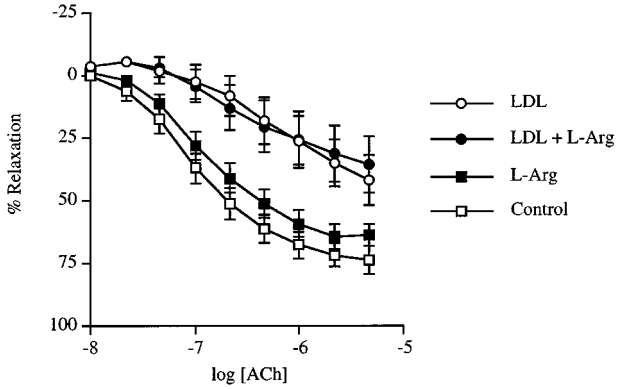

Figure 3 Relaxation of pre-contracted rabbit aortic rings ($n=8$) to acetylcholine at baseline and after 20 min incubation with L-arginine alone (10 mM), LDL alone (150 μg protein ml^{-1}) and LDL plus L-arginine.

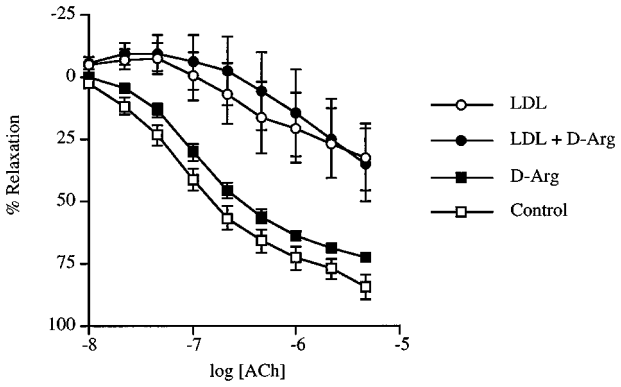

Figure 4 Relaxation of pre-contracted rabbit aortic rings ($n=6$) to acetylcholine at baseline and after 20 min incubation with D-arginine alone (10 mM), LDL alone (150 μg protein ml^{-1}) and LDL plus D-arginine.

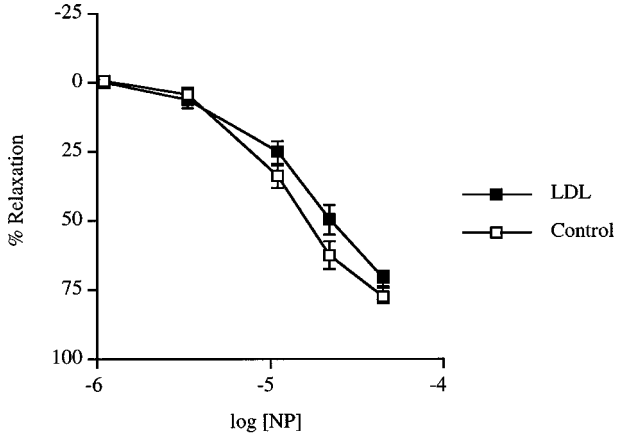

Figure 5 Relaxation of pre-contracted rabbit aortic rings ($n=6$) to sodium nitroprusside before and after 20 min incubation with LDL (150 μg protein ml^{-1}).

Discussion

We have examined effects of lipoproteins on endothelium-dependent relaxation in vessels not previously exposed to raised concentrations of LDL. This allows an important distinction between acute effects of LDL and those related to established hypercholesterolaemia. In the latter condition responsiveness to endothelium-dependent and -independent agonists may be influenced by development of atherosclerosis (Verbeuren *et al*., 1986) and the oxidation of LDL within the vessel wall which may influence signal transduction mechanisms (Liao & Clark, 1995) and the expression of NO synthase (Liao *et al*., 1995; Hirata *et al*., 1995). Our findings that incubation of rabbit aortic rings with native LDL for 20 min inhibits relaxation to acetylcholine but not relaxation to nitroprusside are in agreement with those of other investigators (Jacobs *et al*., 1990; Plane *et al*., 1993). Inhibitory effects of LDL were seen at a lower concentration (150 μg protein ml^{-1}, within the physiological range for the rabbit) of LDL than those used in most previous studies ($\geqslant 500$ μg protein ml^{-1}) and although not as marked were highly significant. The LDL used in this study was likely to be representative of native LDL because it was protected from oxidation and no oxidation products (TBARS) were detectable. Furthermore the characteristics of the inhibition were similar to those reported by other investigators (Jacobs *et al*., 1990; Plane *et al*., 1993) for native LDL. In contrast to the inhibitory properties of native LDL observed in this study, oxidized LDL produces an inhibition of relaxation to acetylcholine which is only partially reversible and it also inhibits relaxation to nitrovasodilators (Jacobs *et al*., 1990). We cannot, however, exclude the presence of minor degrees of oxidation. Variations in the initial state of spontaneous oxidation and in the antioxidant content of the LDL (obtained from different donors) may have accounted for the variability in inhibitory effects of LDL which tended to be greater in the experiments on MnTMPyP. These factors might also explain why not all investigators have observed inhibitory effects of LDL on endothelium-dependent relaxation (Galle *et al*., 1995). In experiments where LDL produced greater inhibitory effects some contraction was observed in response

to acetylcholine. This may have resulted from unopposed actions of endothelium derived constricting factors such as prostaglandin H_2 (Kato *et al*., 1990).

The major novel finding of the present study is that, in contrast to Cu-Zn SOD (Plane *et al*., 1993), the cell permeable SOD mimetic MnTMPyP attenuates the inhibitory effect of LDL on endothelium-dependent relaxation. MnTMPyP is capable of catalyzing the dismutation of O_2^- *in vitro* with a rate constant $\sim 10^7$ M^{-1} s^{-1} and *in vivo* the reduced form of MnTMPyP combines with O_2^- with a rate constant $\sim 10^9$ M^{-1} s^{-1} (Faulkner *et al*., 1994). The effect of MnTMPyP supports the possibility that intracellular generation of O_2^- is responsible, at least in part, for LDL induced endothelial dysfunction. Our findings are consistent with the recent report that, in contrast to authentic SOD, membrane permeable SOD mimetics are capable of restoring endothelium-dependent relaxation following inhibition by an intracellular oxidant stress (MacKenzie & Martin, 1998). The non-enzymic antioxidant vitamin C is also capable of scavenging O_2^- (Som *et al*., 1983). In the present study we found that a high dose of vitamin C partially reversed LDL induced impairment of endothelium-dependent relaxation. The effect was less striking than that obtained with MnTMPyP, perhaps because at this dose vitamin C produced some impairment of endothelium-dependent relaxation in the absence of LDL. In pilot studies we found that higher doses of both vitamin C and MnTMPyP markedly inhibited relaxation to acetylcholine. We do not have a ready explanation for this effect but speculate that, at high concentrations, these antioxidants react directly with NO thus impairing endothelium-dependent relaxation as has been demonstrated in the case of α-tocopherol (Keaney *et al*., 1994). Our findings are consistent with the observation that brachial artery infusion of vitamin C to achieve concentrations within the forearm that approximate 1 mM improves endothelial function within forearm vasculature of hypercholesterolaemic subjects (Ting *et al*., 1996) whereas oral administration of vitamin C (producing only a modest increase in plasma concentrations) does not improve endothelial function in such subjects (Gilligan *et al*., 1994).

One possible source of O_2^- in hypercholesterolaemia is cNOS: when cultured endothelial cells are incubated with LDL for 4 days the activity of cNOS remains constant but NO production decreases and O_2^- generation increases. This is thought to be due to uncoupling of electron transport within cNOS with cNOS catalyzing formation of O_2^- rather than NO (Pritchard *et al*., 1995). The effect is reversed by increasing concentrations of L-arginine. Administration of L-arginine *in vivo* to the cholesterol-fed rabbit (Cooke *et al*., 1991) and to hypercholesterolaemic patients (Drexler *et al*., 1991; Chowienczyk *et al*., 1994) is capable of restoring endothelial function. D-arginine also has potential antioxidant activity (Nagasee *et al*., 1997) and in one clinical study tended to improve endothelial function in hypercholesterolaemic patients (Casino *et al*., 1994). In the present study we found that L- and D- arginine at a dose similar to that used in *in vivo* studies was not effective in reversing endothelial dysfunction resulting from a short period of incubation with LDL. One possible reason for this discrepancy is that, over longer periods, LDL results in increased generation of an endogenous inhibitor of cNOS which competes with L-arginine as a substrate for cNOS (Vallance *et al*., 1992). Increased concentrations of such inhibitors have been demonstrated in cholesterol-fed rabbits (Yu *et al*., 1994; Bode-Böger *et al*., 1996). The restoration of endothelial function by MnTMPyP but not by L-arginine in the present preparation suggests that cNOS may not be the source of the O_2^-. Superoxide-generating systems involving xanthine oxidase and NADH oxidoreductase have been described in rabbit aortic and bovine coronary endothelium (Ohara *et al*., 1993; Mohazzab-H *et al*., 1994). In the aorta of normocholesterolaemic rabbits the major source of O_2^- is an NADPH oxidase located in medial smooth muscle and adventitia (Pagano *et al*., 1995). However in hypercholesterolaemic rabbits increased O_2^- derives mainly from the endothelium (Ohara *et al*., 1993). It is likely, therefore, that lipoproteins stimulate the activity of one or more of these systems or, alternatively, that endogenous SOD activity is compromised.

In conclusion we have demonstrated that the cell permeable SOD mimetic MnTMPyP attenuates the inhibitory effects of LDL on endothelium-dependent relaxation. This suggests a possible therapeutic role for effective intracellular scavenging of O_2^-.

This work was supported by a Lilly Diabetes Grant.

References

BODE-BÖGER, S.M., BOGER, R.H., KIENKE, S., JUNKER, W. & FROLICH, J.C. (1996). Elevated L-arginine/dimethylarginine ratio contributes to enhanced systemic NO production by dietary L-arginine in hypercholesterolaemic rabbits. *Biochem. Biophys. Res. Commun.,* **219,** 598–603.

CASINO, P.R., KILCOYNE, C.M., QUYYUMI, A.A., HOEG, J.M. & PANZA, J.A. (1994). Investigation of decreased availibility of nitric oxide precursor as the mechanism responsible for impaired endothelium-dependent vasodilation in hypercholesterolaemic patients. *J. Am. Coll. Cardiol.,* **23,** 844–850.

CHOWIENCZYK, P.J., WATTS, G.F., COCKCROFT, J.R. & RITTER, J.M. (1992). Impaired endothelium-dependent vasodilation of forearm resistance vessels in hypercholesterolaemia. *Lancet,* **340,** 1430–1432.

CHOWIENCZYK, P.J., WATTS, G.F., COCKCROFT, J.R., BRETT, S.E. & RITTER, J.M. (1994). Sex differences in endothelial function in normal and hypercholesterolaemic subjects. *Lancet,* **344,** 305–306.

CHUNG, B.H., WILKINSON, T., GREER, J.C. & SEGREST, J.P. (1980). Preparative and quantitative isolation of plasma lipoproteins: rapid, single discontinuous density gradient ultracentrifugation in a vertical rotor. *J. Lipid Res.,* **21,** 284–291.

COOKE, J.P., ANDON, N.A., GIRERD, X.J., HIRSCH, A.T. & CREAGER, M.A. (1991). Arginine restores cholinergic relaxation of hypercholesterolaemic rabbit thoracic aorta. *Circulation,* **83,** 1057–1062.

COOKE, J.P. & TSAO, P.S. (1994). Is NO an endogenous antiatherogenic molecule? *Arterioscler. Thromb.,* **14,** 653–655.

DREXLER, H., ZEIHER, A.M., MEINZER, K. & JUST, H. (1991). Correction of endothelial dysfunction in the coronary microcirculation of hypercholesterolaemic patients by L-arginine. *Lancet,* **338,** 1546–1550.

FAULKNER, K.M., LIOCHEV, S.I. & FRIDOVICH, I. (1994). Stable Mn(III) porphyrins mimic superoxide dismutase *in vitro* and substitute for it *in vivo*. *J. Biol. Chem.,* **23,** 23471–23476.

GALLE, J., BENGEN, J., SCHOLLMEYER, P. & WANNER, C. (1995). Impairment of endothelium-dependent dilation in rabbit by oxidised lipoprotein(a). Role of oxygen-derived radicals. *Circulation,* **92,** 1582–1589.

GARCÍA, C.E., KILCOYNE, C.M., CARDILLO, C., CANNON III, R.O., QUYYUMI, A.A. & PANZA, J.A. (1995). Effect of copper-zinc superoxide dismutase on endothelium-dependent vasodilation in patients with essential hypertension. *Hypertension,* **26,** 863–868.

GILLIGAN, D.M., SACK, M.N., GUETTA, V., CASINO, P.R., QUYYUMI, A.A., RADER, D.J., PANZA, J.A. & CANNON III, R.O. (1994). Effect of antioxidant vitamins on low density lipoprotein oxidation and impaired endothelium-dependent vasodilation in patients with hypercholesterolaemia. *J. Am. Coll. Cardiol.,* **24,** 1611 – 1617.

GRYGLEWSKI, R.J., PALMER, R.M.J. & MONCADA, S. (1986). Superoxide anion is involved in the breakdown of endothelium-derived relaxing factor. *Nature,* **320,** 454 – 456.

HALLIWELL, B. & GUTTERIDGE, M.C. (1989). *Free radicals in biology and medicine*, 2nd edn., p. 137, Oxford, Clarendon Press.

HIRATA, K., MIKI, N., KURODA, Y., SAKODA, T., KAWASHIMA, S. & YOKOYAMA, M. (1995). Low concentrations of oxidized low-density lipoprotein and lysophosphatidylcholine upregulate constitutive nitric oxide mRNA expression in bovine aortic endothelial cells. *Circ. Res.,* **76,** 958 – 962.

JACOBS, M., PLANE, F. & BRUCKDORFER, K.R. (1990). Native and oxidized low-density lipoproteins have different inhibitory effects on endothelium-derived relaxing factor in rabbit aorta. *Br. J. Pharmacol.,* **100,** 21 – 26.

KATO, T., IWAMA, Y., OKUMURA, K., HASHIMOTO, H., ITO, T. & SATAKE, T. (1990). Prostaglandin H_2 may be the endothelium-derived contracting factor released by acetylcholine in the aorta of the rat. *Hypertension,* **15,** 475 – 481.

KEANEY, JR. J.F., GAZIANO, J.M. & XU, A. (1994). Low-dose α-tocopherol improves and high dose α-tocopherol worsens endothelial vasodilator function in cholesterol fed rabbits. *J. Clin. Invest.,* **93,** 844 – 851.

LIAO, J.K. & CLARK, S.L. (1995). Regulation of G protein α_{i2} subunit expression by oxidised low-density lipoprotein. *J. Clin. Invest.,* **95,** 1457 – 1463.

LIAO, J.K., SHIN, W.S., LEE, W.Y. & CLARK, S.L. (1995). Oxidised low density lipoprotein decreases the expression of endothelial nitric oxide synthase. *J. Biol. Chem.,* **270,** 319 – 324.

LOWRY, O.H., ROSEBROUGH, N.J., FARR, A.L. & RANDALL, R.J. (1951). Protein measurement with the folin phenol reagent. *J. Biol. Chem.,* **193,** 265 – 275.

MACKENZIE, A. & MARTIN, W. (1998). Loss of endothelium-derived nitric oxide in rabbit aorta by oxidant stress: restoration by superoxide dismutase mimetics. *Br. J. Pharmacol.,* **124,** 719 – 728.

MOHAZZAB-H, K.M., KAMINSKI, P.M. & WOLIN, M.S. (1994). NADH oxidoreductase is a major source of superoxide anion in bovine coronary artery endothelium. *Am. J. Physiol.,* **35,** H2568 – H2572.

NAGASEE, S., TAKEMURA, K., UEDA, A., HIRAYAMA, A., AOYAGI, K., KONDOH, M. & KOYAMA, A. (1997). A novel nonenzymatic pathway for the generation of nitric oxide by the reaction of hydrogen peroxide and D- or L-arginine. *Biochem. Biophys. Res. Commun.,* **233,** 150 – 153.

OHARA, Y., PETERSON, T.E. & HARRISON, D.G. (1993). Hypercholesterolaemia increases endothelial superoxide anion production. *J. Clin. Invest.,* **91,** 2546 – 2551.

PAGANO, P.J., ITO, Y., TORNHEIM, K., GALLOP, P.M., TAUBER, A.I. & COHEN, R.A. (1995). An NADPH oxidase superoxide-generating system in rabbit aorta. *Am. J. Physiol.,* **268,** H2274 – H2280.

PLANE, F., JACOBS, M., MCMANUS, D. & BRUCKDORFER, K.R. (1993). Probucol and other antioxidants prevent the inhibition of endothelium-dependent relaxation by low density lipoproteins. *Atherosclerosis,* **103,** 73 – 79.

PRITCHARD, K.A., GROSZEK, L., SMALLEY, D.M., SESSA, W.C., WU, M., VILLALON, P., WOLIN, M.S. & STEMERMAN, M.B. (1995). Native low-density lipoprotein increases endothelial cell nitric oxide synthase generation of superoxide anion. *Circ. Res.,* **77,** 510 – 518.

SOM, S., RAHA, C. & CHATTERJEE, I.B. (1983). Ascorbic acid: a scavenger of superoxide radical. *Acta. Vitaminol. Enzymol.,* **5,** 243 – 250.

TING, H.H., TIMIMI, F.K., HALEY, E.A., RODDY, M-A., GANZ, P. & CREAGER, M.A. (1996). Vitamin C restores endothelium-dependent vasodilation in patients with hypercholesterolaemia. *Circulation,* **94,** I402.

VALLANCE, P., LEONE, A., CALVER, A., COLLIER, J. & MONCADA, S. (1992). Accumulation of an endogenous inhibitor of nitric oxide synthesis in chronic renal failure. *Lancet*, **339,** 572 – 575.

VERBEUREN, T.J., JORDAENS, F.H., ZONNEKEYN, L.L., VAN HOVE, C.E., COENE, M.-C. & HERMAN, A.G. (1986). Effect of hypercholesterolaemia on vascular reactivity in the rabbit. *Circ. Res.,* **58,** 552 – 564.

YAGI, K. (1976). A simple fluorometric assay for lipoperoxide in blood plasma. *Biochemical Medicine,* **15,** 212 – 216.

YU, X., LI, Y. & XIONG, Y. (1994). Increase of an endogenous inhibitor of nitric oxide synthesis in serum of high cholesterol fed rabbits. *Life Sci.,* **54,** 753 – 758.

ZEIHER, A.M., DREXLER, H., WOLLSCHLÄGER, H. & JUST, H. (1991). Modulation of coronary vasomotor tone in humans. Progressive endothelial dysfunction with different early stages of coronary atherosclerosis. *Circulation,* **83,** 391 – 401.

(Received July 9, 1998
Revised September 23, 1998
Accepted November 3, 1998)

British Journal of Pharmacology (1999) 126, 735–745
http://www.stockton-press.co.uk/bjp

Roles of threonine 192 and asparagine 382 in agonist and antagonist interactions with M_1 muscarinic receptors

[1]Xi-Ping Huang, [1]Peter I. Nagy, [1]Frederick E. Williams, [1]Steven M. Peseckis & *,[1]William S. Messer, Jr

[1]Center for Drug Design and Development, Department of Medicinal & Biological Chemistry, College of Pharmacy, The University of Toledo, 2801 W. Bancroft St., Toledo, Ohio 43606-3390, U.S.A.

1 Conserved amino acids, such as Thr in transmembrane domains (TM) V and Asn in TM VI of muscarinic receptors, may be important in agonist binding and/or receptor activation. In order to determine the functional roles of Thr192 and Asn382 in human M_1 receptors in ligand binding and receptor activation processes, we created and characterized mutant receptors with Thr192 or Asn382 substituted by Ala.

2 HM_1 wild-type (WT) and mutant receptors [HM_1(Thr192Ala) and HM_1(Asn382Ala)] were stably expressed in A9 L cells. The K_d values for ^{3}H-(R)-QNB and K_i values for other classical muscarinic antagonists were similar at HM_1(WT) and HM_1(Thr192Ala) mutant receptors, yet higher at HM_1(Asn382Ala) mutant receptors. Carbachol exhibited lower potency and efficacy in stimulating PI hydrolysis *via* HM_1(Thr192Ala) mutant receptors, and intermediate agonist activity at the HM_1(Asn382Ala) mutant receptors.

3 The Asn382 residue in TM VI but not the Thr192 residue in TM V of the human M_1 receptor appears to participate directly in antagonist binding. Both Thr192 and Asn382 residues are involved differentially in agonist binding and/or receptor activation processes, yet the Asn382 residue is less important than Thr192 in agonist activation of M_1 receptors.

4 Molecular modelling studies indicate that substitution of Thr192 or Asn382 results in the loss of hydrogen-bond interactions and changes in the agonist binding mode associated with an increase in hydrophobic interactions between ligand and receptor.

Keywords: Acetylcholine; arecoline; carbachol; G-protein coupling; M_1 receptor; molecular modelling; muscarinic receptors; oxotremorine-M; phosphatidylinositol turnover; site-directed mutagenesis

Abbreviations: ACh, acetylcholine; APE, arecaidine propagyl ester hydrobromide; 4-DAMP, 4-diphenylacetoxy-N-methylpiperidine methiodide; DMEM, Dulbecco's Modified Eagle Media; EB, binding energy; FBS, foetal bovine serum; GppNHp, guanylylimidodiphosphate; p-F-HHSiD, p-fluoro-hexahydro-sila-difenidol hydrochloride; HM_1, human muscarinic acetylcholine receptor subtype 1; HM_1(Asn382Ala), HM_1 mutant receptor with the mutation of Asn382 to Ala; HM_1(Thr192Ala), HM_1 mutant receptor with the mutation of Thr192 to Ala; KH buffer, Krebs-Henseleit buffer; NMS, N-methyl-scopolamine; PI, phosphatidylinositol; QNB, 3-quinuclidinyl benzilate; TM, Transmembrane; WT, wild-type.

Introduction

Muscarinic acetylcholine receptors are members of the large G protein-coupled receptor family featuring seven transmembrane domains, an extracellular N-terminus and an intracellular C-terminus. In humans, five receptor subtypes (M_1 to M_5) Caulfield & Birdsall, 1998) have been cloned thus far. The M_1, M_3 and M_5 mainly couple to the activation of phospholipase C_β through the pertussis toxin-insensitive $G_{q/11}$ family of G proteins; while M_2 and M_4 preferentially couple to the inhibition of adenylyl cyclase through the pertussis toxin-sensitive $G_{i/0}$ family of G proteins (Hulme *et al*., 1990; Caulfield, 1993). The molecular mechanisms involved in ligand binding and receptor activation processes have been intensively investigated for many years, yet remain unclear (for recent reviews, see Wess 1996; 1997).

Previous molecular modelling studies predicted that conserved amino acids in TM domains of muscarinic receptors, such as an Asp residue in TM III, a Thr residue in TM V, and Asn and Tyr residues in TM VI (see Table 1), were involved in agonist binding and/or receptor activation processes (Trumpp-Kallmeyer *et al*., 1992; Ward *et al*., 1992; Nordvall & Hacksell, 1993). The Asp residue is highly conserved within all G-protein coupled receptors that bind biogenic amines. The carboxylate side chain of the Asp residue serves as a counterion for the quaternary amine headgroup of biogenic amine ligands (Hulme *et al*., 1990; Fraser *et al*., 1994; Schwarz *et al*., 1995). Binding of the endogenous muscarinic agonist acetylcholine (ACh) is initiated by an ion-ion interaction between the negatively charged Asp residue in TM III and the positively charged quaternary amine (Wess *et al*., 1991; 1992; Blüml *et al*., 1994). In addition, other interactions, such as hydrogen-bond and/or hydrophobic interactions between conserved residues and the ester moiety, might be responsible for the selective receptor activation processes. Using site-directed mutagenesis technology and pharmacological studies, Wess and colleagues identified Thr234 in TM V and Tyr506 in TM VI of rat M_3 receptors as important residues in agonist binding and receptor activation processes (Wess *et al*., 1991; 1992). The Thr234 in rat M_3 receptors is equivalent to the Thr192 in M_1 receptors (Table 1). Using Cys scanning mutagenesis, the Thr192 residue was identified to be involved in ACh binding interactions with the acetyl methyl group of ACh (Allman *et al*., 1997). In

* Author for correspondence.

Table 1 Conserved amino acid residues involved in ligand interactions by molecular modelling studies (Trumpp-Kallmeyer *et al*., 1992; Nordvall & Hacksell, 1993; 1995)

Receptor	*Position*	*TM III (part)*	*Position*	*TM V (part)*	*Position*	*TM VI (part)*
Human M_1	105	LAL**D**YVA	192	TFG**T**AMA	382	TPY**N**IMV
Human M_2	103	LAL**D**YVA	190	TFG**T**AIA	404	APY**N**VMV
Rat M_3	147	LSI**D**YVA	234	TFG**T**AIA	507	TPY**N**IMV
Human M_3	148	LAI**D**YVA	235	TFG**T**AIA	508	TPY**N**IMV
Human M_4	112	LAL**D**YVV	199	TFG**T**AIA	417	TPY**N**VMV
Human M_5	110	LAL**D**YVA	197	TFG**T**AIA	459	TPY**N**IMV

Amino acid sequences were retrieved from Watson & Arkinstall (1994) and the GRAP mutant Database: http://mgddk1.niddk.nih.gov:8000/. Numbers indicate the position of the bold and underlined residue in each transmembrane domain.

contrast to the predicted roles by molecular modelling studies based on the M_1 subtype, Asn507 in TM VI of rat M_3 receptors was found to be critical for antagonist binding, yet less involved in agonist binding and receptor activation in COS-7 cells (Blüml *et al*., 1994). The Asn507 in rat M_3 receptors is equivalent to the Asn382 residue in M_1 receptors (Table 1). Previous attempts to determine the functional role of Asn382 in TM VI of M_1 receptors failed, reportedly due to a lack of measurable binding in membrane preparations from COS-7 cells in an Ala scanning mutagenesis study (Ward & Hulme, 1997), raising the possibility that mutation of Asn382 to Ala altered receptor expression and folding. There is a significant discrepancy between the results from three-dimensional molecular modelling studies and from site-directed mutagenesis and pharmacological studies. These discrepancies have received attention in discussions regarding the presumed roles of hydrogen-bond donors/acceptors in TM domains of monoamine receptors in agonist binding and receptor activation processes (Schwartz & Rosenkilde, 1996; Strange, 1996). Thus, further studies are required to investigate the functional role of this highly conserved Asn residue as a potential hydrogen-bond donor and/or acceptor in TM VI in ligand binding and receptor activation processes.

Selective muscarinic agonists may be useful for the treatment of Alzheimer's disease (Growdon, 1997). Understanding the molecular mechanism(s) involved in ligand binding and receptor activation processes would be helpful in designing and developing selective muscarinic agonists. In order to examine the functional roles of the Thr192 and Asn382 residues in HM_1 receptors in ligand binding and receptor activation processes, and to determine if they function as previously reported in rat M_3 receptors or as predicted in molecular modelling studies, a site-directed mutagenesis approach was used to replace Thr192 and Asn382 with Ala in HM_1 receptors. Stable A9 L cell lines expressing HM_1 wild-type [HM_1(WT)] or HM_1 mutant receptors [HM_1(Thr192Ala) and HM_1(Asn382Ala) receptors] were created, and characterized for their ligand binding properties and functional activities. The data reported here indicate that both Thr192 and Asn382 residues are involved in agonist binding and receptor activation processes as predicted in modelling studies, and that Asn382, but not Thr192, directly participates in antagonist binding as reported previously in rat M_3 receptors.

Methods

Materials

Plasmids HM_1pcD1 encoding the human M_1 muscarinic receptor and pcDneo were kindly provided by Dr Tom I. Bonner (NIH) (Bonner *et al*., 1988) and Dr Jürgen Wess (NIDDK), respectively. Dulbeco's Modified Eagle's Medium (DMEM) was purchased from GIBCO BRL (Grand Island, NY, U.S.A.). Foetal bovine serum (FBS) was ordered from HyClone (Logan, UT, U.S.A.). L-Glutamine and penicillin/streptomycins solutions were obtained from GIBCO BRL or Fisher (Pittsburgh, PA, U.S.A.). Geneticin (G418) was ordered from Sigma (St. Louis, MO, U.S.A.) or Fisher (Pittsburgh, PA, U.S.A.).

Acetylcholine, oxotremorine, oxotremorine-M, arecaidine propagyl ester hydrobromide (APE), and pirenzepine (Figure 2) were purchased from Research Biochemicals Intl. (RBI) (Natick, MA, U.S.A.). Carbachol, N-methyl-(−)-scopolamine, *l*-hyoscyamine, lithium chloride, 5′-guanylyl imidodiphosphate (GppNHp) were ordered from Sigma. Poly(ethylenimine) was from Aldrich (Milwaukee, WI, U.S.A.). Both *myo*-^{3}H-inositol and ^{3}H-(R)-quinuclidinyl benzilate (QNB) were purchased from Du Pont-New England Nuclear (Boston, MA, U.S.A.). All other inorganic chemicals were from Fisher.

The QuickChange site-directed mutagenesis kit was purchased from Stratagene (La Jolla, CA, U.S.A.). The Super Separator-24 and T7 Sequenase PCR product sequencing kit were obtained from Amersham (Arlington Heights, IL, U.S.A.). The QIAprep Spin Plasmid Mini- and the QIAGEN Plasmid Maxi-Kits were bought from QIAGEN (Chatsworth, CA, U.S.A). The LIPOFECTIN Reagent was obtained from GIBCO BRL. The SEP-PAK anion exchange cartridges were purchased from Waters (Franklin, MA, U.S.A.). UniverSol ES scintillation cocktail was ordered from ICN Biomedicals (Irvine, CA, U.S.A.). FP-100 Whatman GF/B filters were obtained from Brandel (Gaithersburg, MD, U.S.A.).

Site-directed mutagenesis and stable expression of HM_1(WT) and mutant receptors

Replacement of Thr192Ala in TM V or Asn382Ala in TM VI was carried out using the QuickChange Kit from Stratagene. For the Thr192 to Ala mutation, the sense primer was 5′-ATCACCTTTGGC**GC**CGCCATGGCTGCC-3′ with changed bases in bold, and the antisense primer was 5′-GGCAGCCATGGCGGCGCCAAAGGTGAT-3′. A unique restriction site (*Kas*I) was incorporated for convenient screening. For the Asn382 to Ala mutation, the sense primer was 5′-GACACCGTACG**CCA**TCATGGTGCTG-3′ with mutated bases in bold, the antisense primer was 5′-GCACCATGATGGCGTACGGTGTCCAG-3. A unique restriction site (*Bsi*WI) was incorporated for convenient screening. The mutations were confirmed by unique restriction digestion and dideoxy nucleotide sequencing. A9 L or CHO cells were cotransfected with HM_1pcD1 [or HM_1(Thr192Ala)-pcD1 or HM_1(Asn382Ala)pcD1] and pcDneo (Jürgen Wess, NIDDK) at a ratio of about 10 : 1 using LIPOFECTIN Reagents from GIBCO following the instructions provided by

the manufacturer. Selections were carried out in DMEM (supplemented with 10% FBS, 4 mM L-Glutamine, 50 u ml^{-1} Penicillin, and 50 $\mu g\ ml^{-1}$ Streptomycin) containing 600–800 $\mu g\ ml^{-1}$ Geneticin. Surviving cells were subcultured for functional tests and radioligand binding assays. The creation of stable A9 L cell lines expressing HM_1(WT) was described previously (Huang *et al*., 1998).

PI turnover assays

Cells stably expressing wild-type or mutant receptors were seeded into 24-well tissue culture plates and incubated with ^{3}H-inositol (1 μCi per well) for 48 h to about 80–90% confluence. The cells were washed twice with DMEM and incubated with 450 μl DMEM containing 10 mM LiCl for 30 min. Then 50 μl of different concentrations of test ligands were added in duplicate sets. The plates were incubated for 30 additional mins, and the incubation was terminated by removal of the mixture and addition of 0.75 ml of 5% TCA. The procedures for PI assays conducted in Krebs-Henseleit (KH) buffer were described (Huang *et al*., 1998). The radioactive inositol phosphates in lysate were isolated using SEP-PAK cartridge methods (Wreggett & Irvine, 1987) with minor modifications (Hoss *et al*., 1990). Briefly, the 5% TCA extracts were transferred to balanced SEP-PAK anion exchange cartridges (formate form). The cartridges were then washed with 6 ml distilled water and 10 ml of 5 mM disodium tetraborate. The radioactive ^{3}H-inositol phosphates were eluted from the cartridges by 1 ml of 0.6 M ammonium formate/0.06 M formic acid/5 mM disodium tetraborate (pH 4.75). Then 0.5 ml of eluate was counted in 6 ml of UniverSol ES scintillation cocktail on a 6895 BetaTrac Liquid Scintillation counter. The growth DMEM containing 10 mM LiCl served for determination of basal levels, and activities were presented as the percentage stimulation above basal levels.

Radioligand binding assays

Membrane homogenates were prepared from A9 L or CHO cells stably expressing wild-type or mutant receptors according to procedures reported previously (Dörje *et al*., 1991; Huang *et al*., 1998). Protein concentrations were determined by a modified Lowry method (Lowry *et al*., 1951; Markwell *et al*., 1981). Membrane homogenates were aliquoted and stored at -70°C. All binding assays were conducted in triplicate sets with a final volume of 1 ml. Eight different concentrations of ^{3}H-(R)-QNB were used in radioligand saturation binding assays; while 14 different concentrations of test ligand were used in ligand inhibition binding assays. Total binding and nonspecific binding activities were determined in the absence and presence of 1000 fold excess of cold (R)-QNB, respectively. Reactions started with the addition of membrane proteins to mixtures and were incubated at room temperature for 2 h in the binding buffer (25 mM sodium phosphate, pH 7.4, containing 5 mM magnesium chloride). G-protein coupling properties were examined in the presence of 100 μM GppNHp. The incubations were terminated by addition of 5 ml ice-cold binding buffer and rapid transfer to Whatman GF/B filters which were soaked with cold binding buffer containing 0.3% poly(ethylenimine) immediately before filtration.

Molecular modelling studies

The M_1 receptor model accepted here was proposed by Nordvall & Hacksell (1993). Previously we used a simplified approach (Messer *et al*., 1997) by 'cutting-out' nine amino acids, including Asp105 (TM III), Thr192 (TM V) and Asn382 (TM VI), which were considered to form a cavity for the agonist binding. In contrast, the full M_1 receptor model was utilized here. AMBER charges (Weiner *et al*., 1986) were added to the atoms, and the overall charge of the receptor model was set to zero by neutralizing some side chains on the molecular surface. Asp105 (TM III) in binding cavity bore a unit negative charge.

As described previously in the study with the 9-amino-acid model, molecular modelling for the docking of a ligand within the cavity was performed by using the DOCK procedure of the Sybyl 6.1 modelling package (Tripos, Inc.). The procedure minimizes the energy of the dimer formed of the receptor model and the ligand, by changing their relative positions and allowing geometric changes for both sites. The energy was calculated by using the Tripos molecular mechanics force-field. The minimum energy conformation of each ligand optimized previously was docked to the binding site. Atomic charges for the ligand were obtained from AM1 quantum-chemical calculations (Dewar *et al*., 1985) as implemented in Sybyl.

Energy terms for the dimer, E_D were broken down as follows:

$$E_D = E_L + E_R + E_{LR} \quad (1)$$

where E_L and E_R stand for the stretching, bending, torsional, intramolecular electrostatic or van der Waals energy terms for the ligand and the receptor, respectively, at the geometry taken in the dimer. E_{LR} stands for the ligand-receptor intermolecular energy terms. Applying equation 1, change of a specific term, dE(x), upon dimerization is given by

$$\begin{aligned} dE(x) &= E_D(x) - E_{Lopt}(x) - E_{Ropt}(x) \\ &= (E_L(x) - E_{Lopt}(x)) + (E_R - E_{Ropt}(x)) + E_{LR} \end{aligned} \quad (2)$$

where 'opt' terms refer to the 'x' energy type in the optimized ligand and receptor. The intermolecular term, E_{LR} differs from zero regarding only electrostatic (x = e) and van der Waals (x = W) energies (Table 6). E_{Ropt} was taken from minimization of the pure receptor model. Because of the complexity of its energy surface the found minimum corresponds most likely to a local one. Accordingly, the ($E_R - E_{Ropt}(x)$) terms differ by a constant from their correct values. The differences of these terms, Δ ($E_R - E_{Ropt}$ (x)), however, are correct with different ligands bound to the M_1 receptor model.

Data analysis

Nonlinear least squares curve-fitting was performed using DeltaGraph® version 4.0.1 for the Macintosh (DeltaPoint Inc. 1997). Dose-response data from functional assays were fitted into a one-site stimulation function to obtain S_{max} and EC_{50} values. ^{3}H-(R)-QNB saturation binding data were fitted into a one-site binding model for determining B_{max} and K_d values. Ligand inhibition binding data were fitted into one-site, two-site and three-site binding models. Statistical comparisons were carried out using an F test with P set at the 0.05 level. K_i values were converted from IC_{50} values according to the Cheng & Prusoff (1973) formula.

Results

Receptor expression and antagonist binding

As indicated in Table 2, HM_1(WT) receptors were expressed at relatively higher levels (3.5 fold) in CHO cells than in A9 L cells. HM_1(Thr192Ala) receptors were expressed at higher

levels (2.4 fold) in A9 L cells than in CHO cells. HM_1(Asn382Ala) receptors were generally expressed at relatively low levels both in A9 L cells and CHO cells. When expressed in either A9 L or CHO cells, HM_1(Thr192Ala) and HM_1(WT) receptors exhibited comparable binding affinities for ^{3}H-(R)-QNB, while HM_1(Asn382Ala) mutant receptors showed a marked reduction in binding affinity for ^{3}H-(R)-QNB. Generally, the Asn382Ala substitution produced much greater reductions in antagonist binding affinities than the Thr234Ala mutation (Table 3). Much greater reductions in binding affinities also were observed for structurally different muscarinic antagonists, such as NMS, trihexyphenidyl, and pirenzepine, at HM_1(Asn-382Ala) receptors expressed in A9 L cells (Figure 2). HM_1(Thr192Ala) receptors generally displayed similar binding profiles for these antagonists as HM_1(WT) receptors (Figure 2).

Receptor functional assays

Since A9 L cells provide a suitable system for determining muscarinic agonist activities and G-protein coupling interactions (Brann *et al*., 1987; Messer *et al*., 1997), mutant receptors were compared to HM_1(WT) receptors in A9 L cells for their abilities to mediate phosphatidylinositol (PI) metabolism (Figure 3 and Table 4). Generally, substitution of Thr192 or Asn382 with Ala resulted in different degrees of reduced efficacies and/or potencies for muscarinic agonists. Carbachol showed about 50 and 80% of HM_1(WT) activity at HM_1(Thr192Ala) and HM_1(Asn382Ala), respectively, with significant reductions in potency. The Thr192Ala mutation reduced efficacy and potency, while the Asn382Ala mutation decreased the potency of oxotremorine-M by 20 fold. The tetrahydropyrimidine ester derivative CDD-0034 displayed full agonist activity at HM_1(WT) but showed only 40% efficacies at both mutant receptors, together with significantly reduced potencies. The tetrahydropyrimidine oxadiazole derivative CDD-0102 exhibited decreased efficacies yet increased potencies at both mutant receptors as compared with HM_1(WT) receptors.

The muscarinic natural agonist ACh originally did not show significant stimulation at HM_1(WT) receptors. We then tested ACh and carbachol activities at HM_1(WT) and HM_1(Asn-382Ala) receptors using Krebs-Henseleit (KH) buffer as the incubation media. As indicated in Table 4, ACh exhibited a 10 fold reduction in potency yet with only a slightly lower maximum response at HM_1(Asn382Ala) than at HM_1(WT) receptors.

Interestingly, arecoline, a partial agonist at HM_1(WT) receptors, did not display any agonist activity at HM_1(Asn-382Ala) receptors, although it had almost the same binding affinity to HM_1(Asn382Ala) and HM_1(WT) receptors (see Table 5). To determine if arecoline functioned as an antagonist at HM_1(Asn382Ala) receptors, we tested PI hydrolysis stimulated by ACh in the presence of arecoline. ACh displayed unchanged maximal responses in the presence of 1, 3 and 10 μM of arecoline yet showed significant reduction of potency by 13.3, 18.6 and 22.4 fold, respectively. A Schild plot analysis (Figure 4B) yielded a pA_2 value of 2.8 for arecoline with Schild slope of 0.28.

Table 2 Stable expression of HM_1(WT) and two mutant receptors, HM_1(Thr192Ala) and HM_1(Asn382Ala), in A9 L and CHO cells

Receptor-cell line	B_{max} (fmol mg protein^{-1})	K_d (nM)
HM_1(WT)-A9 L	250±32	0.027±0.0057
HM_1(Thr192Ala)-A9 L	1800±76	0.023±0.0013
HM_1(Asn382Ala)-A9 L	220±30	0.42±0.12
HM_1(WT)-CHO	870±240	0.032±0.0058
HM_1(Thr192Ala)-CHO	760 (n=1)	0.022
HM_1(Asn382Ala)-CHO	85 (n=1)	0.31

Radioligand saturation binding assays were carried out on membrane homogenates in the presence of 5–300 pM of ^{3}H-(R)-QNB for HM_1(WT) and HM_1(Thr192Ala) receptors, and 10–3 nM of ^{3}H-(R)-QNB for HM_1(Asn382Ala) receptors. Data represent the means±s.e.mean from a minimum of three assays or as indicated. B_{max} = maximal specific binding per mg membrane proteins.

Agonist inhibition binding properties

Muscarinic agonists used in functional assays were also tested in inhibition binding assays to determine the effects of mutations on agonist binding interactions (Table 5 and Figures 5 and 6). ACh distinguished three binding sites, while carbachol and oxotremorine-M exhibited two binding sites at HM_1(WT) receptors. These agonists all interacted with two binding sites at the two mutant receptors. Tetrahydropyrimidine derivatives, such as CDD-0034 and CDD-0102, showed two-site binding profiles at HM_1(Asn382Ala) receptors, CDD-0098 showed two-site binding profiles at both HM_1(WT) and HM_1(Thr192Ala) receptors. Mutation of Thr192 or Asn382 to Ala resulted in marked decreases in the binding affinity of ACh, especially in GppNHp-sensitive high affinity (K_H) binding, by 70 to 130 fold. Only small reductions (<2.1 fold) in the lowest affinity binding (K_L) site were

Table 3 Muscarinic antagonist inhibition binding properties of HM_1(WT), HM_1(Thr192Ala) and HM_1(Asn382Ala) receptors, expressed in A9 L cells

	K_i (nM)				
Ligands	*HM_1(WT)*	*HM_1(Thr192Ala)*	*TA/WT (fold)*	*HM_1(Asn382Ala)*	*NA/WT (fold)*
^{3}H-QNB	0.027±0.0057	0.023±0.0013	0.85	0.42±0.12	16
1-Hyoscyamine	0.088±0.0099*	0.21±0.0098	2.4	20±10	230
Scopolamine	0.085±0.016	0.12±0.046	1.4	7.3	86
(−)-NMS	0.022±0.0025*	0.12±0.0021	5.5	50±28	2300
Trihexyphenidyl	0.10±0.0027*	0.063±0.0034	0.63	1100	11000
AF-DX 116	520±52	1400±260	2.7	>30,000	58
Pirenzepine	4.4±0.74*	5.8±0.70	1.3	34,000±5600	7700
p-F-HHSiD	2.6±1.1	4.0±0.31	1.5	110	42
4-DAMP	0.19±0.036	0.19±0.0026	1.0	1.2	6.3

Affinity changes from wild-type are expressed in fold (TA for Thr192Ala; NA for Asn382Ala). ^{3}H-(R)-QNB binding data are from Table 1. Data represent the means±s.e.mean from a minimum of three assays. *Binding data for HM_1(WT) receptors were from Huang *et al*., 1998 and listed for comparison.

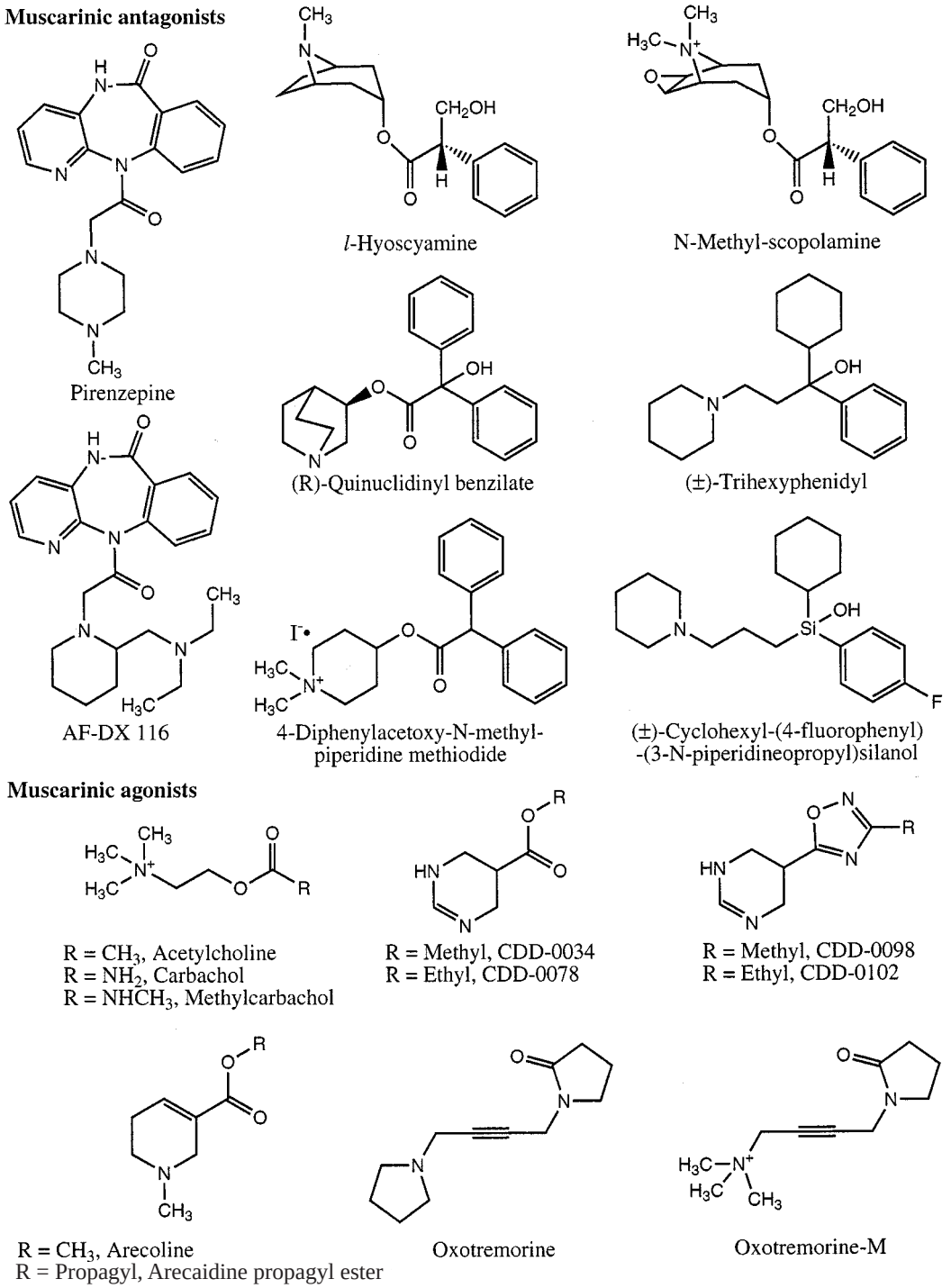

Figure 1 Chemical structures of ligands used in this study.

observed. Carbachol exhibited a greater reduction of K_L than K_H at HM_1(Thr192Ala) mutant receptors, while showing comparable degrees of reduction in both K_H and K_L at HM_1(Asn382Ala) mutant receptors (Table 5). The binding of the structurally-related oxotremorine and oxotremorine-M was more affected by the Asn382Ala mutation than the Thr192Ala mutation. Binding of the structurally related tetrahydropyridine derivatives, arecoline and arecaidine propagyl ester (APE), was not affected significantly by either mutation. All these results indicate that muscarinic agonists with different chemical structures may bind to HM_1(WT) and/or mutant receptors in different modes (geometric positions of the ligand relative to amino acids in the putative binding pocket).

In order to determine if the high-affinity agonist binding was sensitive to guanine nucleotides, ACh binding was assessed in the presence of 100 μM GppNHp. As indicated in Figure 5, the high affinity binding sites at HM_1(WT) and the two mutant receptors were abolished by the addition of GppNHp, indicating the presence of GTP-sensitive coupling between the mutant receptors and G proteins as in HM_1(WT) receptors. In the presence of 100 μM GppNHp, ACh still displayed a 17 fold reduction in binding affinity at

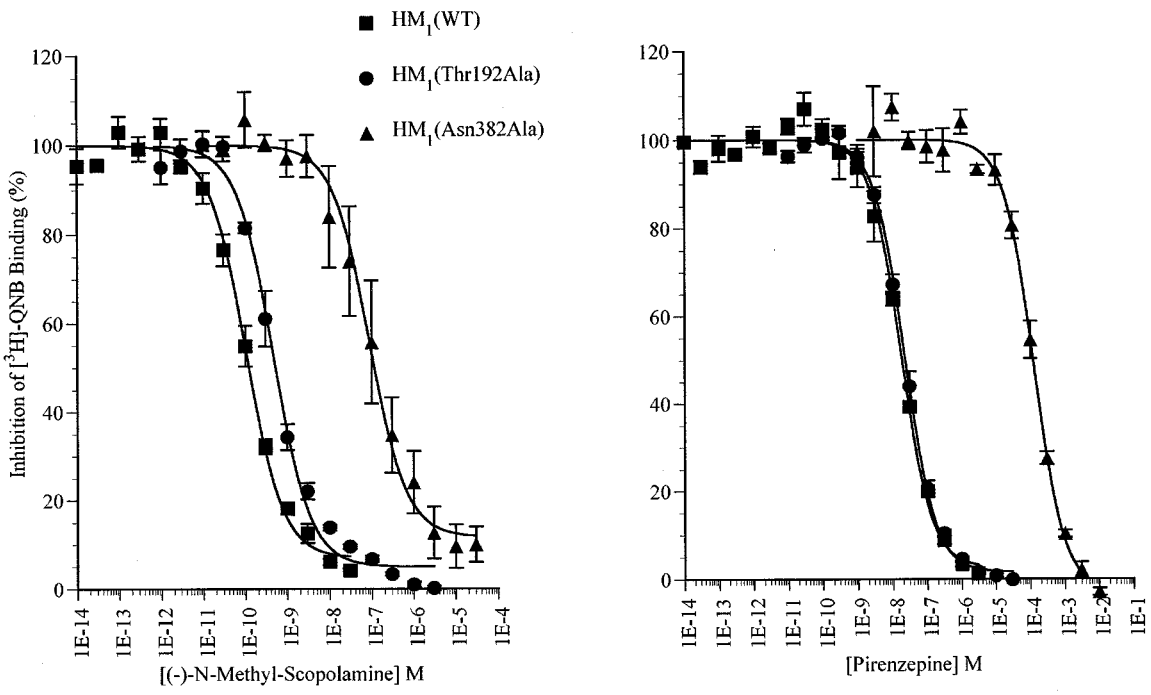

Figure 2 NMS (left) and pirenzepine (right) inhibition binding profiles. Radioligand inhibition binding assays were carried out using membrane homogenates from transfected A9 L cells in the presence of 0.1 nM of ^{3}H-(R)-QNB for HM_1(WT) and HM_1(Thr192Ala) receptors and 1 nM of ^{3}H-(R)-QNB for HM_1(Asn382Ala) receptors. Assays were performed in triplicate sets. Data represent the means$\pm$s.e.mean from a minimum of three assays (Table 3).

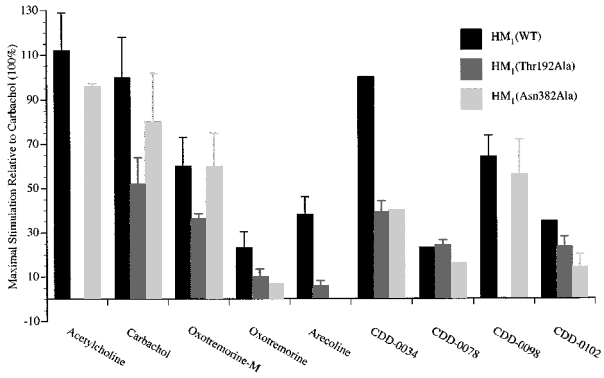

Figure 3 Maximum response of PI hydrolysis mediated by a series of muscarinic ligands at HM_1(WT), HM_1(Thr192Ala), and HM_1(Asn-382Ala) receptors stably expressed in A9 L cells. Receptor expression levels are indicated in Table 2. PI assays were carried out in growth media (DMEM) containing 10% FBS or in KH buffer as described in the Methods section. Data are presented as the percentage relative to the maximal carbachol activity at HM_1(WT) receptors (250$\pm$46% above basal from five assays).

HM_1(Thr192Ala) receptors and 9 fold at HM_1(Asn382Ala) receptors.

Molecular modelling studies

In order to understand the binding interactions between receptors and agonists, molecular modelling studies were carried out by docking agonists carbachol and two tetrahydropyrimidine derivatives, CDD-0034 and CDD-0098, into the putative binding pocket containing the critical residues Asp105 (TM III), Thr192 (TM V), and Asn382 (TM VI) of the HM_1 receptors (Figure 7). The binding energies, EB, were obtained by calculating the minimized energy for the dimer and the monomers. Resulting electrostatic and van der Waals interaction energies between the ligand and receptors are summarized in Tables 6 and 7. Mutation of Thr or Asn to Ala resulted in significantly more negative binding energies, indicating stronger ligand binding. Van der Waals interactions, dE(W), appear to provide the dominant stabilizing contributions to the binding of a ligand by both HM_1(WT) and mutant receptors. In HM_1(WT) receptors, Thr192 had consistent hydrogen-bond interactions with carbachol and the two tetrahydropyrimidine derivatives. As compared with carbachol and CDD-0034, CDD-0098 exhibited two additional strong hydrogen-bond interactions with Asp105 and Asn382 residues. This interaction profile is in good agreement with the fact that CDD-0098 has the highest binding affinity among the three agonists (Table 5).

Hydrogen-bond patterns for ligand-receptor interactions were not significantly affected in the carbachol binding mode by mutation of Thr192 or Asn382 to Ala. These mutations did alter the binding patterns for CDD-0034 and CDD-0098 (Table 7). At HM_1(Thr192Ala) receptors, CDD-0034 lost a hydrogen-bond interaction due to the Thr192 to Ala mutation but gained a strong hydrogen-bond interaction with the Asp105 residue. CDD-0098 lost two hydrogen-bond interactions due to Thr192 to Ala mutation and also lost a strong hydrogen-bond interaction with the Asp105 residue. The different interactions with the Asp105 residue probably result from different binding modes for different agonists.

Discussion

Previous site-directed mutagenesis and pharmacological studies (Wess *et al*., 1991; 1992; Blüml *et al*., 1994) confirmed the role of Thr234 (TM V) but not of Asn507 (TM VI) (number in RM_3 subtype) in agonist binding and receptor

activation as predicted by three dimensional modelling studies (Trumpp-Kallmeyer *et al*., 1992; Ward *et al*., 1992; Nordvall & Hacksell, 1993; 1995) based on the human M_1 receptor subtype. In this study, the roles of the equivalent Thr and Asn in HM_1 receptors in ligand binding and receptor activation were re-examined by stably expressing mutant HM_1 receptors in A9 L cells. Thr192 or Asn382 was replaced by Ala, which has no functional group in its side chain for potential H-bond interactions. A series of muscarinic ligands were characterized at the mutant receptors and HM_1(WT) receptors.

Mutation of Thr192 to Ala did not dramatically change the binding affinities for tested antagonists belonging to different structural classes, indicating that Thr192 may not be involved

Table 4 Potencies of tested ligands at HM_1(WT), HM_1(Thr192Ala) and HM_1(Asn382Ala) receptors expressed in A9 L cells

			EC_{50} (μM)		
Ligands	*HM_1(WT)*	*HM_1(Thr192Ala)*	*TA/WT (fold)*	*HM_1(Asn382Ala)*	*NA/WT (fold)*
Acetylcholine*	2.1±0.65 (n=2)	ND	–	21±2.2	10
Carbachol	12±5.6	140±75	11.6	82±11	6.8
Oxotremorine	ND	82±66	–	>1000	–
Oxotremorine-M	0.68±0.39	2.4±0.39	3.5	14±3.0	20.6
Arecoline	1.3±1.3	>1000	–	>1000	–
CDD-0034	25 (n=1)	150±71	6.0	490 (n=1)	19.6
CDD-0078	34 (n=1)	36±13	1.1	84 (n=1)	2.5
CDD-0098	2.0±1.1	>1000	–	4.4±2.7	2.2
CDD-0102	16 (n=1)	6.2±1.1	0.4	3.1±0.41	0.2

PI assays were conducted in DMEM supplemented with 10% FBS as described in the Methods section. Agonist efficacy was shown in Figure 3. Potency differences between wild-type and mutant receptors are shown in fold (TA, Thr192Ala; NA, Asn382Ala). *Acetylcholine was tested in KH buffer as described in the Methods section. ND, not determined. Data represent the means±s.e.mean from a minimum of two assays or as indicated, each performed in duplicate.

Table 5 Inhibition binding properties of muscarinic agonists at HM_1(WT) and two mutant receptors expressed in A9 L cells

Ligands	*HM_1(WT)*	*HM_1(Thr192Ala)*	*TA/WT (fold)* μM	*HM_1(Asn382Ala)*	*NA/WT (fold)*
Acetylcholine (ACh)*	0.51±0.06	44±4.3	86	12±3.3	24
K_H (%)	17±5.4 nM (30)	1.2±0.94 (16)	71	2.2±1.1 (40)	130
K_M (%)	1.1±0.33 (54)	NA	–	NA	–
K_L	39±14	83±2.9	2.1	65±16	1.7
ACh + 100 μM	3.0±0.30	110±14	37	27±1.4	9.0
GppNHp*	1.4±0.57 (55)	NA	–	NA	–
K_H (%)	13±4.4	NA	–	NA	–
K_L					
Carbachol*	20±4.1	190±42	9.5	74±8.0	3.7
K_H (%)	1.6±0.76 (28)	1.7±0.24 (17)	1.1	6.0±1.2 (27)	3.8
K_L	83±21	320±18	3.9	280±26	3.4
Oxotremorine*	0.18±0.02	0.52±0.09	2.9	11±1.9	61
Oxotremorine-M	2.2±0.40	10±4.2	4.6	18±6.6	8.2
K_H (%)	1.1±0.30 (66)	0.76±0.02 (32)	0.7	2.8±2.3 (40)	2.5
K_L	33±8.3	18±5.3	0.5	92±27	2.8
APE*	0.32±0.030	0.57±0.050	1.8	0.21±0.015	0.6
Arecoline*	4.2±0.41	5.4±0.59	1.3	4.1±1.0	1.0
CDD-0034	39±0.93	140±17	3.6	57±21	1.5
K_H (%)	NA	NA	NA	0.57±0.27 (14)	–
K_L	NA	NA	NA	130±85	–
CDD-0078	5.4±0.46	9.8±0.54	1.8	14±4.5	2.6
CDD-0098	2.9±0.67	8.7±0.72	3.0	1.9±0.12	0.7
K_H (%)	0.12±0.078 (24)	0.24±0.14 (16)	2.0	NA	–
K_L	8.1±1.9	15±1.5	1.9	NA	–
CDD-0102	2.0±0.66	2.3±0.53	1.2	0.42±0.14	0.2
K_H (%)	NA	NA	–	0.27±0.18 (65)	–
K_L	NA	NA	–	44±32	–

Radioligand inhibition binding assays were conducted on membrane homogenates prepared from transfected A9 L cells in the presence of 0.1 nM ^{3}H-(R)-QNB for HM_1(WT) and HM_1(Thr192Ala) receptors and 1.0 nM of ^{3}H-(R)-QNB for HM_1(Asn382Ala) receptors as described in the Methods section. Data for a single site model are shown for comparison. K_H, K_M and K_L are the high, medium and low binding affinities, respectively, with the percentage of the sites in parentheses; NA for not applicable. Affinity changes from wild-type receptor are shown in fold. Data represent the means±s.e.mean from a minimum of three independent assays, each performed in triplicate. *Binding affinity data at HM_1(WT) receptors were from Huang *et al*., 1998 and listed for comparison.

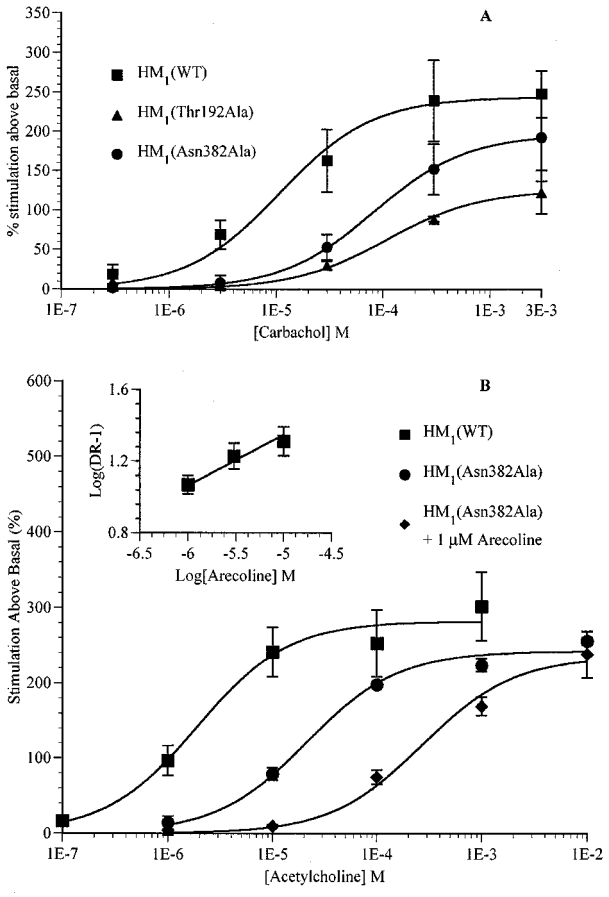

Figure 4 Pharmacology of HM_1(WT) and two mutant receptors stably expressed in A9 L cells. Data (Table 4 and Figure 3) are fitted into a one-site stimulation model. (A) carbachol dose response profiles. PI hydrolysis assays were conducted in growth media (DMEM) containing 10% FBS. (B) acetylcholine dose response at HM_1(WT) receptors and antagonist activity of arecoline at HM_1(Asn382Ala) receptors. PI hydrolysis assays were conducted KH buffer. Insert is a Schild plot analysis of acetylcholine-mediated PI hydrolysis in the presence of 1, 3 and 10 μM of arecoline at HM_1(Asn382Ala) receptors. DR stands for the ratio of EC_{50} values of acetylcholine in the presence of arecoline over that in the absence of arecoline.

in antagonist binding. In contrast, substitution of Asn382 by Ala resulted in much greater reductions in binding affinities for pirenzepine, trihexyphenidyl, and NMS than other antagonists, such as QNB. These data are consistent with previous results on the equivalent mutations in RM_3 receptors (Blüml *et al*., 1994). Therefore, Asn382 played a critical role in the binding of some antagonists, and Thr192 and Asn382 residues in HM_1 receptors appear to have essentially the same functions in antagonist binding as the equivalent residues (Thr234 and Asn507 respectively) in RM_3 receptors.

The selection of ^{3}H-(R)-QNB as radioligand in binding assays appeared to be critical in characterizing the mutant receptors. It would be difficult to use ^{3}H-NMS as the radioactive ligand in assessing receptor binding, since NMS exhibited a 2300 fold reduction in binding affinity at HM_1(Asn382Ala) receptors. This may account for previous failures to detect expression of the same mutant receptors in COS-7 cells (Bourdon *et al*., 1997; Ward & Hulme, 1997).

We were unable to demonstrate dose response curves for the endogenous muscarinic agonist ACh in growth media, possibly due to the presence of cholinesterases in animal serum as we and others (Spalding *et al*., 1995) found previously. In KH buffer, we were able to compare ACh activity at both HM_1(WT) and HM_1(Asn382Ala) receptors and show that substitution of Asn382 with Ala resulted in 10 fold reduction of ACh potency. Interestingly, arecoline, a partial agonist at the HM_1(WT) receptor, can behave as an antagonist at HM_1(Asn382Ala) receptors, by inhibiting ACh stimulation of PI hydrolysis. A Schild plotting analysis indicated that the inhibition may not be competitive.

Substitution of Thr192 or Asn382 with Ala resulted in a greater reduction of binding affinity for classical full agonists (such as ACh, carbachol, oxotremorine-M) than for tetrahydropyridine or tetrahydropyrimidine derivatives (such as arecoline, APE and CDD compounds). The Thr192Ala mutation had a greater effect than the Asn382Ala mutation on reducing binding affinity for acetylcholine and carbachol, but less than the Asn382Ala mutation on reducing binding affinity for oxotremorine-M and oxotremorine. These data indicated that both Thr192 and Asn382 are important for agonist binding.

The natural agonist ACh showed a three-site binding profile to HM_1(WT) receptors, but two binding sites at the mutant receptors. In addition, ACh exhibited much greater reductions in binding affinities at both mutant receptors than any other tested agonists. These data indicate that the mutations had

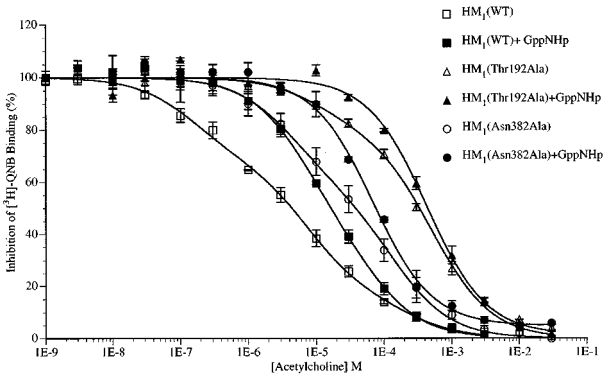

Figure 5 Acetylcholine inhibition binding properties in the absence and presence of 100 μM GppNHp. Radioligand binding experiments were carried out on membrane homogenates in the presence of 0.1 nM of ^{3}H-(R)-QNB for HM_1(WT) and HM_1(Thr192Ala) receptors and 1 nM of ^{3}H-(R)-QNB for HM_1(Asn382Ala) receptors. Data represent the means ± s.e.mean from a minimum of three assays (Table 7).

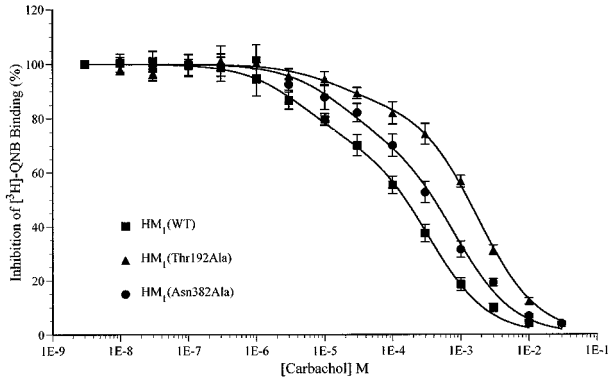

Figure 6 Carbachol inhibition binding properties in the presence of 0.1 nM of ^{3}H-(R)-QNB for HM_1(WT) and HM_1(Thr192Ala) receptors and 1 nM of ^{3}H-(R)-QNB for HM_1(Asn382Ala) receptors. Assays were conducted on membrane homogenates. Data represent the means ± s.e.mean from a minimum of three assays (Table 7).

much more significant effects on the binding of the natural ligand than any other classical agonist. Thus, characterization of mutant receptors with the endogenous agonist is valuable.

The greatest reductions of ACh binding at Thr192Ala mutation (71 fold) and Asn382Ala mutation (130 fold) were associated with the high affinity binding sites. This high affinity binding was found to be GTP sensitive and therefore involved in G protein interactions and receptor activation. In contrast, no significant reduction (1.7–2.1 fold) was observed for the low affinity binding sites. The magnitude of the ACh affinity reduction was much lower in the presence of GppNHp than in the absence of GppNHp. This suggests that both Thr192 and

Figure 7 Docking of CDD-0098 to a model of the M_1 muscarinic receptor (Nordvall & Hacksell, 1993). The backbone of the seven transmembrane domains are shown in white. Key amino acid residues Asp105 (left), Thr192 (right), and Asn382 (top) are coded by atom type (carbon, white; nitrogen, dark blue; oxygen, red; hydrogen, light blue). Colour code for CDD-0098: yellow for the wild-type M_1 receptor, purple for the Thr192Ala mutant receptor, and green for the Asn382Ala mutant receptor.

Table 6 Energy terms for the ligand-receptor interactions at HM_1 receptors

	HM_1(WT)			*HM_1(Thr192Ala)*			*HM_1(Asn382Ala)*		
	Carbachol	*CDD-0034*	*CDD-0098*	*Carbachol*	*CDD-0034*	*CDD-0098*	*Carbachol*	*CDD-0034*	*CDD-0098*
					Kcal mol^{-1}				
EB	−17.9	−16.1	−21.6	−25.8	−26.0	−21.6	−20.9	−20.7	−25.0
dE(e)	−4.0	−3.8	−6.2	−2.8	−7.3	−3.9	−4.1	−3.9	−6.9
dE_L(e)	0.0	0.5	0.1	0.2	0.4	0.1	0.2	0.4	0.1
dE_R(e)	1.0	1.6	1.6	1.6	0.2	1.9	1.2	1.5	1.5
E_{LR}(e)	−5.0	−5.8	−7.9	−4.6	−7.9	−5.9	−5.5	−5.8	−8.4
dE(W)	−15.7	−14.6	−16.7	−22.7	−19.3	−19.2	−17.9	−19.4	−19.7
dE_L(W)	1.2	0.6	0.7	0.5	0.1	0.5	0.5	0.4	0.6
dE_R(W)	6.5	6.2	7.7	2.6	1.8	4.7	5.4	2.2	5.1
E_{LR}(W)	−23.4	−21.4	−25.0	−25.8	−21.2	−24.4	−23.8	−22.0	−25.4

Letters e and W in parentheses stand for the electrostatic and van der Waals interactions, respectively. Letters L and R stand for the ligand and receptor, respectively. EB (binding energy) = E_{dimer}-E_{Lopt}-E_{Ropt}, $dE_L = E_L$-E_{Lopt}, $dE_R = E_R$-E_{Ropt}. For the dE terms see Equation 2.

Table 7 Hydrogen bond patterns for ligand-receptor interactions at HM_1 wild-type and mutant receptors

	HM_1(WT)			*HM_1(Thr192Ala)*			*HM_1(Asn382Ala)*		
Ligand	*Asp105*	*Thr192*	*Asn382*	*Asp105*	*Ala192*	*Asn382*	*Asp105*	*Thr192*	*Ala382*
Carbachol	–	b	c,c	–	–	b,c	–	b,b	–
CDD-0034	–	b	–	a	–	c	c	c	–
CDD-0098	a	b,b	a,c	c	–	a,c	a	b,b,c	–

a = (X···H ⩽ 2.00 Å); b = 2.00 Å < X···H ⩽ 2.50 Å); c = (2.50 Å < X···H ⩽ 3.00 Å) with X = N, O. Distances a and b are considered as strong and medium/weak bonds, respectively. Group c corresponds only to some stabilization upon favourable electrostatic fit.

Asn382 residues are important for the M_1-receptor/ACh complex to interact with G-proteins, indicating that Thr192 and Asn382 are involved in high affinity agonist binding and the receptor activation processes.

Activity differences between M_2 full and partial agonists in mediating the inhibition of adenylyl cyclase were due to reduced affinity of the receptor/agonist complex for G_i, but not the abilities of the receptor/agonist complex to activate G_i (Tota *et al*., 1990). It is possible that mutations in HM_1 receptors may not change receptor binding affinity for agonists but reduce the binding affinity of the mutant receptor/agonist complex for G-proteins and/or decrease the ability of the complex to activate G-proteins.

Mutation of Thr192Ala or Asn382Ala reduced receptor response to agonists. For classical full agonists, such as ACh and carbachol, reduced efficacies and/or potencies were in general agreement with their reduced binding affinities at mutant receptors. However, there was a discrepancy between unchanged or increased agonist binding affinities and reduced agonist activities. Several ligands, such as arecoline and CDD-0034, which showed partial and full agonist activities respectively at HM_1(WT) receptors, exhibited reduced activities at the mutant receptors, with similar binding affinities for HM_1(WT) and the mutant receptors. CDD-0102 displayed two binding affinity states and higher binding affinity at HM_1(Asn382Ala) receptors than HM_1(WT) receptors. Its efficacy at HM_1(Asn382Ala) receptors was only half of that at HM_1(WT) receptors.

HM_1(Thr192Ala) and HM_1(Asn382Ala) receptors are not the only mutant muscarinic receptors that exhibit increased agonist binding affinity and decreased agonist activity. Similar discrepancies were shown previously at RM_1(Asp71Asn) and RM_1(Asp122Asn) (Fraser *et al*., 1989), and RM_3(Pro540Ala) receptors (Wess *et al*., 1993). All these three amino acids are highly conserved in almost all G protein coupled receptors and are believed to be involved in receptor activation by mediating agonist-induced receptor conformational changes (Fraser *et al*., 1989; Wess *et al*., 1993). Our findings support the idea that both Thr192 and Asn382 residues are involved in receptor activation processes.

Molecular modelling studies with carbachol and two tetrahydropyrimidine derivatives, CDD-0034 and CDD-0098, indicated that substitution of Thr192 or Asn382 with Ala removed potential H-bond interactions and changed the agonist binding mode. The changes in binding mode may be energetically beneficial for agonist binding but not effective for receptor activation and G-protein coupling. This is reflected by the discrepancy between reduced efficacies and/or potencies and unchanged binding affinities of muscarinic agonists, such as arecoline.

In conclusion, we have shown here that both Thr192 and Asn382, which are highly conserved within the muscarinic receptor family, are involved in agonist binding and receptor activation processes. Our results are consistent with previous molecular modelling studies. In addition, Asn382 but not Thr192 participated in antagonist binding, presumably by providing H-bond interactions with the ester portion of antagonists (Bourdon *et al*., 1997). Molecular modelling studies suggest that changes in binding mode may contribute to the discrepancies between agonist binding and receptor activity. Site-directed mutagenesis and molecular modelling are an excellent combination in characterizing functionally important amino acid residues in ligand binding and receptor activation. Identification of highly conserved amino acids important in ligand binding and receptor activation processes could aid in the design and development of novel therapeutic drugs for Alzheimer's disease and other neurological disorders.

We thank Dr Tom I. Bonner for kindly providing HM1pcD1 and Dr Jürgen Wess for pcDneo. We also thank Afif A. El-Assadi for his technical assistance. This work was supported by NHS grants NS311T3 and NS 35127.

References

ALLMAN, K., PAGE, K.M. & HULME, E.C. (1997). Cysteine scanning mutagenesis of transmembrane domain V of the M1 muscarinic receptor. *Life Sci.,* **60,** 1177.

BLÜML, K., MUTSCHLER, E. & WESS, J. (1994). Functional role in ligand binding and receptor activation of an asparagine residue present in the sixth transmembrane domain of all muscarinic acetylcholine receptors. *J. Bio. Chem.,* **269,** 18870 – 18876.

BONNER, T.I., YOUNG, A.C., BRANN, M.R. & BUCKLEY, N.J. (1988). Cloning and expression of the human and rat m5 muscarinic acetylcholine genes. *Neuron,* **1,** 403 – 410.

BOURDON, H., TRUMPP-KALLMEYER, S., SCHREUDER, H., HOFLACK, J., HIBERT, M. & WERMUTH, C.G. (1997). Modelling of the binding site of the human M1 muscarinic receptor: Experimental validation and refinement. *J. Comput.-Aided Mol. Des.,* **11,** 317 – 332.

BRANN, M.R., BUCKLEY, N.J., JONES, S.V. & BONNER, T.I. (1987). Expression of a cloned muscarinic receptor in A9 L cells. *Mol. Pharmacol.,* **32,** 450 – 455.

CAULFIELD, M.P. (1993). Muscarinic receptors – characterization, coupling and function. *Pharm. Ther.,* **58,** 319 – 379.

CAULFIELD, M.P. & BIRDSALL, N.J.M. (1998). International union of pharmacology. XVII. Classification of muscarinic acetylcholine receptors. *Pharmacol. Rev.,* **50,** 279 – 290.

CHENG, Y.-C. & PRUSOFF, W.H. (1973). Relationship between the inhibition constant (K_i) and the concentration of inhibitor which causes 50 per cent inhibition (IC_{50}) of an enzymatic reaction. *Biochem. Pharmacol.,* **22,** 3099 – 3108.

DEWAR, M.J.S., ZOEBISCH, E.G., HEALY, E.F. & STEWART, J.J.P. (1985). AM1: A new general purpose quantum mechanical molecular model. *J. Am. Chem. Soc.,* **107,** 3902 – 3909.

DÖRJE, F., WESS, J., LAMBRECHT, G., TACKE, R., MUTSCHLER, E. & BRANN, M.R. (1991). Antagonist binding profiles of five cloned human muscarinic receptor subtypes, *J. Pharmacol. Exp. Ther.,* **256,** 727 – 733.

FRASER, C.M., WANG, C.-D., ROBINSON, D.A., GOCAYNE, J.D. & VENTER, J.C. (1989). Site-directed mutagenesis of M1 muscarinic acetylcholine receptors: conserved aspartic acids play important roles in receptor function. *Mol. Pharmacol.,* **36,** 840 – 847.

GROWDON, J.H. (1987). Muscarinic agonists in Alzheimer's disease. *Life Sci.,* **60,** 993 – 998.

HOSS, W., WOODRUFF, J.M., ELLERBROCK, B.R., PERIYASAMY, S., GHODSI-HOVSEPIAN, S., STIBBE, J., BOHNETT, M. & MESSER, JR W.S. (1990). Biochemical and behavioral responses of pilocarpine at muscarinic receptor subtypes in the CNS. Comparison with receptor binding and low-energy conformations. *Brain Res.,* **533,** 232 – 238.

HUANG, X.-P., WILLIAMS, F.E., PESECKIS, S. & MESSER, JR W.S.. (1998). Pharmacological characterization of human M1 muscarinic acetylcholine receptors with double mutations at the junction of TM VI and the third extracellular domain. *J. Pharmacol. Exp. Ther.,* (in press).

HULME, E.C., BIRDSALL, N.J.M. & BUCKLEY, N.J. (1990). Muscarinic receptor subtypes. *Annu. Rev. Pharmacol. Toxicol.,* **30,** 633 – 673.

LOWRY, O., ROSERBOUGH, N.J., FARR, A.L. & RANALL, R.J. (1951). Protein measurement with the folin phenol reagent. *J. Biol. Chem.,* **193,** 265 – 275.

MARKWELL, M.A., HAAS, S.M., TOLBERT, N.E. & BIEBER, L.L. (1981). Protein determination in membrane and lipoprotein samples: manual and automated procedures. *Methods Enzymol.,* **72,** 296 – 303.

MESSER, JR W.S., ABUH, Y.F., LIU, Y., PERIYASAMY, S., NGUR, D.O., EDGAR, M.A.N., EL-ASSADI, A.A., SBEIH, S., DUNBAR, P.G., ROKNICH, S., RHO, T., FANG, Z., OJO, B., ZHANG, H., HUZL, J.J. III & NAGY, P.I. (1997). Synthesis and biological characterization of 1,4,5,6-tetrahydropyrimidine and 2-amino-3,4,5,6-tetrahydro-pyridine derivatives as selective M1 agonists. *J. Med. Chem.,* **40,** 1230 – 1246.

NORDVALL, G. & HACKSELL, U. (1993). Binding-site modeling of the muscarinic M1 receptor: A combination of homology-based and indirect approaches. *J. Med. Chem.,* **36,** 967 – 976.

NORDVALL, G. & HACKSELL, U. (1995). Binding-site modeling of the muscarinic M1 receptor – molecular interactions with agonists and antagonists. In: Wess, J. (ed.). *Molecular Mechanisms of Muscarinic Acetylcholine Receptor Function*. R.G. Landes Company: Austin, pp 19 – 32.

SCHWARZ, R.D., SPENCER, C.J., JAEN, J.C., MIRZADEGAN, T., MORLAND, D., TECLE, H. & THOMAS, A.J. (1995). Mutations of aspartate 103 in the Hm2 receptor and alterations in receptor binding properties of muscarinic agonists. *Life Sci.,* **56,** 923 – 929.

SCHWARTZ, T.W. & ROSENKILDE, M.M. (1996). Schwartz and Rosenkilde reply: Dogmas versus data in 7TM 'locks' for 'keys'. *Trends Pharmacol. Sci.,* **17,** 347.

SPALDING, T.A., BURSTEIN, E.S., BRAUNER-OSBORNE, H., HILL-EUBANKS, D. & BRANN, M.R. (1995). Pharmacology of a constitutively active muscarinic receptor generated by random mutagenesis. *J. Pharmacol. Exp. Thr.,* **275,** 1274 – 1279.

STRANGE, P.G. (1996). 7TM receptors: 'locks' and 'keys'? Diversity in the interactions of catecholamines with their receptors. *Trends Pharmacol. Sci.,* **17,** 346.

TOTA, M.R. & SCHIMERLINK, M.I. (1990). Partial agonist effects on the interaction between the atrial muscarinic receptor and the inhibitory guanine nucleotide-binding protein in a reconstituted system. *Mol. Pharmacol., 3***7,** 996 – 1004.

TRUMPP-KALLMEYER, S., HOFLACK, J., BRUINVELS, A. & HIBERT, M. (1992). Modeling of G-protein-coupled receptors: Application to dopamine, adrenaline, serotonin, acetylcholine, and mammalian opsin receptors. *J. Med. Chem.,* **35,** 3448 – 3462.

WARD, J.S., MERRITT, L., KLIMKOWSKI, V.J., LAMB, M.L., MITCH, C.H., BYMASTER, F.P., SAWYER, B., SHANNON, H.E., OLESEN, P.H., HONORE, T., SHEARDOWN, M.J. & SAUERBERT, P. (1992). Novel functional M1 selective muscarinic agonists. 2. Synthesis and structure-activity relationships of 3-pyrazinyl-1,2,5,6-tetrahydro-1-methylpyridines. Construction of a molecular model for the M1 pharamcophore. *J. Med. Chem.,* **35,** 4011 – 4019.

WARD, S.D.C. & HULME, E.C. (1997a). Alanine scanning mutagenesis in transmembrane domain six of the rat M1-muscarinic acetylcholine receptor (Rat M1-Receptor). *Br. J. Pharmacol.,* **120,** 284.

WARD, S.D.C. & HULME, E.C. (1997b). Try381 in transmembrane domain six plays a key part in activation of the rat M1-muscarinic acetylcholine receptor. In: *27th Annual Meeting of Society For Neuroscience (Abstracts),* New Orleans: L.A., pp 1750.

WATSON, S. & ARKINSTALL, S. (1994). *The G-protein linked receptor factsbook*. Watson, S. (ed.). Academic Press, London, San Diego.

WEINER, S.J., KOLLMAN, P.A., NGUYEN, D.T. & CASE, D.A. (1986). An all atom force field for simulations of proteins and nucleic acids. *J. Comput. Chem.,* **7,** 230 – 252.

WESS, J. (1996). Molecular biology of muscarinic acetylcholine receptors. *Critical Reviews in Neurobiology,* **10,** 69 – 99.

WESS, J. (1997). G-Protein-coupled receptors: molecular mechanisms involved in receptor activation and selectivity of G-protein recognition. *FASEB J.,* **11,** 346 – 354.

WESS, J., GDULA, D. & BRANN, M.R. (1991). Site-directed mutagenesis of the M3 muscarinic receptor: identification of a series of threonine and tyrosine residues involved in agonist but not antagonist binding. *EMBO J.,* **10,** 3729 – 3734.

WESS, J., MAGGIO, R., PALMER, J.R. & VOGEL, Z. (1992). Role of conserved threonine and tyrosine residues in acetylcholine binding and muscarinic receptor activation. *J. Biol. Chem.,* **267,** 19313 – 19319.

WESS, J., NANAVATI, S., VOGEL, Z. & MAGGIO, R. (1993). Functional role of proline and tryptophan residues highly conserved among G protein-coupled receptors studied by mutational analysis of the m3 muscarinic receptor. *EMBO J.,* **12,** 331 – 338.

WREGGETT, K.A. & IRVINE, R.F.A. (1987). Rapid separation method for inositol phosphates and their isomers. *Biochem. J.,* **245,** 655 – 660.

(Received June 2, 1998
Revised September 10, 1998
Accepted November 5, 1998)

British Journal of Pharmacology (1999) 126, 746–750
http://www.stockton-press.co.uk/bjp

Inhibition of inducible nitric oxide synthase by β-lapachone in rat alveolar macrophages and aorta

*,[1]Shing-Hwa Liu, [1]Huei-Ping Tzeng, [1]Min-Liang Kuo & [1]Shoei-Yn Lin-Shiau

[1]Institute of Toxicology, College of Medicine, National Taiwan University, No. 1, Jen-Ai Road, Section 1, Taipei 10018, Taiwan

1 β-Lapachone, a plant product, has been shown to be a novel inhibitor of DNA topoisomerase. In this study, we performed experiments to examine the effects of β-lapachone on lipopolysaccharide (LPS)-induced inducible nitric oxide (NO) synthase (iNOS) in rat alveolar macrophages and aortic rings.

2 In alveolar macrophages, incubation with LPS (10 μg ml^{-1}) for various time intervals resulted in a significant increase in nitrite production and iNOS protein synthesis, that was inhibited by co-incubation with β-lapachone (1–4.5 μM) without any cytotoxic effects. However, addition of β-lapachone after induction of NO synthase by LPS failed to affect the nitrite production.

3 Treatment with LPS (10 μg ml^{-1}) for 6 h resulted in significant expression of mRNA for iNOS which was significantly inhibited in the presence of β-lapachone (3 μM) in alveolar macrophages.

4 In endothelium-intact rings of thoracic aorta, β-lapachone (1 and 3 μM) markedly inhibited the hypocontractility to phenylephrine in aortic rings treated with LPS (10 μg ml^{-1}) for 4 h. When β-lapachone was added 3 h after LPS into the medium, the contractions evoked by phenylephrine were not significantly different in the presence or absence of β-lapachone.

5 Treatment with LPS (10 μg ml^{-1}) for 4 h resulted in a significant increase in iNOS protein synthesis which was inhibited in the presence of β-lapachone (3 μM), but did not affect the constitutive (endothelial and neuronal) NOS forms in aortic rings.

6 These results indicate that β-lapachone is capable of inhibiting expression and function of iNOS in rat alveolar macrophages and aortic rings. It is considered that β-lapachone can be developed as a potential anti-inflammatory agent in the future.

Keywords: Lipopolysaccharide; nitric oxide; β-lapachone; inducible NO synthase

Introduction

β-Lapachone (3,4 dihydro-2,2-dimethyl-2H-naphtho-[1,2-b] pyran-5,6-dione), a novel DNA topoisomerase inhibitor (Li *et al*., 1993), is synthesized by simple sulphuric acid treatment of a natural plant product 'lapachol', which is readily extracted from *Tabecuia avellanedae* growing mainly in Brazil, or is easily synthesized from lomatiol, isolated from seeds of lomatia growing in Australia (Goncalves *et al*., 1980; Schaffner-Sabba *et al*., 1984). β-Lapachone and its derivatives have been shown to exhibit a number of pharmacological actions including antibacterial, antifungal and antitrypanocidal activities (Goncalves *et al*., 1980; Guiraud *et al*., 1994).

Nitric oxide (NO), induced by bacterial lipopolysaccharide or cytokines, plays an important role in macrophage killing of cells (Hibbs *et al*., 1987; Stuerhr & Nathan, 1989). NO is recognized as an intercellular messenger in the cardiovascular, nervous, muscular and immune systems (Moncada *et al*., 1991; Murphy *et al*., 1993; Kobzik *et al*., 1994). It is through the activation of inducible NO synthase (iNOS) produced in large amounts of NO during endotoxaemia and has been suggested as a mediator of endotoxaemic shock (Lowenstein & Snyder 1992; Vallance & Moncada, 1993) and many other inflammatory conditions (Morris & Billiar, 1994). Drugs, that inhibit iNOS expression or enzyme activity resulting in decreasing NO generation, have beneficial therapeutic effects; examples of such agents include glucocorticoids (Moncada *et al*., 1991), anti-fungal imidazoles (Bogle *et al*., 1994) and some tyrosine kinase inhibitors (Joly *et al*., 1997). In this study, we performed experiments to examine the effects of β-lapachone on the regulation and effects of lipopolysaccharide (LPS)-iNOS in rat alveolar macrophages and aortic rings.

* Author for correspondence.

Methods

Rat alveolar macrophage cultures

Alveolar macrophages were obtained by tracheal lavage using modifications of the technique described by Brain & Frank (1968). Briefly, adult male Wistar rats (250–300 g) were anaesthetized with sodium pentobarbital (50 mg kg^{-1}). The trachea was cannulated, and the lungs lavaged repetitively with 5-ml aliquots of sterile cold phosphate buffer solution (PBS). All aliquots were centrifuged for 10 min at 200 × *g* at 4°C. The cells were resuspended in RPMI 1640 medium with 10% foetal bovine serum, penicillin (100 U ml^{-1}) and streptomycin (100 μg ml^{-1}), and cultured at a density of 1.2×10^6 cells per 60-mm dish at 37°C in 5% CO_2 in moist air. Giemsa staining revealed that the alveolar cells were more than 95% macrophages. Cell viability was measured by exclusion of trypan blue. Macrophages grown and treated with either control vehicle (dimethyl sulphoxide, DMSO, less than 0.1% v/v) or LPS (10 μg ml^{-1}) in the presence or absence of β-lapachone (1–4.5 μM) for various time intervals (3, 6, 12, 24, and 48 h).

Nitrite assay

Measurement of nitrite production as an assay of NO release was performed. Accumulation of nitrite in the medium was determined by colorimetric assay with Griess reagent (Green *et al*., 1982). Aliquots of conditioned media were mixed with an equal volume of Griess reagent (1% sulphanilamide and 0.1% N-(1-naphthyl)-ethylenediamine dihydrochloride in 2% phosphoric acid). Nitrite concentrations were determined by comparison with OD_{550} of standard solutions of sodium nitrite prepared in cell culture medium.

RT–PCR for iNOS expression

The expression of iNOS was determined by reverse transcription-polymerase chain reaction (RT–PCR) analysis. Approximately 3×10^6 alveolar macrophages treated with LPS (10 μg ml^{-1}) in the presence or absence of β-lapachone were homogenized with 1 ml of Trizol reagent (GIBCO-BRL), and total RNA was isolated according to the manufacturer's protocol. The first strand cDNA was synthesized by extension of (dT) primers with 200 U of SuperScript II reverse transcriptase (GIBCO) in a mixture containing 1 μg of total RNA digested by RNase-free DNase (2 U μg^{-1} of RNA) for 15 min at 37°C. The cDNA was then used as a template in a PCR using the Perkin Elmer DNA Thermal Cycler Model 480. PCR was performed in a final volume of 50 μl containing all four dNTPs, $MgCl_2$ (1.5 mM), 2.0 U of AmpliTaq (GIBCO), and each primer (commercial mouse macrophage inducible NO synthase amplimer set, CLONTECH) at 0.4 μM. The amplification cycles were 94°C for 45 s, 65°C for 45 s, and 72°C for 2 min. The PCR products were separated by electrophoresis on a 1.8% agarose gel after 30–35 cycles and visualized by ethidium bromide staining. The mRNA of β-actin served as control for sample loading and integrity.

Rat thoracic aortic rings

Wistar rats (250–300 g) were stunned and killed by exsanguination. Rings, 4–5 mm wide, of thoracic aorta were suspended between two hooks connected to a transducer (Grass FT.03) for the measurement of isometric force. Endothelium-intact rings were used. The rings were suspended in 10 ml organ baths containing oxygenated (95% O_2 + 5% CO_2), warmed (37°C) Krebs solution containing (composition in mM) NaCl 118.3, KCl 4.7, $CaCl_2$ 2.5, KH_2PO_4 1.2, $MgSO_4$ 1.2, $NaHCO_3$ 25.0 and glucose 11.1. Basal tension was set at 1.0 g. The rings were washed every 20 min for three times before a concentration-response curve to phenylephrine was obtained. The rings were incubated with either control vehicle (DMSO), LPS (10 μg ml^{-1}), β-lapachone (1 and 3 μM) or LPS and β-lapachone under resting tension. After 4 h incubation concentration-response curves to phenylephrine (10^{-9}–10^{-5} M) were constructed. In some experiments, β-lapachone (3 μM) was added 3 h after LPS into the medium. On the other hand, for NOSs immunoblotting studies, the rings after 4 h incubation with either control vehicle (DMSO), LPS (10 μg ml^{-1}), β-lapachone (3 μM) or LPS and β-lapachone, were homogenized in buffer containing (composition in mM) Hepes 20, EDTA 0.5, dithiothreitol 2, phenylmethylsulphonyl fluoride (PMSF) 1, sucrose (0.25 M), 10 μg ml^{-1} leupeptin and 10 μg ml^{-1} aprotinin, pH 7.5, and centrifuged at 10,000 r.p.m. for 20 min at 4°C to remove debris. Proteins were determined according to Lowry *et al*. (1951) with bovine serum albumin as standard.

Western blot analysis

A 30–50 μg sample of cellular lysate protein was subjected to electrophoresis on 8% SDS–polyacrylamide gels for detecting inducible (macrophage and aorta samples) and constitutive (endothelial (eNOS) and neuronal (nNOS), aorta sample) NOS forms. The samples were then electroblotted onto nitrocellulose paper. After blocking, blots were incubated with anti-NOSs antibodies (Transduction Laboratories, U.S.A.) in PBS/Tween 20 for 1 h followed by two washes in PBS/Tween 20 and then incubated with horseradish peroxidase-conjugated goat anti-mouse IgG (Cappel, U.S.A.) for 30 min. The levels of NOSs protein expression were determined using the enhanced chemiluminescence kit (Amersham, U.K.). The cellular lysates as positive controls were from LPS-treated RAW 264.7 cells (for iNOS), human endothelial cells (for eNOS) and rat pituitary cells (for nNOS). All these positive controls were provided by Transduction Laboratories (U.S.A.). Moreover, α-tubulin served as control for sample loading and integrity.

Cytotoxicity assay

Cytotoxicity was measured by the tetrazolium salt MTT (3-(4,5-dimethylthiazol-2-yl)-2,5-diphenyl tetrazolium bromide) colorimetric assay using the modifications of the technique described by Mosmann (1983). Briefly, cells were cultured on 96-well plastic plates in a concentration of 10^5 cells per well and allowed to grow overnight in RPMI 1640 medium and 10% foetal bovine serum. At 24 h treatment with tested drugs, MTT solution (0.2 mg ml^{-1}) was added to all wells of an assay, and plates were incubated at 37°C for 4 h. The cells were then treated with DMSO for 30 min. The plates were read on a Dynatech MR5000 multiwell scanning spectrophotometer using a test wavelength of 570 nm.

Materials

β-Lapachone was prepared according to the procedures described by Schaffner-Sabba *et al*. (1984). β-Lapachone was dissolved in DMSO as a stock solution at 10 mM concentration and stored in aliquots at −20°C. The following reagents were obtained from Sigma Chemical (U.S.A.): lipopolysaccharide (*E. coli*, 055:B5, lyophilized powder prepared by TCA extraction procedure), phenylephrine, sodium nitrite, N^G-nitro-L-arginine methyl ester hydrochloride and MTT (tetrazolium salt).

Statistics

The values given are means ± s.e.mean. The significance of difference from the respective controls for each experimental test condition was assessed by using one-way analysis of variance (ANOVA) followed by Dunnett's test for each paired experiment. P values < 0.05 were regarded as indicating significant differences.

Results

Production of nitrite and iNOS expression

The rat alveolar macrophages were used to study the effects of LPS or combination with β-lapachone on the production of nitrite (a stable oxidation product of NO). The exposure of alveolar macrophages to LPS (10 μg ml^{-1}) for several hours

was associated with the accumulation of nitrite in the incubation medium. Treatment of alveolar macrophages with β-lapachone alone had no significant effects on basal levels of nitrite, while elicited a concentration-dependent inhibition of LPS-induced nitrite production (Figure 1a). This inhibitory effect of β-lapachone on LPS-induced nitrite production also appeared to be time dependent. A time course of nitrite accumulation in macrophages treated with LPS (10 μg ml^{-1}) and inhibition by co-incubation with β-lapachone (3 μM) was shown in Figure 1b. However, when macrophages were pre-activated with LPS (10 μg ml^{-1}) for 24 h following which the LPS was removed, and subsequently treated with fresh medium containing β-lapachone (4.5 μM) for a further 24 h, no inhibition of nitrite production was observed (Figure 1c).

For further understanding the effects of β-lapachone on iNOS protein and mRNA expression, Western blot analysis and RT–PCR were used to determine the protein and iNOS mRNA in alveolar macrophages treated with LPS. Exposure of alveolar macrophages to LPS (10 μg ml^{-1}) for 24 h resulted in an induction of iNOS protein. β-Lapachone elicited a concentration-related inhibition of LPS-induced iNOS (Figure 2a). Moreover, as shown in Figure 2b, treatment with LPS (10 μg ml^{-1}) for 6 h resulted in significant expression of mRNA for inducible NO synthase which was significantly inhibited in the presence of β-lapachone (3 μM) in alveolar macrophages.

On the other hand, treatment with LPS (10 μg ml^{-1}), LPS + β-lapachone (3 and 4.5 μM) or β-lapachone alone (3 and 4.5 μM) for 24 h, did not induce the cytotoxicity in alveolar macrophages using the colorimetric MTT assay (Table 1).

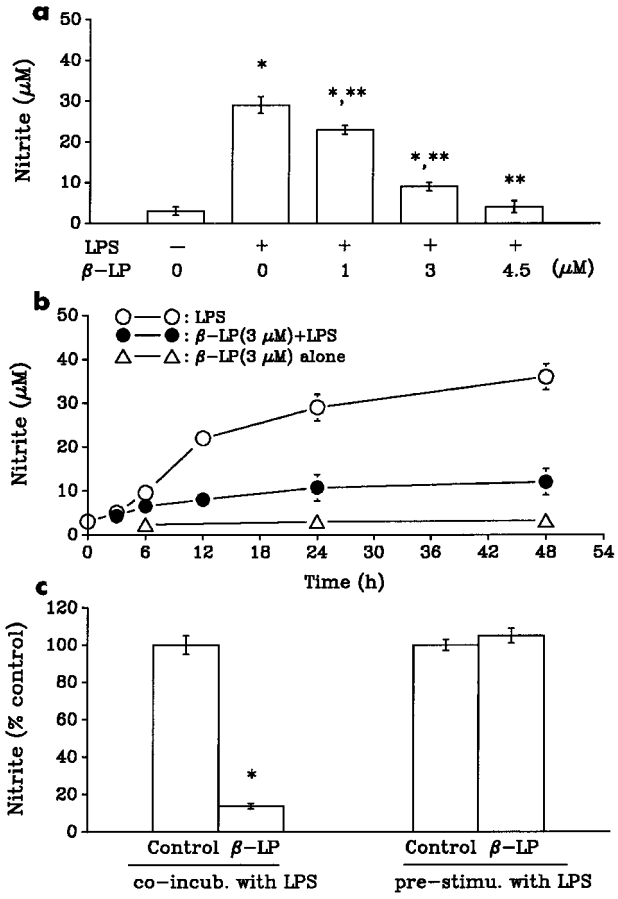

Figure 1 Inhibition of LPS-induced nitrite production. (a) Effects of increasing concentrations of β-lapachone (β-LP) on production of nitrite from alveolar macrophages exposed to LPS (10 μg ml^{-1}) for 24 h. (b) β-LP (3 μM) inhibits the time-dependent increase of LPS-induced NO production in alveolar macrophages. (c) Nitrite production was measured 24 h after co-incubation (co-incub.) of macrophages with LPS and β-LP (4.5 μM) or pre-stimulated (pre-stimu.) of macrophages with LPS for 24 h after which LPS was removed and macrophages subsequently incubated in medium containing β-LP (4.5 μM) for a further 24 h. Data are presented as means ± s.e.mean of 3–5 separate experiments performed in triplicate. *$P<0.05$ as compared with control. **$P<0.05$ as compared with LPS alone.

Studies on rat aortic rings

In intact endothelium aortic rings, phenylephrine caused a concentration-dependent increase in contraction (Figure 3a). Incubation with LPS (10 μg ml^{-1}) for 4 h, shifted the concentration-contraction curve evoked by phenylephrine significantly to the right and decreased the maximal contractile response (Figure 3a). Co-incubation with β-lapachone (1 and 3 μM) significantly reversed the LPS-induced changes in the response to phenylephrine (Figure 3a). The calculated EC_{50} values and maximal contractile responses in these experiments were shown in Table 2. When β-lapachone (3 μM) was added 3 h after LPS into the medium, the contractions evoked by phenylephrine were not significantly different in the presence (pEC_{50}, 6.35 ± 0.05) or absence (pEC_{50}, 6.42 ± 0.06) of β-lapachone. Treatment of aortic rings with β-lapachone (3 μM) alone had no significant effects on contractions evoked by phenylephrine (data not shown).

For further understanding the involvement of NOSs including inducible and constitutive forms in the aortic ring system, Western blot analysis was used to determine the NOSs proteins expression in the LPS-treated aortic rings in the presence or absence of β-lapachone. The results were shown in Figure 3b, treatment with LPS (10 μg ml^{-1}) for 4 h resulted in a significant increase in iNOS protein synthesis which was inhibited in the presence of β-lapachone (3 μM), but did not affect the constitutive NOSs (eNOS and nNOS) in aortic rings.

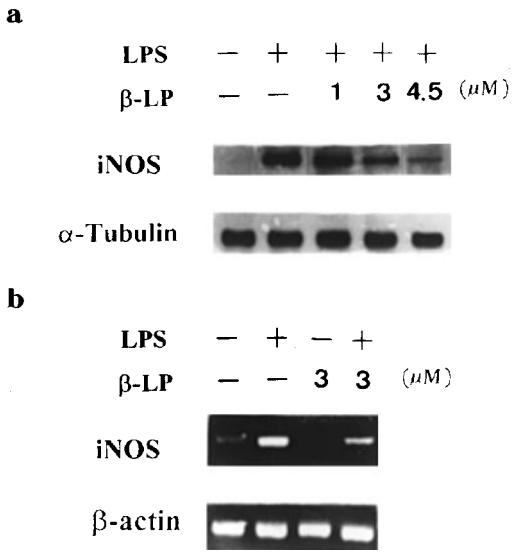

Figure 2 Inhibition of LPS-induced iNOS protein and iNOS mRNA expression. Alveolar macrophages were stimulated with LPS (10 μg ml^{-1}) in the presence or absence of β-lapachone (β-LP, 1–4.5 μM). Cells were harvested at 24 h for Western blot analysis (a) and at 6 h for iNOS mRNA analysis (b). The internal controls of iNOS protein and mRNA were α-tubulin and β-actin respectively. Data are typical of three separate experiments.

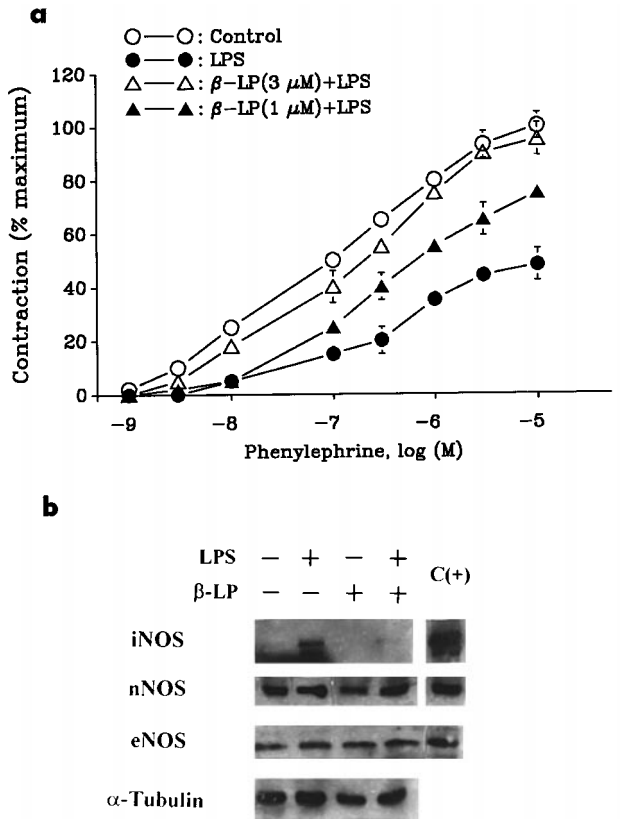

Figure 3 Inhibition of LPS-induced hypovasocontractility and aortic iNOS protein. Rat aortic rings with endothelium were stimulated with LPS (10 μg ml^{-1}) in the presence or absence of β-lapachone (β-LP, 1 and 3 μM) for 4 h. Effects of β-LP on contractions evoked by phenylephrine (a) or inducible and constitutive (endothelial and neuronal) NOS forms (b) in LPS (10 μg ml^{-1})-treated rings were shown. In Western blot analysis, the cellular lysates as positive controls (C(+)) were from LPS-treated RAW 264.7 cells (iNOS), human endothelial cells (eNOS) and rat pituitary cells (nNOS) and α-tubulin served as control for sample loading and integrity. Data are presented as means ± s.e.mean of 3–5 separate experiments in (a) and are typical of three separate experiments in (b).

Discussion

In this study, we performed experiments to examine the effects of β-lapachone on NO production and iNOS expression induced by LPS in rat alveolar macrophages. In addition, the effects of β-lapachone on LPS-induced aortic relaxation and iNOS protein expression were also studied. We found that low concentrations of β-lapachone were capable of inhibiting all of these effects induced by LPS. These results may have implication for the design of a novel anti-inflammatory agent working through the L-arginine-nitric oxide pathway.

The exposure of rat alveolar macrophage to LPS for several hours was associated with the accumulation of nitrite in the incubation medium. β-Lapachone was capable of inhibiting the production of NO in alveolar macrophages when co-incubated with LPS in a time and concentration-dependent manner, without any evidence for a cytotoxic effect, but was ineffective once inducible NO synthase is expressed by pre-activation with LPS. These results imply that β-lapachone may inhibit induction of NO synthase gene expression. To further investigate this possibility, the protein and mRNA for inducible NO synthase was examined. We found that the iNOS protein and gene expression in alveolar macrophages treated with LPS could be inhibited by β-lapachone. These results indicate that β-lapachone inhibits the induction rather than the activity of NO synthase. This profile of action is similar to that of glucocorticoids which probably act by inhibiting gene expression or the transcription of inducible NO synthase mRNA (Radomski *et al*., 1990). On the other hand, there is an iNOS induction leading to widespread vasodilatation and reduced responsiveness to vasoconstrictors in septic shock (Vallance & Moncada, 1993). Our results showed that the stimulation of isolated rat aortic rings with LPS for several hours reduced their responsiveness to phenylephrine, as results similar to previous studies (Bogle & Vallance, 1996; Joly *et al*., 1997), which demonstrated induction of iNOS in vascular rings by LPS. Co-incubation with β-lapachone prevented this vascular hypocontractility. However, β-lapachone failed to inhibit the hypocontractility to phenylephrine once NO synthase was induced by LPS in contrast N^{G}-nitro-L-arginine

Table 1 Cytotoxicity assay for β-lapachone in control and LPS-treated rat alveolar macrophages

	Control	*LPS*	*LPS* + *β-LP*(3)	*LPS* + *β-LP*(4.5)	*β-LP*(3)	*β-LP*(4.5)
OD_{570}	0.38 ± 0.05	0.44 ± 0.07	0.40 ± 0.04	0.41 ± 0.03	0.40 ± 0.06	0.39 ± 0.05

The values of OD_{570} were measured by the colorimetric MTT assay as described in Methods. The alveolar macrophages were treated with control vehicle, LPS (10 μg ml^{-1}), β-lapachone (β-LP, 3 and 4.5 μM) and LPS + β-lapachone for 24 h. Data are presented as means ± s.e.mean of 3–5 separate experiments performed in triplicate.

Table 2 Effects of β-lapachone on vascular reactivity evoked by phenylephrine in LPS-treated rat aorta rings

Treatment	*pEC_{50}*	*Maximum tension (g)*
Control	7.06 ± 0.08	1.34 ± 0.17
LPS	6.42 ± 0.06*	0.72 ± 0.12*
LPS + β-lapachone (1 μM)	6.60 ± 0.03*,**	0.94 ± 0.19*,**
LPS + β-lapachone (3 μM)	6.93 ± 0.06**	1.28 ± 0.11**

Rat thoracic aorta rings were incubated for 4 h with either control vehicle, LPS (10 μg ml^{-1}) or LPS and β-lapachone. Concentration-response curves to phenylephrine were then constructed and curves fitting using a logistic-sigmoid curve weighted for the standard deviation of each experimental value. Data are presented as means ± s.e.mean of 3–5 separate experiments. *$P<0.05$ as compared with control; **$P<0.05$ as compared with LPS alone.

methyl ester (100 μM), an inhibitor of NOS, did significantly inhibit this response (data not shown). Furthermore, treatment with LPS for 4 h resulted in a significant increase in iNOS protein synthesis which was inhibited in the presence of β-lapachone, but did not affect the constitutive NOSs (eNOS and nNOS) in aortic rings. Thus, β-lapachone likely prevents the induction of a functional active iNOS in the vessel wall as well as macrophages and thus might contribute to the anti-inflammatory effect of this drug.

β-Lapachone has been identified as a potent inhibitor of topoisomerase I (Li *et al*., 1993). Recent studies showed that β-lapachone is capable of inducing human promyelocytic leukaemia or human prostate cancer cells to undergo programmed cell death (Planchon *et al*., 1995; Li *et al*., 1995), but it (1–5 μM) did not induce apoptosis in normal human lymphocytes (Chau *et al*., 1998) or rat alveolar macrophages (data not shown). DNA topoisomerase has been reported to be involved in the noncytotoxic and cytotoxic cellular processes mediated by tumour necrosis factor (Baloch *et al*., 1990) or as a cofactor for activator-dependent transcription by RNA polymerase II (Kretzschmar *et al*., 1993). The inhibition of topoisomerase was also implicated as the mechanism of the immunosuppressive activity of streptonigrin on B-cell proliferation induced by LPS (Suzuki *et al*., 1996). Thus, the inhibition of topoisomerase may be involved in the action of β-lapachone on LPS-iNOS. However, further studies are required to determine the precise mechanism by which β-lapachone inhibits the induction of NO synthase activity in alveolar macrophages and aorta.

In conclusion, the results of this study demonstrate that the topoisomerase inhibitor β-lapachone prevents the induction of active NO synthase in rat alveolar macrophages and isolated vessels in response to LPS. This finding provides a potential drug for the development of novel anti-inflammatory agents.

This work was supported by research grants from National Science Council of the Republic of China (NSC 85 - 2331 - B - 002 - 292).

References

BALOCH, Z., COHEN, S. & COFFMAN, F.D. (1990). Synergistic interactions between tumor necrosis factor and inhibitors of DNA topoisomerase I and II. *J. Immunol.,* **145,** 2908–2913.

BOGLE, R.G., SOO, S.-C., WHITLEY, G.ST.J., JOHNSTONE, A.P. & VALLANCE, P. (1994). Effects of anti-fungal imidazoles on mRNA levels and nitric oxide synthesis in cultured murine macrophages. *Br. J. Pharmacol.,* **105,** 919–923.

BOGLE, R.G. & VALLANCE, P. (1996). Functional effects of econazole on inducible nitric oxide synthase: production of a calmodulin-dependent enzyme. *Br. J. Pharmacol.,* **117,** 1053–1058.

BRAIN, J.D. & FRANK, R. (1968). Recovery of free cells from rat lungs by repeated washings. *J. Appl. Physiol.,* **25,** 63–69.

CHAU, Y.P., SHIAH, S.G., DON, M.J. & KUO, M.L. (1998). Involvement of hydrogen peroxide in topoisomerase inhibitor β-lapachone-induced apoptosis and differentiation in human leukaemia cells. *Free Radical Biol. Med.,* **24,** 660–670.

GONCALVES, A.M., VASCONELLOS, M.E., DECOMPO, R., CRUZ, N.S., SOUZA, W.R. & LEON, W. (1980). Evaluation of the toxicity of 3-ally-beta-lapachone against Trypanosoma cruzi bloodstream forms. *Mol. Biochem. Parasitol.,* **1,** 167–176.

GREEN, L.C., WAGNER, D.A., GLOGOWSKI, K., SKIPPER, P.L., WISHNOK, J.S. & TANNENBAUM, S.R. (1982). Analysis of nitrate, nitrite and [^{15}N]nitrate in biological fluids. *Anal. Biochem.,* **126,** 131–138.

GUIRAUD, P., STEIMAN, R., CAMPOS-TAKAKI, G.M., SEIGLE-MURANDI, F. & SIMEN DE BUOCHBERG, M. (1994). Comparison of antibacterial and antifungal activities of lapachol and beta-lapachone. *Planta Med.,* **60,** 373–374.

HIBBS, J.B.J., TAINTOR, R.R. & VAVRIN, F. (1987). Macrophage cytotoxicity: role for L-arginine deiminase and imino nitrogen oxidation to nitrite. *Science,* **235,** 473–476.

JOLY, G.A., AYRES, M. & KILBOURN, R.G. (1997). Potent inhibition of inducible nitric oxide synthase by geldanamycin, a tyrosine kinase inhibitor, in endothelial, smooth muscle cells, and in rat aorta. *FEBS Lett.,* **403,** 40–44.

KOBZIK, L., REID, M.B., BREDT, D.S. & STAMLER, J.S. (1994). Nitric oxide in skeletal muscle. *Nature,* **372,** 546–548.

KRETZSCHMAR, M., MEISTERERNST, M. & ROEDER, R.G. (1993). Identification of human DNA topoisomerase I as a cofactor for activator-dependent transcription by RNA polymerase II. *Proc. Natl. Acad. Sci. U.S.A.,* **90,** 11508–11512.

LI, C.J., AVERBOUKH, L. & PARDEE, A.B. (1993). Beta-lapachone, a novel DNA topoisomerase I inhibitor with a mode of action different from camptothecin. *J. Biol. Chem.,* **268,** 22463–22468.

LI, C.J., WANG, C. & PARDEE, A.B. (1995). Induction of apoptosis by beta-lapachone in human prostate cancer cells. *Cancer Res.,* **55,** 3712–3715.

LOWENSTEIN, C.J. & SNYDER, S.H. (1992). Nitric oxide, a novel biologic messenger. *Cell,* **70,** 705–707.

LOWRY, O.H., ROSENBROUGH, N.J., FARR, A.L. & RANDALL, R.J. (1951). Protein measurement with the Folin phenol reagent. *J. Biol. Chem.,* **193,** 265–275.

MONCADA, S., PALMER, R.M.J. & HIGGS, E.A. (1991). Nitric oxide: Physiology, pathophysiology, and pharmacology. *Pharmacol. Rev.,* **43,** 109–142.

MORRIS, S.M. & BILLIAR, T.R. (1994). New insights into the regulation of inducible nitric oxide synthesis. *Am. J. Physiol.,* **266,** E829–E839.

MOSMANN, T. (1983). Rapid colorimetric assay for cellular growth and survival: application to proliferation and cytotoxicity assays. *J. Immunol. Methods,* **65,** 55–63.

MURPHY, S., SIMMONS, M.L., AGULLO, L., GARCIA, A., FEINSTEIN, D.L., GALEA, E., REIS, D.J., MINC-GOLOMB, D. & SCHWARTZ, J.P. (1993). Synthesis of nitric oxide in CNS glial cells. *Trend Neurosci.,* **16,** 323–328.

PLANCHON, S.M., WUERZBERGER, S., FRYDMAN, B., WITIAK, D.T., HUTSON, P., CHURCH, D.R., WILDING, G. & BOOTHMAN, D.A. (1995). Beta-lapachone-mediated apoptosis in human promyelocytic leukemis (HL-60) and human prostate cancer cells: A p53-independent response. *Cancer Res.,* **55,** 3706–3711.

RADOMSKI, M.W., PALMER, R.M.J. & MONCADA, S. (1990). Glucocorticoids inhibit the expression of an inducible, but not the constitutive, nitric oxide synthase in vascular endothelial cells. *Proc. Natl. Acad. Sci. U.S.A.,* **87,** 10043–10047.

SCHAFFNER-SABBA, K., SCHMIDT-RUPPIN, K.H., WEHRIL, W., SCHUERCH, A.R. & WASLEY, J.W.F. (1984). Beta-lapachone: synthesis of derivatives and activities in tumor models. *J. Med. Chem.,* **27,** 990–994.

STUEHR, D.J. & NATHAN, C.F. (1989). Nitric oxide: a macrophage product responsible for cytostasis and respiratory inhibition in tumor target cells. *J. Exp. Med.,* **169,** 1543–1555.

SUZUKI, H., YAMASHITA, M., LEE, J.C., KATAOKA, T., MAGAE, J. & NAGAI, K. (1996). Immunosuppressive activity of streptonigrin in vitro and in vivo. *Biosci. Biotech. Biochem.,* **60,** 789–793.

VALLANCE, P. & MONCADA, S. (1993). The role of endogenous nitric oxide in septic shock. *New Horizons,* **1,** 77–86.

(Received June 5, 1998
Revised November 3, 1998
Accepted November 6, 1998)

British Journal of Pharmacology (1999) 126, 751–761
http://www.stockton-press.co.uk/bjp

Inhibitory effects of aprindine on the delayed rectifier K^+ current and the muscarinic acetylcholine receptor-operated K^+ current in guinea-pig atrial cells

[1]Yuki Ohmoto-Sekine, [1]Hiroko Uemura, [1]Masaji Tamagawa & *,[1]Haruaki Nakaya

[1]Department of Pharmacology, Chiba University School of Medicine, Inohana 1-8-1, Chuo-ku, Chiba 260-8670, Japan

1 In order to clarify the mechanisms by which the class Ib antiarrhythmic drug aprindine shows efficacy against atrial fibrillation (AF), we examined the effects of the drug on the repolarizing K^+ currents in guinea-pig atrial cells by use of patch-clamp techniques. We also evaluated the effects of aprindine on experimental AF in isolated guinea-pig hearts.

2 Aprindine (3 μM) inhibited the delayed rectifier K^+ current (I_K) with little influence on the inward rectifier K^+ current (I_{K1}) or the Ca^{2+} current. Electrophysiological analyses including the envelope of tails test revealed that aprindine preferentially inhibits I_{Kr} (rapidly activating component) but not I_{Ks} (slowly activating component).

3 The muscarinic acetylcholine receptor-operated K^+ current ($I_{K.ACh}$) was activated by the extracellular application of carbachol (1 μM) or by the intracellular loading of GTPγS. Aprindine inhibited the carbachol- and GTPγS-induced $I_{K.ACh}$ with the IC_{50} values of 0.4 and 2.5 μM, respectively.

4 In atrial cells stimulated at 0.2 Hz, aprindine (3 μM) *per se* prolonged the action potential duration (APD) by 50±4%. The drug also reversed the carbachol-induced action potential shortening in a concentration-dependent manner.

5 In isolated hearts, perfusion of carbachol (1 μM) shortened monophasic action potential (MAP) and effective refractory period (ERP), and lowered atrial fibrillation threshold. Addition of aprindine (3 μM) inhibited the induction of AF by prolonging MAP and ERP.

6 We conclude the efficacy of aprindine against AF may be at least in part explained by its inhibitory effects on I_{Kr} and $I_{K.ACh}$.

Keywords: Antiarrhythmic drug; aprindine; atrial fibrillation; delayed rectifier K^+ current; muscarinic acetylcholine receptor-operated K^+ current

Abbreviations: A_1, amplitude of the fast decay phase; A_2, amplitude of the slow decay phase; AF, atrial fibrillation; AFT, atrial fibrillation threshold; ANOVA, analysis of variance; APD, action potential duration; APD_{50}, APD at 50% repolarization level; APD_{90}, APD at 90% repolarization level; CT, conduction time; ERP, effective refractory period; I_{Ca}, L-type Ca^{2+} current; I_K, delayed rectifier K^+ current; I_{K1}, inward rectifier K^+ current; $I_{K.ACh}$, muscarinic acetylcholine receptor-operated K^+ current; $I_{K,depo}$, time-dependent current of I_K during depolarizing pulses; I_{Kr}, rapid component of I_K; I_{Ks}, slow component of I_K; $I_{K,tail}$, tail current of I_K; I_{Kur}, urtrarapidly activating delayed rectifier current; I_{to}, transient outward current; MAP, monophasic action potentials; MAP_{90}, MAP at 90% repolarization level; RMP, resting membrane potential; τ_1, time constant of the fast decay phase; τ_2, time constant of the slow decay phase; V_{max}, maximum upstroke velocity of the action potential

Introduction

Atrial fibrillation (AF) is not such a benign arrhythmia as thought for a long time, but actually is associated with considerable morbidity and mortality (Brand *et al*., 1985; Kopecky *et al*., 1987; Alpert *et al*., 1988). Therefore the insight is growing that it may not be sufficient to control the ventricular rate during AF, but it may be necessary to cure AF itself in order to prevent the serious adverse outcome. Many investigators were devoted to the mechanisms of AF, and the wavelet hypothesis for AF has emerged from the mapping studies on experimental AF (Allessie *et al*., 1985). It was established that several wavelets and the shortened length of wavelet, i.e., the shortened wavelength, were required for perpetuation of AF. As the wavelength is the product of refractory period and conduction velocity, the pharmacological strategy for prevention of AF is to prolong atrial refractory periods or to increase conduction velocity. Several K^+ currents including the delayed rectifier K^+ current (I_K) and the muscarinic acetylcholine receptor-operated K^+ current ($I_{K.ACh}$) are involved in the repolarization of the action potential in atrial cells (Carmeliet, 1994). Accordingly, drugs which inhibit the repolarizing K^+ currents may be used to prolong refractoriness and therefore to treat AF.

Class I antiarrhythmic drugs have been subdivided according to their effects on action potential duration (APD): class Ia lengthens the duration, Ib shortens it, and Ic has no effects or minimally increases APD. Since aprindine hydrochloride (hereafter abbreviated as aprindine) was demonstrated to depress the maximum upstroke velocity of the action potential (V_{max}) and abbreviate APD in Purkinje and ventricular tissues (Verdonck *et al*., 1974; Steinberg & Greenspan, 1976), it was classified as a class Ib antiarrhythmic drug (Adams *et al*., 1984). It is well established that class Ib drugs such as lignocaine and mexiletine are rarely effective against supraventricular arrhythmias including AF (Hondeghem & Roden, 1995). However, aprindine has been shown to

* Author for correspondence; E-mail: nakaya@med.m.chiba-u.ac.jp

be effective against not only ventricular arrhythmias but also supraventricular arrhythmias including AF (Kesteloot *et al*., 1973; Breithardt *et al*., 1974). Nevertheless, effects of aprindine on repolarizing K^+ currents in atrial cells have not been thoroughly examined. This study was undertaken to examine the effects of aprindine on the K^+ currents in isolated guinea-pig atrial cells using patch clamp techniques. Since aprindine potently inhibited $I_{K.ACh}$ and the rapid component of I_K (I_{Kr}) in this study, we also evaluated the effects of aprindine on the experimental AF in Langendorff-perfused guinea-pig hearts.

Methods

Patch-clamp study

All experiments were performed under the regulations of the Animal Research Committee of the School of Medicine, Chiba University. Single atrial cells of the guinea-pig heart were isolated by an enzymatic dissociation method, as described previously (Tohse *et al*., 1992). The heart was removed from open chest guinea-pigs (250–450 g) anaesthetized with pentobarbitone sodium and mounted on a modified Langendorff perfusion system for retrograde perfusion of the coronary circulation with a normal HEPES-Tyrode's solution. The perfused medium was changed to a nominally Ca^{2+}-free Tyrode's solution and then to the solution containing 0.02% wt vol^{-1} collagenase (Wako, Osaka, Japan). After digestion, the heart was perfused with high K^+, low-Cl^- solution (modified KB solution) (Isenberg & Kloeckner, 1982; Nakaya *et al*., 1993). Atrial tissue was cut into small pieces in the modified KB solution and gently shaken to dissociate cells. The composition of the normal HEPES-Tyrode's solution was (in mM): NaCl 143, KCl 5.4, $CaCl_2$ 1.8, $MgCl_2$ 0.5, NaH_2PO_4 0.33, glucose 5.5, and HEPES-NaOH buffer (pH 7.4) 5.0. The composition of the modified KB solution was (in mM): KOH 70, l-glutamic acid 50, KCl 40, taurine 20, KH_2PO_4 20, $MgCl_2$ 3, glucose 10, EGTA 1.0, and HEPES-KOH buffer (pH 7.4) 10.

Whole-cell membrane currents were recorded by the patch-clamp method (Hamill *et al*., 1981). Single atrial cells were placed in a recording chamber (1 ml volume) attached to an inverted microscope (model IMT-2, Olympus, Tokyo, Japan) and superfused with the HEPES-Tyrode's solution at a rate of 3 ml min^{-1}. The temperature of the external solution was kept constant at 36.0 ± 1.0°C. Patch pipettes were made from glass capillaries with a diameter of 1.5 mm using a vertical microelectrode puller (model PB-7, Narishige, Tokyo, Japan). They were filled with an internal solution, and their resistance was 2–4 MΩ. The composition of the pipette solution was (in mM): potassium aspartate 110, KCl 20, $MgCl_2$ 1.0, potassium ATP 5.0, potassium phosphocreatine 5.0, EGTA 10, and HEPES-KOH buffer (pH 7.4) 5.0. In part of experiments GTP (100 μM) or GTPγS (100 μM) was also added to the pipette solution. The free Ca^{2+} concentration in the pipette solution was adjusted to pCa 8 according to the calculation by Fabiato & Fabiato (1979) with the correction of Tsien & Rink (1980). After the giga-ohm seal between the tip of the electrode and the cell membrane was established, the membrane patch was disrupted by more negative pressure to make the whole-cell voltage-clamp mode. The electrode was connected to a patch-clamp amplifier (model CEZ-2300, Nihon Koden, Tokyo, Japan). Recordings were filtered at 1 kHz bandwidth, and series resistance was compensated. Command pulse signals were generated by a 12-bit digital-to-analog converter controlled by pCLAMP software (Axon Instruments, Inc., Foster City, CA, U.S.A.). Current signals were digitized and stored on the hard disc of an IBM-compatible computer (Compaq Prolinea 4/50 with a 200 Mbyte hard disc, Houston, TX, U.S.A.). A liquid junction potential between the internal solution and the bath solution of −8 mV was corrected.

Membrane currents were recorded by delivering 300 ms depolarizing or hyperpolarizing pulses from a holding potential of −40 mV at a rate of 0.1 Hz, and effects of aprindine on the membrane currents were examined. The I_K was measured by delivering the depolarizing pulses from a holding potential of −40 mV after the inhibition of the L-type Ca^{2+} current (I_{Ca}) by nifedipine. The I_K of guinea-pig atrial myocyte has been reported to consist of two components, rapid (I_{Kr}) and slow component (I_{Ks}) (Sanguinetti & Jurkiewicz, 1991). In order to determine whether aprindine affects I_{Kr} and/or I_{Ks}, effects of aprindine on the I_K elicited by short depolarizing pulses (200 ms) and long depolarizing pulses (3 s) were evaluated. Effect of aprindine on I_K in the presence of E-4031, a prototype I_{Kr} blocker, was also examined. In addition, the envelope of tails test was performed. The ratio of tail current of I_K ($I_{K,tail}$) to the time-dependent current activated during depolarizing pulses of various durations ($I_{K,depo}$) was determined in the absence and presence of aprindine. The $I_{K,tail}$ was measured as a peak current which was actually recorded upon the clamp back to the holding potential. The deactivation kinetics of I_K was also analysed by using an exponential fitting. The exponential analysis of $I_{K,tail}$ after 500 ms and 5 s depolarizing pulses was performed by fitting the deactivation kinetics to an equation of the following form;

$$y = A_1 \exp(-t/\tau_1) + A_2 \exp(-t/\tau_2) + A_0$$

where τ_1 and τ_2 are fast and slow time constants, A_1 and A_2 are the amplitudes of each component and A_0 is the baseline value. The curve-fitting procedure used a non linear least-squares algorithm. We used two exponentials fitting for $I_{K,tail}$ analysis before and after aprindine because we could obtain better least square residual values.

The $I_{K.ACh}$ was activated by the extracellular application of carbachol (1 μM) or adenosine (10 μM) in the GTP-loaded atrial cells or by the intracellular loading of GTPγS, a nonhydrolyzable GTP analogue, in atrial cells held at −40 mV. Effects of various concentrations of aprindine on the $I_{K.ACh}$ activated in three different ways were examined. To calculate per cent inhibition of $I_{K.ACh}$, the difference between the steady-state current in the solution containing either carbachol (1 μM) or adenosine (10 μM) and the current level in the absence of any agonists was taken as 100% in the GTP-loaded cells. In the GTPγS-loaded cells, the difference between the persistent outward current in the absence of agonist and the initial current level just after the break of the patch membrane in the pipette was taken as 100%.

Current-clamp experiments were also performed in the whole-cell recording mode at 36 ± 1°C. External and pipette solutions were the same as those used to record the carbachol-induced $I_{K.ACh}$. The cells were stimulated by passing 2 ms currents through the pipette at a rate of 0.2 Hz. After a stabilization of action potential configuration, effects of aprindine on the action potential in the presence or absence of carbachol (1 μM) were evaluated.

Isolated heart study

The heart was removed from the open-chest guinea-pigs (250–450 g) anaesthetized with pentobarbitone sodium. The aorta was cannulated and perfused at a constant pressure

(800 mmH_2O) of normal Tyrode's solution. The composition of the normal Tyrode's solution was (in mM): NaCl 125, KCl 4, $CaCl_2$ 1.8, $MgCl_2$ 0.5, NaH_2PO_4 1.8, glucose 5.5 and $NaHCO_3$ 25 (pH 7.4). The solution was aerated with a mixture of 95% O_2 and 5% CO_2, and maintained at 36.0 ± 0.5°C.

The right atrium was stimulated with an external bipolar silver electrode. The stimuli were rectangular pulses of 2-ms duration at twice the diastolic threshold, delivered from an electronic stimulator (model SEC-2102, Nihon Kohden). The left atrial electrograms were recorded using an additional bipolar suction electrode for measure of monophasic action potentials (MAP) with a diameter of 2.5 mm, attached to the walls of the left atria. Electrograms were amplified by a bioelectric amplifier (model AB-620G, Nihon Kohden) at a time constant of 3 ms and recorded at a paper speed of 10–100 mm s^{-1} using a chart recorder (model 8K21, NEC San-ei Instruments, Ltd., Tokyo, Japan).

Atrial effective refractory period (ERP) was determined using the standard extrastimulus technique. After every eighth basic right atrial stimulus (S_1S_1 200 ms), an extrastimulus (S_2) was delivered with a shortening of the coupling interval (S_1S_2) in 5-ms steps until the S_2 produced no atrial activity. ERP was defined as the longest S_1S_2 that failed to elicit atrial activity in response to S_2. Conduction time (CT) from the right to the left atrium was measured as the time from the pacing spike to the first upstroke of left atrial action potential on the oscilloscope (model VC-11, Nihon Kohden).

Atrial fibrillation threshold (AFT) was measured by rapid atrial electrical stimulation according to the method of Inoue *et al*. (1994). The fibrillating current consisted of a train of 50 square wave pulses, 2 ms in duration at a frequency of 50 Hz for a duration of 1 s. The pulse train was delivered to the right atrium after every eighth basic paced beat. The current was increased in increments of 0.1 mA from an intensity twice the diastolic threshold. The AFT was defined as the minimum amount of current required to induce AF which was sustained for at least 30 s. Sustained AF was terminated readily by perfusing normal Tyrode's solution. The stimulator used in this study was unable to deliver a current greater than 11 mA. If AF could not be induced by the current as high as 11 mA, the AFT was considered as more than 11 mA.

Initial measurements were made during perfusion with Tyrode's solution (control values). The same measurements were then repeated 10 min after changing to a Tyrode's solution containing carbachol (1 μM) and 10 min after the perfusion of the normal Tyrode's solution containing carbachol (1 μM) and aprindine (3 μM).

Drugs

Drugs used in this study were as follows: aprindine hydrochloride (Mitsui Pharmaceutical Co, Tokyo, Japan), carbachol chloride (Tokyo Kasei, Tokyo, Japan), adenosine, nifedipine (Sigma, U.S.A.), E-4031(N-[4-[[1-[2-(6-methyl-2-pyridinyl)ethyl]-4-piperidinyl]carbonyl]phenyl] methanesulphonamide dihydrochloride dihydrate) (Eisai Co, Tokyo, Japan). Nifedipine was dissolved in ethanol as a stock solution of 10 mM. The final concentration of ethanol was less than 0.1%. It was confirmed that this concentration of ethanol had no influence on the membrane currents. Other drugs were dissolved in distilled water.

Statistics

All values are presented mean ± s.e.mean. Student's *t*-test and ANOVA were used for statistical analyses. *P* value of less than

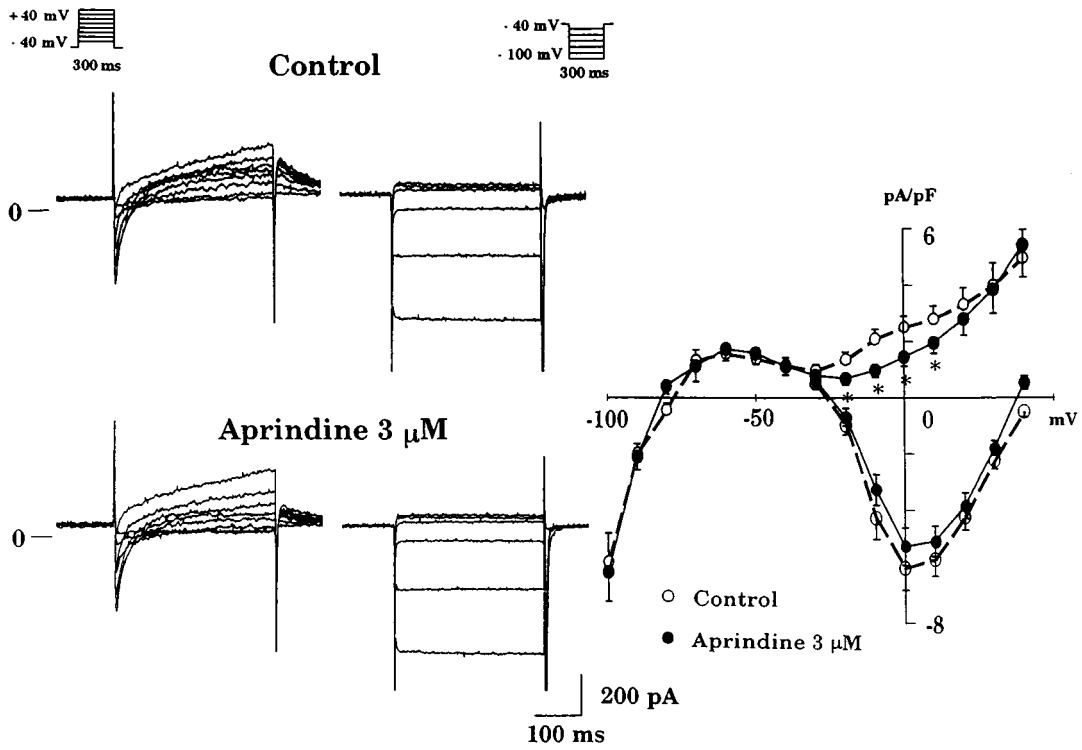

Figure 1 Effects of aprindine on membrane currents in guinea-pig atrial cells. Actual current traces elicited by 300 ms depolarizing and hyperpolarizing pulses from a holding potential of −40 mV before (upper) and after aprindine (3 μM) (lower) in a single atrial cell are shown on left. Cell capacitance was 70 pF. Current-voltage relations for the peak current and the current at the end of 300 ms test pulse in the absence and presence of aprindine, obtained from five cells, are shown on right. $^*P<0.05$ vs control.

0.05 was considered significant. The concentration-effect data were fitted and the IC_{50} values were obtained using Delta Graph Professional (Delta Point, Poloroid computing, Tokyo, Japan).

Results

Effects of aprindine on the delayed rectifier K^+ current

Effects of aprindine on the membrane current system were examined in guinea-pig atrial myocytes. Membrane currents were elicited by 300-ms test pulses to various potentials from a holding potential of −40 mV at 0.1 Hz. Representative changes in the membrane currents and summarized data of current-voltage relations after aprindine (3 μM) are shown in the left and right panels of Figure 1, respectively. We selected a concentration of aprindine, 3 μM, because this concentration of aprindine was reported to suppress V_{max} in isolated ventricular tissues (Kodama *et al.*, 1987a,b) and to be within a therapeutic range in clinical studies (Zipes *et al.*, 1977). Aprindine slightly decreased I_{Ca}, but the changes were statistically insignificant. The steady-state outward and inward currents, elicited by hyperpolarizing test pulses, were hardly affected by aprindine, indicating the lack of the effect on the inward rectifier K^+ current (I_{K1}). However, aprindine decreased the late outward current elicited by depolarizing test pulses to voltage range from −20 mV to +10 mV, concomitantly with the decrease of the outward tail current elicited by the clamp back to the holding potential of −40 mV (Figure 1). These findings suggest that aprindine inhibits I_K in guinea-pig atrial cells.

The I_K of guinea-pig atrial cells has been reported to consist of two components, I_{Kr} and I_{Ks} (Sanguinetti & Jurkiewicz, 1991). I_{Kr} is activated rapidly with mild depolarizations, whereas I_{Ks} is activated slowly with a sigmoidal time course at more positive potentials. To test whether aprindine specifically blocks one or both components of I_K, the following experiments were conducted. After the blockade of I_{Ca} by nifedipine (1 μM) short (200 ms) or long (3 s) depolarizing pulses were applied from a holding potential of −40 mV to various potentials at a rate of 0.1 Hz. The blocking effect of aprindine on I_K was somewhat prominent with short pulses, compared to long pulses (Figure 2). In addition, the aprindine-induced inhibition of I_K at the end of depolarizing pulses was more marked during mild depolarization to potentials ranging from −20 to +20 mV than during strong depolarization to potentials ranging from +30 to +60 mV for both 200 ms and 3 s test pulses. These results suggest that aprindine preferentially inhibits I_{Kr}.

In order to test whether aprindine inhibits I_{Ks} as well as I_{Kr}, we examined the effect of aprindine on I_K in the presence of the I_{Kr} blocker E-4031 (Figure 3). After the full inhibition of I_{Kr} by E-4031 (5 μM), aprindine at a concentration of 3 μM hardly affected the outward current during the depolarizing test pulses of 3 s and the tail current after the clamp back to the holding potential. Aprindine decreased the amplitude of the $I_{K,depo}$ at +60 mV by 4±12% (n.s., $n=4$). Thus, aprindine inhibits I_{Kr} but not I_{Ks}.

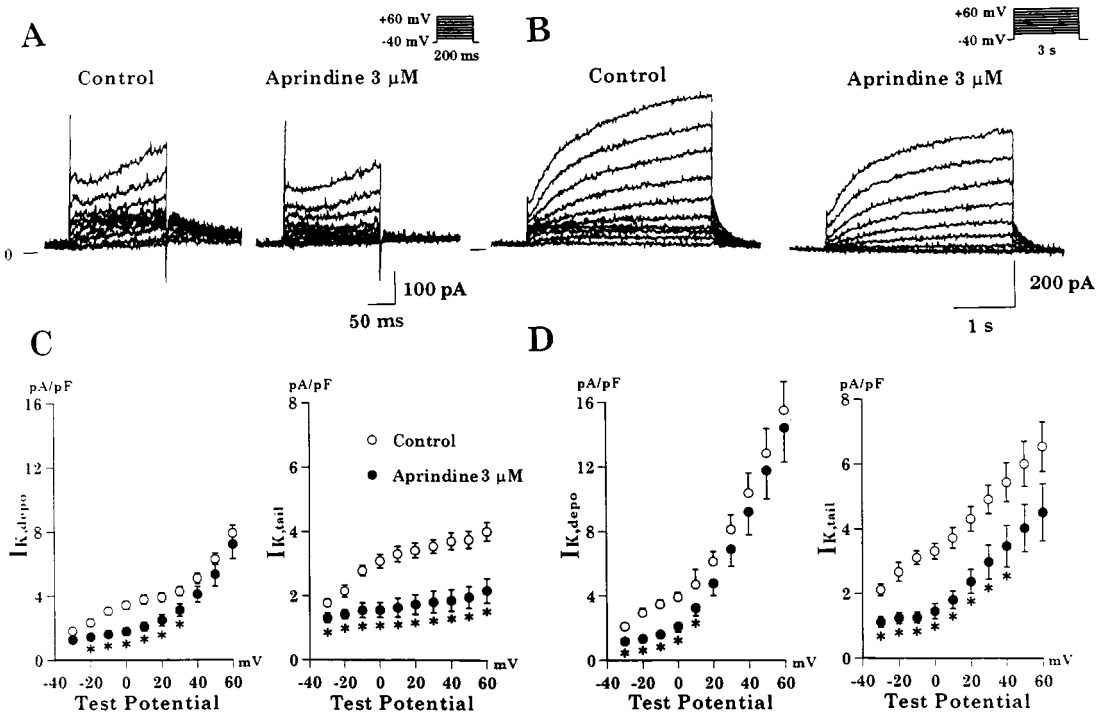

Figure 2 Effects of aprindine on the delayed rectifier K^+ current (I_K) elicited by short and long test pulses. (A) Current traces recorded during 200 ms depolarizing pulses from a holding potential of −40 mV before (left) and after exposure to aprindine (3 μM) (right) in a single atrial cell. The external solution contained nifedipine (1 μM). Cell capacitance was 45 pF. (B) Current traces recorded during 3 s depolarizing pulses from a holding potential of −40 mV before (left) and after exposure to aprindine (3 μM) (right) in a single atrial cell. The external solution contained nifedipine (1 μM). Cell capacitance was 45 pF. (C) Graphs showing I_K measured at the end of 200 ms test pulses to the indicated test potential ($I_{K,depo}$, left) and I_K measured after repolarization to −40 mV from the indicated test potential ($I_{K,tail}$, right). Data represent means±s.e.mean of six cells before and after aprindine (3 μM). (D) Graphs showing I_K measured at the end of 3 s test pulses to the indicated test potential ($I_{K,depo}$, left) and I_K measured after repolarization to −40 mV from the indicated test potential ($I_{K,tail}$, right). Data represent means±s.e.mean of six cells before and after aprindine (3 μM). $^*P<0.05$ vs control.

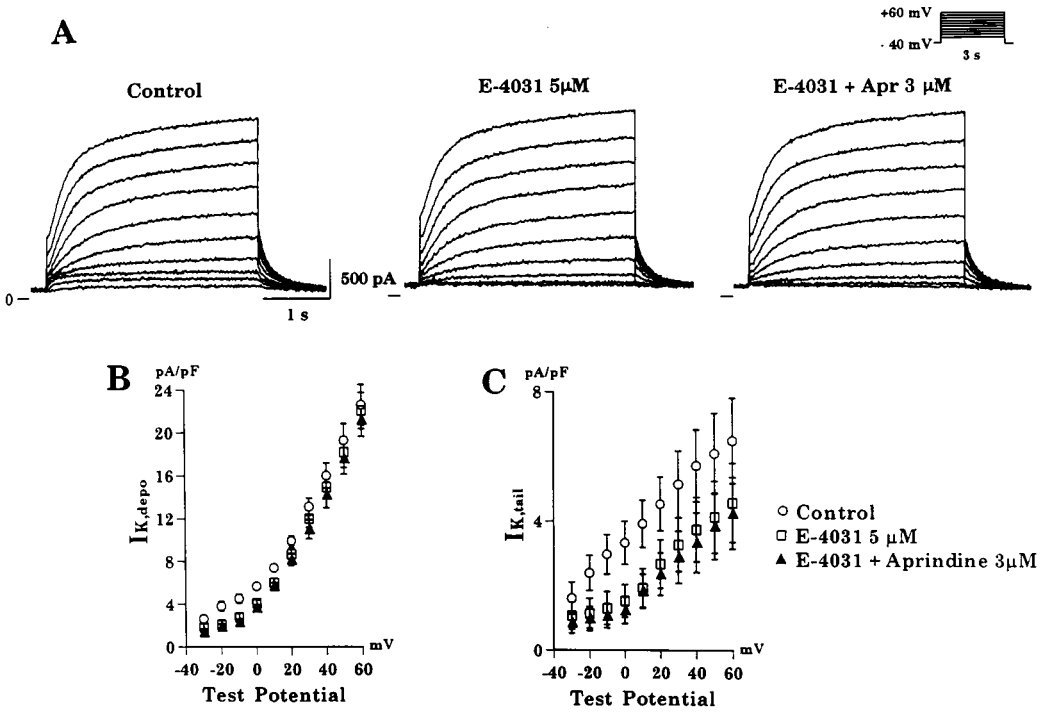

Figure 3 Effects of aprindine (3 μM) on the delayed rectifier K^+ current (I_K) elicited by long test pulses in the presence of E-4031 (5 μM). (A) Current traces recorded during 3 s depolarizing pulses from a holding potential of -40 mV in the control condition (left), in the presence of E-4031 (5 μM) (middle) and after the addition of aprindine (3 μM) (right). The external solution contained nifedipine (1 μM) and the cell capacitance was 45 pF. Graphs showing I_K measured at the end of 3 s test pulses to the indicated test potential ($I_{K,depo}$) (B) and I_K measured after clamp back to -40 mV from the indicated test potential ($I_{K,tail}$) (C) are shown. Data represent means$\pm$s.e.mean of four cells. There was no significant difference between E-4031 alone and E-4031 plus aprindine at any data point.

The envelope of tails test was also performed to confirm this hypothesis. This test predicts that if I_K represents the activation of a single type of channel, then the magnitude of tail current after a given depolarizing pulse of various duration should increase in parallel with the magnitude of outward current during the depolarizing pulse (Sanguinetti & Jurkiewicz, 1990). For a given channel type, the ratio of $I_{K,tail}$; $I_{K,depo}$ should be constant, regardless of the duration of the pulse. Typical recordings elicited by the depolarizing pulses from a holding potentials to $+40$ mV for durations ranging from 100 ms to 5 s before and after exposure to aprindine (3 μM) are shown in Figure 4A, and the ratios of $I_{K,tail}$; $I_{K,depo}$ obtained from the depolarizing pulses of various durations are summarized in Figure 4B. The control ratio of $I_{K,tail}$; $I_{K,depo}$ in guinea-pig atrial cell was dependent on the duration of the pulses, as described previously (Sanguinetti & Jurkiewicz, 1991). After the application of aprindine (3 μM), the ratio of $I_{K,tail}$; $I_{K,depo}$ was almost constant for depolarizing pulses for various durations, suggesting that aprindine preferentially blocks I_{Kr}.

The time course of the deactivating tail currents after 500 ms and 5000 ms during the envelope of tails test was also analysed, as described in previous reports (Chinn, 1993, Valenzuela *et al*., 1994). In the absence of aprindine, the time course of the deactivating tail currents after 500 ms depolarizing pulses was well fitted with a biexponential function, as shown in Figure 5A. The fast (τ_1) and slow time constant (τ_2) of the control deactivation kinetics were 117 ± 3 ms and 514 ± 40 ms and their amplitude (A_1 and A_2) were 113 ± 15 pA and 23 ± 4 pA ($n=6$), respectively. The time course of $I_{K,tail}$ after 5000 ms depolarizing pulses was also well fitted with a biexponential function (Figure 5C). The time constants (τ_1 and τ_2) were 124 ± 6 ms and 531 ± 19 ms ($n=6$), which were not significantly different from those of $I_{K,tail}$ after 500 ms depolarizing pulses, although A_1 (162 ± 31 pA) and A_2 values (97 ± 13 pA) were larger than those obtained after 500-ms depolarizing pulses. In the presence of aprindine (3 μM) the tail currents were fitted by the sum of two exponential better than by one exponential, as shown in Figure 5B and D. After 500-ms depolarizing pulses, τ_1 and τ_2 values were 129 ± 4 ms and 515 ± 26 ms, and A_1 and A_2 values were 60 ± 11 pA and 21 ± 5 pA, respectively. Aprindine significantly decreased the A_1 values ($P<0.05$) without affecting A_2 and $\tau2$ values. The drug insignificantly prolonged the τ_1 value. After 5000-ms depolarizing pulses in the presence of aprindine (3 μM) τ_1 and τ_2 values 131 ± 4 ms and 519 ± 22 ms, respectively. The A_1 values was insignificantly decreased to 123 ± 28 pA while the A_2 values was unchanged (93 ± 13 pA) from the control values. Thus, the amplitude of the fast decay phase was decreased by aprindine while the time constant and the amplitude of the slow decay phase were hardly affected by the drug. These findings suggest that aprindine at a concentration of 3 μM preferentially but incompletely inhibits I_{Kr}.

Effects of aprindine on the muscarinic acetylcholine receptor-operated K^+ current

Since $I_{K.ACh}$ is another important repolarizing current in the atrial action potential, we examined the effect of aprindine on the carbachol-induced $I_{K.ACh}$ in the GTP (100 μM)-loaded atrial cells. Upon application of carbachol (1 μM) to the bath solution, an outward K^+ current was rapidly activated at a holding potential of -40 mV. After the activation, the carbachol-induced K^+ current gradually declined despite the continuous presence of carbachol, possibly because of a desensitization (Carmeliet & Mubagwa. 1986; Kurachi *et al*.,

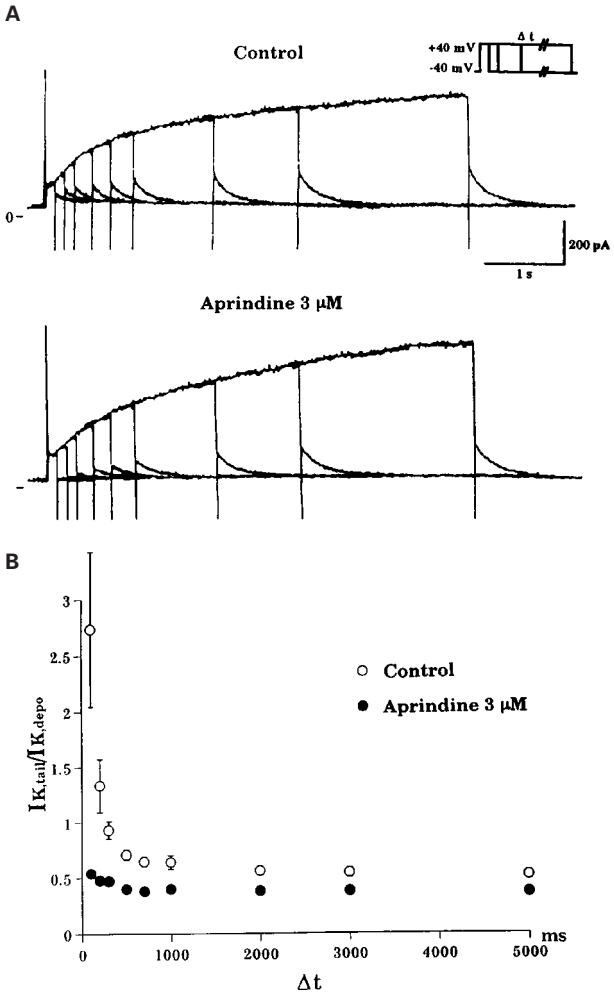

Figure 4 Block of the delayed rectifier K^+ current (I_K) by aprindine evaluated by the envelope of tails test. Envelopes of tail currents were generated by applying depolarizing pulses of variable duration (100–5000 ms) to +40 mV from a holding potential of −40 mV. Typical superimposed tracings before and after aprindine (3 μM) are shown in (A). The external solution contained nifedipine (1 μM) and the cell capacitance was 50 pF. The summarized data of the ratios of the tail current ($I_{K,tail}$) to the time-dependent current activated during the depolarizing pulses ($I_{K,depo}$) are depicted in (B). Open and closed circles indicate the data before (control) and after aprindine (3 μM), respectively. Values are means±s.e.mean of six experiments.

1987). After the current had almost reached a steady level, aprindine was added to the bathing solution. Aprindine depressed the carbachol-induced $I_{K.ACh}$ in a concentration-dependent manner (Figure 6A). Recovery from the inhibition by aprindine was observed after a washout period. The IC_{50} value of aprindine for depressing the carbachol-induced $I_{K.ACh}$ was 0.4 μM (Figure 6D). Although carbachol and adenosine act on different membrane receptors, i.e. M_2 muscarinic-ACh receptor and A_1-adenosine receptor, adenosine can also induce $I_{K.ACh}$ through the activation of pertussis toxin-sensitive GTP-binding protein in atrial cells (Kurachi *et al*., 1986). Aprindine also inhibited adenosine-induced currents less effectively than the carbachol-induced $I_{K.ACh}$ (Figure 6A and B). The IC_{50} value of aprindine for depressing the adenosine-induced $I_{K.ACh}$ was 2.5 μM (Figure 6D). We also evaluated the effects of aprindine on the $I_{K.ACh}$, induced by intracellular loading of GTPγS (100 μM), a nonhydrolyzable GTP analogue. In GTPγS-loaded cells, antagonist-resistant outward current was activated gradually and persisted even in the absence of any agonists. The GTPγS-induced K^+ current was also inhibited by aprindine in a concentration-dependent manner (Figure 6C). The IC_{50} value of aprindine for inhibiting GTPγS-induced $I_{K.ACh}$ was 2.5 μM, which was the same as that of adenosine-induced $I_{K.ACh}$ (Figure 6D). These findings suggest that aprindine may interact with the M_2 muscarinic-ACh receptor in addition to its direct inhibition of K^+ channel itself and/or G proteins.

Effects of aprindine on the action potential

Effects of aprindine on the action potential of guinea-pig atrial cells in the absence and presence of muscarinic stimulation were examined in the current clamp mode. The baseline characteristics of action potentials recorded from single atrial myocytes stimulated at 0.2 Hz were as follows: resting membrane potential (RMP), −75.4±0.8 mV; action potential amplitude, 127.6±1.2 mV; APD at 50% repolarization level (APD_{50}), 61±11 ms; APD at 90% repolarization level (APD_{90}), 87±12 ms ($n=14$). There were no significant differences in any of the baseline values of action potential parameters between the subgroups. In the absence of any muscarinic agonist aprindine prolonged APD, as shown in Figure 7A. Aprindine at a concentration of 3 μM significantly prolonged APD_{50} and APD_{90} by 48±9 and 50±4% from the control, respectively. There were no significant changes in any other action potential parameters after application of aprindine. Carbachol at a concentration of 1 μM markedly shortened APD_{90} from 88±12 to 14±2 ms with a slight and insignificant increase in RMP (from −75.1± 0.9 mV to −78.4±0.6 mV, $n=8$) in GTP-loaded single atrial cells. Aprindine reversed the carbachol-induced action potential shortening in a concentration-dependent manner, as shown in Figure 7B. The carbachol-induced shortening of APD_{90} was reversed to 79±7% of the control after aprindine (3 μM).

Effects of aprindine on experimental atrial fibrillation

In the control condition, AF could not be induced by a train of stimuli at an intensity up to 11 mA in Langendorff-perfused guinea-pig hearts. After the application of carbachol (1 μM), MAP at 90% repolarization level (MAP_{90}) was significantly decreased from 79±2 to 25±3 ms, as shown in Figure 8. Concomitantly, ERP was decreased from 64±3 to 18±1 ms, and AFT was decreased to 1.1±0.1 mA. However, addition of aprindine (3 μM) significantly increased the shortened MAP_{90} and ERP to 78±5 and 112±13 ms, respectively ($P<0.05$, $n=5$). Aprindine also significantly increased CT from the right to the left atrium (Figure 8). After the treatment with aprindine (3 μM), AF could not be induced any longer even in the presence of carbachol. Thus, aprindine suppressed the carbachol-induced AF in the isolated guinea-pig heart.

Discussion

For more than 20 years, clinical use and development of antiarrhythmic drugs have been based on Vaughan-Williams classification (Vaughan Williams, 1970) and that modified by Harisson *et al*. (1981). However, considerable progress in cardiac electrophysiology has lead to greater insights into mechanisms for arrhythmias, identification and cloning of ionic channels and availability of new antiarrhythmic drugs. As a consequence, the classification of antiarrhythmic drugs has become so complex and it has become difficult to link antiarrhythmic drug action to mechanisms of arrhythmias and clinical efficacy. The circumstances have promoted basic and

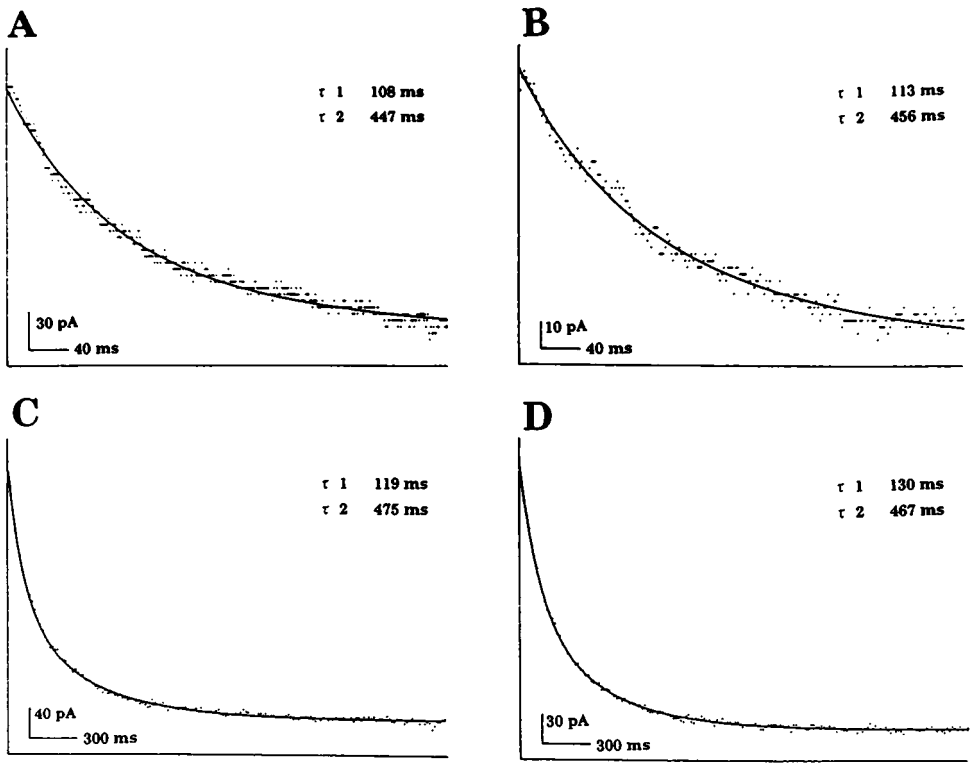

Figure 5 Effects of aprindine (3 μM) on the fast and slow phase of tail current decay after short (500 ms) and long (5000 ms) depolarizing pulses to +40 mV during the envelope of tails test in a single atrial cell. The control tail current traces upon clamp back to −40 mV after short and long depolarizing pulses are shown in A and C, respectively. The tail current traces in the presence of aprindine (3 μM) after short and long depolarizing pulses are shown in B and D, respectively. Time and current scale are indicated at the left side bottom of each panel. The data were fitted by the sum of two exponential functions whose time constants (τ_1, τ_2) are shown. τ_1 and τ_2 are time constants of fast and slow decay phase.

clinical investigators to attempt a new approach for classifying antiarrhythmic drugs, known as Sicilian Gambit (Task Force of the Working Group on Arrhythmias of the European Society of Cardiology, 1991). As information about the action of antiarrhythmic drugs becomes more complete, specific pharmacological management of cardiac arrhythmias will progressively improve. Therefore, it would be of importance to examine the electrophysiological effects of antiarrhythmic drugs available more thoroughly.

Aprindine is a unique class Ib antiarrhythmic drug which is effective for the treatment of supraventricular arrhythmias including AF (Adams *et al*., 1984; Kesteloot *et al*., 1973). However, the reason why aprindine shows some efficacy against atrial arrhythmias has not been fully understood. One possible explanation may be that aprindine exerts class I effect in atrial tissues. The drug is known to be a Na^+-channel blocker having a relatively long time constant for the recovery of V_{max} from the use-dependent block. The recovery time constant from the use-dependent block for aprindine was 4.8–7.8 s, which was much longer than those for the fast kinetic class Ib drugs lignocaine and mexiletine, although aprindine showed high affinity for the inactivated Na^+-channels in a similar fashion to these class Ib drugs (Toyama *et al*., 1987; Kodama *et al*., 1987a,b). Therefore, aprindine may exert Na^+-channel blocking action more readily than lignocaine and mexiletine. Indeed, aprindine prolonged interatrial conduction time in isolated guinea-pig hearts in this study. Another explanation may be that aprindine prolongs APD and thereby atrial refractory period. Aprindine was reported to prolong APD in isolated atrial tissues of guinea-pigs (Shirayama *et al*., 1991). Consistent with this report, the drug *per se* prolonged the action potential recorded from single atrial cells in the current clamp mode in the present study. However, effects of aprindine on membrane currents of atrial myocytes have not been examined.

In isolated atrial myocytes aprindine at a concentration of 3 μM inhibited I_K without any significant influence on I_{Ca} or I_{K1}. Therefore, the inhibition of I_K might be responsible for the aprindine-induced action potential prolongation in guinea-pig atrial cells. Electrophysiological analyses including the envelope of tails test in this study have revealed that aprindine preferentially inhibits I_{Kr}. The ratio of $I_{K,tail}$: $I_{K,depo}$ obtained from the depolarizing pulses of various durations became approximately constant. In addition, the deactivation kinetics of $I_{K,tail}$ after short (500 ms) and long (5000 ms) depolarizing pulses were also analysed. The time constants of the fast and slow phases were similar for depolarizing pulses of various durations. The fast and slow deactivation time constants at −40 mV were somewhat longer than those observed in guinea-pig ventricular cells (Chinn, 1993; Valenzuela *et al*., 1994) but similar to that obtained from guinea-pig atrial cells (Sanguinetti & Jurkiewicz, 1991). Aprindine at a concentration of 3 μM hardly affected the time constant (τ_2) and amplitude (A_2) of the slow phase but decreased the amplitude (A_1) of the fast phase. These findings suggest that the therapeutic concentration of aprindine preferentially inhibits I_{Kr} although the concentration might not be enough for the complete block of I_{Kr}.

It is well known that many class III antiarrhythmic drugs such as sotalol, E-4031 and dofetilide selectively inhibit I_{Kr} (Sanguinetti & Jurkiewicz, 1990; Jurkiewicz & Sanguinetti, 1993). I_{Kr} was also inhibited by class Ia and class Ic

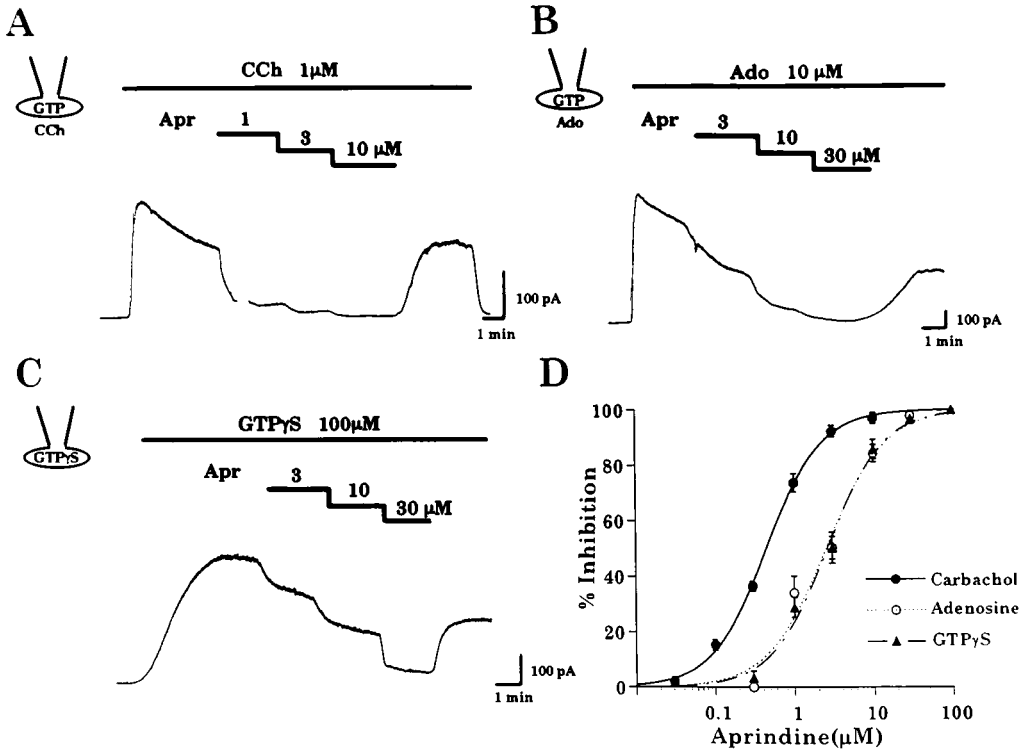

Figure 6 Effects of aprindine on the muscarinic acetylcholine receptor-operated K^+ current ($I_{K.ACh}$) in isolated guinea-pig atrial cells. $I_{K.ACh}$ was activated by the extracellular application of carbachol (CCh) (1 μM) (A), adenosine (Ado) (10 μM) (B) or intracellular loading of GTPγS (100 μM) (C). The holding potential was -40 mV. Intracellular loading of GTPγS, extracellular application of carbachol, adenosine and aprindine are shown by the lines above each original current trace. (D) Concentration-response curves for the inhibitory effects of aprindine on the $I_{K.ACh}$ activated by carbachol, adenosine and GTPγS are shown. Per cent inhibition of the outward current is indicated on the ordinate and the concentrations of aprindine are on the abscissa. Values are expressed as means$\pm$s.e.mean of 6–12 experiments.

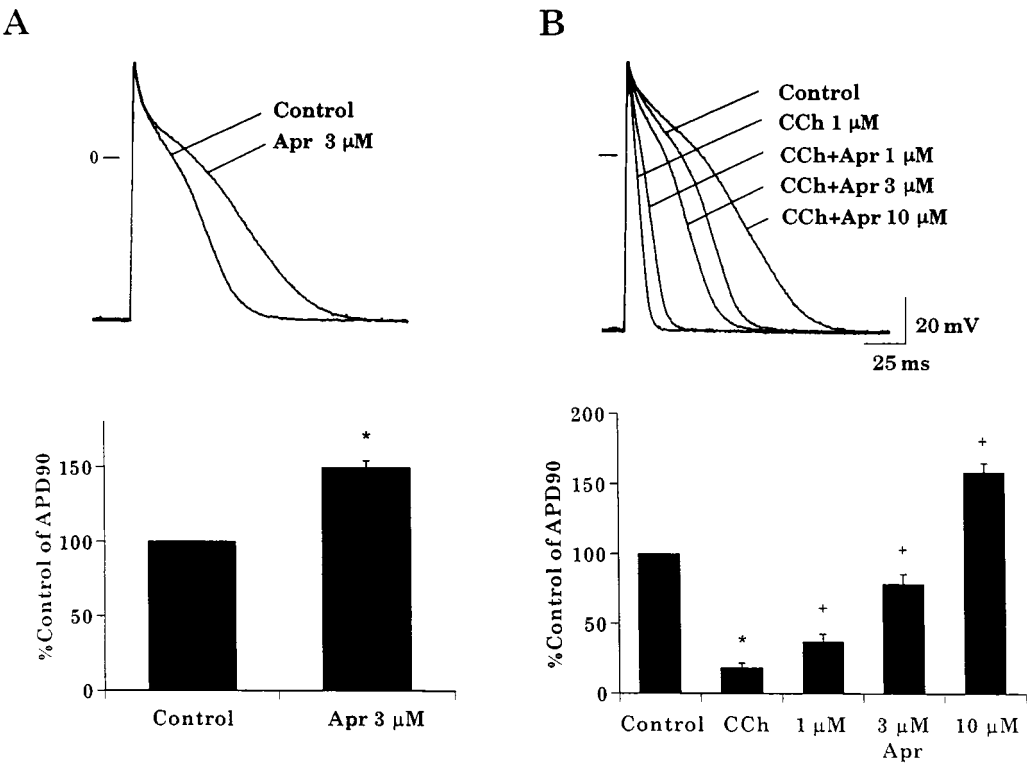

Figure 7 Effects of aprindine on the action potential in the absence (A) and presence of carbachol (1 μM) (B) in guinea-pig atrial cells. Superimposed records of action potentials obtained before (control) and after exposure to aprindine (Apr) (3 μM) (left) or after exposure to carbachol (CCh) (1 μM), and carbachol plus aprindine (right) are shown. Summarized data of changes of action potential duration at 90% repolarization level (APD_{90}) after aprindine in the absence and presence of muscarinic stimulation are shown in lower panels. The values are expressed as means$\pm$s.e.mean of 6–10 experiments. *$P<0.05$ vs control, +$P<0.05$ vs carbachol alone.

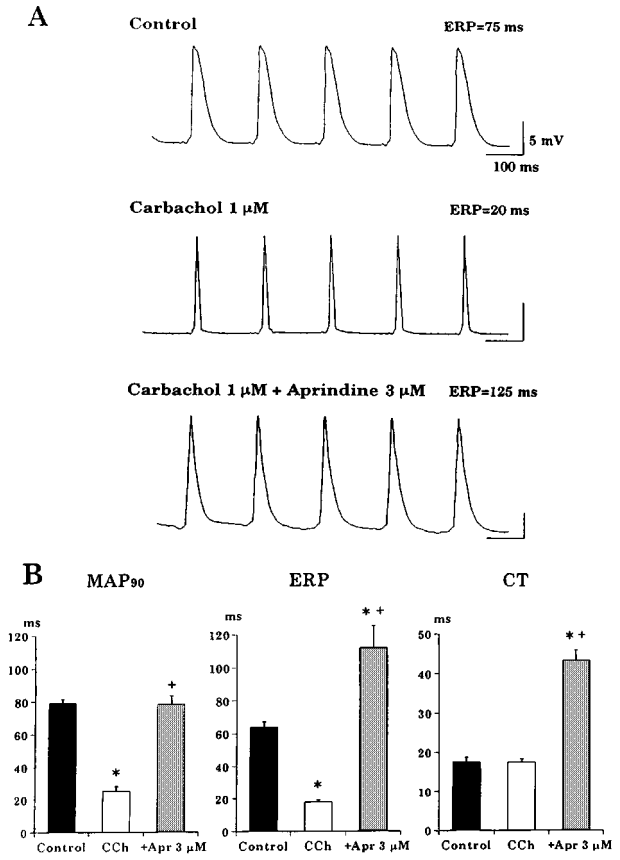

Figure 8 Effects of aprindine (Apr, 3 μM) on the carbachol (CCh, 1 μM)-induced changes in monophasic action potential (MAP), effective refractory period (ERP) and conduction time (CT) in isolated guinea-pig hearts. Actual records of MAP during control period and after carbachol and carbachol plus aprindine are shown in (A). Summarized data of changes of MAP at 90% repolarization level (MAP_{90}), ERP and CT are shown in (B). The values are expressed as means$\pm$s.e.mean of five hearts. $^*P<0.05$ vs control, $^+P<0.05$ vs carbachol alone.

antiarrhythmic drugs. In isolated ventricular cells the class Ic drug flecainide selectively inhibited I_{Kr} (Follmer & Colatsky, 1990) whereas the class Ia drugs quinidine and cibenzoline blocked both I_{Kr} and I_{Ks} (Balser *et al*., 1991; Wang *et al*., 1996). In contrast, mexiletine failed to inhibit either I_{Kr} or I_{Ks} in guinea-pig ventricular cells (Wang *et al*., 1996). Although aprindine but not mexiletine inhibits I_{Kr}, both drugs shortened APD in guinea-pig ventricular muscles (Toyama *et al*., 1987; Valenzuela & Sanchez-Chapula, 1989). In isolated guinea-pig ventricular myocytes the action potential, recorded in the current clamp mode, was not prolonged by aprindine (3 μM) (unpublished observations). It is not clear from the present study why aprindine prolonged APD in atrial cells but not in ventricular cells. There are two possibilities which might explain the differential effects of aprindine on APD in atrial and ventricular cells. The first is that I_{Kr} might play a more important role in the repolarization of action potential in atrial cells than in ventricular cells. It was reported that the current density of I_{Kr} in atrial cells was 2.5 times higher than that measured in ventricular cells of guinea-pigs (Sanguinetti & Jurkiewicz, 1991). Therefore, APD shortening resulting from the blockade of the Na^+ window current by aprindine might predominate in ventricular cells. The second explanation may be that aprindine might show a higher affinity for atrial K^+ channels than for ventricular K^+ channels through which I_{Kr} flows. Whatever the mechanism involved, aprindine may prolong atrial action potential effectively with little likelihood of induction of torsades de pointes.

It is well-known that $I_{K.ACh}$ plays an important role in the repolarization of atrial action potential. Many class I or IV antiarrhythmic drugs were reported to inhibit $I_{K.ACh}$ in isolated guinea-pig atrial cells (Nakajima *et al*., 1989; Ito *et al*., 1989; Inomata *et al*., 1993; Wu *et al*., 1994). We have recently demonstrated that class III antiarrhythmic drugs including amiodarone and d,l-sotalol as well as class I and IV antiarrhythmic drugs such as bepridil also inhibit $I_{K.ACh}$ (Mori *et al*., 1995; Hara & Nakaya, 1995; Watanabe *et al*., 1996). Two mechanisms by which these antiarrhythmic drugs inhibit $I_{K.ACh}$ have been proposed; some drugs block the muscarinic receptors and others inhibit the muscarinic K^+ channel itself and/or GTP-binding proteins. Disopyramide, pilsicainide and d,l-sotalol belong to the former group whereas quinidine, flecainide, propafenone, cibenzoline and amiodarone belong to the latter group (Nakajima *et al*., 1989; Inomata *et al*., 1993; Wu *et al*., 1994; Mori *et al*., 1995; Watanabe *et al*., 1996). Verapamil and E-4031 inhibit not only the muscarinic receptors but also the muscarinic K^+ channel itself and/or GTP-binding proteins (Ito *et al*., 1989; Mori *et al*., 1995). In this study aprindine inhibited not only the current induced by carbachol but also those induced by adenosine and GTPγS, although higher concentrations of aprindine were needed to inhibit the GTPγS and adenosine-induced currents. These findings suggest that aprindine inhibits the K^+ current by blocking the muscarinic receptors and depressing the function of the muscarinic K^+ channel itself and/or GTP-binding proteins.

Under a normal condition AF could not be induced, but during cholinergic stimulation it was easily induced by a high frequency atrial stimulation in isolated guinea-pig heart, which is consistent with previous reports from our and other laboratories (Inoue *et al*., 1994; Watanabe *et al*., 1996). The multiple wavelet hypothesis was proposed to explain the perpetuation of AF by Moe (1962). It was experimentally confirmed by mapping the atrial activation pattern of electrically-induced AF in isolated canine hearts (Allessie *et al*., 1985). From the study the critical number of wavelets needed to sustain AF was estimated to be between four to six, and the number of wavelets could be determined by both the atrial mass and the wavelength of the atrial impulse. The wavelength is the product of atrial refractoriness and conduction velocity (Allessie *et al*., 1985; Rensma *et al*., 1988; Allessie, 1995). Since perfusion of carbachol did not affect CT, the shortening of ERP resulting from the activation of $I_{K.ACh}$ appeared to underlie the shortening of the atrial wavelength and the induction of AF in this study. Addition of aprindine reverted MAP duration to the control level and prolonged ERP to the level exceeding the control. The reversal of MAP duration might be mainly due to inhibition of $I_{K.ACh}$ and partly due to inhibition of I_{Kr}. The excessive prolongation of ERP might be ascribed to the Na^+ channel blocking of aprindine. Aprindine increased the ERP in the presence of carbachol by six times while it decreased the conduction velocity to two fifths. Consequently aprindine increased the wavelength to 2.5 times, which might lead to the failure of AF induction. Thus, the inhibitory effects of aprindine on both K^+ and Na^+ currents might be involved in the antifibrillatory effect in the experimental AF.

Guinea-pig heart may not be the best model to explore the mechanism of antiarrhythmic effects on AF. The transient outward current (I_{to}), which plays an important role in the

repolarization of human atrial action potential (Tseng, 1995; Roden & George, 1997), cannot be readily recorded from guinea-pig atrial cells. In addition, the urtrarapidly activating delayed rectifier current (I_{Kur}), which also plays a significant role in the repolarization of human atrial action potential (Roden & George 1997), cannot be recorded from guinea-pig atrial cells. Therefore, the findings presented here cannot be directly extrapolated to clinical setting. Further studies using the heart and atrial myocytes of other animal species such as dog and rabbit may be warranted.

AF is extremely common cardiac arrhythmias in clinical setting (Pritchett, 1992). In addition, an increase in vagal tone may play an important role in the development of AF (Coumel *et al*., 1979). Aprindine at a concentration of 3 μM, which is clinically within therapeutic range (Zipes *et al*., 1977), can suppress parasympathetic type paroxysmal AF by potently inhibiting $I_{K.ACh}$. Aprindine may be also effective against non-parasympathetic type AF because of its inhibitory effects on I_{Kr} and I_{Na}. The efficacy of aprindine against supraventricular arrhythmias may be, at least in part, explained by its inhibitory action on I_{Kr} and $I_{K.ACh}$ in atrial cells.

The authors thank Mr I. Sakurada and Ms Y. Furusawa for their excellent technical assistance, and Ms I. Sakashita for her secretarial work. We are grateful for the valuable comments of Professor Y. Masuda and S. Kimura.

References

ADAMS, P.C., CAMPBELL, R.W. & JULIAN, D.G. (1984). The clinical pharmacology of antiarrhythmic drugs. *Cardiovasc. Clin.,* **14,** 153 – 190.

ALLESSIE, M. A. (1995). Reentrant mechanisms underlying atrial fibrillation. *In Cardiac Electrophysiology: From Cell to Bedside*. 2nd edn. eds. Zipes, D.P. & Jalife, J. pp. 562 – 566. Philadelphia, PA: W.B. Saunders Company.

ALLESSIE, M.A., LAMMERS, W.J.E.P., BONKE, I.M. & NOLLEN, J. (1985). Experimental evaluation of Moe's multiple wavelet hypothesis of atrial fibrillation. In *Cardiac Arrhythmias*. eds. Zipes D.P. & Jalife J. pp. 265 – 276, New York, Grune & Stratton.

ALPERT, J.S., PETERSON, P. & GODTFREDSEN, J. (1988). Atrial fibrillation: natural history, complication and management. *Ann. Rev. Med.,* **39,** 41 – 52.

BALSER, J.R., BENNETT, P.B., HONDEGHEM, L.M. & RODEN, D.M. (1991). Suppression of time-dependent outward current in guinea pig ventricular myocytes: Action of quinidine and amiodarone. *Circ. Res.,* **69,** 519 – 529.

BRAND, F.N., ABBOTT, R.D., KANNEL, W.B. & WOLF, P.A. (1985). Characteristics and prognosis of lone atrial fibrillation. 30 years follow-up in the Framingham study. *JAMA,* **254,** 3449 – 3453.

BREITHARDT, G., GLECHMANN, U., SEIPEL, L., LOOGEN, F. (1974). Long-term oral antiarrhythmic therapy with aprindine (AC1802). *Acta Cardiol.,* **18,** 341 – 353.

CARMELIET, E. (1994). Action potential duration and refractoriness. In *Electropharmacology Control of Cardiac Arrhythmias: To Delay Conduction or to Prolong Refractoriness?* eds. Singh, B.N., Wellens, H.J.J. & Hiraoka, M. pp. 33 – 44. Mount Kisco, NY: Futura Publising Co.

CARMELIET, E. & MUBAGWA, K. (1986). Desensitization of the acetylcholine-induced increase of potassium conductance in rabbit cardiac Purkinje fibres. *J. Physiol.,* **371,** 239 – 255.

CHINN, K. (1993). Two delayed rectifiers in guinea pig ventricular myocytes distinguished by tail current kinetics. *J. Pharmacol. Exp. Ther.,* **264,** 553 – 560.

COUMEL, P., LECLERCQ, J.F., ATTUEL, P., LAVALLEE, J.P. & FLAMANNG, D. (1979). Autonomic influence in the genesis of atrial arrhythmias: atrial flutter and fibrillation of vagal origin. In *Cardiac Arrhythmias: Electrophysiology, Diagnosis and Management*. ed. Narula, D.S. pp. 243 – 255. Baltimore, MD: Williams & Wilkins Co.

FABIATO, A. & FABIATO, F. (1979). Calculator programs for computing the composition of solutions containing multiple metals and ligands used for experiments in skinned muscle cells. *J. Physiol.,* **75,** 463 – 505.

FOLLMER, C.H. & COLATSKY, T.J. (1990). Block of delayed rectifier potassium current, I_K, by flecainide and E-4031 in cat ventricular myocytes. *Circulation,* **82,** 289 – 293.

HAMILL, O.P., MARTY, A., NEHER, E., SAKMANN, B. & SIGWORTH, F.J. (1981). Improved patch-clamp techniques for high-resolution current recording from cells and cell-free membrane patches. *Pflügers Arch.,* **391,** 85 – 100.

HARA, Y. & NAKAYA, H. (1995). SD-3212, a new class I and IV antiarrhythmic drug: a potent inhibitor of the muscarinic acetylcholine-receptor-operated potassium current in guinea-pig atrial cells. *Br. J. Pharmacol.,* **116,** 2750 – 2756.

HARRISON, D.C., WINKLE, R.A., SAMI, M. & MASON, J.W. (1981). Encainide: a new and potent antiarrhythmic agent. In *Cardiac Arrhythmias, a Decade of Progress*. eds. Harrison, D.C. & Hall, G.K. pp. 315 – 330. Boston, MA: Medical Publishers.

HONDEGHEM, L.M. & RODEN, D.M. (1995). Agents used in cardiac arrhythmias. In *Basic & Clinical Pharmacology*. 6th edn. ed. Katzung, B.G. pp. 205 – 229. Norwalk, CT: Appleton & Lange.

INOMATA, N., OHNO, T., ISHIHARA, T. & AKAIKE, N. (1993). Antiarrhythmic agents act differently on the activation phase of the ACh-response in guinea-pig atrial myocytes. *Br. J. Pharmacol.,* **108,** 111 – 115.

INOUE, M., INOUE, D., ISHIBASHI, K., SAKAI, R., SHIRAYAMA, T., ASAYAMA, J. & NAKAGAWA, M. (1994). Effect of E-4031 on the atrial fibrillation threshold in guinea pig atria: Comparative study with class I antiarrhythmic drugs. *J. Cardiovasc. Pharmacol.,* **24,** 534 – 541.

ISENBERG, G. & KLOECKNER, U. (1982). Calcium tolerant ventricular myocytes prepared by preincubation in a 'KB medium'. *Pflügers Arch.,* **395,** 6 – 18.

ITO, H., TAKIKAWA, R., KURACHI, Y. & SUGIMOTO. T. (1989). Anti-cholinergic effects of verapamil on the muscarinic acetylcholine receptor-gated K^+ channel in isolated guinea-pig atrial myocytes. *Naunyn-Schmiedeberg's Arch. Pharmacol.,* **339,** 244 – 246.

JURKIEWICZ, N.K. & SANGUINETTI, M.C. (1993). Rate-dependent prolongation of cardiac action potentials by a methanesulfonanilide class III antiarrhythmic agent: Specific block of rapidly activating delayed rectifier K^+ current by dofetilide. *Circ. Res.,* **72,** 75 – 83.

KESTELOOT, H., VAN MIEGHEM, W. & DE GEST, H. (1973). Aprindine (AC1802), a new anti-arrhythmic drug. *Acta Cardiol.,* **28,** 145 – 165.

KODAMA, I., TOYAMA, J., TANAKA, C. & YAMADA, K. (1987a). Block of activated and inactivated sodium channels by class-I antiarrhythmic drugs studied by using maximum upstroke velocity (Vmax) of action potential in guinea-pig cardiac muscles. *J. Mol. Cell. Cardiol.,* **19,** 367 – 377.

KODAMA, I., TOYAMA, J. & YAMADA, K. (1987b). Competitive inhibition of cardiac sodium channels by aprindine and lidocaine studied using a maximum upstroke velocity of action potential in guinea-pig ventricular muscles. *J. Pharmacol. Exp. Ther.,* **241,** 1065 – 1071.

KOPECKY, S.L., GERSH, B.J., McGOON, M.D., WHISNANT, J.P., HOLMES, D.R., ILSTRUP, D.M. & FRYE, R.L. (1987). The natural history of lone atrial fibrillation. A population-based study over three decades. *N. Engl. J. Med.,* **317,** 669 – 674.

KURACHI, Y., NAKAJIMA, T. & SUGIMOTO, T. (1986). On the mechanism of activation muscarinic K^+ channels by adenosine in isolated atrial cells: Involvement of GTP-binding proteins. *Pflügers Arch.,* **407,** 264 – 274.

KURACHI, Y., NAKAJIMA, T. & SUGIMOTO, T. (1987). Short-term desensitization of muscarinic K^+ channel current in isolated atrial myocytes and possible role of GTP-binding proteins. *Pflügers Arch.,* **410,** 227 – 233.

MOE, G.K. (1962). On the multiple wavelet hypothesis of atrial fibrillation. *Arch. Int. Pharmacodyn. Ther.,* **140,** 183 – 188.

MORI, K., HARA, Y., SAITO, T., MASUDA, Y. & NAKAYA, H. (1995). Anticholinergic effects of class III antiarrhythmic drugs in guinea-pig atrial cells: different molecular mechanisms. *Circulation,* **91,** 2834 – 2843.

NAKAJIMA, T., KURACHI., Y., ITO, H., TAKIKAWA, R. & SUGIMOTO, T. (1989). Anti-cholinergic effects of quinidine, disopyramide and procainamide in isolated atrial myocytes: mediation by different molecular mechanisms. *Circ. Res.,* **64,** 297 – 303.

NAKAYA, H., TOHSE, N., TAKEDA, Y. & KANNO, M. (1993). Effects of MS-551, a new class antiarrhythmic drug, on action potential and membrane currents in rabbit ventricular myocytes. *Br. J. Pharmacol.,* **109,** 157 – 163.

PRITCHETT, E.L.C. (1992). Management of atrial fibrillation. *N. Engl. J. Med.,* **326,** 1264 – 1271.

RENSMA, P.L., ALLESSIE, M.A., LAMMERS, W.J.E.P., BONKE, F.I.M. & SCHALIJ, M.J. (1988). The length of the excitation wave as an index for the susceptibility to reentrant atrial arrhythmia. *Circ. Res.,* **62,** 395 – 410.

RODEN, D.M. & GEORGE, Jr, A.L. (1997). Structure and function of cardiac sodium and potassium channels. *Am. J. Physiol.,* **273,** H511 – H525.

SANGUINETTI, M.C. & JURKIEWICZ, N.K. (1990). Two components of cardiac delayed rectifier K^+ current: Differential sensitivity to block by class III antiarryhthmic agents. *J. Gen. Physiol.,* **96,** 194 – 214.

SANGUINETTI, M.C. & JURKIEWICZ, N.K. (1991). Delayed rectifier outward K^+current is composed of two currents in guinea-pig atrial cells. *Am. J. Physiol.,* **260,** H393 – H399.

SHIRAYAMA, T., INOUE, D., INOUE, M., TATSUMI, T., YAMAHARA, Y., ASAYAMA, J. & NAKAGAWA, M. (1991). Electrophysiological effects of sodium channel blockers on guinea pig left atrium. *J. Pharmacol. Exp. Ther.,* **259,** 650 – 659.

STEINBERG, M.I. & GREENSPAN, K. (1976). Intracellular electrophysiological alterations in canine cardiac conducting tissue induced by aprindine and lignocaine. *Cardiovasc. Res.,* **10,** 236 – 244.

TASK FORCE OF THE WORKING GROUP ON ARRHYTHMIAS OF THE EUROPEAN SOCIETY OF CARDIOLOGY. (1991). The Sicilian Gambit. A new approach to the classification of antiarrhythmic drugs based on their action on arrhythmogenic mechanisms. *Circulation,* **84,** 1831 – 1851.

TOHSE, N., NAKAYA, H. & KANNO, M. (1992). α1-Adrenoceptor stimulation enhances the delayed K^+ current of guinea-pig ventricular cells through the activation of protein kinase C. *Circ. Res.,* **71,** 1441 – 1446.

TOYAMA, J., KAMIYA, K., KODAMA, I. & YAMADA, K. (1987). Frequency- and voltage-dependent effects of aprindine on upstroke velocity (Vmax) of action potential in guinea-pig ventricular muscles. *J. Cardiovasc. Pharmacol.,* **9,** 165 – 172.

TSENG, G.N. (1995). Potassium channels: Their modulation by drugs. In *Cardiac Electrophysiology: From Cell to Bedside*. 2nd edn. eds. Zipes, D.P. & Jalife, J. pp. 260 – 269. Philadelphia, PA: W.B. Saunders Company.

TSIEN, R.Y. & RINK, T.J. (1980). Neutral carrier ion-sensitive microelectrodes for measurement of intracellular free calcium. *Biochim. Biophys. Acta.,* **559,** 623 – 638.

VALENZUELA, C. & SÁNCHEZ-CHAPULA, J. (1989). Electrophysiologic interactions between mexiletine-quinidine and mexiletine-ropitoin in guinea-pig papillary muscle. *J. Cardiovasc. Pharmacol.,* **14,** 783 – 789.

VALENZUELA, C., SÁNCHEZ-CHAPULA, J., DELPÓN, E., ELIZALDE, A., PÉREZ, O. & TAMARGO, J. (1994). Imipramine blocks rapidly activating and delays slowly activating K^+ current activation in guinea-pig ventricular myocytes. *Circ. Res.,* **74,** 687 – 699.

VAUGHAN WILLIAMS, E.M. (1970). Classification of antiarrhythmic drugs. In *Cardiac Arrhythmias*. eds. Sandoe, E., Flensted-Jensen, E. & Olsen, K. pp. 449 – 472. Sodertalje, Sweden: Astra.

VERDONCK, F., VEREECKE, J. & VLEUGELS, A. (1974). Electrophysiological effects of aprindine on isolated heart preparations. *Eur J. Pharmacol.,* **26,** 338 – 347.

WANG, D.W., KIYOSUE, T., SATO, T. & ARITA, M. (1996). Comparison of the effects of class I anti-arrhythmic drugs, cibenzoline, mexiletine and flecainide, on the delayed rectifier K^+ current of guinea-pig ventricular myocytes. *J. Mol. Cell. Cardiol.,* **28,** 893 – 903.

WATANABE, Y., HARA, Y., TAMAGAWA, M. & NAKAYA, H. (1996). Inhibitory effect of amiodarone on the muscarinic acetylcholine receptor-operated potassium current in guinea-pig atrial cells. *J. Pharmacol. Exp. Ther.,* **279,** 617 – 624.

WU, S.N., NAKAJIMA, T., YAMASHITA, T., HAMADA, E., HAZAMA, H., IWASAWA, K., OMATA, M. & KURACHI, Y. (1994). Molecular mechanism of cibenzoline-induced anticholinergic action in single atrial myocytes: Comparison with effect of disopyramide. *J. Cardiovasc. Pharmacol.,* **23,** 618 – 623.

ZIPES, D.P., GAUM, W.E., FOSTER, P.R., ROSEN, K.M., WU, D., AMAT-Y-LEON, F. & NOBLE, R.J. (1977). Aprindine for treatment of supraventricular tachycardias: With particular application to Wolff-Parkinson-White syndrome. *Am. J. Cardiol.,* **40,** 586 – 596.

(Received May 26, 1998
Revised October 12 1998
Accepted November 4, 1998)

British Journal of Pharmacology (1999) 126, 762–768
http://www.stockton-press.co.uk/bjp

Modulation of ATP-responses at recombinant rP2X$_4$ receptors by extracellular pH and zinc

[1,2]S.S. Wildman, *[,1,2]B.F. King & [1,2]G. Burnstock

[1]Autonomic Neuroscience Institute, Royal Free Hospital School of Medicine, Rowland Hill Street, Hampstead, London NW3 2PF, England and [2]Department of Anatomy & Developmental Biology, University College London, Gower Street, London WC1E 6BT, England

1 The modulatory effects of extracellular H^+ and Zn^{2+} were tested against ATP-responses at rat P2X$_4$ (rP2X$_4$) receptors expressed in *Xenopus* oocytes under voltage-clamp conditions.

2 ATP (0.1–100 μM, at pH 7.5), evoked inward currents *via* rP2X$_4$ receptors (EC_{50} value, 4.1±0.98 μM; n_H, 1.2±0.1). ATP potency was reduced 2 fold, at pH 6.5, without altering maximal activity. ATP potency was reduced by a further 4 fold, at pH 5.5, and the maximal activity of ATP was also reduced. Alkaline conditions (pH 8.0) had no effect on ATP-responses.

3 Zn^{2+} (100 nM–10 μM) potentiated ATP-responses at the rP2X$_4$ receptor by 2 fold, whereas higher concentrations (30 μM–1 mM) inhibited ATP-responses. Zn^{2+} potentiation was due to an increase in ATP potency, whereas its inhibitory action was due to a reduction in ATP efficacy.

4 Zn^{2+} modulation of ATP-responses was pH-dependent. At pH 6.5, the bell-shaped curve for Zn^{2+} was shifted to the right by 1 log unit. At pH 5.5, Zn^{2+} potentiation was abolished and its inhibitory effect reduced considerably.

5 Suramin (50 μM) also potentiated ATP-responses at rP2X$_4$ receptors. Neither H^+ (pH 6.5 and 5.5), Zn^{2+} (10–100 μM) or a combination of both failed to reveal an inhibitory action of suramin at rP2X$_4$ receptors.

6 In conclusion, H^+ and Zn^{2+} exerted opposite effects on the rP2X$_4$ receptor by lowering and raising agonist potency, respectively. H^+ ($\geqslant$3 μM) and Zn^{2+} ($\geqslant$30 μM) also reduces agonist efficacy by lowering the number of rP2X$_4$ receptors available for activation. The striking differences between the modulatory actions of H^+ and Zn^{2+} at rP2X$_4$ and rP2X$_2$ receptors are discussed.

Keywords: Extracellular pH; zinc; ATP; P2X receptor; *Xenopus* oocyte

Abbreviations: ATP, adenosine 5′-triphosphate; EC_{50}, agonist concentration producing 50% of the maximal response; I_{ATP}, ATP-activated membrane current; n_H, Hill co-efficient; pH_e, extracellular pH; PPADS, pyridoxal-α^5-phosphate-6-azophenyl-2′,4′-disulphonic acid; UTP, uridine 5′-triphosphate; V_h, holding potential

Introduction

Adenosine 5′-triphosphate (ATP) can act as a fast excitatory transmitter at neuronal P2X receptors in the central, peripheral and enteric nervous systems (Edwards *et al*., 1992; Evans *et al*., 1992; Silinsky & Gerzanich, 1993; Galligan & Bertrand, 1994; Sperlagh *et al*., 1995; Bardoni *et al*., 1997; Nieber *et al*., 1997). So far, seven P2X receptor subunits (P2X$_{1-7}$) have been identified (North & Barnard, 1997), although the recently-cloned human P2XM subunit may possibly represent the eighth member (Urano *et al*., 1997). Apart from P2X$_7$, transcripts for other P2X subunits have been localized in neuronal tissues.

The P2X$_4$ receptor subunit is concentrated in mammalian nervous systems and, along with P2X$_2$ and P2X$_6$, represent the more common P2X subunits found in adult neural tissues (Bo *et al*., 1995; Buell *et al*., 1996; Collo *et al*., 1996; Séguéla *et al*., 1996; Soto *et al*., 1996; Wang *et al*., 1996; Dhulipala *et al*., 1998; Lê *et al*., 1998). Homomeric P2X$_4$ receptors are characterized by a low sensitivity to P2 receptor antagonists, PPADS (pyridoxal-α^5-phosphate-6-azophenyl-2′,4′-disulphonic acid) and suramin. The blocking activity of PPADS and suramin is greater at human P2X$_4$ (hP2X$_4$) than the rat homologue (rP2X$_4$), yet still lower than at most other human and rat P2X receptor subtypes (Garcia-Guzman *et al*., 1997). The recombinant rP2X$_6$ receptor, however, is also insensitive to PPADS and suramin (Collo *et al*., 1996).

Previously, we have shown that the activity of agonists and antagonists at one neuronal P2X receptor subtype, rP2X$_2$, is exceedingly sensitive to changes to extracellular pH (King *et al*., 1996, 1997). The concentration-response (C/R) curve for ATP (and other agonists) was shifted leftwards under acidic conditions and rightwards under alkaline conditions, without changing the maximal activity of the agonist. Even small changes in pH ($\geqslant$0.03 pH units) significantly altered the amplitude of ATP-responses at rP2X$_2$ (Wildman *et al*., 1997). Additionally, the blocking activity of suramin was greatly enhanced at rP2X$_2$ under acidic conditions and declined under alkaline conditions (King *et al*., 1997). Extracellular zinc (Zn^{2+}) also potentiated agonist and antagonist activity at rP2X$_2$ receptors (Brake *et al*., 1994; Nakazawa & Ohno, 1996, 1997; Wildman *et al*., 1998). However, Zn^{2+} modulation of agonist activity at rP2X$_2$ receptors is more complex than the corresponding H^+ modulation, since the former shows time-dependency and converts to inhibition after prolonged exposure while the latter is constant, time-independent and can overcome Zn^{2+} inhibition (Wildman *et al*., 1998).

ATP-responses at rat and human P2X$_4$ receptors are also affected by extracellular pH (Stoop *et al*., 1997; Clarke *et al*., 1998), but in a different way to rP2X$_2$ receptors. For these P2X$_4$ homologues, acidic and alkaline conditions respectively

*Author for correspondence; E-mail: ucgabfk@ucl.ac.uk

reduced and enhanced ATP-responses although the precise actions on the potency and efficacy of ATP remain to be determined. It has also been reported that ATP activity is potentiated by Zn^{2+} at rat and human $P2X_4$ receptors (Séguéla *et al*., 1996; Soto *et al*., 1996; Garcia-Guzman *et al*., 1997; Nakazawa & Ohno, 1997) although there is no information on how ATP potency and efficacy is altered. Additionally, it remains to be shown if Zn^{2+}-potentiation of agonist activity is time-dependent, as for $P2X_2$, and how Zn^{2+} and H^+ interact at $P2X_4$ receptors. In the present study, therefore, we describe the separate effects of extracellular pH and Zn^{2+} and their joint interaction on both agonist and antagonist activity at a neuronal P2X receptor subunit, the $rP2X_4$ subtype. The striking differences between the modulatory effects of H^+ and Zn^{2+} at $rP2X_4$ and $rP2X_2$ receptors are discussed.

Methods

Oocyte preparation

Xenopus laevis frogs were anaesthetized in Tricaine (0.2% w/v), killed by decapitation, and ovarian lobes surgically removed. Oocytes (stages V and VI) were defolliculated by a 2-step process involving collagenase treatment (Type IA, 2 mg ml^{-1} in a Ca^{2+}-free Ringer's solution, for 2–3 h) followed by stripping away the follicular layer with fine forceps. Defolliculated oocytes were stored in Barth's solution (pH 7.5, at 4°C) containing (mM): NaCl, 110; KCl, 1; $NaHCO_3$, 2.4; Tris HCl, 7.5; $Ca(NO_3)_2$, 0.33; $CaCl_2$, 0.41; $MgSO_4$, 0.82; gentamycin sulphate, 50 $\mu g\ l^{-1}$. Defolliculated oocytes were injected cytosolically with rat $P2X_4$ cRNA (40 nl, 1 $\mu g\ ml^{-1}$), incubated for 48 h at 18°C in Barth's solution then kept at 4°C for up to 12 days until used in electrophysiological experiments.

Electrophysiology

ATP-activated membrane currents (I_{ATP}) ($V_h = -60$ to -90 mV) were recorded from cRNA-injected oocytes using a twin-electrode voltage-clamp amplifier (Axoclamp 2B). The voltage-recording and current-recording microelectrodes (1–5 MΩ tip resistance) were filled with 3.0 M KCl. Oocytes were superfused with Ringer's solution (5 ml min^{-1}, at 18°C) containing (mM): NaCl, 110; KCl, 2.5; HEPES, 5; $BaCl_2$, 1.8, adjusted to pH 7.5. Where stated, the pH of the bathing solution was adjusted using either 1.0 N HCl or 1.0 N NaOH to achieve the desired level. Electrophysiological data were stored on a computer using a MP100 WSW interface (Biopac Systems Inc.) and analysed using the software package Acknowledge III (Biopac).

Solutions

All solutions were nominally Ca^{2+}-free to avoid the activation of a Ca^{2+}-dependent Cl^- current ($I_{Cl,Ca}$) in oocytes (Bo *et al*., 1995). ATP was prepared in a Ca^{2+}-free Ringer's solution (concentrations as stated in the text) and superfused by a gravity-feed continuous flow system which allowed rapid addition and washout. ATP was added for 120 s or until the current reached a peak, then washed out for a period of 15 min. Data were normalized to the maximum current (I_{max}) evoked by ATP at pH 7.5 for agonist concentration-response (C/R) relationships studied at all pH levels. The agonist concentration required to evoke 50% of the maximum response (EC_{50}) was taken from Hill plots, constructed using the formula $\log(I/I_{max} - I)$ where I is the current evoked by each concentration of ATP. High concentrations of ATP (300 μM–3 mM) can activate an inward Na^+-current (I_{Na}) in a small proportion of defolliculated oocytes and this current is inhibited by UTP (300 μM) (Kupitz & Atlas, 1993). To avoid such endogenous currents, UTP (300 μM) was added to the superfusate in experiments (mainly at pH 5.5) where it was necessary to use high concentrations of ATP (>300 μM). UTP (300 μM) had no effect on ATP potency at $rP2X_4$ receptors at pH 7.5 (EC_{50} values: 3.4±1.0 μM *vs* 4.0±1.3 μM, paired data, $n=3$).

The effects of extracellular zinc were investigated on agonist activity in two ways. First, Zn^{2+} was added to ATP solutions and C/R curves for ATP were constructed (data normalized to the maximal ATP-response at pH 7.5). Pre-incubation with Zn^{2+} for 15 min prior to adding ATP solutions had the same effect on agonist responses as did the simultaneous application of Zn^{2+} and ATP. Second, C/R curves for Zn^{2+} were constructed using a submaximal concentration of ATP (EC_{20}) (data normalized to responses to the respective EC_{20} concentration for ATP at pH 8.0, 7.5, 6.5 and 5.5).

Statistics

Data are presented as means±s.e.mean of four sets of data from different oocyte batches. Significant differences were determined by either unpaired Student's *t*-test or one-way analysis of variance (ANOVA) followed by Dunnett's test, using commercially available software (Instat v2.05a, GraphPad).

Drugs

All common salts and reagents were AnalaR grade (Aldrich Chemicals, U.K.). Adenosine 5′-triphosphate disodium salt (ATP), uridine 5′-triphosphate sodium salt (UTP) and zinc chloride were purchased from Sigma Chemical Co. (Poole, Dorset, U.K.). Suramin was a gift from Bayer plc (Newbury, Berkshire, U.K.).

Results

Effect of extracellular pH on I_{ATP}

At pH 7.5, ATP (100 nM–100 μM) evoked inward membrane currents in defolliculated oocytes expressing $rP2X_4$ receptors (EC_{50} value, 4.1±0.98 μM; Hill co-efficient (n_H), 1.2±0.1, $n=4$). At pH 8.0, there was no significant change in ATP potency or maximal activity (EC_{50} value, 2.8±0.6 μM; n_H, 1.1±0.1; $n=4$) (see Figure 1). Acidification of the superfusate significantly reduced ATP potency ($P<0.01$) (pH 6.5: EC_{50} value, 8.4±1.2 μM; n_H, 1.0±0.1, $n=5$; pH 5.5: EC_{50} value, 31.7±4.9 μM; n_H, 1.0±0.1, $n=6$). The efficacy of ATP was diminished only at pH 5.5 (37±4% of maximal ATP-responses at pH 7.5) (see Figure 1). The modulatory effects of H^+ (at either pH 6.5 or 5.5) were reversed after readjusting the superfusate to pH 7.5. Water-injected (control) defolliculated oocytes failed to respond to ATP (100 μM).

Zn^{2+} potentiation of I_{ATP}

Zn^{2+} (0.1–10 μM) potentiated membrane currents to ATP (3 μM) at $rP2X_4$ receptors by approximately 2 fold (EC_{50} value,

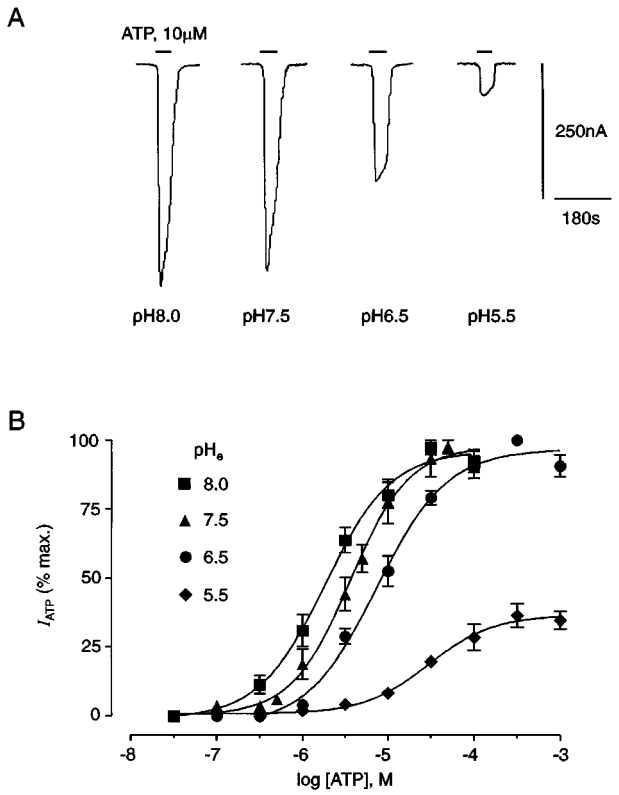

Figure 1 Extracellular pH modulates ATP activity at $rP2X_4$ receptor. (A) Whole-cell currents activated by ATP (10 μM) at four levels of extracellular pH (pH_e) (8.0, 7.5, 6.5, 5.5). All records from the same oocyte ($V_h = -90$ mV). (B) Concentration/response (C/R) curves for ATP (30 nM – 1 mM) at the same four levels of pH_e. Whole-cell currents to ATP (I_{ATP}) were normalized to the maximal ATP-response at pH 7.5. Data points are means ± s.e.mean, $n = 4$.

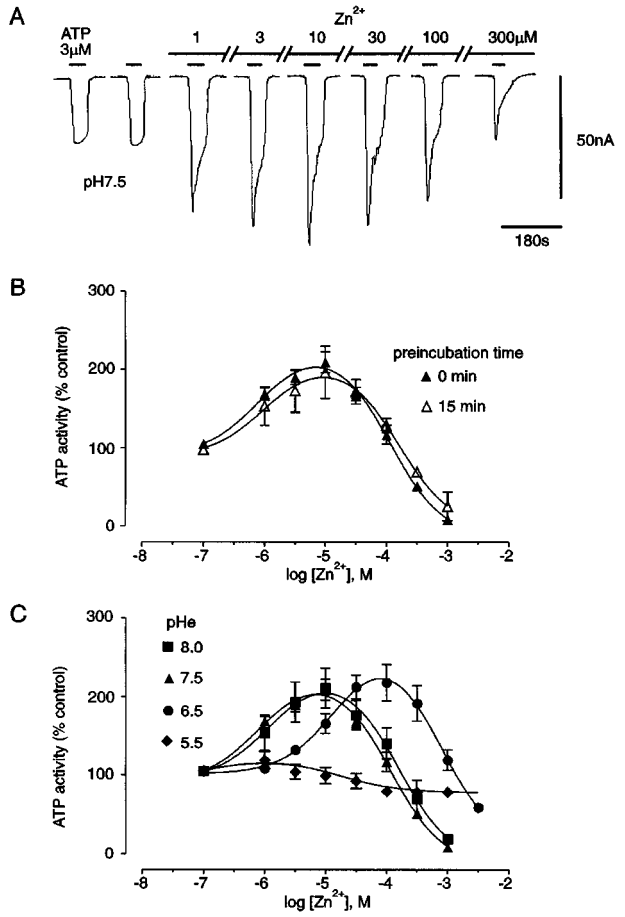

Figure 2 Zn^{2+} modulates ATP activity at $rP2X_4$ receptor. (A) Whole-cell currents to ATP (3 μM) and modulation of agonist activity by Zn^{2+} (1 – 300 μM) added to the superfusate (pH_e, 7.5). All records from the same oocyte ($V_h = -90$ mV). (B) Concentration/response (C/R) curves for Zn^{2+} modulation of whole cell currents at $rP2X_4$ ion-channel activated by three micromolar ATP (at pH 7.5). Zn^{2+} was added to the superfusate and applied either simultaneously with ATP or 15 min prior to, and during, application of ATP. (C) Effect of extracellular pH (pH_e) on the modulatory actions of Zn^{2+} on ATP-responses at $rP2X_4$ receptor. ATP was applied at a concentration equivalent to the EC_{20} value at four levels pH_e (8.0, 7.5, 6.5, 5.5). Data points are means ± s.e.mean, $n = 4$.

1.29 ± 0.2 μM, $n = 4$) (Figure 2A and B). This potentiating effect was not sustained at higher concentrations (30 μM – 1 mM), at which point Zn^{2+} caused an inhibition of ATP-responses (Figure 2A and B). Where Zn^{2+} (0.1 μM – 1 mM) was applied 15 min prior to the addition of ATP, the concentration-dependent potentiating and inhibitory activities of Zn^{2+} remained unaltered (Figure 2B). The potentiating and inhibitory effects of Zn^{2+} were reversed after washout.

Zn^{2+} modulation of ATP-responses was affected by acidifying the extracellular solution. While alkaline conditions (pH 8.0) had no significant effect on Zn^{2+} modulation of ATP-responses, acidification (pH 6.5) displaced the bell-shaped Zn^{2+} curve to the right by 1 log unit without diminishing the extent of Zn^{2+} potentiation (Figure 2C). At pH 5.5, Zn^{2+} failed to potentiate ATP-responses and the inhibitory action of Zn^{2+} was also reduced (Figure 2C).

Effect of Zn^{2+} on concentration dependence of I_{ATP}

The effects of Zn^{2+} on the potency and efficacy of ATP at $rP2X_4$ was studied in detail over a range of pH 7.5 – 5.5. Zn^{2+} was applied at two concentrations at each pH level, the first Zn^{2+} concentration giving maximal potentiation of ATP-responses (pH 7.5, 10 μM; pH 6.5, 100 μM; pH 5.5, 10 μM) and a second concentration causing a significant inhibition of ATP-responses (pH 7.5, 100 μM; pH 6.5, 1000 μM; pH 5.5, 100 μM).

At pH 7.5, the potency of ATP (10 nM – 100 μM) was increased significantly ($P < 0.01$) in the presence of Zn^{2+} (10 μM) (EC_{50} values, 1.0 ± 0.3 μM *vs* 4.1 ± 0.98 μM, $n = 4$). ATP potency was not significantly different at a higher level of Zn^{2+} (100 μM) (EC_{50} value, 1.3 ± 0.3 μM, $n = 4$), but ATP efficacy (i.e., maximal activity) was reduced considerably (59 ± 7% of control) (Figure 3A). Hill co-efficients for ATP curves were similar in the absence and presence of Zn^{2+} (n_H: 0 μM, 1.2 ± 0.1; 10 μM, 1.0 ± 0.1; 100 μM, 1.0 ± 0.1).

Similar effects were seen at pH 6.5. ATP potency was increased significantly ($P < 0.01$) in the presence of Zn^{2+} (100 μM) (EC_{50} values: 1.9 ± 0.5 μM *vs* 8.4 ± 1.2 μM, $n = 4$), whereas ATP potency was not enhanced further by a higher concentration of Zn^{2+} (1000 μM) (EC_{50} 2.1 ± 1.3 μM, $n = 4$) although agonist efficacy was reduced considerably (43 ± 5% of control) (Figure 3B). Hill co-efficients for ATP curves were similar in the absence and presence of Zn^{2+} (n_H: 0 μM, 1.0 ± 0.1; 100 μM, 1.0 ± 0.1; 1000 μM, 0.9 ± 0.1).

At pH 5.5 (and 300 μM UTP present: see Methods), there was no significant change in ATP potency in the presence of Zn^{2+} (10 and 100 μM) (EC_{50} values: 0 μM, 31.7 ± 4.9 μM; 10 μM, 32.6 ± 9.2 μM; 100 μM, 24.9 ± 3.9 μM, $n = 5$). The efficacy of ATP, although reduced considerably at pH 5.5,

was decreased further by Zn^{2+} (peak activity *wrt* maximal ATP activity at pH 7.5: 0 μM, 37±4%; 10 μM, 27±4%; 100 μM, 17±2%) (Figure 3C). Hill co-efficients for ATP curves were similar in the absence and presence of Zn^{2+} (n_H: 0 μM, 1.0±0.1; 100 μM, 0.8±0.2; 1 μM, 0.9±0.1).

Effect of H^+ and Zn^{2+} on suramin blockade

The P2 receptor antagonist, suramin (50 μM), failed to inhibit ATP-responses at $rP2X_4$ receptors at pH 7.5. Instead, suramin caused a modest potentiation of ATP-activated inward currents (Figure 4A). The extent of this potentiation (149±11%, $n=3$) was not significantly altered at pH 6.5 (148±4%, $n=3$) and pH 5.5 (143±13%, $n=3$). In the presence of Zn^{2+} (10 μM) which, of itself, potentiated ATP-responses, suramin (50 μM) failed either to potentiate further or inhibit ATP-activated currents (Figure 4B). This apparent Zn^{2+} antagonism of suramin activity was observed at pH 7.5 and 6.5, but not at 5.5. At this lowest pH level, Zn^{2+} failed to potentiate ATP-responses and also failed to reduce suramin potentiation of ATP-responses. These results suggest that potentiating actions of Zn^{2+} and suramin are not additive at pH 7.5 and pH 6.5. Also, suramin potentiation may involve a mechanism different from Zn^{2+} potentiation, since only the former can occur at pH 5.5.

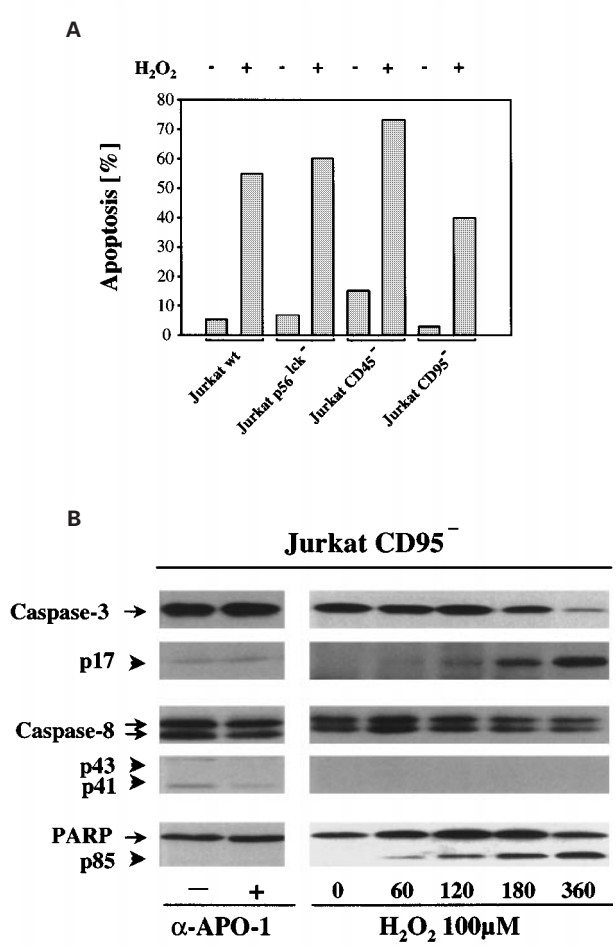

Figure 3 Interaction of H^+ and Zn^{2+} on ATP activity at $rP2X_4$ receptor. Concentration/response (C/R) curves for ATP at three levels of extracellular pH (in A, pH 7.5; in B, pH 6.5; in C, pH 5.5), in the absence then presence of concentrations of Zn^{2+} ions that caused potentiation and inhibition of ATP-responses. Zn^{2+} potentiation was caused by an increase in ATP potency, displacing C/R curves to the left. Zn^{2+} inhibition was due to a decrease in ATP efficacy, without altering agonist potency. Data points are means±s.e.mean, $n=4$.

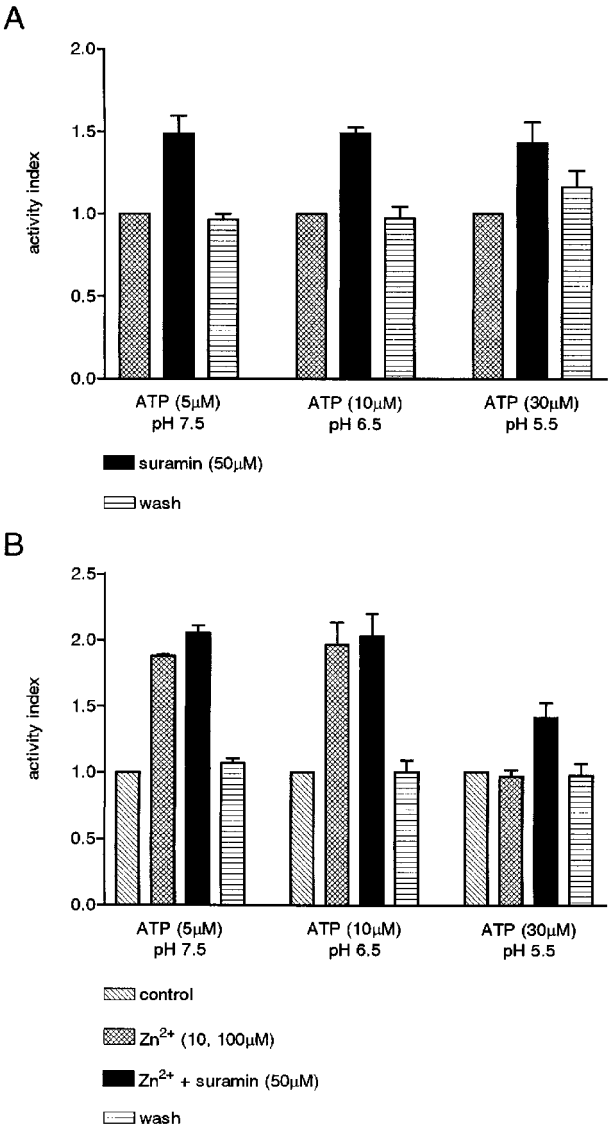

Figure 4 Suramin activity at $rP2X_4$ receptor. (A) Histograms of ATP activity in the absence and presence of suramin (50 μM), and 20 min after washout of suramin. The agonist was applied at the respective EC_{50} value at pH 7.5, 6.5 and 5.5, and control responses were taken as 1 (activity index = 1). (B) Histograms of ATP activity in the absence and presence of Zn^{2+} ions, further addition of suramin (50 μM), and 20 min after washout of suramin and Zn^{2+} ions. Zn^{2+} was applied at 10 μM (pH 7.5 and 5.5) and 100 μM (pH 6.5), these concentrations causing maximal potentiation of ATP-responses at the above pH levels.

Discussion

In the present study, ATP-activated inward currents at the $rP2X_4$ receptor were found to be sensitive to changes in extracellular pH. Acidification of the bathing medium progressively shifted the ATP C/R curve to the right and decreased agonist potency by as much as 8 fold, whereas alkaline changes shifted the C/R curve marginally to the left. Similar phenomena were observed for $rP2X_4$ receptors expressed in either HEK293 cells (Stoop *et al*., 1997) or *Xenopus* oocytes (Clarke *et al*., 1998). We have extended these observations by calculating EC_{50} values and showing that H^+ (at pH 5.5) also reduces the efficacy of ATP. At pH 5.5, H^+ appears to decrease the number of $rP2X_4$ channels available for agonist activation, in a manner comparable to a non-competitive antagonist, although the effects of H^+ were reversed by washout. Can levels as low as pH 5.5 be reached *in vivo*? Localized acidosis has been reported following bone fracture (pH 4.7), during ischaemia (pH 5.7), inflammation (pH 5.4), during epileptic seizures and injuries related to CNS degenerative changes (DeSalles *et al*., 1987; Chesler, 1990; Steen *et al*., 1992; Ransom & Philbin, 1992). It is also evident that acidic shifts occur transiently during CNS neurotransmission (Yanovsky *et al*., 1995).

The above findings at $rP2X_4$ receptors differed radically from the effects of H^+ at $rP2X_2$ receptors (King *et al*., 1996, 1997), where acidic changes to the bathing solution enhanced ATP potency without affecting the efficacy of the agonist. It was further noted that $rP2X_2$ receptors were more sensitive than $rP2X_4$ receptors to small changes in extracellular pH, as confirmed by Stoop *et al*., (1997). At both $rP2X_4$ and $rP2X_2$ receptors, however, the change in amplitude of ATP-activated currents was immediate when changing extracellular pH, did not alter with time and was reversed immediately on washout. The speed with which H^+ exerts its action on these two P2X subtypes suggests H^+ ions act at extracellular site, but there is little structural information to implicate specific (and strategic) amino acid residues. It appears that histidine residues in the extracellular loop of the $rP2X_2$ subunits can be discounted (Stoop *et al*., 1997; King *et al*., 1997).

The software programme, Bound and Determined (BAD), calculates the fractional ratios of ATP species for a given amount of ATP (Brookes & Storey, 1992). We have used this programme beforehand, when studying H^+ modulation of ATP activity at $P2X_2$ receptors, to try to determine the ATP species most likely to activate the $rP2X_2$ subunit (King *et al*., 1996). We have repeated such analysis for $rP2X_4$, comparing EC_{50} values at the four pH_e levels tested against the calculated fractional ratios of ATP species present (data not shown). The fractional amount of free ATP (ATP^{4-}) remained constant (about 30%) for the respective EC_{50} values for ATP over the range of pH 8.0–6.5, but fell sharply (to 8%) at pH 5.5. Thus, it is unlikely that ATP^{4-} alone stimulated the $rP2X_4$ receptor. Of the other ATP species present, the fractional amounts of HATP and BaHATP increased while NaATP, KATP and BaATP decreased with progressive acidification of the superfusate. Such changes in the relative amounts of ATP species could not explain the observed changes in ATP potency over the range of pH 8.0–5.5. As concluded in an earlier paper on $rP2X_2$ receptors (King *et al*., 1996), it is more likely that receptor protonation rather than agonist protonation accounts for the change in ATP potency at $rP2X_4$ receptors.

Other investigators have already shown that extracellular Zn^{2+} can potentiate ATP-responses at rat and human $P2X_4$ receptors (Séguéla *et al*., 1996; Soto *et al*., 1996; Garcia-Guzman *et al*., 1997; Nakazawa & Ohno 1997). Here, we demonstrated the concentration-dependence of this effect and also confirmed that actions of Zn^{2+} were reversed on washout. Additionally, we found that high concentrations of Zn^{2+} can exert an inhibitory effect on ATP activity. A bell-shaped C/R relationship also has been observed for the actions of Zn^{2+} on ATP-activated currents in rat sympathetic neurons (Cloues *et al*., 1993), at which $rP2X_2$ and $rP2X_4$ transcripts have been localized (Collo *et al*., 1996). From studying the effects of both potentiating and inhibitory concentrations of Zn^{2+} on the C/R curve for ATP, it appears that inhibition by Zn^{2+} was due to decrease in agonist efficacy and not a decrease in ATP potency. Thus, high concentrations of Zn^{2+} can reduce the number of $rP2X_4$ receptors available for agonist activation in a manner comparable to a non-competitive antagonist. Since Zn^{2+} further reduced the efficacy of ATP at pH 5.5, it appears that the ability of Zn^{2+} and H^+ to reduce the number of available $rP2X_4$ receptors were additive. The locus for the inhibitory actions of Zn^{2+} and H^+ has not been determined. However, these inhibitory actions raise an interesting issue. Since Zn^{2+} and H^+ are found in synaptic vesicles (Johnson & Scarpa, 1976; Assaf & Chung, 1984) and probably are released along with ATP during central neurotransmission, these modulators at the right concentrations might exert a physiological antagonism of $rP2X_4$ receptors which, otherwise, are insensitive to known P2 receptor antagonists.

Extracellular Zn^{2+} acted differently at $rP2X_4$ and $rP2X_2$ receptors. Both the potentiating and inhibitory actions of Zn^{2+} at $rP2X_4$ were dependent on concentration and independent of time, while the potentiating effect of Zn^{2+} at $rP2X_2$ is dependent on time and, irrespective of concentration, eventually replaced by inhibition (Wildman *et al*., 1998). Additionally, the maximal Zn^{2+} potentiation of ATP-responses is markedly less pronounced at $rP2X_4$ (2 fold) than $rP2X_2$ receptors (15 fold) at pH 7.5 (see Figure 5), and the respective EC_{50} values for Zn^{2+} are somewhat dissimilar ($rP2X_4$, 1.29 ± 0.2 μM; $rP2X_2$, 6.1 ± 1.2 μM). Furthermore, the time-dependent inhibitory actions of Zn^{2+} at $rP2X_2$ involve a reduction in ATP potency and efficacy, whereas inhibition at

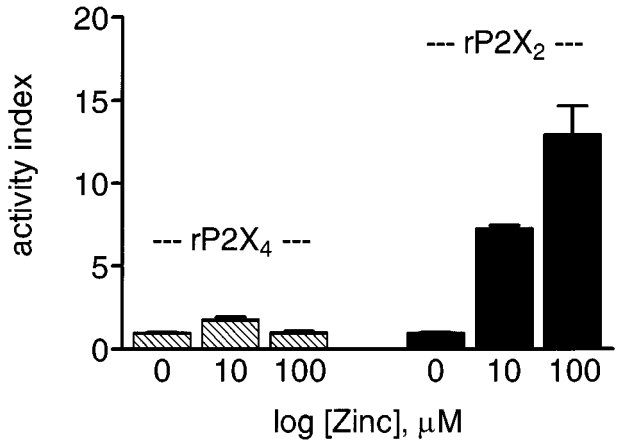

Figure 5 Comparison of Zn^{2+} modulation on ATP-responses at $rP2X_4$ and $rP2X_2$ receptors. Potentiating effects of Zn^{2+} (10 and 100 μM) on the ATP activity at $rP2X_4$ receptor and $P2X_2$ receptor, at pH 7.5. ATP was applied at a concentration just above threshold to give $\sim$5% of the maximal response at each P2X subtype, and these control responses were taken as 1 (activity index = 1). Zn^{2+} had a more profound effect on ATP-responses at $rP2X_2$ receptors at which Zn^{2+} maximally potentiated ATP-responses were increased 15 fold. In contrast, Zn^{2+} maximally potentiated ATP-responses at $rP2X_4$ receptors by 2 fold only.

$rP2X_4$ involves a reduction in ATP efficacy alone. These distinguishing features for Zn^{2+} modulation at $rP2X_2$ and $rP2X_4$ receptors might be useful criteria to determine the presence of either $P2X_2$ or $P2X_4$ subunits in native P2X receptors in neurons in the CNS and periphery. In the same vein, H^+ potentiation of ATP-responses at native P2X receptors is now viewed as signatory for the presence of $P2X_2$ subunits (Stoop *et al*., 1997).

In agreement with earlier reports (Bo *et al*., 1995; Buell *et al*., 1996; Collo *et al*., 1996; Séguéla *et al*., 1996; Soto *et al*., 1996; Wang *et al*., 1996), suramin failed to inhibit ATP-responses at $rP2X_4$ receptors. We attempted to uncover an inhibitory action by suramin by altering pH or adding Zn^{2+}, or using both, on the basis that the blocking activity of suramin is greatly enhanced at $rP2X_2$ at pH 5.5 (King *et al*., 1997) and in the presence of Zn^{2+} (Wildman *et al*., 1998). However, there was no evidence for an inhibitory action by suramin at $rP2X_4$ under such modified conditions. In point of fact, H^+ and Zn^{2+} appeared to be better inhibitors of ATP-responses at $rP2X_4$ than any of the known P2 receptor antagonists.

In conclusion, extracellular pH and Zn^{2+} affect only agonist activity and not antagonist activity at $rP2X_4$ receptors. H^+ and Zn^{2+} exert opposing actions by decreasing and increasing agonist potency, yet both share a common feature of also lowering the efficacy of ATP. These actions are in sharp contrast to the effects of H^+ and Zn^{2+} on agonist and antagonist activity at $rP2X_2$ receptors. Although both $rP2X_4$ and $rP2X_2$ transcripts are found throughout central and peripheral nervous system, their differing activity profiles with H^+ and Zn^{2+} suggest that P2X signalling can be altered in an opposite manner by these modulators. It has been reported for the enteric nervous system that P2X receptors show either a $P2X_2$-like phenotype (Zhou & Galligan, 1996) or a $P2X_4$-like phenotype (Barajas-Lopez *et al*., 1996), although neither H^+ nor Zn^{2+} have been tested on ATP-responses in the ENS. If similar phenotypic subsets of endogenous P2X receptors occur elsewhere throughout the CNS and PNS, the modulatory properties of H^+ and Zn^{2+} may have significant and selective actions on P2X signalling at discrete nuclei and ganglia, and provide the means to amplify or inhibit such signalling.

This work was supported by the British Heart Foundation and Roche Bioscience (Palo Alto, U.S.A.). We are grateful to Dr X. Bo and Dr R. Schoepfer for the gift of cDNA encoding the rat $P2X_4$ receptor.

References

ASSAF, S.Y. & CHUNG, S.H. (1984). Release of endogenous Zn^{2+} from brain tissue during activity. *Nature,* **308,** 734–736.

BARAJAS-LÓPEZ, C., HUIZINGA, J.D., COLLINS, S.M., GERZANICH, V., ESPINOZA-LUNA, R. & PERES, L.A. (1996). P2X-purinoceptors of myenteric neurones from the guinea-pig ileum and their unusual pharmacological properties. *Brit. J. Pharmacol.,* **119,** 1541–1548.

BARDONI, R., GOLDSTEIN, P.A., LEE, C.J., GU, J.G. & MACDERMOTT, A.B. (1997). ATP P2X receptors mediate fast synaptic transmission in the dorsal horn of the rat spinal cord. *J. Neurosci.,* **17,** 5297–5304.

BO, X., ZHANG, Y., NASSAR, M., BURNSTOCK, G. & SCHOEPFER, R. (1995). A P2X purinoceptor cDNA conferring a novel pharmacological profile. *FEBS Lett.,* **375,** 129–133.

BRAKE, A.J., WAGENBACH, M.J. & JULIUS, D. (1994). New structural motif for ligand gated ion channels defined by an ionotropic ATP receptor. *Nature,* **371,** 519–523.

BROOKS, S.P.J. & STOREY, K.B. (1992). Bound and Determined: a computer program for making buffers of defined ion concentrations. *Anal. Biochem.,* **210,** 119–126.

BUELL, G., LEWIS, C., COLLO, G., NORTH, R.A. & SURPRENANT, A. (1996). An antagonist-insensitive P2X receptor expressed in epithelia and brain. *EMBO J.,* **15,** 55–62.

CHESLER, M. (1990). The regulation and modulation of pH in the nervous system. *Prog. Neurobiol.,* **34,** 401–427.

CLARKE, C.E., MEADOWS, H.J., TOMLINSON, W.J., CARPENTER, D., SANGER, G.J. & BENHAM, C.D. (1998). Extracellular acidification inhibits current flow through human $P2X_4$ receptors expressed in *Xenopus* oocytes. *J. Physiol.,* **506,** 44P.

CLOUES, R., JONES, S. & BROWN, D.A. (1993). Zn^{2+} potentiates ATP-activated currents in rat sympathetic neurons. *Pflügers Arch.,* **424,** 152–158.

COLLO, G., NORTH, R.A., KAWASHIMA, E., MERLO-PICH, E., NEIDHART, S., SURPRENANT, A. & BUELL, G. (1996). Cloning of $P2X_5$ and $P2X_6$ receptors and the distribution and properties of an extended family of ATP-gated ion channels. *J. Neurosci.,* **16,** 2495–2507.

DESALLES, A.A., KONTOS, H.A., WARD, J.B., MARMAROU, A. & BECKER, D.P. (1987). Brain tissue pH in severely head injured patients: a report of 3 cases. *Neurosurgery,* **20,** 297–301.

DHULIPALA, P.D.K., WANG, Y.X. & KOTLIKOFF, M.I. (1998). The human $P2X_4$ receptor gene is alternatively spliced. *Gene,* **207,** 259–266.

EDWARDS, F.A., GIBB, A.J. & COLQUHOUN, D. (1992). ATP receptor-mediated synaptic currents in the central nervous system. *Nature,* **359,** 144–147.

EVANS, R.J., DERKACH, V. & SURPRENANT, A. (1992). ATP mediates fast synaptic transmission in mammalian neurons. *Nature,* **357,** 503–505.

GALLIGAN, J.J. & BERTRAND, P.P. (1994). ATP mediates fast synaptic potentials in enteric neurons. *J. Neurosci.,* **14,** 7563–7571.

GARCIA-GUZMAN, M., SOTO, F., GOMEZ-HERNANDEZ, J.M., LUND, P. & STÜHMER, W. (1997). Characterization of recombinant human $P2X_4$ receptor reveals pharmacological differences to the rat homologue. *Mol. Pharmacol.,* **51,** 109–118.

JOHNSON, R.G. & SCARPA, A. (1976). Internal pH of isolated chromaffin granules. *J. Biol. Chem.,* **251,** 2189–2191.

KING, B.F., WILDMAN, S.S., ZIGANSHINA, L.E., PINTOR, J. & BURNSTOCK, G. (1997). Effects of extracellular pH on agonism and antagonism at a recombinant $P2X_2$ receptor. *Brit. J. Pharmacol.,* **121,** 1445–1453.

KING, B.F., ZIGANSHINA, L.E., PINTOR, J. & BURNSTOCK, G. (1996). Full sensitivity of $P2X_2$ purinoceptor to ATP revealed by changing extracellular pH. *Brit. J. Pharmacol.,* **117,** 1317–1373.

KUPITZ, Y. & ATLAS, D. (1993). A putative ATP-activated Na^+ channel involved in sperm-induced fertilization. *Science,* **261,** 484–486.

LÊ, K.T., VILLENEUVE, P., RAMJAUN, A.R., MCPHERSON, P.S., BEADET, A. & SÉGUÉLA, P. (1998). Sensory presynaptic and widespread somatodendritic immunolocalization of central ionotropic P2X ATP receptors. *Neurosci.,* **83,** 177–190.

NAKAZAWA, K. & OHNO, Y. (1996). Dopamine and 5-hydroxytryptamine selectively potentiate neuronal type ATP receptor channels. *Eur. J. Pharmacol.,* **296,** 119–122.

NAKAZAWA, K. & OHNO, Y. (1997). Effects of neuroamines and divalent cations on cloned and mutated ATP-gated channels. *Eur. J. Pharmacol.,* **325,** 101–108.

NIEBER, K., POELCHEN, W. & ILLES, P. (1997). Role of ATP in fast excitatory synaptic potentials in locus ceuruleus neurones of the rat. *Brit. J. Pharmacol.,* **122,** 423–430.

NORTH, R.A. & BARNARD, E.A. (1997). Nucleotide receptors. *Curr. Opin. Neurobiol.,* **7,** 346–357.

RANSOM, B.R. & PHILBIN JR., D.M. (1992). Anoxia-induced extracellular ionic changes in the CNS white matter: the role of glial cells. *Can. J. Physiol. Pharmacol.,* **70,** S181–S189.

SÉGUÉLA, P., HAGHIGHI, A., SOGHOMONIAN, J. & COOPER, E. (1996). A novel neuronal P2X ATP receptor ion channel with widespread distribution in the brain. *J. Neurosci.,* **16,** 448–455.

SILINSKY, E.M. & GERZANICH, V. (1993). On the excitatory effects of ATP and its role as a neurotransmitter in coeliac neurons of the guinea-pig. *J. Physiol.,* **464,** 197–212.

SOTO, F., GARCIA-GUZMAN, M., GOMEZ-HERNANDEZ, J.M., HOLLMANN, M., KARSCHIN, C. & STÜHMER, W. (1996). $P2X_4$: an ATP-activated ionotropic receptor cloned from rat brain. *Proc. Natl. Acad. Sci. U.S.A.,* **93,** 3684–3688.

SPERLAGH, B., KITTEL, A., LAJTHA, A. & VIZI, E.S. (1995). ATP acts as fast neurotransmitter in rat habenula: neurochemical and enzyme cytochemical evidence. *Neurosci.,* **66,** 915–920.

STEEN, K.H., REEH, P.W., ANTON, F. & HANDWERKER, H.O. (1992). Protons selectively induce lasting excitation and sensitization to mechanical stimulation of nociception in rat skin, *in vitro*. *J. Neurosci.,* **12,** 86–95.

STOOP, R., SURPRENANT, A. & NORTH, R.A. (1997). Different sensitivities to pH of ATP-induced currents at four cloned P2X receptors. *J. Neurophysiol.,* **78,** 1837–1840.

URANO, T., NISHIMORI, H., HAN, H.J., FURUHATA, T., KIMURA, Y., NAKAMURA, Y. & TOKINO, T. (1997). Cloning of P2XM, a novel human P2X receptor gene regulated by p53. *Cancer Res.,* **57,** 3281–3287.

WANG, C.Z., NAMBA, N., GONOI, T., INAGAKI, N. & SEINO, S. (1996). Cloning and pharmacological characterization of a fourth P2X subtype widely expressed in brain and peripheral tissues including various endocrine tissues. *Biochem. Biophys. Res. Comm.,* **220,** 196–202.

WILDMAN, S.S., KING, B.F. & BURNSTOCK, G. (1997). Potentiation of ATP-responses at a recombinant $P2X_2$ receptor by neurotransmitters and related substances. *Brit. J. Pharmacol.,* **120,** 221–224.

WILDMAN, S.S., KING, B.F. & BURNSTOCK, G. (1998). Zn^{2+} modulation of ATP-responses at recombinant $P2X_2$ receptors and its dependence on extracellular pH. *Brit. J. Pharmacol.,* **123,** 1214–1220.

YANOVSKY, Y., REYMANN, K. & HAAS, H.L. (1995). pH-dependent facilitation of synaptic transmission by histamine in the CA1 region of mouse hippocampus. *Eur. J. Neurosci.,* **7,** 2017–2020.

ZHOU, X. & GALLIGAN, J.J. (1996). P2X purinoceptor in cultured myenteric neurons of guinea-pig small intestine. *J. Physiol.,* **496,** 719–729.

(Received July 27, 1998
Revised October 14, 1998
Accepted November 11, 1998)

British Journal of Pharmacology (1999) 126, 769–777
http://www.stockton-press.co.uk/bjp

Inhibition of poly(ADP-ribose) synthetase (PARS) and protection against peroxynitrite-induced cytotoxicity by zinc chelation

[1,2]László Virág & *[,1,3]Csaba Szabó

[1]Division of Critical Care Medicine, Children's Hospital Medical Center, 3333 Burnet Avenue, Cincinnati, Ohio 45229-3039, U.S.A.; [2]Department of Pathophysiology, Debrecen University Medical School, Debrecen, Hungary and [3]Inotek Corporation, 3130 Highland Avenue, Cincinnati, Ohio 45219-2374, U.S.A.

1 Peroxynitrite, a potent oxidant formed by the reaction of nitric oxide and superoxide causes thymocyte necrosis, in part, *via* activation of the nuclear enzyme poly(ADP-ribose) synthetase (PARS). The cytotoxic PARS pathway initiated by DNA strand breaks and excessive PARS activation has been shown to deplete cellular energy pools, leading to cell necrosis. Here we have investigated the effect of tetrakis-(2-pyridylmethyl)-ethylenediamine (TPEN) a heavy metal chelator on peroxynitrite-induced cytotoxicity.

2 TPEN (10 μM) abolished cell death induced by authentic peroxynitrite (25 μM) and the peroxynitrite generating agent 3-morpholinosidnonimine (SIN-1, 250 μM). Preincubation of TPEN with equimolar Zn^{2+} but not Ca^{2+} or Mg^{2+} blocked the cytoprotective effect of the chelator.

3 TPEN (10 μM) markedly reduced the peroxynitrite-induced decrease of mitochondrial transmembrane potential, secondary superoxide production and mitochondrial membrane damage, indicating that it acts proximal to mitochondrial alterations.

4 Although TPEN (1–300 μM) did not scavenge peroxynitrite, it inhibited PARS activation in a dose-dependent manner.

5 The cytoprotective effect of TPEN is only partly mediated *via* PARS inhibition, as the chelator also protected PARS-deficient thymocytes from peroxynitrite-induced death.

6 While being cytoprotective against peroxynitrite-induced necrotic death, TPEN (10 μM), similar to other agents that inhibit PARS, enhanced apoptosis (at 5–6 h after exposure), as characterized by phosphatydilserine exposure, caspase activation and DNA fragmentation.

7 In conclusion, the current data demonstrate that TPEN, most likely by zinc chelation, exerts protective effects against peroxynitrite-induced necrosis. Its effects are, in part, mediated by inhibition of PARS.

Keywords: Peroxynitrite; cytotoxicity; zinc; TPEN; poly (ADP-ribose) synthetase

Abbreviations: DiOC6(3), 3,3′dihexyloxacarbocyanine iodide; HE, dyhydroethidium; NAO, nonyl-acridine orange; PARS, poly(ADP-ribose) synthase; PI, propidium iodide; PKC, protein kinase C; SIN-1, 3-morpholinosidnonimine; TPEN, tetrakis-(2-pyridylmethyl)ethylenediamine

Introduction

Peroxynitrite, a potent oxidant formed in the near diffusion-limited reaction of superoxide and nitric oxide (Beckman *et al*., 1994; Beckman & Koppenol, 1996) is a major mediator of tissue injury in various forms of shock, inflammation and ischaemia-reperfusion (Zingarelli *et al*., 1997b; Szabó, 1996). The cytotoxic effect of peroxynitrite is mainly due to the activation of poly(ADP-ribose) synthetase (PARS) (Zingarelli *et al*., 1996; Szabó *et al*., 1996a,b; 1998; Virág *et al*., 1998b). PARS is a DNA nick sensor enzyme which, upon activation by DNA single strand breaks, cleaves NAD to nicotinamide and ADP-ribose and transfers poly(ADP-ribose) adducts to DNA and proteins (Szabó *et al*., 1996a). PARS is thought to play a role in maintaining genome integrity and may facilitate DNA repair (de Murcia *et al*., 1986; 1997; Trucco *et al*., 1998). Excessive PARS activation, however, depletes cellular energy pools and causes cell death (Cochrane, 1991; Szabó *et al*., 1996a; 1998; Virág *et al*., 1998b). The pathophysiological role of the PARS pathway has been demonstrated in various disease states (Szabó *et al*., 1996b; 1997a,c; 1998; for review see: Szabó, 1998; Szabó & Dawson, 1998).

We have previously shown that PARS activation is responsible for the dissipation of mitochondrial membrane potential, secondary superoxide production, mitochondrial membrane damage and the breakdown of plasma membrane integrity in peroxynitrite-treated thymocytes (Virág *et al*., 1998a). Furthermore, we have demonstrated that in the absence of PARS, peroxynitrite induced cell-death is diverted from necrotic to apoptotic death as indicated by increased DNA fragmentation, phosphatidylserine exposure and caspase activation (Virág *et al*., 1998b).

Here we have investigated the effect of tetrakis-(2-pyridylmethyl)ethylenediamine (TPEN), a zinc chelator, on the peroxynitrite-induced cytotoxicity. As PARS activation has been proposed to play a role in peroxynitrite-induced cell death, we also set out to investigate the effect of TPEN on PARS activation.

Methods

Animals

PARS-deficient and wild type mice (breeding pairs: kind gifts of Dr Z.Q. Wang, Inst. Molecular Pathology, Vienna, Austria) were bred at the animal care facility of the Children's Hospital Medical Center and were used at 4–6 weeks of age. Animals received food and water *ad libitum*, and lighting was maintained on a 12 h cycle.

* Author for correspondence; E-mail: szabocsaba@aol.com

Thymocyte preparation and peroxynitrite treatment

Thymi from 4–6-week-old male mice were aseptically removed and placed into ice cold RPMI media supplemented with 10% v v^{-1} foetal calf serum, glutamine (10 mM), HEPES (10 mM), 100 U ml^{-1} penicillin, 100 μg ml^{-1} streptomycin. Single cell suspensions were prepared by sieving the organs through a stainless wire mesh. Cells isolated this way were routinely 95% viable, as assessed by Trypan blue exclusion assay. Thymocytes (10^6 cells in 0.5 ml medium) were seeded in 24-well plates. Peroxynitrite was diluted in phosphate buffered saline (PBS) (pH 8.9) and added to the cells in a bolus of 50 μl. Thymocytes were then incubated for various times (20 min for PARS assay, 3 h for the measurement of mitochondrial parameters, 4 h for propidium iodide and Annexin V staining or 6 h for DNA fragmentation and caspase activation). Decomposed peroxy nitrite (incubated for 30 min at pH 7.0) served as control, and failed to influence any of the parameters studied. In another set of studies, the morpholinosidnonimine compound SIN-1 (250 μM) was used to simultaneously generate NO and superoxide, which then combines to peroxynitrite and induced thymocyte death (see also Virág *et al*., 1998a).

Measurement of mitochondrial membrane potential, superoxide production and cardiolipin content

The mitochondrial membrane potential was quantitated by the flow cytometric analysis of 3,3′dihexyloxacarbocyanine iodide [DiOC6(3)]-stained cells (Zamzami *et al*., 1995). Intramitochondrial generation of reactive oxygen intermediates was determined by analysing with flow cytometry the superoxide-induced conversion of the oxidant-sensitive dye, dihydroethidium to ethidium (Zamzami *et al*., 1995). Mitochondrial membrane damage was determined by measuring the cardiolipin degradation, as described (Zamzami *et al*., 1995). The fluorochrome 10-N nonyl-acridine orange (NAO) stoichiometrically interacts with cardiolipin (1 : 2), the cellular distribution of which is restricted to mitochondria.

Flow cytometry

Thymocytes were stained with 5 μg ml^{-1} PI, 3,3′dihexyloxacarbocyanine iodide [DiOC6(3)] (40 nM), hydroethidine (HE) (2 μM), 10-N nonyl-acridine orange (NAO) (100 nM) for 15 min at 37°C, washed once with PBS and analysed with a FacsCalibur flow cytometer as described (Virág *et al*., 1998a). For the measurement of mitochondrial parameters, forward and side scatters were gated on the major population of normal-sized cells. For the cytotoxicity assay, the percentage of PI-positive cells was calculated from the total (ungated) population.

Samples processed for Annexin V-FITC/propidium iodide staining (Vermes *et al*., 1995) were washed with PBS and 10^5 cells (in 100 μl) were stained with 5 μl Annexin V-FITC and 5 μg ml^{-1} propidium iodide (PI) in annexin binding buffer: (in mM) HEPES (pH 7.4) 10, NaCl 140, $CaCl_2$ 2.5) at room temperature. After 15 min, 400 μl annexin binding buffer was added to the samples which were then immediately analysed with a FacsCalibur flow cytometer (Becton-Dickinson, San Jose, CA, USA).

Dihydrorhodamine assay

The peroxynitrite-dependent oxidation of dihydrorhodamine 123 to rhodamine 123 was measured based on the principles of the method previously described (Szabó *et al*., 1995). Briefly, peroxynitrite (5 μM) was added into phosphate-buffered saline containing 10 μM dihydrorhodamine 123, in the absence or presence of TPEN (3–300 μM). After a 10 min incubation at 22°C, the fluorescence of rhodamine 123 was measured using a Perkin-Elmer fluorimeter (Model LS50B; Perkin-Elmer, Norwalk, CT, USA) at an excitation wavelength of 500 nm, emission wavelength of 536 nm (slit widths 2.5 and 3.0 nm, respectively). In control, reverse-order experiments we have confirmed that TPEN neither showed fluorescence at the above wavelengths, nor was the inhibition of fluorescence by the compounds due to reduction of the rhodamine 123 fluorescence (data not shown).

Cytochrome c oxidation

The peroxynitrite-dependent oxidation of cytochrome c^{2+}, was measured as described (Szabó *et al*., 1997b). Cytochrome c was reduced by sodium dithionite immediately before use and purified by chromatography on Sephadex G-25 using potassium phosphate (100 mM) plus DTPA, pH 7.2 (0.1 mM) as the elution buffer. The concentration of cytochrome c^{2+} was determined spectrophotometrically at 550 nm in the same buffer ($\varepsilon = 21$ mM^{-1} cm^{-1}). Cytochrome c^{2+} oxidation (50 μM) yields upon addition of peroxynitrite (25 μM initial concentration after mixing) were assessed by incubation of reaction mixtures in potassium phosphate (100 mM) plus DTPA, pH 7.2 (0.1 mM) at 22°C for 3 min in the absence or presence of TPEN (1–300 μM). Oxidation of cytochrome c^{2+} was followed at 550 nm using a Beckman DU 640 spectrophotometer (Fullerton, CA, USA). In control, reverse-order experiments we have confirmed that TPEN did not interfere with the spectrophotometric measurements at the above wavelengths. Moreover, in control experiments we have confirmed that the compound tested does not reduce cytochrome c^{3+}.

Measurement of cellular PARS activity

Thymocytes (10^7 cells in 1 ml culture medium) were treated with peroxynitrite. After 20 min, cells were spun, medium was aspirated and cells were resuspended in 0.5 ml assay buffer (in mM) HEPES (pH 7.5) 56, KCl 28, NaCl 28, $MgCl_2$ 2, 0.01% w v^{-1} digitonin and 0.125 μM ^{3}H-NAD (0.5 μCi ml^{-1})]. PARS activity was then measured as previously described (Virág *et al*., 1998b). Briefly, following incubation (10 min at 37°C), 200 μl ice cold 50% w v^{-1} TCA was added and samples incubated for 4 h at 4°C. Samples were then spun (10,000 × *g*, 10 min) and pellets washed twice with ice cold 5% w v^{-1} TCA and solubilized overnight in 250 μl 2% w v^{-1} SDS/0.1 N NaOH at 37°C. Contents of the tubes were added to 6.5 ml ScintiSafe Plus scintillation liquid (Fisher Scientific) and radioactivity was determined using a liquid scintillation counter (Wallac, Gaithersburg, MD, USA).

Detection of internucleosomal DNA fragmentation of thymocytes

Thymocytes were pretreated with TPEN for 20 min and then treated with peroxynitrite (10–80 μM). After 6 h, cells were washed once with cold PBS and pellets resuspended in sample buffer (10 mM Tris, pH 8.0, 5% v v^{-1} glycerol, 0.05% w v^{-1} bromophenol blue, 5 mg ml^{-1} RNase). DNA fragmentation was detected as described (Eastman, 1995). Agarose (2% w v^{-1}) was poured on a horizontal gel support. After solidification of the gel the top part (above the comb) was replaced with 1% w v^{-1} agarose containing 2% w v^{-1} SDS and 64 μg ml^{-1} proteinase K. Cells (2×10^6) were loaded in

20 μl sample buffer. Electrophoresis was carried out at 25 V for 12 h and the gel was stained with 2 μg ml^{-1} ethidium bromide for 1 h.

Measurement of caspase 3-like activity

Caspase activity was measured by the cleavage of the fluorogenic tetrapeptide-amino-4-methylcoumarine conjugate (DEVD-AMC) as described (Vanags *et al*., 1997). Unless otherwise indicated cells ($4-10\times10^6$) were harvested 6 h after peroxynitrite treatment, washed once in PBS and then lysed in a lysis buffer: (in mM) HEPES 10, 0.1% w v^{-1} CHAPS, dithiothreitol 5, EDTA 2, 10 μg ml^{-1} aprotinin, 20 μg ml^{-1} leupeptin, 10 μg ml^{-1} pepstatin A and PMSF, pH 7.25 (1 mM), for 10 min on ice. Cell lysates and substrates (50 μM) were combined in triplicate in the caspase reaction buffer: HEPES (100 mM), 10% w v^{-1} sucrose, dithiothreitol (5 mM), 0.1% w v^{-1} CHAPS, pH 7.25 in the presence or absence of 10 μM of the tetrapeptide caspase 3 inhibitor N-acetyl-aspartyl-glutamyl-valyl-aspartyl-aldehyde (DEVD-CHO) and samples were incubated at 37°C for 60 min. AMC liberation was determined with a Perkin-Elmer fluorimeter using 380 nm excitation and 460 mission wavelength. Data are given as absolute fluorescence units.

Statistical analysis

All values in the figures and text are expressed as mean $\pm$ standard deviation (S.D.) of n observations; $n\geqslant3$. Data sets were examined by analysis of variance and individual group means were then compared with Bonferroni-'s *post hoc* test. A P value less than 0.05 was considered statistically significant. When the results are presented as representative gels, or flow cytometry analyses, results similar to the ones shown were obtained in at least three different experiments.

Materials

Peroxynitrite was a kind gift of Dr H. Ischiropoulos (Inst. Environmental Medicine, University of Pennsylvania, PA, USA). 3-morpholinosidnonimine (SIN-1) was purchased from Calbiochem (San Diego, CA, USA). Tetrakis-(2-pyridyl-methyl)ethylenediamine (TPEN), 3,3′dihexyloxacarbocyanine iodide [DIOC6(3)], dihydroethidium (HE), nonyl-acridine orange (NAO), propidium iodide were obtained from Molecular Probes (Eugene, OR, USA). The tetrapeptide substrate (DEVD-AMC) and inhibitor (DEVD-CHO) of caspase 3 were purchased from Biomol (Plymouth Meeting, PA, USA). Proteinase K was obtained from Life Technologies (Grand Island, NY, USA). Annexin V-FITC was from Pharmingen (San Diego, CA, USA). Tris, magnesium chloride, analytical test filter funnels and Scintisafe scintillation cocktail were from Fisher Scientific (Pittsburgh, PA, USA). ^{3}H-NAD was purchased from DuPont NEN (Boston, MA, USA). All the other chemicals were purchased from Sigma Chemical Co. (St. Louis, MO, USA).

Results

TPEN protects from peroxynitrite-induced cytotoxicity

Treatment of wild-type thymocytes with authentic peroxynitrite (20 μM) or the peroxynitrite releasing agent SIN-1 (250 μM) resulted in cell death, as determined by the uptake of the cell-impermeable fluorescent dye propidium iodide (Figure 1). Pretreatment of the cells with TPEN (10 μM) abolished peroxynitrite-induced cytotoxicity. Preincubation of TPEN with equimolar zinc chloride ($ZnCl_2$) but not calcium chloride ($CaCl_2$) or magnesium chloride ($MgCl_2$) neutralized the protective effect of TPEN, indicating that the effect of TPEN is not related to calcium or magnesium chelation but may result from the chelation of zinc.

TPEN does not scavenge peroxynitrite

TPEN at concentrations of 1–300 μM failed to affect the oxidation of cytochrome c by peroxynitrite (Figure 2A) indicating that the cytoprotective effect of the chelator is not due to a potential peroxynitrite scavenging activity. Similarly, the lack of peroxynitrite-scavenging effect of TPEN has also been confirmed with the dihydrorhodamine assay (Figure 2B): TPEN did not affect the oxidation of dihydrorhodamine 1,2,3 to rhodamine 1,2,3.

TPEN acts proximal to mitochondrial alterations

A central event of the cell death process is the collapse of mitochondrial membrane potential, followed by the production of superoxide anion and the loss of cardiolipin (for review see Kroemer *et al*., 1997). Our previous work has demonstrated that the same sequence of events occur during peroxynitrite-induced cell death (Virág *et al*., 1998a). We have also provided evidence that these mitochondrial alterations

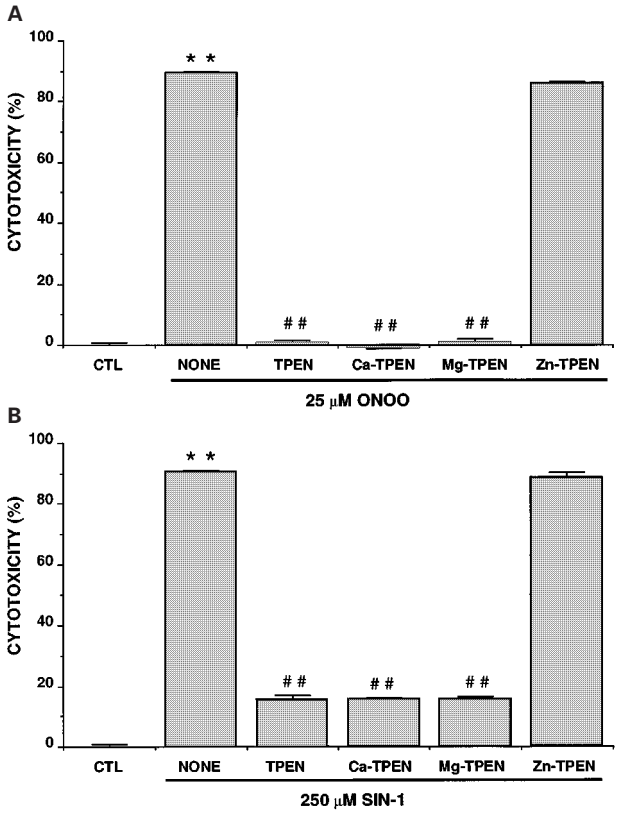

Figure 1 Thymocytes were pretreated with either TPEN (10 μM) or TPEN (10 μM) in the presence or absence of equimolar $CaCl_2$, $MgCl_2$ or $ZnCl_2$ for 30 min and then treated with the indicated concentration of peroxynitrite (ONOO) (A) or SIN-1 (B). After 4 h, cells were stained with propidium iodide and analysed by flow cytometry. Percentage number of PI positive cells $\pm$ s.d. of triplicate samples are shown. **indicates a significant ($P<0.01$) cytotoxic effect of peroxynitrite and ##indicates a significant ($P<0.01$) protection against cytotoxicity.

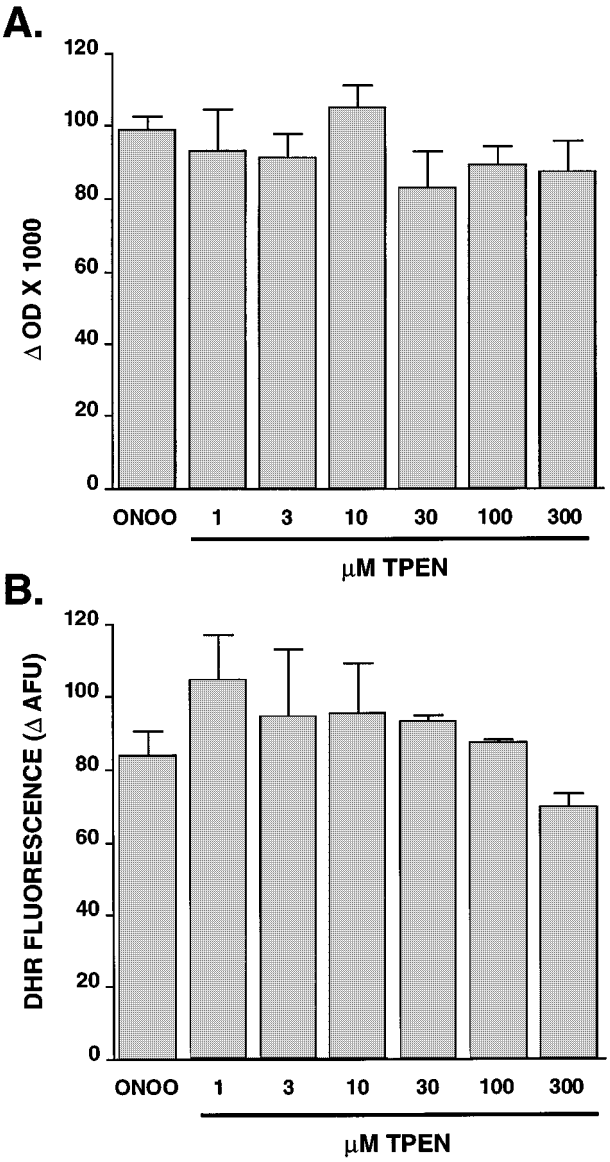

Figure 2 The oxidation of cytochrome c (A) and dihydrorhodamine (B) by peroxynitrite was determined in the presence of various concentrations of TPEN. The peroxynitrite-induced increase in dihydrorhodamine (DHR) fluorescence or decrease in cytochrome c absorbance is shown. Data are given as mean ± s.d. of triplicate experiments.

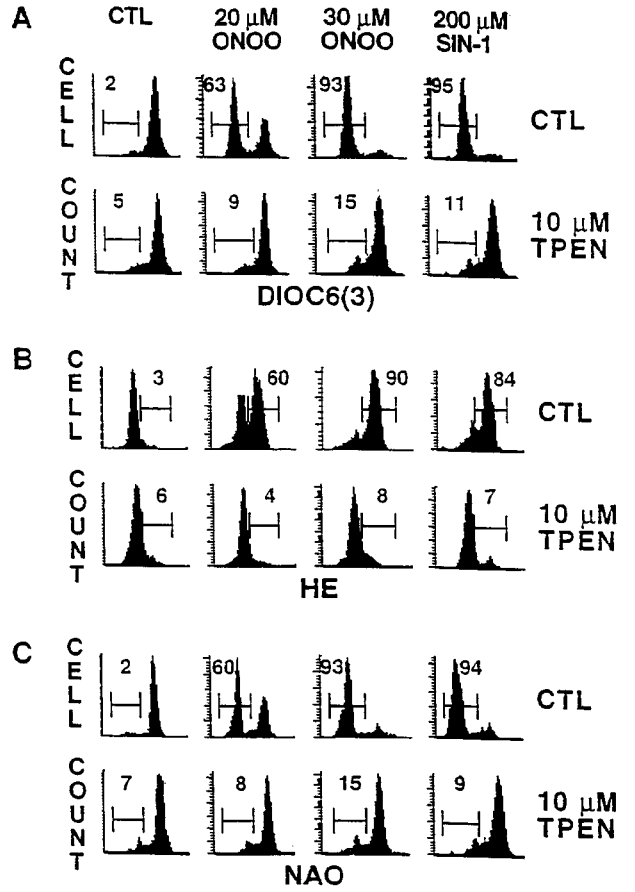

Figure 3 Thymocytes were either left untreated or were pretreated with TPEN (10 μM). Cells were then exposed to peroxynitrite or SIN-1 and incubated for 3 h. Thymocytes were then stained with DiOC6(3), hydroethidine (HE) or nonyl-acridine orange (NAO) for the measurement of mitochondrial membrane potential (A), superoxide production (B) and mitochondrial membrane damage (C), respectively. Histograms presented are representatives of three different experiments. Values shown indicate percentage of cells displaying decreased mitochondrial membrane potential, increased superoxide production and decreased mitochondrial membrane damage.

can be abolished by inactivation of PARS. Here we have determined whether the protective effect of TPEN is proximal or distal to mitochondrial alterations. The peroxynitrite or SIN-1-induced decrease of mitochondrial potential indicated by the decreased DiOC6(3) staining was prevented by TPEN (10 μM) pretreatment (Figure 3A). Similarly, peroxynitrite or SIN-1 induced secondary oxyradical production as measured by HE staining (Figure 3B) as well as the loss of mitochondrial cardiolipin indicated by reduced NAO staining were also markedly inhibited by TPEN (10 μM) (Figure 3C). Prevention of peroxynitrite-induced mitochondrial function alteration suggests that TPEN acts proximal to the mitochondrial phase during peroxynitrite-induced cell death.

TPEN inhibits PARS activation

Since TPEN, similar to compounds that inhibit PARS, blocked peroxynitrite cytotoxicity at a step proximal to mitochondrial perturbations, we have examined the effect of TPEN on PARS activation. TPEN inhibited peroxynitrite-induced PARS activation (Figure 4) in a dose-dependent manner. At the concentration of TPEN used throughout the current study (10 μM), the chelator completely blocked peroxynitrite-induced PARS activity. Higher concentrations of TPEN reduced PARS activity below the baseline levels (Figure 4).

Effect of TPEN on peroxynitrite-induced caspase 3 activation and DNA fragmentation

Our recent work has shown that the cytoprotection provided by PARS inhibition results in a shift from necrosis toward apoptotic cell death (Virág *et al*., 1998b). In the absence of PARS, peroxynitrite (10–80 μM) induced a dose-dependent increase in caspase 3 activity and DNA fragmentation. In the wild type cells, however, only low concentrations (10–20 μM) of peroxynitrite caused DNA fragmentation. At higher doses (40–80 μM) of peroxynitrite, PARS activation led to necrosis without DNA fragmentation (Virág *et al*., 1998b). Here we have investigated the effect of TPEN on two apoptotic parameters of peroxynitrite-treated cells: caspase activation

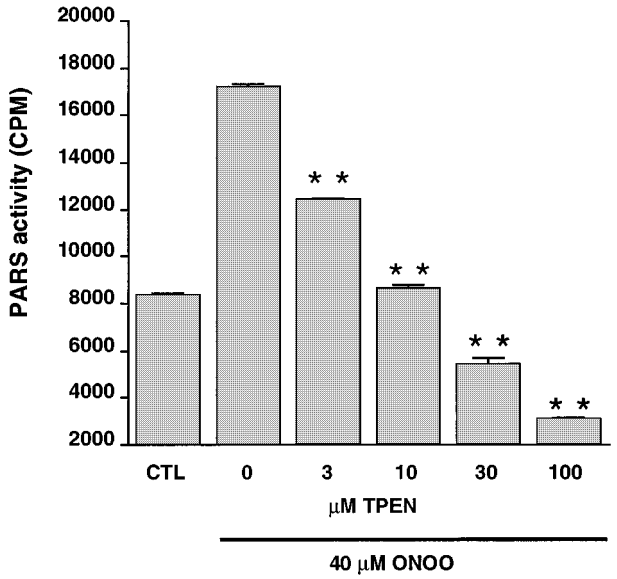

Figure 4 Thymocytes were pretreated for 30 min with TPEN. Cells were then stimulated with peroxynitrite (40 μM) for 20 min and PARS activity was determined with the ^{3}H-NAD assay. Data are given as mean$\pm$s.d. of triplicate experiments. **indicates a significant ($P<0.01$) inhibition of PARS activity.

and DNA fragmentation. In line with the PARS inhibitory effect of TPEN, the chelator prevented the inhibition of DNA fragmentation observed at higher doses (40–80 μM) of peroxynitrite (Figure 5A). TPEN alone (in the absence of peroxynitrite treatment) also induced DNA fragmentation in thymocytes, with DNA laddering first detectable 4 h after TPEN treatment (Figure 5C).

Peroxynitrite caused a dose-dependent increase in caspase activity peaking at 40 μM peroxynitrite (Figure 5B). In addition, TPEN alone also induced a marked increase in caspase-3 like activity, starting at 2 h after exposure (Figure 5D).

Effect of TPEN on phosphatidylserine exposure

Peroxynitrite-induced necrotic and apoptotic cell death was accompanied by the appearance of phosphatidylserine in the outer membrane leaflet, as indicated by Annexin V-FITC binding. Annexin V binding in the absence of PI uptake indicates early apoptotic cells whereas Annexin V/PI double positive cells represent a primary necrotic or late apoptotic population (Virág *et al.*, 1998b). Since phosphatidylserine exposure appears very early in the cytotoxic process, Annexin V/PI double-staining allows a more sensitive detection of cell

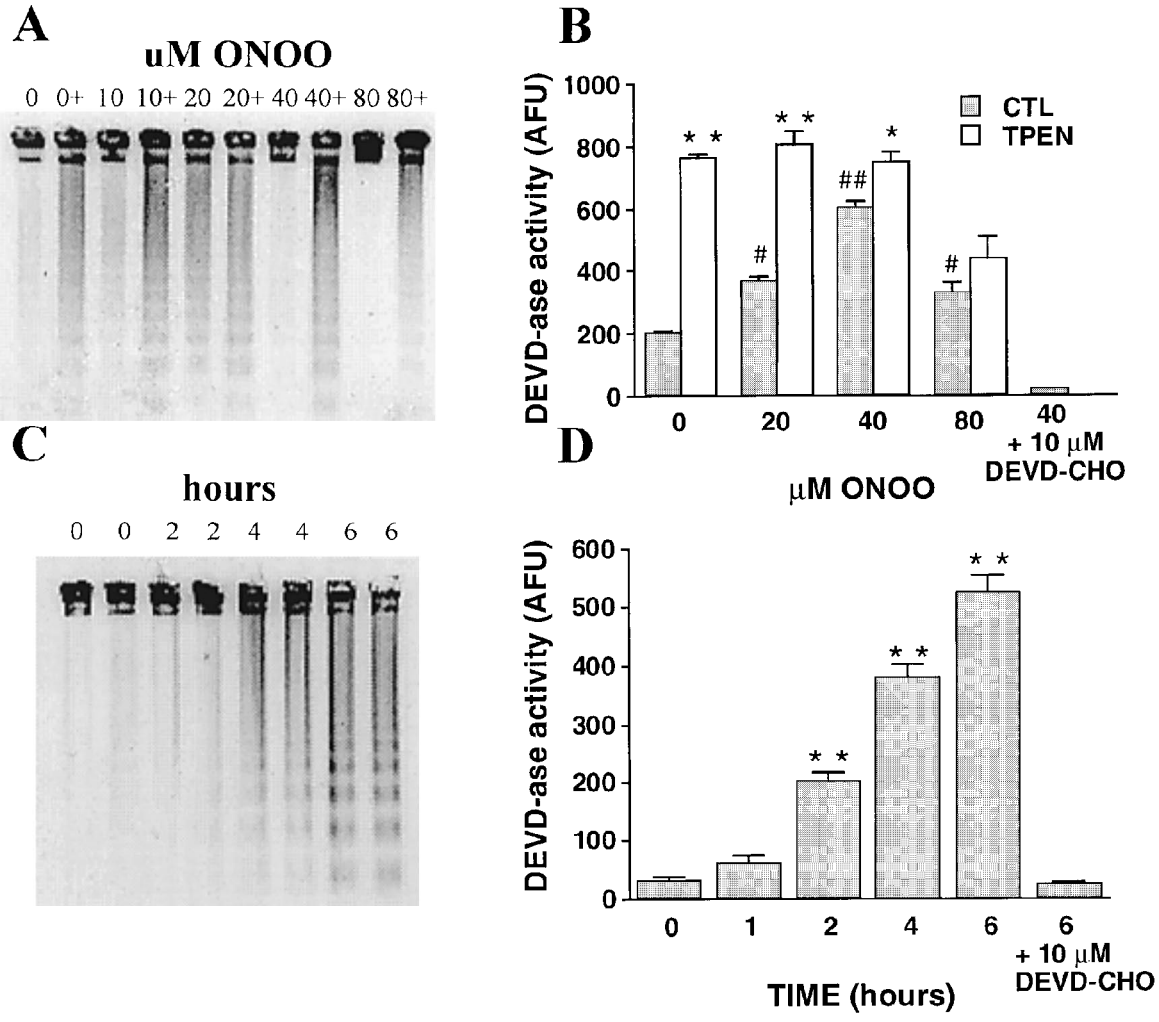

Figure 5 Wild type (W.T.) and PARS knock out (K.O.) thymocytes were either left untreated or pretreated with TPEN (10 μM). Thymocytes were then exposed to the indicated concentrations (μM) of peroxynitrite and incubated for 6 h. DNA fragmentation was visualized by agarose gel electrophoresis (A) (TPEN pretreatment is indicated by '+' sign) and caspase-3 like activity was measured by DEVD-AMC cleavage (B). The time course of TPEN-induced DNA cleavage (C) and DEVD-ase activity (D) has also been determined 0, 2, 4 and 6 h after TPEN exposure. Data of caspase activity are given as mean$\pm$s.d. of triplicate measurements. *, **indicate significant (*$P<0.05$, **$P<0.01$) difference between vehicle and TPEN treated samples. #, # # indicate a significant increase of caspase activity by peroxynitrite when compared to the activity in untreated samples at time 0 (#$P<0.05$ and ##$P<0.01$).

death. Annexin V-FITC/PI double staining revealed that TPEN blocked the breakdown of membrane integrity (PI uptake) both at 3 and 5 h after peroxynitrite treatment. (Figure 6A and B, respectively). TPEN-induced phosphatidylserine exposure could be detected as early as 3 h after peroxynitrite treatment and further increased at 5 h. TPEN markedly antagonized the cytotoxic effect of peroxynitrite at 3 h (Figure 6A). Even at 5 h, when TPEN itself began to induce cytotoxicity, the zinc chelator protected against peroxynitrite-induced cytotoxicity. For example, considering Annexin V/PI double positive cells as dead, Annexin V single positive cells as committed to die, and double negative cells as viable, at 5 h, TPEN induced $40+19=59\%$ and SIN-1 caused $22+63=85\%$ toxicity. In TPEN pretreated cells exposed to SIN-1, however, only $26+11=37\%$ cytotoxicity could be detected (Figure 6).

PARS-independent effect of TPEN in peroxynitrite-induced cytotoxicity

Since PARS-deficient thymocytes were resistant to peroxynitrite-induced cytotoxicity (Virág *et al*., 1998a,b), in order to achieve a similar degree of cell death in these cells, four times higher doses of peroxynitrite (80 μM) were required. TPEN provided significant protection against peroxynitrite-induced cytotoxicity in the PARS-deficient thymocytes (Figure 7), indicating that the chelator also exerts cytoprotective effects independent of PARS inhibition. Similarly to wild type cells, 6 h after TPEN treatment PARS deficient thymocytes showed caspase activation and DNA fragmentation. Peroxynitrite caused DNA fragmentation at the dose of 20–80 μM (Figure 7B), whereas at 160 μM no DNA fragmentation could be detected (not shown). DEVD-ase activity was also increased following treatment with 20–80 μM peroxynitrite (Figure 7C). However, peroxynitrite-induced caspase activation and DNA fragmentation in PARS-deficient cells was unaffected by TPEN pretreatment.

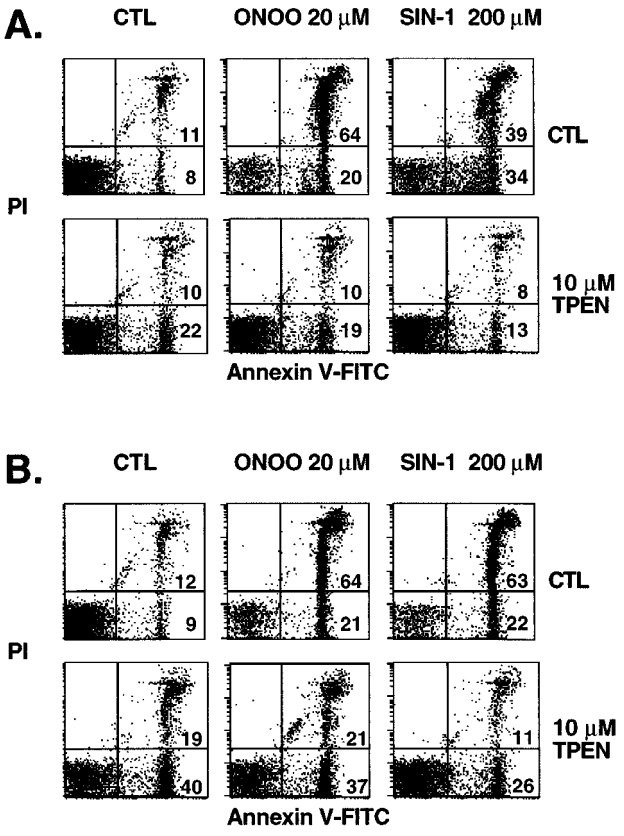

Figure 6 Thymocytes were either left untreated or were pretreated with TPEN (10 μM). Cells were then treated with peroxynitrite or SIN-1 and incubated for 3 h (A) or 5 h (B) followed by Annexin V-FITC/propidium iodide double staining. Numbers indicate percentage of cells in lower right (Annexin V single positive) and upper right (Annexin V/propidium iodide double positive) quadrant. Dot plots shown are representative of three independent experiments.

Discussion

Cytoprotective effect of TPEN via *PARS inhibition*

The present study demonstrates that peroxynitrite-induced thymocyte necrosis can be reduced by chelation of intracellular Zn^{2+}. We have previously shown that, in our experimental system, peroxynitrite-induced PARS activation is responsible for the necrotic death of thymocytes (Virág *et al*., 1998a,b). Thus, it appeared plausible to hypothesize that the zinc chelator directly or indirectly inhibits PARS activation. In our current work we provide evidence that TPEN is a potent inhibitor of PARS activation. Considering that PARS is an enzyme with two zinc finger domains localized in the DNA binding subunit of the enzyme (Mazen *et al*., 1989; Menissier-de Murcia *et al*., 1989), it is plausible to hypothesize that TPEN acts *via* binding to zinc ions in the zinc finger domain of PARS, thereby inhibiting the binding of the enzyme to the single-strand break sites in the DNA.

The mode of the modulation of peroxynitrite-induced cytotoxicity by TPEN (suppression of necrosis, and enhancement of apoptotic DNA fragmentation), is similar to the effect of various PARS inhibitors (see Virág *et al*., 1998a,b). Thus, it is logical to propose that the mode of action of TPEN, in intact cells, is related to inhibition of cellular PARS activity. As discussed earlier (Virág *et al*., 1998a,b), in the absence of functional PARS, the cells are protected against necrotic death by energy failure, but, at the same time, may have preserved sufficient cellular energy reserves to complete the process of apoptosis, which is a known energy-dependent process.

PARS-independent cytoprotection by TPEN

Our results, demonstrating that TPEN protects PARS deficient thymocytes against peroxynitrite-induced necrosis, indicate that, in addition to being an inhibitor of PARS activation, TPEN may also interfere with a yet undefined, PARS-independent cytotoxic pathway. A potential candidate for a target for TPEN in mediating PARS-independent cytoprotection may be another zinc finger protein family, namely the protein kinase C (PKC) family. Although the effect of peroxynitrite on kinase signalling pathways has not yet been investigated, superoxide and nitric oxide have been shown to be involved in N-methyl-D-aspartate receptor mediated PKC activation (Klann *et al*., 1998) and TPEN was reported to inhibit the translocation of PKC from the cytosolic to the membranous fraction in this model (Baba *et al*., 1991). Moreover, hydrogen peroxide, another oxidant known to induce PARS-activation has been shown to induce PKC activation in rat cardiac myocytes (Sabri *et al*., 1998), COS-7 cells (Konishi *et al*., 1997) and in Jurkat T cells (Whisler *et al*., 1995). Identification of the exact mechanism of peroxynitrite cytotoxicity including a possible involvement of PKC activation in this process, however, requires further investigation.

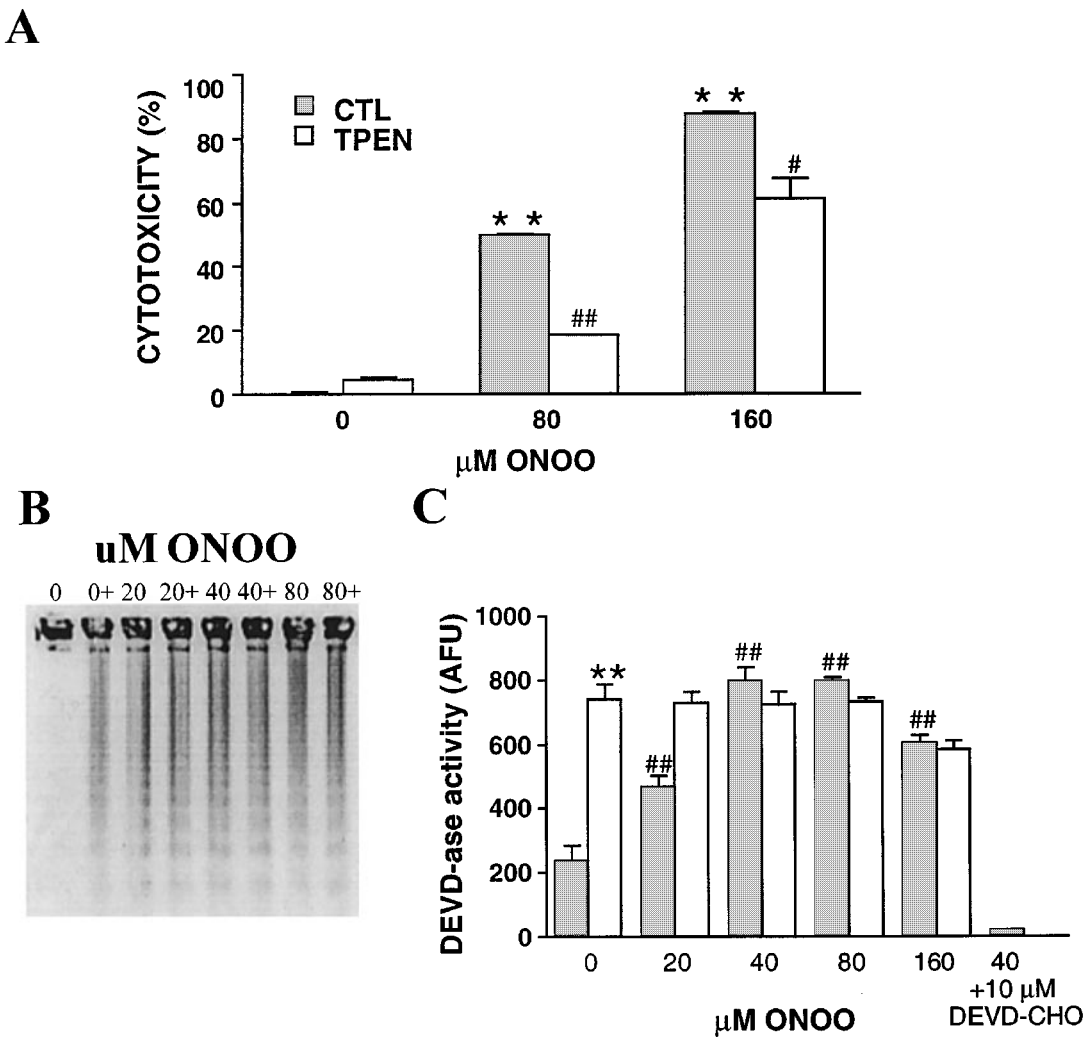

Figure 7 PARS-deficient thymocytes were pretreated with TPEN (10 μM) for 30 min and then treated with the peroxynitrite (ONOO) (80 μM). After 4 h, cells were stained with propidium iodide and analysed by flow cytometry (A). Percentage number of PI positive cells $\pm$ s.d. of triplicate samples are shown. **indicates significant ($P<0.01$) increase in cytotoxicity. #, ## indicate significant (#$P<0.05$ and ##$P<0.01$, respectively) protection against cytotoxicity. The effect of TPEN (10 μM) on peroxynitrite (20–160 μM)-induced DNA fragmentation (B) (TPEN pretreatment is indicated by '+' sign) and caspase-3 like activity (C) was also investigated 6 h after peroxynitrite treatment. **indicates significant ($P<0.01$) difference between vehicle and TPEN treated samples. #, ## indicate a significant increase of caspase activity by peroxynitrite (#$P<0.05$ and ##$P<0.01$).

TPEN-induced apoptosis

While being cytoprotective against peroxynitrite-induced necrotic death *via* PARS inhibition, TPEN itself induces apoptosis in thymocytes, especially at longer times of exposure. It has been known that chelation of Zn^{2+} by TPEN causes apoptosis in thymocytes (McCabe Jr *et al*., 1993; Jiang *et al*., 1995), lymphocytes (Treves *et al*., 1994) and HaCaT keratinocytes (Parat *et al*., 1997) as evidenced by DNA fragmentation and appearance of apoptotic nuclear morphology (nuclear condensation). Although exogenous Zn^{2+} has been shown to prevent apoptosis by inhibiting caspases (Perry *et al*., 1997), the effect of Zn^{2+} chelation on caspase activation has not yet been examined. Here we have shown that during TPEN-induced apoptosis a markedly elevated caspase-3 like activity could be detected as measured by DEVD-AMC cleavage. Although the mechanism of caspase activation in the course of TPEN-induced programmed cell death requires further elucidation, we hypothesize that caspases may represent primary targets of TPEN for the initiation of apoptosis. Recently, a new family of endogenous apoptosis inhibitors called IAP-s (inhibitors of apoptosis proteins) have been described (Rothe *et al*., 1995). Some members of this family including XIAP, cIAP-1 and c-IAP-2 can bind and selectively inhibit caspases (Deveraux *et al*., 1997; Roy *et al*., 1997). A common structural element of these caspase-inhibiting IAP family proteins is a RING zinc finger domain. Although this domain is not directly involved in binding to and inhibiting caspases (Takahashi *et al*., 1998), it may serve as a regulator of IAP protein function and thus chelation of Zn^{2+} in the zinc finger domain may inhibit the function of caspase-inhibiting IAP family members.

Effect of TPEN on the mode of peroxynitrite-induced cell death

Low doses (10–25 μM) of peroxynitrite induce DNA fragmentation in thymocytes, whereas higher doses (40–80 μM) inhibit oligonucleosomal DNA cleavage (Virág *et al*., 1998b). This latter effect is mediated by PARS activation (Virág *et al*., 1998b). In line with the PARS-inhibitory effect of TPEN, the chelator reversed the inhibition of DNA

fragmentation observed at high doses of peroxynitrite. Theoretically, it is possible that a very rapid TPEN-induced caspase activation (see above) 'switches on' DNA fragmentation before PARS activation occurs which would result in inhibition of DNA laddering. However, the time-course of PARS activation (10–20 min) and TPEN-induced caspase activation (starting at 2 h) and DNA fragmentation (starting at 4 h) argues against this scenario and favours the hypothesis that TPEN reverses the peroxynitrite-induced inhibition of DNA cleavage due to its function as a PARS inhibitor.

Conclusions and implications

Taken together, the conclusions of the present study are the following: (1) TPEN suppresses peroxynitrite-induced cell necrosis; (2) TPEN inhibits peroxynitrite-induced PARS activation and (3) TPEN also exerts PARS-independent cytoprotective effects. TPEN has previously been shown to protect spinal cord neurons from oxyradical-induced cytotoxicity (Michikawa *et al*., 1994) and prevent ATP depletion in hydrogen peroxide-treated Ac2F cells (Musicki & Behrman, 1993). Furthermore, treatment with TPEN proved beneficial *in vivo* in protecting from CCl_4-induced liver injury (Moon *et al*., 1998), and from arrhythmia caused by myocardial ischaemia-reperfusion (Ferdinandy *et al*., 1998; Chevion, 1991). Regarding the cardioprotective effect of TPEN, it is noteworthy that *in vivo* peroxynitrite formation and PARS activation was proposed to mediate myocardial injury after ischaemia-reperfusion (Zingarelli *et al*., 1997a,b; 1998). Although the effect of TPEN on PARS activation in these experiments has not been investigated, it is conceivable that the protection against necrosis by TPEN *in vivo* is, at least in part, related to inhibition of PARS activation.

The authors wish to thank Mr Paul Hake for technical assistance, Dr Harry Ischiropoulos (Inst. Environmental Medicine, University of Pennsylvania, PA, U.S.A.) for generously donating authentic peroxynitrite, Dr Z.Q. Wang (Inst. Molecular Pathology, Vienna, Austria) for the PARS-deficient mice and Dr G.S. Scott for critically reading the manuscript. This work was supported by grants from the National Institutes of Health (R29GM54773 and R01HL59266) to C.S., L.V. was supported by a fellowship from the Ida and Zoltan Dobsa Foundation.

References

BABA, A., ETOH, S. & IWATA, H. (1991). Inhibition of NMDA-induced protein kinase C translocation by a Zn^{2+} chelator: implication of intracellular Zn^{2+}. *Brain Res.,* **557,** 103–108.

BECKMAN, J.S., CHEN, J., ISCHIROPOULOS, H. & CROW, J.P. (1994). Oxidative chemistry of peroxynitrite. *Meth. Enzymol.,* **233,** 229–240.

BECKMAN, J. S. & KOPPENOL, W.H. (1996). Nitric oxide, superoxide, and peroxynitrite: the good, the bad, and ugly. *Am. J. Physiol.,* **271,** C1424–C1437.

CHEVION, M. (1991). Protection against free radical-induced and transition metal-mediated damage: the use of 'pull' and 'push' mechanisms. *Free Radic. Res. Commun.,* **12–13,** 691–696.

COCHRANE, C. (1991). Mechanisms of oxidant injury of cells. *Mol. Aspects Med.,* **12,** 137–147.

DE MURCIA, G., HULETSKY, A., LAMARRE, D., GAUDREAU, A., POUYET, J., DAUNE, M. & POIRIER, G.G. (1986). Modulation of chromatin superstructure induced by poly(ADP-ribose)polimerase synthesis and degradation. *J. Biol. Chem.,* **261,** 7011–7017.

DE MURCIA, J.M., NIEDERGANG, C., TRUCCO, C., RICOUL, M., DUTRILLAUX, B., MARK, M., OLIVER, F.J., MASSON, M., DIERICH, A., LEMEUR, M., WALTZINGER, C., CHAMBON, P. & DE MURCIA, G. (1997). Requirement of poly(ADP-ribose) polymerase in recovery from DNA damage in mice and in cells. *Proc. Natl. Acad. Sci. U.S.A.,* **94,** 7303–7307.

DEVERAUX, Q.L., TAKAHASHI, R., SALVESEN, G.S. & REED, J.C. (1997). X-linked IAP is a direct inhibitor of cell-death proteases. *Nature,* **388,** 300–304.

EASTMAN, A. (1995). Assays of DNA fragmentation, endonucleases, and intracellular pH and Ca^{2+} associated with apoptosis. *Methods Cell Biol.,* **46,** 41–55.

FERDINANDY, P., APPELBAUM, Y., CSONKA, C., BLASIG, I.E. & TOSAKI, A. (1998). Role of nitric oxide and TPEN, a potent metal chelator, in ischaemic and reperfused hearts. *Clin. Exp. Pharmacol. Physiol.,* **25,** 496–502.

JIANG, S., CHOW, S.C., MCCABE JR, M.J. & ORRENIUS, S. (1995). Lack of Ca^{2+} involvement in thymocyte apoptosis induced by chelation of intracellular Zn^{2+}. *Lab. Invest.,* **73,** 111–117.

KLANN, E., ROBERSON, E.D., KNAPP, L.T. & SWEATT, J.D. (1998). A role for superoxide in protein kinase C activation and induction of long-term potentiation. *J. Biol. Chem.,* **273,** 4516–4522.

KONISHI, H., TANAKA, M., TAKEMURA, Y., MATSUZAKI, H., ONO, Y., KIKKAWA, U. & NISHIZUKA, Y. (1997). Activation of protein kinase C by tyrosine phosphorylation in response to H_2O_2. *Proc. Natl. Acad. Sci. U.S.A.,* **94,** 11233–11237.

KROEMER, G., ZAMZAMI, N. & SUSIN, S. A. (1997). Mitochondrial control of apoptosis. *Immunol. Today,* **18,** 44–51.

MAZEN, A., MENISSIER-DE MURCIA, J. MOLINETE, M., SIMONIN, F., GRADWOHL, G., POIRIER, G. & DE MURCIA, G. (1989). Poly (ADP-ribose) polymerase: a novel finger protein. *Nucleic Acids Res.,* **17,** 4689–4698.

MENISSIER-DE MURCIA, J., MOLINETE, M., GRADWOHL, G., SIMONIN, F. & DE MURCIA, G. (1989). Zinc-binding domain of poly(ADP-ribose)polymerase participates in the recognition of single strand breaks on DNA. *J. Mol. Biol.,* **210,** 229–233.

MCCABE JR, M.J., JIANG, S.A. & ORRENIUS, S. (1993). Chelation of intracellular zinc triggers apoptosis in mature thymocytes. *Lab. Invest.,* **69,** 101–110.

MICHIKAWA, M., LIM, K.T., MCLARNON, J.G. & KIM, S.U. (1994). Oxygen radical-induced neurotoxicity in spinal cord neuron cultures. *J. Neurosci. Res.,* **37,** 62–70.

MOON, J.O., PARK, S.K. & NAGANO, T. (1998). Hepatoprotective effect of Fe-TPEN on carbon tetrachloride induced liver injury in rats. *Biol. Pharm. Bull.,* **21,** 284–288.

MUSICKI B. & BEHRMAN, H.R. (1993). Metal chelators reverse the action of hydrogen peroxide in rat luteal cells. *Mol. Cell. Endocrinol.,* **92,** 215–220.

PARAT, M.O., RICHARD, M.J., POLLET, S., HADJUR, C., FAVIER, A. & BEANI, J.C. (1997). Zinc and DNA fragmentation in keratinocyte apoptosis: its inhibitory effect in UVB irradiated cells. *J. Photochem. Photobiol. B.,* **37,** 101–106.

PERRY, D.K. SMYTH, M.J., STENNICKE, H.R., SALVESEN, G.S., GURIEZ, P., POIRIER, G.G. & HANNUN, Y.A. (1997). Zinc is a potent inhibitor of the apoptotic protease, caspase-3. A novel target for zinc in the inhibition of apoptosis. *J. Biol. Chem.,* **272,** 18530–18533.

ROTHE, M., PAN, M.G., HENZEL, W.J., AYRES, T.M. & GOEDDEL, D.V. (1995). The TNFR2-TRAF signaling complex contains two novel proteins related to baculoviral inhibitor of apoptosis proteins. *Cell,* **83,** 1243–1252.

ROY, N. DEVERAUX, Q.L., TAKAHASHI, R., SALVESEN, G.S. & REED, J.C. (1997). The c-IAP-1 and c-IAP-2 proteins are direct inhibitors of specific caspases. *EMBO J.,* **16,** 6914–6925.

SABRI, A., BYRON, K.L., SAMAREL, A.M., BELL, J. & LUCCHESI, P.A. (1998). Hydrogen peroxide activates mitogen-activated protein kinases and Na+-H+ exchange in neonatal rat cardiac myocytes. *Circ. Res.,* **82,** 1053–1062.

SZABÓ, C. (1996). The pathophysiological role of peroxynitrite in shock, inflammation, and ischemia-reperfusion injury. *Shock,* **6,** 79–88.

SZABÓ, C. (1998). Role of poly (ADP-ribose) synthetase in inflammation. *Eur. J. Pharmacol.,* **350,** 1–19.

SZABÓ, C., CUZZOCREA, S., ZINGARELLI, B., O'CONNOR, M. & SALZMAN, L.A. (1997a). Endothelial dysfunction in a rat model of endotoxic shock. Importance of the activation of poly (ADP-ribose) synthetase by peroxynitrite. *J. Clin. Invest.,* **100,** 723–735.

SZABÓ, C. & DAWSON, V.L. (1998). Role of poly (ADP-ribose) synthetase activation in inflammation and reperfusion injury. *Trends Pharmacol. Sci.,* **19,** 287–298.

SZABÓ, C., FERRER-SUETA, G., ZINGARELLI, B., SOUTHAN, G.J., SALZMAN, A.L. & RADI, R. (1997b). Mercaptoethylguanidine and related guanidine nitric oxide synthase inhibitors react with peroxynitrite and protect against peroxynitrite-induced oxidative damage. *J. Biol. Chem.,* **272,** 9030 – 9036.

SZABÓ, C., LIM, L.H., CUZZOCREA, S., GETTING, S.J., ZINGARELLI, B., FLOWER, R.J., SALZMAN, A.L. & PERRETTI, M. (1997c). Inhibition of poly (ADP-ribose) synthetase exerts anti-inflammatory effects and inhibits neutrophil recruitment. *J. Exp. Med.,* **186,** 1041 – 1049.

SZABÓ, C., SALZMAN, A.L. & ISCHIROPOULOS, H. (1995). Endotoxin triggers the expression of an inducible isoform of nitric oxide synthase and the formation of peroxynitrite in the rat aorta in vivo. *FEBS Letters,* **363,** 235 – 238.

SZABÓ, C., VIRÁG, L., CUZZOCREA, S., SCOTT, G.J., HAKE, P., O'CONNOR, M.P., ZINGARELLI, B., SALZMAN, A.L. & KUN, E. (1998). Protection against peroxynitrite-induced fibroblast injury and arthritis development by inhibition of poly (ADP-ribose) synthetase. *Proc. Natl. Acad. Sci. U.S.A.,* **95,** 3867 – 3872.

SZABÓ, C., ZINGARELLI, B., O'CONNOR, M. & SALZMAN, A.L.. (1996a). DNA strand breakage, activation of poly (ADP-ribose) synthetase, and cellular energy depletion are involved in the cytotoxicity of macrophages and smooth muscle cells exposed to peroxynitrite. *Proc. Natl. Acad. Sci. U.S.A.,* **93,** 1753 – 1758.

SZABÓ, C., ZINGARELLI, B. & SALZMAN, A.L. (1996b). Role of poly-ADP ribosyltransferase activation in the vascular contractile and energetic failure elicited by exogenous and endogenous nitric oxide and peroxynitrite. *Circ. Res.,* **78,** 1051 – 1063.

TAKAHASHI, R., DEVERAUX, Q., TAMM, I., WELSH, K., ASSA-MUNT, N., SALVESEN, G.S. & REED, J.S. (1998). A single BIR domain of XIAP sufficient for inhibiting caspases. *J. Biol. Chem.,* **273,** 7787 – 7790.

TREVES, S., TRENTINI, P.L., ASCANELLI, M., BUCCI, G. & DI VIRGILIO, F. (1994). Apoptosis is dependent on intracellular zinc and independent of intracellular calcium in lymphocytes. *Exp. Cell Res.,* **211,** 339 – 343.

TRUCCO, C., OLIVER, F.J., DE MURCIA, G. & MENISSIER-DE MURCIA, J. (1998). DNA repair defect in poly(ADP-ribose) polymerase-deficient cell lines. *Nucleic Acids Res.,* **26,** 2644 – 2649.

VANAGS, D.M., PÖRN-ARES, M., COPPOLA, S., BURGESS, D.H. & ORENIUS, S. (1997). Protease involvement in fodrin cleavage and phosphatidylserine exposure in apoptosis. *J. Biol. Chem.,* **271,** 31075 – 31085.

VERMES, I., HAANEN, C., STEFFENS-NAKKEN, H.& REUTELING-SPERGER, C. (1995). A novel assay for apoptosis. Flow cytometric detection of phosphatidylserine expression on early apoptotic cells using fluorescein labelled Annexin V. *J. Immunol. Methods,* **184,** 39 – 51.

VIRÁG, L., SALZMAN A.L. & SZABÓ, C. (1998a). Poly (ADP-ribose) synthetase activation mediates mitochondrial injury during oxidant-induced cell death. *J. Immunol.,* **161,** 3753 – 3759.

VIRÁG, L., SCOTT, G., CUZZOCREA, S., MARMER, D., SALZMAN, A.L. & SZABÓ, C. (1998b). Peroxynitrite-induced thymocyte apoptosis: the role of caspases and poly-(ADP-ribose) synthetase (PARS) activation. *Immunology,* **94,** 345 – 355.

WHISLER, R.L., GOYETTE, M.A., GRANTS, I.S. & NEWHOUSE, Y.G. (1995). Sublethal levels of oxidant stress stimulate multiple serine/threonine kinases and suppress protein phosphatases in Jurkat T cells. *Arch. Biochem. Biophys.,* **319,** 23 – 25.

ZAMZAMI, N., MARCHETTI, P., CASTEDO, M., ZANIN, C., VAYS-SIERE, J.L., PETIT, P.X. & KROEMER, G. (1995). Reduction in mitochondrial potential constitutes an early irreversible step of programmed lymphocyte death in vivo. *J. Exp. Med.,* **181,** 1661 – 1672.

ZINGARELLI, B., CUZZOCREA, S., ZSENGELLÉR, Z., SALZMAN, A.L. & SZABÓ, C. (1997a). Protection against myocardial ischemia and reperfusion injury by 3-aminobenzamide, an inhibitor of poly (ADP-ribose) synthetase. *Cardiovasc. Res.,* **36,** 205 – 215.

ZINGARELLI, B., DAY, B.J., CRAPO, J.D., SALZMAN, A.L. & SZABÓ, C. (1997b). The potential role of peroxynitrite in the vascular contractile and cellular energetic failure in endotoxic shock. *Br. J. Pharmacol.,* **120,** 259 – 267.

ZINGARELLI B., O'CONNOR, M., WONG, H., SALZMAN, A.L. & SZABÓ, C. (1996). Peroxynitrite-mediated DNA strand breakage activates poly-ADP ribosyl synthetase and causes cellular energy depletion in macrophages stimulated with bacterial lipopolysaccharide. *J. Immunol.,* **156,** 350 – 358.

ZINGARELLI B., SALZMAN, A.L. & SZABÓ, C. (1998). Genetic disruption of poly (ADP ribose) synthetase inhibits the expression of P-selectin and intercellular adhesion molecule-1 in myocardial ischemia-reperfusion injury. *Circ. Res.,* **83,** 85 – 94.

(Received August 17, 1998
Revised October 30, 1998
Accepted November 4 1998)

British Journal of Pharmacology (1999) 126, 778–784
http://www.stockton-press.co.uk/bjp

Roles of oxygen radicals and elastase in citric acid-induced airway constriction of guinea-pigs

*,[1]Y.-L. Lai, [1]W.-Y. Chiou, [2]F.J. Lu, & [3]L. Y. Chiang

[1]Department of Physiology, College of Medicine, National Taiwan University, No.1, Sec.1, Jen-Ai Road, Taipei, Taiwan, R.O.C.; [2]Department of Biochemistry, College of Medicine, National Taiwan University, Taipei, Taiwan, R.O.C.; and [3]Center For Condensed Matter Sciences, National Taiwan University, No. 1, Sec. 4, Roosevelt Road, Taipei, Taiwan, R.O.C.

1 Antioxidants attenuate noncholinergic airway constriction. To further investigate the relationship between tachykinin-mediated airway constriction and oxygen radicals, we explored citric acid-induced bronchial constriction in 48 young Hartley strain guinea-pigs, divided into six groups: control; citric acid; hexa(sulphobutyl)fullerenes + citric acid; hexa(sulphobutyl)fullerenes + phosphoramidon + citric acid; dimethylthiourea (DMTU) + citric acid; and DMTU + phosphoramidon + citric acid. Hexa(sulphobutyl)fullerenes and DMTU are scavengers of oxygen radicals while phosphoramidon is an inhibitor of the major degradation enzyme for tachykinins.

2 Animals were anaesthetized, paralyzed, and artificially ventilated. Each animal was given 50 breaths of 4 ml saline or citric acid aerosol. We measured dynamic respiratory compliance (Crs), forced expiratory volume in 0.1 ($FEV_{0.1}$), and maximal expiratory flow at 30% total lung capacity ($\dot{V}_{max30}$) to evaluate the degree of airway constriction.

3 Citric acid, but not saline, aerosol inhalation caused marked decreases in Crs, $FEV_{0.1}$ and $\dot{V}_{max30}$, indicating marked airway constriction. This constriction was significantly attenuated by either hexa(sulphobutyl)fullerenes or by DMTU. In addition, phosphoramidon significantly reversed the attenuating action of hexa(sulphobutyl)fullerenes, but not that of DMTU.

4 Citric acid aerosol inhalation caused increases in both lucigenin- and t-butyl hydroperoxide-initiated chemiluminescence counts, indicating citric acid-induced increase in oxygen radicals and decrease in antioxidants in bronchoalveolar lavage fluid. These alterations were significantly suppressed by either hexa(sulphobutyl)fullerenes or DMTU.

5 An elastase inhibitor eglin-c also significantly attenuated citric acid-induced airway constriction, indicating the contributing role of elastase in this type of constriction.

6 We conclude that both oxygen radicals and elastase play an important role in tachykinin-mediated, citric acid-induced airway constriction.

Keywords: Airway constriction; bronchial reactivity; oxygen radicals; tachykinins

Abbreviations: BAL, bronchoalveolar lavage; Crs, dynamic respiratory compliance; DMTU, dimethylthiourea; $FEV_{0.1}$, forced expiratory volume in 0.1 s; FRC, functional residual capacity; MEFV, maximal expiratory flow-volume; NK, neurokinin; PBS, physiological buffer solution; TBHP, t-butyl hydroperoxide; TLC, total lung capacity; $\dot{V}_{max30}$, maximal expiratory flow at 30% total lung capacity

Introduction

Satoh *et al.* (1993) found that citric acid-induced airway constriction is mediated *via* tachykinin neurokinin-2 (NK-2) but not NK-1 receptors. We demonstrated previously that oxygen radicals are involved in the activation of afferent C-fibres which release tachykinins. The involvement of oxygen radicals has been found in several types of noncholinergic airway constriction such as that caused by capsaicin (Lai, 1990), hyperventilation (Fang & Lai, 1993) and exsanguination (Zhang & Lai, 1994). However, it is not clear whether oxygen radicals are involved in citric acid-induced airway constriction. This study was thus conducted to test the role of oxygen radicals by direct measurement of their activities and using antioxidants to antagonize the radicals (Halliwell, 1992).

Two types of antioxidants were employed in this study. We demonstrated previously that water-soluble derivatives, such as fullerenol-1 synthesized by Chiang *et al.* (1995), ameliorate airway constriction induced by exsanguination (Lai & Chiang, 1997) and by xanthine-xanthine oxidase (Lai *et al.*, 1997). The former, but not the latter, airway constriction was mediated by release of tachykinins from C-fibres. Fullerenol-1 was later modified to become hexa(sulphobutyl)fullerenes (Chi *et al.*, 1998), which is more potent and has fewer side effects compared to fullerenol-1. Similarly, we found that dimethylthiourea (DMTU) inhibits tachykinin-mediated noncholinergic airway constriction induced by capsaicin (Lai, 1990) and hyperventilation (Fang & Lai, 1993). To further investigate the relationship between tachykinin-mediated airway constriction and oxygen radicals, novel water-soluble hexa(sulphobutyl)fullerenes and DMTU were used in this study.

In a previous study using an elastase inhibitor eglin-c (Lai & Lin, 1998), we found that endogenous elastase plays an important role in hyperpnea-induced airway constriction. It is not clear whether elastase plays a role in citric acid-induced airway constriction. It is possible that endogenous elastase could cause airway constriction directly (Suzuki *et al.*, 1996) or indirectly *via* its enhancement of the release of bronchoconstrictors and/or oxygen radicals. To test this hypothesis, eglin-c was used to suppress endogenous elastase and to see if this suppression attenuates citric acid-induced airway constriction.

*Author for correspondence; E-mail: tiger@ha.mc.ntu.edu.tw

Methods

Animal preparations

Forty-eight young Hartley strain guinea-pigs weighing 217 ± 9 g were divided into six groups of eight animals each: control; citric acid; hexa(sulphobutyl)fullerenes + citric acid; hexa(sulphobutyl)fullerenes + phosphoramidon + citric acid; DMTU + citric acid; DMTU + phosphoramidon + citric acid. Following anaesthesia with sodium pentobarbitone (30–40 mg kg^{-1}), each animal's trachea, carotid artery and jugular vein were cannulated. After being paralyzed with gallamine triethiodide (4 mg kg^{-1}), the animal was artificially ventilated. To ensure that the animal was anaesthetized during paralysis, we administered gallamine according to the following plans. (l) Gallamine was only given when its active period (40 min) was within the effective duration of pentobarbitone (1–2 h). If it was necessary to administer gallamine beyond this effective period of the anaesthetic, supplemental doses of pentobarbitone were given before any more gallamine treatment. (2) If an additional dose of gallamine was needed after a single dose, we first examined the level of anaesthesia and made sure that the expected anaesthesia could be maintained longer than the effective duration of gallamine. The second injection of gallamine was then given to the animal. Each animal in the control group received 50 breaths of 4 ml saline aerosol while those in all citric acid groups were given citric acid aerosol (50 breaths of 4 ml aerosol generated from 0.6M citric acid). Both aerosols were generated from a nebulizer (Ultra-Neb99, DeVilbiss Co., Somerset, PA, U.S.A.). According to our previous method of administering fullerenol-1 (Lai & Chiang, 1997), each animal in all hexa(sulphobutyl)fullerenes groups was injected peritoneally with hexa(sulphobutyl)fullerenes (10 mg kg^{-1}) for 2 days prior to the functional study. In addition, 2 mg kg^{-1} of hexa(sulphobutyl)fullerenes were also injected intravenously 30 min prior to citric acid aerosol inhalation. Phosphoramidon, the inhibitor of neutral endopeptidase (the degradation enzyme for tachykinins), was intravenously injected (1 mg kg^{-1}) 5 min prior to the citric acid aerosol inhalation. DMTU was given to the animals by intraperitoneal injection for 3 days before the study. The three consecutive daily doses of DMTU were 750, 250 and 250 mg kg^{-1} (Lai, 1990).

Evaluation of bronchial function

Each anaesthetized-paralyzed and ventilated animal was placed supine inside a whole-body plethysmograph. The flow rate was monitored with a Validyne DP45 differential pressure transducer as the pressure dropped across three layers of 325-mesh wire screen in the wall of the plethysmograph. Lung volume change was obtained *via* integration of flow. Airway opening pressure was measured with a Statham PM 131 pressure transducer. Maximal expiratory flow-volume (MEFV) manoeuvres were performed using the Buxco Pulmonary Maneuvers system (Sharon, CT, U.S.A.). The system consists of a pressure panel and a fast solenoid manifold, both of which are operated by a BioSystem for Manoeuvres software program in a 586 computer. Tracings of pressure, flow, volume, and the MEFV curve appeared on the computer screen and these tracings were stored and printed. For the MEFV manoeuvre, the lungs were inflated to total lung capacity (TLC, lung volume at airway opening pressure = 30 cmH_2O) four times. At peak volume during the fourth inflation, the solenoid valve for inflation was shut off and immediately another solenoid valve for deflation was automatically turned on. The deflation valve was connected to a 20-L container, which maintained a subatmospheric pressure of −40 cmH_2O. The negative pressure of 40 cmH_2O produced maximal expiratory flow (Lai, 1988). During the baseline period, we first performed MEFV manoeuvres two to three times to obtain the baseline TLC. Subsequently, MEFV manoeuvres were carried out 20 min after inhalation of saline or citric acid aerosol and maximal expiratory flow at 30% vital capacity ($\dot{V}_{max30}$) was obtained. At the same time, the program picked the forced expiratory volume in 0.1 s ($FEV_{0.1}$) from the volume-time tracing. Airway opening pressure (Pao) and tidal volume (V_T) were measured during artificial ventilation, and both parameters were recorded on a polygraph. Dynamic respiratory compliance (Crs) was calculated as the ratio of the V_T-to-Pao difference between the end of expiration and the end of inspiration. Before and after each MEFV manoeuvre, functional residual capacity (FRC) (the lung volume at Pao = 0) was determined using a modified neon dilution method (Lai, 1988). Starting from FRC, the lungs were inflated with a standard neon (0.5%) gas mixture to 50% vital capacity. Gas in the lungs, in the dead space of the instrument, and in the syringe was mixed thoroughly by repeating the injection and withdrawal of the gas mixture 10–20 times. The equilibrated gas mixture was withdrawn and analysed with a Varian gas chromatograph (Model 3300). The total volume (including FRC and instrumental dead space) was calculated. The FRC was obtained by subtracting the instrumental dead space from the total volume.

The general experimental procedure consisted of obtaining the values of Crs, $FEV_{0.1}$ and $\dot{V}_{max30}$ both before and 20 min after inhalation of saline or citric acid aerosol.

Collection of bronchoalveolar lavage (BAL) fluid

An additional 24 young guinea-pigs were divided into four groups of six animals each: saline control; citric acid; hexa(sulphobutyl)fullerenes + citric acid; and DMTU + citric acid. Preparations for these four groups of animals were the same as those described above. BAL fluid was collected about 3 min following saline or citric acid aerosol inhalation. To obtain BAL fluid, 3 ml of saline was instilled *via* the trachea 2 min after the inhalation of saline or citric acid aerosol. Saline in the lungs was withdrawn about 40 s following the instillation. Furthermore, to detect temporal changes in the production of oxygen radicals, an additional 12 animals were divided into two groups: saline control and citric acid. These animals were treated as described above except that BAL fluid was sampled 10 min after inhalation of either saline or citric acid aerosol. The obtained BAL fluid was immediately wrapped with aluminium foil and kept in the ice box until testing for chemiluminescence, which was usually done within 2 h.

Measurements of lucigenin-initiated and lucigenin-amplified t-butyl hydroperoxide (TBHP)-initiated chemiluminescence

Determinations of both lucigenin-initiated and lucigenin-amplified TBHP-initiated BAL fluid chemiluminescence were performed with the method of Sun *et al*. (1998) with some modifications. 0.1 ml physiological buffer solution (PBS, pH 7.4) was added to 0.2 ml BAL fluid in a stainless cell (5 cm in diameter). The chemiluminescence was then measured in an absolutely dark chamber of the Chemiluminescence Analyzing System (Tohoku Electronic Industrial Co., Sendai, Japan). This system contains a photon detector (Model CLD-

110), chemiluminescence counter (Model CLC-10), water circulator (Model CH-20), and 32-bit IBM personal computer system. A cooler circulator was connected to the model CLD-110 photon detector to keep the temperature at 5°C. The Model CLD-110, according to the manufacturer's specifications, is so sensitive it is able to detect as low as 10^{-15} W of radiant energy. Photon emission from the BAL fluid was counted at 10-s intervals at 37°C and atmospheric conditions. At the 100-s time point, 1.0 ml of lucigenin (0.01 mM) in PSB was injected into the cell. The chemiluminescence in the BAL sample was continuously measured for a 600-s time period. Subsequently, at the 700-s time point, 0.1 ml of TBHP (Sigma Co., St. Louis, MO, U.S.A.) in PBS (pH = 7.4) was injected into the cell. The chemiluminescence in the sample was continuously measured for a total of 200-s. The total amount of chemiluminescence was calculated by integrating the area under the curve and subtracting it from the background level, which was equivalent to the dark average. The assay was performed in duplicate for each sample and was expressed as chemiluminescence counts per 10 s.

Elastase inhibitor and citric acid-induced airway constriction

An additional 18 guinea-pigs were evenly divided into two groups: saline control and eglin-c. Each animal was intratracheally instilled with 0.25 ml of either saline or eglin-c (37.5 mg kg^{-1}) 10 min prior to citric acid aerosol inhalation. The dose of eglin-c was according to our previous studies (Lai & Diamond, 1990; Lai & Zhou, 1997). The functional testing of airways was performed before as well as 10 and 20 min after the inhalation of citric acid aerosol, in the same fashion as that described above.

Drugs and chemicals

Hexa(sulphobutyl)fullerenes was synthesized by Chi *et al.* (1998). Eglin-c was kindly provided by Dr Hans Peter Schnebli, Ciba-Geigy Research Department, Basel, Switzerland. Citric acid, dimethylthiourea, gallamine triethiodide, lucigenin, phosphoramidon, sodium pentobarbitone, and t-butyl hydroperoxide were obtained from the Sigma Chemical Company (St. Louis, MO, U.S.A.).

Statistical analysis

All values are reported as means ± s.e.mean. Analysis of variance was used to establish the statistical significance of differences among groups. If significant differences among groups were obtained using the analysis of variance, Duncan's multiple range test was used to differentiate differences between groups. Differences were considered significant if $P < 0.05$.

Results

Body weight and baseline respiratory parameters in the guinea-pigs used for examining effects of antioxidants are listed in Table 1. Body weights, but not respiratory parameters, of animals treated with DMTU were lower than those of the animals in other groups. Differences in body weight between groups were caused by pretreatment with various drugs. To account for individual differences, we compared the results using per cent baseline values for each animal.

Effect of citric acid on bronchial function

Saline aerosol inhalation did not induce any significant change (expressed as per cent baseline values) in Crs (Figure 1). On the other hand, citric acid aerosol inhalation caused a marked decrease in Crs (expressed as per cent baseline value), indicating severe airway constriction in the citric acid group (Figure 1). This constriction was significantly attenuated either by hexa(sulphobutyl)fullerenes or by DMTU; this attenuating effect was significantly larger with DMTU than with hexa(sulphobutyl)fullerenes. In addition, phosphoramidon significantly reversed the attenuating action of hexa(sulphobutyl)fullerenes but not that of DMTU (Figure 1). Using $FEV_{0.1}$ (Figure 2) and $\dot{V}_{max30}$ (Figure 3) as indicators, the effects of hexa(sulphobutyl)fullerenes and DMTU, as well as supplemental influences of phosphoramidon, appeared to be in the same manner as those of Crs values shown above.

Effect of citric acid on BAL samples

In the BAL samples obtained about 3 min after inhalation of saline or citric acid aerosol, the addition of lucigenin caused a small rise while adding TBHP caused an even larger increase in the chemiluminescence signal (Figure 4). Both increases were larger in the BAL fluid obtained from the animals who inhaled citric acid than that from the animals who inhaled saline aerosol (Figure 4). Group data of BAL samples obtained 3 min after aerosol inhalation are shown in Table 2. Inhalation of citric acid aerosol induced significant increases in both lucigenin- and TBHP-initiated chemiluminescence counts.

Table 1 Body weight and baseline respiratory parameters in guinea-pigs

	n	*BW* (g)	*TLC* (ml)	*FRC* (ml)	*Crs* (ml cmH_2O^{-1})	$FEV_{0.1}$ (ml)	$\dot{V}_{max30}$ (ml s^{-1})
Saline control	8	239 ± 10	8.5 ± 0.3	2.7 ± 0.1†	0.24 ± 0.01	3.8 ± 0.3	47.8 ± 6.7
Citric acid	8	221 ± 7‡	7.8 ± 0.3†‡	2.5 ± 0.1†‡	0.23 ± 0.01	3.5 ± 0.2†‡	39.2 ± 4.9†‡
Hexa(sulphobutyl)fullerenes + citric acid	8	236 ± 6†‡	8.3 ± 0.3	2.6 ± 0.1†‡	0.22 ± 0.01	3.5 ± 0.2†‡	46.7 ± 3.2
Hexa(sulphobutyl)fullerenes + phosphoramidon + citric acid	8	221 ± 11‡	8.3 ± 0.4	2.5 ± 0.1†‡	0.21 ± 0.01	3.2 ± 0.2*†‡	40.8 ± 5.4†‡
Dimethylthiourea + citric acid	8	199 ± 13*	9.2 ± 0.3	3.2 ± 0.1	0.24 ± 0.01	4.6 ± 0.2*	56.8 ± 2.1
Dimethylthiourea + phosphoramidon + citric acid	8	189 ± 8*	9.0 ± 0.3	2.9 ± 0.1	0.23 ± 0.01	4.6 ± 0.1*	58.4 ± 0.9

Values are the means ± s.e.mean. *n*, the number of animals; BW, body weight; TLC, total lung capacity; FRC, functional residual capacity; $FEV_{0.1}$, forced expiratory volume in 0.1 s; $\dot{V}_{max30}$, maximal expiratory flow rate at 30% of baseline vital capacity. Statistical differences ($P < 0.05$) between groups: *compared to the saline group; †compared to the dimethylthiourea + citric acid group; and ‡compared to the dimethylthiourea + phosphoramidon + citric acid group.

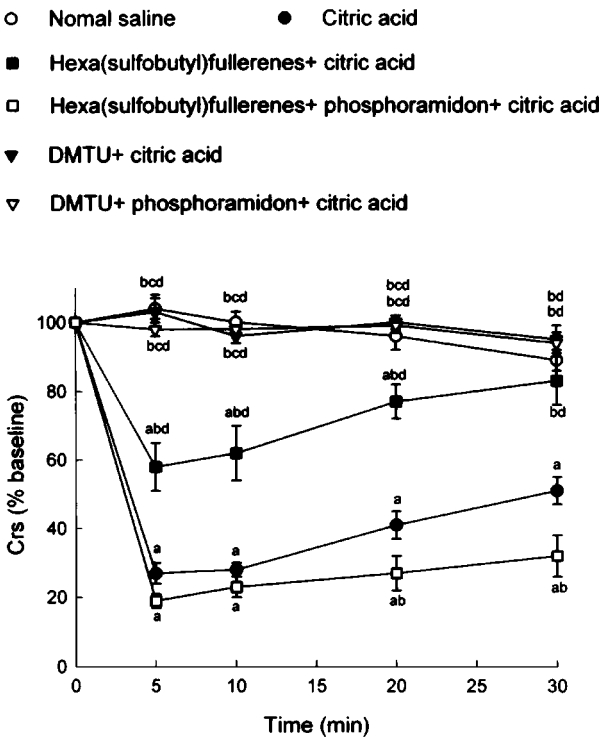

Figure 1 Citric acid-induced alterations in dynamic respiratory compliance (Crs), expressed as per cent baseline values, in six groups of guinea-pigs. DMTU = dimethylthiourea. Statistical differences ($P<0.05$) between groups: [a]compared to the saline control group; [b]compared to the citric acid group; [c]compared to the hexa(sulphobutyl)fullerenes + citric acid group; and [d]compared to the hexa(sulphobutyl)fullerenes + phosphoramidon + citric acid group.

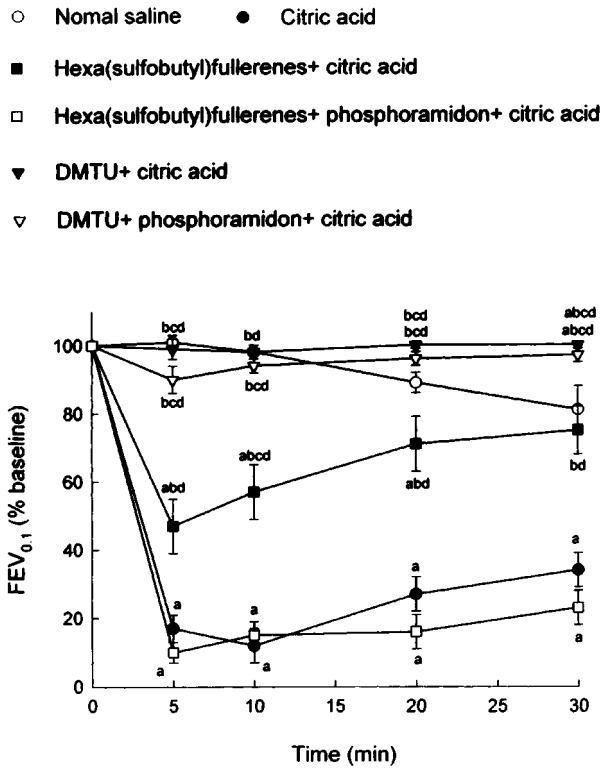

Figure 2 Citric acid-induced alterations in forced expiratory volume in 0.1 s ($FEV_{0.1}$), expressed as per cent baseline values, in six groups of guinea-pigs. DMTU = dimethylthiourea. Statistical differences ($P<0.05$) between groups: [a]compared to the saline control group; [b]compared to the citric acid group; [c]compared to the hexa(sulphobutyl)fullerenes + citric acid group; and [d]compared to the hexa(sulphobutyl)fullerenes + phosphoramidon + citric acid group.

These increases were, however, significantly attenuated by either hexa(sulphobutyl)fullerenes or DMTU.

In the BAL samples obtained 10 min after inhalation of citric acid aerosol, the addition of lucigenin and TBHP caused smaller increases in the chemiluminescence signals compared to those of the 3 min samples. Chemiluminescence counts (per 10 s) initiated by lucigenin were: saline control, 78 ± 12; and citric acid, 156 ± 41. At the same time, TBHP-initiated chemiluminescence counts per 10 s were: saline control, 287 ± 50; and citric acid, 328 ± 107. No significant differences were found in the above two values between the citric acid and saline control groups.

Effect of eglin-c on citric acid-induced airway constriction

Body weight and baseline respiratory parameters in guinea-pigs used for examining the effects of the elastase inhibitor eglin-c are listed in Table 3. No significant differences in either body weight or respiratory parameters between groups were found. Similar to Figure 1, citric acid caused marked decreases in Crs (Figure 5), $FEV_{0.1}$ (Figure 6) and $\dot{V}_{max30}$ (Figure 7), indicating severe airway constriction in saline control animals. This airway constriction was significantly attenuated by pretreatment with eglin-c at 20 and/or 30 min time points (Figure 5–7).

Discussion

We demonstrated that citric acid-induced bronchoconstriction was significantly attenuated by hexa(sulphobutyl)fullerenes and DMTU, the attenuating effect of DMTU being more potent than that of the hexa(sulphobutyl)fullerenes. In addition, the inhibitor for neutral endopeptidase (the major degradation enzyme of tachykinins) significantly reversed the attenuating effect of hexa(sulphobutyl)fullerenes but not that of DMTU. Furthermore, citric acid aerosol inhalation caused increases in lucigenin- and TBHP-induced chemiluminescence. We showed also that eglin-c suppressed citric acid-induced airway constriction. Several features of these results will be discussed below.

Tachykinins in citric acid-induced airway constriction

It is known that acid aspiration induces airway constriction (Goldman *et al*., 1992). Inhalation of citric acid aerosol causes coughing (Girard *et al*., 1995), airway hyperresponsiveness (Girard *et al*., 1996), bronchoconstriction (Satoh *et al*., 1993), and plasma extravasation in the lungs (Satoh *et al*., 1993). These effects of citric acid-induced alterations have been attenuated or prevented by capsaicin pretreatment to deplete tachykinins (Girard *et al*., 1996; Satoh *et al*., 1993), the selective capsaicin antagonist capsazepine (Satoh *et al*., 1993), and the NK-2 receptor antagonist SR 48968 (Girard *et al*., 1996; Satoh *et al*., 1993). Capsazepine interferes with proton-sensitive ion channels (Bevan & Yeats, 1991) *via* occupation of the proposed capsaicin receptor site (Szallasi & Blumberg, 1990). Thus, the above citric acid-induced changes are related closely with the activation of afferent C-fibres in the lungs *via* capsaicin receptors. The sequence of this action may be depicted as follows. Citric acid stimulates afferent C-fibres which, in turn, release tachykinins. Released tachykinins act on

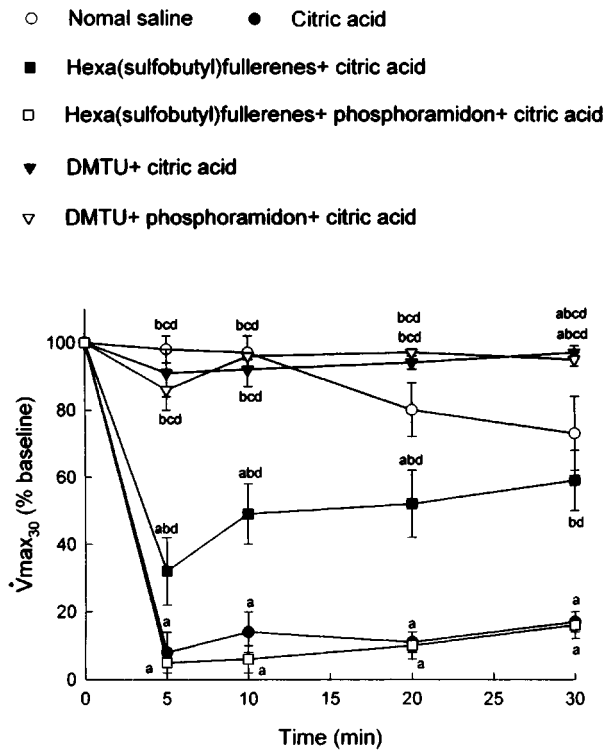

Figure 3 Citric acid-induced alterations in maximal expiratory flow at 30% vital capacity (V_{max30}), expressed as per cent baseline values, in six groups of guinea-pigs. DMTU = dimethylthiourea. Statistical differences ($P<0.05$) between groups: [a]compared to the saline control group; [b]compared to the citric acid group; [c]compared to the hexa(sulphobutyl)fullerenes + citric acid group; and [d]compared to the hexa(sulphobutyl)fullerenes + phosphoramidon + citric acid group.

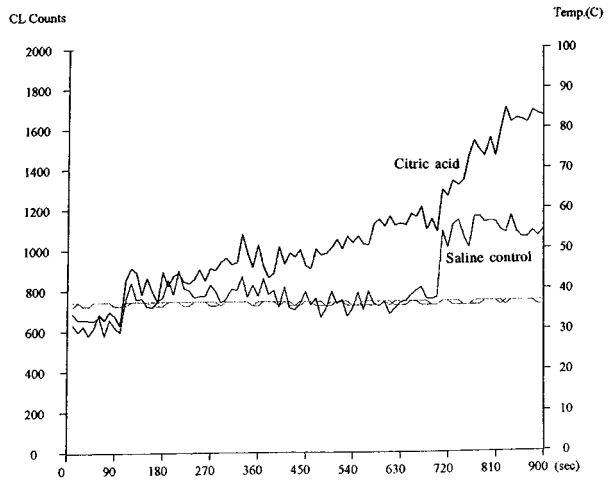

Figure 4 Examples of lucigenin-initiated (100–700-s) and lucigenin-amplified, t-butyl hydroperoxide (TBHP)-initiated (700–900-s) chemiluminescence signals of bronchoalveolar (BAL) lavage fluid obtained from a saline control and citric acid-treated animals. Lucigenin was added at 100-s and TBHP added at 700-s time points. BAL samples were maintained constantly around 37°C as shown in the two temperature lines parallel to the x-axis baseline.

effectors *via* three types of neurokinin (NK) receptors: NK-1, NK-2, and NK-3 (Khawaja & Rogers, 1996). NK-2 receptor can be blocked by SR 48968, which prevents citric acid-induced airway constriction (Girard *et al*., 1996; Satoh *et al*., 1993). However, the NK-1 receptor antagonist CP 96345 did not prevent this type of airway constriction, indicating the specific NK-2 receptor in mediating the constriction. In addition to airway constriction, released tachykinins cause also coughing and characteristics of neurogenic inflammation, including increases in airway responsiveness (Girard *et al*., 1996), plasma extravasation (Lei *et al*., 1996; Martling & Lundberg, 1988), and airway secretion (Ramnarine *et al*., 1994).

Table 2 Lucigenin-initiated and lucigenin-amplified TBHP-initiated chemiluminescence in bronchoalveolar fluid

	n	*Lucigenin-initiated* (counts per 10 s)	*Lucigenin-amplified TBHP-initiated* (counts per 10 s)
Saline control	6	83 ± 22*	400 ± 63*
Citric acid	6	237 ± 23	734 ± 119
Hexa(sulphobutyl)-fullerenes + citric acid	6	140 ± 33*	258 ± 67*
Dimethylthiourea + citric acid	6	55 ± 27*†	170 ± 39*

Values are means ± s.e.mean. n = the number of animals; TBHP = t-butyl hydroperoxide. Statistical differences ($P<0.05$) between groups: *compared to the citric acid group; and †compared to the hexa(sulphobutyl)fullerenes + citric acid group.

Phosphoramidon is an inhibitor for neutral endopeptidase which is the major degradation enzyme for tachykinins (Borson, 1991). Theoretically, administration of phosphoramidon should prevent the degradation of tachykinins and thus augment citric acid-induced airway constriction. In the presence of hexa(sulphobutyl)fullerenes, our results were according to this expectation. Again, this fact supports the idea that citric acid-induced airway constriction is mediated *via* tachykinins. Following DMTU treatment, however, phosphoramidon did not augment citric acid-induced airway constriction. The failure of phosphoramidon to augment the airway constriction might be related to an adrenergic β_2-agonist property of DMTU (Lin & Lai, 1998).

Oxygen radicals in tachykinin-mediated, citric acid-induced airway constriction

Goldman *et al*. (1992) found that acid aspiration caused increases in both reactive oxygen species and lung permeability. In agreement with their results, we observed that citric acid inhalation induced an increase in chemiluminescence counts and airway constriction. Lucigenin-initiated chemiluminescence is an effective monitor of mitochondrial superoxide generation (Rembish & Trush, 1994). On the other hand, TBHP-initiated chemiluminescence is an effective monitor of lipid peroxide generation (Boveris *et al*., 1980; Nakano *et al*., 1975; Sugioka & Nakano, 1976) and has been used to detect decreased levels of endogenous antioxidants in liver and cardiac tissues (Cadenas *et al*., 1981; Prasad *et al*., 1992). From the present study, it is suggested that the decreased antioxidant activity following citric acid inhalation is partially caused by the superoxide pathway, while remote pathophysiological events are mediated by defective scavenging defences. The generation of free radicals in the presence of defective scavenging defences might be the cause of the stimulation of afferent C-fibres, resulting in noncholinergic airway constriction.

Table 3 Body weight and baseline respiratory parameters in guinea-pigs

	n	*BW* (g)	*TLC* (ml)	*FRC* (ml)	*Crs* (ml cmH_2O^{-1})	$FEV_{0.1}$ (ml)	$\dot{V}_{max30}$ (ml s^{-1})
Citric acid	9	260±6	10.0±0.4	2.7±0.1	0.26±0.01	4.2±0.2	64.1±3.7
Eglin-c+citric acid	9	265±9	10.1±0.7	2.7±0.1	0.28±0.01	4.1±0.1	63.1±4.8

Values are means±s.e.mean. *n*, the number of animals; BW, body weight; TLC, total lung capacity; FRC, functional residual capacity; $FEV_{0.1}$, forced expiratory volume in 0.1 s; $\dot{V}_{max30}$, maximal expiratory flow rate at 30% of baseline vital capacity. There are no significant differences in any parameter between groups.

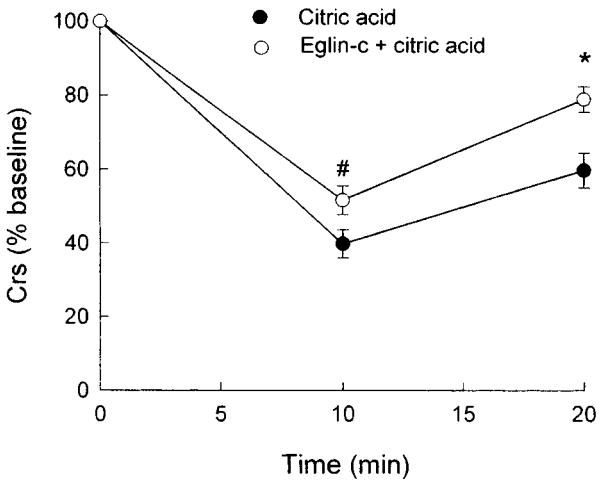

Figure 5 Citric acid-induced alterations in dynamic respiratory compliance (Crs), expressed as per cent baseline values, in two groups of guinea-pigs. Statistical differences between groups: $\#P<0.05$; $*P<0.01$.

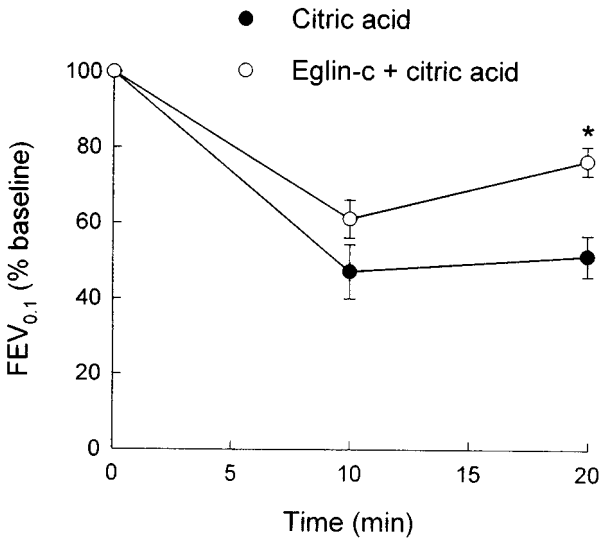

Figure 6 Citric acid-induced alterations in forced expiratory volume in 0.1 s ($FEV_{0.1}$), expressed as per cent baseline values, in two groups of guinea-pigs. Statistical differences between groups: $*P<0.01$.

It is not clear why there was a time-lag between the increase in oxygen radical production and airway constriction. We detected increases in oxygen radicals within 3 min, but not at 10 min, and airway constriction was detected between 3 min to 20 min after the citric acid inhalation. It is apparent that oxygen radicals are needed for the initiation of the release of tachykinins and subsequent airway constriction. This is believed because the action of oxygen radicals was significantly prevented by either DMTU or hexa(sulphobutyl)fullerenes (Figure 1–3). Compared to hexa(sulphobutyl)fullerenes, DMTU caused a larger inhibition of citric acid-induced increases in oxygen radicals and airway constriction. This effect of DMTU might be related to its smaller molecular size and its ability to penetrate the cell (Fox, 1984). In addition, DMTU might have the properties of an adrenergic β_2-agonist (Lin & Lai, 1998), which suppresses both the production of oxygen radicals and airway constriction.

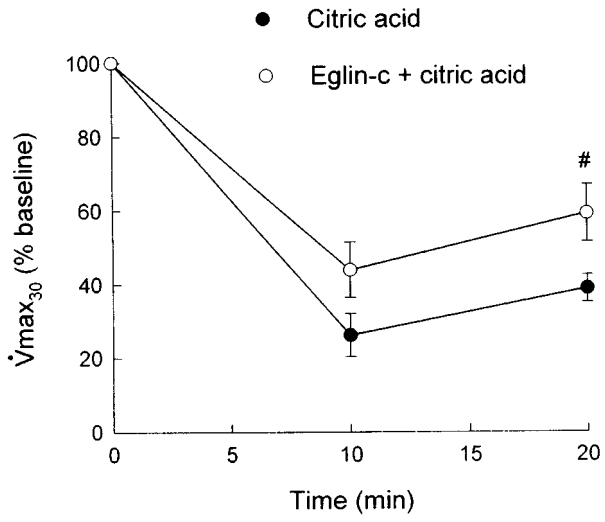

Figure 7 Citric acid-induced alterations in maximal expiratory flow at 30% vital capacity ($\dot{V}_{max30}$), expressed as per cent baseline values, in two groups of guinea-pigs. Statistical differences between groups: $\#P<0.05$.

Elastase in citric acid-induced bronchoconstriction

We found that eglin-c inhibits citric acid-induced airway constriction, indicating the important role of endogenous elastase in this type of bronchoconstriction. It is possible that endogenous elastase may cause airway constriction in two ways. In addition to a direct constricting effect of elastase (Suzuki *et al*., 1996), serine elastase can enhance the release of bronchoconstrictors. For example, serine proteinases augment the release of histamine in sheep (Molinari *et al*., 1996), rats (Emadi-Khiav & Pearce, 1994) and humans (Hultsch *et al*., 1988). It is interesting to mention that this type of released histamine causes bronchoconstriction *in vivo* in sheep (Molinari *et al*., 1996). Beside its direct action, histamine can also trigger the release of tachykinins (Saria *et al*., 1988). The source for endogenous elastase is speculative. It is possible that

citric acid aerosol induces mucosal injury as well as degranulations of mast cells and leukocytes, which release elastase. It is not clear, however, whether there are simultaneous releases of elastase and oxygen radicals. Compared to the effect of antioxidants [hexa(sulphobutyl)fullerenes and DMTU] (Figure 1–3), however, eglin-c produced a smaller magnitude of suppression of citric acid-induced airway constriction (Figure 5–7). This may imply that oxygen radicals may be the main contributing factor to elicit tachykinin release following inhalation of citric acid aerosol.

In summary, we conclude that both oxygen radicals and elastase play an important role in tachykinin-mediated, citric acid-induced airway constriction.

We deeply appreciate Dr Hans Peter Schnebli, Ciba-Geigy Research Department, Basel, Switzerland for providing eglin-c for this study. This investigation was supported by the National Science Council (NSC 87-2314-B002-349 and NSC 87-2314-B002-121M41) and the Department of Health (DOH88-HR-833) and help from NHRI.

References

BEVAN, S. & YEATS, J. (1991). Protons activate a cation conductance in a sub-population of rat dorsal root ganglion neurons. *J. Physiol.,* **433,** 145–161.

BORSON, D.B. (1991). Roles of neutral endopeptidase in airways. *Am. J. Physiol.,* **260,** L212–L225.

BOVERIS, A., CADENAS, E., REITER, R., FILIPKOWSKI, M., NAKASE, Y. & CHANCE, B. (1980). Organ chemiluminescence: noninvasive assay for oxidative radical reaction. *Proc. Natl. Acad. Sci. U.S.A.,* **77,** 347–351.

CADENAS, E., WEFERS, H. & SIES, H. (1981). Low-level chemiluminescence of isolated hepatocytes. *Eur. J. Biochem.,* **119,** 531–536.

CHI, Y., BHONSLE, J.B., CANTEENWALA, T., HUANG, J.-P., SHIEA, J., CHEN, B.-J. & CHIANG, L.Y. (1998). Novel water-soluble hexa(sulphobutyl)fullerenes as potent free radical scavengers. *Chem. Lett.,* 465–466.

CHIANG, L.Y., LU, F.-J. & LIN, J.-T. (1995). Free radical scavenging activity of water-soluble fullerenols. *J. Chem. Soc. Chem. Commun.,* 1283–1284.

EMADI-KHIAV, B. & PEARCE, F.L. (1994). Involvement of a serine protease in mast cell activation. *Agents Actions,* **41,** C37–C38.

FANG, Z.X. & LAI, Y.-L. (1993). Oxygen radicals in bronchoconstriction of guinea-pigs elicited by isocapnic hyperpnea. *J. Appl. Physiol.,* **74,** 627–633.

FOX, R.B. (1984). Prevention of granulocyte-mediated oxidant lung injury in rats by a hydroxyl radical scavenger, dimethylthiourea. *J. Clin. Invest.,* **74,** 1456–1464.

GIRARD, V., NALINE, E., VILAIN, P., EMOND-ALT, X. & ADVENIER, C. (1995). Effect of the two tachykinin antagonists, SR 48968 and SR 140333, on cough induced by citric acid in the unanesthetized guinea-pig. *Eur. Respir. J.,* **8,** 1110–1114.

GIRARD, V., YAVO, J., EMOND-ALT, X. & ADVENIER, C. (1996). The tachykinin NK_2 receptor antagonist SR 48968 inhibits citric acid-induced airway hyperresponsiveness in guinea-pigs. *Am. J. Respir. Crit. Care Med.,* **153,** 1496–1502.

GOLDMAN, G., WELBOURN, R., KOBZIK, L., VALERI, C.R., SHERPO, D. & HECHTMAN, H.B. (1992). Reactive oxygen species and elastase mediate lung permeability after acid aspiration. *J. Appl. Physiol.,* **73,** 571–575.

HALLIWELL, B. (1992). Reactive oxygen species and the central nervous system. *J. Neurochem.,* **59,** 1609–1623.

HULTSCH, T., ENNIS, M. & HEIDTMANN, H.H. (1988). The role of chymase in ionophore-induced histamine release from human pulmonary mast cells. *Adv. Exper. Med. Biol.,* **240,** 133–136.

KHAWAJA, A.M. & ROGERS, D.F. (1996). Tachykinins: receptor to effector. *Int. J. Biochem. Cell Biol.,* **28,** 721–738.

LAI, Y.-L. (1988). Maximal expiratory flow in the guinea-pig. *Lung,* **166,** 303–313.

LAI, Y.-L. (1990). Oxygen radicals in capsaicin-induced bronchoconstriction. *J. Appl. Physiol.,* **68,** 568–573.

LAI, Y.-L. & LIN, Y.J. (1998). Elastase in hyperpnea-induced guinea-pig airway constriction. *Eur. J. Pharmacol.,* (In press).

LAI, Y.-L. & CHIANG, L.Y. (1997). Water-soluble fullerene derivatives attenuate exsanguination-induced bronchoconstriction of guinea-pigs. *J. Autonom. Pharmacol.,* **17,** 229–235.

LAI, Y.-L., CHIOU, W.-Y. & CHIANG, L.Y. (1997). Fullerene derivatives attenuate bronchoconstriction induced by xanthine-xanthine oxidase. *Fullerene Sci. Technol.,* **5,** 1057–1065.

LAI, Y.-L. & DIAMOND, L. (1990). Inhibition of porcine pancreatic elastase-induced pulmonary emphysema by eglin-c. *Exp. Lung Res.,* **16,** 547–557.

LAI, Y.-L. & ZHOU, K.-R. (1997). Eglin-c prevents monocrotaline-induced ventilatory dysfunction. *J. Appl. Physiol.,* **82,** 324–328.

LEI, Y.-H., BARNES, P.J. & ROGERS, D.F. (1996). Involvement of hydroxyl radicals in neurogenic airway plasma exudation and bronchoconstriction in guinea-pigs *in vivo*. *Br. J. Pharmacol.,* **117,** 449–454.

LIN, C.-W. & LAI, Y.-L. (1998). Tachykinins in propranolol-augmented, hyperpnea-induced bronchoconstriction in Taida guinea-pigs: effects of dimethylthiourea. *J. Autonom. Pharmacol.,* **18,** 139–147.

MARTLING, C.-R. & LUNDBERG, J.M. (1988). Capsaicin sensitive afferents contribute to acute airway edema following tracheal instillation of hydrochloric acid or gastric juice in the rat. *Anesthesiology,* **68,** 350–356.

MOLINARI, J.F., SCURI, M., MOORE, W.R., CLARK, J., TANAKA, R. & ABRAHAM, W.M. (1996). Inhaled trypase causes bronchoconstriction in sheep via histamine release, *Am. J. Respir. Crit. Care Med.,* **154,** 649–653.

NAKANO, M., NOGUCHI, T., SUGIOKA, K., FUKUYAMA, H. & SATO, M. (1975). Spectroscopic evidence for the generation of singlet oxygen in the reduced nicotinamide adenine dinucleotide phosphate-dependent microsomal lipid peroxidation system. *J. Biol. Chem.,* **250,** 2404–2406.

PRASAD, K., LEE, P., MANTHA, S., KALRA, J., PRASAD, M. & GUPTA, J.B. (1992). Detection of ischemia-reperfusion cardiac injury by cardiac muscle chemiluminescence. *Molec. Cell Biochem.,* **115,** 49–58.

RAMNARINE, S.I., HIRAYAMA, Y., BARNES, P.J. & ROGERS, D.F. (1994). 'Sensory-efferent' neural control of mucus secretion: characterization using tachykinin receptor antagonists in ferret trachea *in vitro*. *Br. J. Pharmacol.,* **113,** 1183–1190.

REMBISH, S.J. & TRUSH, M.A. (1994). Further evidence that lucigenin-derived chemiluminescence monitors mitochondrial superoxide generation in rat alveolar macrophages. *Free Radical Biol. Med.,* **17,** 117–126.

SARIA, A., MARTLING, C.-R., YAN, X., THEODORSSON-NORHEIM, E., GAMSE, R. & LUNDBERG, J.M. (1988). Release of multiple tachykinins from capsaicin-sensitive sensory nerves in the lung by bradykinin, histamine, dimethylphenyl piperazinium, and vagal nerve stimulation. *Am. Rev. Respir. Dis.,* **137,** 1330–1335.

SATOH, H., LOU, Y.P. & LUNDBERG, J.M. (1993). Inhibitory effects of capsazepine and SR 48968 on citric acid-induced bronchoconstriction in guinea-pigs. *Eur. J. Pharmacol.,* **236,** 367–372.

SUGIOKA, K. & NAKANO, M. (1976). A possible mechanism of the generation of singlet molecular oxygen in NADPH-dependent microsomal lipid peroxidation. *Biochem. Biophys. Acta,* **423,** 203–216.

SUN, J.-S., TSUANG, Y.-H., CHEN, I.-J., HUANG, W.-C., HANG, Y.-H. & LU, F.-J. (1998). An ultra-weak chemiluminescence study on oxidative stress in rabbits following acute thermal injury. *Burns,* **24,** 225–232.

SUZUKI, T., WANG, W., LIN, J.T., SHIRATO K., MITSUHASHI, H. & INOUE, H. (1996). Aerosolized human neutrophil elastase induces airway constriction and hyperresponsiveness with protection by intravenous pretreatment with half-length secretory leukoprotease inhibitor. *Am. J. Respir. Crit. Care Med.,* **153,** 1405–1411.

SZALLASI, A. & BLUMBERG, P.M. (1990). Specific binding of resiniferatoxin, an ultrapotent capsaicin analog, by dorsal root ganglion membranes. *Brain Res.,* **524,** 106–111.

ZHANG, H.-Q. & LAI, Y.-L. (1994). Intratracheal antioxidants attenuate exsanguination-induced bronchoconstriction in guinea-pigs. *J. Appl. Physiol.,* **76,** 553–559.

(Received August 10, 1998
Revised November 9, 1998
Accepted November 10, 1998)

British Journal of Pharmacology (1999) 126, 785–793
http://www.stockton-press.co.uk/bjp

Effects of vasopressin on the sympathetic contraction of rabbit ear artery during cooling

[1]A.L. García-Villalón, [2]J. Padilla, [1]L. Monge, [1]N. Fernández, [1]M.A. Sánchez, [1]B. Gómez & *,[1]G. Diéguez

[1]Departamento de Fisiología, Facultad de Medicina, Universidad Autónoma, Arzobispo Morcillo 2, 28029 Madrid, Spain; and [2]Departamento de Biología, Universidad del Atlántico, Barranquilla, Colombia

1 In order to analyse the effects of arginine-vasopressin on the vascular contraction to sympathetic nerve stimulation during cooling, the isometric response of isolated, 2-mm segments of the rabbit central ear (cutaneous) artery to electrical field stimulation (1–8 Hz) was recorded at 37 and 30°C.

2 Electrical stimulation (37°C) produced frequency-dependent arterial contraction, which was reduced at 30°C and potentiated by vasopressin (10 pM, 100 pM and 1 nM). This potentiation was greater at 30 than at 37°C and was abolished at both temperatures by the antagonist of vasopressin V_1 receptors d$(CH_2)_5$ Tyr(Me)AVP (100 nM). Desmopressin (1 μM) did not affect the response to electrical stimulation.

3 At 37°C, the vasopressin-induced potentiation was abolished by the purinoceptor antagonist PPADS (30 μM), increased by phentolamine (1 μM) or prazosin (1 μM) and not modified by yohimbine (1 μM), whilst at 30°C, the potentiation was reduced by phentolamine, yohimbine or PPADS, and was not modified by prazosin.

4 The Ca^{2+}-channel blockers, verapamil (10 μM) and $NiCl_2$ (1 mM), abolished the potentiating effects of vasopressin at 37°C whilst verapamil reduced and $NiCl_2$ abolished this potentiation at 30°C. The inhibitor of nitric oxide synthesis, L-NOARG (100 μM), or endothelium removal did not modify the potentiation by vasopressin at 37 and 30°C.

5 Vasopressin also increased the arterial contraction to the α_2-adrenoceptor agonist BHT-920 (10 μM) and to ATP (2 mM) at 30 and 37°C, but it did not modify the contraction to noradrenaline (1 μM) at either temperature.

6 These results suggest that in cutaneous (ear) arteries, vasopressin potentiaties sympathetic vasoconstriction to a greater extent at 30 than at 37°C by activating vasopressin V_1 receptors and Ca^{2+} channels at both temperatures. At 37°C, the potentiation appears related to activation of the purinoceptor component and, at 30°C, to activation of both purinoceptor and α_2-adrenoceptor components of the sympathetic response.

Keywords: Cutaneous arteries; temperature; vasopressin V_1 receptors; alpha-adrenoceptor vasoconstriction; purinoceptor vasoconstriction; nitric oxide; endothelium; Ca^{2+}-channels; cooling

Abbreviations: BHT-920, 5-allyl-2-amino-5,6,7,8-tetrahydro-4H-thiazolo-[4,5]-dazepin hydrochloride; d$(CH_2)_5$ Tyr(Me)AVP, b-Mercapto-b,b-cyclopenta-methylenepropionyl[1],O-Me-Tyr[2],Arg[8])-vasopressin; L-NOARG, L-N^G-nitro-arginine; PPADS, pyridoxalphosphate-6-azophenyl-2-4′-disulphonic acid

Introduction

Vasopressin is known to exert powerful vasoconstrictor activity in a variety of vascular beds (Altura & Altura, 1977). However, a key issue is whether the vasoconstrictor action of vasopressin can be achieved with vasopressin concentrations that are physiologically or pathophysiologically achievable, as many studies of the vascular actions of vasopressin have employed large, unphysiological doses of this hormone (Share, 1988). It has been shown that vasopressin, in addition to its direct vasoconstrictor effect, may enhance the vascular response to exogenous catecholamines at low, subthreshold, doses of this peptide (Bartlestone *et al*., 1967), although others have not confirmed this phenomenon (Altura & Altura, 1977). Although this subject may be of interest for understanding the role of vasopressin in controlling vascular function, it has received little attention from investigators.

In a previous study (Padilla *et al*., 1997), we found that vasopressin potentiated the vasoconstrictor response of the rabbit central ear artery, a cutaneous blood vessel, to sympathetic stimulation at 30 but not at 37°C. We therefore suggested that vasopressin may play a role in the regulation of the cutaneous circulation during changes in temperature, by enhancing the sympathetic nerve-induced contraction that occurs during cooling in cutaneous blood vessels. The objective of the present study was to analyse further this potentiating action of vasopressin. Vasopressin receptors have been classified into V_1 and V_2 subtypes, and in a previous study we have found that the constriction in several types of arteries from the rabbit is mediated by the V_1 subtype and may be modulated by endothelial nitric oxide (García-Villalón, 1996). Also, the vasoconstriction to vasopressin may be produced by mobilization of intracellular Ca^{2+} (McDonald *et al*., 1994) and/or by facilitating the entry of extracellular Ca^{2+} through membrane channels (Altura & Altura, 1977). Therefore, in the present study we have analysed the subtype of vasopressin receptor mediating the potentiating effects of vasopressin on sympathetic contraction, and have determined whether this potentiating effect is

* Author for correspondence; E-mail: godofredo.dieguez@uam.es

dependent on Ca^{2+} channels or is modulated by the endothelium and nitric oxide.

It has been previously reported that sympathetic vasoconstriction in rabbit ear arteries may be mediated by release of noradrenaline and ATP from perivascular nerve terminals (Kennedy *et al*., 1986). These transmitters then produce constriction by acting on postjunctional α-adrenoceptors and purinoceptors, respectively. In the present study we have also analysed whether the potentiation by vasopressin of the sympathetic contraction is mediated by α-adrenoceptors and purinoceptors.

The present studies have been performed at 37 and 30°C in the rabbit central ear artery, a superficial, cutaneous blood vessel which is involved in thermoregulation (Harker & Vanhoutte, 1988; Patton & Wallace, 1978; Roberts & Zygmunt, 1984).

Methods

Thirty-eight New Zealand White rabbits, weighing 2–2.5 kg, were killed by intravenous injection of sodium pentobarbital (100 mg kg^{-1}). Central ear arteries were dissected free and cut into cylindrical segments 2 mm in length. Each segment was prepared for isometric tension recording in a 6-ml organ bath containing modified Krebs-Henseleit solution with the following composition (millimolar): NaCl, 115; KCl, 4.6; KH_2PO_4, 1.2; $MgSO_4$, 1.2; $CaCl_2$, 2.5; $NaHCO_3$, 25; glucose, 11.1. The solution was equilibrated with 95% oxygen and 5% carbon dioxide to give a pH of 7.3–7.4, which was measured with a pH-meter micropH 2001 (Crison Instruments). Briefly, the method consists of passing two fine, stainless steel pins, 150 μm in diameter, through the lumen of the vascular segment. One pin is fixed to the organ bath wall, while the other is connected to a strain gauge for isometric tension recording, thus permitting the application of passive tension in a plane perpendicular to the long axis of the vascular cylinder. The recording system included a Universal Transducing Cell UC3 (Statham Instruments, Inc.), a Statham Microscale Accessory UL5 (Statham Instruments, Inc.) and a Beckman Type RS Recorder (model R-411, Beckman Instruments, Inc.). A previously determined resting passive tension of 0.5 g was applied to the vascular segments, and then they were allowed to equilibrate for 60–90 min before any drug was added. The temperature of the bath was adjusted from the beginning of the experiment at 37 and 30°C, and the arteries remained at the chosen temperature throughout the duration of the experiment.

Electrical field stimulation (1, 2, 4 and 8 Hz, 0.2 ms pulse duration, at a supramaximal voltage of 70 V, during 5 s) was applied to the arteries with two platinum electrodes placed on either side of the artery and connected to a CS-14 stimulator (Cibertec). An interval of at least 5 min was imposed between stimulation periods to allow recovery of the response, and the stimulation trains were repeated until the responses were reproducible over at least 40 min under control conditions. Thereafter, the effect of vasopressin (10 pM, 100 pM and 1 nM) on the arterial response to electrical stimulation was studied by cumulative addition of this peptide to the organ bath. The segments were incubated with each vasopressin concentration for 5 min before electrical stimulation. One stimulation series (1–8 Hz) was applied to the arteries after each dose of the peptide. Each arterial segment was treated with every dose of vasopressin. The effect of vasopressin on the response to electrical stimulation was studied in arterial segments at 37 or 30°C. Each arterial segment was tested at one temperature only.

To investigate the nature of the vasopressin receptor subtypes involved, the effect of vasopressin on the arterial response to electrical stimulation was recorded in the presence of the V_1 vasopressin antagonist, $d(CH_2)_5$ Tyr(Me)AVP (100 nM). In addition, the effect of the V_2 agonist, desmopressin (1 μM) on the response to electrical stimulation was studied.

The relative contribution of the sympathetic neurotransmitters noradrenaline and ATP in the effect of vasopressin on the arterial response to electrical stimulation was studied by performing a series of experiments in the presence of the α_1- and α_2-adrenoceptor antagonist, phentolamine (1 μM), of the α_1-adrenoceptor antagonist, prazosin (1 μM), of the α_2-adrenoceptor antagonist, yohimbine (1 μM), of the purinoceptor antagonist, pyridoxalphosphate-6-azophenyl-2,4′-disulphonic acid (PPADS, 30 μM), and of phentolamine (1 μM) plus PPADS (30 μM).

The effect of vasopressin on the response to electrical stimulation was also recorded in the presence of $NiCl_2$ (1 mM) and verapamil (10 μM), which are non-specific (Narahashi *et al*., 1987) and L-type-specific (McDonald *et al*., 1994) Ca^{2+}-channel blockers, respectively.

To analyse the role of nitric oxide and the vascular endothelium, the effects of vasopressin on the response of the artery to electrical stimulation at 37 and at 30°C were studied in arteries without endothelium or in arteries with endothelium pretreated with the inhibitor of nitric oxide synthesis L-N^G-nitro-arginine (L-NOARG, 100 μM). Endothelium removal was accomplished by gentle rubbing of the vascular lumen with a steel rod, and tested, after finishing the experiment with vasopressin and electrical stimulation, by the abolition of the relaxing response to acetylcholine (10 μM) after precontraction with endothelin-1 (100 nM). This peptide was used to precontract the arteries as in our experimental conditions it produces more stable contractions than other vasoactive drugs such as noradrenaline or serotonin.

Reproducible responses to electrical stimulation (1–8 Hz) were obtained over a period of 40 min. Thereafter, an antagonist was added to the organ bath, and two series of electrical stimulation (1–8 Hz) were applied in the presence of the antagonist. After these series of electrical stimulations, vasopressin (10 pM, 100 pM and 1 nM) was added to the organ bath cumulatively and the response to electrical stimulation was recorded in the arteries in the presence of each concentration of vasopressin plus the antagonist previously applied. Each of the antagonists used was added to the bath 40 min before applying vasopressin. As a control, one vascular segment (each temperature) was treated with vasopressin but not antagonist.

To examine the site of the effect of vasopressin (i.e., pre- or post-junctional) on the arterial response to electrical stimulation, the response of ear arteries to exogenous noradrenaline, ATP or to the α_2-adrenoceptor agonist BHT-920 were studied at 37 or 30°C, in the absence (control) and in the presence of vasopressin (10 pM, 100 pM and 1 nM). The response to BHT-920 was always studied in the presence of prazosin (1 μM) to block a possible α_1 agonist effect of this agonist. A single submaximal concentration (García-Villalón *et al*., 1997b) of noradrenaline (1 μM), BHT-920 (10 μM) or ATP (2 mM) was used, and it was applied to the arteries every 15 min, each time followed by washing, until a consistent response was obtained over at least 40 min. After

this period, vasopressin, in increasing concentrations (10 pM, 100 pM and 1 nM), was added to the bath, and 15 min thereafter noradrenaline, BHT-920 or ATP were again applied to the arteries, followed by washout and addition of the next vasopressin concentration.

Data are expressed as means ± s.e.mean, and were evaluated by analysis of variance (ANOVA) applied to each group of data. To compare the response in the presence and the absence of vasopressin, paired Student's *t*-test after analysis of variance was applied to the absolute contraction values at each temperature. Then, to compare the effects of vasopressin found at 37 and 30°C, the increments or decrements in the contraction of arteries to sympathetic stimulation were calculated (i.e., the difference between the control response and the response in the presence of vasopressin) and three-way analysis of variance was applied to these data: in this case one factor was stimulation frequency, another factor was vasopressin concentration and another was temperature. To analyse the effects of the antagonists on the potentiation by vasopressin, the increments or decrements in the contraction produced by electrical stimulation were also calculated and analysed by three-way analysis of variance, in which one factor

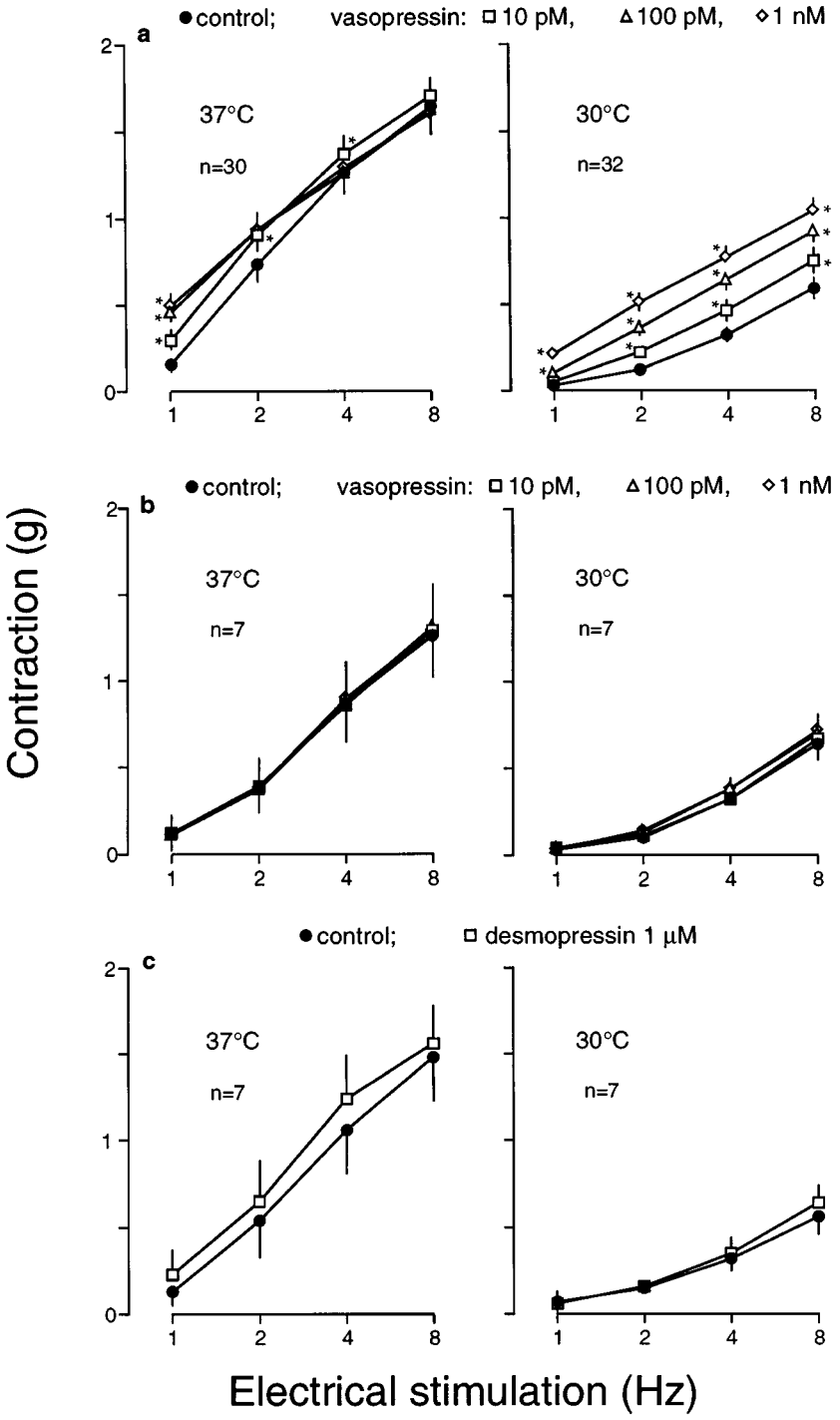

Figure 1 Contraction of rabbit ear arteries at 37 and 30°C to electrical field stimulation (1–8 Hz, 0.2 ms pulse duration, 70 V, for 5 s) in arteries: (a) in the absence (control) and in the presence of vasopressin (10 pM–1 nM); (b) pretreated with the antagonist of vasopressin V_1 receptors $d(CH_2)_5$ Tyr(Me)AVP (100 nM) in the absence (control) and in the presence of vasopressin (10 pM–1 nM); and (c) in the absence (control) and in the presence of desmopressin (1 μM). Points are means ± s.e.mean. * Significantly different ($P<0.01$) from the control. n = number of animals.

was stimulation frequency, another factor was vasopressin concentration and another presence or absence of the antagonist. A probability value of less than 0.05 was considered significant.

Drugs used were: [Arg^8]-vasopressin acetate; [deamino-Cys^1, D-Arg^8]-vasopressin (desmopressin) acetate; the V_1 antagonist (b-Mercapto-b,b-cyclopenta-methylenepropionyl^1, O-Me-Tyr^2,Arg^8)-vasopressin [d(CH$_2$)$_5$Tyr(Me)AVP]; adenosine 5′-triphosphate, disodium salt (ATP); (−)-arterenol, bitartrate salt (noradrenaline); L-N^G-nitro-arginine (L-NOARG); nickel chloride hexahydrate ($NiCl_2$); phentolamine hydrochloride; prazosin hydrochloride; verapamil hydrochloride; and yohimbine hydrochloride; all from Sigma; pyridoxalphosphate-6-azophenyl-2′,4′-disulphonic acid (PPADS tetrasodium salt) from Tocris Cookson Ltd.; and 5-allyl-2-amino-5,6,7,8-tetrahydro-4H-thiazolo-[4,5]-dazepin hydrochloride (BHT-920) was a gift from Europharma S.A.

Results

Response to electrical field stimulation

Electrical stimulation (1–8 Hz) produced frequency-dependent contraction of the vascular segments at 37 and 30°C, but at 30°C the response was significantly lower ($P<0.001$) than at 37°C, at every frequency of stimulation (Figure 1). For example, the arterial contraction (8 Hz) at 30°C was 0.59 ± 0.06 g ($n=32$) and at 37°C was 1.6 ± 0.12 g ($n=30$: $P<0.01$).

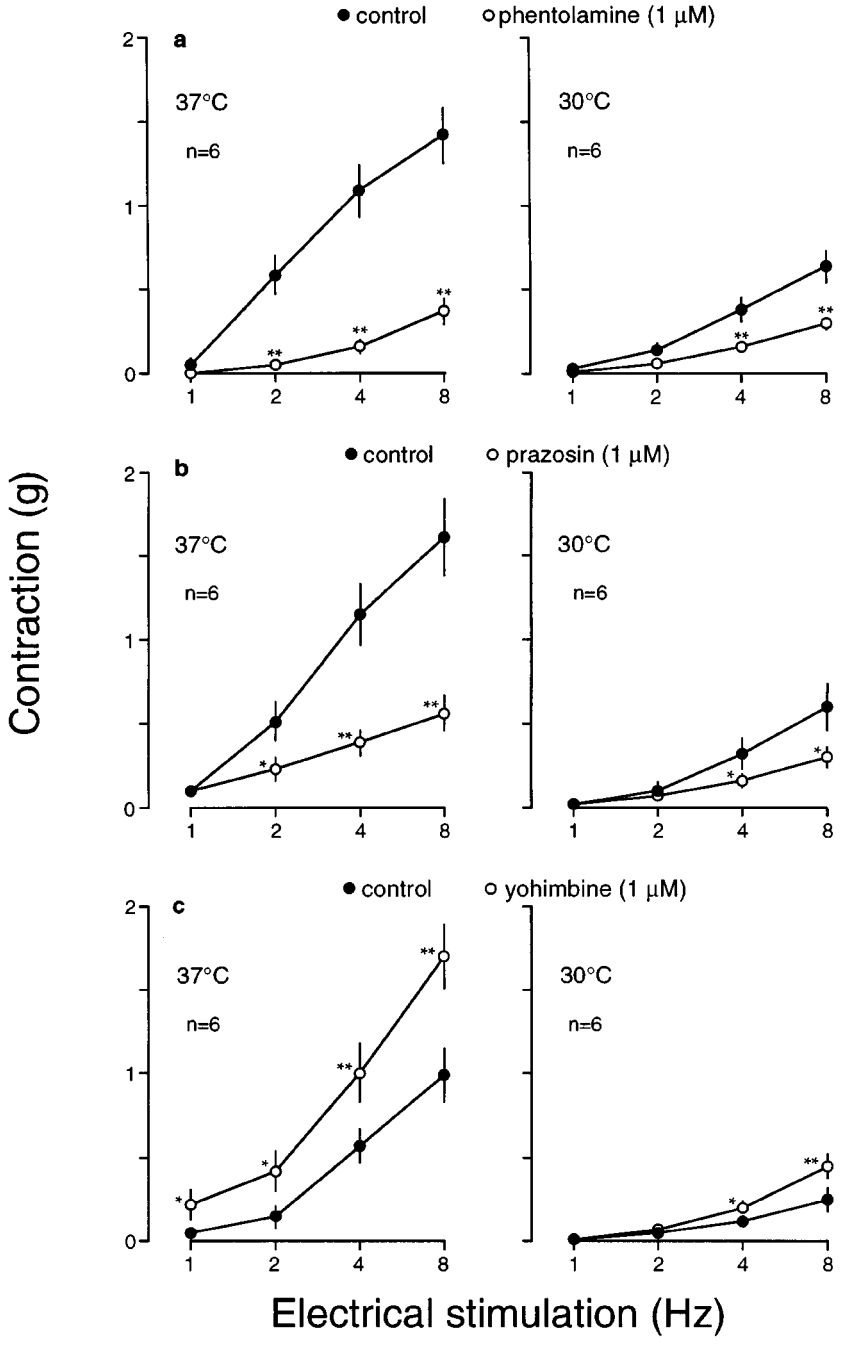

Figure 2 Contraction of rabbit ear arteries at 37 and 30°C to electrical field stimulation (1–8 Hz, 0.2 ms pulse duration, 70 V, for 5 s) in the absence (control) and in the presence of: (a) phentolamine (1 μM); (b) prazosin (1 μM); and (c) yohimbine (1 μM). Points are means ± s.e.mean. *, **, Significantly different from the control (*$P<0.05$, **$P<0.01$). n = number of animals.

Effects of vasopressin on the response to electrical field stimulation

Control Vasopressin, at the concentrations used, did not produce contraction, or in some cases produced a contraction that markedly diminished after applying electrical stimulation. If the contraction induced by vasopressin did not return to less than 25% of the maximal response to electrical stimulation, these data were discarded following the protocol used in a previous study (Padilla *et al*., 1997).

In the presence of vasopressin (10 pM, 100 pM and 1 nM) the contraction to electrical stimulation was greater than that in the absence of the peptide (Figure 1a). At 37°C, the potentiating effect of vasopressin was significant ($P<0.01$) only at 1 Hz for every vasopressin concentration, at 2 Hz for vasopressin at 10 and 100 pM, and at 4 Hz only for vasopressin at 10 pM. At 30°C, vasopressin increased the contraction to electrical stimulation in a concentration-dependent manner, and this increase was significant ($P<0.01$) at every stimulation frequency and vasopressin concentration. The increments induced by vasopressin at 30°C were significantly higher ($P<0.01$) than at 37°C for 4 and 8 Hz frequencies and 100 pM and 1 nM vasopressin concentrations; for 1 Hz it was higher ($P<0.05$) at 37°C for all vasopressin concentrations (Table 1).

Table 1 Vasopressin-induced increments in g, of the contraction of rabbit central ear arteries to electrical field stimulation (1–8 Hz, 0.2 ms pulse duration, 70 V for 5 s) at 37 and 30°C

	37°C (n=30)				*30°C (n=32)*			
Vasopressin	*1Hz*	*2Hz*	*4Hz*	*8Hz*	*1Hz*	*2Hz*	*4Hz*	*8Hz*
10 pM	0.14±0.03	0.16±0.03	0.11±0.04	0.05±0.04	0.02±0.01**	0.1±0.02	0.15±0.02	0.16±0.02*
100 pM	0.31±0.04	0.22±0.05	0.04±0.05	0.01±0.06	0.07±0.01**	0.24±0.02	0.32±0.03**	0.34±0.03**
1 nM	0.33±0.08	0.14±0.12	−0.01±0.13	−0.06±0.1	0.18±0.03*	0.39±0.04*	0.45±0.04**	0.45±0.03**

Values are means±s.e.mean. *,**, significantly different from 37°C (*$P<0.05$; **$P<0.01$). n=number of animals.

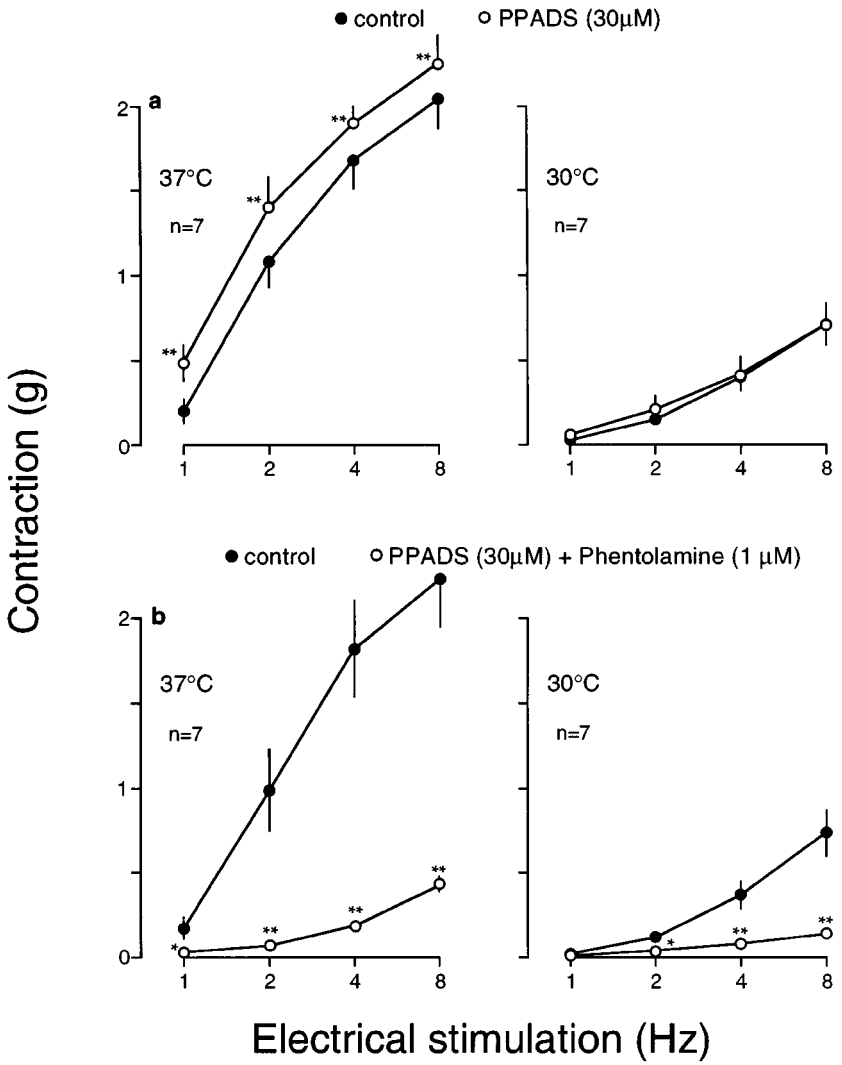

Figure 3 Contraction of rabbit ear arteries at 37 and 30°C to electrical field stimulation (1–8 Hz, 0.2 ms pulse duration, 70 V, for 5 s) in the absence (control) and in the presence of: (a) PPADS (30 μM); and (b) PPADS (30 μM) plus phentolamine (1 μM). Points are means±s.e.mean. *, **, Significantly different from the control (*$P<0.05$, **$P<0.01$). n=number of animals.

Vasopressin receptor subtypes involved The antagonist of V_1 vasopressin receptors d(CH_2)$_5$Tyr(Me)AVP (100 nM) by itself did not modify the contraction to electrical stimulation (data not shown). In the presence of this antagonist, the potentiation of the response to electrical stimulation produced by vasopressin in control conditions was not present either at 37 or 30°C (Figure 1b) ($n=7$).

The agonist of vasopressin V_2 receptors desmopressin did not produce any contraction of rabbit ear artery and did not modify the contraction to electrical stimulation at 37 and 30°C (Figure 1c) ($n=7$).

Adrenoceptor and purinoceptor blockade The contraction of the ear artery to electrical stimulation was significantly reduced by application of phentolamine (1 μM, Figure 2a, $P<0.01$, $n=6$) or prazosin (1 μM, Figure 2b, $P<0.05$, $n=6$), and was significantly increased ($P<0.01$) by yohimbine (1 μM, Figure 2c, $n=6$), at both 37 and 30°C. However, application of PPADS (30 μM, $n=7$) slightly increased the response at 37°C ($P<0.01$) and did not affect the response at 30°C (Figure 3a). Application of PPADS plus phentolamine markedly reduced ($P<0.01$, $n=7$) the contraction to electrical stimulation at both temperatures (Figure 3b).

At 37°C, the potentiation of the arterial contraction to electrical stimulation by vasopressin was increased ($P<0.001$) by phentolamine (Figure 4a, $n=6$) or prazosin (Figure 4b, $n=6$) but was not modified by yohimbine (Figure 4c, $n=6$). At this temperature PPADS ($P<0.001$, Figure 4d, $n=7$) or PPADS plus phentolamine ($P<0.001$, Figure 4e, $n=7$) changed the effect of vasopressin on the contraction to

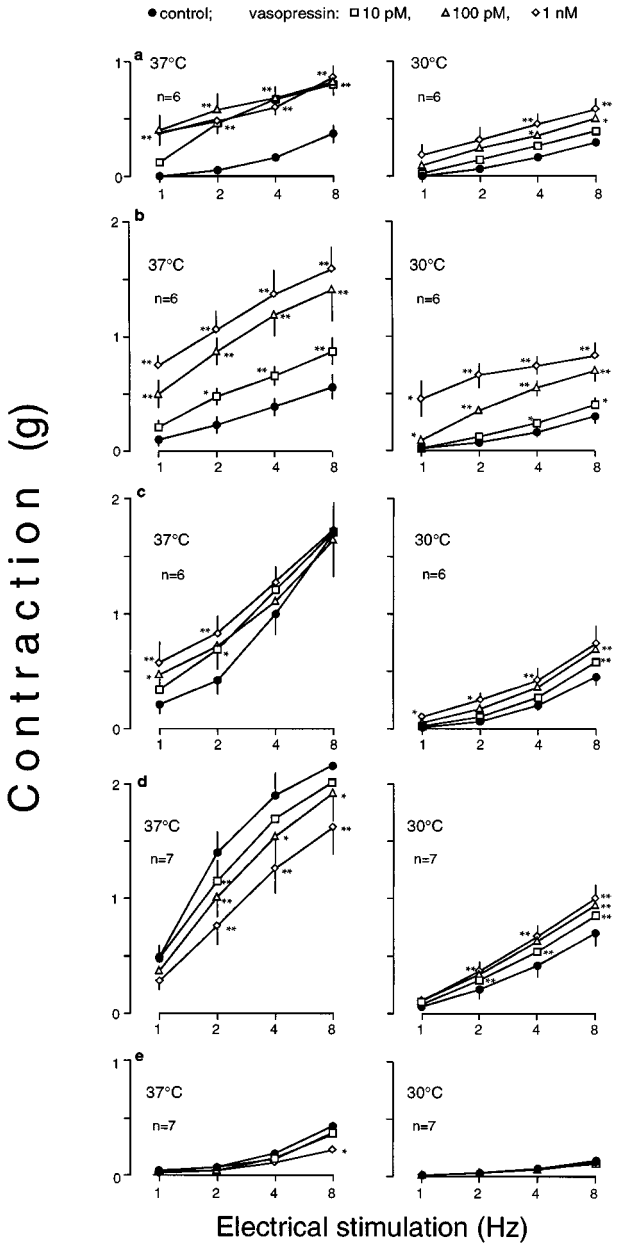

Figure 4 Contraction of rabbit ear arteries at 37 and 30°C to electrical field stimulation (1–8 Hz, 0.2 ms pulse duration, 70 V, for 5 s) in the absence (control) and in the presence of vasopressin (10 pM–1 nM) in arteries pretreated with: (a) phentolamine (1 μM); (b) prazosin (1 μM); (c) yohimbine (1 μM); (d) PPADS (30 μM); and (e) PPADS (30 μM) plus phentolamine (1 μM). Points are means ±s.e.mean. *, **, Significantly different from the control (*$P<0.05$, **$P<0.01$). n=number of animals.

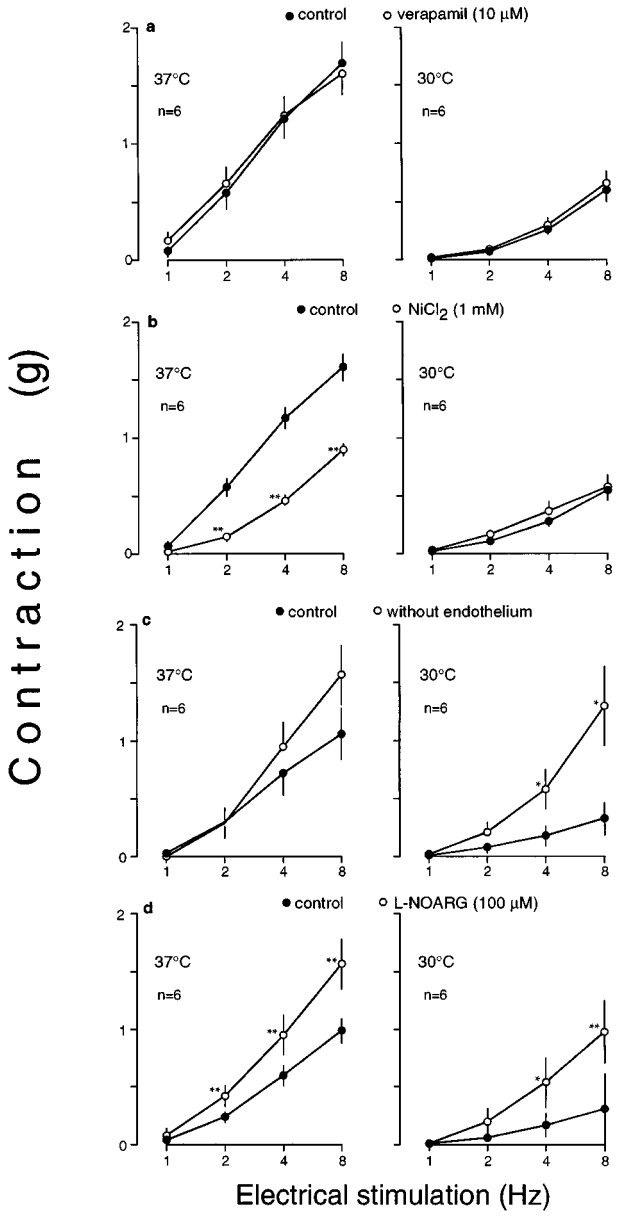

Figure 5 Contraction of rabbit ear arteries at 37 and 30°C to electrical field stimulation (1–8 Hz, 0.2 ms pulse duration, 70 V, for 5 s) in arteries under control conditions and in arteries: (a) pretreated with verapamil (10 μM); (b) pretreated with $NiCl_2$ (1 mM); (c) without endothelium; and (d) pretreated with L-NOARG (100 μM). Points are means±s.e.mean. *, **, Significantly different from the control (*$P<0.05$, **$P<0.01$). n=number of animals.

electrical stimulation, as during these two treatments vasopressin reduced the response to electrical stimulation. At 30°C, the potentiation produced by vasopressin was reduced by phentolamine ($P<0.05$, Figure 4a, $n=6$), yohimbine ($P<0.05$, Figure 4c, $n=6$) or PPADS ($P<0.001$, Figure 4d, $n=7$), was abolished by phentolamine plus PPADS ($P<0.001$, Figure 4e, $n=7$) and was not modified by prazosin (Figure 4c, $n=6$).

Role Ca^{2+} channels The specific blocker of L-type Ca^{2+} channels verapamil (1 μM) did not modify the response of vascular segments to electrical stimulation at 37 or 30°C (Figure 5a, $n=6$), whereas the non-specific Ca^{2+} channel blocker, $NiCl_2$ (1 mM) reduced the arterial response at 37°C ($P<0.01$, $n=6$) but not at 30°C (Figure 5b, $n=6$). At 30°C, the potentiating effect of vasopressin on the contraction of ear arteries to electrical stimulation was reduced by verapamil ($P<0.001$, $n=6$) and abolished by $NiCl_2$ ($P<0.001$, $n=6$). At 37°C, in the arteries pretreated with verapamil ($n=6$) or $NiCl_2$ ($n=6$) vasopressin did not potentiate but reduced ($P<0.001$) the contraction to electrical stimulation (Figure 6a and b).

Nitric oxide synthesis inhibition and endothelium removal The contraction of rabbit ear artery to electrical stimulation was increased by endothelium removal at 30°C ($P<0.01$, $n=6$) but not at 37°C (Figure 5c, $n=6$), and was increased by pretreatment of the arteries with L-NOARG (100 μM) at both temperatures ($P<0.01$, Figure 5d, $n=6$). However, the potentiation by vasopressin was not significantly modified by endothelium removal ($n=6$) or L-NOARG ($n=6$) (Figure 6c and d) compared to intact, non treated arteries, at both temperatures.

Effect of vasopressin on the contraction to noradrenaline, BHT-920 and ATP

A submaximal concentration of noradrenaline (1 μM) produced contraction of ear arteries, which was not significantly different ($P>0.05$) at 37°C (2.78 ± 0.3 g, $n=6$) and 30°C (2.23 ± 0.19 g, $n=6$), and this contraction was not modified in the presence of vasopressin, either at 37 or 30°C (Figure 7a, $n=6$).

The selective α_2-adrenoceptor agonist, BHT-920 (10 μM) after treatment with prazosin (1 μM), produced a small contraction at 37°C (0.09 ± 0.03 g, $n=6$) and no observable response at 30°C in control arteries (Figure 7b, $n=6$). However, after pretreatment with both prazosin (1 μM) and vasopressin, the response to BHT-920 was markedly increased ($P<0.01$, $n=6$) at 37°C, and this adrenoceptor agonist produced a clear contraction at 30°C ($n=6$).

A submaximal concentration of ATP (2 mM) contracted arterial segments at 37°C (0.69 ± 0.07 g, $n=6$) and 30°C (0.47 ± 0.07 g, $n=6$). There was not statistically significant

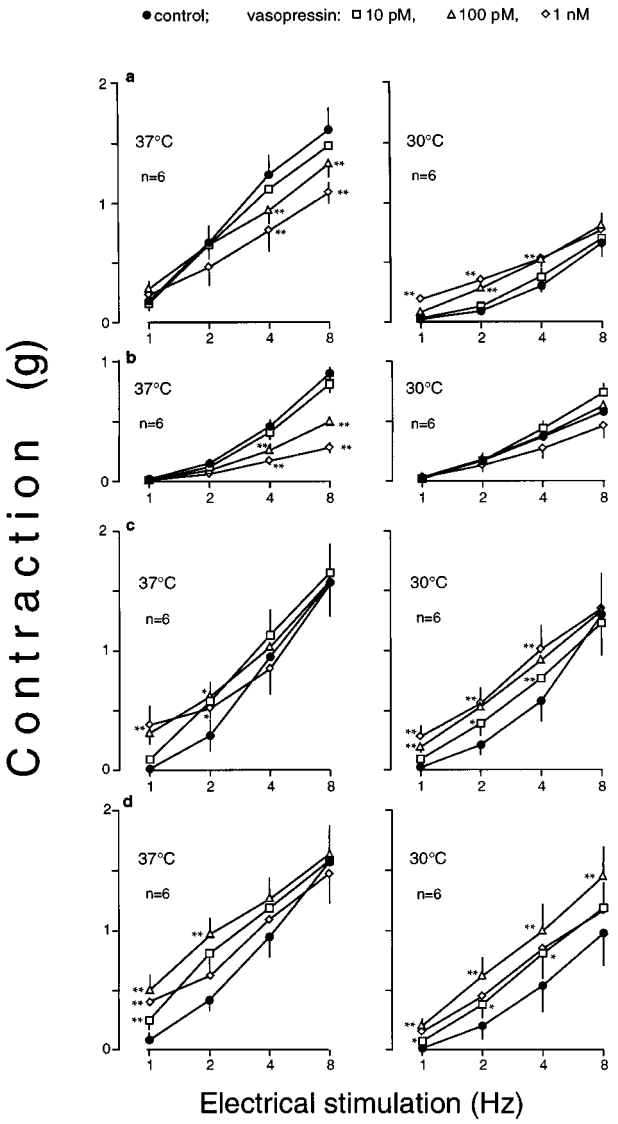

Figure 6 Contraction of rabbit ear arteries at 37 and 30°C to electrical field stimulation (1–8 Hz, 0.2 ms pulse duration, 70 V, for 5 s) in arteries in the absence (control) and in the presence of vasopressin (10 pM–1 nM): (a) pretreated with verapamil (10 μM); (b) pretreated with $NiCl_2$ (1 mM); (c) without endothelium; and (d) pretreated with L-NOARG (100 μM). Points are means$\pm$s.e.mean. *, **, Significantly different from the control (*$P<0.05$, **$P<0.01$). n = number of animals.

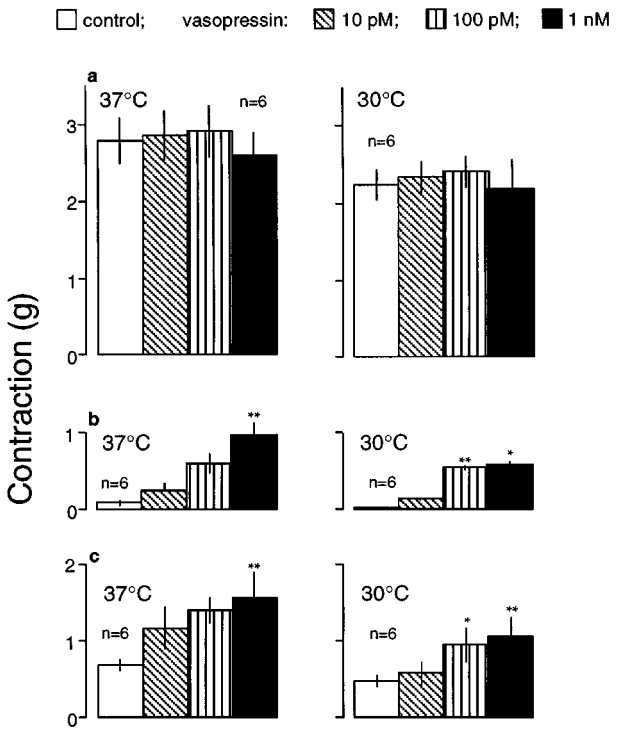

Figure 7 Contraction of rabbit central ear arteries at 37 and 30°C, in the absence (control) and in the presence of vasopressin (10 pM–1 nM), in response to: (a) noradrenaline (1 μM); (b) BHT-920 (10 μM) in the presence of prazosin (1 μM); and (c) ATP (2 mM). Values are means$\pm$s.e.mean. *Significantly different from its control (*$P<0.01$). n = number of animals.

difference in the response at these temperatures ($P>0.05$). The presence of vasopressin in the organ bath increased ($P<0.01$) the arterial contraction to ATP. The magnitude of this increment was similar at both 37 and 30°C (Figure 7c, $n=6$).

Discussion

The results of this study indicate that the contractile response of rabbit ear arteries to sympathetic nerve stimulation was reduced at 30°C compared to 37°C and that vasopressin potentiated this response to a greater extent at 30 than at 37°C, for most of the frequencies of electrical stimulation used. These results thus confirm a previous study from our laboratory (Padilla *et al*., 1997). The main aim of this study was to analyse the mechanisms underlying the potentiating effect of vasopressin on sympathetic vasoconstriction.

Under control conditions, the characteristics of the response of ear arteries to sympathetic stimulation at 37 and at 30°C are qualitatively similar to those reported in previous studies (García-Villalón *et al*., 1997a,b). In those studies we suggested that the reduction in the sympathetic response of these arteries at 30°C may be mainly due to a diminished participation of postjunctional α_1-adrenoceptors. Also, we suggested that a purinoceptor component, in addition to the α_1-adrenoceptor component, may be present in the sympathetic response of these arteries at 30°C, and that this response is modulated by endothelial nitric oxide release, to a greater extent at 30 than at 37°C. The results of the present study and of one of those studies (García-Villalón *et al*., 1997b) also suggest that there may be inhibitory prejunctional α_2-adrenoceptors and/or purinoceptors in the nerve terminals of the rabbit ear artery since the arterial response to electrical stimulation was increased by purinoceptor inhibition at 37°C, and by yohimbine at both 30 and 37°C. According to previous studies from our and other laboratories, the concentrations of the receptor antagonists or enzyme inhibitors used in the present study are likely to be selective and/or effective: antagonists for vasopressin V_1 receptors (100 nM, García-Villalón *et al*., 1996; Martínez *et al*., 1994), phentolamine (1 μM, García-Villalón *et al*., 1997b), prazosin (1 μM, García-Villalón *et al*., 1997b; Lefebvre & Smits, 1992), yohimbine (1 μM, DeMan *et al*., 1994; García-Villalón *et al*., 1997b), PPADS (30 μM, García-Villalón *et al*., 1997b), verapamil (10 μM, unpublished observations from our laboratory), $NiCl_2$ (1 mM; Hirano *et al*., 1989) and L-NOARG (100 μM; Padilla *et al*., 1998).

With regard to the mechanisms underlying the potentiation of the sympathetic contraction of ear arteries by vasopressin, our results suggest that this potentiation is mediated by activation of vasopressin V_1 receptors, because this potentiation was abolished by the vasopressin V_1 receptor antagonist $d(CH_2)_5$ Tyr(Me)AVP, whilst desmopressin, an agonist of vasopressin V_2 receptors, did not affect the response of these arteries to sympathetic stimulation. These results agree with those found in mesenteric arteries of humans (Medina *et al*., 1997) or rats (Noguera *et al*., 1997) in which vasopressin also potentiated the contraction to adrenoceptor stimulation by activation of vasopressin V_1 receptors.

Another aspect of the present work is the role of adrenoceptors and purinoceptors in the potentiation of the sympathetic contraction by vasopressin. In the rabbit ear artery it has been shown previously that the constriction to sympathetic stimulation may be mediated by release of both noradrenaline and ATP from perivascular sympathetic nerve terminals (Kennedy *et al*., 1986), and these transmitters then act on α-adrenoceptors and purinoceptors, respectively. The present study suggests that, at 37°C, vasopressin did not potentiate the response to α_1-adrenoceptor activation. This suggestion is supported by the observations that phentolamine or prazosin increased instead of reduced the potentiating effect of vasopressin on the response to nerve stimulation, and that vasopressin did not modify the arterial contraction to exogenous noradrenaline (this amine contracts rabbit ear arteries by activating mainly α_1-adrenoceptors, García-Villalón *et al*., 1992). On the other hand, at 37°C, the potentiating effect of vasopressin on nerve stimulation was abolished by PPADS, and at the same time, vasopressin increased the contraction to exogenous ATP. This suggests that vasopressin, at this temperature, potentiates the contraction to sympathetic stimulation mainly by facilitating the response to purinoceptor activation. This might explain why the potentiation by vasopressin at 37°C is greater at the lower stimulation frequencies than at the higher ones (Table 1), as the purinergic component of the sympathetic response may be more apparent at lower frequencies of stimulation (Kennedy *et al*., 1986). The involvement of α_2-adrenoceptors in the potentiating effect of vasopressin at 37°C is unclear, since this effect of vasopressin was not modified by yohimbine, but vasopressin did potentiate the contraction to BHT-920.

At 30°C, the mechanisms underlying the vasopressin effect on sympathetic stimulation may differ from those at 37°C. Our data with PPADS and ATP suggest that at 30°C, vasopressin potentiated the purinoceptor component of the sympathetic contraction, and that this potentiation for high stimulation frequencies (4 and 8 Hz) was more marked at 30 than at 37°C. Moreover, our results at 30°C suggest that, in addition to potentiating the purinoceptor component, vasopressin may also potentiate the response to α_2-adrenoceptor activation. This is suggested by the observation at 30°C that the potentiation of the sympathetic response by vasopressin was reduced by phentolamine and yohimbine but not by prazosin, and that the potentiating effect of vasopressin still present after PPADS treatment was abolished by phentolamine. This is in line with the results of Guc *et al*. (1992) who observed, in pithed rats, that vasopressin increased the pressor effects of noradrenaline, but not that due to selective stimulation of α_1-adrenoceptors.

Regarding the role of Ca^{2+} channels, our results at 37 and 30°C suggest that the potentiation of the vasoconstriction to sympathetic stimulation by vasopressin is mediated by entry of extracellular Ca^{2+}, at least in part through Ca^{2+} channels of the L-type, because the vasopressin effect was reduced by the Ca^{2+} channels blockers verapamil and $NiCl_2$, at both temperatures. Results reported in the literature in this respect show that the potentiating effect of vasopressin on the contraction to adrenoceptor stimulation was mediated by L-type Ca^{2+} channels in rat (Medina *et al*., 1997) but not in human (Noguera *et al*., 1997) mesenteric arteries, suggesting that species differences may be involved. Our results also suggest that T-type Ca^{2+} channels might be also involved in the potentiating effect of vasopressin at 30°C, since at this temperature $NiCl_2$ was more effective than verapamil in inhibiting the potentiation by vasopressin. To clarify this question, however, antagonists more specific for this subtype of Ca^{2+} channels should be used.

In relation to the role of the vascular endothelium and nitric oxide, we have found in a previous study (García-Villalón *et al*., 1996) that the modulatory role of nitric oxide in the effect of vasopressin on rabbit arteries varies widely between vascular beds, and that this modulatory role of nitric oxide was particularly small in ear arteries. In line with this, the present results at 37 and 30°C suggest that the role of the

endothelium and nitric oxide may be of relatively little importance for the potentiating effect of vasopressin on the sympathetic contraction of ear arteries, as this potentiation was not modified by endothelium removal nor by nitric oxide synthase inhibition, at both temperatures. However, nitric oxide may modulate, at both temperatures, the response of ear arteries to sympathetic stimulation, since nitric oxide synthase inhibition in the absence of vasopressin did increase the response to electrical stimulation. Thus, it is suggested that, at 37 and 30°C, nitric oxide release may be stimulated by sympathetic stimulation to a similar extent in the absence and in the presence of vasopressin.

Therefore, it may be suggested that vasopressin potentiates the contraction of cutaneous (ear) arteries to sympathetic stimulation, to a greater extent at 30 than at 37°C. At both temperatures, this potentiating effect of vasopressin may be mediated by activation of vasopressin V_1 receptors and Ca^{2+} channels, and it may be independent of endothelial nitric oxide. The increased potentiating effect of vasopressin at 30°C may not be due to cooling-induced changes of vasopressin receptor subtype, nor to changes of Ca^{2+} channels or endothelial nitric oxide effects. It may be hypothesized, instead, that cooling (30°C) changes the facilitating action of vasopressin on the receptors that mediate the sympathetic response of cutaneous arteries, so at normal temperature (37°C) vasopressin would potentiate mainly purinoceptor effects whereas during cooling (30°C) it would potentiate both purinoceptor and α_2-adrenoceptor effects.

The authors are grateful to Mrs M.E. Martínez and H. Fernández-Lomana for technical assistance. This work was supported, in part, by FIS ((6/0474), DGICYT (PM 95/0032), and CAM (AE 263/95).

References

ALTURA, B.M. & ALTURA, B.T. (1977). Vascular smooth muscle and neurohypophyseal hormones. *Fed. Proc.,* **36,** 1853–1860.

BARTLESTONE, H.J., NASMYTH, P.A. & TELFORD, J.M. (1967). The significance of adenosine cyclic 3′5′-monophosphate for the contraction of smooth muscle. *J. Physiol.,* **188,** 159–176.

DEMAN, J.G., BOECKXSTAENS, G.E., HERMAN, A.G. & PELCKMANS, P.A. (1994). Effect of potassium channel blockade and α_2-adrenoceptor activation on the release of nitric oxide from non-adrenergic non-cholinergic nervers. *Br. J. Pharmacol.,* **112,** 341–345.

GARCÍA-VILLALÓN, A.L., GARCÍA, J.L., FERNÁNDEZ, N., MONGE, L., GÓMEZ, B. & DIÉGUEZ, G. (1996). Regional differences in the arterial response to vasopressin: role of endothelial nitric oxide. *Br. J. Pharmacol.,* **118,** 1848–1854.

GARCÍA-VILLALON, A.L., MONGE, L., MONTOYA, J.J., GARCÍA, J.L., FERNÁNDEZ, N., GÓMEZ, B. & DIÉGUEZ, G. (1992). Cooling and response to adrenoceptor agonists of rabbit ear and femoral artery: role of the endothelium. *Br. J. Pharmacol.,* **106,** 727–732.

GARCÍA-VILLALÓN, A.L., PADILLA, J., FERNÁNDEZ, N., MONGE, L., GÓMEZ, B. & DIÉGUEZ, B. (1997a). Role of endothelin receptors, calcium and nitric oxide in the potentiation by endothelin-1 of the sympathetic contraction of rabbit ear artery during cooling. *Br. J. Pharmacol.,* **121,** 1659–1664.

GARCÍA-VILLALÓN, A.L., PADILLA, J., MONGE, L., FERNÁNDEZ, N., GÓMEZ, B. & DIÉGUEZ, B. (1997b). Role of the purinergic and noradrenergic components in the potentiation by endothelin-1 of the sympathetic contraction of the rabbit central ear artery during cooling. *Br. J. Pharmacol.,* **122,** 172–178.

GUC, M.O., FURMAN, B.L. & PARRAT, J.R. (1992). Modification of α-adrenoceptor-mediated pressor responses by N^G-nitro-L-arginine methyl ester and vasopressin in endotoxin-treated pithed rats. *Eur. J. Pharmacol.,* **224,** 63–69.

HARKER, C.T. & VANHOUTTE, P.M. (1988). Cooling the central ear artery of the rabbit: myogenic and adrenergic responses. *J. Pharmacol. Exp. Ther.,* **245,** 89–93.

HIRANO, Y., FOZZARD, H.A. & JANUARY, C.T. (1989). Characteristics of L- and T-type Ca^{2+} currents in canine cardiac Purkinje cells. *Am. J. Physiol.,* **256,** H1478–H1492.

KENNEDY, C., SAVILLE, V.L. & BURNSTOCK, G. (1986). The contribution of noradrenaline and ATP to the responses of the rabbit central ear artery to sympathetic nerve stimulation depend on the parameters of stimulation. *Eur. J. Pharmacol.,* **122,** 291–300.

LEFEBVRE, R.A. & SMITS, G.J.M. (1992). Modulation of non-adrenergic non-cholinergic inhibitory neurotransmission in rat gastric fundus by the α_2-adrenoceptor agonist, UK-14,304. *Br. J. Pharmacol.,* **107,** 256–261.

MARTÍNEZ, M.C., ALDASORO, M., VILA, J.M., MEDINA, P. & LLUCH, S. (1994). Responses to vasopressin and desmopressin of human cerebral arteries. *J. Pharmacol. Exp. Ther.,* **270,** 622–627.

MCDONALD, T., PELZER, S., TRAUTWEIN, W. & PELZER, D.J. (1994). Regulation and modulation of calcium channels in cardiac, skeletal, and smooth muscle cells. *Physiol. Rev.,* **74,** 365–507.

MEDINA, P., NOGUERA, I., ALDASORO, M., VILA, J.M., FLOR, B. & LLUCH, S. (1997). Enhancement by vasopressin of adrenergic responses in human mesenteric arteries. *Am. J. Physiol.,* **272,** H1087–H1093.

NARAHASHI, T., TSUNOO, A. & YOSHII, M. (1987). Characterization of two types of calcium channels in mouse neuroblastoma cells. *J. Physiol.,* **383,** 231–249.

NOGUERA, I., MEDINA, P., SEGARRA, G., MARTÍNEZ, M.C., ALDASORO, M., VILA, J.M. & LLUCH, S. (1997). Potentiation by vasopressin of adrenergic vasoconstriction in the rat isolated mesenteric artery. *Br. J. Pharmacol.,* **122,** 431–438.

PADILLA, J., GARCÍA-VILLALÓN, A.L., FERNÁNDEZ, N., MONGE, L., GÓMEZ, B. & DIÉGUEZ, G. (1998). Effects of hyperthermia on the contraction and dilatation of rabbit femoral arteries. *J. Appl. Physiol.,* in press.

PADILLA, J., GARCÍA-VILLALÓN, A.L., MONGE, L., GARCÍA, J.L., FERNÁNDEZ, N., GÓMEZ, B. & DIÉGUEZ, G. (1997). Peptidergic modulation of the sympathetic contraction in the rabbit ear artery: effects of temperature. *Br. J. Pharmacol.,* **121,** 21–28.

PATTON, J.N. & WALLACE, W.F.M. (1978). Response of isolated rabbit ear arteries to intra-and extraluminal L- and D-noradrenaline and histamine in the temperatures range 37–3°C. *Ir. J. Med. Sci.,* **147,** 313–317.

ROBERTS, M.F. & ZYGMUNT, A.C. (1984). Reflex and local thermal control of rabbit ear blood flow. *Am. J. Physiol.,* **246,** R979–R984.

SHARE, L. (1988). Role of vasopressin in cardiovascular regulation. *Physiol. Rev.,* **68,** 1248–1284.

(Received May 20, 1998
Revised October 1, 1998
Accepted November 6, 1998)

British Journal of Pharmacology (1999) 126, 794–800
http://www.stockton-press.co.uk/bjp

Hyperbaric oxygen increases plasma exudation in rat trachea: involvement of nitric oxide

*,[1]M. Bernareggi, [1]S. Radice, [1]G. Rossoni, [2]G. Oriani, [1]E. Chiesara & [1]F. Berti

[1]Department of Pharmacology, Chemotherapy and Medical Toxicology 'E. Trabucchi', University of Milan, Via Vanvitelli 32, 20129 Milan, Italy; [2]Galeazzi Ortopedics Institute, Milan, Italy

1 This study investigates the microvascular permeability changes in tracheal tissue of rats exposed to hyperbaric oxygen (HBO).

2 Rats, following exposure to HBO or ambient air (control animals) for 1.5, 3 and 6 h, were prepared for recording of nitric oxide exhaled (FENO) in air using a chemiluminescence analyser. The level of FENO was not statistically different in the two groups. Plasma exudation, evaluated by measuring the leakage of Evans blue (EB) dye into the tracheal tissue, was significantly elevated (48, 86 and 105% at 1.5, 3 and 6 h, respectively) in HBO-treated rats.

3 Plasma exudation in the trachea of control rats was significantly increased (42%, $P<0.05$) by N^G-nitro-L-arginine methyl ester (L-NAME), whereas it was significantly reduced (31%, $P<0.05$) in rats exposed to HBO for 3 h.

4 N-acetylcysteine (NAC) and flunisolide significantly prevented the increase in plasma leakage in HBO-treated rats. In contrast, indomethacin was devoid of anti-exudative activity in these experiments.

5 Western immunoblot showed a significant increase in the level of inducible nitric oxide synthase (iNOS) protein in the tracheal homogenates of HBO-treated rats, as compared to basal levels.

6 These results indicate that nitric oxide (NO) is involved in the maintenance of microvascular permeability in tracheal tissue of rats. The protective effect observed with the steroid seems to support this hypothesis. Furthermore, the beneficial action of NAC underlines that reactive oxygen species participate in the microvascular permeability changes observed in tracheal tissue of rats exposed to HBO.

Keywords: Hyperoxia; microvascular permeability; expired nitric oxide (FENO); oxygen free radicals; L-NAME; flunisolide; indomethacin; N-acetylcysteine

Abbreviations: ATA, atmospheres absolute pressure; cNOS, constitutive nitric oxide synthase; EB, Evans blue; FENO, fractional expired nitric oxide; HR, heart rate; HBO, hyperbaric oxygen; iNOS, inducible nitric oxide synthase; IFNγ, interferon gamma; LPS, lipopolysaccaride; MABP, mean arterial blood pressure; NAC, N-acetylcysteine; D/L-NAME, N^G-nitro-D/L-arginine methyl ester; p.p.b, parts per billion; p.p.m., parts per million; ROS, reactive oxygen species

Introduction

It is known that the lungs are particularly sensitive to oxidant damage during prolonged exposure to environments with increased oxygen content at 1 a.t.m. (normobaric hyperoxia) or when the exposure to pure oxygen is carried out at more than 1 a.t.m. (hyperbaric oxygen) and for several days. In fact, alterations in lung structure and function such as tissue and alveolar oedema, surfactant dysfunction, lung inflammation and decreased pulmonary compliance have been reported (Amin *et al*., 1993; Jenkinson, 1993). In recent years, an increasing number of patients has been subjected to HBO therapy in order to supplement blood oxygen content to control different types of ischaemic organ damage with particular reference to wound healing problems and infectious diseases (Amin *et al*., 1993). However, increased oxygen ambient pressure is a significant factor that could aggravate normobaric pulmonary oxygen toxicity and lead to the development of chronic lung disease or death. Although the exact mechanisms of pulmonary oxygen toxicity are unknown, Gerschman (1964) first suggested that oxygen toxicity may be mediated in large part by the production of reactive oxygen species (ROS) that act through peroxidation of membrane lipids, oxidation of membrane proteins and breakage of DNA strands (Wispè & Roberts, 1987). Acute HBO exposure of rats markedly alters pulmonary vascular responses following extravascular fluid accumulation (Amin *et al*., 1993). In rabbits, HBO treatment for 1 h causes marked pulmonary hypertension and lung weight gain (Jacobson *et al*., 1992). In a recent study by our group (Radice *et al*., 1997) we reported an impairment of vascular endothelium-dependent relaxant mechanisms in coronary artery of isolated hearts obtained from HBO exposed rats. This event, associated with a worsening of myocardial ischaemia-reperfusion damage, was attributed to increased free radicals formation and was prevented by N-acetylcysteine (Rossoni *et al*., 1997).

Nitric oxide (NO) is a potent autacoid formed from L-arginine and molecular oxygen by the constitutive nitric oxide synthase (cNOS) in a variety of cells, particularly pulmonary vascular endothelium and human lung epithelial cells (Szabò 1995; Robbins *et al*., 1994). In addition, an inducible NO synthase (iNOS) is expressed in different models of inflammation (Vane *et al*., 1994; Tomlinson *et al*., 1994; Hutcheson *et al*., 1990). In rats, lipopolysaccaride (LPS) treatment results in an increased expression of iNOS mRNA in homogenates of whole lung (Liu *et al*., 1994) or in iNOS induction in tracheal tissue (Bernareggi *et al*., 1997). Exposure of mice to normobaric hyperoxia has been demonstrated to be associated with a significant increase in NO production, measured as total

*Author for correspondence; E-mail: berti@immiucca.csi.unimi.it
MB and SR contributed to this work.

nitrite and nitrate in bronchoalveolar lavage fluid (Arkovitz *et al*., 1997). Oxidant stress, as well, has recently been shown to induce iNOS in pulmonary alveolar epithelial cells (Adcock *et al*., 1994).

Plasma exudation in the tracheaeobronchial airways represents a mucosal defence mechanism. However, under certain conditions, plasma leakage from tracheobronchial vessels may also result in inflammatory consequences that are important in airway disease (Persson, 1986). In fact, it has been demonstrated that when NO is constitutively present in the airways it may play a protective role, but when iNOS is expressed the increased production of NO may be responsible of deleterious effects. In fact, the NOS inhibitor, L-NAME, increases plasma leakage into the trachea in rat airways, whereas it inhibits LPS-induced vascular damage (Bernareggi *et al*., 1997).

Although several studies have demonstrated that the lungs are particularly susceptible to oxidant injury during acute or prolonged exposure to hyperbaric oxygen (Amin *et al*., 1993; Jacobson *et al*., 1992), there is limited information regarding what contribution NO and ROS may have on plasma leakage in the large airways. We have, therefore, examined the relationship between acute HBO exposure and the consequent microvascular leakage in the tracheal tissue of rats. In addition, we have investigated the relevance of NO and ROS formations to the HBO-induced plasma exudation in the airway tissues.

Methods

Hyperbaric oxygen treatment

Male albino rats of the Sprague-Dawley strain (Charles River Italia, Calco, CO, Italy), weighing 250–300 g were introduced (two animals each time) into a small (25 cm diameter, 50 cm long) hyperbaric chamber with one compartment (Sistemi Iperbarici Integrati S.p.A., Rome, Italy) and exposed for a period of 1.5, 3 and 6 h to HBO (100% oxygen; 2.5 atmospheres absolute pressure, ATA). In order to eliminate carbon dioxide accumulation, the chamber was flushed with 100% oxygen for 1 min every 30 min during exposure. All experimental protocols were approved by the Review Committee of the Department of Pharmacology and met the Italian guidelines for laboratory animals which conform with the European Communities Directive of November 1986 (86/609/EEC).

At the end of HBO or ambient air exposure, the animals were anaesthetized with pentobarbitone sodium (60 mg kg^{-1} i.p.) and prepared for recording of systemic blood pressure and heart rate by placing a catheter in the right carotid artery. The trachea was cannulated for mechanical ventilation with synthetic ultrapure air (NO-free air, Air SP, Sapio, Monza, MI, Italy) performed by a pump (mod. 29488, U. Basile, Comerio, VA, Italy) operating on a partially closed circuit (10 ml kg^{-1} stroke volume; 70 cycles min^{-1}). To avoid spontaneous breathing, the animals were treated with pancuronium bromide injected *via* the jugular vein at a dose of 1 mg kg^{-1} and heparin (10 UI kg^{-1}) was then administered intravenously. Changes in blood pressure were measured by pressure transducers (mod. 7016 U. Basile) and signals displayed on a two-channel pen recorder (mod. Gemini, U. Basile).

After completion of the surgical procedure, expired NO detection and vascular permeability measurements were carried out in less than 20 min. Due to the short duration of the experiment, the dose of pentobarbitone sodium used was sufficient to maintain a deep anaesthesia throughout the protocol.

Expired nitric oxide measurements

Fractional expired NO (FENO) was continuously measured using a chemiluminescence analyser (Model 280A; Sievers, Boulder, CO). This device uses ozone to oxidize NO to NO_2 in an excited state. Light is emitted when transition of NO_2 from excited to ground state occurs. The detection limit of the NO analyser is <1 p.p.b. with a repeatability of ± 1 p.p.b over a linear range $<1-500{,}000$ p.p.b. The response time is 200 ms. The analyser was designed for on-line recording of simultaneous measurements of the gas. This feature obviates the need for collection in a reservoir, with its variable loss of reactive NO and gives greater sensitivity and reproducibility (Kharitonov *et al*., 1994). A certified standard mixture of 100.1 p.p.m. NO in nitrogen (N_2) was used to calibrate the instrument and linearity was checked by serial dilution with N_2. Ambient air NO concentration was recorded and the absolute zero was adjusted before each measurement by flushing the NO analyser with NO-free certified compressed air. The instrument permitted digital conversion of the analogue signals for data storage and off-line analysis. Gas was drawn continuously from a teflon catheter positioned within the tracheostomy tube and recorded on a breath by breath basis. The peaks average concentration of NO at end expiration over 70 ± 1 breaths was used as the FENO concentration (expressed as p.p.b.).

Vascular permeability measurements

Protein leakage, a marker of vascular permeability, was evaluated by measuring the leakage of Evans blue (EB) dye (Belvisi *et al*., 1989) into the tracheal tissue. This method has been previously shown to correlate well with the leakage of radiolabelled albumin (Rogers *et al*., 1989) in guinea-pig airways. Specifically, the EB dye (20 mg kg^{-1}) was injected in the jugular vein at time 0 and its tissue content was determined 5 min after the injection by perfusing the systemic circulation with saline to remove intravascular dye. Specifically, the left ventricle was incised, a blunt ended needle inserted into the aorta and the ventricles cross-clamped. Blood was expelled from the incised right atrium at 100 mmHg pressure until the perfusate was clear (125 ml infused). The trachea was removed, blotted dry and weighed. EB dye was extracted in formamide at 37°C for 18 h and its concentration was determined with a spectrophotometer (Shimadzu UV-160A Shimadzu, Tokyo, Japan) at the absorbance maximum of 620 nm wavelength. The tissue content of the EB dye (ng EB mg^{-1} wet wt. tissue) was calculated from a standard curve of EB dye concentration in the range of $0.12-20$ μg ml^{-1}.

Experimental protocol

Effect of HBO treatment on time-dependent plasma leakage in rat trachea After exposing rats to HBO or ambient air for 1.5, 3 and 6 h, EB dye (20 mg kg^{-1} i.v.) was injected *via* a jugular vein and plasma leakage was determined. The results obtained from this experiment allowed us to choose the optimal time of HBO treatment for use in the following experiments.

Effect of L-NAME, D-NAME and flunisolide on plasma leakage into the trachea of control and HBO-treated rats To investigate the role of NO in plasma leakage into the rat

trachea under control and HBO-treated conditions, L-NAME (100 mg kg^{-1} i.p.), an inhibitor of both constitutive and inducible isoforms of NOS (Rees *et al*., 1990), D-NAME (100 mg kg^{-1} i.p.), its inactive enantiomer, and isotonic sterile saline (1 ml kg^{-1} i.p.) were injected 1 h before exposure to ambient air (3 h) or HBO (3 h).

In other experiments, rats were pre-treated for 1 h prior to either ambient air exposure (3 h) or HBO exposure (3 h) with flunisolide (1 mg kg^{-1} i.p.) or its vehicle (1 ml kg^{-1} i.p.).

Effect of N-acetylcysteine and indomethacin on plasma leakage into the trachea of control and HBO-treated rats To investigate the potential contribution of oxygen free radicals to the increase in vascular permeability observed in rat trachea after HBO treatment, animals received NAC (1 g kg^{-1} p.o.) or isotonic sterile saline (1 ml kg^{-1} p.o.) once a day for 2 days and immediately before exposure to ambient air (3 h) or HBO (3 h).

To assess the relative contribution of prostanoids to the increased plasma leakage observed in trachea after HBO treatment, rats were treated with indomethacin (5 mg kg^{-1} i.p.) or isotonic sterile saline (1 ml kg^{-1} i.p.) 30 min before exposure to ambient air (3 h) or HBO (3 h).

Western immunoblot analysis

In separate experiments, iNOS protein expression was measured in the trachea of six rats exposed to HBO or ambient air for 3 h. At the end of exposure, the animals were killed by cervical dislocation, tracheal tissue was then removed and homogenates from tracheal tissues were centrifuged at 5000 × *g* for 15 min at 4°C. Proteins were boiled (10 min) in gel loading buffer in a ratio of 1 : 1 (v/v) and a determined amount (10 μg) was subjected to electrophoresis on sodium dodecyl sulphate 10% polyacrylamide gels according to the method of Maizel (1979). Western immunoblot analysis was performed as described by Towbin *et al*. (1979). The separated proteins were transferred electrophoretically from the polyacrylamide gel to nitrocellulose sheet in a blotting buffer (25 mM Tris, 192 mM glycine and 20% methanol, pH 8.3), using a mini-transblot apparatus. The proteins were transferred onto nitrocellulose membrane. The membrane was saturated by incubation at 4°C overnight with Marvell (powered milk) solution (5% Marvell, 0.05% Tween 20) and then primed with a primary polyclonal anti-iNOS. The primary antibody was located with an alkaline phosphatase-conjugated second antibody with BCIP (5-bromo-4-chloro-3-indoylphosphate p-toluidine salt) and NTB (p-nitro blue tetrazolium chloride) colour development reagents. All antibodies were used at 1 : 1000 diluition.

Materials

The following drugs were used: formamide (Merck, Darstad, FRG); Evans blue, indomethacin, N^G-nitro-D/L-arginine methyl ester (Sigma Chem. Co., St. Louis, MO, U.S.A); pancuronium bromide (N.V. Organon, Oss, The Netherlands); N-acetylcysteine (Zambon, Italia srl, Bresso, Milano, Italy); flunisolide idrate (Valeas SpA, Milan, Italy); pentobarbital sodium (Abbott SpA, Campoverde di Aprilia, LT, Italy); heparin (Squibb, LT, Italy); anti-iNOS antibody (Transduction Laboratories, Lexington, U.K.).

Statistics

Results are expressed as the mean ± s.e.mean of *n* animals. In all experiments, the differences between control and treatment groups were analysed for statistical significance using a one-way analysis of variance (ANOVA) and Student's two tailed *t*-test for paired or unpaired samples as appropriate; $P<0.05$ was accepted as significant.

Results

Effect of HBO treatment on haemodynamic parameters

The exposure of rats to HBO regimen (1.5, 3 and 6 h) did not induce a status of aggressivity to handling and did not modify the haemodynamic parameters when measured in anaesthetized animals. In fact, baseline values for MABP and HR of control rats (147 ± 4 mmHg; $n=18$; 418 ± 8 b min^{-1}; $n=18$) were not significantly different ($P>0.05$) from those of rats exposed to HBO (144 ± 4 mmHg; $n=18$; 400 ± 9 b min^{-1}; $n=18$). These parameters were constant throughout the duration of the experiment.

Effect of HBO treatment on FENO concentrations

The HBO treatment did not provide any statistical modification of the basal concentration of FENO when compared to that in the expired gas of control rats ($P>0.05$). In fact, the basal FENO values in the control rats were 5.0 ± 0.81 p.p.b ($n=13$) and in HBO exposed rats were 5.0 ± 0.75 p.p.b ($n=14$).

Effect of HBO treatment on plasma leakage in rat trachea

Figure 1 shows plasma leakage in tracheal tissue of control and HBO-treated rats at 1.5, 3 and 6 h. HBO exposure caused a significant increase in plasma leakage of 48, 86 and 105% in HBO exposed animals compared with controls at 1.5, 3 and 6 h exposure, respectively. Since the HBO treatment at 3 h was significantly different from 1.5 h ($P<0.05$) but not from 6 h, a 3 h exposure was used in the following experiments.

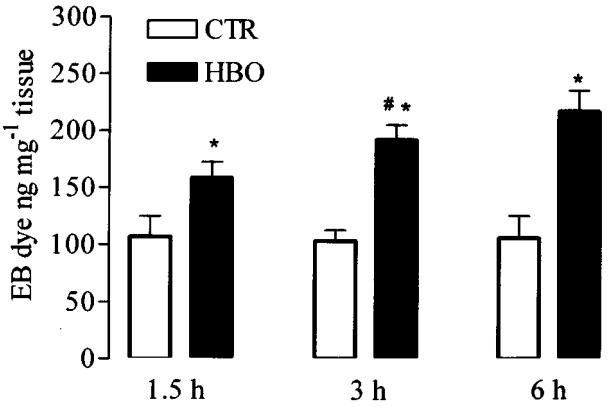

Figure 1 Effect of duration of exposure to hyperbaric oxygen on plasma leakage in rat tracheal tissue. Rats were exposed to hyperbaric oxygen (HBO, 100% oxygen; 2.5 ATA) treatment or ambient air for 1.5, 3 and 6 h. At the end of the exposure rats were anaesthetized and protein leakage was evaluated by measuring the leakage of Evans blue (EB) dye into the tracheal tissue. Columns represent the mean value ± s.e.mean of six experiments at each time point. CTR, rats not exposed to HBO; HBO, rats exposed to hyperbaric oxygen. Significant differences between control and HBO-treated groups at each time points are demonstrated as $*P<0.05$ according to one-way ANOVA. Significant differences between 1.5 and 3 h HBO-treated rats are demonstrated as # $P<0.05$ according to one-way ANOVA.

Effect of L-NAME, D-NAME and flunisolide on tracheal plasma leakage in control and HBO-treated rats

In the trachea of rats exposed for 3 h to ambient air L-NAME significantly increased plasma leakage by 42% ($P<0.05$). In contrast, L-NAME significantly inhibited the HBO-induced plasma leakage in the trachea by 31% ($P<0.05$) (Figure 2). D-NAME did not modify EB dye leakage in the trachea of control (vehicle for D-NAME, 99.5 ± 6.8 ng mg^{-1}, $n=4$; D-NAME-treated, 108.3 ± 19.3 ng mg^{-1}, $n=6$, $P>0.05$) and HBO-treated rats (vehicle for D-NAME, 195.8 ± 10.5 ng mg^{-1}, $n=4$; D-NAME-treated, 187.4 ± 19.3 ng mg^{-1}, $n=6$, $P>0.05$).

In the trachea of HBO-treated rats, flunisolide inhibited plasma leakage by 41% ($P<0.05$) so that the leakage resembled that found in vehicle for flunisolide-treated control rats. Flunisolide had no effect on leakage in control rats (Figure 3).

Effect of N-acetylcysteine and indomethacin on tracheal plasma leakage in control and HBO-treated rats

In the trachea of HBO-treated rats, NAC significantly inhibited plasma leakage by 42% ($P<0.05$) so that the phenomenom resembled that found in vehicle for NAC-treated control rats. NAC had no effect on tracheal leakage in control rats (Figure 4).

Indomethacin had no effect on plasma leakage in the trachea of either control rats (vehicle for indomethacin, 100.4 ± 6.5 ng mg^{-1}, $n=4$; indomethacin-treated, 116.7 ± 16.8 ng mg^{-1}, $n=6$, $P>0.05$) or HBO-treated rats (vehicle for indomethacin, 182.8 ± 13.5 ng mg^{-1}, $n=4$; indomethacin-treated, 171.9 ± 20.2 ng mg^{-1}, $n=6$, $P>0.05$).

Western immunoblot analysis

The levels of iNOS protein from tracheal homogenates of rats exposed for 3 h to HBO were investigated by Western immunoblot analysis. Low levels of iNOS protein expression were detectable in control rats (lane b). The 3 h exposure to HBO resulted in an increase of iNOS protein expression (lane c) (Figure 5).

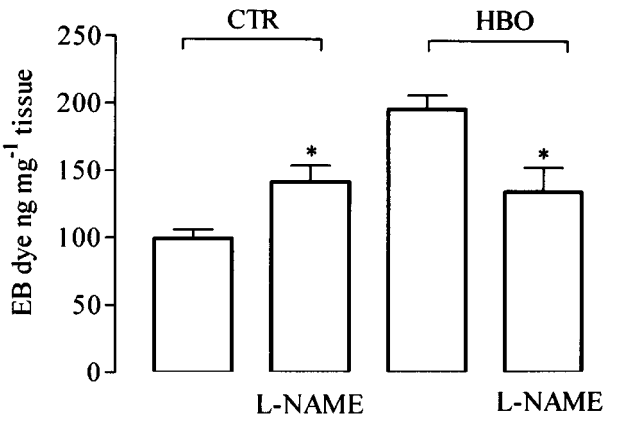

Figure 2 Effect of L-NAME on plasma leakage of tracheal tissue in control and HBO-treated rats. Rats were treated with L-NAME (100 mg kg^{-1} i.p.) 1 h prior to exposure to HBO or ambient air for 3 h. Columns represent the mean value$\pm$s.e.mean of 4–6 experiments. CTR, rats not exposed to HBO for 3 h. HBO, rats exposed to hyperbaric oxygen for 3 h. Significant differences between L-NAME-treated and untreated rats in both control and HBO-treated groups are demonstrated as $*P<0.05$ according to one-way ANOVA.

Discussion

Pulmonary oxygen toxicity is the primary limiting factor in the therapeutic administration of oxygen (Winter *et al*., 1972; Jenkinson, 1993). The diffuse cellular infiltration of lungs, proteinaceous exudate and consequent hypoxemia concurrent with high inspired concentration of O_2 has been shown to be harmful (Vacchiano & Tempel, 1994).

The present results clearly demonstrate that the microvascular permeability of the large airways of rats is increased when the animals are exposed for a limited period of time (3 h) to HBO. The mechanism/s involved in this phenomenon is difficult to understand. However a large contribution of free radicals appears a reasonable hypothesis. In fact, neutrophilis, macrophages and vascular endothelial cells, all found in abundance in airways, can produce a variety of free radicals when appropriately stimulated (Radi *et al*., 1991). Rat lung homogenates and mitochondrial particles exposed to high oxygen concentration showed increased superoxide anion (O^{-}_{2}) and hydrogen peroxide (H_2O_2) production. In addition, increased lipid peroxidation in the presence of hyperoxia has been reported (Freeman *et al*., 1982; Turrens *et al*., 1982). The fact that NAC administration to rats prior to HBO exposure abolished the increase in plasma exudate indicates for a large contribution of free radicals in the permeability changes of the tracheal vasculature. Beneficial effects of NAC in several ischaemia reperfusion models have been mostly referred not only to its antioxidant activity but also to its direct scavenging action on hydroxyl radicals (Villa & Ghezzi, 1995; Brunet *et al*., 1995).

Another finding emerging from the present experiments refers to the opposite effect on plasma exudation observed in rats treated with the inhibitor of NO synthase, L-NAME. This compound given to control rats brings about a significant increase in plasma extravasation in tracheal tissue, whereas it inhibits this event in rats exposed to HBO. The demonstration that in the trachea under 'physiological' conditions NOS

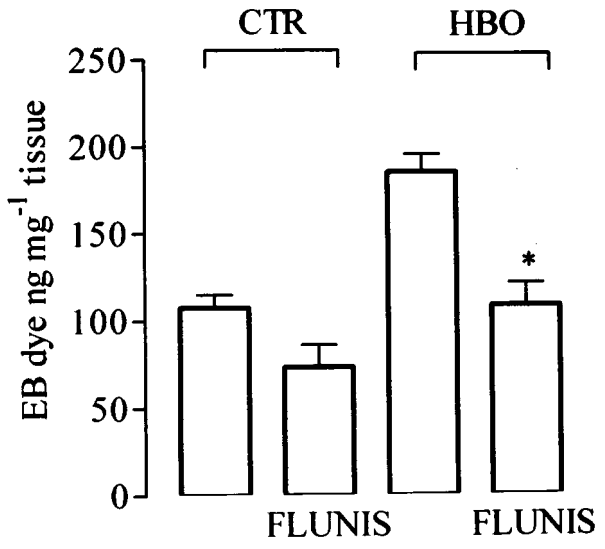

Figure 3 Effect of flunisolide on plasma leakage of tracheal tissue in control and HBO-treated rats. Rats were treated with flunisolide (FLUNIS, 1 mg kg^{-1} i.p.) 1 h prior to exposure to HBO or ambient air for 3 h. Columns represent the mean value$\pm$s.e.mean of 4–6 experiments. CTR, rats not exposed to HBO for 3 h; HBO, rats exposed to hyperbaric oxygen for 3 h. Significant differences between FLUNIS-treated and untreated rats in both control and HBO-treated groups are demonstrated as $*P<0.05$ according to one-way ANOVA.

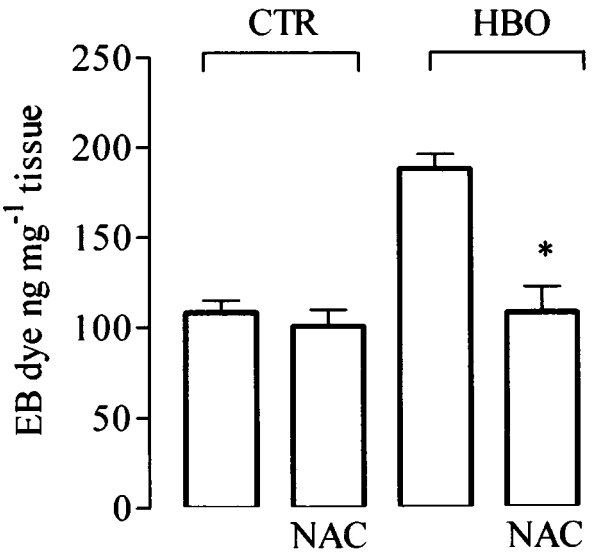

Figure 4 Effect of N-acetylcysteine (NAC) on plasma leakage of tracheal tissue in control and HBO-treated rats. Rats were treated with NAC (1 g kg^{-1} p.o.) once a day for 2 days and immediately prior to exposure to HBO or ambient air for 3 h. Columns represent the mean value$\pm$s.e.mean of 4–6 experiments. CTR, rats not exposed to HBO for 3 h. HBO, rats exposed to hyperbaric oxygen for 3 h. Significant differences between NAC-treated and untreated rats in both control and HBO-treated groups are demonstrated as $^*P<0.05$ according to one-way ANOVA.

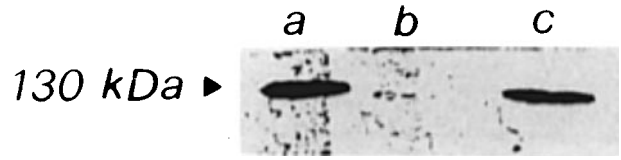

Figure 5 Western immunoblot analysis of iNOS protein in tracheal tissue of control and HBO-treated rats. Expression of iNOS protein from cytosolic fraction of tracheal homogenates of rats exposed for 3 h to HBO or ambient air (control) was investigated by Western blot analysis. The iNOS antibody recognized a protein at a molecular weight of 130 kDa. The immunoblot presents mouse macrophage cells stimulated with IFNγ (10 ng ml^{-1}) and LPS (1 μg ml^{-}) for 12 h (positive control; lane a), control (lane b) and HBO-treated (lane c). This immunoblot is representative of six separate experiments.

inhibition causes plasma leakage suggests a possible role for NO in the maintenance of microvascular integrity. In fact, different studies have suggested a protective role in the airways for constitutively formed NO (Laszlo *et al*., 1995a). L-NAME, for instance, increases plasma exudation into the trachea of vehicle for LPS-treated rats (Bernareggi *et al*., 1997). Furthermore, it has already been suggested that the maintenance of intestinal microvascular and mucosal integrity depends on the beneficial actions of NO (Laszlo *et al*., 1995b). On the contrary, as a consequence of HBO exposure, an inducible NO synthase generate a greater amount of NO which in turn is responsible for the increased tracheal vascular permeability. This hypothesis is supported by at least two observations from the present study: (1) the Western immunoanalysis of tracheal homogenates from rats exposed to HBO resulted in a significant increase in inducible NO synthase protein expression; (2) treatment of these animals with flunisolide caused a complete inhibition of the increased plasma extravasation, which is consistent with a well recognized primary mode of action of the glucocorticoids (suppression of inducible NO synthase expression) (Radomsky *et al*., 1990).

The protective effect of NAC in limiting the HBO-induced plasma leakage in rat trachea associated to the anti-exudative activity shown by L-NAME in the same group of animals suggests not also that oxygen free radicals and NO contribute largely to the injury of the large airways but that they are both related to each other. In fact, Adcock *et al*. (1994) have already demonstrated that oxidative stress induce iNOS in pulmonary alveolar epithelial cells. Even though we did not measure the expression of iNOS protein by immunoblot analysis with antibodies against iNOS in NAC-treated rats, and this should be performed in the future experiments, still NAC has been proven to significantly inhibit NO production, iNOS activity and iNOS gene expression in rat peritoneal macrophages stimulated by endotoxin (Pahan *et al*., 1998). This inhibitory effect was evident as early as 2 h pre-treatment and decreased progressively with the increase in time interval. In our study, NAC was given chronically once a day for 2 days and immediately before HBO exposure. Therefore, we could postulate that NAC would have decreased iNOS expression in tracheal homogenates of HBO-treated rats.

In our study, we were expecting that the rats exposed to HBO could demonstrate an increase in FENO, but this was not the case. The basal level of FENO in control rats was not different from that recorded in HBO exposed animals. These negative results are difficult to explain. However, we could speculate that the absence of NO in exhaled air depends on the redox, pH and biochemical milieu in the mucosa and the lining fluid of the respiratory tract resulting in other nitrogen-oxygen species than gaseous NO (Gaston *et al*., 1994; Cross *et al*., 1994a, b). Other possible interpretations might be the effects of the close relation to oxygenated haemoglobin in the lungs or the presence of radicals in the lining fluid of the respiratory tract that act as rapid scavengers for the NO formed. In fact, Schedin *et al*. (1997) were unable to obtain accumulation of NO during nose occlusion in the pig, perhaps due to local inactivation of NO by e.g. superoxide or haemoglobin. However, further experiments are needed in order to investigate if chronic exposure to HBO could increase the levels of FENO. The fact that we were able to show, indirectly, the involvement of NO in the maintenance of a normal vascular permeability does not necessarily mean that there should exist a link between exhaled NO and systemic NO production. In fact, Dillon *et al*. (1996) have already demonstrated the absence of a correlation between oral NO levels and plasma and urine nitrate and nitrite concentrations in humans suggesting that breath NO reflects local rather systemic NO production.

In this study we have found that indomethacin, a non-specific cyclo-oxygenase-1 and -2 inhibitor (Mitchell *et al*., 1993), was devoid of any inhibitory activity on the HBO-induced increase in plasma leakage in rat trachea. In agreement with our data, Mialon & Barthelemy (1991) have shown that eicosanoids do not play a major role in HBO seizures in rats. This is in contrast with another study which demonstrated that indomethacin completely eliminated the pulmonary hypertension and oedema induced by exposing rabbits for 1 h to 100% oxygen at 4 a.t.m. barometric pressure (Jacobson *et al*., 1992). Alternatively, the results presented here suggest that cyclo-oxygenase products do not play a direct role in the HBO-induced plasma leakage in tracheal tissue of rats and the major role is imputable to oxygen free radicals and NO. However, it is now recognized that cyclo-oxygenase, the first enzyme in the pathway of prostaglandin and thromboxane A_2 biosynthesis from arachidonic acid, exists in both

constitutive (COX-1) and inducible (COX-2) isoforms (Mitchell *et al*., 1995). Therefore, the development of further experiments with COX-2 selective inhibitors should be performed.

In summary, we have shown that acute exposure to HBO induces increases in rat tracheal plasma leakage. The beneficial action of NAC underlines that reactive oxygen species participate in the microvascular permeability changes observed in rat tracheal tissue. Furthermore, the inhibitory action of NOS inhibition in the HBO-induced vascular damage supports the idea that the increased production of NO, as a consequence of iNOS expression, leads to the deleterious effects observed. However, the very recent development of a new selective iNOS inhibitor, 1400W (Garvey *et al*., 1997), offers a new important tool to better characterize the role of NO when induced by HBO exposure in further experiments.

References

ADCOCK, I.M, BROWN, C.R., KWON, O. & BARNES, P.J. (1994). Oxidative stress induces NF kappa B DNA binding and inducible NOS mRNA in human epithelial cells. *Biochem. Biophys. Res. Commun.,* **199,** 1518 – 1524.

AMIN, H.M., CIGADA, M., HAKIM, T.S. & CAMPORESI, E.M. (1993). Pulmonary mechanical and vascular responses after acute hyperbaric oxygen exposure. *Can. J. Physiol. Pharmacol.,* **71,** 592 – 596.

ARKOVITZ, M.S., SZABO, C., GARCIA, V.F., WONG, H.R. & WISPE, J.R. (1997). Differential effects of hyperoxia on the inducible and constitutive isoforms of nitric oxide synthase in the lung. *Shock,* **7,** 345 – 350.

BELVISI, M.G., ROGERS, D.F. & BARNES, P.J. (1989). Neurogenic plasma extravasation: inhibition by morphine in guinea pig airways in vivo. *J. Appl. Physiol.,* **66,** 268 – 272.

BERNAREGGI, M., MITCHELL, J.A., BARNES, P.J. & BELVISI, M.G. (1997). Dual action of nitric oxide on airway plasma leakage. *Am. J. Respir. Crit. Care Med.,* **155,** 869 – 874.

BRUNET, J., BOILY, MJ., CORDEAU, S. & DES ROSIERS, C. (1995). Effects of N-acetylcysteine in the rat heart reperfused after low-flow ischemia: evidence for a direct scavenging of hydroxyl radicals and a nitric oxide-dependent increase in coronary flow. *Free Radical Biol. Med.,* **19,** 627 – 638.

CROSS, C.E., VAN DER VLIET, A., O'NEILL, C.A. & EISERICH, J.P. (1994a). Reactive oxygen species and the lung. *Lancet,* **344,** 930 – 933.

CROSS, C.E., VAN DER VLIET, A., O'NEILL, C.A., LOUIE, S. & HALLIWELL, B. (1994b). Oxidants, antioxidants and respiratory tract lining fluids. *Environ. Health Perspect.,* **102,** 185 – 191.

DILLON, W.C., HAMPL, V., SHULTZ, P.J., RUBINS, J.B. & ARCHER, S.L. (1996). Origins of breath nitric oxide in humans. *Chest,* **110,** 930 – 938.

FREEMAN, B.A., TOPOLOSKY, M.K. & CRAPO, J.D. (1982). Hyperoxia increases oxygen radical production in rat lung homogenates. *Arch. Biochem. Biophys.,* **216,** 477 – 484.

GARVEY, E.P., OPLINGER, J.A., FURFINE, E.S., KIFF, R.J., LASZLO, F., WHITTLE, B.J.R. & KNOWLES, R.G. (1997). 1400W is a slow, tight binding, and highly selective inhibitor of inducible nitric-oxide synthase in vitro and in vivo. *J. Biol. Chem.,* **272,** 4959 – 4963.

GASTON, C.E., DRAZEN, J.M., LOSCALZO, J. & STAMLER, JS. (1994). The biology of nitrogen oxides in the airways. *Am. J. Respir. Crit. Care Med.,* **149,** 538 – 551.

GERSCHMAN, R. (1964). *Oxygen in the animal organism*. ed. Dickens, F. & Neil, E. pp. 475 – 494. New York: Macmillan.

HUTCHESON, I.R., WHITTLE, B.J.R. & BOUGHTON-SMITH, N.K. (1990). Role of nitric oxide in maintaining vascular integrity in endotoxin-induced acute intestinal damage in the rat. *Br. J. Pharmacol.,* **101,** 815 – 820.

JACOBSON, J.M., MICHAEL, J.R., MEYERS, R.A., BRADLEY, M.B., SCIUTO, A.M. & GURTNER, G.H. (1992). Hyperbaric oxygen toxicity: role of thromboxane. *J. Appl. Physiol.,* **72,** 416 – 422.

JENKINSON, S. (1993). Oxygen toxicity. *New Horizons,* **1,** 504 – 511.

KHARITONOV, S.A., YATES, D., ROBBINS, R.A., LOGAN-SINCLAIR, R., SHINEBOURNE, E.A. & BARNES, P.J. (1994). Increased nitric oxide in exhaled air of asthmatic patients. *Lancet,* **343,** 133 – 135.

LASZLO, F., WHITTLE, B.J.R., EVANS, S.M. & MONCADA, S. (1995a). Association of microvascular leakage with induction of nitric oxide synthase: effects of nitric oxide synthase inhibitors in various organs. *Eur. J. Pharmacol.,* **283,** 47 – 53.

LASZLO, F., WHITTLE, B.J.R. & MONCADA, S. (1995b). Interactions of constitutive nitric oxide with PAF and thromboxane on rat intestinal vascular integrity in acute endotoxaemia. *Br. J. Pharmacol.,* **113,** 1131 – 1136.

LIU, S., ADCOCK, I.M., OLD, R.W., BARNES P.J. & EVANS, T.W. (1994). Lipopolysaccaride treatment in vivo induces widespread tissue expression of inducible nitric oxide synthase mRNA. *Biochem. Biophys. Res. Commun.,* **196,** 1208 – 1213.

MAIZEL, J.B. (1979). Polyacrylamide gel electrophoresis of viral proteins. In *Methods in virology*. ed. Marasmorosch K.& Kopprowski, N. pp. 355 – 375. New York: Academic Press.

MIALON, P. & BARTHELEMY, L. (1991). The influence of one hyperbaric oxygen-induced seizure on brain eicosanoid content. *Mol. Chem. Neuropathol.,* **15,** 1 – 11.

MITCHELL, J.A., AKARASEREENONT, P., THIEMERMANN, C. & VANE, J.R. (1993). Selectivity of non-steroid anti-inflammatory drugs as inhibitors of constitutive and inducible cyclooxygenase. *Proc. Natl. Acad. Sci.,* **90,** 11693 – 11697.

MITCHELL, J.A., LARKIN, S. & WILLIAMS, T.J. (1995). Cycloxygenase 2: regulation and relevance in inflammation. *Biochem. Pharmacol.,* **50,** 1535 – 1542.

PAHAN, K., SHEIKH, F.G., NAMBOODIRI, A.M.S. & SINGH, I. (1998). N-acetyl cysteine inhibits induction of NO production by endotoxin or cytokine stimulated rat peritoneal macrophages, C_6 glial cells and astrocytes. *Free Rad. Biol. Med.,* **24,** 39 – 48.

PERSSON, C.G.A. (1986). Role of plasma exudation in asthmatic airways. *Lancet,* **2,** 1126 – 1129.

RADI, R., BECKMAN, J.S., BUSH, K.M. & FREEMAN, B.A. (1991). Peroxynitrite-induced membrane lipid peroxidation: the cytotoxic potential of superoxide and nitric oxide. *Arch. Biochem. Biophys.,* **288,** 481 – 487.

RADICE, S., ROSSONI, G., ORIANI, G., MICHAEL, M., CHIESARA, E. & BERTI, F. (1997). Hyperbaric oxygen worsens myocardial low flow ischeamia-reperfusion injury in isolated rat heart. *Eur. J. Phramacol.,* **320,** 43 – 49.

RADOMSKY, M.W., PALMER, R.M.J. & MONCADA, S. (1990). Glucocorticoids inhibit the expression of an inducible but not the constitutive nitric oxide synthase in vascular endothelial cells. *Proc. Natl. Acad. Sci. U.S.A.,* **87,** 2593 – 2597.

REES, D.D., PALMER, M.J., SCHULZ, R., HODSON, H.F. & MONCADA, S. (1990). Characterisation of three inhibitors of endothelial nitric oxide synthase in vitro and in vivo. *Br. J. Pharmacol.,* **101,** 746 – 752.

ROBBINS, R.A., BARNES, P.J., SPRINGALL, D.R., WARREN, J.B., KWON, O.J., BUTTERY, L.D.K., WILSON, A.J., GELLER, D.A. & POLAK, J.M. (1994). Expression of inducible nitric oxide in human lung epithelial cells. *Biochem. Biophys. Res. Comm.,* **203,** 209 – 218.

ROGERS, D.F., BOSCHETTO, P. & BARNES, P.J. (1989). Plasma exudation: correlation between Evans blue dye and radiolabeled albumin in guinea pig airways in vivo. *J. Pharmacol. Methods,* **21,** 309 – 315.

ROSSONI, G., RADICE, S., BERNAREGGI, M., POLVANI, G., ORIANI, G., CHIESARA, E. & BERTI, F. (1997). Influence of acetylcysteine on aggravation of ischemic damage in ex vivo hearts exposed to hyperbaric oxygen. *Arzneim.-Forsch./Drug Res.,* **47,** 710 – 715.

SCHEDIN, U., RÖKEN, B.O., NYMAN, G., FROSTELL, C. & GUSTAFSSON, L.E. (1997). Endogenous nitric oxide in the airways of different animal species. *Acta Anaesthesiol. Scand.,* **41,** 1133 – 1141.

SZABÓ, C. (1995). Alterations in nitric oxide production in various forms of circulatory shock. *New Horizons,* **3,** 2 – 32.

TOMLINSON, A., APPLETON, A.R., MOORE, A.R., GILROY, D.W., WILLIS, D., MITCHELL, J.A. & WILLOUGHBY, D.A. (1994). Cyclooxygenase and nitric oxide synthase isoforms in rat-carrageenin-induced pleurisy. *Br. J. Phramacol.,* **113,** 693 – 698.

TOWBIN, H., STAEHELIN, T. & GORDON, J. (1979). Electrophoretic transfer of proteins from polyacrylamide gels to nitrocellulose sheets: procedure and some applications. *Biochemistry,* **76,** 4350–4354.

TURRENS, J.F., FREEMAN, B.A., LEVITT, J.G. & CRAPO, J.D. (1982). The effect of hyperoxia on superoxide production by lung submitochondrial particles. *Arch Biochem. Biophys.,* **217,** 401–410.

VACCHIANO, C.A. & TEMPEL, G.E. (1994). Role of nonenzymatically generated prostanoid, 8-iso-$PGF_{2\alpha}$, in pulmonary oxygen toxicity. *J. Appl. Physiol.,* **77,** 2912–2917.

VANE, J.R., MITCHELL, J.A., APPLETON, A., TOMLINSON, A., BISHOP-BAILEY, D., CROXTALL, J. & WILLOUGHBY, D.A. (1994). Inducible isoforms of cyclooxygenase and nitric oxide synthase in inflammation. *Proc. Natl. Acad. Sci. U.S.A.,* **91,** 2046–2050.

VILLA, P. & GHEZZI, P. (1995). Effect of N-acetyl-L-cysteine on sepsis in mice. *Eur. J. Pharmacol.,* **292,** 341–344.

WINTER, P.M. & SMITH, G. (1972). The toxicity of oxygen. *Anaesthesiology,* **37,** 210–242.

WISPÈ, J.R. & ROBERTS, R. (1987). Molecular basis of pulmonary oxygen toxicity. *Clin. Pediatr.,* **14,** 651–666.

(Received August 3, 1998
Revised November 4, 1998
Accepted November 10, 1998)

British Journal of Pharmacology (1999) 126, 801–809
http://www.stockton-press.co.uk/bjp

Mode of action of ICS 205,930, a novel type of potentiator of responses to glycine in rat spinal neurones

*,[1]D. Chesnoy-Marchais

[1]Laboratoire de Neurobiologie, Ecole Normale Supérieure, 46 rue d'Ulm, 75005 Paris, France

1 The effect of a novel potentiator of glycine responses, ICS 205,930, was studied by whole-cell recordings from spinal neurones, and compared with that of other known potentiators, in an attempt to differentiate their sites of action.

2 The ability of ICS 205,930 (0.2 μM) to potentiate glycine responses persisted in the presence of concentrations of Zn^{2+} (5–10 μM) that were saturating for the potentiating effect of this ion.

3 Preincubation with 10 μM Zn^{2+} before application of glycine plus Zn^{2+} had an inhibitory effect, which did not result from Zn^{2+} entry into the neurone, since it persisted with either 10 mM internal EGTA or 10 μM internal Zn^{2+}. To test whether the potentiating effects of ICS 205,930 and Zn^{2+} interact, both compounds were applied without preincubation.

4 The potentiating effect of ICS 205,930 was similar for responses to glycine and for responses to glycine plus Zn^{2+}, provided the concentrations of agonist were adjusted so as to induce control responses of identical amplitudes.

5 ICS 205,930 remained able to potentiate glycine responses in the presence of ethanol (200 mM).

6 ICS 205,930 also retained its potentiating effect in the presence of the anaesthetic propofol (30–90 μM), which strongly potentiated glycine responses but, in contrast with ICS 205,930, also markedly increased the resting conductance.

7 The anticonvulsant chlormethiazole (50–100 μM) neither potentiated glycine responses nor prevented the effect of ICS 205,930, even though it increased the resting conductance and potentiated $GABA_A$ responses.

8 The mechanism of action of ICS 205,930 appears to be different from those by which Zn^{2+}, propofol or ethanol potentiate glycine responses.

Keywords: Glycine; 5-HT_3 antagonists; ICS 205,930; Zn^{2+}; ethanol; propofol; chormethiazole; anaesthetics; spinal neurones

Abbreviations: ATP, adenosine triphosphate; DMSO, dimethyl sulphoxide; EGTA, ethylenediaminetetraacetic acid; GABA, γ-amino-n-butyric acid; GTP, guanosine triphosphate; HEPES, N-[2-hydroxyethyl]piperazine-N′-[2-ethanesulphonic acid]; TTX, tetrodotoxin

Introduction

In a previous study performed in ventral spinal cord neurones in primary culture, the chloride conductance increase induced by glycine was shown to be potentiated by three molecules previously known as 5-HT_3 antagonists (ICS 205,930, MDL 72222, LY 278,584). The ability of these compounds to potentiate glycine responses, however, appeared to be independent of their 5-HT_3 antagonist properties, and to result from their capacity to increase the apparent affinity of the receptors for glycine (Chesnoy-Marchais, 1996). Responses to glycine have also been reported to be potentiated by other compounds, such as Zn^{2+} ions (Akagi *et al*., 1993; Bloomenthal *et al*., 1994; Laube *et al*., 1995; Zhang & Berg, 1995; Kumamoto & Murata, 1996; Trombley & Shepherd, 1996), various types of anaesthetics, such as propofol (Hales & Lambert, 1991; Mascia *et al*., 1996a; 1997; Pistis *et al*., 1997) or inhalation anaesthetics (Wakamori *et al*., 1991; Harrison *et al*., 1993; Downie *et al*., 1996; Mihic *et al*., 1997), and alcohols (Celentano *et al*., 1988; Aguayo & Pancetti, 1994; Mascia *et al*., 1996a,b; Mihic *et al*., 1997; Ye *et al*., 1998). The identification of the site(s) of action of potentiators of glycine receptors is currently under study in several laboratories. In the case of Zn^{2+}, the role of some extracellular domains has been demonstrated (Laube *et al*., 1995), and in the case of volatile anaesthetics and high concentrations of ethanol, a residue present in the second transmembrane segment of α subunits has been shown to play a critical role (Mihic *et al*., 1997). It is well-known that different potentiators of a given receptor can involve different sites of action (for reviews concerning the potentiations of $GABA_A$ responses by benzodiazepines, barbiturates, steroids and other agents, see MacDonald & Olsen, 1994 or Whiting *et al*., 1995). The mode of action of propofol on $GABA_A$ receptors, for example, has been shown to be different from that of many other potentiators, including ethanol (Mihic *et al*., 1997) and some other general anaesthetics, such as volatile anaesthetics (Mihic *et al*., 1997; Krasowski *et al*., 1998) or etomidate (Hill-Venning *et al*., 1997). In the present paper, whole-cell recordings from ventral spinal cord neurones and combined applications of ICS 205,930 with either Zn^{2+}, ethanol or propofol were used in order to determine whether the mechanism of potentiation of glycine responses by low concentrations of ICS 205,930 can be discriminated from the mechanisms involved in the effects of these other modulators. The effects of chlormethiazole, another molecule reported to potentiate glycine responses (Gent & Wacey, 1983; Hales & Lambert, 1992), were also reinvestigated.

Methods

The experiments were performed at room temperature (20–23°C) on primary cultures of ventral spinal cord neurones from

* Author for correspondence; E-mail: chesnoy@biologie.ens.fr

rat embryos, using the whole-cell configuration of the patch-clamp technique.

Cell preparation

Female rats (OFA, Iffa Credo) carrying E15 or E16 embryos were killed by CO_2-induced anoxia. No anaesthetic was used. The embryos were rapidly removed and decapitated. Their spinal cords were taken out and dissected under a microscope in a phosphate buffer saline (PBS without Ca and Mg, Gibco) supplemented with glucose (33 mM). After removal of the meninges, the ventral part of the spinal cord was excised and cut in small pieces in order to dissociate the neurones as previously described (Chesnoy-Marchais, 1996). Recordings from cells were performed between day 11 and day 15 in culture.

Experimental solutions

Before recording, the culture medium was replaced by the external solution to be used during the recording which contained (in mM): NaCl 150, KCl 2.5, $CaCl_2$1.8, $MgCl_2$ 1, glucose 20 and HEPES-NaOH 10 pH 7.4. The internal solution used to fill the recording electrode in most experiments, internal solution 1, contained (in mM): Cs methanesulphonate 145, CsCl 15, $MgCl_2$ 1, EGTA 0.1, ATP-Mg 3, GTP-Na 0.3 and HEPES-CsOH 10 pH 7.2. A few experiments were also performed either with internal solution 2, containing (in mM): Cs methanesulphonate 130, CsCl 15, $MgCl_2$ 1, EGTA 10, $CaCl_2$ 1, ATP-Mg 3, GTP-Na 0.3 and HEPES-CsOH 10 (pH 7.2) or with internal solution 3, identical to solution 1 except that it did not contain EGTA and was supplemented with 10 μM $ZnCl_2$.

Drugs

Stock solutions of ICS-205,930 (3-tropanyl-indole-3-carboxylate hydrochloride, RBI) were prepared before use at 1 mM in distilled water. Stock solutions of propofol were prepared in DMSO, at either 60 or 180 mM. In all the experiments where its modulatory effects were tested, all the solutions applied by the fast perfusion system contained the same amount of DMSO (1/1000). A stock solution of $ZnCl_2$ (Sigma) was prepared at 50 mM in dilute HCl (2 mM) and kept at -20°C. Chlormethiazole edisylate was a gift from Astra and was diluted before use at 10 mM in water. A given stock solution of glycine (Sigma), prepared at 10 mM in distilled water and kept at -20°C, was used for several weeks.

Perfusion system

The culture dish was continuously perfused with the external solution. In addition, a fast perfusion system was used for rapid application of glycine and modulators. All solutions applied *via* this system contained tetrodotoxin (TTX) 0.2 μM. As previously explained, the fast perfusion system was made of two glass barrels and lateral movements of the two barrels were controlled by a computer-driven motor in order to apply the solution of the desired barrel to the cell; only one of the barrels contained glycine and the cell was continuously perfused with one of the solutions that could be applied by this system (either the control solution containing TTX or a solution also containing a modulator and/or glycine, see Chesnoy-Marchais, 1996 for more details concerning this perfusion system). All tubings were in Teflon, and traces of chemicals previously used were eliminated by extensive washing.

At the low concentrations of glycine used in most experiments (below 20 μM), successive responses recorded in the same solution were usually quite stable when tested every 40 s. Repetitive measurements of successive glycine responses at a fixed interval have been systematically performed in order to separate true modulatory effects from possible slow spontaneous changes in the response. When a high concentration of glycine was used (100–200 μM), the interval between successive tests was longer (100 s) in order to allow recovery from desensitization.

When a modulator of glycine responses was applied 'with preincubation', it was applied continuously between and during the successive glycine applications, that is in both barrels of the fast perfusion system; when applied 'without preincubation', it was present only in the glycine-containing barrel. In several experiments, ICS 205,930 was applied only during glycine applications, since its potentiating effect was previously shown to be identical whether it was applied without or with preincubation (see Figure 5b in Chesnoy-Marchais, 1996). ICS 205,930 has been preferred to the two other 5-HT_3 antagonists tested previously (LY 278,584 and MDL 72222; Chesnoy-Marchais, 1996) because it is active at much lower concentrations than LY 278,584 and because it is water-soluble and has faster effects than MDL 72222.

Recording

Patch-clamp micropipettes were made from hard glass (Kimax 51); the shank of each pipette was covered with Sylgard and the tip was fire-polished. The resistance of these electrodes filled with the usual internal solution was between 5 and 10 MΩ. The cells were voltage-clamped by an EPC7 List amplifier, controlled by a TANDON 38620 computer, *via* a Cambridge Electronic Design (CED) 1401 interface, using CED patch- and voltage-clamp software. The current monitor output of the amplifier was filtered at 0.3 kHz before being sampled on-line at 0.6 kHz. The bath was connected to the ground *via* an agar bridge. Membrane potentials were corrected for the junction potential of 10 mV amplitude that was measured between the recording pipette and the usual external solution.

The series resistance (*Rs*) was systematically measured several times during each experiment. Particular care was taken to eliminate experiments in which *Rs* changed suddenly. *Rs* was between 10 and 20 MΩ. These values are high enough to introduce a difference of a few mV between the voltage applied to the electrode and that actually applied to the inside of the cell (error of maximum 10 mV for the largest responses). Usually, no correction has been used to compensate for these errors. However, the current modulations observed occurred without any simultaneous change in *Rs* and thus cannot result from changes in the applied voltage.

The zero indicated on current traces is the absolute zero current level.

All values are expressed as mean $\pm$ s.d. (number of observations).

Results

Additivity of the potentiating effects of ICS 205,930 and Zn^{2+} on glycine responses

The effect of ICS 205,930 (0.2 μM) on the response to a low concentration of glycine (10 μM) was first tested during continuous application of Zn^{2+} at concentrations (5 or 10 μM)

known to induce the maximal potentiation that can be evoked by this ion (Laube *et al.*, 1995). Such an experiment is illustrated in Figure 1a and b and shows that coapplication of ICS 205,930 with glycine potentiated the response in the continuous presence of 5 μM Zn^{2+}; in the absence of ICS 205,930, increasing the concentration of Zn^{2+} during glycine applications from 5 to 10 μM did not affect the response, which confirmed that 5 μM was saturating for the rapid potentiating effect of these ions. The persistence of the potentiating effect of ICS 205,930 in the presence of Zn^{2+} was confirmed in experiments such as that illustrated in Figure 1c, where the effect of ICS 205,930 was successively tested on the same cell in the absence of Zn^{2+} and in the presence of Zn^{2+}. In three such experiments, using either 5 or 10 μM Zn^{2+}, the percentage of potentiation induced by ICS 205,930 was $98 \pm 29\%$ and $40 \pm 9\%$, in the absence and presence of Zn^{2+}, respectively.

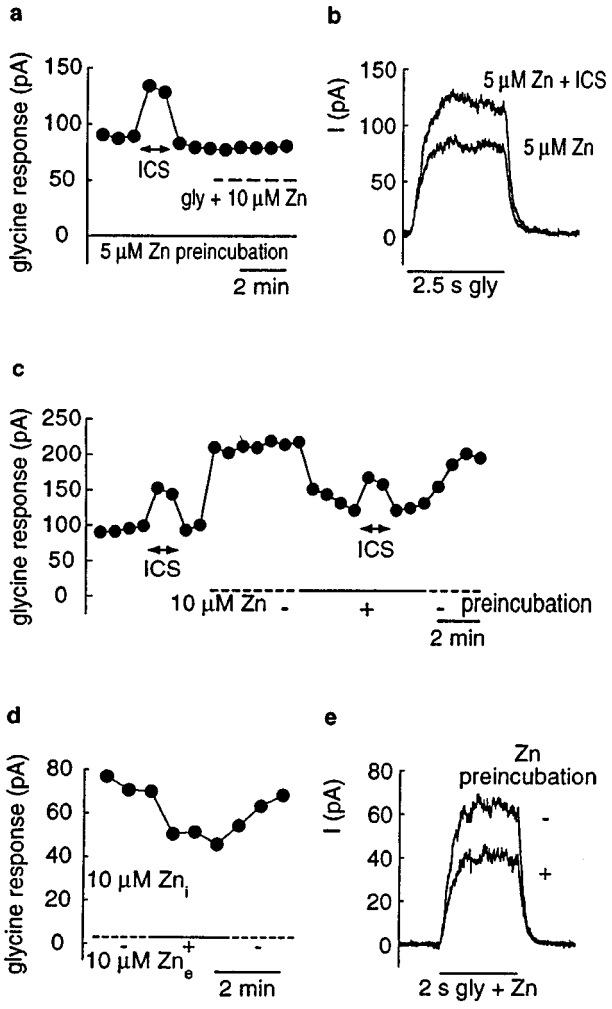

Figure 1 Potentiating effect of ICS 205,930 in the continuous presence of Zn^{2+} and inhibitory effect of Zn^{2+} preincubation on glycine responses. (a) Amplitude of successive peak responses to 10 μM glycine recorded at -30 mV, without or with 0.2 μM ICS 205,390, Zn^{2+} being initially applied at 5 μM both between and during glycine applications; then, the concentration of Zn^{2+} applied together with glycine was increased to 10 μM (which did not affect the response). (b) Mean of two glycine responses recorded in the continuous presence of 5 μM Zn^{2+}, without or with ICS 205,930 (same cell as in (a)). (c) Amplitude of successive peak responses to 10 μM glycine recorded at -30 mV in another cell, first in the absence of Zn^{2+}, then when Zn^{2+} was applied at 10 μM, either without or with preincubation; when indicated, ICS 205,930 was added to the corresponding glycine-containing solution. (d) Amplitude of successive peak responses of another neurone to simultaneous applications of 10 μM glycine and 10 μM Zn^{2+} at -30 mV using internal solution 3 (containing no EGTA and supplemented with 10 μM Zn^{2+}); 10 μM Zn^{2+} was applied in the external solution without or with preincubation, as indicated. (e) Mean of two current traces recorded in the same neurone without or with Zn^{2+} preincubation. Note that under the conditions used here, Zn^{2+} preincubation did not affect the current recorded in the absence of glycine (as shown in (e) by the superposition of the holding currents before glycine applications).

The experiment of Figure 1c also revealed an unexpected result: an inhibitory effect of Zn^{2+} preincubation. In six such experiments (performed at -30 mV with the usual internal solution 1) the response to the simultaneous application of glycine (10 μM) and Zn^{2+} (10 μM) was reduced by $45 \pm 8\%$ when Zn^{2+} (10 μM) was also added between the glycine pulses. This inhibitory effect of Zn^{2+} preincubation was slowly reversible. It was also observed below the reversal potential of glycine responses, at a holding potential of -90 mV (reduction by $29 \pm 5\%$ (4), using again 10 μM glycine, 10 μM Zn^{2+} and internal solution 1). In order to test the hypothesis according to which this inhibitory effect could result from an entry of Zn^{2+} into the cell, two types of experiments were performed. First, the concentration of EGTA in the internal solution was increased up to 10 mM (internal solution 2) in order to better buffer Zn^{2+} possibly entering into the cell. The inhibitory effect of preincubation with Zn^{2+} (10 μM) persisted (not illustrated), the degree of inhibition being of $36 \pm 8\%$ (4) after 9–15 min of cell dialysis with 10 mM EGTA. A second series of experiments was performed using internal solution 3 that contained no buffer of divalent ions and was already supplemented with 10 μM Zn^{2+}. Again, the inhibitory effect of Zn^{2+} preincubation persisted, as illustrated by Figures 1d–e: reduction of $44 \pm 6\%$ (4) by Zn^{2+} preincubation after 5–9 min of cell dialysis. These results indicate that the inhibitory effect of Zn^{2+} preincubation is not due to an entry of Zn^{2+} into the cells. Preincubation with 10 μM Zn^{2+} also reduced the peak responses to the simultaneous application of a high concentration of glycine (100 or 200 μM) and 10 μM Zn^{2+} (responses that were close to saturating, not shown); however the degree of inhibition induced in these experiments, $16 \pm 6\%$ (3) for responses to 200 μM glycine and Zn^{2+}, $22 \pm 5\%$ (6) for responses to 100 μM glycine and Zn^{2+}, was significantly smaller (Student's t-test $P < 0.0005$) than in the experiments using only 10 μM glycine.

In order to avoid the inhibitory effect of Zn^{2+} preincubations, the additional experiments designed to look for possible interferences between the potentiating effects of ICS 205,930 and Zn^{2+} were performed by applying both modulators without preincubation.

In a first series of experiments (performed at -30 mV), the effect of ICS 205,930 was tested on each cell both on the control response to glycine (10 μM) and when the same concentration of glycine was applied with Zn^{2+} (5 or 10 μM). The results from six cells (not illustrated) showed that ICS 205,930 potentiated the control response by $100 \pm 31\%$ and potentiated the response to the simultaneous application of glycine and Zn^{2+} by $41 \pm 14\%$. Thus, even though the potentiation was clear, it was smaller than that observed in the same cells in the absence of Zn^{2+}. The ratio of the percentage of potentiation induced by ICS 205,930 in the presence of Zn^{2+} over the percentage measured in the same cell in the absence of Zn^{2+} was 0.41 ± 0.05 (6), which is significantly different from 1 (Student's t-test, $P < 0.000005$).

Both the potentiating effect of Zn^{2+} (Laube *et al.*, 1995) and the potentiating effect of ICS 205,930 (Chesnoy-Marchais, 1996) are known to result from decreases in the EC_{50} for glycine without changes in the maximal response. In agreement

with these published observations, it was confirmed in four experiments that the responses to a high concentration of glycine (200 μM) were very little affected by the simultaneous application of ICS 205,930 (0.2 μM) and Zn^{2+} (10 μM): peak responses were enhanced by only $8 \pm 4\%$. In order to compare the potentiating effect of ICS 205,930 on responses of comparable amplitude without or with Zn^{2+}, a second series of experiments was performed in which the concentration of glycine was lower when applied with Zn^{2+} than in the absence of Zn^{2+}. The reduction was such that the response in the presence of Zn^{2+} had a size similar to that induced in the same cell by application of 10 μM glycine alone (Figure 2). In four such experiments, in which the responses obtained by applying 5 μM glycine together with 10 μM Zn^{2+} were very similar to the control responses obtained by applying 10 μM glycine alone ($90 \pm 14\%$ of these control responses), ICS 205,930 potentiated the responses to 10 μM glycine by $57 \pm 11\%$ whereas it potentiated the responses to 5 μM glycine plus 10 μM Zn^{2+} by $72 \pm 16\%$. Thus, the ability of ICS 205,930 to potentiate glycine responses of similar amplitudes was not significantly different in control and in the presence of a saturating concentration of Zn^{2+} (paired Student's t-test $P > 0.1$).

In four experiments, the potentiating effects of Zn^{2+} (1 or 10 μM) on responses to glycine were tested on the same cell at two membrane potentials (-90 mV and either -30 or -10 mV) and no voltage-dependence was detected (not illustrated). In contrast, the potentiating effect of ICS 205,930 was slightly but reproducibly more pronounced at -90 mV than at -30 mV: in 14 experiments (see also Chesnoy-Marchais, 1996) the response to glycine (15 or 20 μM) was alternately recorded on each cell at -90 and -30 mV, before, during and after a given application of ICS 205,930 (at either 0.1, 0.2 or 1 μM according to the experiment). The ratio of the response recorded in the presence of ICS 205,930 over the control response was 1.14 ± 0.07 (14) times higher at -90 mV than at -30 mV (which is significantly different from 1, paired Student's t-test, $P < 0.000005$).

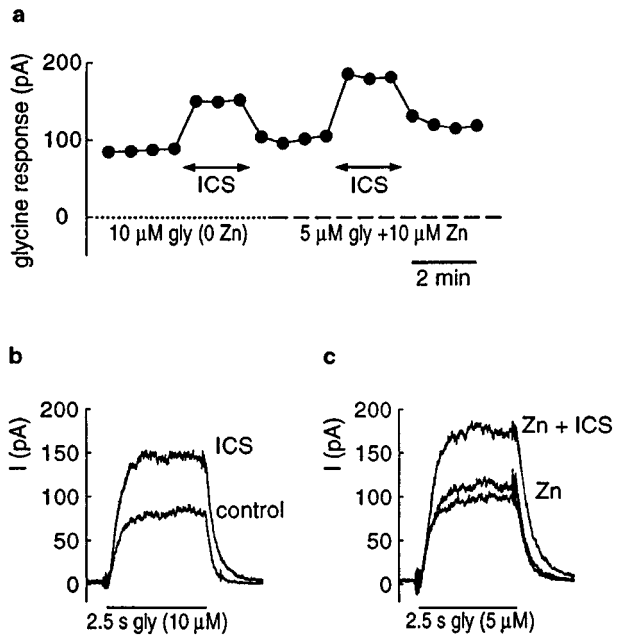

Figure 2 Comparison of the effects of ICS 205,930 on responses of similar amplitudes recorded in the absence or presence of Zn^{2+}. (a) Amplitude of successive peak responses to glycine recorded at -30 mV without or with 0.2 μM ICS 205,930, glycine being first applied at 10 μM without Zn^{2+}, then at 5 μM with 10 μM Zn^{2+}. (b) Mean of two responses to 10 μM glycine recorded in the absence of Zn^{2+}, without and with ICS 205,930. (c) Mean of two responses to 5 μM glycine recorded in the presence of 10 μM Zn^{2+}, without ICS 205,930 (before and after its application) and with ICS 205,930. (a), (b) and (c) from the same cell.

Potentiating effect of ICS 205,930 in the presence of 200 mM ethanol

As already observed by other authors (see Introduction) and shown by Figures 3a and b, ethanol can potentiate responses to low concentrations of glycine. The potentiation of glycine responses has been reported to increase with the concentration of ethanol (Aguayo & Pancetti, 1994; Mascia *et al*., 1996a,b) and it does not seem possible to saturate this effect. Despite this limitation, a few experiments were performed in order to determine whether or not the presence of a high concentration of ethanol (200 mM) would impair the potentiating effect of ICS 205,930 on glycine responses. As illustrated by Figures 3c and d, in the continuous presence of 200 mM ethanol, the responses to 10 μM glycine were still potentiated by 0.2 μM ICS 205,903, by $78 \pm 28\%$ (5). The mean potentiation observed in the absence of ethanol from a large number of other cells was of $91 \pm 34\%$ (27) (see Discussion).

Potentiating effect of ICS 205,930 in the presence of high concentrations of propofol

The intravenous general anaesthetic propofol is known to induce several effects in neurones. Propofol potentiates the chloride responses to subthreshold concentrations of GABA (see Sanna *et al*., 1995 and references therein) and is one of the few agents known as able to potentiate glycine responses (see Hales & Lambert, 1991 for spinal neurones; see Mascia *et al*.,

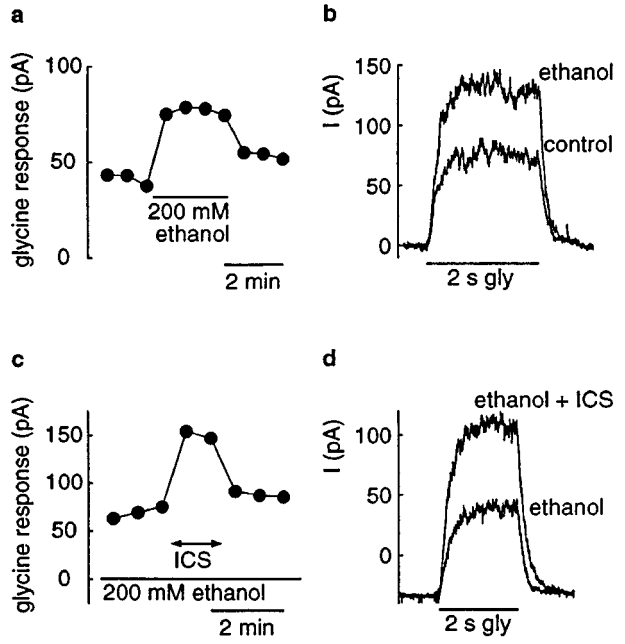

Figure 3 High concentrations of ethanol potentiate glycine responses and do not prevent the potentiating effect of ICS 205,930. (a) and (b) Potentiating effect of 200 mM ethanol (applied continuously) on the response to 10 μM glycine recorded at -10 mV. (a) Amplitude of successive peak responses. (b) Mean of four responses recorded with or without ethanol (two before, two after ethanol application). (c) and (d) Persistence of the potentiating effect of 0.2 μM ICS 205,930 on the response to 10 μM glycine recorded in another cell at -30 mV in the continuous presence of 200 mM ethanol. (c) Amplitude of successive peak responses. (d) Mean of two responses recorded with or without ICS 205,930 (one before, one after ICS 205,930 application).

1996a and Pistis *et al*., 1997 for cloned glycine receptors). In chromaffin cells (Hales & Lambert, 1991), hippocampal neurones (Hara *et al*., 1993; Orser *et al*., 1994) and hypothalamic neurones (Adodra & Hales, 1995), propofol has also been shown to activate a chloride conductance in the absence of GABA and glycine, and since this effect could be partly blocked by addition of bicuculline, it was interpreted as resulting, at least partly, from the direct activation of $GABA_A$ receptors.

Initial experiments performed in ventral spinal cord neurones confirmed the ability of propofol to potentiate glycine responses and to activate a chloride conductance. The lowest concentrations of propofol (between 0.5 and 1 μM) inducing a detectable potentiation of responses to 10 μM glycine already induced an increase in chloride conductance in the absence of glycine (not shown). Thus, in order to estimate the potentiating effect of higher concentrations of propofol on glycine responses, propofol had to be applied both in the absence and presence of glycine. Initially, glycine responses were measured at a constant holding potential, different from the chloride equilibrium potential. It appeared that, under such conditions, the reversal potential of glycine responses could be appreciably modified by chloride fluxes through the large conductance activated by propofol in the absence of glycine, which prevented a reliable estimation of the potentiating effect of propofol on the glycine-induced conductance. Therefore, the protocol was modified in order to minimize the propofol-activated chloride fluxes and to better control the reversal potential. In order to reduce the conductance directly activated by propofol, bicuculline (10 μM) was added in all the solutions applied by the fast perfusion; this was not sufficient however to induce a complete blockade (see Discussion). Thus, in addition, the holding potential was set close to the reversal potential of the propofol-induced current, and the conductance in the absence of glycine and during the glycine responses was measured by using either voltage-jumps (see Figure 4a) or brief voltage ramps (see Figures 4d–f) which allowed direct measurement of reversal potentials. Using these methods, it was possible to reliably measure glycine responses in the continuous presence of high concentrations of propofol (30–90 μM) and to study the effects of the addition of ICS 205,930 (0.2 μM) after a maximal potentiation by propofol. Note that in these experiments, ICS 205,930 was applied both between and during glycine applications, in order to look for possible modifications of the conductance recorded with propofol in the absence of glycine. In several experiments, the addition of ICS 205,930 in the presence of propofol induced a very small conductance increase in the absence of glycine (not shown), which was taken into account when measuring glycine responses in the simultaneous presence of propofol and ICS 205,930.

Figure 4a illustrates the effects of 30 and 60 μM propofol on the response to glycine and on the conductance measured in the absence of glycine (see figure legend). The glycine response was potentiated by 362±43% by 30 μM propofol in three similar experiments and increasing the propofol concentration from 30 to 60 μM did not have a significant additional effect either on glycine responses (see also Figure 4c) or on the conductance measured in the absence of glycine (see also Figure 4f). The experiment illustrated by Figure 4b shows that ICS 205,930 clearly potentiated the response to a low concentration of glycine in the continuous presence of a very high concentration (90 μM) of propofol (for clarity only the currents recorded at the test potential are displayed).

The results of an experiment using voltage ramps, alternately applied in the absence and presence of glycine in different solutions, are illustrated by Figures 4c–f. Glycine responses were measured during the ramps (after subtraction of the corresponding traces obtained in the absence of glycine) first in the absence of any modulator, then in the presence of

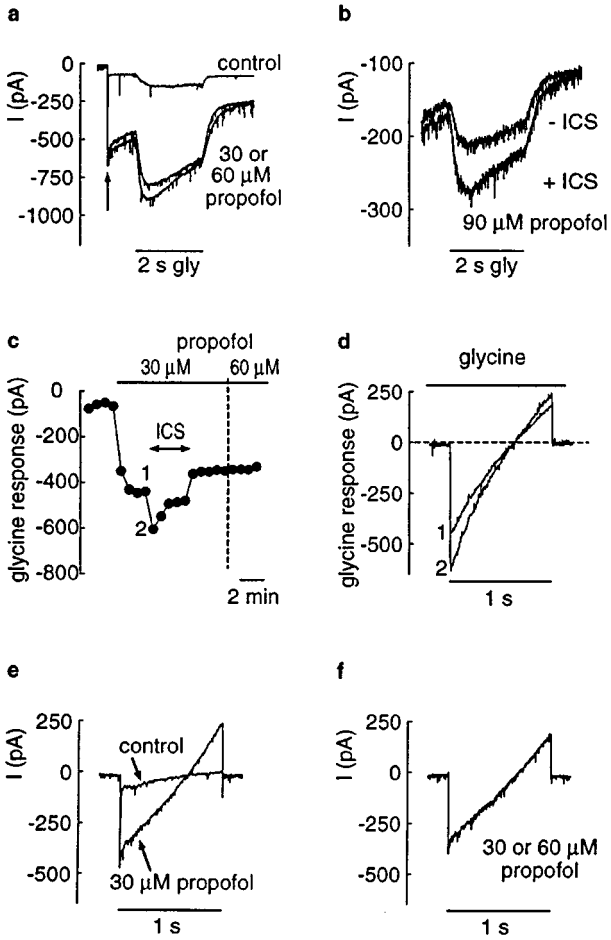

Figure 4 High concentrations of propofol, which increase the leak currents and glycine responses, do not prevent the potentiating effect of ICS 205,930. (a) Current traces recorded in the absence of propofol and in the continuous presence of either 30 or 60 μM propofol, during voltage jumps from −52 to −92 mV (regularly applied for 4 s every 40 s), 10 μM glycine being systematically applied at −92 mV. The conductance of the neurone in the absence of glycine is shown by the instantaneous current change induced by the voltage jump. (b) Current traces recorded at −95 mV in the absence or continuous presence of 0.2 μM ICS 205,930 in another cell continuously perfused with 90 μM propofol, 5 μM glycine being regularly applied as in (a) (that is every 40 s, 900 ms after the beginning of each voltage jump, from −55 to −95 mV for this cell). (c) and (d) Persistence of the potentiating effect of 0.2 μM ICS 205,930 in the presence of a saturating concentration of propofol. (c) Amplitude of successive responses to 10 μM glycine measured close to −90 mV (after subtraction of the leak current) in a cell held at −50 mV to which voltage ramps from −90 to −30 mV were alternately applied in the absence and presence of glycine; propofol was continuously applied at either 30 μM or 60 μM as indicated; ICS 205,930 was also continuously applied during the arrow. (d) Records corresponding to the points indicated in (c), obtained during the voltage ramps, after subtraction of the corresponding traces recorded in the absence of glycine; the application of glycine began 1.3 s before the ramp and, as expected, the response was not detectable at the holding potential (that was close to the chloride equilibrium potential). (e) and (f) Leak current traces recorded in the same cell in the absence of glycine, (e) at the beginning of the experiment either without or with 30 μM propofol, (f) in the presence of either 30 or 60 μM propofol (two traces superimposed). In these experiments, all the solutions applied by the fast perfusion contained TTX, a final dilution of 1/1000 DMSO and 10 μM bicuculline.

30 μM propofol (trace 1 in Figure 4d), then in the presence of both 30 μM propofol and 0.2 μM ICS 205,930, which further potentiated the response without changing the reversal potential (trace 2 in Figure 4d); finally, after wash of ICS 205,903, the propofol concentration was increased to 60 μM, and this did not affect the response. Current traces recorded during the ramps applied in the absence of glycine are also illustrated (Figures 4e and f); addition of 30 μM propofol induced a clear conductance increase (despite the presence of bicuculline, Figure 4e), and increasing the propofol concentration to 60 μM did not further affect the conductance in the absence of glycine (Figure 4f, two traces superimposed).

The results (confirmed in several other experiments using 5 μM glycine and a propofol concentration of either 30 μM (three cells) or 90 μM (four cells including that of Figure 4b) clearly show that ICS 205,930 remains capable of potentiating glycine responses in the presence of concentrations of propofol which were saturating both for the potentiation of glycine responses and for the direct conductance activation by this anaesthetic.

Chlormethiazole does not affect glycine responses

In order to study possible interferences between the effects of ICS 205,930 and chlormethiazole, experiments were first performed to confirm the ability of this anticonvulsant to potentiate glycine responses. Surprisingly (see Introduction), 50 μM chlormethiazole (applied either continuously or only with glycine) did not affect the responses to glycine (10 μM) in six different cells (Figures 5a and b). However, the leak current recorded in these cells in the absence of glycine was systematically increased by chlormethiazole, as indicated by the slight reversible increase in outward current observed above E_{Cl} (Figures 5b and c). Chlormethiazole potentiated the responses of the same neurones to a low concentration (2.5 μM) of GABA (Figures 5d and e; potentiation of $124 \pm 6\%$ in three similar experiments). The inability of chlormethiazole to affect glycine responses (on either side of E_{Cl}) was confirmed by using a higher concentration (100 μM) in seven additional cells, continuously perfused with bicuculline (5 μM) in order to block GABA responses and to prevent the leak current increase usually induced by chlormethiazole (Figure 5f). Figure 5f also shows that, as expected, the continuous presence of chlormethiazole and bicuculline did not affect the ability of ICS 205,930 to potentiate the responses of these cells to glycine, a result confirmed in four similar experiments.

Discussion

In the first part of the present paper, it has been shown that the potentiating effect of ICS 205,930 on responses to low concentrations of glycine persists in the presence of high concentrations of Zn^{2+} (5 or 10 μM), whatever the method used for Zn^{2+} applications (with or without preincubation). From the study of Laube *et al.* (1995), these concentrations were known to be saturating for their potentiating effect, either in spinal neurones (Zn^{2+} ions being then applied without preincubation) or in *Xenopus* oocytes expressing $\alpha 1$, $\alpha 1\beta$ or $\alpha 2$ receptors (Zn^{2+} being then applied with a preincubation of 15 s). This has been confirmed by the present results (Figure 1a). Even though the potentiating effect of ICS 205,930 was shown to persist in the presence of Zn^{2+}, the percentage of

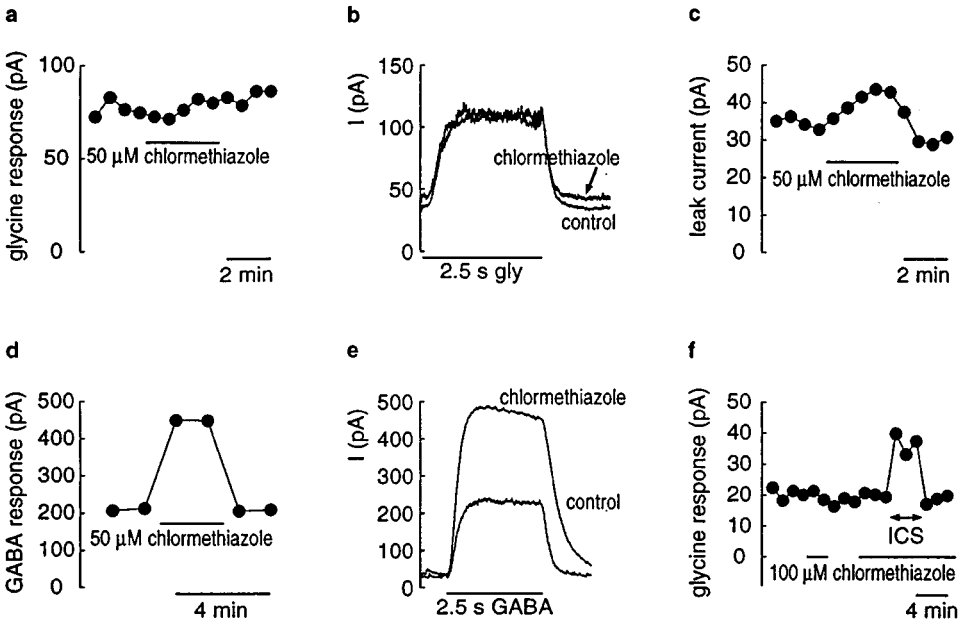

Figure 5 High concentrations of chlormethiazole, increasing the leak current and potentiating GABA responses, do not affect glycine responses and do not prevent the potentiating effect of ICS 205,930. (a), (b) and (c) from a same experiment. (a) Amplitude of successive peak response to 10 μM glycine recorded at -20 mV in an experiment during which 50 μM chlormethiazole was applied with preincubation. (b) Mean of four glycine responses recorded with or without chlormethiazole (two before, two after the chlormethiazole application). (c) Current recorded in the absence of glycine at -20 mV; note the small reversible increase in outward current induced by chlormethiazole (that was also visible in (b) before or after the glycine application). (d) and (e) Experiment showing that the same chlormethiazole concentration potentiated the responses to 2.5 μM GABA (same culture, -30 mV). (d) Amplitude of successive peak GABA responses. (e) Mean of two GABA responses recorded without or with chlormethiazole. (f) Amplitude of successive peak responses to 10 μM glycine recorded at -30 mV in another cell continuously perfused with 5 μM bicuculline; neither of the two applications of 100 μM chlormethiazole (with preincubation) affected the response, whereas 0.2 μM ICS 205,930 applied with preincubation during the second test of chlormethiazole did potentiate the response, without affecting the current recorded in the absence of glycine (not illustrated).

increase of the response to a given concentration of glycine was lower in the presence than in the absence of Zn^{2+}. This apparent reduction of the potentiating effect of ICS 205,930 results from the fact that both ICS 205,930 and Zn^{2+} potentiate glycine responses by increasing the apparent affinity of the receptors for glycine. Indeed, the percentage of increase induced by ICS 205,930 became very similar in the absence and presence of Zn^{2+} when the controls used were responses of identical amplitudes, either to glycine alone (10 μM) or to an equipotent mixture of a lower concentration of glycine plus 10 μM Zn^{2+} (Figure 2). These results show that the sites of action of ICS 205,930 and Zn^{2+} are different. This conclusion is also in agreement with the observation that potentiating effect of ICS 205,930 shows a slight (but reproducible) voltage-sensitivity, which is lacking in the potentiating effect of Zn^{2+} (despite the presence of a larger positive charge), as previously noticed in other neurones (Kumamoto & Murata, 1996; Trombley & Shepherd, 1996) and as expected if the site involved is extracellular (Laube *et al*., 1995).

During the comparison of the potentiating effects of ICS 205,930 and Zn^{2+}, the existence of an inhibitory effect of Zn^{2+} on glycine responses (Bloomenthal *et al*., 1994; Laube *et al*., 1995) was confirmed. In previous investigations, when these ions were applied on spinal neurones without preincubation, their inhibitory effect had been detected only with very high concentrations (above 100 μM: see Figure 1b in Laube *et al*., 1995). The present study has shown that preincubation with Zn^{2+} already reveals a pronounced inhibitory effect of these ions at 10 μM (see for example Figure 1c). The strong effect of preincubation with Zn^{2+} ions might have resulted from their slow entry into the neurones, since various routes of entry for these ions have been described in neurones (see for example Sensi *et al*., 1997). Several experiments, using different internal solutions (containing either a buffer for divalent ions or a high concentration of Zn^{2+}, see Figures 1d and e) have shown that the inhibitory effect of Zn^{2+} preincubation does not result from an entry of Zn^{2+}. It probably results from the existence of a second binding site for these ions that is only slowly accessible: this site would not be occupied by Zn^{2+} during the short applications of low concentrations of glycine and Zn^{2+} used in the present study (of a few seconds duration), but would be occupied when Zn^{2+} is applied between these applications (here, during at least 30 s). Zn^{2+} preincubation also showed a slight inhibitory effect on the peak response to high concentrations of glycine applied with Zn^{2+}; however, since this effect was smaller than the inhibitory effect observed when using only 10 μM glycine and Zn^{2+}, some competition between glycine and Zn^{2+} could account, at least partly, for the inhibitory effect of Zn^{2+} preincubation. Further studies will be necessary to better characterize the mechanism responsible for this inhibitory effect. The Zn^{2+}-sensitivity of responses to glycine recorded in some neuronal preparations, such as septal cholinergic neurones (Kumamoto & Murata, 1996) or olfactory bulb neurones (Trombley & Shepherd, 1996), in particular the absence of inhibitory effects of Zn^{2+} below 100 μM in these studies, has been used to support the idea that the glycine receptors expressed in the corresponding neurones are different from those previously studied in spinal neurones and from α1- or α2-containing receptors expressed in *Xenopus* oocytes. These data, obtained without Zn^{2+} preincubation, should now be reconsidered taking into account the strong influence of the protocol used (presence or absence of Zn^{2+} preincubation) on the Zn^{2+}-sensitivity of glycine responses (as revealed by the present study).

Various compounds which potentiate glycine responses also act, like Zn^{2+} and ICS 205,930, by shifting the dose-response curve for glycine to the left. This has been shown for some alcohols, including ethanol (Mascia *et al*., 1996a,b; Ye *et al*., 1998) and for an intravenous general anaesthetic, propofol (Pistis *et al*., 1997). Note that the behavioural action of propofol has been shown to involve its effect on glycine receptors: for example Mascia *et al*. (1997) showed that the difference in sleep time induced by administration of propofol between two lines of mice, the 'long-sleep' mice and the 'short-sleep' mice, is correlated with a genetic difference in propofol-sensitivity of their glycine receptors (without any difference in propofol-sensitivity of their $GABA_A$ receptors). As discussed below, the results obtained in the present study indicate that ICS 205,930 acts on glycine receptors at a site different from the site(s) of action of either ethanol or propofol.

In the presence of 200 mM ethanol, ICS 205,930 remained able to increase the response to 10 μM glycine (Figure 3). It can be argued that the concentration of ethanol used was not saturating for the potentiation of glycine responses and indeed, one cannot exclude that higher concentrations of ethanol would interfere with the site of action of ICS 205,930. It was shown above, in the case of Zn^{2+}, that the degree of potentiation induced by ICS 205,930 (for a given concentration of glycine) can be lowered by another potentiator that also shifts to the left the dose-response curve for glycine. One might have expected such a result in the case of ethanol. However, the experiments concerning the effect of ICS 205,930 in the presence of ethanol did not include tests of the effect of ICS 205,930 on the same cells in the absence of ethanol; thus, because of the variability of the effect of ICS 205,930 among different cells (already reported in Chesnoy-Marchais, 1996), these experiments did not exclude the possible reduction by ethanol of the degree of potentiation induced by ICS 205,930. These experiments merely showed the persistence of a significant potentiating effect of ICS 205,930 in the presence of ethanol. The strong variability of the effect of ICS 205,930 among different cells is unlikely to result from variations between individual dose-response curves for glycine (in view of previous results obtained from these neurones and in view of the absence of pronounced difference in the EC_{50} for glycine between different types of recombinant glycine receptors; see for example Pribilla *et al*., 1992); preliminary results obtained in *Xenopus* oocytes expressing recombinant glycine receptors (given by Pr. H. Betz) indicate that this variability is more likely to result from a different ICS 205,930-sensitivity of the different types of glycine receptors expressed in cultured neurons (unpublished results obtained in collaboration with S. Supplisson).

In the case of propofol, it was shown that even at very high concentrations, which were saturating for the potentiation of glycine responses, this anaesthetic did not prevent the potentiating effect of ICS 205,930 (Figure 4). Thus, propofol and ICS 205,930 also seem to potentiate glycine responses by different mechanisms. The results obtained in the present study have confirmed in native neurones the initial observation by Hales & Lambert (1991) of the potentiating effect of propofol on glycine responses. In agreement with the recent demonstration (Pistis *et al*., 1997) that propofol induces a shift to the left of the dose-response curve for glycine, the potentiations induced by propofol in the present study, using 5–10 μM glycine, were much larger than those observed in the initial study (Hales & Lambert, 1991) using 100 μM glycine. It was also confirmed that whereas ICS 205,930 does not affect the basal conductance in the absence of glycine (Chesnoy-Marchais, 1996), propofol markedly increases this conductance, even in the presence of bicuculline, known to block most responses involving $GABA_A$ receptors. The bicuculline-

resistant conductance increase induced by propofol could result from the activation of bicuculline-resistant $GABA_A$ receptors in the absence of GABA, such as some homomeric β receptors (Sanna *et al*., 1995; Krishek *et al*., 1996; see also Davies *et al*., 1997) and/or from the activation of some glycine receptors in the absence of glycine (Pistis *et al*., 1997). This last hypothesis could explain why in several experiments performed in the presence of propofol, ICS 205,930 induced a small conductance increase in the absence of glycine: this compound might have potentiated the basal activity of glycine receptors induced by propofol in the absence of glycine. In agreement with the results obtained in the present study, even in cases where bicuculline was reported to 'suppress' the propofol-induced current, the blockade induced by 10 or 20 μM bicuculline was not complete (see Figure 3 in Hara *et al*., 1993, where the propofol concentration was only 20 μM). As explained in the Results section, the large conductance increase induced by propofol in the absence of neurotransmitter made the experiments concerning propofol particularly difficult. Some of the difficulties encountered, such as the progressive change of the baseline current and the imperfect stability of the responses to glycine applications in the presence of propofol, could not be avoided. These changes may result partly from desensitization-like effects, as shown in hippocampal neurones for the baseline current induced by propofol (Hara *et al*., 1993) and as suggested by the fact that $GABA_A$ responses can be desensitized by preincubations with high concentrations of propofol (Orser *et al*., 1994). Thus, with the methods used in the present study, it would not have been reasonable to try to perform a more quantitative study of possible interferences between the potentiating effects of propofol and ICS 205,930. However, the data obtained indicate that these two drugs act by different mechanisms.

Contrary to some previous observations (Gent & Wacey, 1983; Hales & Lambert, 1992), chlormethiazole could not potentiate responses to glycine in the present study. Several possibilities could explain this apparent discrepancy. As already pointed out (Hales & Lambert, 1992), the potentiating effect of chlormethiazole previously reported might result from an effect on glycine uptake mechanisms rather than from a direct effect on glycine receptors. It is also possible that chlormethiazole has a direct potentiating effect on some subtypes of glycine receptors that would be different from those which are predominant in the preparation used in the present study. Such a subunit selectivity could explain the previously noticed variability in the degree of potentiation induced by chlormethiazole on the electrical activity of brainstem neurones (Gent & Wacey, 1983).

In conclusion, it has been shown that ICS 205,930 is a novel type of potentiator of glycine responses. Not only is it efficient at remarkably low concentrations without affecting the resting conductance, but it also uses a site that is different from the site(s) responsible for the potentiating effects of several other modulators.

This work was supported by CNRS (URA 1857) and by the European Commission (BMH4-CT97-2374). I wish to thank P. Ascher and J.S. Kehoe for helpful advice and D. Lévy for culturing the cells. I also wish to thank Astra France Production for having kindly provided chlormethiazole.

References

ADODRA, S. & HALES, T.G. (1995). Potentiation, activation and blockade of $GABA_A$ receptors of clonal murine hypothalamic GT1-7 neurones by propofol. *Br. J. Pharmacol.,* **115,** 953 – 960.

AGUAYO, L.G. & PANCETTI, F.C. (1994). Ethanol modulation of the γ-aminobutyric $acid_A$- and glycine-activated Cl^- current in cultured mouse neurons. *J. Pharmacol. Exp. Ther.,* **270,** 61 – 69.

AKAGI, H., MAJIMA, T., HIRAI, K. & HISHINUMA, F. (1993). Extracellular zinc ion increases Cl^- currents generated through cloned glycine receptor channels expressed in Xenopus oocytes. *Neurosci. Res.,* **18,** S45.

BLOOMENTHAL, A.B., GOLDWATER, E., PRITCHETT, D.B. & HARRISON, N.L. (1994). Biphasic modulation of the strychnine-sensitive glycine receptor by Zn^{2+}. *Mol. Pharmacol.,* **46,** 1156 – 1159.

CELENTANO, J.J., GIBBS, T.T. & FARB, D.H. (1988). Ethanol potentiates GABA- and glycine-induced chloride currents in chick spinal cord neurons. *Brain Res.,* **455,** 377 – 380.

CHESNOY-MARCHAIS, D. (1996). Potentiation of chloride responses to glycine by three 5-HT_3 antagonists in rat spinal neurons. *Br. J. Pharmacol.,* **118,** 2115 – 2125.

DAVIES, P.A., KIRKNESS, E.F. & HALES, T.G. (1997). Modulation by general anaesthetics of rat $GABA_A$ receptors comprised of $\alpha1\beta3$ and $\beta3$ subunits expressed in human embryonic kidney 293 cells. *Br. J. Pharmacol.,* **120,** 899 – 909.

DOWNIE, D.L., HALL, A.C., LIEB, W.R. & FRANKS, N.P. (1996). Effects of inhalational general anaesthetics on native glycine receptors in rat medullary neurones and recombinant glycine receptors in Xenopus oocytes. *Br. J. Pharmacol.,* **118,** 493 – 502.

GENT, J.P. & WACEY, T.A. (1983). The effects of chlormethiazole on single unit activity in rat brain; interactions with inhibitory and excitatory neurotransmitters. *Br. J. Pharmacol.,* **80,** 439 – 444.

HALES, T.G. & LAMBERT, J.J. (1991). The actions of propofol on inhibitory amino acid receptors of bovine adrenomedullary chromaffin cells and rodent central neurones. *Br. J. Pharmacol.,* **104,** 619 – 628.

HALES, T.G. & LAMBERT, J.J. (1992). Modulation of $GABA_A$ and glycine receptors by chlormethiazole. *Eur. J. Pharmacol.,* **210,** 239 – 246.

HARA, M., KAI, Y. & IKEMOTO, Y. (1993). Propofol activates $GABA_A$ receptor-chloride ionophore complex in dissociated hippocampal pyramidal neurons of the rat. *Anesthesiology,* **79,** 781 – 788.

HARRISON, N.L., KUGLER, J.L., JONES, M.V., GREENBLATT, E.P. & PRITCHETT, D.B. (1993). Positive modulation of human gamma-aminobutyric acid type A and glycine receptors by the inhalation anesthetic isoflurane. *Mol. Pharmacol.,* **44,** 628 – 632.

HILL-VENNING, C., BELELLI, D., PETERS, J.A. & LAMBERT, J.J. (1997). Subunit-dependent interaction of the general anaesthetic etomidate with the γ-aminobutyric acid type A receptor. *Br. J. Pharmacol.,* **120,** 749 – 756.

KRASOWSKI, M.D., KOLTCHINE, V.V., RICK, C.E., YE, Q., FINN, S.E. & HARRISON, N.L. (1998). Propofol and other intravenous anesthetics have sites of action on the γ-aminobutyric acid type A receptor distinct from that of isoflurane. *Mol. Pharmacol.,* **53,** 530 – 538.

KRISHEK, B.J., MOSS, S.J. & SMART, T.G. (1996). Homomeric $\beta1$ γ-aminobutyric $acid_A$ receptor-ion channels: evaluation of pharmacological and physiological properties. *Mol. Pharmacol.,* **49,** 494 – 504.

KUMAMOTO, E. & MURATA, Y. (1996). Glycine current in rat septal cholinergic neurons in culture: monophasic positive modulation by Zn^{2+}. *J. Neurophysiol.,* **76,** 227 – 241.

LAUBE, B., KUHSE, J., RUNDSTRÖM, N., KIRSCH, J., SCHMIEDEN, V. & BETZ, H. (1995). Modulation by zinc ions of native rat and recombinant human inhibitory glycine receptors. *J. Physiol.,* **483,** 613 – 619.

MACDONALD, R.L. & OLSEN, R.W. (1994). $GABA_A$ receptor channels. *Ann. Rev. Neurosci.,* **17,** 569 – 602.

MASCIA, M.P., BLECK, V.G. & HARRIS, R.A. (1997). Glycine receptors from long-sleep and short-sleep mice: genetic differences in drug sensitivity. *Mol. Brain Research,* **45,** 169 – 172.

MASCIA, M.P., MACHU, T.K. & HARRIS, R.A. (1996a). Enhancement of homomeric glycine receptor function by long-chain alcohols and anaesthetics. *Br. J. Pharmacol.,* **119,** 1331 – 1336.

MASCIA, M.P., MIHIC, S.J., VALENZUELA, C.F., SCHOFIELD, P.R. & HARRIS, R.A. (1996b). A single amino acid determines differences in ethanol actions on strychnine-sensitive glycine receptors. *Mol. Pharmacol.,* **50,** 402–406.

MIHIC, S.J., YE, Q., WICK, M.J., KOLTCHINE, V.V. KRASOWSKI, M.D., FINN, S.E., MASCIA, M.P., VALENZUELA, C.F., HANSON, K.K., GREENBLATT, E.P., HARRIS, R.A. & HARRISON, N.L. (1997). Sites of alcohol and volatile anaesthetic action on $GABA_A$ and glycine receptors. *Nature,* **389,** 385–389.

ORSER, B.A., WANG, L.-Y., PENNEFATHER, P.S. & MACDONALD, J.F. (1994). Propofol modulates activation and desensitization of $GABA_A$ receptors in cultured murine hippocampal neurons. *J. Neurosci.,* **14,** 7747–7760.

PISTIS, M., BELELLI, D., PETERS, J.A. & LAMBERT, J.J. (1997). The interaction of general anaesthetics with recombinant $GABA_A$ and glycine receptors expressed in Xenopus laevis oocytes: a comparative study. *Br. J. Pharmacol.,* **122,** 1707–1719.

PRIBILLA, I., TAKAGI, T., LANGOSCH, D., BORMANN, J. & BETZ, H. (1992). The atypical M2 segment of the β subunit confers picrotoxinin resistance to inhibitory glycine receptor channels. *EMBO J.,* **11,** 4305–4311.

SANNA, E., GARAU, F. & HARRIS, R.A. (1995). Novel properties of homomeric $\beta 1$ γ-aminobutyric acid type A receptors: actions of the anesthetics propofol and pentobarbital. *Mol. Pharmacol.,* **47,** 213–217.

SENSI, S.L., CANZONIERO, L.M.T., YU, S.P., YING, H.S., KOH, J.Y., KERCHNER, G.A. & CHOI, D.W. (1997). Measurement of intracellular free zinc in living cortical neurons: routes of entry. *J. Neurosci.,* **17,** 9554–9564.

TROMBLEY, P.Q. & SHEPHERD, G.M. (1996). Differential modulation by zinc and copper of amino acid receptors from rat olfactory bulb neurons. *J. Neurophysiol.,* **76,** 2536–2546.

WAKAMORI, M., IKEMOTO, Y. & AKAIKE, N. (1991). Effects of two volatile anaesthetics and a volatile convulsant on the excitatory and inhibitory amino acid responses in dissociated CNS neurons of the rat. *J. Neurophysiol.,* **66,** 2014–2021.

WHITING, P.J., MCKERNAN, R.M. & WAFFORD, K.A. (1995). Structure and pharmacology of vertebrate $GABA_A$ receptor subtypes. *Int. Rev. Neurobiol.,* **38,** 95–138.

YE, Q., KOLTCHINE, V.V., MIHIC, S.J., MASCIA, M.P., WICK, M.J., FINN, S.E., HARRISON, N.L. & HARRIS, R.A. (1998). Enhancement of glycine receptor function by ethanol is inversely correlated with molecular volume at position $\alpha 267$. *J. Biol. Chem.,* **273,** 3314–3319.

ZHANG, Z.-W. & BERG, D.K. (1995). Patch-clamp analysis of glycine-induced currents in chick ciliary ganglion neurons. *J. Physiol.,* **487,** 395–405.

(Received July 13, 1998
Revised November 4, 1998
Accepted November 20, 1998)

British Journal of Pharmacology (1999) 126, 810–818
http://www.stockton-press.co.uk/bjp

Signalling by CXC-chemokine receptors 1 and 2 expressed in CHO cells: a comparison of calcium mobilization, inhibition of adenylyl cyclase and stimulation of GTPγS binding induced by IL-8 and GROα

*,[1]David A. Hall, [1]Isabel J.M. Beresford, [1]Christopher Browning & [1]Heather Giles

[1]Receptor Pharmacology Unit, Glaxo Wellcome Medicines Research Centre, Gunnels Wood Road, Stevenage, Herts SG1 2NY, England, U.K.

1 The effect of interleukin-8 (IL-8) and growth-related oncogene α (GROα) on [^{35}S]-guanosine 5′-*O*-(3-thiotriphosphate) ([^{35}S]GTPγS) binding, forskolin-stimulated cyclic AMP accumulation and cytosolic calcium concentration were determined in recombinant CHO cells expressing HA-tagged CXC-chemokine receptors 1 and 2 (CXCR1 and CXCR2).

2 Radioligand binding assays confirmed that the binding profiles of the recombinant receptors were similar to those of the native proteins. IL-8 displaced [^{125}I]-IL-8 binding to CXCR1 and CXCR2 with pK_i values of 8.89 ± 0.05 and 9.27 ± 0.03, respectively. GROα, a selective CXCR2 ligand, had a pK_i value of 9.66 ± 0.39 at CXCR2 but a $pK_i > 8$ at CXCR1. Calcium mobilization experiments were also consistent with previous reports on native receptors.

3 Activation of both receptors resulted in stimulation of [^{35}S]GTPγS binding and inhibition of adenylyl cyclase.

4 A comparison of the functional data at CXCR1 showed that a similar potency order (IL-8 > > GROα) was obtained in all three assays. However, at CXCR2 whilst the potency orders for calcium mobilization and inhibition of adenylyl cyclase were similar (IL-8 ≥ GROα), the order was reversed for stimulation of [^{35}S]GTPγS binding (GROα > IL-8).

5 All of the functional responses at both receptors were inhibited by pertussis toxin (PTX), suggesting coupling to a Gi/Go protein. However, the calcium mobilization induced by IL-8 at CXCR1 was not fully inhibited by PTX, suggesting an interaction with a G-protein of the Gq family. Our results with pertussis toxin also suggested that, in the [^{35}S]GTPγS binding assay, CXCR1 displays some constitutive activity.

6 Thus, we have characterized the binding and several functional responses at HA-tagged CXCRs 1 and 2 and have shown that their pharmacology agrees well with that of the native receptors. We also have preliminary evidence that CXCR1 displays constitutive activity in our cell line and that CXCR2 may traffic between different PTX sensitive G-proteins.

Keywords: Interleukin-8; GROα; chemokine receptors; [^{35}S]GTPγS binding

Abbreviations: B_{max}, the maximal level of binding; BSA, bovine serum albumin; cyclic AMP, cyclic adenosine monophosphate; CHO cells, Chinese hamster ovary cells; CXCR1 and 2, CXC-chemokine receptors 1 and 2; DMEM F-12, a 1 : 1 mixture of Dulbecco's modified Eagle medium and HAMS F-12 nutrient mixture; DMSO, dimethylsulphoxide; EDTA, ethylenediaminetetraacetic acid; EGTA, [ethylene-bis(oxyethylenenitrilo)]tetraacetic acid; FBS, foetal bovine serum; GROα, growth-related oncogene α; GTPγS, guanosine 5′-O-(3-thiotriphosphate); HA-tagged, haemagglutinin-tagged; HEPES, N-2-hydroxyethylpiperazine-N′-ethanesulphonic acid; IBMX, isobutylmethylxanthine; IL-8, interleukin-8; PBS, phosphate buffered saline; PTX, pertussis toxin; SPA, scintillation proximity assay; WGA, wheat-germ agglutinin

Introduction

The chemokines are a group of proteins which act as leukocyte chemotactic factors. They can be divided into two main families on the basis of the relative positions of the first two of four conserved cysteine residues (Power & Wells, 1996). In the CXC chemokines, these cysteines are separated by an intervening amino acid residue, whilst in the CC-chemokines they are adjacent. Interleukin-8 (IL-8) and the related peptide, growth-related oncogene α (GROα) (also termed melanocyte growth stimulatory activity, MGSA), are members of the CXC-chemokine family and are potent chemotactic factors for neutrophils (Baggiolini & Clark-Lewis, 1992). The effects of IL-8 on human neutrophils are mediated by two receptors, CXC-chemokine receptors 1 and 2 (CXCR1 and 2); previously known as IL-8 receptors A and B. CXCR1 is highly selective for IL-8, virtually all of the other CXC-chemokines having much lower binding affinities and functional potencies at this receptor (e.g. Lee *et al*., 1992; Petersen *et al*., 1994; Ahuja & Murphy, 1996). CXCR2 is less ligand selective than CXCR1, being a receptor for IL-8 and a number of other CXC-chemokines (including GROα), all of which contain the sequence glu-leu-arg (ELR) immediately preceding the first of the conserved cysteine residues (Loetscher *et al*., 1994; Petersen *et al*., 1994; Ahuja & Murphy, 1996). CXC-chemokines without this ELR sequence appear to lack activity at CXCR1 and CXCR2 (Petersen *et al*., 1996; Clark-Lewis *et al*., 1993; Proost *et al*., 1993).

*Author for correspondence.

The functional significance of the presence of two receptors for IL-8 on human neutrophils is as yet unclear, for example mouse neutrophils possess only one CXCR (Lee *et al*., 1995), and there appears to be a large degree of overlap between the signalling pathways activated by the two receptors. In recombinant systems, activation of either receptor induces chemotaxis and calcium mobilization (Lee *et al*., 1992; Loetscher *et al*., 1994; Wu *et al*., 1996). Both receptors have also been shown to be able to couple to both pertussis toxin (PTX) sensitive and insensitive G-proteins (of the Gq family) when co-transfected into COS7 cells (Wu *et al*., 1993). However, responses to IL-8 and GROα in human neutrophils, including chemotaxis and calcium mobilization, are markedly inhibited by PTX (Bacon & Camp, 1990; Thelen *et al*., 1988; Wuyts *et al*., 1997), suggesting either that the PTX sensitive pathways are predominant or that there is synergy between the PTX sensitive and insensitive signalling mechanisms. Interestingly, in neutrophils, whilst both IL-8 and GROα induce calcium mobilization and chemotaxis (Walz *et al*., 1991; Schroder *et al*., 1990), only IL-8 is able to activate phospholipase D (L'Heureux *et al*., 1995), implying some signalling specificity for CXCR1 (or its co-activation with CXCR2). Also, calcium mobilization in response to IL-8 and GROα appears to occur through different mechanisms: GROα has been reported to cause the influx of extracellular calcium as well as release of calcium from intracellular stores (Damaj *et al*., 1996b), whilst in the same study IL-8 was only able to elicit intracellular store release. One study using blocking antibodies selective for either CXCR1 or CXCR2 has suggested that the major receptor for IL-8 on the human neutrophil is CXCR1 (Hammond *et al*., 1995). In this study, an anti-CXCR2 antibody virtually abolished chemotaxis to GROα, whilst only weakly affecting that to IL-8, whereas an anti-CXCR1 antibody markedly inhibited chemotaxis in response to IL-8 but had no significant effect on that to GROα.

Whilst the signalling pathways activated in response to stimulation of CXCR1 and CXCR2 have been studied to some extent, there have been few reports in which systematic pharmacological comparisons have been made between agonists at either receptor. In the present study we have examined the binding of IL-8 and GROα to haemagglutinin (HA)-tagged CXCR1 and CXCR2 expressed in Chinese hamster ovary (CHO) cells and have compared the abilities of these agonists to elicit a number of functional responses. Calcium mobilization was measured as this assay has been widely used to study the activation of CXCRs (see above) and was, therefore, used to assess the authenticity of the pharmacology of the tagged receptors. Also, calcium mobilization is thought to be involved in a number of neutrophil responses (Maxfield, 1993, Sengelov *et al*., 1993). We have also determined the ability of the agonists to inhibit forskolin-stimulated cyclic adenosine monophosphate (cyclic AMP) accumulation and to stimulate [^{35}S]-guanosine 5′-O-(3-thiotriphosphate) (GTPγS) binding. CXCRs have been shown to couple to Gi proteins (Wu *et al*., 1993; Damaj *et al*., 1996a) and would thus be expected to inhibit forskolin-stimulated cyclic AMP accumulation in CHO cells. The inhibition of adenylyl cyclase is thought to be mediated by the α-subunit of Gi proteins whilst PTX sensitive calcium mobilization is generally thought to involve the activation of phospholipase C-β isoforms by the βγ-subunit (Morris & Scarlata, 1996). The measurement of both of these responses will, therefore, allow the comparison of two signal transduction events occurring at different points along the transduction pathways arising from the activation of the same G-protein. Stimulation of [^{35}S]GTPγS binding measures one of the first signalling events initiated by G-protein coupled receptors and it was, therefore, of interest to compare it with the other two functional assays. This assay also has the advantage of being a functional assay which can be performed on membrane preparations in a radioligand binding format.

Methods

Cell culture

CHO-K1 cells were transfected with cDNA encoding CXCR1 or CXCR2 (derived from human neutrophils) using previously published methods (Solari *et al*., 1997). The cells were grown at 37°C in a 5% CO_2 atmosphere in a 1 : 1 mixture of Dulbecco's modified Eagle medium and HAMS F-12 nutrient mixture (DMEM F-12) containing 10% foetal bovine serum (FBS), 2 mM L-glutamine and 300 μg ml^{-1} geneticin (to maintain selection pressure). Cells were passaged every 3–4 days. Untransfected CHO cells were grown in the same medium but in the absence of geneticin.

Measurement of increases in cytosolic calcium concentration

Confluent 175-cm^2 flasks of cells were harvested by treatment with 5 mM ethylenediaminetetraacetic acid (EDTA) in phosphate buffered saline ((mM) NaCl 137, KCl 2.7, KH_2PO_4 1.5, Na_2HPO_4 8) (PBS-EDTA) followed by centrifugation at $500 \times g$ for 5 min. The cell pellet was resuspended in 10 ml HEPES-saline ((mM) NaCl 145, KCl 5, $MgCl_2$ 1, $CaCl_2$ 1, glucose 10, N-2-hydroxyethylpiperazine-N′-ethanesulphonic acid (HEPES) 10, 2 mg ml^{-1} bovine serum albumin (BSA), 2.5 mM probenecid (to prevent export of fura2 from the cells; Edelman *et al*., 1994), pH 7.4) and the resulting cell suspension was incubated at 37°C for 45 min in the presence of 4 μM fura2-AM. The fura2-loaded cells were then centrifuged at $500 \times g$ for 5 min and resuspended at 3×10^5 ml in HEPES-saline. The cells were maintained at 37°C and aliquots were transferred to a Perkin-Elmer LS50 fluorimeter for calcium measurement. The response was measured as the ratio of emitted light intensities at 510 nm after alternate excitation at 340 or 380 nm (Grynkiewicz *et al*., 1985). The fluorescence intensity ratios were calibrated as previously described (Hall & Hourani, 1993). In experiments using PTX, the medium in the culture flask was replaced with fresh medium or fresh medium containing 100 ng ml^{-1} PTX 16–20 h prior to harvesting the cells.

Responses were quantified as the maximal increase in cytosolic calcium concentration after addition of agonist. Concentration-response curves were analysed by fitting the data with a four parameter logistic equation to determine pEC_{50} values and maximal increases in cytosolic calcium concentration.

Measurement of cyclic AMP accumulation

Cells were seeded into 96-well plates and incubated (37°C) in culture medium for 16–20 h before the medium was replaced with DMEM F-12 (160 μl) containing 300 μM isobutylmethylxanthine (IBMX), a phosphodiesterase inhibitor. After incubation for 60 min at 37°C, forskolin (final concentration 10 μM, which had been shown in control experiments to be the EC_{50}) and appropriate concentrations of chemokines were added in 40 μl of DMEM F-12 containing 0.5% dimethylsulphoxide (DMSO). The final DMSO concentration in all

wells was 0.1%. Cyclic AMP was allowed to accumulate for 15 min, after which the assay was terminated by aspiration of the medium and addition of 200 μl ice-cold 95% ethanol. The cells were incubated at 4°C for 45 min and 25 μl aliquots of the ethanol extract were transferred to 96-well scintillation proximity assay (SPA) plates and dried under a stream of air. The dry extract was then dissolved in 25 μl of cyclic AMP assay buffer (as provided with the Amersham kit) and the cyclic AMP content was determined using an Amersham scintillation proximity assay (SPA) kit, following the manufacturer's instructions. The cyclic AMP content of each sample was corrected to give the amount of cyclic AMP (pmol) per well.

In experiments using PTX, the cells were seeded into 96-well plates and incubated for 4 h at 37°C in culture medium to allow them to adhere. The medium was then replaced with fresh medium alone or fresh medium containing 100 ng ml^{-1} of PTX and the cells incubated for a further 16 h and treated as described above.

Concentration-response curves were fitted with four-parameter logistic equations to obtain estimates of the pEC_{50}, maximal inhibition and Hill coefficient. For pooling of concentration-response curves, the data were converted to percentage inhibitions of the forskolin control after subtraction of cyclic AMP accumulation in the presence of IBMX alone.

Measurement of GTPγS binding in cell membrane preparations

The optimization of this assay protocol has previously been reported (Hall *et al*., 1998).

For preparation of cell membranes, cells were harvested from confluent 850-cm^2 roller bottles by treatment with PBS-EDTA and centrifugation at $500 \times g$ for 5 min. The cell pellet was resuspended in homogenization buffer ((mM) HEPES 20, EDTA 1, [ethylene-bis(oxyethylenenitrilo)]tetraacetic acid (EGTA) 1, $MgCl_2$ 6, pH 7.4) and the cells left to swell on ice for 20 min before homogenization in a Waring blender (3×15 s, with 2 min incubation on ice between each bout). The homogenate was centrifuged at $1000 \times g$ for 10 min and the resulting supernatant was centrifuged at $48{,}000 \times g$ for 20 min at 4°C. The supernatant was discarded and the pellet was resuspended in 5 ml homogenization buffer per roller bottle. The membrane suspension was then frozen in aliquots at −80°C until required. The protein concentration was determined by the Bradford method using BSA as a standard.

For measurement of agonist-stimulated GTPγS binding, membranes from CHO-CXCR1 (25 μg protein ml^{-1}) or CHO-CXCR2 (50 μg protein ml^{-1}) were incubated in GTPγS binding buffer ((mM) HEPES 20, $MgCl_2$ 10, NaCl 100, pH 7.4) at 30°C for 20 min in the presence of GDP (10 μM). Agonists were added and followed 10 min later by [^{35}S]GTPγS (100 pM). The total volume was 250 μl. The reaction was allowed to proceed for 20 min, with shaking, before the mixture was harvested through Whatman GF/C filters on a Brandel cell harvester. The filters were washed four times with 1 ml of ice cold milliQ water, transferred to scintillation vials, soaked in 4 ml of scintillation fluid overnight and the bound radioactivity determined by liquid scintillation counting. Non-specific binding was determined in the presence of 100 μM GTP. In experiments using PTX, cells were treated with 100 ng ml^{-1} of toxin for 16 h prior to membrane preparation.

After subtraction of non-specific binding, the raw d.p.m. data were fitted with four parameter logistic equations. When the data were pooled, the [^{35}S]GTPγS bound in the presence of agonist was divided by that in the absence of agonist and is presented as a percentage of the basal.

Radioligand binding assays

Membranes were prepared as described for GTPγS binding assays above. The radioligand binding experiments were performed using a SPA protocol. Membranes (10 or 100 μg protein for CXCR1 or CXCR2, respectively) were mixed with 0.5 mg wheat-germ agglutinin (WGA) SPA bead and increasing concentrations of [^{125}I]IL-8 (for saturation binding assays) or 50 pM [^{125}I]IL-8 and increasing concentrations of unlabelled IL-8 or GROα (for competition experiments). The plates were incubated at room temperature for 8 h and counted on a Microbeta plate counter. The total assay volume was 100 μl. Non-specific binding was determined in the presence of 100 or 10 nM unlabelled IL-8 for CXCR1 and CXCR2, respectively. Saturation binding data were analysed by directly fitting the sum of a rectangular hyperbola and a straight line to the total binding data. Competition binding data were analysed by fitting the data with a four parameter logistic equation.

Statistics

All statistical comparisons were made using Student's *t*-test unpaired, P values less than 0.05 were considered significant.

Materials

IL-8 was obtained from the Geneva Biomedical Research Institute. GROα was purchased from Peprotech EC Ltd. Fatty acid-free BSA, DMEM F-12, EDTA, EGTA, FBS, fura2-AM, guanine nucleotides, HEPES, IBMX, PTX and probenecid were obtained from Sigma. [^{35}S]GTPγS (1250 Ci mmol^{-1}) was obtained from NEN, [^{125}I]IL-8 (2000 Ci mmol^{-1}), Biotrak SPA cyclic AMP assay kits and WGA SPA beads were from Amersham International. SPA plates were from Wallac. Geneticin was from Gibco BRL and L-glutamine was from Hyclone. Protein assay dye reagent was obtained from BioRad. All other reagents were AnalaR grade from BDH.

Results

Calcium mobilization

There was no significant difference between the potencies of IL-8 at CXCR1 and CXCR2 in the calcium mobilization assay (Figure 1, Table 1), however, IL-8 did induce a significantly greater maximal increase in calcium concentration in the CHO-CXCR1 cells (Figure 1, Table 1). GROα was a full agonist at CXCR2 (Figure 1b, Table 2), inducing a maximal increase in calcium concentration which was not significantly different from that of IL-8 in these cells. The potency of GROα at CXCR2 was not significantly different from that of IL-8. However, GROα had a low potency at CXCR1, only consistently mobilizing calcium at concentrations greater than 100 nM (Figure 1a). Treatment with PTX (100 ng ml^{-1}, 16 h) effectively abolished calcium mobilization in response to IL-8 in the CHO-CXCR2 cells (Figure 1d). However, PTX-treated CHO-CXCR1 cells were still responsive to IL-8 (Figure 1c) with a pEC_{50} of 7.20 ± 0.11 ($n = 3$), which was more than 60 fold less potent than in untreated cells, and a significantly reduced maximal increase in cytosolic calcium concentration (180 ± 44 nM, $n = 3$). The effect of IL-8 (up to 10 μM) in

untransfected CHO cells was indistinguishable from that of the vehicle (water) control (data not shown).

Cyclic AMP accumulation

IL-8 potently inhibited forskolin-stimulated cyclic AMP accumulation in both CHO cell lines, causing greater than 90% inhibition in both cases (Figure 2a,b, Table 1). IL-8 was slightly (3.3 fold) but significantly more potent in CHO-CXCR1 than in the CXCR2 cells. In the CXCR1 cells, GROα showed no significant inhibitory activity at up to 100 nM (Figure 2a), but it caused a potent inhibition of forskolin-stimulated cyclic AMP accumulation in the CXCR2 cells (Figure 2b, Table 2). The potency and maximal inhibitory effect of GROα in CXCR2 cells were not significantly different from those of IL-8. Treatment of either cell line with PTX completely abolished IL-8 mediated inhibition of forskolin-stimulated cyclic AMP accumulation. In the PTX treated cells, there appears to be a slight stimulation of cyclic AMP production at high concentrations of IL-8 (Figure 2c and d), however, this effect was not statistically significant. Also, in the absence of forskolin, IL-8 (up to 1 μM) was without effect on cyclic AMP levels in PTX-treated cells (data not shown). There was no effect of IL-8 on forskolin-stimulated cyclic AMP accumulation in untransfected CHO cells (data not shown).

GTPγS binding

IL-8 induced marked increases in GTPγS binding in membranes prepared from both CHO-CXCR1 and -CXCR2 cells (Figure 3a,b, Table 1). IL-8 was 320 fold more potent at CXCR1 than CXCR2 in this assay. However, interestingly, the maximal stimulation of binding in CHO-CXCR2 membranes was significantly greater than that in CHO-CXCR1. GROα was significantly (approximately 3 fold) more potent than IL-8

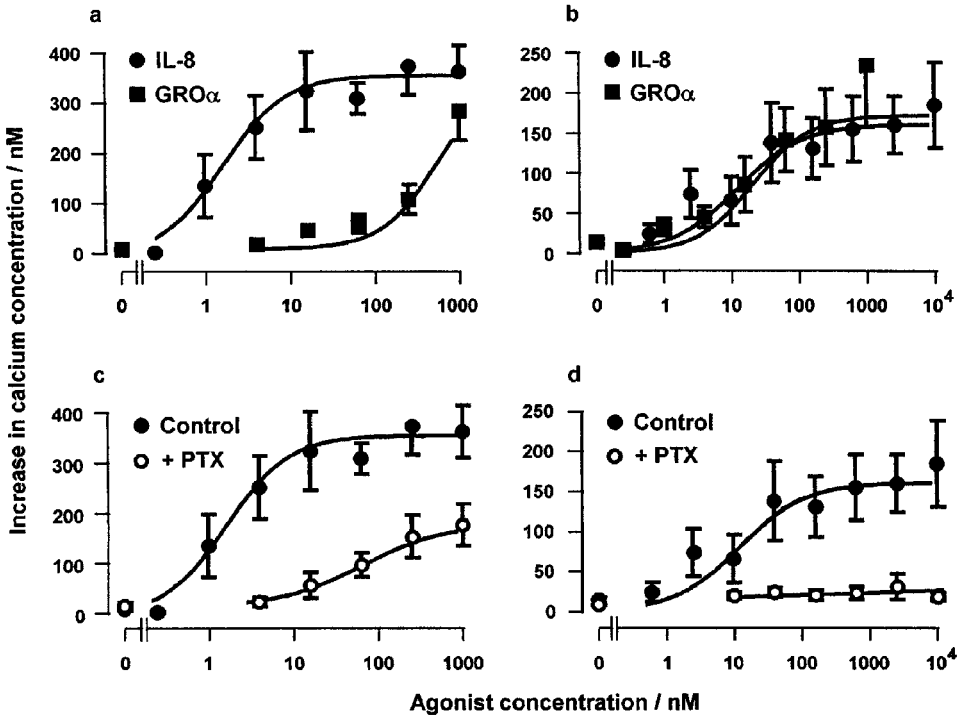

Figure 1 Effect of IL-8 and GROα on cytosolic calcium concentration in CHO-CXCR1 (a) or CHO-CXCR2 (b) cells or of IL-8 in control or PTX-treated CHO-CXCR1 (c) or CHO-CXCR2 (d). Values are the means±s.e.mean of three separate determinations. Vertical bars show the s.e.mean. The curves plotted through the data points are four parameter logistic equations fitted to the mean data.

Table 1 The pEC_{50} or pK_i values, E_{max} values and Hill coefficients (n_H) for IL-8 in the functional and binding assays at CXCR1 and CXCR2

	CXCR1			*CXCR2*		
Assay	*pEC_{50}/pK_i* (n)†	*E_{max}**	*n_H*	*pEC_{50}/pK_i* (n)†	*E_{max}**	*n_H*
Calcium	8.70±0.23 (3)	364±43	1.33±0.23	7.91±0.34 (3)	175±43	0.88±0.33
Cyclic AMP	8.66±0.16 (8)	95.2±0.7	1.29±0.16	8.14±0.10 (11)	94.1±1.5	1.05±0.12
GTPγS	8.64±0.11 (9)	266±17	1.20±0.08	6.15±0.05 (7)	600±48	0.85±0.06
Binding	8.89±0.05 (3)	100	0.99±0.02	9.27±0.03 (3)	100	0.92±0.04

*E_{max} for the different assays refers to the maximal increase in cytosolic calcium concentration (in nM), the maximal percentage inhibition of forskolin-stimulated cyclic AMP accumulation or the maximal increase in [^{35}S]GTPγS binding (as a percentage of the basal level of binding). In the binding assays IL-8 was used to estimate the non-specific binding and therefore, by definition, caused a maximum of 100% displacement.
†The number of replicate determinations.

at CXCR2, but was more than two orders of magnitude less potent than IL-8 in CXCR1 membranes (Figure 3a,b, Table 2). In the CXCR2 membranes, the maximal response to GROα was not well defined, however, the maximal response from the fitted curves was not significantly different from that of IL-8 suggesting that GROα was a full agonist. No response to IL-8 was seen in PTX-treated membranes from either cell line (Figure 3c and d). Interestingly, there was a significantly lower basal level of [^{35}S]GTPγS binding in the PTX-treated CXCR1 membranes than in the untreated control membranes. There was no response to IL-8 in membranes from untransfected CHO cells (not shown).

Radioligand binding

[^{125}I]IL-8 bound saturably to membranes from both CHO-CXCR1 and -CXCR2 (data not shown). At CXCR1 the pK_D was 9.64 ± 0.03, the Hill coefficient was 1.17 ± 0.01 and the maximal level of binding (B_{max}) was estimated as 20 ± 2 pmol.mg protein^{-1}; at CXCR2 the pK_D was 9.41 ± 0.03, the Hill coefficient was 0.95 ± 0.02 and the B_{max} was estimated as 1.1 ± 0.1 pmol.mg protein^{-1}. These B_{max} estimates indicate that the CHO-CXCR1 cell line was expressing an 18 fold greater density of receptors than CHO-CXCR2.

Table 2 The pEC_{50} or pK_i values, E_{max} values and Hill coefficients (n_H) for GROα in the functional and binding assays at CXCR1 and CXCR2

	CXCR1			*CXCR2*		
Assay	*pEC_{50}/pK_i* (n)†	*E_{max}**	*n_H*	*pEC_{50}/pK_i* (n)†	*E_{max}**	*n_H*
Calcium	<7 (3)	–	–	7.51±0.12 (3)	185±32	1.04±0.37
Cyclic AMP	<7 (3)	–	–	7.73±0.15 (3)	89.6±3.8‡	1.19±0.26
GTPγS	<7 (3)	–	–	6.60±0.05 (3)	612.8±115	1.30±0.18
Binding	<8 (3)	–	–	9.66±0.39 (3)	104.5±5.4	0.99±0.05

*E_{max} for the different assays refers to the maximal increase in cytosolic calcium concentration (in nM), the maximal percentage inhibition of forskolin-stimulated cyclic AMP accumulation, the maximal increase in [^{35}S]GTPγS binding (as a percentage of the basal level of binding) or the maximal percentage inhibition of specific [^{125}I]-IL-8 binding. Due to the incomplete curves obtained for GROα at CXCR1 it was not possible to determine maximal effects (or Hill coefficients) at this receptor.
†The number of replicate determinations.
‡The effect of the highest concentration of GROα in these experiments was not significantly different from that of a maximally active concentration of IL-8, therefore the GROα curves were constrained to the IL-8 maximum.

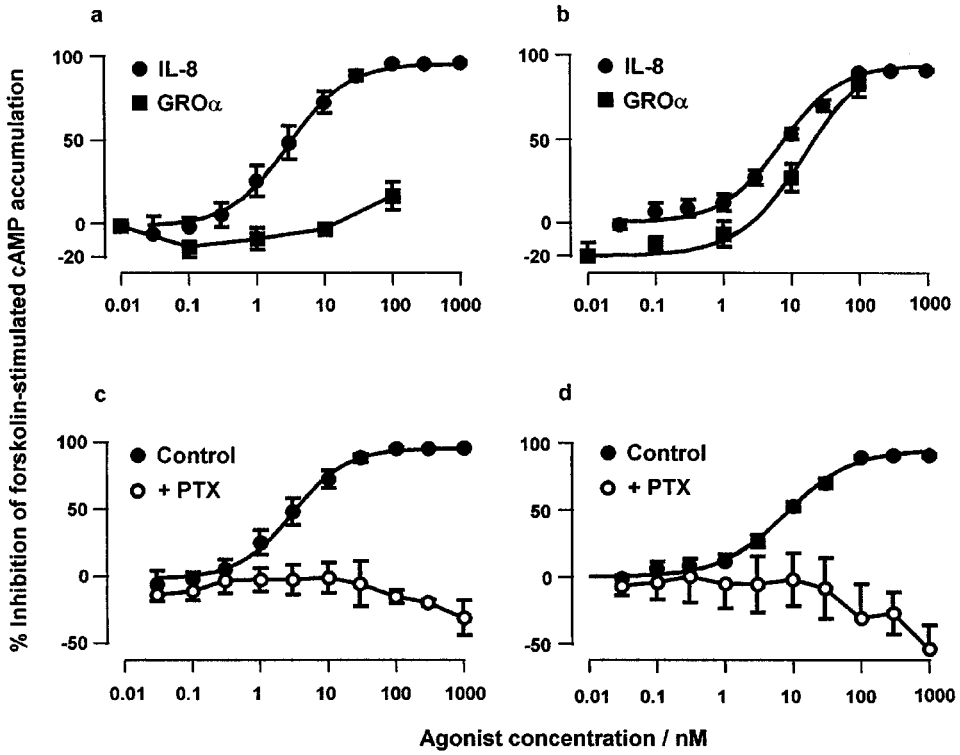

Figure 2 Effect of IL-8 and GROα on forskolin-stimulated cyclic AMP accumulation in CHO-CXCR1 (a) or CHO-CXCR2 (b) cells or of IL-8 in control or PTX-treated CHO-CXCR1 (c) or CHO-CXCR2 (d). Values are the means±s.e.mean of 3–11 separate determinations in duplicate. Vertical bars show the s.e.mean. The curves plotted through the data points are four parameter logistic equations fitted to the mean data.

The data from competition binding assays with IL-8 and GROα are summarized in Tables 1 and 2 and illustrated in Figure 4. The affinity of IL-8 was greater at CXCR2 than CXCR1. The affinity of GROα was similar to that of IL-8 at CXCR2 but markedly less at CXCR1.

Discussion

In this study we have compared the ability of IL-8 receptors to interact with two commonly measured signalling systems, calcium mobilization and cyclic AMP production, and their ability to stimulate [^{35}S]GTPγS binding, one of the earliest measurable consequences of receptor activation.

[^{125}I]IL-8 bound saturably to both cell lines with affinities in the nanomolar range. The estimated B_{max} values should be treated with caution as they were obtained using an agonist radioligand and in a SPA format. However, the data do suggest a higher density of receptor in the CXCR1 compared to the CXCR2 cells. Competition binding experiments confirmed that the affinities of the recombinant receptors for IL-8 and GROα were similar to those reported by others both in recombinant cell lines and in neutrophils (Ahuja & Murphy, 1996; Lee *et al*., 1992; Loetscher *et al*., 1994; Wu *et al*., 1996), all of which were in the low nanomolar range. Similarly, the potency orders of these peptides (IL-8 > > GROα at CXCR1; IL-8 ≈ GRO-α at CXCR2) in our calcium mobilization experiments are consistent with their potencies for the mobilization of calcium and the induction of chemotaxis in recombinant cells (Ahuja *et al*., 1996; Loetscher *et al*., 1994). Both of these observations suggest that the HA-tagged receptors in these cell lines exhibit native pharmacology.

IL-8-induced calcium mobilization at both receptors was sensitive to PTX. This is consistent with the effect of PTX in neutrophils and indicates that the calcium mobilization in our cell lines was predominantly mediated by Gi/Go proteins (and presumably therefore by the βγ subunit). There was, however, a residual calcium mobilization in response to IL-8 after PTX treatment in CHO-CXCR1. This is unlikely to be due to the use of an insufficiently high concentration of toxin as the concentration used (100 ng ml^{-1}) was sufficient to fully block the inhibition of cyclic AMP accumulation and stimulation of [^{35}S]GTPγS binding in these cells. The PTX insensitive component of the response is likely therefore to represent an interaction with a PTX-insensitive class of G-protein, presumably of the Gq family. The ability of both CXCR1 and CXCR2 to interact with several members of the Gq family, when co-expressed in COS7 cells, has been reported (Wu *et al*., 1996). It is not clear why CXCR2 was unable to couple to the PTX insensitive pathway in our cell line. It may represent a difference in the coupling of the two receptors in CHO cells, however, CHO-CXCR2 expresses a lower density of receptor than CHO-CXCR1. If the receptors interact with relatively low efficiency with this pathway (as seems to be the case from the much lower EC_{50} of IL-8 at CXCR1 after PTX treatment), then the level of receptor present in CHO-CXCR2 may be insufficient to activate it. The maximal response to IL-8 in CHO-CXCR1 was larger than that in CHO-CXCR2 (see Table 1) but it is interesting to note that the size of the PTX-sensitive component of the response in the CXCR1 cells (~184 nM) is similar to that induced by IL-8 in CHO-CXCR2 (175±43 nM), which was fully PTX-sensitive. This may imply that the PTX-sensitive pathways activated by these two receptors are similar.

The relative agonist potencies in the cyclic AMP accumulation assays were similar to those in the calcium mobilization assays. However, in contrast with the calcium response, inhibition of adenylyl cyclase by IL-8 was abolished by PTX

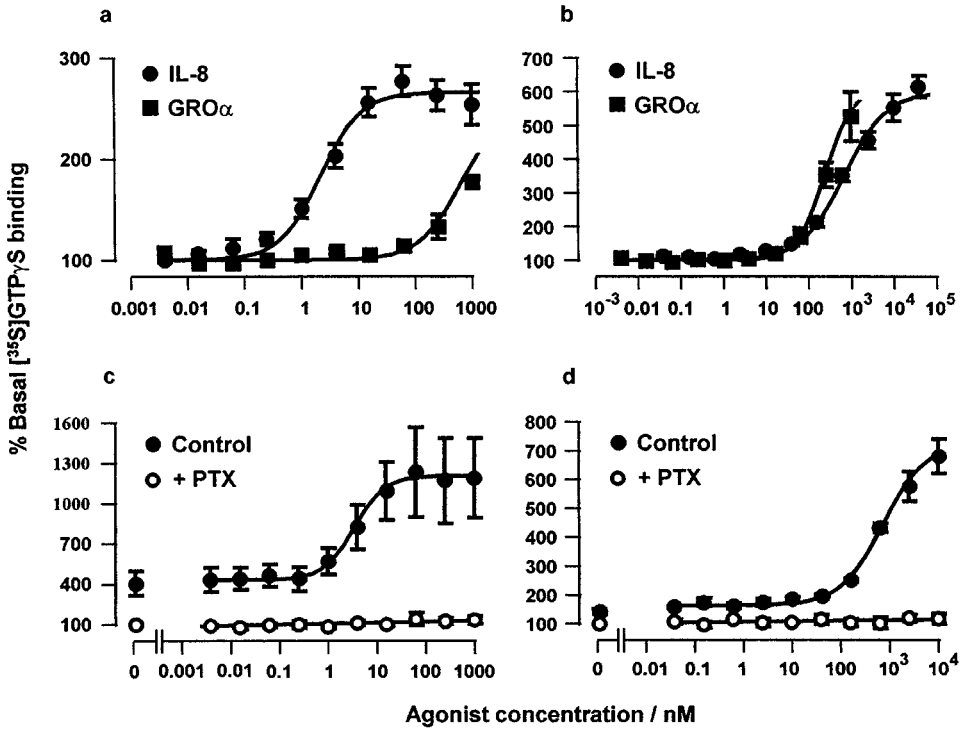

Figure 3 Effect of IL-8 and GROα on the binding of [^{35}S]GTPγS to membranes from CHO-CXCR1 (a) or CHO-CXCR2 (b) cells or of IL-8 in control or PTX-treated CHO-CXCR1 (c) or CHO-CXCR2 (d) membranes. Values are the means±s.e.mean of 3–9 separate determinations in duplicate. Vertical bars show the s.e.mean. In (c) and (d) the values are presented as a percentage of the basal in the PTX-treated membranes. The curves plotted through the data points are four parameter logistic equations fitted to the mean data.

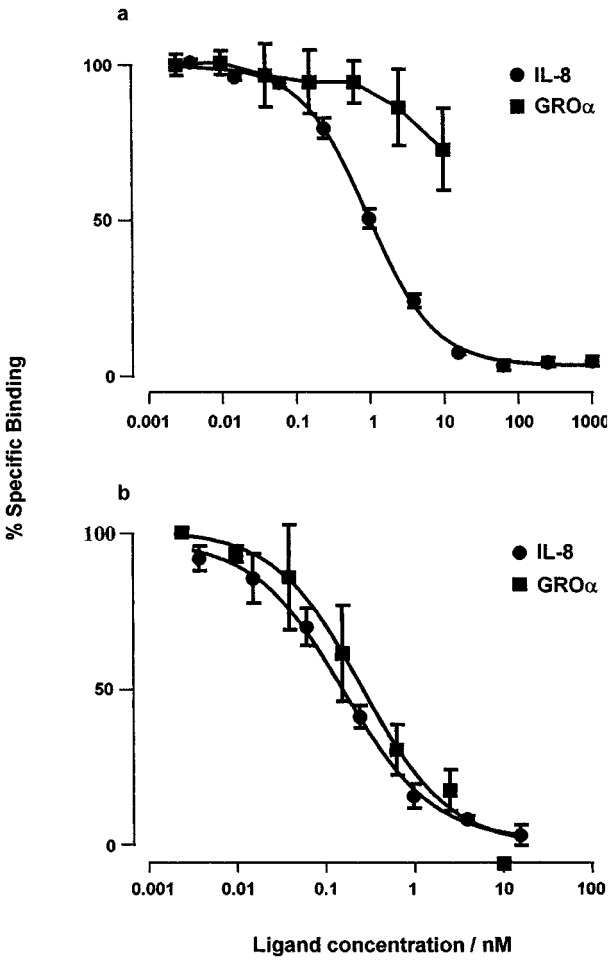

Figure 4 Competition binding curves for IL-8 and GROα versus [^{125}I]IL-8 in membranes from CHO-CXCR1 (a) or CHO-CXCR2 (b). Values are the means ± s.e.mean of three separate determinations. Vertical bars show the s.e.mean. The curves plotted through the data points are four parameter logistic equations fitted to the mean data.

in both cell lines (there was no PTX insensitive component in CHO-CXCR1) and the maximal levels of inhibition induced by IL-8 were similar. In both cell lines, the potencies of IL-8 (and GROα in CHO-CXCR2) in the cyclic AMP accumulation assays were very similar to those in the calcium mobilization assays. The relative potencies for inhibition of adenylyl cyclase and calcium mobilization in response to Gi-coupled receptor activation seem to vary depending on the cell line (Dickenson & Hill, 1995; Sharp *et al.*, 1996; Schoeffter *et al.*, 1997). However, in CHO cells, stimulation of the endogenous 5-HT_{1B}-like receptor activates these two pathways with equal potency (Dickenson & Hill, 1995) which is consistent with our data.

The effects of the peptides in CHO-CXCR1 membranes in the [^{35}S]GTPγS binding assay were also similar to those in the other two functional assays. In CXCR2 membranes, however, the potency order of the peptides was reversed, GROα was ~3 fold more potent at stimulating [^{35}S]GTPγS binding than IL-8. This difference in potency is relatively small but it is highly statistically significant ($P<0.01$). One possible explanation is that the G-proteins measured in the [^{35}S]GTPγS binding assay are distinct from those which mediate the downstream responses. The difference in agonist potency series between [^{35}S]GTPγS binding and the downstream responses would then imply some form of agonist trafficking (Kenakin, 1995). Another possibility is that the G-proteins interact less efficiently with the downstream effectors when the receptor is activated by GROα than when it is activated by IL-8. It has recently been shown, for the β_2 adrenoceptor, that an agonist was able to stimulate the activity of adenylyl cyclase even when the G-protein pool was saturated with guanine nucleotides (Ugur & Onaran, 1997) implying that an agonist can influence the activity of signalling pathways by a mechanism additional to catalysis of nucleotide exchange. Different agonists would not necessarily have similar orders of efficacy for these two effects resulting potentially in differences in potency orders between [^{35}S]GTPγS binding and downstream effects. However, further experiments would be necessary to distinguish between and provide firm support for either of these hypotheses.

PTX abolished the effect of IL-8 on [^{35}S]GTPγS binding in both cell lines. Additionally, in the CHO-CXCR1 membranes there was a marked reduction in the basal level of binding in the PTX-treated membranes (Figure 3c). A smaller effect, which was not statistically significant, was also seen in the CXCR2 membranes. This effect of PTX may suggest that there is some constitutive activity of CXCR1 in this cell line resulting in a significant level of G-protein activation in the absence of agonist. The significant effect in the CHO-CXCR1 membranes is consistent with the greater level of receptor expression in this cell line. It could be argued that the PTX sensitive basal activity in these membranes was due to the activity of other (endogenous) Gi coupled receptors in this cell line. However, if this were the case PTX might have been expected to have a similar magnitude of effect in CHO-CXCR2. The abolition by PTX of the [^{35}S]GTPγS binding response in the CHO-CXCR1 cells also implies that the PTX-insensitive component of the calcium response at CXCR1 is mediated by a G-protein which is not detected in [^{35}S]GTPγS binding assays or that it is not G-protein mediated.

In marked contrast to the other two functional responses, there was a very large difference in the potencies of IL-8 at CXCR1 and CXCR2 in the [^{35}S]GTPγS binding assays. The potency of IL-8 at CXCR1 was very similar to that in the other assays whilst at CXCR2 it was some two orders of magnitude weaker. The close agreement of the pEC_{50} values for IL-8 in the three assay systems is somewhat surprising, particularly for the [^{35}S]GTPγS binding assay at CXCR1. Each of the functional responses we have measured occur at different stages along the signal transduction pathway and would be expected to exhibit different levels of receptor reserve. [^{35}S]GTPγS binding is a measure of nucleotide exchange on the G-protein and is one of the earliest measurable consequences of receptor activation. As this response occurs very early in the transduction pathway it would be expected to show the least amplification and agonists would therefore be expected to evoke this response with lower potencies than those further downstream. This was observed here for CXCR2 and has been observed for other receptors such as the D_2 dopamine receptor (Gardner *et al.*, 1997). The very similar pEC_{50} values for IL-8 at the three responses in the CXCR1 cells may suggest that CXCR1 interacts with a G-protein which is only poorly coupled to the downstream responses (particularly in comparison with CXCR2). This would result in a much smaller leftward shift in the dose-response curves between [^{35}S]GTPγS binding and the downstream responses for CXCR1 than CXCR2. It would also suggest that the two receptors activate different G-proteins in the [^{35}S]GTPγS binding assay.

However, this difference could also be due to the higher level of receptor expression in CHO-CXCR1 cells. From the

effect of PTX in the [^{35}S]GTPγS binding assays, CXCR1 may exhibit constitutive activity whilst CXCR2 does not. However, there did not seem to be any evidence of constitutive activity of CXCR1 in the whole cell assays, e.g. PTX treatment did not cause an increase in forskolin-stimulated cyclic AMP accumulation in CHO-CXCR1 cells. This may imply that, in the whole cell assays, the constitutive receptor activity had caused a homeostatic uncoupling of the G-protein from the effector pathways. The much lower levels of receptor in CXCR2 (which do not show significant constitutive activity in the [^{35}S]GTPγS binding assay) would presumably not induce this uncoupling and would be expected to show a much greater level of amplification from G-protein to effectors, as indeed was observed. It is, of course, also possible that the G-proteins which are being measured in the [^{35}S]GTPγS binding assay are not the G-proteins responsible for the downstream responses (see above). The constitutive activation of the G-protein would simply not be transmitted to the downstream effectors in this case. It may be possible to address some of these issues by performing adenylyl cyclase assays in membranes rather than in whole cells. This would allow the direct comparison of the adenylyl cyclase activity in membranes from the two cell lines after the various treatments, e.g. does PTX treatment affect the activity of adenylyl cyclase in the CXCR1 cells?

It is unwise to compare the functional potencies of the agonists in this study with their binding affinities as the latter were determined using an agonist radioligand. These affinities presumably therefore represent binding of the peptides to the high affinity state of the receptor whilst the low affinity state of the receptor is thought to be important for functional responses. For example, Gardner *et al.* (1997) were able to simultaneously measure agonist binding affinity and functional potency in a [^{35}S]GTPγS binding assay and showed that for D_2 dopamine receptors the affinities of agonists in the assay (which lay to the right of their functional potencies) corresponded to their low affinity states from competition binding assays.

In conclusion, we have characterized the binding and three functional responses of HA-tagged CXC-chemokine receptors 1 and 2 and shown that, in general, their pharmacology agrees well with that reported for the native receptors. The only anomaly was the stimulation of [^{35}S]GTPγS binding at CXCR2 where the potency order of IL-8 and GROα was reversed. This may represent trafficking of the receptor between distinct signalling pathways in our cell lines for this receptor or may indicate subtle differences in the effects of the peptides at different stages of the activation process. We also have preliminary evidence that at relatively high expression levels CXCR1 displays constitutive coupling to PTX-sensitive G-proteins.

We would like to thank Tania Chernov-Rogan of Affymax Incorporated for providing the recombinant cell lines used in this study, Kerri-Ann Cartwright for technical assistance and Murray Mackinnon and Helen Connor for helpful discussions during the writing of this manuscript.

References

AHUJA, S.K., LEE, J.C. & MURPHY, P.M. (1996). CXC chemokines bind to unique sets of selectivity determinants that can function independently and are broadly distributed on multiple domains of human interleukin-8 receptor B. *J. Biol. Chem.,* **271,** 225 – 232.

AHUJA, S.K. & MURPHY, P.M. (1996). The CXC chemokines growth-related oncogene (GRO) α, GROβ, GROγ, neutrophil-activating peptide-2 and epithelial cell-derived neutrophil-activating peptide-78 are potent agonists for the type B, but not type A, human interleukin-8 receptor. *J. Biol. Chem.,* **271,** 20545 – 20550.

BACON, K.B. & CAMP, R.D.R. (1990). Interleukin (IL)-8-induced *in vitro* human lymphocyte migration is inhibited by cholera and pertussis toxins and inhibitors of protein kinase C. *Biochem. Biophys. Res. Commun.,* **169,** 1099 – 1104.

BAGGIOLINI, M. & CLARK-LEWIS, I. (1992). Interleukin-8, a chemotactic and inflammatory cytokine. *FEBS Lett.,* **307,** 97 – 101.

CLARK-LEWIS, I., DEWALD, B., GEISER, T., MOSER, B. & BAGGIOLINI, M. (1993). Platelet factor 4 binds to IL-8 receptors and activates neutrophils when its N-terminus is modified with glu-leu-arg. *Proc. Natl. Acad. Sci. U.S.A.,* **90,** 3574 – 3577.

DAMAJ, B.B., MCCOLL, S.R., MAHANA, W., CROUCH, M.F. & NACCACHE, P.H. (1996a). Physical association of $G_{12}\alpha$ with interleukin-8 receptors. *J. Biol. Chem.,* **271,** 12783 – 12789.

DAMAJ, B.B., MCCOLL, S.R., NEOTE, K., HEBERT, C.A. & NACCACHE, P.H. (1996b). Diverging signal transduction pathways activated by interleukin 8 (IL-8) and related chemokines in human neutrophils: IL-8 and Gro-α differentially stimulate calcium influx through IL-8 receptors A and B. *J. Biol. Chem.,* **271,** 20540 – 20544.

DICKENSON, J.M. & HILLS, S.J. (1995). Coupling of an endogenous 5-HT_{1B}-like receptor to increases in intracellular calcium through a pertussis toxin-sensitive mechanism in CHO-K1 cells. *Br. J. Pharmacol.,* **116,** 2889 – 2896.

EDELMAN, J.L., KAJIMURA, M., WOLDEMUSSIE, E. & SACHS, G. (1994). Differential effects of carbachol on calcium entry and release in CHO cells expressing m3 muscarinic receptor. *Cell Calcium,* **16,** 181 – 193.

GARDNER, B.R., HALL, D.A. & STRANGE, P.G. (1997). Agonist action at D2(short) dopamine receptors determined in ligand binding and functional assays. *J. Neurochem.,* **69,** 2589 – 2598.

GRYNKIEWICZ, G., POENIE, M. & TSIEN, R.Y. (1985). A new generation of Ca^{2+} indicators with greatly improved fluorescence properties. *J. Biol. Chem.,* **260,** 3440 – 3450.

HALL, D.A., BERESFORD, I.J.M. & GILES, H. (1998). Characterisation of a [^{35}S]GTPγS binding assay for chemokine CXC 1 and 2 (IL-8 A and B) receptors expressed on CHO cells. *Br. J. Pharmacol.,* in press.

HALL, D.A. & HOURANI, S.M.O. (1993). Effect of analogues of adenine nucleotides on increases in intracellular calcium concentration mediated by P_{2T}-purinoceptors on human blood platelets. *Br. J. Pharmacol.,* **108,** 728 – 733.

HAMMOND, M.E.W., LAPOINTE, G.R., FEUCHT, P.H., HILT, S., GALLEGOS, C.A., GORDON, C.A., GIEDLIN, M.A., MULLENBACH, G. & TEKAMP-OLSON, P. (1995). IL-8 induces neutrophil chemotaxis predominantly via type I IL-8 receptors. *J. Immunol.,* **155,** 1428 – 1433.

KENAKIN, T. (1995). Agonist-receptor efficacy II: Agonist trafficking of receptor signals. *Trends Pharmacol. Sci.,* **16,** 232 – 238.

LEE, J., CACALANO, G., CAMERATO, T., TOY, K., MOORE, M.W. & WOOD, W.I. (1995). Chemokine binding and activities by the mouse IL-8 receptor. *J. Immunol.,* **155,** 2158 – 2164.

LEE, J., HORUK, R., RICE, G.C., BENNETT, G.L., CAMERATE, T. & WOOD, W.I. (1992). Characterisation of two high affinity human interleukin-8 receptors. *J. Biol. Chem.,* **267,** 16283 – 16287.

L'HEUREUX, G., BOURGOIN, S., JEAN, N., MCCOLL, S.R. & NACCACHE, P.H. (1995). Diverging signal transduction pathways activated by interleukin-8 and related chemokines in human neutrophils: Interleukin-8, but not NAP-2 or GROα, stimulates phospholipase D activity. *Blood,* **85,** 522 – 531.

LOETSCHER, P., SEITZ, M., CLARK-LEWIS, I., BAGGIOLINI, M. & MOSER, B. (1994). Both interleukin-8 receptors independently mediate chemotaxis. Jurkat cells transfected with IL-8R1 or IL-8R2 migrate in response to IL-8, GROα and NAP-2. *FEBS Lett.,* **341,** 187 – 192.

MAXFIELD, F.R. (1993). Regulation of leukocyte locomotion by Ca^{2+}. *Trends Cell Biol.,* **3,** 386 – 391.

MORRIS, A.J. & SCARLATA, S. (1996). Regulation of effectors by G-protein α- and $\beta\gamma$-subunits: Recent insights from studies of the phospholipase C-β isoenzymes. *Biochem. Pharmacol.,* **54,** 429 – 435.

PETERSEN, F., FLAD, H.-D. & BRANDT, E. (1994). Neutrophil-activating peptides NAP-2 and IL-8 bind to the same sites on neutrophils but interact in different ways. Discrepancies in binding affinities, receptor densities and biologic effects. *J. Immunol.,* **152,** 2467 – 2478.

PETERSEN, F., LUDWIG, A., FLAD, H.D. & BRANDT, E. (1996). TNF-α renders human neutrophils responsive to platelet factor 4: Comparison of PF-4 and IL-8 reveal different activity profiles of the two chemokines. *J. Immunol.,* **156,** 1954 – 1962.

POWER, C.A. & WELLS, T.N.C. (1996). Cloning and characterisation of human chemokine receptors. *Trends Pharmacol. Sci.,* **17,** 209 – 213.

PROOST, P., DE WOLF-PEETERS, C., CONINGS, R., OPDENAKKER, G., BILLIAU, A. & VAN DAMME, J. (1993). Identification of a novel granulocyte chemotactic peptide (GCP-2) from human tumour cells: In vitro and in vivo comparison with natural forms of GRO, IP-10 and IL-8. *J. Immunol.,* **150,** 1000 – 1010.

SCHOEFFTER, P., BOBIRNAC, I., BODDECKE, E. & HOYER, D. (1997). Inhibition of cAMP accumulation via recombinant human serotonin 5-HT_{1A} receptors: Considerations on receptor effector coupling across systems. *Neuropharmacol.,* **36,** 429 – 437.

SCHRODER, J.-M., PERSOON, N.L.M. & CHRISTOPHERS, E. (1990). Lipopolysaccharide-stimulated human monocytes secrete, apart from neutrophil-activating peptide 1/ interleukin 8, a second neutrophil activating protein: NH_2-terminal amino acid sequence identity with melanocyte growth stimulatory activity. *J. Exp. Med.,* **171,** 1091 – 1100.

SENGELOV, H., KJELDSEN, L. & BORREGAARD, N. (1993). Control of exocytosis in early neutrophil activation. *J. Immunol.,* **150,** 1535 – 1543.

SHARP, B.M., SHAHABI, N.A., HEAGY, W., MCALLEN, K., BELL, M., HUNTOON, C. & MCKEAN, D.J. (1996). Dual signal transduction through delta opioid receptors in a transfected human T-cell line. *Proc. Natl. Acad. Sci. U.S.A.,* **93,** 8294 – 8299.

SOLARI, R., OFFORD, R.E., REMY, S., AUBRY, J.-P., WELLS, T.N.C., WHITEHORN, E., OUNG, T. & PROUDFOOT, A.E.I. (1997). Receptor-mediated endocytosis of CC-chemokines. *J. Biol. Chem.,* **15,** 9617 – 9620.

THELEN, M., PEVERI, P., KERNEN, P., VON TSCHARNER, V., WALZ, A. & BAGGIOLINI, M. (1988). Mechanism of neutrophil activation by NAF, a novel monocyte-derived peptide agonist. *FASEB J.,* **2,** 2702 – 2706.

UGUR, Ö. & ONARAN, H.O. (1997). Allosteric equilibrium model explains steady-state coupling of β-adrenergic receptors to adenylate cyclase in turkey erythrocyte membranes. *Biochem. J.,* **323,** 765 – 776.

WALZ, A., MELONI, F., CLARK-LEWIS, I., VON TSCHARNER, V. & BAGGIOLINI, M. (1991). $[Ca^{2+}]_i$ changes and respiratory burst in human neutrophils and monocytes induced by NAP1/interleukin-8, NAP-2, and *gro*/MGSA. *J. Leukocyte Biol.,* **50,** 279 – 286.

WU, D., LAROSA, G.J. & SIMON, M.I. (1993). G-protein-coupled signal transduction pathways for IL-8. *Science,* **261,** 101 – 103.

WU, L., RUFFING, N., NEWMAN, W., SOLER, D., MACKAY, C.R. & QIN, S. (1996). Discrete steps in binding and signalling of interleukin-8 with its receptor. *J. Biol. Chem.,* **271,** 31202 – 31209.

WUYTS, A., VAN OSSELAER, N., HAELENS, A., SAMSON, I., HERDEWIJN, P., BEN-BURACH, A., OPPENHEIM, J.J., PROOST, P. & VAN DAMME, J. (1997). Characterization of synthetic human granulocyte chemotactic protein 2: usage of chemokine receptors CXCR1 and CXCR2 and *in vivo* inflammatory properties. *Biochem.,* **36,** 2716 – 2723.

(Received June 15, 1998
Revised October 27, 1998
Accepted November 3, 1998)

British Journal of Pharmacology (1999) 126, 819–825
http://www.stockton-press.co.uk/bjp

Functional and molecular biological evidence for a possible β_3-adrenoceptor in the human detrusor muscle

*,[1]Yasuhiko Igawa, [2]Yoshinobu Yamazaki, [2]Hiroo Takeda, [2]Kohichi Hayakawa, [2]Masuo Akahane, [2]Yukiyoshi Ajisawa, [1]Takehisa Yoneyama, [1]Osamu Nishizawa & [3]Karl-Erik Andersson

[1]Department of Urology, Shinshu University School of Medicine, 3-1-1, Asahi, Matsumoto 390-8621, Japan; [2]Division of Discovery Research, Kissei Pharmaceutical Co., Ltd., Hotaka, Nagano 399-8304, Japan; [3]Department of Clinical Pharmacology, Lund University Hospital, S-221 85 Lund, Sweden

1 The possible existence of a β_3-adrenergic receptor (β_3-AR) in the human detrusor muscle was investigated by *in vitro* functional studies and analysis of mRNA expression.

2 Isoprenaline, noradrenaline and adrenaline each produced a concentration-dependent relaxation of the human detrusor. The rank order for their relaxing potencies was isoprenaline (pD_2 6.37 ± 0.07) $\geqslant$ noradrenaline (pD_2 6.07 ± 0.12) $\geqslant$ adrenaline (pD_2 5.88 ± 0.11).

3 Neither dobutamine (β_1- and β_2-AR agonist) nor procaterol (β_2-AR agonist) produced any significant relaxation at concentrations up to 10^{-5} M. BRL37344A, CL316243 and CGP-12177A (β_3-AR agonists), relaxed the preparations significantly at concentrations higher than 10^{-6} M. The pD_2 values for BRL37344A, CL316243 and CGP-12177A were 6.42 ± 0.25, 5.53 ± 0.09 and 5.74 ± 0.14, respectively.

4 CGP-20712A (10^{-7}–10^{-5} M), a β_1-AR antagonist, did not affect the isoprenaline-induced relaxation. On the other hand, ICI-118,551, a β_2-AR antagonist, produced a rightward parallel shift of the concentration-relaxation curve for isoprenaline only at the highest concentration used (10^{-5} M) and its pK_B value was 5.71 ± 0.19. Moreover, SR58894A (10^{-7}–10^{-5} M), a β_3-AR antagonist, caused a rightward shift of the concentration-relaxation curve for isoprenaline in a concentration-dependent manner. The pA_2 value and slope obtained from Schild plots were 6.24 ± 0.20 and 0.68 ± 0.31.

5 The β_1-, β_2- and β_3-AR mRNAs were all positively expressed in detrusor smooth muscle preparations in a reverse transcription polymerase chain reaction assay.

6 In conclusion, the present results provide the first evidence for the existence of the β_3-AR subtype in the human detrusor. They also suggest that the relaxation induced by adrenergic stimulation of the human detrusor is mediated mainly through β_3-AR activation.

Keywords: Human bladder; β-adrenoceptor subtypes; functional analysis; mRNA analysis

Abbreviations: AMV, avian myeloblastosis virus; β-AR, β-adrenoceptor; DMSO, dimethyl sulphoxide; G3PDH, glyceraldehyde-3-phosphate dehydrogenase; RT-PCR, reverse transcription-polymerase chain reaction

Introduction

There is much evidence indicating that, at least in animals, activation of the sympathetic nervous system contributes to urine storage by relaxing the detrusor muscle *via* activation of β-adrenoceptors (β-ARs; see review by Andersson, 1993). Although β-ARs were originally subclassified into β_1- and β_2-subtypes (Lands *et al*., 1967a,b), another subtype, the β_3-subtype, has since been reported (Emorine *et al*., 1989; 1994). Furthermore, it has been known for some years that there are species differences in the subtypes of β-ARs involved in the relaxation of the detrusor (Elmér, 1974; Nergårdh *et al*., 1977; Anderson & Marks, 1984; Levin *et al*., 1988; Li *et al*., 1992; Goepel *et al*., 1997; Seguchi *et al*., 1998). Recently, we reported that part of the relaxation induced by adrenergic stimulation in the rat and canine detrusor was mediated by β_3-AR (Yamazaki *et al*., 1998).

In humans, although the β-ARs present in the detrusor muscle have been shown to have functional characteristics typical of neither β_1- nor β_2-ARs (Nergårdh *et al*., 1977; Larsen, 1979), receptor-binding studies carried out using selective radio-ligands have indicated a predominance of the β_2-subtype (Levin *et al*., 1988). It is still unclear whether β_3-ARs are present in the human detrusor and, if they are, what function they perform. In the present study, we set out to determine which β-AR subtypes are involved in the relaxation of the human detrusor that occurs on adrenergic stimulation. We were particularly interested in β_3-ARs, and we used *in vitro* functional studies and mRNA analysis. Some of the results have been presented in a preliminary communication (Igawa *et al*., 1998).

Methods

Patients and specimens

The study involved 56 patients (44 men and 12 women; aged 66.2 ± 1.5, range 23–82 years) undergoing open pelvic surgery at Shinshu University Hospital, 38 for bladder carcinoma, eight for renal pelvic or ureteral carcinoma, two for prostatic carcinoma, three for bladder stone, three for benign prostatic hyperplasia, and two for vesico-ureteral reflex. On the basis of preoperative urodynamic studies and neurological examina-

*Author for correspondence; E-mail: yxigawa@gipac.shinshu-u.ac.jp

tions, all patients were judged to have normal bladder function. None of the patients had diseases known to interfere with the β-AR system or had received medication known to interfere with that system. General anaesthesia was induced with a short-acting barbiturate and was maintained with fentanyl and a mixture of oxygen, nitrous oxide and isoflurane. Written informed consent was obtained from all patients before their operation. The study was approved by the Ethics Committee of Shinshu University School of Medicine.

All specimens were taken from macroscopically normal tissue in the anterior or posterior wall of the bladder body *via* a longitudinal incision. In all cases, except when total cystectomy was performed for bladder carcinoma, specimens were obtained from the margin of the longitudinal incision in the anterior bladder wall during the operation itself. For functional studies, the specimens were placed immediately after excision in pre-oxygenated Krebs solution (for composition see below) at 4°C and transported to the laboratory. The specimens for RNA analysis were frozen immediately after excision and stored in liquid nitrogen.

Functional studies

After the mucosa and adventitia had been removed, detrusor muscle strips measuring approximately $10 \times 5 \times 3$ mm were isolated. Each preparation was suspended in a 10 ml organ bath containing Krebs solution; this was maintained at 37°C and continuously gassed with a mixture of 95% oxygen and 5% carbon dioxide. One end of each strip was connected to a force-displacement transducer (SB-1T, Nihon-Kohden, Tokyo, Japan) and changes in muscle tension were measured and recorded on a pen-writing oscillograph (Rectigraph 8S, NEC Sanei, Tokyo, Japan). The preparation was gradually stretched until a stable tension of 10 mN was obtained. Concentration-response curves for β-AR agonists were obtained by cumulative addition of the appropriate drug to the bathing fluid. Each preparation was used in only one experiment, i.e. to obtain one concentration-curve for one of the agonists. To test the antagonistic potency of β-AR antagonists against isoprenaline, one of the antagonists was added to the bath 30 min before the addition of isoprenaline. Concentration-response curves for isoprenaline were thus obtained in the presence of the antagonist. All experiments were conducted in the presence of 10^{-6} M phentolamine, an α-adrenoceptor antagonist.

Analysis of functional data

The results are expressed as means $\pm$ s.e.mean. The relaxing effect of each agonist is expressed as a percentage of the maximal relaxation induced by 10^{-5} M forskolin, which was used as a reference drug. The pD_2 value, which is the negative logarithm of the EC_{50} value, was calculated for each agonist from its concentration-relaxation curve. The pA_2 value for each antagonist, as defined by Arunlakshana & Schild (1959), was obtained from linear regression analysis of the plot of mean values of log (CR-1) vs the negative log of the antagonist concentration. When a parallel rightward shift of the concentration-relaxation curve was observed only at the highest concentration of antagonist used, the pK_B value (the negative logarithm of (antagonist concentration/CR-1)) was calculated from the pD_2 values in the presence (at the highest concentration) and absence of antagonist. Statistical analysis was performed using a Student's two-tailed *t*-test. A probability level of less than 0.05 was accepted as significant.

mRNA analysis

All procedures were carried out according to the manufacturer's instructions unless otherwise specified. Total RNA was extracted from human detrusor smooth muscle (approximate 1 g) using TRIzol® (Gibco-BRL, Rockville, MD, U.S.A.). The total RNA preparations were digested by RQ1 RNase-free DNase (Promega, Madison, WI, U.S.A.) to remove contaminating genomic DNA. The amount of the total RNA was determined by a spectrophotometer (DU-640, Beckman Instruments Inc., Fullerton, CA, U.S.A.).

Primers (Sawady Technology Inc., Tokyo, Japan) for β_1-, β_2-, and β_3-AR were used according to a previous report (Krief *et al*., 1993) and primers for glyceraldehyde-3-phosphate dehydrogenase (G3PDH), as an internal standard, were designed in base on a DNA sequence (Tso *et al*., 1985). The sequences of these primers are shown in Table 1. The reverse transcription-polymerase chain reaction (RT-PCR) was carried out using Titan™ one tube RT-PCR system (Boehringer-Mannheim, Mannheim, Germany). The PCR mixtures consisted of $1 \times$ the RT-PCR buffer (containing $MgCl_2$ (1.5 mM) and dimethyl sulphoxide (DMSO); Boehringer-Mannheim), dNTPs (0.2 mM), 0.4 μM each of PCR primers, DTT (5 mM), 5 U RNasin® RNase inhibitor (Promega, U.S.A.), 1 μl enzyme mix (expand™ high fidelity enzyme mix and avian myeloblastosis virus (AMV)-reverse transcriptase) and 1 μg total RNA, in a volume of 50 μl. cDNA synthesis and PCR amplification was continuously performed without opening the reaction tubes in a thermal cycler (Gene Amp® 2400, PE Applied-Biosystems, Foster City, CA, U.S.A.).

cDNA synthesis was performed at 50°C for 30 min with reverse transcriptase and PCR primer. Following initial heating of samples at 94°C for 2 min, 10 cycles were performed, which consisted of denaturation (30 s at 94°C), annealing (30 s at 58°C) and elongation (1 min at 68°C).

Table 1 Oligonucleotides used as RT-PCR primers

	Strand	*Sequence*	*Location**
β_1-adrenoceptor	Forward	5′-TCGTGTGCACCGTGTGGGCC-3′	J03019
	Reverse	5′-AGGAAACGGCGCTCGCAGCTGTCG-3′	(619–883)
β_2-adrenoceptor	Forward	5′-GCCTGCTGACCAAGAATAAGGCC-3′	Y00106
	Reverse	5′-CCCATCCTGCTCCACCT-3′	(1221–1549)
β_3-adrenoceptor	Forward	5′-GCTCCGTGGCCTCACGAGAA-3′	X70811
	Reverse	5′-CCCAACGGCCAGTGGCCAGTCAGCG-3′	(129–442)
G3PDH	Forward	5′-ACCACAGTCCATGCCATCAC-3′	X01677
	Reverse	5′-TCCACCACCCTGTTGCTGTA-3′	(586–1037)

*Genbank accession number and nucleotide numbers within corresponding entry.

Furthermore, the PCR amplification was repeated for 25 cycles for β_1-, β_2- and β_3-AR and for 14 cycles for G3PDH in the same manner except that the elongation time was added 5 s for each cycle (These numbers of repeated cycles and the elongation times were determined by results of pilot experiments).

A portion (10 μl) of PCR-products were visualized by electrophoresis of 3% LO3 agarose gels (TAKARA-Shuzo, Ohtsu, Japan) with 0.5 μg ml^{-1} ethidium bromide (Gibco-BRL). To identify these PCR-products, direct sequencing of PCR-products was performed according to the dideoxy chain termination method. The PCR-products were labelled by Big-dye terminator (PE Applied-Biosystems) using the sense and anti-sense PCR primers, and analysed by DNA sequencer (ABI PRISM^{TM} 310, PE Applied-Biosystems).

Drugs and solutions

The following drugs were used; (±)-isoprenaline hydrochloride, forskolin (Wako Pure Chemical, Osaka, Japan), (±)-dobutamine hydrochloride, BRL37344A ((±)-(R*,R*)-[4-[2-[[2-(3-chlorophenyl)-2-hydroxyethyl]-amino]propyl]phenoxy]-acetic acid sodium), (±)-CGP-12177A hydrochloride ((±)-4-(3-t-butylamino-2-hydroxypropoxy) benzimidazol-2-one hydrochloride), ICI-118,551 hydrochloride (erythro-(±)-1-(7-methylindan-4-yloxy)-3-isopropylaminobutan-2-ol hydrochloride) (Funakoshi, Tokyo, Japan), procaterol hydrochloride (Sigma Chemical, St. Louis, MO, U.S.A.), (±)-noradrenaline (Sankyo, Tokyo, Japan), (−)-adrenaline (Daiichi, Tokyo, Japan), phentolamine mesylate (Ciba-Geigy, Basel, Switzerland) and dimethyl sulphoxide (DMSO) (Nacalai tesque, Kyoto, Japan). CL316243((R,R)-5-[2-[[2-(3-chlorophenyl)-2-hydroxyethyl]-amino]propyl]- 1,3-benzodioxole-2,2-dicarboxylate), CGP-20712A (2-hydroxy-5(2-((2-hydroxy-3-(4-((1-methyl-4-trifluoromethyl)1H-imidazole-2-yl)-phenoxy)propyl) amino) ethoxy)-benzamide monomethane sulphonate) and SR58894A (3-(2-allylphenoxy)-1-[(1S)-1,2,3,4-tetrahydronaphth-1-ylamino]-(2 S)-2-propanol hydrochloride) were synthesized in our laboratories (Kissei, Hotaka, Japan). The drugs were dissolved as follows: forskolin, in 100% DMSO; the other drugs, in distilled water. The solutions were prepared on the day of the experiment and kept in dark vessels to minimize light-induced degradation. Subsequent dilutions of the drugs were prepared in distilled water. The reported concentrations are the calculated final concentrations in the bath solution. The Krebs solution used had the following composition (mM): NaCl 118.1, KCl 4.7, $CaCl_2$ 2.5, $MgSO_4$ 1.2, $NaHCO_3$ 25.0, KH_2PO_4, 1.2 and glucose 11.1 (pH 7.4).

Results

Relaxation responses to β-AR agonists

A distinct relaxation of the human detrusor preparation was produced by forskolin (10^{-5} M), the tension decreasing to 47.3±2.4% ($n=60$) of the initial tension. Isoprenaline (10^{-10}–10^{-4} M), a non-selective β-AR agonist, produced relaxation in a concentration-dependent manner (Figure 1). The maximal effect, which was observed at a concentration of 10^{-4} M, averaged 78.7±1.4% ($n=29$) of the forskolin (10^{-5} M)-induced maximal relaxation. Both noradrenaline (10^{-10}–10^{-4} M) and adrenaline (10^{-10}–10^{-4} M) also relaxed the preparations in a concentration- dependent manner. The rank order for the relaxing activity of these drugs was isoprenaline ⩾ noradrenaline ⩾ adrenaline, the pD_2 values being 6.37±0.07 ($n=29$), 6.07±0.12 ($n=6$) and 5.88±0.11 ($n=6$), respectively (Figure 2). The difference in pD_2 value between isoprenaline and adrenaline was statistically significant ($P<0.05$). However, there was no statistically significant difference in pD_2 value between isoprenaline and noradrenaline, or between noradrenaline and adrenaline.

On the other hand, neither dobutamine (10^{-10}–10^{-4} M), which stimulates both β_1- and β_2-ARs, nor procaterol (10^{-10}–10^{-4} M), a selective β_2-AR agonist, produced any significant relaxation at concentrations up to 10^{-5} M (Figure 2). When

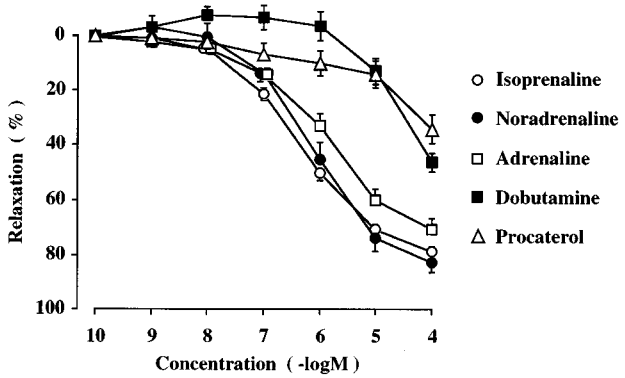

Figure 2 Effects of isoprenaline, noradrenaline, adrenaline, dobutamine, and procaterol on resting tension in human detrusor preparations. All experiments were performed in the presence of 10^{-6} M phentolamine. Each point represents the mean±s.e.mean of 6–29 experiments. Data are expressed as a percentage of the maximal relaxation induced by 10^{-5} M forskolin.

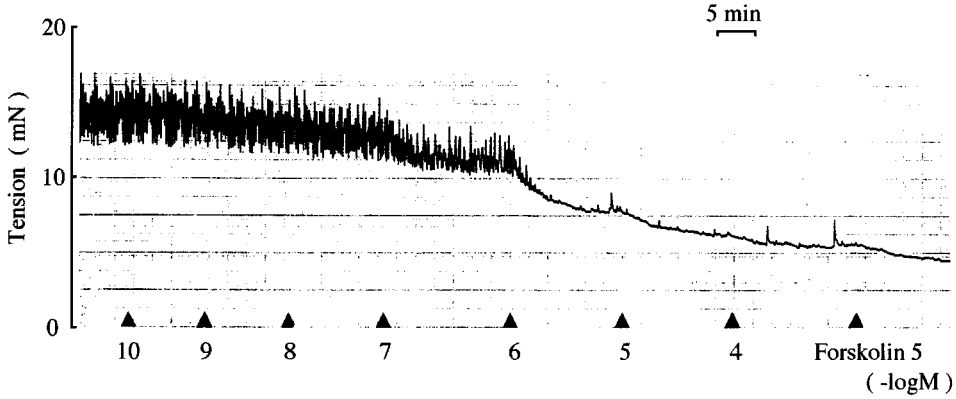

Figure 1 Representative recording of the effect of isoprenaline on resting tension in a human detrusor preparation.

applied at 10^{-4} M, dobutamine and procaterol produced relaxing effects that were the equivalent of $46.2 \pm 3.4\%$ ($n=8$) and $34.2 \pm 5.2\%$ ($n=11$), respectively, of the forskolin (10^{-5} M)-induced relaxation. However, neither of these effects reached a maximum at a concentration of 10^{-4} M and so the pD_2 values were not determined.

Both BRL37344A (10^{-10}–10^{-4} M) and CL316243 (10^{-10}–10^{-4} M), selective β_3-AR agonists, and CGP-12177A (10^{-10}–10^{-4} M), a selective β_3-AR partial agonist and β_1-/β_2-AR antagonist, relaxed the preparation when applied at concentrations greater than 10^{-6} M (Figure 3). The pD_2 values (and maximal relaxation at 10^{-4} M) were 6.42 ± 0.25 ($47.4 \pm 4.5\%$; $n=7$) for BRL37344A, 5.53 ± 0.09 ($43.7 \pm 6.4\%$; $n=7$) for CL316243 and 5.74 ± 0.14 ($33.3 \pm 4.2\%$; $n=11$) for CGP-12177A, respectively.

Effect of β-AR antagonists on the isoprenaline-induced relaxation

CGP-20712A (10^{-7}–10^{-5} M; $n=5$–6), a selective β_1-AR antagonist, failed to affect the concentration-relaxation curve for isoprenaline (Figure 4a). At concentrations from 10^{-7} M to 3×10^{-6} M, ICI-118,551 ($n=6$–7), a selective β_2-AR antagonist, did not affect the relaxation induced by isoprenaline. However, at 10^{-5} M ICI-118,551 produced a rightward parallel shift of the isoprenaline concentration-response curve (Figure 4b). The pK_B value determined by using 10^{-5} M ICI-118,551 was 5.71 ± 0.19.

In the presence of both CGP-20712A (10^{-7} M) and ICI-118,551 (10^{-7} M), on the other hand, addition of SR58894A (10^{-7}–10^{-5} M; $n=7$–12), a selective β_3-AR antagonist, caused a rightward shift of the concentration-relaxation curve for isoprenaline in a concentration-dependent manner (Figure 5a). A Schild plot analysis yielded a pA_2 value of 6.24 ± 0.20 and a slope of 0.68 ± 0.31 (Figure 5b). The slope did not differ from unity for this antagonist.

Expression of β-AR mRNA in human detrusor

RT-PCR amplification was carried out using specific primers corresponding to β_1-, β_2- and β_3-AR sequences and, as a template, mRNA obtained from human detrusor preparations from three patients. As shown in Figure 6, PCR products for β_1-, β_2- and β_3-AR were detected identically in all the preparations and the expected size of PCR products for β_1-, β_2- and β_3-AR were 265, 329 and 314 bp, respectively. The PCR product for G3PDH, an internal standard, was detected also in each preparations obtained from all the three patients and its expected size was 452. The sequences of the PCR products analysed by DNA sequencer were identified with their reported sequences as regards the detectable signals.

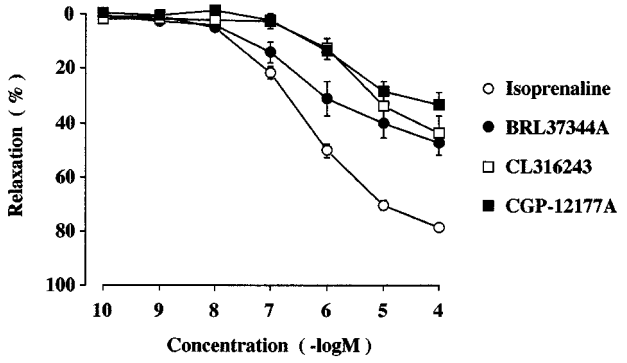

Figure 3 Effects of isoprenaline, BRL37344A, CL316243 and CGP-12177A on resting tension in human detrusor preparations. All experiments were performed in the presence of 10^{-6} M phentolamine. Each point represents the mean ± s.e.mean of 7–29 experiments. Data are expressed as a percentage of the maximal relaxation induced by 10^{-5} M forskolin.

Discussion

The present study, combining functional and molecular biological investigations, provides evidence for the existence of β_3-AR in the human detrusor. It further suggests that the major β-AR subtype involved in the relaxation of the human detrusor smooth muscle observed on adrenergic stimulation is neither the β_1- nor the β_2-AR, but most probably the β_3-AR.

First, we examined the relative potencies with which endogenous and synthetic catecholamines relaxed the human detrusor muscle. The rank order of potency for the three catecholamines producing β-AR-mediated responses has been reported to be isoprenaline > noradrenaline > adrenaline for β_1- and β_3-ARs, but isoprenaline > adrenaline > noradrenaline for β_2-AR (Lands *et al*., 1967a; Emorine *et al*., 1989). In the present study, the rank order of potency in relaxing human detrusor was isoprenaline ⩾ noradrenaline ⩾ adrenaline. Although the pD_2 value for noradrenaline was greater than that for adrenaline, the difference was not statistically

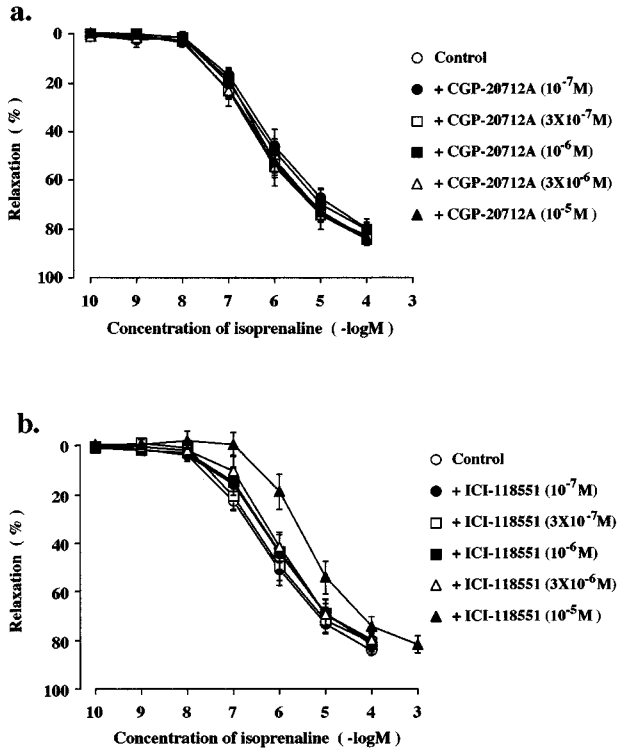

Figure 4 Effects of CGP-20712A (a) and ICI-118,551 (b) on the isoprenaline-induced relaxation of human detrusor muscle preparations. (a) Concentration-response relationships for isoprenaline, either alone or in the presence of CGP-20712A 10^{-7} M, 3×10^{-7} M, 10^{-6} M, 3×10^{-6} M or 10^{-5} M. Each point represents the mean ± s.e.mean ($n=5$–6). (b) Concentration-response relationships for isoprenaline, either alone or in the presence of ICI-118,551 10^{-7} M, 3×10^{-7} M, 10^{-6} M, 3×10^{-6} M, or 10^{-5} M. Each point represents the mean ± s.e.mean ($n=6$–7). All experiments were carried out in the presence of 10^{-6} M phentolamine. Data are expressed as a percentage of the maximal relaxation induced by 10^{-5} M forskolin.

significant. Thus, no difinitive conclusions in terms of a functional predominance of either subtype of β-AR in the human detrusor can be drawn.

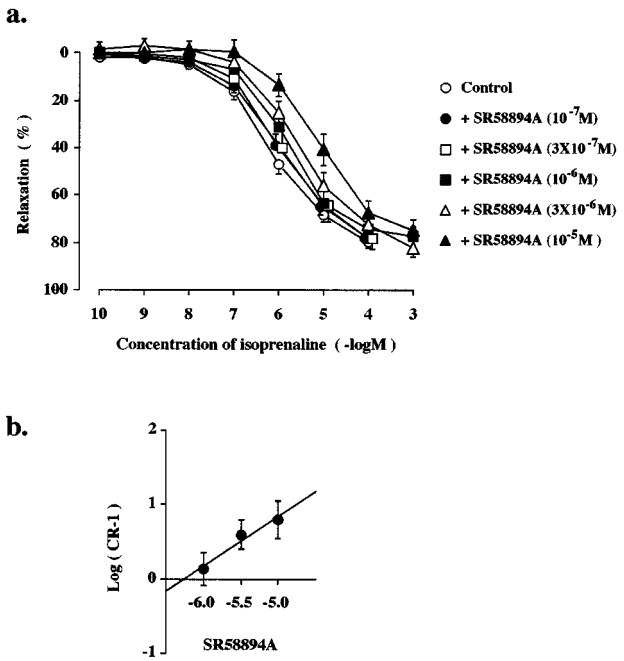

Figure 5 Effect of SR58894A on the isoprenaline-induced relaxation of human detrusor muscle preparations. All experiments were carried out in the presence of CGP-20712A (10^{-7} M), ICI-118,551 (10^{-7} M) and phentolamine (10^{-6} M). (a) Concentration-response relationships for isoprenaline, either alone or in the presence of SR58894A 10^{-7} M, 3×10^{-7} M, 10^{-6} M, 3×10^{-6} M or 10^{-5} M. Each point represents the mean $\pm$ s.e.mean ($n=7-12$). Data are expressed as a percentage of the maximal relaxation induced by 10^{-5} M forskolin. (b) Schild plot for the inhibition of the isoprenaline-induced relaxation produced by SR58894A.

Second, we tested the potencies with which selective agonists for the β-AR subtypes relaxed the human detrusor muscle. Neither dobutamine, which stimulates both β_1- and β_2-ARs (Ozaki *et al*., 1982; Ruffolo *et al*., 1984; Ruffolo, 1987; Aikawa *et al*., 1996), nor procaterol, a β_2-AR agonist, produced any significant relaxation at up to 10^{-5} M. In fact, the concentration at which dobutamine and procaterol did induce a relaxing effect in our preparation was around 10^{-4} M. At this concentration, it is doubtful that the drugs stimulated any β-AR subtype selectively.

We then examined the relaxing effects of the selective β_3-AR agonists, BRL37344A (Oriowo *et al*., 1996), CL316243 (Bloom *et al*., 1992) and CGP-12177A. CGP-12177A has been reported to be a partial agonist for the β_3-AR and an antagonist for β_1- and β_2-ARs (Kaumann, 1996). These β_3-AR agonists were more potent in relaxing our preparations than either dobutamine or procaterol. Thus, these findings suggest that the β_3-AR is functionally predominant over β_1- and β_2-ARs in the human detrusor. Although the β_3-AR agonists, BRL37344A and CL316243, produced relaxations in the human detrusor at concentrations over 10^{-6} M, the maximal relaxations induced by these β_3-AR agonists were only half of the maximal relaxation induced by isoprenaline. This suggests that other β-ARs than the β_3-AR may coexist and contribute to the relaxation of the human detrusor.

Confirmation of the predominant role of the β_3-AR in the human detrusor was obtained in our investigation of the potencies with which several β-AR antagonists counteracted the isoprenaline-induced relaxation of our preparations. In fact, CGP-20712A, a selective β_1-AR antagonist, did not affect the isoprenaline-induced relaxation. Moreover, ICI-118,551, a selective β_2-AR antagonist, shifted the concentration-relaxation curve for isoprenaline only at a high concentration (10^{-5} M). But, the shift was parallel and its pK_B value (5.71) was comparable to the pA_2 value of 5.31 for the antagonist in antagonizing isoprenaline-induced relaxation of rat oesophageal muscularis mucosae, which is known to be mediated predominantly through β_3-ARs (De Boer *et al*., 1993) and the

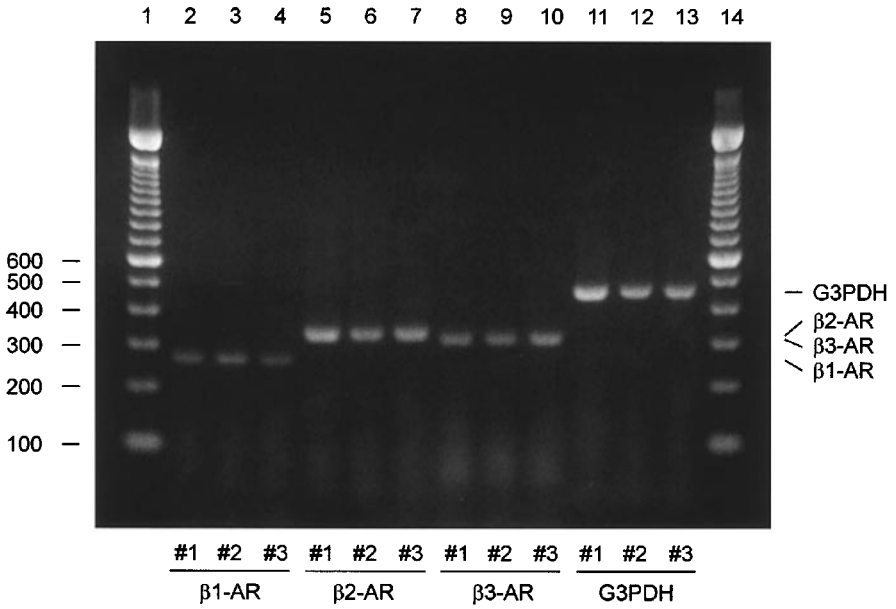

Figure 6 Detection of β_1-, β_2- and β_3-AR mRNA in human detrusor tissue by RT-PCR. Detrusor preparations were obtained from three different patients (#1, #2 and #3). PCR amplification for β_1- (lanes 2–4), β_2- (lanes 5–7), β_3-AR (lanes 8–10) and G3PDH (lanes 11–13) were carried out for 35, 35, 35 and 24 cycles, respectively. Expected size of PCR-products for β_1-, β_2-, β_3- AR and G3PDH were 265, 329, 314 and 452, respectively. Lanes 1 and 14 show 100 bp DNA ladder (Gibco-BRL).

pK_B value of <5.5 for rat cardiac putative β_4-AR (Kaumann, 1997). This suggests that the functional β-ARs in the human detrusor belong to neither the β_1- nor β_2-AR subtypes, but probably to some other subtype (β_3- or β_4).

We then studied the antagonistic activity of SR58894A, a recently developed β_3-AR selective antagonist (Manara *et al*., 1996), against the isoprenaline-induced relaxation. In the presence of 10^{-7} M CGP-20712A (β_1-AR antagonist) and 10^{-7} M ICI-118,551 (β_2-AR antagonist), SR58894A counteracted the isoprenaline-induced relaxation of the human detrusor. This finding provides functional evidence for β_3-ARs in the human detrusor. It has been reported that bupranolol, a non-selective β-AR antagonist, has an antagonistic action at β_1- and β_2-ARs at low concentrations (nM), whereas at higher concentrations (μM) it also affects the β_3-AR (Kaumann, 1989; Koike *et al*., 1995). In a preliminary study (Igawa *et al*., 1998), pretreatment with bupranolol at 10^{-7}, 10^{-6} and 10^{-5} M produced an apparent rightward shift of the concentration-response curve for isoprenaline. Its pA_2 value for this effect was 7.27, which is comparable to the pA_2 values (about 7.3–7.5) for β_3-AR reported by Langin *et al*. (1991). Thus, the findings with bupranolol further support the view that the relaxation induced by adrenergic stimulation in the human detrusor is mediated mainly by β_3-ARs, rather than by β_1- or β_2-ARs. However, the slope for SR58894A, obtained from Schild plots, was 0.68. This suggests that other β-ARs, possibly the putative β_4-AR (Kaumann, 1997) and/or atypical β-ARs, may coexist and play a functional role in the relaxation of the human detrusor. Indeed, the presence of atypical β-ARs has been postulated in human colonic smooth muscle (De Ponti *et al*., 1996). Further studies are needed to determine whether such ARs exist also in the human detrusor.

To obtain a biological correlate of the pharmacological evidence for a functional β_3-AR in the human detrusor, we used a PCR assay to study the expression of the mRNA for each of the various β-AR genes. In fact, the mRNAs for all three β-AR subtypes were demonstrated in the human detrusor in the present study. The DNA sequencer analysis performed subsequently confirmed that each sequence of these PCR products was identified with its reported sequence. Although the distribution of the β_3-AR mRNA has been investigated in a variety of human tissues, such as white fat, gall bladder, small intestine, stomach and prostate (Krief *et al*., 1993; Berkowitz *et al*., 1995), to our knowledge, this is the first report of a distribution of β_3-AR mRNA in the human urinary bladder. A putative β_4-AR has been reported in the human heart (Kaumann, 1997). If β_4-AR cDNA is isolated and its DNA sequence is determined, more detailed analysis of the expression of β-AR would be possible.

Taken together, the results of the present pharmacological study and those of the mRNA analysis indicate the presence of the β_3-AR in the human detrusor. They further suggest that the relaxation of the human detrusor produced by adrenergic stimulation is mediated mainly by the β_3-AR.

This work was supported by the Swedish Medical Research Council (grant no 6837).

References

AIKAWA, J., FUKAZAWA, M., ISHIKAWA, M., MOROI, M., NAMIKI, A. & YAMAGUCHI, T. (1996). Vascular smooth muscle relaxation by α-adrenoceptor blocking action of dobutamine in isolated rabbit aorta. *J. Cardiovasc. Pharmacol.,* **27,** 33–36.

ANDERSON, G.F. & MARKS, B.H. (1984). Beta adrenoreceptors in the rabbit bladder detrusor muscle. *J. Pharmacol. Exp. Ther.,* **228,** 283–286.

ANDERSSON, K.-E. (1993). Pharmacology of lower urinary tract smooth muscles and penile erectile tissues. *Pharmacol. Rev.,* **45,** 253–308.

ARUNLAKSHANA, O. & SCHILD, H.O. (1959). Some quantitative uses of drug antagonists. *Br. J. Pharmacol.,* **14,** 48–52.

BERKOWITZ, D.E., NARDONE, N.A., SMILEY, R.M., PRICE, D.T., KREUTTER, D.K., FREMEAU, R.T. & SCHWINN, D.A. (1995). Distribution of β_3-adrenoceptor mRNA in human tissues. *Eur. J. Pharmacol.,* **289,** 223–228.

BLOOM, J.D., DUTIA, M.D., JOHNSON, B.D., WISSNER, A., BURNS, M.G., LARGIS, E.E., DOLAN, J.A. & CLAUS, T.H. (1992). Disodium (*R,R*)-5-[2-[[2-(3-Chlorophenyl)-2-hydroxyethyl]-amino] propyl]-1,3-benzodioxole 2,2-dicarboxylate (CL316,243). A potent β-adrenergic agonist virtually specific for β_3 receptors. A promising antidiabetic and antibesity agent. *J. Med. Chem.,* **35,** 3081–3084.

DE BOER, R.E.P., BROUWER, F. & ZAAGSMA, J. (1993). The β-adrenoceptors mediating relaxation of rat oesophageal muscularis mucosae are predominantly of the β_3-, but also of the β_2-subtype. *Br. J. Pharmacol.,* **110,** 442–446.

DE PONTI, F., GIBELLI, G., CROCI, T., ARCIDIACO, M., CREMA, F. & MANARA, L. (1996). Functional evidence of atypical β_3-adrenoceptors in the human colon using the β_3-selective adrenoceptor antagonist, SR 59230A. *Br. J. Pharmacol.,* **117,** 1374–1376.

ELMÉR, M. (1974). Inhibitory β-adrenoceptors in the urinary bladder of the rat. *Life Sci.,* **15,** 273–280.

EMORINE, L.J., BLIN, N. & STROSBERG, A.D. (1994). The human β_3-adrenoceptor: the search for a physiological function. *Trends Pharmacol. Sci.,* **15,** 3–7.

EMORINE, L.J., MARULLO, S., BRIEND-SUREN, M.M., PATEY, G., TATE, K., DELAVIER-KLUTCHKO, C. & STROSBERG, A.D. (1989). Molecular characterization of the human β_3-adrenergic receptor. *Science,* **245,** 1118–1121.

GOEPEL, M., WITTMANN, A., RUBBEN, H. & MICHEL, M.C. (1997). Comparison of adrenoceptor subtype expression in porcine and human bladder and prostate. *Urol. Res.,* **25,** 199–206.

IGAWA, Y., YAMAZAKI, Y., TAKEDA, H., AKAHANE, M., AJISAWA, Y., YONEYAMA, T. & NISHIZAWA, O. (1998). Possible β_3-adrenoceptor-mediated relaxation of the human detrusor. *Acta. Physiol. Scand.,* **164,** 117–118.

KAUMANN, A.J. (1989). Is there a third heart β-adrenoceptor? *Trends Pharmacol. Sci.,* **10,** 316–320.

KAUMANN, A.J. (1996). (−)-CGP 12177-induced increase of human atrial contraction through a putative third β-adrenoceptor. *Br. J. Pharmacol.,* **117,** 93–98.

KAUMANN, A.J. (1997). Four β-adrenoceptor subtypes in the mammalian heart. *Trends Pharmacol. Sci.,* **18,** 70–76.

KOIKE, K., HORINOUCHI, T. & TAKAYANAGI, I. (1995). Possible mechanisms of β-adrenoceptor-mediated relaxation induced by noradrenaline in guinea pig taenia caecum. *Eur. J. Pharmacol.,* **279,** 159–163.

KRIEF, S., LÖNNQVIST, F., RAIMBAULT, S., BAUDE, B., SPRONSEN, A.V., ARNER, P., STRÖSBERG, A.D., RICQUIER, D. & EMORINE, L.J. (1993). Tissue distribution of β_3-adrenergic receptor mRNA in man. *J. Clin. Invest.,* **91,** 344–349.

LANDS, A.M., ARNOLD, A., MCAULIFF, J.P., LUDUENA, F.P. & BROWN JR, T.G. (1967a). Differentiation of receptor systems activated by sympathomimetic amines. *Nature,* **214,** 597–598.

LANDS, A.M., LUDUENA, F.P. & BUZZO, H.J. (1967b). Differentiation of receptors responsive to isoproterenol. *Life Sci.,* **6,** 2241–2249.

LANGIN, D., PORTILLO, M.P., SAULNIER-BLACHE, J.-S. & LAFONTAN, M. (1991). Coexistence of three β-adrenoceptor subtypes in white fat cells of various mammalian species. *Eur. J. Pharmacol.,* **199,** 291–301.

LARSEN, J.-J. (1979). α- and β-adrenoceptors in the detrusor muscle and bladder base of the pig and β-adrenoceptors in the detrusor muscle of man. *Br. J. Pharmacol.,* **65,** 215–222.

LEVIN, R.M., RUGGIERI, M.R. & WEIN, A.J. (1988). Identification of receptor subtypes in the rabbit and human urinary bladder by selective radio-ligand binding. *J. Urol.,* **139,** 844–848.

LI, J.H., YASAY, G.D. & KAU, S.T. (1992). β-Adrenoceptor subtypes in the detrusor of guinea-pig urinary bladder. *Pharmacology,* **44,** 13–18.

MANARA, L., BADONE, D., BARONI, M., BOCCARDI, G., CECCHI, R., CROCI, T., GIUDICE, A., GUZZI, U., LANDI, M. & FUR, G.L. (1996). Functional identification of rat atypical β-adrenoceptors by the first β_3-selective antagonists, aryloxypropanolaminotetralins. *Br. J. Pharmacol.,* **117,** 435–442.

NERGÅRDH, A., BORÉUS, L.O. & NAGLO, A.-S. (1977). Characterization of the adrenergic beta-receptor in the urinary bladder of man and cat. *Acta. Pharmacol. Toxicol.,* **40,** 14–21.

ORIOWO, M.A., CHAPMAN, H., KIRKHAM, D.M., SENNITT, M.V., RUFFOLO JR, R.R. & CAWTHORNE, M.A. (1996). The selectivity *in vitro* of the stereoisomers of the *beta*-3 adrenoceptor agonist BRL37344. *J. Pharmacol. Exp. Thera.,* **277,** 22–27.

OZAKI, N., KAWAKITA, S. & TODA, N. (1982). Effects of dobutamine on isolated canine cerebral, coronary, mesenteric, and renal arteries. *J. Cardiovasc. Pharmacol.,* **4,** 456–461.

RUFFOLO, R.R. (1987). The pharmacology of dobutamine. *Am. J. Med. Sci.,* **294,** 244–248.

RUFFOLO JR, R.R., MESSICK, K. & HORNG, J.S. (1984). Interactions of the three inotropic agents, ASL-7022, dobutamine, and dopamine, with α- and β-adrenoceptors in vitro. *Naynyn-Schmiedeberg's Arch. Pharmacol.,* **326,** 317–326.

SEGUCHI, H., NISHIMURA, J., ZHOU, Y., NIIRO, N., KUMAZAWA, J. & KANAIDE, H. (1998). Expression of β_3-adrenoceptors in rat detrusor smooth muscle. *J. Urol.,* **159,** 2197–2201.

TSO, J.Y., SUN, X.H., KAO, T.H., REECE, K.S. & WU, R. (1985). Isolation and characterization of rat and human glyceraldehyde-3-phosphate dehydrogenase cDNAs: geomic complexity and molecular evolution of the gene. *Nucleic Acids Res.,* **13,** 2485–2502.

YAMAZAKI, Y., TAKEDA, H., AKAHANE, M., IGAWA, Y., NISHIZAWA, O. & AJISAWA, Y. (1998). Species differences in the distribution of β-adrenoceptor subtypes in bladder smooth muscle. *Br. J. Pharmacol.,* **124,** 593–599.

(Received July 20, 1998
Revised November 6, 1998
Accepted November 11, 1998)

British Journal of Pharmacology (1999) 126, 826–832
http://www.stockton-press.co.uk/bjp

The subtype 2 of angiotensin II receptors and pressure-natriuresis in adult rat kidneys

*,[1]K.L. Liu, [1]M. Lo, [2]E. Grouzmann, [3]M. Mutter & [1]J. Sassard

[1]Département de Physiologie et Pharmacologie Clinique, CNRS ESA 5014, IFR 39, Faculté de Pharmacie, 69008 Lyon, France; [2]Division d'Hypertension, Centre Hospitalier Universitaire Vaudois, Université de Lausanne, Lausanne, Switzerland; [3]Institut de Chimie Organique, Université de Lausanne, Lausanne, Switzerland

1 The present work examined the effects of the subtype 2 of angiotensin II (AT_2) receptors on the pressure-natriuresis using a new peptide agonist, and the possible involvement of cyclic guanosine 3′, 5′ monophosphate (cyclic GMP) in these effects.

2 In adult anaesthetized rats (Inactin, 100 mg kg^{-1}, i.p.) deprived of endogenous angiotensin II by angiotensin converting enzyme inhibition (quinapril, 10 mg kg^{-1}, i.v.), T_2-(Ang II 4-8)$_2$ (TA), a highly specific AT_2 receptor agonist (5, 10 and 30 μg kg^{-1} min^{-1}, i.v.) or its solvent was infused in four groups. Renal functions were studied at renal perfusion pressures (RPP) of 90, 110 and 130 mmHg and urinary cyclic GMP excretion when RPP was at 130 mmHg. The effects of TA (10 μg kg^{-1} min^{-1}) were reassessed in animals pretreated with PD 123319 (PD, 50 μg kg^{-1} min^{-1}, i.v.), an AT_2 receptor antagonist and the action of the same dose of PD alone was also determined.

3 Increases in RPP from 90 to 130 mmHg did not change renal blood flow (RBF) but induced 8 and 15 fold increases in urinary flow and sodium excretion respectively. The 5 μg kg^{-1} min^{-1} dose of TA was devoid of action. The 10 and 30 μg kg^{-1} min^{-1} doses did not alter total RBF and glomerular filtration rate, but blunted pressure-diuresis and natriuresis relationships. These effects were abolished by PD.

4 TA decreased urinary cyclic GMP excretion. After pretreatment with PD, this decrease was reversed to an increase which was also observed in animals receiving PD alone.

5 In conclusion, renal AT_2 receptors oppose the sodium and water excretion induced by acute increases in blood pressure and this action cannot be directly explained by changes in cyclic GMP.

Keywords: Angiotensin II; AT_2 receptors; cyclic GMP; pressure-natriuresis

Abbreviations: ACE, angiotensin converting enzyme; AI, angiotensin I; AII, angiotensin II; AT_1, subtype 1 of angiotensin II receptor; AT_2, subtype 2 of angiotensin II receptor; cyclic GMP, cyclic guanosine 3′, 5′ monophosphate; NO, nitric oxide; RPP, renal perfusion pressure; TA, T_2-(Ang II 4-8)$_2$

Introduction

At the renal level, angiotensin II (AII) exerts potent vasoconstrictor effects and enhances the tubular sodium reabsorption, thus lowering the pressure-natriuresis (Mattson *et al*., 1991; Van Der Mark & Kline, 1994) which is a major determinant of the long-term blood pressure level (Guyton, 1990). Most of the renal actions of AII are mediated through subtype 1 receptors (AT_1). The role of the receptors belonging to the subtype 2 (AT_2) remains poorly defined. In the whole organism, mice lacking the AT_2 receptor gene exhibit increases in the blood pressure response to AII (Hein *et al*., 1995; Ichiki *et al*., 1995) thus suggesting that AT_2 receptors oppose the AT_1-mediated vasoconstriction. In the kidneys where AT_2 receptors represent 5–10% of the total AII receptors (Chang & Lotti, 1991; Zhuo *et al*., 1992; 1993; Ozono *et al*., 1997), the reported vascular effects are controversial. PD 123319, an AT_2 receptor antagonist was found to block the AII-induced renal vasoconstriction (Chatziantoniou & Arendshorst, 1993) and intracellular calcium mobilization in vascular smooth muscle cells (Zhu & Arendshorst, 1996). In contrast, other studies showed that PD 123319 augmented the AII-induced vasoconstriction in both pre- and post-glomerular arterioles (Arima *et al*., 1996; Endo *et al*., 1997). Concerning the excretory functions, AT_2 receptor blockade with PD 123319 increased the urine volume, chloride and bicarbonate excretion in anaesthetized rats (Cogan *et al*., 1991) and increased free water formation in anaesthetized dogs (Keiser *et al*., 1992). We previously observed that, in rats infused with AII and the AT_1 receptor antagonist losartan, the blockade of AT_2 receptors with PD 123319 increased the pressure-natriuresis while CGP 42112B, an AT_2 receptor ligand with agonistic properties, lowered the pressure-natriuresis (Lo *et al*., 1995). Since the interpretation of the above reported data relies upon the selectivity of the various ligands, our attention was drawn by a new compound T_2-(Ang II 4-8)$_2$ (TA), which is the most specific peptide agonist available for AT_2 receptors (Grouzmann *et al*., 1995). We therefore thought it is of interest to examine its effects on the pressure-natriuresis. In addition, since it has been suggested that AT_2 receptors may interact with the formation of cyclic guanosine 3′, 5′ monophosphate (cyclic GMP) which mediates the renal vasodilatation and natriuresis induced by nitric oxide (NO) (Siragy *et al*., 1992) and atrial natriuretic peptide (Margulies & Burnett, 1994), we measured urinary excretion of cyclic GMP so as to approach the intracellular mechanisms of the effects of AT_2 receptor stimulation.

*Author for correspondence at: Département de Physiologie et Pharmacologie Clinique, CNRS ESA 5014, Faculté de Pharmacie, 8 avenue Rockefeller, 69373 Lyon Cedex 08, France.
E-mail: klliu@rockefeller.univ-lyon1.fr

Methods

Animals

Ten week-old male Sprague-Dawley rats (Iffa-Credo, Les Oncins, France) were used. They were housed in controlled conditions (temperature: $21 \pm 1°C$; humidity: $60 \pm 10\%$; lighting: 8–20 h), and fed a standard rat chow containing 0.3% sodium (Elevage UAR, Villemoisson sur Orge, France) and tap water *ad libitum*. The studies were conducted in agreement with our institutional guidelines for animal care.

AT_2 receptor ligands

TA (T_2-(Ang II 4–8)$_2$) is a template-assembled peptide agonist for AT_2 receptors (Institute of Organic Chemistry, Lausanne, Switzerland). It is made of two angiotensin II 4–8 pentapeptide fragments (Ang II 4–8)$_2$, attached to a carrier molecule (T_2) which alone did not bind to either AT_1 or AT_2 receptors (Grouzmann *et al*., 1995). Binding assays showed that in the presence of an AT_1 antagonist, TA completely inhibited the specific binding of ^{125}I-AII to the AT_2 receptors of a rat adrenal membrane preparation and that half-maximal inhibition (IC_{50}) occurred at the concentration of 2×10^{-7} M. In contrast, TA at the concentration of 10^{-5} M did not bind to AT_1 receptors of rat aortic smooth muscle cells (Grouzmann *et al*., 1995). PD 123319 (Parke-Davis, Ann Arbor, MI, U.S.A.), a non-peptide AT_2 receptor antagonist, exhibits an IC_{50} of 0.5×10^{-7} M for AT_2 receptors and did not bind to AT_1 receptors of rat aortic smooth muscle cells at the concentration of 10^{-5} M (Grouzmann *et al*., 1995). PD 123319 was dissolved in saline and infused at the dose of 50 μg kg^{-1} min^{-1} which, according to Macari *et al*. (1993), yields plasma concentrations close to 3×10^{-6} M, i.e. a value which remains highly specific for AT_2 receptors. TA was dissolved in a 12% solution of dimethyl sulphoxide in saline and three doses (5, 10 and 30 μg kg^{-1} min^{-1}, i.v.) were chosen according to preliminary experiments.

Surgical preparation

Pressure-natriuresis was studied using the method of Roman & Cowley (1985). The right kidney and adrenal gland were removed and the rats allowed 7–10 days to recover. On the day of experiment, the rats were anaesthetized with Inactin (100 mg kg^{-1}, i.p., Research Biochemicals, Natick, MA, U.S.A.) and placed on a heating blanket (Model 50-6980, Harvard Apparatus, Edenbrige, KY, U.S.A.) to maintain the rectal temperature at $37 \pm 0.5°C$. After tracheotomy, the left jugular vein was cannulated for infusion. Catheters were placed into the left carotid and femoral arteries to sample blood and to record the mean arterial blood pressure through a pressure transducer (Model P23ID, Statham Instrument Division, Gould Inc., Cleveland, OH, U.S.A.). After an abdominal incision, the left kidney was exposed and denervated by stripping all the visible renal nerves and coating the renal artery with a 10% solution of phenol in ethanol. The remaining adrenal gland was then removed and the left ureter cannulated for urine collection. Two adjustable silastic balloon cuffs were placed around the aorta, one above the renal artery between the superior mesenteric and celiac arteries, the other below the left renal artery so that the renal perfusion pressure (RPP) could be fixed at different levels. Silk ligatures were placed loosely around the superior mesenteric and celiac arteries and tighten to further elevate the RPP. An ultrasonic flow probe (1RB) was placed around the left renal artery so as to continuously record the total renal blood flow using a transonic transit-time flowmeter (Model T106, Transonic Systems Inc., Ithaca, NY, U.S.A.). After a priming dose (250 mg kg^{-1}, i.v.) of polyfructosan (Inutest, Laevosan, Linz, Austria), a hormone-cocktail (Mattson *et al*., 1991; Liu *et al*., 1996) designed to fix the circulating levels of the most important sodium- and water-retaining hormones was infused at a rate of 330 μl kg^{-1} min^{-1} (Pump Model 2400-001, Harvard Apparatus, South Natick, MA, U.S.A.). It contained d-aldosterone (66 ng kg^{-1} min^{-1}), hydrocortisone (33 ng kg^{-1} min^{-1}), norepinephrine (333 ng kg^{-1} min^{-1}) and Arg^8-vasopressin acetate (0.17 ng kg^{-1} min^{-1}). Drugs were obtained from Sigma Chemicals (St. Louis, MO, U.S.A.) and dissolved in 0.9% sodium chloride containing 1% bovine serum albumin (Fraction V) and 1.25% polyfructosan. At the end of the experiment, the left kidney was decapsulated, removed, cut in half, blotted dry and weighed.

Renal parameters

RPP (mmHg) was estimated as the mean femoral artery pressure when the suprarenal aortic cuff was inflated and as the mean carotid artery pressure when the infrarenal aortic cuff was inflated. Glomerular filtration rate (ml min^{-1} g^{-1}) was measured by polyfructosan clearance. Urine flow (μl min^{-1} g^{-1}) was determined by weighing, and sodium concentration by flame photometry (IL meter, model 243, Lexington, MA, U.S.A.) so as to calculate urinary sodium excretion (μmoles min^{-1} g^{-1}). Urinary concentration of cyclic GMP was determined by an enzyme immunoassay kit (Cayman Chemical Company, Ann Arbor, MI, U.S.A.) (Pradelles *et al*., 1989) with which the minimum detectable concentration approched 0.04 pmol ml^{-1} and the coefficient of variation was below 5%. All the parameters were normalized per gram of the left kidney weight.

Experimental protocol

The endogenous production of AII was blocked by an angiotensin converting enzyme (ACE) inhibitor, quinapril (10 mg kg^{-1}, i.v.) (Parke-Davis, Ann Arbor, MI, U.S.A.) so as to eliminate any interference due to changes in renal renin release. The efficiency of this inhibition during the whole of the experimental period is shown in Figure 1. The injection of angiotensin I (AI, 750 ng kg^{-1}) in five animals increased mean blood pressure by $37 \pm 5\%$ and lowered renal blood flow by $82 \pm 5\%$. These responses were fully abolished during the 2 h following quinapril injection.

Sixty minutes after the hormonal-cocktail infusion begun, quinapril (10 mg kg^{-1}, i.v.) was given 30 min prior to the start of the study. In a first protocol, four groups of animals were used. Controls received dimethyl sulphoxide (the solvent for TA) at the rate corresponding to that infused with the different doses of TA. Three doses of TA (5, 10 and 30 μg kg^{-1} min^{-1}, i.v) were randomly allocated each to one group of rats 10 min prior to the start of the study. To confirm the specificity of the findings, TA (10 μg kg^{-1} min^{-1}) was given to another group of animals in which PD 123319 (50 μg kg^{-1} min^{-1}) was infused starting 15 min before. Finally, so as to check whether PD 123319 by itself could influence renal functions, an additional group of rats received PD 123319 alone at the same dose of 50 μg kg^{-1} min^{-1}. In both protocols, the renal functions were studied at a RPP of 90 mmHg, a level close to the basal mean blood pressure level, and, later on, at 110 and 130 mmHg. Urines were collected for 20, 10 and 10 min respectively. Arterial blood (200 μl) was sampled at the end of

each period. Urines collected at RPP of 130 mmHg were used for cyclic GMP assay, since at the lower levels of pressure the volume of urines did not allow all the measurements to be done.

Statistical analysis

Values are means ± s.e.mean. Two-way analysis of variance (ANOVA) was used to statistically evaluate the differences between groups over the whole range of RPP. The differences at a given level of RPP were assessed using the Student's *t*-test for unpaired data. A difference was considered statistically significant at $P<0.05$.

Results

Effects of AT_2 receptor ligands on renal functions

The renal functions observed at a RPP of 90 mmHg, a level close to the basal mean blood pressure level in rats deprived of endogenous AII are shown in Table 1. Neither the infusion of TA nor that of PD 123319 changed significantly these baseline renal functions.

Figure 2 shows that in control animals, a stepwise elevation in RPP from 90 to 130 mmHg, did not change total renal blood flow and glomerular filtration rate, but induced 8 and 15 fold increases in urine flow and sodium excretion respectively. The lowest dose of TA (5 μg kg^{-1} min^{-1}) did not modify the effects of increasing renal perfusion pressure. When infused at the rate of 10 μg kg^{-1} min^{-1}, TA did not affect, over the whole range of pressures, total renal blood flow and glomerular filtration rate, while it significantly decreased pressure-diuresis (ANOVA, $P<0.001$) and natriuresis relationships (ANOVA, $P<0.03$) by increasing the tubular sodium reabsorption (98.0 ± 0.2 and 99.0 ± 0.3% in control and TA-treated animals respectively at the RPP of 130 mmHg, $P<0.05$). The 30 μg kg^{-1} min^{-1} dose of TA induced effects similar to those of 10 μg kg^{-1} min^{-1}.

Figure 3 shows that, in animals deprived of endogenous AII, pressure-diuresis and natriuresis observed during the infusion of PD 123319 alone did not differ from those of controls although glomerular filtration rate was significantly increased (ANOVA, $P<0.01$). The combined infusion of PD 123319 and TA did not change the relationships between RPP, renal blood flow and glomerular filtration rate. The decreases in pressure-diuresis and -natriuresis observed during infusion of TA (10 μg kg^{-1} min^{-1}) were fully abolished by PD 123319.

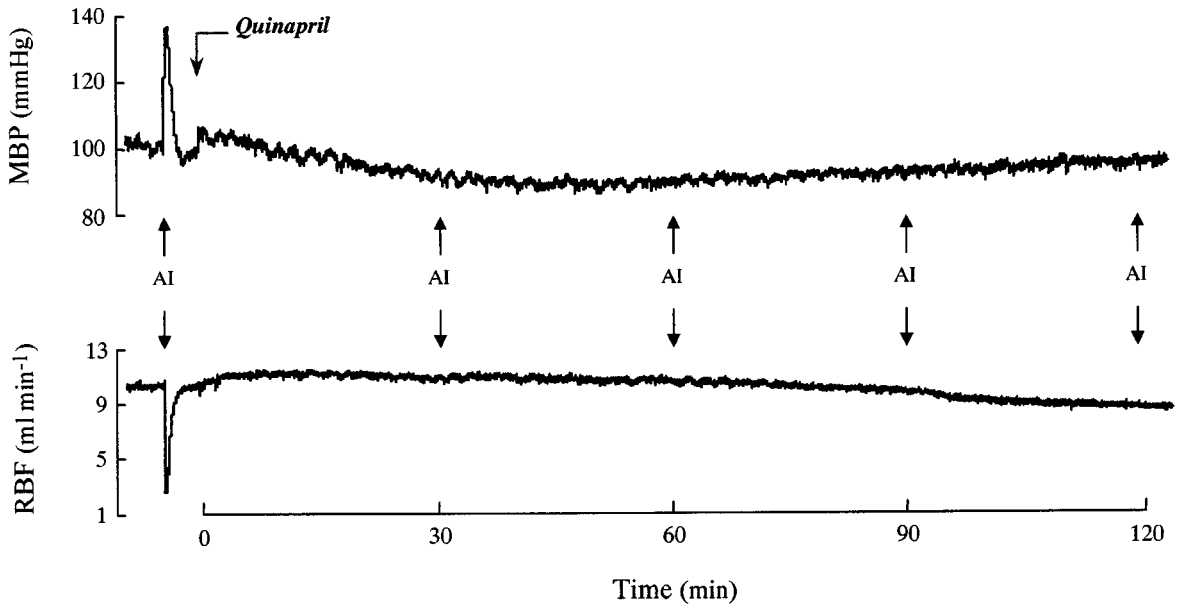

Figure 1 Averaged values ($n=5$) of mean blood pressure (MBP) and renal blood flow (RBF) in response to angiotensin I (AI) injections (750 ng kg^{-1}) before, 30, 60, 90 and 120 min after angiotensin converting enzyme inhibition by quinapril (10 mg kg^{-1}).

Table 1 Effects of AT_2 receptor ligands on baseline renal functions

	n	*MBP* (mmHg)	*RBF* (ml min^{-1} g^{-1})	*GFR* (ml min^{-1} g^{-1})	*V* (μl min^{-1} g^{-1})	*UNaV* (μmol min^{-1} g^{-1})
Controls	9	91 ± 1	6.5 ± 0.5	0.9 ± 0.1	4.1 ± 0.5	0.17 ± 0.04
TA-5	6	90 ± 1	6.5 ± 0.5	1.1 ± 0.3	3.7 ± 0.8	0.20 ± 0.04
TA-10	9	91 ± 1	6.4 ± 0.4	0.9 ± 0.1	3.5 ± 0.3	0.20 ± 0.05
TA-30	4	93 ± 2	7.4 ± 0.3	1.0 ± 0.1	4.2 ± 0.5	0.17 ± 0.05
PD	7	88 ± 2	5.9 ± 0.2	0.9 ± 0.1	3.0 ± 0.4	0.15 ± 0.02
PD + TA-10	7	91 ± 2	6.2 ± 0.4	1.2 ± 0.2	4.3 ± 0.5	0.25 ± 0.10

Mean blood pressure (MBP), renal blood flow (RBF), glomerular filtration rate (GFR), urine flow (V) and urinary sodium excretion (UNaV) observed at prevailing blood pressure in rats deprived of endogenous angiotensin II and infused with solvent (Controls) or TA at the dose of 5, 10 or 30 μg kg^{-1} min^{-1} (TA-5, TA-10 and TA-30) or PD 123319 (50 μg kg^{-1} min^{-1}, PD) or PD 123319 combined to TA (PD + TA-10).

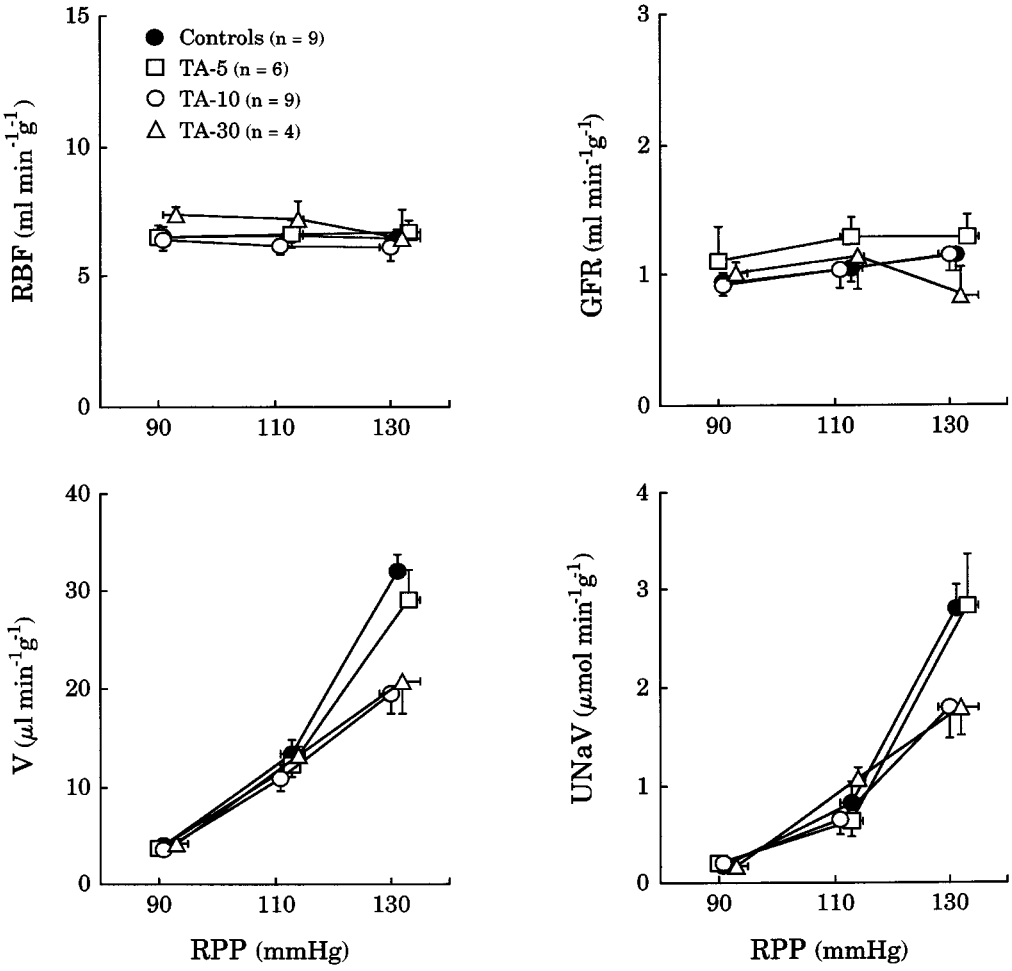

Figure 2 Effects of TA on the relationships between renal perfusion pressure (RPP), renal blood flow (RBF), glomerular filtration rate (GFR), urine flow (V) and sodium excretion (UNaV) in rats deprived of endogenous angiotensin II and infused with solvent (Controls) or TA at the doses of 5, 10 or 30 μg kg^{-1} min^{-1} (TA-5, TA-10 and TA-30).

Effect of AT_2 receptor stimulation on urinary excretion of cyclic GMP

As shown in Figure 4, urinary excretion of cyclic GMP, measured at the renal perfusion pressure of 130 mmHg, was significantly decreased during the infusion of TA alone (10 μg kg^{-1} min^{-1}). This decrease was transformed into an increase when TA was given in rats pretreated with PD 123319. Interestingly, PD 123319 alone also tended to increase the urinary excretion of cyclic GMP.

Discussion

The present work shows that the acute stimulation of AT_2 receptors with a new highly specific peptide agonist in adult rats, blunts pressure-natriuresis and -diuresis, and suggests that these effects of AT_2 receptors do not directly involve changes in cyclic GMP release.

The method developed by Roman & Cowley (1985) is one of the most widely used to study the acute pressure-natriuresis in anaesthetized rats. We applied this technique after ACE inhibition so as to block the endogenous production of AII and possibly enhance the renal sensitivity to AII (Richer *et al.*, 1983). The efficiency of ACE inhibition in this work was demonstrated by the lack of pressor response to AI injections during the whole experimental period. Among the compounds having agonistic properties for AT_2 receptors, TA seems the most selective as it leaves intact AT_1 receptors at concentration above 10^{-5} M, while CGP 42112, starts having significant interactions with AT_1 receptors at the concentration of 10^{-6} M (Grouzmann *et al.*, 1995). Using this compound, we observed that at the doses of 5, 10 and 30 μg kg^{-1} min^{-1}, TA had no effect on the total renal blood flow. Since this latter is mainly controlled by AT_1 receptors (Keiser *et al.*, 1992; Lo *et al.*, 1995), this result suggests that even the highest dose of TA used, remained fully specific for AT_2 receptors. Contrasting with this lack of overall vascular effect, TA lowered pressure-natriuresis and -diuresis. These effects were dose-dependent partially only since, the 5 μg kg^{-1} min^{-1} dose was devoid of action while the maximum effect was obtained with the 10 μg kg^{-1} min^{-1} dose. Such a narrow dose-response relationship is difficult to explain. It might relate to the low number of AT_2 receptors available or to the high sensitivity of AT_2 receptors in our experimental conditions. The specificity of the observed effects of TA on natriuresis and diuresis was further confirmed by their disappearance after infusion of PD 123319 at a dose which does not affect AT_1 receptors (Macari *et al.*, 1993). Thus AT_2 receptor stimulation lowers pressure-natriuresis. According to this finding, Madrid *et al.*, (1997a) recently reported that in rats in which NO synthesis was blocked with N$^{\omega}$-nitro-L-arginine methyl ester, AT_1 receptor blockade had no effect on the slope of the pressure-natriuresis curve, while PD 123319 normalized it thus indicating that the

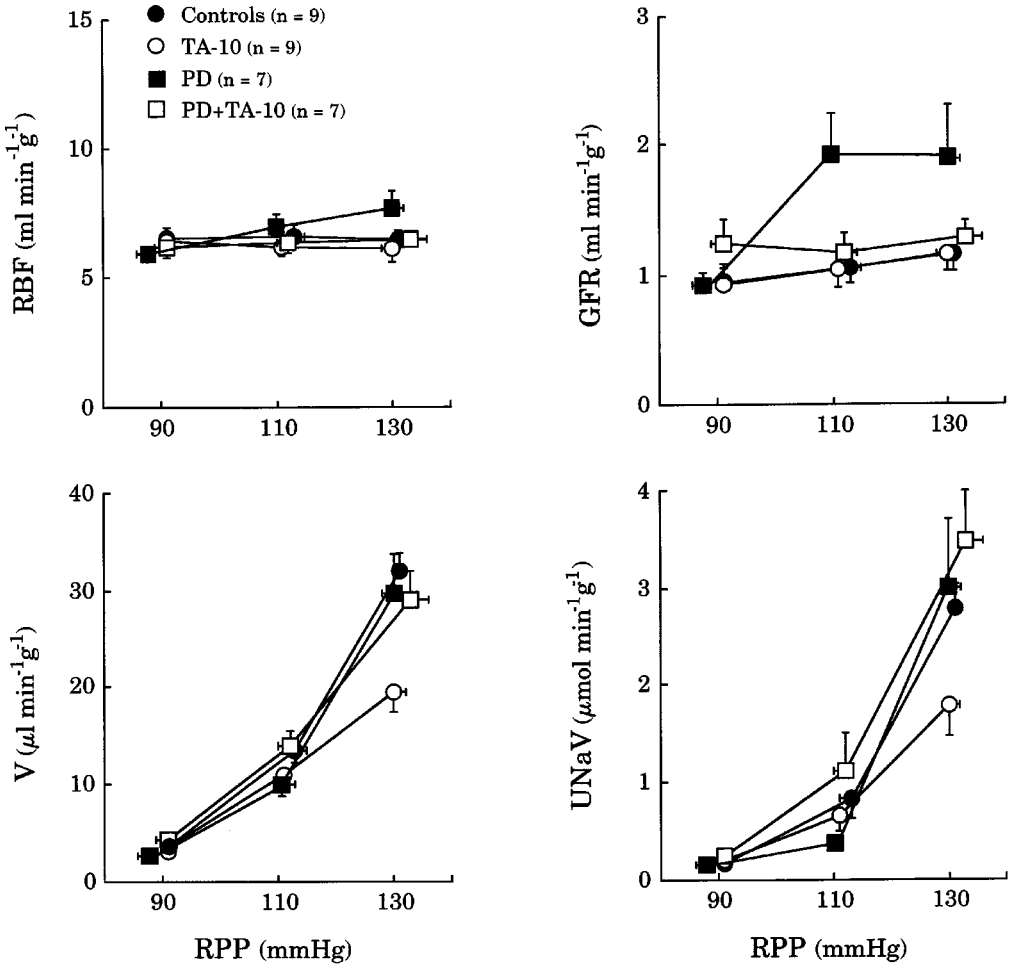

Figure 3 Effects of renal perfusion pressure (RPP) on renal blood flow (RBF), glomerular filtration rate (GFR), urine flow (V) and sodium excretion (UNaV) in rats deprived of endogenous angiotensin II and infused with solvent (Controls) or TA (10 μg kg^{-1} min^{-1}, TA-10) or PD 123319 (50 μg kg^{-1} min^{-1}, PD) or PD 123319 combined to TA (PD+TA-10).

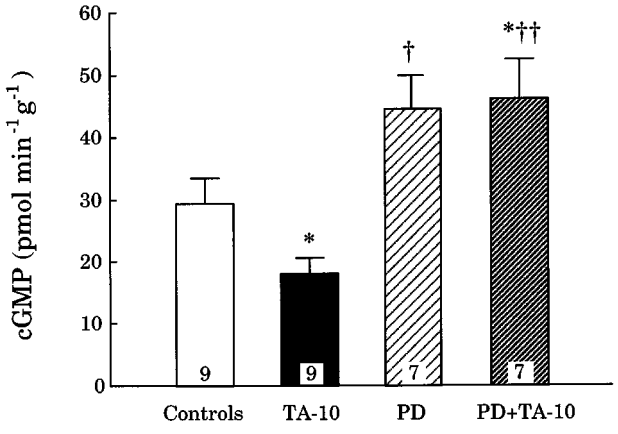

Figure 4 Urinary excretion of cyclic guanosine 3′, 5′ monophosphate (cyclic GMP) in rats deprived of endogenous angiotensin II and infused with solvent (Controls) or TA (10 μg kg^{-1} min^{-1}, TA-10) or PD 123319 (50 μg kg^{-1} min^{-1}, PD) or PD 123319 combined to TA (PD+TA-10). The renal perfusion pressure was set at 130 mmHg. $^{*}P<0.05$ vs controls; $^{\dagger}P<0.05$, $^{\dagger\dagger}P<0.01$ vs TA-10.

pressure-natriuresis was under the control of AT_2 receptors. Such a function of AT_2 receptors is also in accordance with the fact that in acute conditions, AII lowers the pressure-natriuresis (Mattson *et al*., 1991) while AT_1 receptor blockade with losartan given acutely does not affect the pressure-natriuresis in rats (Kline & Liu, 1994; Lo *et al*., 1995). In addition, recent studies showing that dietary sodium depletion increases the density of AT_2 receptors in adult rat kidneys (Ozono *et al*., 1997) and decreases that of AT_1 receptors (Ruan *et al*., 1997) reinforce the hypothesis that AT_2 receptors could be involved in sodium preservation. In that respect, since in the present experiment, as well as in our previous one (Lo *et al*., 1995), the effects of AT_2 receptor stimulation or blockade were more marked when renal perfusion pressure was elevated, it can be speculated that AT_2 receptors contribute to prevent the sodium losses which would follow acute increases in blood pressure.

The mechanisms of this action are difficult to approach, because little is known about not only the intracellular signaling pathways of AT_2 receptors but also about the mechanisms involved in pressure-natriuresis. Concerning the signaling pathways of AT_2 receptors *in vitro* studies conducted in tissues that selectively or mainly express these receptors, show that the activation of AT_2 receptors in R3T3 fibroblasts stimulates a phosphotyrosine phosphatase (Tsuzuki *et al*., 1996) and decreases cyclic GMP formation in rat adrenal gland (Israel *et al*., 1995). More recently, several kinases belonging to transduction cascades were shown to be altered by AT_2 receptor stimulation (Fischer *et al*., 1998). Concerning the mechanisms involved in pressure-natriuresis, the most widely accepted hypothesis is that, in rats, they implicate increases in

the poorly regulated papillary blood perfusion (Roman *et al*., 1988a) leading to rises in renal interstitial pressure (Granger, 1992) which will reduce the tubular sodium and fluid reabsorption. In that respect, the reported effects of AII on renal medullary circulation varied upon the experimental conditions. The intravenous infusion of AII at high doses did not modify (Nobes *et al*., 1991) or increased (Parekh & Zou, 1996) medullary blood flow, an effect which was mediated by the release of vasodilator prostaglandins. The intrarenal infusion of AII at a physiological dose (0.5 ng kg^{-1} min^{-1}) decreased papillary flow without altering cortical renal blood flow and glomerular filtration rate (Faubert *et al*., 1987). Consistently, AII receptor blockade with saralasin as well ACE inhibition increased papillary blood flow in rats having received a bradykinin antagonist (Roman *et al*., 1988b). Since AT_1 receptor blockade was found devoid of action on papillary blood flow (Madrid *et al*., 1997b), it can be postulated that AII constricts medullary vessels through AT_2 receptors. Another possible mechanism is that AT_2 receptor stimulation might blunt NO release. This is suggested by the fact that, in the present work, as well as in our previous one (Lo *et al*., 1995), AT_2 receptors were found more efficient at high than at normal pressure, a condition which, through elevated shear-stress, stimulates NO production, and might contribute to pressure-induced natriuresis by impairing the autoregulation of papillary flow (Fenoy *et al*., 1995). To test this hypothesis and although it is known that cyclic GMP is under the control of several circulating agents such as atrial natriuretic peptide, we used its urinary excretion as an index of renal NO synthesis (Siragy *et al*., 1992). We observed that urinary excretion of cyclic GMP decreased during infusion of TA alone. However, when TA was given after PD 123319, urinary cyclic GMP excretion reached greater values than in controls. Finally, since PD 123319 given alone which, despite a surprising and unexplained increase in glomerular filtration rate, was devoid of effect on pressure-diuresis and -natriuresis, also increased urinary cyclic GMP, it became obvious that antinatriuretic properties of AT_2 receptor stimulation could not be explained by a decreased formation or release of cyclic GMP in the kidney.

In conclusion, using a new highly specific agonist, we confirm that AT_2 receptor stimulation blunts pressure-natriuresis, and can contribute to prevent the sodium losses induced by acute increases in blood pressure.

This work was supported by Centre National de la Recherche Scientifique. It has been presented as an oral communication at the Eighth European Meeting on Hypertension, Milan, Italy (June, 1997). We gratefully acknowledge J. Sacquet for her technical assistance. PD 123319 and quinapril were generous gifts of Parke-Davis Laboratories.

References

ARIMA, S., ITO, S., OMATA, K., TSUNODA, K., YAOITA, H. & ABE, K. (1996). (abstract). Activation of angiotensin II type 2 receptor (AT_2) causes epoxyeicosatrienoic acids (EETs)-dependent vasodilation in the micro-perfused rabbit afferent arterioles. *Hypertension,* **28,** 515.

CHANG, R.S.L. & LOTTI, V.J. (1991). Angiotensin receptor subtypes in rat, rabbit, and monkey tissues: Relative distribution and species dependency. *Life Sci.,* **49,** 1485–1490.

CHATZIANTONIOU, C. & ARENDSHORST, W.J. (1993). Angiotensin receptor sites in renal vasculature of rats developing genetic hypertension. *Am. J. Physiol.,* **265,** F853–F862.

COGAN, M.G., LIU, F.Y., WONG, P.C. & TIMMERMANS, P.B.M.W.M. (1991). Comparison of inhibitory potency by nonpeptide angiotensin II receptor antagonists PD 123177 and Dup 753 on proximal nephron and renal transport. *J. Pharmacol. Exp. Ther.,* **259,** 687–691.

ENDO, Y., ARIMA, S., YAOITA, H., OMATA, K., TSUNODA, K., TAKEUCHI, K., ABE, K. & ITO, S. (1997). Function of angiotensin II type 2 receptor in the postglomerular efferent arteriole. *Kidney Int.,* **52,** (Suppl. 63), S205–S207.

FAUBERT, P.F., CHOU, S.Y. & PORUSH, J.G. (1987). Regulation of papillary plasma flow by angiotensin II. *Kidney Int.,* **32,** 472–478.

FENOY, F.J., FERRER, P., CARBONELL, L. & SALOM, M.G. (1995). Role of nitric oxide on papillary blood flow and pressure natriuresis. *Hypertension,* **25,** 408–414.

FISCHER, T.A., SINGH, K., HARA, D.S., KAYE, D.M. & KELLY, R.A. (1998). Role of AT_1 and AT_2 receptors in regulation of MAPKs and MKP-1 by ANG II in adult cardiac myocytes. *Am. J. Physiol.,* **275,** H906–H916.

GRANGER, J.P. (1992). Pressure natriuresis: role of renal interstitial hydrostatic pressure. *Hypertension,* **19,** (Suppl I), I9–I17.

GROUZMANN, E., FELIX, D., IMBODEN, H., RAZANAME, A. & MUTTER, M. (1995). A specific template-assembled peptidic agonist for the angiotensin II receptor subtype 2 (AT_2) and its effect on inferior olivary neurones. *Eur. J. Biochem.,* **234,** 44–49.

GUYTON, A.C. (1990). Long-term arterial pressure control: an analysis from animal experiments and computer and graphic models. *Am. J. Physiol.,* **259,** R865–R877.

HEIN, L., BARSH, G.S., PRATT, R.E., DZAU, V.J. & KOBILKA, B.K. (1995). Behavioural and cardiovascular effects of disrupting the angiotensin II type-2 receptor gene in mice. *Nature,* **377,** 744–747.

ICHIKI, T., LABOSKY, P.A., SHIOTA, C., OKUYAMA, S., IMAGAWA, Y., FOGO, A., NIIMURA, F., ICHIKAWA, I., HOGAN, B.L.M. & INAGAMI, T. (1995). Effects on blood pressure and exploratory behaviour of mice lacking angiotensin II type-2 receptor. *Nature,* **377,** 748–750.

ISRAEL, A., STROMBERG, C., TSUTSUMI, K., GARRIDO, M.R., TORRES, M. & SAAVEDRA, J.M. (1995). Angiotensin II receptor subtypes and phosphoinositide hydrolysis in rat adrenal medulla. *Brain Res. Bull.,* **38,** 441–446.

KEISER, J.A., BJORK, F.A., HODGES, J.C. & TAYLOR, JR. D.G. (1992). Renal hemodynamics and excretory responses to PD 123319 and losartan, non-peptide AT_1 and AT_2 subtype-specific angiotensin II ligands. *J. Pharmacol. Exp. Ther.,* **262,** 1154–1160.

KLINE, R.L. & LIU, F. (1994). Modification of pressure natriuresis by long-term losartan in spontaneously hypertensive rats. *Hypertension,* **24,** 467–473.

LIU, K.L., SASSARD, J. & BENZONI, D. (1996). In the Lyon hypertensive rat, renal function alterations are angiotensin II dependent. *Am. J. Physiol.,* **271,** R346–R351.

LO, M., LIU, K.L., LANTELME, P. & SASSARD, J. (1995). Subtype 2 of angiotensin II receptors controls pressure-natriuresis in rats. *J. Clin. Invest.,* **95,** 1394–1397.

MACARI, D., BOTTARI, S., WHITEBREAD, S., DE GASPARO, M. & LEVENS, N. (1993). Renal actions of the selective angiotensin AT_2 receptor ligands CGP 42112B and PD 123319 in the sodium-depleted rat. *Eur. J. Pharmacol.,* **249,** 85–93.

MADRID, M.I., SALOM, M.G., TORNEL, J., GASPARO, M. & FENOY, F.J. (1997a). Effect of interaction between nitric oxide and angiotensin II on pressure diuresis and natriuresis. *Am. J. Physiol.,* **273,** R1676–R1682.

MADRID, M.I., SALOM, M.G., TORNEL, J., GASPARO, M. & FENOY, F.J. (1997b). Interactions between nitric oxide and angiotensin II on renal cortical and papillary blood flow. *Hypertension,* **30,** 1175–1182.

MARGULIES, K.B. & BURNETT, JR. J.C. (1994). Inhibition of cyclic GMP phosphodiesterases augments renal responses to atrial natriuretic factor in congestive heart failure. *J. Card. Fail.,* **1,** 71–80.

MATTSON, D.L., RAFF, H. & ROMAN, R.J. (1991). Influence of angiotensin II on pressure natriuresis and renal hemodynamics in volume-expanded rats. *Am. J. Physiol.,* **260,** R1200–R1209.

NOBES, S., HARRIS, P.J., YAMADA, H. & MENDELSOHN, F.A.O. (1991). Effects of angiotensin II on renal cortical and papillary blood flows measured by laser-Doppler flowmetry. *Am. J. Physiol.,* **261,** F998 – F1006.

OZONO, R., WANG, Z.Q., MOORE, A.F., INAGAMI, T., SIRAGY, H.M. & CAREY, R.M. (1997). Expression of the subtype 2 angiotensin (AT_2) receptor protein in rat kidney. *Hypertension,* **30,** 1238 – 1246.

PAREKH, N. & ZOU, A.P. (1996). Role of prostaglandins in renal medullary circulation: response to different vasoconstrictors. *Am. J. Physiol.,* **271,** F653 – F658.

PRADELLES, P., GRASSI, J., CHABARDES, D. & GUISO, N. (1989). Enzyme immunoassays of adenosine cyclic 3′,5′-monophosphate and guanosine cyclic 3′,5′-monophosphate using acetylcholinesterase. *Anal. Chem.,* **61,** 447 – 453.

RICHER, C., DOUSSAU, M.P. & GIUDICELLI, J.F. (1983). Effects of captopril and enalapril on regional vascular resistance and reactivity in spontaneously hypertensive rats. *Hypertension,* **5,** 312 – 320.

ROMAN, R.J. & COWLEY, JR. A.W. (1985). Characterization of a new model for the study of pressure-natriuresis in the rat. *Am. J. Physiol.,* **248,** F190 – F198.

ROMAN, R.J., COWLEY, JR. A.W., GARCIA-ESTAN, J. & LOMBARD, J. (1988a). Pressure-diuresis in volume-expanded rats: cortical and medullary hemodynamics. *Hypertension,* **12,** 168 – 176.

ROMAN, R.J., KALDUNSKI, M.L., SCICLI, A.G. & CARRETERO, O.A. (1988b). Influence of kinins and angiotensin II on the regulation of papillary blood flow. *Am. J. Physiol.,* **255,** F690 – F698.

RUAN, X., WAGNER, C., CHATZIANTONIOU, C., KURTZ, A. & ARENDSHORST, W.J. (1997). Regulation of angiotensin II receptor AT_1 subtypes in renal afferent arterioles during chronic changes in sodium diet. *J. Clin. Invest.,* **99,** 1072 – 1081.

SIRAGY, H.M., JOHNS, R.A., PEACH, M.J. & CAREY, R.M. (1992). Nitric oxide alters renal function and guanosine 3′,5′-cyclic monophosphate. *Hypertension,* **19,** 775 – 779.

TSUZUKI, S., MATOBA, T., EGUCHI, S. & INAGAMI, T. (1996). Angiotensin II type 2 receptor inhibits cell proliferation and activates tyrosine phosphatase. *Hypertension,* **28,** 916 – 918.

VAN DER MARK, J. & KLINE, R.L. (1994). Altered pressure natriuresis in chronic angiotensin II hypertension in rats. *Am. J. Physiol.,* **266,** R739 – R748.

ZHU, Z. & ARENDSHORST, W.J. (1996). Angiotensin II-receptor stimulation of cytosolic calcium concentration in cultured renal resistance arterioles. *Am. J. Physiol.,* **271,** F1239 – F1247.

ZHUO, J., ALCORN, D., HARRIS, P.J. & MENDELSOHN, F.A.O. (1993). Localization and properties of angiotensin II receptors in rat kidney. *Kidney Int.,* **44,** (Suppl 42): S40 – S46.

ZHUO, J., SONG, K., HARRIS, P.J. & MENDELSOHN, F.A.O. (1992). In vitro autoradiography reveals predominantly AT_1 angiotensin II receptors in rat kidney. *Renal Physiol. Biochem.,* **15,** 231 – 239.

(Received October 19, 1998
Revised November 12, 1998
Accepted November 13, 1998)

British Journal of Pharmacology (1999) 126, 833–839
http://www.stockton-press.co.uk/bjp

Beta-adrenoceptor agonist stimulation of pulmonary nitric oxide production in the rabbit

*,[1]L. Christofer Adding, [1]Per Agvald, [1]Andreas Artlich, [1]Magnus G. Persson & [1,2]Lars E. Gustafsson

[1]Department of Physiology and Pharmacology, Karolinska Institute, S-171 77 Stockholm, Sweden; [2]Institute of Environmental Medicine, Karolinska Institute, S-171 77 Stockholm, Sweden

1 Nitric oxide (NO) is continuously produced in the lung and is present in exhaled air. We examined the effect of β-adrenoceptor stimulation on the production of pulmonary NO in rabbits.

2 Exhaled NO was measured by chemiluminescence in anaesthetized and mechanically ventilated rabbits and in buffer-perfused rabbit lungs.

3 Intravenous infusions of adrenaline ($0.1-10$ μg kg^{-1} min^{-1}) elicited dose-dependent increases in exhaled NO. The increases in exhaled NO comprised an initial peak followed by a lower plateau level. The increase in exhaled NO was inhibited by propranolol (1 mg kg^{-1}) but not by phentolamine (1 mg kg^{-1}).

4 Prenalterol, a β_1-adrenoceptor agonist, and terbutaline, a β_2-adrenoceptor agonist, also caused dose-dependent increases in exhaled NO. However, prenalterol was >100 times more potent than terbutaline.

5 Infusions of forskolin ($0.01-0.03$ μmol kg^{-1} min^{-1}), an adenylate cyclase stimulator, elicited dose-dependent decreases in blood pressure and concomitant increases in heart rate but caused no alterations in exhaled NO.

6 Nimodipine, a L-type calcium channel blocker, antagonized the increases in exhaled NO in response to prenalterol infusions.

7 The increases in exhaled NO in response to adrenaline and prenalterol were also present in blood-free, buffer perfused lungs during constant-flow conditions.

8 These results demonstrate that pulmonary nitric oxide production can be enhanced by β-adrenoceptor stimulation. Furthermore, the results indicate that the β-adrenergic stimulation of pulmonary NO production is not critically dependent on cyclic AMP formation but may require intact calcium-channels.

Keywords: β-adrenergic receptors; epinephrine; forskolin; lung; nimodipine; nitric oxide; perfusion; prenalterol; terbutaline

Introduction

Nitric oxide (NO) is derived from the amino acid L-arginine (Palmer *et al*., 1987; Marletta, 1989) and has many regulatory functions in the body, including the circulatory, immune and nervous systems (Moncada, 1994; Moncada *et al*., 1991).

In the lungs NO is continuously formed and its production can directly be monitored by analysing the concentrations of NO in the exhaled air (Gustafsson *et al*., 1991). Important functions for NO in the lungs are ventilation-perfusion matching (Persson *et al*., 1990), host-defense (Gustafsson *et al*., 1991; Wei *et al*., 1995), and anti-obstructive airway effects (Persson *et al*., 1995a). Furthermore NO contributes to the adaptation of the pulmonary circulation to extra-uterine life (Abman *et al*., 1990).

Several cell-types in the lung may contribute to the production of NO detected in exhaled air since the enzyme NO-synthase (NOS) can be found in epithelial, endothelial and neuronal cells in the lungs (Kobzik *et al*., 1993; Shaul *et al*., 1994; Asano *et al*., 1994; Lawrence *et al*., 1996). The NOS responsible for this NO production is constitutively expressed and is at least in part calcium-dependent (Persson *et al*., 1994a). Nitregic nerves in the lower airways might have a bronchodilator function (Belvesi *et al*., 1992) but it is not known whether this NO contributes to exhaled NO.

Factors influencing the NO formation in the lungs have only partially been characterized. Airway hypoxia and hypercapnea reduce NO in exhaled air (Gustafsson *et al*., 1991; Strömberg *et al*., 1997; Bannenberg *et al*., 1997). Infusions or orally administered L-arginine increase NO in exhaled air (Gustafsson *et al*., 1991; Kharitonov *et al*., 1995). Stretching the lungs of rabbits and guinea-pigs increases concentrations of exhaled nitric oxide (Persson *et al*., 1995b; Strömberg *et al*., 1997; Bannenberg & Gustafsson, 1997). Exhaled nitric oxide falls, whereas excretion rate increases, in response to exercise (Persson *et al*., 1993; Maroun *et al*., 1995) and high concentrations of nitric oxide are present in the upper airways of healthy newborn infants (Schedin *et al*., 1995). A common feature during the two latter conditions is an increased sympathetic activity with high concentrations of adrenaline in the blood (Lagercrantz & Slotkin, 1986). Recently it was reported that cultured tracheal epithelial cells generate nitric oxide in response to isoproterenol and cyclic AMP stimulation (Tamaoki *et al*., 1995a). β-adrenoceptor stimulating agents are thought to relax airways through stimulation of cyclic AMP formation in the smooth musculature. However, we found it of interest to investigate the possibility of a relationship between β-adrenoceptor activation and NO generation, since NO as mentioned above is a known bronchodilator and at least epithelial cells increase their NO production when stimulated with β-agonists. The aim of the present study was to determine whether β-adrenoceptor stimulation can affect NO production in the intact respiratory

*Author for correspondence.

system, and if such a stimulation might be exerted through cyclic AMP- or calcium-dependent mechanisms.

Methods

The experiments were approved by the local animal ethics committee. Male New Zealand white rabbits (2–3 kg) were anaesthetized with pentobarbitone sodium (6 mg ml^{-1}, 40–60 mg kg^{-1} body weight) *via* an ear vein and placed in the supine position on the operating table and were tracheotomized. The animals were ventilated *via* a two way valve (model 2200 A, Hans Rudolph Inc., Kansas City, MO, U.S.A.) by means of a Harvard model 683 rodent ventilator (Harvard Apparatus, South Natick, Massachusetts, U.S.A.). The ventilator was supplied with NO-free air using a charcoal filter (150 × 12 cm). Ventilation rate was 40 min^{-1} and the tidal volume was adjusted to keep end-tidal CO_2 at 4.0–5.0% as determined by a ventilatory monitor (Oscar-Oxy, Datex, Helsinki, Finland) connected to the tracheal cannula. The animals were paralyzed by injection of pancuronium bromide (0.5 mg kg^{-1}). Polythene catheters were inserted in the right femoral artery and the left jugular vein for recordings of mean arterial blood pressure, heart rate, sampling of blood gases and administration of drugs. A continuous infusion of glucose (2.75 g 100 ml^{-1}), dextran 70 (Macrodex® 2.8 g 100 ml^{-1}), $NaHCO_3$ (0.7 g 100 ml^{-1}) and pentobarbitone sodium (480 mg 100 ml^{-1}) was administered i.v. at a rate of 5 ml kg^{-1} h^{-1} by means of an infusion pump (Terumo STC-521, Terumo Inc., Tokyo, Japan). Body temperature, measured rectally, was maintained at 37–38°C by means of a heating pad connected to a thermostat (Heater control LB 700, PRODAB, Uppsala, Sweden). Insufflation pressure was recorded by a pressure transducer connected to a side arm of the tracheal cannula.

Cardiac output was measured as previously described (Adding *et al*., 1998). Briefly, a median sternotomy was performed and an ultrasonic flow probe (S6, Transonic Systems Inc., Cornell Research Park, Ithaca, NY, U.S.A.) was applied to the ascending aorta and connected to a blood flow meter (Transonic T-201). Blood flow in the ascending aorta was taken as a measure of cardiac output. The stroke volume was calculated by dividing cardiac output by heart rate. Total peripheral resistance was calculated from the expression (mean arterial blood pressure/cardiac output).

Perfusion experiments

The rabbits were prepared as above, sternotomized and then anticoagulated with heparin 1000 IU kg^{-1} body weight. The lungs were perfused *in situ via* the common pulmonary artery, at a constant rate of 45 ml min^{-1}, by means of a peristaltic pump (Sigmamotor, Middleport, NY, U.S.A.). The perfusion-buffer was not recirculated. The perfusion catheter was inserted in the pulmonary artery *via* a puncture wound in the right ventricle. Drainage catheters were placed in the left atrium and ventricle. The buffer perfusate contained (concentrations in mM); NaCl 125, KCl 4.3, $CaCl_2$ 2.4, $MgCl_2$ 1.3, NaH_2PO_4 1.2, glucose 8.3, and $NaHCO_3$ 35 and bubbled with 7% CO_2 in N_2. Temperature of the perfusate was maintained at 37°C by pre-heating the container of perfusion buffer in a water bath and by leading the perfusate through a jacketed spiral glass tubing connected to a thermostat-controlled water bath. A positive end-expiratory pressure of 3 cm H_2O was maintained throughout the perfusion experiments and left atrial pressure was set at 1.0–2.0 cm H_2O. Pressures in the pulmonary artery and the left atrium were measured in side-arms of the perfusion catheters by means of small saline-filled catheters connected to pressure transducers. The lungs were perfused with at least two litres of buffer fluid so that on visual inspection the post-lung perfusate appeared clear and colourless.

Drugs were administered by a microinfusion pump (CMA 100, Carnegie Medicine, Stockholm, Sweden) *via* a side-arm in the pulmonary artery catheter.

NO measurements in exhaled air

NO concentration was continuously measured in respiratory gas with a single-breath analysis system (Aerocrine AB, Danderyd, Sweden). Sampling was from the tracheal cannula, and sampling flow rate was 70 ml min^{-1}. Detection limit was 1.5 p.p.b. and response time was 0.35 s. At the given respiratory rate of 40 min^{-1} this setting resulted in a stabilization of NO concentrations during expiration. The NO analyzer was calibrated with dilutions of NO in filtered air using certified NO standard gas in nitrogen (AGA Specialgas, Lidingö, Sweden) and precision mass flow controllers (Bronkhorst, Ruurlo, Holland). The NO concentration in inhaled and exhaled air was, together with other parameters, continuously recorded on a Grass model 7 Polygraph (Grass Instruments, Quincy, MA, U.S.A.).

Experimental protocol

In vivo *experiments* After completion of the instrumentation the rabbits were allowed to rest until stable circulatory conditions and stable concentrations of exhaled NO were obtained. At this point an arterial blood gas sample was taken and analysed.

In the first set of rabbits ($n=7$) we studied the effect of adrenaline on pulmonary NO production and investigated the effect of β-adrenoceptor blockage. Adrenaline (3 μg kg^{-1} min^{-1}) was infused for 6 min before and after a bolus injection of propranolol (1 mg kg^{-1}). Nitric oxide in exhaled air, arterial blood pressure, heart rate and insufflation pressure were registered throughout the experiments and an arterial blood gas sample was performed during the infusion. In two rabbits, prior to β-adrenoceptor blockade, we examined the effect of α-adrenoceptor inhibition with phentolamine (1 mg kg^{-1}) on the response to adrenaline infusion.

Haemodynamic effects of adrenaline infusion (3 μg kg^{-1} min^{-1}) were studied by measuring cardiac output in open-chest rabbits ($n=3$) and calculating stroke volume and total peripheral resistance.

The subtype of β-adrenoceptors involved were investigated in rabbits receiving 3 min infusions at 15 min intervals of the β_1-adrenoceptor agonist prenalterol (0.01–30 μg kg^{-1} min^{-1}; $n=6$) or the β_2-adrenoceptor agonist terbutaline (0.01–30 μg kg^{-1} min^{-1}; $n=12$) in random fashion.

To elucidate the mechanism whereby β-adrenergic stimulation increased pulmonary NO production we repeated the infusions of prenalterol (0.01–30 μg kg^{-1} min^{-1}) during concomitant continuous infusion of nimodipine (0.6 μg kg^{-1} min^{-1}; $n=5$) a L-type calcium-channel blocker and examined the effect of forskolin infusions (0.01 and 0.03 μmol kg^{-1} min^{-1}; $n=4$) on exhaled nitric oxide concentrations.

Perfusion experiments After completion of the perfusion setup the lungs were allowed to rest until stable concentrations of exhaled NO and pulmonary artery pressure were obtained. Graded adrenaline infusions (0.03–10 μg kg^{-1} min^{-1}) were then administered to establish a dose-response curve for the

effect of adrenaline on pulmonary NO production in the *in situ* buffer-perfused lung ($n=4$). The effect of β-adrenoceptor blockade was also investigated by infusing adrenaline (100 μg kg^{-1} min^{-1}) in conjunction with saline or propranolol (0.5 mg kg^{-1} min^{-1}) at 15 min intervals ($n=4$). Subsequently, influence on exhaled NO by α-adrenoceptor stimulation, also causing an effect on pulmonary arterial resistance, was analysed by simultaneous phentolamine infusion (0.5 mg kg^{-1} min^{-1}).

Statistics

Data are expressed as means ± s.e.mean and *n* denotes number of animals or perfused lungs studied. One-way ANOVA and Student's paired *t*-test (normality distribution test passed) were used for statistical analysis of data using a computer program (SigmaStat, Jandel Corp. San Rafael, CA, U.S.A.).

Drugs

Adrenaline was from NM Pharma AB, Stockholm, Sweden; Nimodipine (Nimotop®) from Bayer Sverige AB, Göteborg, Sweden; HEPES and Propranolol from Sigma Chemical Company, St Louis, MO, U.S.A.; Prenalterol (Hyprenan®) from Hässle Läkemedel AB, Mölndal, Sweden; Terbutaline (Bricanyl®) from Draco Läkemedel AB, Lund, Sweden; Phentolamine (Regitina®) from Ciba-Geigy Ltd., Basel, Switzerland; Heparin from Kabi Vitrum, Stockholm, Sweden; Pancuronium bromide (Pavulon®) from Organon, Oss, Holland; Pentobarbitone sodium from Apoteksbolaget, Stockholm, Sweden; Dextran 70 (Macrodex®) from Pharmacia Infusion, Uppsala, Sweden.

General aspects

All pressure recordings were performed by means of Statham pressure transducers (Hato Rey, Puerto Rico). Samples (0.3 ml) for blood gas or perfusate gas analysis were drawn from the femoral and the left atrial catheter respectively, or from the perfusion reservoir, and were analysed on a Radiometer ABL 300 acid-base laboratory blood gas analyzer (Radiometer, Copenhagen, Denmark).

Results

Effects of adrenaline, prenalterol and terbutaline infusions in vivo

Mean arterial blood pressure, heart rate, cardiac output, insufflation pressure, and end-tidal CO_2 were stable during control conditions. Furthermore, stable NO concentrations of 28 ± 2 p.p.b. could be determined breath-by-breath in exhaled air (Figure 1), with a brief plateau towards the end of expiration (data not shown).

Dose-dependent increases in the concentration of NO in exhaled air were detected upon infusions of adrenaline (0.01–10 μg kg^{-1} min^{-1}). The increase in exhaled NO concentration was rapid and biphasic in its time-course, exhibiting an initial maximum within 30 s after start of infusion and was followed by a lower stable plateau level of NO concentration in exhaled air (Table 1; Figures 1 and 2). In addition to the changes in exhaled NO concentrations adrenaline infusion (3 μg kg^{-1} min^{-1}) increased mean arterial blood pressure and insufflation pressure but caused no significant change in heart rate (Table 1).

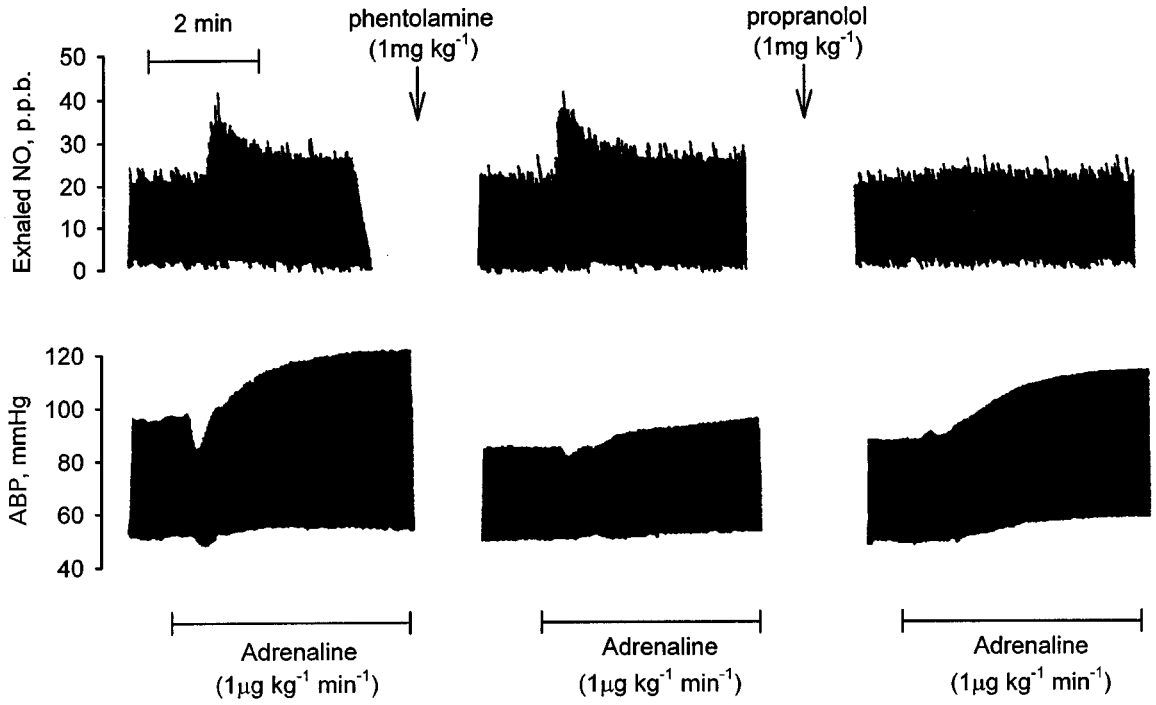

Figure 1 Representative recording of the effect of three consecutive adrenaline infusions (1 μg kg^{-1} min^{-1}) on exhaled nitric oxide measured breath by breath and arterial blood pressure (ABP) in a pentobarbitone anaesthetized rabbit. The first infusion was made during control conditions, the second infusion after treatment with phentolamine (1 mg kg^{-1}) and the third infusion was after propranolol (1 mg kg^{-1}). Note the rapid increase in exhaled NO in response to adrenaline infusion and how this effect was unaltered by phentolamine but abolished with propranolol pretreatment.

In the open-chest rabbits, where cardiac output was measured, adrenaline infusion (3 μg kg^{-1} min^{-1}) increased total peripheral resistance (by 61±4%, $P<0.01$) and stroke volume (by 12±2%, $P<0.05$), at 3 min after start of the infusion. At this time NO concentration in exhaled air had stabilized and was increased (by 22±2%, $P<0.01$) compared to control prior to infusion.

The effect of adrenaline infusions on exhaled NO concentration could not be altered by pretreatment with phentolamine (1 mg kg^{-1}) even though there was a marked reduction in the increase of mean arterial blood pressure (Figure 1) and insufflation pressure (data not shown). However, pretreatment with propranolol (1 mg kg^{-1}) significantly reduced the increments in exhaled NO concentrations in response to adrenaline (Figures 1 and 2; Table 1). Propranolol augmented the increase in arterial blood pressure (from 115±21 to 147±19%, $P<0.01$) and insufflation pressure (from 12±2 to 24±2%, $P<0.01$) in response to adrenaline (Table 1).

Infusions of prenalterol (0.01–10 μg kg^{-1} min^{-1}) or terbutaline (0.1–100 μg kg^{-1} min^{-1}) caused dose-dependent increases in exhaled NO concentrations (Figures 3 and 4). Prenalterol was more than 100 times as potent in stimulating pulmonary nitric oxide production compared to terbutaline (Figure 3). Prenalterol infusions in the higher doses (>3 μg kg^{-1} min^{-1}) caused slight reductions in mean arterial

Table 1 Effects of adrenergics on exhaled NO and haemodynamics

	NO (p.p.b.)	*MABP* (cmH_2O)	*HR* (min^{-1})	*IP* (cmH_2O)
No pretreatment				
Control	28±2	86±9	284±19	6.2±0.3
Adrenaline	37±2*	175±5*	290±7	6.9±0.4*
Control	28±2	108±2	311±12	8.8±0.7
Prenalterol	33±2*	104±2	313±10	8.8±0.7
Propranolol pretreatment				
Control	25±2	78±8	227±10#	6.2±0.3
Adrenaline	27±2#	186±5*	231±11#	7.7±0.3*#

Adrenaline and prenalterol infusions (3 μg kg^{-1} min^{-1}) were studied during measurements of exhaled nitric oxide (NO), mean arterial blood pressure (MABP), heart rate (HR) and insufflation pressure (IP) in pentobarbitone anaesthetized rabbits (no pretreatment). Adrenaline infusion was also studied after a bolus dose of propranolol (1 mg kg^{-1}). Values were obtained immediately before (control) and 3 min after start of respective infusion (during the exhaled NO plateau level). Data denoted with (*) indicates $P<0.05$ for difference from control value. Data denoted with (#) indicates $P<0.05$ for difference in adrenaline effect after propranolol treatment, as compared to no pretreatment. Repeated measures ANOVA. Values represent means±s.e.mean ($n=6$).

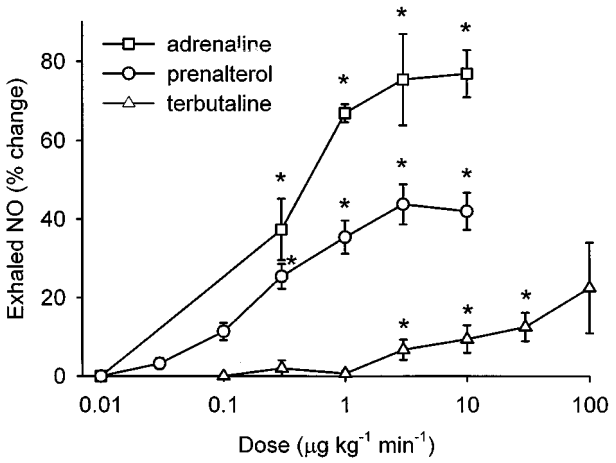

Figure 3 Pentobarbitone anaesthetized rabbits. Dose-response curves for the effect of adrenaline, prenalterol, and terbutaline infusions on exhaled nitric oxide. Measurements were obtained at the initial peak of exhaled nitric oxide concentrations. Level of significance denoted as (*) indicates $P<0.05$ for comparison with control. Mean±s.e.mean ($n=3-9$).

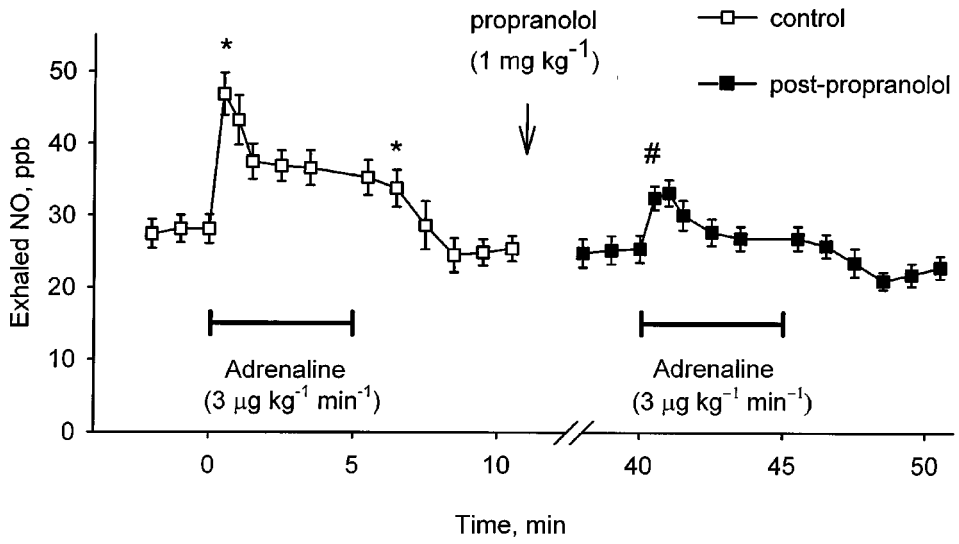

Figure 2 Time course of the effect of adrenaline infusion (3 μg kg^{-1} min^{-1}) on exhaled nitric oxide during control condition and after propranolol treatment (1 mg kg^{-1}) in pentobarbitone anaesthetized rabbits. Level of significance denoted as (*) indicates $P<0.05$ compared with control value at 0 min (repeated measurements one-way ANOVA). (#) indicates $P<0.05$ for peak values compared before and after propranolol (paired t-test). Mean±s.e.mean ($n=7$).

blood pressure but no changes in heart rate or in insufflation pressure (Table 1 and data not shown). Terbutaline infusions caused dose-dependent and sustained reductions in mean arterial blood pressure and increases in heart rate but no changes in insufflation pressure (Figure 4 and data not shown). Continuous infusion of nimodipine (0.6 μg kg^{-1} min^{-1}) did not alter the concentrations of exhaled NO during control conditions (data not shown). However, nimodipine reduced the increments in exhaled NO concentrations in response to prenalterol infusions (3 μg kg^{-1} min^{-1}, from 45$\pm$4 to 19$\pm$2%, $P<0.05$). Infusion of forskolin (0.01 μmol kg^{-1} min^{-1}) caused reductions in mean arterial blood pressure and concomitant increases in heart rate. However, there was no change in concentration of NO in exhaled air (Figure 4).

Effect of adrenaline administration on exhaled NO in the in situ *buffer perfused lung*

During control conditions the plateau concentration of exhaled NO measured breath-by-breath in the perfused lung averaged 51$\pm$4 p.p.b. Administration of adrenaline (0.03–10 μg kg^{-1} min^{-1}) increased exhaled NO concentrations in a dose-dependent manner (Figure 5). Concomitant dose-dependent increases in mean pulmonary artery pressure were also present, but there were no increases in left atrial pressure or in insufflation pressure (data not shown).

Administration of adrenaline (100 μg kg^{-1} min^{-1}) increased exhaled NO concentration (by 55$\pm$2%, $P<0.001$) during control conditions. However, during co-infusion of propranolol (0.5 mg kg^{-1} min^{-1}) exhaled NO concentration in response to adrenaline increased only by 16$\pm$6% ($P<0.001$). Co-infusion of phentolamine (0.5 mg kg^{-1} min^{-1}) abolished the increase in pulmonary artery pressure in response to adrenaline infusion but did not alter the concentration of NO in the exhaled air (data not shown).

Discussion

The present study clearly demonstrates that pulmonary NO production can be enhanced by adrenaline, and that the effect is exerted through activation of β-adrenoceptors. Furthermore, the results indicate that the mechanism is in part dependent on intact calcium-channel activity but may not be critically dependent on an increase in cyclic AMP levels.

Pulmonary NO is enzymatically produced from one of the guanidino nitrogens of L-arginine and molecular oxygen in an oxidation reaction. The enzyme responsible for this NO production, NO synthase, is a haeme-containing protein, expressed in three different isoforms (Bredt *et al*., 1991), two of which are dependent on calcium for their activation, nNOS and eNOS. The third isoform, iNOS, is calcium-independent and can be expressed in high concentrations after induction with cytokines.

Nitric oxide is a lipophilic molecule with a modest solubility in aqueous solutions. Therefore, in the respiratory system, where NO is continuously produced, the NO molecules readily diffuse across cell-membranes and escape into the airspace of the lungs. This provides the basis for the unique circumstance that direct measurement of endogenous NO *in vivo* is possible by analysing the concentrations of NO in exhaled air (Gustafsson *et al*., 1991). Such measurements have indicated that pulmonary NO production increases during physical exercise (Persson *et al*., 1993; Maroun *et al*., 1995) and in response to severe haemorrhage (Carlin *et al*., 1997) and that high levels of exhaled nitric oxide are present already at birth (Schedin *et al*., 1995). Adrenaline in high concentrations is known to be released into the blood stream in response to physical exercise, blood loss, and at birth (see Hoffman & Lefkowitz, 1994). Asphyxiated infants have a 200 fold increase

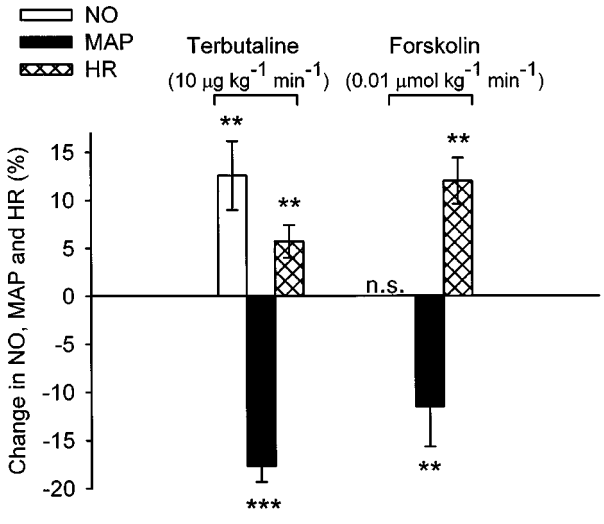

Figure 4 Pentobarbitone anaesthetized rabbits. Comparison between the effect of terbutaline (10 μg kg^{-1} min^{-1}) and forskolin (0.01 μmol kg^{-1} min^{-1}) infusions on exhaled nitric oxide, mean arterial blood pressure, and heart rate at 3 min after start of respective infusion. Note the increase in exhaled nitric oxide in response to terbutaline infusion in contrast to unchanged levels of exhaled nitric oxide in response to forskolin infusion, yet the haemodynamic effects were similar during respective infusion. Level of significance denoted as (**) indicates $P<0.01$ and (***) indicates $P<0.001$ for comparison with control value at 0 min. (n.s. denotes non significant change). Mean$\pm$s.e.mean ($n=4$).

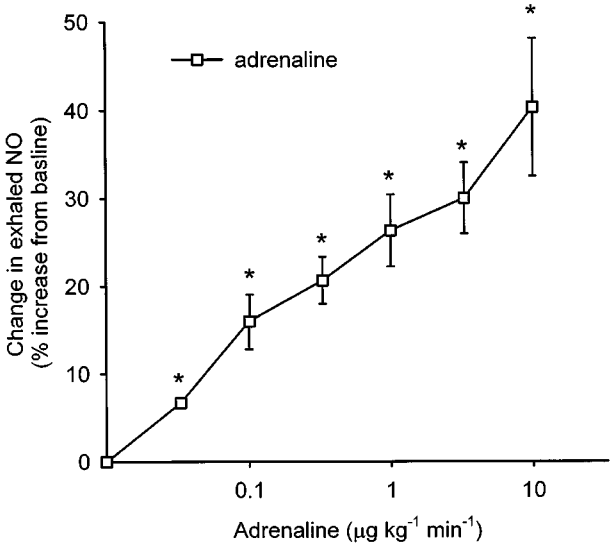

Figure 5 *In situ* Krebs-Henseleit-buffer perfused rabbit lungs. Dose-response curve for the effect of adrenaline infusions on change in exhaled nitric oxide. Measurements were obtained at the initial peak of exhaled nitric oxide concentrations. Level of significance denoted as (*) indicates $P<0.05$ for comparison with control. Mean$\pm$s.e.mean ($n=4$), missing error bars fall inside symbol.

in the plasma adrenaline concentration during delivery (see Lagercranz & Slotkin, 1986).

In the present study adrenaline induced dose-dependent increments in exhaled NO concentration both *in vivo* and in the buffer-perfused lung. Adrenaline was administered in doses known to increase the plasma adrenaline concentrations more than 15 fold in the rabbit (Maze *et al*., 1985). Since adrenaline also induced changes in arterial blood pressure and cardiac output one might suspect that the observed changes in exhaled NO concentrations were due to indirect pulmonary haemodynamic changes. However, the fact that similar responses could be elicited after α-receptor blockade with phentolamine and in the blood-free, buffer-perfused lung strongly suggests that the increase in NO concentration reflects an increased NO production within the pulmonary system, independent of haemodynamic alterations or changes in insufflation pressure.

Blockade of β-adrenoceptors reduced the increase in NO production in response to adrenaline, which however was unaffected by α-adrenoceptor antagonism. Administration of selective β_1- and β_2-adrenoceptor agonists increased pulmonary NO production although to a lesser degree than did adrenaline. The β_1-agonist was more than 100 times more potent than the β_2-agonist in stimulating NO production. This might be explained by the fact that β-adrenoceptors on the tracheobronchial tree of rabbit are mainly of the β_1-adrenoceptor subtype. Nevertheless it cannot be excluded that another subtype of β-adrenoceptor, e.g. the β_3-adrenoceptor, is involved.

Administration of the calcium-channel blocker nimodipine reduced the stimulatory effect on NO production in response to β_1-adrenoceptor activation. This suggests that the β-adrenoceptor stimulated NO production involves a calcium dependent NOS. This is in accordance with the observation that the major part of exhaled NO in rabbits is derived from a calcium dependent NOS (Persson *et al*., 1994a). A recent *in vitro* study of cultured tracheal epithelial cells concluded that isoproterenol, an unselective β-adrenoceptor agonist, could stimulate NO production. However, the NOS responsible for this NO generation was cyclic AMP dependent but calcium independent (Tamaoki *et al*. 1995b). In our study forskolin (an activator of adenylate cyclase), in concentrations causing profound hypotension and tachycardia, did not stimulate NO production. This negative finding was also confirmed in the perfused lung (data not shown). The discrepancy between the results of the two studies possibly reflects the involvement of different cell types. Exhalation profiles for NO in single breaths indicate that the major formation of NO present in exhaled air occurs in the airways, e.g., the respiratory bronchioles (Persson *et al*., 1993) where other epithelial cell types (Clara cells, small granular cells etc.) are present than in the alveoli. The lack of effect of an adenylate cyclase stimulator suggests that elevation of cyclic AMP is not a key event. Taken together our data rather suggest that pulmonary β-adrenoceptors are able to activate calcium influx. Indeed, there is evidence for the existence of β_1-adrenoceptors with direct G-protein coupling to calcium-channels (Brown & Birnbaumer, 1988).

Recently it has been shown that β-adrenoceptor stimulation induces arterial vasodilatation dependent on intact NO formation in the human forearm, the canine coronary artery and in the pial artery of newborn pigs (Dawes *et al*., 1997; Ming *et al*., 1997; Rebich *et al*., 1995). In the respiratory system NO plays a prominent role in relaxing vascular and bronchial smooth muscle. Nitric oxide is a powerful vasodilator during the circulatory adaptation at birth (Abman *et al*., 1990) and NO aids in maintaining the low pulmonary vascular resistance in adult life (Stamler *et al*,. 1994, Cooper *et al*., 1996). Allergen-induced bronchial obstruction is counteracted by NO (Persson *et al*., 1995a). Furthermore, β-adrenoceptor stimulated NO might increase ciliary beating activity in airway epithelial cells (Jain *et al*., 1993). In this study we show that pulmonary NO production may be enhanced as a consequence of β-adrenoceptor stimulation *in vivo*. We observed that when adrenaline caused an increase in blood pressure and insufflation pressure, a further increase was attained in the presence of propranolol suggesting a vaso- and bronchodilator β-adrenoceptor effect balancing the constrictive effects. Whether this involves β-adrenoceptor mediated stimulation of NO production merits further investigation. Though the physiological implication of β-stimulated NO production is not obvious, we speculate that β-adrenoceptor stimulated NO production might be of great importance in the adaptation to stress responses, e.g. birth, heavy exercise, blood loss and asthmatic attacks.

In conclusion, we demonstrate that endogenous pulmonary nitric oxide production can be activated by β-adrenoceptor stimulation. The effect is dependent on calcium flux but may not be critically dependent on changes in cyclic AMP levels. This suggests that circulating catecholamines as well as adrenergic nerve activity might influence pulmonary nitric oxide production.

The authors thank Prof P. Thorén for valuable discussions and Mr A. Guhl for excellent technical assistance. Supported by Stiftelsen Vårdal, the Swedish MRC (7919), Karolinska Institutet, the AGA Medical Research Fund, and the Swedish Heart-Lung Foundation. Dr A. Artlich's tenure was supported by the Deutsche Forschungsgemeinschaft grant AR 205/2-1.

References

ABMAN, S.H., CHATFIELD, B.A., HALL, S.L. & MCMURTRY, I.F. (1990). Role of endothelium derived relaxing factor during transition of pulmonary circulation at birth. *Am. J. Physiol.,* **259,** H1921 – H1927.

ADDING, L.C., BANNENBERG, G.L. & GUSTAFSSON, L.E. (1998). Gadolinium inhibition of pulmonary nitric oxide production and effects on pulmonary circulation in the rabbit. *Pharmacol. Toxicol.,* **83,** 8 – 15.

ASANO, K., CHEE, C.B., GASTON, B., LILLY, C.M., GERARD, C., DRAZEN, J.M. & STAMLER, J.S. (1994). Constitutive and inducible nitric oxide synthase gene expression, regulation, and activity in human lung epithelial cells. *Proc. Nat. Acad. Sci. U.S.A.,* **91,** 10089 – 10093.

BANNENBERG, G.L. & GUSTAFSSON, L.E. (1997). Stretch-induced stimulation of lower airway nitric oxide formation in the guinea-pig; inhibition by gadolinium chloride. *Pharmacol. Toxicol.,* **81,** 13 – 18.

BANNENBERG, G.L., GIAMMARRESI, C. & GUSTAFSSON, L.E. (1997). Inhaled carbon dioxide inhibits lower airway nitric oxide formation in the guinea-pig. *Acta Physiol. Scand.,* **160,** 401 – 405.

BELVISI, M.G., STRETTON, C.D., YACOUB, M. & BARNES, P.J. (1992). Nitric oxide is the endogenous neurotransmitter of bronchodilator nerves in humans. *Eur. J. Pharmacol.,* **210,** 221 – 222.

BREDT, D.S., HWANG, P.M., GLATT, C.E., LOWENSTEIN, C., REED, R.R. & SNYDER, S.H. (1991). Cloned and expressed nitric oxide synthase structurally resembles cytochrome P-450 reductase. *Nature,* **351,** 714 – 718.

BROWN, A.M. & BIRNBAUMER, L. (1988). Direct G protein gating of ion channels. *Am. J. Physiol.,* **254,** H401 – H410.

CARLIN, R.E., MCGRAW, D.J., CAMPORESI, E.M. & HAKIM, T.S. (1997). Increased nitric oxide in exhaled gas is an early marker of hypovolemic states. *J. Surgical Res.,* **69,** 362 – 366.

COOPER, C.J., LANDZBERG, M.J., ANDERSON, T.J., CHARBONNEAU, F., CREAGER, M.A., GANZ, P. & SELWYN, A.P. (1996). Role of nitric oxide in the local regulation of pulmonary vascular resistance in humans. *Circulation.,* **93,** 266 – 271.

DAWES, M., CHOWIENCZYK, P.J. & RITTER, J.M. (1997). Effects of inhibition of the L-Arginine/nitric oxide pathway on vasodilatation caused by beta-adrenergic agonists in human forearm. *Circulation,* **95(9),** 2293 – 2297.

GUSTAFSSON, L.E., LEONE, A.M., PERSSON, M.G., WIKLUND, N.P. & MONCADA, S. (1991). Endogenous nitric oxide is present in the exhaled air of rabbits, guinea-pigs and humans. *Biochem. Biophys. Res. Commun.,* **181,** 852 – 857.

HOFFMAN, B.B. & LEFKOWITZ, R.J. (1994). Catecholamines, Sympathomimetic Drugs, and Adrenergic receptor Antagonists. In *Goodman & Gilman's The Pharmacological Basics of Therapeutics*. eds. Hoffman, B.B. & Gilman, A.A. pp. 199 – 220. 9th edn. London: McGraw-Hill.

JAIN, B., RUBINSTEIN, I., ROBBINS, R.A., LEISE, K.L. & SISSON, J.H. (1993). Modulation of airway epithelial cell ciliary beat frequency by nitric oxide. *Biochem. Biophys. Res. Commun.,* **191,** 83 – 88.

KHARITONOV, S.A., LUBEC, G., HJELM, M. & BARNES, P.J. (1995). L-Arginine increases exhaled nitric oxide in normal human subjects. *Clin. Sci.,* **88,** 135 – 139.

KOBZIK, L., BREDT, D.S., LOWENSTEIN, C.J., DRAZEN, J., GASTON, B., SUGARBAKER, D. & STAMLER, S. (1993). Nitric oxide synthase in human and rabbit lung: immunocytochemical and histochemical localization. *Am. J. Respir. Cell Mol. Biol.,* **9,** 371 – 377.

LAGERCRANTZ, H. & SLOTKIN, T.A. (1986). The 'stress' of being born. *Sci. Am.,* **274,** 100 – 107.

LAWRENCE, A.J., KRSTEW, E. & JARROT, B. (1996). Actions of nitric oxide and expression of the mRNA encoding nitric oxide synthase in rat vagal afferent neurons. *Eur. J. Pharmacol.,* **315(2),** 127 – 133.

MARLETTA, M.A. (1989). Nitric oxide: Biosynthesis and biological significance. *TIBS,* **14,** 488 – 492.

MAROUN, M.J., MEHTA, S., TURCOTTE, R., COSIO, M.G. & HUSSAIN, S.N.A. (1995). Effects of physical conditioning on endogenous nitric oxide output during exercise. *J. Appl. Physiol.,* **79,** 1219 – 1225.

MAZE, M., SPISS, C.K., TSUJIMOTO, G. & HOFFMAN, B.B. (1985). Epinephrine infusion induces hyporesponsiveness of vascular smooth muscle. *Life Sci.,* **37,** 1571 – 1578.

MING, Z., PARENT, R. & LAVALLEE, M. (1997). Beta 2-adrenergic dilation of resistance coronary vessels involves KATP channels and nitric oxide in conscious dogs. *Circulation,* **95,** 1568 – 1576.

MONCADA, S. (1994). Nitric oxide gas: mediator, modulator, and pathophysiologic entity. *J. Lab. Clin. Med.,* **120,** 187 – 191.

MONCADA, S., PALMER, R.M.J. & HIGGS, E.A. (1991). Nitric oxide: Physiology, pathophysiology and pharmacology. *Pharmacol. Rev.,* **43,** 109 – 141.

PALMER, R.M.J., FERRIGE, A.G. & MONCADA, S. (1987). Nitric oxide release accounts for the biological activity of endothelium-derived relaxing factor. *Nature,* **327,** 524 – 526.

PERSSON, M.G., FRIBERG, S.G., GUSTAFSSON, L.E. & HEDQVIST, P. (1995a). The promotion of patent airways and inhibition of antigen-induced bronchial obstruction by endogenous nitric oxide. *Br. J. Pharmacol.,* **116,** 2957 – 2962.

PERSSON, M.G., GUSTAFSSON, L.E., WIKLUND, N.P., MONCADA, S. & HEDQVIST, P. (1990). Endogenous nitric oxide as a probable modulator of pulmonary circulation and hypoxic pressor response *in vivo*. *Acta Physiol. Scand.,* **140,** 449 – 457.

PERSSON, M.G., LÖNNQVIST, P.A. & GUSTAFSSON, L.E. (1995b). Positive end-expiratory pressure ventilation elicits increases in endogenously formed nitric oxide as detected in exhaled air of rabbits. *Anesthesiology,* **82,** 969 – 974.

PERSSON, M.G., MIDTVEDT, T., LEONE, A.M. & GUSTAFSSON, L.E. (1994a). Ca^{2+}-dependent and Ca^{2+}-independent exhaled nitric oxide, presence in germ-free animals, and inhibition by arginine analogues. *Eur. J. Pharmacol.,* **264,** 13 – 20.

PERSSON, M.G., WIKLUND, N.P. & GUSTAFSSON, L.E. (1993). Endogenous nitric oxide in single exhalations and the change during exercise. *Am. Rev. Respir. Dis.,* **148,** 1210 – 1214.

REBICH, S., DEVINE, J.O. & ARMSTEAD, W.M. (1995). Role of nitric oxide and cAMP in beta-adrenoceptor-induced pial artery vasodilation. *Am. J. Physiol.,* **268,** H1071 – H1076.

SCHEDIN, U., NORMAN, M., GUSTAFSSON, L.E., HERIN, P., JACOBSSON, J., ANDERSSON, G. & FROSTELL, C. (1995). Endogenous nitric oxide in the upper airways of healthy newborn infants. *Pediatric Res.,* **40,** 148 – 151.

SHAUL, P.W., NORTH, A.J., WU, L.C., WELLS, L.B., BRENNON, T.S., LAU, K.S., MICHEL, T., MARGRAF, L.R. & STAR, R.A. (1994). Endothelial nitric oxide synthase is expressed in cultured human bronchiolar epithelium. *J. Clin. Invest.,* **94,** 2231 – 2236.

STAMLER, J.S., LOH, E., RODDY, M-A., CURRIE, K. & CREAGER, M.A. (1994). Nitric oxide regulates basal systemic and pulmonary vascular resistance in healthy humans. *Circulation,* **89,** 5.

STRÖMBERG, S. LÖNNQVIST, P.A. PERSSON, M.G. & GUSTAFSSON, L.E. (1997). Lung distension and carbon dioxide affect pulmonary nitric oxide formation in the anaesthetized rabbit. *Acta Physiol. Scand.,* **159,** 59 – 67.

TAMAOKI, J., CHIYOTANI, A., KONDO, M. & KONNO, K. (1995a). Role of NO generation in beta-adrenoceptor-mediated stimulation of rabbit airway ciliary motility. *Am. J. Physiol.,* **268,** C1342 – C1347.

TAMAOKI, J., KONDO, M., TAKEMURA, H., CHIYOTANI, A., YAMAWAKI, I. & KONNO, K. (1995b). Cyclic adenosine monophosphate-mediated release of nitric oxide from canine cultured tracheal epithelium. *Am. J. Respir. Crit. Care Med.,* **152,** 1325 – 1330.

WEI, X.Q., CHARLES, I.G., SMITH, A., URE, J., FENG, G.J., HUANG, F.P., XU, D., MULLER, W., MONCADA, S. & LIEW, F.Y. (1995). Altered immune responses in mice lacking inducible nitric oxide synthase. *Nature,* **375,** 408 – 411.

(Received April 24, 1998
Revised October 10, 1998
Accepted November 17, 1998)